CARDE TECH. LETTER N-47-19

[redacted]

SECOND QUARTERLY REPORT

on

CF-105 WEAPON SYSTEM ASSESSMENT

by

J.T. Baker
R.S. Mitchell
J.T. MacFarlane

CANADIAN ARMAMENT RESEARCH AND DEVELOPMENT ESTABLISHMENT

Valcartier, Quebec

November 1958

CANADIAN ARMAMENT RESEARCH AND DEVELOPMENT ESTABLISHMENT
DEFENCE RESEARCH BOARD

Technical Letter No. N-47-12 Date 15 November 1956 Copy No. 22

Author J.T. Baker Approved by [signature] Sheet Title of 701

PROJECT
CF-105 ASSESSMENT

SECOND QUARTERLY REPORT

Period 1 August to 31 October 1956

Compiled by: - J.T. Baker
R.S. Mitchell
J.T. Macfarlane

Systems Group

[signature]
Chief Superintendent

TABLE OF CONTENTS

..../2

TABLE OF CONTENTS(Cont'd)

10. APPENDICES

SUMMARY

This technical letter has been issued as an interim progress report on the work being done at CARDE in connection with the CF 105 Weapon System assessment.

The objectives of this study are stated and the methods of approach to the problem are described.

Technical appendices dealing with various facets of the work are included. These are not intended to describe completed sections of the assessment, but rather to familiarize the reader with the task and the methods of investigation which have been adopted.

SECOND QUARTERLY REPORT
on
CF 105 WEAPON SYSTEM ASSESSMENT

1. INTRODUCTION

The engagement of high speed targets by supersonic interceptors armed with air-to-air missiles introduces a variety of new problems which cannot be assessed by extrapolation of data arising from experience with conventionally armed subsonic aircraft.

For this reason, CARDE has been requested by the RCAF to carry out an evaluation study of the effectiveness of a supersonic interceptor weapon system based on the AVRO CF-105 aircraft armed with Sparrow II or Sparrow III air-to-air missiles.

The primary objectives of the study as stated by the RCAF are:

(i) To evaluate the combat effectiveness of the system with different types of armament, beginning with the Sparrow series, for probable bomber threats including the Bison, Badger and Bear.

(ii) To investigate the effect of variation in fire control parameters such as A.I. radar range and look angle.

(iii) To establish the minimum acceptable level of aerodynamic performance and to investigate the effect of possible design changes in the aircraft and engine configuration, insofar as these changes affect combat performance.

(iv) To determine the effect of variations in G.C.I. placement accuracy.

(v) To explore possible tactics and suggest optimum modes of attack.

In order to arrive at an accurate assessment of the overall combat effectiveness of this weapon system, the many inter-dependent sub-systems of which it is composed require analysis, first individually and then collectively, so that the relative importance of the principal parameters can be established. Naturally, an exploratory study of this nature is quite involved and certainly time-consuming, if it is to be sufficiently exhaustive to achieve the above-stated objectives. Further, the task is rendered difficult in that very little preliminary information is available on which to base investigations, as it is evident that the establishment of such data is perhaps the primary object of the study.

The general approach then has been to adopt a range of parameters which should encompass final characteristics, then to conduct an analysis based on these and thus establish their validity and importance in the particular

sub-system, as well as their influence on the effectiveness of the system as a whole. In this way overall effectiveness can be established as a function of the parameters of individual sub-systems and optimum design values indicated.

Although this method is elongated and somewhat tedious, an important compensatory feature lies in the fact that the most critical areas requiring further study are highlighted.

2. INITIATION OF STUDY

CARDE Technical Letter N-47-3, May 56, gives a review of the general interceptor-weapon problem with particular reference to the proposed CF-105 system, and also sets out in some detail a proposal for the prosecution of studies to attain the objectives since enumerated by the RCAF. A directive to initiate the CF-105 Weapon System Assessment Study was received on May 29, 1956 and work has actively continued in accordance with the original program as set out in CARDE Tech. Letter N-47-3, May 4, 1956.

3. MANPOWER ALLOCATION

This work is being carried out by specialist sections within the various Wings of CARDE, under the co-ordination and direction of the Systems Group which is generally responsible for the task.

During the period under review a total of 17 professional personnel have been engaged on the work. The degree of participation was as follows:

	Full time	Part time
Systems Group	3	2
B Wing	1	-
D Wing	1	-
G Wing	7	3
TOTAL	12	5

This team has now been enlarged by some 5 engineers whose services became available for the CF 105 Assessment Study on 1st November. This additional effort will be applied in the Fire Control and Analogue Computing groups of "G" Wing.

4. GENERAL REVIEW OF PROBLEM

Generally, the work to date has progressed smoothly with emphasis on the study of the interceptor placement problem. This is a pivot point in assessing the capability of a fighter and is an area in which work could readily proceed with the data at hand. This work has been concentrated on studying the interception of a high altitude, super-sonic target, since it was the most unfamiliar situation and required an extensive parametric study.

This work has provided much basic data which is required to correlate the effects of aircraft manoeuvre, speed ratios, AI range and G.C.I. accuracies.

Work on other aspects of the system such as warhead lethality, target vulnerability, effects of ECM and fire control problems has proceeded satisfactorily during the period covered by the report. However two serious

obstructions, lack of basic information and inadequate computing facilities somewhat hampered progress but have now been overcome.

4.1 Computing Facilities

During the period under review the analogue computing equipment at CARDE has been expanded by more than 100%. Unfortunately, delayed deliveries and faulty equipment in the new plant have so far precluded the use of the expanded facility for problems associated with the CF 105 Assessment. However most of the new equipment has now been delivered and the eradication of defects is proceeding satisfactorily.

At the same time, repeated extension of delivery dates by the manufacturers of this equipment has rendered it necessary to modify the original schedule in order to obtain a maximum of useful results for inclusion in the present study. It is confidently hoped however, that the new equipment will be in full working order at an early date and that the revised program will be followed without further degradation.

4.2 Basic Information

When the CF 105 study was planned in early spring of 1956 it was evident that certain basic data relating to the proposed weapons would be needed from US sources. It was also thought that much complementary information resulting from similar studies conducted in the USA may well be available.

To establish the validity of these assumptions, an unclassified exploratory tour of various departments in Washington was made by a member of the Systems Group during the week of June 25, 1956. As a result of this visit, clearances were formally requested in July for a small party of CARDE personnel to visit selected U.S. Establishments commencing September 10.

On September 7, the US Navy requested a two week postponement and on September 21 suggested that the proposed party should visit various offices in Washington to ascertain whether the data required could not be obtained there.

Such a visit was made during the week of October 8. The information obtained was not directly applicable to the CF 105 Study and agreement was reached with some of the people interviewed that the type of information sought could best be obtained from the establishments for which clearances had been requested originally. Appendix A.

Further negotiations with the U.S. Navy became necessary which have culminated in the approval of the original request. The series of visits will now take place commencing December 3, 1956.

Unfortunately the unavoidable postponement of these visits has made it necessary to pursue the study using estimated characteristics of the missile and AI equipment. Also it is felt that discussions with personnel who have participated in similar studies in the U.S.

might well have provided reassuring confirmation of our data, assumptions and procedures employed.

5. ACTIVITIES August - October 1956

5.1 Information Sources

Reference has already been made herein to delays in arranging for certain personnel engaged on the study to visit U.S. establishments for consultations on basic data. (4.2).

In the meantime it must be stated that liaison arrangements with AVRO Aircraft Ltd. Toronto and N.A.E. have functioned smoothly resulting in a steady flow of information on CF 105 Aerodynamics as it becomes available. Appendix B.

A somewhat similar arrangement has been established with R.C.A. Waltham, and it is hoped that this channel of communication will be used to the full from now on.

Valuable cooperation has been achieved with DSI and DAI, RCAF Headquarters, particularly in relation to information and advice on aspects of enemy aircraft, equipment and tactics.

During the period covered by this report the Systems Group was fortunate in having an opportunity for discussions with several scientists from RAE Farnborough and other U.K. establishments who were visiting Canada and rearranged their programs for this purpose.

5.2 Placement Problem

5.2.1 Two Dimensional Placement (Mild Evasion)

Placement charts for gently evading targets have been prepared by the REAC group. These, together with charts for non evading targets have been analysed and curves showing the variation of probability of successful placement as a function of various parameters have been drawn. Appendix K.

It must be stressed that the analysis of these results is by no means complete. However they are published so as to provide as much advance information as possible to interested parties.

5.2.2 Interceptor Simulation

Aerodynamics of the CF 105 were set up on the REAC in two dimensional form and trajectories of decelerating turns were drawn in space and target co-ordinates. Preliminary results are published in Appendix C. These trochoids will be used in preparation of further, more accurate placement charts for the aircraft decelerating against non evading targets.

5.2.3 Two Dimensional Placement (Full Evasion)

The two dimensional placement analysis has continued with more pronounced target evasion injected. Increased computer

facilities, now becoming available will expedite this work. Placement charts will be prepared for the decelerating interceptor against targets using more pronounced evasion.

5.2.4 Three Dimensional Placement

The proposal for three dimensional simulation on the REAC has been checked and is currently being instrumented. (Ref. 1 Appendix G.). Simulation of aerodynamics and other REAC work is reviewed in Appendix D.

5.2.5 AI Acquisition

Work carried out to date confirms that A.I. acquisition capability is an important and sensitive parameter in assessing the effectiveness of this Weapon System. Unfortunately, it is also a function of one of the most controversial facets of Radar engineering - Target Reflection Area. For this reason, the values used as basic data for a theoretical study of this type can be decided upon only after careful consideration of various opinions as to the interpretation of the scant experimental data which is available.

Since publication of the First Quarterly Report on this project, helpful discussion has led to revision of some of the assumed target reflection areas used in computing contours of AI range capability. Appendix E deals more fully with this subject and includes the modified contours.

5.3 Missile Studies

The results obtained from REAC Studies carried out in the first period, Appendices J and K, Ref. 1., have been examined in conjunction with information of a similar nature acquired from other sources.

Work, based on this data is proceeding in order to generate missile launch zones for use in the main three dimensional study. Ref. 5.2.4.

5.4 E.C.M. Aspects

During the period under review effort has been applied in two separate directions in order to accumulate data in a suitable form to feed into the systems study.

1. Studies are being conducted within the Systems group to explore the possibilities of defeating some forms of ECM, notably AI jamming, by tactical or manoeuvre methods.

2. Assessments of the susceptibility of individual components and subsystems to expected forms of ECM are proceeding in collaboration with DRTE.

Some results of the work carried out so far by the Systems group are given in Appendices F and G.

No results of the work with DRTE are yet available but these should be on hand shortly.

During the period of this report investigations of ECM techniques generally have continued. These tend to confirm the content of the preliminary survey published as Appendix L of the first progress report. Ref. 1. Valuable informal discussions with visitors from the U.K. who are intimately associated with this aspect of Weapon System Engineering also confirmed the validity of the basic assumptions on which the detailed ECM studies are proceeding. As great importance is attached to defeating "range denial" occasioned by some forms of jamming, particularly as it applies to the AI equipment of the fighter, work is continuing to explore every possibility of achieving this.

5.5 Fire Control Studies

Unanticipated delay in obtaining the services of additional suitably qualified personnel somewhat retarded progress of these studies until the latter part of the period under review. Two additional engineers have now been allocated to this group and work on the fire control problem generally is well underway. An outline of the program and present status of the work is given in Appendix H.

5.6 Lethality

Work in this field is proceeding satisfactorily but as yet insufficient quantitative results have been obtained to warrant publication. This area of the study has been broken down into separate considerations of:

(a) Warheads

(b) Fuzes

(c) Vulnerability of Targets

As these separate investigations progress, the trends and results obtained will be correlated with other pertinent information to establish system lethality.

5.6.1 Warhead

Since publication of the first progress report, Ref. 1, (Appendix N), informal talks with certain members of the U.K. Lethality Mission who visited CARDE have served to generally confirm that continuous rod warheads appear superior to fragmenting types for the weapon system under consideration.

Until recently great difficulty has been experienced in obtaining data on the warheads which have, and are being developed for the Sparrow II and III missiles, as a result of which it was necessary to resort to using estimated characteristics in the present work. However, CARDE representation on the Tripartite Lethality Conference held recently in the U.S.A. has proved well worthwhile. During these sessions data relating to Sparrow II and III Warhead design and performance was obtained which generally confirms the estimated figures now being used for the CF 105 Systems Study.

5.6.2 Target Vulnerability

Vulnerability assessments of current and future enemy bomber aircraft present problems which are not readily solvable by methods used previously.

However a program is underway to investigate the vulnerability of two representative types of Russian heavy bombers which are expected to be operational during the period 1958-1965.

Appendix J of this report outlines in more detail the approach to vulnerability studies which has been adopted, and also describes the Terminal - Engagement Simulator which will be used to correlate results of warhead, fuze, vulnerability and guidance studies which are now proceeding.

This simulator was recently designed at CARDE and, together with scale models of the bombers to be studied, is nearing completion.

Co-operation with DAI, RCAF and informal talks with visiting personnel of R.A.E. Farnborough have been of great value in obtaining basic data for this section of the study.

6. PRESENT INDICATIONS

The following are noted as tentative trends arising from the work so far.

6.1 Sub-Sonic Target Case

The placement aspects of the present study have received most emphasis in relation to super-sonic targets. These studies have confirmed, however, that treatment of sub-sonic targets will require a modified approach. Work in this connection will now commence in order to balance the effort already expended on super-sonic target cases.

6.2 Target Evasion

Even gentle evasion reduces the probability of successful placement considerably, if it can be assumed that intelligent evasion always takes place. Consideration will therefore have to be given to target evasion philosophy as it has become clear that the situation is more complex than a simple extension of the 'non evasion' case.

6.3 Launch Zones

As the work progresses it is becoming more clear that variations of launch zones are relatively unimportant as a contributing factor of placement probability.

6.4 Warheads

Investigations to date indicate that fragmenting type warheads, of the size that can be carried by Sparrow Missiles, tend towards uselessness against the targets under consideration. The continuous rod type, however, shows some promise and will be thoroughly studied. In the course of discussions with members of the UK Lethality Mission it was learnt that continuous rod warheads present no major production problems aside from the fact that extreme care in excess of anything encountered elsewhere is required in welding the ends of the individual rods.

6.5 Placement Probability

In the case of non evading and gently evading targets, AI range, ground control positioning accuracy, and fighter turn capability are three mutually related variables. In general, deficiencies in one of these parameters may be made up by improvements in one of the others.

For poor ground control accuracy, probability of success in positioning is almost a linear function of AI range capability; as ground control accuracy is improved a knee occurs in the curve, indicating that beyond a certain value, increased AI range will not greatly increase probability of successful positioning.

The same sort of limiting process seems to operate with regard to g-capability: that is, for good ground control accuracy, there is a value of fighter turn capability beyond which increase in this parameter does not materially increase probability of successful placement.

However, work to date has not included deceleration of the interceptor which accompanies pronounced manoeuvre, thus it is not yet known whether this maximum useful value of fighter g capability could be achieved by the CF 105 even with very good ground control accuracy.

7. FUTURE PROGRAM

During the current quarter, November 1 to January 31, emphasis will be placed on the following facets of the work.

(a) Further analysis of results of graphical placement work.

(b) Studies of placement probabilities for an evading target taking into account evasion philosophy.

(c) Two dimensional placement studies incorporating aircraft aerodynamics.

(d) Obtaining preliminary results of three dimensional placement work now proceeding.

(e) Evaluation of the defence afforded by the system against subsonic targets (USSR Bear).

(f) Studies of Target Vulnerability to obtain data in a suitable form for use in the System Lethality assessment.

(g) Carrying out runs with the Terminal Engagement Simulator as part of the Lethality assessment study.

(h) Conducting study of intended fire control system and correlating results with those of (d) above.

(i) Continued work on ECM to establish:

(i) System vulnerability.

(ii) Ways of defeating or reducing the adverse effects of ECM tactically or otherwise.

(iii) The best means of reflecting the results of (i) and (ii) in the overall study.

(j) Visits to U.S. Establishments. These are now scheduled to commence December 3rd and will be computed by 18th.

8. REFERENCE No. 1.

CARDE Technical Letter N-47-8, "First Progress Report on CF 105 Weapon System Assessment", by Baker, Mitchell & Macfarlane.

9. DISTRIBUTION

Recipient	Copy No.
Chief Supt CARDE	1
D/Chief Supt "	2
A/Chief Supt "	3
Supt A Wing "	4
" B " "	5
" C " "	6
" D " "	7
" E " "	8
" F " "	9
" G " "	10
Librarian "	11
Document Library CARDE	12-15

..../22

DISTRIBUTION (Cont'd)

Recipient	Copy No.
Systems Group	16-18
DWR, DRB H/Q	19-20
Chief Scientist DRB	21
CH. of Establishments DRB	22
DRM, London	23-24
DRM, Washington	25-26
DSIS, DRB	27-29
D.Eng.R. DRB	30
D.Phys.R. DRB	31
RCAF HQ Attn COR/DSE	32-33
" " Attn S/L Peek 2630 A Bldg	34-36
" " Attn C.Arm.Eng.	37-39
" " S.A.C.A.S.	40
S/N.A.E.	41
S/O.R.G.	42
S/D.R.T.E.	43
DRB Liaison Officer, Lincoln Lab,MIT	44
Systems Group	
Mr. R.S. Mitchell	45
Mr. J.T. Baker	46
Mr. J.T. Macfarlane	47
Mr. F. Slingerland	48
Contributors	
Mr. D. Mc Kinnon	49
Mr. D. Ferguson	50
Mr. C. Wilson	51
Mr. B. Cheers	52
Mr. J. Regniere	53
For Information	
Dr. G.V. Bull	54
Mr. Y. Caron	55
Mr. L. Robichaud	56
Spares	57-100

APPENDIX A

SUMMARY OF REPORT ON VISIT TO WASHINGTON, D.C.
(9 - 12 October, 1956)

1.0 PURPOSE OF VISIT

A request to visit a number of U.S. establishments as outlined in CARDE Technical Letter N-47-7 was submitted in July. The U.S. Navy requested that a classified visit first be made to certain of their Washington offices so that they might better ascertain the needs of the study in question and to make certain the information required was not at Washington. The organizations that were visited at the Navy's suggestion were:

Operations Evaluation Group

Bureau of Aeronautics (Research Section and Guided Missile Section)

Office of Naval Research (Operations Research Section)

2.0 GENERAL RESULTS OF VISIT

The people interviewed were very cooperative and helpful, and discussions ranged over the topics of methods, interception studies and weapon characteristics. However, although useful guiding information was given, detailed technical material of the type required was not obtainable at the places visited. The personnel at these Naval offices agreed that the information desired was best obtained by visiting the establishments or contractors concerned. An outline is given below of the type of deficiencies that were encountered in the information gathered during this visit.

2.1 System and Interception Studies

Most of the groups visited were not working on interception problems or aircraft weapon systems for the same time period as is of concern in the CF-105 study. Although the discussions were not without interest the problems covered were on systems which are one, two or three generations behind the 1960-1965 era. For the type of assessment that is required in the CF-105 study it is necessary to deal with futuristic thinking and planning of the interception problem.

2.2 The F4H

The aircraft system in the U.S. that most resembles the CF-105 is understood to be the F4H. Information on this system was not available on this visit, but is most emphatically desired as it would appear to bear the closest relation to the Canadian study.

2.3 Methods

Unfortunately most of the studies discussed related to systems far removed from the era of interest, as the groups visited were engaged in general operational research. For this reason their approach to the problems was of a broader but simplified nature compared to that required for the CF 105 study. No opportunity offered for detailed discussions on digital or analogue computation methods.

2.4 Missiles

Some information was obtained on Sparrow II and Sparrow III, both present versions and supersonic launch versions. Types of additional information that would be required from contractors would be:

(a) Variations in launch zone data outlined in brochures when target and launching speeds are changed or when the missile characteristics are altered, such as by increase in manoeuvre capabilities. (The actual launch zones discussed were all subsonic launch).

(b) Effect of programmed boost manoeuvres for Sparrow III.

(c) Expected distribution of miss distance.

(d) Analogue computor methods, especially with respect to approximation to three-dimensional cases by two-dimensional runs.

(e) Transfer function of Sparrow III, in sufficient detail that if the launch zone data has to be extended a simplified simulation of Sparrow III could be undertaken at CARDE.

2.5 Lethality

No detailed information was obtained on lethality studies. It is desired to discuss this subject at establishments that have incorporated this phase of the work in interception studies, such as the Armament Lab. at NADC, and appropriate personnel at Rand and Bell Telephone.

2.6 Fuzing

The problem of fuzing was mentioned only briefly. An aspect of the problem which is of concern in the CF-105 study is how the kill probability varies with angle of approach of missile to target, and what the distribution of fuze triggering points might be.

2.7 E.C.M.

Because of security restrictions the question of E.C.M. was discussed only in the most general terms. However it 's a factor which could drastically alter the effectiveness of the system, and will eventually have to be included.

3.0 CONCLUSION

As a result of this visit it was decided to resubmit the requests for visits to U.S. Establishments. These requests were held in abeyance by the U.S. Navy.

4.0 SUMMARY OF INFORMATION OBTAINED

Several points of interest which were discussed at the various offices are outlined below. For a more detailed account CARDE Technical Letter N-47-11 should be consulted.

4.1 Operations Evaluation Group

People interviewed had recently conducted a study for the U.S. Navy on Short Term Improvements in Fleet Air Defence. (OEG Report No. 74). This study was the only OEG work that was even remotely concerned with the type of work of interest in the CF-105 study. It considered point defence of a convoy against radial attacks. The target penetration was the main criterion of success.

It was found that the average experimental tally-ho occurred at the ideal collision point and the distribution was normally distributed with a standard deviation of 10-11 miles.

It was found that within the range of velocities considered this standard deviation was independent of speed ratio and also of range of target at assignment and range of interceptor at assignment.

Figures for penetration between detection and intercept obtained for jet attackers were:

50% less than 10 miles

80% less than 15 miles

On these trials 75% of tally-ho's were converted to firing passes.

4.2 Bureau of Aeronautics

One office visited has cognizance of, among other things, Sparrow II and Sparrow III programs. Here there was conducted a general discussion on Sparrow family missiles.

Supersonic Launch - Present configuration is aerodynamically acceptable for launch Mach numbers up to 2.2 and altitudes up to 70,000 ft. Main problems are temperature and erosion of radome of externally carried missiles. Sparrow II D is built with a cooling duct through the centre line of the guidance head. Liquid cooling would be used. A semi submerged method of carrying the missiles was to be considered.

Missile is being progressively modified for supersonic launch. These weapons will retain subsonic launch capabilities.

Three-Dimensional Simulation - It was stated that Raytheon and NADC have so far done only 2-D missile trajectory studies in vertical and horizontal planes. Both have analysed snap up capabilities of various aircraft missile combinations. (Sparrow I/F7U, Sparrow II/F3H2). NADC did one complete 3-D analysis and showed that 2-D analysis gave an acceptable approximation.

The Sparrow III can be made to slave the autopilot gyro reference to the AI look angle so that the missile is commanded to this space course during boost. This does not prevent blind launch since the missile dish is independently stabilized to the line of sight.

Preparation Time - Warm-up time 3 minutes for Sparrow III or II. Normally the missiles would be put on stand-by at take-off. Committment time for Sparrow II is 2 seconds, for Sparrow III, 1 second.

Some graphs for Mach 2 launch were obtained and are shown in Figures A-1 and A-2.

Another office visited was the Mathematics Section. Here their method for computation of probabilities of detection and conversion was described. Placement diagrams are drawn by superimposing space trajectories of fighter missile and target for both evading and non evading targets. The resulting diagrams are the same as those produced at CARDE. Probabilities are determined by integrating along the manoeuvre barriers the cumulate probability of detection given as

$$P_{DC} = \int_{-\infty}^{+\infty} P_D(Z) \frac{e^{-Z^2/2\sigma^2}}{2\pi\sigma} dZ$$

The diagrams were drawn graphically and the integration performed on a digital computer. The standard deviation used for vectoring accuracy was 3 miles.

A curve was obtained of experimental AI Detection probability based on 350 operational interceptions using F2 H aircraft of the VC4 squadron in Atlantic City, equipped with E10 system (250 kw 24 in dish). This is shown in Figure A-3.

It was stated that for the system, considering take-off to missile impact, the expected reliability figure was between 70 to 80%. This was based on present day figures of 40-50% with an extrapolation for expected improvements. The time-scale for this improvement was estimated as 2 - 3 years after squadron introduction.

4.3 Operations Research Division, ONR

Activities of ONR are to plan the U.S. Navy's research and development program.

ORG has done two studies for ONR.

ORG 1 - Problems of Introduction of Air-to-air Missile Systems for Fleet Air Defence. August 17, 1955. Secret. Contract N5-ori-07887. This considered Sparrow I with F7U3M and FJ4/Sidewinder. These are day fighters (F7U = Cutlass)(FJ4 = Fury). This report was seen and is summarized in CARDE Technical Letter N-47-11.

ORG 2 - This report is in draft form only to date. Its title is "Operational Problems of Sparrow III/F3 H2 Missile System". This study was completed in April 1956 but is not yet published. A summary of the contents was given. Some points to note are outlined below.

Various AI detection contours were used to account for uncertainties in AI effectiveness. These contours were ellipses with major and minor axis (in miles) given by

$7\frac{1}{2} \times 5$

15×10

20×15

Two values (1 and 4 miles) of C1C vectoring error were considered.

Figure A-1.

M_L .9, 1.2 and 2.0

M_T .8, .9, 1.5 2.0

Sp. III B
Alt. 50 K ft ML = 2.0
T = 9264 lb t = 1.8 sec.
(8889 @ SL) Noise .6729 per plane

M .9	5K	30K	50K
Noise	2.8	.928	.408
M 1.2	2.85	-	-
M 20		1.62	.672

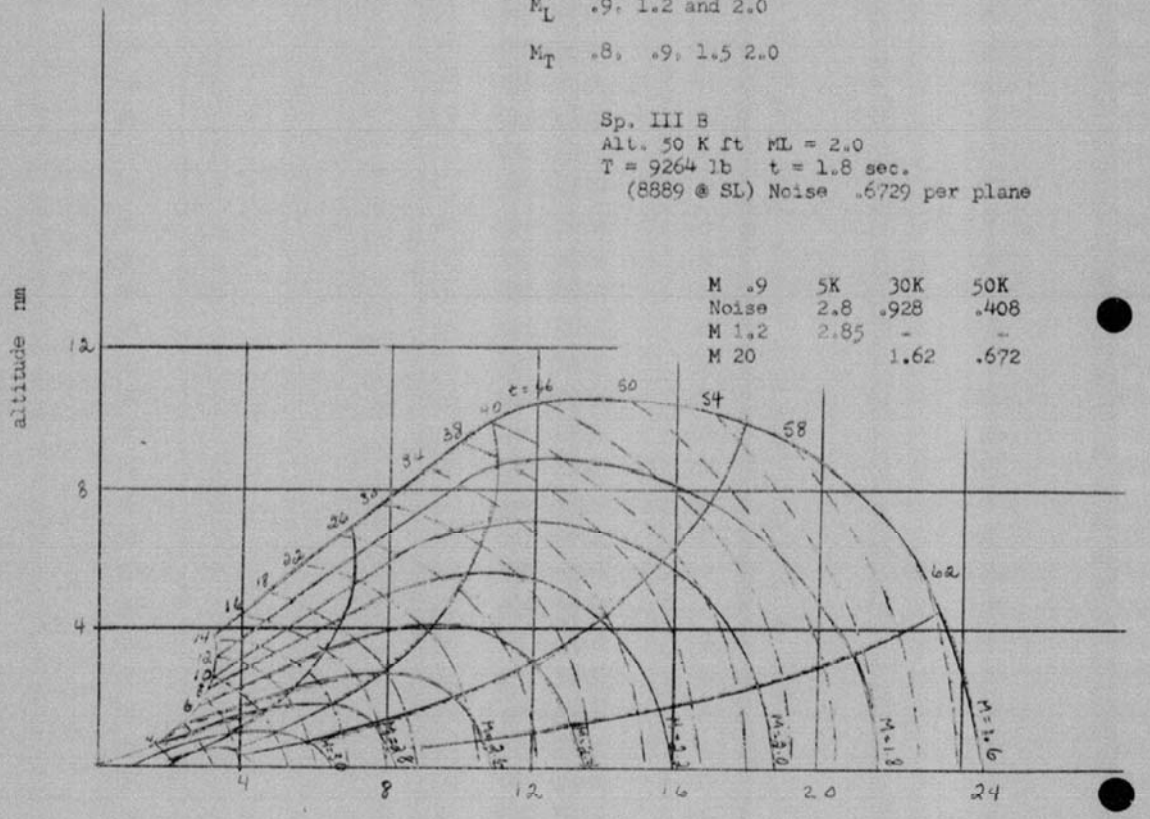

Figure A-2

Ref. Raytheon Memo.
No. MS 396
Feb. 24, 1956.

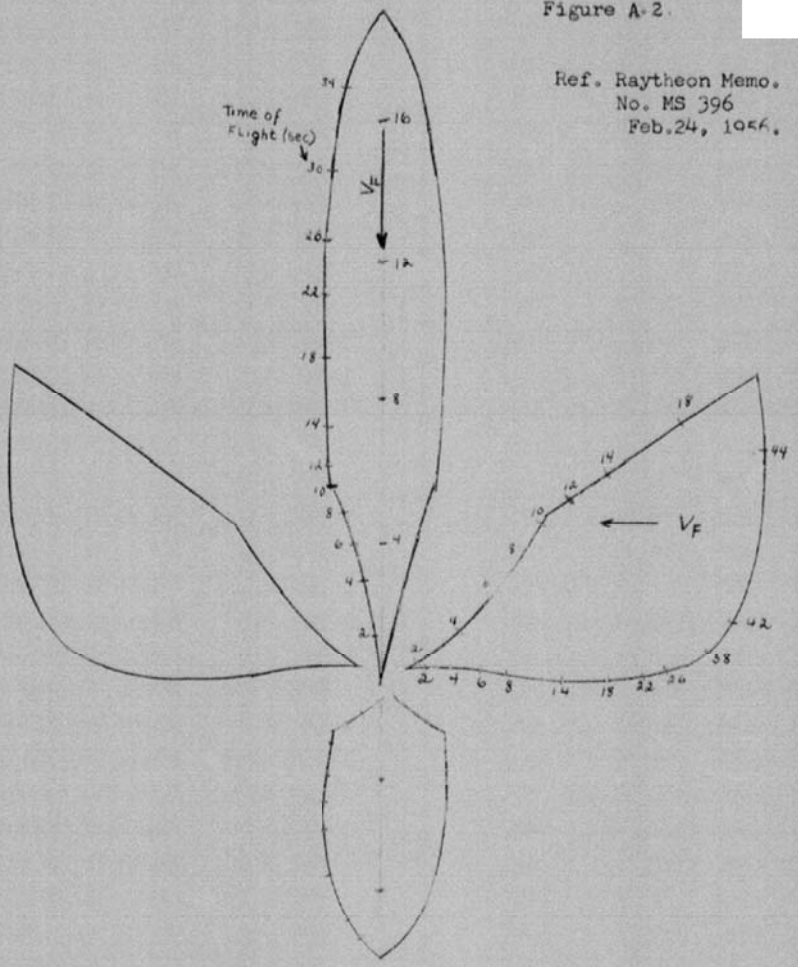

Sp. III B
Zones of Tactical Effectiveness

Tgt at origin
Alt. 50K
M_T = 1.5
M_L = 2.0

Control after .3 sec.
Final Mach No. 2.0
Manoeuvring Tgt - 4 gs.

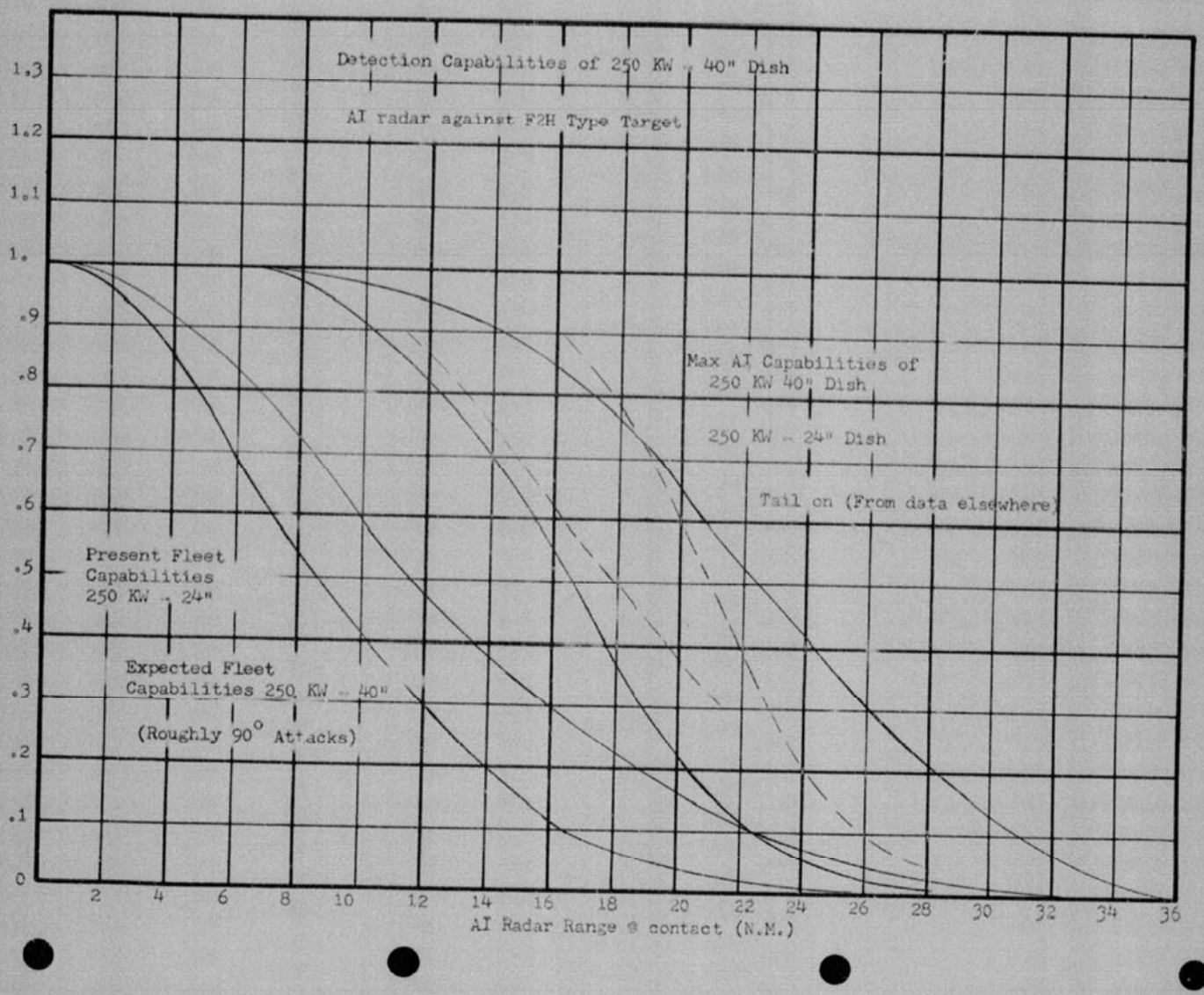
Detection Capabilities of 250 KW - 40" Dish
AI radar against F2H Type Target
Max AI Capabilities of 250 KW 40" Dish
250 KW - 24" Dish
Tail on (From data elsewhere)
Present Fleet Capabilities 250 KW - 24"
Expected Fleet Capabilities 250 KW - 40"
(Roughly 90° Attacks)
Cumulative Probability of Detection
AI Radar Range @ contact (N.M.)
1.3
1.2
1.1
1.
.9
.8
.7
.6
.5
.4
.3
.2
.1
0
2
4
6
8
10
12
14
16
18
20
22
24
26
28
30
32
34
36

-30-
Figure A-3.

APPENDIX B

Aerodynamics

B. Cheers

1.0 Introduction

During the past quarter there was a considerable increase in the amount of information obtained on recent estimates of the aerodynamic characteristics of the CF-105.

The main items of interest are the thrust and drag functions and flight envelope limitations to be used in the "Total Energy Height" equation for the simulation of the high-altitude performance of the aircraft, now being carried out on the REAC.

Sets of these functions and limitations have been calculated by N.A.E. and CARDE., for various C.G. positions, using both N.A.E. and AVRO estimates. The methods used and the results obtained are given below.

2.0 "Total Energy Height" Functions

2.1 General

The method being used on the REAC in the simulation of the high-altitude performance of the CF-105 is basically that proposed by R.J. Templin Ref. (1) and outlined in Appendix B of the first Quarterly Progress Report, but the actual form of the functions to be used on the REAC is somewhat changed [K. Acton, Ref. (2)].

Templin assumes that the relation between drag coefficient and lift coefficient, for a trimmed condition, is parabolic for the range of C_L in which the aircraft is considered to be flying: i.e. for any M,

$$C_D = C_{D_o} + K_1 C_L + K_2 C_L^2 = C_{D_{min}} + K_2 (C_L - C_{L_{C_{D_{min}}}})^2$$

Acton [Ref. (2)] converts the coefficients into $\frac{\text{force}}{\text{ambient pressure}}$

[by the relation $C_F = \frac{F}{p} \cdot \frac{1}{\frac{1}{2}\gamma M^2 S}$]

and obtains:

$$\frac{D}{p} = \frac{D_o}{p} + K_1 \frac{L}{p} + \mathcal{F} \frac{L^2}{p^2} = \frac{D_{min}}{p} + \mathcal{F}\left(\frac{L}{p} - \frac{L_{D_{min}}}{p}\right)^2$$

The functions f_1, f_2, f_3 in Ref. (1) and $\frac{D_o}{\rho}$, K_1 and $\mathcal{Y}$ in Ref.(2) are related in the following way:

$$\frac{D_o}{\rho} = 3.225 \times 10^{-2} \frac{f_1}{M}$$

$$K_1 = \frac{f_2}{971 M}$$

$$\mathcal{Y} = 32.92 \times 10^{-6} \frac{f_3}{M}$$

Because of non-linearities in the lift coefficient for this aircraft the drag-polars actually consist of an approximation to two parabolae, each parabola applying over a certain range of $\frac{L}{\rho}$. This effect is shown up very clearly by plotting $\sqrt{\frac{D}{\rho} - \frac{D_{min}}{\rho}}$ against $\frac{L}{\rho}$, a typical plot being given in the figure below, where

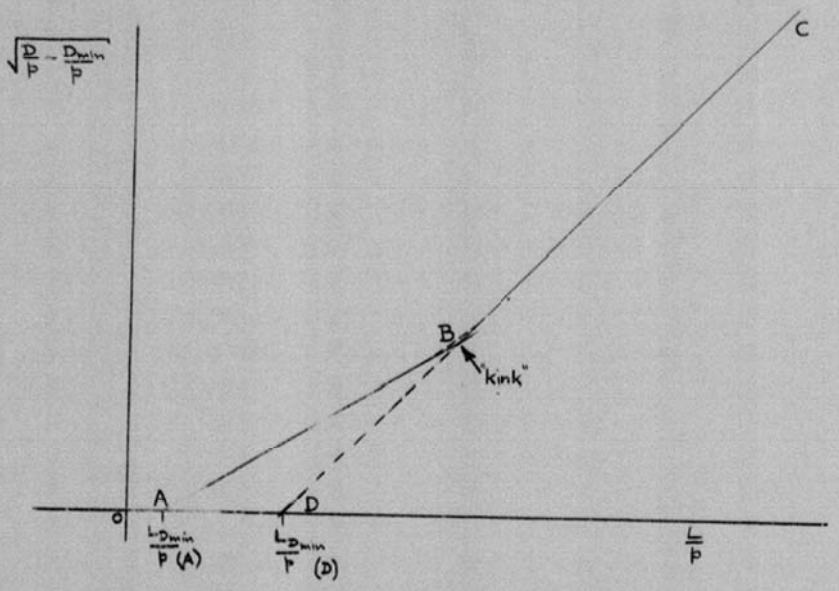

we obtain two straight lines AB and BC with different slopes and different intercepts on the L/ρ axis $\left[\frac{L_{D_{min}}}{\rho}(A) \text{ \& } \frac{L_{D_{min}}}{\rho}(D)\right]$. In all the calculations of the functions $\frac{D_o}{\rho}$, K_1, $\mathcal{Y}$, it is considered that the aircraft is flying at values of lift coefficient greater than that corresponding to the "kink" (i.e. along the line BC).

If the Drag-Lift-Mach Number carpets are available, the functions $\frac{D_o}{p}$, K_1 and $\mathcal{J}$ may be obtained in the following manner from the plot of $\sqrt{\frac{D}{p} - \frac{D_{min}}{p}}$ vs $\frac{L}{p}$

$$\mathcal{J} = (\text{slope of line BC})^2$$

$$K_1 = -2\mathcal{J}\frac{L_{Dmin}}{p}_{(D)}$$

$$\frac{D_o}{p} = \frac{D_{min}}{p} + \mathcal{J}\left(\frac{L_{Dmin}}{p}_{(D)}\right)^2$$

The functions f_1, f_2, f_3 may be obtained in a similar manner. The thrust function $\frac{T_m}{p}$ Ref.(2) is related to Templin's f_T function in the following way:

$$\frac{T_m}{p} = 3{\cdot}225 \times 10^{-2}\,\frac{f_T}{M}$$

2.2 NAE Calculations

Values of the functions f_T, f_1, f_2, f_3 have been calculated by N.A.E. for C.G. positions of 28% and 34% MAC using both "Optimistic" and "Pessimistic" extrapolated estimates for high values of lift coefficient (above the "Kink") [O.E. Michaelsen Ref (3)]. The thrust function f_T is obtained directly from AVRO Monthly Performance Report No. 8 (for PS-13 engines) and there is no "Optimistic" or "Pessimistic" in this case.

The values of the functions as calculated by N.A.E. were obtained using the following formula for drag coefficient:

$$C_D = C_{D_o} + K_1 C_L + K_2 C_L^2$$

where :

$$C_{D_o} = \frac{2}{\rho_o a^3 M^3}\left(\frac{W}{S}\right) f_1 = C_{D_{min}} + \frac{dC_D}{dC_L^2}\left(C_{L_{C_{D_{min}}}} + C_{L_o}\right)^2$$

$$+ C_{L_o}^2\left(\frac{K}{C_{L_\delta}} - \frac{1 + K\frac{C_{h_\alpha}}{C_{h_\delta}}}{C_{L_\alpha}}\right) + C_{L_o}\left[\alpha_o\left(1 + K\frac{C_{h_\alpha}}{C_{h_\delta}}\right) + K\frac{C_{h_o}}{C_{h_\delta}} + \Delta\alpha_{ref.}\right]$$

$$K_1 = \frac{f_2}{aM} = 2\frac{dC_D}{dC_L^2}\left(C_{L_{C_{D_{min}}}} + C_{L_0}\right)(\xi - 1) + 2\xi C_{L_0}\left(\frac{K}{C_{L_\delta}} - \frac{1 + K\frac{C_{h_\alpha}}{C_{h_\delta}}}{C_{L_\alpha}}\right)$$
$$+ C_{L_0}\left[\frac{1 + K\frac{C_{h_\alpha}}{C_{h_\delta}}}{C_{L_\alpha}}\right] + \xi\left[\alpha_0\left(1 + K\frac{C_{h_\alpha}}{C_{h_\delta}}\right) + K\frac{C_{h_0}}{C_{L_\delta}} + \Delta\alpha_{ref}\right]$$

$$K_2 = \frac{\rho_0 aM}{2}\left(\frac{S}{W}\right)f_3 = \frac{dC_D}{dC_L^2}(\xi - 1)^2 + \xi^2\left(\frac{K}{C_{L_\delta}} - \frac{1 + K\frac{C_{h_\alpha}}{C_{h_\delta}}}{C_{L_\alpha}}\right) + \xi\left[\frac{1 + K\frac{C_{h_\alpha}}{C_{h_\delta}}}{C_{L_\alpha}}\right]$$

and:
$$C_{L_0} = \frac{C_{m_0}}{cp_e - ac} \qquad \Delta\alpha_{ref} = -.0143$$
$$\xi = \frac{cg - ac}{cp_e - ac}$$
$$K = \frac{\Delta C_{L_{\delta_{ref}}}}{C_{L_\delta}} = 1 - \frac{c_f}{\pi\beta b_f}$$

$\begin{cases} c_f = \text{elevator chord} \\ b_f = \text{elevator span} \end{cases}$

2.2.1 "Pessimistic" Values

The "Pessimistic" values as calculated from the above expressions were obtained using quantities calculated from a combination of Wind-tunnel tests (Cornell Aeronautical Laboratory $M \leq 1.23$, Langley Field (NACA) $M = 1.41$ and NAE half-model tests $M > 1.2$, for a C.G. position of 28% MAC) and linearized extrapolations, to obtain the functions f_1, f_2, f_4 for C.G. positions of 28% and 34% MAC.

These functions have been converted into $\frac{D_a}{r}$, K_1 and $\mathcal{F}$, and are shown plotted in figures 1, 2 and 3.

The flight envelope limitations were calculated for stall, buffet, maximum elevator hinge moment (60,000 lb.ft.) and maximum elevator deflection (-30°).

The elevator limits were obtained from the following relations:

Maximum deflection

$$C_{L_{trim_{max}}} = -\frac{1}{\frac{dC_m}{dC_L}}\left(30^\circ C_{m_{\delta_{C_L}}} + C_{m_0}\right)$$

Maximum hinge moment

$$C_{L_{HM}} = \frac{\frac{0.191}{\sigma M^2} - C_{h_{C_L=0}}}{\frac{dC_m}{dC_L}}$$

The "Pessimistic" Load factors (28% and 34% MAC) are shown in figure 4 (for a combat weight of 50,000 lb. and 50,000 ft. altitude). N.A.E. consider the "Pessimistic" values to be their own estimates.

2.2.2 "Optimistic" Values

The "Optimistic" values were obtained in a manner similar to that used for the "Pessimistic" ones with the exception that AVRO estimates were used more extensively, and wherever non-linearities appeared in any of the quantities the most "optimistic" linearization was always used. For $M \leq 1.23$ the high C_L values as obtained from the Cornell A.L. Wind-tunnel tests were used. For $M > 1.23$ the AVRO estimates, already obtained for low C_L, were extrapolated to match up with the Cornell values (for high C_L) at $M = 1.23$.

The "Optimistic" functions $\frac{D_e}{p}$, K_1 and $\mathcal{F}$ are shown in figures 1, 2 and 3. The flight envelope limitations were calculated using the same relations as in 2.2.1 for maximum elevator hinge moment and deflection, but AVRO values were inserted.

2.3 AVRO Data

2.3.1 Latest Values

The supersonic performance of the CF-105 which has been given previously by AVRO, has been largely based on estimates and extrapolations from transonic wind-tunnel data. Recently, however, the results of supersonic wind-tunnel and free-flight tests, conducted at the Langley Laboratories of NACA, have become available, and have been used to revise the estimated performance. These revised estimates show a deterioration in performance.

The revised estimates were first presented, as "rigid" characteristics, based solely on these tests, and the functions $\frac{D_e}{p}$, K_1 and $\mathcal{F}$ have been calculated using these data (2.3.2).

However, corrections have been applied and certain configuration changes have been made by AVRO. The resulting estimates ("elastic" characteristics) are considered by AVRO to be final (with the possible exception of minor amendments).

The drag carpets where these changes have been included were received very recently and the functions $\frac{D_o}{P}$, K_1 and γ are being calculated. If they are available before publication of this Quarterly, the results will be plotted on the relevant graphs (Figures 1, 2 and 3).

The corrections and changes are summarized below:

Weight

The combat weight has increased because of both an increase in empty weight and in the fuel for the mission. The empty weight increase is divided between structure and equipment (mainly due to installation of ASTRA I). The increase in mission fuel is due to increased empty weight and the increased drag.

Increase in empty weight	lb.
Structure	850
Equipment	1250
Increase in combat fuel	250
Total increase	2350

This gives a new combat weight (with PS-13 engines) of 51,050 lb.

Minimum Profile Drag

The minimum profile drag coefficient based on a wing area of 1225 sq. ft. at M = 1.5 :

	$C_{D_{min}}$
Previous value	.0206
Obtained from free-flight model	.0223
Addition for semi-submerged missiles	.0007
New value	.0230

Trim Drag

The trim drag is a function of the elevator angle to trim. The wind-tunnel derivatives were corrected to the exact distance of the C.G. below the reference axis. The effects of structural elasticity and of the thrust momentum change between model and full-scale aircraft have also been included.

As the trim drag of the elevator is proportional to the square of the deflection it has been proposed by AVRO that the ailerons give some assistance to the elevators in producing a trimming moment, in order to give a net reduction in drag. The proposal is then to trim the ailerons symmetrically up to accomplish this, this to apply only at altitudes greater than 40,000 ft.

Engine Changes

It has been proposed by AVRO that the performance of the PS-13 engine can be increased by as much as 20% at M = 2.0, whilst leaving it virtually unchanged below M = 1.5 , by using a variable ejector and rematching the HP and LP compressors to give greater mass flow.

This will result in an increase in operational ceiling at M = 2.0, from 57,800 ft. to 63,900 ft. and an increase in steady "g" available at 50,000 ft. and M = 2.0, from 1.48 to 2.00.

The extra weight of the variable ejectors is 550 lb.

2.3.2 Total Energy Height Functions (Rigid Aircraft Characteristics)

The Total Energy Height Functions have been calculated at CARDE from the drag carpets of AVRO P/AERO DATA/74, using the graphical method described in Section 2.1.

The functions obtained ($\frac{P_o}{P}$, K, and $\mathcal{F}$) have been calculated for values of C_L above the "Kink" and the ranges of C_L in which they are applicable are given in the table below (together with the corresponding values of load factor (n) for W = 50,000 lb., h = 50,000 ft).

M	C_L (low)	C_L (high)	n(low)	n(high)
0.5	.16	.49	.16	.48
0.6	.11	.45	.16	.64
0.7	.08	.33	.16	.64
0.8	.13	.57	.32	1.44
0.9	.15	.50	.48	1.60
1.0	.16	.41	.64	1.60
1.1	.13	.34	.64	1.60
1.2	.18	.31	1.06	1.76
1.3	.20	.41	1.44	2.72
1.4	.10	.35	.80	2.72
1.5	.09	.31	.80	2.72
1.6	.08	.29	.80	2.88
1.7	.07	.22	.80	2.72
1.8	.06	.20	.80	3.20
1.9	.12	.22	1.60	3.20
2.0	.10	.20	1.60	3.20
2.1	.09	.18	1.60	3.20

2.4 Missiles Extended

The tests in the Cornell Aeronautical Laboratories Wind-tunnel have shown that the increase in drag coefficient (ΔC_D) is

$$\Delta C_D = .0042 \quad \text{at} \quad M = 0.95$$

$$\Delta C_D = .0047 \quad \text{at} \quad M = 1.20$$

There is no information on the effects of the extension of the missiles at Mach Numbers greater than 1.23, but a programme is being drawn up by AVRO for further tests, using more sophisticated techniques, to be carried out at C.A.L. (for $M \leq 1.23$).

3.0 Aircraft Radar

The look angles and physical dimensions of the aircraft radar are given in latest proposals by RCA for ASTRA I. They are as follows:

Look angles	Elevation	$\begin{cases} 75^\circ \text{ up} \\ 45^\circ \text{ down} \end{cases}$
	Azimuth	$\pm\ 70^\circ$
Diameter of the dish		32 "
Cone angle		30°

The axis of the cone is at $3^\circ\ 26'$ (nose down) to the aircraft datum line.

4.0 References

1. R.J. Templin: NAE Lab. Memo AE-82 (Jun 12, 1956).

2. K. Acton: CARDE Memo, to C.J. Wilson S/N-47-3 (dated Oct 4,1956).

3. O.E. Michaelsen: NAE Lab. Memo AE-46 g (Aug 24, 1956)

List of Symbols

C_D = total drag coefficient (trimmed condition)

D = drag in lb.

p = ambient pressure (lb/sq.ft.)

S = reference area = 122 sq.ft.

C_L = trimmed lift coefficient

D_o = drag at zero lift

D_{min} = minimum drag

$L_{D_{min}}$ = lift at minimum drag

ρ_o = standard density at sea-level (slugs/cu.ft.)

W = combat weight (assumed to be 50,000 lb.)

$C_{L_\delta} = \frac{\partial C_L}{\partial \delta}$

$C_{L_\alpha} = \frac{\partial C_L}{\partial \alpha}$

$C_{h_\alpha} = \frac{\partial C_h}{\partial \alpha}$ = rate of change of hinge moment coefficient with angle of attack

$C_{h_\delta} = \frac{\partial C_h}{\partial \delta}$ = rate of change of hinge moment coefficient with elevator deflection

$\sigma = p/\rho_o$ = $\frac{\text{ambient density}}{\text{density at sea-level}}$

n = normal load factor = $\frac{L}{W}$

Figure 1.

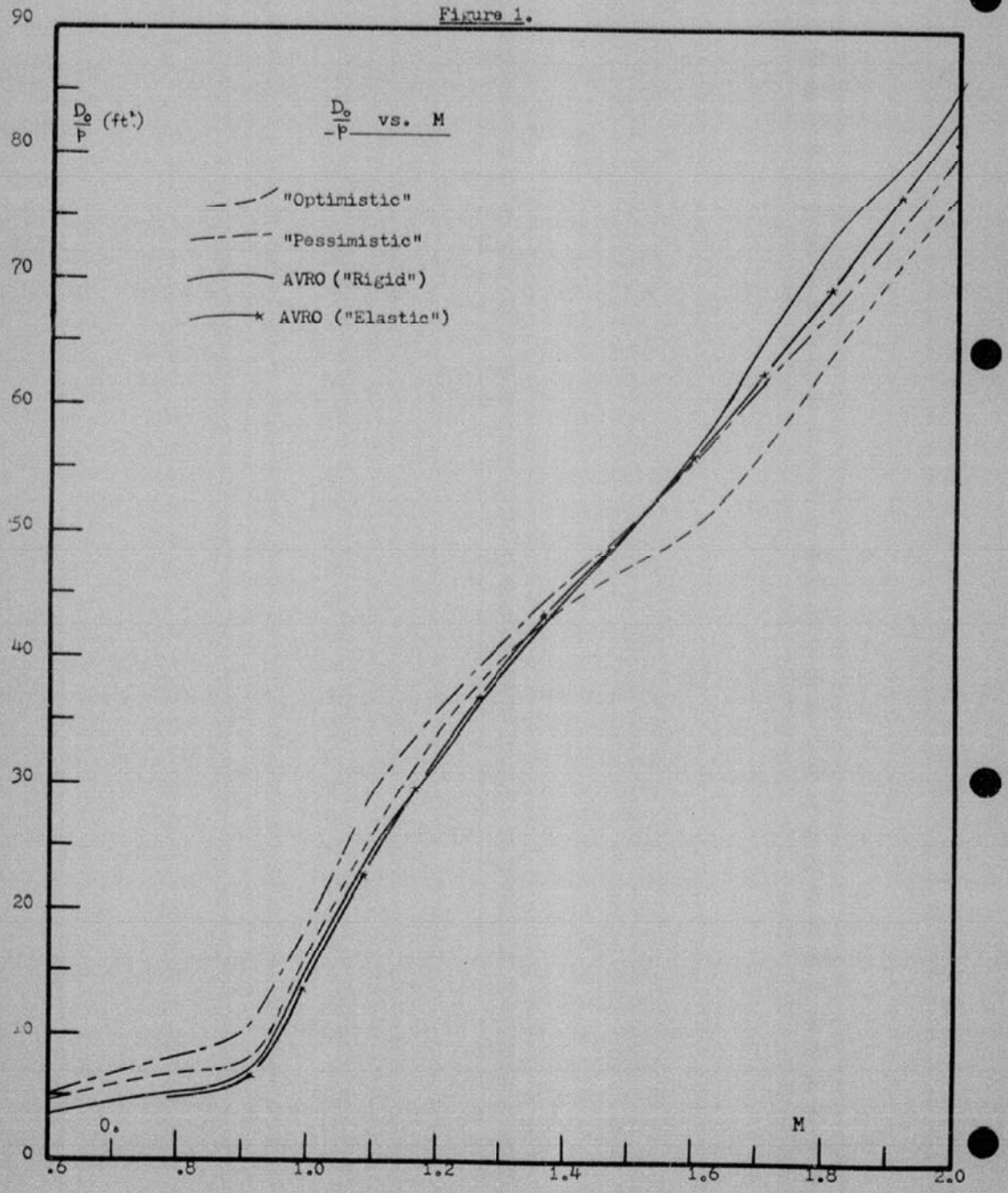
$\frac{D_o}{P}$ (ft²)
$\frac{D_o}{P}$ vs. M
"Optimistic"
"Pessimistic"
AVRO ("Rigid")
AVRO ("Elastic")
90
80
70
60
50
40
30
20
10
0
0.
M
.6
.8
1.0
1.2
1.4
1.6
1.8
2.0

Figure 2.

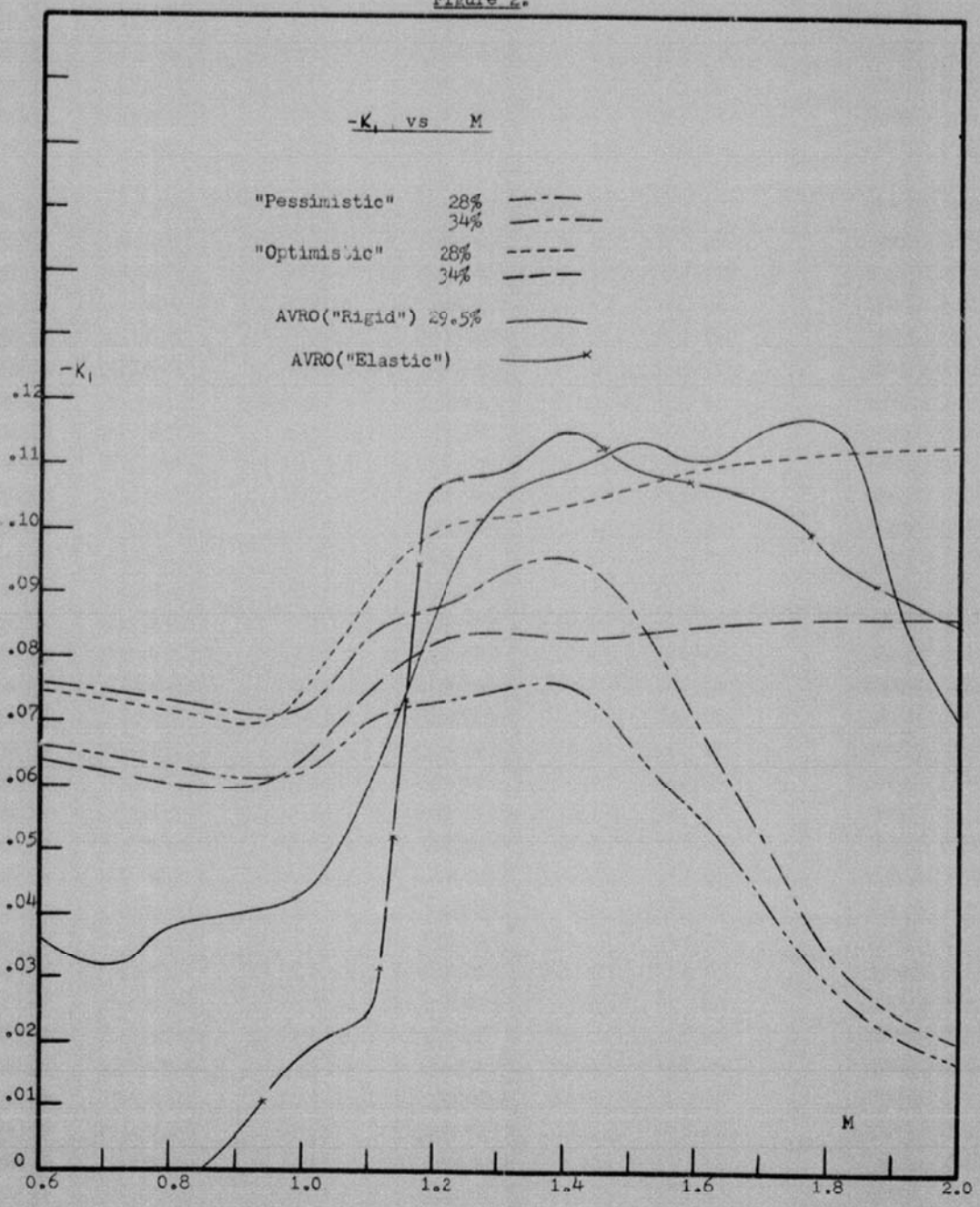
-K1 vs M
"Pessimistic" 28%
34%
"Optimistic" 28%
34%
AVRO("Rigid") 29.5%
AVRO("Elastic")
-K1
.12
.11
.10
.09
.08
.07
.06
.05
.04
.03
.02
.01
0
M
0.6
0.8
1.0
1.2
1.4
1.6
1.8
2.0

Figure 3.

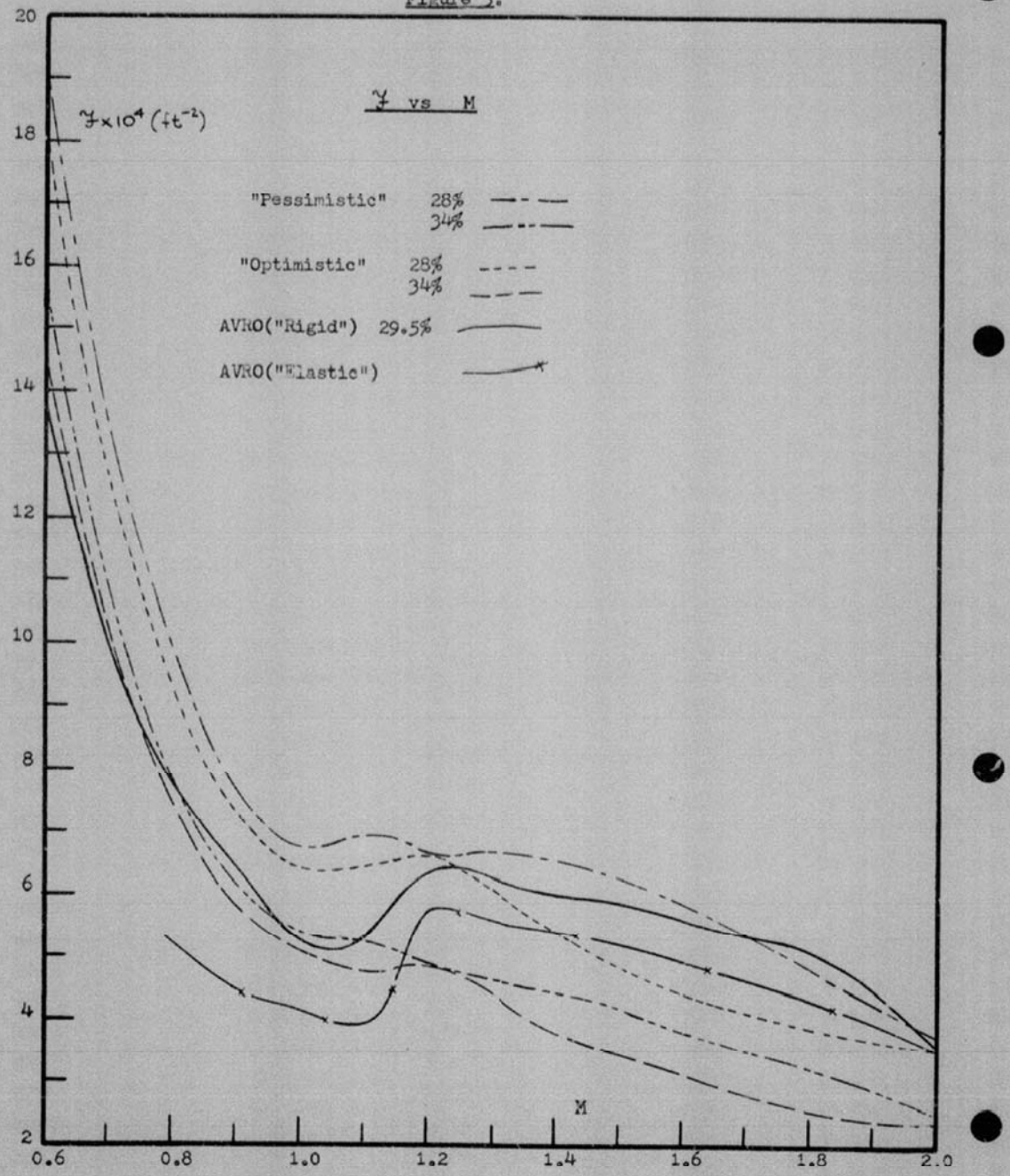
γ vs M
γ×10⁴ (ft⁻²)
"Pessimistic" 28%
34%
"Optimistic" 28%
34%
AVRO("Rigid") 29.5%
AVRO("Elastic")
M
20
18
16
14
12
10
8
6
4
2
0.6
0.8
1.0
1.2
1.4
1.6
1.8
2.0

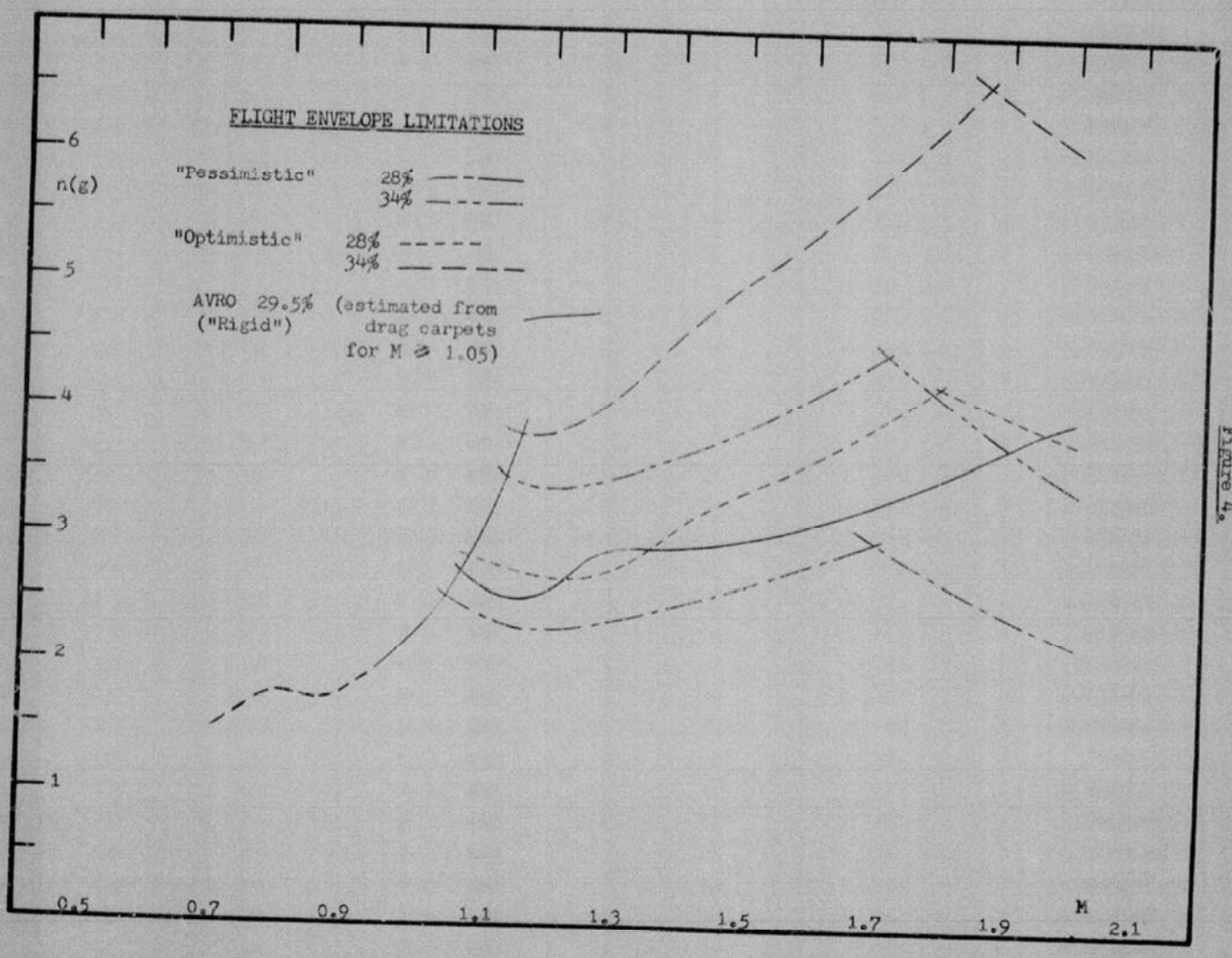
FLIGHT ENVELOPE LIMITATIONS
"Pessimistic" 28%
34%
"Optimistic" 28%
34%
AVRO 29.5% ("Rigid") (estimated from drag carpets for M ≥ 1.05)
n(g)
6
5
4
3
2
1
0.5
0.7
0.9
1.1
1.3
1.5
1.7
1.9
2.1
M

Figure 4.

APPENDIX C

Deceleration Trajectories - CF105

B. Hughes

Appendix D, following, describes methods used by the analysis group at CARDE for simulation of trajectories of the CF105 in two dimensions. To date, work has been completed for one set of aerodynamic characteristics: the so-called "pessimistic" aerodynamics for 28% centre of gravity position (Reference Appendix B). The aircraft is considered to use the maximum amount of turn permitted.

This appendix gives a collection of trajectories in target coordinates, for positive and negative interceptor turns with respect to the target, drawn to a scale of 15,000 feet per inch. One value only of interceptor weight, 50,000 lbs, has been chosen. Six values of initial course difference, from 75° to 180°, were used. Initial interceptor Mach number is 1.5 in all cases; the targets considered have Mach numbers 0.85, 1.2, 1.5, and 2.0. Altitudes of 40,000 and 50,000 ft. are considered for the subsonic target, and of 50,000 and 60,000 ft. for the supersonic targets.

Trajectories are marked in elapsed time in seconds, at five second intervals, zero time representing the start of the turn. Values of interceptor instantaneous load factor g's, of interceptor instantaneous Mach number, and of change in course difference, are tabulated in the tables which precede the graphs. Interceptor velocity and load factor may be taken directly from the table; the instantaneous value of course difference is obtained by subtracting the difference value given in the table from the initial course difference.

Each trajectory is identified by the value of initial course difference which is indicated on the figure. A sketch shows the direction of the interceptor turn, towards or away from the target, in each case. The reference direction, which is the target velocity direction, is shown in each case by an arrow on the sheet.

Decelerating Turns in Two Dimensions

Kinematic Quantities

Altitude 40,000 ft.

Time (Seconds)	Interceptor Mach No.	Load Factor (g's)	(degrees)
0	1.5	3.85	0
5	1.38	3.95	20
10	1.30	3.70	49
15	1.23	3.60	73
20	1.11	3.60	99
25	1.01	3.45	135
30	0.968	2.95	165
35	0.916	2.35	191
40	0.896	2.75	229
45	0.865	2.70	249
50	0.803	2.72	281
55	0.742	2.56	297
60	0.710	2.35	343
65	0.66	2.20	365
70	0.638	2.05	395

Altitude 50,000 ft.

Time (seconds)	Interceptor Mach No.	Load Factor (g's)	(degrees)
0	1.5	2.775	0
5	1.36	2.675	15
10	1.30	2.6	31
15	1.215	2.5	51
20	1.131	2.45	65
25	1.07	2.4	85
30	0.989	2.35	109
35	0.928	2.05	123
40	0.886	1.95	143
45	0.845	1.9	159
50	0.784	1.9	179
55	0.742	1.825	195
60	0.680	1.675	211
65	0.638	1.55	231
70	0.557	1.35	249

Altitude 60,000 ft.

Time (seconds)	Interceptor Mach No.	Load Factor (g's)	(degrees)
0	1.5	1.8	0
5	1.46	1.8	10
10	1.38	1.75	20
15	1.32	1.7	30
20	1.26	1.7	40
25	1.19	1.7	50
30	1.11	1.75	60
35	1.05	1.65	72
40	0.99	1.4	86
45	0.95	1.35	96
50	0.91	1.3	108
55	0.84	1.35	116
60	0.78	1.37	128
65	0.72	1.2	138
70	0.66	1.05	148

110°

$M_T = 0.85$

$M_{I_0} = 1.5$

$H = 40K$

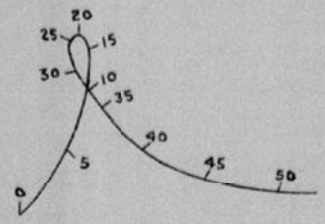

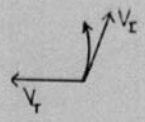

90°

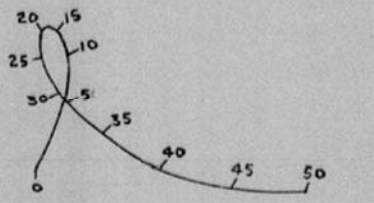

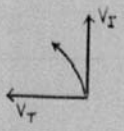

75°

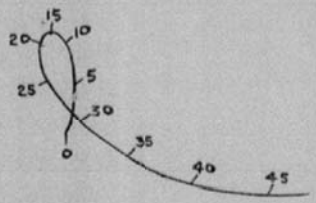

135°

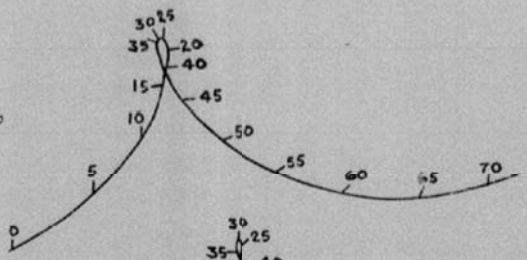

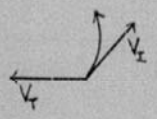

160°

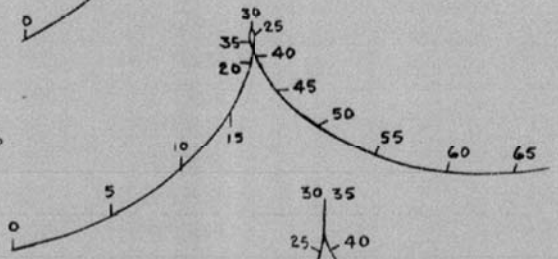

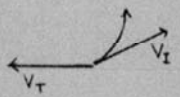

180°

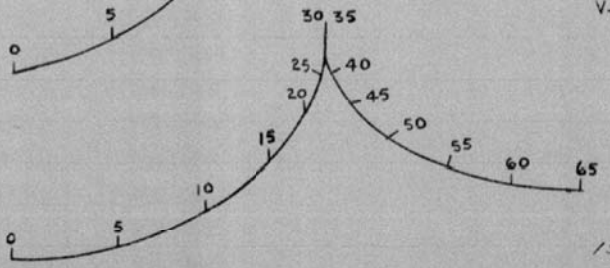

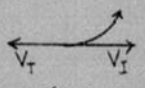

15000 / inch.

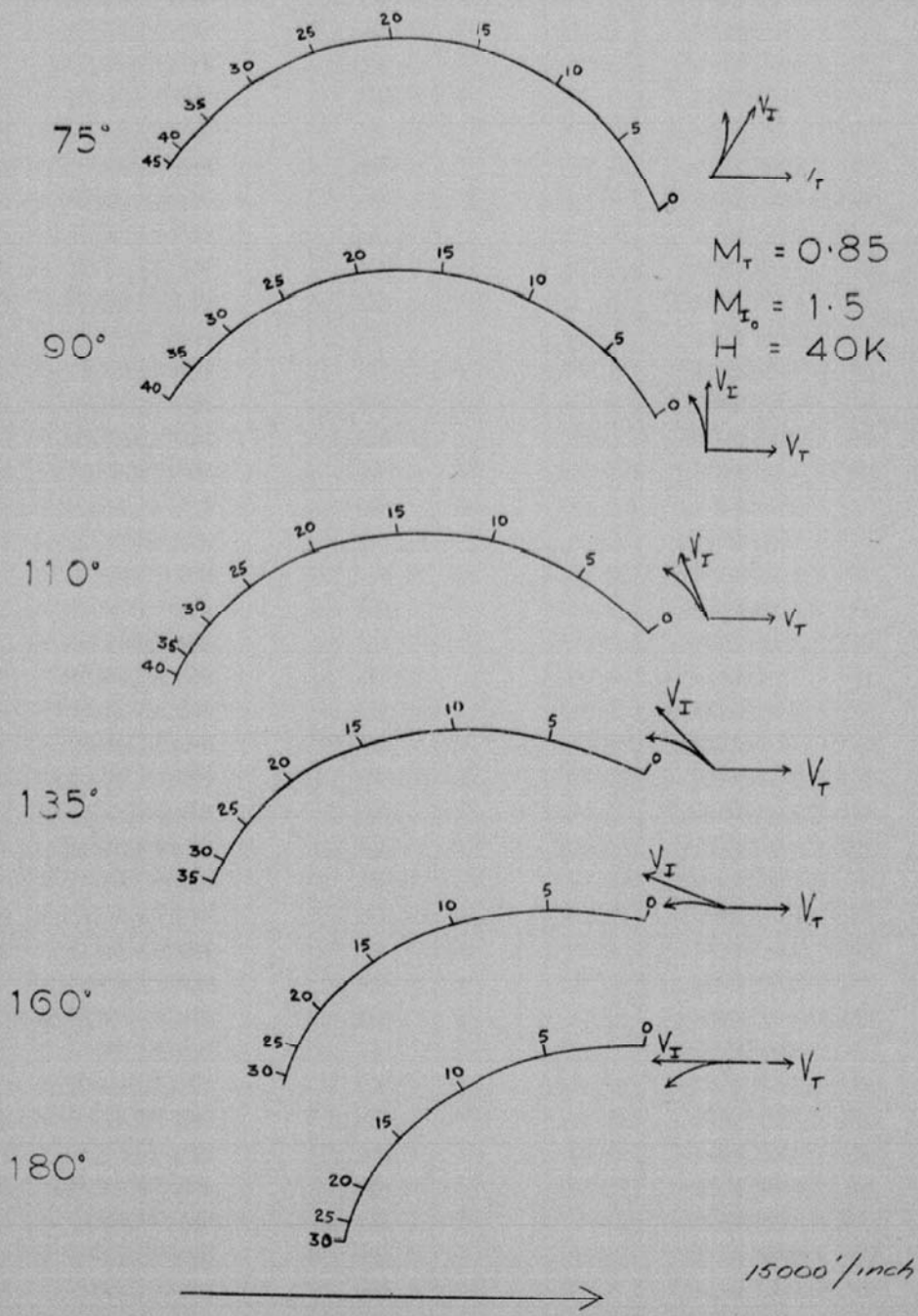
75°
90°
110°
135°
160°
180°
V_I
V_T
$M_T = 0.85$
$M_{I_0} = 1.5$
$H = 40K$
15000'/inch

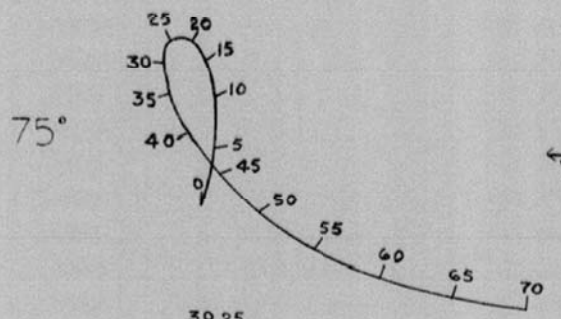

75°

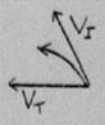

$M_T = 0.85$

$M_{I_0} = 1.5$

$H = 50\ K$

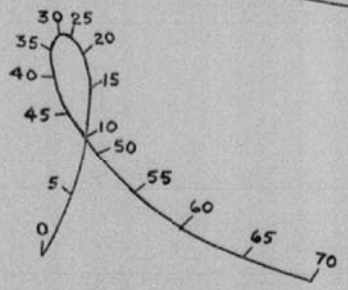

90°

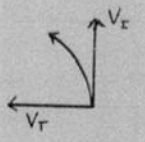

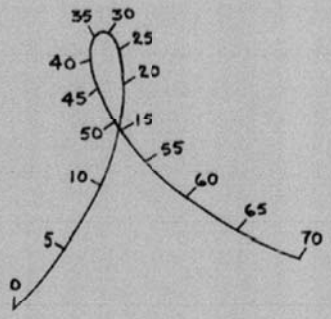

110°

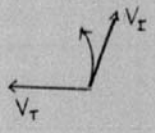

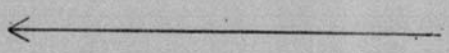

15000'/inch.

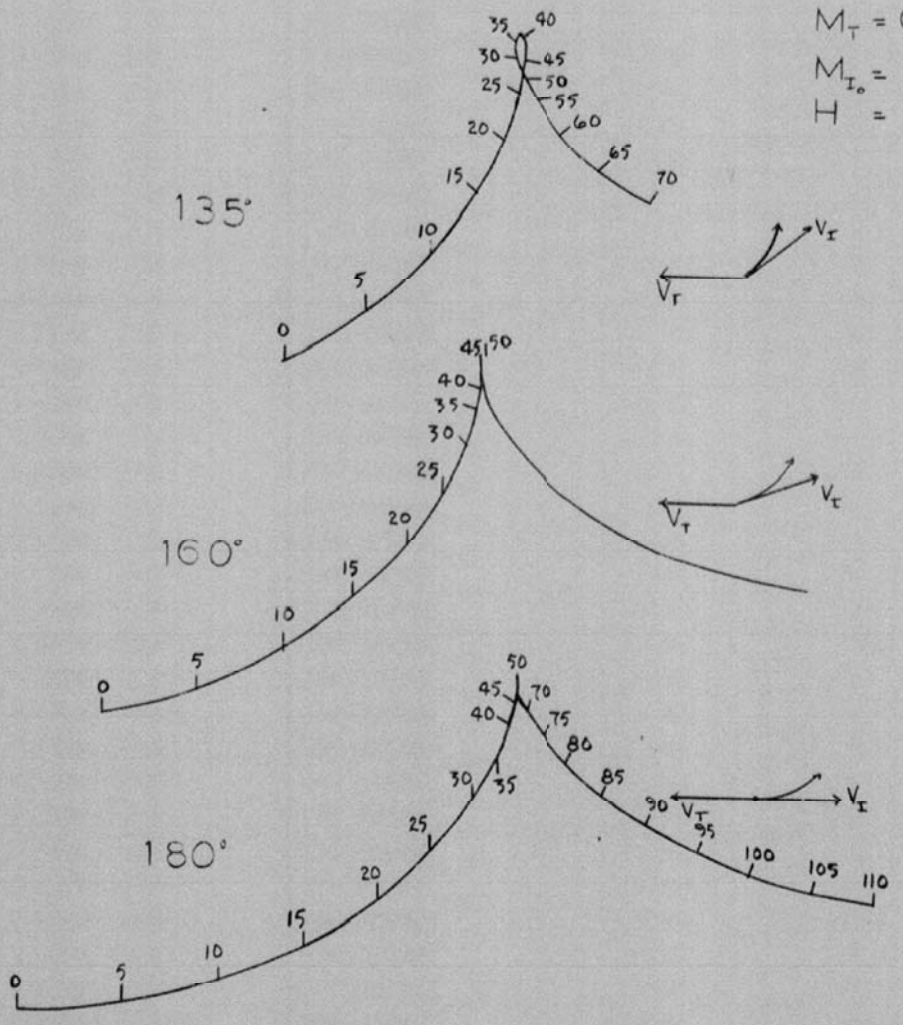
$M_T = 0.85$
$M_{I_o} = 1.5$
H = 50K
135°
160°
180°
V_I
V_T
15000'/inch.

$M_T = 0.85$

$M_{I_0} = 1.5$

$H = 50K$

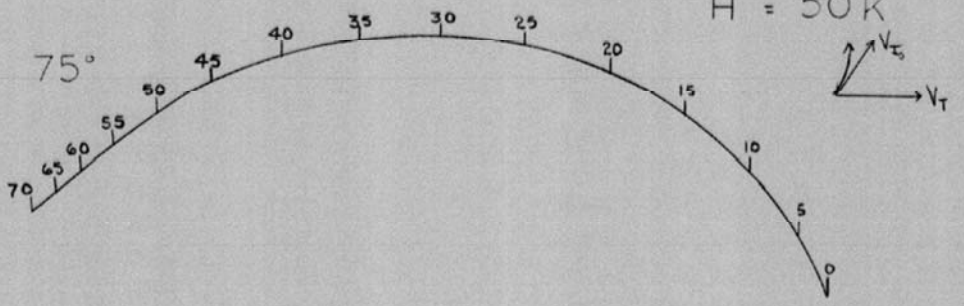

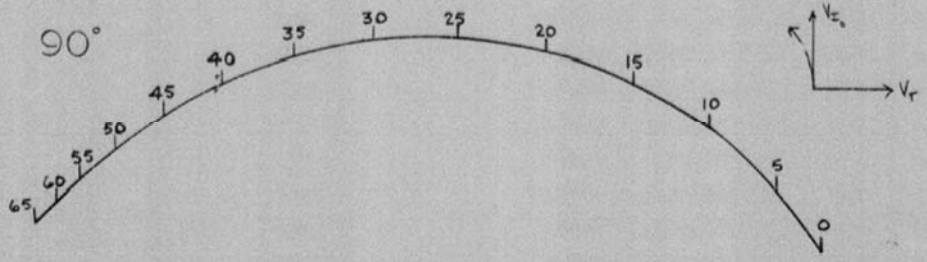

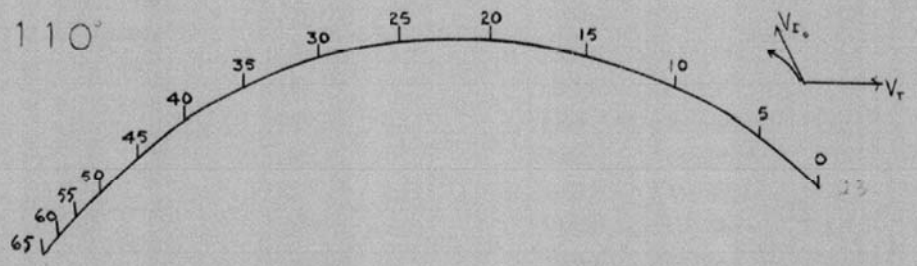

15000'/inch.

$M_T = 0.85$
$M_{I_o} = 1.5$
$H = 50K$

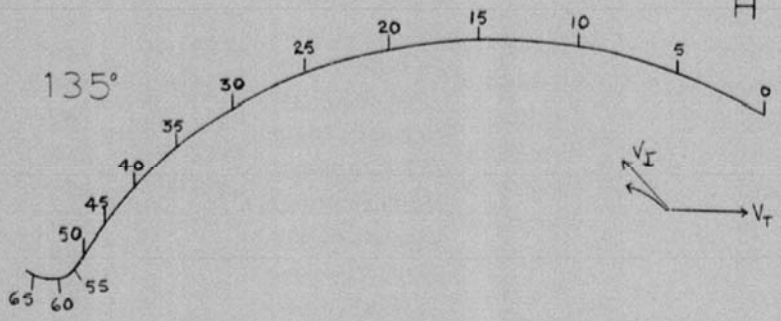

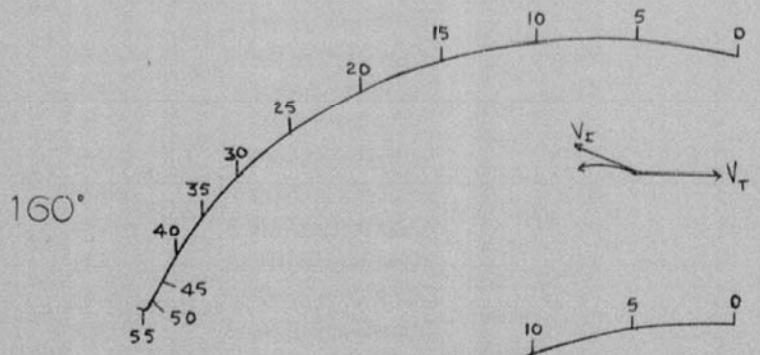

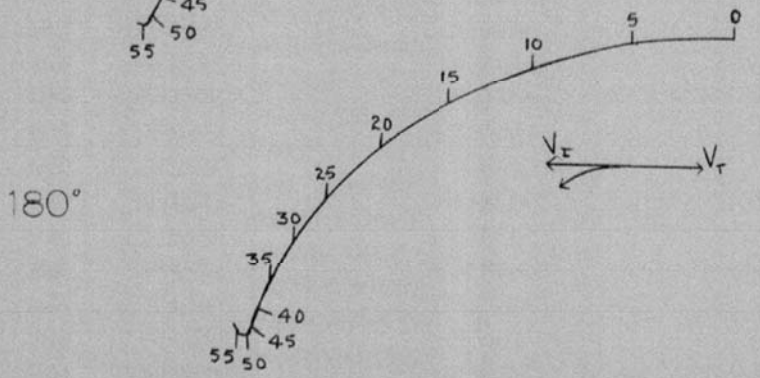

15000'/inch.

$M_T = 1.2$
$M_{T_o} = 1.5$
$H = 50K$

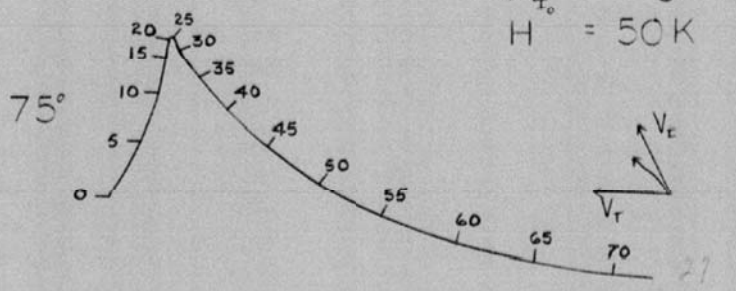

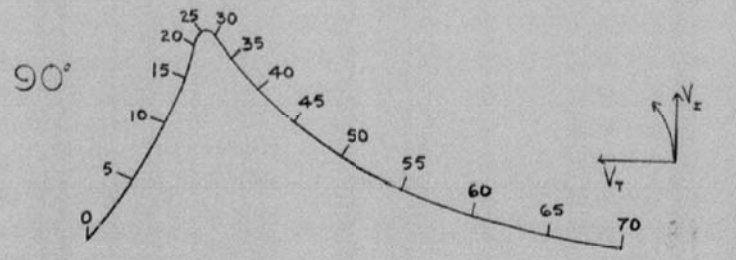

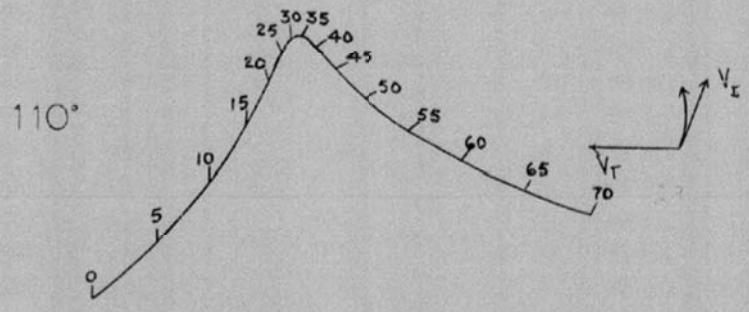

15000'/inch

$M_T = 1.2$

$M_{I_o} = 1.5$

$H = 50K$

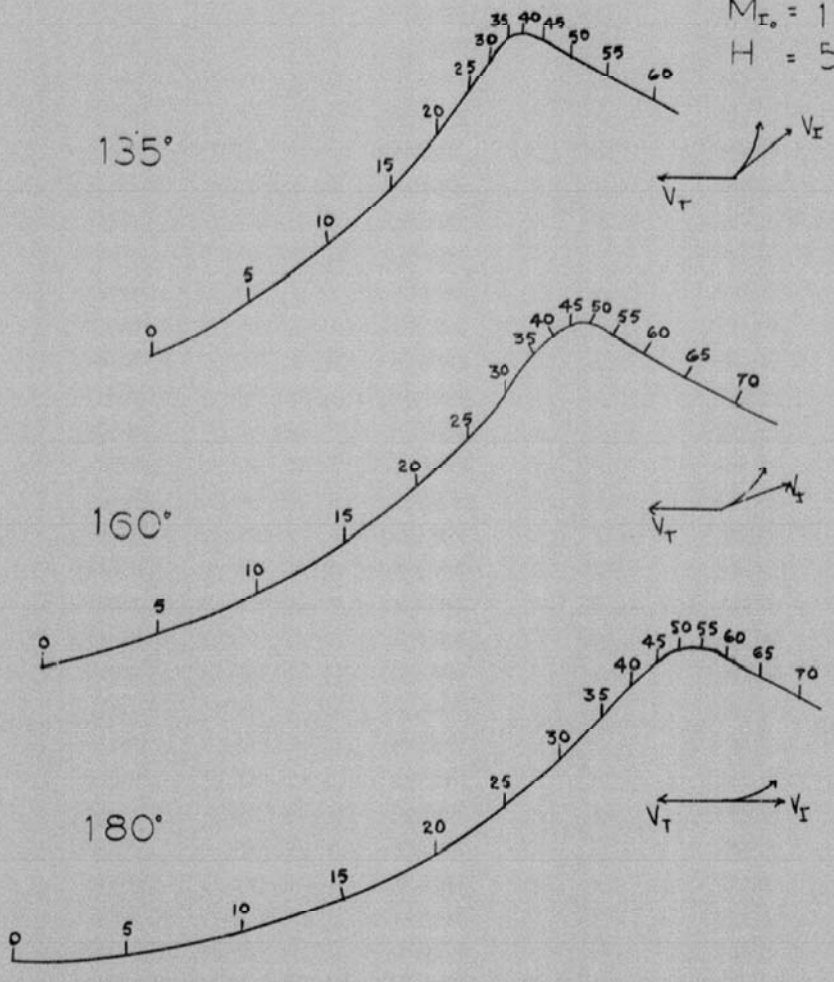

15000'/inch

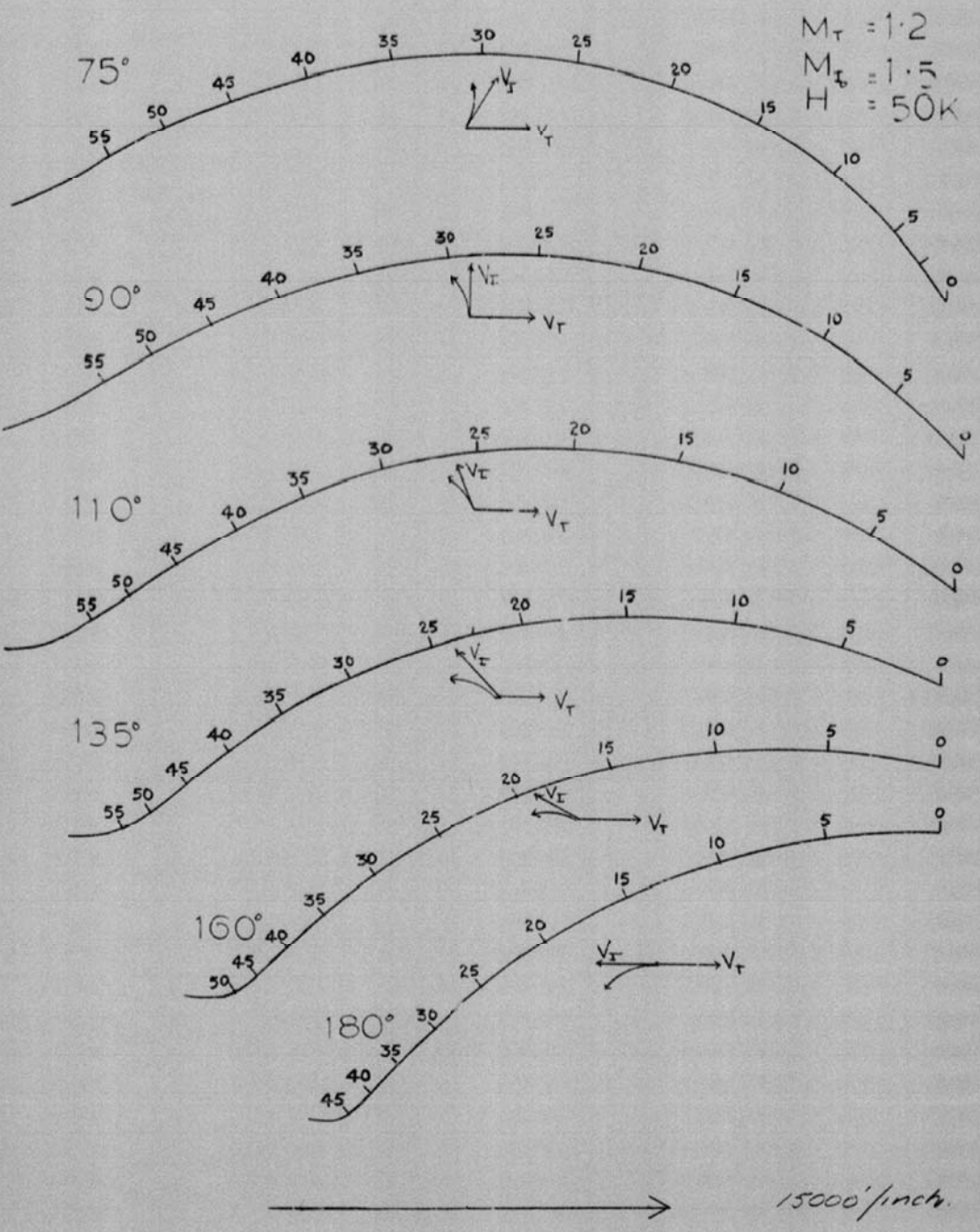
M_T = 1·2
M_I = 1·5
H = 50K
75°
90°
110°
135°
160°
180°
V_I
V_T
15000'/inch.

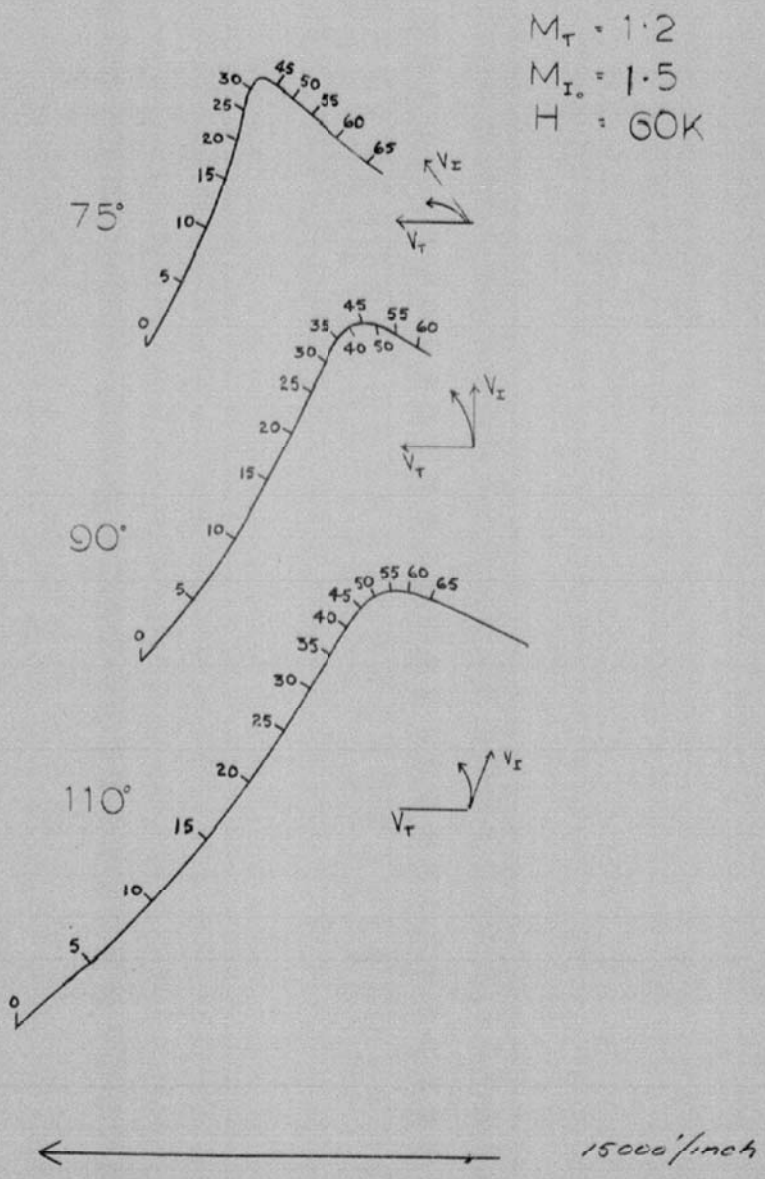
M_T = 1·2
M_{I_∞} = 1·5
H = 60K
75°
90°
110°
V_I
V_T
15000'/inch

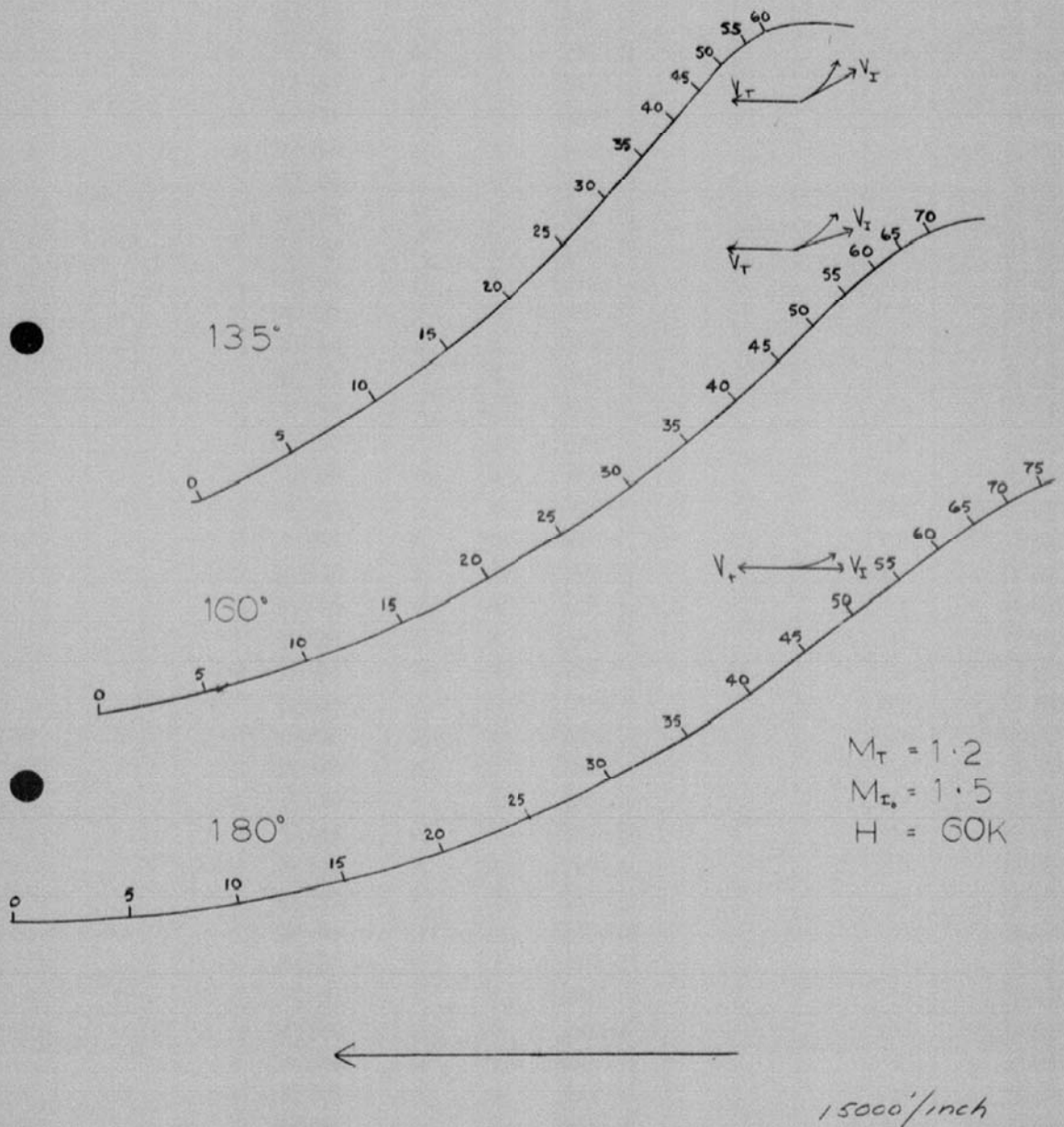
135°
160°
180°
V_T
V_I
$M_T = 1.2$
$M_{I_0} = 1.5$
H = 60K
15000'/inch

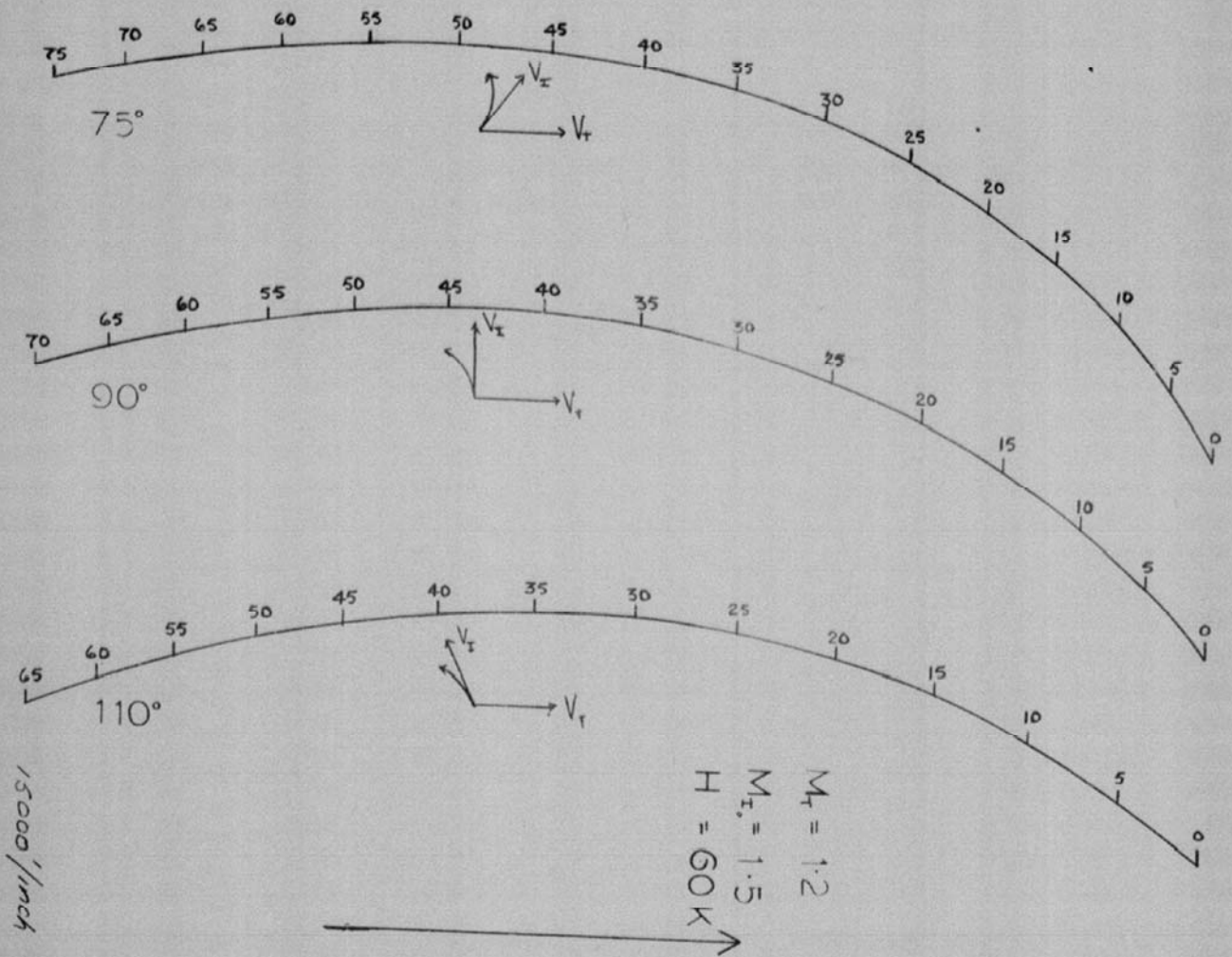

$M_T = 1.2$

$M_{I_0} = 1.5$

$H = 60K$

15000'/inch

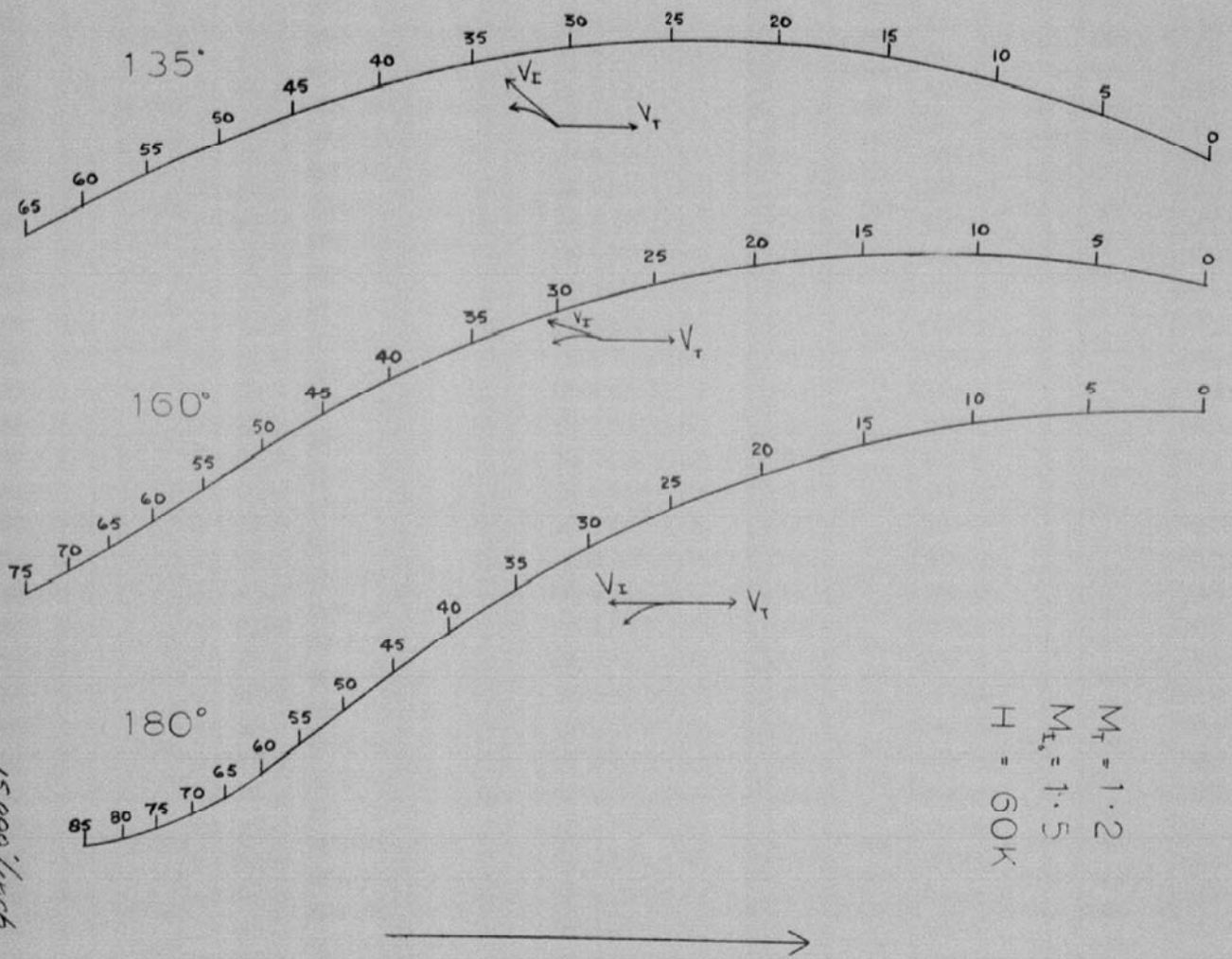

$M_T = 1.2$
$M_{T_0} = 1.5$
H = 60K

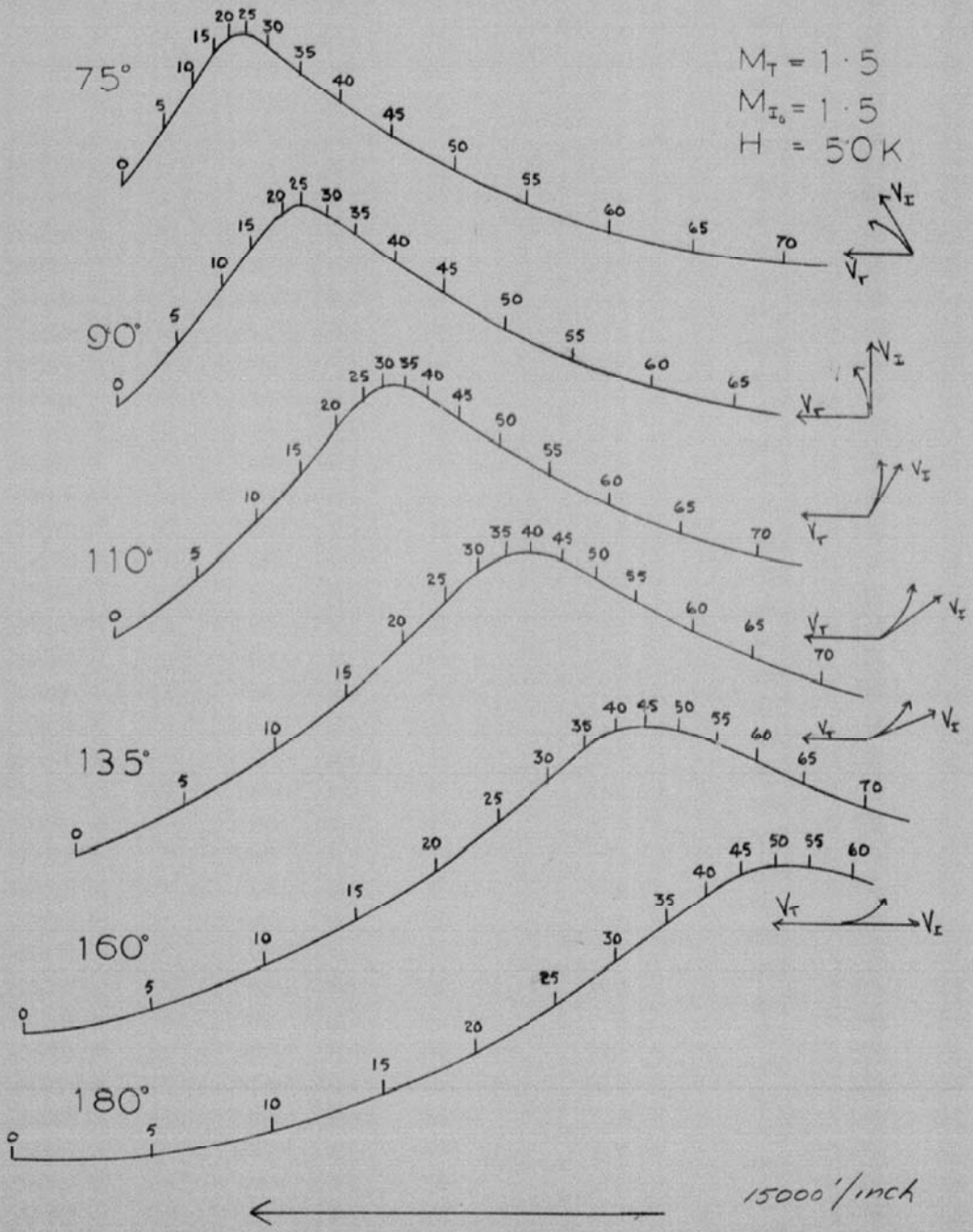
75°
90°
110°
135°
160°
180°
$M_T = 1.5$
$M_{I_0} = 1.5$
H = 50K
V_I
V_T
15000'/inch

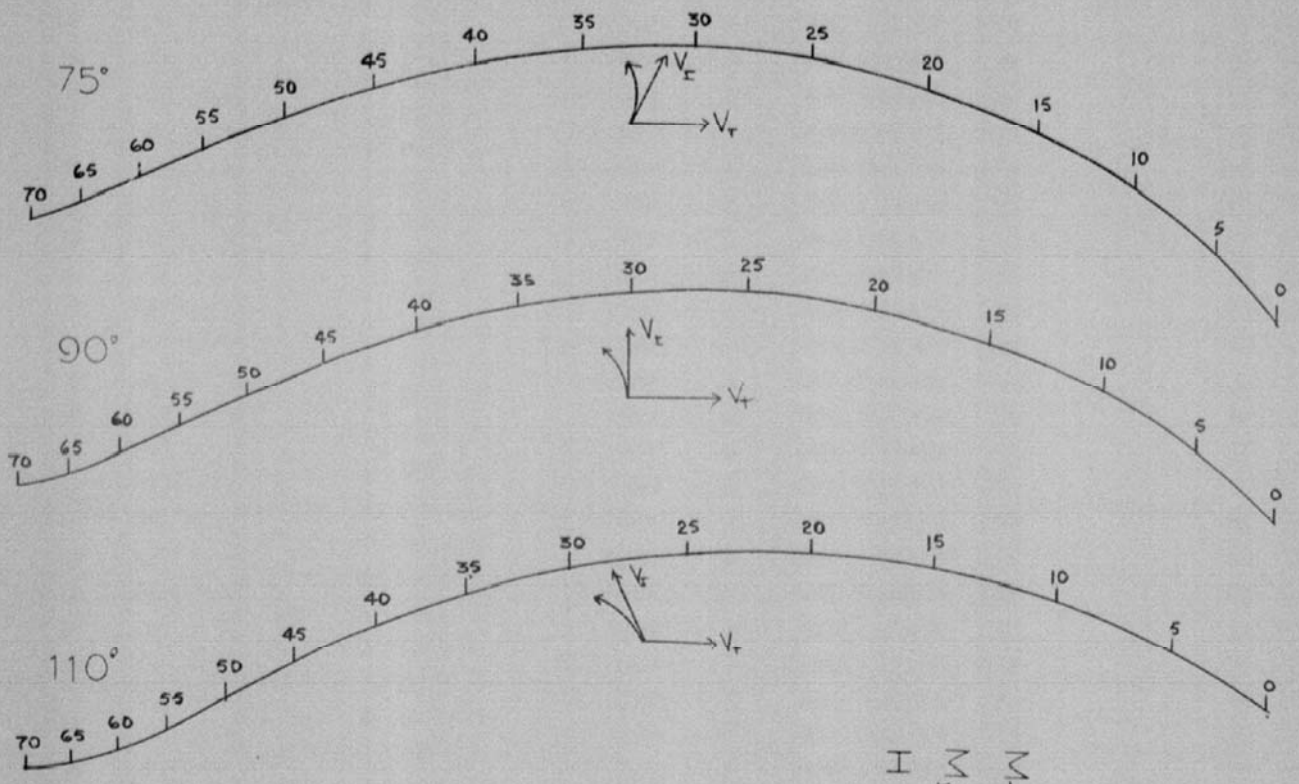

$M_T = 1.5$
$M_I = 1.5$
$H = 50K$

15000'/inch

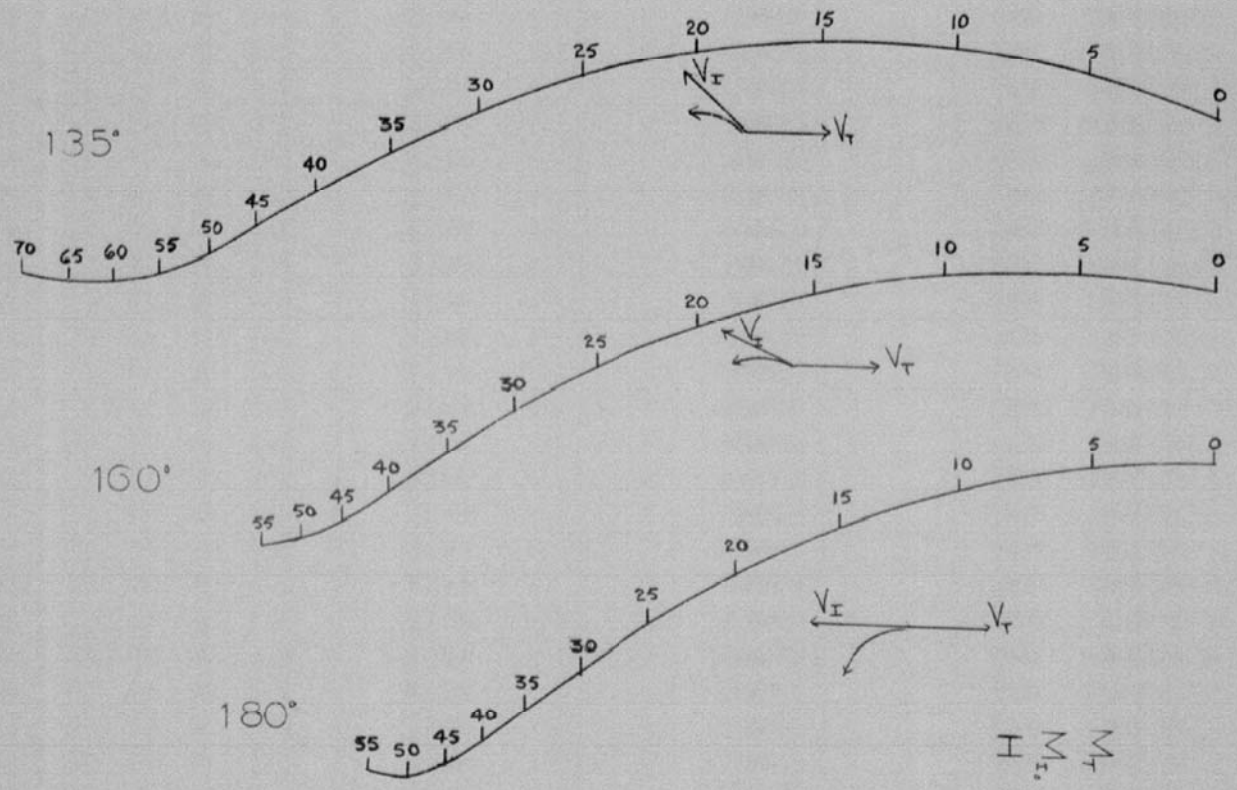

$M_T = 1.5$
$M_{I_0} = 1.5$
$H = 50K$

15000'/inch.

$M_T = 1.5$

$M_{I_0} = 1.5$

$H = 60\,K$

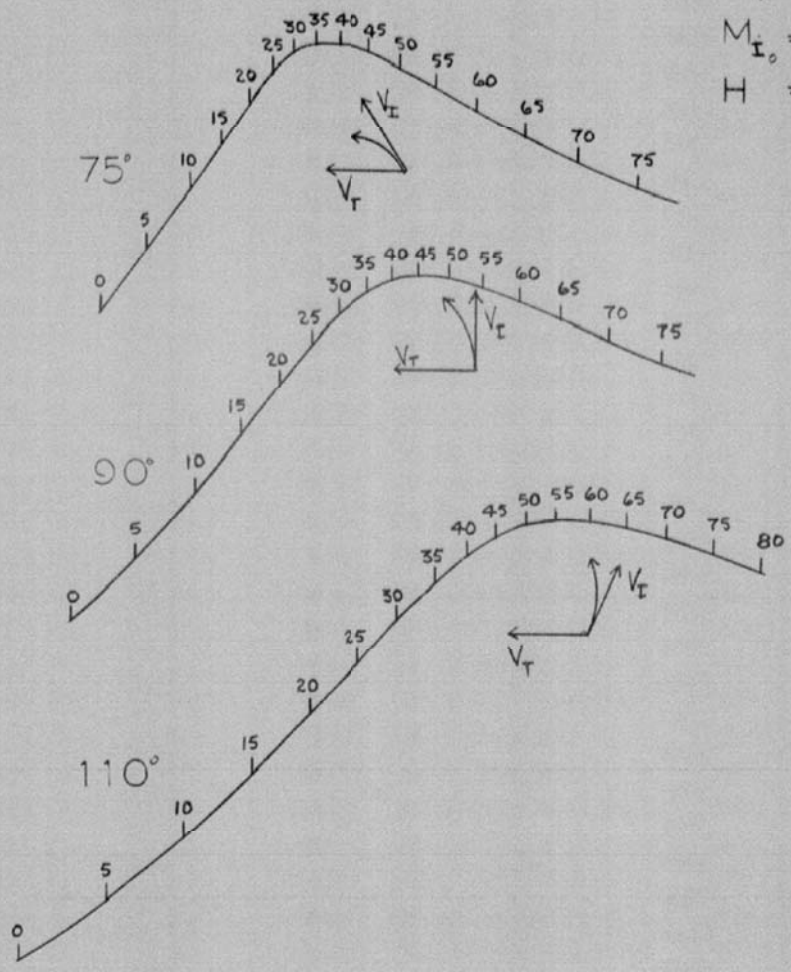

15000'/inch.

15000 ft/inch

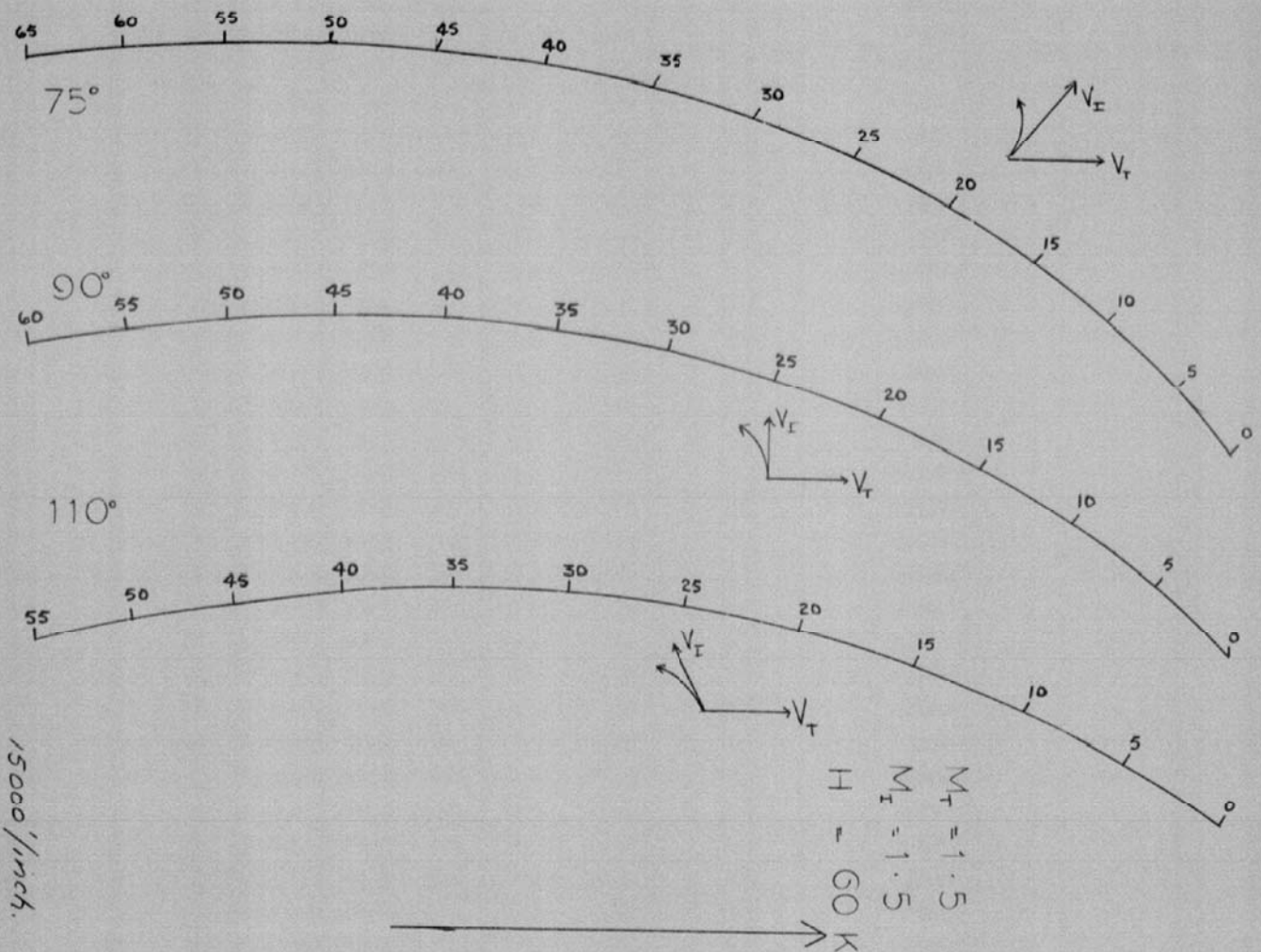
65 60 55 50 45 40 35 30 25 20 15 10 5 0
75°
V_I
V_T
60 55 50 45 40 35 30 25 20 15 10 5 0
90°
V_I
V_T
55 50 45 40 35 30 25 20 15 10 5 0
110°
V_I
V_T
$M_T = 1.5$
$M_I = 1.5$
H = 60 K
15000'/inch.

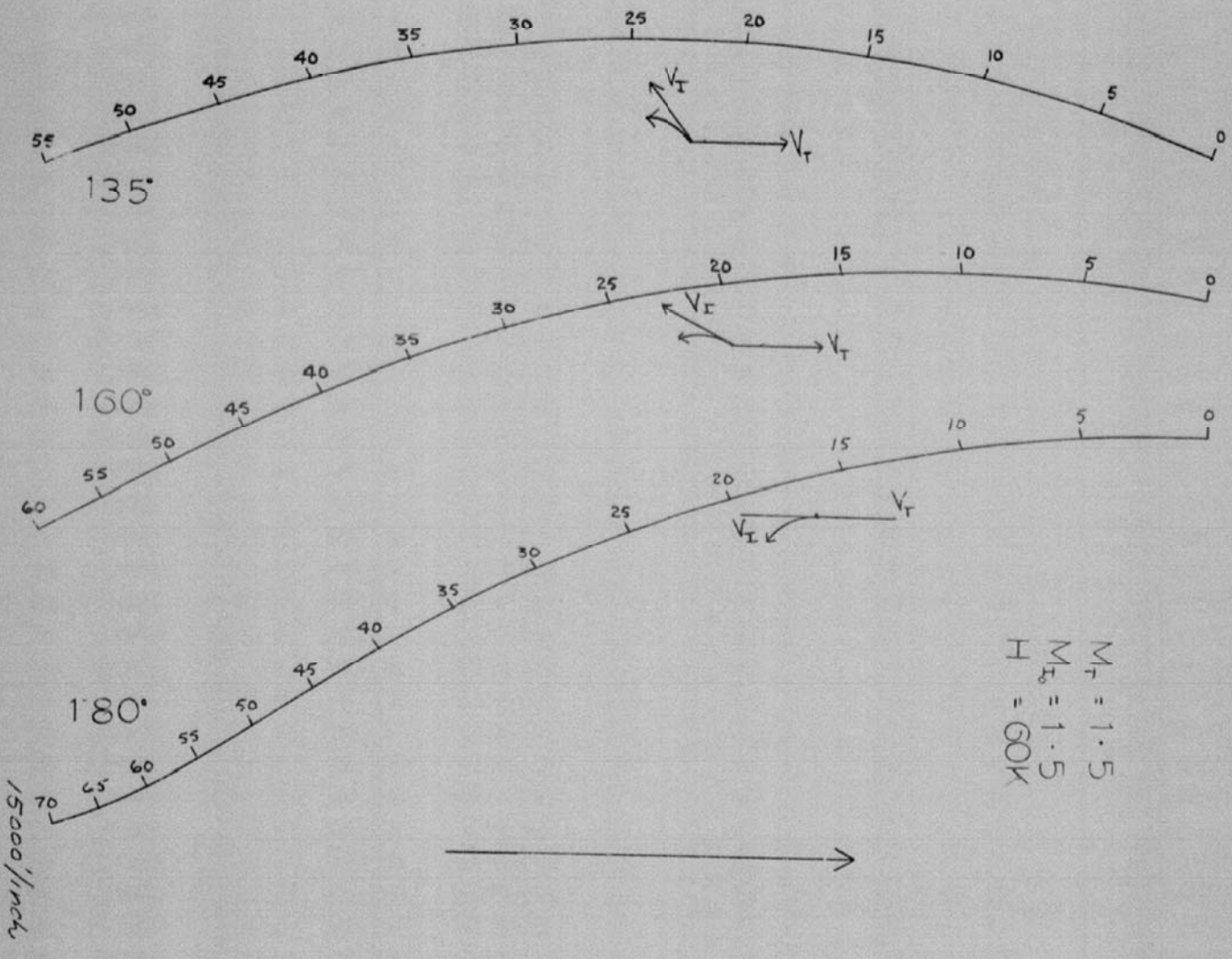
135°
160°
180°
V_I
V_T
$M_T = 1.5$
$M_{I_0} = 1.5$
H = 60K
15000'/inch

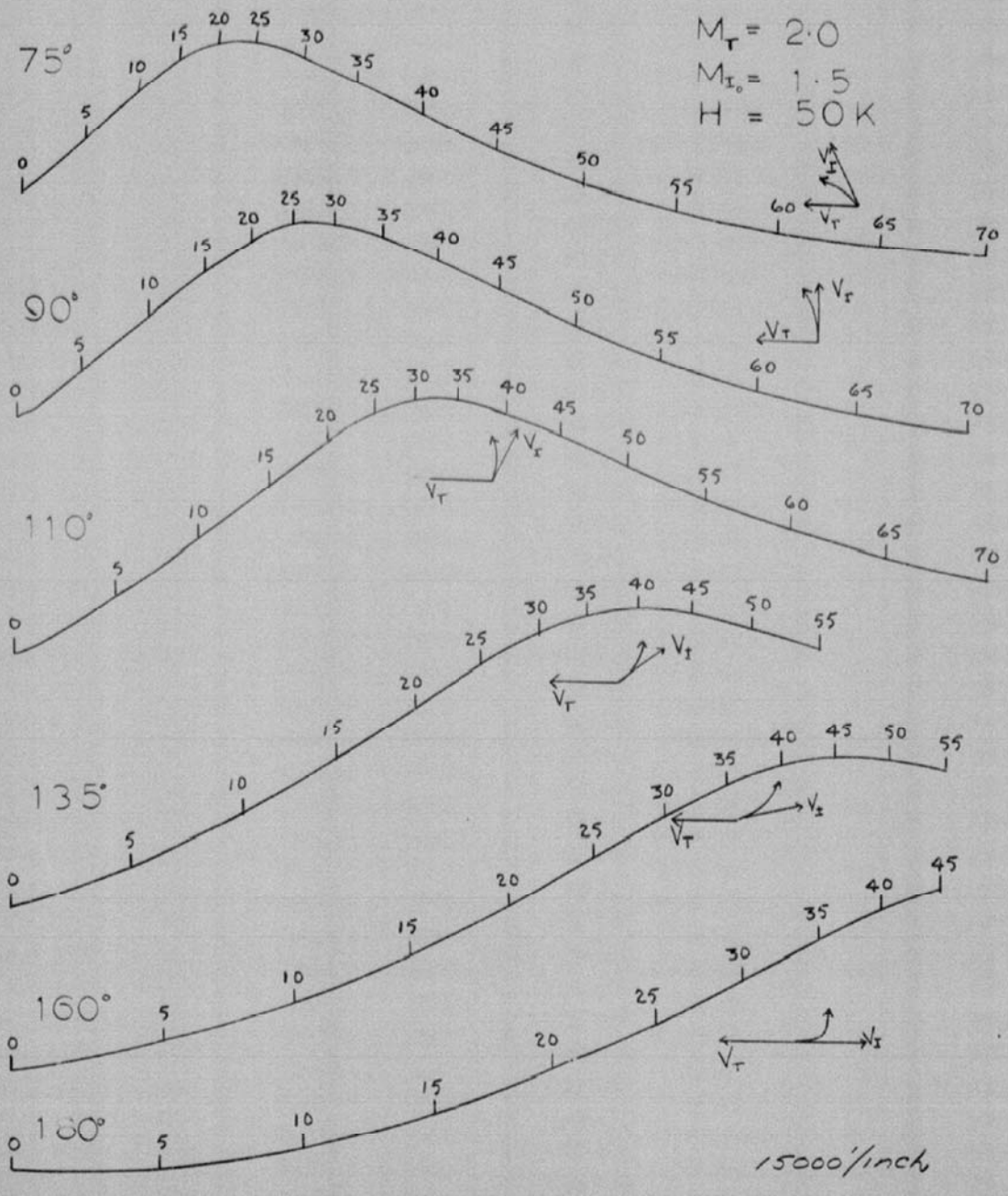
M_T = 2.0
M_{I_o} = 1.5
H = 50K
75°
90°
110°
135°
160°
180°
V_I
V_T
15000'/inch

75°
50
45
40
35
30
25
20
15
10
5
0
V_I
V_T
90°
45
40
35
30
25
20
15
10
5
0
V_I
V_T
110°
45
40
35
30
25
20
15
10
5
0
V_I
V_T
$M_T = 2.0$
$M_I = 1.5$
$H = 50K$
15000'/inch

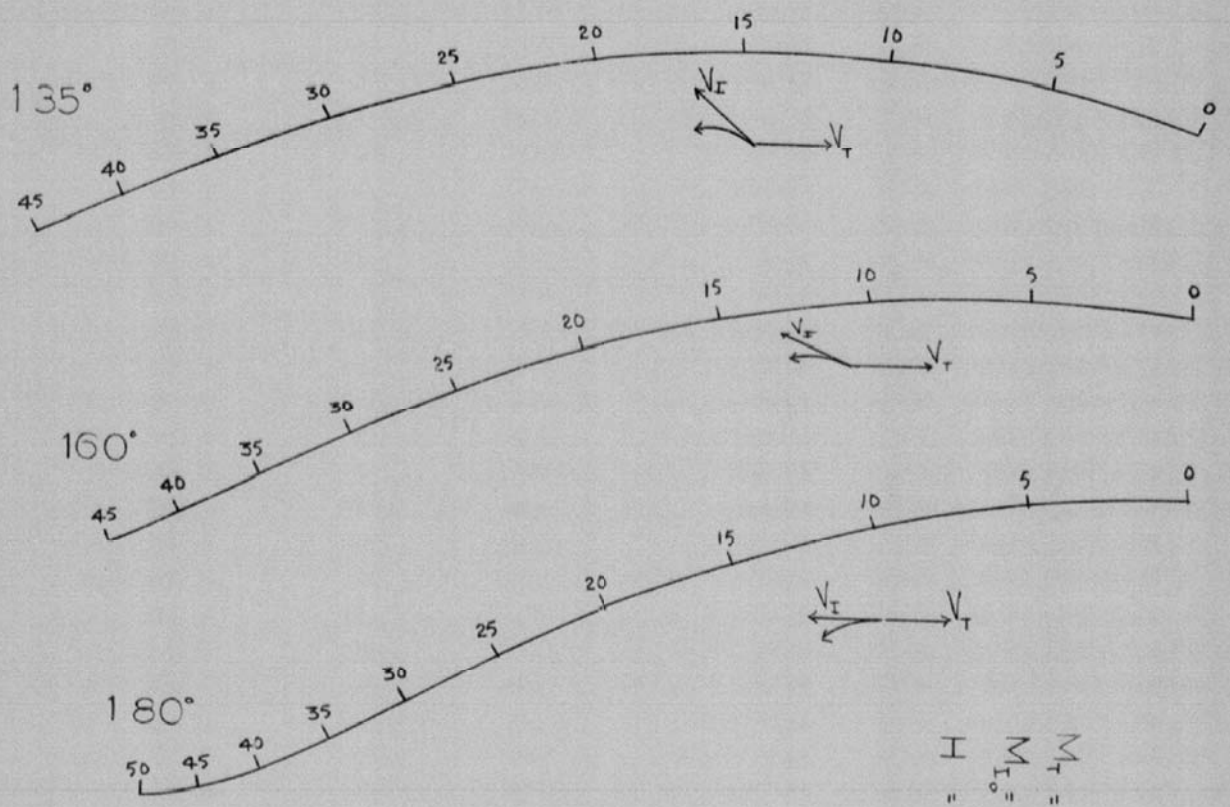

$M_T = 2.0$
$M_{I_o} = 1.5$
$H = 50K$

15000'/inch

75°
90°
110°
0
5
10
15
20
25
30
35
40
45
50
55
60
65
70
75
80
V_I
V_T
$M_T = 2.0$
$M_I = 1.5$
$H = 60K$
knots/1000 ft

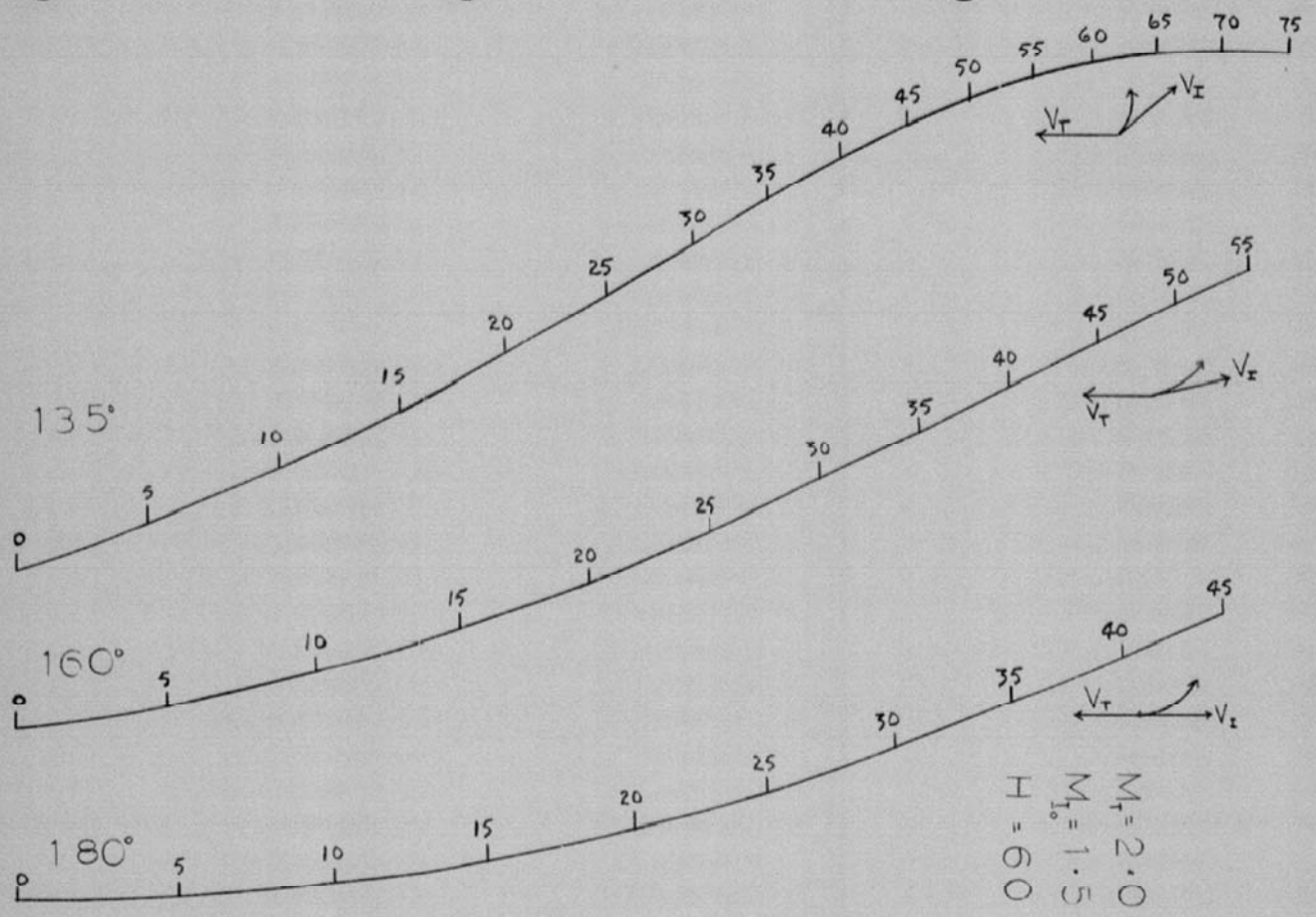

$M_T = 2.0$
$M_{T_\infty} = 1.5$
$H = 60\,K$

15000'/mm

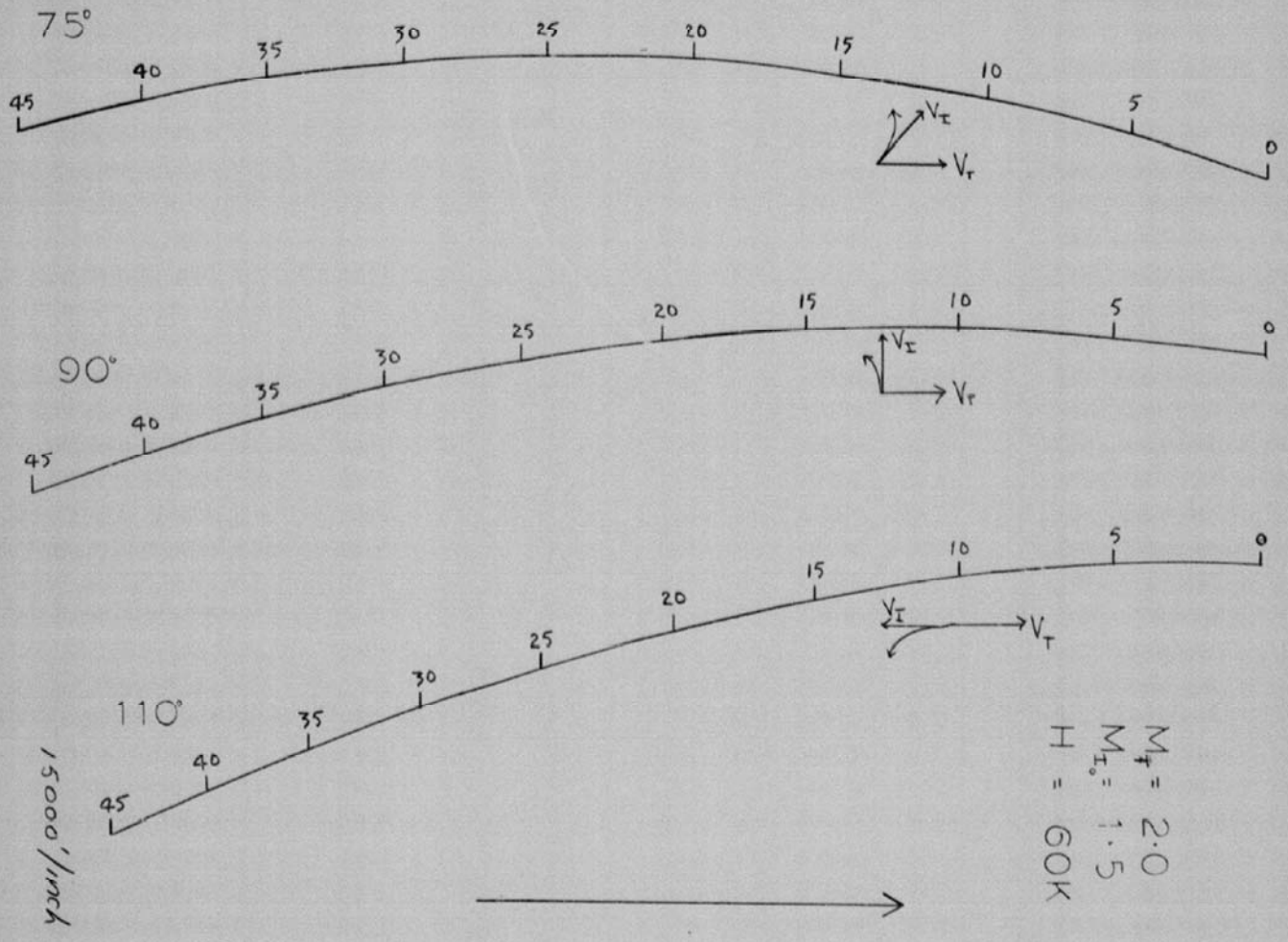

$M_r = 2.0$
$M_{I_\infty} = 1.5$
$H = 60K$

15000 ft/min

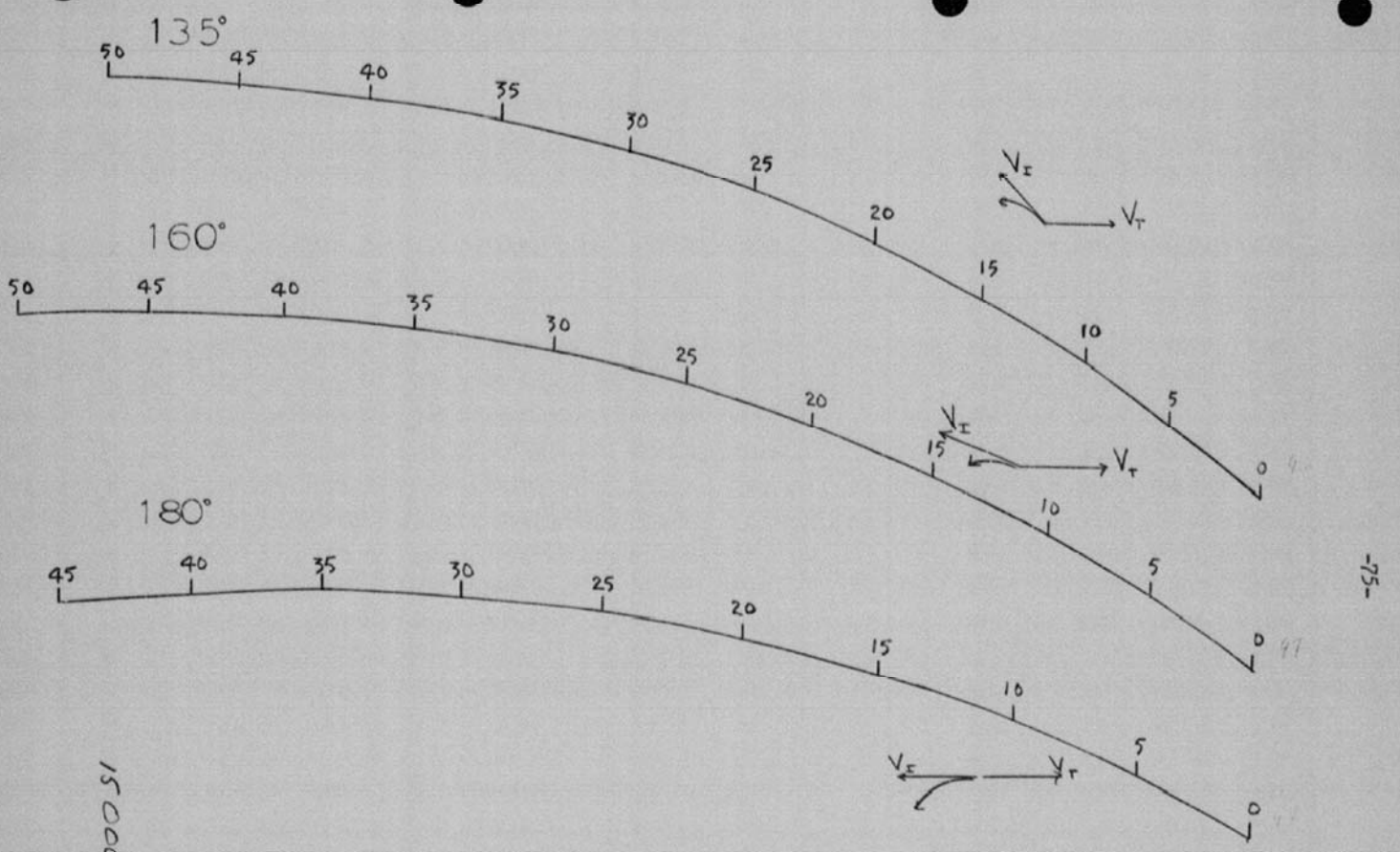

15000'/inch.

$M_T = 2.0$
$M_1 = 1.5$
H = 60K

APPENDIX D

Fighter Placement Studies with Use of Realistic Performance Estimates for the CF 105 Aircraft

C.J. Wilson

The Performance Estimates

Estimated figures for the steady state aerodynamic performance of the CF 105 are available at CARDE in two forms. Information from AVRO reports is in the form of drag carpets; NAE have processed their own data into a form more suitable for use in an analogue computer simulation of the fighter performance (Refs. 1 and 2). NAE have given two sets of estimates, pessimistic and optimistic, for each of two positions of the center of gravity, at 28% and 34% of the mean chord; they have indicated that they have more confidence in their pessimistic figures being fulfilled. At present the position of the center of gravity and probable variations of its position during flight are not known exactly, although AVRO have said that 29.5% of the mean chord will be the aft limit with optimum fuel programming, before the missiles are fired. The c. of g. moves back by 1.5% of the mean chord when the missiles are fired, but these circumstances are not of interest for a Placement Study. The latest AVRO drag carpets do assume 29.5% of the mean chord for the c. of g. position.

The Placement Studies

The two dimensional Placement Study described in Appendix D of Tech. Letter N-47-8 has been finished. A simulation of the CF 105 is now being incorporated into a similar study. (This was suggested in para. 3 of Appendix E of N-47-8). In the previous work the fighter flew always at constant speed, and was therefore restricted to power limited manoeuvres. The effects of the decelerations which occur as a result of tight turns on the system effectiveness have to be assessed. In the initial work on the REAC the NAE pessimistic data, with 28% c. of g. position is being used. An aircraft weight of 50,000 lbs. is assumed.

The three dimensional Placement Study which was outlined in Appendix G of N-47-8 also includes a model of the fighter based on the same N.A.E. 28% pessimistic data. This work has been held up by the delays experienced in obtaining aerodynamic data, and more recently by the delays in installing CARDE's new REAC equipment in operating condition.

The complete range of estimates of CF 105 aerodynamic performance is being used in an extension of the paper and pencil method for Placement Studies in order to evaluate the effects which the differences between these estimates will produce. For this purpose it is necessary to know the trajectory of the fighter in target coordinates when it is manoeuvring to the

limit in a horizontal turn. These curves are based upon corresponding trajectories in space in the same manner as the cycloids used in the constant speed studies are based on circular turns in space. A set of these trajectories for each of the different sets of N.A.E. figures and also for the latest AVRO figures is being prepared using both the REAC and numerical computation. The aircraft weight changes substantially with fuel load, and future developments may also affect the combat weight of the machine. Some trajectories in space coordinates have been drawn for aircraft weights of 46,500 lbs. and 53,500 lbs. as well as for the standard 50,000 lbs. *See note.

These curves are attached to show how the CF 105 might fly a maximum manoeuvre horizontal turn. (Figures 1 to 9). The figures on these curves represent elapsed time in seconds, and tables are given showing the angle turned, the velocity and the load factor at these time intervals (Tables 1 to 9). The fighter has been assumed to begin the turn at a speed of M. 2.0, with full reheat. It is evident that speed is lost rapidly during such a turn.

At present these curves cover only a limited part of the aerodynamic data. An estimate of the changes which other sets of aerodynamics will make can be derived from Figure 10 which displays the aerodynamic limits on load factor (buffet, elevator deflection and hinge moment) for the N.A.E. data, with some corresponding net drag (i.e. the difference between drag and thrust) figures (Table 10). This figure and these data assume 50,000 ft. altitude, 50,000 lbs. aircraft weight and maximum thrust with full reheat.

Method of Simulating the Performance of the CF 105 Aircraft on the REAC

A simulation of the steady-state behaviour of the aircraft is made. This does not imply that everything is held constant, but merely that all considerations of stability and transient behaviour are ignored. The fighter is always assumed to be making coordinated turns and its acceleration or retardation along the direction of the velocity vector is determined by the thrust and drag forces.

The Maximum Lift

The maximum lift available is a function of aircraft speed and altitude. The lift is limited by a number of factors viz. stall, buffet, maximum control deflection and maximum control hinge moment.

It is assumed that the upper lift limit due to stall, buffet and maximum control deflection is given by

$$L_{mB} = \left(\frac{L_{mB}}{p_o}\right) p_o$$

Where $\frac{L_{mB}}{p_o}$ is a function of Mach number only, p_o is the air pressure.

* Note: Appendic C gives the corresponding fighter turns in target coordinates.

The upper limit due to restrictions on the available hinge moment is given by

$$L_{mHM} = L_{mHM_1} + \left(\frac{L_{mHM_2}}{p_o} \right) . \; p_o$$

Where L_{mHM_1} and $\frac{L_{mHM_2}}{p_o}$ are functions of Mach No. only.

The maximum available lift is the smaller of L_{mB} and L_{mHM}

i.e. $L_{max} \leq L_{mB}$

$L_{max} \leq L_{mHM}$

Fighter Turns

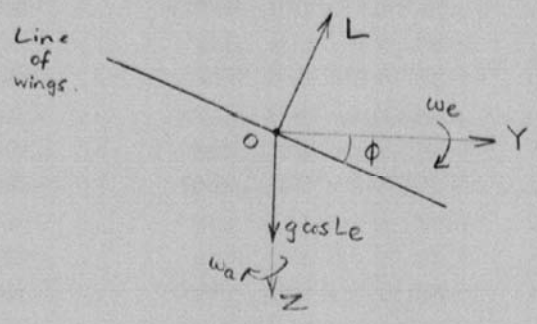

Fig. 11.

A right-handed set of mutually perpendicular axes OXYZ is chosen with OX along the fighter's velocity vector, OXZ a vertical plane containing this velocity vector, OZ downwards, and OY horizontal. OX makes an angle L_e with a horizontal plane when the fighter is climbing at an inclination L_e.

If ω_e and ω_a are the components of the fighter's angular velocity about OY and OZ respectively, V_f the velocity, ϕ the bank angle, L the lift force and W the weight of the aircraft, (see Figure 11), then

$$(L \cos \phi - W \cos L_e)\, g = W V_f \omega_e$$

$$L \sin \phi\, g = W V_f \omega_a$$

If the turn demands are such that L is less than L_{max} they can be satisfied. If they are too large the demands will be reduced by a factor K'/K such that

$$(L_{max} \cos \phi - W \cos L_e)\, g = W V_f K'/K\, \omega_e$$

$$L_{max} \sin \phi\, g = W V_f K'/K\, \omega_a$$

Where, now, ω_e and ω_a are the turn demands, and $K'/K\, \omega_e$ and $K'/K\, \omega_a$ are turn rates achieved. In the first set of equations L and ϕ are determined, given ω_e, ω_a and V_f, but in the second set K'/K and ϕ are determined, with the same inputs ω_e, ω_a and V_f.

Engine Thrust

The thrust of a jet engine at full throttle is assumed to be

$$T = (T/p_o)\, p_o$$

and the maximum boost in thrust when using reheat is

$$\Delta T_r = \left(\frac{\Delta T_r}{p_o}\right) p_o$$

where T/p_o and $\frac{\Delta T_r}{p_o}$ are functions of Mach number only.

The maximum possible thrust is thus given by

$$T_{max} = (T/p_o)\, p_o + \left(\frac{\Delta T_r}{p_o}\right) p_o$$

Drag

It is assumed that the drag, a function of altitude, Mach number and lift, takes the form

$$D = (D_o/p_o)\, p_o + K_1 L + \frac{\mathcal{F}_1 L^2}{p_o}$$

where $\frac{D_o}{p_o}$, K_1 and $\mathcal{F}_1$ are functions of Mach number only.

The functions of Mach number, $\frac{L_{mB}}{p_o}$, L_{mHM_1}, $\frac{L_{mHM_2}}{p_o}$, T/p_o, $\frac{\Delta T_r}{p_o}$, $\frac{D_o}{p_o}$, K_1 and $\mathcal{F}_1$ have values based on the pessimistic set of data provided by N.A.E. for 28% of mean chord c. of g. position.

A block diagram illustrates the method of mechanization (Fig.12).

Attention is drawn to Appendix B.

References

1. N.A.E. Lab. Memo No. AE-82 "The Problem of Representing the High-Altitude Performance of a Turbo-jet Aircraft on an Analogue Computer" by R.J. Templin. CONFIDENTIAL.

2. N.A.E. Lab. Memo No. AE-46g "High Altitude Performance Data for the CF 105 Aircraft" by O.E. Michaelsen. SECRET.

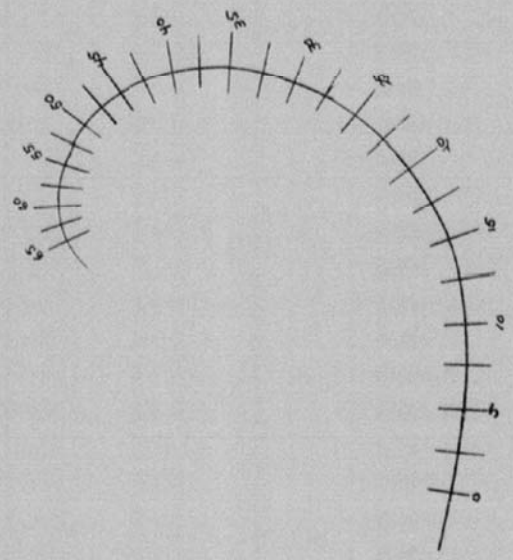

Figure 1
Ht. = 50,000 ft.
Wt. = 46,500 lbs
Scale 1 inch = 5,000 yds.

Table 1

Height = 50,000 ft.
Weight = 46,500 lbs.
N.A.E. = 28% pessimistic data.

t	0	5	10	15	20	25	30	35	40
V_f	2	1.94	1.88	1.77	1.65	1.55	1.44	1.35	1.25
N	2.25	2.45	2.68	2.98	2.9	2.8	2.7	2.58	2.5
Γ	0	10	22	34	52	66	84	104	119

t	45	50	55	60	65	70	75	80
V_f	1.15	1.03	.97	.90	.82	.72	.64	.54
N	2.58	2.35	2.0	1.9	2.0	1.78	1.45	1.15
Γ	139	162	189	199	218	242	260	274

t = elapsed time (in seconds)

V_f = velocity of fighter (Mach no.)

N = load factor

Γ = angle turned (in degrees)

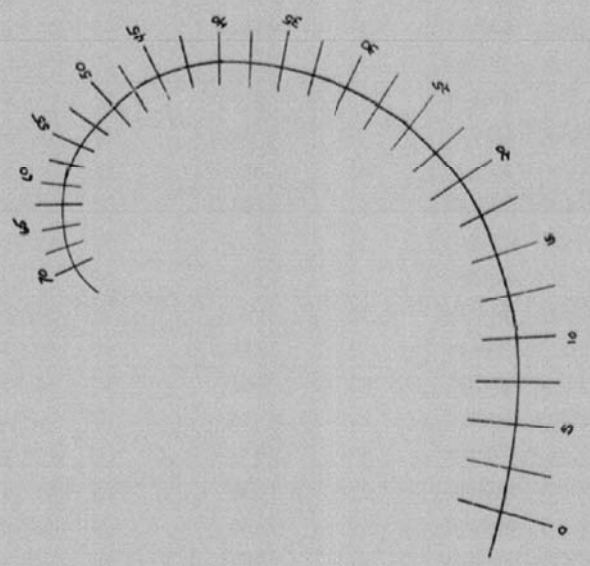

Figure 2

Ht. 50,000 ft.
Wt. 50,000 lbs.
Scale 1 inch = 5,000 yds.

Table 2

Height = 50,000 ft.
Weight = 50,000 lbs.
N.A.E. = 28% pessimistic data

t	0	5	10	15	20	25	30	35	40
V_f	2	1.95	1.90	1.81	1.70	1.61	1.50	1.41	1.34
N	2.13	2.3	2.48	2.7	2.8	2.7	2.6	2.5	2.43
Γ	0	10	20	33	47	63	77	93	111

t	45	50	55	60	65	70	75
V_f	1.26	1.17	1.07	1.00	.95	.90	.82
N	2.4	2.4	2.48	2.0	1.85	1.8	1.9
Γ	125	145	163	183	201	212	235

t = elapsed time (in seconds)

V_f = velocity of fighter (Mach no.)

N = load factor

Γ = angle turned (in degrees)

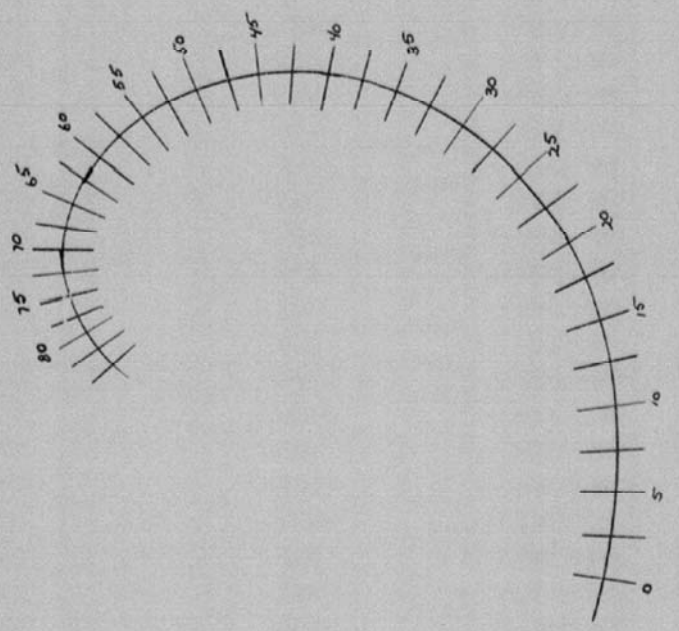

Figure 3

Ht. = 50,000 ft.
Wt. = 53,500 lbs.
Scale 1 inch = 5,000 yds.

Table 3

Height = 50,000 ft.
Weight = 53,500 lbs.
N.A.E. = 28% pessimistic data.

t	0	5	10	15	20	25	30	35	40
V_f	2	1.96	1.90	1.85	1.79	1.72	1.64	1.57	1.49
N	1.97	2.1	2.2	2.4	2.5	2.6	2.53	2.45	2.38
Γ	0	8	16	25	38	52	64	80	94

t	45	50	55	60	65	70	75	80	85
V_f	1.44	1.37	1.32	1.26	1.19	1.12	1.05	1.00	.97
N	2.30	2.25	2.2	2.2	2.2	2.28	2.2	1.83	1.75
Γ	106	122	136	152	167	184	204	220	234

t = elapsed time (in seconds)

V_f = velocity of fighter (Mach no.)

N = load factor

Γ = angle turned (in degrees)

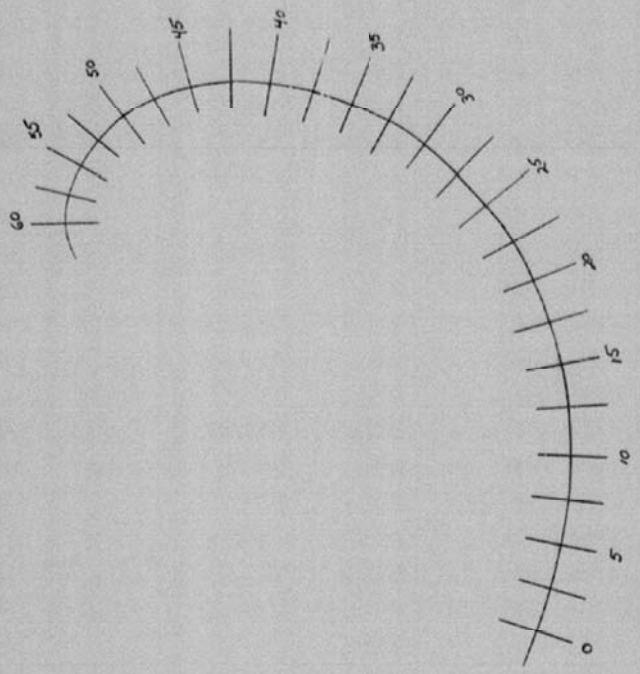

Figure 4

Ht = 40,000 ft
Wt = 46,500 lbs
Scale 1 inch = 5,000 yds

Table 4

Height = 40,000 ft.
Weight = 46,500 lbs.
N.A.E. = 28% pessimistic data.

t	0	5	10	15	20	25	30	35	40
V_f	2	1.98	1.96	1.94	1.89	1.86	1.83	1.78	1.73
N	2.23	2.32	2.45	2.56	2.65	2.78	2.88	3.0	3.19
Γ	0	7	18	29	40	54	66	81	98

t	45	50	55	60	65	70	75
V_f	1.68	1.59	1.48	1.35	1.23	1.09	.99
N	3.40	3.78	4.08	3.40	3.85	4.0	3.09
Γ	117	137	160	187	220	255	285

t = elapsed time (in seconds)

V_f = velocity of fighter (Mach no.)

N = load factor

Γ = angle turned (in degrees)

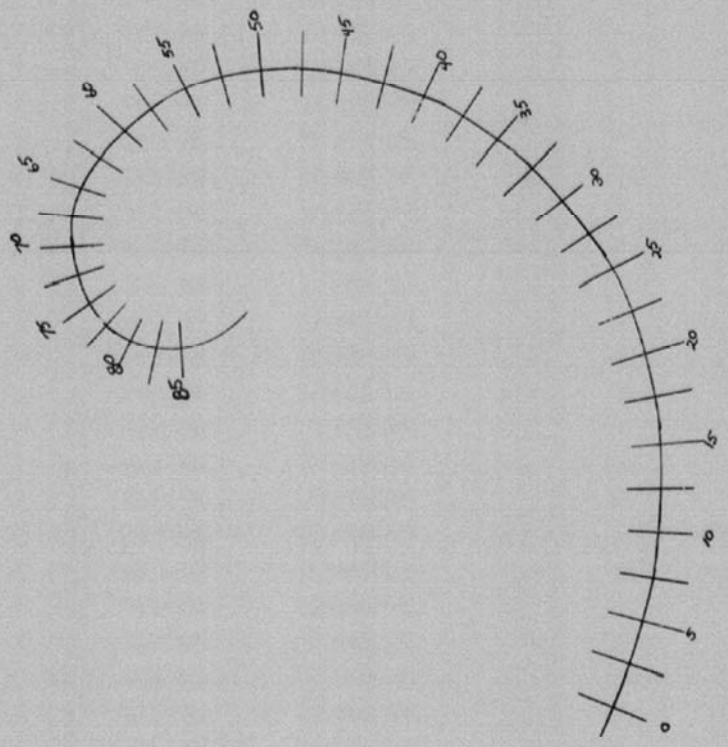

Figure 5

Ht. = 40,000 ft.
Wt. = 50,000 lbs.
Scale 1 inch = 5,000 yds.

Table 5

Height = 40,000 ft.
Weight = 50,000 lbs.
N.A.E. = 28% pessimistic data.

t	0	5	10	15	20	25	30	35	40
V_f	2	1.99	1.97	1.94	1.92	1.89	1.87	1.84	1.81
N	2.1	2.2	2.3	2.4	2.4	2.5	2.6	2.68	2.78
Γ	0	6	18	30	38	51	62	76	89

t	45	50	55	60	65	70	75	80	85
V_f	1.77	1.73	1.67	1.60	1.50	1.40	1.30	1.19	1.07
N	2.9	3.0	3.2	3.5	3.82	3.8	3.68	3.66	3.77
Γ	103	118	138	156	180	204	232	258	288

t = elapsed time (in seconds)

V_f = velocity of figher (Mach no.)

N = load factor

Γ = angle turned (in degrees)

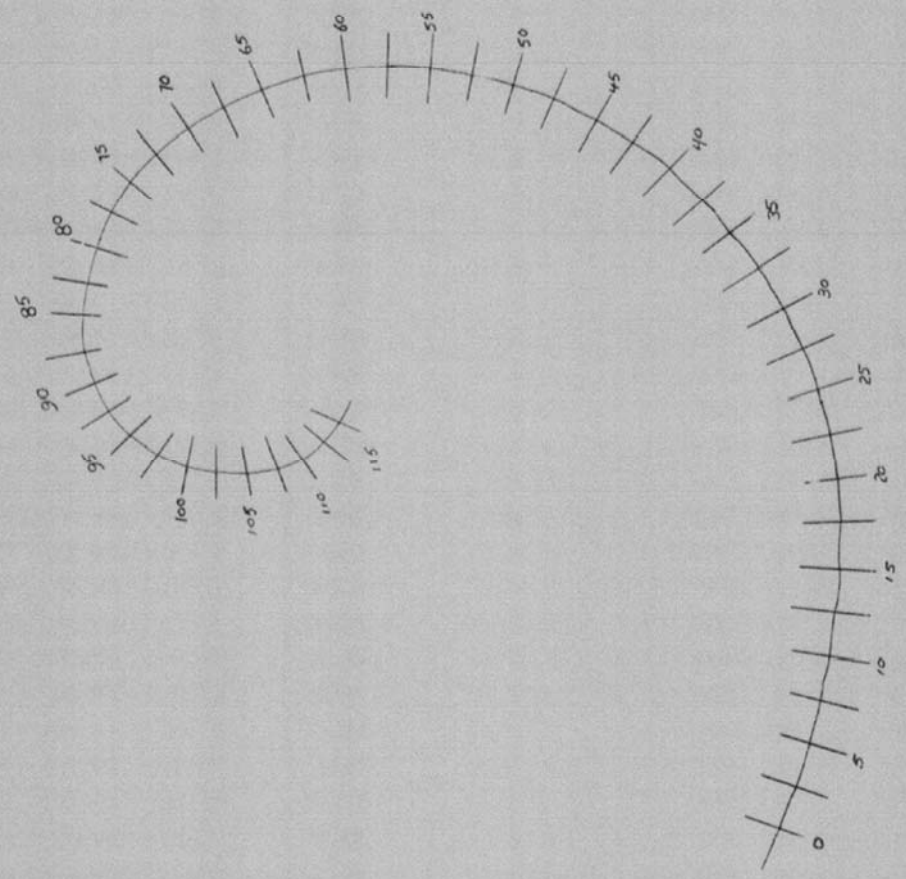

Figure 6

Ht. = 40,000 ft
Wt. = 53,000 lbs
Scale 1 inch = 5,000 yds

Table 6

Height : 40,000 ft.
Weight : 53,500 lbs.
N.A.E. : 28% pessimistic data.

t	0	5	10	15	20	25	30	35	40
V_f	2	1.99	1.98	1.96	1.95	1.94	1.92	1.89	1.87
N	1.9	1.98	2.0	2.1	2.2	2.2	2.3	2.3	2.4
Γ	0	8	16	28	36	44	54	66	77

t	45	50	55	60	65	70	75	80	85
V_f	1.85	1.82	1.81	1.78	1.75	1.73	1.69	1.64	1.58
N	2.4	2.5	2.53	2.60	2.7	2.78	2.9	3.05	3.19
Γ	88	98	113	126	138	153	170	186	206

t	90	95	100	105	110	115
V_f	1.50	1.42	1.36	1.28	1.19	1.09
N	3.48	3.5	3.4	3.4	3.4	3.48
Γ	226	248	273	298	324	352

t = elapsed time (in seconds)

V_f = velocity of fighter (Mach no.)

N = load factor

Γ = angle turned (in degrees)

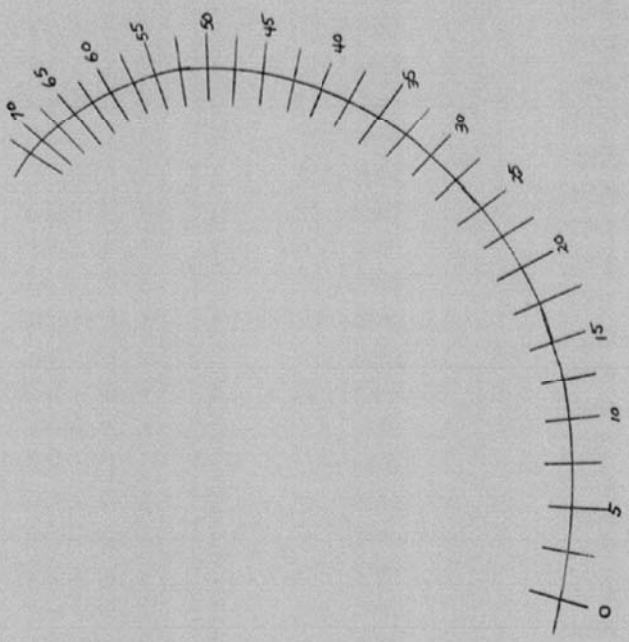

Figure 7

Ht. = 60,000 ft.
Wt. = 46,500 lbs.
Scale 1 inch = 5,000 yds.

Table 7

Height = 60,000 ft.
Weight = 46,500 lbs.
N.A.E. = 28% pessimistic data.

t	0	5	10	15	20	25	30	35	40
V_f	2	1.93	1.80	1.71	1.63	1.54	1.45	1.38	1.30
N	2.45	2.21	2.10	2.0	1.91	1.85	1.8	1.74	1.70
⌐	0	11	20	28	38	49	60	69	80

t	45	50	55	60
V_f	1.24	1.15	1.06	.99
N	1.70	1.74	1.73	1.40
⌐	91	102	117	130

t = elapsed time (in seconds)

V_f = velocity of fighter (Mach no.)

N = load factor

⌐ = angle turned (in degrees)

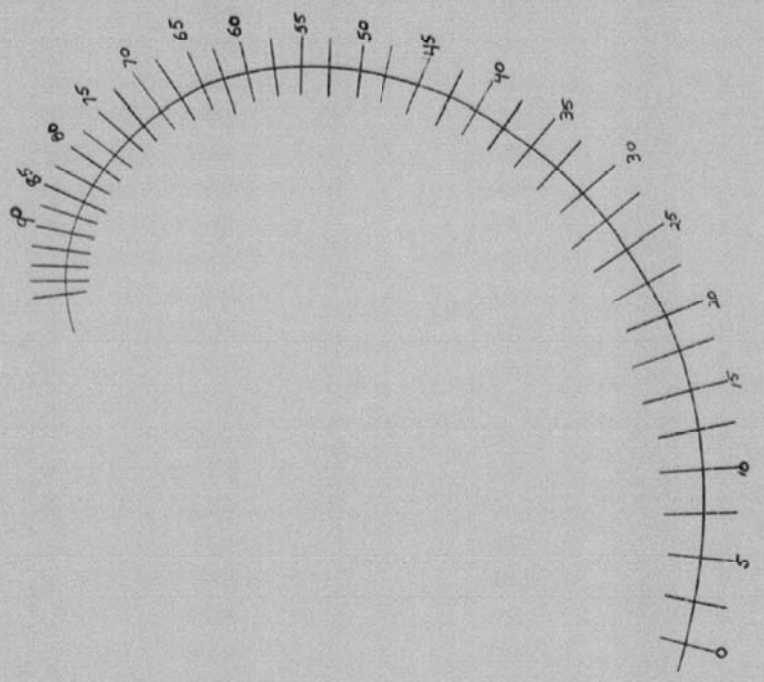

Figure 8

Ht. = 60,000 ft
Wt. = 50,000 lbs
Scale 1 inch = 5,000 yds.

Table 8

Height = 60,000 ft.
Weight = 50 000 lbs.
N.A.E. = 28% pessimistic data.

t	0	5	10	15	20	25	30	35	40
V_f	2	1.92	1.82	1.74	1.67	1.59	1.51	1.44	1.38
N	2.33	2.13	2.0	1.9	1.85	1.80	1.74	1.70	1.65
Γ	0	11	20	29	39	48	58	67	76

t	45	50	55	60	65
V_f	1.32	1.26	1.18	1.11	1.03
N	1.61	1.60	1.60	1.67	1.5
Γ	86	97	108	120	132

t = elapsed time (in seconds)

V_f = velocity of fighter (Mach no.)

N = load factor

Γ = angle turned (in degrees)

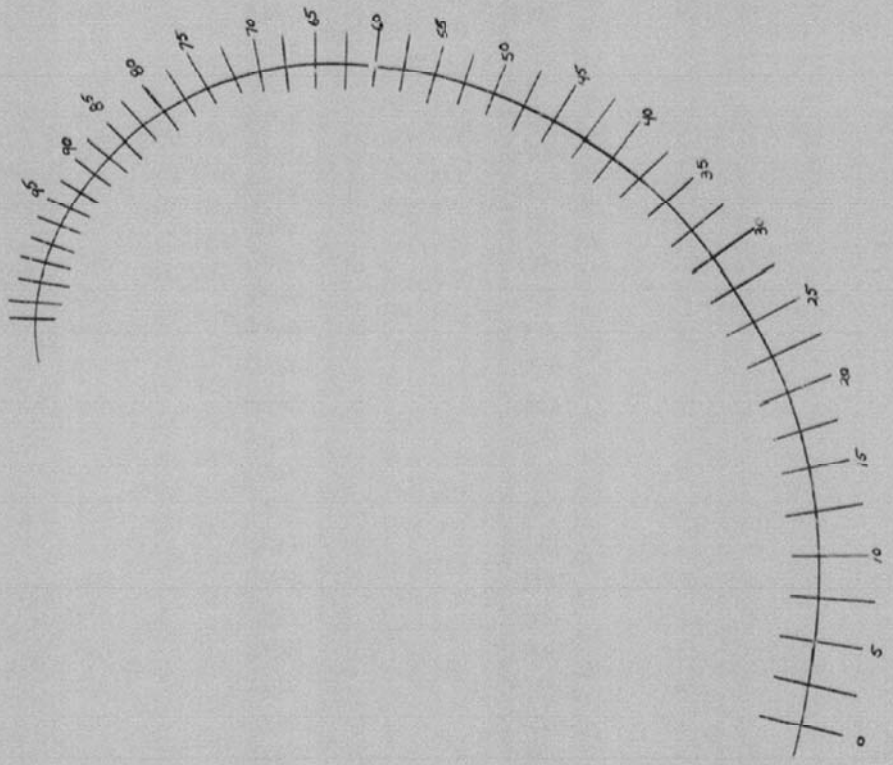

Figure 9

Ht. = 60,000 ft.
Wt. = 53,000 lbs.
Scale 1 inch = 5,000 yds.

Table 9

Height = 60,000 ft.
Weight = 53,500 lbs.
N.A.E. = 28% pessimistic data.

t	0	5	10	15	20	25	30	35	40
V_f	2	1.92	1.85	1.78	1.72	1.65	1.55	1.53	1.48
N	2.1	1.95	1.85	1.78	1.73	1.69	1.64	1.60	1.58
Γ	0	10	19	27	35	44	52	60	67

t	45	50	55	60	65	70	75	80	85
V_f	1.43	1.38	1.33	1.28	1.24	1.18	1.12	1.06	1.01
N	1.54	1.61	1.49	1.48	1.47	1.49	1.51	1.50	1.28
Γ	75	84	93	102	111	120	131	141	153

t = elapsed time (in seconds)

V_f = velocity of fighter (Mach no.)

N = load factor

Γ = angle turned (in degrees)

CF-105 lift limits at 50,000 ft.
From N.A.E. Lab. Memo AE 46 g

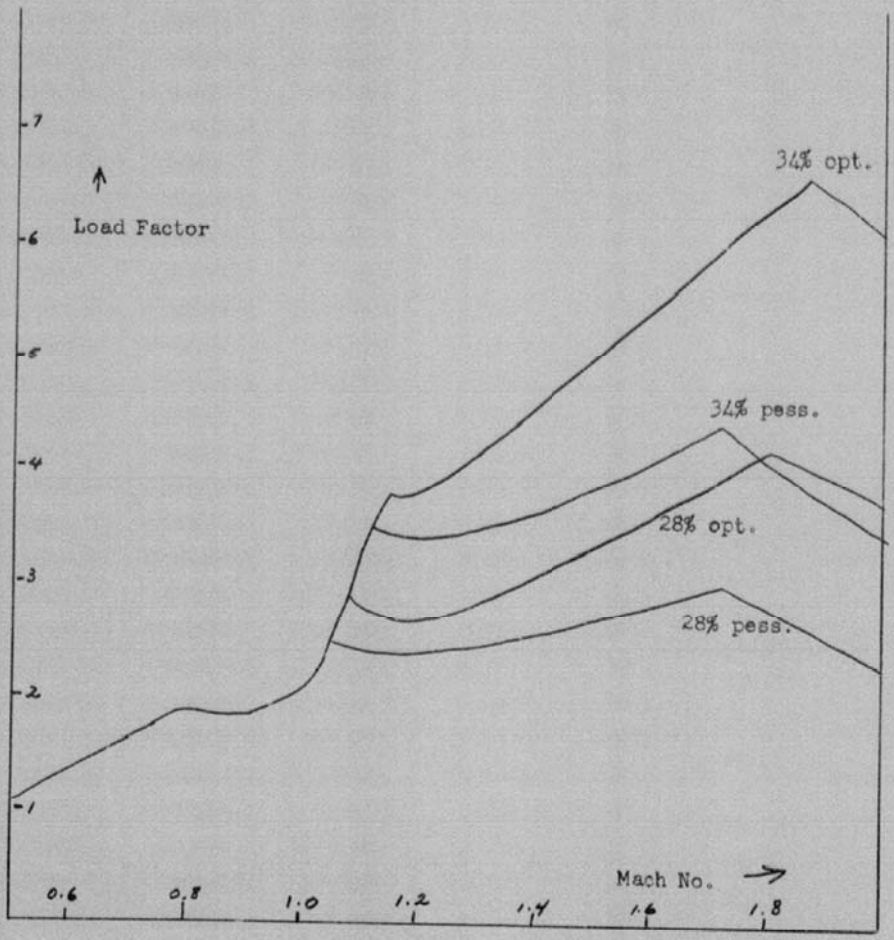

Figure 10

Table 10

NET DRAG (TOTAL DRAG MINUS THRUST) AT THE LIFT LIMITS OF FIGURE 10

Height = 50,000 ft.
Weight = 50,000 lbs.
Throttle - Full reheat.

MACH NO.	28% PESS.	28% OPT.	34% PESS.	34% OPT.
0.5	17570	15750	12050	11290
0.8	21610	18920	14930	15040
0.9	13310	10370	8700	7456
1.0	16360	14080	11160	9532
1.1	27280	34250	41530	35860
1.2	24610	30580	41530	51920
1.4	26470	29410	41850	54800
1.6	32910	35070	50860	64730
1.8	27810	41830	44690	76310
2.0	16540	29100	25890	62607

NOTE: These net drag figures apply at the lift limits (see figure 10). These lift limits differ widely at high Mach no. and cause the large differences in drag.

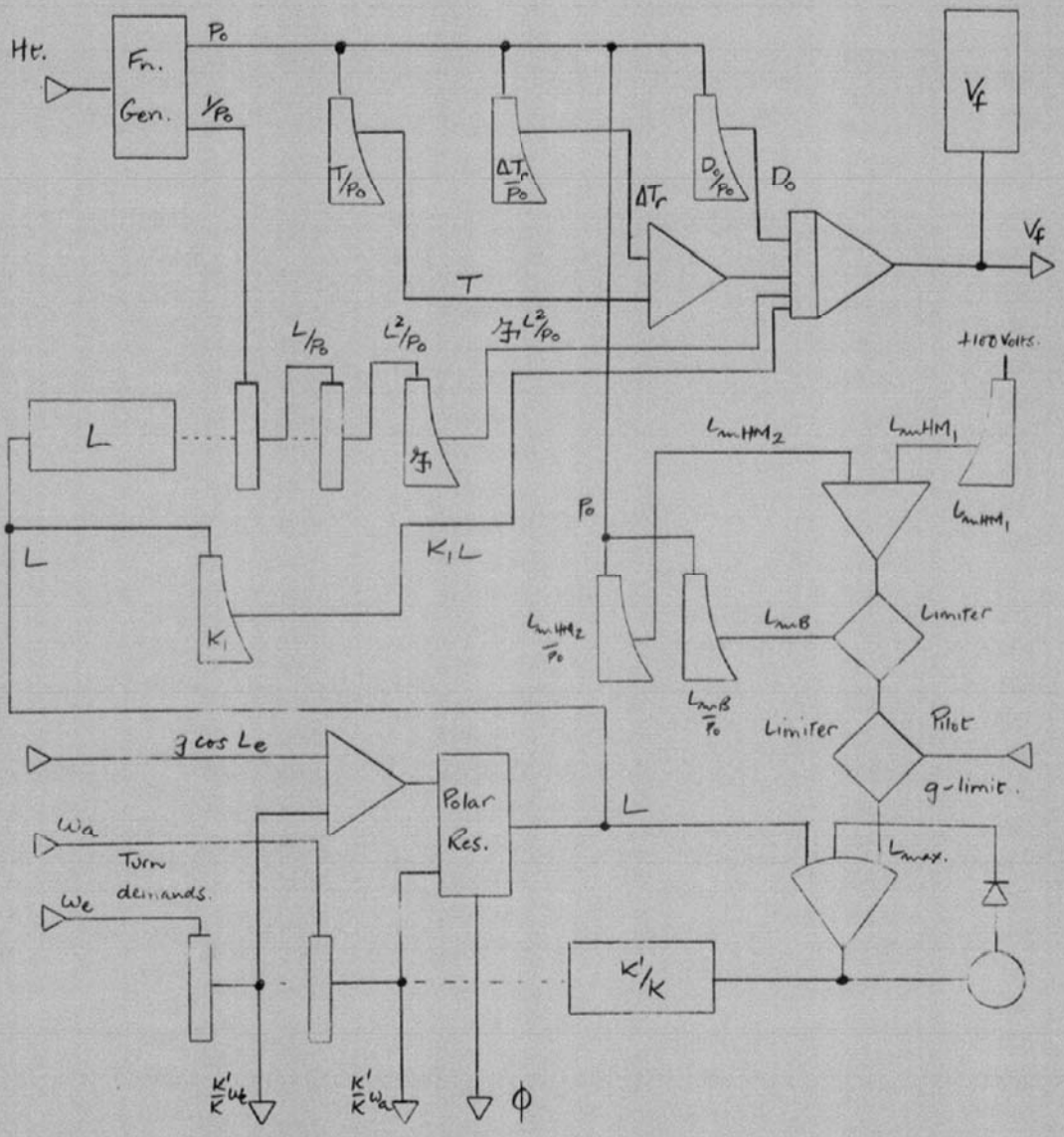

Achieved turns

REAC Simulation of Aircraft Behaviour

Figure 12

APPENDIX

AI ACQUISITION RANGE

J.T. Macfarlane

1. Calculation of placement probability for an interceptor requires knowledge of the available acquisition range of the A.I. radar. This quantity varies with aspect for a given target and is different of course for different targets.

2. The RCAF Specification Air 7-6 states a range of 25 nautical miles for 80% probability of detection of a target having 5 square meters reflection area. This figure has been used in computing expected acquisition range as a function of aspect for three targets: a subsonic swept-wing bomber, a delta-winged medium bomber, and a supersonic straight-winged bomber.

3. Graphs of expected acquisition range for the three targets were originally published in a previous CARDE Technical Letter (Reference 1). Subsequent discussion has led to modification of some of the assumed target reflection areas, and revised contours are given here.

4. The reflection area values used for computing the revised acquisition range contours are given in Table I below. Values originally used are given in parentheses for comparison.

The values for the B-52 aircraft are derived in part from those given in University of Michigan reports on Radar Cross Sections. Any sharp peaks have been reduced or eliminated since such peaks, if only a few degrees wide, are of no use in positioning an aircraft by ground control because of the obtainable accuracy in placement and the variability in the position of these peaks due to pitch and yaw of the target and interceptor. The minimum value of reflection area for any aspect was taken to be 4 square meters.

Radar cross-section values used for the delta-winged aircraft are those for the Avro Vulcan medium bomber, taken from RRE published reports. The median values were used. No change has been made in these values since publication of Reference 1.

Reflection area values for a straight-winged supersonic aircraft are purely hypothetical and represent a possible case. The values used for the revised contours are greater than those originally used, since it has been pointed out by DRTE that very small areas (about one square meter) are very unlikely at X-band.

Table I

Reflection Areas in Square Meters

Aspect	B-52	Delta	Straight Wing
0	4 (.8)	17.5	2.5 (0.5)
10	4 (.9)		
20	4 (1.03)		
30	4 (1.1)	16.6	2.25 (0.45)
37.5	Peak		
40	4 (3.0)		
50	4.3		
60	10	18.7	2.75 (0.55)
70	30		
80	100		
90	Peak	200	
100	140		12.0 (2.4)
110	25		
120	4.5	22.4	4.0 (0.8)
130	4 (1.1)		
140	4 (1.1)		
150	4 (0.6)	5.9	1.0 (0.2)
152	Peak		
160	4 (0.4)		
170	4 (0.35)		
180	4 (0.4)	8.0	1.0 (0.2)

5. Figures 1, 2, and 3 below give polar graphs of expected acquisition range. Polar graphs are drawn since these may be used as overlays on positioning diagrams drawn in target coordinates. Contours are given for various degrees of radar performance, marked as follows:

S	Range required in RCAF Specification
1.92S	Range proposed by RCA for final development
1.28S	Range proposed for the degraded system by RCA
0.85S 0.6 S 0.4 S	Various degradations of the Specification

6. Semicircles are drawn on the graphs to indicate the 30 n.m. lock-on range required by the specification, and the 60 n.m. range of the search presentation.

References:

1. CARDE Technical Letter N-47-8, First Quarterly Report on CF-105 Weapon System Assessment.

2. University of Michigan Report 2260-1-T, Studies in Radar Cross Sections XV.

3. RRE Memos 1078, 1015.

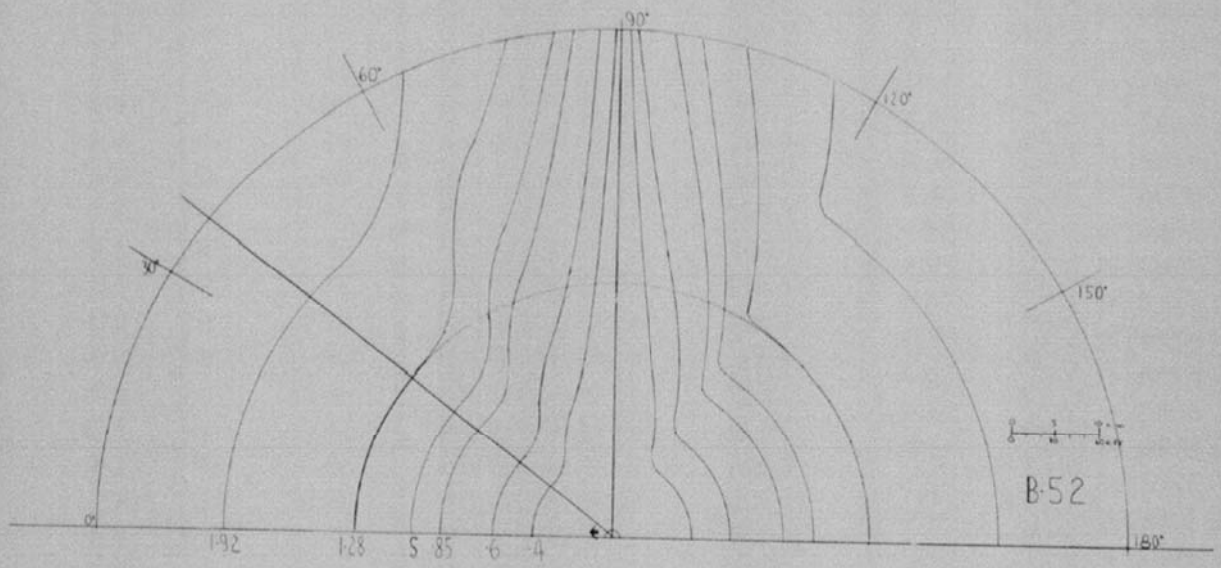
90°
60°
120°
30°
150°
B·52
0°
1·92
1·28
S ·85
·6
·4
180°

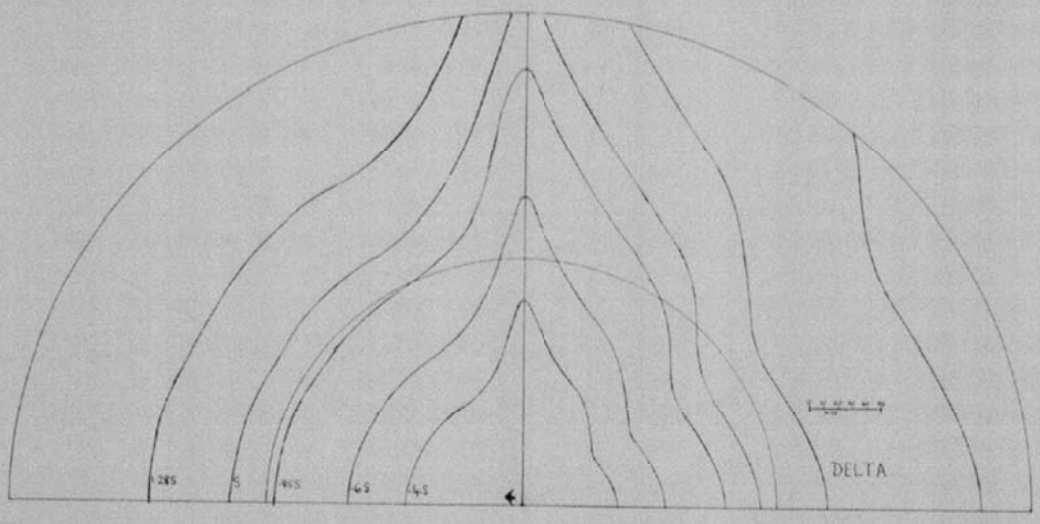
.285
.5
.665
.65
.45
DELTA

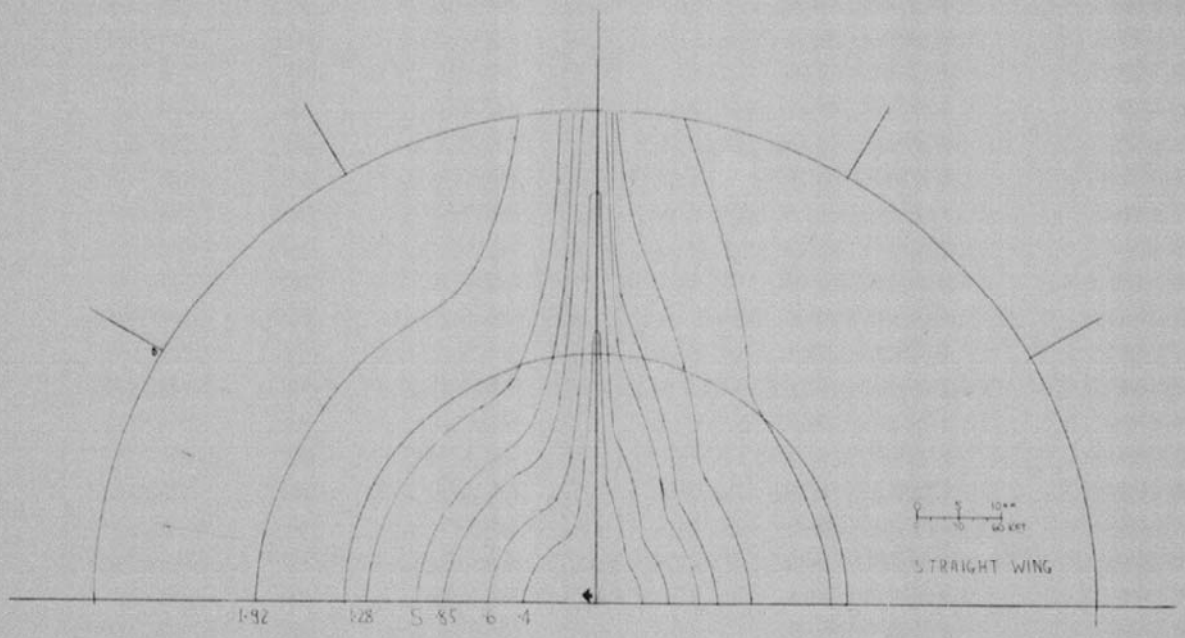
STRAIGHT WING
1·92
1·28
5·85
6·4

APPENDIX

"AI HOMING ON JAMMER AIRCRAFT"

D.J. Mc Kinnon

Sections:

A. Scope of the Study

B. Results of Theoretical Study

C. Range Finding

A. SCOPE OF STUDY

1. INTRODUCTION

The radar to be carried by the all weather type of interceptor planned for the future is expected to suffer from the effects of electronic jamming. This will produce difficulty in launching guided missiles successfully unless some method of overcoming the effects of jamming is discovered.

This study approaches the subject from a tactical rather than a technical view point. Possible enemy strategy in the use of jamming was examined and tactical procedures were designed to overcome the most obvious jamming applications.

The procedures recommended to combat the effects of jamming were designed with the need for simplification and standardization in mind. Hence, each procedure is really a "rule of thumb" which reduces any tendency toward confusion under the strain of combat conditions. The subject matter is discussed under three main topics.

I - Scope of the Study - The reader is familiarized with the general problems involved in launching air-to-air missiles against a jamming aircraft. The recommended homing method and the conditions under which it would be applied are described in general terms.

II - Results of Theoretical Study - The homing method is discussed here in detail. The various factors influencing the success of the method are examined individually. Their influence is shown in a graphical or numerical form whenever possible.

III - Range Finding - This section contains the results of a sub-study of various range finding methods. Although range finding is intimately connected with the homing method the results of the sub-study are more conveniently contained as a separate section, following the detailed description of the homing method.

In the process of developing successful procedures a number of unsuccessful means of acquiring information were examined and these results are also included.

2. BASIC ASSUMPTIONS

2.1 Interceptor Aircraft - The CF-105 interceptor was chosen as representative of an aircraft capable of maintaining a speed of Mach 1.5 while straight and level for a duration of several minutes. The airborne radar considered was the RCA set proposed for the CF-105. Certain modifications are stipulated to assist the homing technique.

2.2 Enemy Bomber Aircraft - The enemy aircraft were considered as being capable of speeds ranging from Mach 0.85 to 2.0 and heights of up to 60,000 feet.

2.3 Missile Armament - The Sparrow family of missiles was chosen in accordance with planning for the CF-105.

2.4 Jamming of GCI - The GCI frequencies were regarded as being continuously jammed throughout the entire period of the attack. This will substantially reduce the capability of GCI to position interceptors precisely on a large raiding force.

2.5 Jamming of Interceptor - The jamming of the AI and the missile radar frequencies occurred whenever it served the enemy to the greatest advantage.

3. GCI CAPABILITY

3.1 A continuously jammed GCI site can provide only a bearing indication but no range. Two sites can, by triangulating the bearing indications, provide an approximate range. This triangulation of bearings will provide the GCI controller with the following information. The accuracies quoted are only an estimation and are not based on actual results of a trial. They are considered to be pessimistic if anything.

(a) Target speed to ± 30 percent.
(b) Target heading to ± 30 degrees.
(c) Target geographical position to ± 30 nautical miles.
(d) No height indication.

3.2 The GCI controller must be able to direct the interceptor to the target. Some means of communication is therefore essential. Several facilities are available although all are subject to varying degrees of enemy counter-measures.

a) V.H.F. and U.H.F.

Some present day installations are capable of transmitting and receiving on any one of over a thousand frequency selections. Spot frequency jamming is difficult against this installation as the selections are so numerous that it would be difficult to follow. If a prearranged switching sequence is followed by the GCI site and the interceptor, it may be possible to get heading corrections through to the interceptor.

Rapid switching of V.H.F. or U.H.F. frequencies is not always desirable. A sequence must be followed and under combat conditions the interceptor and GCI site may become separated on different frequencies. Getting back on the same frequency again often presents a practical problem unless the rules of the switching sequence are very comprehensive.

One method of simplifying the switching sequence would be to have the GCI site transmit information simultaneously on several frequencies spaced throughout the entire VHF or UHF band. This would force the enemy to act in one of the following ways.

(i) Spot jam each individual frequency. The interceptor would switch its radio to another frequency each time jamming was encountered. To completely jam the VHF and UHF radio communications the enemy would have to "listen out" and find all the frequencies in use and then transmit on each one.

(ii) Wide band jam the entire band of GCI frequencies. This is considered to be within the enemy capability but it must be remembered that if the enemy is forced to spread its jamming power over a wider band of frequencies the power density will be correspondingly reduced. This is advantageous to the interceptor. Unfortunately, although the jamming density may be reduced to a very low figure, the close proximity of the interceptor to the jammer during the final stages of the attack may cause the jammer signal to override the GCI transmission.

b) Radio Compass

This installation is used primarily as a navigation aid and as such can receive commercial radio stations.

In event of war, the commercial stations of high power could transmit instructions to the fighter.

The usefulness of the radio compass receiver has not been fully explored in this study. It would appear, however, that if the broadcast frequencies were jammed, the jamming signal could be substantially reduced by manually rotating the loop antenna until the bearing of the jamming aircraft coincided with the null position of the loop. If the broadcast station is anywhere other than on a line running through the jammer and the interceptor, the instructions broadcast should be readable.

Simultaneous transmission from two or more broadcast stations would improve the reliability of the system whereas jamming from several sources would reduce it. The jamming interference could not be nulled out if the jamming sources were widely divergent in bearing from the interceptor.

A brief test programme is presently underway to assess the ability of the radio compass to receive distant broadcast stations. The test will consist of the radar observer in an airborne CF-100 tuning in distant stations and recording the strength and readability of the received signal. Readings will be taken using all the various antenna features in order to discover the best mode of operation.

The tests are being conducted during convenient intervals on flights scheduled for other purposes. It is anticipated that tests on several flights will be necessary before any conclusive evidence can be obtained which will show the effects of distance, altitude and weather phenomena. No estimate can be placed on the data at which the tests will be completed.

c) Ground Scramble Instructions

When scramble instructions are issued to the interceptor, a heading and distance to close would be included. The heading is only approximate but if care is taken initially by the GCI controller, it should bring the fighter very close to the raid, providing evasive action has not commenced. If the enemy aircraft decide to jam the AI radar before the interceptor closes to its detection range, then the interceptor's chances of finding the target are enhanced. Larger formations of targets and greater maximum detection ranges by the interceptor's radar also assist. It would appear that in many cases the pretake-off instructions will prove to be entirely adequate.

4. ENEMY JAMMING STRATEGY

The attacking enemy bomber has a choice of three times at which to commence jamming.

4.1 Geographical Location - AI jamming may commence when the enemy reaches a geographical location where an attack from the defending interceptors is physically possible. This denies the interceptors a range measurement at all times. It also provides a signal on which to home from ranges greatly exceeding that of normal acquisition. This action will tend to draw interceptors to the jammers at an early stage in the raid. Since the homing will be on a collision course using the homing method, the interceptor will be able to close to the bomber in the shortest time physically possible and hence make the best use of its available airborne time.

4.2 At AI Detection - The enemy bomber can "listen out" for the AI radar signal upon entering an area where an attack is expected. The first indication of interceptors in the area will be short intervals of received signal. Each short interval will represent the narrow beam of the interceptors radar passing across the bomber. The intervals need not be spaced systematically. More than one interceptor may be in the area.

When the signal becomes steady, instead of an intermittent paint, it can be assumed that the interceptor has detected the bomber. Although not necessarily locked on, it has at least a range and azimuth reading. If a lock-on was obtained a rate of closure would also be observed. To begin jamming at this point denies the interceptor any further range readings but would not necessarily prevent it from launching its missiles successfully.

This particular subject is dealt with in greater detail in section 14.

4.3 At Measured Signal Strength - The strength of the signal received from the interceptor can be measured by the bomber during the "listening out" period. The strength of the signal represents the range of the interceptor from the bomber. Jamming can be switched on when the received signal strength rises to a level where the interceptor is nearing detection range.

4.4 It can be shown (see section 9) that the maximum range at which a jamming signal can be detected is in the order of several hundred miles, even at low jamming power densities. Considering this, it would appear that choice 4.3 is the most beneficial to the bomber. The possibility of drawing a number of interceptors from considerable distances is reduced by holding off the initiation of jamming until an attack is imminent and at the same time it denies the interceptor any form of radar ranging.

5. LAUNCHING CONSIDERATIONS

A brief resume of missile requirements is necessary before outlining the homing method. The requirements can be broken down into the following general headings.

5.1 Missile Time of Flight - A maximum and minimum time of flight exist for the missile. For this study a maximum time of 25 seconds was chosen. After 25 seconds the missile speed drops rapidly, the guidance system becomes sluggish, and the oil supply may be exhausted. The minimum flight time varies but it is generally in the order of 10 seconds, depending on the minimum lead angle tolerances necessary for launching the missile.

5.2 Maximum Height Differential at Launch - The Sparrow missiles were taken as being capable of homing on a target that is ten thousand feet higher or lower than the interceptor.

5.3 Lead Angle Tolerance - Launching a missile at the target on a missile collision course would be ideal. It would mean the missile need theoretically make no corrections of heading to strike the target. However, because of the missile's ability to change heading, it can be launched at lead angles only approximating the ideal and still hit the target.

It can be said, in general, that the lead angle error tolerance at the maximum launching range will be the largest and that the tolerance will diminish as the range is shortened. A point will be reached where the range is so short that the missile must be launched on a missile collision heading. Any further reductions in launching range will prevent a successful launch unless the interceptor's heading is perfect.

This is true for a 25 second time of missile flight but not true if the time of flight is extended. The effect on lead angle tolerance for the entire range of missile flight times is illustrated by the accompanying diagram.

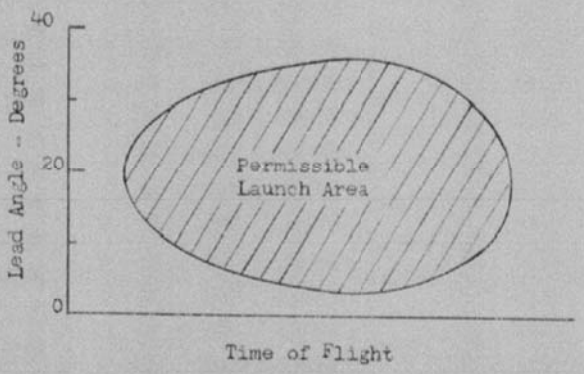

For this study it was arbitrarily decided that combat aircrew would be unable to consistently launch at ranges where the lead angle tolerance was less than 5 degrees from the ideal.

6. COLLISION COURSE COMPUTER

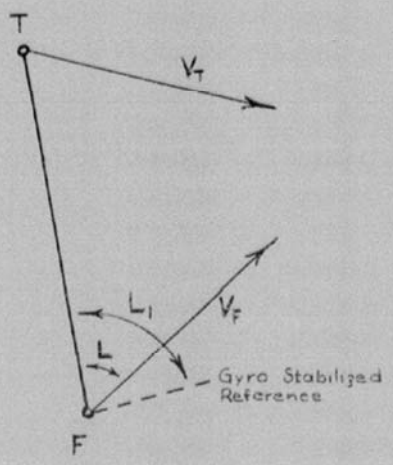

For a true aircraft collision course interception, the line of sight, measured from F to T, must not rotate in space. Angle L is the horizontal radar look angle relative to the nose of the fighter. If the rate of rotation of L is measured, random variations in interceptor heading will produce changes in L and this would be interpreted as a change in the actual line-of-sight. Since most aircraft have systematic motions in the yawing and pitching planes, the steering indication would be "noisy". One method of overcoming this is to measure the radar look angle from a gyro stabilized reference. Angle L_1 will not be influenced by changes in fighter heading.

The rate of change of L_1 would be the basis of the collision course computer. The magnitude and direction of the rate could be displayed in the form of a dot displaced from the reference circle of the pilot's AI radar scope. To place the interceptor on a collision course it would be necessary to turn toward the dot and pull it into the centre of the reference circle. This, in effect, reduces the angular rate of rotation of the line-of-sight to zero.

Both vertical and horizontal steering indications can be provided in this manner if angle L is resolved into its vertical and horizontal components and the resultant angles applied to their respective gyro stabilized references. It is not expected that this would be an involved process to instrument in the ASTRA I.

7. BASIC HOMING METHOD

A simple case will serve to illustrate the basic homing method. The action sequence is broken down into separate steps for the sake of clarity.

7.1 GCI Detection and Identification - The GCI sites will detect a jamming signal from one or more enemy aircraft forming a raid. By triangulation of bearings from two or more ground sites, the raid's approximate heading and speed are determined.

7.2 Scramble - The defending interceptors are scrambled. The scramble instructions should include

a) Heading to steer
b) Speed
c) Altitude or, if unknown, a most suitable altitude
d) The raider's speed and direction
e) Estimated size of the raid.

7.3 Pre-attack Planning - During the interval between the issue of the scramble instructions and the actual commencement of the attack the radar observer should note from a small table the lead angle necessary to launch the missile. All that he needs to know about the target is the approximate speed he was given with the scramble instructions. This angle will be referred to hence forth as the Predetermined Launching Lead Angle or PLLA.

7.4 Target Detection - The target will become aware of the interceptor's presence in the area when it receives the AI radar signal. Jamming may commence at any of the times outlined in section 4. As soon as it does, the radar observer in the interceptor must isolate a suitable jamming signal and lock-onto it. The pilot will adjust the interceptor's speed to Mach 1.5 immediately, unless the target speed is estimated by GCI to be greater than Mach 1.2. For target speeds above Mach 1.2 the speed should be adjusted to the target speed plus Mach 0.3 if at all possible.

After lock-on is accomplished, the pilot must turn the interceptor, using a maximum rate turn, until his Jammer Homing Computer indicates that the aircraft is on a collision course heading with the target. This collision course heading could be shown as the centering of a dot on a visual display. Any corrections necessary to maintain the collision course could be made using less severe rates of turn, the rate depending on the extent of the correction required.

If an altitude correction is indicated it should be made as quickly as conditions allow. Range at this point is not known and the altitude separation of the two aircraft must not exceed 10,000 feet when the missile is launched.

7.5 Launching Sequence - The launching sequence depends on the lead angle required by the interceptor to produce a collision course. The sequence is varied to accommodate two situations.

(a) If the aircraft collision course produces a lead angle equal to, or less than, the PLLA the missile can be launched manually anywhere between the maximum and minimum permissable launch ranges. The missile itself must be locked-onto the target before minimum range is reached. After the missile is launched the interceptor should make a maximum rate turn, preferably toward the target, to break the collision course and insure the survival of the interceptor aircraft. Turning toward the target causes the interceptor to pass behind the debris.

(b) If the collision course heading yields a lead angle larger than the PLLA, a maximum rate corrective turn must be made toward the target to reduce the lead angle to the PLLA just before launching. When the PLLA is achieved the bank is removed and the missile launched providing it is locked-on. If the missile is not locked-on, then sufficient bank must be applied in the opposite direction to maintain the PLLA until the range is reduced sufficiently to produce missile lock-on. Again after missile launching the interceptor should break in the target's direction to avoid collision with the debris.

B. RESULTS OF THEORETICAL STUDY

8. EFFECTS OF JAMMING POWER DENSITY

The effects of jamming power density were considered under five separate headings.

8.1 Maximum Detection Range - The range of a jamming signal source from the interceptor in free space can be conveniently expressed as:

$$R = \left[\frac{D_J B_R G_J G_T \lambda^2}{(4\pi)^2 \; P_J \; L_J} \right]^{\frac{1}{2}} \qquad \ldots\ldots(1)$$

where

D_J = Jamming power density in watts per megacycle of bandwidth.

B_R = receiver bandwidth, in megacycles.

G_J = antenna gain of the jammer antenna over an isotropic radiator, in the direction of the interceptor.

G_T = antenna gain of the interceptor's antenna as per G_J but in the direction of maximum gain.

λ = wavelength of the transmitted radiation, in same units as R.

P_J = received jammer power in watts.

L_J = system losses of the interceptor's radar for the jamming signal only.

The constants for the RCA radar to be placed in the CF-105 are expected to be approximately as follows:

B_R = 5.0 mcs

G_T = 35 dB or 3160

L_J = 5.0 dB or 3.16

λ = 3.20 cms

The minimum received power to detect a return on the scope is theoretically:

P_J = -98 dBM or 1.584×10^{-13} watts.

The jamming radiator is considered to be a low gain type. An antenna gain of 10 dB or 10 was chosen as a representative figure.

The system losses L_J can be broken down into:[2]

Collapsing loss	=	0.45 dB
Beam shaping loss	=	2.5
Waveguide loss	=	1.8
Radome loss	=	0.5
		5.0 dB

The maximum detection ranges expected from the RCA proposed radar system are plotted on figure 1.

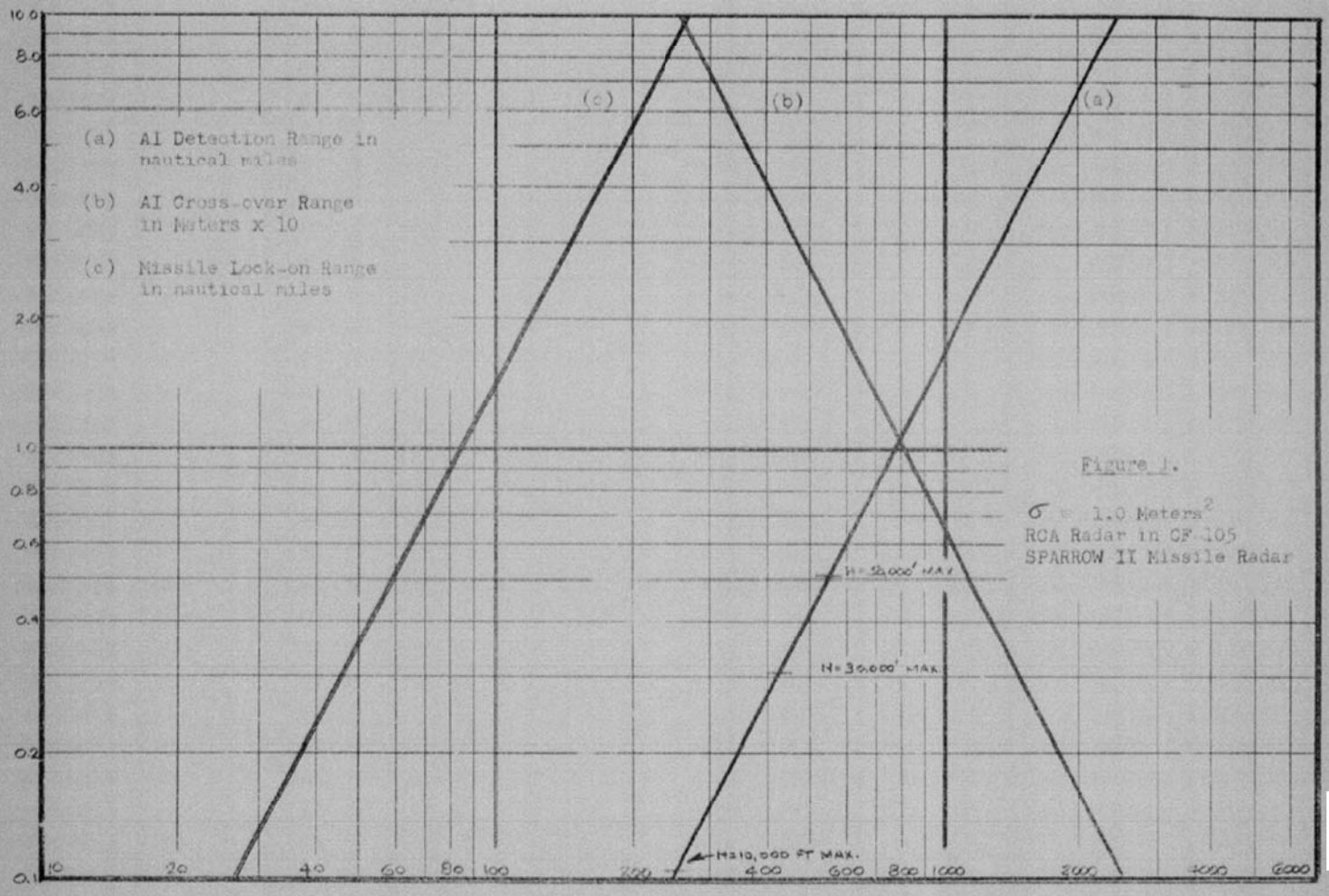

Figure 1.

σ = 1.0 Meters^2
RCA Radar in CF-105
SPARROW II Missile Radar

8.2 Maximum Missile Lock-on Range - Equation (1) can be used to find the lock-on range of the missile on a jamming signal. Constants for the Sparrow II were used for the plot of lock-on range versus jamming power density in Figure 1.

B_R = 10 Mcs

G_J = 10 dB or 10

G_T = 27.6 dB or 575

λ = 1.25×10^{-2} meters

$P_{J_{Min}}$ = -93.5 dBM or 4.47×10^{-13} watts

L_J = 7 dB or 5.02

8.3 Line-of-Sight Limitation - The extreme ranges of detection are noteworthy. Because of these long ranges the earth's curvature becomes a limiting factor since the jamming signal is nearly a line-of-sight transmission.

To account for the refraction of the transmitted wave the earth's radius can be taken as four thirds of its actual value. Thus the enlarged radius R equals 4586 nautical miles.

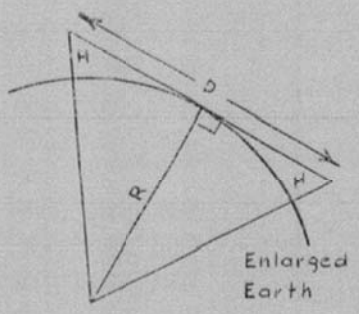

Fig. 2. - Line-of-Sight Range

From Figure 2 it is easily established that the line-of-sight distance

$$D = 2\sqrt{2RH + H^2} \qquad \text{.....(2)}$$

when target and interceptor are at the same altitude H.

Values of D were calculated for three altitudes and are shown on Figure 1. It should be noted that these values of D assume a perfectly smooth spherical earth. D will be reduced by any terrain rising above the surface considered which happens to block the line-of-sight.

8.4 Cross-over Point - Rearranging equation (1), the power received from the jamming transmission is:

$$P_J = \frac{D_J B_R G_J G_T \lambda^2}{(4\pi)^2 R^2 L_J} \quad \text{watts} \qquad \text{.....(3)}$$

If the interceptor's radar is locked-onto the jamming signal the power received as a reflected echo from the target is:

$$P_R = \frac{P_T G_T^2 \lambda \sigma}{(4\pi)^3 R^4 L_T} \quad \text{watts} \qquad \text{.....(4)}$$

where

P_T = peak transmitted power in watts

σ = target scattering cross-section, in the same units as R^2

R = range from target to interceptor, in suitable units

L_T = system losses of the interceptor's radar for echo only.

Depending on the various constants of each equation, a range may occur, at or below which, P_R may be larger than P_J and the target will be visible on the interceptor's radar scope. This is known as the cross-over range. Should this occur at great enough ranges the missile can be launched on accurate range information.

It is estimated that the ASTRA I will require that P_R exceed P_J by 3 dB to distinguish the echo from the jamming presentation while locked-on. Hence at the cross-over range

$$Rx = \left[\frac{0.502\ P_T G_T \sigma L_J}{4\pi\ L_R D_J B_R G_J \lambda}\right]^{\frac{1}{2}} \qquad \text{.....(5)}$$

Suitable values for the ASTRA I and the hypothetical jamming aircraft previously considered can be taken as:

P_T = 1.0×10^6 watts

G_T = 35 dB or 3160

L_R = 5.75 dB or 3.75

B_R = 5.0 mcs

G_J = 10 dB or 10

L_J = 5.0 dB or 3.16

σ = variable area depending on aircraft type and aspect angle

D_J = variable jamming power, watts/mc

The system losses L_R and L_J are assumed identical except for the collapsing loss where values of 0.95 dB were used for L_R and 0.45 dB for L_J.

Figure 1 shows a plot of cross-over range versus jamming power density using these values and σ = 1.0 square meter. The cross-over range is below 9000 yds for jamming power densities greater than one watt per megacycle. Since this density is possible, it is doubtful if a useful cross-over range will be achieved under realistic jamming conditions. An increased value of σ increases the range but at the present time the values of σ for potential enemy aircraft are not accurately known. A value of 1.0 square metre was arbitrarily chosen as a representative figure which may prove to be pessimistic when better estimates are available. From equation (5) it will be noted that Rx varies as $\sqrt{\sigma}$.

9. PREDETERMINED LAUNCHING LEAD ANGLE (PLLA)

9.1 Conditions - The study used an interceptor capable of Mach 1.5. As stated earlier, this speed need not be adhered to but, if it is not, then higher speeds should be used rather than lower ones because of the effects of target evasive manoeuvres.

9.2 Method - The lead angle required by the interceptor was plotted against the aspect of the fighter's approach to the target on a true aircraft collision course for a particular target speed. This involved resolving the normal velocity triangle of figure 3 for various aspect angles.

L.A. = Lead Angle
A = Aspect Angle
V_T = Target Velocity
V_I = Interceptor Velocity
ϕ = Course Difference.

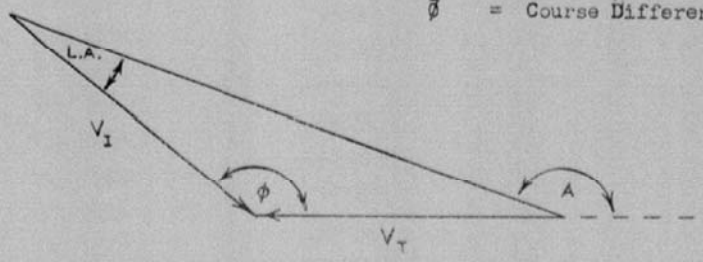

Figure 3. True Collision Velocity Traiangle

A maximum lead angle of 60° is permissible. Greater lead angles exceed the maximum look angle of the Sparrow II and lock-on will be impossible unless the lead angle is reduced to 60 degrees or less.

The exact lead angle and the allowable lead angles required by the missile were also plotted against aspect angle. Figure 4 is a plot for V_T and V_I equal to Mach 1.5. The average missile velocity for 25 seconds time of flight was Mach 2.6.

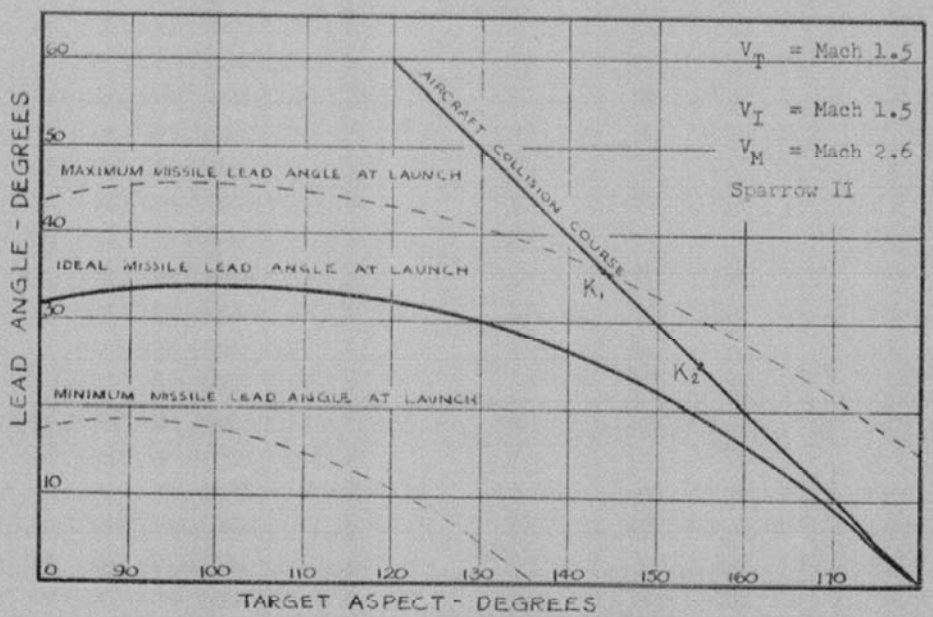

Fig. 4. Lead Angle vs Target Aspect.

It is evident that at large aspect angles the aircraft collision course lead angles satisfy the lead angle requirements of the missile if launched at its maximum range. In Figure 4 this first occurs at the aspect corresponding to point K_1 . If the launching range is reduced, the allowable error is reduced and point K_1 moves to point K_2 and a larger aspect angle. This means that for smaller error allowances the launch must be made nearer the nose aspect of the target to satisfy the missile.

It was stated previously that it was not reasonable to try and launch at ranges less than the 5 degree error range. Thus, when considering launching at minimum range, the actual aircraft lead angle must be within 5 degrees of the ideal lead angle for the particular aspect at which launching occurs. The interceptor is not aware of this ideal lead angle and the fire control system cannot compute it as range is unknown. Therefore, it is necessary to choose a standard lead angle (PLLA) for launching which will place the fighter within the launch errors permissible for any aspect.

A PLLA of 30 degrees was selected for the case where V_T and V_I are both Mach 1.5. If the aircraft collision lead angle is 30 degrees or less, no turn is required before launching. This situation applies for aspects between 150 and 180 degrees. At 150 degrees the lead angle error is 8° so launching must occur at or before reaching a range allowing for 8° error. At an aspect of 156 degrees the error is reduced to 5 degrees and the missile can be launched at the 5 degrees error range contour.

On aircraft collision courses for aspects of 120 to 150 degrees the interceptor must turn toward the target to reduce the lead angle to 30 degrees before launching. Launching can occur on the 5 degree range contour at the end of the turn at all times.

9.3 Recommended PLLA's - The method of section 9.2 was applied to four separate target speeds. The interceptor speed was Mach 1.5. Table I shows the recommended PLLA's.

TARGET MACH NO.	PLLA
0.85	15°
1.2	20°
1.5	30°
2.0	30°

Table I - Predetermined Launching Lead Angles.

9.4 Effect of Overturning or Underturning - This effect is only serious when launching must occur at or near the 5 degree error range contour. If launching occurs at ranges where 10 degree errors are acceptable then a 5 degree error in either estimating the PLLA or in actually turning to the PLLA is acceptable. Depending on the aspect at which launching occurs, the inaccuracy in the PLLA may either add to or subtract from the error inherent in the general method. Consequently, all around accuracy is very beneficial but the limits of accuracy are not so stringent that they will be difficult to fulfill.

10. TERMINAL MANOEUVRE BARRIERS

10.1 Bomber Coordinates - The bomber coordinate system as outlined in reference 2 was employed to produce a series of manoeuvre barrier diagrams as illustrated by Figure 5.

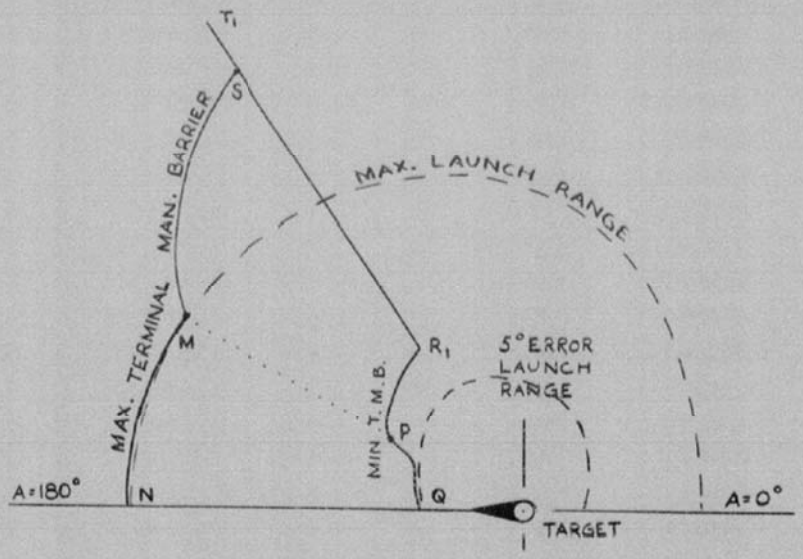

Fig. 5. Terminal Manoeuvre Barriers.

10.2 Launch Zone Contours - The prime source of the launch zone contours was reference 1, which considers an evading target only. Certain alterations to the evading target contours were made to produce representative contours for the non-evading targets. These alterations were as follows:

(a) Maximum Range, Non Evading - The maximum range was based on 25 seconds time of missile flight. A pure ballistic range contour was constructed, using an average missile velocity of Mach 2.6, and the result scaled down in range by 10 percent to allow for the homing action and the lead angle errors acceptable to the missile.

(b) Maximum Range, Evading - Reference 1 gives contours for 20 seconds time of missile flight. The 20 second ballistic flight contour was constructed and the percentage reduction in range calculated for the evading contour over a number of aspects. These percentage reductions were applied to the 25 second ballistic flight contour to obtain the 25 second evading contour.

(c) Minimum Range, Non Evading - The material upon which the contours of reference 1 were based would indicate that the effect of evasion is most pronounced at target aspects on the tail and least pronounced on the nose. The evading contours were reduced by three seconds time of missile flight on the tail. No reduction was applied to the nose. Intermediate aspects were scaled accordingly.

(d) Minimum Range, Evading - The contours of Reference 1 were used unaltered.

10.3 Terminal Manoeuvre Barriers - Figure 5 shows a representative set of terminal manoeuvre barriers. Line T_1R_1 represents the look angle barrier imposed by the Sparrow II missile which has a maximum look angle of 60 degrees on either side of the dead ahead position. If an interceptor falls behind line T_1R_1 (i.e. to the right of line T_1R_1) and takes up a collision course then the missile seeker will not see the target and cannot lock-on.

10.4 Crossing line MN on a collision course involves no turning of the interceptor to meet a PLLA as the look angle is already less than the predetermined value. If the missile is locked-on, it can be launched at line MN or anywhere in area MNPQ. Launching at ranges less than line PQ will not fulfill the error tolerances of the missile. Launching at ranges greater than line MN result in extending the missile time of flight excessively.

10.5 The initial collision courses which give lead angles greater than the PLLA cause the interceptor to cross line MS. At line MS the interceptor can turn toward the target at a particular rate of turn and the PLLA will be acquired at exactly the maximum launch range. Initiating the turn at line PR_1 will acquire the PLLA on the 5 degree error launch contour if commenced near R_1. If initiated near P, it will be at error range contours greater than 5 degrees but not exceeding the error contour that runs through

point P. Thus, a turn to the PLLA initiated anywhere in area MSRP will result in meeting the missiles launching requirements at the instant the PLLA is acquired.

11. FACTORS AFFECTING TERMINAL MANOEUVRE BARRIERS

11.1 Terminal manoeuvre barriers are shown for three cases in Figures 6, 7 and 8. Several factors affect the barriers.

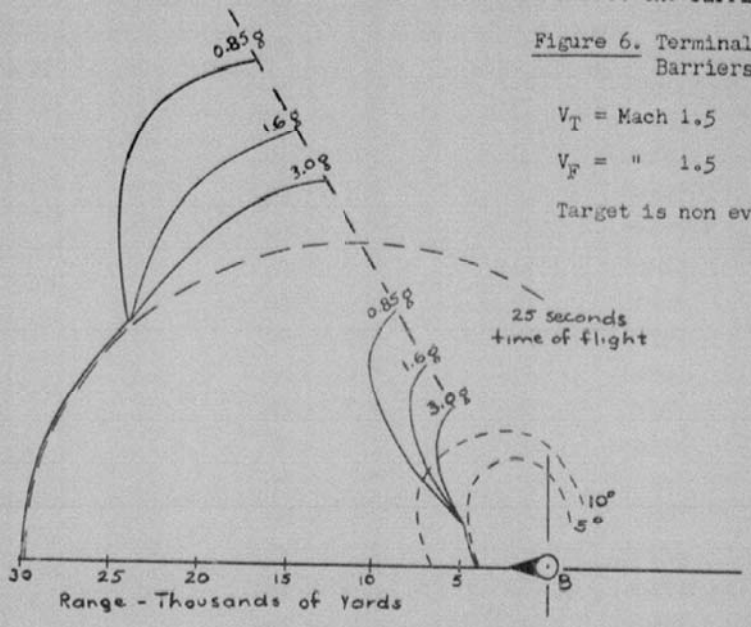

Figure 6. Terminal Manoeuvre Barriers.

V_T = Mach 1.5 H = 50 K ft.

V_F = " 1.5

Target is non evading

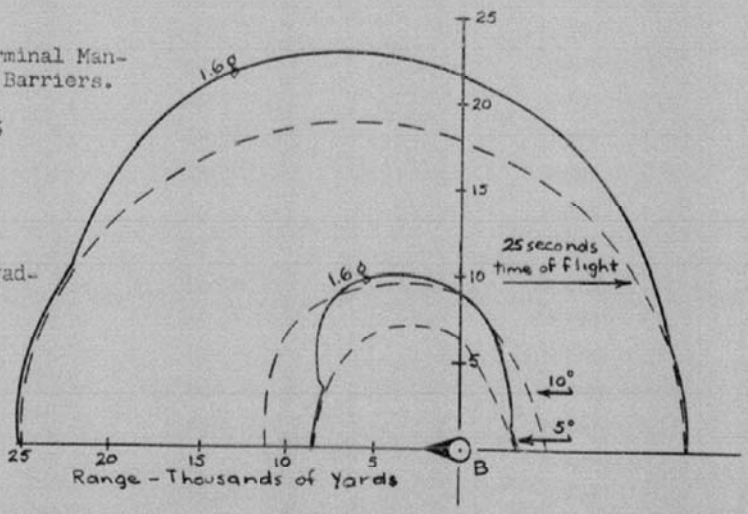

Figure 7. Terminal Manoeuvre Barriers.

V_T = Mach 0.85

V_F = " 1.5

H = 50 K ft.

Target is non evading.

Figure 8.
Terminal Manoeuvre Barriers

V_T = Mach 0.95 H = 50 K ft.
V_I = " 1.5

Target evasion = 2 g

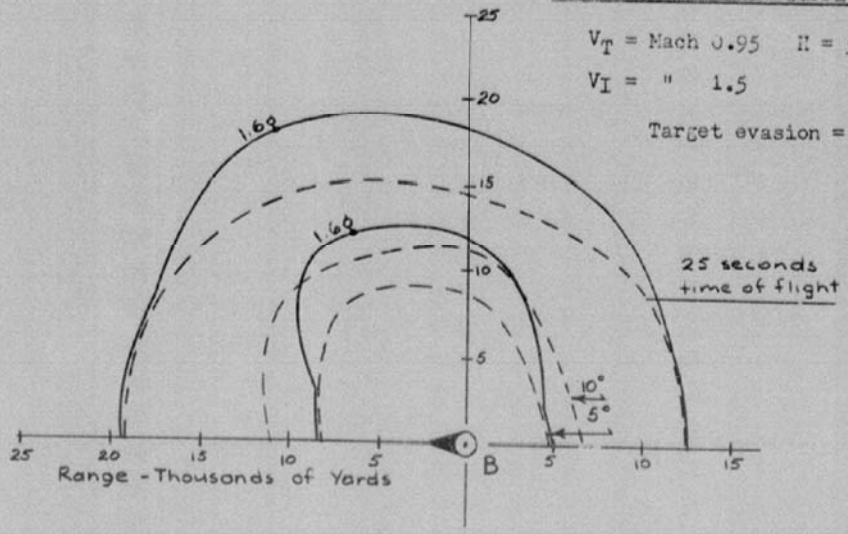

V_T = Mach 1.2 H = 50 K ft.
V_F = " 1.5

Target evasion = $\frac{3}{4}$ g

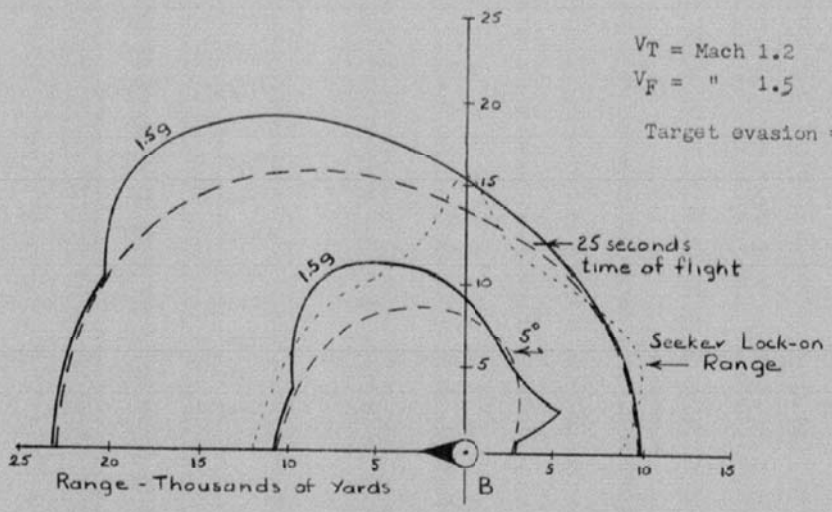

Figure 9.

Terminal Manoeuvre Barriers

11.2 Target Speed - The most prominent effect is the addition of the missile look angle barrier at higher speeds. A secondary effect is an increase in range for head-on attacks and shortening of range for tail attacks as the target speed is increased.

G Limitation of Interceptor - The ability of an interceptor to turn rapidly reduces the range used up in the turn before launching. Thus, higher G limitations

a) move the minimum terminal barriers nearer the target.

b) move the maximum terminal barriers nearer the maximum launch range contour.

Target Evasive Action - A comparison of Figures 7 and 8 indicates that if the target is evading

a) the minimum launch range contours and the minimum terminal barriers are increased in range

b) the maximum launch range contour and the maximum terminal barriers are decreased in range.

Effects (a) and (b) produce a large reduction in range separation between the maximum and minimum terminal barriers.

Altitude - The terminal barriers are enlarged at higher altitudes because the launch range contours are enlarged. This is attributable mainly to

a) a higher average missile velocity for any specific duration of flight

b) the reduced turning ability of the missile in the atmosphere.

Seeker Lock-on Range - One method of range finding employs the missile seeker lock-on characteristics. If the missile guidance system is not being jammed, then the seeker will lock-on when its maximum range limits are reached. The lock-on range contour may fall between the maximum and minimum terminal barriers. If it does, then the interceptor can immediately initiate the launching sequence. Hence, the missile lock-on range contour becomes the maximum manoeuvre barrier. Figure 9 shows a case where this applies.

Seeker lock-on is not a reliable terminal barrier. A more detailed discussion in included in section 14.3.

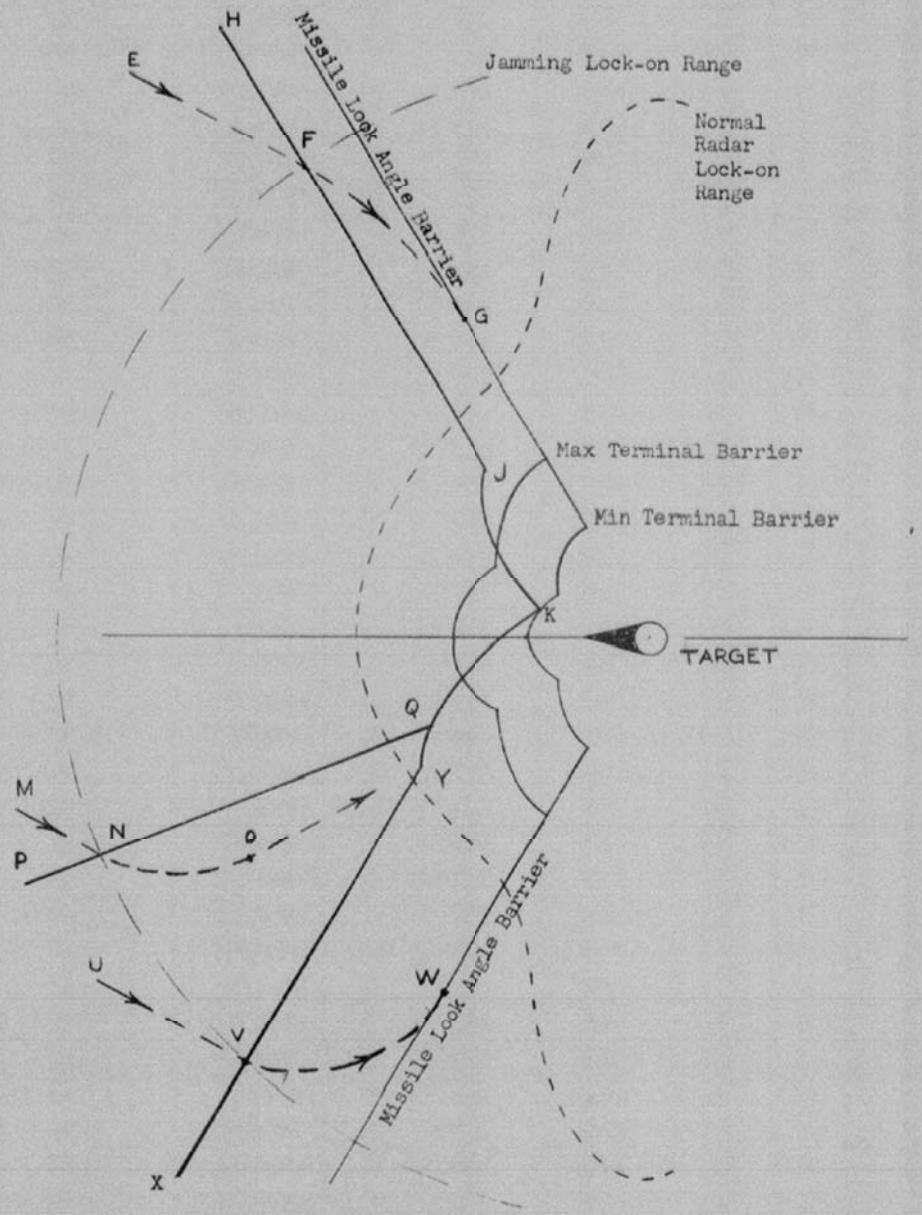

Figure 10. - GCI Positioning Contours.

12. GCI POSITIONING LANES

12.1 When the target is slower than the interceptor, the GCI controller can salvage an interception where the interceptor is badly positioned by ordering a stern chase. The amount of mispositioning acceptable depends on the amount of time available before the targets destruction must be assured. However, a stern chase is useless when the interceptor does not enjoy a speed advantage. Hence, for slower interceptors, GCI positioning lanes exist which must conform to a number of limitations.

12.2 Figure 10 shows the possible barriers imposed by the various limitations for a single heading difference between interceptor and target.

12.3 Consider the interceptor moving along the path EF. At F it locks-onto the jamming signal and commences turning to a collision course heading. At G it reaches the collision course heading with a lead angle of 60 degrees, the maximum allowable value. Point F is a point on the actual lane limit for the jamming lock-on range shown in Figure 10. Variation of the range moves point F in or out along line HJ which is parallel to the missile look angle barrier. The outward extremity H depends on the jamming lock-on range.

12.4 Line HJ generally crosses the normal non-jammed radar lock-on range contour. If jamming does not occur by this range then the target will be detected and locked-onto normally and the attack continued without regard to jamming techniques.

12.5 Interceptions are still possible although the interceptor has crossed the target's nose before detecting the jamming signal. The amount of mispositioning allowable in this situation is determined by two things for any fixed values of interceptor turn rate and target speed.

(a) The maximum lock angle (70 degrees) of the interceptor's radar must not be exceeded or the jamming signal will never be detected. The interceptor, advancing from M to N, must turn after locking-onto the jamming signal at N. If it advances beyond N without turning, the jamming signal will no longer be on the operators scope. Thus the AI radar look angle barrier PQ is the limit of the lane.

(b) If the course difference is large enough, limitation (a) will not apply and barrier PQ does not exist. An interceptor moving from U to V must initiate its turn at V so as to obtain a collision course heading at W on the missile look angle barrier. XY is the corresponding lane limit for various detection ranges.

12.6 One more possibility remains unexplored. Two circumstances, if both applicable at any one time, produce the limits on Figure 10 denoted as lines JK and YQK.

a) Radar detection range very low

b) Jamming delayed until the range is less than the average expected detection range.

Under these circumstances the interceptor, still unaware of the true range, will apply the homing "rule of thumb" as soon as it is locked-onto the jamming signal. Lines JK and YQK show the most extreme limits for the course difference considered. The interceptor, in turning to an aircraft collision course, just reaches this course at the moment it crosses the minimum terminal barrier.

13. GCI POSITIONING PROBABILITY - NON EVADING TARGET

13.1 Positioning lanes were worked out at representative course differences for two target speeds. Both were non-evading.

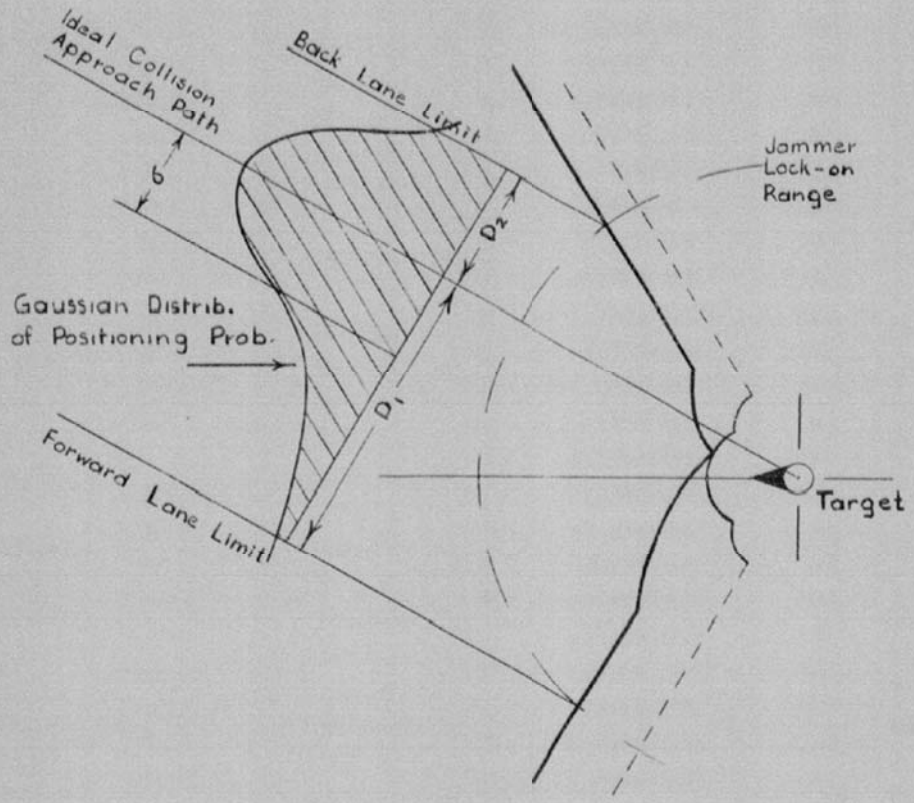

Fig. 11 - Application of Probability Distribution to GCI Approach Lanes.

13.2 Figure 11 shows a sample GCI positioning lane for one course difference. The GCI operator attempts to direct the interceptor in along the ideal approach path but can be in error by as much as distances D_1 and D_2 without completely jeopardizing the attack. A standard deviation σ of 10 nautical miles from the ideal was chosen in the absence of any more reliable experimental value.

13.3 A standard Gaussian distribution curve of probability was fitted, as shown, to the ideal approach path. The area under the curve contained in the approach lane, denoted by hatched lines, indicates the total probability of positioning.

13.4 Figs. 12 & 13 page 26 show a plot of GCI positioning probability against jamming signal lock-on range.

It should be noted that GCI positioning probability is not coincident with the probability of successful launching. The probability of successful launching is contingent on acquiring a range measurement just previous to launching. The GCI positioning probability concerns only the probability of the controller placing the interceptor in a position where it can commence homing on a jamming signal.

13.5 As expected, the probability of positioning was lowest on:

(a) High Speed Targets - The positioning contours are narrowed by kinematic considerations where the interceptor suffers from a speed disadvantage. Slowing the target down opens the contours and increases the probability of positioning.

If the interceptor has a speed advantage then a probability of 100% exists theoretically but in practice it is reduced by the time available to the interceptor.

(b) Reduction of Course Differences - At small course differences, the ideal approach path and the rear approach lane limit are very close together, reducing the permissable error the GCI controller can make in direction D_2.

(c) Short Jamming Lock-on Ranges - Shortening the jamming range narrows the lane width according to the configuration of the GCI positioning contour. If the range was eventually reduced to the minimum terminal manoeuvre barrier, the probability would reduce to zero. This assumes, of course, no normal radar detection of the target prior to this range.

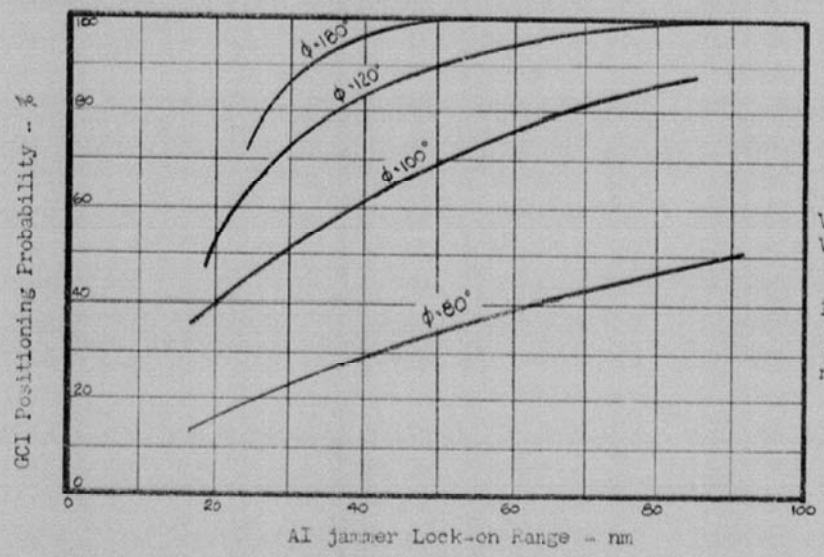

V_T = Mach 2.0
V_I = " 1.5
H = 50 K ft
1.6 g turn
σ = 10 n.m.
no evasion

Fig. 12. - GCI Positioning Probability

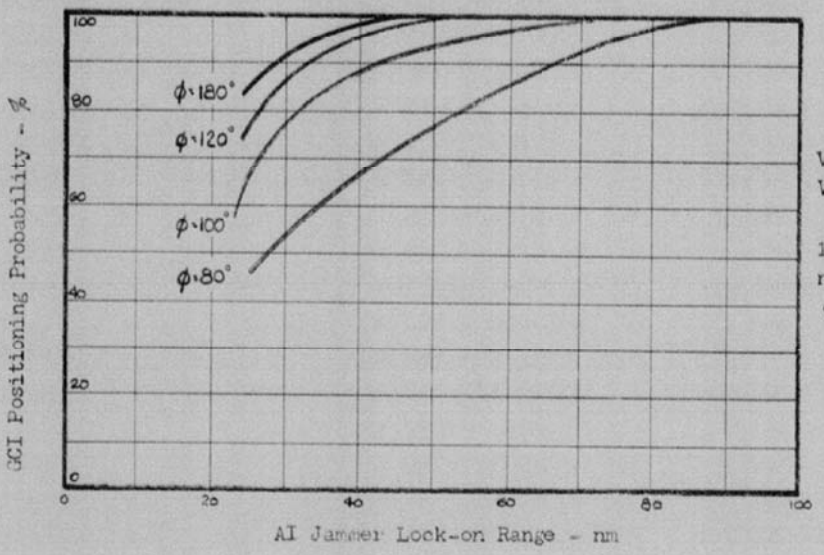

V_T = Mach 1.5
V_I = " 1.5
H = 50 K ft
1.6 g turn
no evasion
σ = 10 n.m.

Fig. 13. - GCI Positioning Probability

13.6 Evasion at Long Range - A target commencing evasion at a long range can place the interceptor in an untenable situation. Consider the case of the Mach 1.5 target and 1.5 interceptor in a head-on attack. The interceptor locks-onto the jamming signal at long range and applies the homing method. The target evades by altering heading slightly over 60 degrees. If the pilot of the interceptor responds perfectly and keeps the interceptor on a collision heading throughout the turn the interceptor will end up closing on a target aspect of less than 120 degrees. At this aspect the missile cannot lock-on because its look angle limitation of 60 degrees has been exceeded although the fighter can still close on the target unless the target alters heading by 90 degrees or more. Should the alteration be greater than 90° it would be kinematically impossible to close on the target even under GCI control.

A general rule governs the amount of evasive turn required to place the interceptor in a hopeless position.

$$\text{Turn required} = A_o - A_{min}$$

where A_o = Aspect of fighter at beginning of the turn

A_{min} = Aspect of missile look angle barrier.

This rule when applied to a Mach 2.0 target shows that the target need never turn more than 41 degrees to escape any single attacking interceptor with a speed of Mach 1.5. This is not a large deviation from the target's track if it is maintained for only a few minutes.

This disadvantage can only be overcome by increasing the speed of the interceptor. An interceptor with a speed advantage can catch it's slower target if the time available is sufficient. The time available depends on the allowable target penetration distance and the airborne time still remaining to the interceptor.

Where the speed advantage is not pronounced a large evasive turn may be sufficient. For head-on attacks however the target must turn through nearly 180 degrees to place the interceptor dead astern. A turn of this magnitude will not be advantageous to the target for obvious reasons. In evading, the enemy must consider the amount of turn required and weigh its advantages against the disadvantages suffered from loss of forward speed.

A head-on attack provides the best insurance against the effects of evasion in all cases. It makes the target turn the most and allows it less time to accomplish the turn.

A single aircraft can make evasive manoeuvres almost at random but a large formation does not have this option. This is especially true at night. Again, if interceptors are vectored on a raid from both sides of the targets mean line of approach, evasive turns away from one side will turn the raid toward the other interceptors. No prediction can be made as to the enemy's intentions but it would appear that evasion may not be as productive for large raids as a steady course designed to punch a narrow lane through the defense lines.

C RANGE FINDING

14. INTRODUCTION

The success of the homing method employed in this study is ultimately dependent on the ability of the interceptor to obtain some form of range measurement. With this in mind, a sub-study of range finding methods was performed. Special attention was paid to finding ranges in the vicinity of the terminal manoeuvre barriers.

All the methods explored are outlined here. Some are of no practical value but are included to familiarize the reader with the problems involved.

14.1 Radar Range - Radar range will be denied the interceptor if the enemy uses its jamming judiciously. However, the situation may occasionally arise where the enemy fails to jam until the interceptor has made a contact and obtained a range measurement. From this range measurement a "time-to-go" until the two aircraft would actually collide can be made using the GCI estimate of target speed and direction passed on with the scramble instructions.

In a pure head-on attack, a Mach 0.85 target and a Mach 1.5 interceptor will close from 30 nautical miles in 80 seconds. This is reduced to 54 seconds for a Mach 2.0 target. The missile can be launched successfully between approximately 15 and 30 seconds "time-to-go" in all cases.

A true tail chase on a Mach 0.85 bomber would take about 190 seconds to close from 20 miles. The missile could be launched successfully between approximately 25 and 60 seconds "time-to-go".

The radar operator could start a stop watch at the time jamming began and calculate the "time-to-go" from the last known range - i.e. where he started timing. He would have to use a small chart to find the rate of closure and then divide this rate into the total range to obtain "time-to-go". The launch sequence could be initiated at say 25 seconds so he would subtract 25 seconds from the "time-to-go" and when the stop watch reached this figure he would tell the pilot to initiate the launch sequence.

The radar operator could manually calculate the "time-to-go" but he would require several seconds of uninterrupted time to do so. It is felt that it could be accomplished satisfactorily on attacks from the tail quarter but not on beam or head-on attacks because of the short time available.

The alternative to the time consuming hand calculation is to instrument the aircraft to compute the speed of closure and apply it to the range to give a visual indication of "time-to-go".

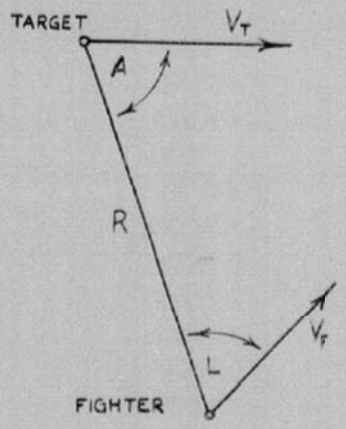

Figure 14.

Figure 14 shows the interceptor and target separated by distance R . The rate of closure of the aircraft

$$\dot{R} = V_F \cos L + V_T \cos A$$

where

V_F = interceptor velocity

V_T = target

L = interceptor radar look angle

A = aspect of fighter from target.

For this set of circumstances the interceptor can be considered as being on a collision heading. This is not strictly true but it would apply over the greater portion of the attack. For a collision course

$$V_T \sin A = V_F \sin L$$

$$A = \sin^{-1}\left(\frac{V_F}{V_T} \sin L\right)$$

Hence

$$\dot{R} = V_F \cos L + V_T \cos \left[\sin^{-1}\left(\frac{V_F}{V_T} \sin L\right)\right]$$

It is significant that if V_T is fed into the computor by manually setting a control on the radar operators consol the value of R can be continuously computed. All the remaining variables are measurable in the interceptor itself.

The interceptor is interested in knowing "time-to-go" as opposed to rate of closure. This could be computed simply using the following general circuit.

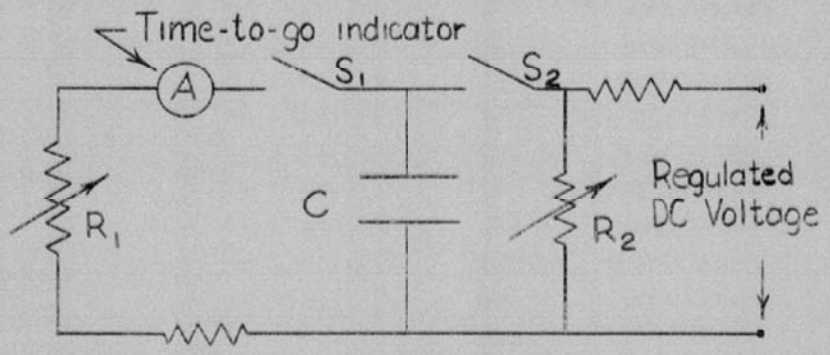

Fig. 15 - "Time-to-go" computer - simplified diagram

Previous to the attack the radar operator feeds the estimated value of V_T into the $\dot{R}$ computer. The value of $\dot{R}$ is then taken from this computer and used to control the value of the variable resistor R_1. Thus R_1 will be set correctly as long as V_T has been inserted in the computer.

Under normal non-jamming conditions switch S_1 would be open and S_2 closed. When jamming commenced the radar operator would set the value of the last known range on the range knob. This sets the value of R_2. Capacitor C would charge to the value of the voltage across R_2.

Immediately after setting R_2 the operator would push a button that would open S_2 and close S_1. The capacitor would begin to discharge through R_1 at a rate that would depend on the voltage across C and the value of R_1. The rate of discharge is a direct measure of "time-to-go". The ammeter would be calibrated in seconds and displayed to the interceptor aircrew as "time-to-go".

14.2 Radar Cross-Over - The target return will be visible to the radar operator at ranges below the cross-over range. Figure 1 shows cross-over ranges for a target with an echoing cross-section of one square meter.

No definite values are known for the cross-sections of potential enemy bombers. Attempts have been made to estimate the cross-sections of the B-47 and the B-52. Reference 2 gives the following values.

AIRCRAFT ASPECT	Nose 0°	30°	60°	Beam 90°
B-47 Max. sq. m.	5.0	3.2	14	500,000
B-47 Min. sq. m.	1.26	1.0	3.16	1,590
B-52 Avg. sq. m.	0.8	1.6	10	500,000

Table 2. - Radar Echoing Cross-Section.

The radar cross-over range must exceed the range of the minimum terminal barriers if it is to be useful. This falls between 10,000 and 15,000 yards for most cases. To produce such a cross-over range, the target echoing cross-section must be in the order of 10 square meters. This is only possible on the 60 to 90 degree beam aspects according to Table 2. Cross-over ranges at other aspects would be too short.

This method of range finding cannot be considered satisfactory. Nevertheless it must be remembered that some course difference cause the fighter to close to the target on 60 to 90 degree aspects. The radar operator should at all times be vigilant in case cross-over does occur at a useful range.

14.3 Missile Lock-on - The missile guidance system must be locked-onto the target before launching. It is capable of locking-onto jamming signals at ranges greatly exceeding the terminal manoeuvre barriers - see Fig.1. However, if the missile is not being jammed it may lock-onto the target echo at ranges that are useful to the interceptor pilot.

A missile lock-on range contour is shown in Figure 9. The contour is an estimation of the lock-on capability of a Sparrow II missile on an AVRO Vulcan bomber. While the Vulcan is not a supersonic aircraft it was felt to be a reasonable representation of an aerodynamic shape capable of doing Mach 1.2.

The pilot can initiate the launching sequence immediately after the missile locks-onto the non-jamming target. Launching will be successful everywhere except in a narrow slice near 150 degrees aspect.

Not all the lock-on contours are as convenient as the one shown in Figure 9. Figure 16 shows the case of a hypothetical bomber capable of Mach 2.0. It is assumed to have short stubby wings and a long cigar shaped body. The anticipated lock-on contour is much different in shape from that of the delta winged Vulcan. The lock-on range is very short on the nose. This restricts the launching aspects so severely that the fighter must close to the target on an aircraft collision course of not less than 160 degrees aspect.

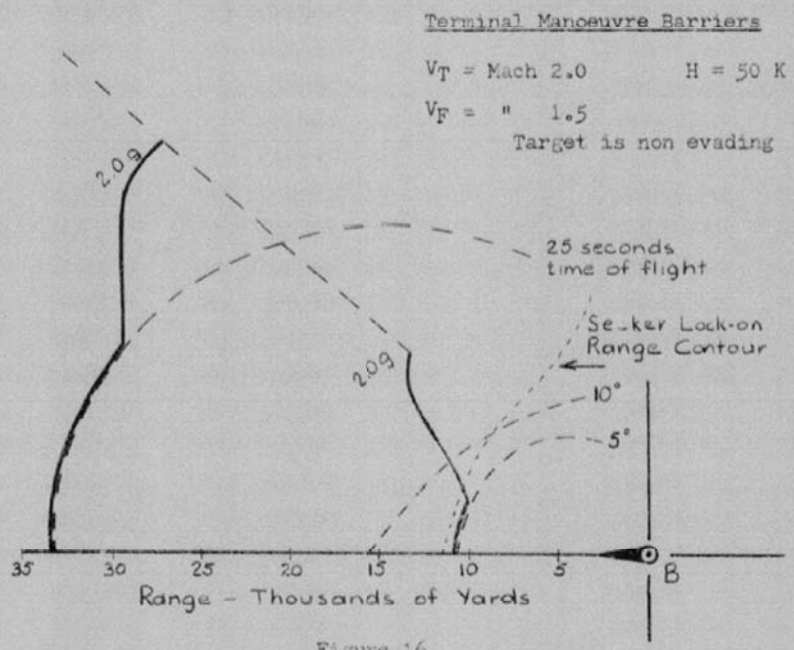

Figure 16.

The solution to the difficulty in Figure 16 would appear to be an increase in the lock-on range of the missile. For this particular set of circumstances it would be satisfactory. For Figure 9 it would not be. An increase in lock-on range would permit launching at aspects near 150 degrees but would cause the fighter to initiate the launching sequence too early at beam and tail aspects if the sequence is initiated solely on the basis of seeker lock-on indication.

It is clear that the interceptor pilot cannot rely on initiating the launching sequence immediately after a missile lock-on indication because

(a) The missile may be locked onto a jamming signal at excessively long range.

(b) Even if the pilot were aware that it was not on a jamming signal he still has no guarantee that lock-on occurred somewhere between the maximum and minimum terminal manoeuvre barriers.

Designing the missile to provide range information to the control radar would overcome the effects of (b). The control radar only requires range measurements in addition to what information it already has to compute for normal launching. If the AI radar is jammed the pilot could just switch in missile range measurements. The usefulness of the range obtained would depend on the missile lock-on range. Of course, if both are jammed another method of range finding must be utilized.

14.4 Visual - Visual estimation may be possible if the attack occurs during daylight or twilight hours. The pilot knows exactly where to look if he uses the information afforded by the radar set which is locked-onto the jamming signal. He should be able to pick up a large bomber of the B-52 type in excess of 10 miles during broad daylight.

To launch successfully the pilot should have some appreciation of the positions of the terminal manoeuvre barriers. Figures 6, 7, 8 and 9 show the ranges at which the launch sequence must be initiated. The minimum ranges vary between about three miles and seven miles. The limits between the maximum and minimum barriers are liberal so with some practice at range estimation it is felt that a pilot could successfully launch the missile against a clearly defined target.

Conditions of reduced visibility and hours of darkness obviously limit the use of this method. Visibility, even in broad daylight, is reduced at high altitudes because the dark colour of the sky reduces the contrast between the target and its background. Fortunately normal weather phenomena such as clouds and haze are seldom experienced at these altitudes. Below 35,000 feet weather would be a major problem.

Contrails can be seen for many miles, even in twilight conditions, but the aircraft itself is often difficult to actually spot. Without seeing the aircraft it is difficult to judge distance as there is no standard of comparison against which to judge the size of the contrail.

Visual ranging is not recommended if a more reliable method is available but it may prove useful if all else fails.

14.5 Triangulation - Single Aircraft Method

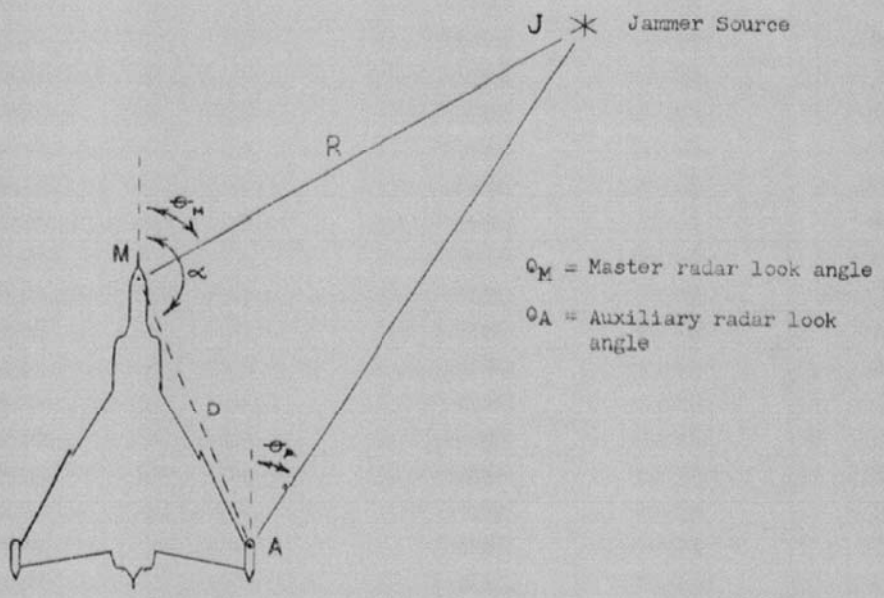

Fig. 17. - Range by Triangulation - Single Aircraft.

Figure 17 shows a CF-105 equipped with an auxiliary radar set on each wingtip. The auxiliaries are of much smaller power than the master set in the nose. A type similar to that used in the guidance system of the Velvet Glove missile was envisioned.

A range finding system was explored using any two of the three radars locked-onto a single source of jamming.

From the triangle MJA the range

$$R = D \left[\sin (\pi - \alpha + \theta_M) \cot (\theta_M - \theta_A) - \cos (\pi - \alpha + \theta_M) \right]$$

The second term cos ($\pi - \alpha + \theta_M$) will always be insignificant compared to the first. Hence

$$R = D \sin (\pi - \alpha + \theta_M) \cot (\theta_M - \theta_A)$$

The accuracy of R depends on the precision to which the term cot ($\theta_M - \theta_A$) can be measured. This measurement problem was referred to the CARDE Dynamics and Control group for investigation. An excerpt is taken from the formal report prepared by Mr. C.R. Iverson in which he assesses the feasibility of the technique.

"If one were to employ the triangulation system outlined in the a/m reference (triangulation technique), in order to attain a range accuracy of ± 250 yards, then the following convergence angle measurement accuracies must be attained:

For a range of 1,000 yds. - ± 0.1 degree.

For a range of 10,000 yds - ± 0.001 degree.

The ability to attain these high angular accuracy measurements by subtracting the angles as viewed by two radars is beyond the state of the art by one or more orders of magnitude.

The ASTRA I system as proposed has an angular measurement accuracy of from ± 0.12 to ± 0.5 degrees depending upon the target evasion characteristics.

A seeker of the Velvet Glove type would have to be mounted on a 2-axis servo mount. To expect a nulling servo with information provided by a V.G. seeker to have an angular accuracy of better than ½ degree would be very optimistic. The discriminator and cathod follower output drifts combined would result in uncertainties of up to ± ¼ degree. Also due to the non-circular polarization characteristics of the V.G. antenna, considerable second harmonic of the scan frequency exists at the null region which makes it difficult for the discriminator to accurately indicate a null position with a high degree of accuracy.

The distortion of the CF-105 airframe from nose to wing tips would undoubtedly rule out extremely high accuracy measurements, especially during manoeuvres. Vibration would also be a problem."

14.6 Triangulation - Two Aircraft

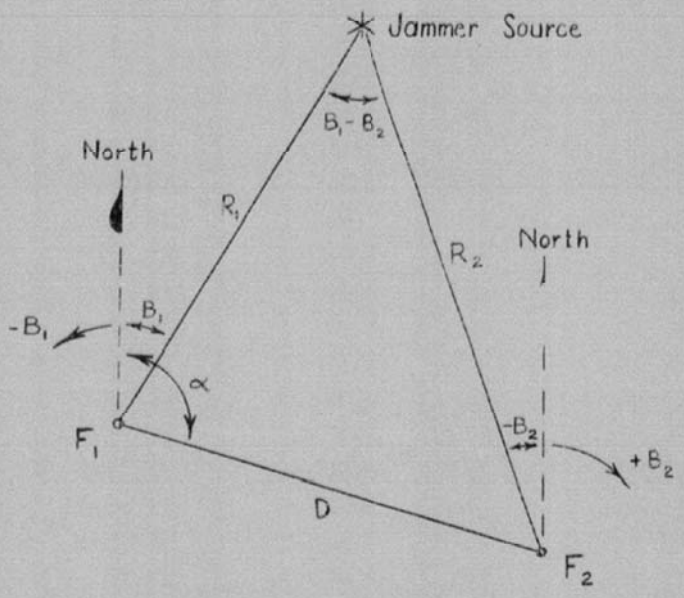

Fig. 18. - Range by Triangulation - Two Aircraft.

An attempt was made to enlarge the convergence angle by using two aircraft separated by several miles if necessary.

The two interceptors fly on approximately parallel courses, maintaining as constant a separation distance D as normal flying allows. Both interceptors then lock-onto a single jamming signal. If distance D is known and angles α, B_1 and B_2 can be measured then the ranges R_1 and R_2 can be computed.

Distance D could be measured accurately using a transponder system such as DME (Distance Measuring Equipment). The airborne DME currently in service would have to be modified to measure the distance separating the aircraft directly.

Angles B_1 and B_2 are actually the interceptors' line-of-sight to the jammer oriented to represent a line in space. They could be measured by applying the radar look angle to the aircraft gyro compass reading.

No solution for finding angle α was found. It would appear that this measurement may be difficult to obtain. Since the range finding method proved unsuitable for other reasons only a cursory inspection was made of the problem.

A data link between aircraft would have to be provided. The information could be fed to a computer to give instantaneous range values which in turn would be used as a substitute for the AI range denied by the jamming action.

If the necessary technical obstacles are overcome the range to the jammer can be measured to the degree of accuracy required for missile launching. A tactical problem enters the situation however. To obtain a large convergence angle the separation distance D and angle α must be suitably oriented. If turns are made by each aircraft they must be co-ordinated in such a fashion that the interceptors do not fall on a straight line with the target and hence reduce the convergence angle to zero. This may prove a major problem under combat conditions, especially at night.

The critical problem in using two aircraft is that of solving the ambiguity involved in identifying a particular target that is part of a large formation of targets. The probability of both interceptors being able to lock-onto the same target is very low if the targets are numerous and relatively closely formated.

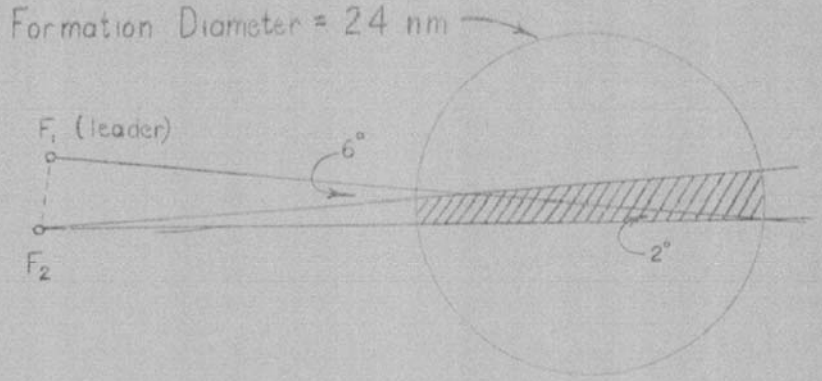

Fig. 19. - Ambiguity in Location of a Single Target.

A hypothetical case is considered where 200 jamming bombers enter the defence zone. They are spaced an average of three miles apart giving a bomber density of one bomber per nine square miles. If the formation is considered circular then the diameter is 24 nautical miles.

Figure 19 illustrates a situation where two interceptors have acquired the jamming formation at a range of 30 miles and are attempting to single out one particular target to attack.

A simple rule is being used to reduce the ambiguity. The interceptor designated as the "leader" locks-onto a jamming signal and the second interceptor tries to locate the same signal by placing the convergence angle between certain limits. For this analysis a maximum of 6 degrees and a minimum of 2 were chosen. Any signals producing convergence angles outside the limits would be disregarded.

The "leader" is locked-onto a target in the centre of the formation. The second aircraft, in attempting to apply the rule, sweeps the hatched area. This is an area of 68 square miles and contains at least 7 targets. By sheer good luck the same target may be selected by both interceptors but the probability is so low that it renders this method of range finding tactically useless during a multiple aircraft raid.

Selecting the extreme right or left hand azimuth indication does not solve the ambiguity. The interceptors are separated in space and this indication may well represent different targets to each.

Another degrading factor can enter during the attack. If the same target was selected by each interceptor at the beginning of the attack there is no guarantee that the radar will remain locked-onto the same target throughout the entire run. The occasion may arise where two or more jammers lie along the radar line of sight. Should the line of sight change, the radar will remain locked-onto one of the targets but it would be uncertain as to just which target the radar would choose to follow.

It should be noted that since two aircraft are required to destroy one target the overall efficiency of the defending force is substantially reduced. For a small defending force this would be a major consideration in evaluating the systems over-all effectiveness.

14.7 Triangulation -GCI - It was stated in section 3.1 that the GCI controller can only be expected to estimate the position of a jamming formation to ± 30 nautical miles by triangulating bearings from neighboring sites. This degree of accuracy is not adequate for missile launch as the interceptor must know the range, not to the formation, but to a particular target within the formation. It would be impossible for the GCI controller to isolate a particular target in a formation using triangulation of bearings alone.

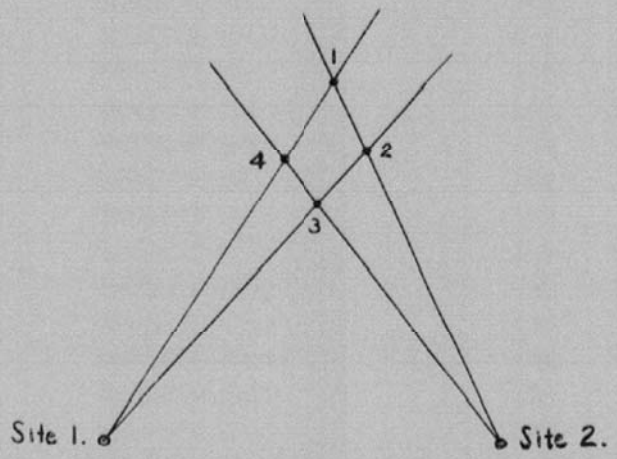

Fig. 20. - Ambiguity Introduced by Triangulation of bearings on Two Targets.

Figure 20 shows the ambiguity introduced by triangulation on only two jammers. The positions could be taken as the intersections 1,2,3 or 4. In general, n^2 intersections are formed by triangulation from 2 sites on n jammers.

Some hope is offered in the case of a single isolated jamming aircraft. It is considered highly unlikely that a jammer would operate as a single unit during wartime but certain results are included here to bring out some difficulties that will face the GCI operator in trying to triangulate on a single jammer.

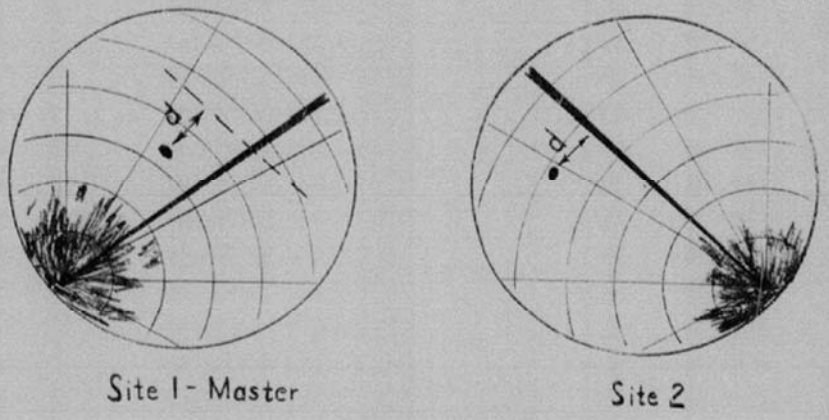

Fig. 21. - GCI Scope Presentation.

If one GCI controller could view the scope presentations from two radar sites simultaneously he could do the triangulation very quickly. The scope presentations are shown in Figure 21. Each scope shows one interceptor and a bearing indication on a single jammer. The origin of the presentation has been shifted to a corner and the range expanded by the controller for his convenience.

Transferring the bearing of the jammer from site 2 to the master scope directly can result in a considerable positioning error for the following reasons:

(a) A small error exists between the bearing measured by the antenna and that presented on the scope display. If this alignment error amounts to one degree it places any aircraft position in error by two miles at a distance of 120 miles from the sight.

(b) Sizeable plotting errors can develop. The ground position of the second site must be plotted on the master scope and the attendant bearings plotted from that position. If the ground position were plotted perfectly but the bearing plotted in error by one degree the target position would again be in error by two miles at a distance of 120 miles.

Errors (a) and (b) can be substantially reduced by using the interceptor's position as the reference point instead of the positions of the ground radar sites. The bearing on the second scope should be transferred to the master scope as a line properly oriented in direction but a distance d from the interceptor. d is measured normal to the bearing as shown in Figure 21.

This method practically eliminates both errors (a) and (b). Even a small misalignment of the second bearing during the transfer action amounts to small errors in the intersection providing the angle of cut is over 30 degrees. A controller should be able to transfer distance d to an accuracy of one mile.

Another significant plotting error is involved in both methods of triangulation. For perfect plotting both radars should sweep through the jamming signal at the same instant. If the two radars are not in synchronism and the bearing and distance d is transferred directly to the master scope, the two arms of the intersection will not represent the same instant of time. This has a considerable effect on the plotting accuracy.

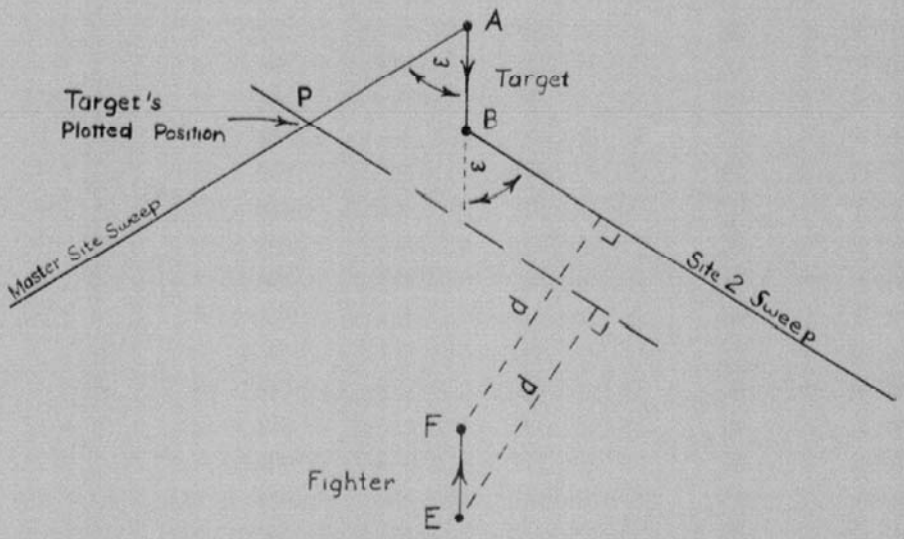

Fig. 22. - Plotting error from asynchronous radars.

GCI sites commonly use a sweep rate of 6 r.p.m. Thus each radar would paint the jammer every 10 seconds. Figure 22 illustrates a case where an interceptor is closing on a target from a head-on aspect. The target is positioned at A and the interceptor at B at the moment the master radar sweeps the target. Five seconds later the other radar sweeps the target which has now moved to position B. Meanwhile the interceptor has advanced to F. Distance d is measured on the second scope from F to the second strobe running through B. It is transferred to the master scope and applied to the last known position of the interceptor - position E. This results in plotting the bearing such that it intersects the master bearing at point P instead of A.

Point P is an incorrect position and will give the controller a false picture of the relative positioning of the aircraft. However, the only information the interceptor requires just prior to launching is the target range. The controller would normally measure from E to P and pass this distance to the interceptor.

The distance from F to B is the range that should be passed as it corresponds to the true range at the time of the second bearing. Distance E to P is the measured value and will differ from the true range by an amount depending on course difference, the aircraft speeds, and the angle of bearing cut.

The largest errors occur on head-on attacks at high speeds. Table 3 shows the errors involved when a Mach 2.0 target and a Mach 1.5 interceptor converge head-on. Each bearing intersects the target's track at the same angle ω (see Figure 22).

RANGE (N.M.)	$\omega = 60^\circ$		$\omega = 45^\circ$		$\omega = 15^\circ$	
True Range E to A	15.0	10.0	15.0	10.0	15.0	10.0
True Range F to B	11.8	6.7	11.8	6.7	11.8	6.7
Measured Range E to P	14.7	10.3	13.5	8.5	13.3	8.3
Range Error (F-P)-(F-B)	+2.9	+3.6	+1.7	+1.8	+1.5	+1.6

Table 3.

For this set of circumstances the measured range is too long. To make the situation even worse the error will be increased by the range closed during the interval occupied in plotting the second bearing and transmitting the information to the interceptor.

A beam attack reduces the error. Table 4 lists the errors for the same conditions as Table 3 but using a 90 degree course difference.

RANGE (N.M.)	$\omega = 60^\circ$		$\omega = 45^\circ$		$\omega = 15^\circ$	
True Range E to A	15.0	10.0	15.0	10.0	15.0	10.0
True Range F to B	12.7	7.7	12.7	7.7	12.7	7.7
Measured Range E to P	11.8	7.2	12.8	7.8	11.7	6.8
Range Error (F-P)-(F-B)	-0.9	-0.5	+0.1	+0.1	-1.0	-0.9

Table 4.

It is estimated from the results of a brief trial that a controller could plot the second bearing and pass the range to the interceptor within 7 seconds after the second strobe had passed the jammer. In this interval the aircraft previously considered would close an additional 4.5 miles during a head-on attack.

Thus if the measured range was 10.3 miles (Table 3) the true range at the time of transmission would actually be 2.1 miles. A launch at this range would be unsuccessful. However the picture is not as bleak as it might appear. The fighter can launch as far out as 16.5 miles (see Fig.14). If it launched on the measured range of 16.5 miles then the launch would be successful.

Another practical point arises in the form of slow radar sweep rates. At 6 rpm a complete target plot could only be obtained every 10 seconds. This corresponds to a head-on range closure of 6.5 miles between plots. At minimum ranges it would be difficult to give the ranges fast enough for the interceptor pilot to launch at the most auspicious moment.

The time element is a restricting one in this method of range finding. The controller would have to be very versatile to plot and pass on information simultaneously. It would be better to use two plotters and one controller. The plotters could do all the manual plotting leaving the controller free to communicate with the interceptor. He would have time to form some estimate of the course difference and could lead the target plot by a suitable number of miles and reduce the inherent errors in the method. After a number of plots he could estimate the range of closure between plots and when the interceptor approached the maximum terminal barrier he could start telling off the range as a continuous "count down", gauging his rate to coincide with the values of range obtained on each successive plot.

The method is considered feasible when used against a single jammer but of no use against multiple aircraft. The controller and plotters would require some practice to raise their proficiency to an acceptable level not only in the matter of speed but in the manipulation of the radar scope controls to obtain the narrowest jammer bearing indication.

Little has been said of the communication problems involved but it is essential that some form of communication exist. It is vitally important that it be continuously available during the period during which the ranges just previous to launching are being transmitted.

15. REFERENCES

1. CARDE Technical Letter N-47-2 "Launch Zones for a Hypothetical Constant - Bearing Missile" by J.T. Macfarlane.

2. CARDE Technical Memorandum 119/55 "A Study to Determine the Effectiveness of the CF-100 MK 4B Armed with Sparrow II Missiles Against a Type 37 Bomber" complied by S.Z. Mack; in particular Appendix E, Appendix J by W.J. Surtees and Appendix M by F.W. Slingerland.

APPENDIX G

Study of a Range Finding Proposal in Two Dimensions

D. Ferguson

Summary

In this report the possibility of obtaining approximate range information against a jamming target by turning onto or off a collision course heading is investigated. The motivation being to determine whether or not the suggested method, apart from the problem of modified instrumentation, is sufficiently accurate and operationally feasible to allow for the successful launching of air-to-air guided missiles.

It is shown how the errors, as caused by radar inaccuracies and an approximating assumption, in the approximate range estimate may be calculated in terms of:

(a) the speed of the interceptor and target,

(b) the lateral acceleration of the interceptor,

(c) the amount of turn the interceptor executes in order to get on a collision course or the amount he turns off a collision course,

(d) the course difference when on the collision course.

Suggestions and reasons for a following numerical study are given together with the practical conclusions that could be obtained from such an investigation.

1.0 Introduction

1.1 General

The basic problem, from which this study arose, is that of determining the range from an interceptor to a target when the target has successfully jammed the interceptor's A.I. (Airborne Interceptor) radar. Now in present and proposed A.I. radar sets the only information which is known once the interceptor has been successfully jammed is:

1.1-A. The azimuth and elevation angles of the target relative to the interceptor;

1.1-B. The time rate of change of the angles mentioned in 1.1-A;

1.1-C. The interceptor's heading and time rate of change of the interceptor's heading in space;

1.1-D. The true airspeed of the interceptor.

None the less, even in the much simplified case where the interceptor and target are at the same altitude, the problem of specifying the exact range, from the information in 1.1-A to 1.1-D, has not been solved by the author nor has the solution been found in current literature. However, in Reference 1 approximate methods for determining the range have been outlined.

At this point we might note that in the event of successful target jamming the finite aerodynamic range of "all" present air-to-air missiles makes it quite necessary that range information, from sources other than A.I. radar, be gathered to some specified degree of accuracy if it is felt desirable that the missile(s) be "launched" and not "thrown" from the interceptor. Consequently, it is the aim of this study to determine whether or not the methods, outlined in Reference 1, will suffice to give a value of range which is sufficiently accurate for the purposes of missile launch.

1.2 Errors

If an interceptor were instrumented to calculate an approximate value of range, denoted $\tilde{R}_e$, then the variance of $\tilde{R}_e$ from the true range, denoted R, will be termed the "range error". Now this range error may be attributed as being due to three independent sources of error, namely:

1.2-A errors in the input information 1.1-A, 1.1-B, 1.1-C and 1.1-D due to radar inaccuracies.

1.2-B errors in the processing of the input information.

1.2-C error due to the fact that even in the event of no errors of the type 1.2-A and 1.2-B, there would still be a variance between $\tilde{R}_e$ and R due to the approximations made in Reference 1.

Errors of the type 1.2-A and 1.2-B shall be collectively referred to as "input error" and of the type 1.2-C as "intrinsic error". In this study it shall be shown how both the input and intrinsic error may be determined and consequently the range error.

1.3 Attitude and Content of Sections

The attitude of this study from the point of development is analytic and little recourse has been made to drawing conclusions from purely intuitive reasoning. This analytic development will be found in full and,

it is hoped, explicit detail in the mathematical addenda to be found in Section 5.0.

A few introductory remarks explaining notations, conventions and symbols are to be found in Section 2.0, along with those assumptions which are made throughout the study. The interested reader is well advised to familiarize himself with Section 2.0, before continuing on to Section 3.0 where the mathematical results along with their physical explanation are to be found. Also in Section 3.0 will be found: the approximate range equation which would have to be instrumented in the interceptor in order to calculate the approximate value of range $\tilde{R}_c$, the equations

from which the range error could be calculated for a particular radar set having stated accuracies. Suggestions for an ensuing digital analysis, the reasons and value of such an analysis are then given in Section 4.0. The number of digital computations necessary in order to obtain sufficient information as to the accuracy of the method and an estimate of the amount of time required to complete these suggested computations on the Alwac Digital Computer is also included in Section 4.0.

2.0 Preliminary Remarks

2.1 Notations and Conventions

A somewhat unusual notation for designating angles is employed and shall now be explained. Consider any two vectors $\underline{f}_1$ and $\underline{f}_2$ in space and the symbol $(\underline{f}_1 : \underline{f}_2)$. Let $\Pi(\underline{f}_1, \underline{f}_2)$ be the plane defined by the vectors $\underline{f}_1$ and $\underline{f}_2$, i.e. both $\underline{f}_1$ and $\underline{f}_2$ lie in $\Pi(\underline{f}_1, \underline{f}_2)$. Then the angle formed by the counterclockwise rotation of the first-mentioned vector $\underline{f}_1$ into the "sense" of the second-mentioned vector $\underline{f}_2$, as performed in the plane $\Pi(\underline{f}_1, \underline{f}_2)$ shall be denoted $(\underline{f}_1 : \underline{f}_2)$. In the above we have differentiated between the works "sense" and "direction" in the description of vectors. Figure 1 is meant to illustrate this point.

The positions of the interceptor and target in space at an arbitrary instant of time t shall be the points $I(t)$ and $T(t)$ respectively. The point 0 shall be fixed in plane of interception, and therefore in space, and shall be chosen as the origin of space-fixed coordinates.

2.2 Explanation of Symbols Used

With reference to the remarks in 2.1 we shall, without further ado, define the following symbols where t is to be an arbitrary instant of time. Note that these definitions are quite mathematical and to obtain an intuitive grasp of their significance we refer the reader to Figure 2.

$\underline{z}(t) = \overrightarrow{O, I(t)}$, the time rate of change of this vector

$\dot{\underline{z}}(t)$ is clearly the vector velocity of the interceptor at time t and thus the speed of the interceptor at time t is $\dot{z}(t)$;

$\underline{y}(t) = \overrightarrow{O, T(t)}$, the time rate of change of this vector

$\underline{y}(t)$ is clearly the vector velocity of the target at time t, and thus the speed of the target at time t is $y(t)$;

$R(t) = |\overrightarrow{I(t), T(t)}|$, indeed this is the range from the interceptor to target at the instant t;

$\underline{i}_1(t) = \dfrac{\overrightarrow{I(t), T(t)}}{R(t)}$, this is a unit vector directed along the line of sight and having the sense from interceptor to target;

$\theta(t) = \left(\underline{\dot{y}}(t) : \underline{i}_1(t)\right)$, this angle is often called the "angle-off" in the sense that it is the angle which the interceptor subtends "off" the tail of the target;

$\alpha(t) = \left(\dot{\underline{z}}(t) : \underline{i}_1(t)\right)$, this angle is referred to as the "squint" or "look" angle and is really the azimuth angle of the target relative to the interceptor;

$\phi(t) = \left(\underline{\dot{y}}(t) : \dot{\underline{z}}(t)\right)$, this angle has generally been given the name "course difference";

$\lambda(t) = \dfrac{\dot{y}(t)}{\dot{z}(t)}$, this is the ratio of target speed to interceptor speed;

$\underline{m}_1$ = a unit vector fixed in the plane of the interception and therefore is fixed in space;

$\beta(t) = (\underline{m}_1 : \underline{i}_1(t))$, This angle gives the orientation of the line of sight in space and hence $\dot{\beta}(t)$ gives the rate of rotation of the line of sight in space;

g = the numerical value of the acceleration due to gravity in units of feet per second per second;

$n(t)$ = a positive number representing the maximum possible lateral acceleration of the interceptor expressed in units of g's at the speed $\dot{z}(t)$ and particular altitude of the plane of interception;

$\Delta\phi_i = \phi(t_c) - \phi(t_i)$, the numerical value of $\Delta\phi_i$ represents the amount by which the interceptor turns in order to get on a collision course or the amount he turns off the collision course;

$\Delta\theta_i = \theta(t_c) - \theta(t_i)$, the numerical value of $\Delta\theta_i$ represents the amount by which the line of sight rotates in space during the interval of time when the interceptor is manoeuvring onto or off the collision course.

In dealing with general scalar or vector symbols like $h(t_c)$ and $\underline{f}(t_c)$, we shall usually write:

$$h(t_c) = h_c \quad ; \qquad \underline{f}(t_c) = \underline{f}_c \quad ;$$

when it is felt that no confusion will result in the simplified notation.

2.3 Assumptions

The interception shall be assumed to take place in a horizontal plane relative to the earth's surface and further assumptions are:

$\dot{\underline{y}}(t) = \dot{\underline{y}}$ = constant vector, $\therefore$ $\dot{y}$ = constant;

$\dot{z}(t) = \dot{z}$ = constant;

$\therefore$ $\lambda(t) = \lambda$ = constant;

$\therefore \quad n(t) = n = \text{constant.}$

Further when interceptor lateral acclerations are to be applied it will be assumed that there is no time lag.

2.4 Figures

It is to be noted that the figures accompanying this study have NOT been drawn to scale, and in fact in all cases have been grossly exaggerated. They have been included to appeal to the reader's intuition only and do not embody any of the results of this study.

3.0 RESULTS

3.1 The Approximate Range Equations

Consider the following possible requence of events. Suppose that at time t_1 the interceptor's AI radar picks up the target but is found to be jammed. Now generally he will NOT be on a course such that $\dot{\beta}(t) = 0$ at the instant t_1 and assume that this is the case in fact. Then the interceptor can subsequently manoeuvre until he does achieve a collision course by noting when the rate of rotation of the line of sight $\dot{\beta}(t)$ does reduce to zero, if some means of presenting $\dot{\beta}(t)$ to the interceptor crew is provided.

Suppose that at the instant t_c the interceptor has finally manoeuvred such that:

$$\dot{\beta}(t_c) = 0.$$

If subsequently, i.e. for $t > t_c$, he turns so that $\dot{\beta}(t)$ again becomes non-zero then we again consider the kinematic situation at a time t_2, $(t_2 - t_c)$ seconds after the instant t_c. Thus we have now established a physical interpretation of the time sequence t_1, t_c, t_2. The actual ranges at these points of time are given by:

$$R_i = \frac{\dot{z} \sin \alpha(t_i) - \dot{y} \sin \theta(t_i)}{\dot{\beta}(t_i)} \quad , \quad i = 1, 2 \; ; \qquad 3.1\text{-}1.$$

$$R_c = R_1 + \int_{t_1}^{t_c} \dot{R}(t)\, dt \; ; \qquad 3.1\text{-}2.$$

However, neither of the Equations 3.1-1 and 3.1-2 can be evaluated since the quantities $\dot{y}$, $\theta(t_i)$ and $\dot{R}(t)$ for $t_1 \leq t \leq t_c$ cannot be specified. However, approximations to R_1 to R_2, denoted $\tilde{R}_1$ and $\tilde{R}_2$ respectively, can be given(as outlined in Section 5.3) by the formulae:

$$\tilde{R}_i = \frac{\dot{x}}{\dot{\beta}(t_i)} \left\{ \sin \alpha(t_i) - \sin \alpha(t_c) \right\}, \quad i = 1, 2 \; ; \qquad 3.1.3.$$

Thus we can see that instrumentation of an equation of the form of Equations 3.1-3 would lead to an approximate value of range, denoted $\tilde{R}_e(t_i)$, since all quantities entering in 3.1-3 are measurable in the interceptor. It is important to note the difference in meaning between the symbols $\tilde{R}_e(t_i)$ and $\tilde{R}(t_i) \equiv \tilde{R}_i$. Indeed, $\tilde{R}_e(t_i)$ is the approximate value of range which would be computed by an actual radar-computer system having inaccuracies in radar information as well as in actual computation, whereas $\tilde{R}_i$ is the approximate value of range which would be computed by an ideal radar-computer system having no inaccuracies either in radar information or in computation.

However, the pertinent question which must be asked is: "How approximate will this value $\tilde{R}_e(t_i)$ be ?" We shall answer this question in the sections to follow, but before continuing on let us note:

The range estimate $\tilde{R}_e(t_1)$ is not available at the instant t_1 but rather is computed at the later time t_c, whereas $\tilde{R}_e(t_2)$ is available at the instant t_2. The proper derivation of the above equations will be found in Section 5.3.

3.2 <u>The Intrinsic Error</u>

From Equations 3.1-1 and 3.1-3, we get on subtracting that:

$$\Delta R_i = R_i - \tilde{R}_i = \frac{\dot{x} \sin \alpha(t_c) - \dot{y} \sin \theta(t_i)}{\dot{\beta}(t_i)} .$$

Now the term $(R_i - \tilde{R}_i)$ in the above equation is the difference between the true range and the approximate range estimate which would be computed by an ideal radar-computer system having no inaccuracies. In other words, the term $(R_i - \tilde{R}_i)$ represents the intrinsic error and shall be henceforth denoted ΔR_i . It is found that ΔR_i can be found analytically from the following sequence of equations:

$$\lambda = \frac{\dot{y}}{\dot{z}} \quad , \qquad 3.2.1$$

$$\nu = + \sqrt{1 + \lambda^2 - 2\lambda \cos \phi_c} \quad , \qquad 3.2.2$$

$$\sigma_i = \frac{\Delta \phi_i}{|\Delta \phi_i|} \quad , \qquad 3.2.3$$

$$d_i = \frac{(-1)^i \sigma_i \dot{z}^2}{ng\nu} \left\{ (1 - \cos \Delta\phi_i)(1 - \lambda \cos \phi_c) + \lambda \sin \phi_c \sin \Delta \phi_i \right\} \quad , \qquad 3.2.4$$

$$\sin \Delta\theta_i = - \frac{d_i}{R_i} + \frac{(-1)^i \sigma_i \dot{z}^2}{ng\nu R_i} \lambda \Delta\phi_i \sin \phi_c \quad , \qquad 3.2.5$$

$$\cos \Delta\theta_i = + \sqrt{1 - \sin^2 \Delta\theta_i} \quad , \qquad 3.2.6$$

$$A_i = \lambda \sin \phi_c (1 - \cos \Delta\phi_i) - (1 - \lambda \cos \phi_c) \sin \Delta \phi_i \quad , \qquad 3.2.7$$

$$B_i = \lambda(\lambda - \cos \phi_c) - \lambda \sin \phi_c \sin \Delta \phi_i + (1 - \lambda \cos \phi_c) \cos \Delta \phi_i \quad , \qquad 3.2.8$$

$$\frac{\Delta R_i}{R_i} = \frac{\lambda(\lambda - \cos\phi_c)\sin\Delta\theta_i - \lambda\sin\phi_c(1 - \cos\Delta\theta_i)}{A_i\cos\Delta\theta_i + B_i\sin\Delta\theta_i}, \qquad 3.2.9$$

where in each of the above equations the subscript i can take on either the value + 1 or + 2.

If one examines the above sequence of equations, it will be found that they express ΔR_i in terms of the variables: R_i, n, $\dot{z}$, $\dot{y}$, ϕ_c and $\Delta\phi_i$, i.e. in terms of the variables: true range, maximum possible lateral acceleration of the interceptor in units of g's at the particular interceptor speed $\dot{z}$ and altitude considered, speed of the interceptor, speed of the target, course difference when the rate of change of the line of sight in space is zero and the angular amount the interceptor turns during the time sequence t_1, t_0 or the time sequence t_c, t_2. Now the manner in which the equations have been set up, allows us to vary at random the variables R_i, n, $\dot{z}$, $\dot{y}$, ϕ_c and $\Delta\phi_i$ except for the dependency of n upon $\dot{z}$ for a particular interceptor. Consequently, the intrinsic error that would result in actual instances can be calculated from the above and for both methods of determining an approximate range as outlined in Reference 1 and repeated in this study in Section 5.3.

3.3 Clarification of Equations

In an attempt to give a physical meaning to the stream of equations from 3.2-1 to 3.2-9, let us consider the following examples in conjunction with Figures 3 and 4.

$\dot{y}$ = Mach 1.50 at 50,000 feet,

$\dot{z}$ = Mach 1.20 at 50,000 feet,

n = 1.75 g's.

Thus the variables λ and n have been specified and ΔR_i as seen from Equations 3.2-1 to 3.2-9 becomes a function of R_i, ϕ_c and $\Delta\phi_i$.

Suppose that as values of the variables R_i, ϕ_c and $\Delta\phi_i$ we were to choose:

$$R_1 = 60 \text{ n.m.}; \qquad \phi_c = 90^\circ; \qquad \Delta\phi_1 = -60^\circ$$

Then what is the interpretation of the value of ΔR_1 as computed by

Equations 3.2-1 to 3.2-9 ? It is this:

At the instant t_1 the interceptor is situated (unknowlingly) 60 n.m. from the target and is headed (unknowingly) such that his course difference is $\phi_1 = \phi_c - \Delta\phi_1 = 150^\circ$. At this instant he also realizes his A.I. radar is jammed and that the rate of rotation of the line of sight in space is not zero. Consequently, he immediately applies a maximum rate starboard turn (since unknowingly $\Delta\phi_1 < 0$) and $(t_c - t_1)$ seconds later finds that he has reduced $\dot{\beta}(t)$ to zero and also finds that his heading in space has changed by $+60^\circ$, i.e. he finds that he has changed (unknowingly) his course difference from $\phi_1 = 150^\circ$ to $\phi_c = 90^\circ$. At the instant t_c his course difference is (unknowingly) $\phi_c = 90^\circ$ and an approximate value $\tilde{R}_1$ of his range at the earlier time t_1 will then be computed at the time t_c and the amount by which it would be in error with the true range R_1 at time t_1 (if the radar-computer system was ideal) will be given on computing ΔR_1 from Equations 3.2-1 to 3.2-9.

Suppose now that as values of the variables R_i , ϕ_c and $\Delta\phi_i$ we were to choose:

$$R_2 = 60 \text{ n.m.}, \qquad \phi_c = 90^\circ, \qquad \Delta\phi_2 = -60^\circ ,$$

then again we ask as to what is the interpretation of the value of ΔR_2 as computed by Equations 3.2-1 to 3.2-9? The interpretation of ΔR_2 is radically different from that given in the above paragraph for ΔR_1 , and in fact is:

At the instant t_c the interceptor finds that the rate of change of the line of sight in space is zero, i.e. $\dot{\beta}(t_c) = 0$. His course difference at this instant is (unknowingly) $\phi_c = 90^\circ$, and he decides that in order to get an estimate of range from the jamming target he will execute a maximum rate port turn (i.e. $\Delta\phi_2 < 0$). Then $(t_2 - t_c)$ seconds later after having completed a turn of 60° port, i.e. after having changed (unknowingly) his course difference from $\phi_c = 90^\circ$ to $\phi_2 = 150^\circ$, he will be situated (unknowingly) 60 n.m. from the target and an ideal radar set would compute an approximate value $\tilde{R}_2$ of his range at the time t_2 and this value would also be computed at the instant t_2. The amount by which this approximate range $\tilde{R}_2$ at time t_2 (if the radar-computer system was ideal) would be in error with the true range R_2 at time t_2 will then be given on computing ΔR_2 from Equations 3.2-1 to 3.2-9.

In summary we might point out that the determination of the intrinsic error is important from the point of view that it will be the same regardless of what radar set should be chosen to instrument the interceptor. A proper derivation of the Equations 3.2-1 to 3.2-9 will be found in Section 5.4; however, before continuing on it is of some small interest to note the correspondence between

resultant port or starboard turns and the sign of the variable $\Delta\phi_i$. Let the symbol $\sim$ be read as if it were the words "corresponds to". Then the above mentioned correspondence can be explained by:

$\Delta\phi_1 > 0 \quad \sim$ a port turn by the interceptor .

$\Delta\phi_1 < 0 \quad \sim$ a starboard turn by the interceptor .

$\Delta\phi_2 > 0 \quad \sim$ a starboard turn by the interceptor .

$\Delta\phi_2 < 0 \quad \sim$ a port turn by the interceptor.

Figure 5 is included to further clarify the above remarks.

3.4 The Input Error

Repeating what has been said in 3.1 the approximate range equations are:

$$\tilde{R}_i = \frac{\dot{z}}{\dot{\beta}(t_i)}\left\{\sin\alpha_i - \sin\alpha_c\right\}, \quad i = 1,2 ; \qquad 3.4\text{-}1.$$

In accordance with the usual first order approximations the differentials of the variables in 3.4-1 can be considered as representing a small change in those variables. Consequently, if $d\dot{\beta}(t_i)$, $d\dot{z}$, $d\alpha_i$ and $d\alpha_c$ represent small changes in the variables $\dot{\beta}(t_i)$, $\dot{z}$, α_i and α_c then the resulting change in $\tilde{R}_i$, namely $d\tilde{R}_i$ will be given by:

$$d\tilde{R}_i = \frac{(\sin\alpha_i - \sin\alpha_c)}{\dot{\beta}(t_i)}\left\{d\dot{z} - \frac{\dot{z}}{\dot{\beta}(t_i)}d\dot{\beta}(t_i)\right\}$$

$$+ \frac{\dot{z}}{\dot{\beta}(t_i)}\left\{\cos\alpha_i\, d\alpha_i - \cos\alpha_c\, d\alpha_c\right\}, \quad i = 1,2 ; \qquad 3.4\text{-}2$$

If the errors of computation involved in computing Equations 3.4-1 are ignored for the moment then Equations 3.4-2 can be looked upon as giving the input error in $\tilde{R}_i$ due to the radar inaccuracies $d\dot{\beta}$, $d\dot{z}$, $d\alpha_i$ and $d\alpha_c$.

Now there is a subtle difference between the terms $d\alpha_i$ and $d\alpha_c$ although at first this may not be apparent. The error in α_i i.e. $d\alpha_i$ is clearly a matter of how accurately the angle α can be measured due to the effects of radar noise and so on. However, this

is not the case with $d\alpha_c$, for in addition to the inaccuracies in measuring α we cannot specify exactly the instant t_c, at which we wish to take a measurement of α . Consider Figure 6 where a hypothetical time history of $\dot{\beta}(t)$ has been plotted. Now in actuality when the voltage pulse representing $\dot{\beta}(t)$ falls below a certain minimum value, B volts, then the value of $\dot{\beta}(t)$ would be taken to be zero, when in actuality this would not be the case. However, the value of $\tilde{R}_i$ definitely is dependent upon $\dot{\beta}(t)$ actually reducing to zero and since the radar set would indicate that this condition was achieved at the instant t^* (or at very best with some further modifications t^{**}) instead of the instant t_c (see Figure 6), further unknown inaccuracies in the approximate range $\tilde{R}_i$ would enter. However, this may be overcome in practice by having the interceptor maintain $\dot{\beta}(t)$, as displayed to the interceptor crew, equal to zero for τ seconds after the indicated instant t^* (or t^{**}), where τ would be chosen large enough so that:

$$t^* + \tau \geq t_c \quad \text{or} \quad t^{**} + \tau \geq t_c \ ;$$

for all possible cases. Then we would be assured that at the instant $(t^* + \tau)$ or $(t^{**} + \tau)$:

$$\dot{\beta}(t^* + \tau) = 0, \quad \text{or} \quad \dot{\beta}(t^{**} + \tau) = 0.$$

It is felt that one of $(t^* + \tau)$ or $(t^{**} + \tau)$ would serve as a true value of t_c and therefore the inaccuracy in determining t_c would be eliminated. For this reason, the error in α_c is merely the error in the measurement of α . Consequently, the error in α_c would be exactly the same as that in α_i and thus we can write $d\alpha_c = d\alpha_i = d\alpha$ in Equation 3.4-2 and get:

$$d\tilde{R} = \frac{(\sin\alpha_i - \sin\alpha_c)}{\dot{\beta}(t_i)} \left\{ d\dot{z} - \frac{\dot{z}}{\dot{\beta}(t_i)} d\dot{\beta}(t_i) \right\}$$

$$+ \frac{(\cos\alpha_i - \cos\alpha_c)}{\dot{\beta}(t_i)} \dot{z}\, d\alpha \ ; \qquad 3.4\text{-}3.$$

Now it will be shown in Section 5.5 that the unknown quantities entering into 3.4-3 can be found from the following sequence of equations:

$$C_i = \lambda \sin\phi_c \sin\Delta\phi_i - (1 - \lambda\cos\phi_c)\cos\Delta\phi_i \ , \qquad 3.4\text{-}4$$

$$D_i = \lambda \sin\phi_c \cos\Delta\phi_i + (1 - \lambda\cos\phi_c)\sin\Delta\phi_i \ , \qquad 3.4\text{-}5$$

$$\sin\alpha_i - \sin\alpha_c = \frac{1}{v}\left\{C_i \sin\Delta\theta_i + D_i \cos\Delta\theta_i - \lambda \sin\phi_c\right\} , \qquad 3.4\text{-}6$$

$$\sin\alpha_i - \cos\alpha_c = \frac{1}{v}\left\{D_i \sin\Delta\theta_i - C_i \cos\Delta\theta_i - (1 - \lambda\cos\phi_c)\right\} , \qquad 3.4\text{-}7$$

$$A_i = \lambda \sin\phi_c - D_i , \qquad 3.4\text{-}8$$

$$B_i = \lambda(\lambda - \cos\phi_c) - C_i , \qquad 3.4\text{-}9$$

$$\dot{\beta}(t_i) = -\frac{\dot{z}}{v R_i}\left\{A_i \cos\Delta\theta_i + B_i \sin\Delta\theta_i\right\} , \qquad 3.4\text{-}10$$

where the quantities λ, v, σ_i, d_i, $\sin\Delta\theta_i$ and $\cos\Delta\theta_i$ have already been given in Equations 3.2-1 to 3.2-6 respectively. Now on examining Equations 3.4-3 to 3.4-10 and 3.2-1 to 3.2-6, it will be seen that once estimates of the errors $d\dot{z}$, $d\alpha$ and $d\dot{\beta}(t_i)$ have been made for the particular radar set under consideration, then the resulting value of $d\bar{R}_i$ can be computed on stating the values of the variables: R_i, n, $\dot{z}$, $\dot{y}$, ϕ_c and $\Delta\phi_i$. It is clear that for a different radar set different values of $d\dot{z}$, $d\alpha$ and $d\dot{\beta}(t_i)$ may be necessary.

In the above, the matter of input error arising due to errors in the subsequent computations after the input information $\dot{z}, \alpha_i, \alpha_c$ and $\dot{\beta}(t)$ has been gathered by radar has been ignored. Of course such error may well be significant, however, in this study we shall ignore such effects and thus we can consider the input error in $\bar{R}_e(t_i)$ to be $d\bar{R}_i$.

4.0 Concluding Remarks

4.1 The Need and Value of a Digital Analysis

If we are to consider a particular interceptor instrumented by a particular radar set and carrying out an interception at a particular altitude, then this immediately specifies the values of $\dot{z}$ and therefore n, $d\dot{\beta}(t_i)$, $d\alpha$ and $d\dot{z}$. Consequently,

the intrinsic and input errors become functions of the variables R_i, $\dot{y}$, ϕ_c and $\Delta\phi_i$. Now from the complexity of the equations expressing the intrinsic and input errors in terms of these variables R_i, $\dot{y}$, ϕ_c and $\Delta\phi_i$ and due to the fact that so many (four) variables can vary markedly it is not at all evident how ΔR_i and $d\tilde{R}_i$ will vary with changes in R_i, $\dot{y}$, ϕ_c and $\Delta\phi_i$. It is felt that the only way in which a grasp can be got as to the values of ΔR_i and $d\tilde{R}_i$ for various conditions is to actually calculate both ΔR_i and $d\tilde{R}_i$ for various ranges of the variables R_i, $\dot{y}$, ϕ_c and $\Delta\phi_i$ and possibly for more than one interceptor. If such calculations were to be made then it is suggested that the following list of quantities become outputs on the flexowriter for each set of conditions.

4.1-A $$\Delta R_i,\ d\tilde{R}_i,\ \beta(t_i),\ |t_c - t_i|,\ R_i,\ n,\ \dot{z},\ \dot{y},\ \phi_c,\ \Delta\phi_i.$$

Now by simply investigating tables of the above results it would be possible to answer the following questions:

4.1-B "For a particular interceptor instrumented with a particular radar set, IS it possible to specify how large $\beta(t_i)$ must be in order that the resulting approximate value of range $R_e(t_i)$ obtained after turning onto a collision course will be sufficiently accurate for the purposes of missile launch against a target which is flying rectilinearly in a speed range $a_1 \leq \dot{y}(t) \leq a_2$?"

Question 4.1-B is the pertinent question if the manoeuvre we are thinking of is represented by the time sequence t_1, t_c. However, if the manoeuvre we have in mind is represented by the time sequence t_c, t_2 then the question in point is:

4.1-C "For a particular interceptor instrumented with a particular radar set, is it possible to specify how much the interceptor must turn off the collision course in order that the resulting approximate value of range $R_e(t_2)$ will be sufficiently accurate for the purposes of missile launch against a target which is flying rectilinearly in a speed range $a_1 \leq \dot{y}(t) \leq a_2$?"

Since the GCI should be able to make an intelligent guess as to the value of $\dot{y}$, the range $a_1 \leq a \leq a_2$ would appear not to be restrictively large.

Should the answer to questions 4.1-B and 4.1-C happen to be negative then the only practical result that would be obtained would be the remark: "The discussed approximate methods for determining range are not adequate for practical purposes." Of course, it is

possible that the answer to the above questions may be in the affirmative and yet the proposal may be unacceptable for operational reasons. For example, if in order to obtain sufficient accuracy the interceptor was required to turn 80° off the collision course, it is doubtful that this would be considered a practicable manoeuvre.

4.2 Suggested Computations

As a very minimum variation of the variables concerned we suggest the following table:

Table 4.2-1

Variable	Suggested Range of the Variable	Suggested Interval of the variable	Resulting No. of values of the variable
$\dot{z}$	$\dot{z}$ = Mach 1.50	Mach 0.00	1
n	1.25 g's $\leqslant$ n $\leqslant$ 1.85 g's	1.60 g's	2
$\dot{y}$	Mach 1.80 $\leqslant \dot{y} \leqslant$ Mach 2.20	Mach 0.20	3
R_i	10 n.m. $\leqslant R_i \leqslant$ 70 n.m.	20 n.m.	4
ϕ_c	$60° \leqslant \phi_c \leqslant 180°$	30°	5
$\Delta\phi_i$	$15° \leqslant \lvert\Delta\phi_i\rvert \leqslant 60°$	15°	8

It is apparent from the above table that such an extent of investigation would require 1920 runs, a "run" being the various calculations that would have to be made in order that the computer produce the outputs ΔR_i, $d\dot{R}_i$, $\beta(t_i)$, $|t_c - t_i|$ from the inputs $\dot{z}$, $\dot{y}$, n, R_i, ϕ_c, $\Delta\phi_i$, $d\beta(t_i)$, $d\dot{z}$ and $d\alpha$.

In consultation with Mr. Harry Sussman the conclusion was reached that as a maximum, the time required for the Alwac Digital Computer at CARDE to complete a single run once properly programmed would be 120 seconds. Consequently 64 hours of computer time would represent the maximum amount of time to complete the suggested 1920 runs. This as indicated does not include time required to program the computer. If the decision should be made to investigate but a single interceptor (i.e. only one value of n) then the suggested number of runs would be cut to 960.

The reader may have noticed that no numerical results giving evidence as to the validity of the theory have been included. However, such verification is presently being carried out by comparing the analytic results with those obtained from a more intuitive geometric procedure for finding ΔR_i.

5.0 Analytic Development

It is the sole object of this section to explain, in a complete analytic manner, how the results given in Section 3.0 were obtained. The development has been written, it is hoped, so that the interested reader can follow along without experiencing an excessive number of omissions in reasoning and the necessity to discover for himself what manipulations the author has undergone in order to obtain a certain result.

5.1 Measurement of Angles in Two Dimensions

The basic purport of this section is to outline a systematic method which will result in a consistent sign convention regarding the measurement of angles, without the necessity of consulting several geometric diagrams before concluding that your result is sufficiently general.

Throughout this section let:

$\underline{f}$, $\underline{g}$, and $\underline{h}$ be arbitrary, non-zero vectors which are furthermore coplanar. Now in Section 2.1 a rather vague definition of the angle $(\underline{f} : \underline{g})$ was given. We shall now give a more complete definition, namely:

Definition 5.1-A The symbol $(\underline{f} : \underline{g})$, called the angle between the vectors $\underline{f}$ and $\underline{g}$, shall be that "positive" and "non-zero" real number which corresponds to the "minimum" number of radians through which the first-mentioned vector $\underline{f}$ must be rotated counterclockwise in order that the sense of $\underline{f}$ may become identical with the sense of the second-mentioned vector $\underline{g}$ (see Figure 7).

The word "sense" as used in the above definition has been adequately explained in Figure 1. We shall use the symbol $\mathcal{I}$ to represent the set of integers and the zero scalar, and when we write:

$$\xi \in \mathcal{I} ,$$

this shall indicate that ξ is an integer or zero, i.e. ξ belongs to the set $\mathcal{I}$. From Definition 5.1-A, it should be clear that:

$$(\underline{f} : \underline{g}) > 0 ,$$

for all angles $(\underline{f} : \underline{g})$. The following equations 5.1-1 and 5.1-2

may be looked upon as postulates determining the nature of angles or as quite evident results of geometric intuition:

$$(\underline{f} : \underline{f}) = 2\pi \quad ; \qquad 5.1\text{-}1,$$

$$(\underline{f} : -\underline{f}) = \pi \quad ; \qquad 5.1\text{-}2.$$

We shall now prove an important theorem.

Theorem 5.1-I

Hypotheses: 1.) $\underline{f}$, $\underline{g}$ and $\underline{h}$ are arbitrary, non-zero, coplanar vectors.

Conclusions: 1.) There exists $m \in \Pi$ which will satisfy the condition:

$$(\underline{f} : \underline{g}) = (\underline{f} : \underline{h}) + (\underline{h} : \underline{g}) + 2\pi m \quad ; \qquad 5.1\text{-}3.$$

Proof: First we show that if m is not restricted to the set Π , but is allowed to be a real number, then indeed such an m does exist. For in fact take:

$$m = \frac{(\underline{f} : \underline{g}) - (\underline{f} : \underline{h}) - (\underline{h} : \underline{g})}{2\pi} ,$$

then certainly such an m is a real number and also satisfies 5.1-3. We now must show that m belongs to Π , and to this end let us assume that m does not belong to Π . Thus since $\underline{f}$, $\underline{g}$ and $\underline{h}$ are arbitrary suppose that $\underline{g} = \underline{h}$, for then 5.1-3 becomes:

$$(\underline{f} : \underline{h}) = (\underline{f} : \underline{h}) + (\underline{h} : \underline{h}) + 2\pi m ,$$

$$\therefore \quad 0 = +(\underline{h} : \underline{h}) + 2\pi m \quad ; \qquad 5.1\text{-}4,$$

for some real number m which does not belong to Π . However, using 5.1-1, Equation 5.1-4 yields:

$$0 = 2\pi + 2\pi m ,$$

$$m = -1 ,$$

but this is a contradiction since m was not to belong to Π . Consequently, the existence of $m \in \Pi$ is irrevocably established.

5.2 Preliminary Mathematical Results

Before continuing on with the development of the range equations and the various errors, it is desirable to define various symbols which shall be used constantly throughout that which follows. In Section 2.0 a number of symbols, notations and conventions have been outlined. However, in the more complete development to be found in this section it is necessary to define a greater number of symbols. We shall do this immediately, but not before remarking that the definitions given here shall appear in mathematical form only and will not be complimented with illustrative verbage as in Section 2.2. Of course, it is not possible to define everything mathematical wise and consequently some of the definitions will necessarily appear in verbal form. Whenever it has been found necessary to define a symbol by means of two equations, this has been done by placing the two equations on the same line and separated by a comma. An attempt has been made to present the definitions in such a sequence that a new symbol appearing in Definition 5.2- Dn is explicitly defined in terms of one or more of the definitions from 5.2- D1 to 5.2- D(n-1). Simplifications in notation have been indicated by replacing the "euqal to" sign = by the "identically equal to" sign $\equiv$. In order to maintain a continuity in the sequence of definitions given here, many of those symbols already defined in Section 2.0 have been redefined. He who desires a more physical interpretation is referred to Figures 8 and 9. The definitions are:

t = an arbitrary instant of time during the interception..5.2-D1

$I(t), T(t)$ = the space positions of the centers of gravity of the interceptor and target respectively at the instant t; 5.2-D2

O = a point fixed in the plane of interception and consequently fixed in space ; 5.2-3D

$\underline{\rho}(t) \equiv \overrightarrow{O, I(t)}$; 5.2-D4

$\underline{\rho}(t) \equiv \overrightarrow{O, T(t)}$; 5.2-D5

$R(t) \equiv \left|\overrightarrow{I(t), T(t)}\right|$; 5.2-D6

$\underline{m}_1$ = a fixed unit vector in the plane of interception .. 5.2-D7

$(\underline{m}_1 : \underline{m}_2) \equiv \frac{\pi}{2}$, $\underline{m}_2 \cdot \underline{m}_2 = 1$; 5.2-D8

$\underline{i}_1(t) \equiv \frac{\overrightarrow{I(t), T(t)}}{R(t)}$; 5.2-D9

$$\left(\underline{i}_1(t) : \underline{i}_2(t)\right) = \frac{\pi}{2} \qquad \underline{i}_2(t) \cdot \underline{i}_2(t) = 1 ; \qquad \text{5.2-D10}$$

$$\underline{p}_1(t) = \frac{\dot{\underline{z}}(\tau)}{\dot{z}(t)} ; \qquad \text{5.2-D11}$$

$$\left(\underline{p}_1(t) : \underline{p}_2(t)\right) = \frac{\pi}{2} , \quad \underline{p}_2(t) \cdot \underline{p}_2(t) = 1 ; \qquad \text{5.2-D12}$$

$$\left.\begin{aligned} \underline{k}_1(t) &= \frac{\dot{\underline{y}}(t)}{\dot{y}(t)} ; \\ \left(\underline{k}_1(t) : \underline{k}_2(t)\right) &= \frac{\pi}{2} , \quad \underline{k}_2(t) \cdot \underline{k}_2(t) = 1 ; \end{aligned}\right\} \qquad \text{5.2-D13}$$

$$\theta(t) = \left(\dot{\underline{y}}(t) : \underline{i}_1(t)\right) ; \qquad \text{5.2-D14}$$

$$\alpha(t) = \left(\dot{\underline{z}}(t) : \underline{i}_1(t)\right) ; \qquad \text{5.2-D15}$$

$$\phi(t) = \left(\dot{\underline{y}}(t) : \dot{\underline{z}}(t)\right) ; \qquad \text{5.2-D16}$$

$$\gamma(t) = \left(\dot{\underline{z}}(t) : \underline{m}_1\right) ; \qquad \text{5.2-D17}$$

$$\psi(t) = \left(\dot{\underline{y}}(t) : \underline{m}_1\right) ; \qquad \text{5.2-D18}$$

$$\beta(t) = \left(\underline{m}_1 : \underline{i}_1(t)\right) ; \qquad \text{5.2-D19}$$

$$\lambda_1(t) = \underline{z}(t) \cdot \underline{m}_1 ; \qquad \text{5.2-D20}$$

$$\lambda_2(t) = \underline{z}(t) \cdot \underline{m}_2 ; \qquad \text{5.2-D21}$$

$$\mu_1(t) = \underline{y}(t) \cdot \underline{m}_1 ; \qquad \text{5.2-D22}$$

$$\mu_2(t) = \underline{y}(t) \cdot \underline{m}_2 ; \qquad \text{5.2-D23}$$

$$\xi_1(t) = \left\{\underline{z}(t) - \underline{y}(t)\right\} \cdot \underline{k}_1(t) ; \qquad \text{5.2-D24}$$

$$\xi_2(t) = \left\{\underline{z}(t) - \underline{y}(t)\right\} \cdot \underline{k}_2(t) \quad ; \qquad \text{. . . . . 5.2-D25}$$

$P(t)$ for $(-1)^i t_c \leq t \leq (-1)^i t_i$, $i = 1,2$ is that

point in the plane of interception about which the interceptor is executing a circular turn where t_c and t_i are to have the meaning given in Section 3.1 . . . . . 5.2-D26

$$\underline{b}(t) = \overrightarrow{P(t) \cdot I(t)} \quad ; \qquad \text{. . . . . 5.2-D27}$$

$$\underline{j}_1(t) = \frac{\underline{b}(t)}{b(t)} \quad ; \qquad \text{. . . . . 5.2-D28}$$

$$\left(\underline{j}_1(t) : \underline{j}_2(t)\right) = \frac{\pi}{2} \quad , \quad \underline{j}_2(t) \cdot \underline{j}_2(t) = 1 \; ; \qquad \text{. . . . . 5.2-D29}$$

$$\rho(t) = \left(\underline{j}_1(t) : -\underline{k}_1(t)\right) \; ; \qquad \text{. . . . . 5.2-D30}$$

$$\Delta\phi_i = \phi(t_c) - \phi(t_i) \equiv \phi_c - \phi_i \; ; \qquad \text{. . . . . 5.2-D31}$$

$$\Delta\alpha_i = \alpha(t_c) - \alpha(t_i) \equiv \alpha_c - \alpha_i \; ; \qquad \text{. . . . . 5.2-D32}$$

$$\Delta\theta_i = \theta(t_c) - \theta(t_i) \equiv \theta_c - \theta_i \; ; \qquad \text{. . . . . 5.2-D33}$$

$$\sigma_i = \frac{\Delta\phi_i}{|\Delta\phi_i|} \quad ; \qquad \text{. . . . . 5.2-D34}$$

$$\Delta\lambda_1 = \lambda_1(t_c) - \lambda_1(t_i) \; ; \qquad \text{. . . . . 5.2-D35}$$

$$\Delta\lambda_2 = \lambda_2(t_c) - \lambda_2(t_c) \; ; \qquad \text{. . . 5.2-D36}$$

$$v = \frac{1}{\dot{z}} \sqrt{\left\{\dot{\underline{z}}(t) - \dot{\underline{y}}(t)\right\} \cdot \left\{\dot{\underline{z}}(t) - \dot{\underline{y}}(t)\right\}} \quad ; \qquad \text{. . 5.2-D37}$$

$$\sigma(t) = \frac{\dot{\phi}(t)}{|\dot{\phi}(t)|} \quad ; \qquad \text{. . . . . 5.2-D38}$$

$$\Delta\mu_1 = \mu_1(t_c) - \mu_1(t_i) \; ; \qquad \text{. . . . . 5.2-D39}$$

$\Delta\mu_2 = \mu_2(t_c) - \mu_2(t_i)$; 5.2-D40

$\Delta\xi_1 = \xi_1(t_c) - \xi_1(t_i)$; 5.2-D41

$\Delta\xi_2 = \xi_2(t_c) - \xi_2(t_i)$; 5.2-D42

$\mathcal{J}$ = The set of all integers and zero 5.2-D43

$\mathcal{N}$ = The set of all positive integers 5.2-D44

Λ = The set of all negative integers 5.2-D45

$Q(t_i)$ = That point on the line joining the points $I(t_c)$ and $T(t_c)$ at the instants t_i and having the unique property that

$$\overrightarrow{I(t_i), Q(t_i)} \cdot \underline{i}_1(t_c) = 0 \quad ; \qquad 5.2\text{-}D46$$

d_i = That scalar which will satisfy the relation $\overrightarrow{I(t_i), Q(t_i)} = d_i\, \underline{i}_2(t_c)$; 5.2-D47

η_i = That scalar which will satisfy the relation $\overrightarrow{T(t_c), Q(t_i)} = \eta_i\, \underline{i}_1(t_c)$; 5.2-D48

$$\lambda = \frac{\dot{y}}{\dot{z}} \quad ; \qquad \text{. . . . . } \quad 5.2\text{-}D49$$

By repeated use of theorem 5.1-1, the well known fact that any vector $\underline{f}$ can be expressed as $\underline{f} = \underline{a}_1(\underline{a}_1 \cdot \underline{f}) + \underline{a}_2(\underline{a}_2 \cdot \underline{f})$ where

$\underline{a}_1$ and $\underline{a}_2$ are non-colinear vectors and the above definitions; many useful results can be obtained by ordinary vector methods. However, the process of obtaining such results is thought to be too well known to be included here and hence we shall but state the results:

TABLE 5.2-1

UNIT VECTOR $\underline{a}$	Components of the unit vector $\underline{a}$ when expressed in terms of the dyad: $\underline{m}_1, \underline{m}_2$	$\underline{i}_1(t), \underline{i}_2(t)$	$\underline{P}_1(t), \underline{P}_2(t)$	$\underline{k}_1, \underline{k}_2$	$\underline{j}_1(t), \underline{j}_2(t)$
$\underline{m}_1$	$1, 0$	$\cos\beta(t), -\sin\beta(t)$	$\cos\gamma(t), \sin\gamma(t)$	$\cos\psi(t), \sin\psi(t)$	$-\sigma\sin\gamma(t), \sigma\cos\gamma(t)$
$\underline{m}_2$	$0, 1$	$\sin\beta(t), \cos\beta(t)$	$-\sin\gamma(t), \cos\gamma(t)$	$-\sin\psi(t), \cos\psi(t)$	$-\sigma\cos\gamma(t), -\sigma\sin\gamma(t)$
$\underline{i}_1(t)$	$\cos\beta(t), \sin\beta(t)$	$1, 0$	$\cos\alpha(t), \sin\alpha(t)$	$\cos\theta(t), \sin\theta(t)$	$-\sigma\sin\alpha(t), \sigma\cos\alpha(t)$
$\underline{i}_2(t)$	$-\sin\beta(t), \cos\beta(t)$	$0, 1$	$-\sin\alpha(t), \cos\alpha(t)$	$-\sin\theta(t), \cos\theta(t)$	$-\sigma\cos\alpha(t), -\sigma\sin\alpha(t)$
$\underline{P}_1(t)$	$\cos\gamma(t), -\sin\gamma(t)$	$\cos\alpha(t), -\sin\alpha(t)$	$1, 0$	$\cos\phi(t), \sin\phi(t)$	$0, \sigma$
$\underline{P}_2(t)$	$\sin\gamma(t), \cos\gamma(t)$	$\sin\alpha(t), \cos\alpha(t)$	$0, 1$	$-\sin\phi(t), \cos\phi(t)$	$-\sigma, 0$
$\underline{k}_1$	$\cos\psi(t), -\sin\psi(t)$	$\cos\theta(t), -\sin\theta(t)$	$\cos\phi(t), -\sin\phi(t)$	$1, 0$	$-\cos\rho(t), -\sin\rho(t)$
$\underline{k}_2$	$\sin\psi(t), \cos\psi(t)$	$\sin\theta(t), \cos\theta(t)$	$\sin\phi(t), \cos\phi(t)$	$0, 1$	$\sin\rho(t), -\cos\rho(t)$
$\underline{j}_1(t)$	$-\sigma\sin\gamma(t), -\sigma\cos\gamma(t)$	$-\sigma\sin\alpha(t), -\sigma\cos\alpha(t)$	$0, -\sigma$	$-\cos\rho(t), \sin\rho(t)$	$1, 0$
$\underline{j}_2(t)$	$\sigma\cos\gamma(t), -\sigma\sin\gamma(t)$	$\sigma\cos\alpha(t), -\sigma\sin\alpha(t)$	$\sigma, 0$	$-\sin\rho(t), -\cos\rho(t)$	$0, 1$

SECRET

TABLE 5.2-2

UNIT VECTOR $\underline{a}$	Time rate of change of the Unit Vector $\frac{d\underline{a}}{dt}$	Unit Vector $\underline{a}$	Time rate of change of the Unit Vector $\frac{d\underline{a}}{dt}$
$\underline{m}_1$	$\underline{0}$	$\underline{P}_2(t)$	$\dot{\gamma}(t)\ \underline{P}_1(t)$
$\underline{m}_2$	$\underline{0}$	$\underline{k}_1$	$\underline{0}$
$\underline{i}_1(t)$	$\dot{\beta}(t)\ \underline{i}_2(t)$	$\underline{k}_2$	$\underline{0}$
$\underline{i}_2(t)$	$-\dot{\beta}(t)\ \underline{i}_1(t)$	$\underline{j}_1(t)$	$-\dot{\rho}(t)\ \underline{j}_2(t)$
$\underline{P}_1(t)$	$-\dot{\gamma}(t)\ \underline{P}_2(t)$	$\underline{j}_2(t)$	$\dot{\rho}(t)\ \underline{j}_1(t)$

$$\theta(t) = \psi(t) + \beta(t) + 2\pi m\ ,\ m \in \mathbb{J}\ ; \qquad \ldots\ 5.2\text{-}1$$

$$\alpha(t) = \gamma(t) + \beta(t) + 2\pi m\ ,\ m \in \mathbb{J}\ ; \qquad \ldots\ 5.2\text{-}2$$

$$\theta(t) - \alpha(t) = \psi(t) - \gamma(t) + 2\pi m\ ,\ m \in \mathbb{J}\ ; \qquad \ldots\ 5.2\text{-}3$$

$$\phi(t) = \psi(t) - \gamma(t) + 2\pi m\ ,\ m \in \mathbb{J}\ ; \qquad \ldots\ 5.2\text{-}4$$

$$\theta(t) = \alpha(t) + \phi(t) + 2\pi m\ ,\ m \in \mathbb{J}\ ; \qquad \ldots\ 5.2\text{-}5$$

$$\rho(t) + \phi(t) = 2\pi m - \frac{\pi}{2}\sigma(t)\ ,\ m \in \mathbb{J}\ ; \qquad \ldots\ 5.2\text{-}6$$

Let us but point out again that the above are analytic and quite rigorous results.

5.3 Analytic Development of the Approximate Range Equations

As a general vector relation between the interceptor and target which holds true for all possible situations we can write:

$$\overrightarrow{O,I(t)} + \overrightarrow{I(t),T(t)} = \overrightarrow{O,T(t)} \ ,$$

and from 5.2-D4, 5.2-D5 and 5.2-D9 the above becomes:

$$\underline{Z}(t) + R(t)\underline{i}_1(t) = \underline{y}(t) \ ; \qquad 5.3\text{-}1$$

Now on differentiating 5.3-1 and using the results of Table 5.2-2 we get:

$$\dot{\underline{Z}}(t) + \dot{R}(t)\underline{i}_1(t) + R(t)\dot{\beta}(t)\underline{i}_2(t) = \dot{\underline{y}}(t) \ ; \qquad 5.3\text{-}2$$

Equation 5.3-2 gives the general kinematic relationships between the interceptor and target. Resolving the vectors in Equation 5.3-2, as seen in Figure 2, perpendicular to the line of sight there results:

$$R(t)\dot{\beta}(t) = \dot{Z}(t)\sin\alpha(t) - \dot{y}(t)\sin\theta(t) \ ; \qquad 5.3\text{-}3$$

Indeed, it is thus seen that the condition $\dot{\beta}(t) = 0$ is sufficient to insure the interceptor that he is on a collision course even in the case of an arbitrarily manoeuvring target, the only additional provision being that $\dot{R}(t) < 0$ must be maintained.

Now let t_1, t_c, t_2 be the time sequence as explained in Section 3.1, then we have that $\dot{\beta}(t_c) = 0$ and thus 5.3-3 yields

$$\dot{Z}(t_c)\sin\alpha(t_c) = \dot{y}(t_c)\sin\theta(t_c) \ ; \qquad 5.3\text{-}4$$

Now at the times t_1, t_2 we have that:

$$\dot{\beta}(t_i) \neq 0 \ , \quad i = 1,2;$$

and hence from 5.3-3 we get:

$$R(t_i) = \frac{\dot{Z}(t_i)\sin\alpha(t_i) - \dot{y}(t_i)\sin\theta(t_i)}{\dot{\beta}(t_i)} \qquad i = 1,2. \qquad 5.3\text{-}5$$

Now in 5.3-5 the quantities $\dot{y}(t_i)$; $\sin\theta(t_i)$ cannot be determined in the case of the successfully jamming target. Consequently, at best some approximation to the terms $\dot{y}(t_i)$; $\sin\theta(t_i)$ can be made. The suggested approximation in Reference 1. and the one that shall therefore be made in this study, is that:

$$\dot{y}(t_i)\sin\theta(t_i) \cong \dot{y}(t_c)\sin\theta(t_c), \quad i = 1,2; \qquad 5.3\text{-}6$$

Now if Equation 5.3-4, which is a perfectly rigorous and valid result, is substituted into 5.3-6 then we have:

$$\dot{y}(t_i)\sin\theta(t_i) \cong \dot{\tilde{z}}(t_c)\sin\alpha(t_c), \quad i = 1,2; \qquad 5.3\text{-}7$$

Now if in 5.3-5 we would substitute from 5.3-7 then an approximate value of the true range $R(t_i)$ should be obtained. Let this approximate value be denoted $\tilde{R}(t_i)$, then indeed $\tilde{R}(t_i)$ will be given by:

$$\tilde{R}(t_i) = \frac{\dot{\tilde{z}}(t_i)\sin\alpha(t_i) - \dot{\tilde{z}}(t_c)\sin\alpha(t_c)}{\beta(t_i)}, \quad i = 1,2 \qquad 5.3\text{-}8$$

Now let us note a few things about Equation 5.3-8. Firstly, it has been developed without any special assumptions as to whether or not the target is manoeuvring. Secondly, it has been developed without any special assumptions as to the nature of the interceptor's manoeuvre. Now since the approximation 5.3-6 does in no way depend upon the speed of the interceptor, we thus see that the variance between $R(t_i)$ and $\tilde{R}(t_i)$ is not affected by even marked differences between $\dot{\tilde{z}}(t_i)$ and $\dot{\tilde{z}}(t_c)$. Consequently, it is suggested that Equation 5.3-8 be the one which is instrumented in an actual interceptor rather than the somewhat simpler equation which results for the simpler case of the constant speed interceptor. However, the variance of $\tilde{R}(t_i)$ as given by 5.3-8 from the true range $R(t_i)$ might be markedly affected by target manoeuvres. However, in this study we are concerned only with the simplest case where the vector velocity of the target is constant and also the speed of the interceptor is a constant.

Consequently, we have that $\dot{z}(t_i) = \dot{z}(t_c)$ and we put $\dot{z} = \dot{z}(t_i) = \dot{z}(t_c)$ and thus 5.3-8 becomes

$$\tilde{R}_i = \frac{\dot{z}}{\beta(t_i)} \left\{ \sin\alpha_i - \sin\alpha_c \right\} , \quad i = 1, 2 ; \qquad 5.3\text{-}9$$

Equations 5.3-9 are the approximate range equations which shall be analyzed in this study.

5.4 Analytic Development of the Intrinsic Error

On subtracting Equation 5.3-8 from 5.3-5 we obtain:

$$R(t_i) - \tilde{R}(t_i) = \frac{\dot{z}(t_c)\sin\alpha(t_c) - \dot{y}(t_i)\sin\theta(t_i)}{\beta(t_i)} ,$$

and dividing both sides of the above by $R(t_i)$ we get:

$$\frac{R(t) - \tilde{R}(t_i)}{R(t_i)} = \frac{\dot{z}(t_c)\sin\alpha(t_c) - \dot{y}(t_i)\sin\theta(t_i)}{\dot{z}(t_i)\sin\alpha(t_i) - \dot{y}(t_i)\sin\theta(t_i)} ,$$

and using the simplifications of notation indicated in Section 5.3 the above submits to the form:

$$\frac{\Delta R_i}{R_i} = \frac{\lambda \sin\theta_i - \sin\alpha_c}{\lambda \sin\theta_i - \sin\alpha_i} , \quad i = 1, 2 ; \qquad 5.4\text{-}1$$

Now in order to solve for ΔR_i from 5.4-1, we might consider solving one or both of the following problems:

Problem 5.4-1

"Given the values of R_i, α_i, θ_i subsequently determine the corresponding value of α_c".

Problem 5.4-2

"Given the values of R_i, $\Delta\phi_i$; ϕ_c subsequently determine the corresponding values of θ_i, α_i and α_c".

It would seem that the latter of the two questions would present the more formidable problem; however, this has not found to be the case and a solution to Problem 5.4-2 will shortly be offered, whereas a solution of Problem 5.4-1 has as yet not been found.

We shall now attack Problem 5.4-2 having in mind that theoretically we can specify the values of $\dot{z}$, $\dot{y}$, η, R_c, $\Delta\phi_i$ and ϕ_c. Our first move shall be to show that the terms $\sin\theta_i$ and $\sin\alpha_i$ in 5.4-1 can be expressed in terms of α_c, $\Delta\phi_i$ and $\Delta\theta_i$. From the definitions given in Section 5.2 and well known trigonometric expressions it immediately follows that:

$$\begin{aligned} \sin\alpha_i &= \sin\{\alpha_c - (\Delta\theta_i - \Delta\phi_i)\}, \\ \sin\alpha_i &= \sin\alpha_c \cos(\Delta\theta_i - \Delta\phi_i) \\ &\quad - \cos\alpha_c \sin(\Delta\theta_i - \Delta\phi_i); \end{aligned} \qquad 5.4\text{-}3$$

$$\begin{aligned} \sin\theta_i &= \sin(\theta_c - \Delta\theta_i) \\ \sin\theta_i &= \sin\theta_c \cos\Delta\theta_i - \cos\theta_c \sin\Delta\theta_i \end{aligned} \qquad 5.4\text{-}4$$

We shall now outline how $\sin\theta_c$, $\cos\phi_c$, $\sin\alpha_c$ and $\cos\alpha_c$ can be expressed in terms of $\dot{z}$, $\dot{y}$ and ϕ_c. Recalling that $\beta(t_c) = 0$ we have from Equation 5.3-2 that:

$$\underline{\dot{z}}(t_c) - \underline{\dot{y}}(t_c) = -\dot{R}(t_c)\,\underline{i}_1(t_c) \qquad 5.4\text{-}5$$

Now taking the dot product of Equation 5.4-5 with the vectors $\underline{i}_1(t_c)$, $\underline{R}(t_c)$, $\underline{R}(t_c)$ and $\underline{k}_1$, and using the results in Table 5.2-1 there results:

$$\left.\begin{aligned} \dot{z}\sin\alpha_c &= \dot{y}\sin\theta_c \\ \dot{y}\sin\phi_c &= -\dot{R}(t_c)\sin\alpha_c \\ \dot{z} &= \dot{y}\cos\phi_c - \dot{R}(t_c)\cos\alpha_c \\ \dot{y} &= \dot{z}\cos\phi_c + \dot{R}(t_c)\cos\theta_c \end{aligned}\right\} \qquad 5.4\text{-}6$$

On manipulating Equations 5.4-6 algebraically it is possible to show:

$$\left.\begin{aligned} \cos\theta_c &= -\frac{1}{\nu}(\lambda - \cos\phi_c)\ ; \\ \sin\theta_c &= \frac{1}{\nu}\sin\phi_c\ ; \\ \cos\alpha_c &= \frac{1}{\nu}(1 - \lambda\cos\phi_c)\ ; \\ \sin\alpha_c &= \frac{\lambda}{\nu}\sin\phi_c\ ; \end{aligned}\right\} \qquad 5.4\text{-}7$$

where for simplicity of notation we have put:

$$\nu = +\sqrt{1+\lambda^2 - 2\lambda\cos\phi_c}\ .$$

At this point we realize, from Equations 5.4-1, 5.4-3, 5.4-4 and 5.4-7 that we have now expressed ΔR_i in terms of the variables $R_i, \lambda, \phi_c, \Delta\phi_i$ and $\Delta\theta_i$, all of which are specified or known excepting $\Delta\theta_i$. Thus it now but remains to solve for $\Delta\theta_i$ in terms of the known variables $R_i, \eta, \dot{z}, \dot{y}, \phi_c$ and $\Delta\phi_i$. First let us substitute in 5.4-1 from 5.4-3 and 5.4-4 and after a few trigonometric expansions we can write $\frac{\Delta R_i}{R_i}$ in the form:

$$\frac{\Delta R_i}{R_i} = \frac{\lambda\sin\theta_c\cos\Delta\theta_i - \lambda\cos\theta_c\sin\Delta\theta_i - \sin\alpha_c}{\left[\begin{aligned} &\{\cos\Delta\theta_i\}\{\lambda\sin\theta_c - \sin\alpha_c\cos\Delta\phi_i - \cos\alpha_c\sin\Delta\phi_i\} \\ -&\{\sin\Delta\theta_i\}\{\lambda\cos\theta_c + \sin\alpha_c\sin\Delta\phi_i - \cos\alpha_c\cos\Delta\phi_i\}\end{aligned}\right]}$$

5.4-8

From 5.4-8 we now see that we need only determine $\cos\Delta\theta_i$ and $\sin\Delta\theta_i$ (this in effect determines $\Delta\theta_i$) in order that ΔR_i be expressed as a function of $R_i, \eta, \dot{z}, \dot{y}, \phi_c$ and $\Delta\phi_i$. We shall now proceed with the determination of $\cos\Delta\theta_i$ and $\sin\Delta\theta_i$. However, as will be seen, the road leading to the determination of $\sin\Delta\theta_i$ and $\cos\Delta\theta_i$ will be rather circuitous, and for some time it will appear that we are ranting and raging with no good purpose in mind.

Now the position of the interceptor in space at the instants t_i is given by the vector $\underline{Z}(t_i)$ which may be written in the form:

$$\underline{Z}(t_i) = \underline{m}_1\left\{\underline{m}_1\cdot\underline{Z}(t_i)\right\} + \underline{m}_2\left\{\underline{m}_2\cdot\underline{Z}(t_i)\right\}$$

and from 5.2-D20 and 5.2-D21 the above takes the form:

$$\underline{Z}(t_i) = \underline{m}_1\lambda_1(t_i) + \underline{m}_2\lambda_2(t_i)\ , \qquad i = 1,2\ ; \qquad 5.4\text{-}9$$

However, we have that:

$$\overrightarrow{O,I(t_i)} = \overrightarrow{O,P(t_i)} + \overrightarrow{P(t_i),I(t_i)} ;$$

$$\therefore \quad \underline{r}(t_i) = \overrightarrow{O,P(t_i)} + b\,\underline{j}_1(t_i)$$

and substituting this expression for $\underline{r}(t_i)$ in Equation 5.4-9 and subsequently solving for $\lambda_1(t_i)$, $\lambda_2(t_i)$ we get:

$$\left.\begin{aligned} \lambda_1(t_i) &= \underline{m}_1 \cdot \overrightarrow{O,P(t_i)} - b\,\sigma(t_i)\sin\varphi(t_i) ; \\ \lambda_2(t_i) &= \underline{m}_2 \cdot \overrightarrow{O,P(t_i)} - b\,\sigma(t_i)\cos\varphi(t_i) ; \end{aligned}\right\} \qquad 5.4\text{-}10.$$

In a similar manner we obtain

$$\left.\begin{aligned} \lambda_1(t_c) &= \underline{m}_1 \cdot \overrightarrow{O,P(t_c)} - b\,\sigma(t_c)\sin\varphi(t_c) \\ \lambda_2(t_c) &= \underline{m}_2 \cdot \overrightarrow{O,P(t_c)} - b\,\sigma(t_c)\cos\varphi(t_c) \end{aligned}\right\} \qquad 5.4\text{-}11.$$

We must realize that $P(t_c)$ and $P(t_i)$ are the same point throughout $(-1)^i t_c \leq (-1)^i t \leq (-1)^i t_1$ and hence on subtraction of 5.4-10 and 5.4-11 we have:

$$\left.\begin{aligned} \Delta\lambda_1 &= b\left\{\sigma(t_i)\sin\varphi_i - \sigma(t_c)\sin\varphi_c\right\} ; \\ \Delta\lambda_2 &= b\left\{\sigma(t_i)\cos\varphi_i - \sigma(t_c)\cos\varphi_c\right\} ; \end{aligned}\right\} \qquad 5.4\text{-}12.$$

Since the target flies such that $\ddot{\underline{y}} = \underline{0}$ we therefore have that $\psi(t)$ is a constant, and since $\underline{m}_1$ may be arbitrarily chosen we take $\underline{m}_1$ such that $\psi(t) = 2\pi$ for all t.

Thus from Equation 5.2-4 we get that:

$$\left.\begin{aligned} \cos\phi(t) &= \cos\varphi(t) ; \\ \sin\phi(t) &= -\sin\varphi(t) ; \end{aligned}\right\} \qquad 5.4\text{-}13.$$

and subsequent use of 5.4-13 in 5.4-12 yields:

$$\left.\begin{aligned}\Delta\lambda_1 &= b\left\{\sigma(t_c)\sin\phi_c - \sigma(t_i)\sin\phi_i\right\}\\ \Delta\lambda_2 &= b\left\{\sigma(t_i)\cos\phi_i - \sigma(t_c)\cos\phi_c\right\}\end{aligned}\right] \qquad 5.4\text{-}14$$

Now during the time intervals $(-1)^i t_c \leq (-1)^i t \leq (-1)^i t_i$ the interceptor will be executing either a port or starboard turn and hence $\dot{\phi}(t)$ will be of the same sign throughout this interval of time. Consequently $\dot{\phi}_i$ and $\dot{\phi}_c$ will be of the same sign and thus:

$$\sigma(t_i) = \sigma(t_c) = \sigma(t) \quad , \quad \text{for } (-1)^i t_c \leq (-1)^i t \leq (-1)^i t_i \qquad \text{and thus}$$

Equations 5.4-14 become:

$$\left.\begin{aligned}\Delta\lambda_1 &= b\,\sigma(t)\left\{\sin\phi_c - \sin\phi_i\right\};\\ \Delta\lambda_2 &= b\,\sigma(t)\left\{\cos\phi_i - \cos\phi_c\right\};\end{aligned}\right] \qquad 5.4\text{-}15$$

Recalling some of the results in Section 3.2 we have:

a port turn by interceptor $\sim$ $\begin{cases}\Delta\phi_1 > 0;\\ \Delta\phi_2 < 0;\end{cases}$

however, $\dot{\phi}(t) > 0$ or $\sigma(t) = 1$ corresponds to a port turn and hence we can write:

$\sigma(t) = 1$, when $\begin{cases}\Delta\phi_1 > 0;\\ \Delta\phi_2 < 0.\end{cases}$

If we wish the above may be made to read:

$\sigma(t) = 1$ when $-(-1)^i \Delta\phi_i > 0$, $i = 1,2$;

and consequently:

$\sigma(t) = 1$ when $-(-1)^i \dfrac{\Delta\phi_i}{|\Delta\phi_i|} = 1$, $i = 1,2$;

and thus we can write:

$$\sigma(t) = -(-1)^i \frac{\Delta\phi_i}{|\Delta\phi_i|} \quad , \; i = 1,2; \text{ if the interceptor is in a port turn.}$$

Using an analogue train of reasoning we can show that:

$$\sigma(t) = -(-1)^i \frac{\Delta\phi_i}{|\Delta\phi_i|} \quad , \; i = 1,2; \text{ if the interceptor is in a starboard turn.}$$

We now decide to put $\sigma_i = \frac{\Delta\phi_i}{|\Delta\phi_i|}$ and hence 5.4-15 becomes:

$$\left.\begin{aligned} \Delta\lambda_1 &= (-1)^i b\sigma_i \{\sin\phi_i - \sin\phi_c\} \\ \Delta\lambda_2 &= (-1)^i b\sigma_i \{\cos\phi_c - \cos\phi_i\} \end{aligned}\right\} \qquad 5.4\text{-}16.$$

Now the transformation equations between space and target co-ordinates in the special case of the non-accelerating target are easily shown to be:

$$\left.\begin{aligned} \xi_1(t) &= \lambda_1(t) - \mu_1(t) \; ; \\ \xi_2(t) &= \lambda_2(t) - \mu_2(t) \; ; \end{aligned}\right\} \qquad 5.4\text{-}17.$$

with the further stipulation that $\psi(t) = 2\pi$.

On evaluating Equations 5.4-17 at the instants t_c and t_i and subtracting the resulting equations we obtain:

$$\left.\begin{aligned} \Delta\xi_1 &= \Delta\lambda_1 - \Delta\mu_1 \; : \\ \Delta\xi_2 &= \Delta\lambda_2 - \Delta\mu_2 \; ; \end{aligned}\right\} \qquad 5.4\text{-}18.$$

The displacement of the non-accelerating target in space during the interval of time $(-1)^i t_c \leqslant (-1)^i t \leqslant (-1)^i t_i$ is given by:

$$\left.\begin{aligned} \Delta\mu_1 &= \dot{y}\,(t_c - t_i) \; ; \\ \Delta\mu_2 &= 0 \qquad\quad : \end{aligned}\right\} \qquad 5.4\text{-}19.$$

Without a great deal of effort we can show that:

$$t_c - t_i = \frac{\Delta\phi_i}{\dot{\phi}(t)} \; ; \; (-1)^i t_c \leqslant (-1)^i t \leqslant (-1)^i t_i \; ; \qquad 5.4\text{-}20.$$

$$\frac{1}{\dot{\phi}(t)} = \frac{b}{\dot{z}}\sigma_i (-1)(-1)^i, \; (-1)^i t_c \leqslant (-1)^i t \leqslant (-1)^i t_i \; ; \qquad 5.4\text{-}21.$$

Now substituting in 5.4-19 from 5.4-20 and 5.4-21 we get:

$$\left.\begin{aligned} \Delta\mu_1 &= -(-1)^i \lambda\, b\, \sigma_i\, \Delta\phi_i \quad ; \\ \Delta\mu_2 &= 0 \qquad\qquad\quad ; \end{aligned}\right\} \qquad 5.4\text{-}21.$$

If we now substitute into Equations 5.4-18 from Equations 5.4-16 and 5.4-21 there results:

$$\left.\begin{aligned} \Delta\xi_1 &= -(-1)^i b\, \sigma_i \{\sin\phi_c - \sin\phi_i - \lambda\,\Delta\phi_i\} \; ; \\ \Delta\xi_2 &= -(-1)^i b\, \sigma_i \{\cos\phi_i - \cos\phi_c\} \; ; \end{aligned}\right\} \qquad 5.4\text{-}22.$$

Now let $Q(t_i)$ be some point on the line joining the points $T(t_c)$ and $I(t_c)$ at the instant t_i (see Figure 10). Now further demand that the point $Q(t_i)$ be chosen such that:

$$\overrightarrow{I(t_i), Q(t_i)} \cdot \underline{i}_1(t_c) = 0 \, .$$

and realize that in general we may write (see Figure 11):

$$\overrightarrow{T(t_i), I(t_i)} + \overrightarrow{I(t_i), Q(t_i)} = \overrightarrow{T(t_i), T(t_c)} + \overrightarrow{T(t_c), Q(t_i)} \, ,$$

which may be written in the form:

$$-\overrightarrow{I(t_i), T(t_i)} + \overrightarrow{I(t_i), Q(t_i)} = \overrightarrow{T(t_c), Q(t_i)} + \overrightarrow{O, T(t_c)}$$

$$+ (-1)\ \overrightarrow{O, T(t_i)} \; ; \qquad 5.4\text{-}23.$$

Now since $\overrightarrow{I(t_i), Q(t_i)}$ is perpendicular to $\underline{i}_1(t_c)$ it can therefore be expressed in the form:

$$\overrightarrow{I(t_i), Q(t_i)} = d_i\, \underline{i}_2(t_c) \; ; \qquad 5.4\text{-}24,$$

for some real scalar d_i. Now since $\overrightarrow{T(t_c), Q(t_i)}$ is parallel to the line through $I(t_c)$ and $T(t_c)$ it is therefore parallel to the vector $\underline{i}_1(t_c)$ and hence a scalar η_i will exist such that:

$$\overrightarrow{T(t_c), Q(t_i)} = \eta_i\, \underline{i}_1(t_c) \; ; \qquad 5.4\text{-}25.$$

Now using 5.4-24, 5.4-25 and the definitions 5.2-D5 and 5.2-D9, Equations 5.4-23 take the form:

$$-R_i\,\underline{i}_1(t_i) + d_i\,\underline{i}_2(t_c) = \left\{\underline{y}(t_c) - \underline{y}(t_i)\right\} + \eta_i\,\underline{i}_1(t_c)\ ,$$

and subsequently we can show that the above takes the form:

$$-R_i\,\underline{i}_1(t_i) + d_i\,\underline{i}_2(t_c) = -(-1)^i \sigma_i\, b\,\lambda\,\Delta\phi_i\,\underline{m}_1 + \eta_i\,\underline{i}_1(t_c)\ ; \qquad 5.4\text{-}26.$$

Now resolving the vectors in 5.4-26 perpendicular to the line of sight existing at the instant t_c (see Figure 11) we get:

$$\sin\left(\underline{i}_1(t_i) : \underline{i}_1(t_c)\right) = -\frac{d_i}{R_i} + \frac{(-1)^i \sigma_i \lambda\, b}{v R_i}\,\Delta\phi_i \sin\phi_c\ ; \qquad 5.4\text{-}27,$$

where we have used the additional fact that

$$\sin\beta_c = \sin\theta_c = \frac{\sin\phi_c}{v}\ .$$

Now by repeated use of Theorem 5.1-1 it is possible to show:

$$\Delta\theta_i = 2\pi m + \left(\underline{i}_1(t_i) : \underline{i}_2(t_c)\right)\ ,\quad m \in \mathrm{JI}\ ;$$

and on taking the sine of this last equation we can then put 5.4-27 in the form:

$$\sin\,\Delta\theta_i = -\frac{d_i}{R_i} + (-1)^i \frac{\sigma_i \lambda\, b}{v R_i}\,\Delta\phi_i \sin\phi_c\ ; \qquad 5.4\text{-}28.$$

Thus far we have been merely able to show how $\sin\Delta\theta_i$ may be expressed in terms of known quantities save d_i and b. It now remains to find d_i and b in terms of known quantities. First, in order to obtain d_i consider Equation 5.3-1 in the form:

$$\underline{z}(t) - \underline{y}(t) = -R(t)\,\underline{i}_1(t)\ ; \qquad 5.4\text{-}29.$$

On evaluating Equation 5.4-29 at the instants t_c and t_i and then subtracting the resulting equations we have:

$$\left\{\underline{z}(t_c) - \underline{y}(t_c)\right\} - \left\{\underline{z}(t_i) - \underline{y}(t_i)\right\} = -R(t_c)\,\underline{i}_1(t_c) + R_i\,\underline{i}_1(t_i)\ ; \qquad 5.4\text{-}30.$$

Now clearly we can write:

$$\underline{z}(t) - \underline{y}(t) = \underline{k}_1 \left\{ \underline{k}_1 \cdot \left(\underline{z}(t) - \underline{y}(t) \right) \right\} + \underline{k}_2 \left\{ \underline{k}_2 \cdot \left(\underline{z}(t) - \underline{y}(t) \right) \right\} ,$$

and using 5.2-D24 and 5.2-D25 this yields:

$$\underline{z}(t) - \underline{y}(t) = \underline{k}_1 \xi_{1_2}(t) + \underline{k}_2 \xi_{2_2}(t) \; ; \qquad 5.4\text{-}31.$$

Now on evaluating 5.4-31 at the instants t_c and t_i, subtracting the resulting equations and finally substituting back into 5.4-30 we arrive at:

$$\underline{k}_1 \left\{ \xi_{1_1}(t_c) - \xi_{1_1}(t_i) \right\} + \underline{k}_2 \left\{ \xi_{2_2}(t_c) - \xi_{2_2}(t_i) \right\} = - R(t_c) \; \underline{i}_1(t_c) + R_i \; \underline{i}_1(t_i) ,$$

wherein we now substitute from 5.4-26 to get:

$$\underline{k}_1 \Delta \xi_{1_1} + \underline{k}_2 \Delta \xi_{2_2} = (- R(t_c) - \eta_i) \, \underline{i}_1(t_c) + d_i \, \underline{i}_2(t_c) + (-1)^i \sigma_i \Delta \phi_i \lambda b \, \underline{m}_1 \qquad 5.4\text{-}32.$$

On resolving the vectors in 5.4-32 perpendicular to the line of sight existing at the instant t_c one can show:

$$d_i = - \sin\theta_c \; \Delta \xi_{1_1} + \cos\theta_c \; \Delta \xi_{2_2} + (-1)^i \sigma_i b \lambda \Delta \phi_i \sin\beta_c ,$$

and further since $\sin\beta_c = \sin\theta_c$ and substituting from 5.4-22 there results:

$$d_i = -(-1)^i b \sigma_i \Big[- \sin\theta_c \left\{ \sin\phi_c - \sin(\phi_c - \Delta\phi_i) - \lambda \Delta\phi_i \right\} + \cos\theta_c \left\{ \cos(\phi_c - \Delta\phi_i) - \cos\phi_c \right\} \Big] + (-1)^i \sigma_i b \lambda \Delta\phi_i \sin\theta_c \; ; \qquad 5.4\text{-}33.$$

If now we apply Equations 5.4-7, then 5.4-33 becomes:

$$d_i = \frac{(-1)^i \sigma_i \dot{z}^2}{ngv} \left\{ (1 - \cos\Delta\phi_i)(1 - \lambda\cos\phi_c) - \lambda \sin\phi_c (\Delta\phi_i - \sin\Delta\phi_i) \right\} + \frac{(-1)^i \sigma_i \dot{z}^2}{ngv} \; \lambda \Delta\phi_i \sin\phi_c \; ; \qquad 5.4\text{-}34.$$

In obtaining 5.4-34 we note that the relation $b = \frac{\dot{z}^2}{ng}$ has been used. Now 5.4-34 can further be reduced to the form:

$$d_i = \frac{(-1)^i \sigma_i \dot{z}^2}{ng\nu}\left\{(1-\cos\Delta\phi_i)(1-\lambda\cos\phi_c) + \lambda\sin\phi_c\sin\Delta\phi_i\right\};$$

5.4-35.

If we were to have $\cos\Delta\theta_i < 0$ then this in turn would imply that:

$$\frac{\pi}{2} < |\Delta\theta_i| < \frac{3\pi}{2}$$

and this inequality certainly represents a ridiculous physical situation and thus we must have that $\cos\Delta\theta_i > 0$ and thus:

$$\cos\Delta\theta_i = \sqrt{1-\sin^2\Delta\theta_i}\ ;$$

5.4-36.

At this point the problem of determining ΔR_i in terms of the variables $R_i, n, \dot{z}, \dot{y}, \phi_c$ and $\Delta\phi_i$ is complete as seen from the Equations 5.4-7, 5.4-8, 5.4-35, 5.4-28 and 5.4-36. However, this can be seen much more easily if the pertinent equations already developed are presented in a more revealing sequence, namely:

$$\lambda = \frac{\dot{y}}{\dot{z}}\ ,$$

$$\nu = +\sqrt{1+\lambda^2-2\lambda\cos\phi_c}\ ,$$

$$\sigma_i = \frac{\Delta\phi_i}{|\Delta\phi_i|}\ ,$$

$$d_i = \frac{(-1)^i\sigma_i\dot{z}^2}{ng\nu}\left\{(1-\cos\Delta\phi_i)(1-\lambda\cos\phi_c)+\lambda\sin\phi_c\sin\Delta\phi_i\right\},$$

$$\sin\Delta\theta_i = -\frac{d_i}{R_i} + \frac{(-1)^i\sigma_i\Delta\phi_i\lambda\dot{z}^2}{ng\nu R_i}\sin\phi_c\ ,$$

$$\cos\Delta\theta_i = +\sqrt{1-\sin^2\Delta\theta_i}\ ,$$

$$A_i = \lambda \sin\phi_c(1-\cos\Delta\phi_i) - (1-\lambda\cos\phi_c)\sin\Delta\phi_i \; ; \qquad 5.4\text{-}37 ,$$

$$B_i = \lambda(\lambda-\cos\phi_c) - \lambda\sin\phi_c \sin\Delta\phi_i + (1-\lambda\cos\phi_c)\cos\Delta\phi_i \; ; \qquad 5.4\text{-}38 .$$

$$\frac{\Delta R_i}{R_i} = \frac{\lambda(\lambda-\cos\phi_c)\sin\Delta\theta_i - \lambda\sin\phi_c(1-\cos\Delta\theta_i)}{A_i\cos\Delta\theta_i + B_i\sin\Delta\theta_i} \; ; \qquad 5.4\text{-}39.$$

The last three equations evolve by substituting into 5.4-8 from 5.4-7 and a moderate amount of algebra following. However, the form in which the above equations have been presented is admittedly rather arbitrary; however, the criterion, by reason of which the above form has been choosen, is that the evaluation of a trigonometric function is a much more complicated computation digitally than are the basic arithmetic computations. Consequently, the number of sine and cosine functions having different arguments has been kept to a minimum.

5.5 Analytic Development of the Input Error

As given in Section 5.3 in Equation 5.3-9 the approximate range equations to be analyzed here are:

$$\tilde{R}_i = \frac{\dot{z}}{\dot{\beta}(t_i)} \left\{ \sin\alpha_i - \sin\alpha_c \right\}, \; i = 1,2 \; ; \quad \ldots \quad 5.5\text{-}1 .$$

Now if for the moment, we assume that the variables $\dot{z}$, $\dot{\beta}(t_i)$, α_i and α_c are independent then from the calculus we have:

$$d\tilde{R}_i = \frac{\partial\tilde{R}_i}{\partial\dot{z}}\, d\dot{z} + \frac{\partial\tilde{R}_i}{\partial\dot{\beta}(t_i)}\, d\dot{\beta}(t_i) + \frac{\partial\tilde{R}_i}{\partial\alpha_i}\, d\alpha_i + \frac{\partial\tilde{R}_i}{\partial\alpha_c}\, d\alpha_c ,$$

and performing the indicated computations the above takes the form:

$$d\tilde{R}_i = \frac{(\sin\alpha_i - \sin\alpha_c)}{\dot{\beta}(t_i)} \left\{ d\dot{z} - \frac{\dot{z}\, d\dot{\beta}(t_i)}{\dot{\beta}(t_i)} \right\}$$

$$+ \frac{(\cos\alpha_i\, d\alpha_i - \cos\alpha_c\, d\alpha_c)}{\dot{\beta}(t_i)}\, \dot{z} \; ; \qquad 5.5\text{-}2 .$$

However, as explained in Section 3.4 we can put $d\alpha_i = d\alpha_c = d\alpha$ and interpret the differentials in 5.5-2 as physically corresponding to small changes or errors in the input information:

$\dot{z}$, $\dot{\beta}(t_i)$, α_i and α_c. Thus we have:

$$d\tilde{R}_i = \frac{(\sin\alpha_i - \sin\alpha_c)}{\dot{\beta}(t_i)}\left\{d\dot{z} - \dot{z}\,\frac{d\dot{\beta}(t_i)}{\dot{\beta}(t_i)}\right\}$$

$$+ (\cos\alpha_i - \cos\alpha_c)\,\frac{\dot{z}\,d\alpha}{\dot{\beta}(t_i)} \quad ; \qquad 5.5\text{-}3.$$

Now from Equations 5.4-3 and 5.4-7, the expression $(\sin\alpha_i - \sin\alpha_c)$ can be put in the form:

$$\sin\alpha_i - \sin\alpha_c = \frac{1}{\nu}\left\{C_i \sin\Delta\theta_i + D_i\cos\Delta\theta_i - \lambda\sin\phi_c\right\} ; \qquad 5.5\text{-}4,$$

where C_i and D_i are given by:

$$C_i = \lambda\sin\phi_c\sin\Delta\phi_i - (1-\lambda\cos\phi_c)\cos\Delta\phi_i \quad ; \qquad 5.5\text{-}5,$$

$$D_i = \lambda\sin\phi_c\cos\Delta\phi_i + (1-\lambda\cos\phi_c)\sin\Delta\phi_i \quad ; \qquad 5.5\text{-}6.$$

and where $\sin\Delta\theta_i$, $\cos\Delta\theta_i$ and ν have been determined as in Section 5.4.

On employing Equations 5.4-13 and the definitions in Section 5.2 the expression $(\cos\alpha_i - \cos\alpha_c)$ takes the form:

$$\cos\alpha_i - \cos\alpha_c = \frac{1}{\nu}\left\{D_i\sin\Delta\theta_i - C_i\cos\Delta\theta_i - (1-\lambda\cos\phi_c)\right\} ;$$

5.5-7

For a particular radar set $d\dot{z}$, $d\alpha$ and $d\dot{\beta}(t_i)$ will be given and hence in Equation 5.5-3 we see that all terms have been expressed in terms of R_i , n , $\dot{z}$, $\dot{y}$, ϕ_c and $\Delta\phi_i$, excepting $\dot{\beta}(t_i)$. Now from Equation 5.3-6 we can write:

$$\dot{\beta}(t_i) = -\frac{\dot{z}}{R_i}\left\{\lambda \sin\theta_i - \sin\alpha_i\right\} ; \qquad \ldots . \quad 5.5\text{-}8.$$

However, the term ($\lambda \sin \theta_i - \sin \alpha_i$) is the denominator of $\frac{\Delta R_i}{R_i}$ as seen in 5.4-1, and in 5.4-39 this has proven to take the form

$$\frac{1}{v}\left(A_i \cos\Delta\theta_i + B_i \sin\Delta\theta_i\right),$$

where A_i, B_i are given in 5.4-37, 5.4-38 respectively and $\sin \Delta\theta_i$, $\cos \Delta\theta_i$ from 5.4-28, 5.4-36 respectively. We have now shown that the input error $d\bar{R}_i$ can be expressed in terms of the known quantities R_i , n , $\dot{z}$, $\dot{y}$, ϕ_c , $\Delta\phi_i$, $d\dot{z}$ and $d\alpha$, $d\dot{\beta}(t_i)$. However, as in Section 5.4 we shall now give a sequence of equations which will make this fact much more evident.

$$\lambda = \frac{\dot{y}}{\dot{z}} ,$$

$$\sigma_i = \frac{\Delta\phi_i}{|\Delta\phi_i|} ,$$

$$v = +\sqrt{1 + \lambda^2 - 2\lambda\cos\phi_c} ,$$

$$d_i = \frac{(-1)^i \sigma_i \dot{z}^2}{n g v}\left\{(1-\cos\Delta\phi_i)(1-\lambda\cos\phi_c) + \lambda \sin\phi_c \sin\Delta\phi_i\right\},$$

$$\sin\Delta\theta_i = -\frac{d_i}{R_i} + \frac{(-1)^i \sigma_i \dot{z}^2 \Delta\phi_i}{n g v R_i} \sin\phi_c ,$$

$$\cos\Delta\theta_i = +\sqrt{1 - \sin^2\Delta\theta_i} ,$$

$$C_i = \lambda \sin\phi_c \sin\Delta\phi_i - (1-\lambda\cos\phi_c)\cos\Delta\phi_i ,$$

$$D_i = \lambda \sin\phi_c \cos\Delta\phi_i + (1-\lambda\cos\phi_c)\sin\Delta\phi_i .$$

$$\sin\alpha_i - \sin\alpha_c = \frac{1}{v}\left\{D_i\cos\Delta\theta_i + C_i\sin\Delta\theta_i - \lambda\sin\phi_c\right\},$$

$$\cos\alpha_i - \cos\alpha_c = \frac{1}{v}\left\{D_i\sin\Delta\theta_i - C_i\cos\Delta\theta_i - (1-\lambda\cos\phi_c)\right\},$$

$$A_i = \lambda\sin\phi_c - D_i ,$$

$$B_i = \lambda(\lambda - \cos\phi_c) - C_i ,$$

$$\dot{\beta}(t_i) = -\frac{\dot{z}}{v R_i}\left\{A_i\cos\Delta\theta_i + B_i\sin\Delta\theta_i\right\},$$

$$d\bar{R}_i = \frac{(\sin\alpha_i - \sin\alpha_c)}{\dot{\beta}(t_i)}\left\{d\dot{z} - \frac{\dot{z}\,d\dot{\beta}(t_i)}{\dot{\beta}(t_i)}\right\} + \frac{\{\cos\alpha_i - \cos\alpha_c\}\dot{z}\,d\alpha}{\dot{\beta}(t_i)}.$$

6.0 REFERENCES

1. Project Lamp Light, Volume II; Appendices 9-P and 9-R; March 15, 1955; D.R.B. Acc. No. 55/4751; SECRET.

2. Vector and Tensor Analysis, H. Lass; McGraw Hill, 1950; UNCLASSIFIED.

3. A Study to Determine the Effectiveness of the CF-100 Mk. 4B Armed with Sparrow II Missiles Against a Type 37 Bomber, Appendix M; CARDE Tech. Memo No. 119/55, October 1955; SECRET.

FIGURE 1

(a) $\phi > 0$, HENCE THE SENSE OF BOTH VECTORS IS THE SAME

(b) $\phi < 0$, HENCE THE SENSE OF ONE VECTOR IS OPPOSITE THE SENSE OF THE OTHER

FIGURE 2

(SPACE COORDINATES)

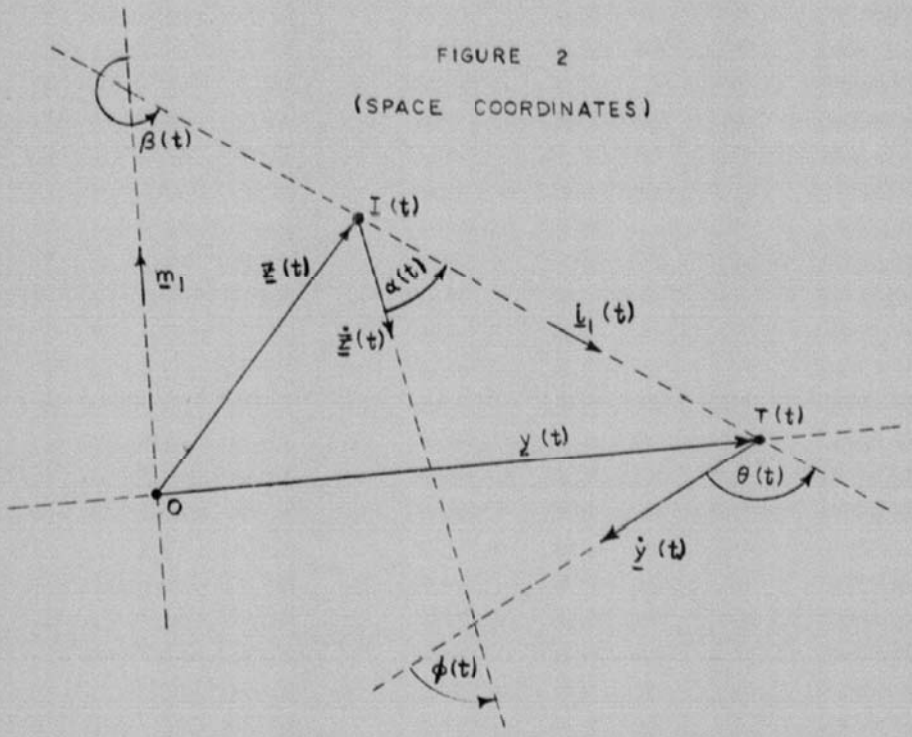

FIGURE 3

(IN TARGET COORDINATES)

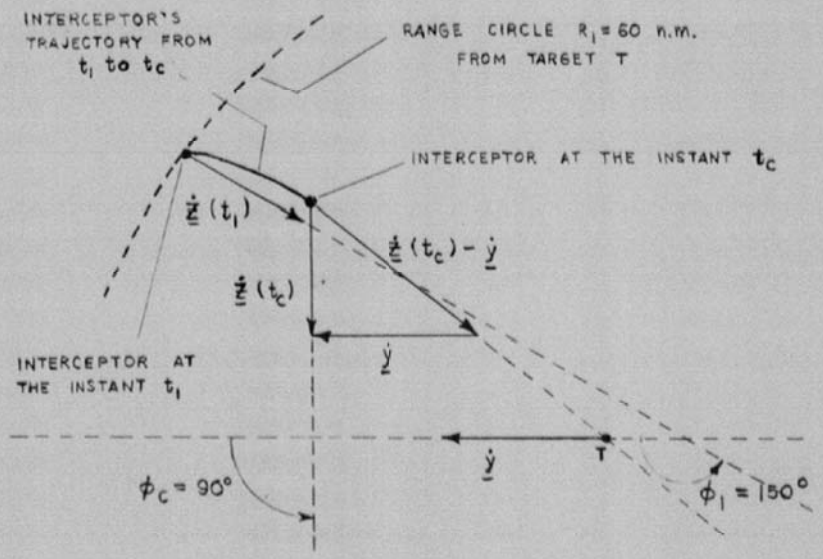

FIGURE 4

(IN TARGET COORDINATES)

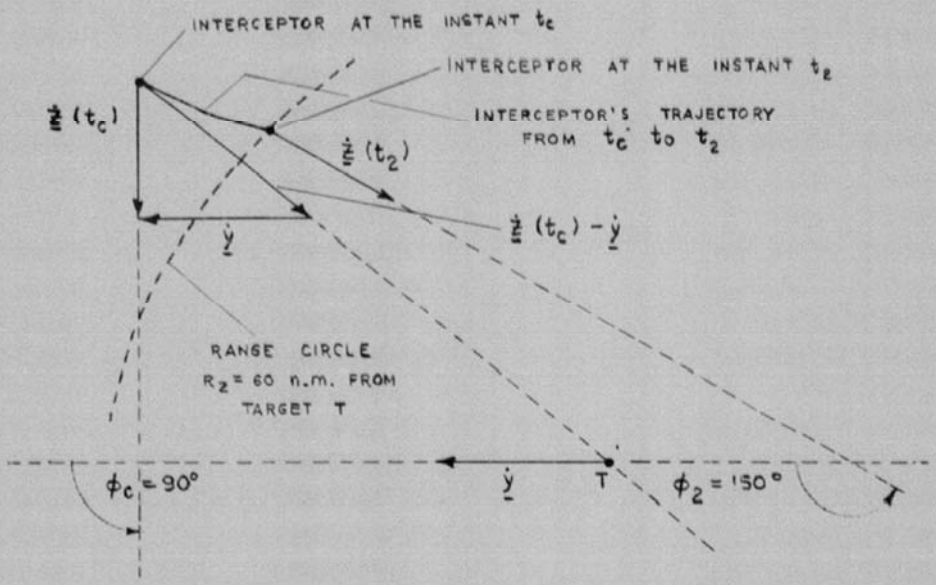

FIGURE 5

(SPACE COORDINATES)

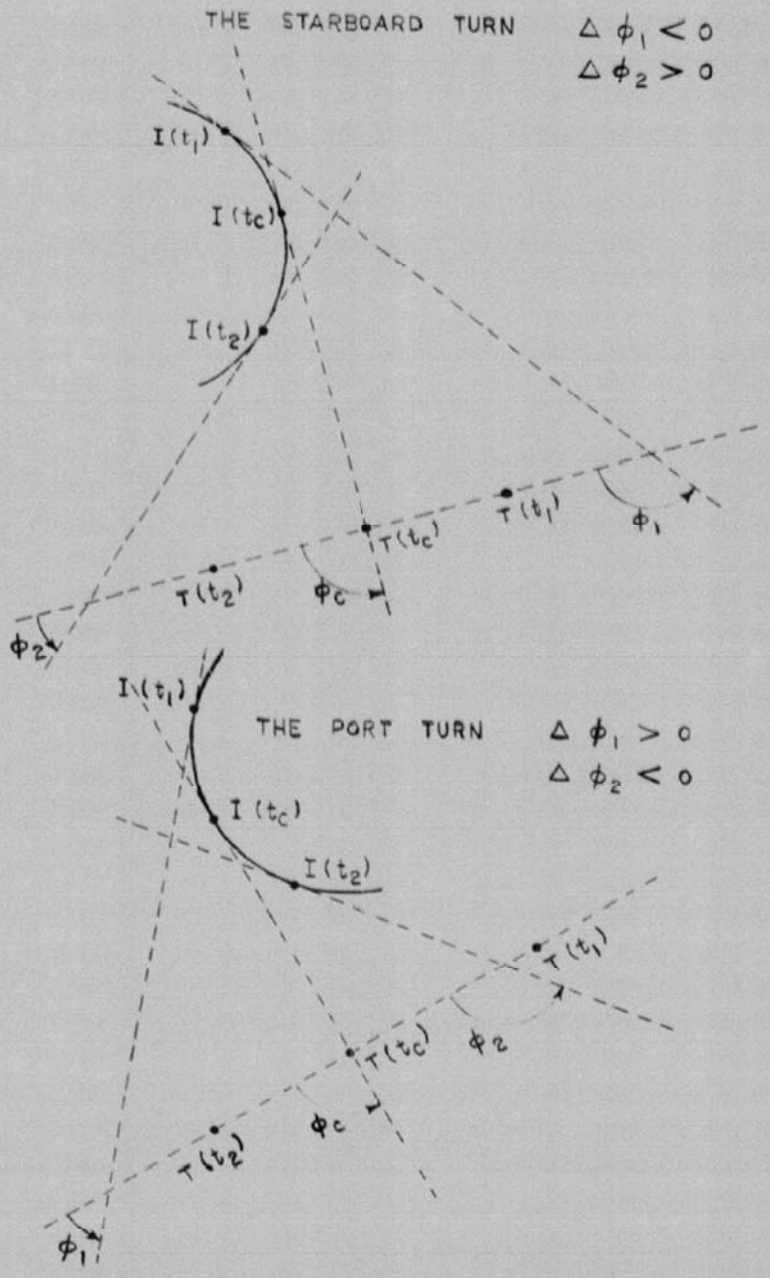

FIGURE 6

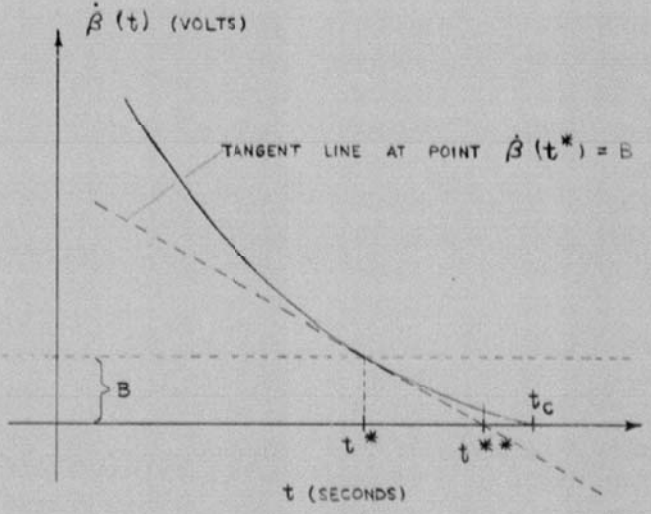

FIGURE 7

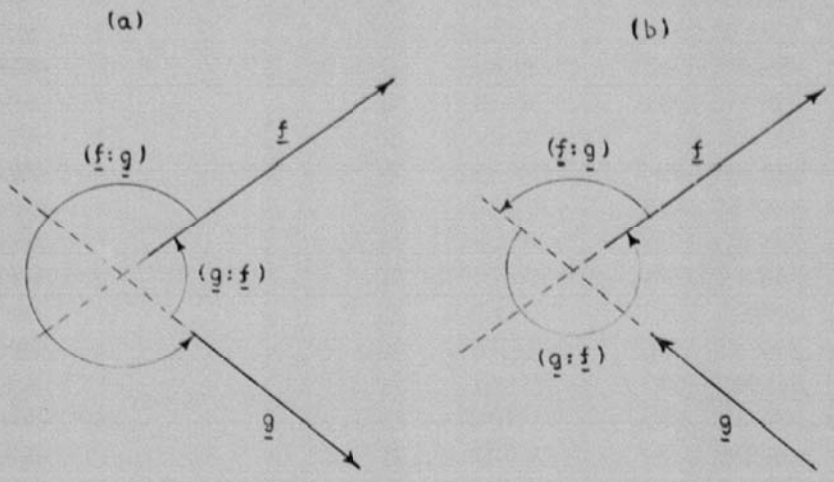

FIGURE 8

(SPACE COORDINATES)

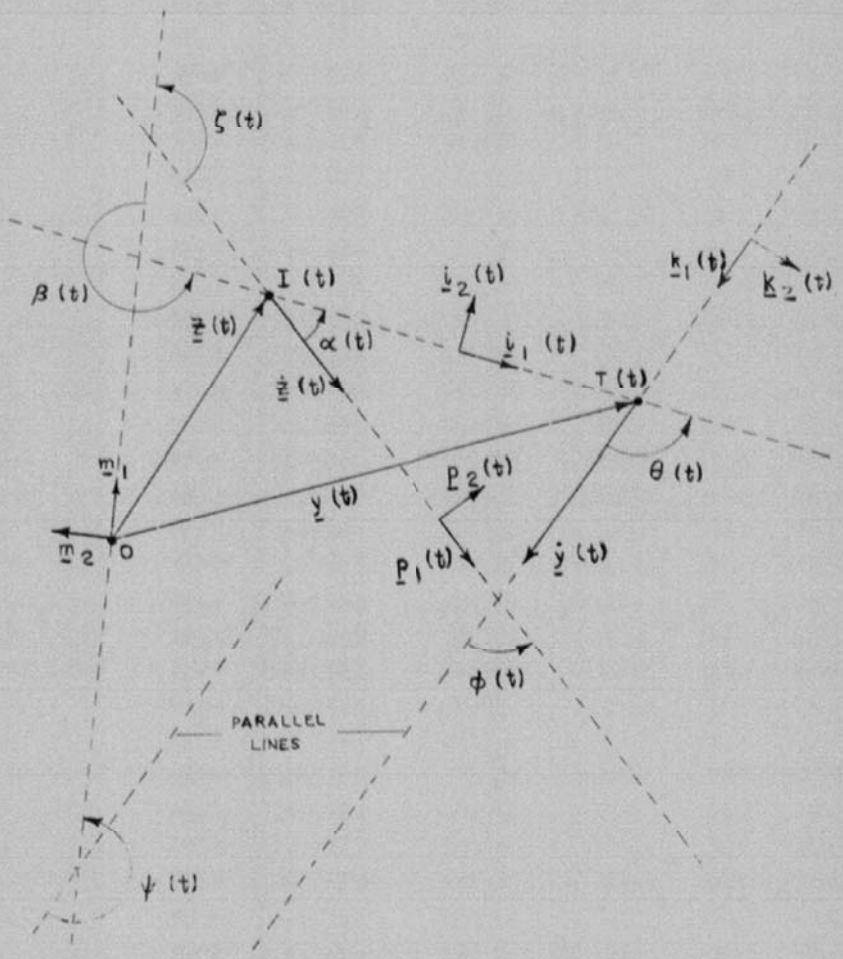

FIGURE 9

(SPACE COORDINATES)

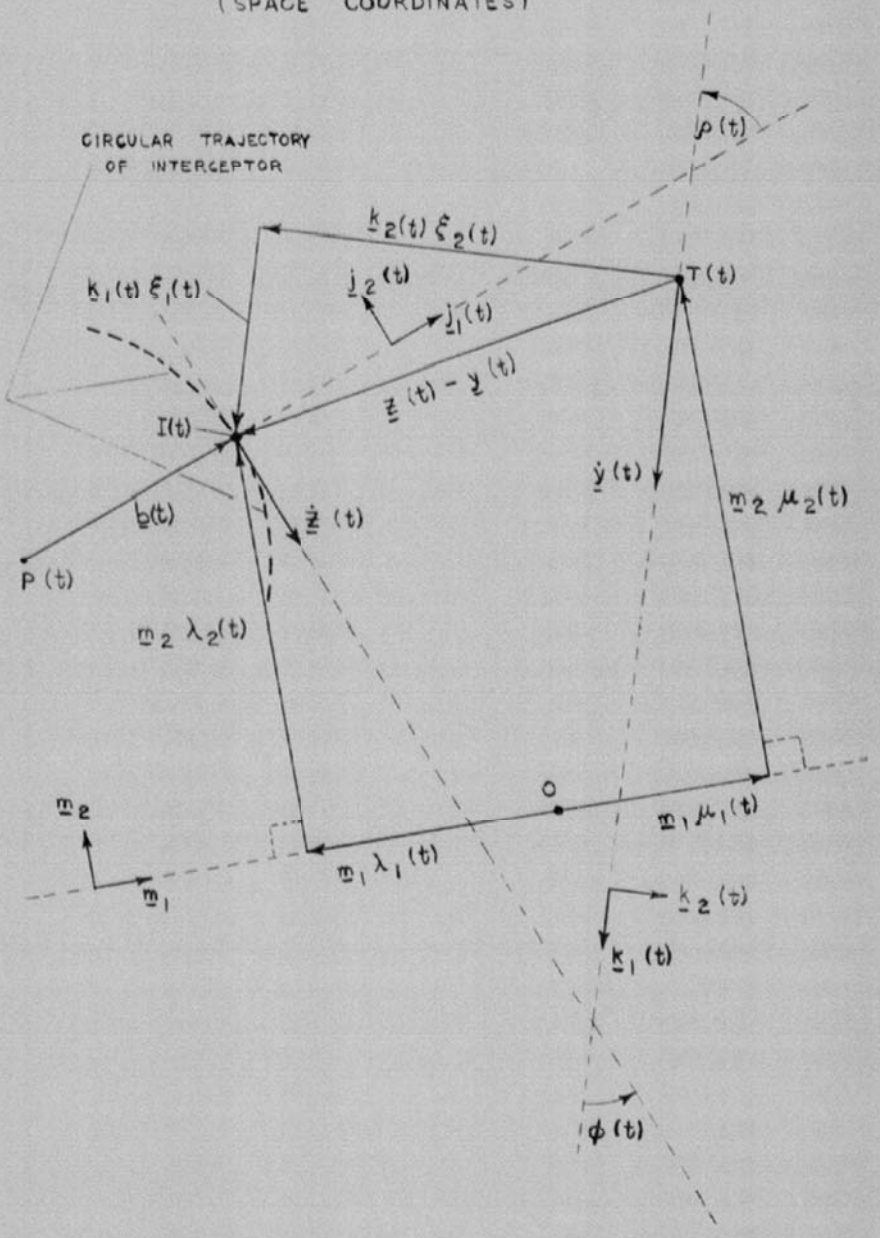

FIGURE 10
(SPACE COORDINATES)

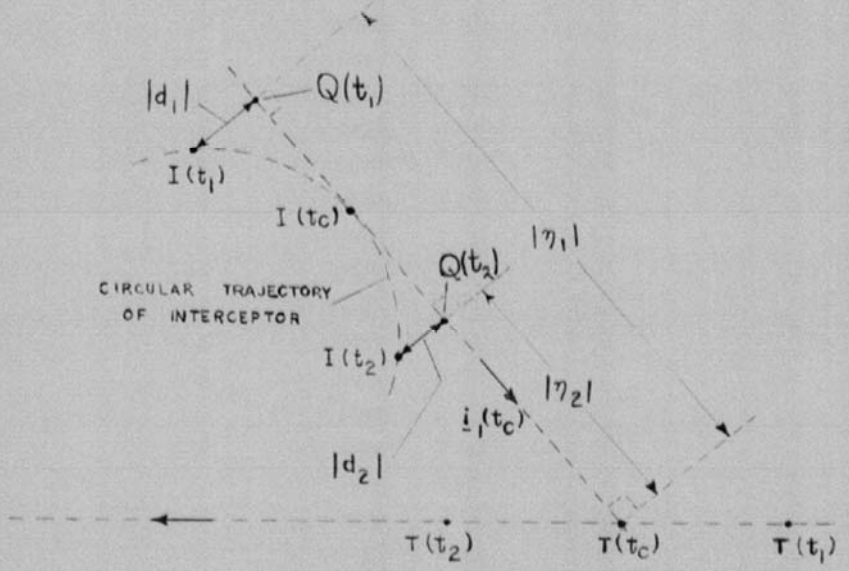

FIGURE 11
(SPACE COORDINATES)

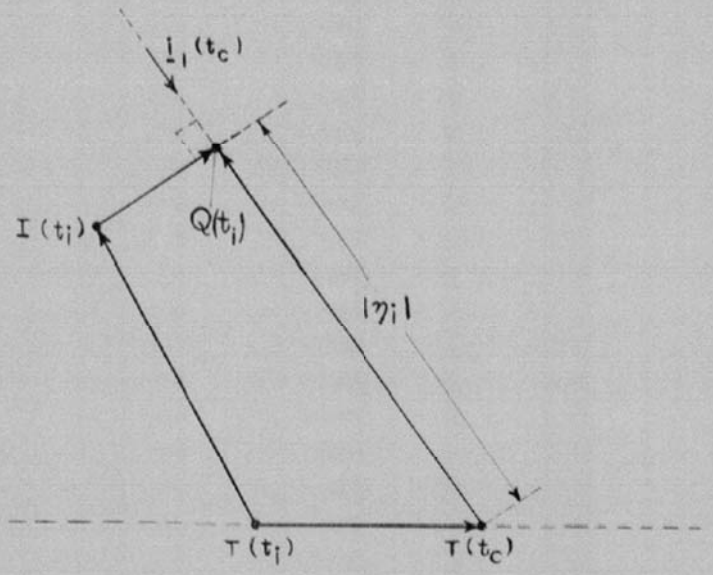

APPENDIX

Fire Control

J.P. Regniere

The shortage in personnel reported in our last progress report has finally been cured by the addition of two engineers to the fire control group. This addition was made rather late in the reported period, but active work on the fire control problem is now well underway.

The program has been divided into two phases which were determined by the time limitations imposed on the study. The first phase is based upon the evaluation of the RCA Proposal as compared to the RCAF Specification Air 7-6, with emphasis being put on the Astra I system. This phase of the study has been progressing satisfactorily. The second phase will be applied to more futuristic thinking along the lines of the Astra II system.

Since the basic governing factors of a fire control system are determined by the geometry of the interception, it appears that the most pressing subject of investigation should be computer modes of operation in order to find out which modes would be more desirable and to evaluate if the proposed modes are sufficient and adequate.

The Basic Modes Proposed are:

1) Lead Pursuit

2) Lead Collision

3) Snap up

4) Optical

A quick survey of the above mentioned modes seems to indicate that the exclusive use of one does not result in a completely satisfactory approach for missiles, but that a combination of two or more of them is preferable. Lead pursuit courses naturally tend to bring the interceptor into a tail chase and result in long interception times and become totally ineffective when the target flies faster than the interceptor. The lead collision course does not present those disadvantages but results in a single firing point and hence, does not utilize the full capability of the missile launch zone. Therefore it has been suggested that a combination of the two modes be used; that is, the interceptor would fly a lead-collision course until it reached the missile's maximum launch range and then a lead-pursuit until minimum launch range.

Some work has already been done on this subject and some experimental results have been obtained in a previous CF-100 study, but not enough data are available in order to make a decision in favour of one or another form of navigation. The most desirable means of acquiring this information would be the use of the REAC but since this facility might not be available for this work until the end of December, it is proposed to obtain all possible information by modification and extension of the present graphical two-dimensional placement method, and by analytical studies.

Some problems can not be answered by two-dimensional analysis, and three-dimensional studies will be needed. An attempt will be made to determine whether it is preferable to compute and fly in the inclined plane or the horizontal plane. This will bring in new tactics such as pitch-up and snap-up. These special tactics will require careful attention, both in terms of the possibility and ease of mechanization. Snap-up will be studied carefully since it is suggested in the RCA proposal. Studies should determine what course is to be flown to reach the predicted point where snap-up should commence, when the manoeuvre should be initiated, what steering signals should be given during snap-up and after the missiles are launched. Liaison with RCA will be essential if CARDE is to be up-to-date on the contractor's developments.

The second phase of the study is not well defined as yet. Among the problems likely to be studied are:

1) The effect of aspect angle on miss distance and lethality

2) Snap-up attack

3) Possibility and importance of speed-control tie-in with fire control, especially for nose or head-on attacks

4) Special manoeuvres to obtain range on a jammer

5) The effect of having a variable F rather than a fixed F in the computation of the lead-collision course.

This phase is left undetermined intentionally so that the results of phase I may be used and also to permit the introduction of any new problems which may arise as a result of phase I.

APPENDIX J

Vulnerability Considerations

J.T. Baker

Introduction

Considerations of combat aircraft vulnerability to attack may, in a broad sense, embrace many aspects of military strategy. Such studies affect the prediction of attrition rates, armament design, combat tactics, the design of the aircraft itself and lethality evaluations of weapon systems intended to destroy it.

In a more confined sense the term "aircraft vulnerability" may designate the extent to which an aircraft is likely to sustain certain specified categories of damage when the weapon directed against it either strikes or explodes within some prescribed zone around it. It is in this more particular sense that the term is used herein.

Current Vulnerability Studies

Studies are proceeding, within the Systems Group, to establish reliable methods of assessing the vulnerability of present and near future enemy aircraft targets such as the USSR "Bear" and projected supersonic bombers of the 1960-65 era.

It is of course necessary to stipulate the nature of the weapon with which the target under consideration is opposed, as it is clear that the degree of vulnerability of various sections and components of the target is dependent upon the size, energy and general nature of the weapon acting to destroy it. For instance, penetration of the crew pressure cabin by a single $\frac{1}{4}$ oz fragment would cause only negligible damage while penetration by a small H.E. sub-projectile, which explodes upon entry, may well result in a K K Kill. It is evident therefore, that some weapon reference is necessary as the basis for such assessments.

As a weapon reference for the present work, warheads of the Controlled Fragmenting and Continuous Rod types having a total weight of approximately 65 lbs are implied as the payload of the weapon system.

Further, in view of the bomb types likely to be carried by such targets, considerations of vulnerability will be restricted to the following categories of damage.

KK. Immediate disintegration

K. Immediate loss of control

A. Loss of control within five minutes

Possible Methods of Vulnerability Assessment

Until comparatively recently vulnerability assessments have been arrived at by employing one of the following basic approaches.

The first of these consists of analysing operational statistics, available at the conclusion of a period of war, and correlating with this, data acquired by inspection of damage inflicted on aircraft which returned during the combat period under consideration. The second takes the form of analysing the results of ground firing trials conducted against representative aircraft and aircraft components. Unfortunately results obtained by these methods alone are by no means conclusive and at best relate only to the specific aircraft and weapons used.

When faced with the problem of evaluating the vulnerability of modern near sonic and supersonic enemy bomber targets it is not possible to rely on statistical data pertaining to World War II losses, as such information bears very little or no relation to the problem. Further, data of this nature is not readily amenable to extrapolation over the intervening decade, as vast changes have taken place in the concept of the heavy bomber and weapon systems to counter it.

Present day and near future targets are approximately twice the size, about three times the weight, fly roughly twice as fast with about double the altitude capability besides employing a form of propulsion which uses much safer fuels. Furthermore, these aircraft have been built with vulnerability considerations well integrated into their design.

Weapon systems too, have changed radically being far more complex in nature, and it is hoped, more effective than those employed in World War II.

For similar reasons results produced as a result of firing trials against aircraft and their components are equally unrealistic unless it is possible to obtain samples of modern enemy aircraft for trial purposes. However, even if this were feasible, reliable data could only be collected by an exhaustive program conducted under realistic conditions. This would necessarily involve the target aircraft being manned and flown under combat conditions.

In view of the foregoing, it would seen that the best approach to vulnerability assessments of modern enemy aircraft is to proceed by means of analytical processes using as basic data, technical information available from intelligence sources and supplementing this where necessary with data pertaining to our own contemporary aircraft of similar design.

This approach is being followed in the current studies but as yet insufficient quantative data has been generated to warrant publication in this appendix.

Close co-operation with the Directorate of Air Intelligence R.C.A.F. has resulted in the accumulation of much useful information on the structure, equipment and performance of certain Russian heavy bombers including the Bear and Bison. This data is being closely studied and supplemented where necessary from other sources to permit a quantitative vulnerability assessment of individual components and "areas" of the target.

Quantitative investigations are proceeding to establish penetration and shatter performances of fragments possessing various energies and of the "chopping" capability of rod rings against the various materials of which the target structure is built up.

When the results of these investigations are available more detailed studies of the probability of inflicting kills on individual vital components, systems and structures can be proceeded with, as the energy of fragments or rods after penetration of the aircraft skin and protective casings will then be known.

For purposes of vulnerability analysis, an aircraft may be considered as made up of the following sub-systems, any of which if damaged sufficiently may lead to destruction of the aircraft itself.

a. Pressure Cabin (Crew)

b. Fuel System

c. Power Plant

d. Airframe (Main structure)

e. Flight controls and essential ancillary equipment such as cabin pressurization apparatus.

The sensitivity of these sub-systems to damage is therefore receiving close attention.

Terminal Engagement Simulator

In order to correlate the data which will be generated as a result of vulnerability, fuze, warhead and guidance studies which are now proceeding, a terminal-engagement simulator for use with $\frac{1}{48}$ scale models has been designed.

This equipment, to-gether with scale models of the USSR Bear and a hypothetical supersonic, missile-shaped bomber will be ready for use during the current period.

A sketch of the simulator is given in Figure 1. The apparatus was designed to afford the target rotational freedom in three mutually perpendicular planes, A, B and C Fig. 1. The warhead has freedom of translational movement also in three planes, D, E, F .

By means of a programmed, sequential use of the degrees of movement available, the warhead can be systematically positioned at any desired distance and aspect relative to the target.

Simulation of the warhead burst pattern, which is a function of target/fragment relative velocity is achieved by means of a light source surrounded by a metal hemisphere, suitably drilled to produce rays of light representing the path of each fragment. The requisite kinematic configuration of burst patterns for various sets of conditions to be investigated will be simulated by using several suitably drilled interchangeable hemispheres.

Figure 2. gives a sketch of the warhead assembly and shows simulated fragment holes produced by a near "burst".

Simulation of continuous rod warhesds will be achieved in a similar fashion, the metal hemisphere being suitably slotted to produce kinematic representation of the expanding ring of rods.

Use of this simulator will permit examination of the individual distributions of fragments or rod cuts on the target, and will facilitate correlation of the data accumulated on guidance accuracy, fuze triggering point and warhead characteristics to assess terminal lethality.

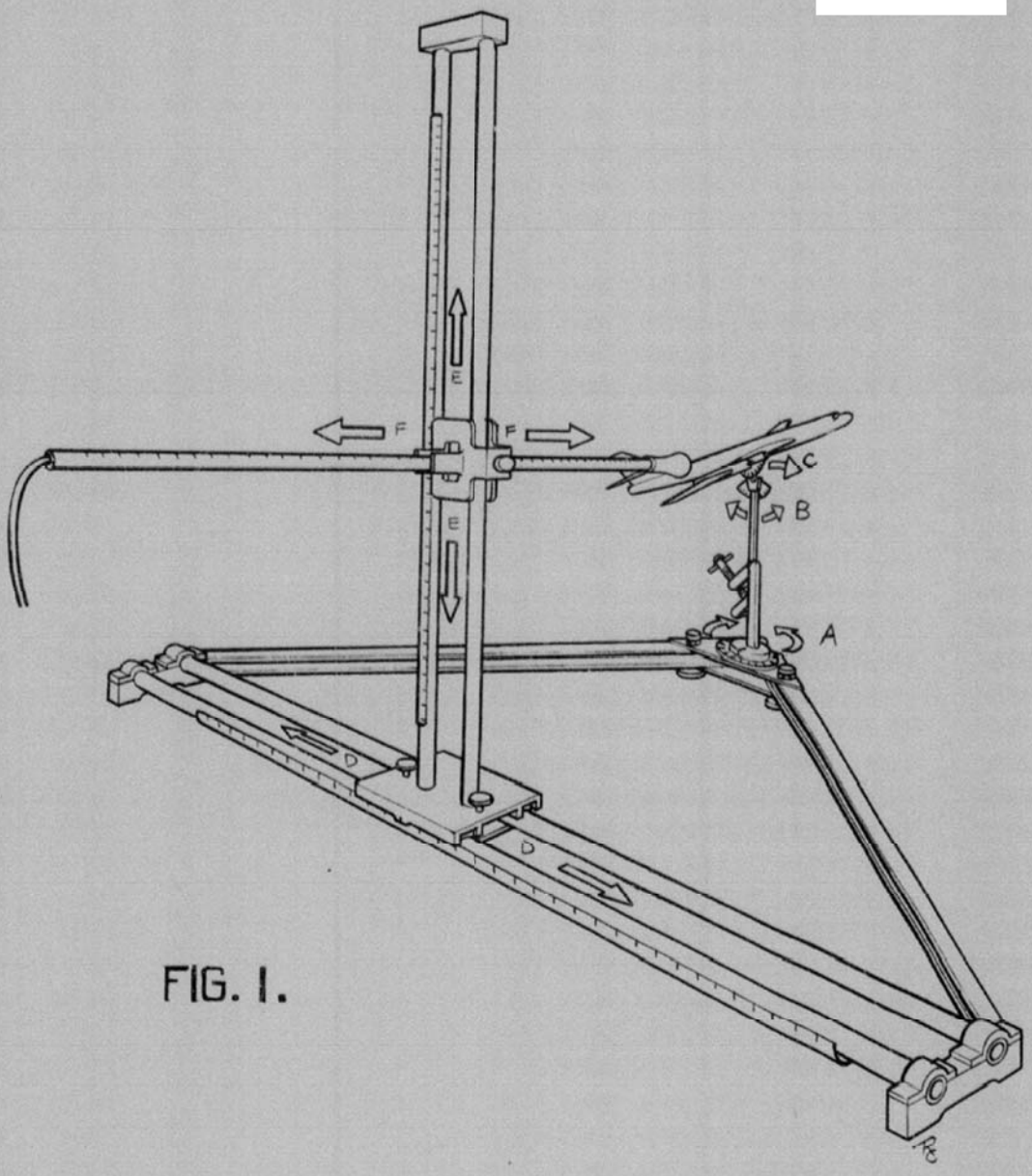

FIG. 1.

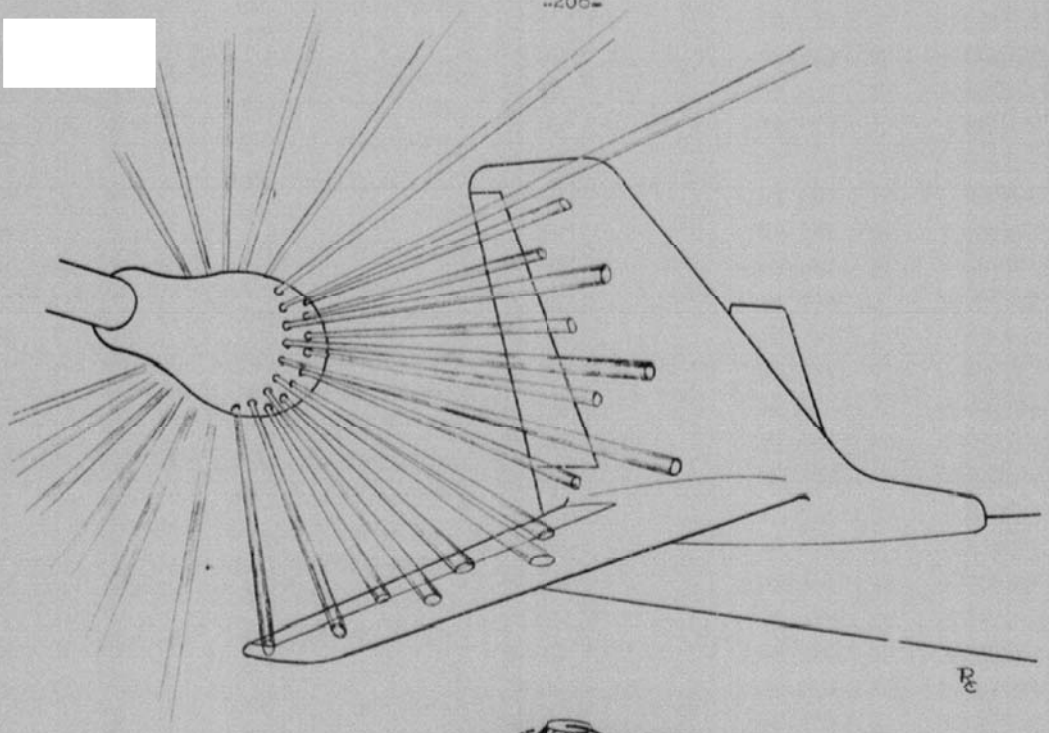

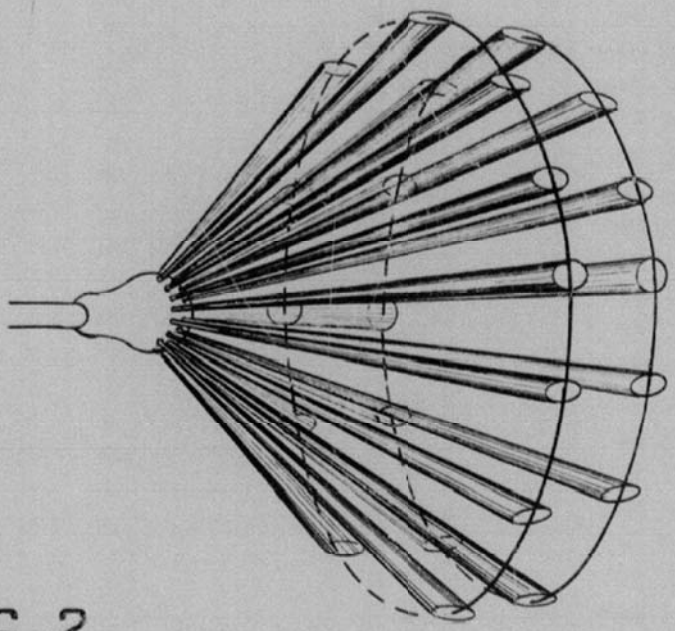

FIG. 2.

APPENDIX K

Placement Probability (Supersonic Targets)

J. MacFarlane

NOTE: Publication of this body of results on placement probabilities is undertaken at this time in order to show the progress which has been made in the study. The results have not been exhaustively analysed; CARDE prefers to wait until work on evading targets has been completed in order to discuss fully interceptor effectiveness against supersonic targets.

1.0 The methods used at CARDE in deriving placement probabilities have been discussed in previous publications (References 1 and 2). In order that this appendix may be read with some understanding of the underlying work, these are reviewed here.

2.0 The Placement Chart

The first step in computing probability of placement for an interceptor is preparation of a placement chart. This is a way of showing into what region of space relative to a target, the ground control must be capable of putting an interceptor, if the aircraft is to be able to get into position for launching its missiles. The chart is drawn in target coordinates for a given set of values of a large number of parameters. Quantities which must be defined before the positioning diagram may be drawn are:

Target Mach Number M_T
Interceptor Mach Number M_I
Initial course difference of interceptor and target ϕ_i
Target evasion n_T
Interceptor lateral acceleration n_I
AI radar look angle γ
Missile launch zone

2.1 Missile Launch Zone. The missile launch zone must be known. The information needed includes the value of correct heading of the missile at launch as a function of aspect with respect to the target, and the allowable launch heading error at various ranges and aspects. The launch zones which were used at CARDE were based on those published in a previous CARDE Technical Letter (Reference 3). Figures L-1 to L-13 at the end of this appendix give the actual zones which were used for the various cases.

2.2 Interceptor Turns. In preparation of placement charts, the trajectory in target coordinates of an interceptor making a circular horizontal turn must be available in the form of a template. This may be prepared by a simple method described in reference 1. The curve is called a trochoid.

3.0 Preparation of Placement Chart for Non-Evading Target

3.1 The Fall Back Barrier. This is a kinematic barrier existing in cases where the interceptor speed is equal to or less than the target speed; it is a line in target space behind which the interceptor must not fall, if it is to be able to make an interception. Its position varies with speed ratio of target and interceptor. When the interceptor is on this limiting line, its relative velocity with respect to the target is perpendicular to the interceptor velocity vector. The course difference for which this occurs may be called the critical course difference ϕ_c, whose value is arc cos (V_I/V_T). The corresponding "angle-off" of the interceptor from the target is θ_c = arc sin (V_I/V_T). The line along which the interceptor can drift into the target at this critical course difference and end up at a correct launch point is the fall-back barrier. It is drawn by finding the point on the launch zone for which the correct course difference is ϕ_c, and drawing through it a line making the angle θ_c with the target path. If missile heading error allowance ϵ is to be considered, the point $(\phi_c - \epsilon)$ on the launch zone is taken instead.

In preparation of a chart for a particular initial course difference ϕ_i of the interceptor, the line at which the aircraft must commence its turn so as to end up on the fall-back barrier with the critical course difference is found by using the turn trochoid. It is held tangent to the fall-back barrier, at the point ϕ_c on the trochoid. Then the point ϕ_i on the trochoid is a point on the effective barrier.

3.2 The Rear Look Angle Barrier. In general for an interceptor on course difference ϕ there is a line through the target at an angle $\Psi = 180° - (\phi + \gamma)$ behind which the interceptor must not be if it is to see the target. Many such lines may be drawn for various course differences. Now to each value of ϕ there corresponds an approach line, passing through a point on the launch zone for which ϕ is the correct course difference. This approach line makes an angle Θ with the target path, Θ being thus the angle between the target velocity vector and the relative velocity vector. Where each approach line meets the corresponding look angle line drawn at an angle Ψ through the target, is a point on the basic look angle barrier. If a few points on the barrier are found it may then be drawn. It is to be noted that each point on it corresponds to some value of course difference ϕ of the interceptor after its correcting turn.

The effective look angle barrier for an interceptor with initial course difference ϕ_i is then found by applying the turn trochoid to each point on the basic barrier, holding it tangent to the barrier with corresponding ϕ-values of the trochoid and look angle barrier in contact. A point on the effective look angle barrier is then ϕ_i on the trochoid.

3.3 The Rear Manoeuvre Barrier. To find the locus of points at which the interceptor must start its final correcting turn in order just to possess the correct course difference when it enters the launch zone, the following procedure is used. For a given point on the launch zone, behind that for correct launch on the interceptor's original course difference, the correct course difference is ϕ_L and the heading error allowed is ϵ. The turn trochoid is aligned for a starboard turn, with its reference direction along the target path, with the point $(\phi_L - \epsilon)$ of the trochoid on the point ϕ_L of the launch zone. Then ϕ_i on the trochoid is a point of the manoeuvre barrier.

3.4 The Front Manoeuvre Barrier. The same procedure is followed for launch points in front of ϕ_i on the launch zone, with the trochoid set for a port turn, and using the point $(\phi_L + \epsilon)$ on it.

3.5 The Front Look-Angle Barrier. This is a straight line passing through the target, making an angle $(180° - \phi_i - \gamma)$ with the target path.

3.6 The Composite Barrier. The region of space in which the interceptor must be placed is that bounded by the five barriers described above. Figure 1 shows a representative set of barriers.

4.0 The Evading Target.

Barrier systems for evading targets are found by a trial and error method, using the REAC to simulate the interceptor's flight. The equations used have been described in Reference 2, Appendix D. The REAC method gives the same result as the graphical method for non-evading targets with one exception: the circuit which has been used to date does not permit missile launch from the rear half of the launch zone. Thus the portion of the manoeuvre barrier close to the launch zone as found by the REAC method is pessimistic, that is farther away from the target than it would be if rear zone launch were permitted. The REAC circuit has only been used with initial course difference $110°$ or more, so that the effect is not great. Figure 2 shows the effect. For large AI ranges no error appears in the final results due to this factor.

5.0 Placement Probability

Transparent overlays have been prepared of the AI Acquisition contours which are being assumed (See Appendix E). They are used in the following manner. The ideal approach line for the given initial course difference is drawn on the placement chart. The acquisition contour is then superimposed, and the width of the placement zone at the AI Range considered is noted. Actually, since the ideal line may not be in the centre of the zone, the widths of the zone between the ideal line, and the forward and rear barriers, are separately noted. Now if the standard deviation σ of placement accuracy of the ground control system is known. The probability of the interceptor being placed inside the required zone at the AI Range considered can be found from a table of the probability integral. A good table is that on page 407 of the book "Introduction to Mathematical Probability" by Uspensky.

If the AI contour is used in this fashion, it is assumed to give the range at which the pilot can start acting on the radar information: this may be for example three seconds or six seconds after actual acquisition.

6.0 Results of Placement Studies to Date

6.1 To date, the cases which have been studied consider a supersonic interceptor, making constant speed circular turns, attacking a supersonic target. Various values of interceptor load factor are used: the available power limited turn of the CF-105 will fall within the range of values chosen.

6.2 Evasion. Two groups of results are presented - a group for non-evading targets, and a group for gently evading targets. Work on more pronounced evasion is continuing but is not far enough advanced to be reported here.

The amount of target evasion which has been applied for the Mach 1.5 target was 0.15 lateral g's, corresponding to a load factor of 1.02: this amount of evasion can be applied by the target with no penalty in range or fuel consumption. This evasion corresponds to a turn radius of 73 miles, and a turn rate of .19 degrees per second.

The amount of target evasion which has been applied for the Mach 2 target was 0.1 lateral g's; thus represents a turn radius of 182 miles and a turn rate of 0.1 degrees per second.

It is seen that the amount of evasion considered here is in reality so small that the results obtained for this case may represent closely the probability of success in an apparently non-evading case in practice.

Work which is at present in progress uses evasion of 0.5 lateral g's for the Mach 2 target and 0.75 lateral g's for the Mach 1.5 target.

6.3 AI Acquisition Range. Two sets of AI acquisition contours have been used, so that results for two different types of target may be compared. These are for the delta-winged and straight winged targets, described in Appendix E . The difference in the two cases which is of interest, is in the ratio of front to beam range which is obtainable.

Where AI acquisition range is plotted in the graphs it is represented in terms of the Specification range, and not in nautical miles. The graphs were completely drawn at the time when alteration in the AI range assumptions became necessary - thus the range scale on the graphs for the straight wing case is not the same as that for the delta case.

6.4 Interceptor Turn Capability. For convenience in computation, the interceptor turn capability has been stated in g's of lateral acceleration. A table of conversion from lateral acceleration to load factor is given here;

Lateral g's	Load Factor g's
0	1
0.66	1.2
0.75	1.25
0.85	1.31
1.0	1.41
1.12	1.5
1.25	1.6
1.50	1.8
1.60	1.88
1.73	2.0
2.0	2.23
2.4	2.60
3.0	3.16
3.6	3.75
4.0	4.12

6.5 Standard Deviation of Placement Accuracy. Since the characteristics of the ground control system in which the CF-105 will operate are not known, a range of values of σ, the standard deviation of placement accuracy, has been used. The values included range from 1.5 nautical miles which is thought to be a most optimistic estimate, to 9 nautical miles. This rather large value may very well represent the accuracy of placement obtainable under conditions of severe degradation, whether due to e.c.m, climatic conditions, or equipment malfunction.

6.6 Target and Interceptor Kinematics. Two target velocities are considered in the work described here - these are Mach 1.5 and Mach 2. For both cases the interceptor is assumed to have a speed of Mach 1.5. In addition, for the Mach 2.0 target, an interceptor Mach number 1.8 is considered. The missile launch zone varies with interceptor and target speeds, and also depends on altitude. In this work the only significance of an altitude value is in the designation of missile launch zone.

7.0 The basic set of graphs which are drawn gives probability of successful placement as a function of AI acquisition range. The results for the two different contours are numbered similarly, with a letter prefix D for the Delta case, and S for the Straight wing case. This will facilitate intercomparison.

These curves all have the same general shape: probability rises almost linearly from zero at some AI range which corresponds to the range at which the missile must be prepared for launch; the curve reaches a "knee" which is more or less pronounced, so that beyond a certain range capability increase in this parameter is of little value.

7.1 Graphs of P_p/ AI Range for M_T=1.5 M_I =1.5. Figures D1 to D24 give the results for the non-evading target at a nominal altitude of 50,000 feet. Launch zone L-1 is used. Six values of course difference from 80° to 180° are used, and four values of interceptor lateral g-capability from 0.85 to 3.0. Most of the curves are drawn for launch at maximum range with 15° heading error. For one value of course difference the case of launch at minimum range with 10° heading error allowance is studied for comparison. Although decreasing the launch range should improve probability, the corresponding decrease in heading error more than offsets this improvement, and the net result is worse, even for the best interceptor turn capability considered.

Even for the largest value of σ used, the worst value of P, for AI range of 0.6S, is 48%.

Figures D25-D42 give P_p/range for the non-evading target at 60,000 feet nominal altitude. The launch zone used here is L-2: higher altitude missile capability is considered to be worse: a larger minimum range is used with only 5° heading error allowance, and at maximum range only 10° heading error is thought usable. The same range of values of course difference and interceptor turn capability are used. In two cases the graphs for launch at minimum range are given for comparison.

Figures D43-D55 give P_p/range for a gently evading target at 50,000 feet nominal altitude. The launch zone used in the REAC work is L-12. The amount of evasion used here involves almost no drag or fuel penalty for the target, and yet does reduce by a small amount the placement success. Four values of course difference from 110° to 180° are considered, and three values of interceptor turn capability. For the case with intermediate fighter turn g's the effect of considering a late target turn is shown: the target is assumed to start evading at a fixed range of 150,000 feet. This produces very little difference in probability of placement.

In several cases, the results were calculated for target evasion in one direction only: this gives results comparable to those for a non-evading target. Also, this is not thought to be a realistic way of computing results; it is felt that a better assumption to make is that the target will always evade in the most profitable manner.

Figures D56-D66 give the results for the evading target at nominal altitude of 60,000 feet. (Launch zone L-13). Three values of fighter g capability and four values of course difference are used.

7.2 Graphs of P_p/AI range for $M_T = 2.0$, $M_I = 1.5$. Figures D-67 to D-84 give P/range curves for this case at 50,000 feet nominal altitude. Launch zone L-3 is used. Three values of interceptor turn capability, and six values of course difference are considered.

Figures D-85 to D-90 repeat for one value of interceptor g's the same kinematic case, with a different launch zone, where maximum launch range is reduced due to, say, reduced missile guidance range. A large reduction in probability is obtained in this case, the maximum being about 50% for the best σ.

Figures D91-D99 give the P/AI range curves for the gently evading target at nominal altitude 50,000 feet. Launch zone is L-10. For a few cases, the curves are drawn for the target evading in a fixed direction only for comparison with results for the target evading in the optimum manner. Four values of course difference and only two values of interceptor turn capability are used.

Figures D100-D114 give the P/AI range curves for the non-evading Mach 2 target at nominal altitude 60,000 feet. Some variation of launch zone was made here, in order to determine effect of this on the final results. Launch zone L-9 corresponds at 60,000 feet to zone L-3 at 50,000 feet, and represents a reasonable launch zone for this altitude. Results were obtained with this launch zone for two values of fighter lateral g's only, and five of course difference. These are labelled with suffic (a) from D100 to 109. Launch zone L-5 assumes the same maximum and minimum ranges, but a slower missile, so that the ideal course difference for launch at any target aspect is different. Quite different, (and, with this value of target/interceptor speed rate, quite inferior) results are obtained. These results are presented with the same figure number, with suffix b or c.

For one value of interceptor lateral g's a larger maximum launch range was used. The results of this are given in figures 105 to 109, lettered d. Very little difference is noted in the resulting probabilities. For the smallest value of interceptor turn capability, 1.12 lateral g's, only the launch zone L-5 was used, so that no values using the more correct launch zone L-9 are available.

Figures D115-126 give P/AI range for the gently evading target at 60,000 feet nominal altitude. Launch zone L-11 was used. Three values of interceptor lateral g's, and four values of course difference are considered. In most cases, target evasion was 0.1 g's, with results being given in a few cases for 0.2 g's.

7.3 Graphs of P_p/AI Range for $M_T = 2.0$ $M_I = 1.8$. This case was considered only at nominal altitude 60,000 feet, using launch zone L-8 and for the non-evading target only. Results are given in figures D127-144. It is to be noted that launch is not permitted for forward aspects with the proposed launch zone.

High closing speed on frontal approach results in a minimum missile launch range which is greater than the obtainable guidance range. This explains the somewhat anomalous results of the case, and indicates that increased interceptor speed capability will not improve interception chance unless the missile's guidance range is sufficient.

8.0 Figures A1 to 7 give some examples of graphs of Probability of successful placement as a function of the σ of GCI accuracy. It is seen that P_p decreases as σ increases, the curve having the shape of a segment of the Gaussian error curve, in the concave region for small values of AI range, and convex for layer values.

9.0 Figures G1-27 give examples for various cases of the variation of placement probability with lateral g capability of the interceptor. The cases plotted include samples of the three speed ratios, and several values of course difference. It is seen that in general, P_p increases with g-capability. However, the rate of increase of P_p with g-capability decreases as the g-value increases. Thus there exists for any value of σ and of AI range capability a value of lateral g capability beyond which further increase is not very profitable. For the mildly evading or straight flying targets, it is seen from the results here that this critical value of lateral g's is about 1.5.

10.0 Figures C1-42 give graphs of the variation of placement probability with course difference, for a representative group of cases. It is seen that the optimum value of course difference is a function of speed ratio, as may be expected; the optimum value, or the amount by which it gives improvement, is a function of lateral g-capability and of AI Range capability.

11.0 Some studies were done, in one case only, to note the effect of heading error allowance at missile launch. These results are given in figures E-1, 2, 3. The trends shown here may not be conclusive since they may be sensitive to launch zone size and shape. In general, if AI range is great enough the heading error is not an important parameter.

12.0 Some studies were done for one speed ratio only and one launch zone on the effect of an error in the choice of ideal approach line by the GCI. This was found to reduce the probabilities by almost half for small values of g-capability, but to be of little importance for better g-capability. These results are shown in figures F1 - 8.

References

1. CARDE Technical Memorandum 119/55, A Study to Determine the Effectiveness of the CF 100 Armed with Sparrow II Missiles (S.Z. Mack).

2. CARDE Technical Letter M/47-8, First Quarterly Report on CF 105 Assessment Study. (Baker, Mitchell, MacFarlane).

3. CARDE Technical Letter M/47-2, Launch Zones for a Hypothetical Constant Bearing Missile (J.T. MacFarlane).

TABLE OF FIGURES

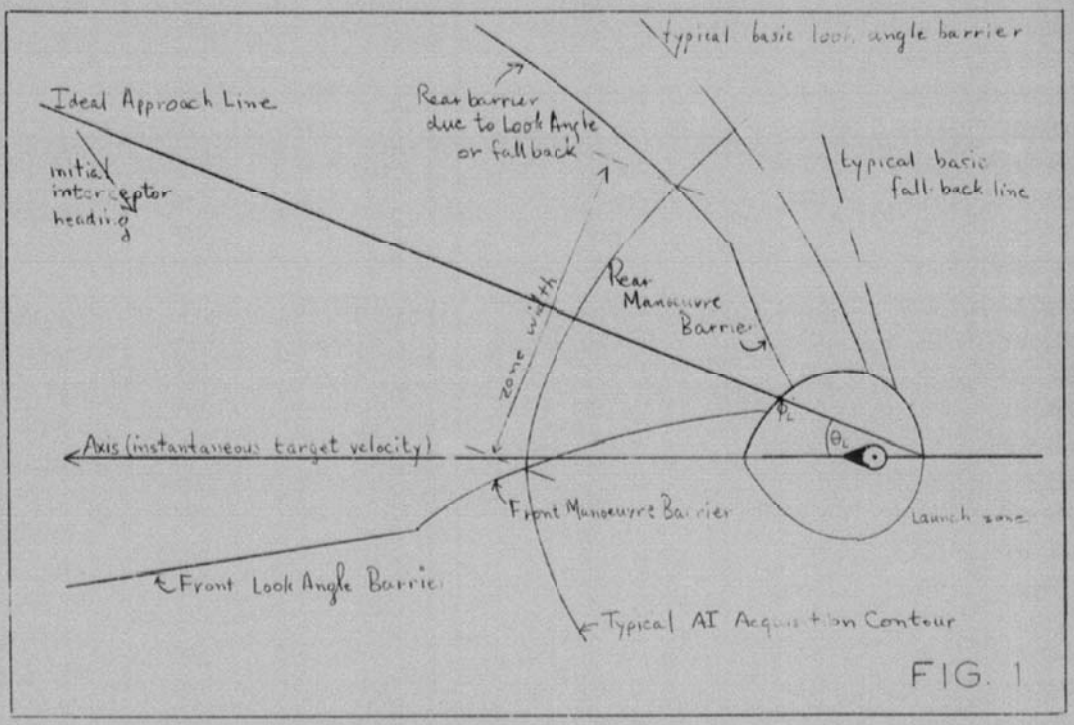
typical basic look angle barrier
Ideal Approach Line
Rear barrier due to Look Angle or fall back
initial interceptor heading
typical basic fall back line
Rear Manoeuvre Barrier
zone width
Axis (instantaneous target velocity)
Front Manoeuvre Barrier
Launch zone
Front Look Angle Barrier
Typical AI Acquisition Contour

FIG. 1

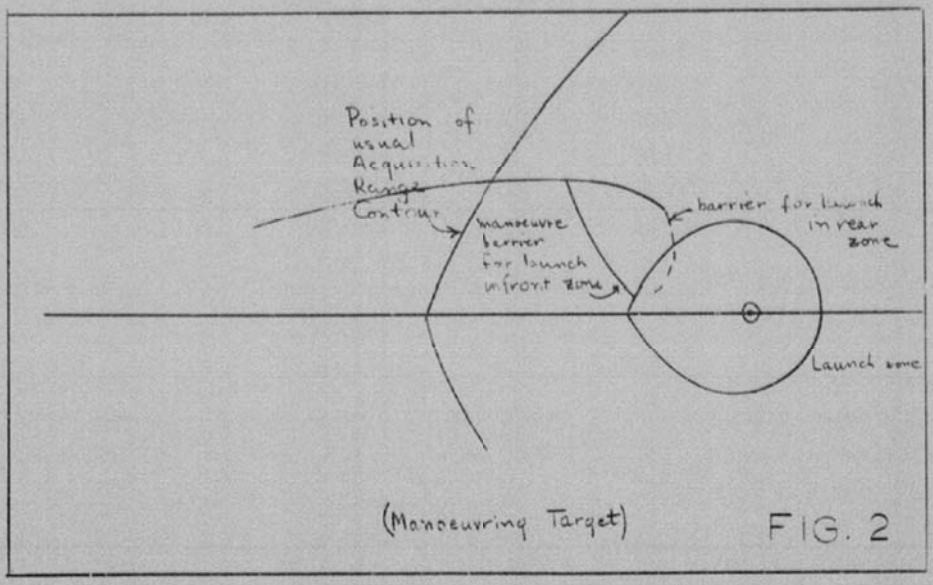
Position of usual Acquisition Range Contour
manoeuvre barrier for launch in front zone
barrier for launch in rear zone
Launch zone
(Manoeuvring Target)

FIG. 2

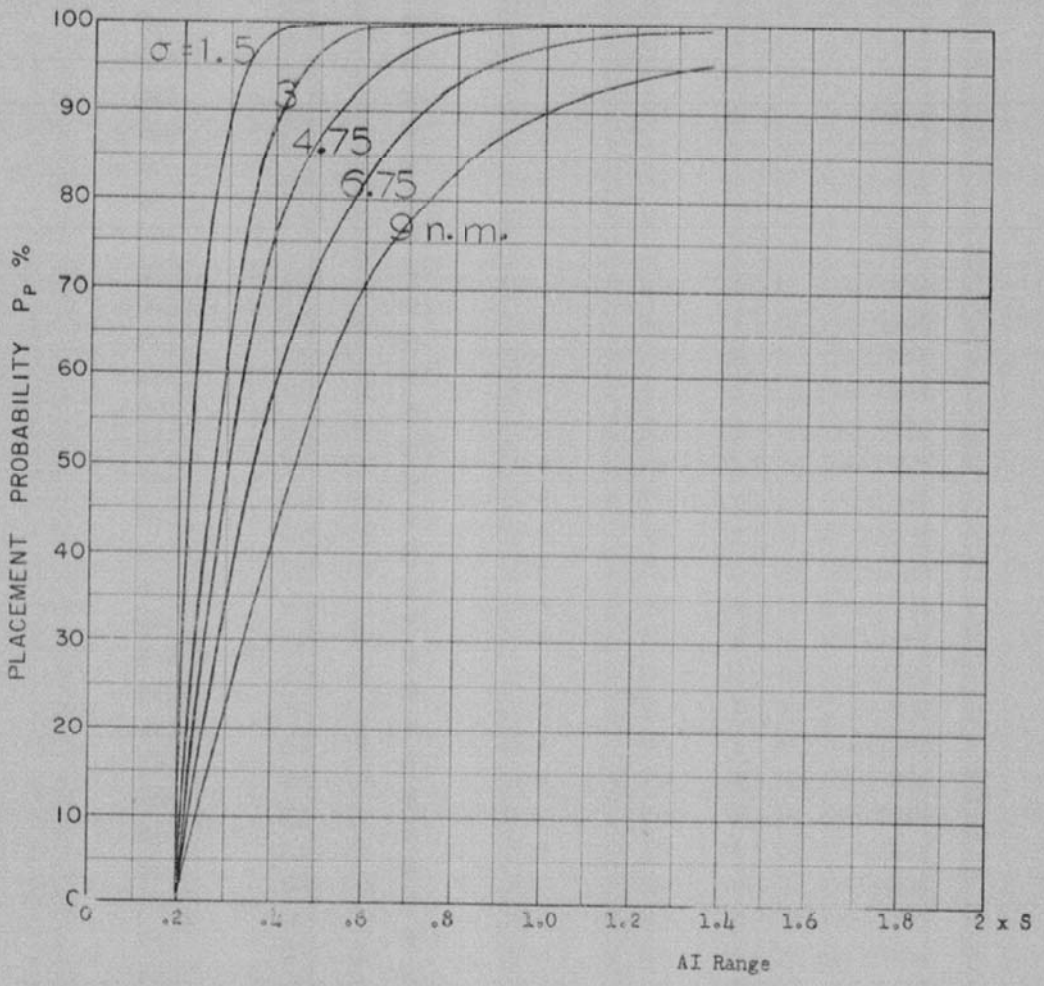

COURSE DIFFERENCE: 80°
TARGET EVASION: 0
TARGET MACH NO.: 1.5
INTERCEPTOR LATERAL G's: .85
INTERCEPTOR MACH NO.: 1.5
σ OF G.C.I. ACCURACY: Five values
A.I. DETECTION RANGE AS FRACTION OF SPECIFICATION RANGE, S: Abscissa
A.I. DETECTION RANGE CONTOUR: Delta
ALTITUDE: 50 K

D-1

Launch zone of figure L-I, missile launched at maximum range with 15° heading error.

34 b x d p r

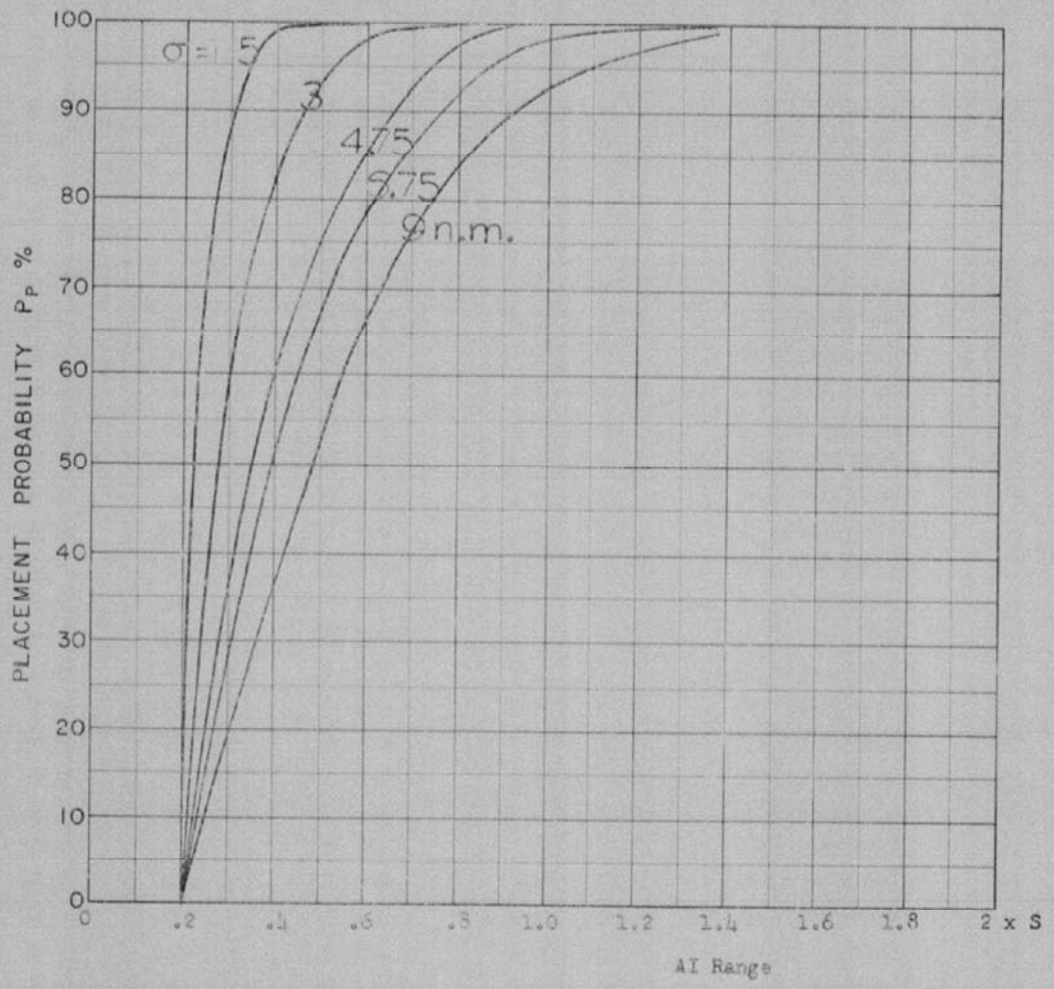

COURSE DIFFERENCE: 100°
TARGET EVASION: 0
TARGET MACH NO.: 1.5
INTERCEPTOR LATERAL G's: 0.85
INTERCEPTOR MACH NO.: 1.5
σ OF G.C.I. ACCURACY: Five values
A.I. DETECTION RANGE AS FRACTION OF SPECIFICATION RANGE, S: Abscissa
A.I. DETECTION RANGE CONTOUR: Delta
ALTITUDE: 50 K

(D-2a)

Launch zone of figure L-I, missile launched at maximum range with 15° heading error.

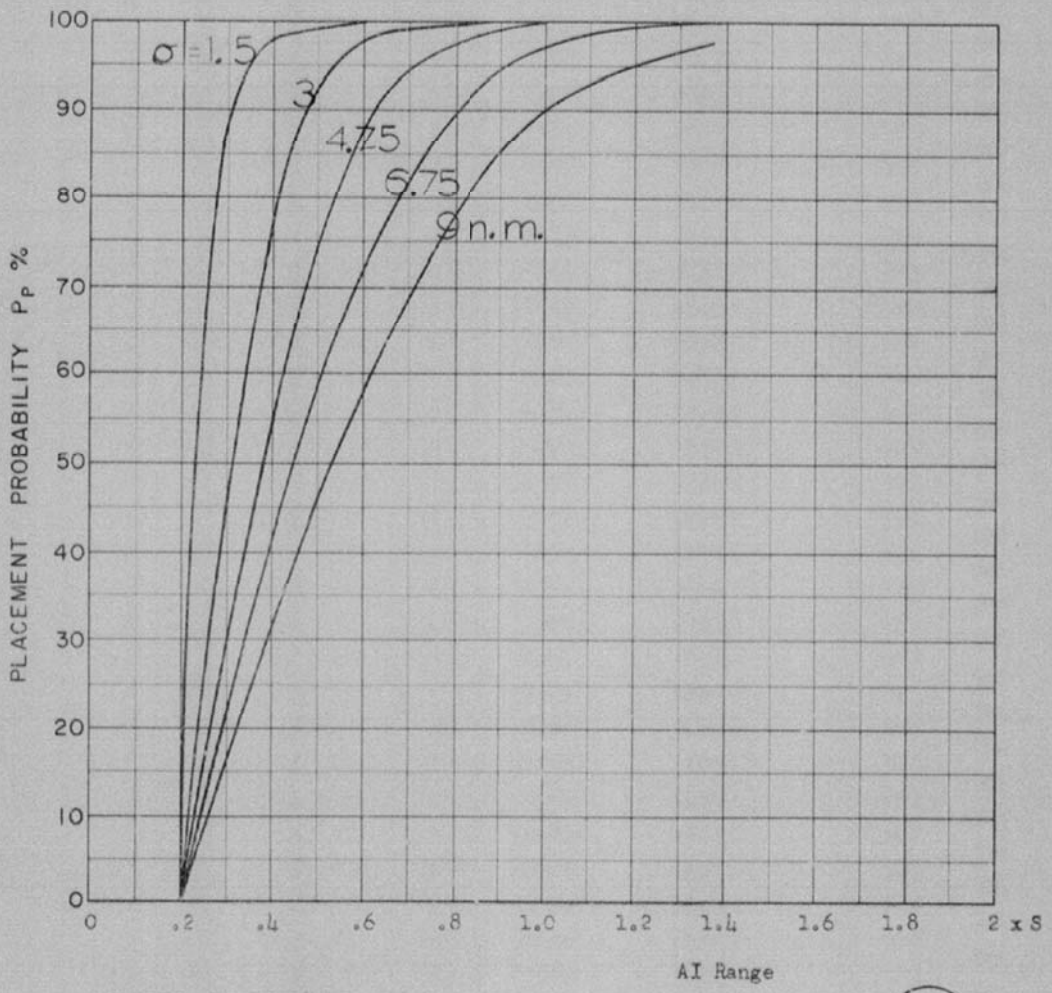

COURSE DIFFERENCE: 100°
TARGET EVASION: 0
TARGET MACH NO.: 1.5
INTERCEPTOR LATERAL G's: 0.85
INTERCEPTOR MACH NO.: 1.5
σ OF G.C.I. ACCURACY: Five values
A.I. DETECTION RANGE AS FRACTION OF SPECIFICATION RANGE, S: Abscissa
A.I. DETECTION RANGE CONTOUR: Delta
ALTITUDE: 50 K

D-2b

Launch zone figure L-I, missile launched at minimum range with 10° heading error allowance.

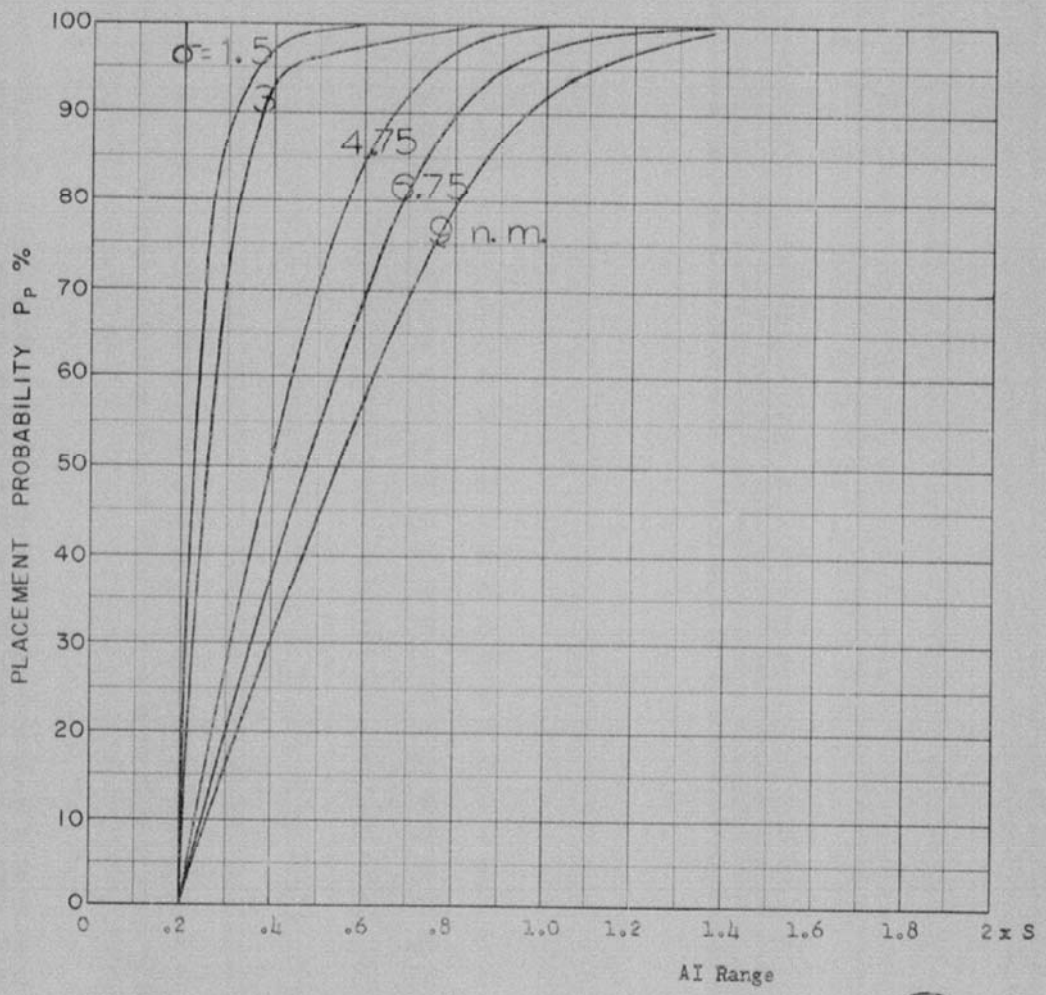

COURSE DIFFERENCE: 120°
TARGET EVASION: 0
TARGET MACH NO.: 1.5
INTERCEPTOR LATERAL G's: 0.85
INTERCEPTOR MACH NO.: 1.5
σ OF G.C.I. ACCURACY: Five values
A.I. DETECTION RANGE AS FRACTION OF SPECIFICATION RANGE, S: Abscissa
A.I. DETECTION RANGE CONTOUR: Delta
ALTITUDE: 50 K

D-3

Launch zone of figure L-1, missile launched at maximum range with 15° heading error.

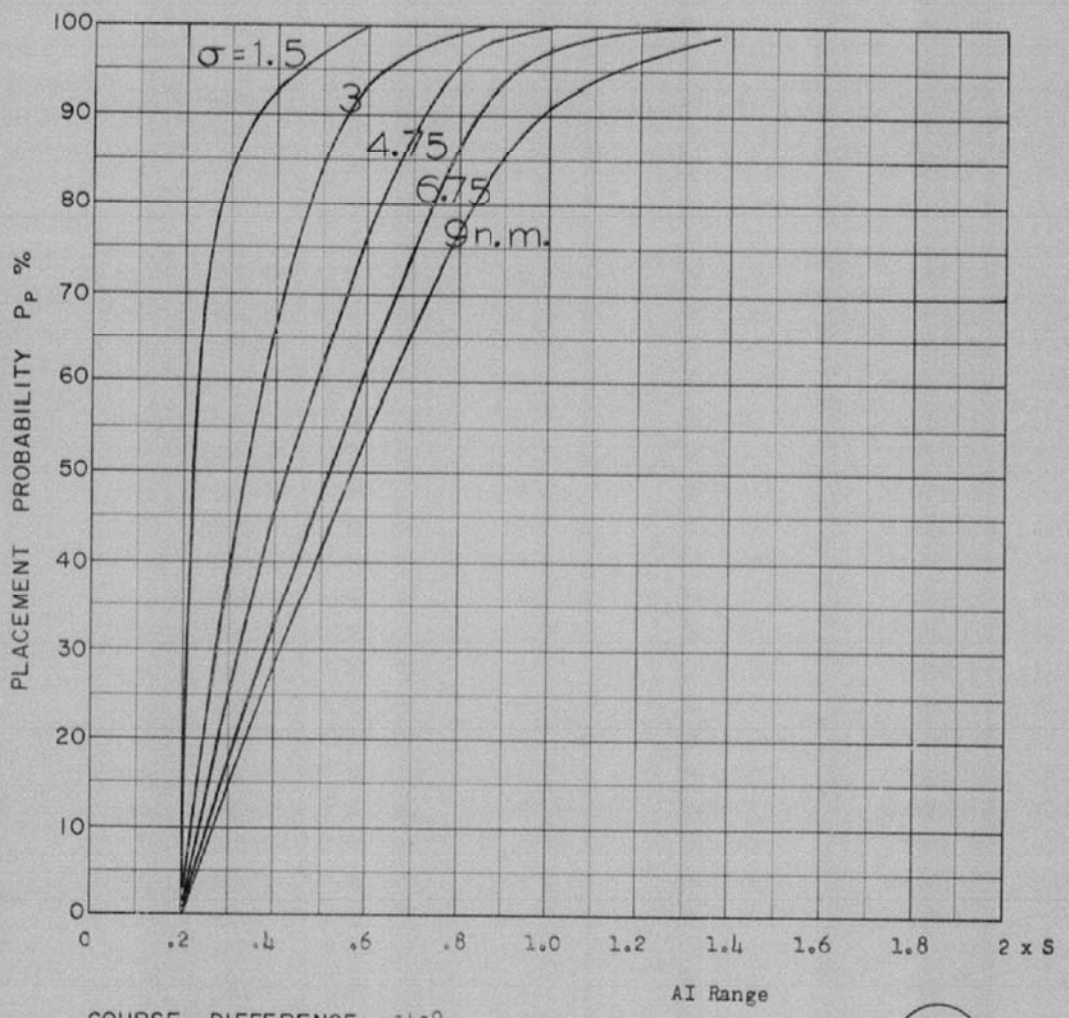

COURSE DIFFERENCE: 140°
TARGET EVASION: 0
TARGET MACH NO.: 1.5
INTERCEPTOR LATERAL G's: 0.85
INTERCEPTOR MACH NO.: 1.5
σ OF G.C.I. ACCURACY: Five values
A.I. DETECTION RANGE AS FRACTION OF SPECIFICATION RANGE, S: Abscissa
A.I. DETECTION RANGE CONTOUR: Delta
ALTITUDE: 50K

D-4

Launch zone of figure L-I, missile launched at maximum range with 15° heading error.

34 e x d p r

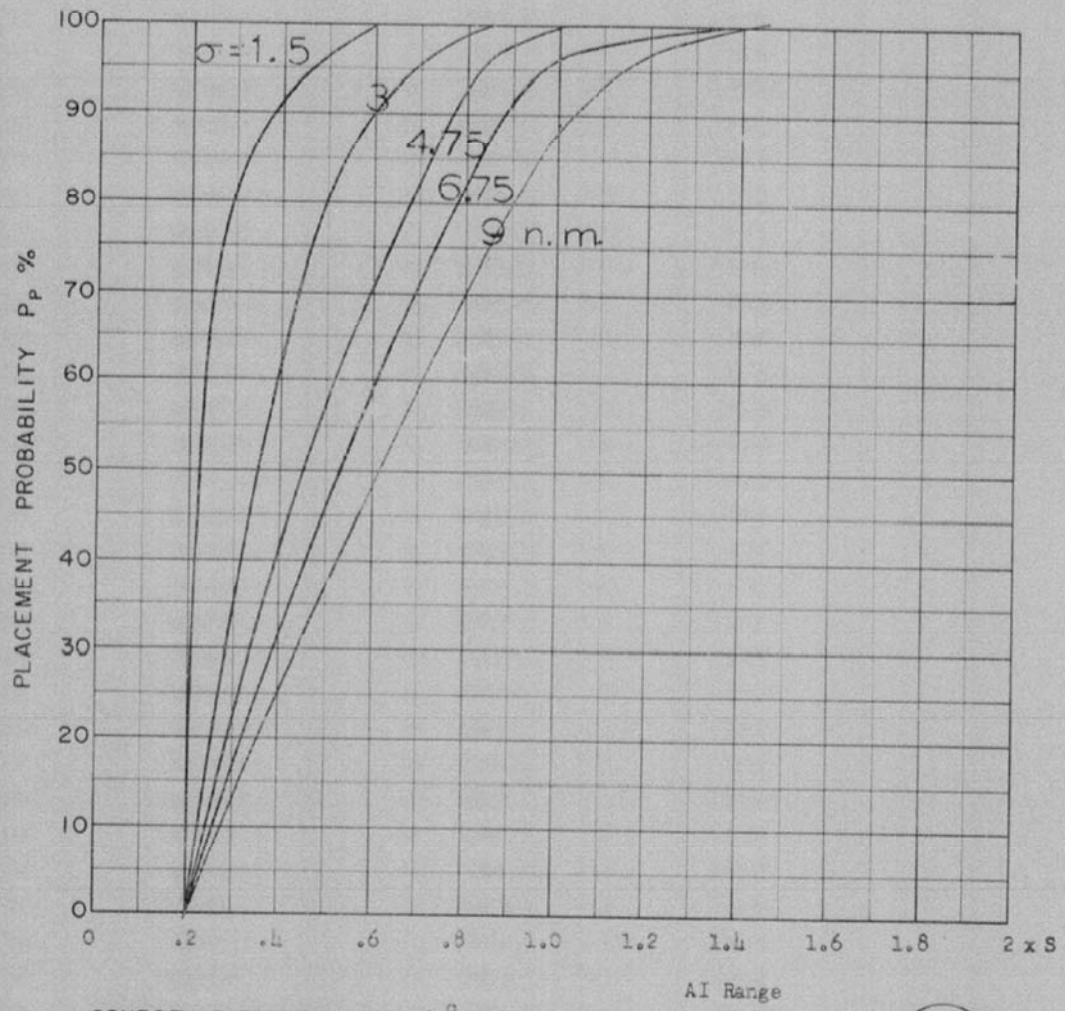

COURSE DIFFERENCE: 160°
TARGET EVASION: 0
TARGET MACH NO.: 1.5
INTERCEPTOR LATERAL G's: 0.85
INTERCEPTOR MACH NO.: 1.5
σ OF G.C.I. ACCURACY: Five values
A.I. DETECTION RANGE AS FRACTION OF SPECIFICATION RANGE, S: Abscissa
A.I. DETECTION RANGE CONTOUR: Delta
ALTITUDE: 50 K

D-5

Launch zone of figure L-I, missile launched at maximum range with 15° heading error.

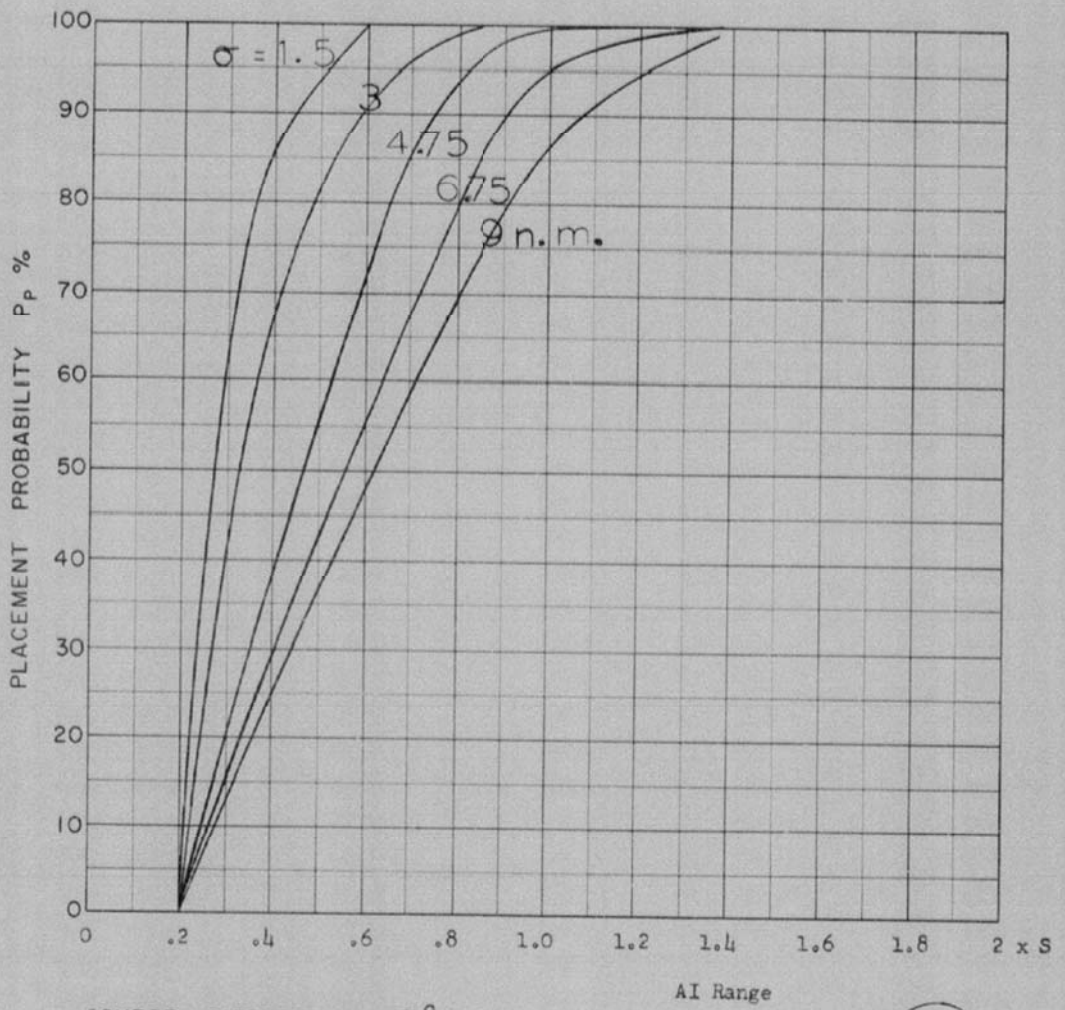

COURSE DIFFERENCE: 180°
TARGET EVASION: 0
TARGET MACH NO.: 1.5
INTERCEPTOR LATERAL G's: 0.85
INTERCEPTOR MACH NO.: 1.5
σ OF G.C.I. ACCURACY: Five values
A.I. DETECTION RANGE AS FRACTION OF SPECIFICATION RANGE, S: Abscissa
A.I. DETECTION RANGE CONTOUR: Delta
ALTITUDE: 50 K

D-6

Launch zone of figure L-I, missile launched at maximum range with 15° heading error.

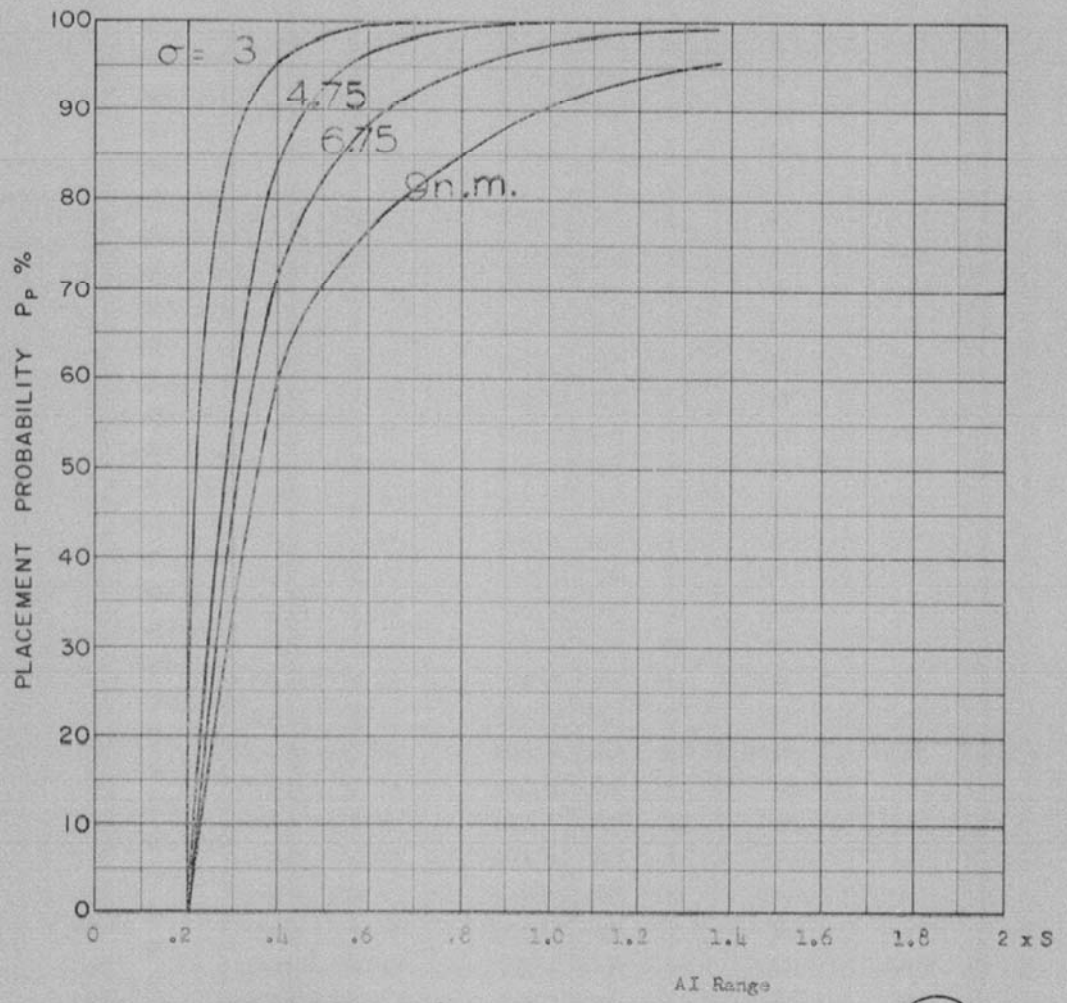

COURSE DIFFERENCE: 80°
TARGET EVASION: 0
TARGET MACH NO.: 1.5
INTERCEPTOR LATERAL G's: 1.25
INTERCEPTOR MACH NO.: 1.5
σ OF G.C.I. ACCURACY: Four values
A.I. DETECTION RANGE AS FRACTION OF SPECIFICATION RANGE, S: Abscissa
A.I. DETECTION RANGE CONTOUR: Delta
ALTITUDE: 50 K

D-7

Launch zone figure L-1, missile launched at maximum range with 15° heading error allowance.

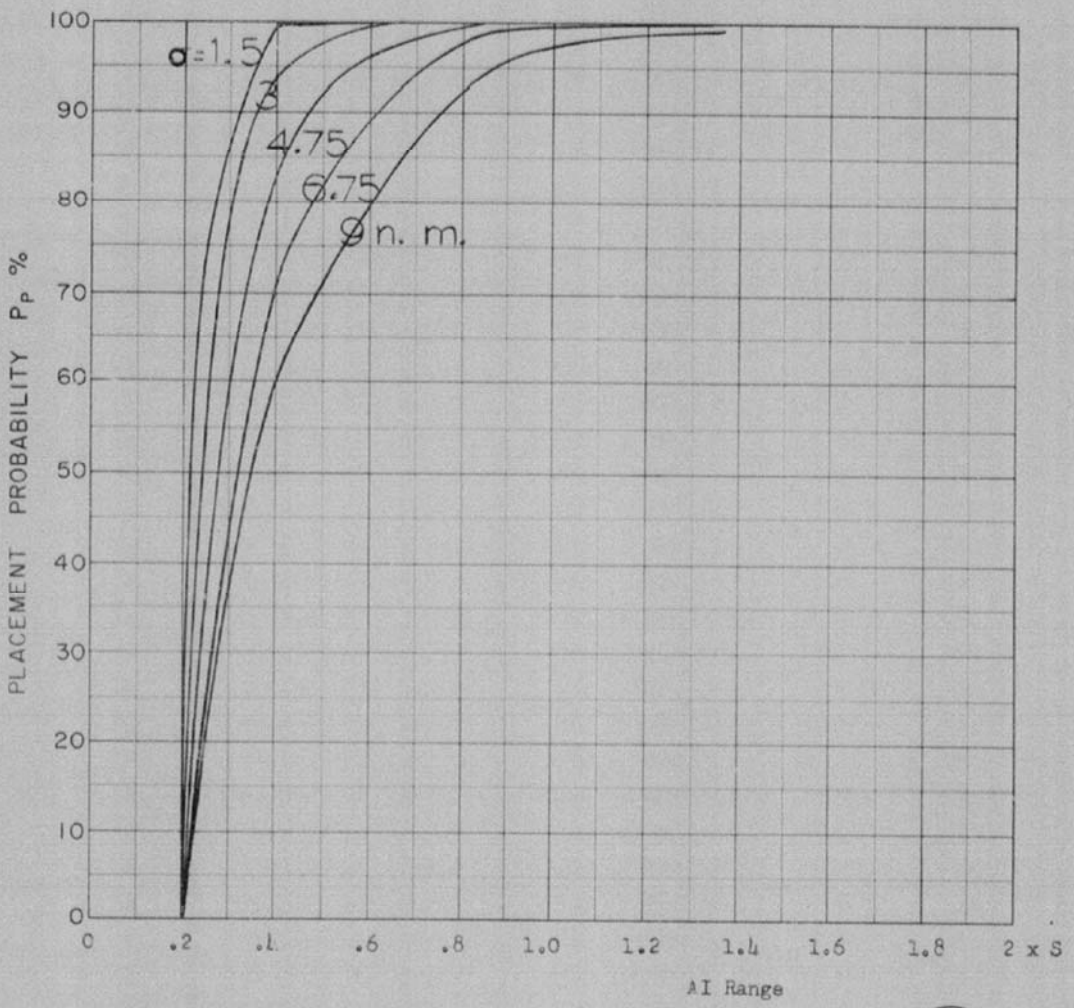

COURSE DIFFERENCE: 100°
TARGET EVASION: 0
TARGET MACH NO.: 1.5
INTERCEPTOR LATERAL G's: 1.25
INTERCEPTOR MACH NO.: 1.5
σ OF G.C.I. ACCURACY: five values
A.I. DETECTION RANGE AS FRACTION OF SPECIFICATION RANGE, S: Atscissa
A.I. DETECTION RANGE CONTOUR: Delta
ALTITUDE: 50 K

D-8a

Launch zone figure L-I, missile launched at maximum range with 15° heading error allowance.

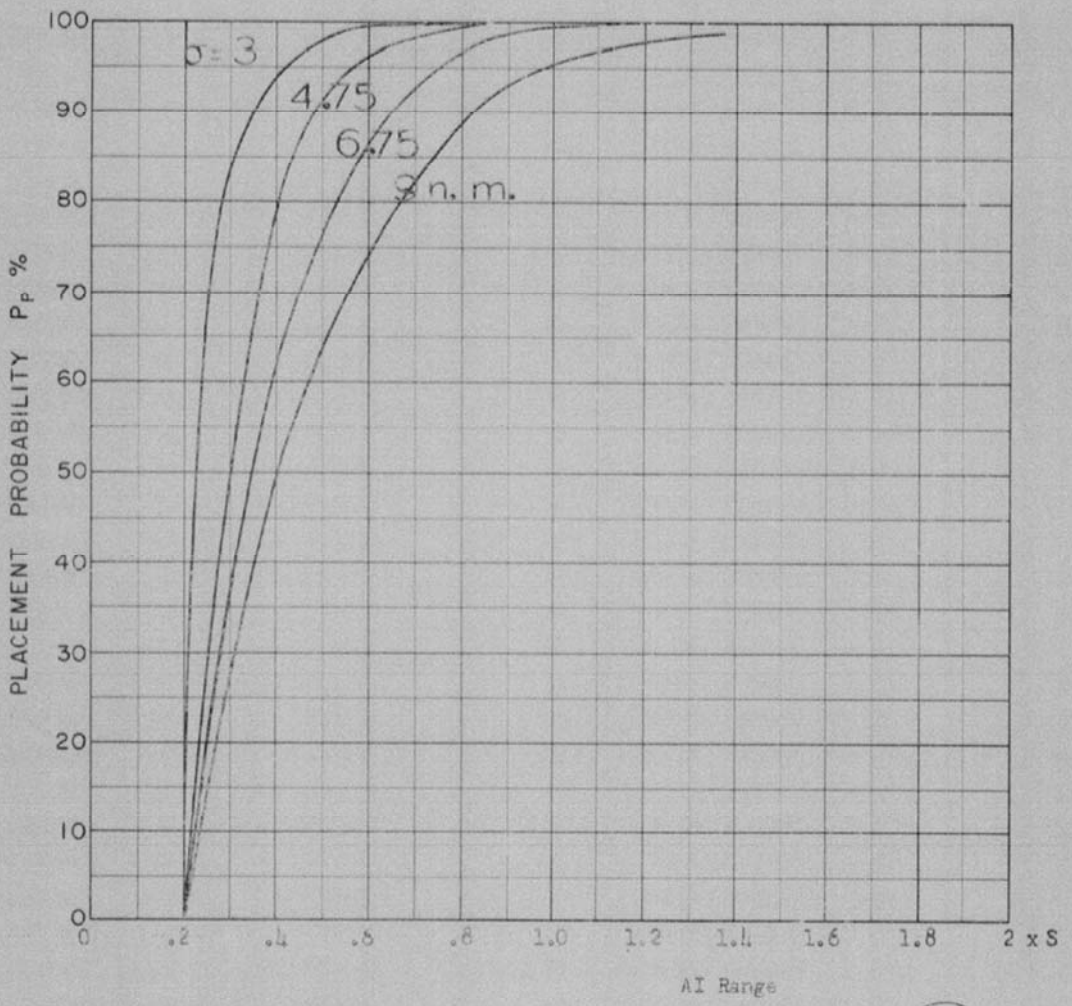

COURSE DIFFERENCE: 100°
TARGET EVASION: 0
TARGET MACH NO.: 1.5
INTERCEPTOR LATERAL G's: 1.25
INTERCEPTOR MACH NO.: 1.5
σ OF G.C.I. ACCURACY: Four values
A.I. DETECTION RANGE AS FRACTION OF SPECIFICATION RANGE, S: Abscissa
A.I. DETECTION RANGE CONTOUR: Delta
ALTITUDE: 50 K

D-86

Launch zone of figure L-1, missile launched at minimum range with 10° heading error allowance.

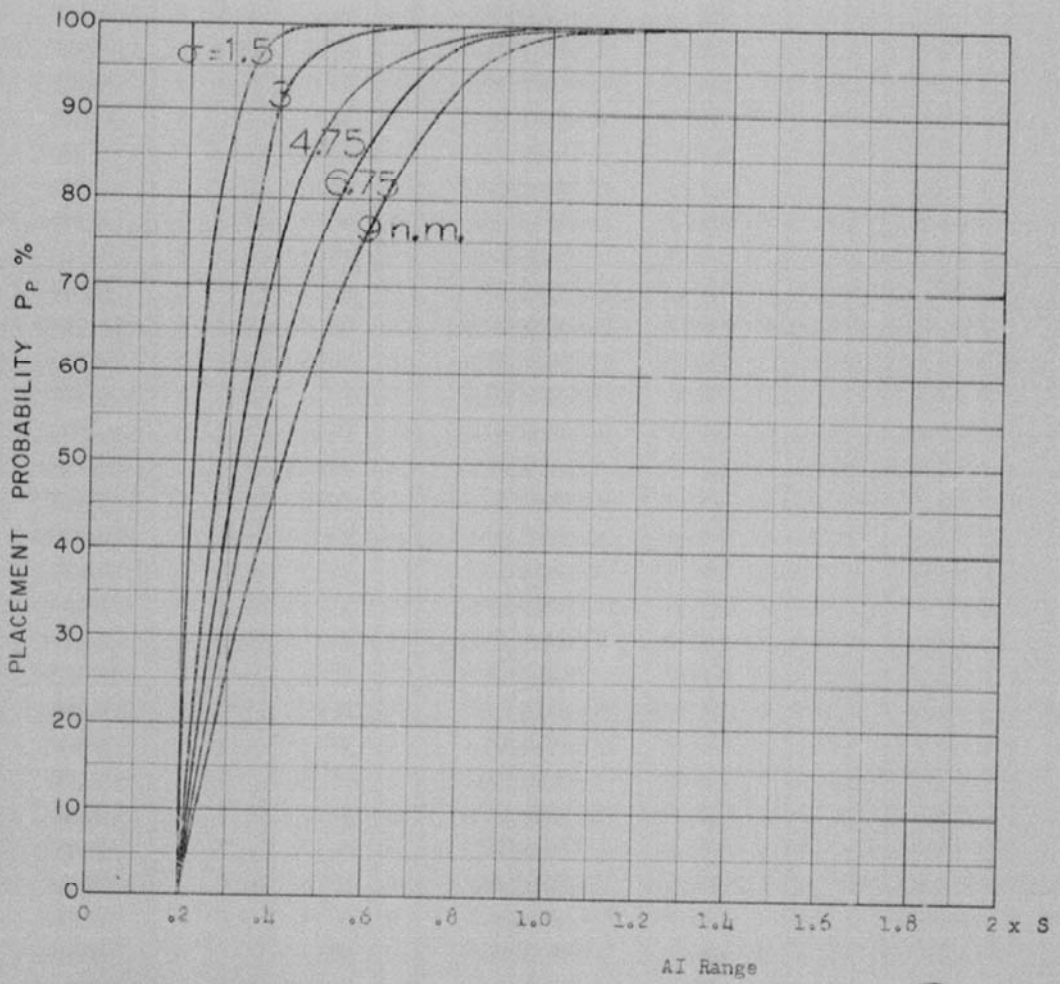

COURSE DIFFERENCE: 120°
TARGET EVASION: 0
TARGET MACH NO.: 1.5
INTERCEPTOR LATERAL G's: 1.25
INTERCEPTOR MACH NO.: 1.5
σ OF G.C.I. ACCURACY: Five values
A.I. DETECTION RANGE AS FRACTION OF SPECIFICATION RANGE, S: Abscissa
A.I. DETECTION RANGE CONTOUR: Delta
ALTITUDE: 50 K

D-9

Lauch zone figure I-I, missile launched at maximum range with 15° heading error allowance.

35 d x d p r

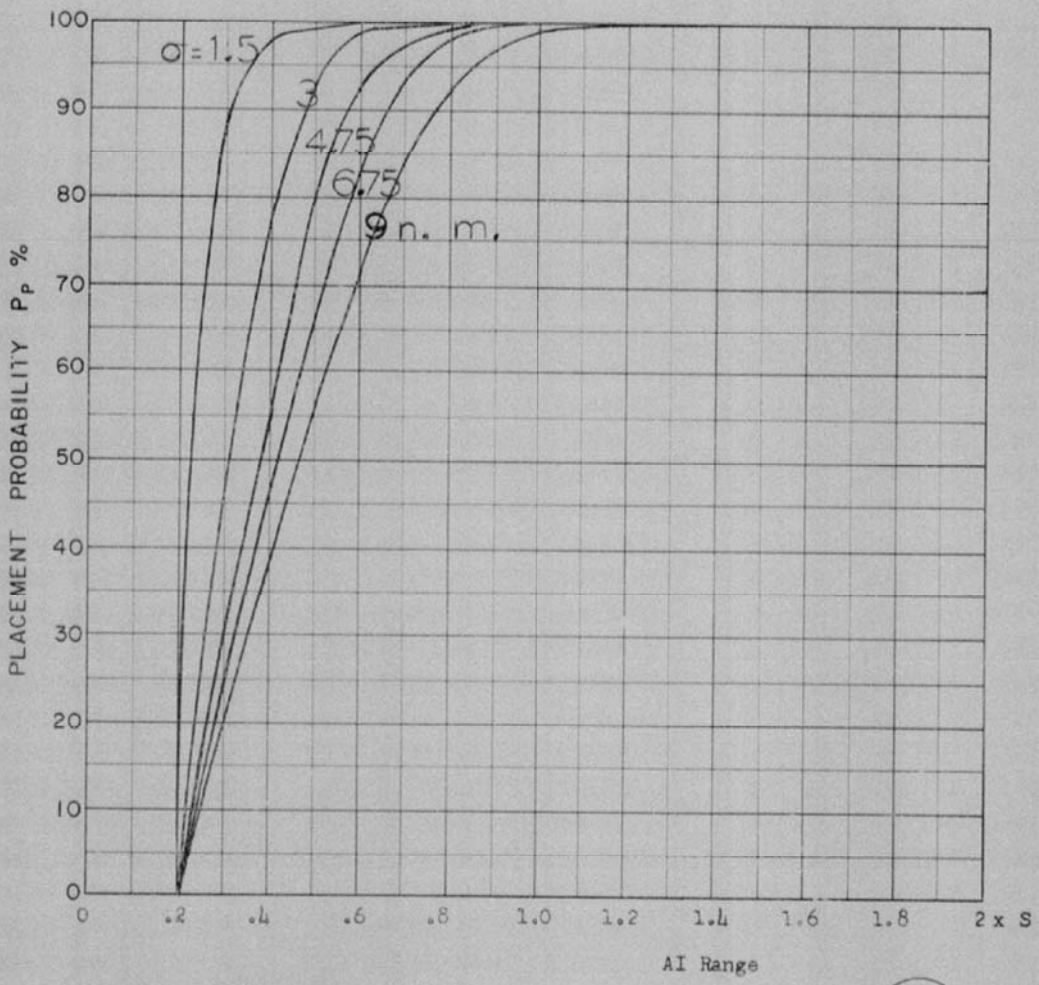

COURSE DIFFERENCE: 140°
TARGET EVASION: 0
TARGET MACH NO.: 1.5
INTERCEPTOR LATERAL G's: 1.25
INTERCEPTOR MACH NO.: 1.5
σ OF G.C.I. ACCURACY: Five values
A.I. DETECTION RANGE AS FRACTION OF SPECIFICATION RANGE, S: Abscissa
A.I. DETECTION RANGE CONTOUR: Delta
ALTITUDE: 50 K

D-10

Launch zone figure L-I, missile launched at maximum range with 15° heading error allowance.

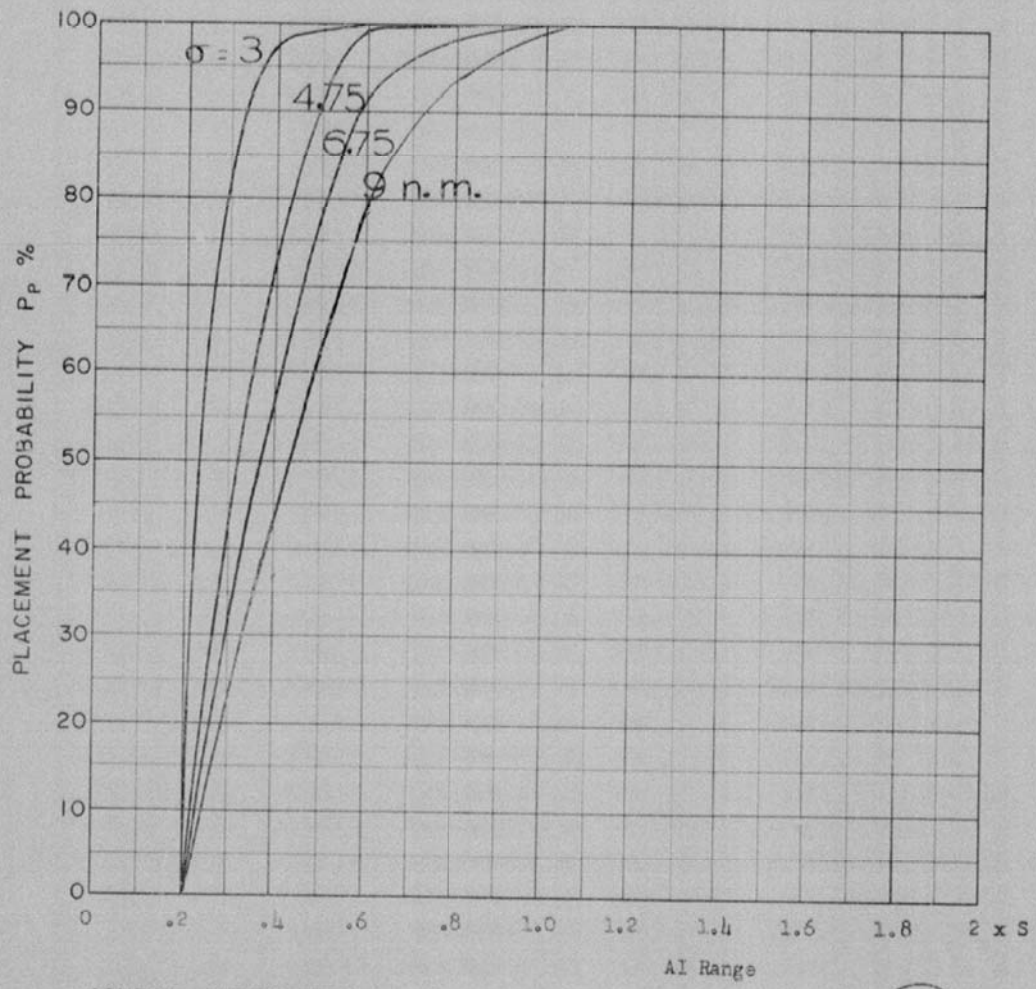

COURSE DIFFERENCE: 160°
TARGET EVASION: 0
TARGET MACH NO.: 1.5
INTERCEPTOR LATERAL G's: 1.25
INTERCEPTOR MACH NO.: 1.5
σ OF G.C.I. ACCURACY: Four values
A.I. DETECTION RANGE AS FRACTION OF SPECIFICATION RANGE, S: Abscissa
A.I. DETECTION RANGE CONTOUR: Delta
ALTITUDE: 50 K

D-11

Launch zone figure L-I, missile launched at maximum range with 15° heading error allowance.

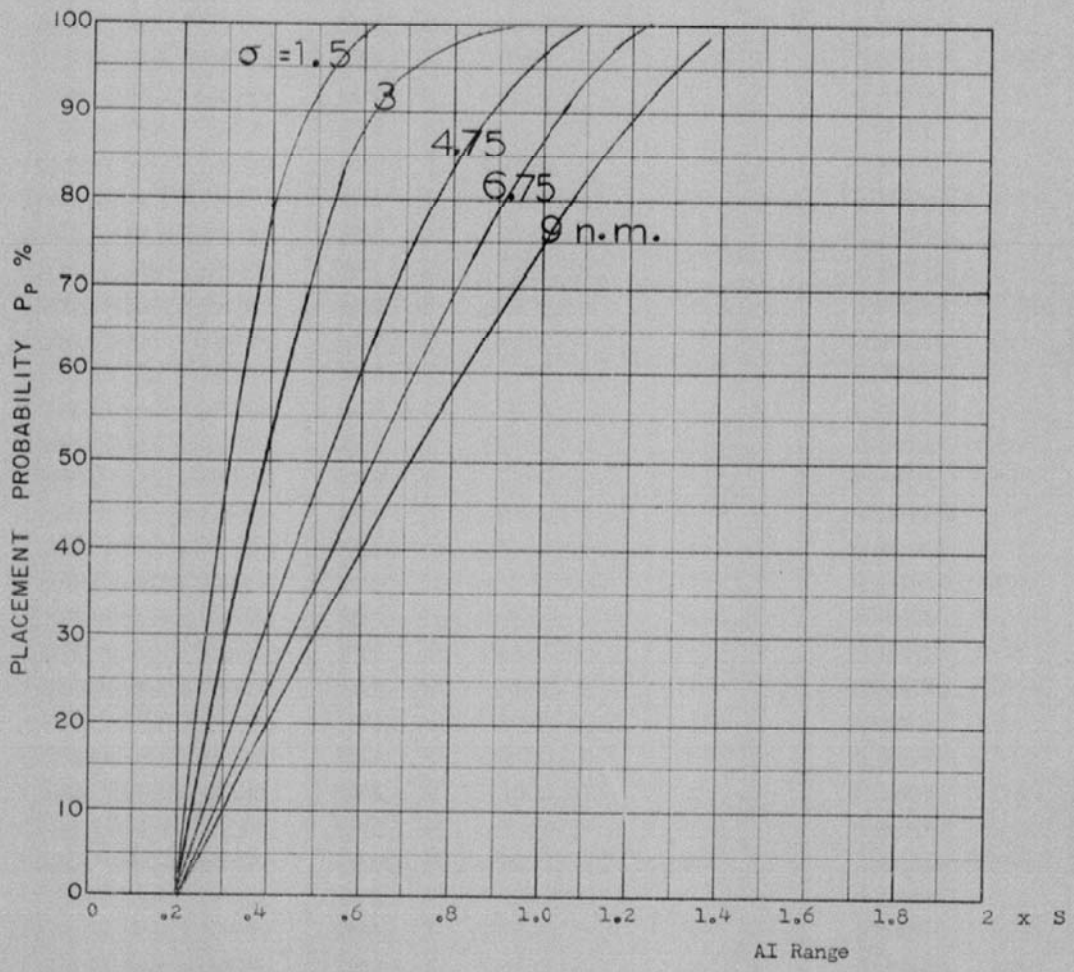

COURSE DIFFERENCE: 180°
TARGET EVASION: 0
TARGET MACH NO.: 1.5
INTERCEPTOR LATERAL G's: 1.25
INTERCEPTOR MACH NO.: 1.5
σ OF G.C.I. ACCURACY: Five values
A.I. DETECTION RANGE AS FRACTION OF SPECIFICATION RANGE, S: Abscissa
A.I. DETECTION RANGE CONTOUR: Delta
ALTITUDE: 50 K

(D-12)

Launch zone of figure I-1. Missile launched at maximum range, with 15° heading error allowance.

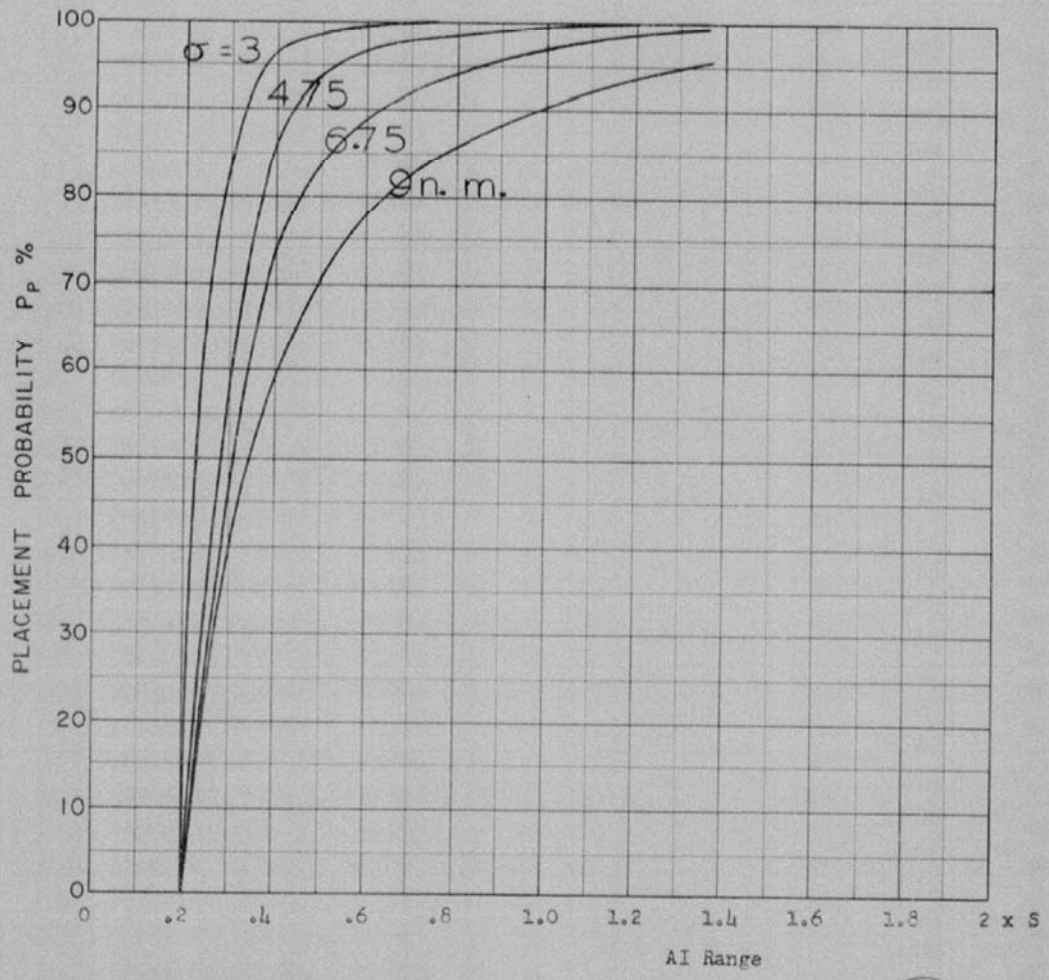

COURSE DIFFERENCE: 80°
TARGET EVASION: 0
TARGET MACH NO.: 1.5
INTERCEPTOR LATERAL G's: 1.6
INTERCEPTOR MACH NO.: 1.5
σ OF G.C.I. ACCURACY: Four values
A.I. DETECTION RANGE AS FRACTION OF SPECIFICATION RANGE, S: Abscissa
A.I. DETECTION RANGE CONTOUR: Delta
ALTITUDE: 50 K

D-13

Launch zone of figure L-1, missile launched at maximum range with 15° heading error allowance.

36 b x d p r

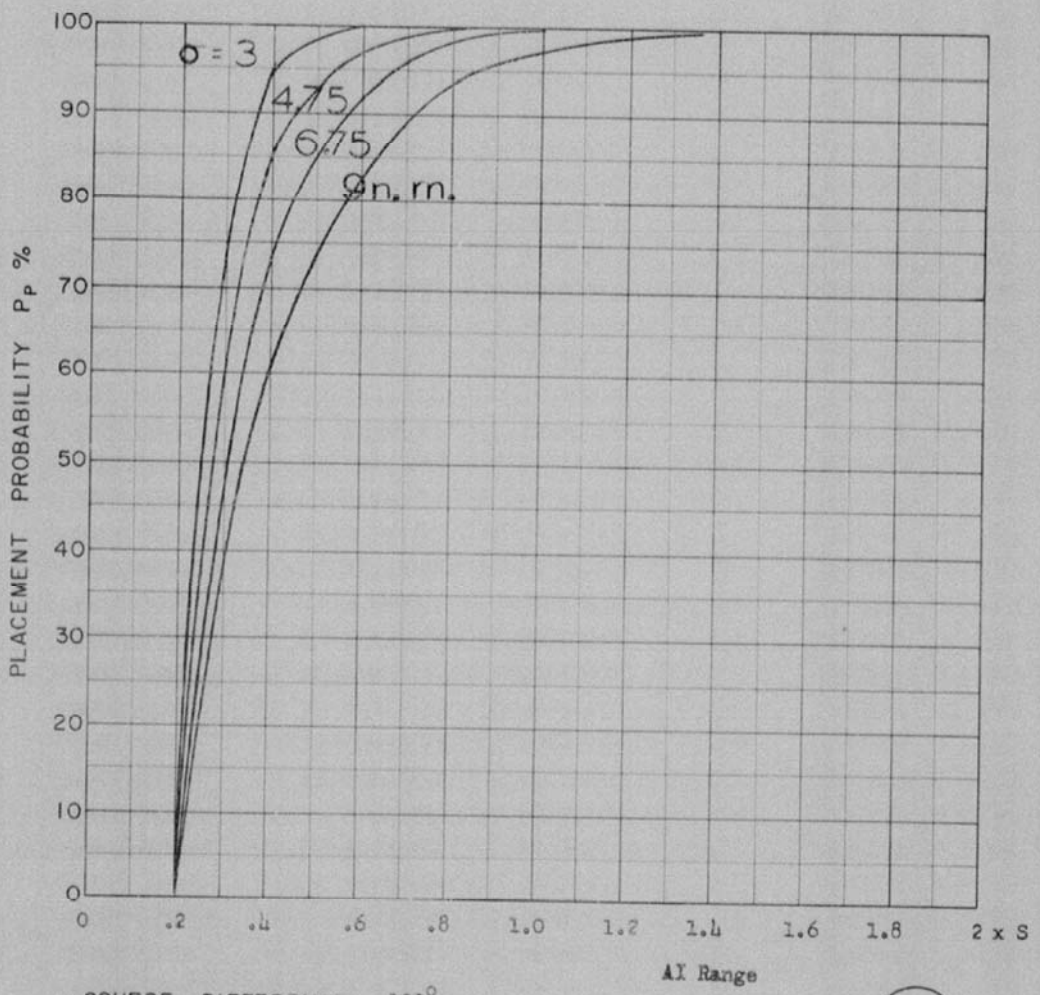

COURSE DIFFERENCE: 100°
TARGET EVASION: 0
TARGET MACH NO.: 1.5
INTERCEPTOR LATERAL G's: 1.6
INTERCEPTOR MACH NO.: 1.5
σ OF G.C.I. ACCURACY: Four values
A.I. DETECTION RANGE AS FRACTION OF SPECIFICATION RANGE, S: Abscissa
A.I. DETECTION RANGE CONTOUR: Delta
ALTITUDE: 50 K

D-14a

Launch zone of figure L-1, missile launched at maximum range with 15° heading error allowance.

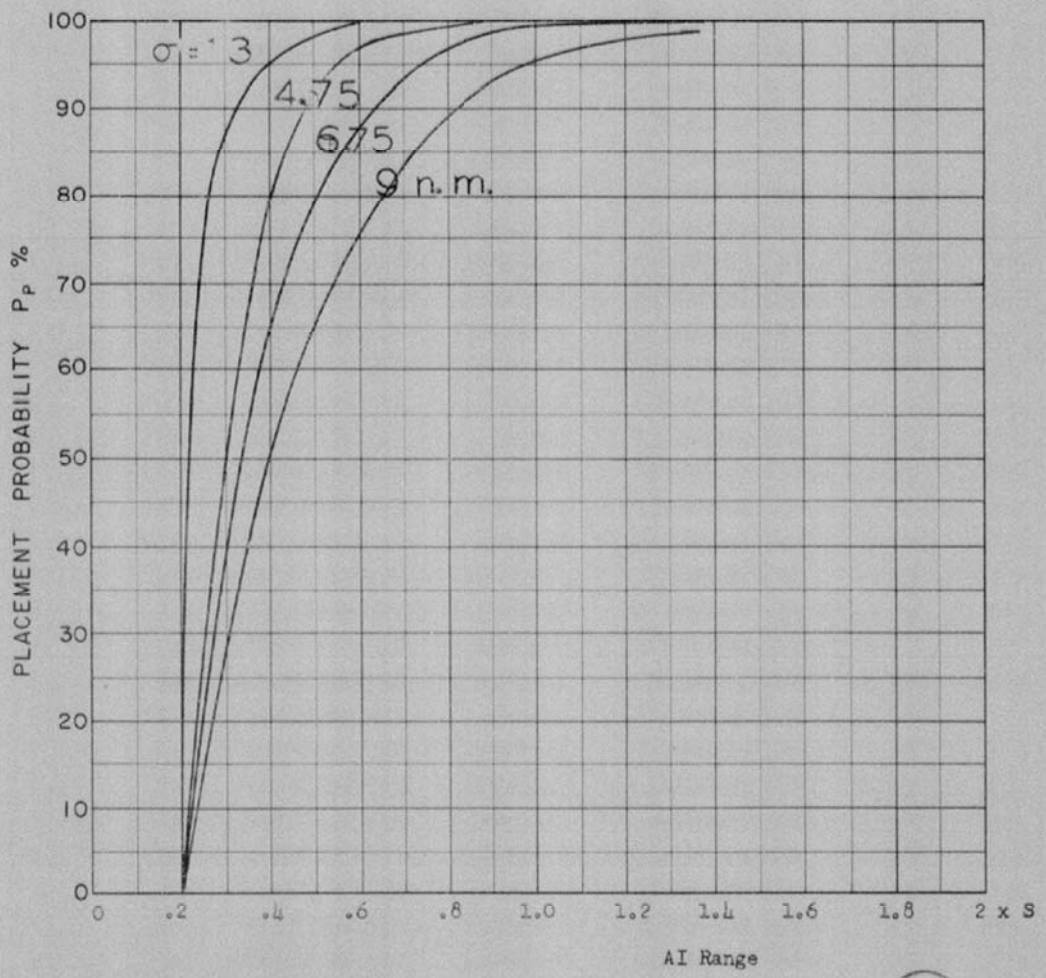

COURSE DIFFERENCE: 100°
TARGET EVASION: 0
TARGET MACH NO.: 1.5
INTERCEPTOR LATERAL G's: 1.6
INTERCEPTOR MACH NO.: 1.5
σ OF G.C.I. ACCURACY: Four values
A.I. DETECTION RANGE AS FRACTION OF SPECIFICATION RANGE, S: Abscissa
A.I. DETECTION RANGE CONTOUR: Delta
ALTITUDE: 50 K

D-146

Launch zone of figure L-I, missile launched at minimum range with 10° heading error allowance.

37 b x d p r

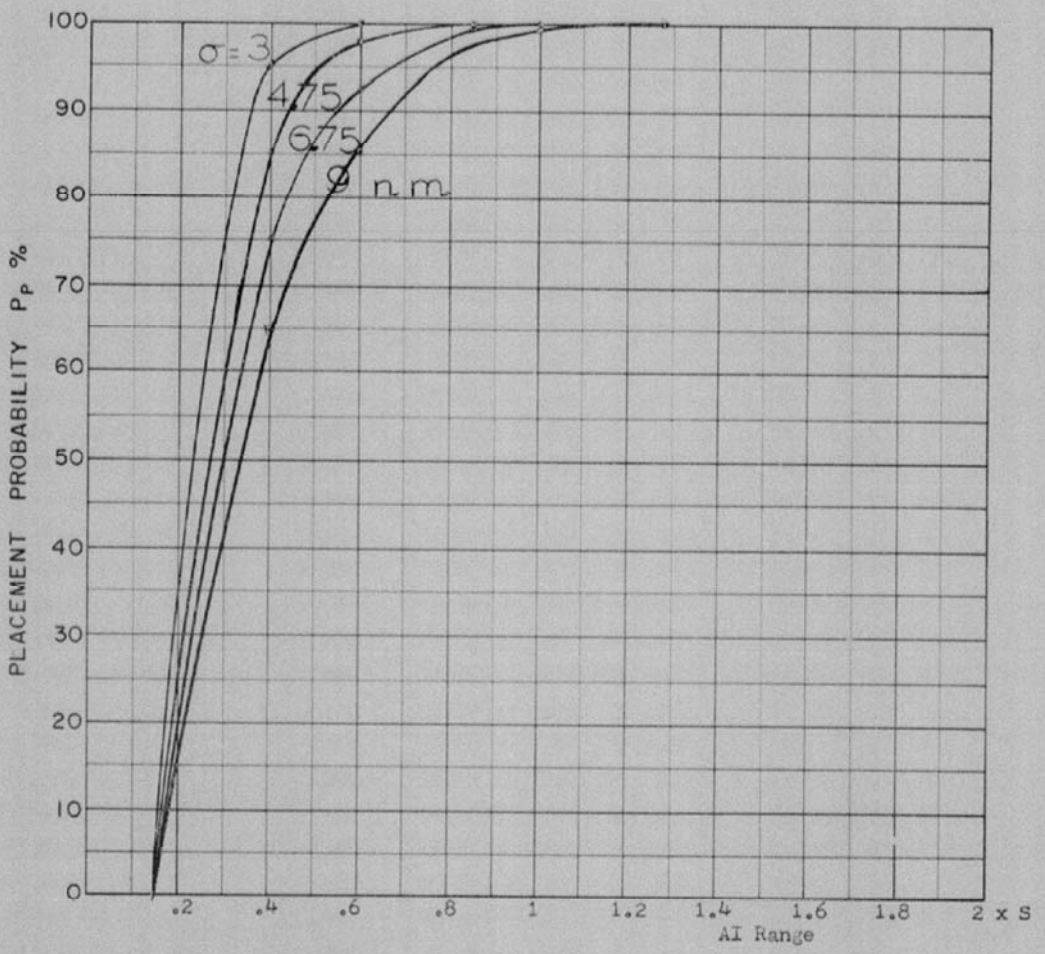

COURSE DIFFERENCE: 100°
TARGET EVASION: 0
TARGET MACH NO.: 1.5
INTERCEPTOR LATERAL G's: 1.6
INTERCEPTOR MACH NO.: 1.5
σ OF G.C.I. ACCURACY: 4 values
A.I. DETECTION RANGE AS FRACTION OF SPECIFICATION RANGE, S: Abscissa
A.I. DETECTION RANGE CONTOUR: Delta
ALTITUDE: 50 K

D14c

Look Angle Limit 80°. Missile Launch zone L-1, missile launched at maximum range.

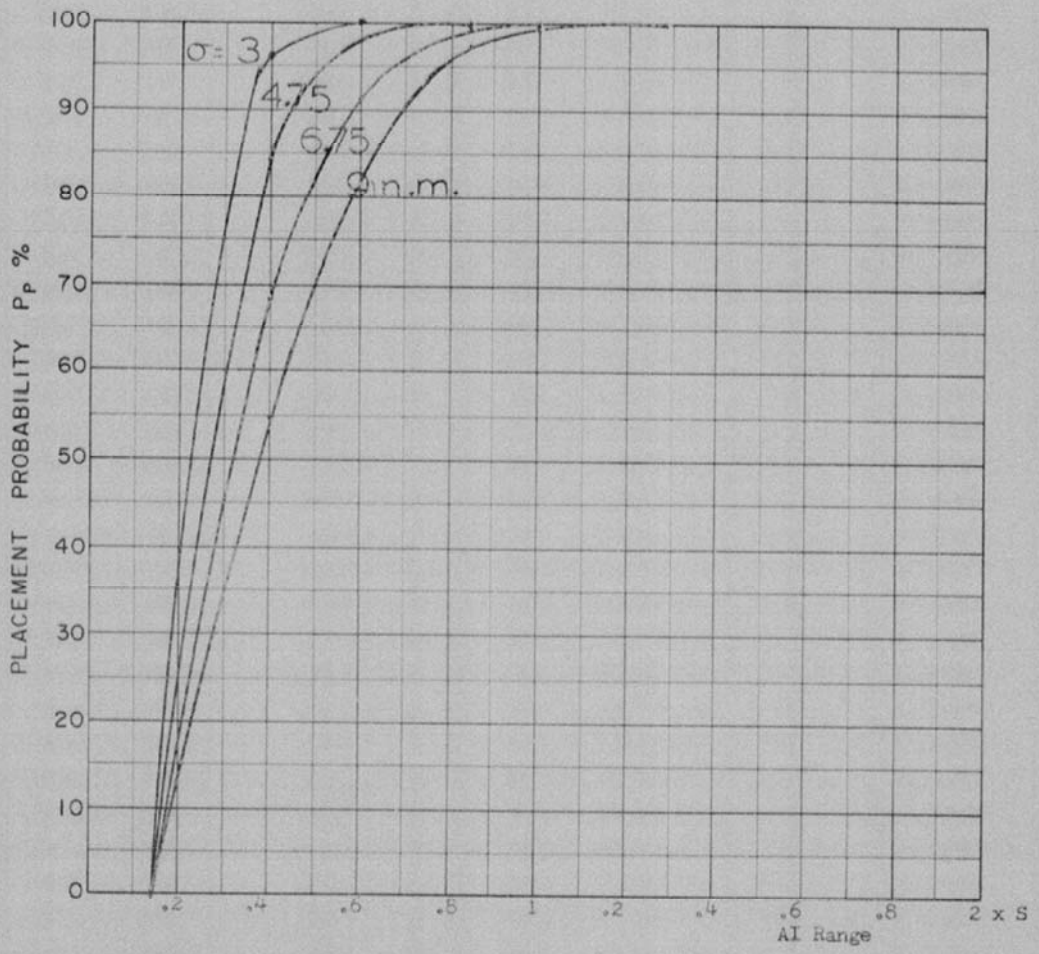

COURSE DIFFERENCE: 100°
TARGET EVASION: 0
TARGET MACH NO.: 1.5
INTERCEPTOR LATERAL G's: 1.6
INTERCEPTOR MACH NO.: 1.5
σ OF G.C.I. ACCURACY: 4 values
A.I. DETECTION RANGE AS FRACTION OF SPECIFICATION RANGE, S: Abscissa
A.I. DETECTION RANGE CONTOUR: Delta
ALTITUDE: 50 K

D14d

Look Angle Limit 80°. Missile Launch zone L-1, missile launched at minimum range.

36 c x d p r

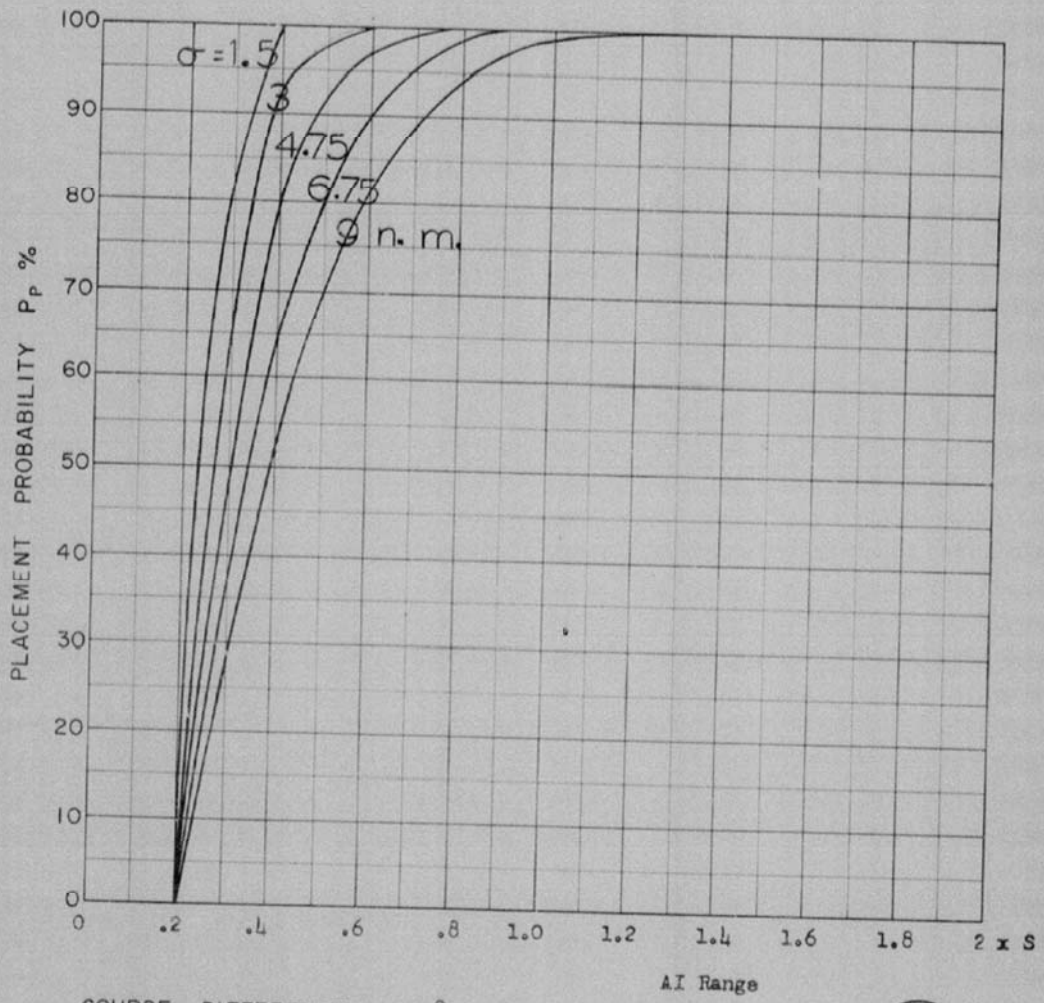

COURSE DIFFERENCE: 120°
TARGET EVASION: 0
TARGET MACH NO.: 1.5
INTERCEPTOR LATERAL G's: 1.6
INTERCEPTOR MACH NO.: 1.5
σ OF G.C.I. ACCURACY: Five values
A.I. DETECTION RANGE AS FRACTION OF SPECIFICATION RANGE, S: Abscissa
A.I. DETECTION RANGE CONTOUR: Delta
ALTITUDE: 50 K

D-15

Launch zone of figure L-1, missile launched at maximum range with 15° heading error allowance.

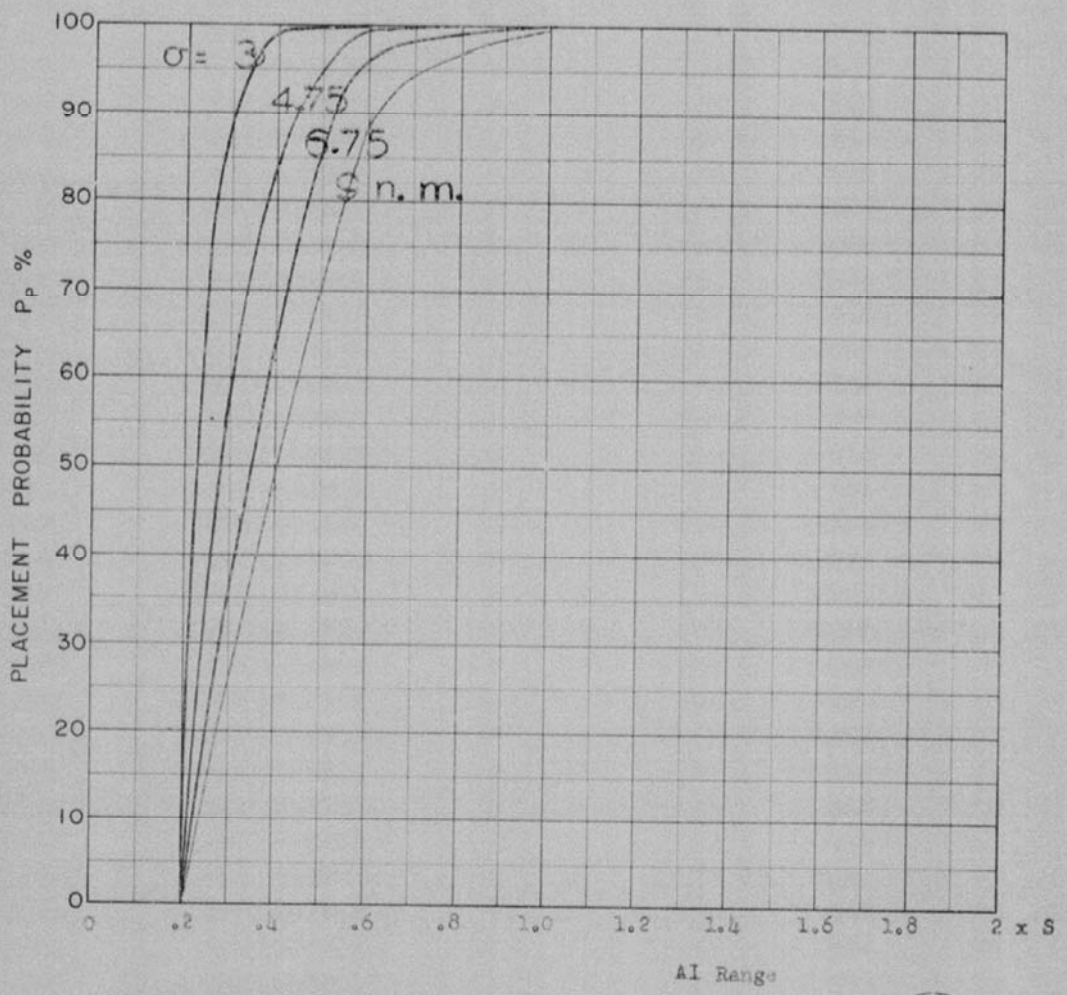

COURSE DIFFERENCE: 140°
TARGET EVASION: 0
TARGET MACH NO: 1.5
INTERCEPTOR LATERAL G's: 1.6
INTERCEPTOR MACH NO.: 1.5
σ OF G.C.I. ACCURACY: Four values
A.I. DETECTION RANGE AS FRACTION OF SPECIFICATION RANGE, S: Abcissa
A.I. DETECTION RANGE CONTOUR: Delta
ALTITUDE: 50 K

D-16

Launch zone of figure I-1, missile launched at maximum range with 15° heading error allowance.

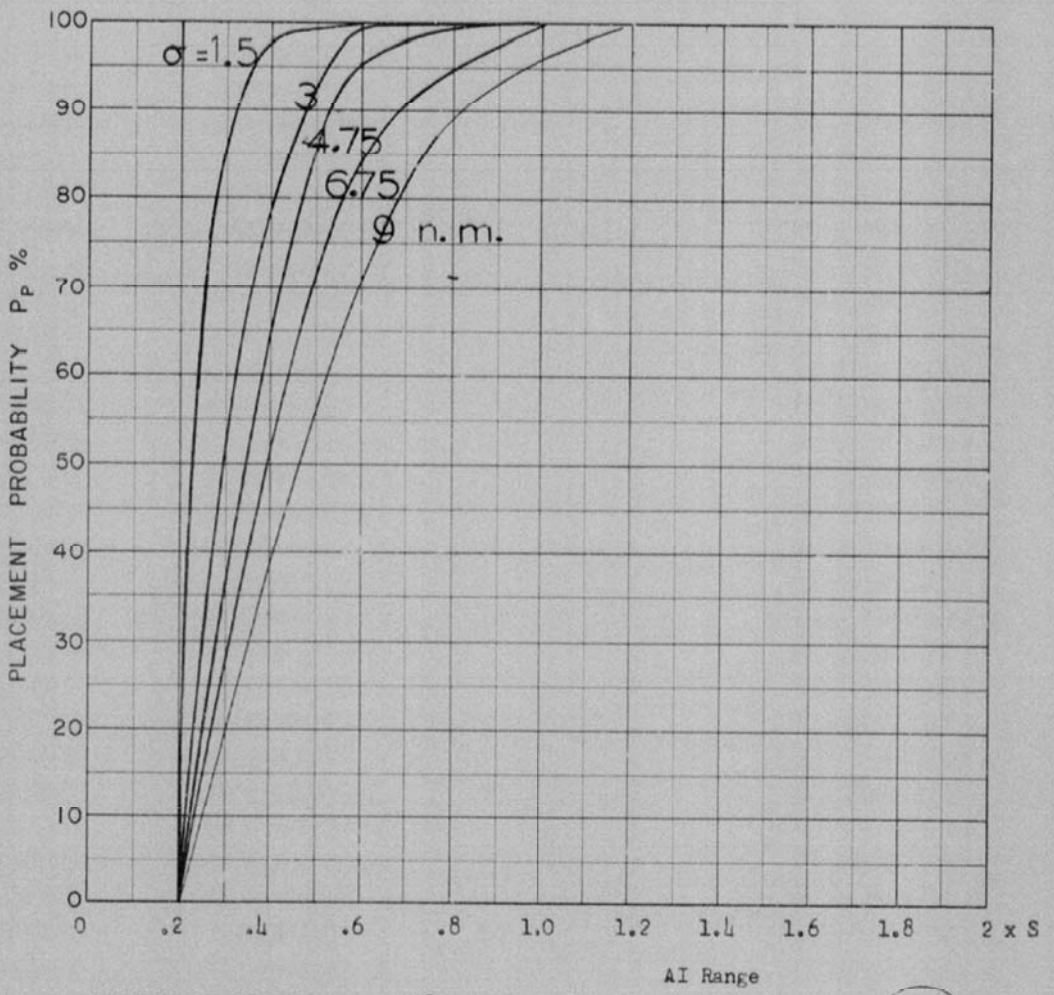

COURSE DIFFERENCE: 160°
TARGET EVASION: 0
TARGET MACH NO.: 1.5
INTERCEPTOR LATERAL G's: 1.6
INTERCEPTOR MACH NO.: 1.5
σ OF G.C.I. ACCURACY: Five values
A.I. DETECTION RANGE AS FRACTION OF SPECIFICATION RANGE, S*Abscissa
A.I. DETECTION RANGE CONTOUR: Delta
ALTITUDE: 50 K

(D 17)

Launch zone of figure L-1, missile launched at maximum range with 15° heading error allowance.

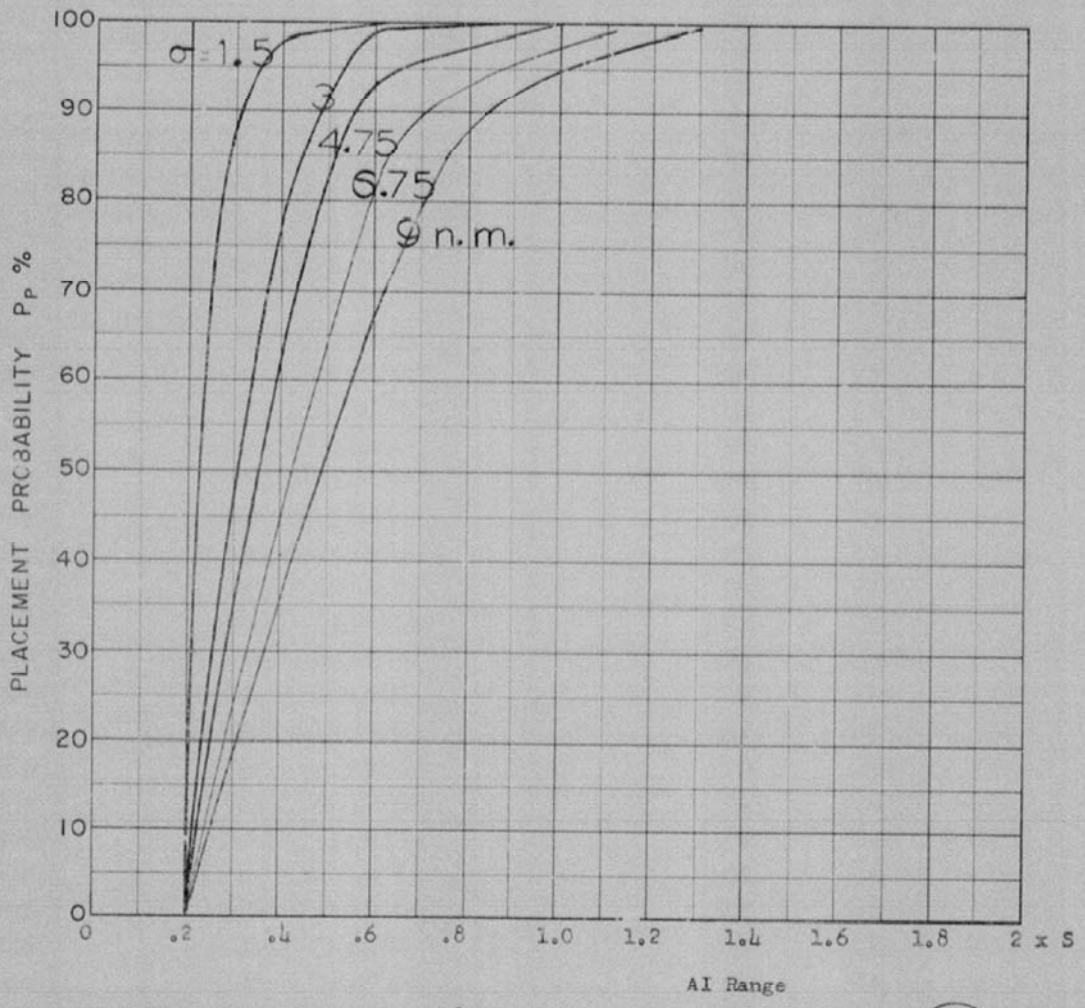

COURSE DIFFERENCE: 180°
TARGET EVASION: 0
TARGET MACH NO.: 1.5
INTERCEPTOR LATERAL G's: 1.6
INTERCEPTOR MACH NO.: 1.5
σ OF G.C.I. ACCURACY: Five values
A.I. DETECTION RANGE AS FRACTION OF SPECIFICATION RANGE, S: Abscissa
A.I. DETECTION RANGE CONTOUR: Delta
ALTITUDE: 50 K

D-18

Launch zone of figure L-1, missile launched at maximum range with 15° heading error allowance.

38 axdpr

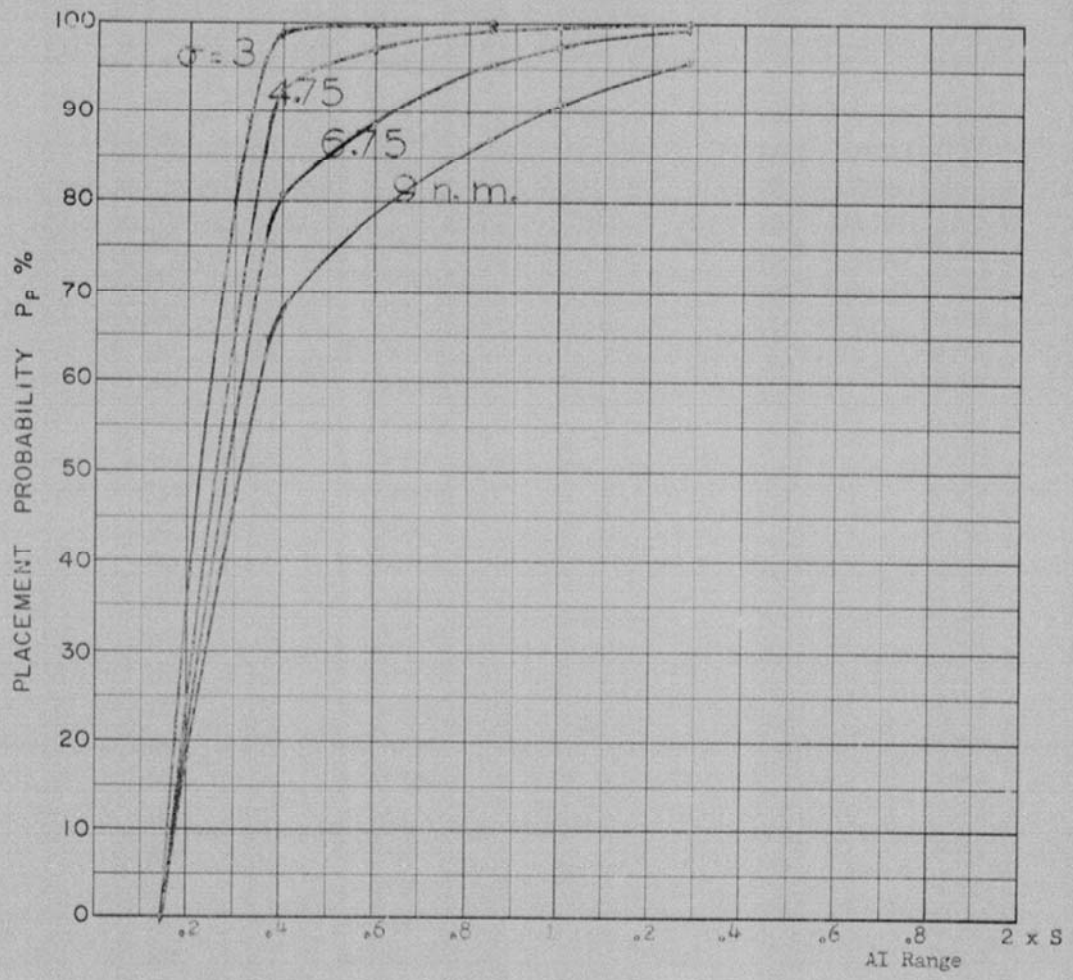

COURSE DIFFERENCE: 80°
TARGET EVASION: 0
TARGET MACH NO.: 1.5
INTERCEPTOR LATERAL G's: 3.0
INTERCEPTOR MACH NO.: 1.5
σ OF G C.I. ACCURACY: 4 values
A.I. DETECTION RANGE AS FRACTION OF SPECIFICATION RANGE, S: Abscissa
A.I. DETECTION RANGE CONTOUR: Delta
ALTITUDE: 50 K

D-19a

Missile launch zone L-1

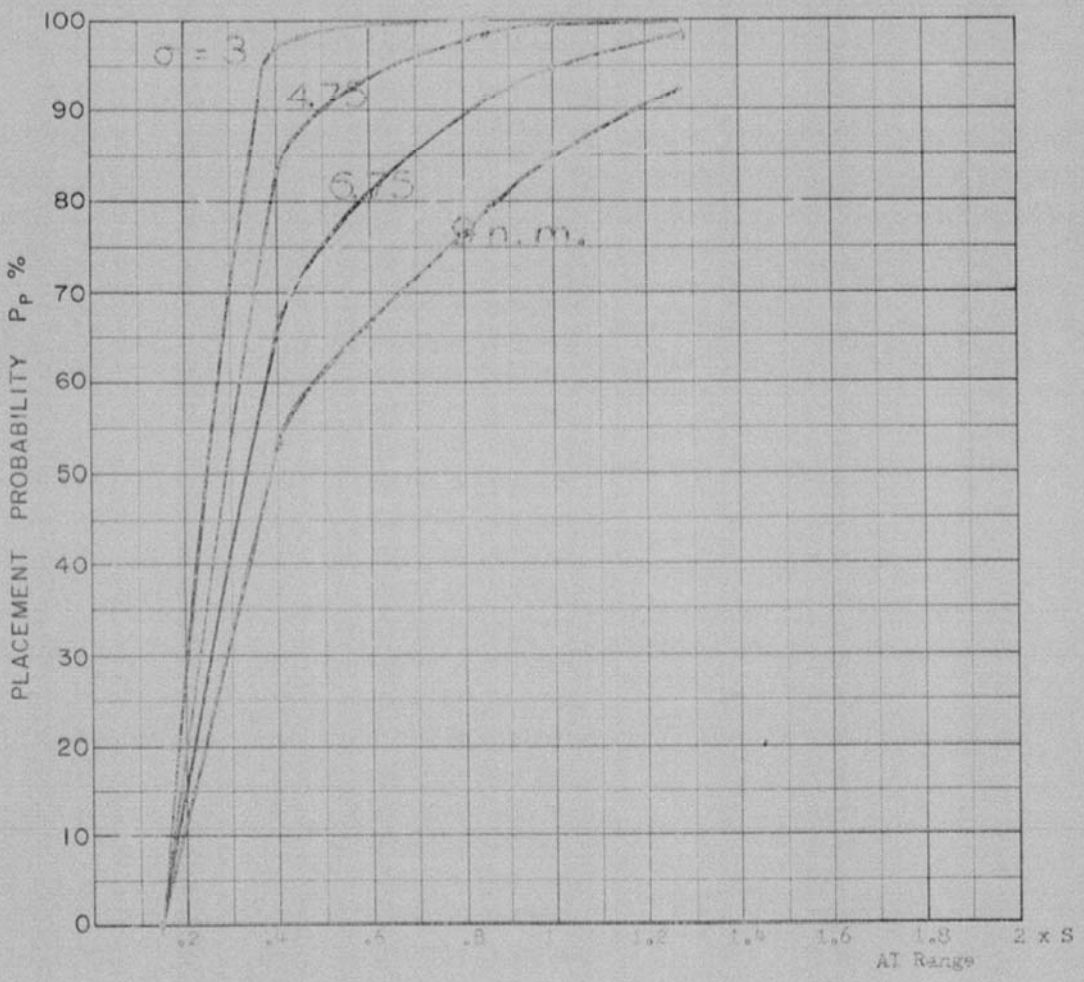

COURSE DIFFERENCE: 80°
TARGET EVASION: 0
TARGET MACH NO.: 1.5
INTERCEPTOR LATERAL G's: 3.0
INTERCEPTOR MACH NO.: 2.5
σ OF G.C.I. ACCURACY: 4 values
A.I. DETECTION RANGE AS FRACTION OF SPECIFICATION RANGE, S: Abscissa
A.I. DETECTION RANGE CONTOUR: Delta
ALTITUDE: 50 K

D 196

Missile launch zone L-1

38 bxdpr

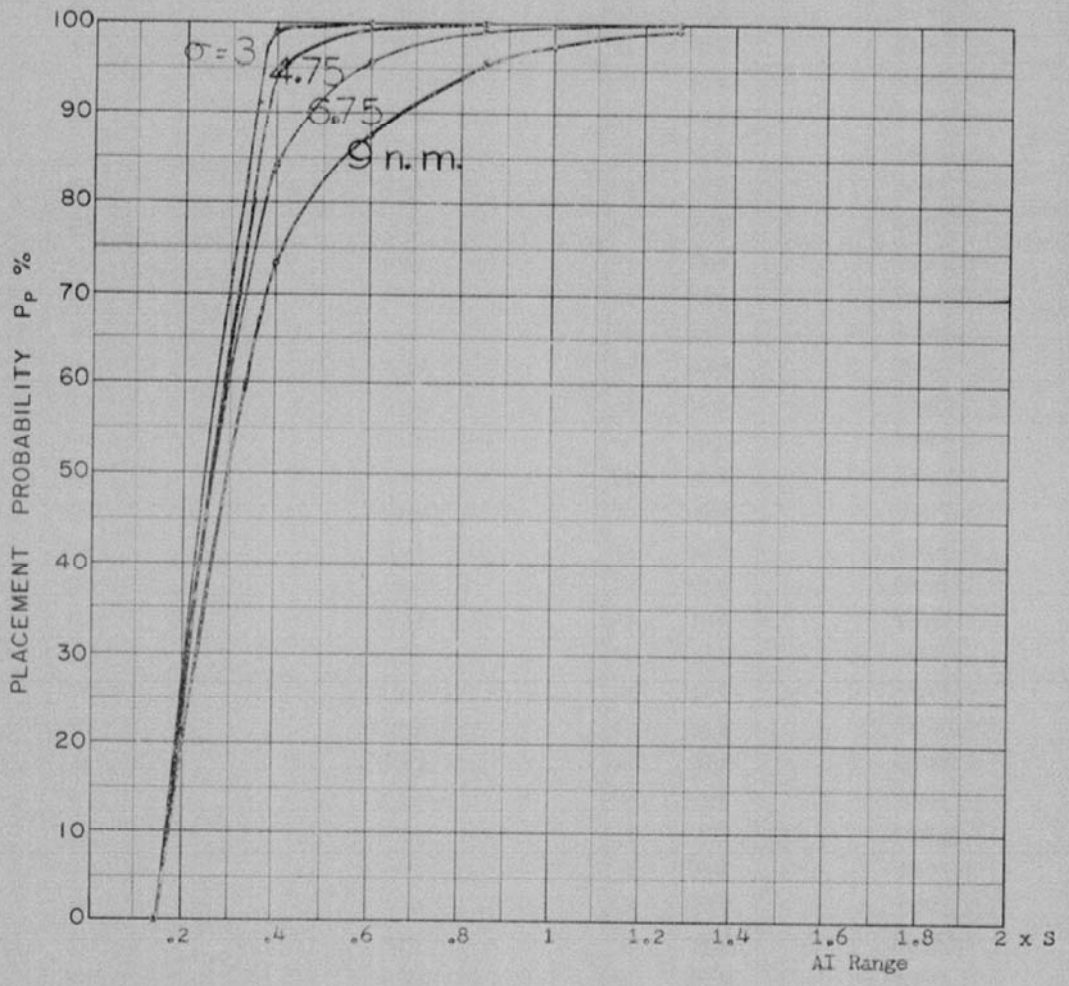

COURSE DIFFERENCE: 100°
TARGET EVASION: 0
TARGET MACH NO.: 1.5
INTERCEPTOR LATERAL G's: 3.0
INTERCEPTOR MACH NO.: 1.5
σ OF G.C.I. ACCURACY: 4 values
A.I. DETECTION RANGE AS FRACTION OF SPECIFICATION RANGE, S: Abscissa
A.I. DETECTION RANGE CONTOUR: Delta
ALTITUDE: 50 K

Missile Launch zone L-1

D 20a

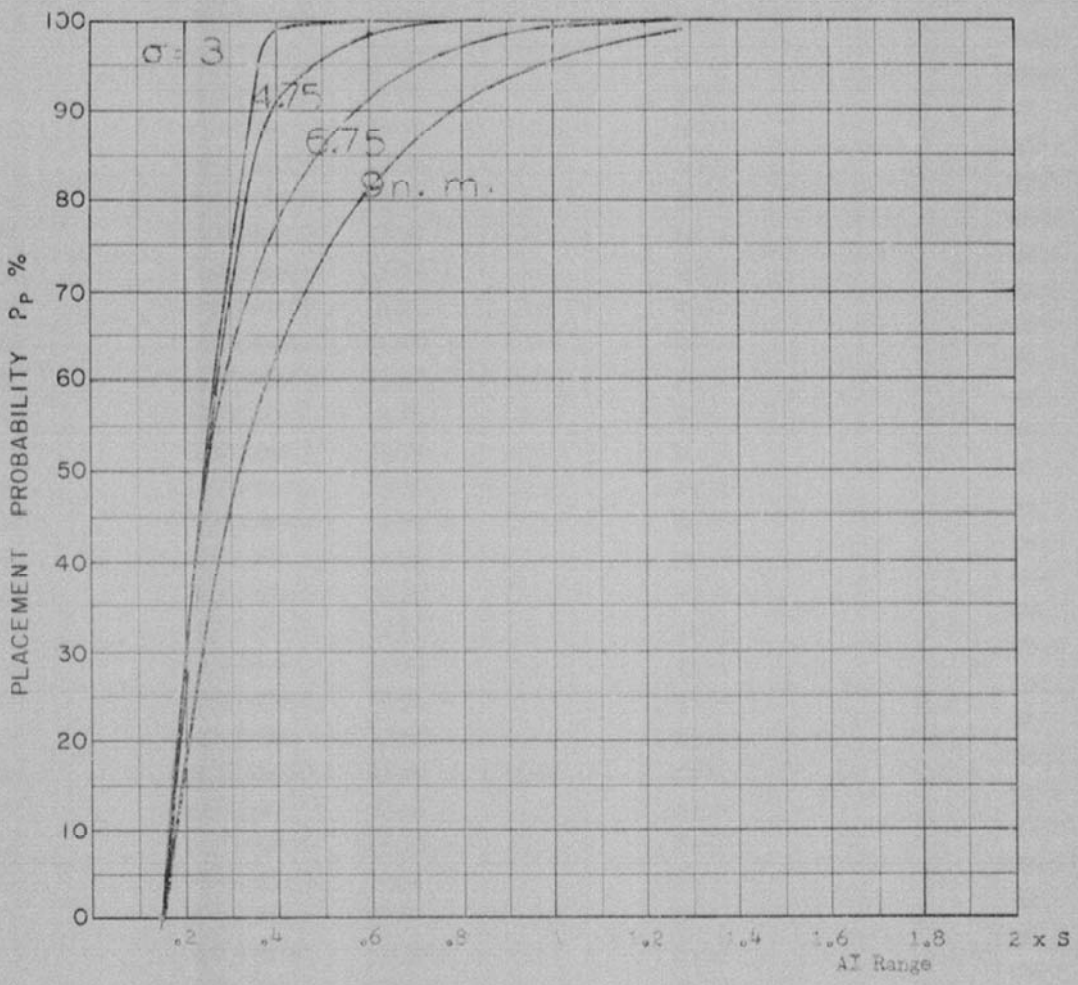

COURSE DIFFERENCE: 100°
TARGET EVASION: 0
TARGET MACH NO.: 1.5
INTERCEPTOR LATERAL G's: 3.0
INTERCEPTOR MACH NO.: 1.5
σ OF G.C.I. ACCURACY: 4 values
A.I. DETECTION RANGE AS FRACTION OF SPECIFICATION RANGE, S: Abscissa
A.I. DETECTION RANGE CONTOUR: Delta
ALTITUDE: 50 K

Missile launch zone L-1

(D 20b)

38 cxdpr

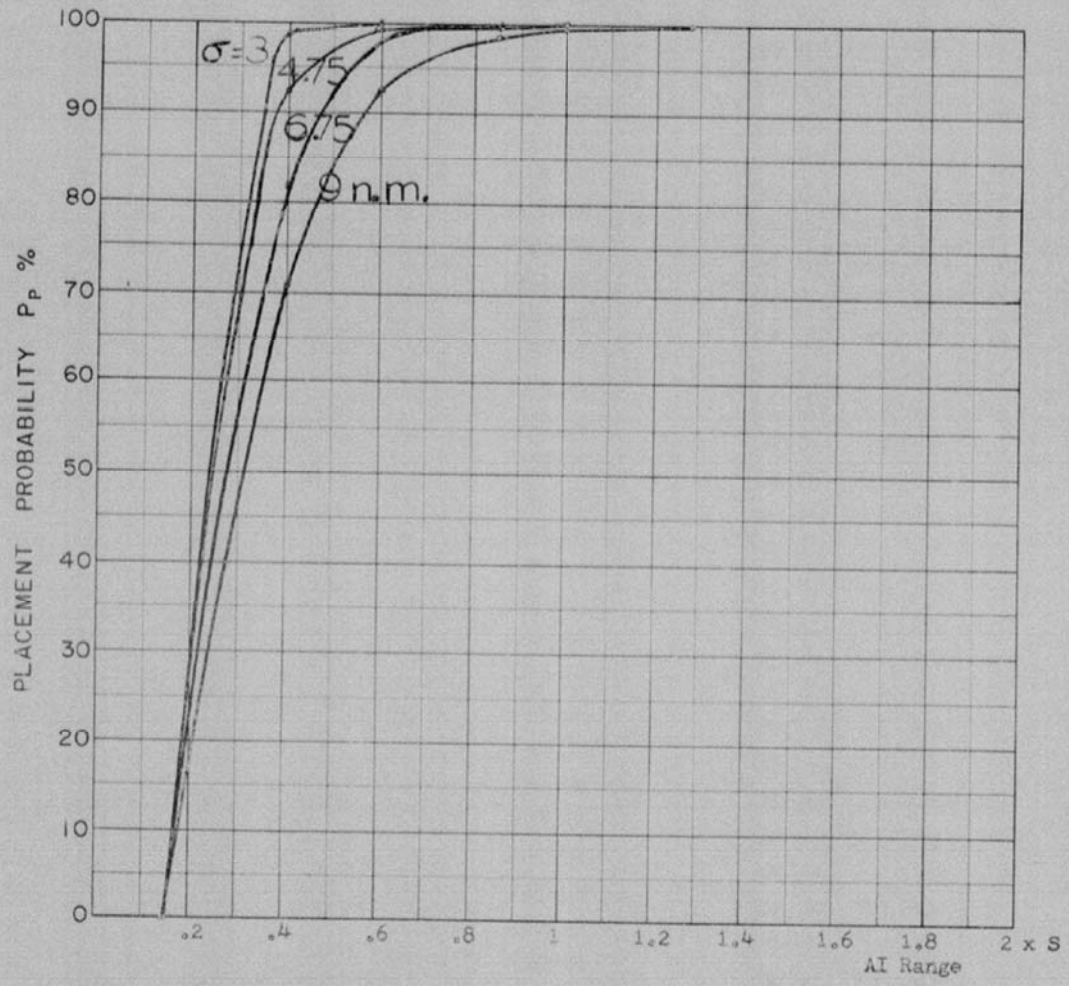

COURSE DIFFERENCE: 120°
TARGET EVASION: 0
TARGET MACH NO.: 1.5
INTERCEPTOR LATERAL G's: 3.0
INTERCEPTOR MACH NO.: 1.5
σ OF G.C.I. ACCURACY: 4 values
A.I. DETECTION RANGE AS FRACTION OF SPECIFICATION RANGE, S: Abscissa
A.I. DETECTION RANGE CONTOUR: Delta
ALTITUDE: 50 K

D21a

Missile launch zone L-1

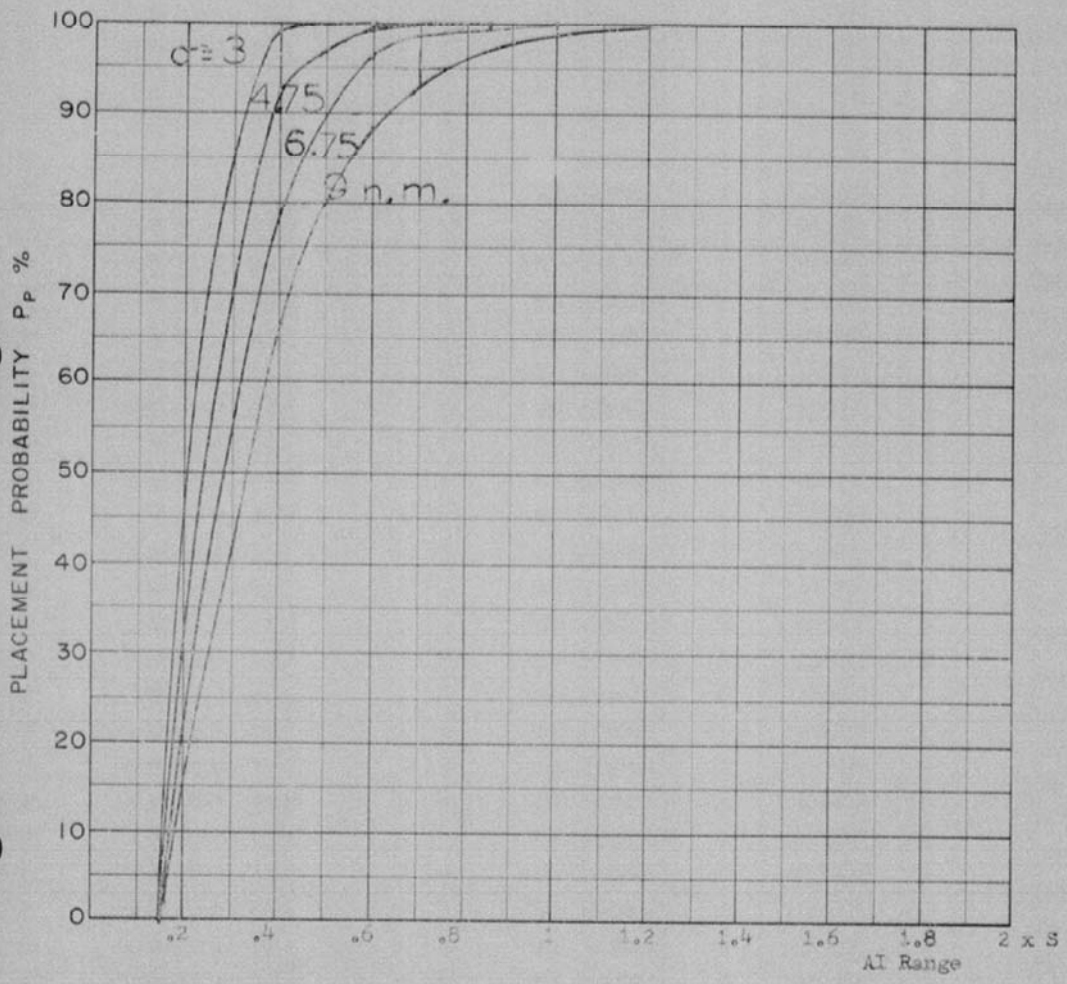

COURSE DIFFERENCE: 120°
TARGET EVASION: 0
TARGET MACH NO.: 1.5
INTERCEPTOR LATERAL G's: 3.0
INTERCEPTOR MACH NO.: 1.5
σ OF G.C.I. ACCURACY: 4 values
A.I. DETECTION RANGE AS FRACTION OF SPECIFICATION RANGE, S: Abscissa
A.I. DETECTION RANGE CONTOUR: Delta
ALTITUDE: 50 K

D216

Missile launch zone L-1

38 dxdpz

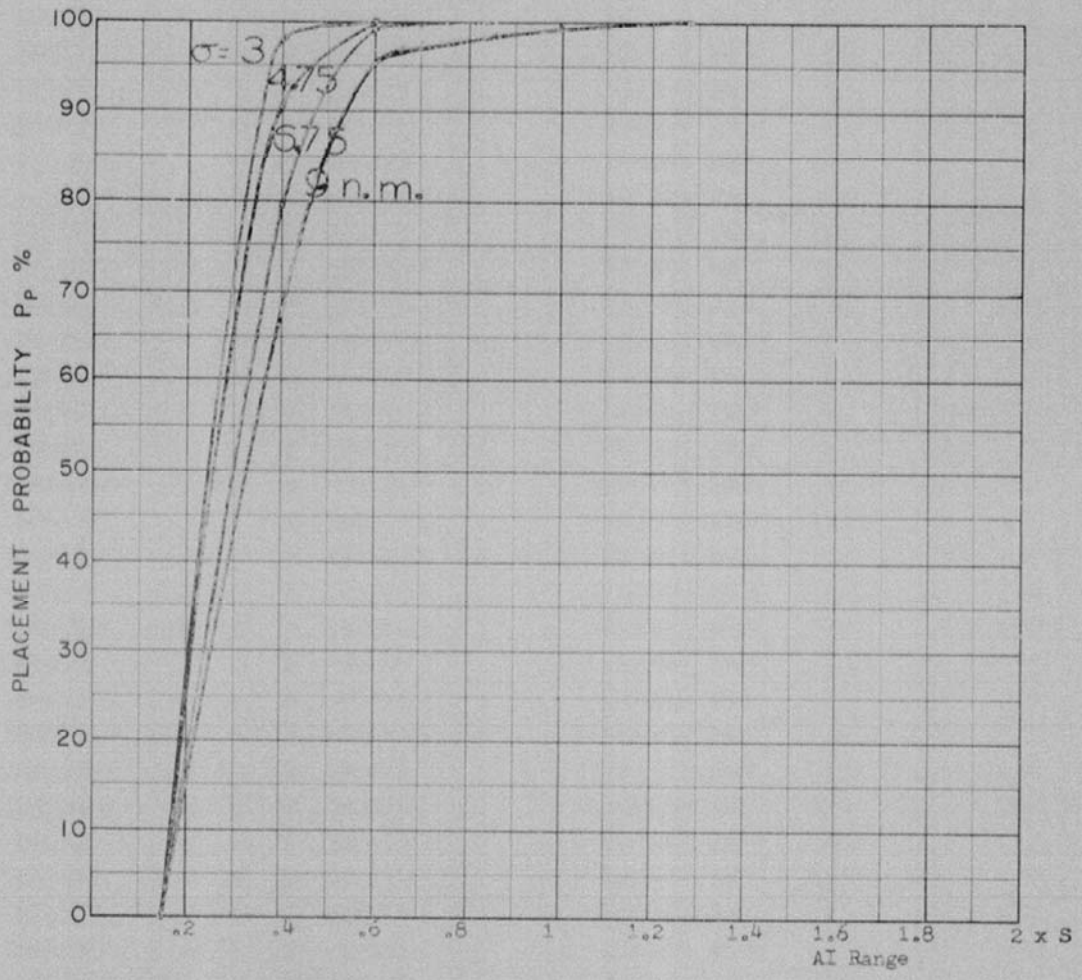

COURSE DIFFERENCE: 140°
TARGET EVASION: 0
TARGET MACH NO.: 1.5
INTERCEPTOR LATERAL G's: 3.0
INTERCEPTOR MACH NO.: 1.5
σ OF G.C.I. ACCURACY: 4 values
A.I. DETECTION RANGE AS FRACTION OF SPECIFICATION RANGE, S: Abscissa
A.I. DETECTION RANGE CONTOUR: Delta
ALTITUDE: 50 K

D 22

Missile launch zone L.1

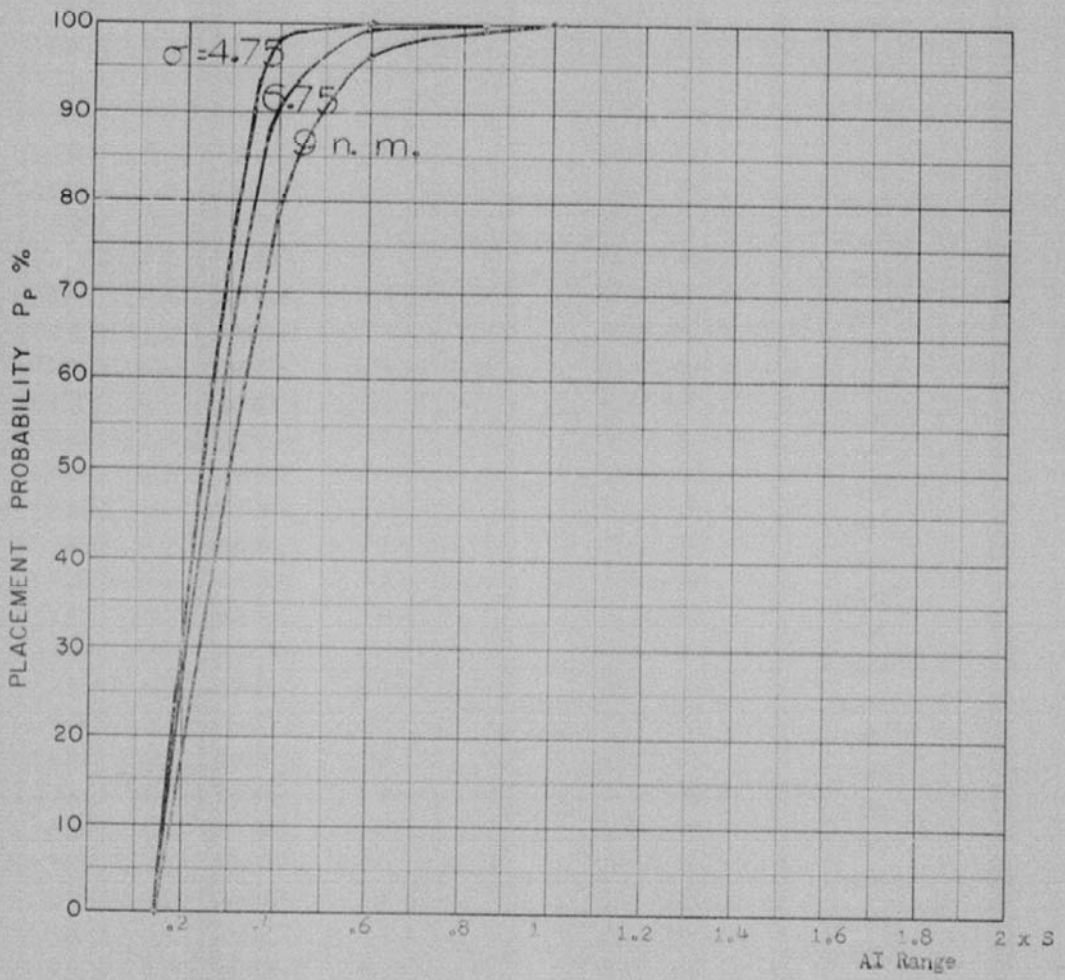

COURSE DIFFERENCE: 160°
TARGET EVASION: 0
TARGET MACH NO.: 1.5
INTERCEPTOR LATERAL G's: 3.0
INTERCEPTOR MACH NO.: 1.5
σ OF G.C.I. ACCURACY: 3 values
A.I DETECTION RANGE AS FRACTION OF SPECIFICATION RANGE, S Abscissa
A.I. DETECTION RANGE CONTOUR: Delta
ALTITUDE: 50 K

D 23

Missile launch zone L-1

38 fxdpr

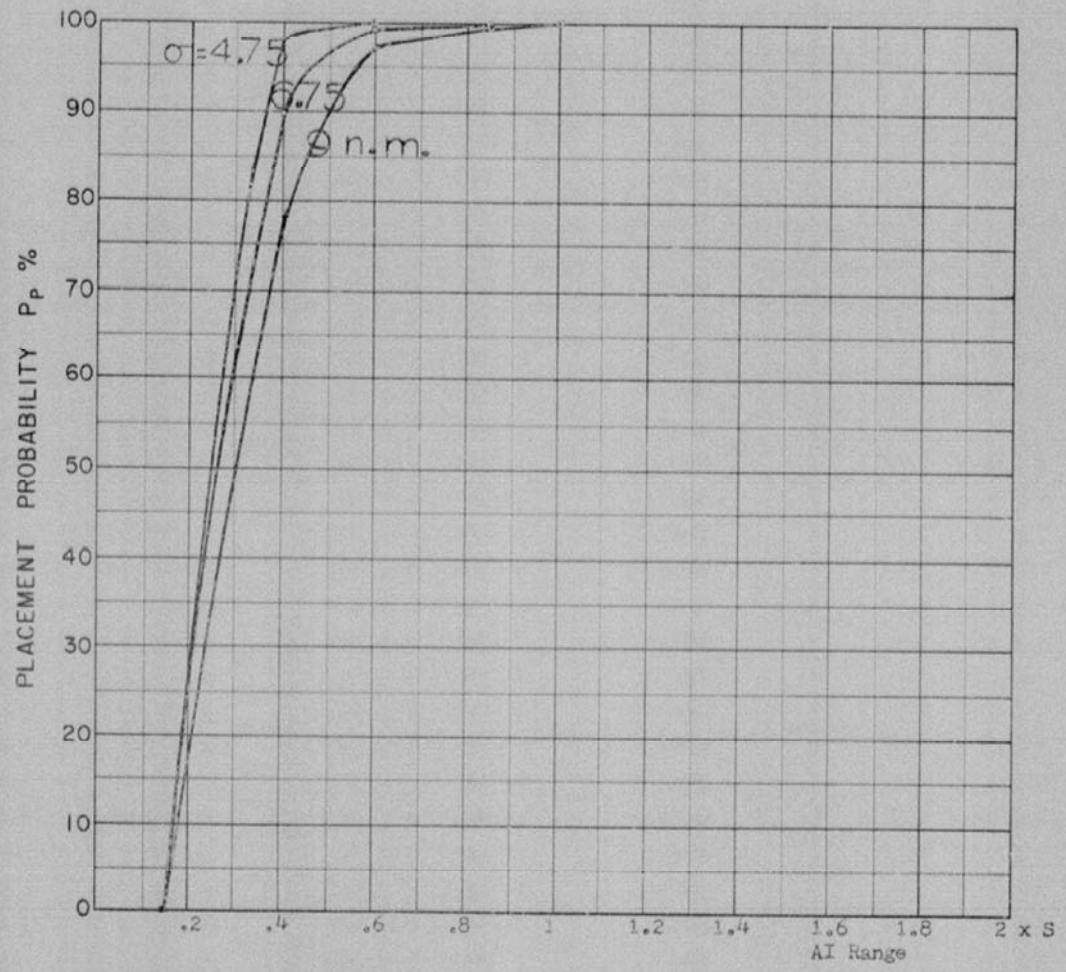

COURSE DIFFERENCE: 180°
TARGET EVASION: 0
TARGET MACH NO.: 1.5
INTERCEPTOR LATERAL G's: 3.0
INTERCEPTOR MACH NO.: 1.5
σ OF G.C.I. ACCURACY: 3 values
A.I. DETECTION RANGE AS FRACTION OF SPECIFICATION RANGE, S: Absciasa
A.I. DETECTION RANGE CONTOUR: Delta
ALTITUDE: 50 K

Missile launch zone L-1

D 24

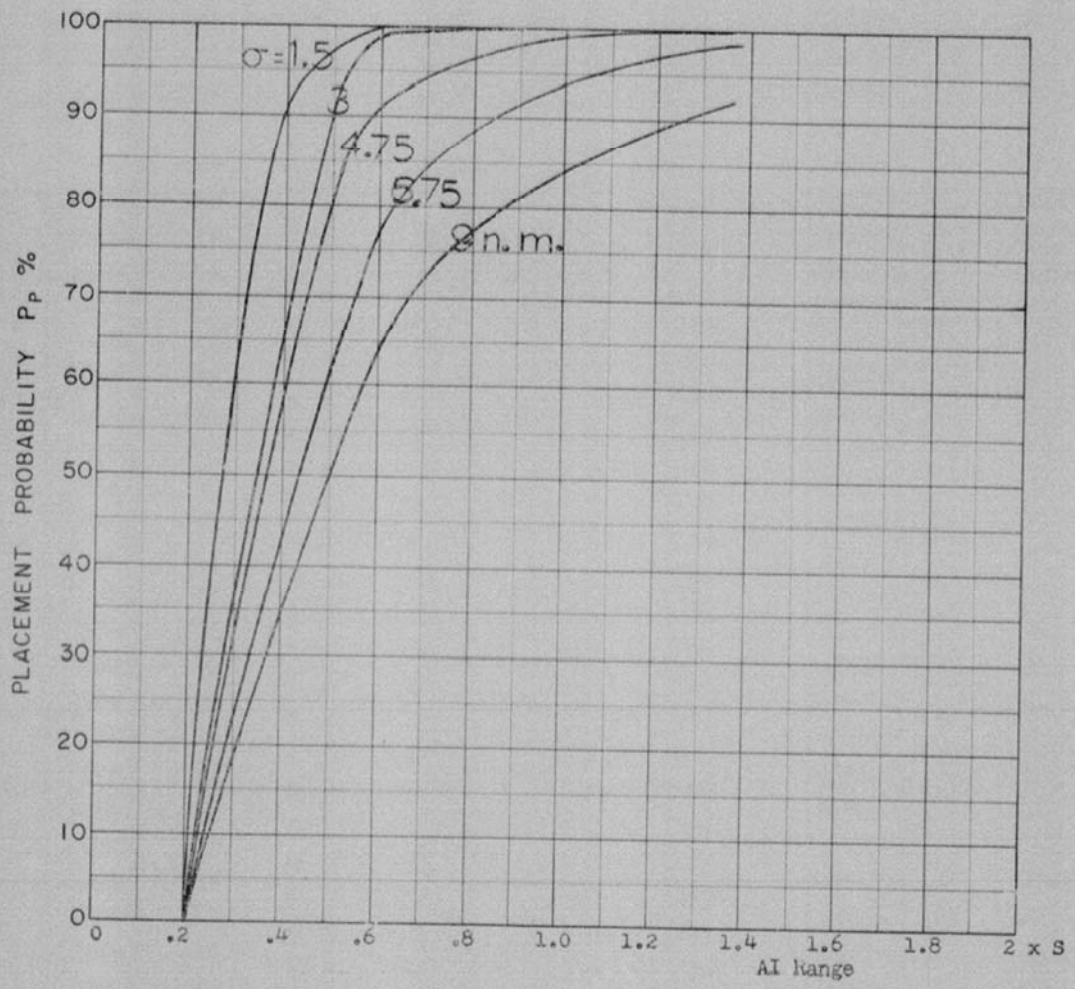

COURSE DIFFERENCE: 80°
TARGET EVASION: 0
TARGET MACH NO.: 1.5
INTERCEPTOR LATERAL G's: 0.66
INTERCEPTOR MACH NO.: 1.5
σ OF G.C.I. ACCURACY: Five values
A.I. DETECTION RANGE AS FRACTION OF SPECIFICATION RANGE, S Abscissa
A.I. DETECTION RANGE CONTOUR: Delta
ALTITUDE: 60 K

(D 25)

Launch zone of figure L-2, missile launched at maximum range with 10° heading error allowance.

32 b x d p r

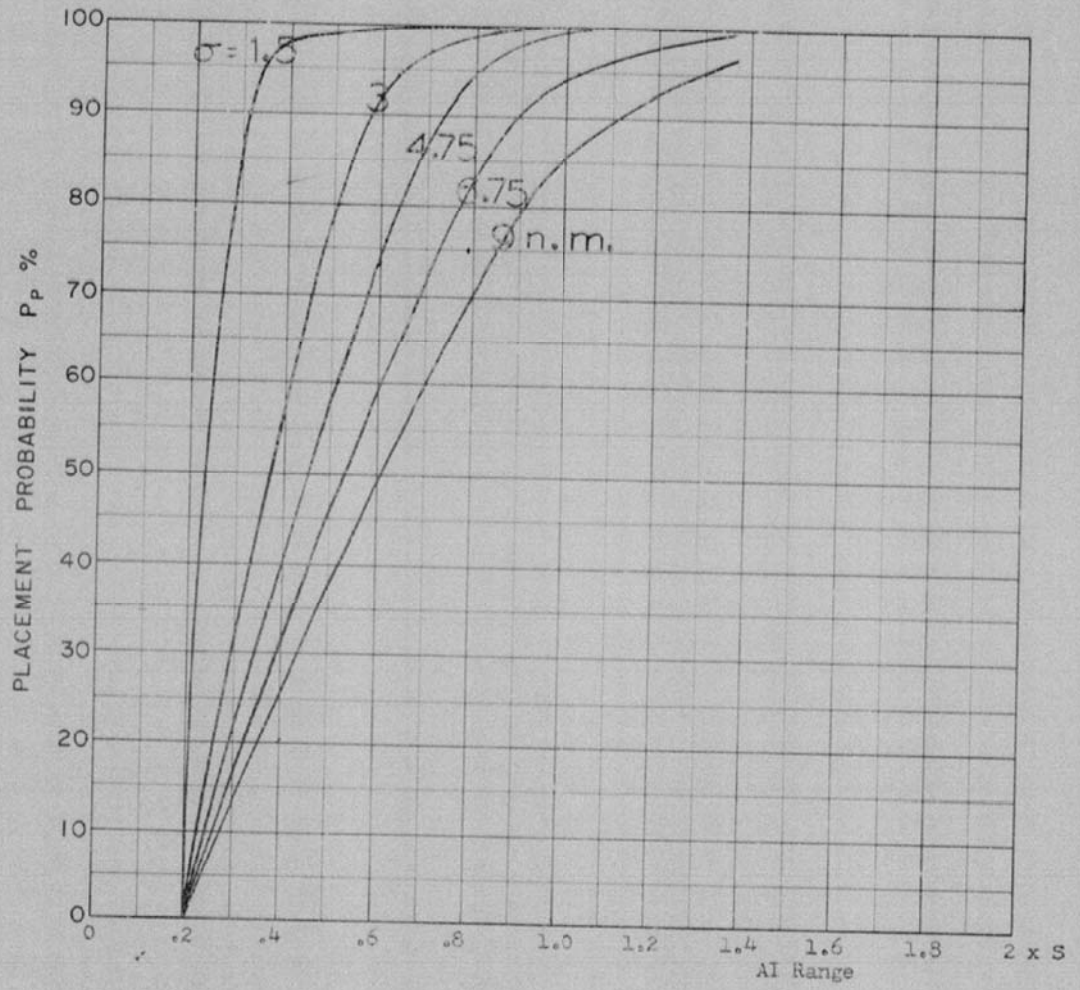

COURSE DIFFERENCE: 100°
TARGET EVASION: 0
TARGET MACH NO.: 1.5
INTERCEPTOR LATERAL G's: 0.66
INTERCEPTOR MACH NO.: 1.5
σ OF G.C.I. ACCURACY: Five values
A.I. DETECTION RANGE AS FRACTION OF SPECIFICATION RANGE, S: Abscissa
A.I. DETECTION RANGE CONTOUR: Delta
ALTITUDE: 60 K

D.26a

Launch zone of figure L-2, missile launched at maximum range with 10° heading error allowance.

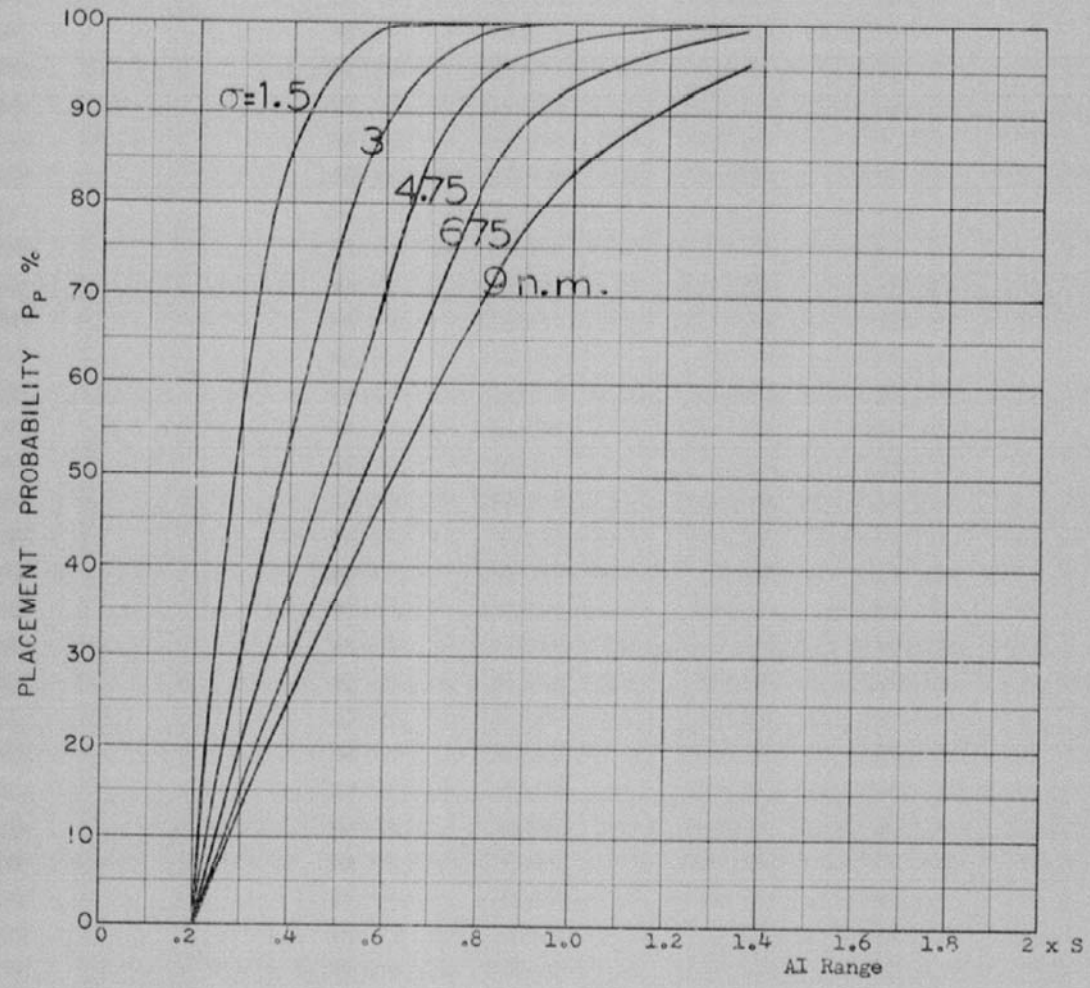

COURSE DIFFERENCE: 100°
TARGET EVASION: 0
TARGET MACH NO.: 1.5
INTERCEPTOR LATERAL G's: 0.66
INTERCEPTOR MACH NO.: 1.5
σ OF G.C.I. ACCURACY: Five values
A.I. DETECTION RANGE AS FRACTION OF SPECIFICATION RANGE, S: Abscissa
A.I. DETECTION RANGE CONTOUR: Delta
ALTITUDE: 60 K

D266

Launch zone of figure L-2

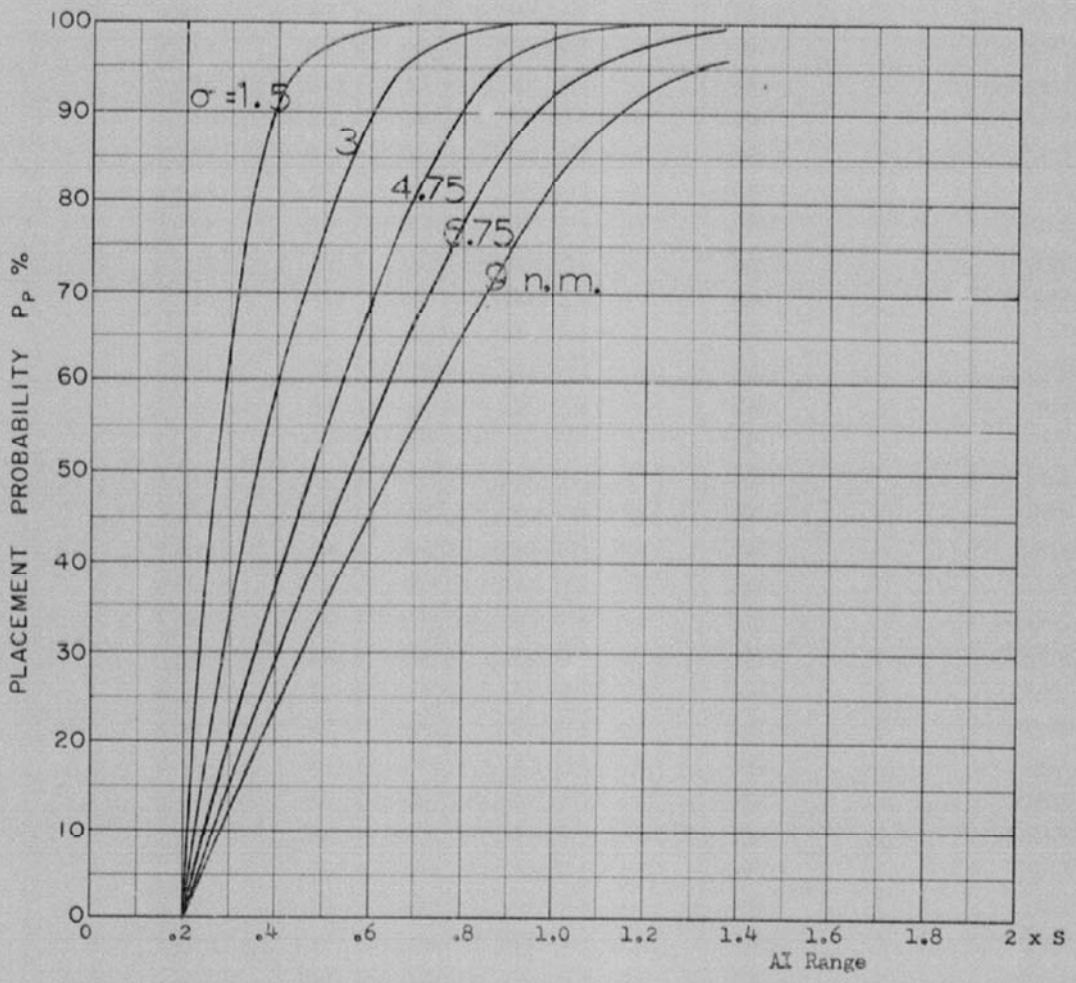

COURSE DIFFERENCE: 120°
TARGET EVASION: 0
TARGET MACH NO.: 1.5
INTERCEPTOR LATERAL G's: 0.66
INTERCEPTOR MACH NO.: 1.5
σ OF G.C.I. ACCURACY: Five values
A.I. DETECTION RANGE AS FRACTION OF SPECIFICATION RANGE, S Abscissa
A.I. DETECTION RANGE CONTOUR: Delta
ALTITUDE: 60 K

(D 27)

Launch zone of figure L-2, missile launched at maximum range with 10° heading error allowance.

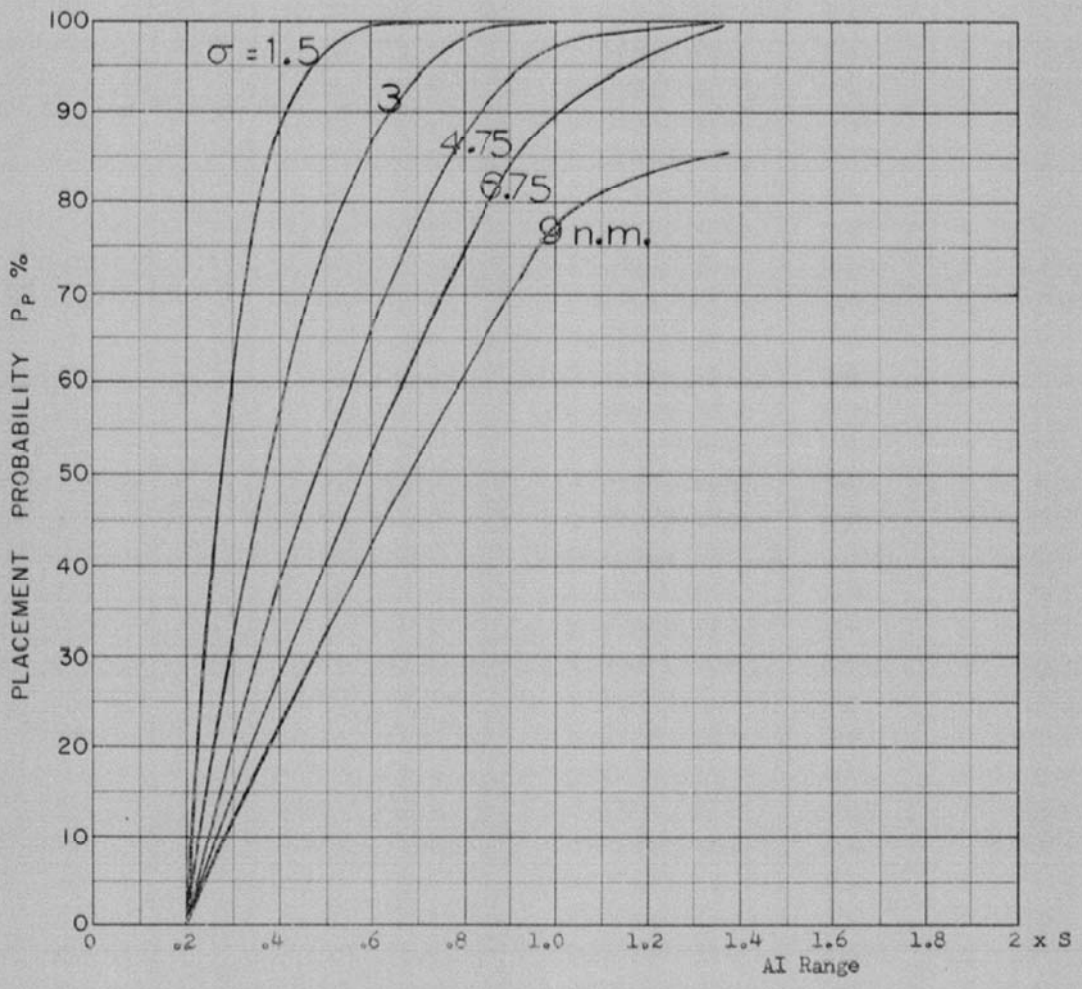

COURSE DIFFERENCE: 140°
TARGET EVASION: 0
TARGET MACH NO.: 1.5
INTERCEPTOR LATERAL G's: 0.66
INTERCEPTOR MACH NO.: 1.5
σ OF G.C.I. ACCURACY: Five values
A.I. DETECTION RANGE AS FRACTION OF SPECIFICATION RANGE, S Abscissa
A.I. DETECTION RANGE CONTOUR: Delta
ALTITUDE: 60 K

D 28

Launch zone of figure L-2, missile launched at maximum range with 10° heading error allowance.

32 e x d p r

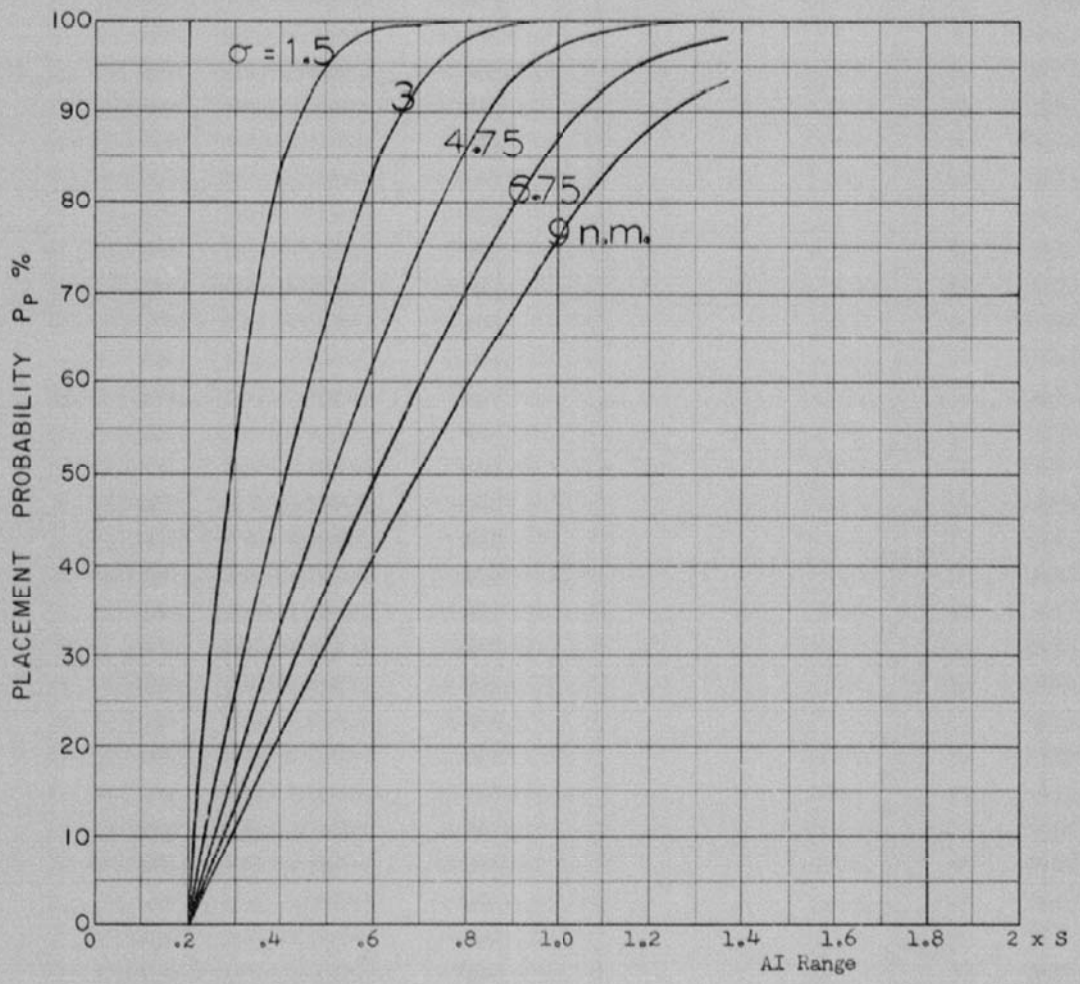

COURSE DIFFERENCE: 160°
TARGET EVASION: 0
TARGET MACH NO.: 1.5
INTERCEPTOR LATERAL G's: 0.66
INTERCEPTOR MACH NO.: 1.5
σ OF G.C.I. ACCURACY: Five values
A.I. DETECTION RANGE AS FRACTION OF SPECIFICATION RANGE, S Abscissa
A.I. DETECTION RANGE CONTOUR: Delta
ALTITUDE: 60 K

D-29

Launch zone of figure L-2, missile launched at maximum range with 10° heading error allowance.

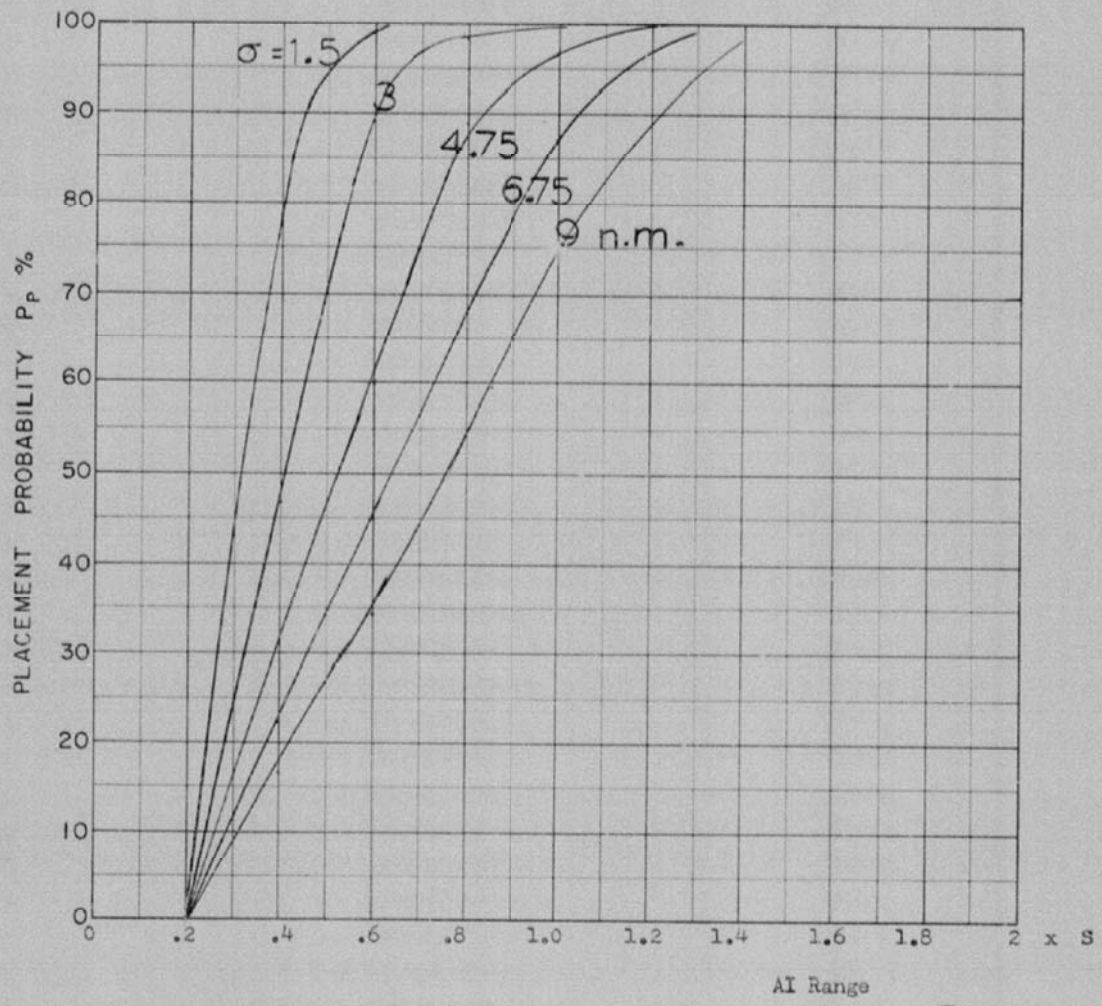

COURSE DIFFERENCE: 180°
TARGET EVASION: 0
TARGET MACH NO.: 1.5
INTERCEPTOR LATERAL G's: 0.66
INTERCEPTOR MACH NO.: 1.5
σ OF G.C.I. ACCURACY: Five values
A.I. DETECTION RANGE AS FRACTION OF SPECIFICATION RANGE, S: Abscissa
A.I. DETECTION RANGE CONTOUR: Delta
ALTITUDE: 60 K

(D-30)

Launch zone of figure L-2, missile launched at maximum range with 10° heading error allowance.

33 a x d p r

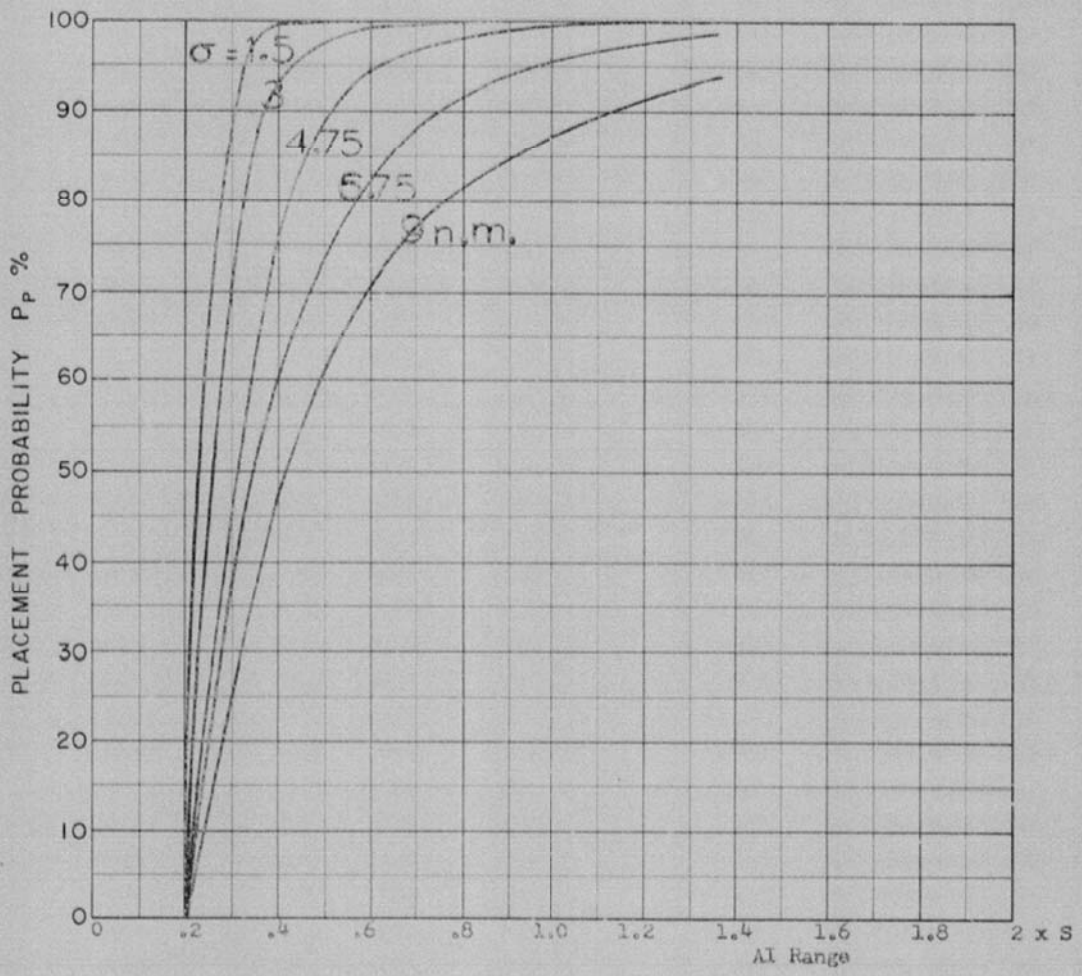

COURSE DIFFERENCE: 80°
TARGET EVASION: 0
TARGET MACH NO.: 1.5
INTERCEPTOR LATERAL G's: 1.6
INTERCEPTOR MACH NO.: 1.5
σ OF G.C.I. ACCURACY: Five values
A.I. DETECTION RANGE AS FRACTION OF SPECIFICATION RANGE, S: Abscissa
A.I. DETECTION RANGE CONTOUR: Delta
ALTITUDE: 60 K

(D31)

Launch zone of figure L-2, missile launched at maximum range with 10° heading error allowance.

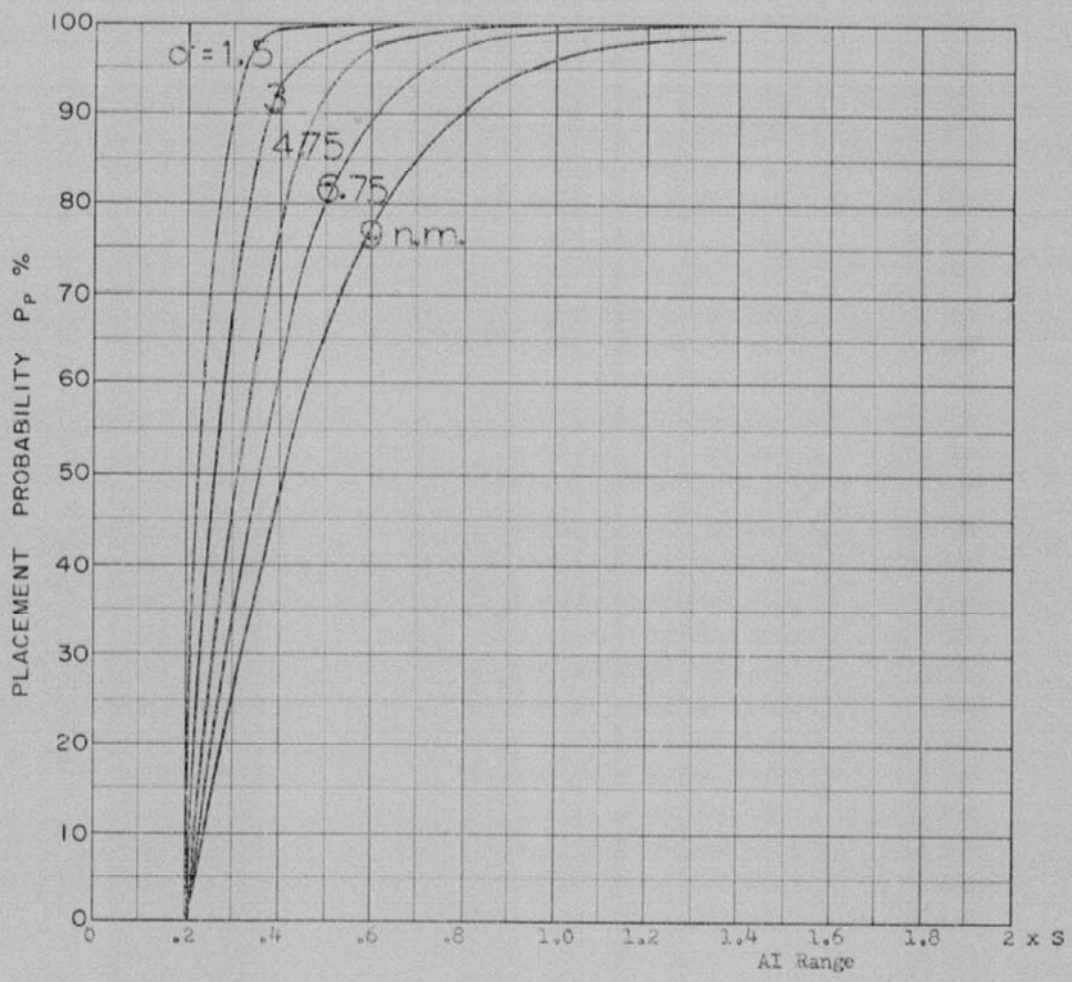

COURSE DIFFERENCE: 100°
TARGET EVASION: 0
TARGET MACH NO.: 1.5
INTERCEPTOR LATERAL G's: 1.6
INTERCEPTOR MACH NO.: 1.5
σ OF G.C.I. ACCURACY: Five values
A.I. DETECTION RANGE AS FRACTION OF SPECIFICATION RANGE, S Abscissa
A.I. DETECTION RANGE CONTOUR: Delta
ALTITUDE: 60 K

D-32

Launch zone of figure L-2. missile launched at maximum range with 10° heading error allowance.

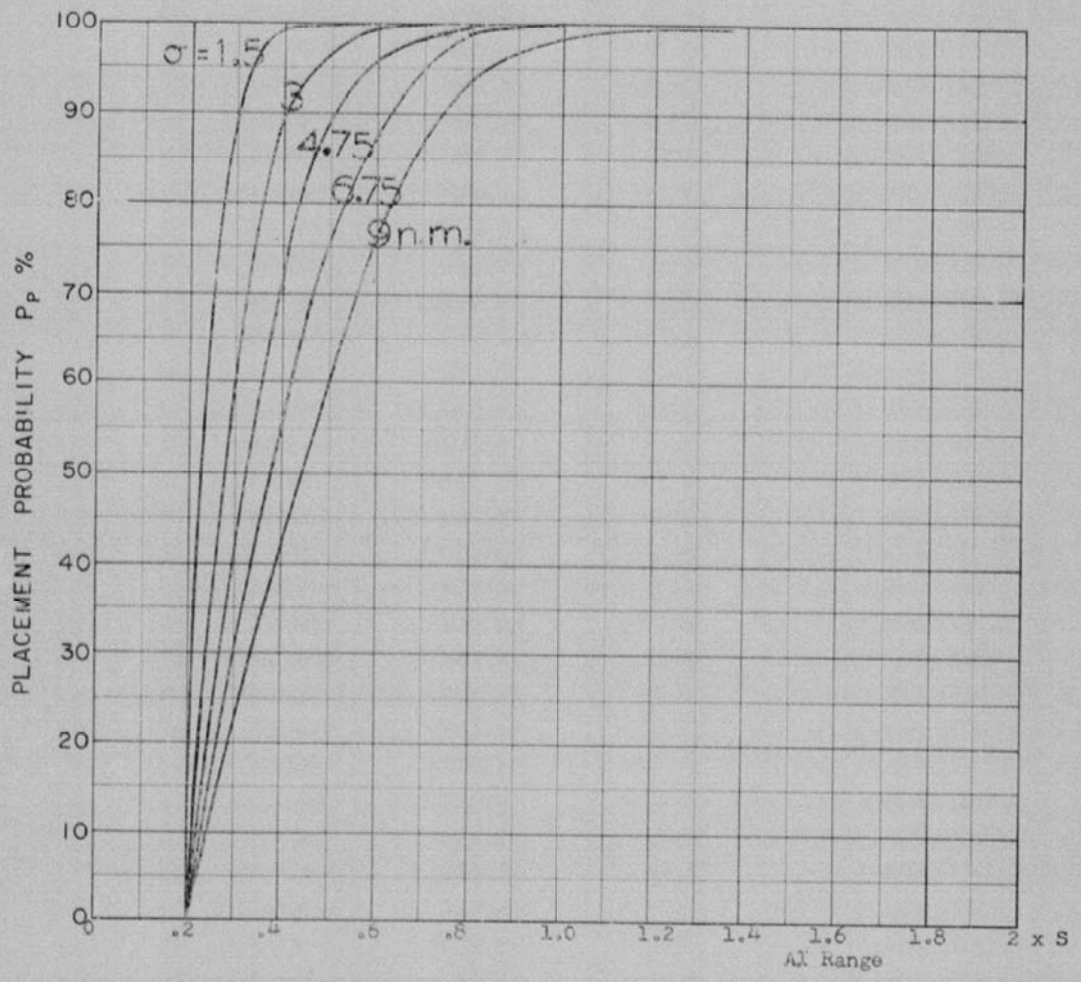

COURSE DIFFERENCE: 120°
TARGET EVASION: 0
TARGET MACH NO.: 1.5
INTERCEPTOR LATERAL G's: 1.6
INTERCEPTOR MACH NO.: 1.5
σ OF G.C.I. ACCURACY: Five values
A.I. DETECTION RANGE AS FRACTION OF SPECIFICATION RANGE, S Abscissa
A.I. DETECTION RANGE CONTOUR: Delta
ALTITUDE: 60 K

D-33

Launch zone of figure L-2, missile launched at maximum range with 10° heading error allowance.

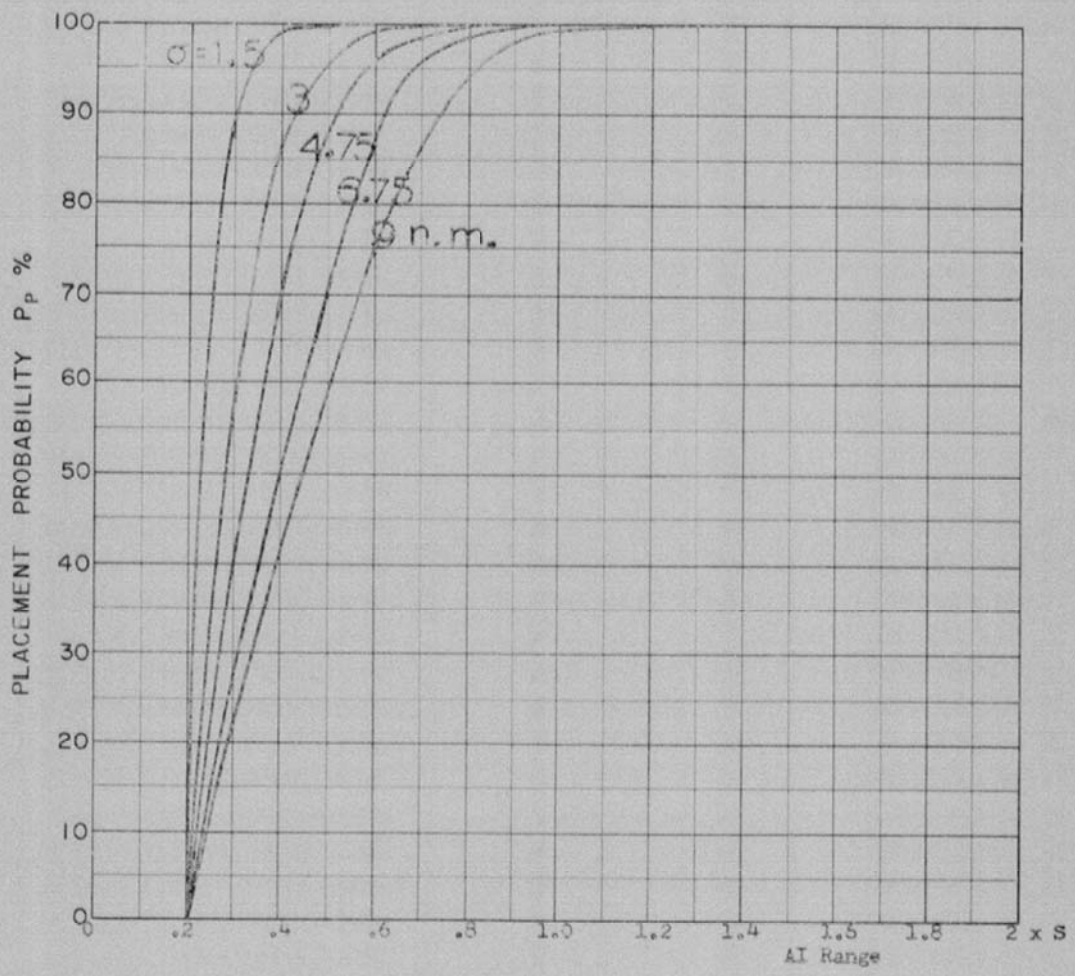

COURSE DIFFERENCE: 140°
TARGET EVASION: 0
TARGET MACH NO.: 1.5
INTERCEPTOR LATERAL G's: 1.6
INTERCEPTOR MACH NO.: 1.5
σ OF G.C.I. ACCURACY: Five values
A.I. DETECTION RANGE AS FRACTION OF SPECIFICATION RANGE, S Abscissa
A.I. DETECTION RANGE CONTOUR: Delta
ALTITUDE: 60 K

D-34

Launch zone of figure L-2, missile launched at maximum range with 10° heading error allowance.

33 e x d p r

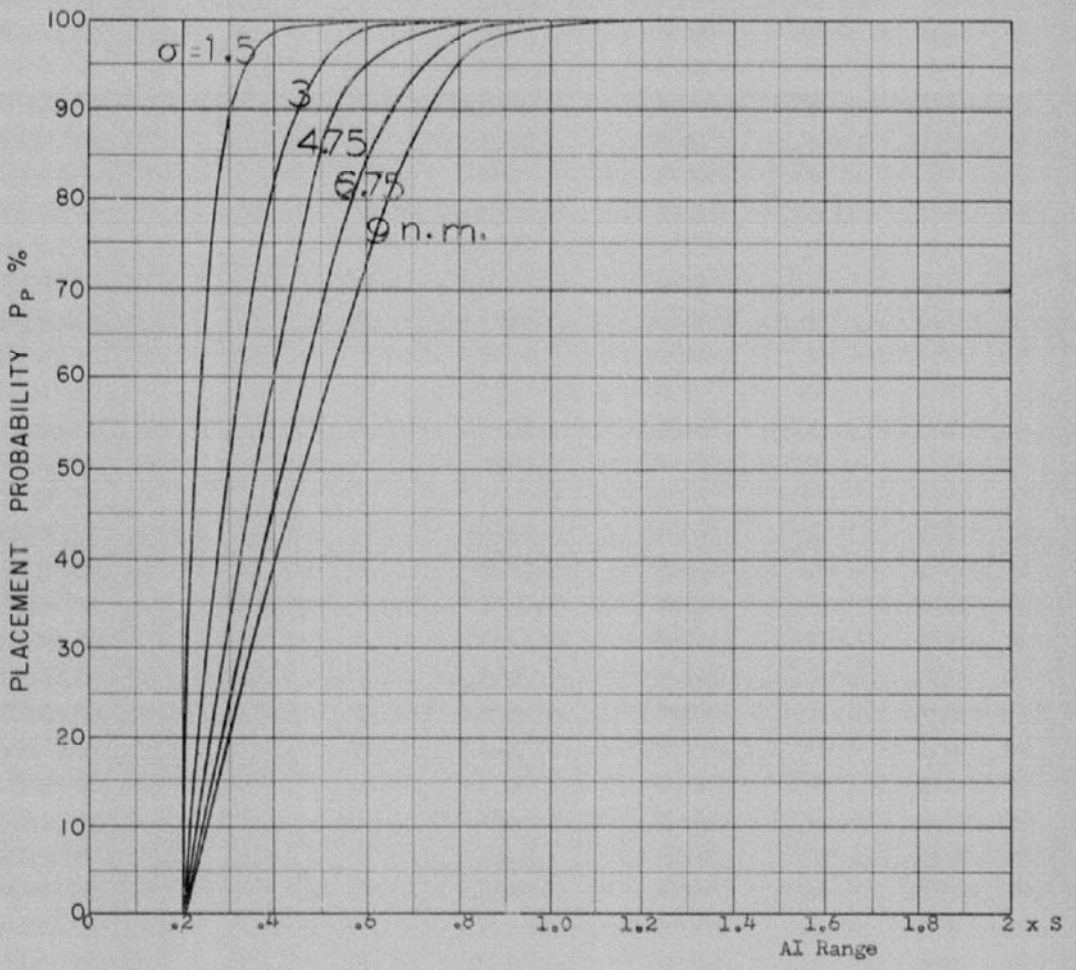

COURSE DIFFERENCE: 160°
TARGET EVASION: 0
TARGET MACH NO.: 1.5
INTERCEPTOR LATERAL G's: 1.6
INTERCEPTOR MACH NO.: 1.5
σ OF G.C.I. ACCURACY: Five values
A.I. DETECTION RANGE AS FRACTION OF SPECIFICATION RANGE, S abscissa
A.I. DETECTION RANGE CONTOUR: Delta
ALTITUDE: 60 K

D-35

Launch zone of figure L-2, missile launched at maximum range with 10° heading error allowance.

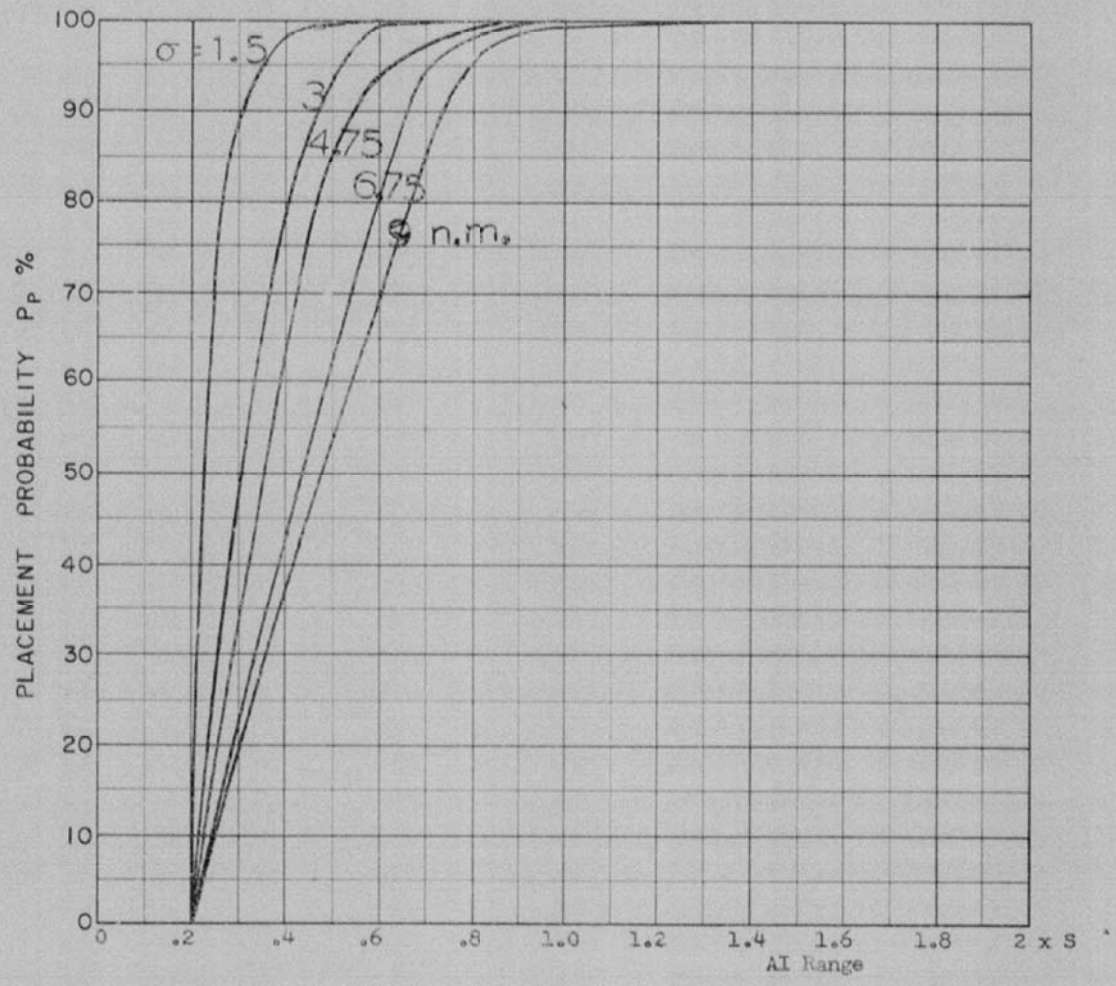

COURSE DIFFERENCE: 180°
TARGET EVASION: 0
TARGET MACH NO.: 1.5
INTERCEPTOR LATERAL G's: 1.6
INTERCEPTOR MACH NO.: 1.5
σ OF G.C.I. ACCURACY: Five values
A.I. DETECTION RANGE AS FRACTION OF SPECIFICATION RANGE, S: Abscissa
A.I. DETECTION RANGE CONTOUR: Delta
ALTITUDE: 60 K

D-36

Launch zone of figure L-2, missile launched at maximum range with 10° heading error allowance.

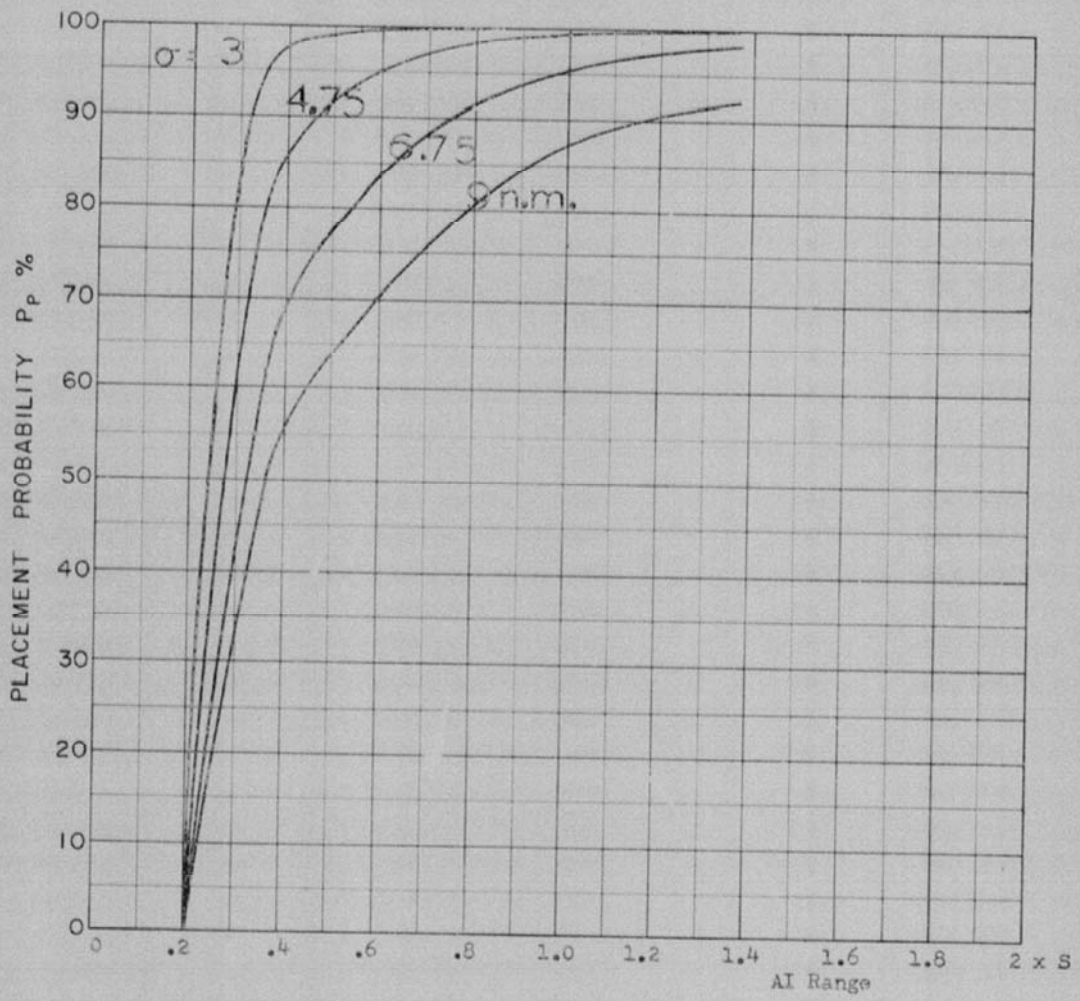

COURSE DIFFERENCE: 80°
TARGET EVASION: 0
TARGET MACH NO.: 1.5
INTERCEPTOR LATERAL G's: 3.0
INTERCEPTOR MACH NO.: 1.5
σ OF G.C.I. ACCURACY: Four values
A.I. DETECTION RANGE AS FRACTION OF SPECIFICATION RANGE, S: Abscissa
A.I. DETECTION RANGE CONTOUR: Delta
ALTITUDE: 60 K

D-37

Launch zone L-2, missile launched at maximum range with 10° heading error allowance.

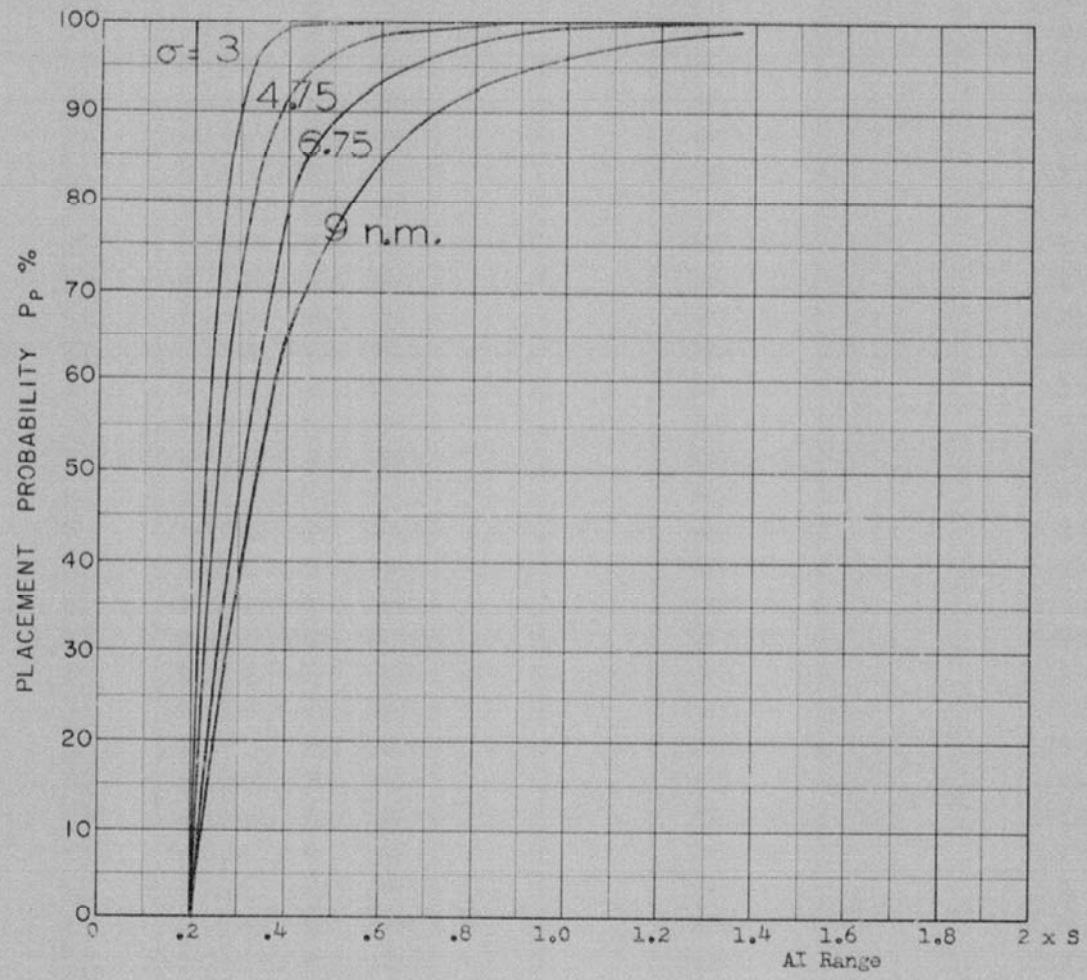

COURSE DIFFERENCE: 100°
TARGET EVASION: 0
TARGET MACH NO.: 1.5
INTERCEPTOR LATERAL G's: 3.0
INTERCEPTOR MACH NO.: 1.5
σ OF G.C.I. ACCURACY: Four values
A.I. DETECTION RANGE AS FRACTION OF SPECIFICATION RANGE, S Abscissa
A.I. DETECTION RANGE CONTOUR: Delta
ALTITUDE: 60 K

D-38

Launch zone L-2, missile launched at maximum range with 10° heading error allowance.

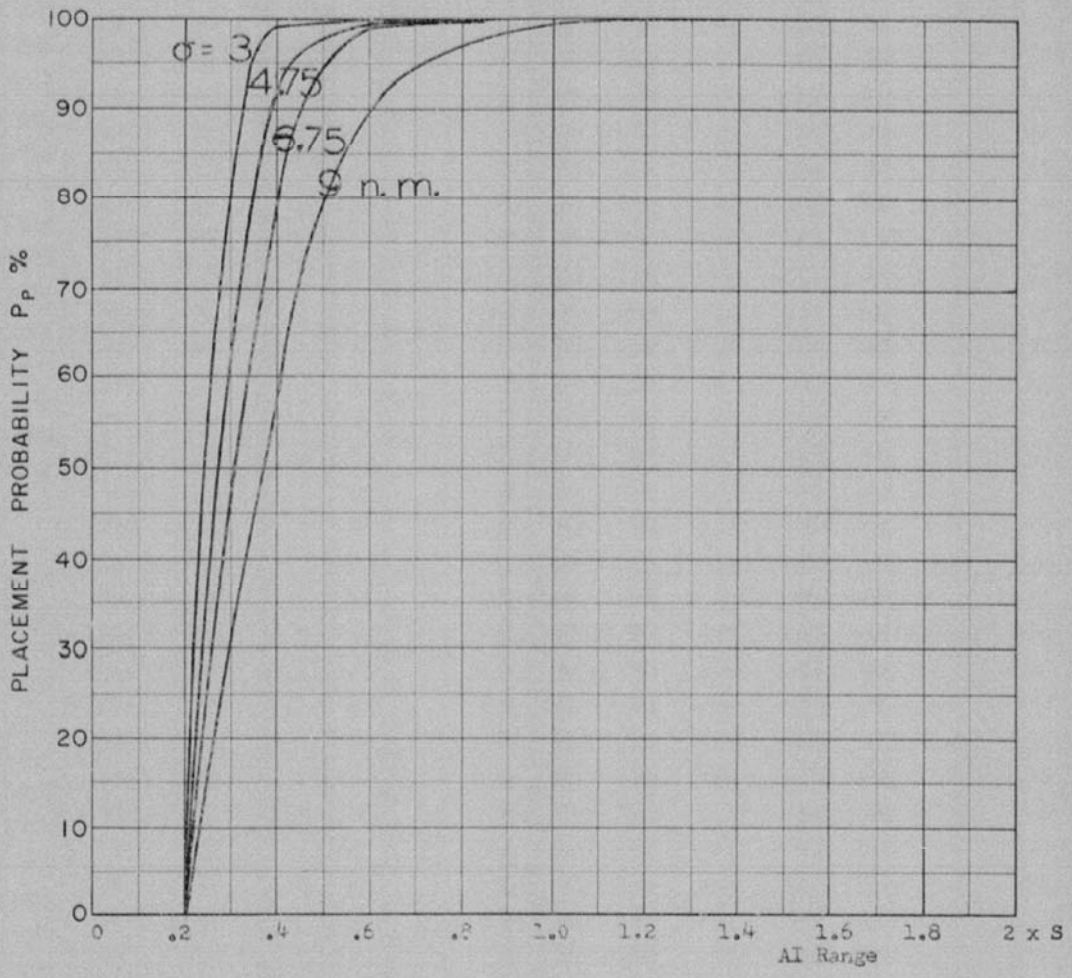

COURSE DIFFERENCE: 120°
TARGET EVASION: 0
TARGET MACH NO.: 1.5
INTERCEPTOR LATERAL G's: 3.0
INTERCEPTOR MACH NO.: 1.5
σ OF G.C.I. ACCURACY: Four values
A.I. DETECTION RANGE AS FRACTION OF SPECIFICATION RANGE, S: Abscissa
A.I. DETECTION RANGE CONTOUR: Delta
ALTITUDE: 60 K

D-39a

Launch zone L-2, missile launched at maximum range with 10° heading error allowance.

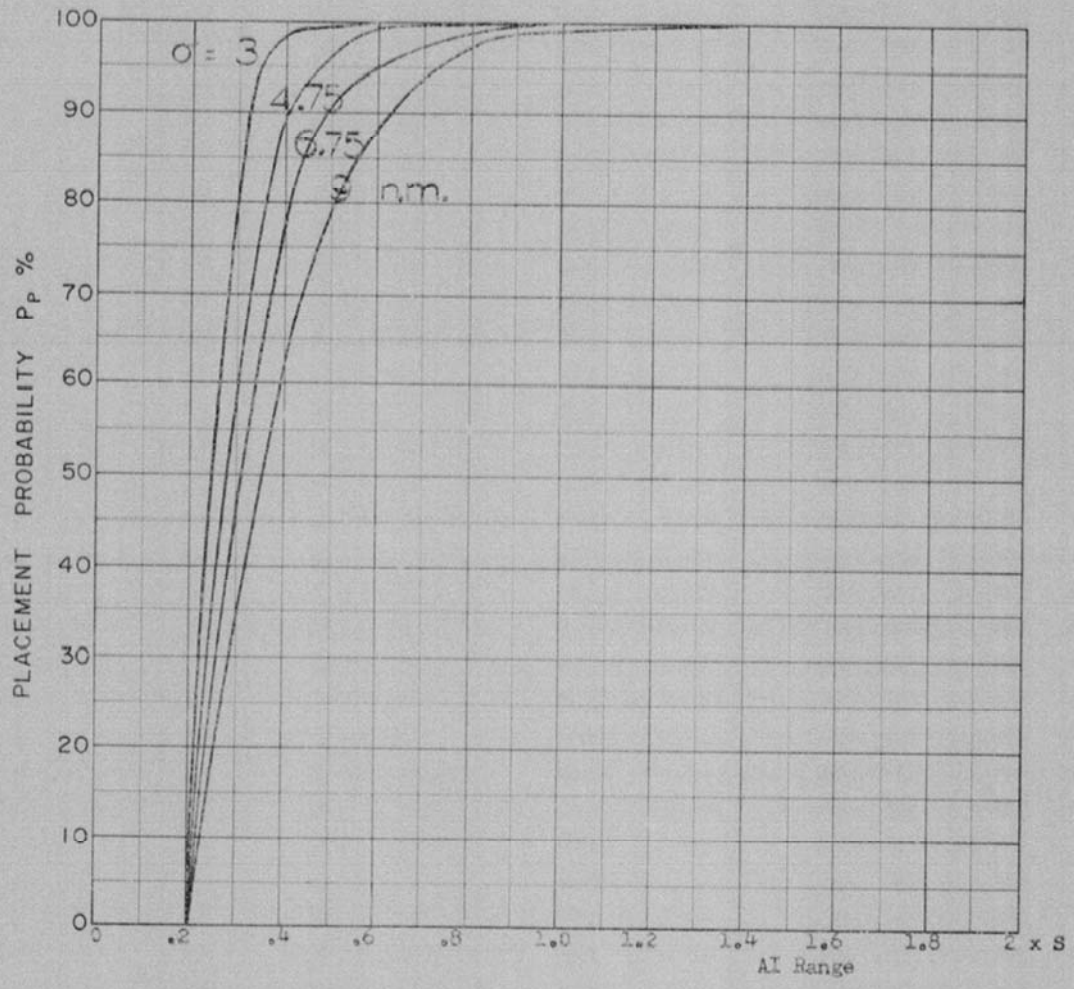

COURSE DIFFERENCE: 120°
TARGET EVASION: 0
TARGET MACH NO.: 1.5
INTERCEPTOR LATERAL G's: 3.0
INTERCEPTOR MACH NO.: 1.5
σ OF G.C.I. ACCURACY: Four values
A.I. DETECTION RANGE AS FRACTION OF SPECIFICATION RANGE, S: Abscissa
A.I. DETECTION RANGE CONTOUR: Delta
ALTITUDE: 60 K

D 39b

Launch zone of figure L-2, missile launched at minimum range with 5° heading error.

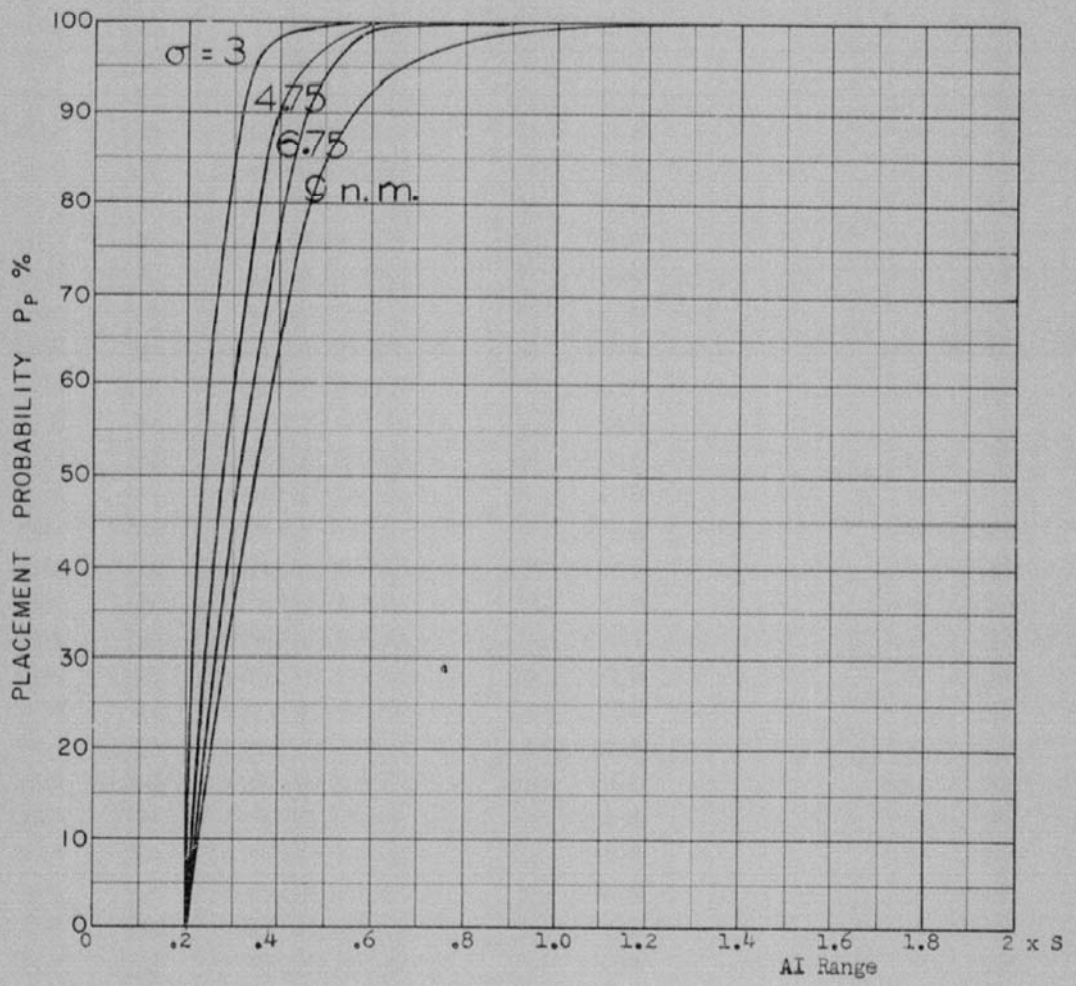

COURSE DIFFERENCE: 140°
TARGET EVASION: 0
TARGET MACH NO.: 1.5
INTERCEPTOR LATERAL G's: 3.0
INTERCEPTOR MACH NO.: 1.5
σ OF G.C.I. ACCURACY: Four values
A.I. DETECTION RANGE AS FRACTION OF SPECIFICATION RANGE, S Abscissa
A.I. DETECTION RANGE CONTOUR: Delta
ALTITUDE: 60 K

D 40

Launch zone $L_o 2$, missile launched at maximum range with 10° heading error allowance.

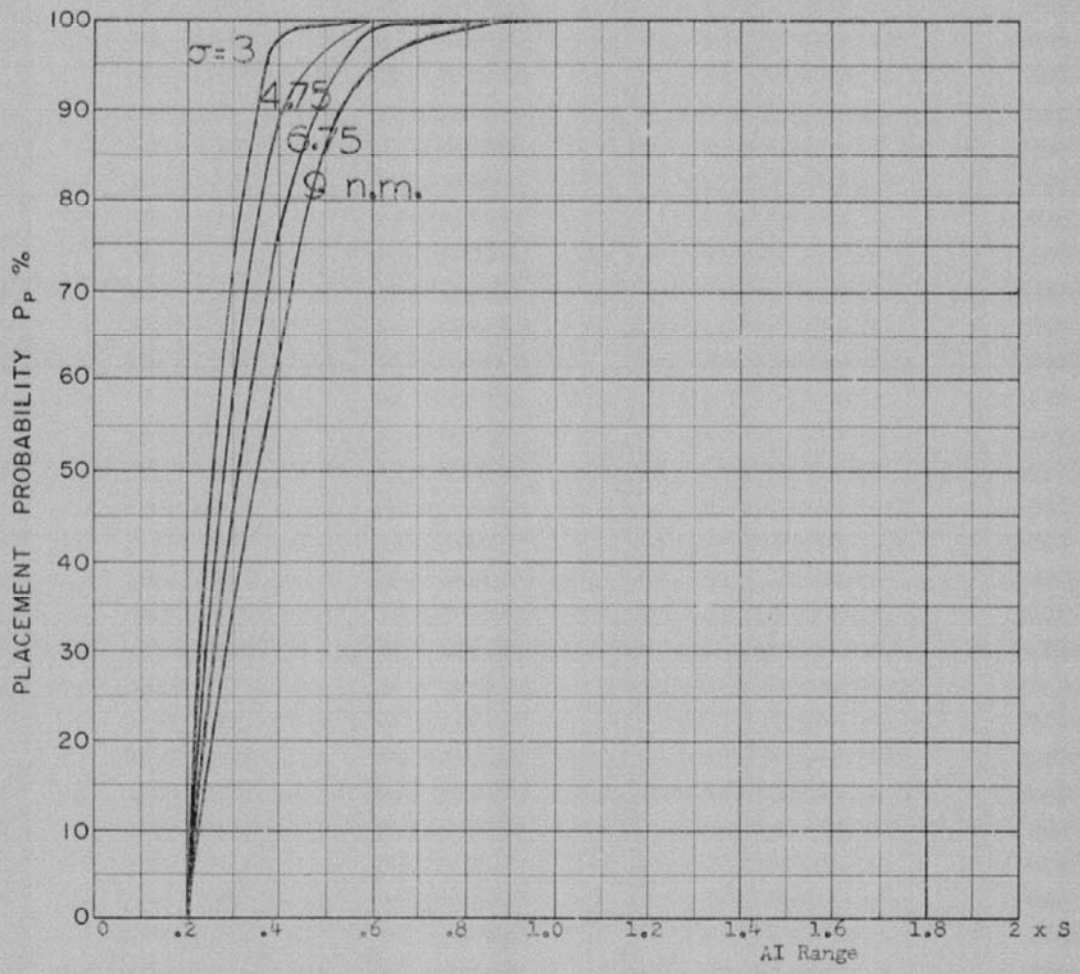

COURSE DIFFERENCE: 160°
TARGET EVASION: 0
TARGET MACH NO.: 1.5
INTERCEPTOR LATERAL G's: 3.0
INTERCEPTOR MACH NO.: 1.5
σ OF G.C.I. ACCURACY: Four values
A.I. DETECTION RANGE AS FRACTION OF SPECIFICATION RANGE, S: Abscissa
A.I. DETECTION RANGE CONTOUR: Delta
ALTITUDE: 60 K

(D-41)

Launch zone L-2, missile launched at maximum range with 10° heading error allowance.

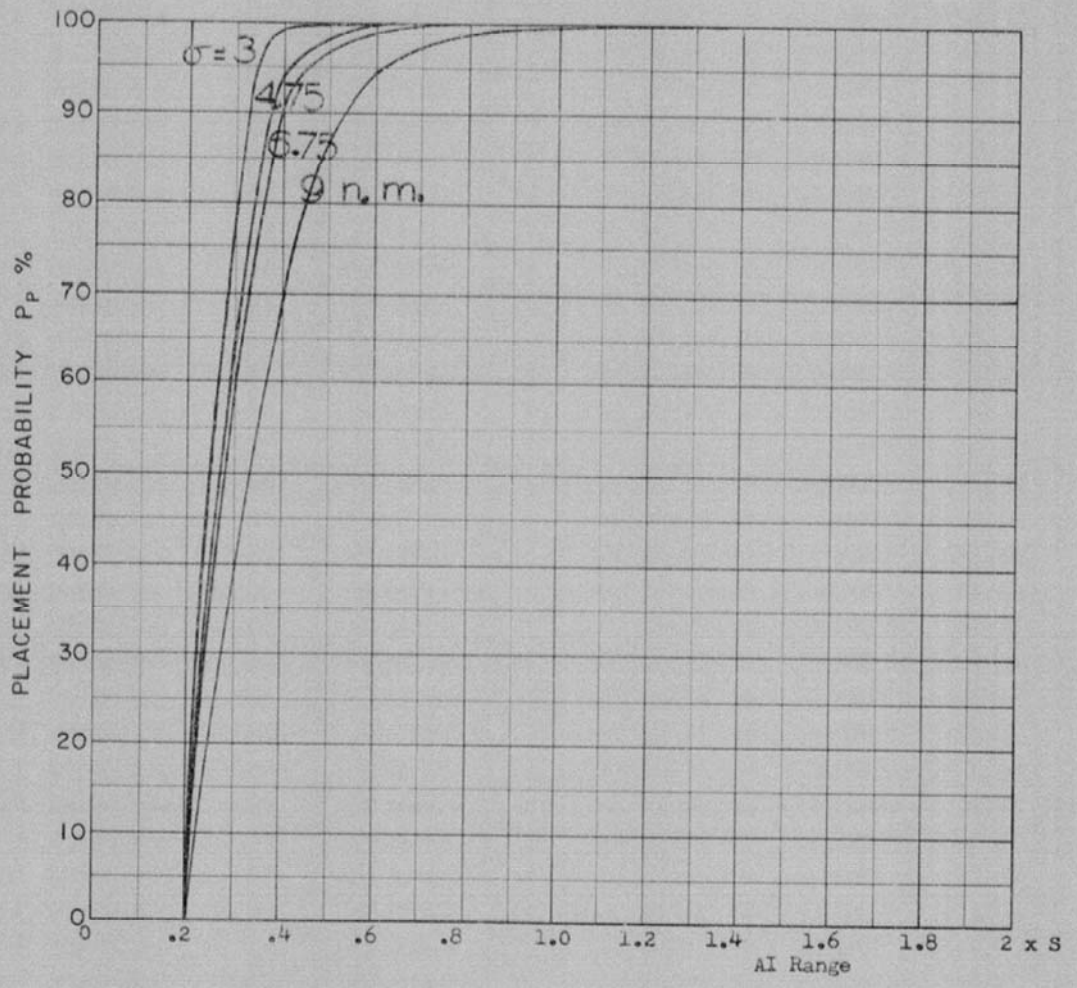

COURSE DIFFERENCE: 180°
TARGET EVASION: 0
TARGET MACH NO.: 1.5
INTERCEPTOR LATERAL G's: 3.0
INTERCEPTOR MACH NO.: 1.5
σ OF G.C.I. ACCURACY: Four values
A.I. DETECTION RANGE AS FRACTION OF SPECIFICATION RANGE, S: Abscissa
A.I. DETECTION RANGE CONTOUR: Delta
ALTITUDE: 60 K

D-42

Launch zone L_2, missile launched at maximum range with 10° heading error allowance.

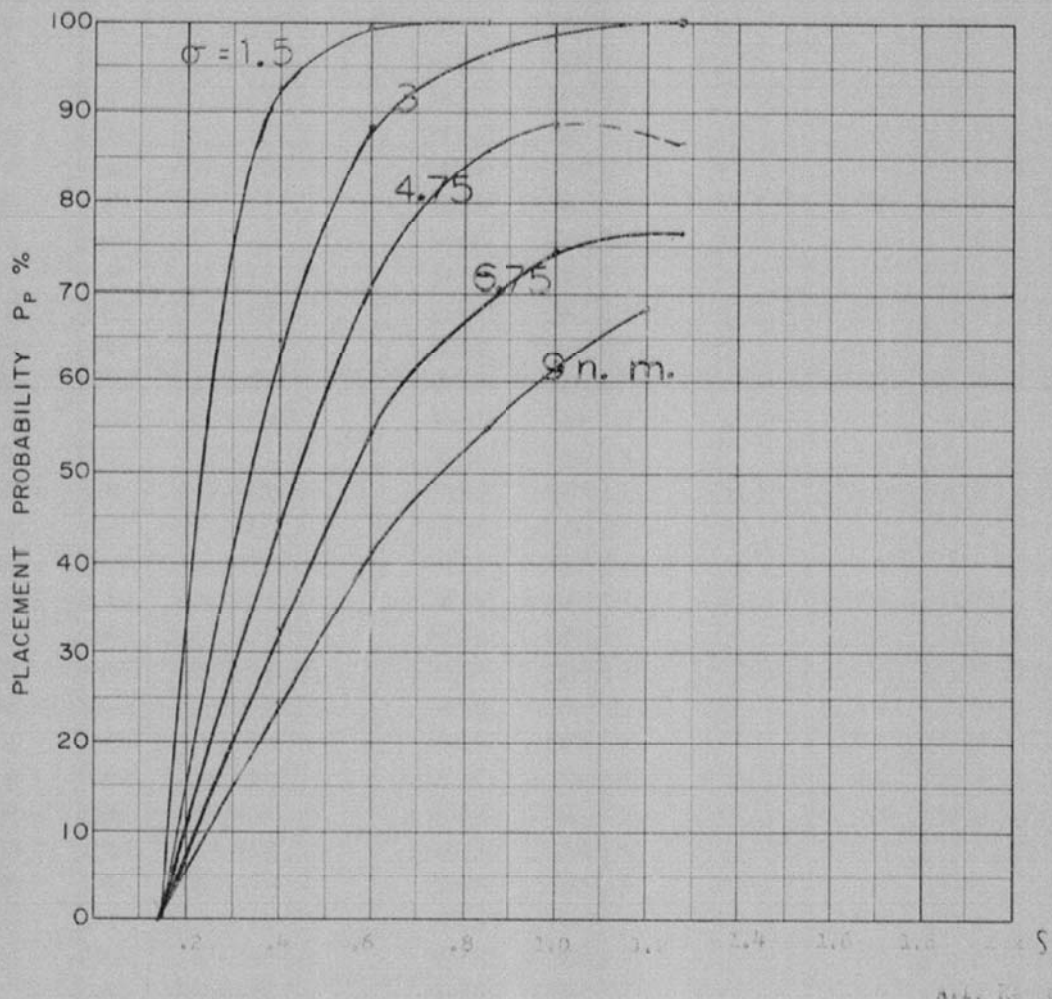

A.I. Range

COURSE DIFFERENCE: 110°
TARGET EVASION: 0.25 lateral g's
TARGET MACH NO.: 1.5
INTERCEPTOR LATERAL G's: 0.85
INTERCEPTOR MACH NO.: 2.5
σ OF G.C.I. ACCURACY: five values
A.I. DETECTION RANGE AS FRACTION OF SPECIFICATION RANGE, S: abscissa
A.I. DETECTION RANGE CONTOUR: Delta
ALTITUDE: 50K

D-43

Launch zone figure L 12

157 dpr

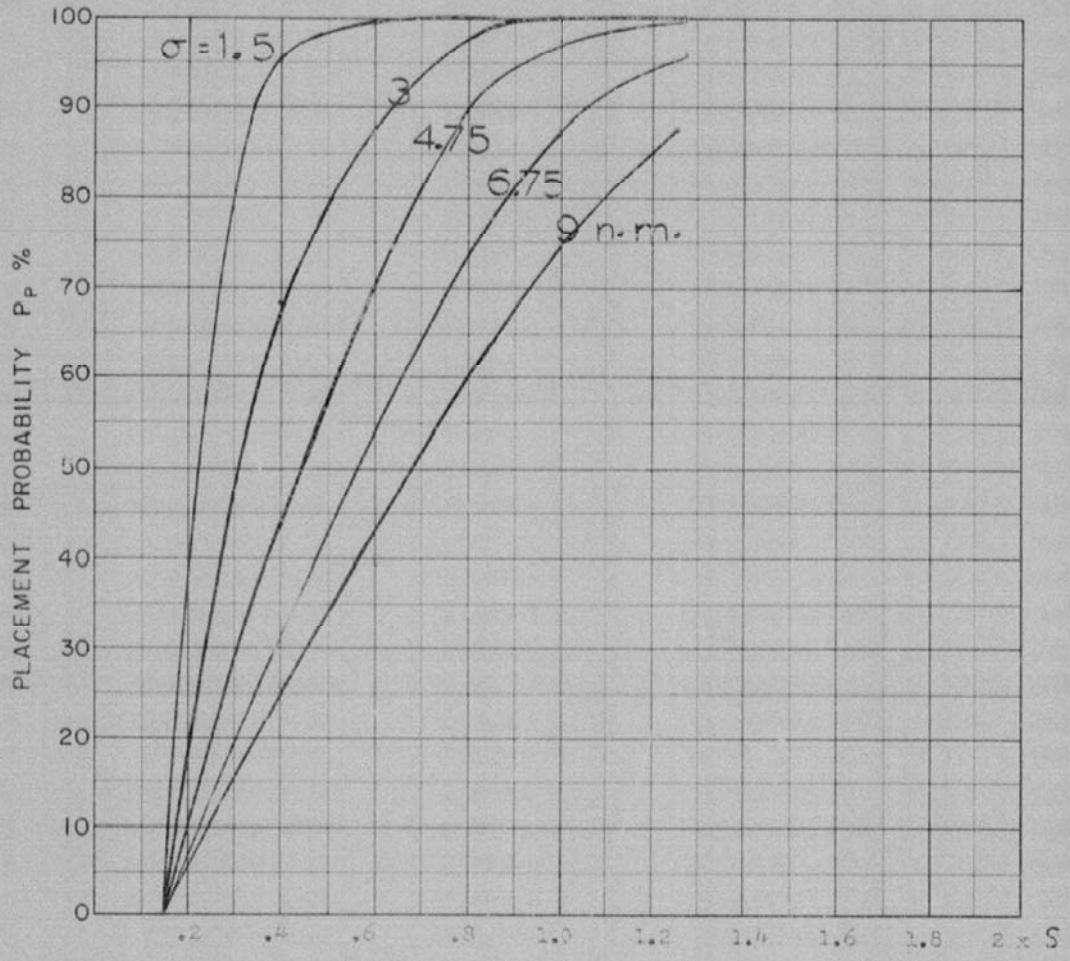

COURSE DIFFERENCE: 135°
TARGET EVASION: 0.15 lateral g's
TARGET MACH NO.: 1.5
INTERCEPTOR LATERAL G's: 0.85
INTERCEPTOR MACH NO.: 1.5
σ OF G.C.I. ACCURACY: five values
A.I. DETECTION RANGE AS FRACTION OF SPECIFICATION RANGE, S: abscissa
A.I. DETECTION RANGE CONTOUR: Delta
ALTITUDE: 50K

D-44

Launch zone figure L 12

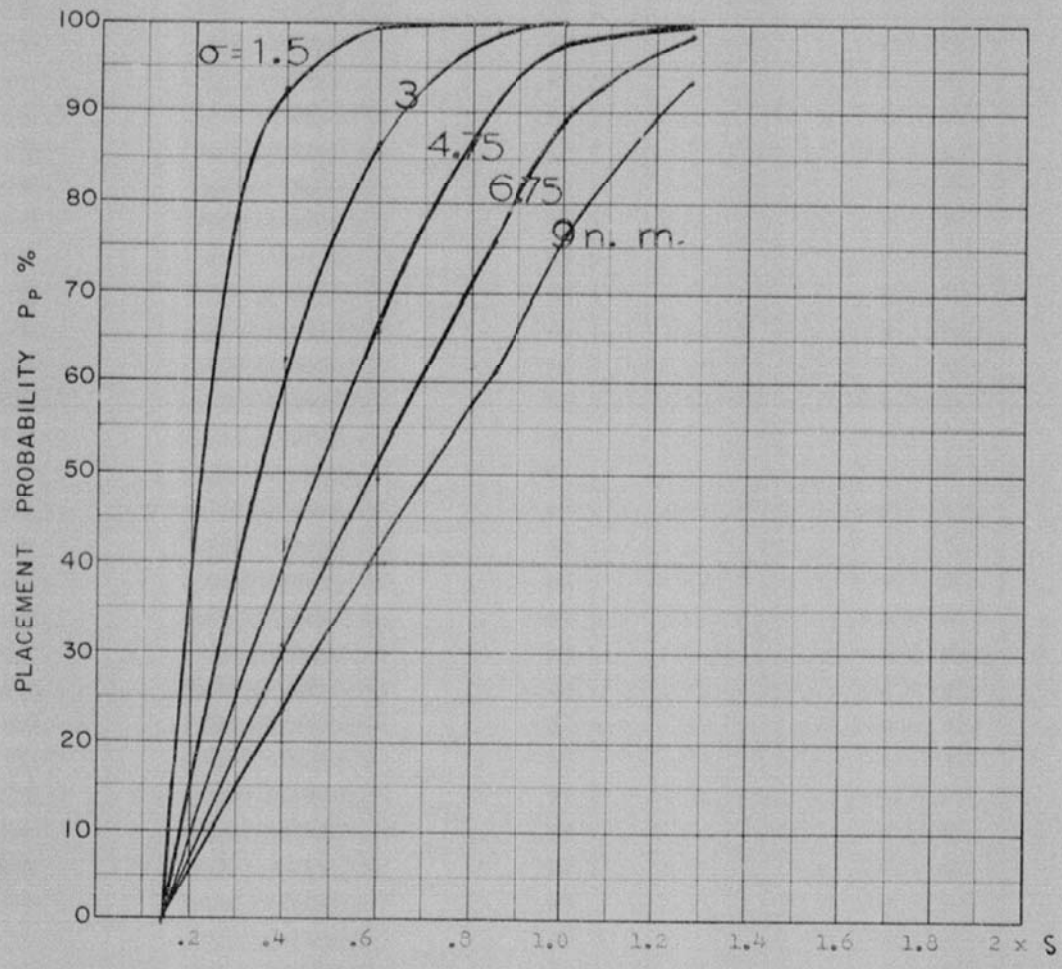

COURSE DIFFERENCE: 160°
TARGET EVASION: 0.15 lateral g's
TARGET MACH NO.: 1.5
INTERCEPTOR LATERAL G's: 0.85
INTERCEPTOR MACH NO.: 1.5
σ OF G.C.I. ACCURACY: five values
A.I. DETECTION RANGE AS FRACTION OF SPECIFICATION RANGE, S: abscissa
A.I. DETECTION RANGE CONTOUR: Delta
ALTITUDE: 50K

D.45

Launch zone figure L 12

161 dpr

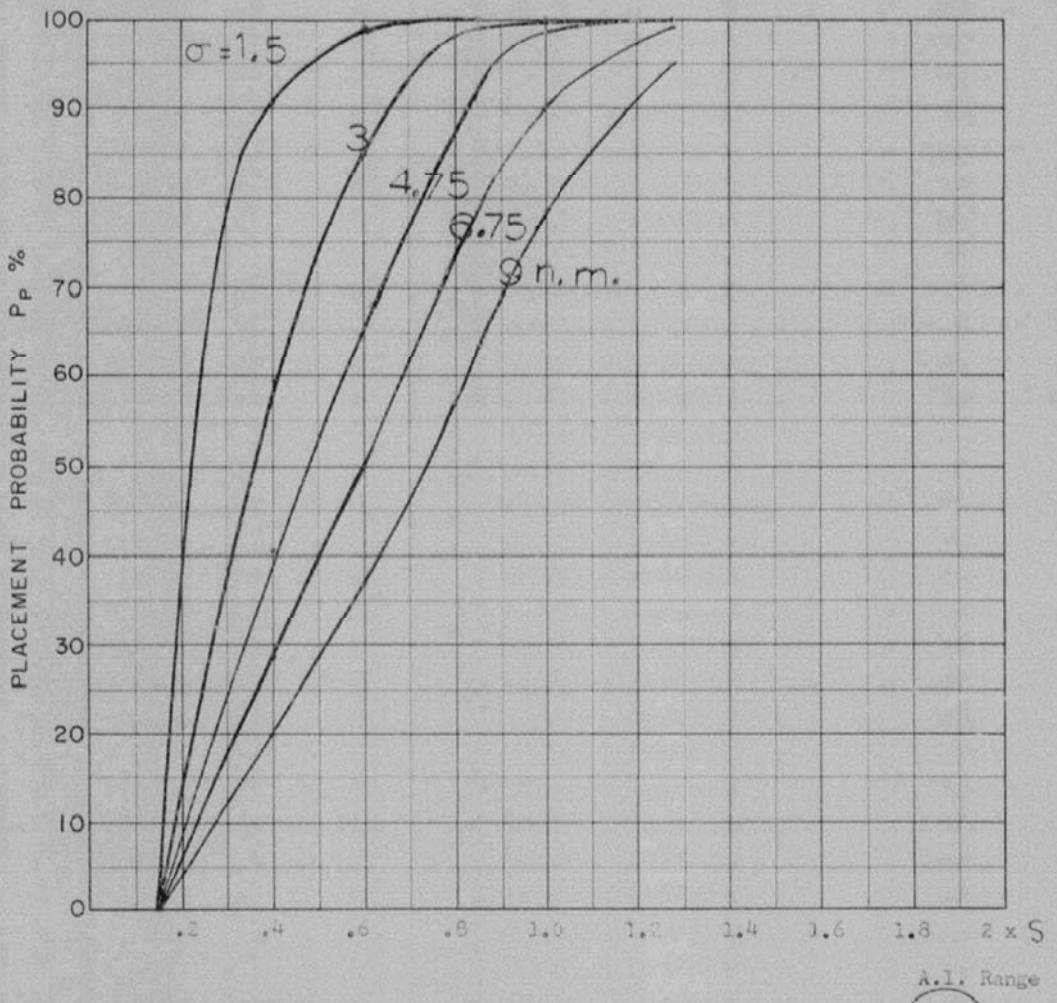

COURSE DIFFERENCE: 180°
TARGET EVASION: 0.15 lateral g's
TARGET MACH NO.: 1.5
INTERCEPTOR LATERAL G's: 0.85
INTERCEPTOR MACH NO.: 1.5
σ OF G.C.I. ACCURACY: five values
A.I. DETECTION RANGE AS FRACTION OF SPECIFICATION RANGE, S: abscissa
A.I. DETECTION RANGE CONTOUR: Delta
ALTITUDE: 50K

(D.46)

Launch zone of figure L 12

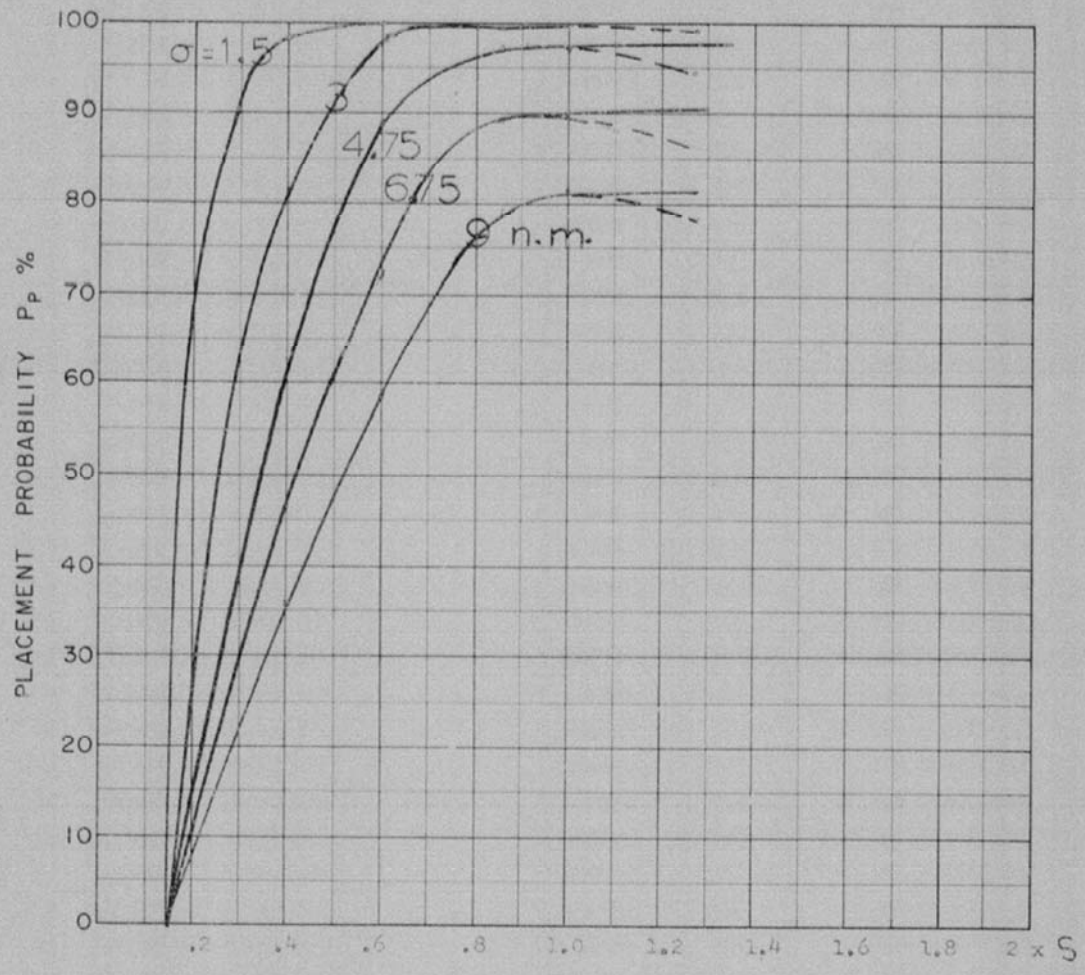

D 47a

COURSE DIFFERENCE: 110°
TARGET EVASION: 0.15 lateral g's
TARGET MACH NO.: 1.5
INTERCEPTOR LATERAL G's: 1.6
INTERCEPTOR MACH NO.: 1.5
σ OF G.C.I. ACCURACY: five values
A.I. DETECTION RANGE AS FRACTION OF SPECIFICATION RANGE, S: abscissa
A.I. DETECTION RANGE CONTOUR: Delta
ALTITUDE: 50K

Launch zone figure L 12

164 adpx

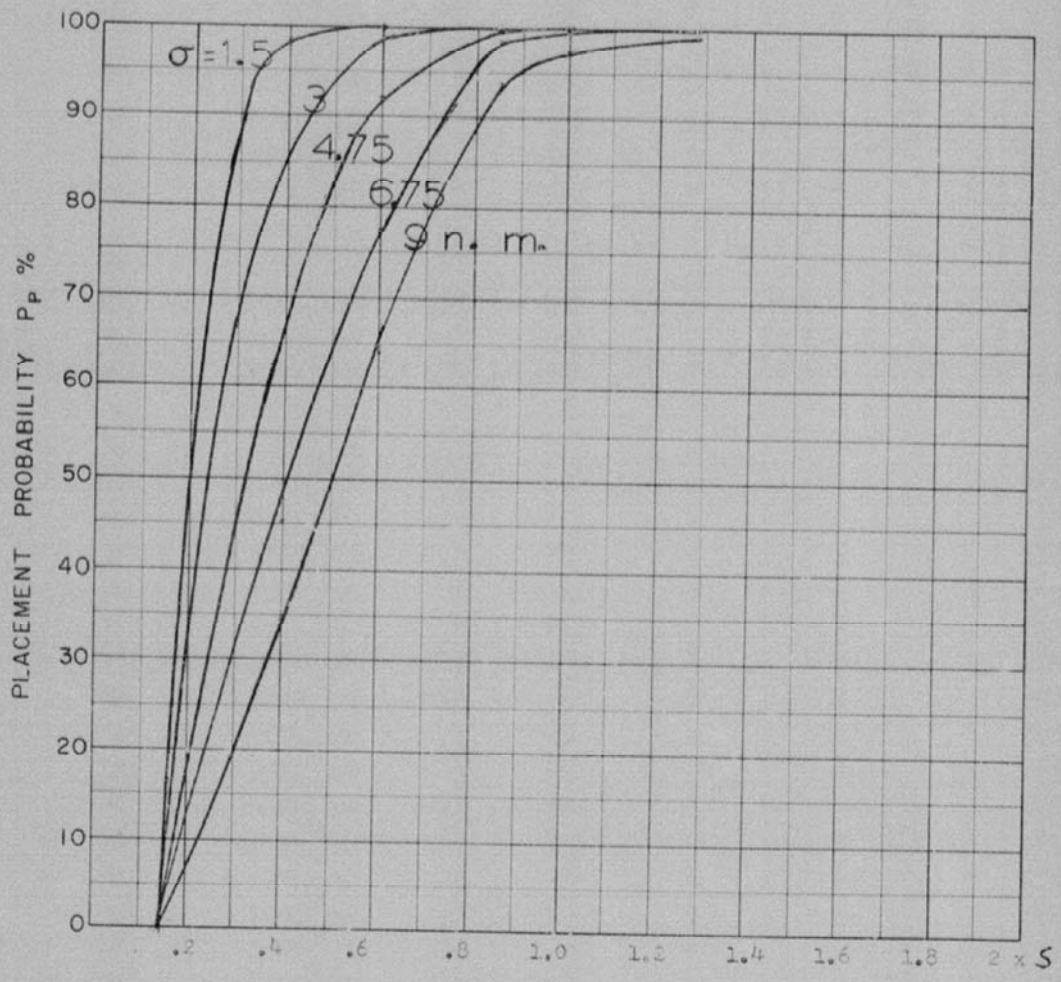

COURSE DIFFERENCE: 110°
TARGET EVASION: .15 lateral g's (turn away)
TARGET MACH NO.: 1.5
INTERCEPTOR LATERAL G's: 1.6
INTERCEPTOR MACH NO.: 1.5
σ OF G.C.I. ACCURACY: five values
A.I. DETECTION RANGE AS FRACTION OF SPECIFICATION RANGE, S: abscissa
A.I. DETECTION RANGE CONTOUR: Delta
ALTITUDE: 50K

D 476

Launch zone of figure I 12

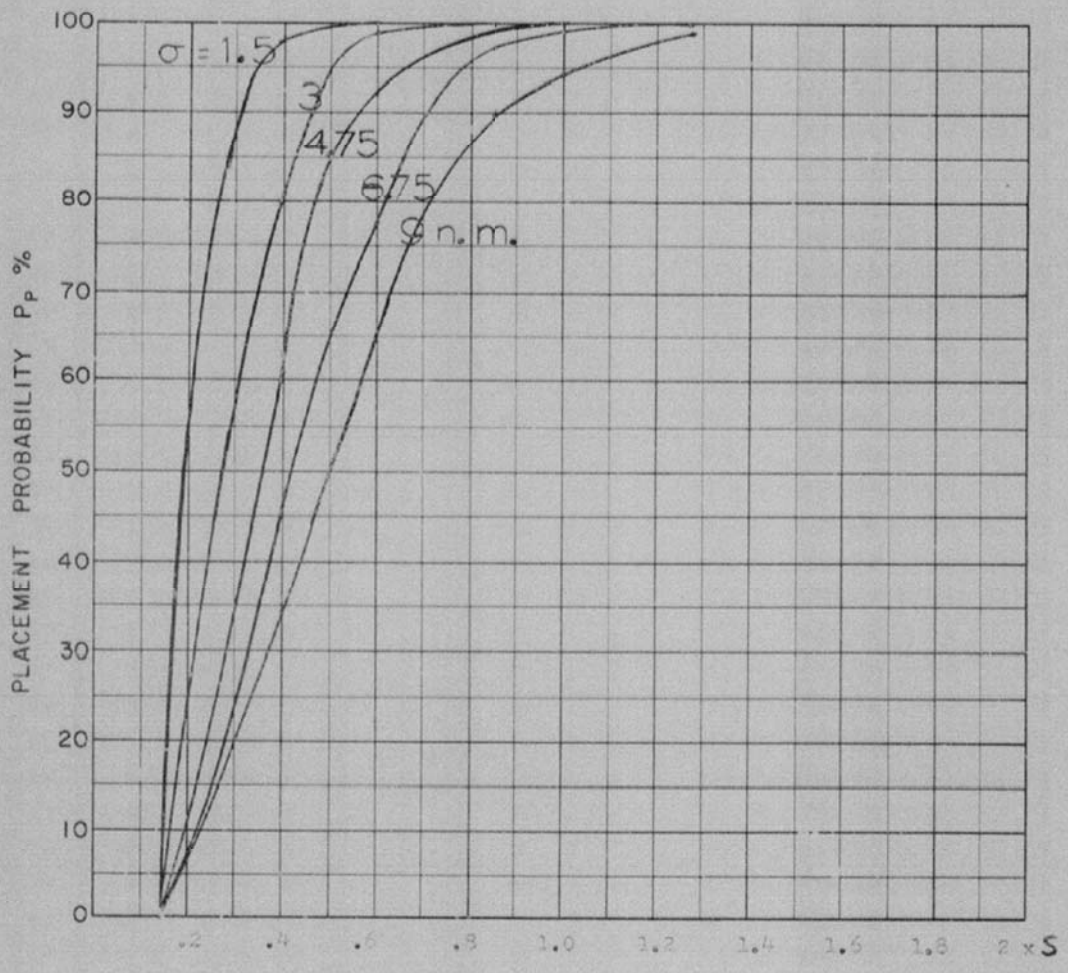

COURSE DIFFERENCE: 110°
TARGET EVASION: .15 lateral g's beginning at 150,000 ft. range (turn away)
TARGET MACH NO.: 1.5
INTERCEPTOR LATERAL G's: 1.6
INTERCEPTOR MACH NO.: 1.5
σ OF G.C.I. ACCURACY: five values
A.I. DETECTION RANGE AS FRACTION OF SPECIFICATION RANGE, S: abscissa
A.I. DETECTION RANGE CONTOUR: Delta
ALTITUDE: 50K

(D-47c)

Launch zone figure L 12

166 dpr

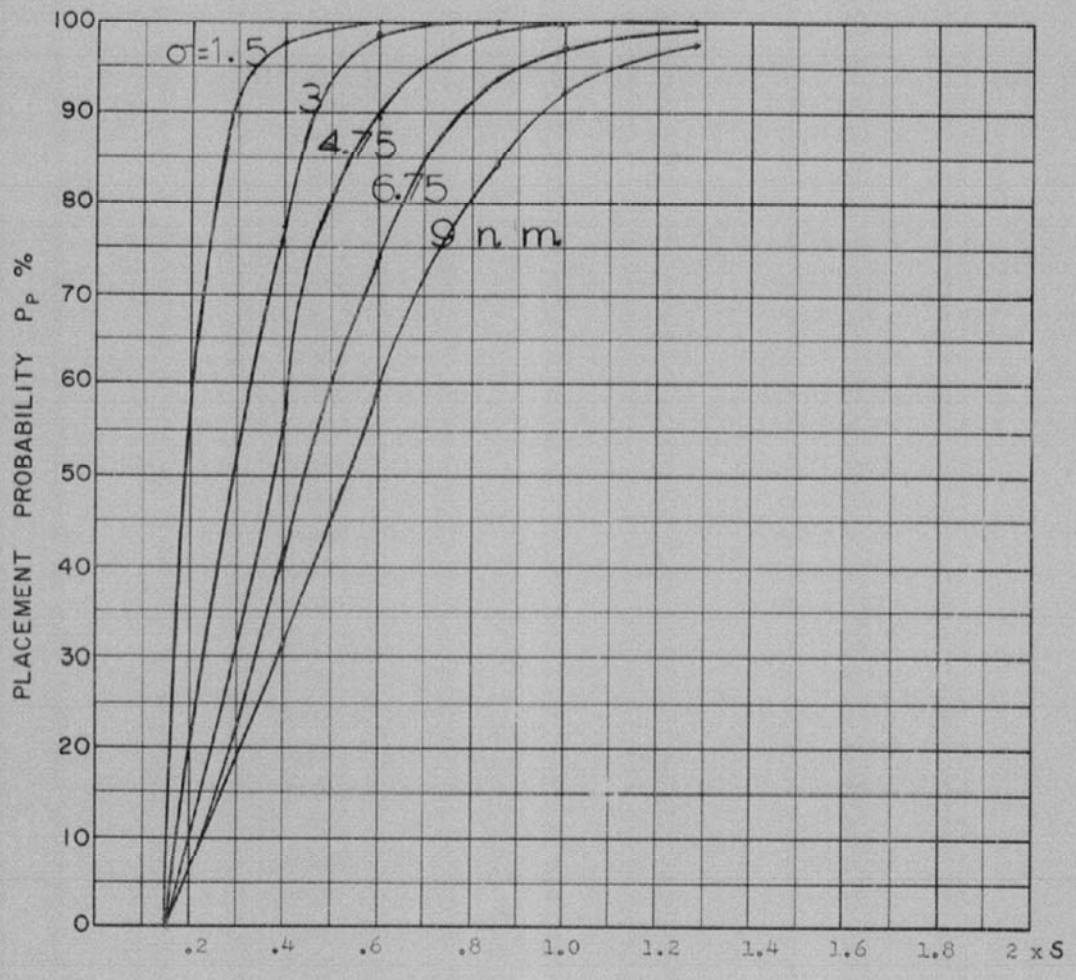

A.I. Range

D-48

COURSE DIFFERENCE: 135°
TARGET EVASION: 0.15 lateral g's
TARGET MACH NO.: 1.5
INTERCEPTOR LATERAL G's: 1.6
INTERCEPTOR MACH NO.: 1.5
σ OF G.C.I. ACCURACY: five values
A.I. DETECTION RANGE AS FRACTION OF SPECIFICATION RANGE, S: abscissa
A.I. DETECTION RANGE CONTOUR: Delta
ALTITUDE: 50K

Launch zone figure L 12

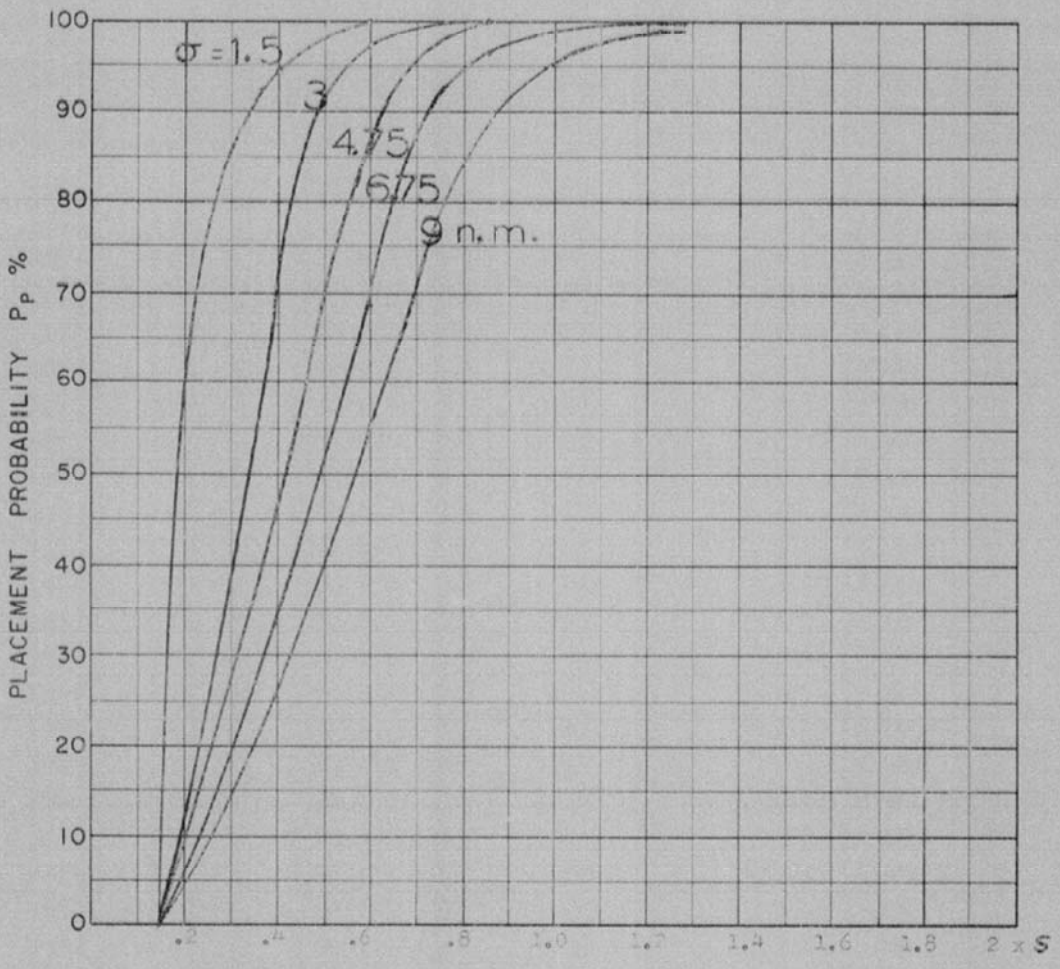

COURSE DIFFERENCE: 160°
TARGET EVASION: 0.25 lateral g's
TARGET MACH NO.: 1.5
INTERCEPTOR LATERAL G's: 1.6
INTERCEPTOR MACH NO.: 1.5
σ OF G.C.I. ACCURACY: five values
A.I. DETECTION RANGE AS FRACTION OF SPECIFICATION RANGE, S: abscissa
A.I. DETECTION RANGE CONTOUR: Delta
ALTITUDE: 50K

D-49a

Launch zone figure L 12

170 adpr

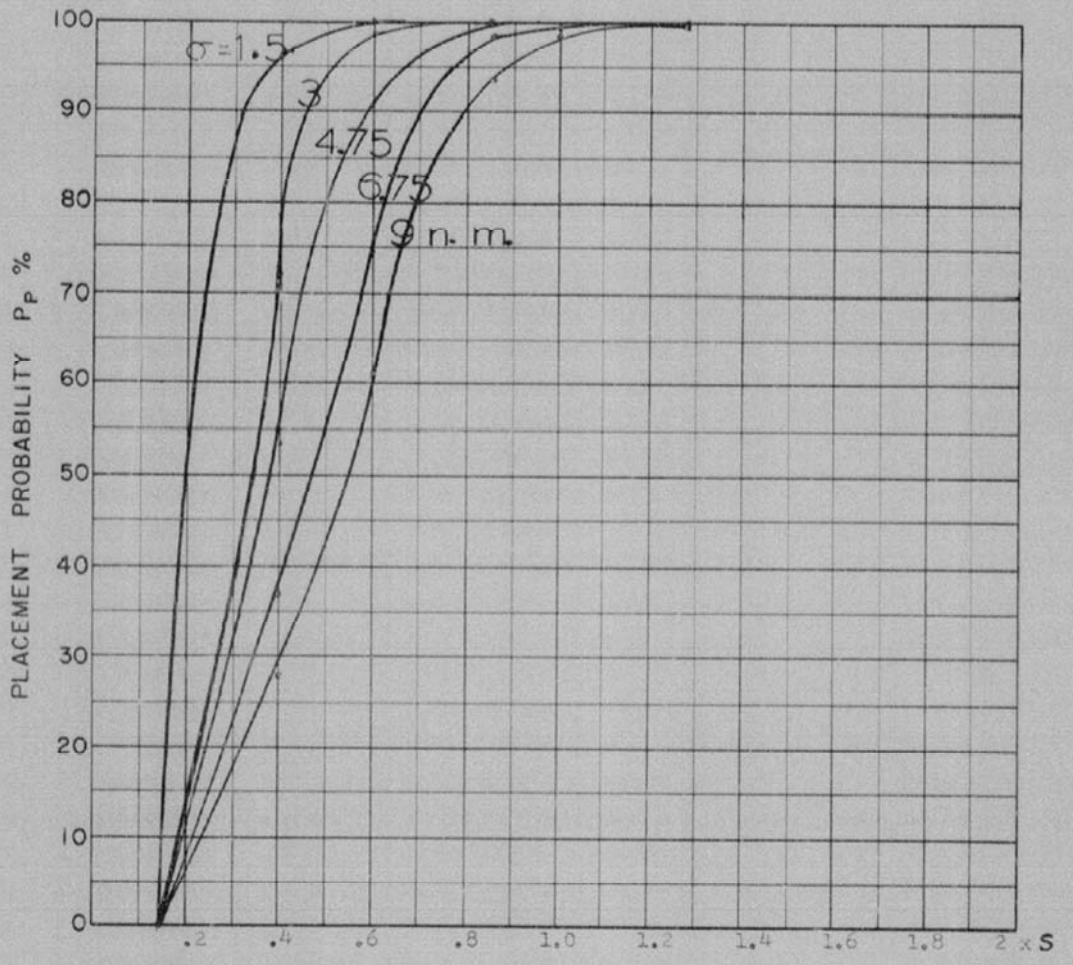

COURSE DIFFERENCE: 160°
TARGET EVASION: 0.15 lateral g's (turn away)
TARGET MACH NO.: 1.5
INTERCEPTOR LATERAL G's: 1.6
INTERCEPTOR MACH NO.: 1.5
σ OF G.C.I. ACCURACY: five values
A.I. DETECTION RANGE AS FRACTION OF SPECIFICATION RANGE, S: abscissa
A.I. DETECTION RANGE CONTOUR: Delta
ALTITUDE: 50K

D 496

Launch zone figure L 12

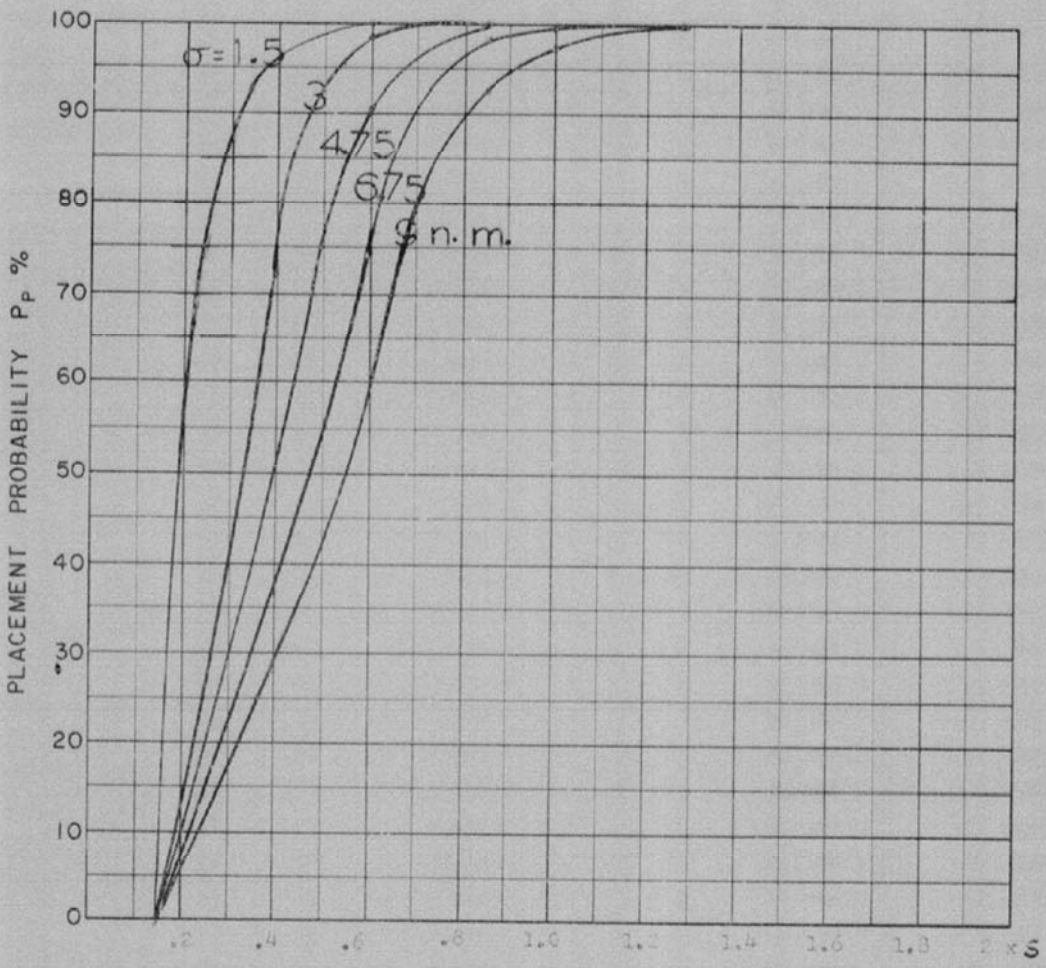

COURSE DIFFERENCE: 180°
TARGET EVASION: 0.15 lateral g's, beginning at range 150,000 ft. (turn away)
TARGET MACH NO.: 1.5
INTERCEPTOR LATERAL G's: 1.6
INTERCEPTOR MACH NO.: 1.5
σ OF G.C.I. ACCURACY: five values
A.I. DETECTION RANGE AS FRACTION OF SPECIFICATION RANGE, S: abscissa
A.I. DETECTION RANGE CONTOUR: Delta
ALTITUDE: 50K

D49c

Launch zone figure I 12

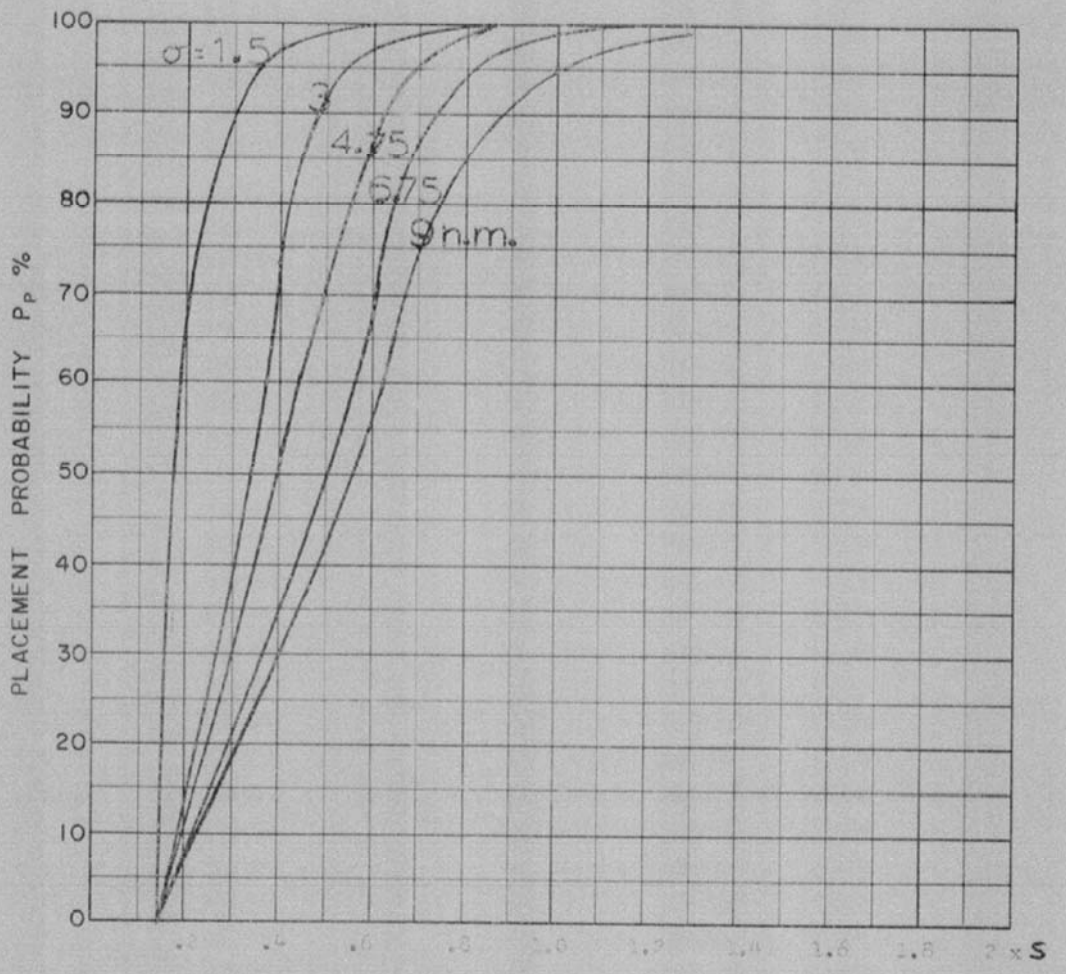

COURSE DIFFERENCE: 180°
TARGET EVASION: 0.15 lateral g's
TARGET MACH NO.: 1.5
INTERCEPTOR LATERAL G's: 4.6
INTERCEPTOR MACH NO.: 1.5
σ OF G.C.I. ACCURACY: five values
A.I. DETECTION RANGE AS FRACTION OF SPECIFICATION RANGE, S: abscissa
A.I. DETECTION RANGE CONTOUR: Delta
ALTITUDE: 50K

D50a

Launch zone figure L 12

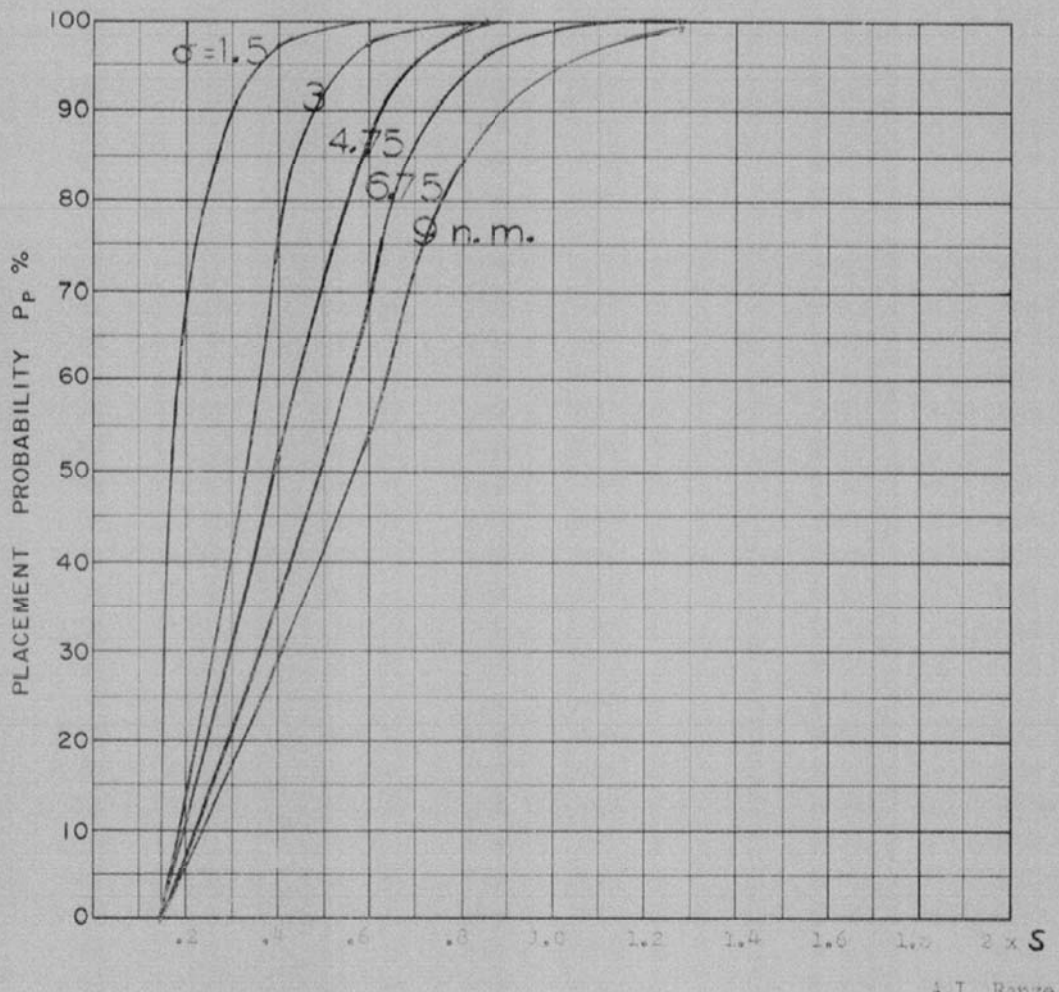

COURSE DIFFERENCE: 180°
TARGET EVASION: 0.15 lateral g's, beginning at 200,000 ft. range
TARGET MACH NO.: 1.5
INTERCEPTOR LATERAL G's: 1.6
INTERCEPTOR MACH NO.: 1.5
σ OF G.C.I. ACCURACY: five values
A.I. DETECTION RANGE AS FRACTION OF SPECIFICATION RANGE, S: abscissa
A.I. DETECTION RANGE CONTOUR: Delta
ALTITUDE: 50K

D506

Launch zone figure L 12

172 adpr

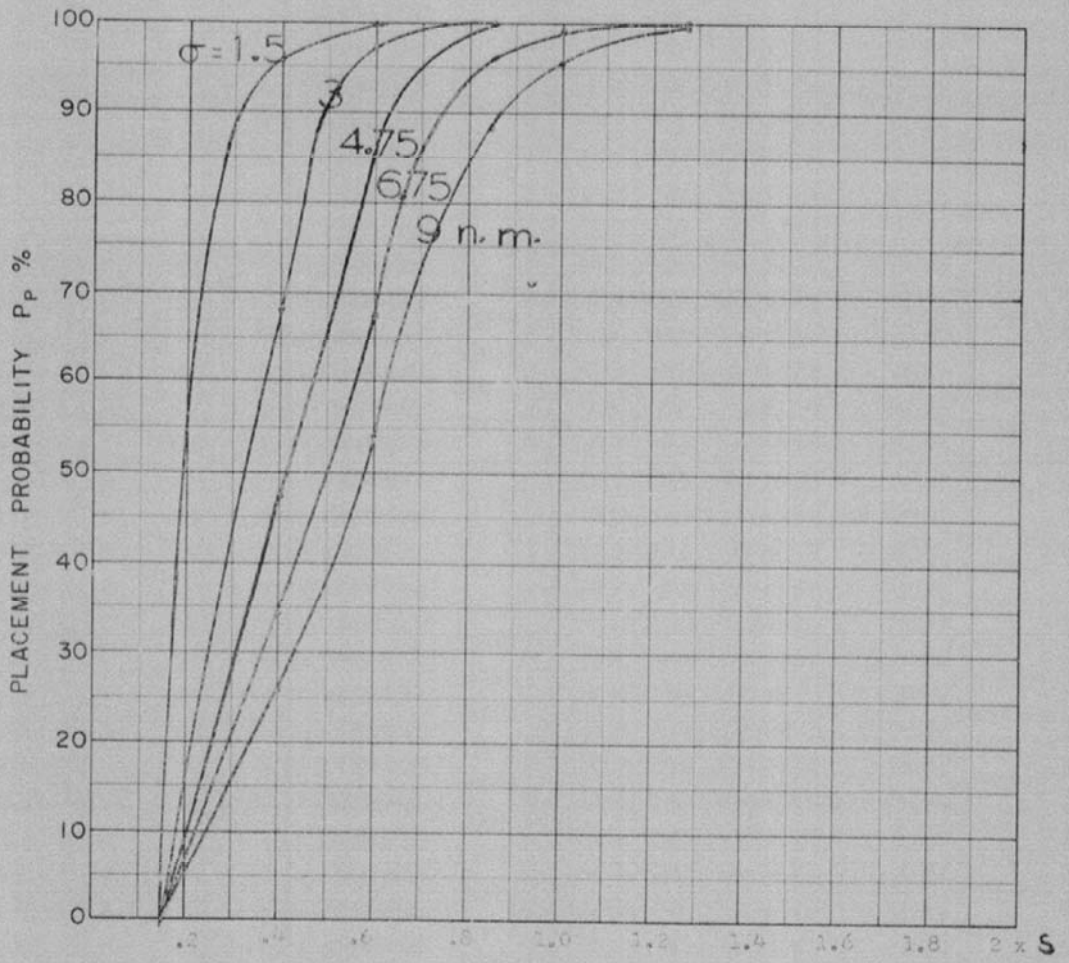

COURSE DIFFERENCE: 180°
TARGET EVASION: 0.15 lateral g's, beginning at 150,000 ft. range
TARGET MACH NO.: 1.5
INTERCEPTOR LATERAL G's: 1.6
INTERCEPTOR MACH NO.: 1.5
σ OF G.C.I. ACCURACY: five values
A.I. DETECTION RANGE AS FRACTION OF SPECIFICATION RANGE, S: abscissa
A.I. DETECTION RANGE CONTOUR: Delta
ALTITUDE: 50K

(D-50c)

Launch zone figure I 12

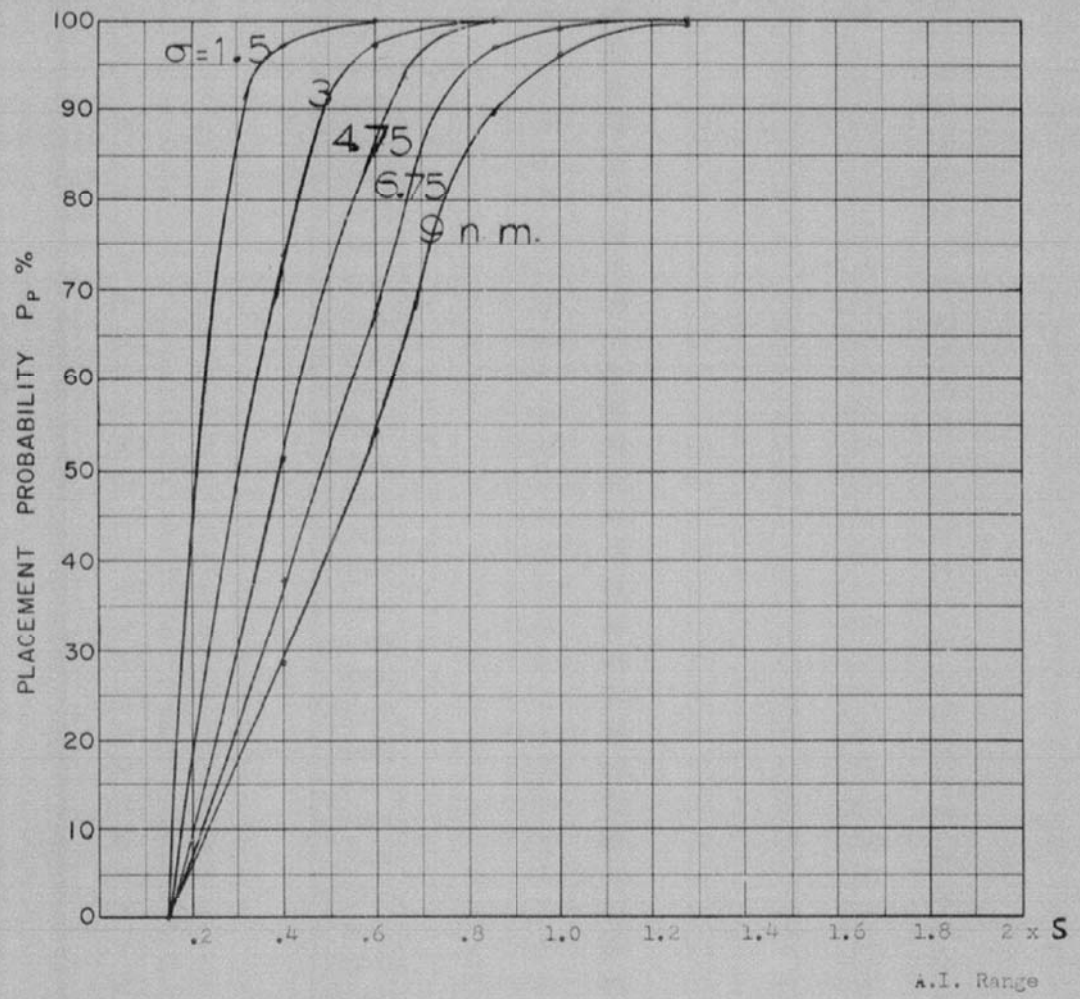

COURSE DIFFERENCE: 180°
TARGET EVASION: 0.15 lateral g's, beginning at 100,000 ' . range
TARGET MACH NO.: 1.5
INTERCEPTOR LATERAL G's: 1.6
INTERCEPTOR MACH NO.: 1.5
σ OF G.C.I. ACCURACY: five values
A.I. DETECTION RANGE AS FRACTION OF SPECIFICATION RANGE, S: abscissa
A.I. DETECTION RANGE CONTOUR: Delta
ALTITUDE: 50K

D.50d

Launch zone figure L 12

172 bdpr

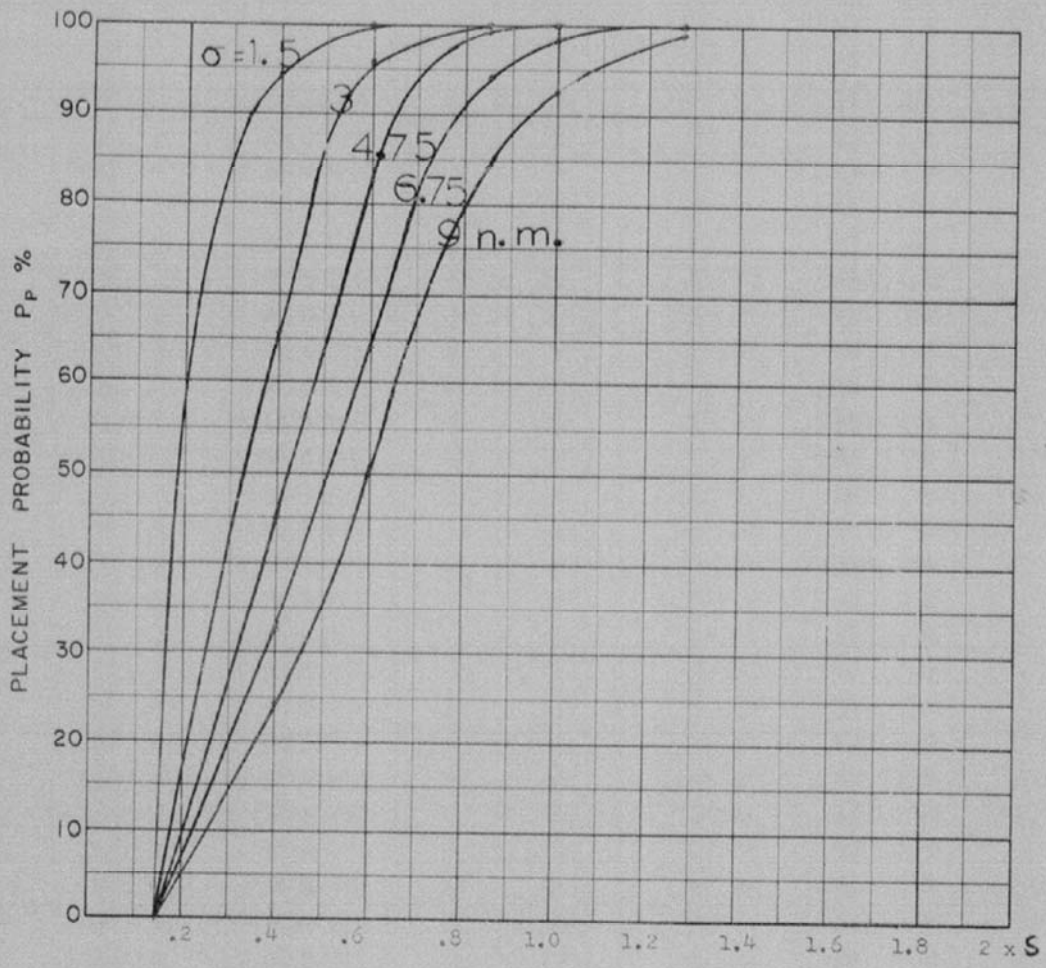

COURSE DIFFERENCE: 180°
TARGET EVASION: 0.3 lateral g's, beginning at 150,000 ft. range
TARGET MACH NO.: 1.5
INTERCEPTOR LATERAL G's: 1.6
INTERCEPTOR MACH NO.: 1.5
σ OF G.C.I. ACCURACY: five values
A.I. DETECTION RANGE AS FRACTION OF SPECIFICATION RANGE, S: abscissa
A.I. DETECTION RANGE CONTOUR: Delta
ALTITUDE: 50K

D50e

Launch zone figure L 12

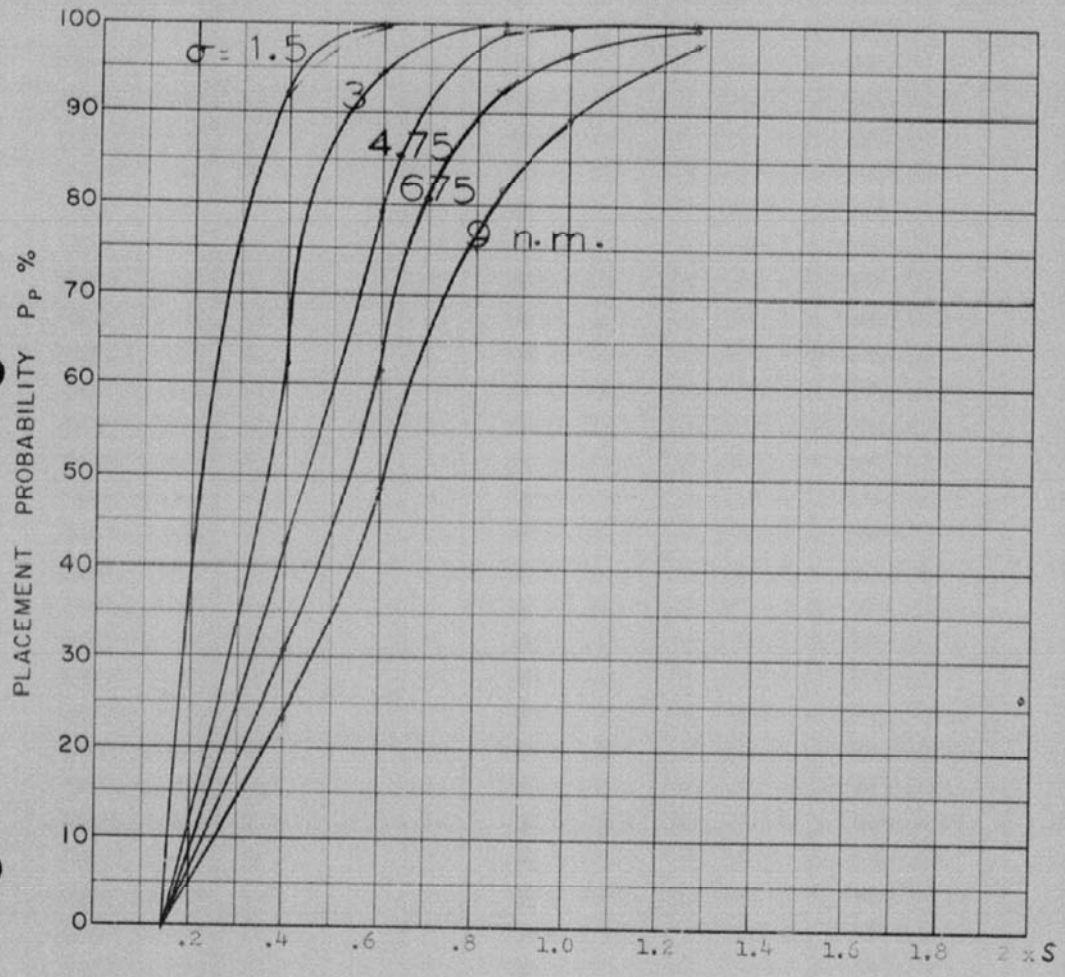

COURSE DIFFERENCE: 180°
TARGET EVASION: 0.45 lateral g's, beginning at 150,000 ft. range
TARGET MACH NO: 1.5
INTERCEPTOR LATERAL G's: 1.6
INTERCEPTOR MACH NO.: 1.5
σ OF G.C.I. ACCURACY: five values
A.I. DETECTION RANGE AS FRACTION OF SPECIFICATION RANGE, S: nosciscn
A.I. DETECTION RANGE CONTOUR: Delta
ALTITUDE: 50K

D50f

Launch zone figure L 12

173 dpr

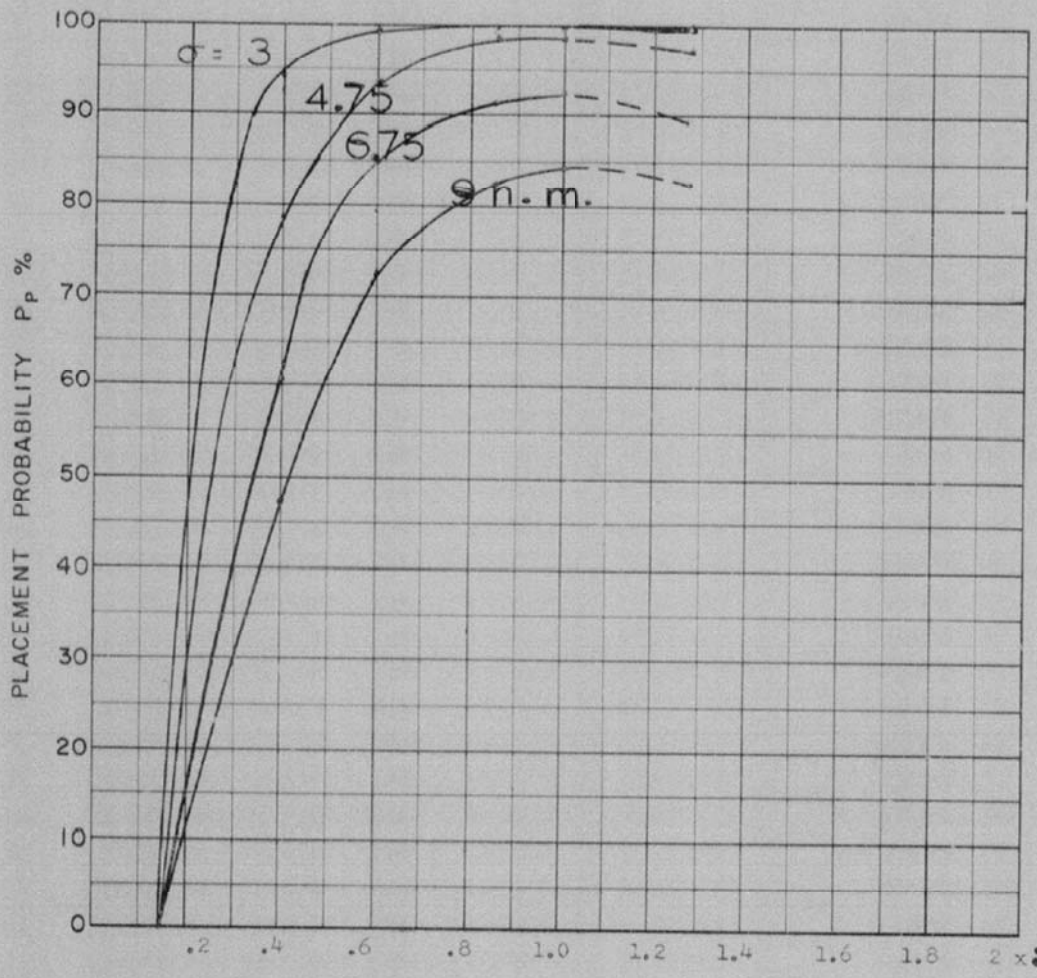

A.I. Range

(D51)

COURSE DIFFERENCE: 110^0
TARGET EVASION: 0.15 lateral g's
TARGET MACH NO.: 1.5
INTERCEPTOR LATERAL G's: 3.0
INTERCEPTOR MACH NO.: 1.5
σ OF G.C.I. ACCURACY: five values
A.I. DETECTION RANGE AS FRACTION OF SPECIFICATION RANGE, S: abscissa
A.I. DETECTION RANGE CONTOUR: Delta
ALTITUDE: 50K

Launch zone figure L 12

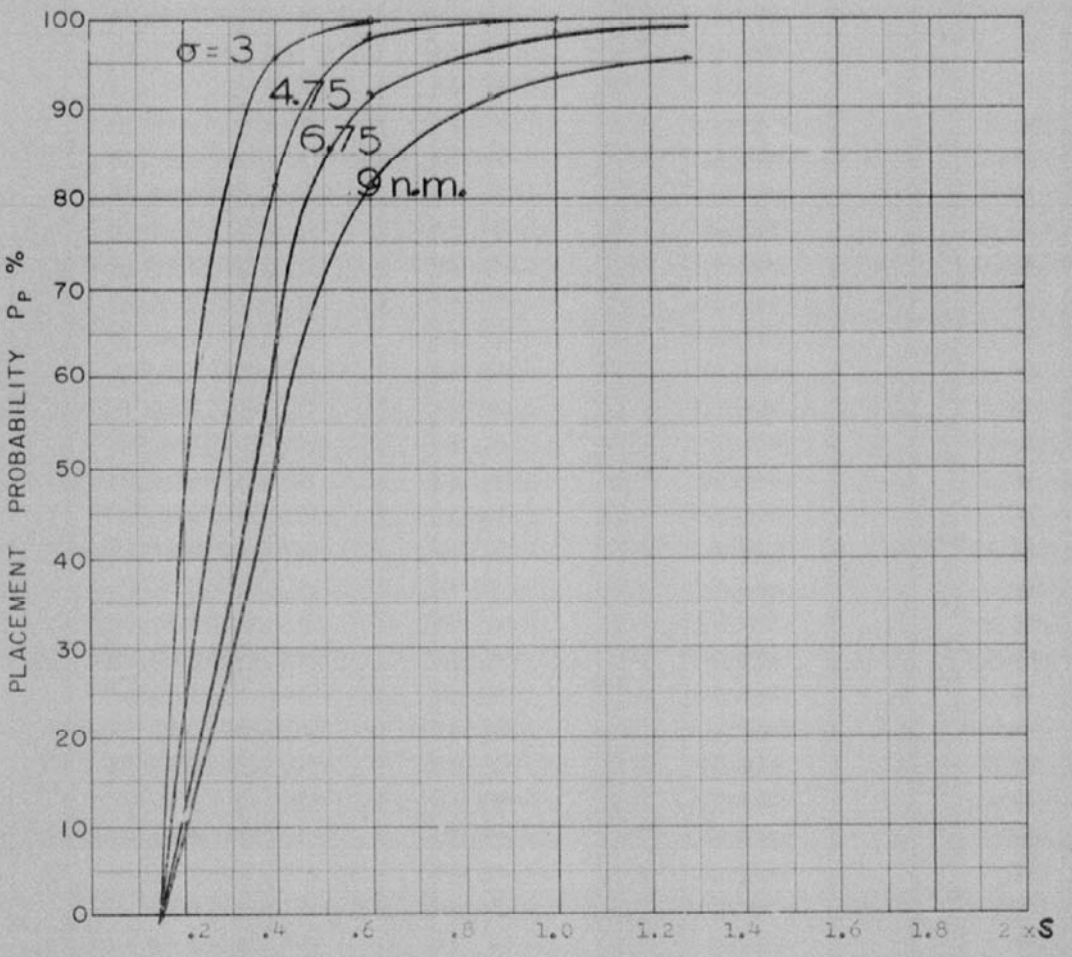

D52

COURSE DIFFERENCE: 135°
TARGET EVASION: 0.15 lateral g's
TARGET MACH NO.: 1.5
INTERCEPTOR LATERAL G's: 3.0
INTERCEPTOR MACH NO.: 1.5
σ OF G.C.I. ACCURACY: five values
A.I. DETECTION RANGE AS FRACTION OF SPECIFICATION RANGE, S: abscissa
A.I. DETECTION RANGE CONTOUR: Delta
ALTITUDE: 50K

Launch zone figure L 12

177 dpr

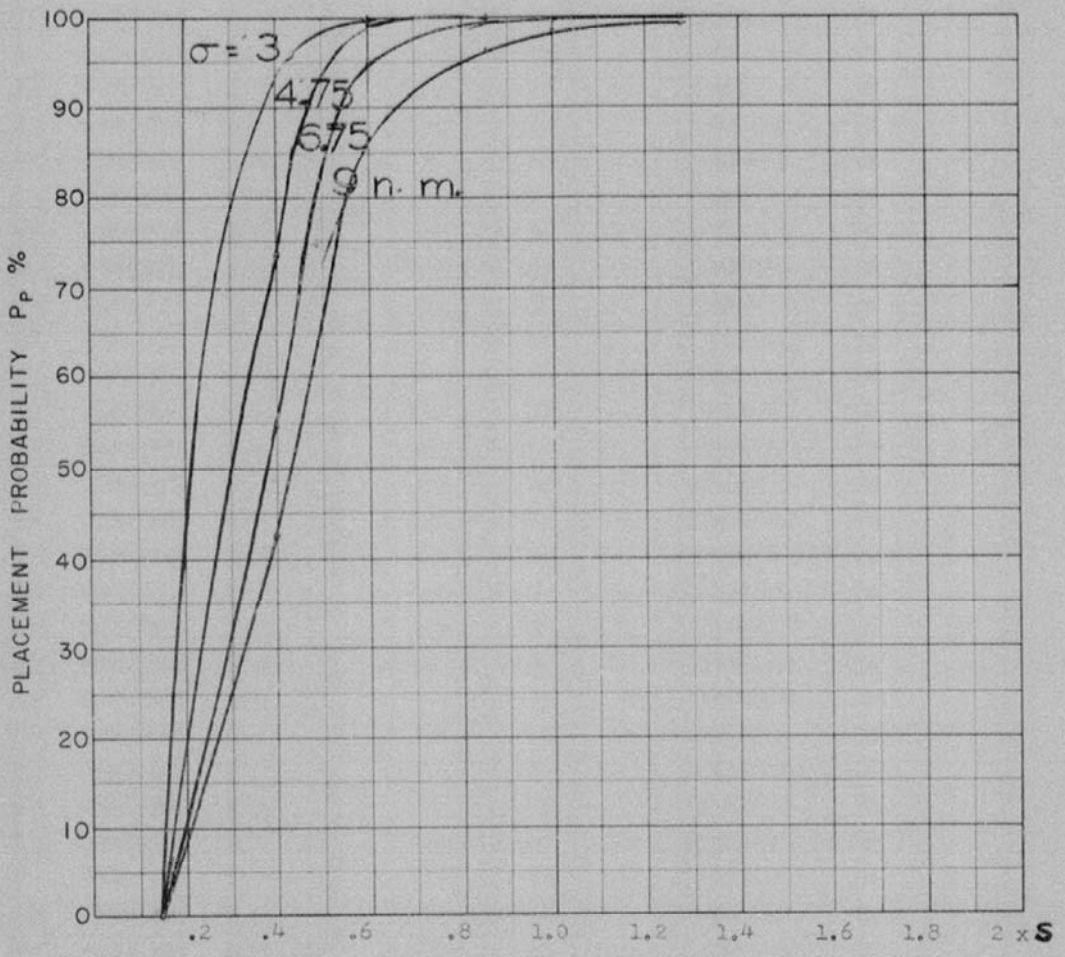

D-53

COURSE DIFFERENCE: 160°
TARGET EVASION: 0.15g
TARGET MACH NO.: 1.5
INTERCEPTOR LATERAL G's: 3.0
INTERCEPTOR MACH NO.: 1.5
σ OF G.C.I. ACCURACY: four values
A.I. DETECTION RANGE AS FRACTION OF SPECIFICATION RANGE, S: abscissa
A.I. DETECTION RANGE CONTOUR: Delta
ALTITUDE: 50K

Launch zone figure L 12

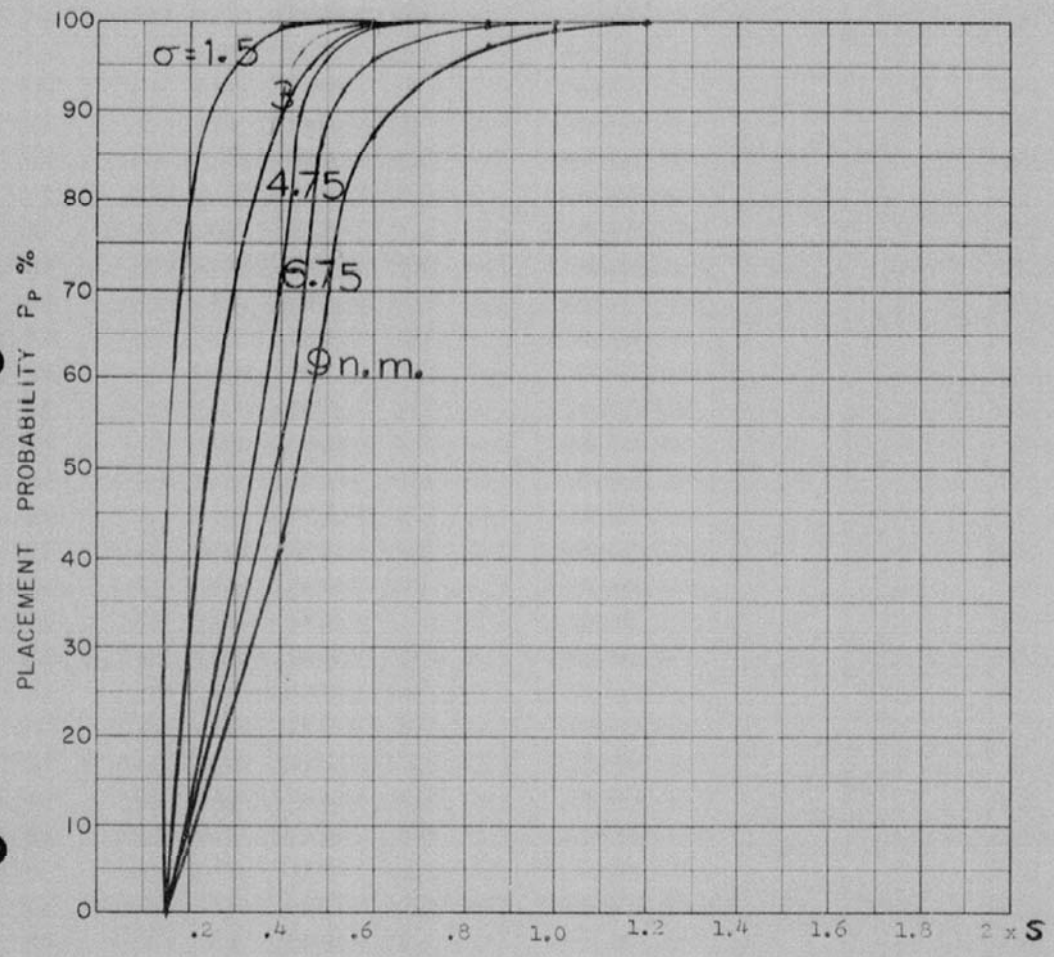

COURSE DIFFERENCE: 180°
TARGET EVASION: 0.15 lateral g's
TARGET MACH NO.: 1.5
INTERCEPTOR LATERAL G's: 3.0
INTERCEPTOR MACH NO.: 1.5
σ OF G.C.I. ACCURACY: five values
A.I. DETECTION RANGE AS FRACTION OF SPECIFICATION RANGE, S: abscissa
A.I. DETECTION RANGE CONTOUR: Delta
ALTITUDE: 50K

D-54

Launch zone figure L 12

180 dpr

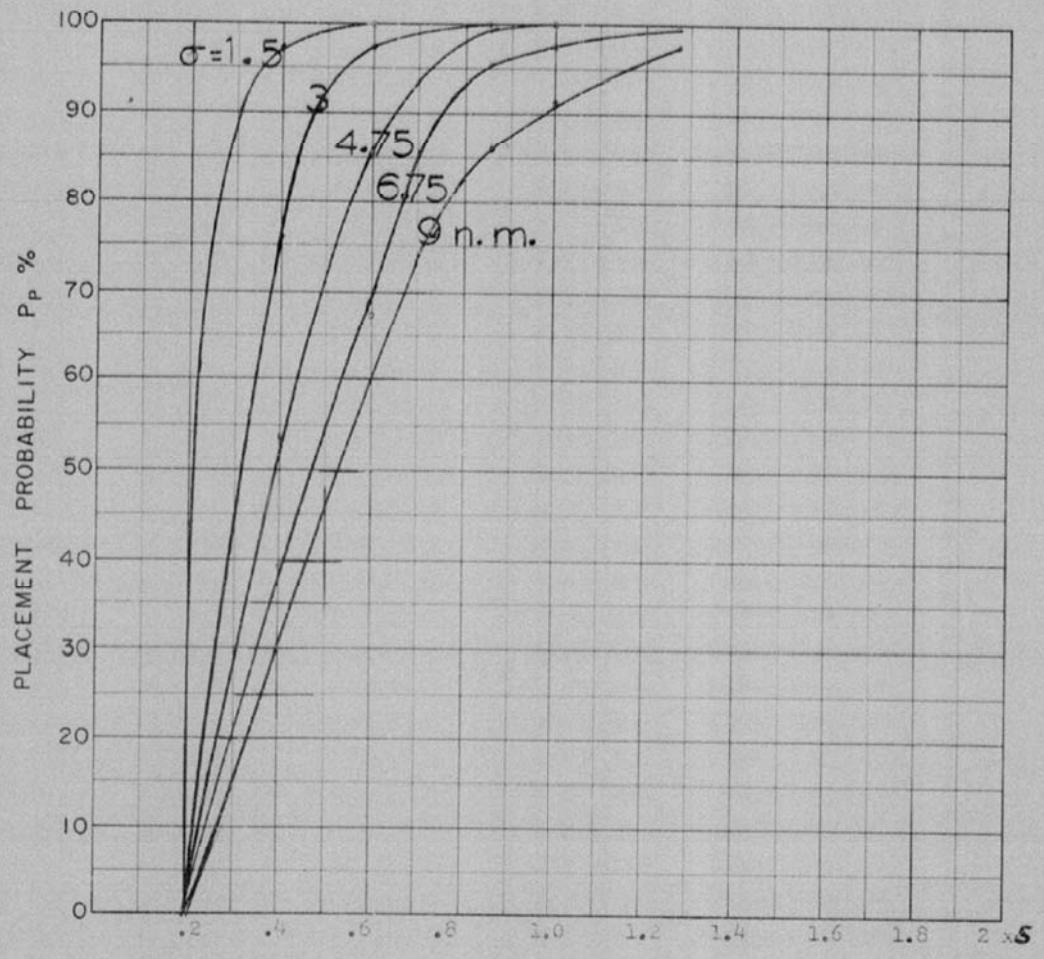

COURSE DIFFERENCE: 180°
TARGET EVASION: 0.15 lateral g's
TARGET MACH NO.: 1.5
INTERCEPTOR LATERAL G's: 1.6
INTERCEPTOR MACH NO. 1.5
σ OF G.C.I. ACCURACY: five values
A.I. DETECTION RANGE AS FRACTION OF SPECIFICATION RANGE, S abscissa
A.I. DETECTION RANGE CONTOUR: Delta
ALTITUDE: 50K

D-55

Launch zone

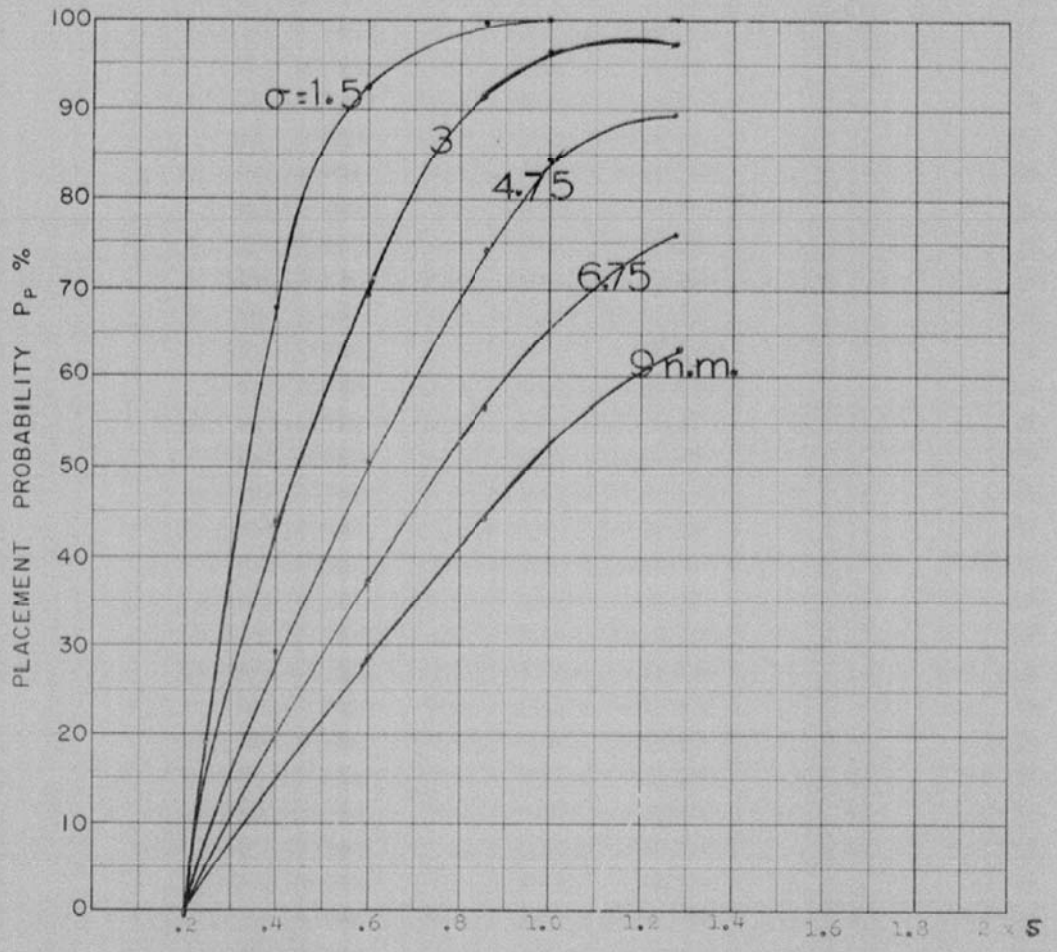

COURSE DIFFERENCE: 110°
TARGET EVASION: 0.1g lateral g's
TARGET MACH NO.: 1.5
INTERCEPTOR LATERAL G's: 0.66
INTERCEPTOR MACH NO.: 1.5
σ OF G.C.I. ACCURACY: five values
A.I. DETECTION RANGE AS FRACTION OF SPECIFICATION RANGE, S: abscissa
A.I. DETECTION RANGE CONTOUR: Delta
ALTITUDE: 60K ft

D-56

Missile launch zone L 13

183 dp:

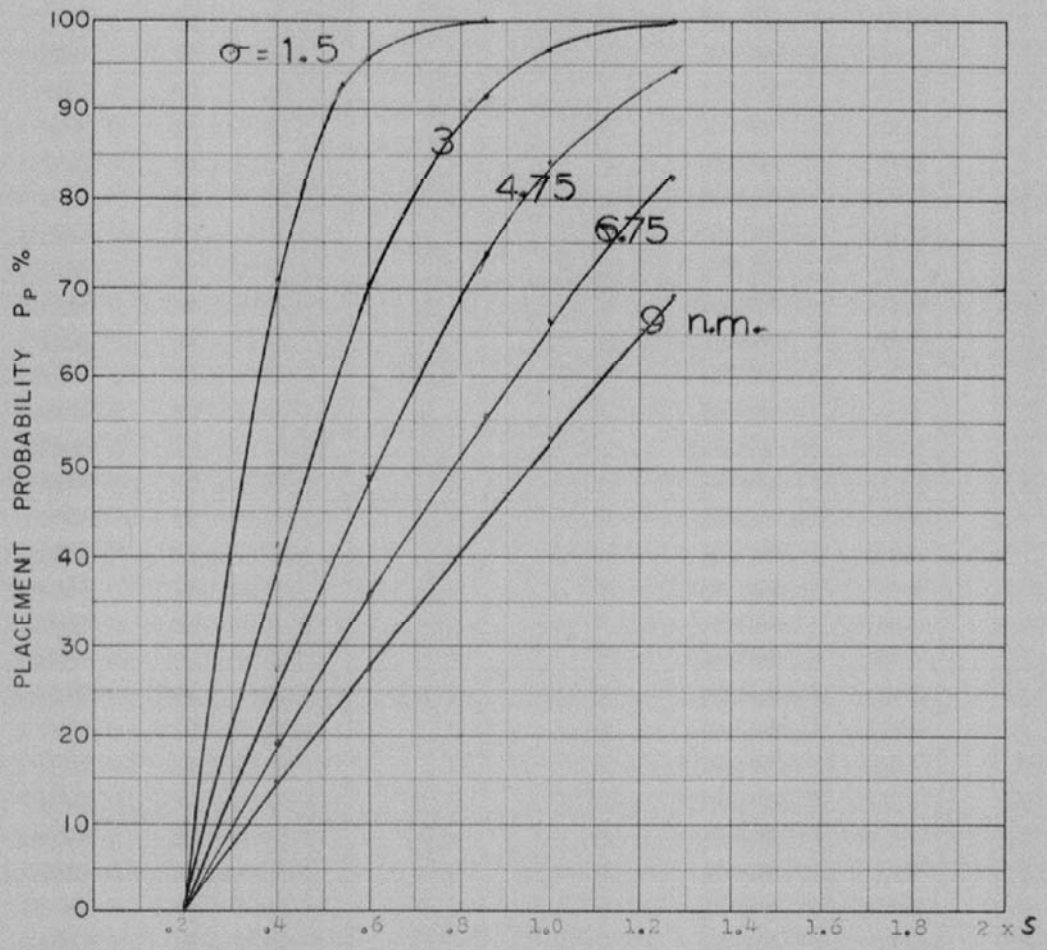

D-57

COURSE DIFFERENCE: 135°
TARGET EVASION: 0.15 lateral g's
TARGET MACH NO.: 1.5
INTERCEPTOR LATERAL G's: 0.66
INTERCEPTOR MACH NO.: 1.5
σ OF G.C.I. ACCURACY: five values
A.I. DETECTION RANGE AS FRACTION OF SPECIFICATION RANGE, S: abscissa
A.I. DETECTION RANGE CONTOUR: Delta
ALTITUDE: 60K

Missile Launch zone L 1)

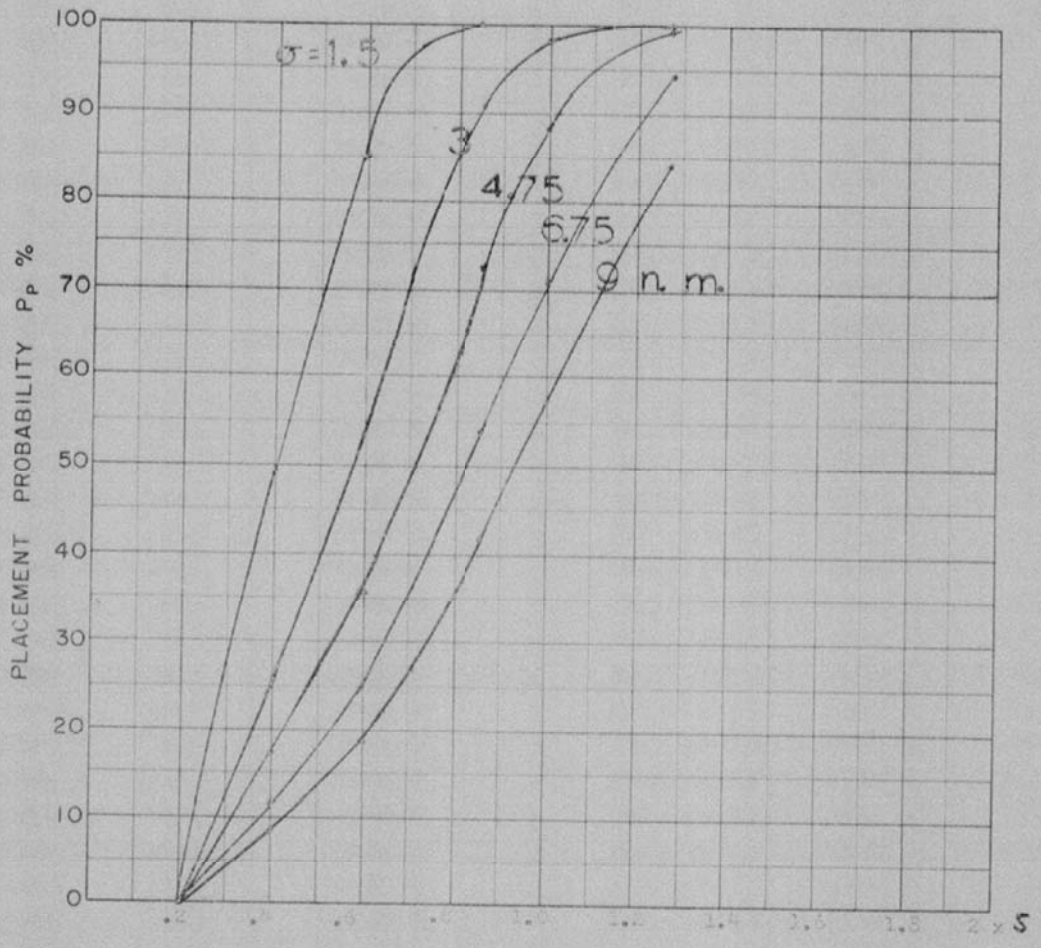

A.I. Range

COURSE DIFFERENCE: 180°
TARGET EVASION: 0.15 Lateral g's
TARGET MACH NO.: 1.5
INTERCEPTOR LATERAL G's: 0.66
INTERCEPTOR MACH NO.: 1.5
σ OF G.C.I. ACCURACY: five values
A.I. DETECTION RANGE AS FRACTION OF SPECIFICATION RANGE, S Abscissa
A.I. DETECTION RANGE CONTOUR: Delta
ALTITUDE: 40K

Missile launch zone L 13

D-58

187 dpn

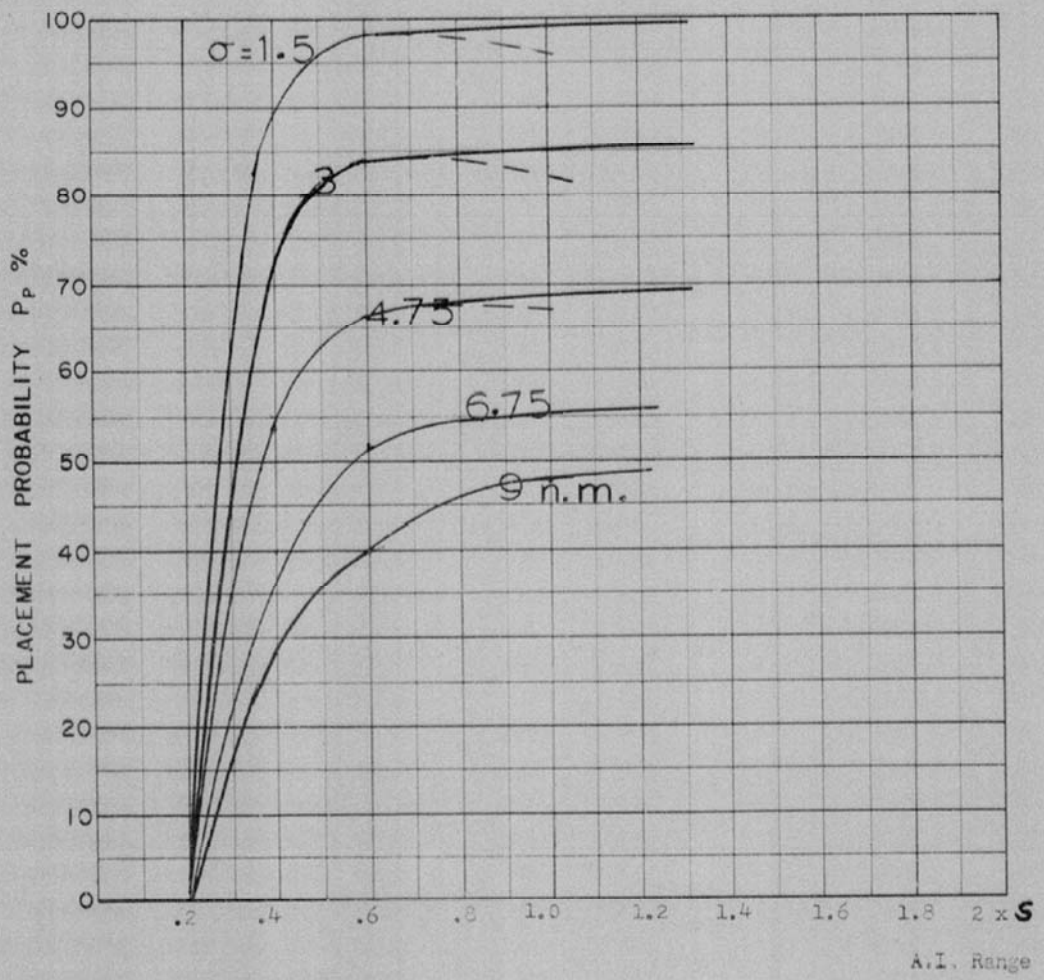

COURSE DIFFERENCE: 110°
TARGET EVASION: 0.15 lateral g's
TARGET MACH NO.: 1.5
INTERCEPTOR LATERAL G's: 1.5
INTERCEPTOR MACH NO.: 1.5
σ OF G.C.I. ACCURACY: five values
A.I. DETECTION RANGE AS FRACTION OF SPECIFICATION RANGE, S: abscissa
A.I. DETECTION RANGE CONTOUR: Delta
ALTITUDE: 60K

D59

Launch zone L 13

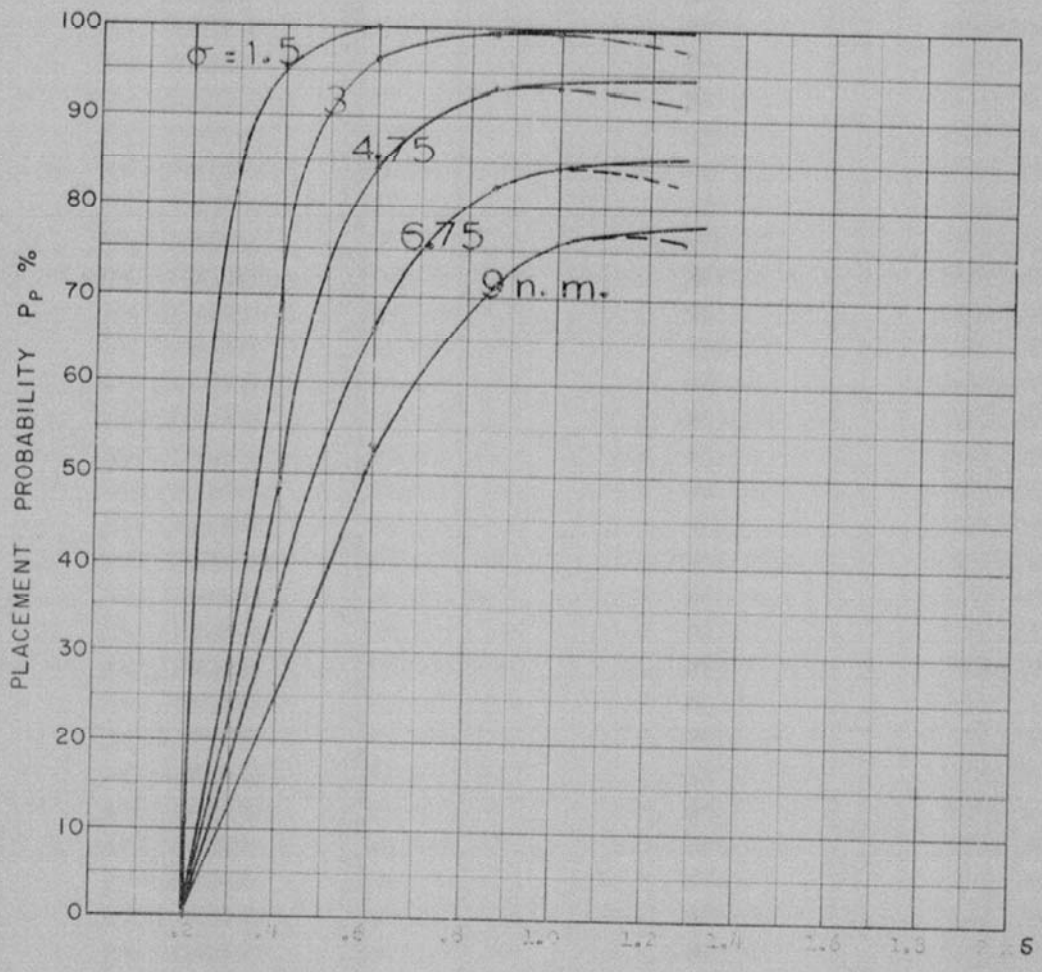

COURSE DIFFERENCE: 135°
TARGET EVASION: 0.15 lateral g's
TARGET MACH NO.: 1.5
INTERCEPTOR LATERAL G's: 1.5
INTERCEPTOR MACH NO.: 1.5
σ OF G.C.I. ACCURACY: Sliv values
A.I. DETECTION RANGE AS FRACTION OF SPECIFICATION RANGE, S abscissa
A.I. DETECTION RANGE CONTOUR: Delta
ALTITUDE: 60K ft.

D-60

Missile launch zone L13

191 dpn

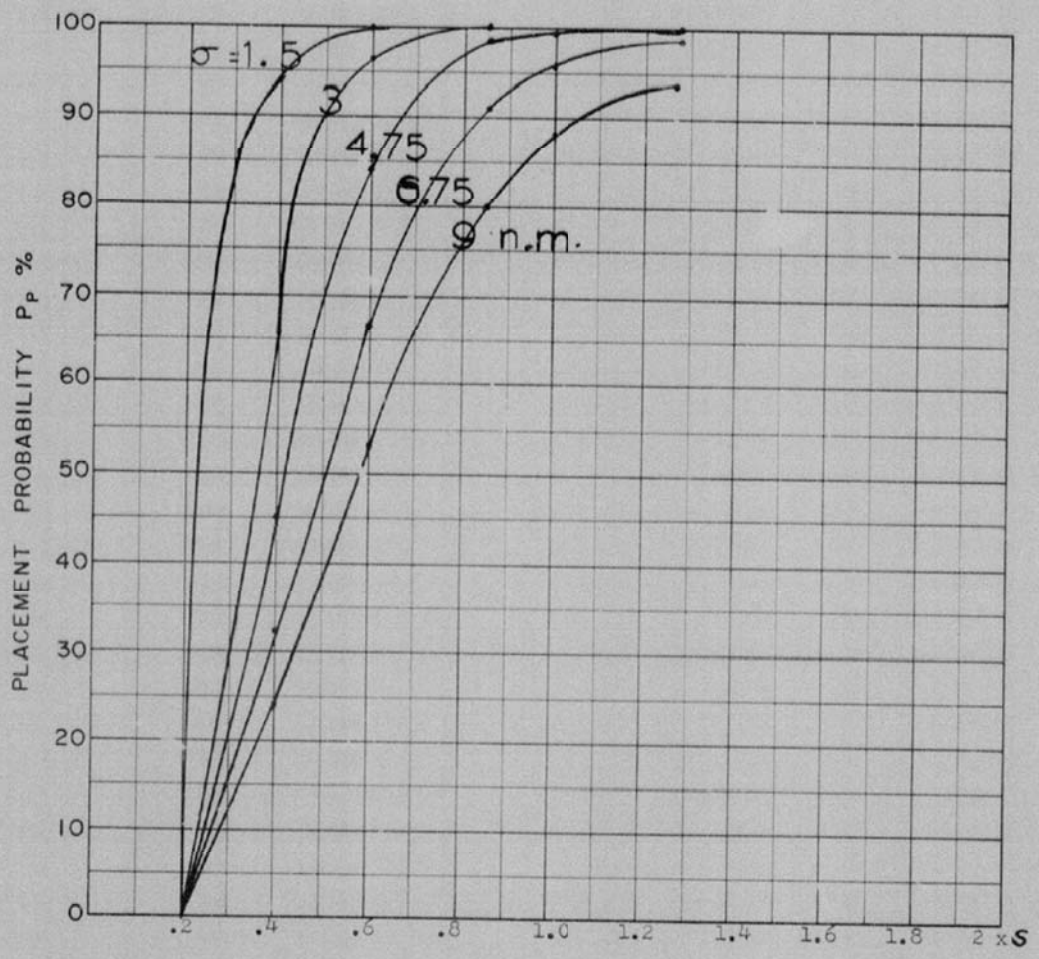

COURSE DIFFERENCE: 160°
TARGET EVASION: 0.15 lateral g's
TARGET MACH NO.: 1.5
INTERCEPTOR LATERAL G's: 1.5
INTERCEPTOR MACH NO.: 1.5
σ OF G.C.I. ACCURACY: five values
A.I. DETECTION RANGE AS FRACTION OF SPECIFICATION RANGE, S: abscissa
A.I. DETECTION RANGE CONTOUR: Delta
ALTITUDE: 60K

D61

Missile launch zone L 13

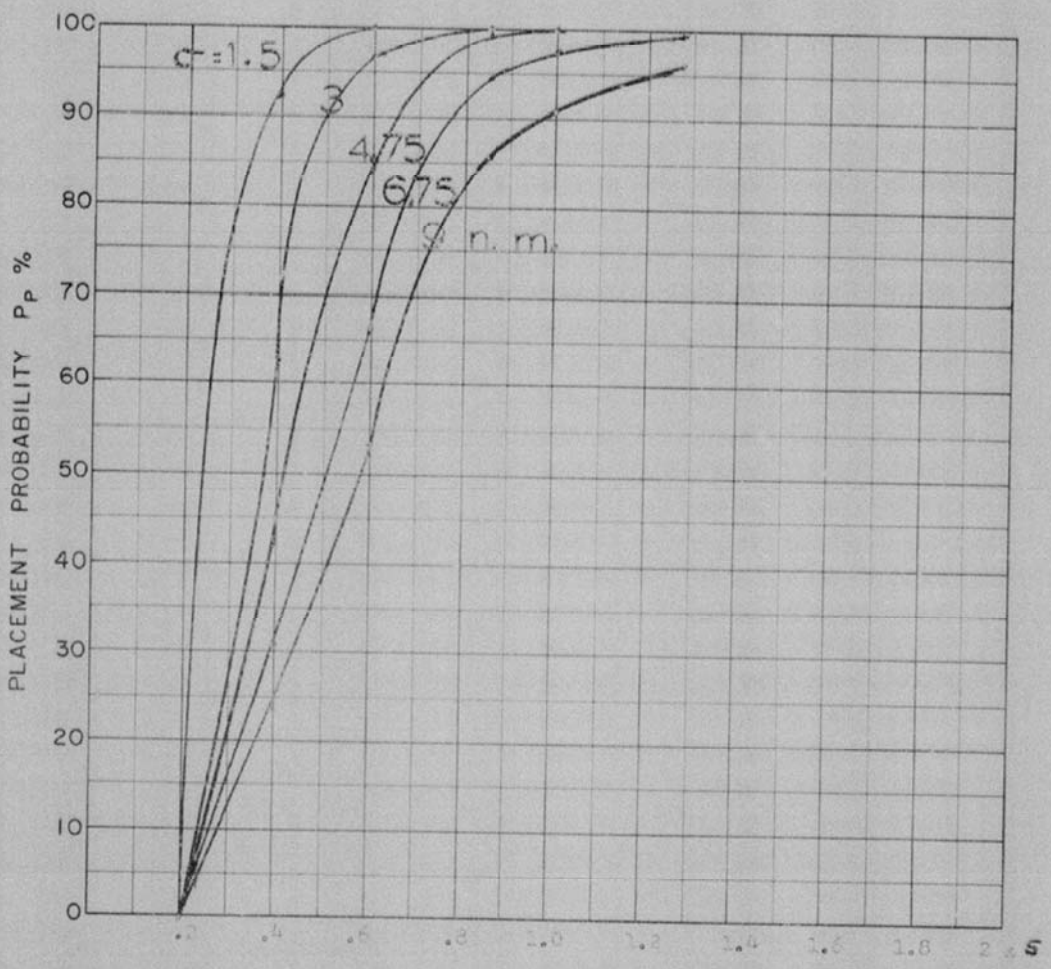

COURSE DIFFERENCE: 180°
TARGET EVASION: 0.15 lateral g's
TARGET MACH NO.: 1.5
INTERCEPTOR LATERAL G's: 1.5
INTERCEPTOR MACH NO.: 1.5
σ OF G.C.I. ACCURACY: five values
A.I. DETECTION RANGE AS FRACTION OF SPECIFICATION RANGE, S: abscissa
A.I. DETECTION RANGE CONTOUR: Delta
ALTITUDE: 60K

D 62

Missile launch zone L 13

294 dpn

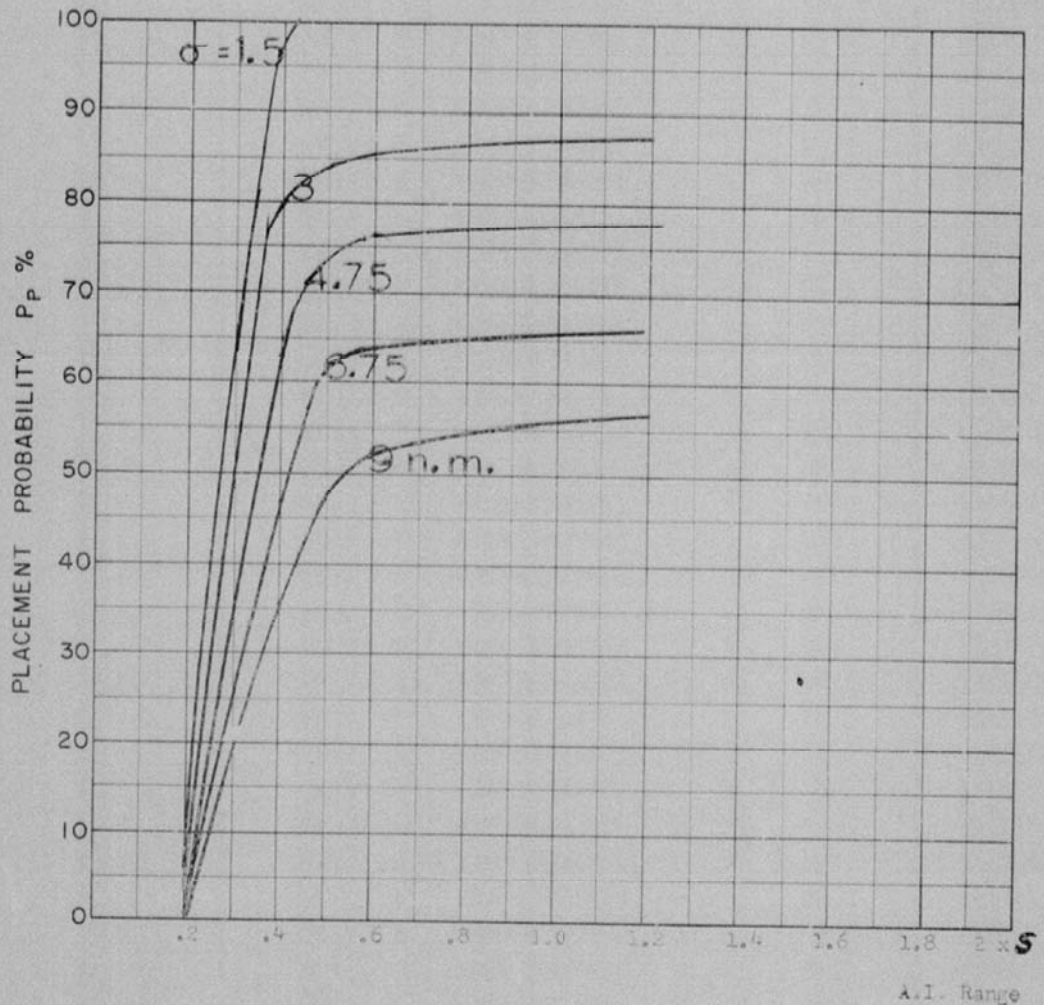

COURSE DIFFERENCE: 110°
TARGET EVASION: 0.15 lateral g's
TARGET MACH NO.: 1.5
INTERCEPTOR LATERAL G's: 2.4
INTERCEPTOR MACH NO.: 1.5
σ OF G.C.I. ACCURACY: five values
A.I. DETECTION RANGE AS FRACTION OF SPECIFICATION RANGE, S abscissa
A.I. DETECTION RANGE CONTOUR: Delta
ALTITUDE: 60K

D-63

Missile Launch Zone L13

196 dpm

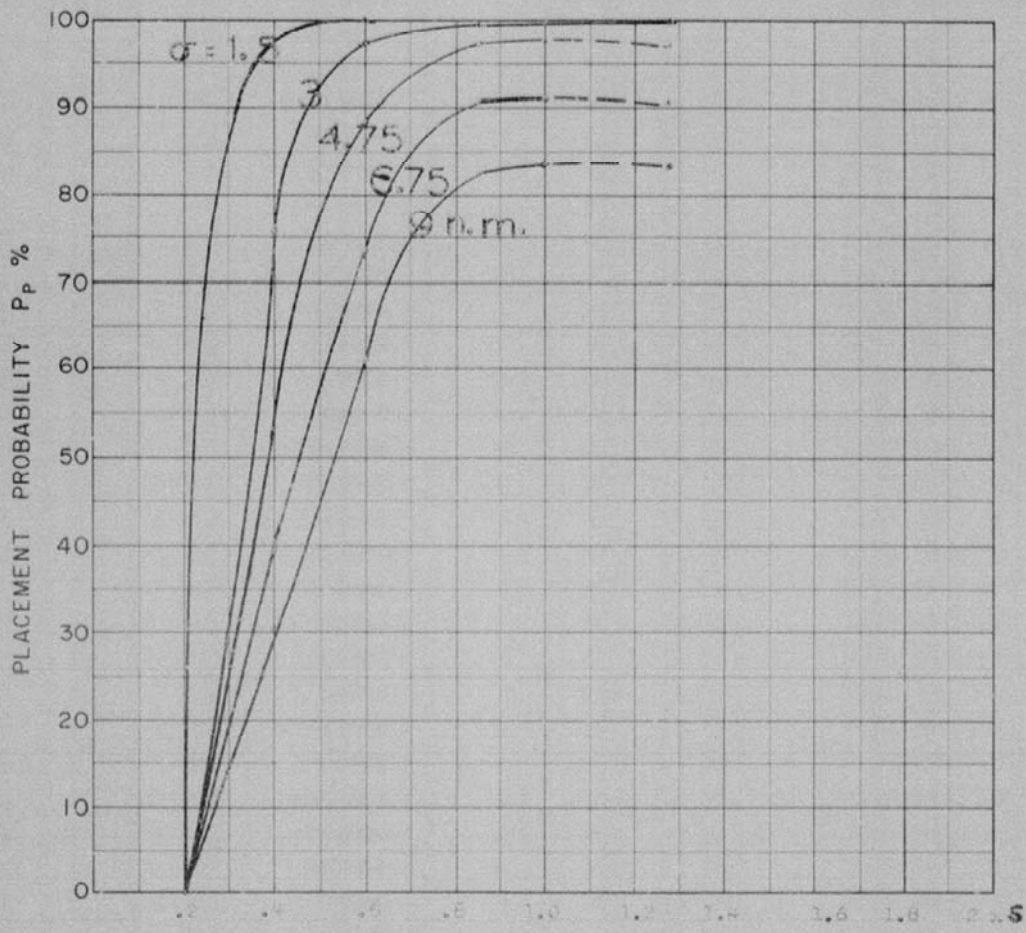

COURSE DIFFERENCE: 135°
TARGET EVASION: 0.15 lateral g's
TARGET MACH NO.: 1.5
INTERCEPTOR LATERAL G's: 2.4
INTERCEPTOR MACH NO.: 1.5
σ OF G.C.I. ACCURACY: five values
A.I. DETECTION RANGE AS FRACTION OF SPECIFICATION RANGE, S: abscissa
A.I. DETECTION RANGE CONTOUR: Delta
ALTITUDE: 60K

D.64

Missile launch zone L-13

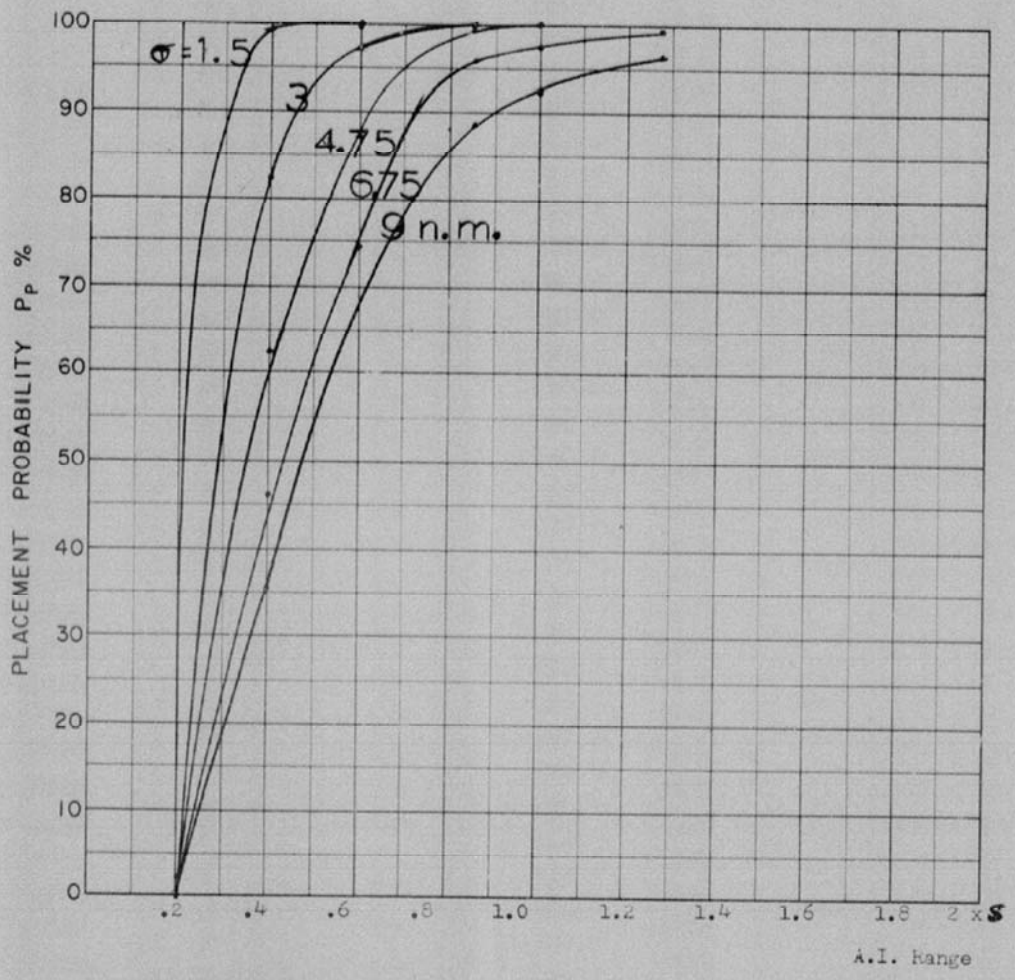

COURSE DIFFERENCE: 160°
TARGET EVASION: 0.15 lateral g's
TARGET MACH NO.: 1.5
INTERCEPTOR LATERAL G's: 2.4
INTERCEPTOR MACH NO.: 1.5
σ OF G.C.I. ACCURACY: five values
A.I. DETECTION RANGE AS FRACTION OF SPECIFICATION RANGE, S abscissa
A.I. DETECTION RANGE CONTOUR: Delta
ALTITUDE: 60K

D 65

Missile launch zone L 13

200 dpn

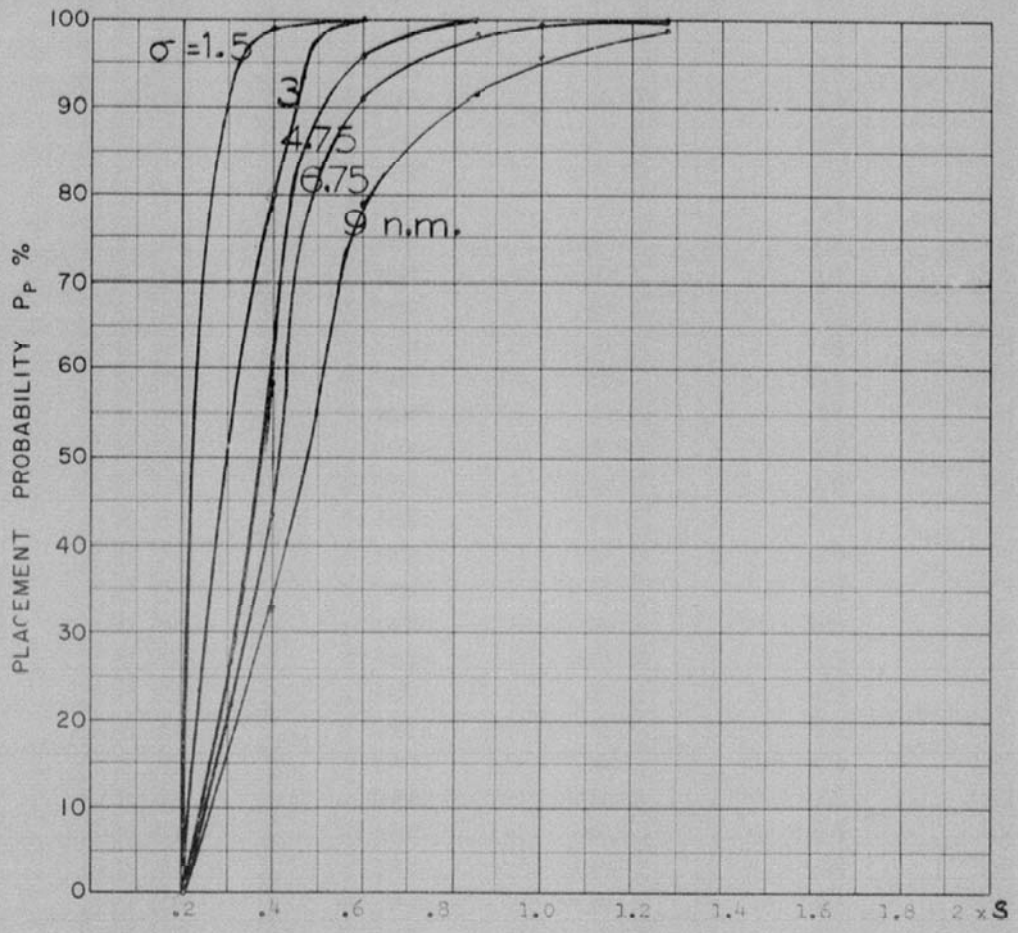

COURSE DIFFERENCE: 180°
TARGET EVASION: 0.15 lateral g's
TARGET MACH NO.: 1.5
INTERCEPTOR LATERAL G's: 2.4
INTERCEPTOR MACH NO.: 1.5
σ OF G.C.I. ACCURACY: five values
A.I. DETECTION RANGE AS FRACTION OF SPECIFICATION RANGE, S: abscissa
A.I. DETECTION RANGE CONTOUR: Delta
ALTITUDE: 60K

D-66

Missile launch zone L 13

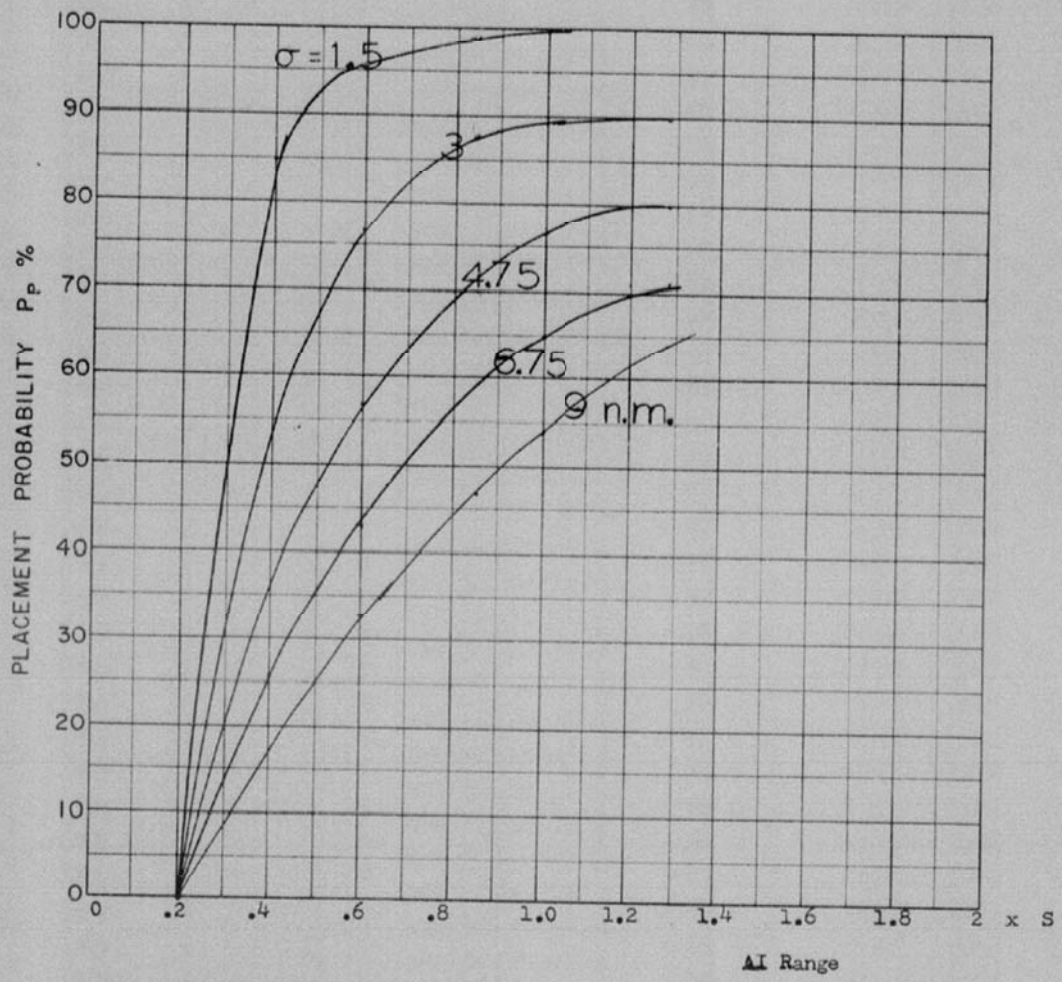

COURSE DIFFERENCE: 75°
TARGET EVASION: 0
TARGET MACH NO.: 2.0
INTERCEPTOR LATERAL G's: 0.85
INTERCEPTOR MACH NO.: 1.5
σ OF G.C.I. ACCURACY: Five values
A.I. DETECTION RANGE AS FRACTION OF SPECIFICATION RANGE, S: Abscissa
A.I. DETECTION RANGE CONTOUR: Delta
ALTITUDE: 50 K

(D 67)

Launch zone figure L-3, missile launched at maximum range with 10° heading error.

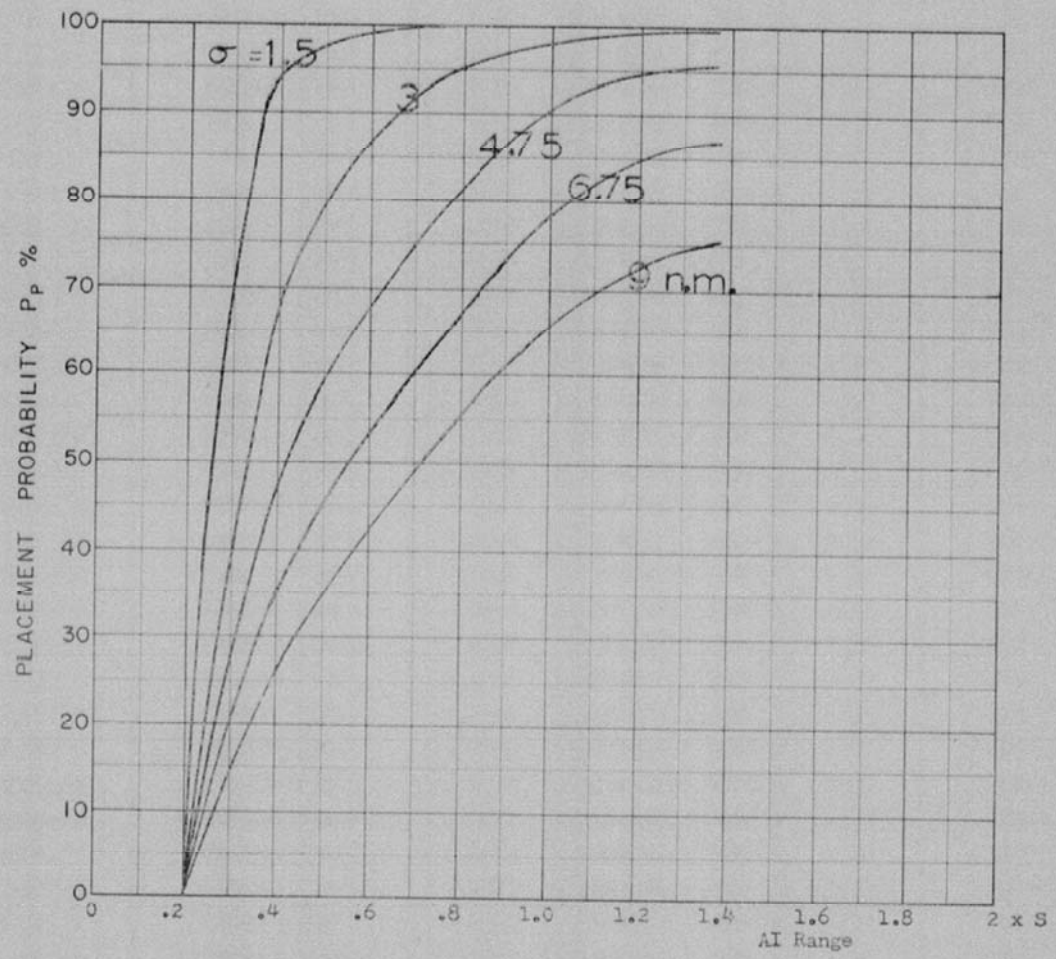

COURSE DIFFERENCE: 90°
TARGET EVASION: 0
TARGET MACH NO.: 2.0
INTERCEPTOR LATERAL G's: 0.85
INTERCEPTOR MACH NO.: 1.5
σ OF G.C.I. ACCURACY: Five values
A.I. DETECTION RANGE AS FRACTION OF SPECIFICATION RANGE, S Abscissa
A.I. DETECTION RANGE CONTOUR: Delta
ALTITUDE: 50 K

D68a

Launch zone figure L-3, missile launched at maximum range with 10° heading error.

29 b n d p r

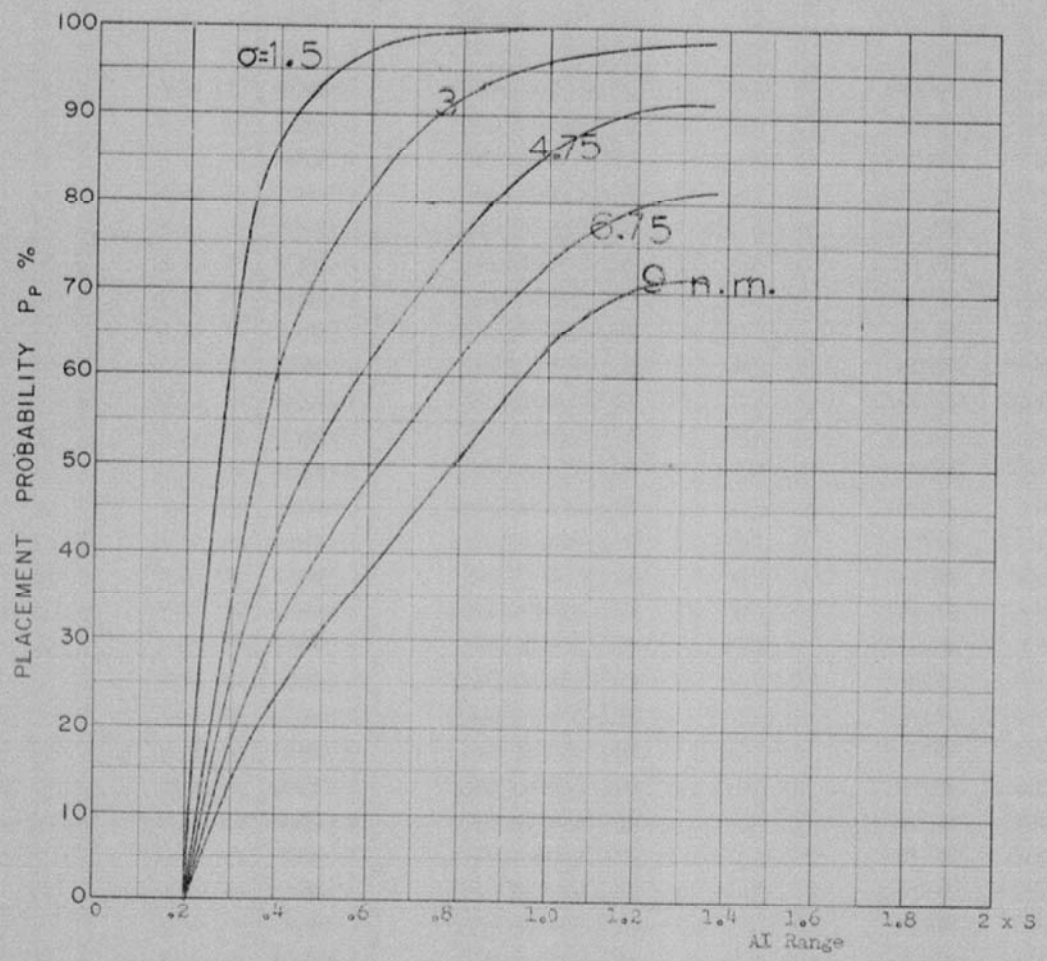

COURSE DIFFERENCE: 90°
TARGET EVASION: 0
TARGET MACH NO.: 2.0
INTERCEPTOR LATERAL G's: 0.85
INTERCEPTOR MACH NO.: 1.5
σ OF G.C.I. ACCURACY: Five values
A.I. DETECTION RANGE AS FRACTION OF SPECIFICATION RANGE, S: Abscissa
A.I. DETECTION RANGE CONTOUR: Delta
ALTITUDE: 50 K

D686

Launch zone figure I-3, missile launched at minimum range with 5° heading error.

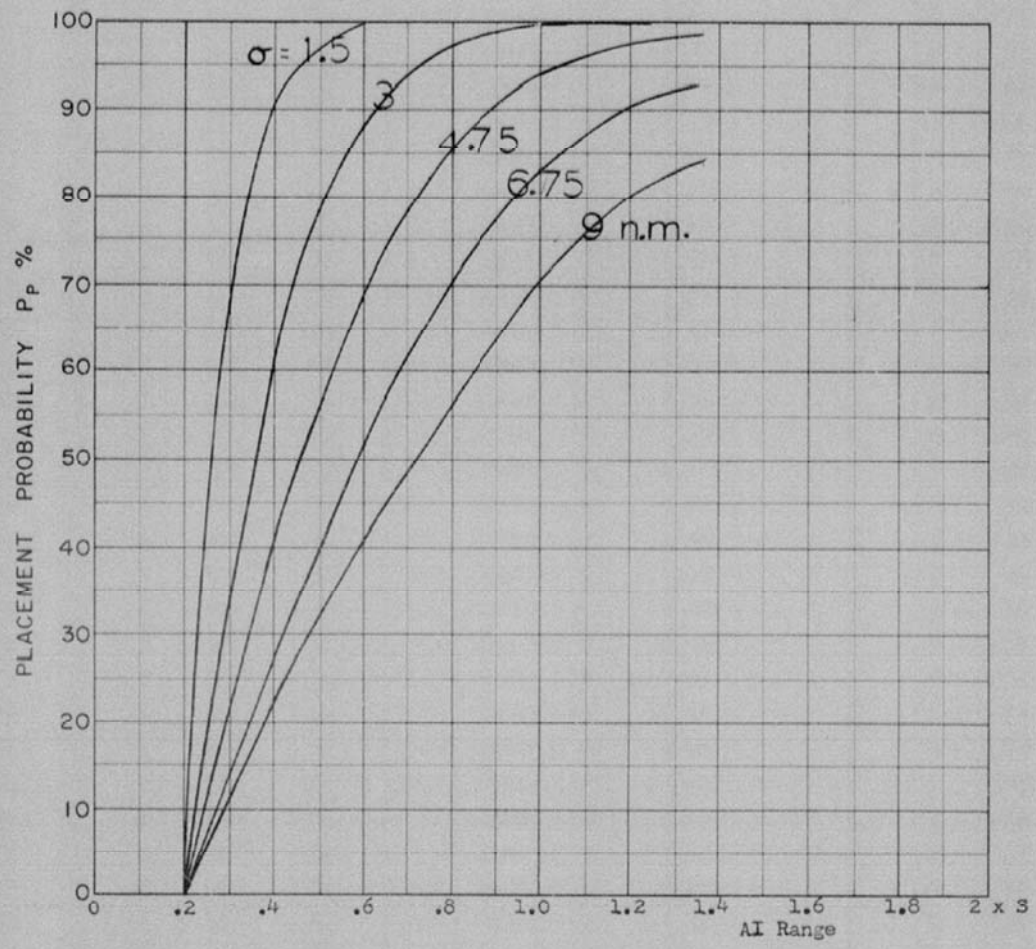

COURSE DIFFERENCE: 100°
TARGET EVASION: 0
TARGET MACH NO.: 2.0
INTERCEPTOR LATERAL G's: 0.85
INTERCEPTOR MACH NO.: 1.5
σ OF G.C.I. ACCURACY: Five values
A.I. DETECTION RANGE AS FRACTION OF SPECIFICATION RANGE, SAbscissa
A.I. DETECTION RANGE CONTOUR: Delta
ALTITUDE: 50 K

(D 69)

Launch zone figure L-3, missile launched at maximum range with 10° heading error.

29 d x d p r

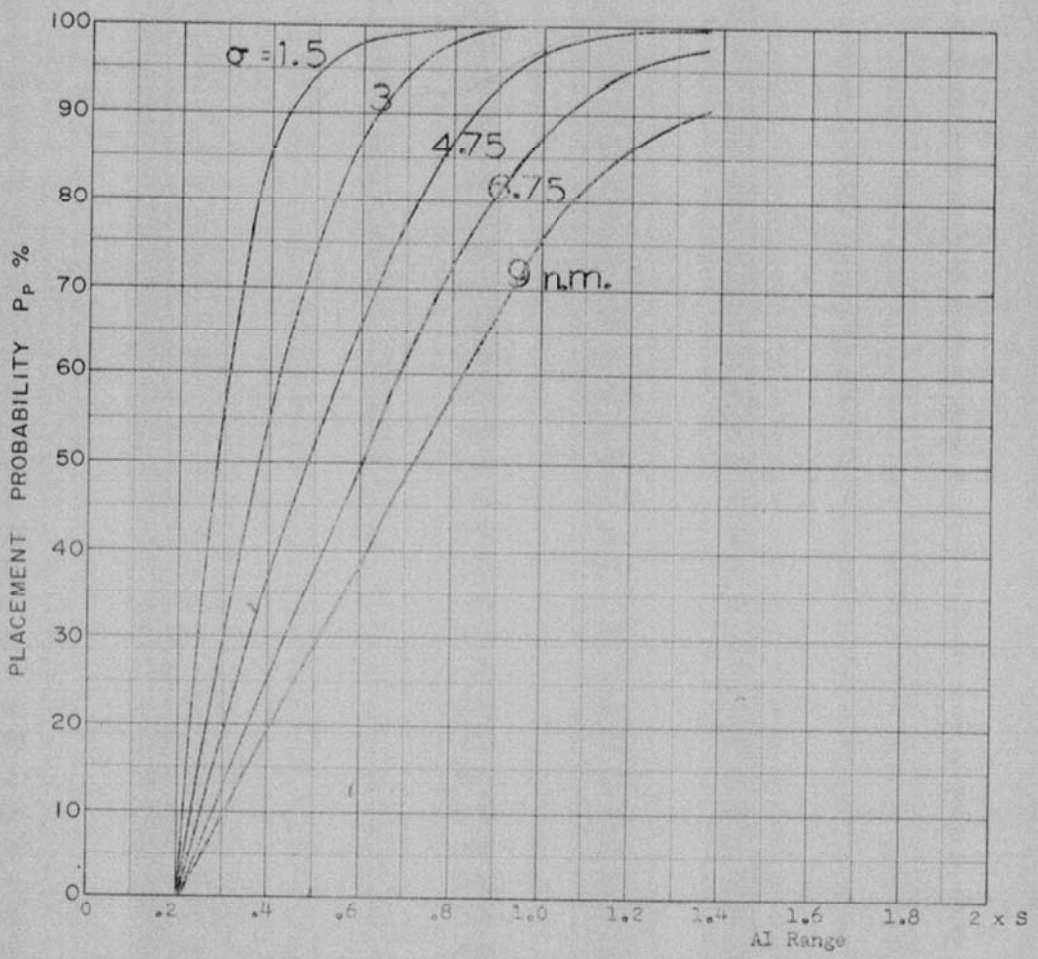

COURSE DIFFERENCE: 120°
TARGET EVASION: 0
TARGET MACH NO.: 2.0
INTERCEPTOR LATERAL G's: 0.85
INTERCEPTOR MACH NO.: 1.5
σ OF G.C.I. ACCURACY: Five values
A.I. DETECTION RANGE AS FRACTION OF SPECIFICATION RANGE, S: Abscissa
A.I. DETECTION RANGE CONTOUR: Delta
ALTITUDE: 50 K

D 70

Launch zone figure L-3, missile launched at maximum range with 10° heading error.

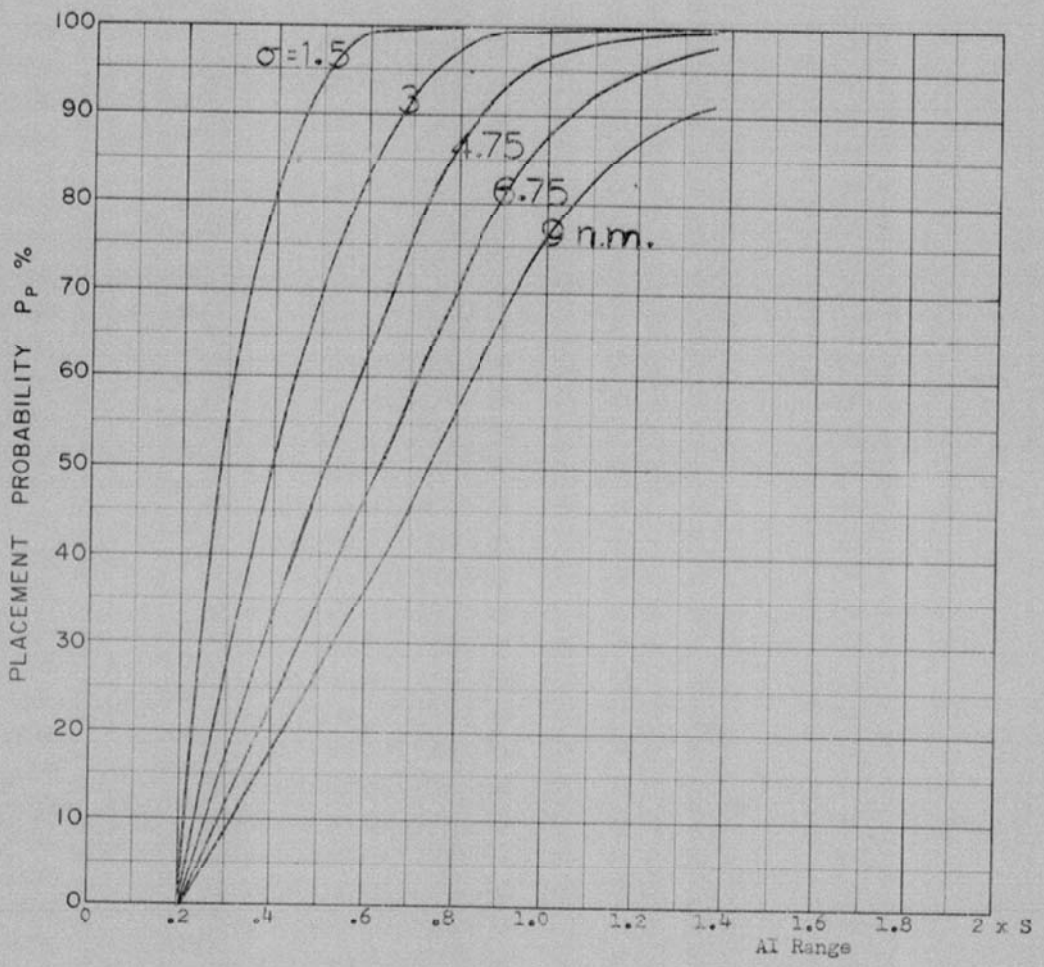

COURSE DIFFERENCE: 135°
TARGET EVASION: 0
TARGET MACH NO.: 2.0
INTERCEPTOR LATERAL G's: 0.85
INTERCEPTOR MACH NO.: 1.5
σ OF G.C.I. ACCURACY: Five values
A.I. DETECTION RANGE AS FRACTION OF SPECIFICATION RANGE, S: Abscissa
A.I. DETECTION RANGE CONTOUR: Delta
ALTITUDE: 50 K

(D 71)

Launch zone figure L-3, missile launched at maximum range with 10° heading error.

29 f x d p r

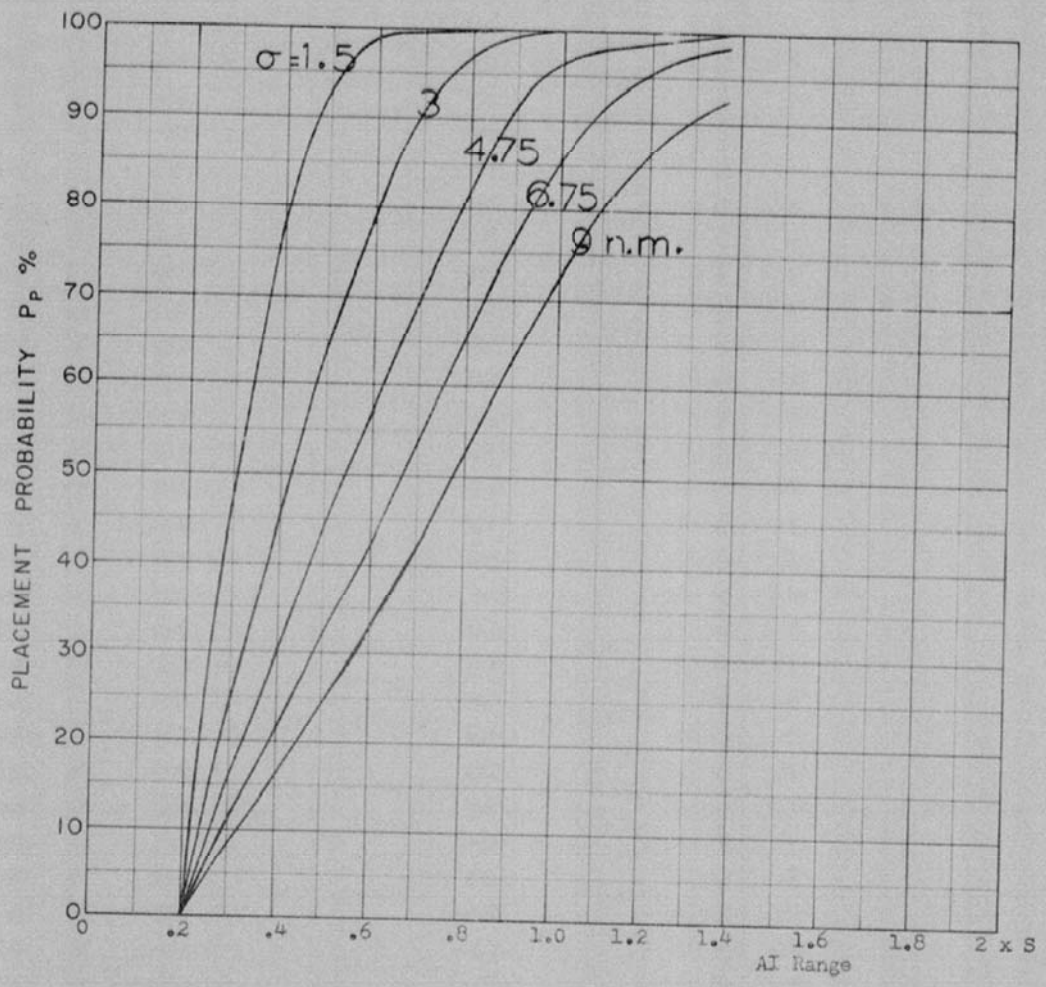

COURSE DIFFERENCE: 160°
TARGET EVASION: 0
TARGET MACH NO.: 2.0
INTERCEPTOR LATERAL G's: 0.85
INTERCEPTOR MACH NO.: 1.5
σ OF G.C.I. ACCURACY: Five values
A.I. DETECTION RANGE AS FRACTION OF SPECIFICATION RANGE, S: Abscissa
A.I. DETECTION RANGE CONTOUR: Delta
ALTITUDE: 50 K

D 72

Launch zone figure L-3, missile launched at maximum range with 10° heading error.

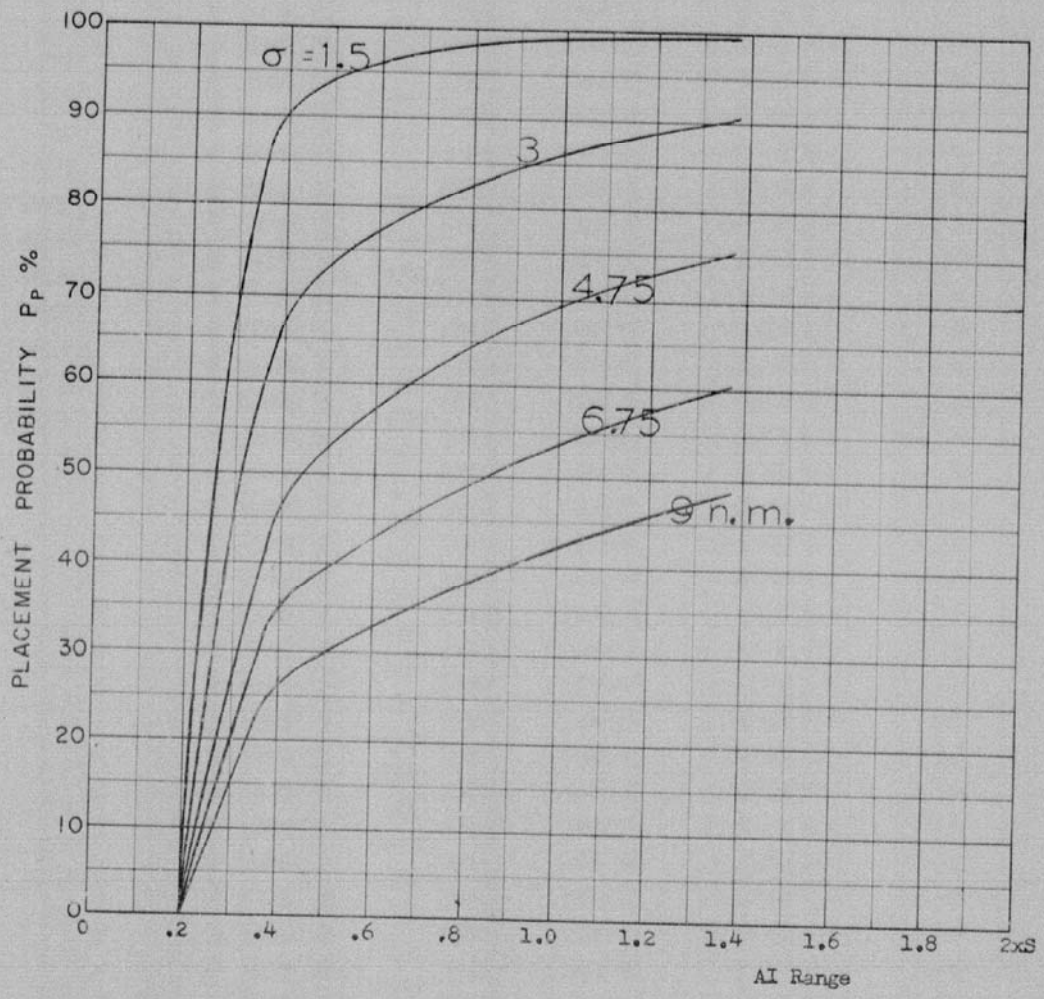

COURSE DIFFERENCE: 75°
TARGET EVASION: 0
TARGET MACH NO.: 2.0
INTERCEPTOR LATERAL G's: 1.6
INTERCEPTOR MACH NO.: 1.5
σ OF G.C.I. ACCURACY: Five values
A.I. DETECTION RANGE AS FRACTION OF SPECIFICATION RANGE, S Abscissa
A.I. DETECTION RANGE CONTOUR: Delta
ALTITUDE: 50 K

D-73

Launch zone figure L-3, missile launched at maximum range with 10° heading error.

27 b x d p r

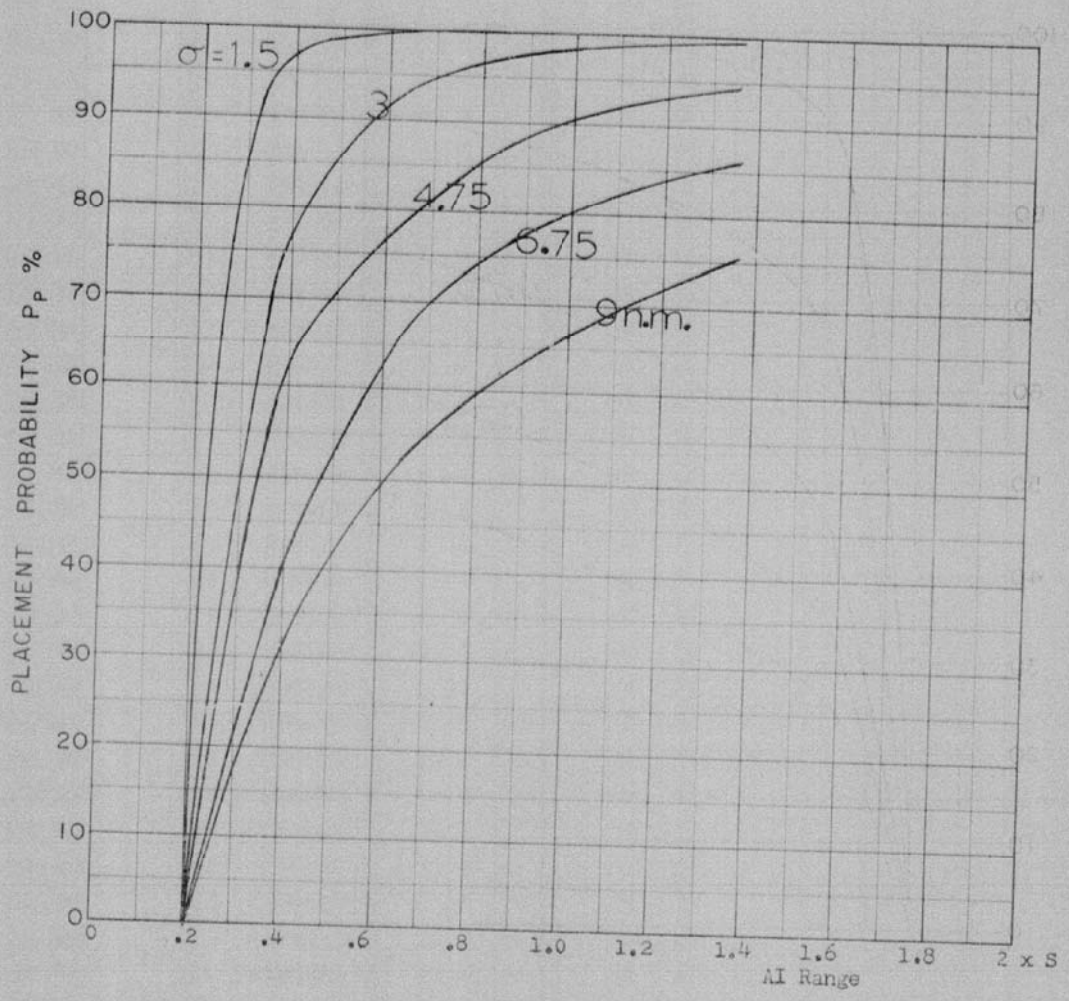

COURSE DIFFERENCE: 90°
TARGET EVASION: 0
TARGET MACH NO.: 2.0
INTERCEPTOR LATERAL G's: 1.6
INTERCEPTOR MACH NO: 1.5
σ OF G.C.I. ACCURACY: Five values
A.I. DETECTION RANGE AS FRACTION OF SPECIFICATION RANGE, S: Abscissa
A.I. DETECTION RANGE CONTOUR: Delta
ALTITUDE: 50 K

D74a

Launch zone figure L-3, missile launched at maximum range with 10° heading error.

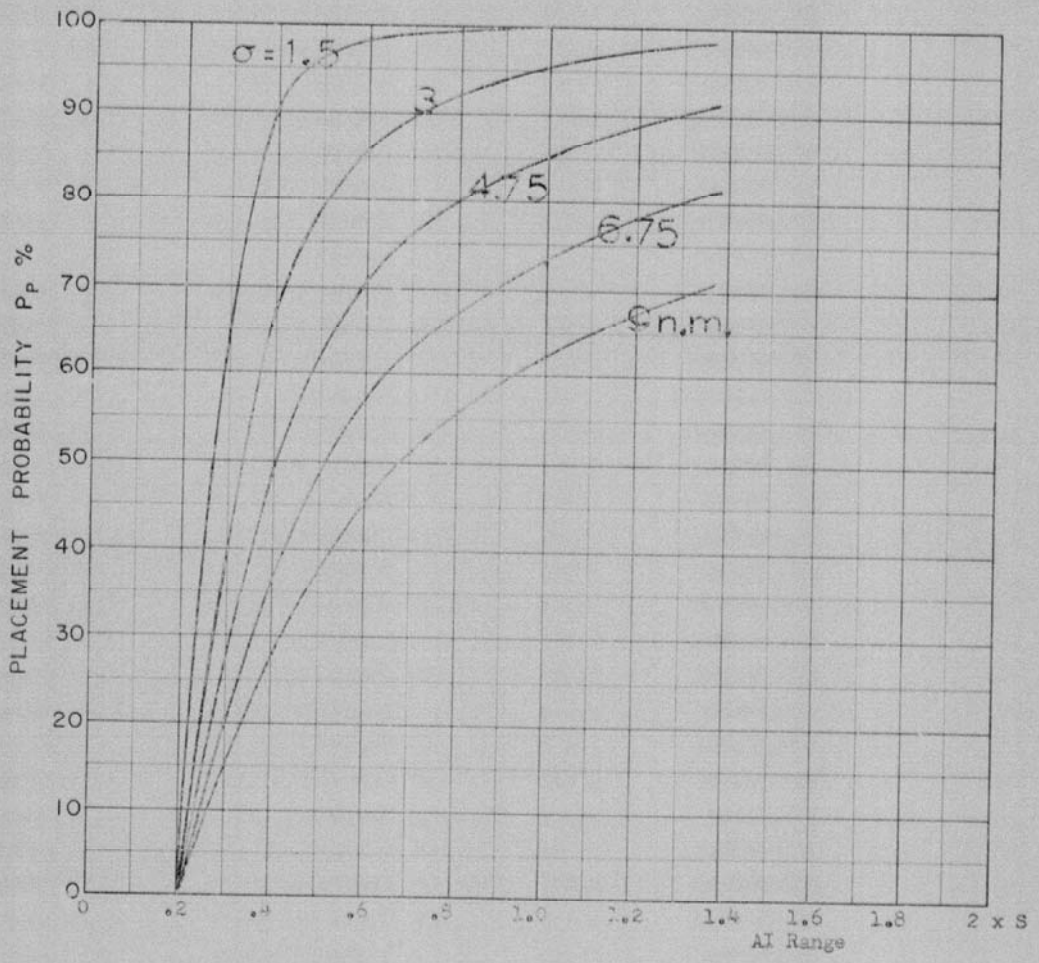

COURSE DIFFERENCE: 90°
TARGET EVASION: 0
TARGET MACH NO.: 2.0
INTERCEPTOF LATERAL G's: 1.6
INTERCEPTOR MACH NO.: 1.6
σ OF G.C.I. ACCURACY: Five Values
A.I. DETECTION RANGE AS FRACTION OF SPECIFICATION RANGE, S Abscissa
A.I. DETECTION RANGE CONTOUR: Delta
ALTITUDE: 50 K

D746

Launch zone figure L-3, missile launched at short range with 5° heading error allowance.

27 c x d p r

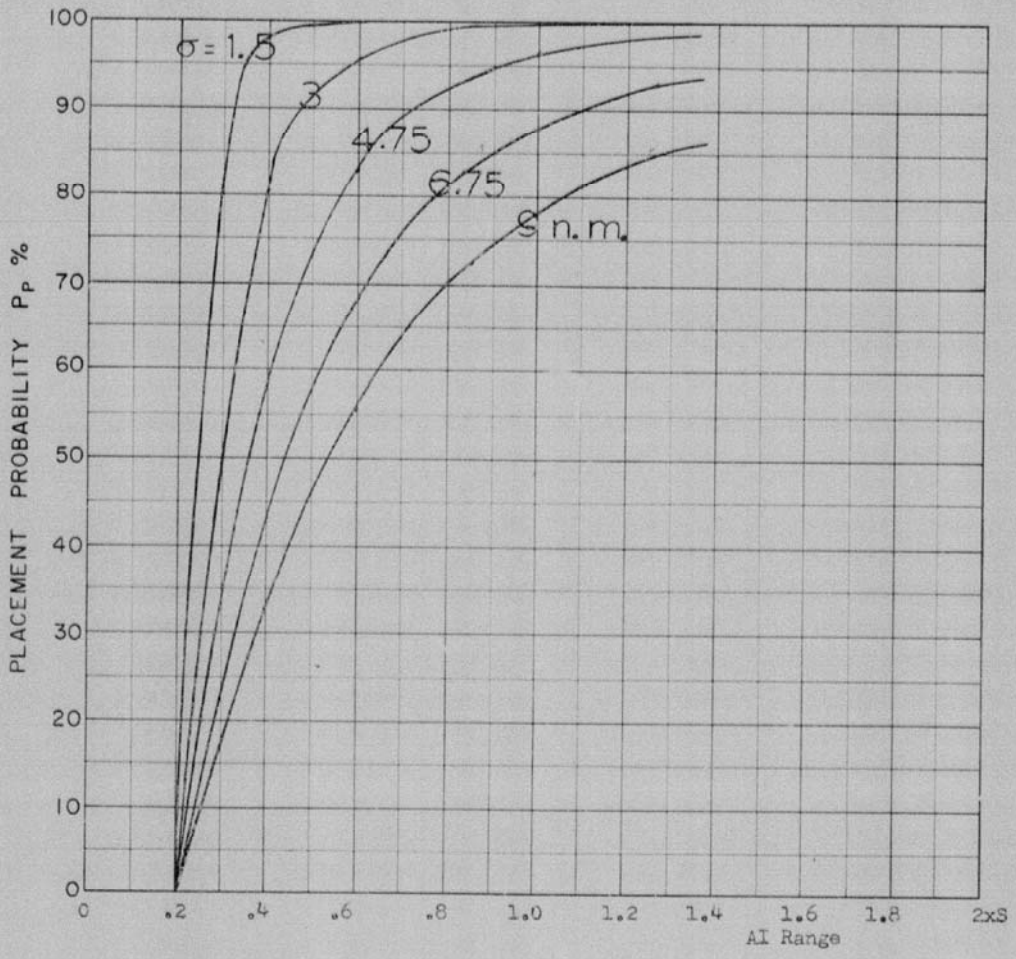

COURSE DIFFERENCE: 100°
TARGET EVASION: 0
TARGET MACH NO.: 2.0
INTERCEPTOR LATERAL G's: 1.6
INTERCEPTOR MACH NO.: 1.5
σ OF G.C.I. ACCURACY: Five values
A.I. DETECTION RANGE AS FRACTION OF SPECIFICATION RANGE, S Abscissa
A.I. DETECTION RANGE CONTOUR: Delta
ALTITUDE: 50 K

D75

Launch zone figure L-3, missile launched at maximum range with 10° heading error.

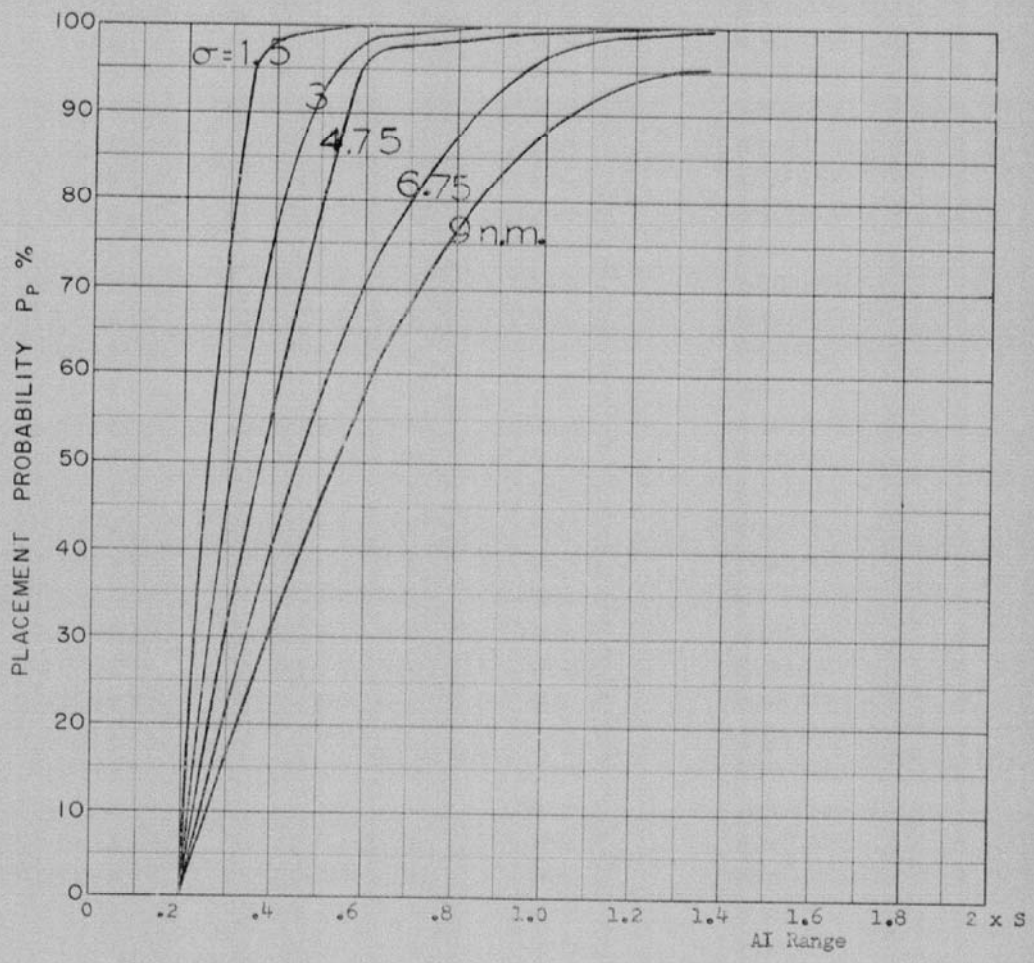

COURSE DIFFERENCE: 120°
TARGET EVASION: 0
TARGET MACH NO.: 2.0
INTERCEPTOR LATERAL G's: 1.6
INTERCEPTOR MACH NO.: 1.5
σ OF G.C.I. ACCURACY: Five values
A.I. DETECTION RANGE AS FRACTION OF SPECIFICATION RANGE, S Abscissa
A.I. DETECTION RANGE CONTOUR: Delta
ALTITUDE: 50 K

D.76a

Launch zone figure L-3, missile launched at maximum range with 10° heading error.

28 d n d p r

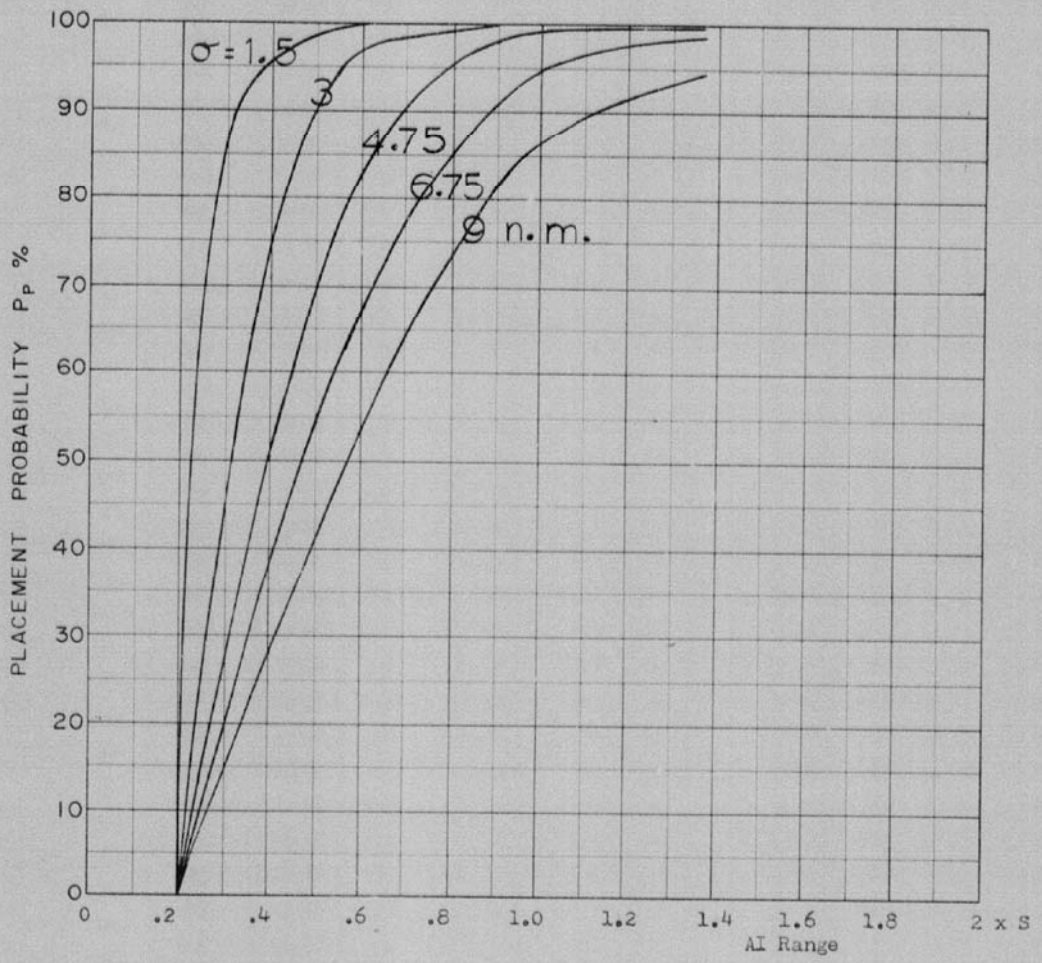

COURSE DIFFERENCE: 120°
TARGET EVASION: 0
TARGET MACH NO.: 2.0
INTERCEPTOR LATERAL G's: 1.6
INTERCEPTOR MACH NO.: 1.5
σ OF G.C.I. ACCURACY: Five values
A.I. DETECTION RANGE AS FRACTION OF SPECIFICATION RANGE, S Abscissa
A.I. DETECTION RANGE CONTOUR: Delta
ALTITUDE: 50 K

D766

Launch zone figure L-3, missile launched at short range with 5° heading error allowance.

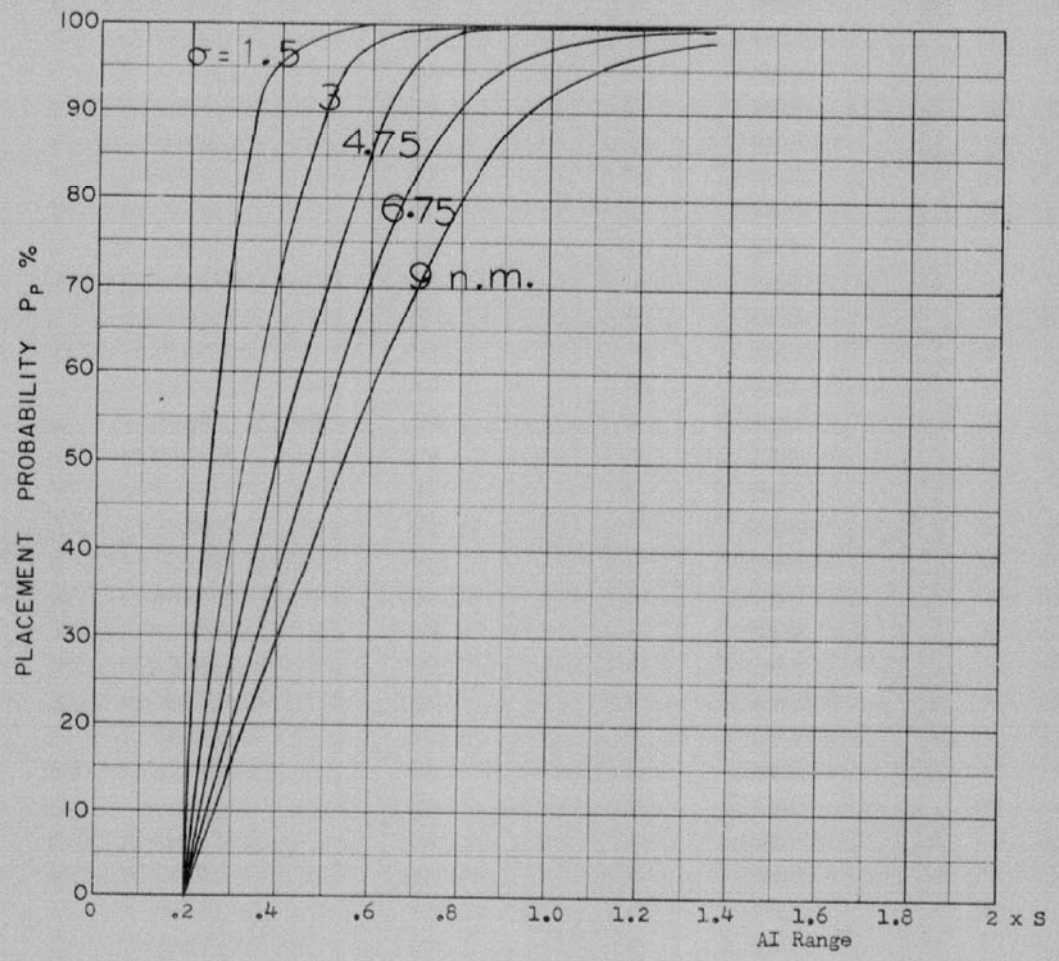

COURSE DIFFERENCE: 135°
TARGET EVASION: 0
TARGET MACH NO.: 2.0
INTERCEPTOR LATERAL G's: 1.6
INTERCEPTOR MACH NO.: 1.5
σ OF G.C.I. ACCURACY: Five values
A.I. DETECTION RANGE AS FRACTION OF SPECIFICATION RANGE, S Abscissa
A.I. DETECTION RANGE CONTOUR: Delta
ALTITUDE: 50 K

(D77)

Launch zone figure L-3, missile launched at maximum range with 10° heading error.

27 f x d p r

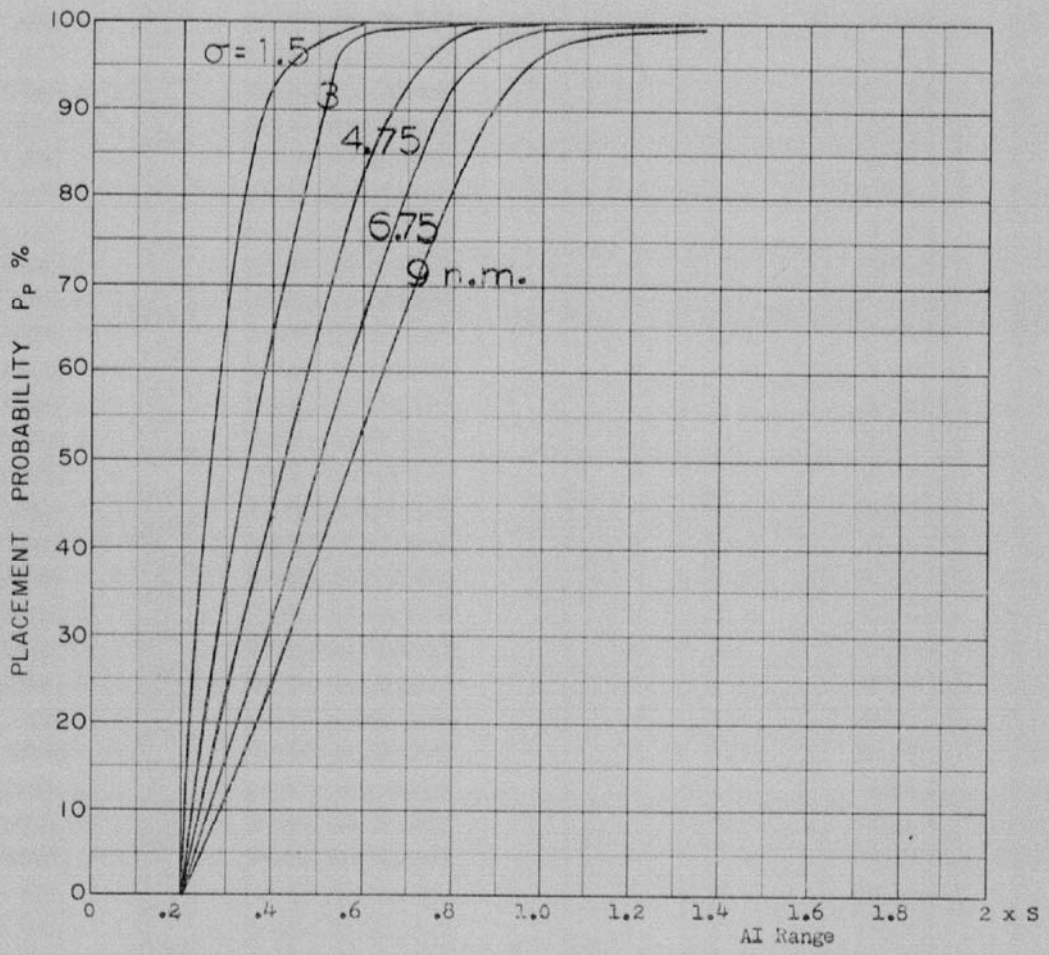

COURSE DIFFERENCE: 160°
TARGET EVASION: 0
TARGET MACH NO.: 2.0
INTERCEPTOR LATERAL G's: 1.6
INTERCEPTOR MACH NO.: 1.5
σ OF G.C.I. ACCURACY: Five values
A.I. DETECTION RANGE AS FRACTION OF SPECIFICATION RANGE, S: Abscissa
A.I. DETECTION RANGE CONTOUR: Delta
ALTITUDE: 50 K

D 78

Launch zone figure L-3, missile launched at maximum range with 10° heading error.

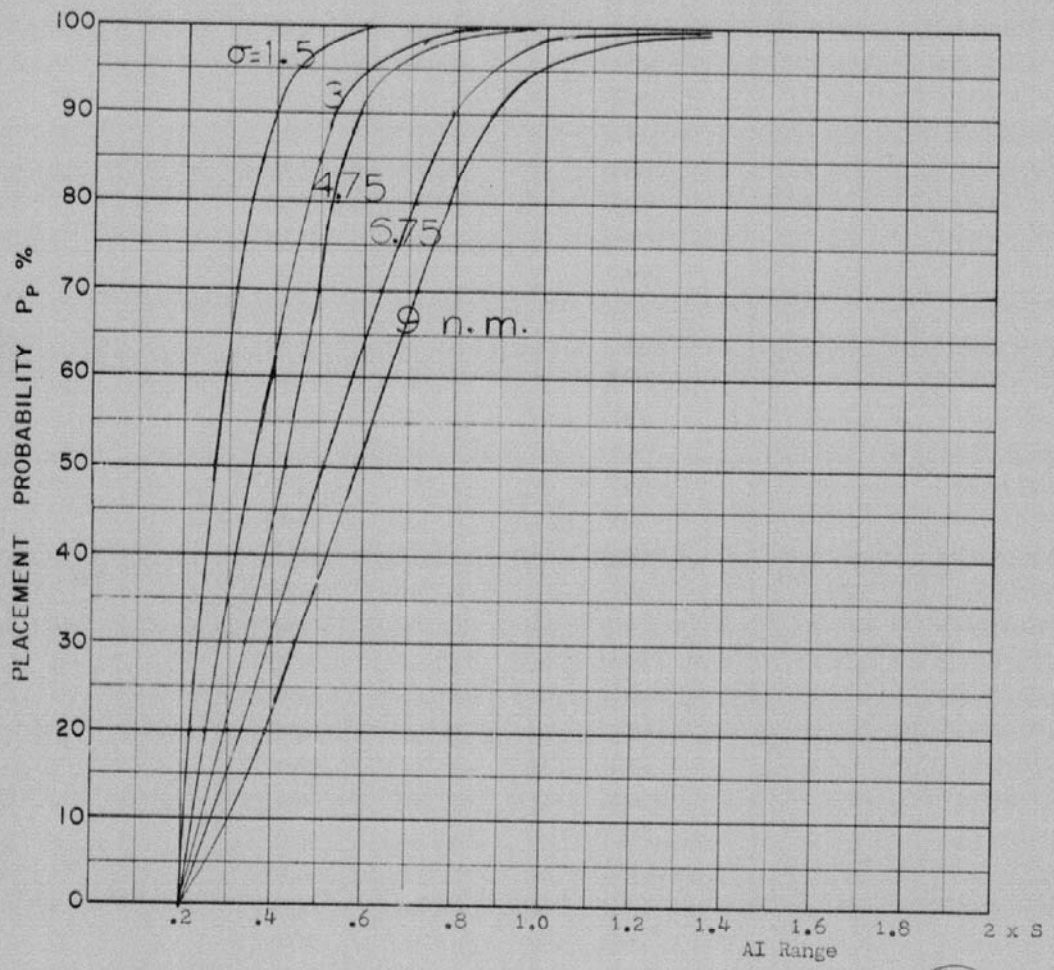

D.79

COURSE DIFFERENCE: 160°
TARGET EVASION: 0
TARGET MACH NO.: 2.0
INTERCEPTOR LATERAL G's: 1.6
INTERCEPTOR MACH NO.: 1.5
σ OF G.C.I. ACCURACY: Five values
A.I. DETECTION RANGE AS FRACTION OF SPECIFICATION RANGE, S: Abscissa
A.I. DETECTION RANGE CONTOUR: Delta
ALTITUDE: 50 K

Launch zone figure L-3, missile launched at short range with 5° heading error allowance.

25 a x d p r

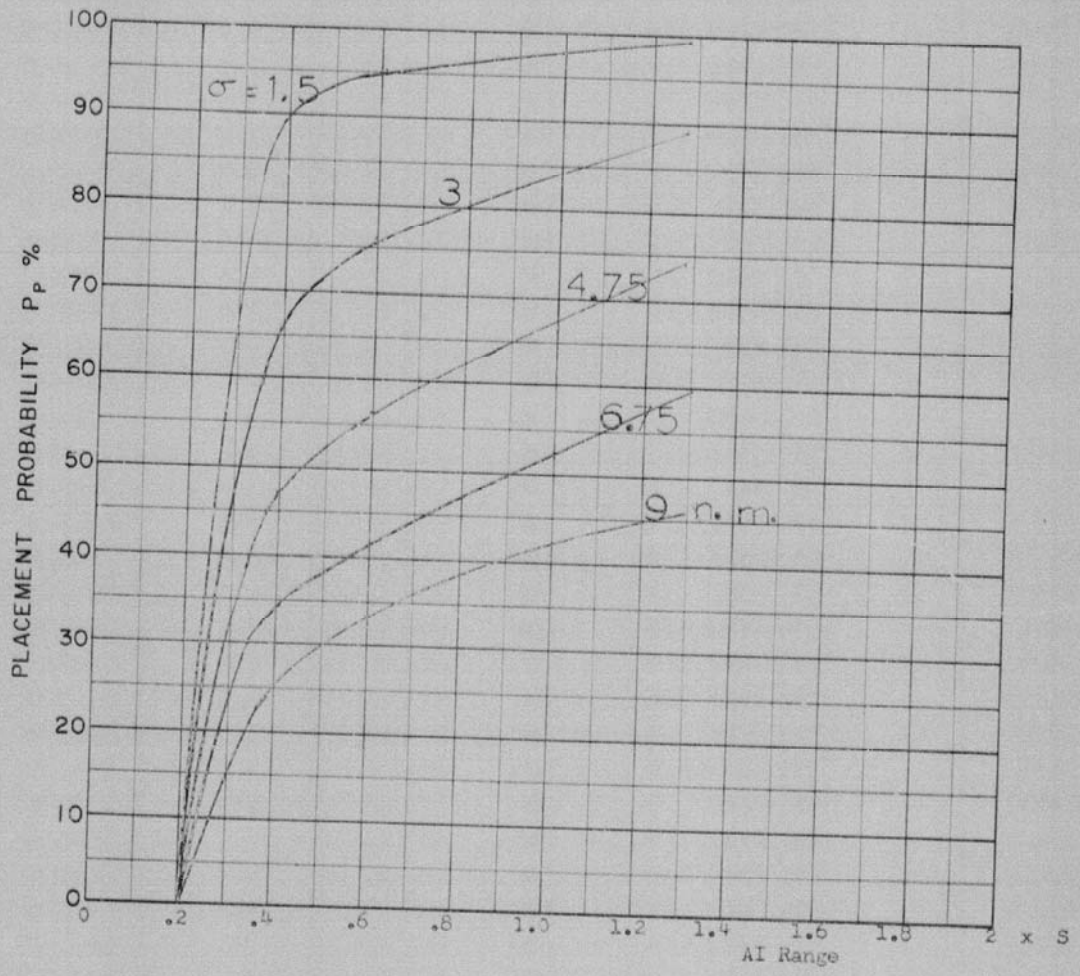

COURSE DIFFERENCE: 75°
TARGET EVASION: 0
TARGET MACH NO.: 2.0
INTERCEPTOR LATERAL G's: 3.0
INTERCEPTOR MACH NO.: 1.5
σ OF G.C.I. ACCURACY: Five values
A.I. DETECTION RANGE AS FRACTION OF SPECIFICATION RANGE, S: Abscissa
A.I. DETECTION RANGE CONTOUR: Delta
ALTITUDE: 50 K

D80a

Launch zone figure L-3, missile launched at maximum range with 10° heading error allowance.

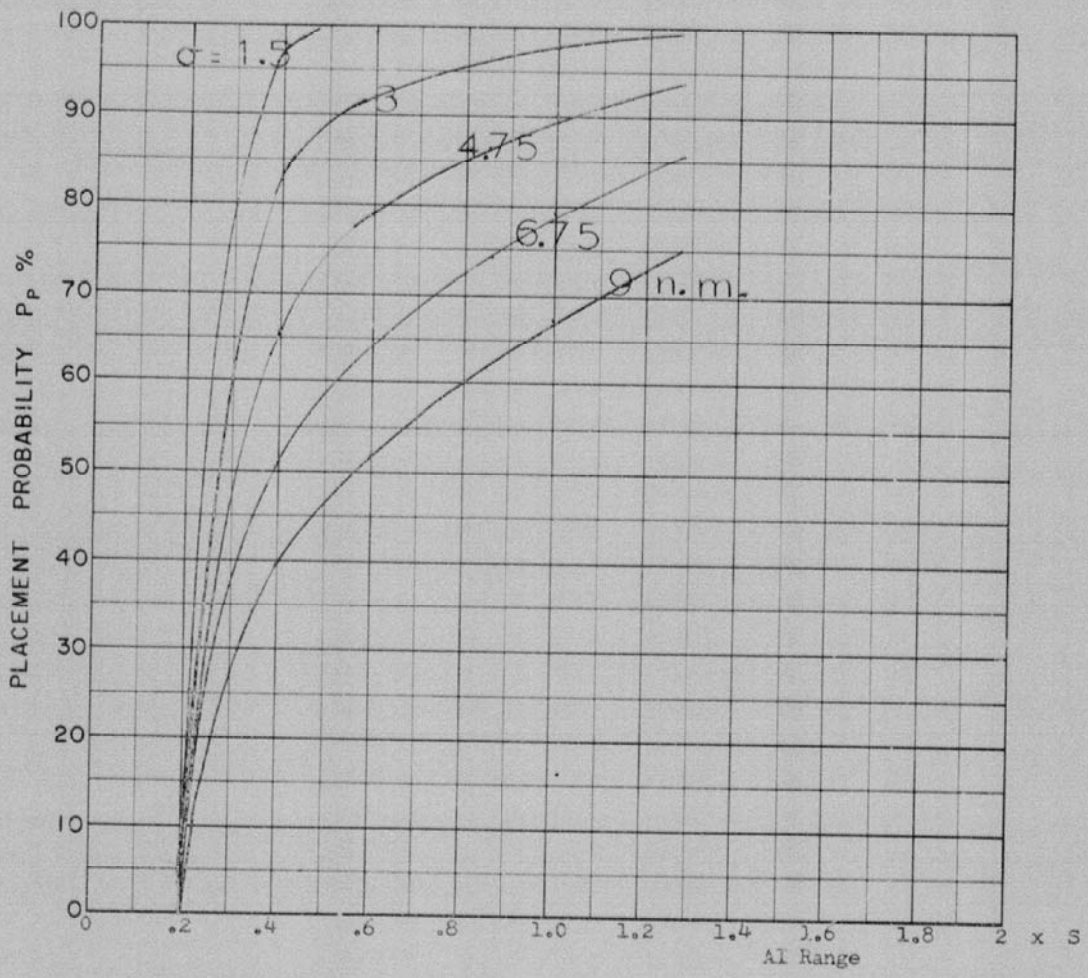

COURSE DIFFERENCE: 90°
TARGET EVASION: 0
TARGET MACH NO.: 2.0
INTERCEPTOR LATERAL G's: 3.0
INTERCEPTOR MACH NO.: 1.5
σ OF G.C.I. ACCURACY: Five values
A.I. DETECTION RANGE AS FRACTION OF SPECIFICATION RANGE, S: Abscissa
A.I. DETECTION RANGE CONTOUR: Delta
ALTITUDE: 50K

D80b

Launch zone figure L-3, missile launched at maximum range with 10° heading error allowance.

25 c x d p r

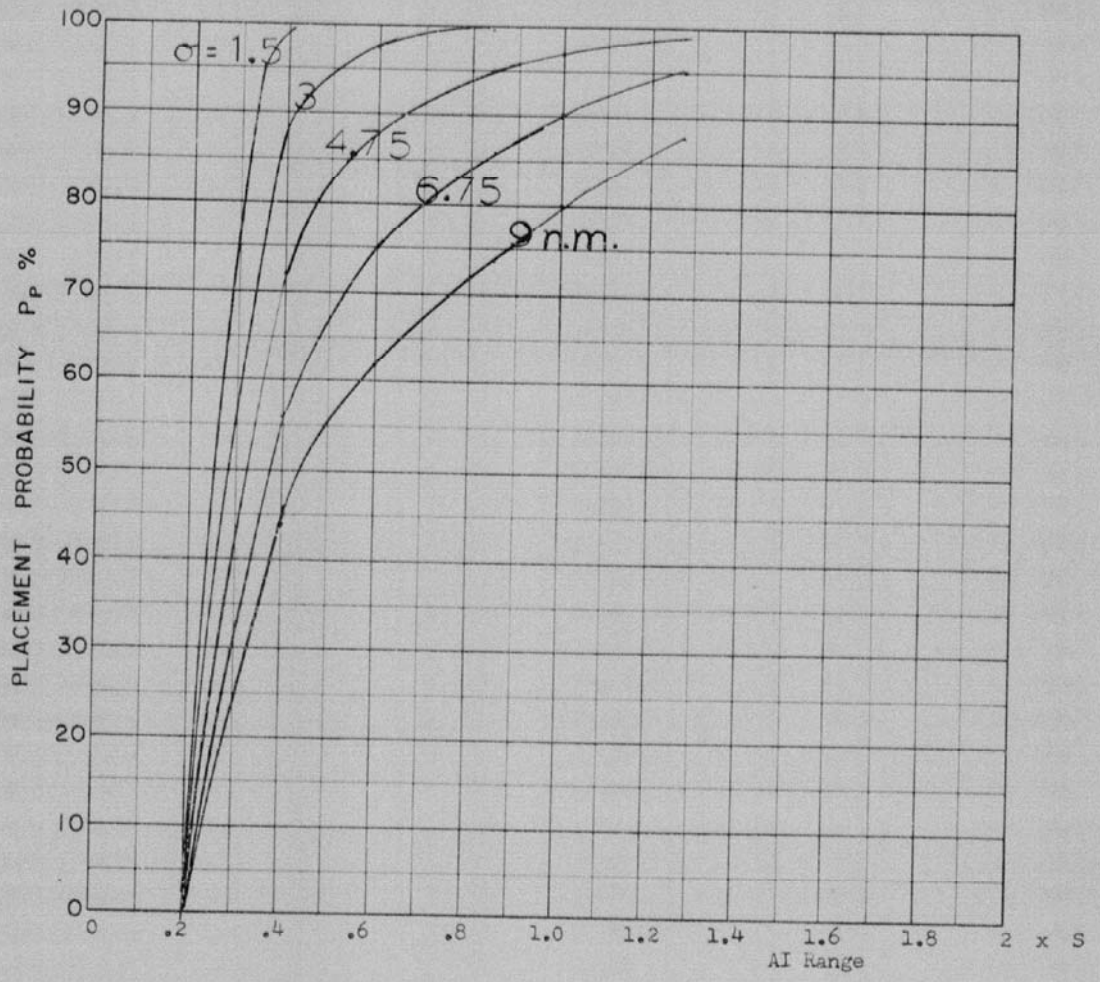

COURSE DIFFERENCE: 100°
TARGET EVASION: 0
TARGET MACH NO.: 2.0
INTERCEPTOR LATERAL G's: 3.0
INTERCEPTOR MACH NO.: 1.5
σ OF G.C.I. ACCURACY: Five values
A.I. DETECTION RANGE AS FRACTION OF SPECIFICATION RANGE, S: Abscissa
A.I. DETECTION RANGE CONTOUR: Delta
ALTITUDE: 50 K

D81

Launch zone figure L-3, missile launched at maximum range with 10° heading error allowance.

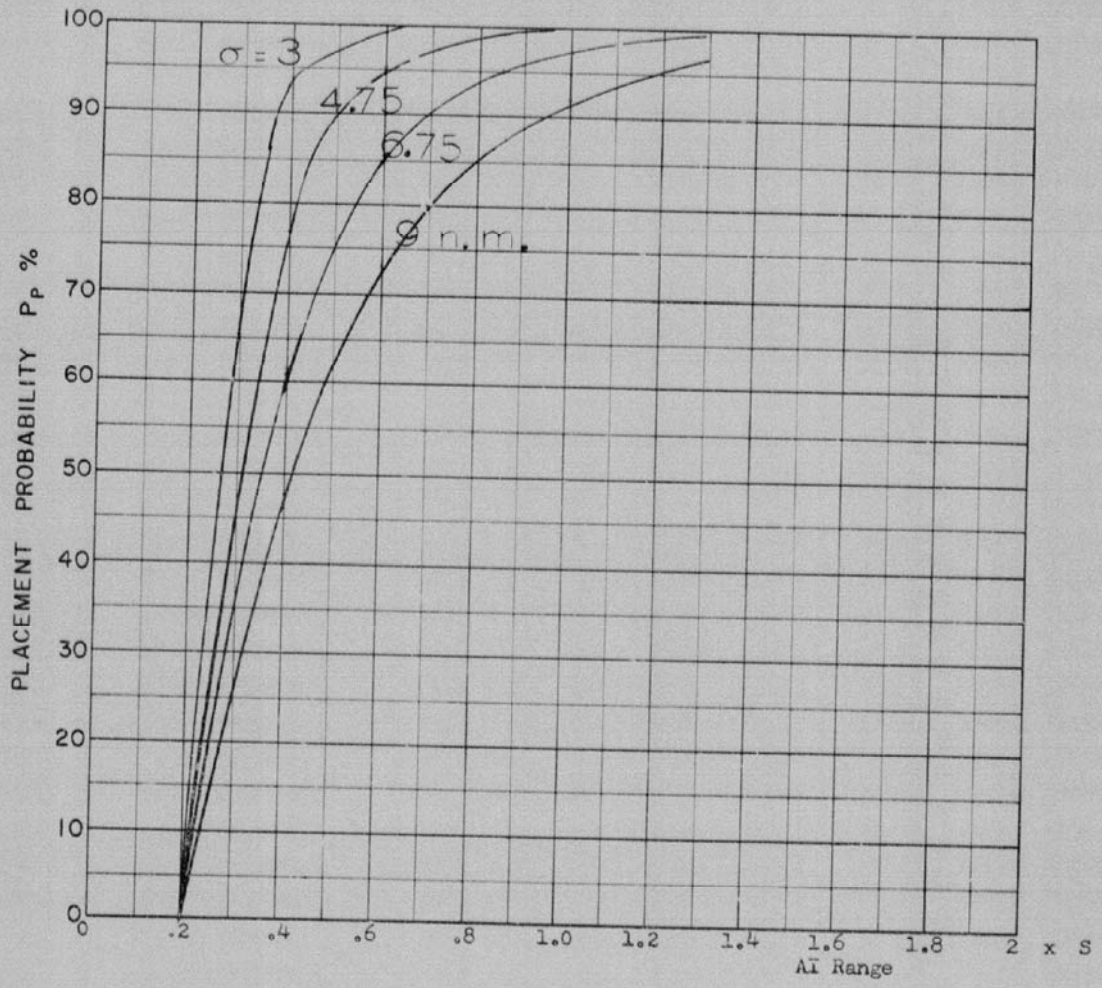

COURSE DIFFERENCE: 120°
TARGET EVASION: 0
TARGET MACH NO.: 2.0
INTERCEPTOR LATERAL G's: 3.0
INTERCEPTOR MACH NO.: 1.5
σ OF G.C.I. ACCURACY: Four values
A.I. DETECTION RANGE AS FRACTION OF SPECIFICATION RANGE, S: Abscissa
A.I. DETECTION RANGE CONTOUR: Delta
ALTITUDE: 50 K

D82

Launch zone figure L-3, missile launched at maximum range with 10° heading error allowance.

25 e x d p r

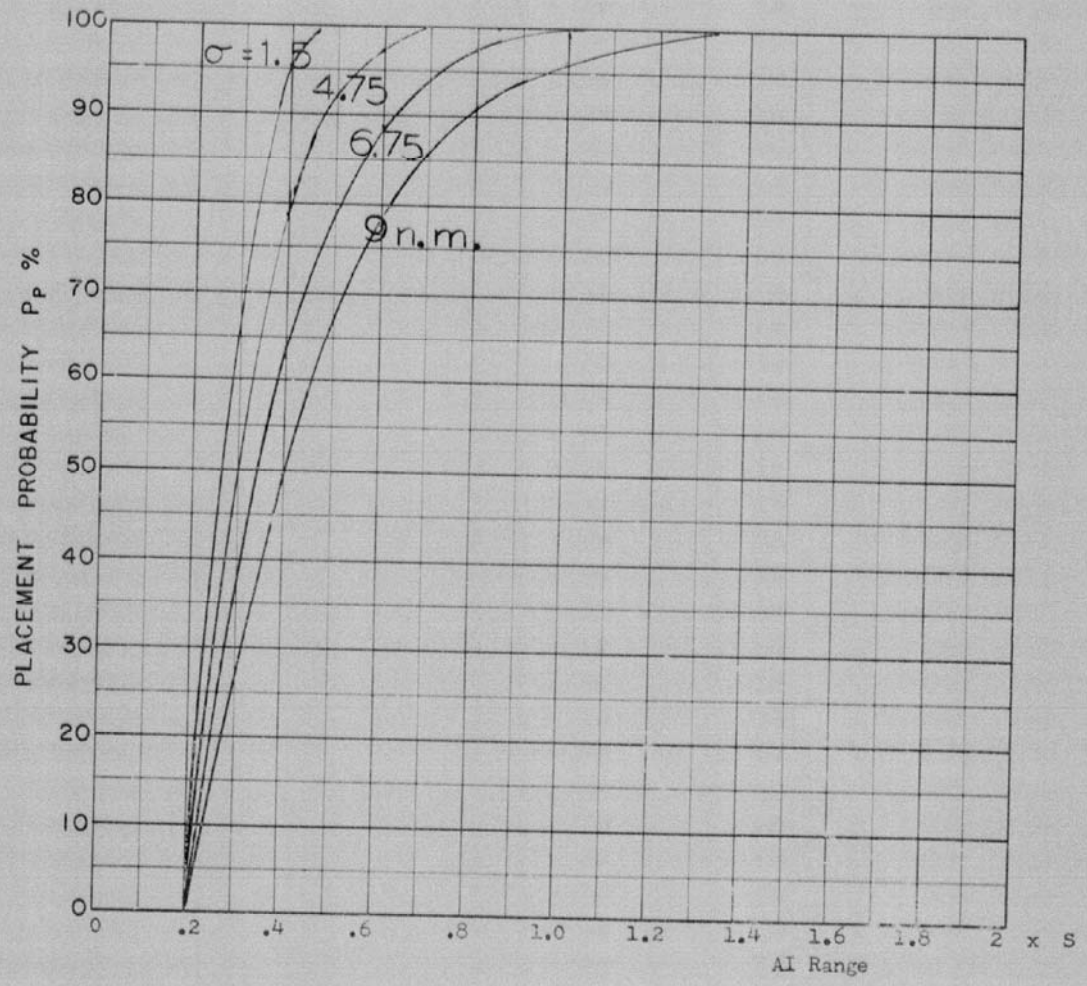

COURSE DIFFERENCE: 135°
TARGET EVASION: 0
TARGET MACH NO.: 2.0
INTERCEPTOR LATERAL G's: 3.0
INTERCEPTOR MACH NO.: 1.5
σ OF G.C.I. ACCURACY: Four values
A.I. DETECTION RANGE AS FRACTION OF SPECIFICATION RANGE, S: Abscissa
A.I. DETECTION RANGE CONTOUR: Delta
ALTITUDE: 50 K

D83

Launch zone figure L-3, missile launched at maximum range with 10° heading error allowance.

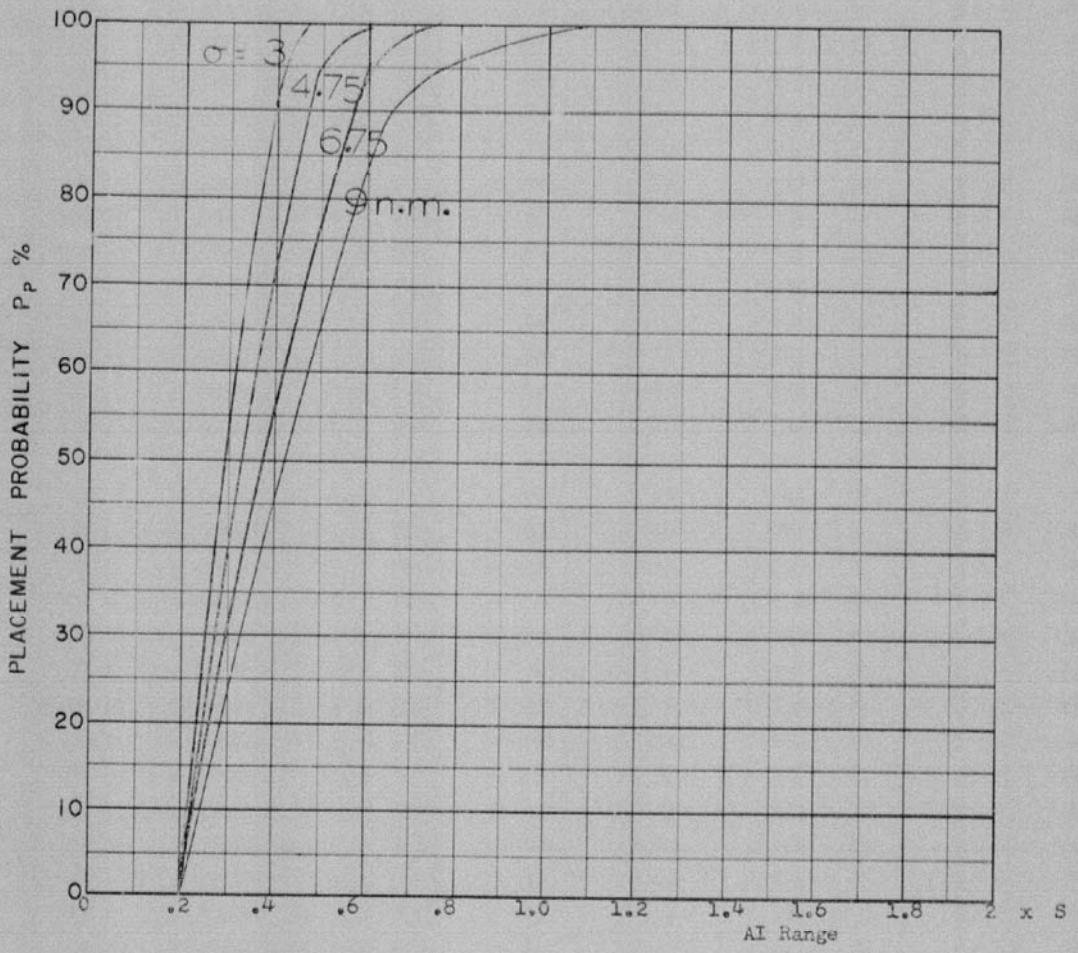

COURSE DIFFERENCE: 160°
TARGET EVASION: 0
TARGET MACH NO.: 2.0
INTERCEPTOR LATERAL G's: 3.0
INTERCEPTOR MACH NO.: 1.5
σ OF G.C.I. ACCURACY: Four values
A.I. DETECTION RANGE AS FRACTION OF SPECIFICATION RANGE, S: Abscissa
A.I. DETECTION RANGE CONTOUR: Delta
ALTITUDE: 50 K

D84

Launch zone figure L-3, missile launched at maximum range with 10° heading error allowance.

30 a x d p r

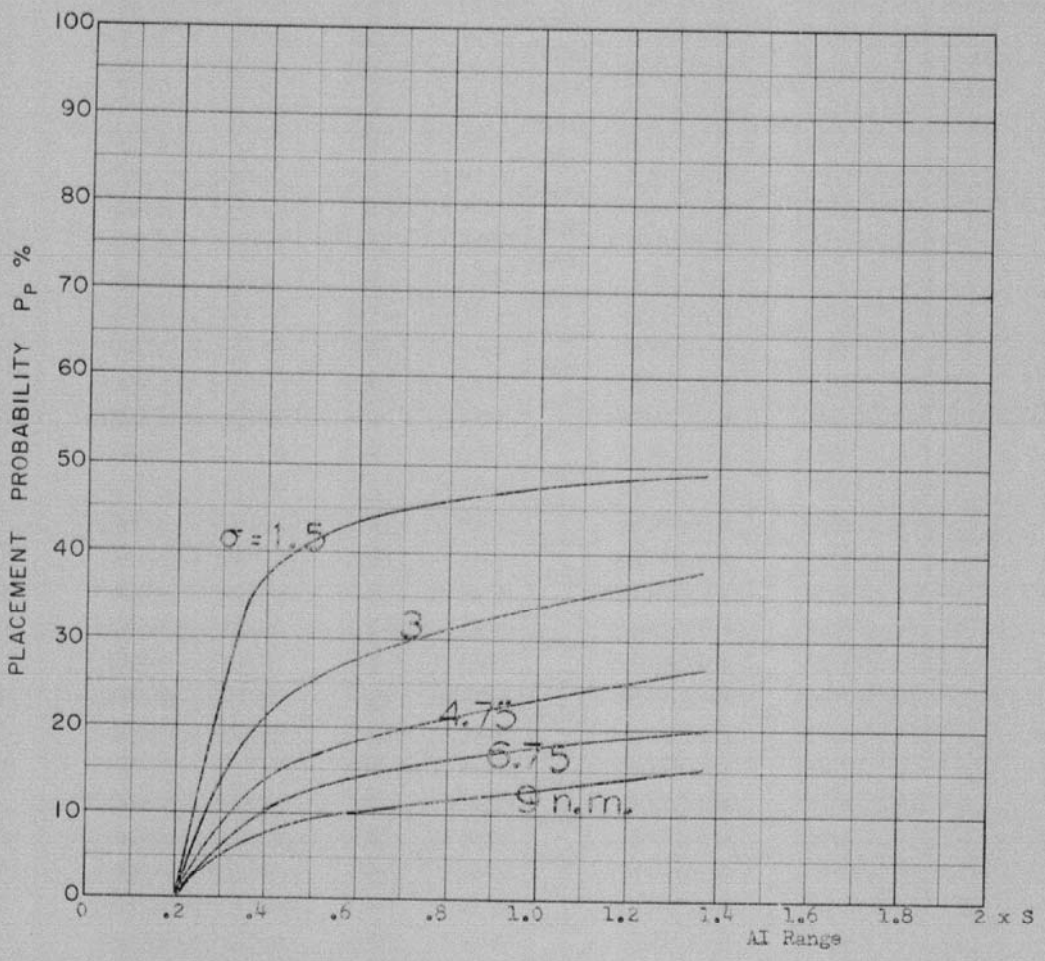

COURSE DIFFERENCE: 75°
TARGET EVASION: 0
TARGET MACH NO.: 2.0
INTERCEPTOR LATERAL G's: 1.6
INTERCEPTOR MACH NO.: 1.5
σ OF G.C.I. ACCURACY: Five values
A.I. DETECTION RANGE AS FRACTION OF SPECIFICATION RANGE, S Abscissa
A.I. DETECTION RANGE CONTOUR: Delta
ALTITUDE: 50 K

D85

Launch zone L-4, missile launched at long range with 10° heading error allowance.

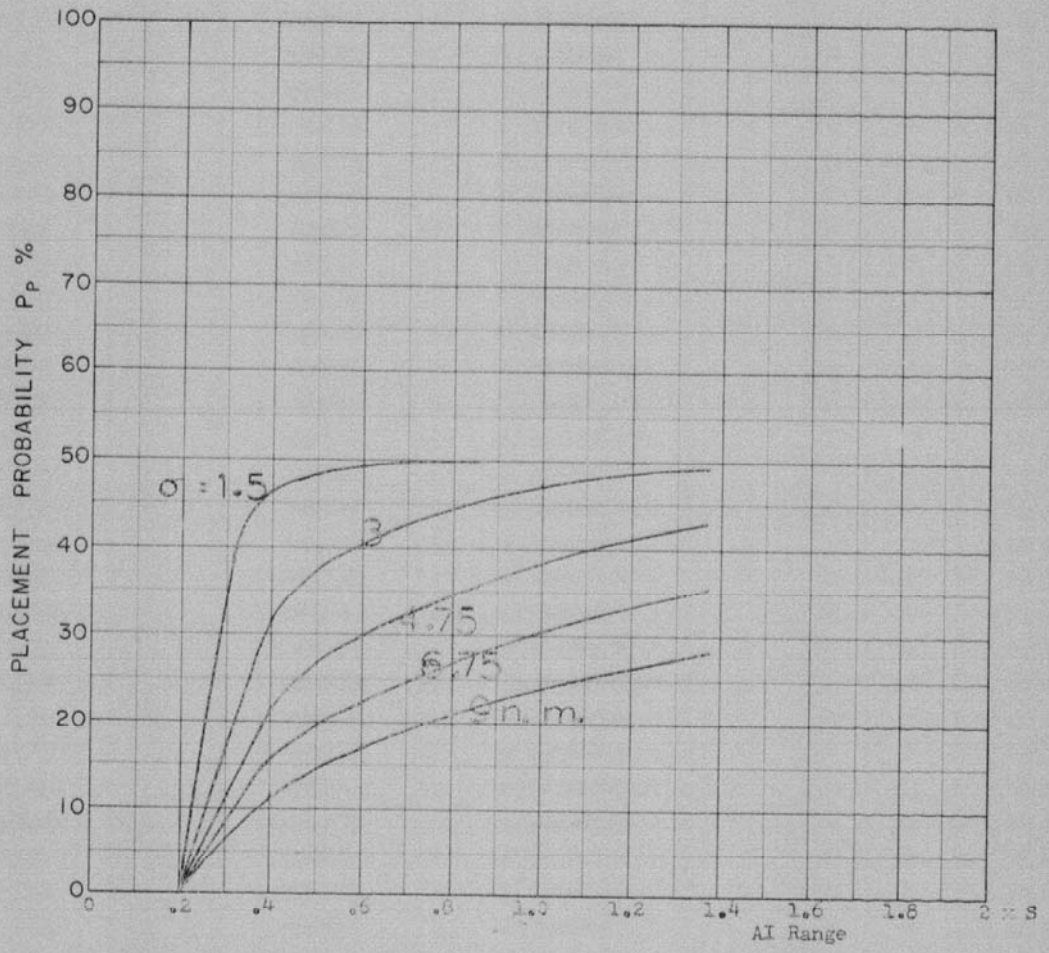

COURSE DIFFERENCE: 90°
TARGET EVASION: 0
TARGET MACH NO.: 2.0
INTERCEPTOR LATERAL G's: 1.6
INTERCEPTOR MACH NO.: 1.5
σ OF G.C.I. ACCURACY: Five values
A.I. DETECTION RANGE AS FRACTION OF SPECIFICATION RANGE, S Abscissa
A.I. DETECTION RANGE CONTOUR: Delta
ALTITUDE: 50 K

(D86)

Launch zone L4, missile launched at long range with 10° heading error allowance.

30 c x d p r

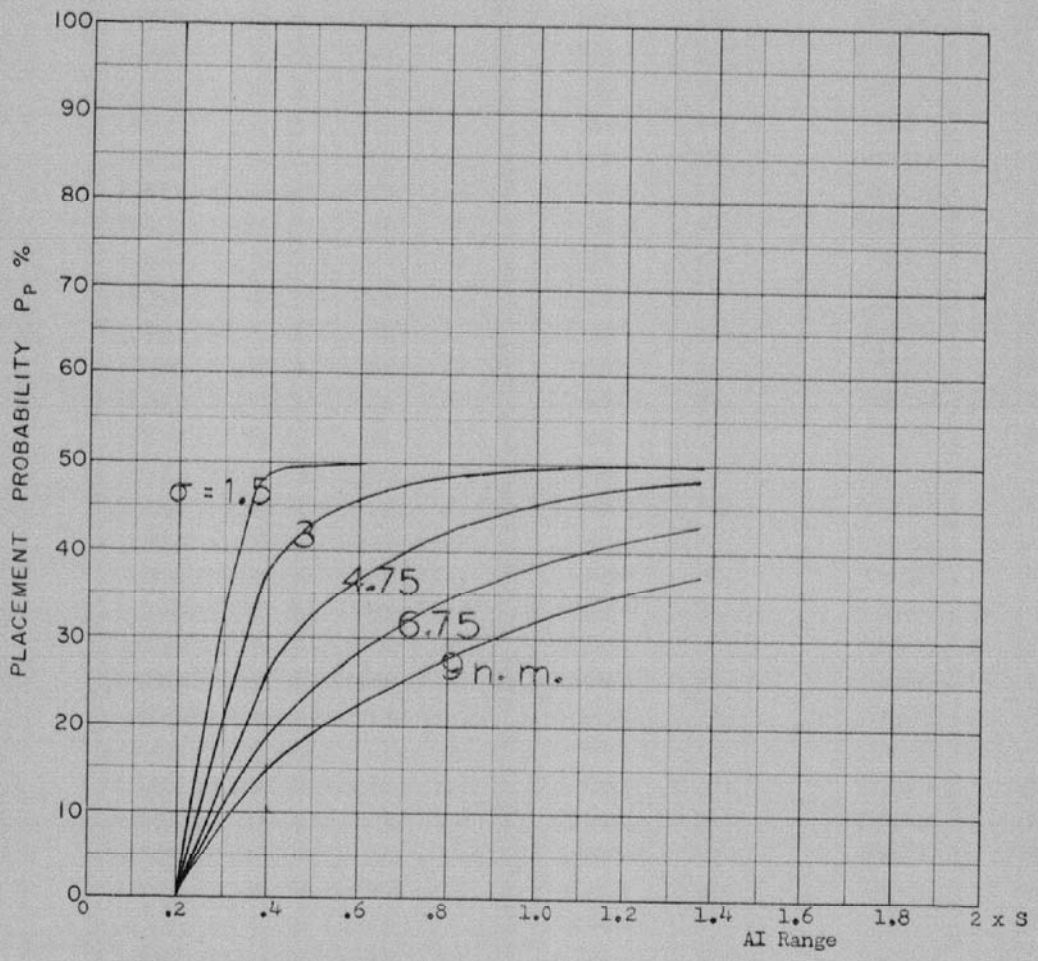

COURSE DIFFERENCE: 100°
TARGET EVASION: 0
TARGET MACH NO.: 2.0
INTERCEPTOR LATERAL G's: 1.6
INTERCEPTOR MACH NO.: 1.5
σ OF G.C.I. ACCURACY: Five values
A.I. DETECTION RANGE AS FRACTION OF SPECIFICATION RANGE, S: Abscissa
A.I. DETECTION RANGE CONTOUR: Delta
ALTITUDE: 50 K

D87

Launch zone L_8^4, missile launched at long range with 10° heading error allowance.

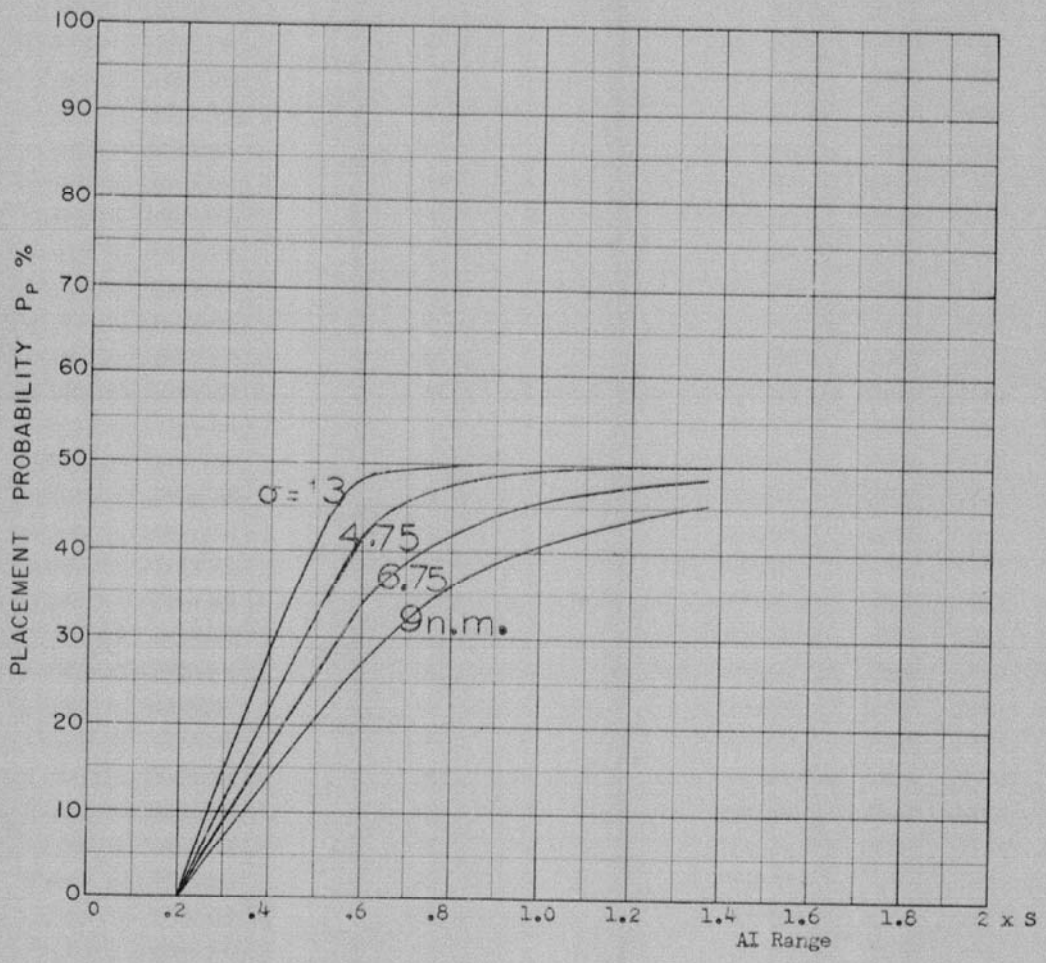

COURSE DIFFERENCE: 120°
TARGET EVASION: 0
TARGET MACH NO.: 2.0
INTERCEPTOR LATERAL G's: 1.6
INTERCEPTOR MACH NO.: 1.5
σ OF G.C.I. ACCURACY: Four values
A.I. DETECTION RANGE AS FRACTION OF SPECIFICATION RANGE, S Abscissa
A.I. DETECTION RANGE CONTOUR: Delta
ALTITUDE: 50 K

D88

Launch zone L-4, missile launched at long range with 10° heading error allowance.

30 e x d p r

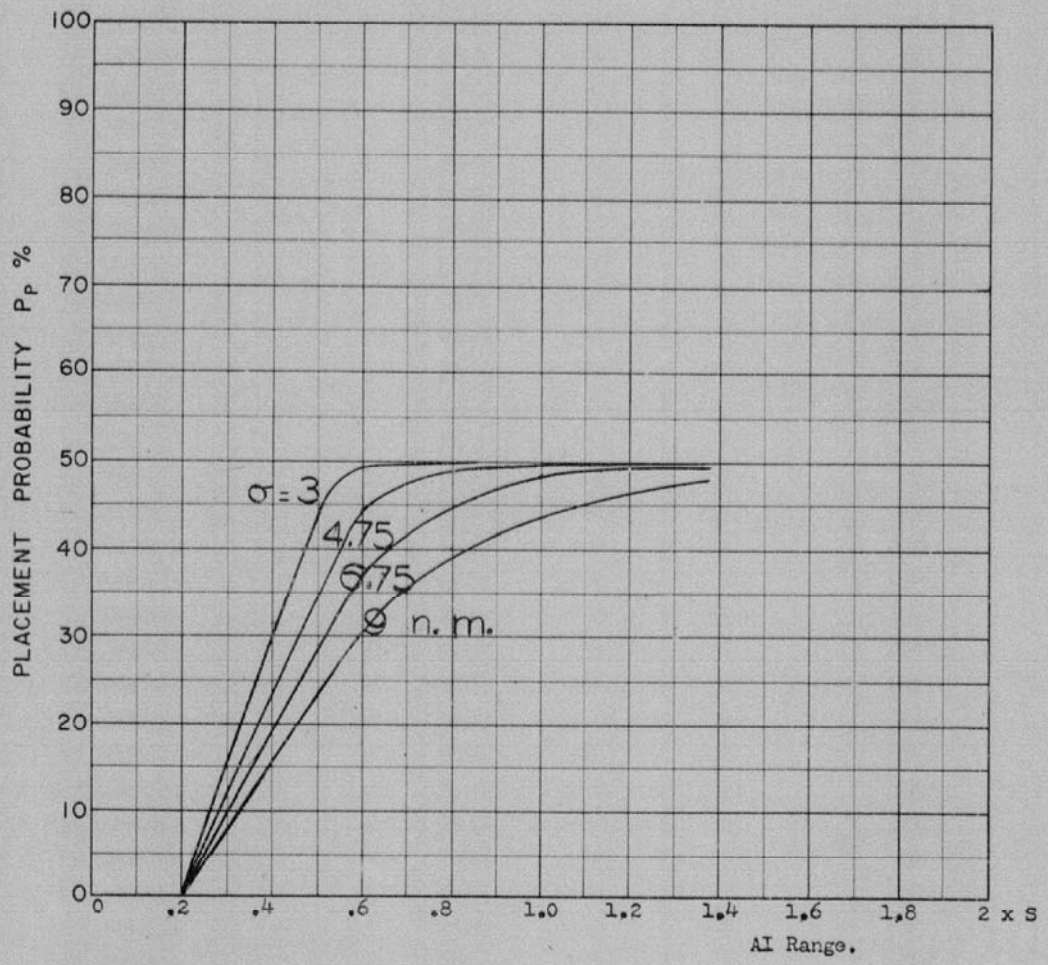

COURSE DIFFERENCE: 135°
TARGET EVASION: 0
TARGET MACH NO.: 2.0
INTERCEPTOR LATERAL G's: 1.6
INTERCEPTOR MACH NO.: 1.5
σ OF G.C.I. ACCURACY: Four values
A.I. DETECTION RANGE AS FRACTION OF SPECIFICATION RANGE, S: Abscissa
A.I. DETECTION RANGE CONTOUR: Delta
ALTITUDE: 50 K

D89

Launch zone L-4, missile launched at long range with 10° heading error allowance.

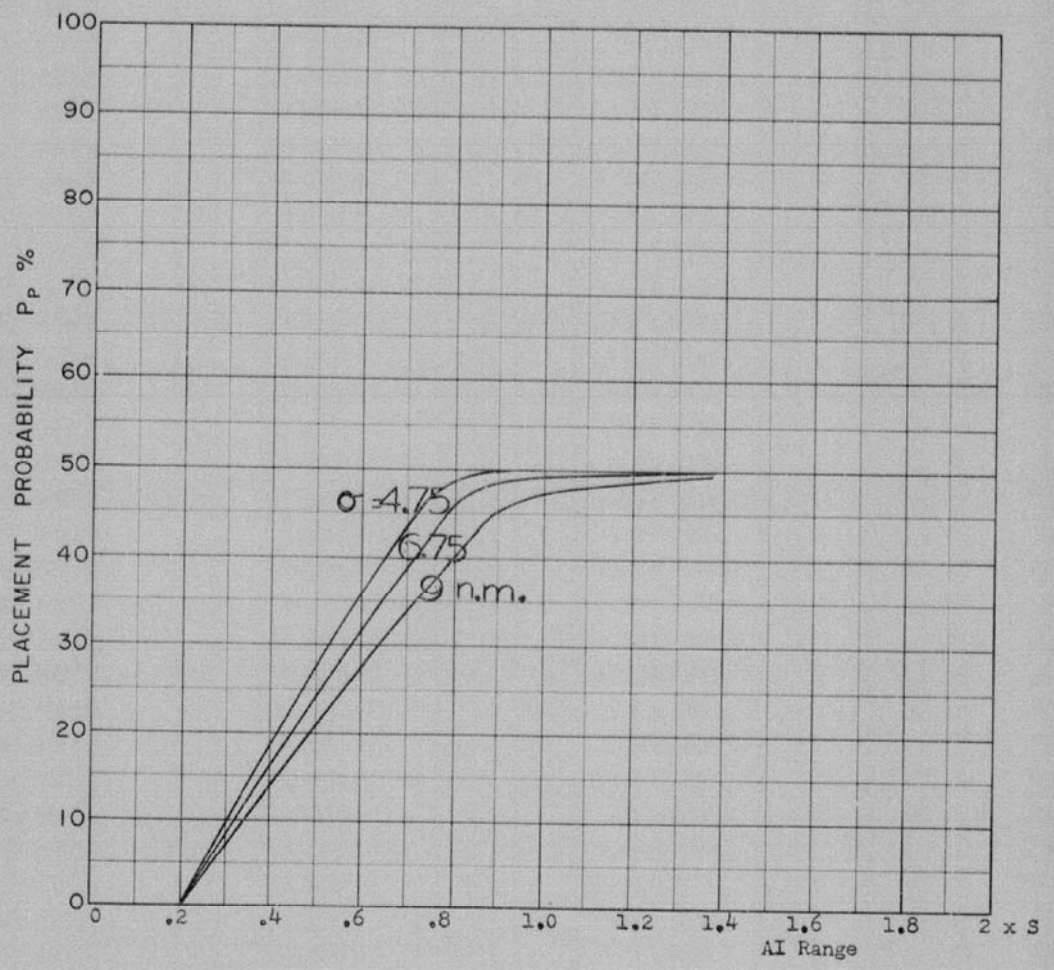

COURSE DIFFERENCE: 160°
TARGET EVASION: 0
TARGET MACH NO.: 2.0
INTERCEPTOR LATERAL G's: 1.6
INTERCEPTOR MACH NO.: 1.5
σ OF G.C.I. ACCURACY: Three values
A.I. DETECTION RANGE AS FRACTION OF SPECIFICATION RANGE, S: Abscissa
A.I. DETECTION RANGE CONTOUR: Delta
ALTITUDE: 50 K

D90

Launch zone L4, missile launched at long range with 10° heading error allowance.

110 dpr

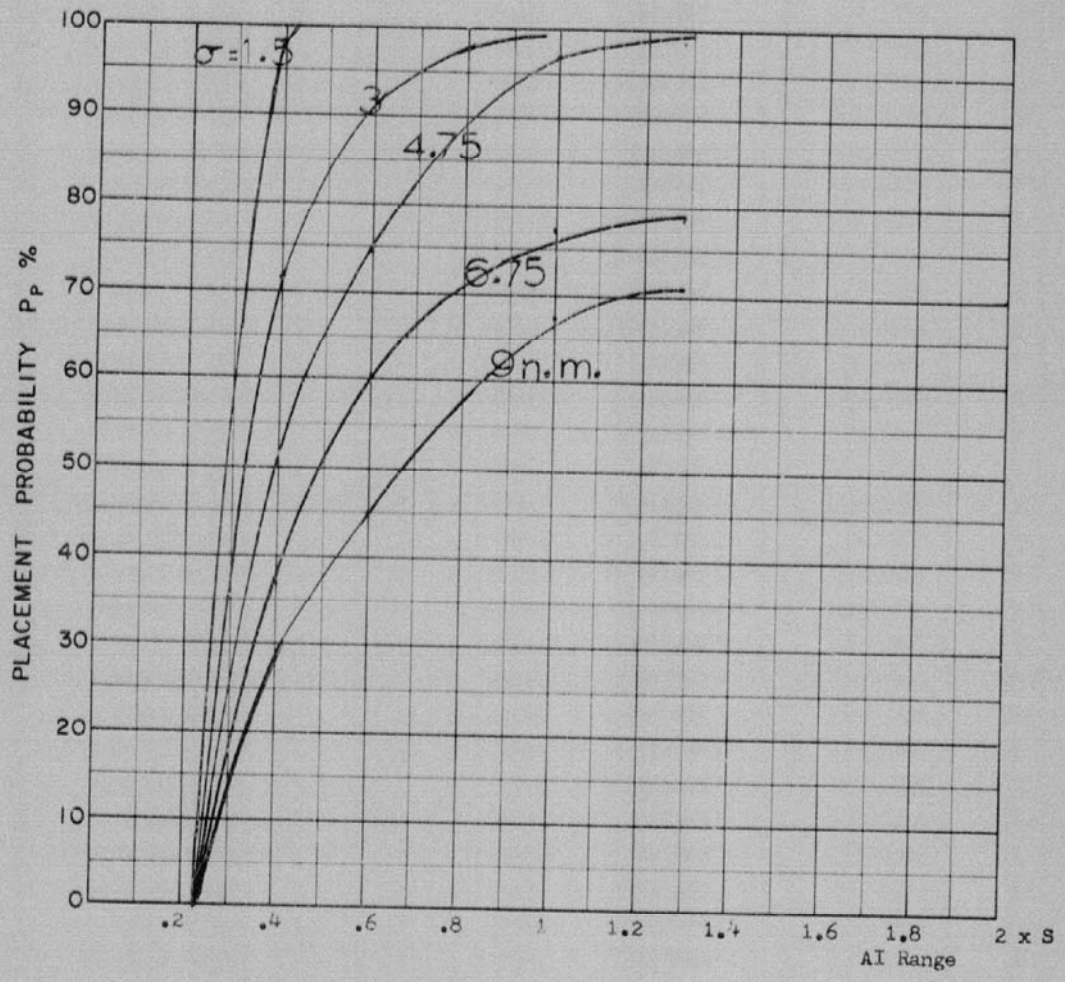

COURSE DIFFERENCE: 110°
TARGET EVASION: 0.1 lateral g's
TARGET MACH NO.: 2.0
INTERCEPTOR LATERAL G's: 1.6
INTERCEPTOR MACH NO.: 1.5
σ OF G.C.I. ACCURACY: 5 values
A.I. DETECTION RANGE AS FRACTION OF SPECIFICATION RANGE, S: Abscissa
A.I. DETECTION RANGE CONTOUR: Delta
ALTITUDE: 50 K

Missile launch zone L-10

D91a

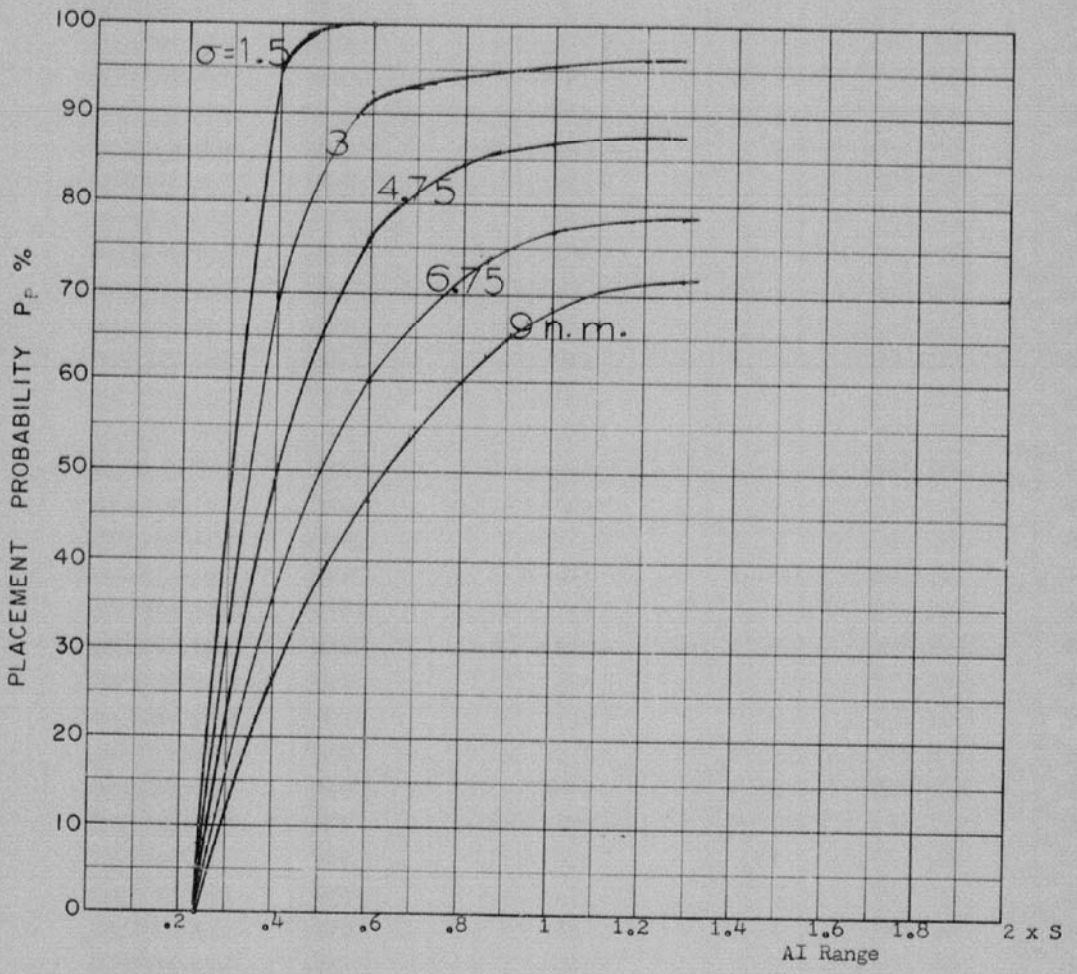

COURSE DIFFERENCE: 110°
TARGET EVASION: 0.1 lateral g's towards interceptor only
TARGET MACH NO.: 2.0
INTERCEPTOR LATERAL G's: 1.6
INTERCEPTOR MACH NO.: 1.5
σ OF G.C.I. ACCURACY: 5 values
A.I. DETECTION RANGE AS FRACTION OF SPECIFICATION RANGE, S: Abscissa
A.I. DETECTION RANGE CONTOUR: Delta
ALTITUDE: 50 K

D916

Missile launch zone L-10

104 dpr

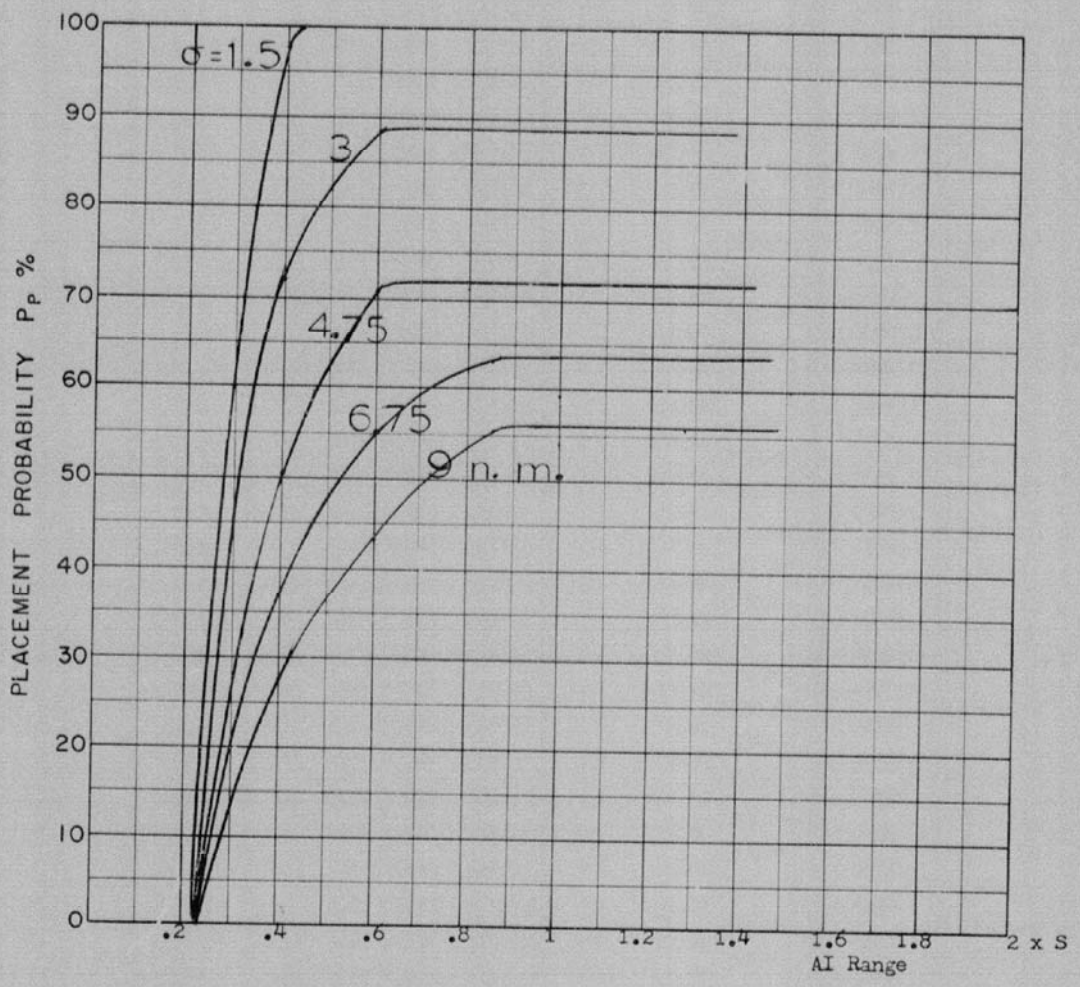

COURSE DIFFERENCE: 110°
TARGET EVASION: 0.2 lateral g's, towards interceptor only
TARGET MACH NO.: 2.0
INTERCEPTOR LATERAL G's: 1.6
INTERCEPTOR MACH NO.: 1.5
σ OF G.C.I. ACCURACY: 5 values
A.I. DETECTION RANGE AS FRACTION OF SPECIFICATION RANGE, S: Abscissa
A.I. DETECTION RANGE CONTOUR: Delta
ALTITUDE: 50 K

D92

Missile launch zone L-10

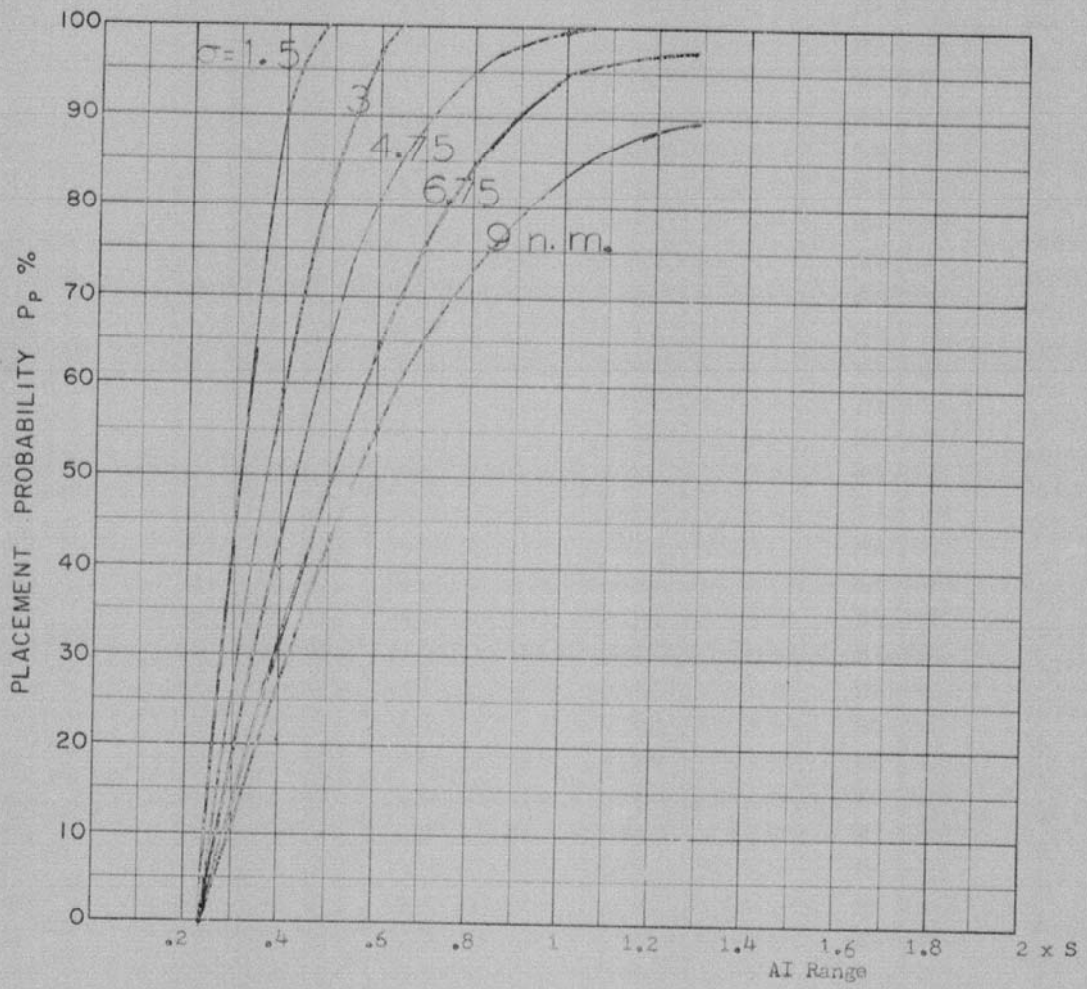

COURSE DIFFERENCE: 135°
TARGET EVASION: 0.1 lateral g's
TARGET MACH NO.: 2.0
INTERCEPTOR LATERAL G's: 1.6
INTERCEPTOR MACH NO.: 1.5
σ OF G.C.I. ACCURACY: 5 values
A.I. DETECTION RANGE AS FRACTION OF SPECIFICATION RANGE, S: Abscissa
A.I. DETECTION RANGE CONTOUR: Delta
ALTITUDE: 50 K

Missile launch zone L.10

D93

114 dpr

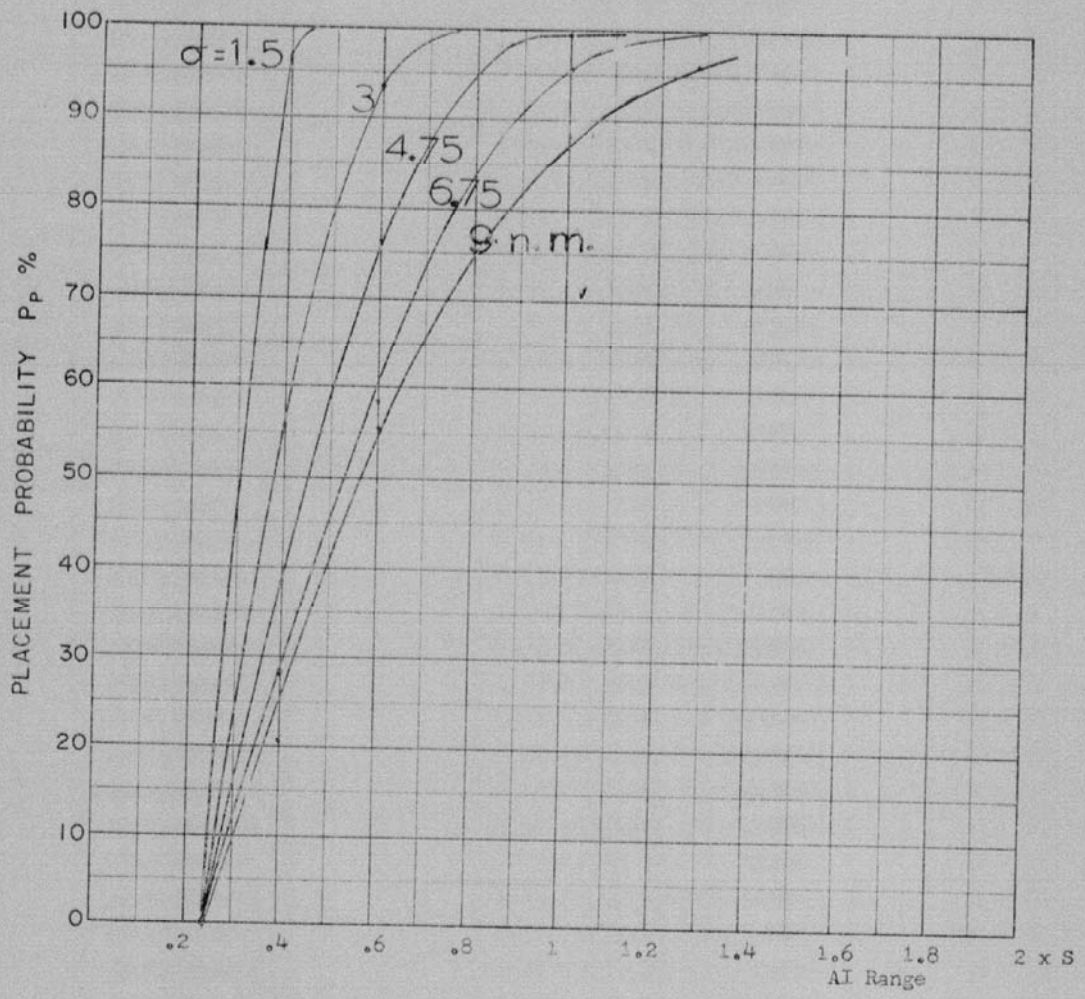

COURSE DIFFERENCE: 160°
TARGET EVASION: 0.1 lateral g's
TARGET MACH NO.: 2.0
INTERCEPTOR LATERAL G's: 1.6
INTERCEPTOR MACH NO.: 1.5
σ OF G.C.I. ACCURACY: 5 values
A.I. DETECTION RANGE AS FRACTION OF SPECIFICATION RANGE, S: Abscissa
A.I. DETECTION RANGE CONTOUR: Delta
ALTITUDE: 50 K

D94a

Missile launch zone L-10

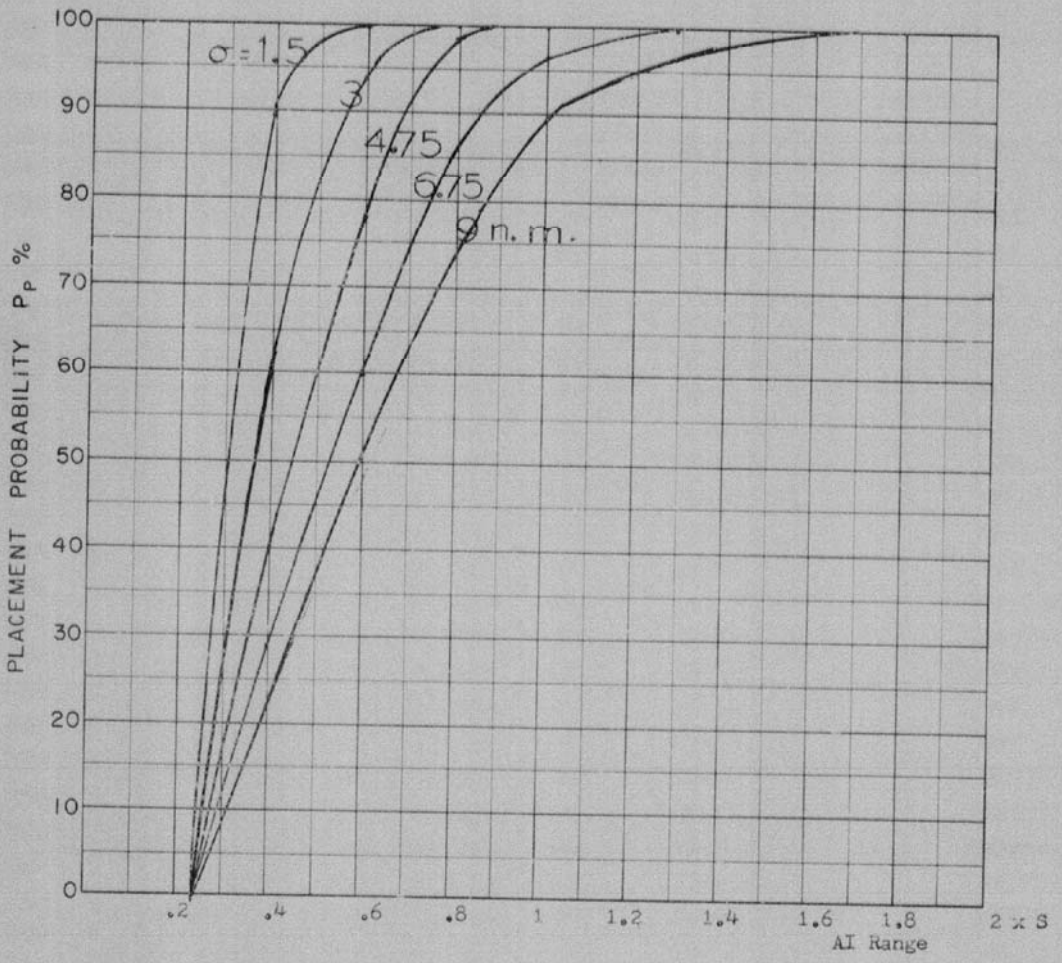

COURSE DIFFERENCE: 160°
TARGET EVASION: 0.1 lateral g's, towards interceptor only
TARGET MACH NO.: 2.0
INTERCEPTOR LATERAL G's: 1.6
INTERCEPTOR MACH NO.: 1.5
σ OF G.C.I. ACCURACY: 5 values
A.I. DETECTION RANGE AS FRACTION OF SPECIFICATION RANGE, S: Abscissa
A.I. DETECTION RANGE CONTOUR: Delta
ALTITUDE: 50 K

D94b

Missile launch zone L-10

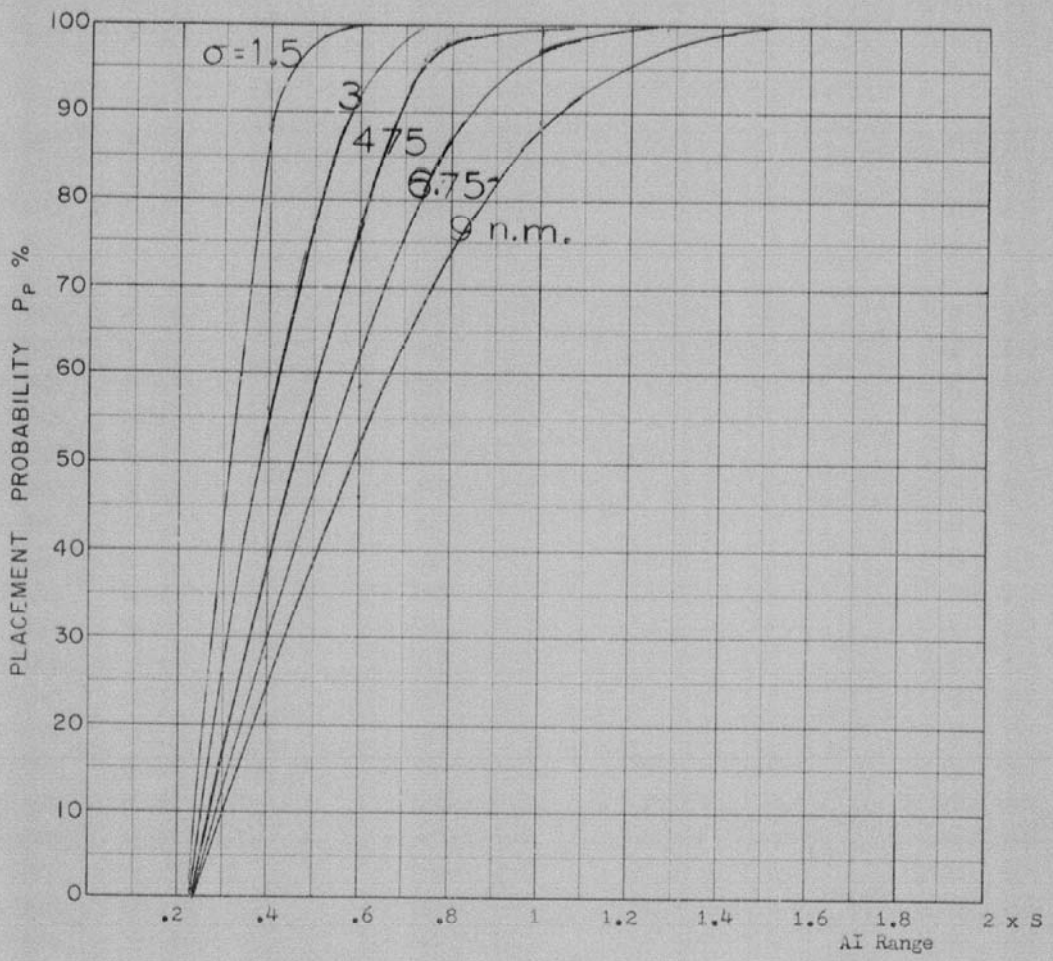

COURSE DIFFERENCE: 180°
TARGET EVASION: 0.1 lateral g's
TARGET MACH NO.: 2.0
INTERCEPTOR LATERAL G's: 1.6
INTERCEPTOR MACH NO.: 1.5
σ OF G.C.I. ACCURACY: 5 values
A.I. DETECTION RANGE AS FRACTION OF SPECIFICATION RANGE, S: Abscissa
A.I. DETECTION RANGE CONTOUR: Delta
ALTITUDE: 50 K

Missile launch zone L-10

D95

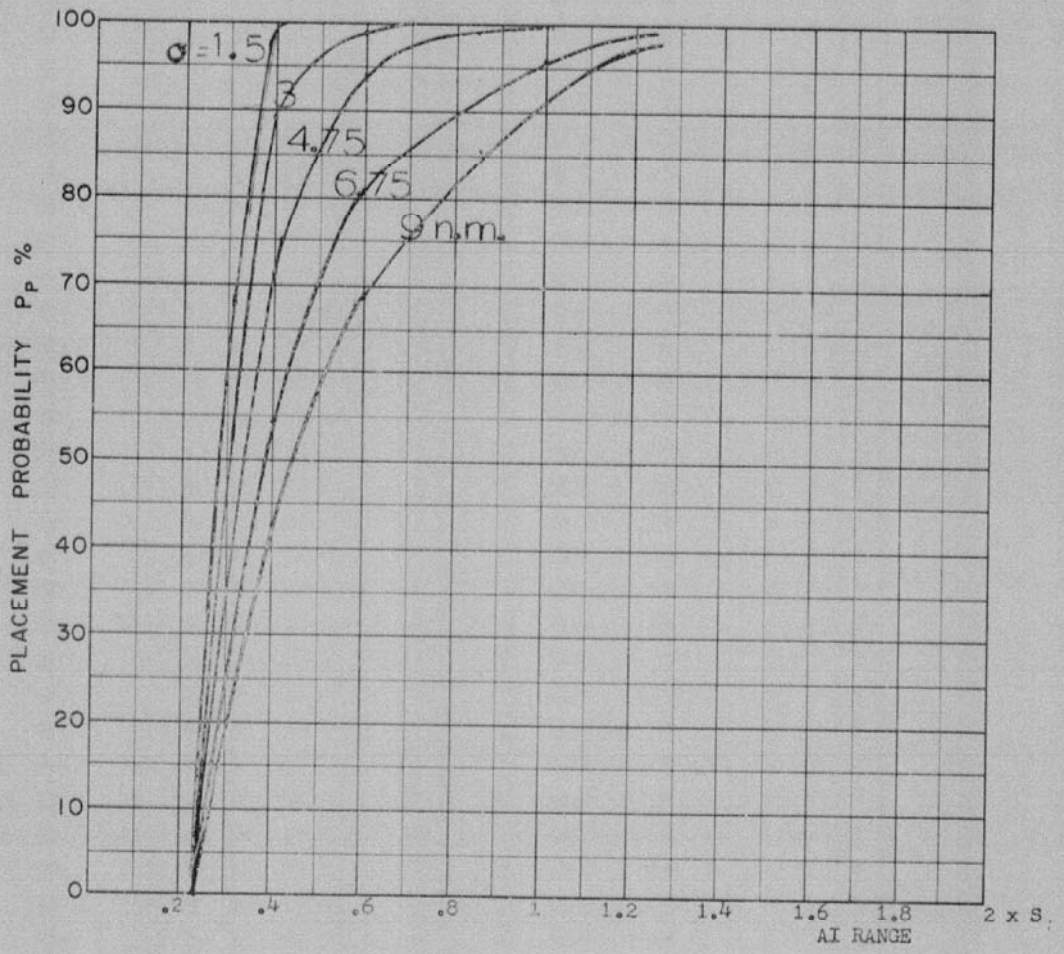

COURSE DIFFERENCE: 135°
TARGET EVASION: 0.1 lateral g's
TARGET MACH NO.: 2.0
INTERCEPTOR LATERAL G's: 3.0
INTERCEPTOR MACH NO.: 1.5
σ OF G.C.I. ACCURACY: 5 values
A.I. DETECTION RANGE AS FRACTION OF SPECIFICATION RANGE, S: Abscissa
A.I. DETECTION RANGE CONTOUR: Delta
ALTITUDE: 50 K

D97a

Missile launch zone L-10
AI Look angle 75°

107 dpr

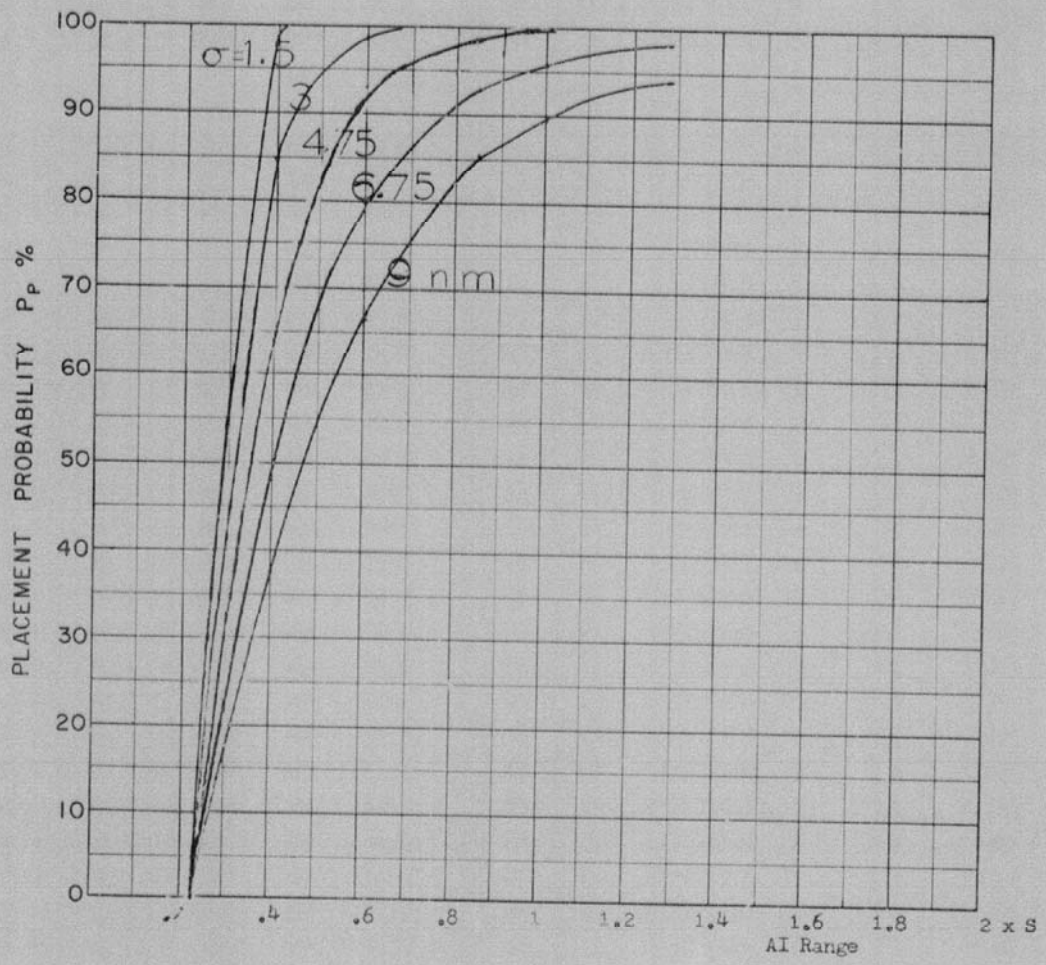

COURSE DIFFERENCE: 135°
TARGET EVASION: 0.1 lateral g's
TARGET MACH NO.: 2.0
INTERCEPTOR LATERAL G's: 3.0
INTERCEPTOR MACH NO.: 1.5
σ OF G.C.I. ACCURACY: 5 values
A.I. DETECTION RANGE AS FRACTION OF SPECIFICATION RANGE, S: Abscissa
A.I. DETECTION RANGE CONTOUR: Delta
ALTITUDE: 50 K

Missile launch zone L-10

D976

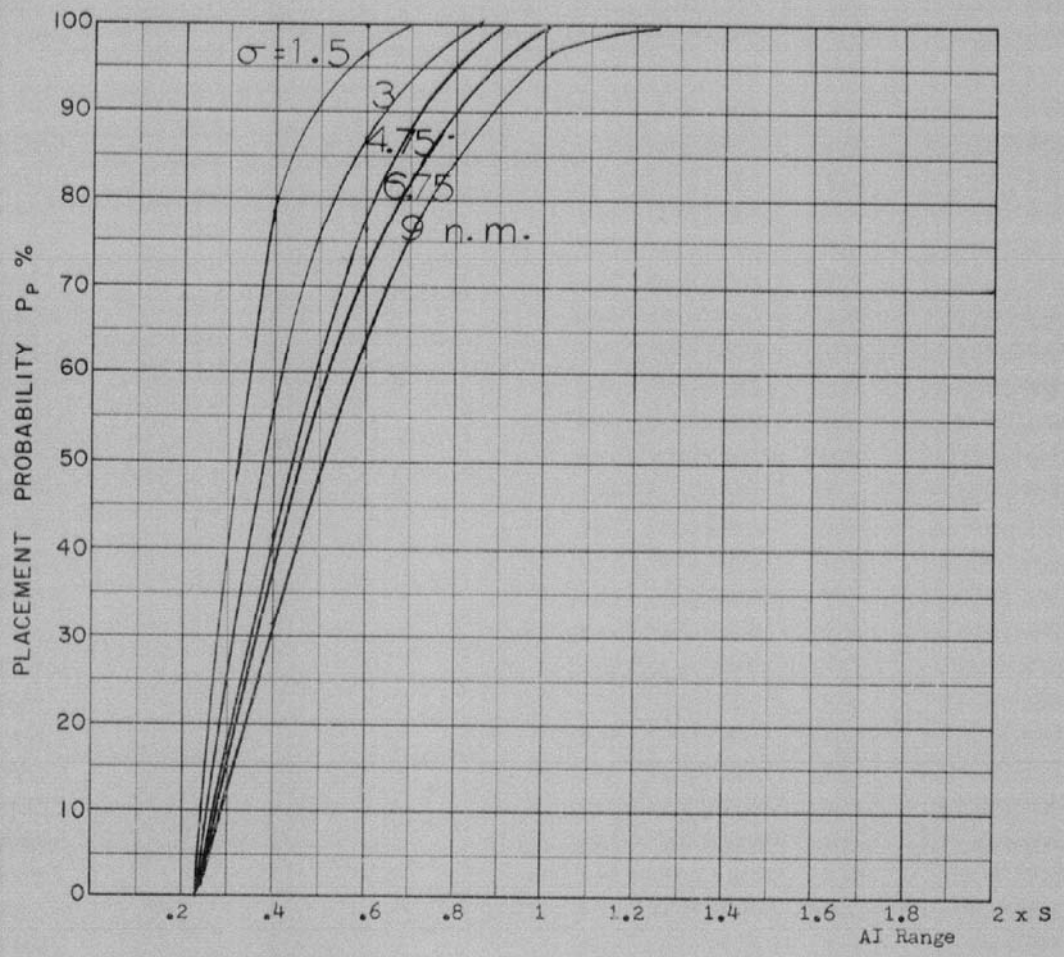

COURSE DIFFERENCE: 160°
TARGET EVASION: 0.1 g's
TARGET MACH NO.: 2.0
INTERCEPTOR LATERAL G's: 3.0
INTERCEPTOR MACH NO.: 1.5
σ OF G.C.I. ACCURACY: 5 values
A.I. DETECTION RANGE AS FRACTION OF SPECIFICATION RANGE, S: Abscissa
A.I. DETECTION RANGE CONTOUR: Delta
ALTITUDE: 50 K

Missile launch zone L-10

D98a

101 adpr

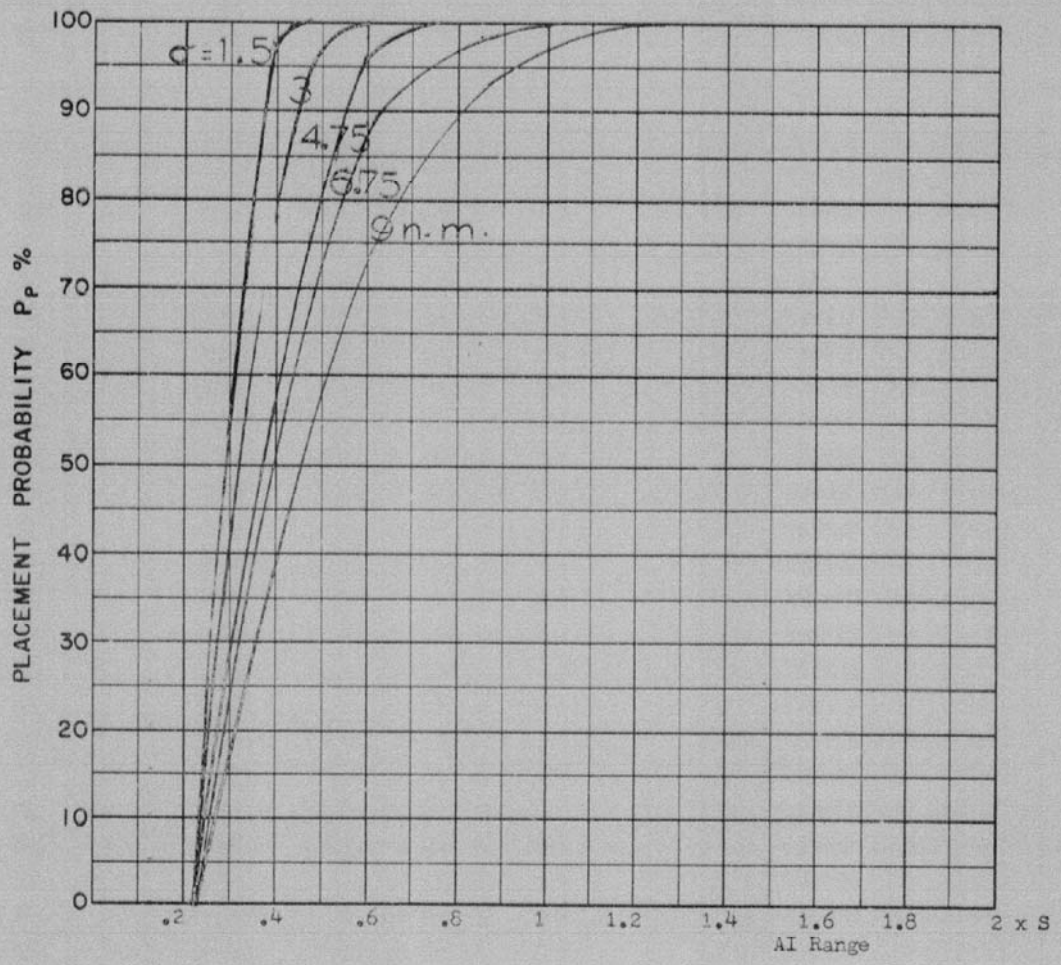

COURSE DIFFERENCE: 160°
TARGET EVASION: 0.1 lateral gs, towards interceptor only
TARGET MACH NO.: 2.0
INTERCEPTOR LATERAL G's: 3.0
INTERCEPTOR MACH NO.: 1.5
σ OF G.C.I. ACCURACY: 5 values
A.I. DETECTION RANGE AS FRACTION OF SPECIFICATION RANGE, S: Abscissa
A.I. DETECTION RANGE CONTOUR: Delta
ALTITUDE: 50 K

D98b

Missile launch zone L-10

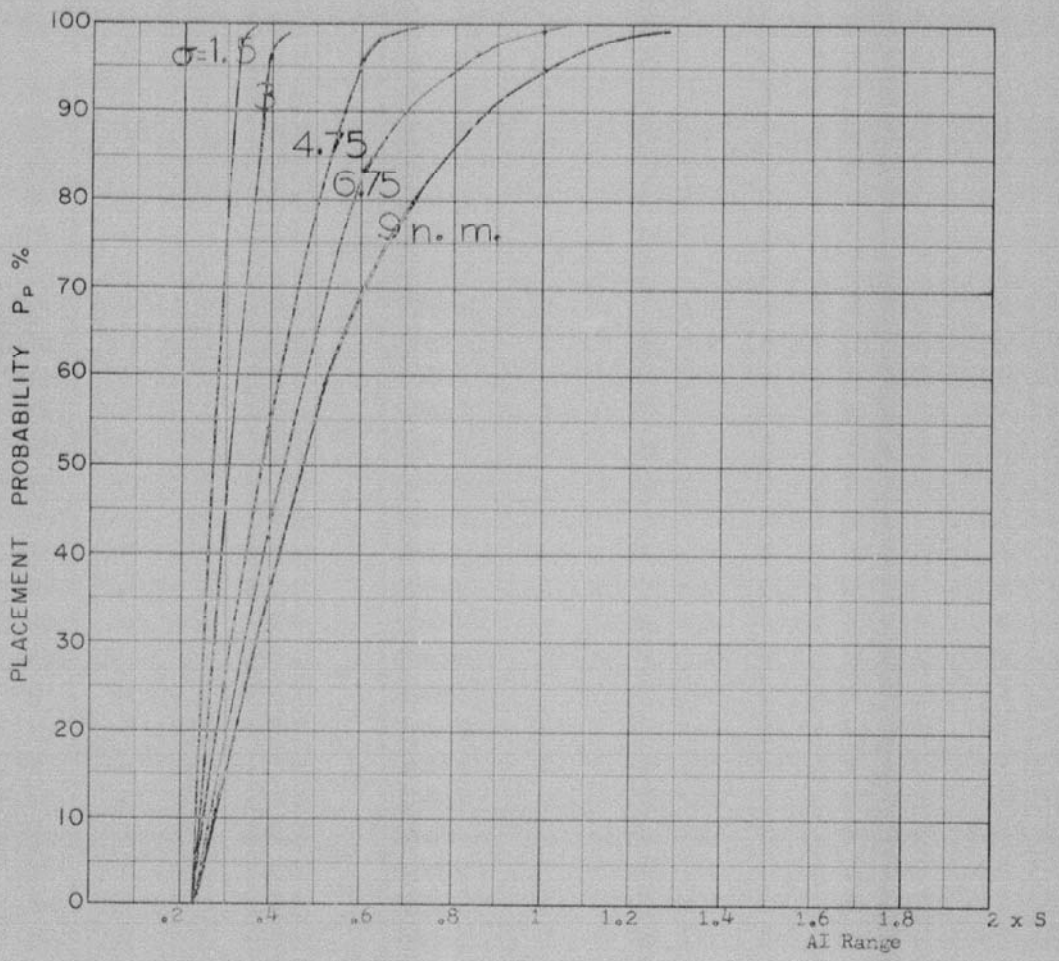

COURSE DIFFERENCE: 180°
TARGET EVASION: 0.1 lateral G's
TARGET MACH NO.: 2.0
INTERCEPTOR LATERAL G's: 3.0
INTERCEPTOR MACH NO.: 1.5
σ OF G.C.I. ACCURACY: 5 values
A.I. DETECTION RANGE AS FRACTION OF SPECIFICATION RANGE, S: Abscissa
A.I. DETECTION RANGE CONTOUR: Delta
ALTITUDE: 50 K

D99

Missile launch zone L-10

12 a x d p r

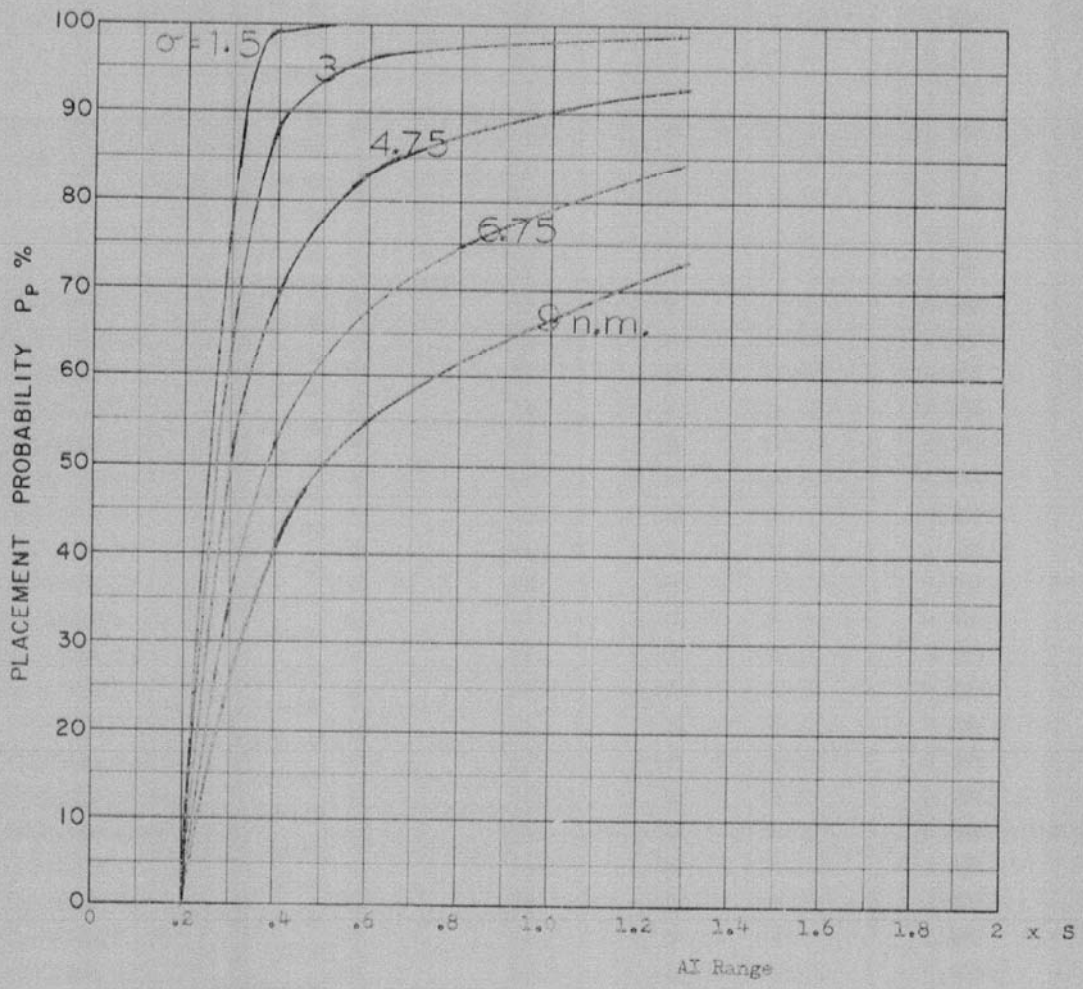

COURSE DIFFERENCE: 90°
TARGET EVASION: 0
TARGET MACH NO.: 2.0
INTERCEPTOR LATERAL G's: 2.0
INTERCEPTOR MACH NO.: 1.5
σ OF G.C.I. ACCURACY: Five values
A.I. DETECTION RANGE AS FRACTION OF SPECIFICATION RANGE, S: Abscissa
A.I. DETECTION RANGE CONTOUR: Delta
ALTITUDE: 60 K

D100a

Launch zone of figure L-8, missile launched at maximum range with 8° heading error.

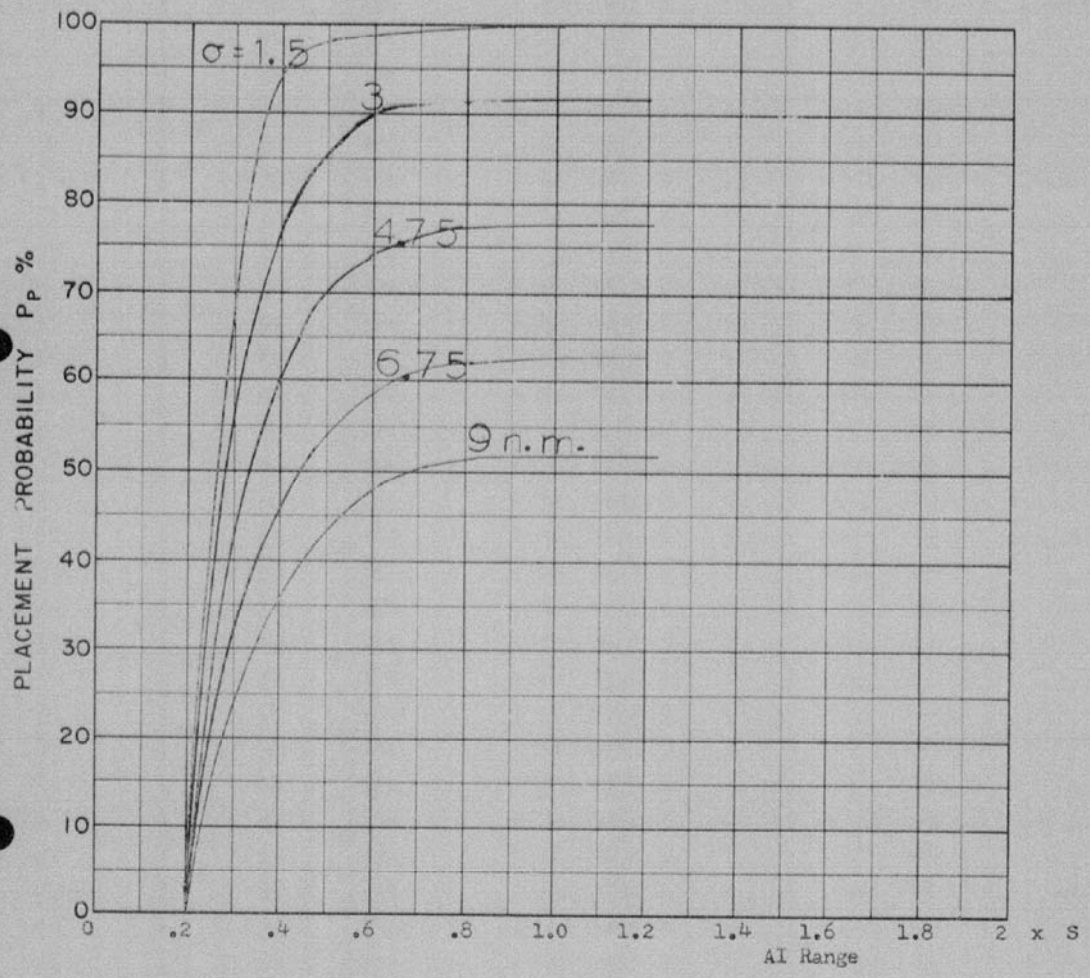

COURSE DIFFERENCE: 90°
TARGET EVASION: 0
TARGET MACH NO.: 2.0
INTERCEPTOR LATERAL G's: 2.0
INTERCEPTOR MACH NO.: 1.5
σ OF G.C.I. ACCURACY: Five values
A.I. DETECTION RANGE AS FRACTION OF SPECIFICATION RANGE, S: Abscissa
A.I. DETECTION RANGE CONTOUR: Delta
ALTITUDE: 60 K

D 100b

Launch zone of figure L-5, missile launched at maximum range with 8° heading error allowance.

12 b x d p r

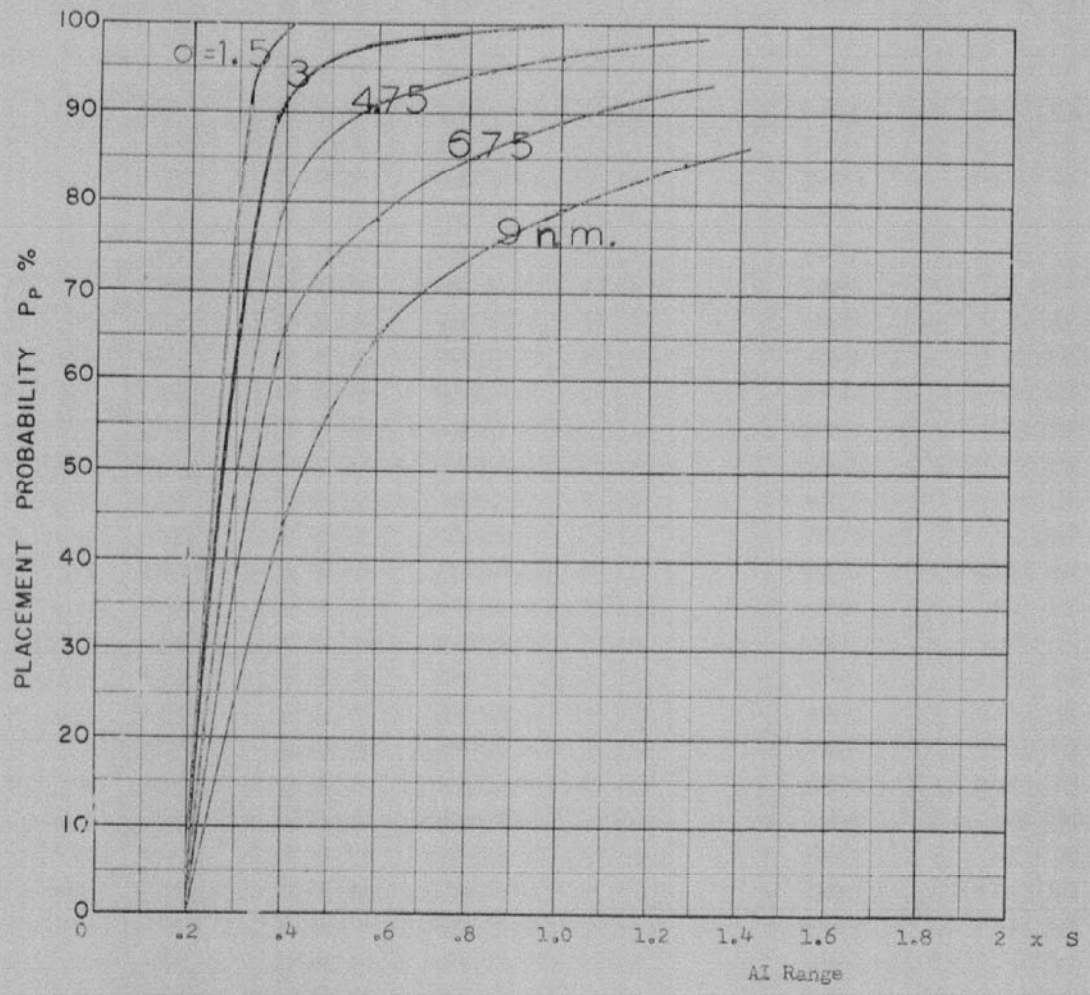

COURSE DIFFERENCE: 100°
TARGET EVASION: 0
TARGET MACH NO.: 2.0
INTERCEPTOR LATERAL G's: 2.0
INTERCEPTOR MACH NO.: 1.5
σ OF G.C.I. ACCURACY: Five values
A.I. DETECTION RANGE AS FRACTION OF SPECIFICATION RANGE, S: Abscissa
A.I. DETECTION RANGE CONTOUR: Delta
ALTITUDE: 60 K

D10a

Launch zone of figure L.8, missile launched at maximum range with 8° heading error.

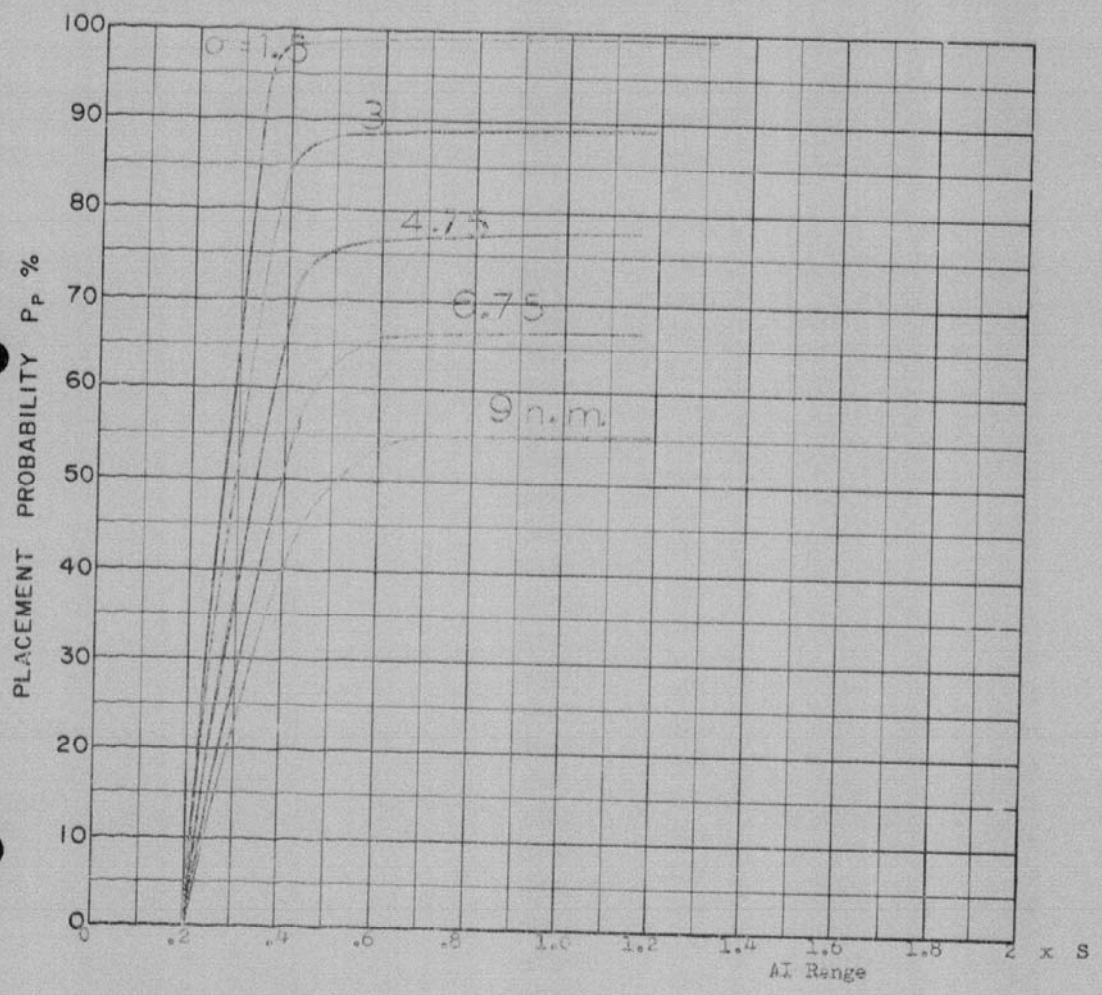

COURSE DIFFERENCE: 100°
TARGET EVASION: 0
TARGET MACH NO.: 2.0
INTERCEPTOR LATERAL G's: 2.0
INTERCEPTOR MACH NO.: 1.5
σ OF G.C.I. ACCURACY: Five values
A.I DETECTION RANGE AS FRACTION OF SPECIFICATION RANGE, S: Abscissa
A.I. DETECTION RANGE CONTOUR: Delta
ALTITUDE: 60 K

D101b

Launch zone of figure L-5, missile launched at maximum range with 8° heading error allowance.

12 s x d p r

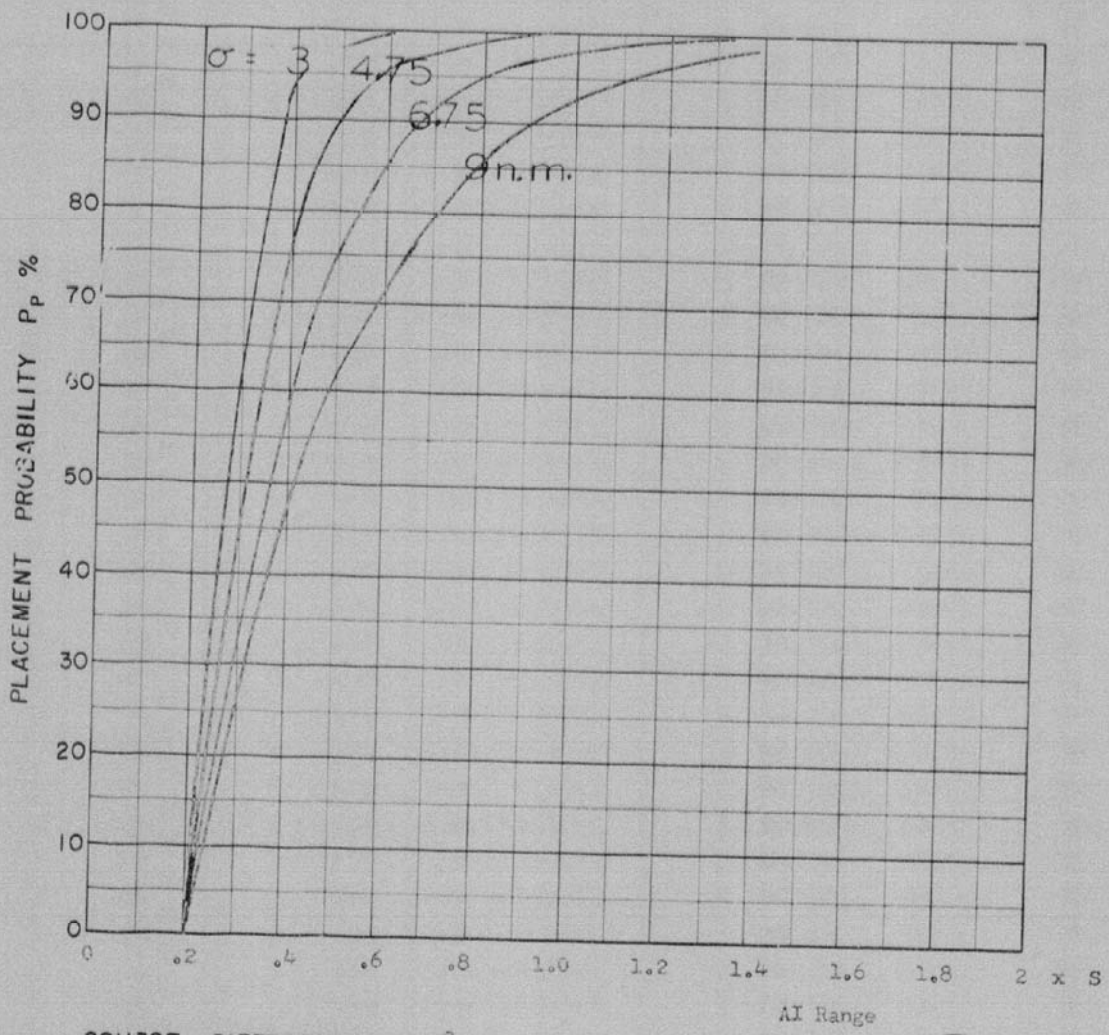

COURSE DIFFERENCE: 120°
TARGET EVASION: 0
TARGET MACH NO.: 2.0
INTERCEPTOR LATERAL G's: 2.0
INTERCEPTOR MACH NO.: 1.5
σ OF G.C.I. ACCURACY: Four values
A.I. DETECTION RANGE AS FRACTION OF SPECIFICATION RANGE, S: Abscissa
A.I. DETECTION RANGE CONTOUR: Delta
ALTITUDE: 60 K

D:02a

Launch zone of figure L-8; missile launched at maximum range with 8° heading error.

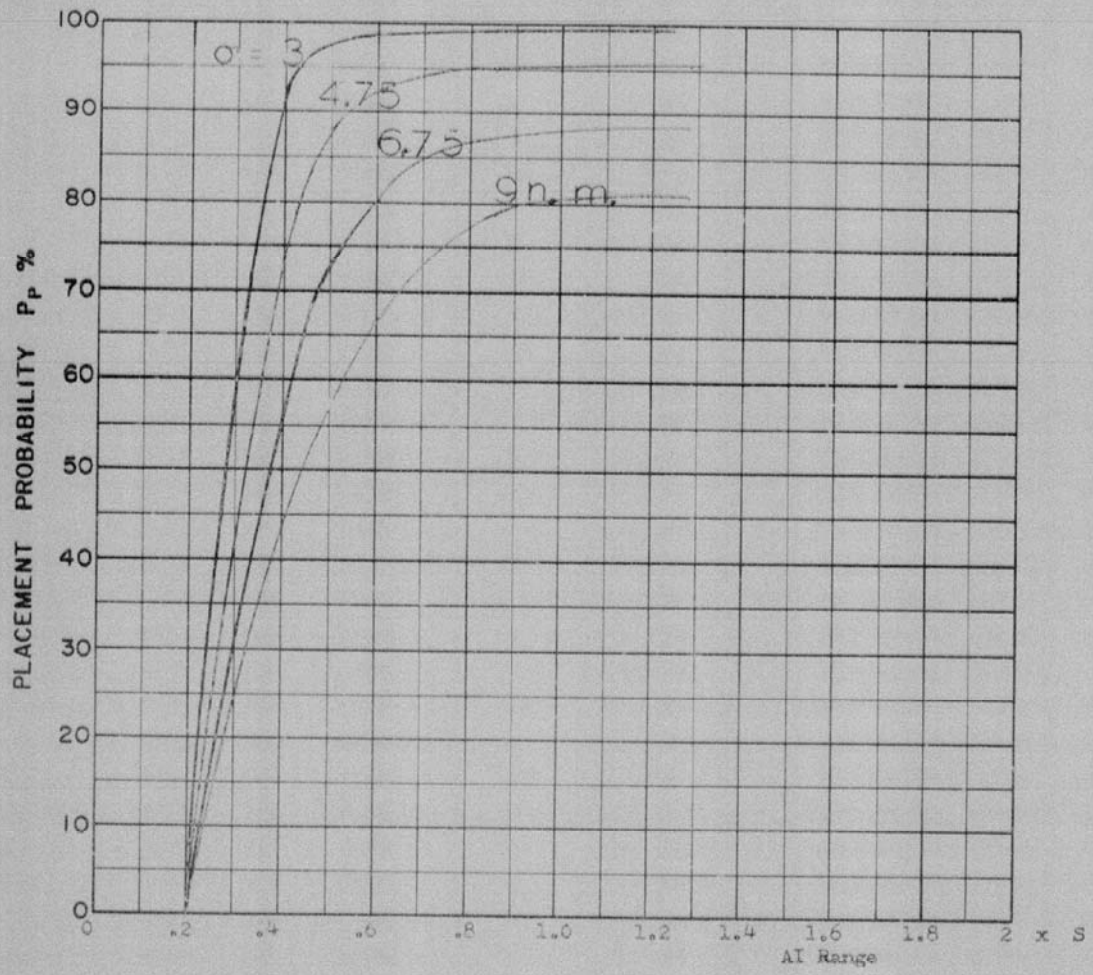

COURSE DIFFERENCE: 120°
TARGET EVASION: 0
TARGET MACH NO.: 2.0
INTERCEPTOR LATERAL G's: 2.0
INTERCEPTOR MACH NO.: 1.5
σ OF G.C.I. ACCURACY: Four values
A.I. DETECTION RANGE AS FRACTION OF SPECIFICATION RANGE, S: Abscissa
A.I. DETECTION RANGE CONTOUR: Delta
ALTITUDE: 60 K

D102b

Launch zone of figure L-5, missile launched at maximum range with 8° heading error allowance.

12 d x d p r

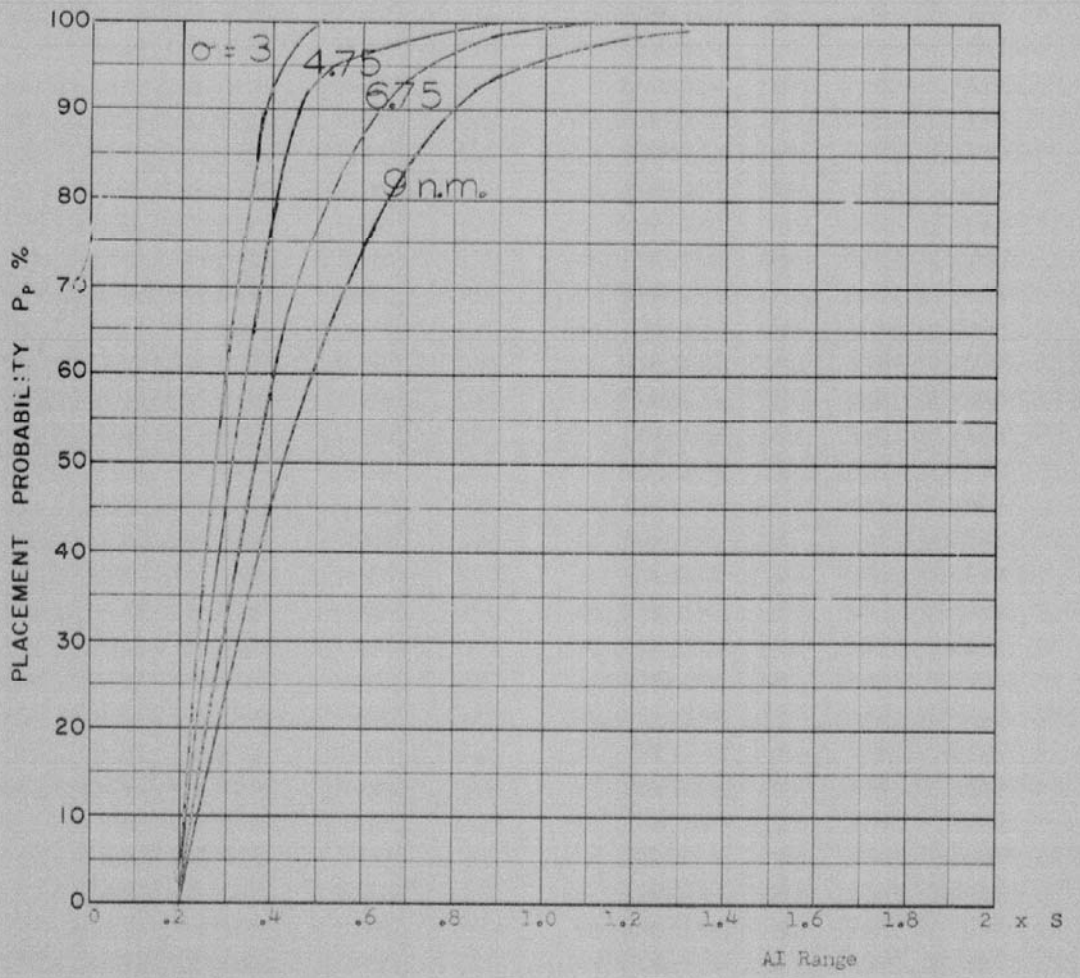

COURSE DIFFERENCE: 135°
TARGET EVASION: 0
TARGET MACH NO.: 2.0
INTERCEPTOR LATERAL G's: 3.0
INTERCEPTOR MACH NO.: 1.5
σ OF G.C.I. ACCURACY: Four values
A.I. DETECTION RANGE AS FRACTION OF SPECIFICATION RANGE, S: Abscissa
A.I. DETECTION RANGE CONTOUR: Delta
ALTITUDE: 60 K

(D103a)

Launch zone of figure L-8. missile launched at maximum range with 8° heading error.

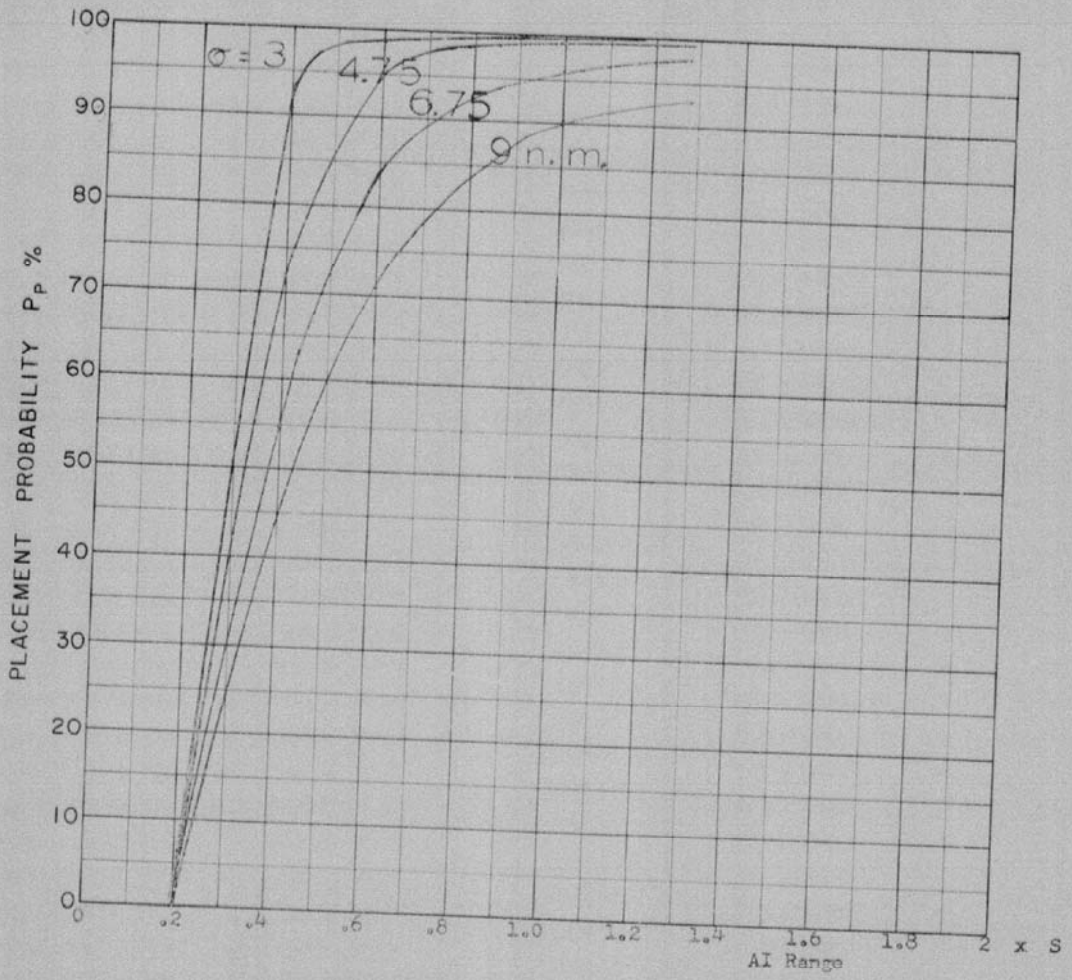

COURSE DIFFERENCE: 135°
TARGET EVASION: 0
TARGET MACH NO.: 2.0
INTERCEPTOR LATERAL G's: 2.0
INTERCEPTOR MACH NO.: 1.5
σ OF G.C.I. ACCURACY: Four values
A.I. DETECTION RANGE AS FRACTION OF SPECIFICATION RANGE, S: Abscissa
A.I. DETECTION RANGE CONTOUR: Delta
ALTITUDE: 60 K

D1036

Launch zone of figure L-5, missile launched at maximum range with 8° heading error allowance.

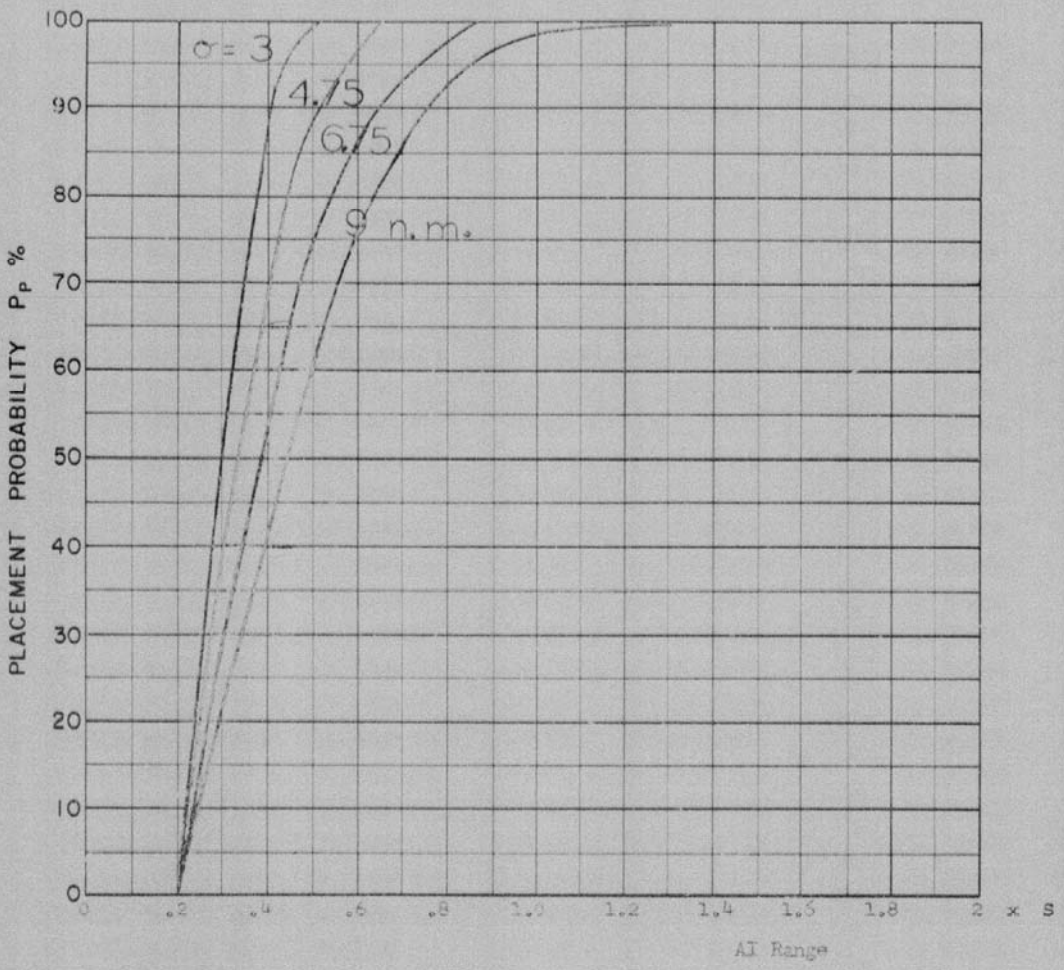

COURSE DIFFERENCE: 160°
TARGET EVASION: 0
TARGET MACH NO.: 2.0
INTERCEPTOR LATERAL G's: 2.0
INTERCEPTOR MACH NO.: 1.5
σ OF G.C.I. ACCURACY: Four values
A.I. DETECTION RANGE AS FRACTION OF SPECIFICATION RANGE, S: Abscissa
A.I. DETECTION RANGE CONTOUR: Delta
ALTITUDE: 60 K

D104a

Launch zone of figure L-8; missile launched at maximum range with 8° heading error.

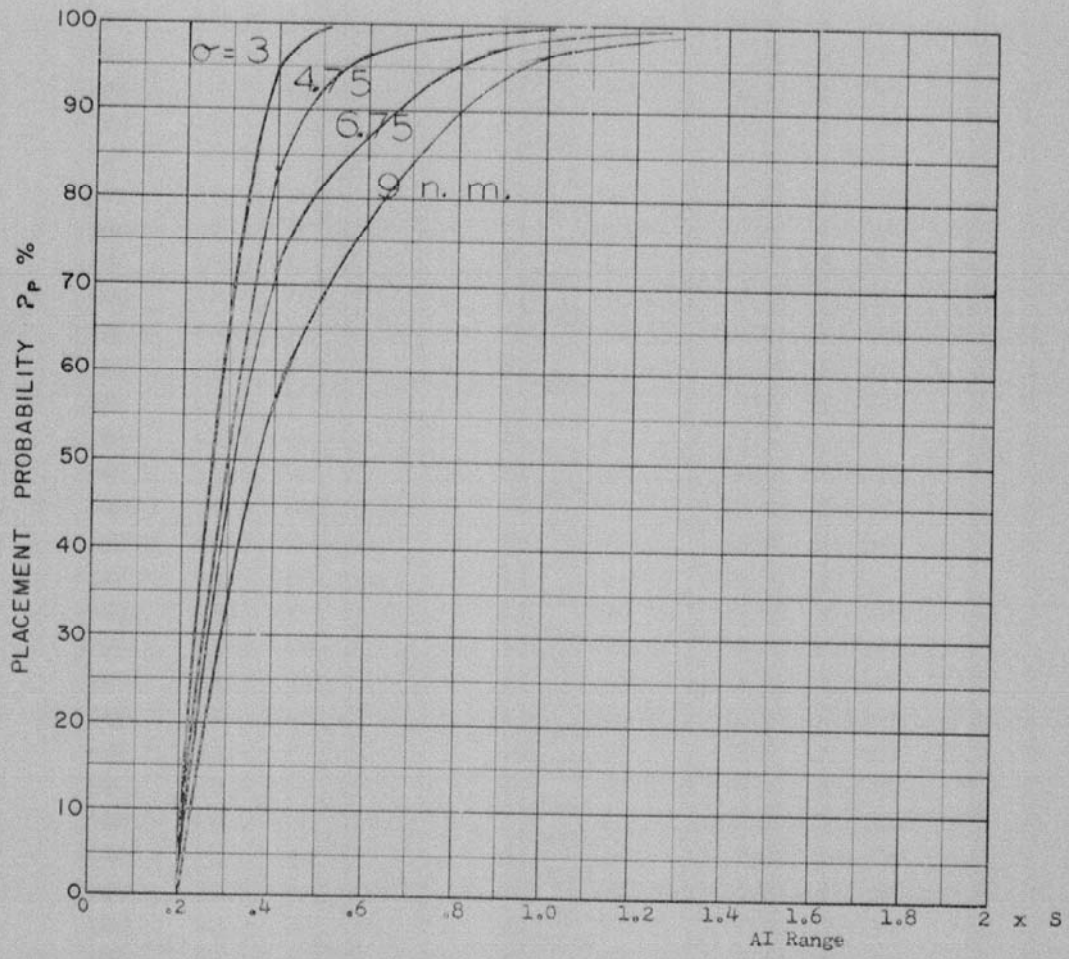

COURSE DIFFERENCE: 160°
TARGET EVASION: 0
TARGET MACH NO.: 2.0
INTERCEPTOR LATERAL G's: 2.0
INTERCEPTOR MACH NO.: 1.5
σ OF G.C.I. ACCURACY: Four values
A.I. DETECTION RANGE AS FRACTION OF SPECIFICATION RANGE, S: Abscissa
A.I. DETECTION RANGE CONTOUR: Delta
ALTITUDE: 60 K

D1046

Launch zone of figure L-5, missile launched at maximum range with 8° heading error allowance.

13 a x d p r

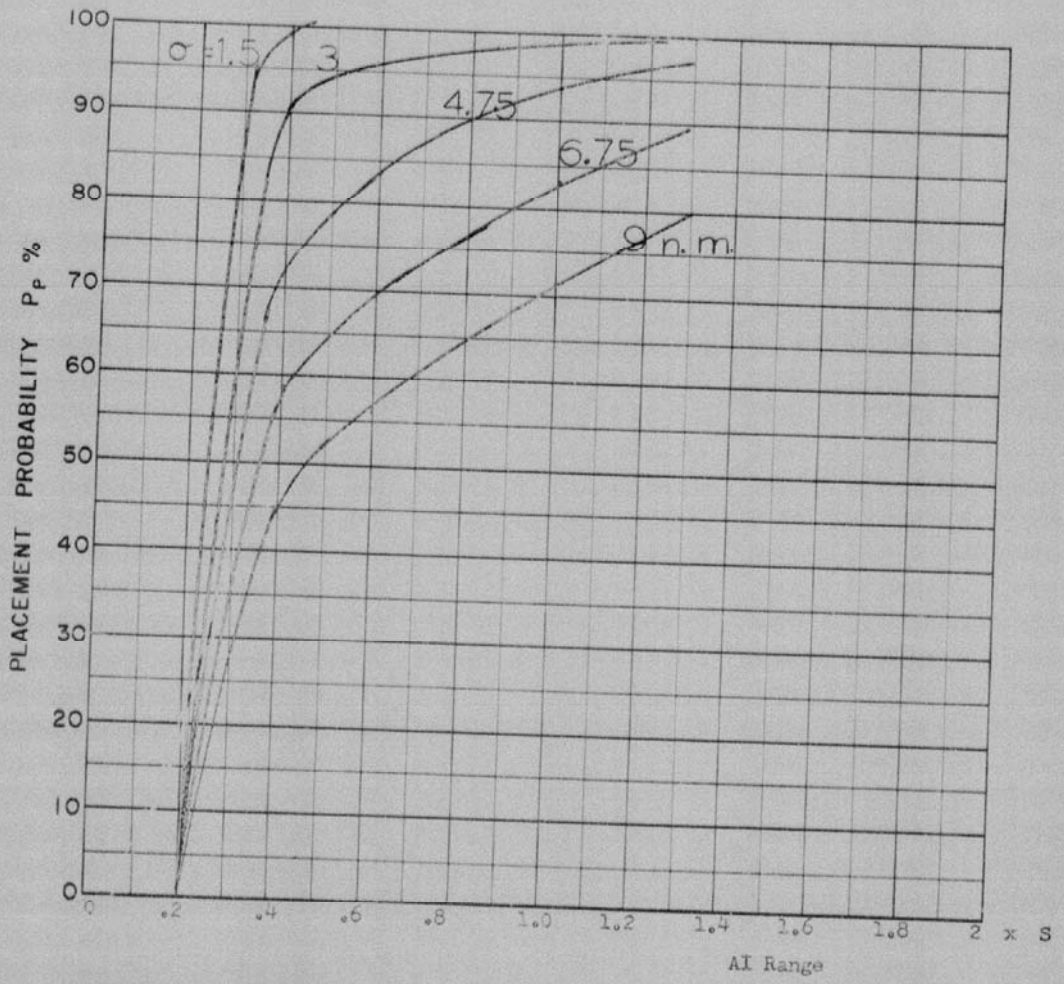

COURSE DIFFERENCE: 90°
TARGET EVASION: 0
TARGET MACH NO.: 2.0
INTERCEPTOR LATERAL G's: 3.35
INTERCEPTOR MACH NO.: 1.5
σ OF G.C.I. ACCURACY: Five values
A.I. DETECTION RANGE AS FRACTION OF SPECIFICATION RANGE, S: Abscissa
A.I. DETECTION RANGE CONTOUR: Delta
ALTITUDE: 60 K

D105a

Launch zone of figure L-9, missile launched at maximum range with 8° heading error allowance.

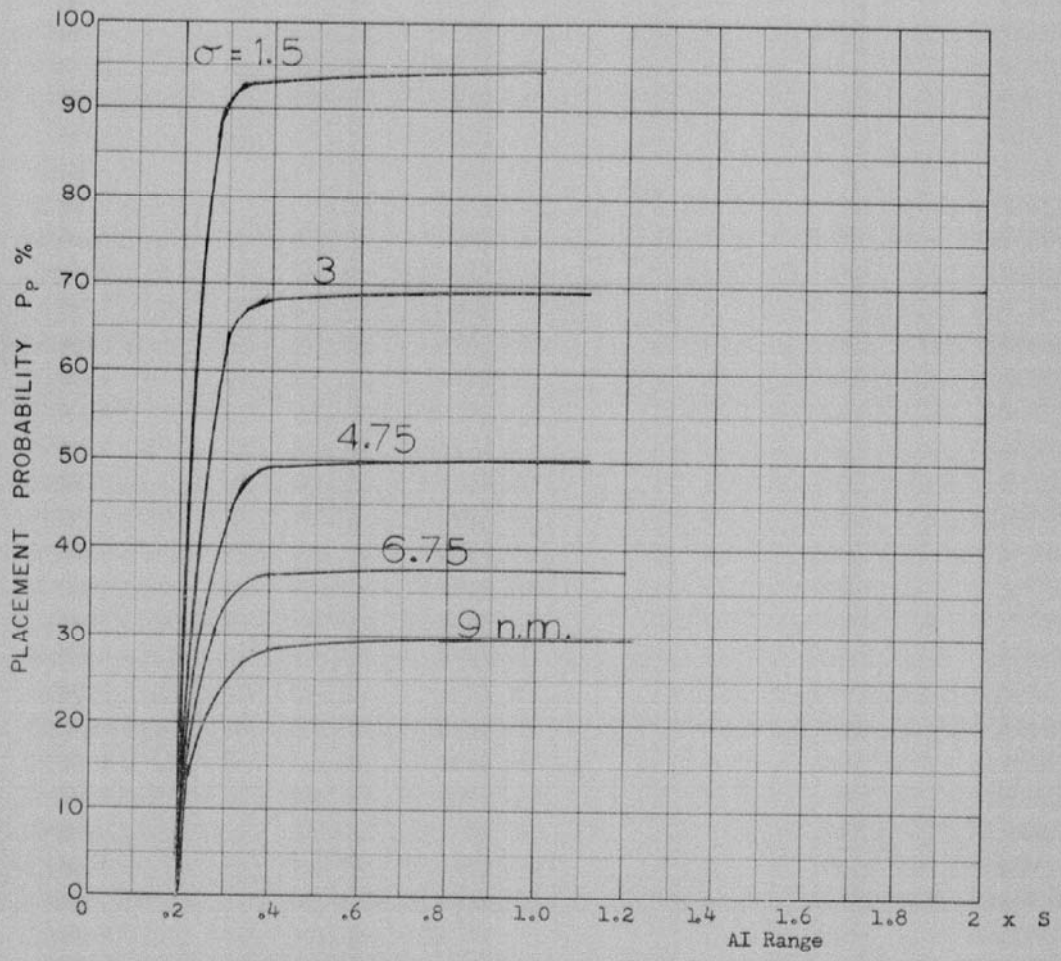

COURSE DIFFERENCE: 90°
TARGET EVASION: 0
TARGET MACH NO.: 2.0
INTERCEPTOR LATERAL G's: 3.35
INTERCEPTOR MACH NO.: 1.5
σ OF G.C.I. ACCURACY: Five values
A.I. DETECTION RANGE AS FRACTION OF SPECIFICATION RANGE, S: Abscissa
A.I. DETECTION RANGE CONTOUR: Delta
ALTITUDE: 60 K

(D105b)

Launch zone of figure L-5, missile launched at minimum range with 8° heading error allowance.

6 a d p r

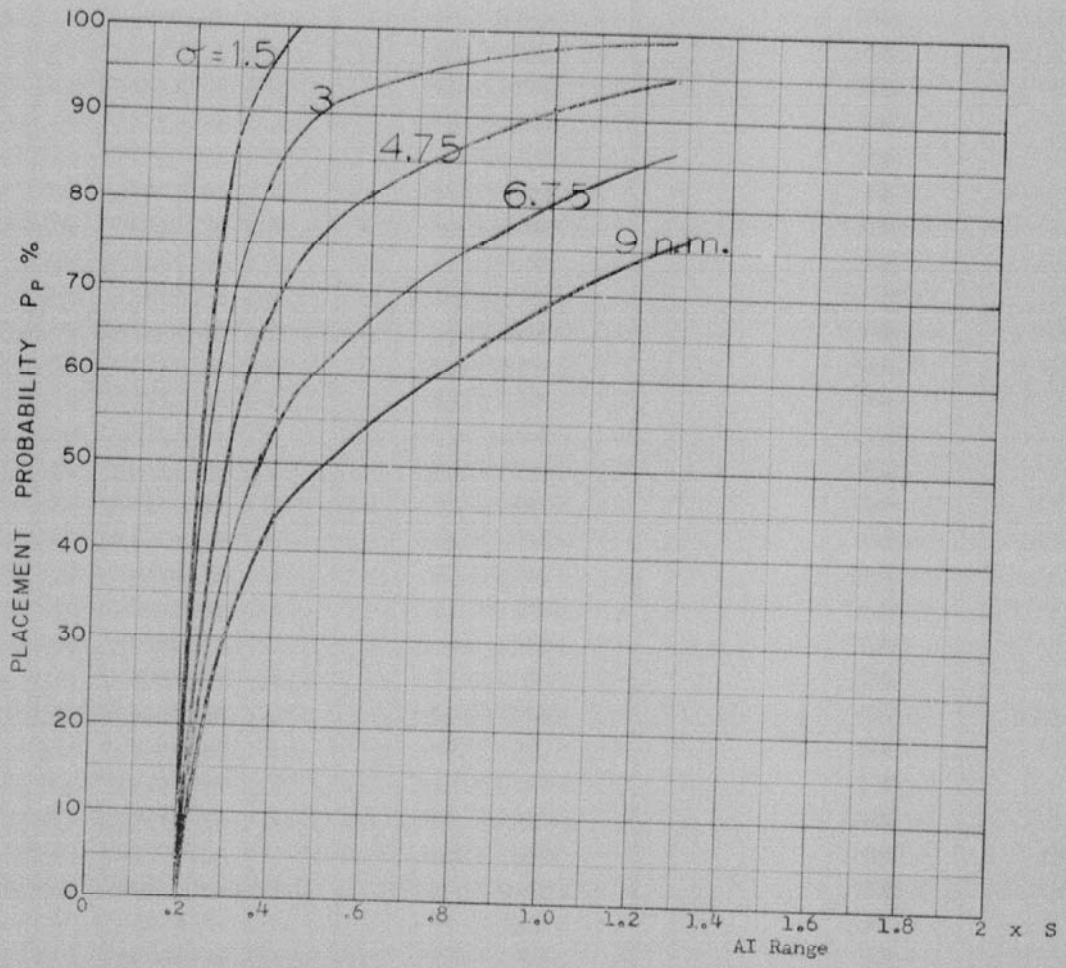

COURSE DIFFERENCE: 90°
TARGET EVASION: 0
TARGET MACH NO.: 2.0
INTERCEPTOR LATERAL G's: 3.35
INTERCEPTOR MACH NO.: 1.5
σ OF G.C.I. ACCURACY: Five values
A.I. DETECTION RANGE AS FRACTION OF SPECIFICATION RANGE, S: Abscissa
A.I. DETECTION RANGE CONTOUR: Delta
ALTITUDE: 60 K

D105c

Launch zone of figure L-5, missile launched at minimum range with 5° heading error allowance.

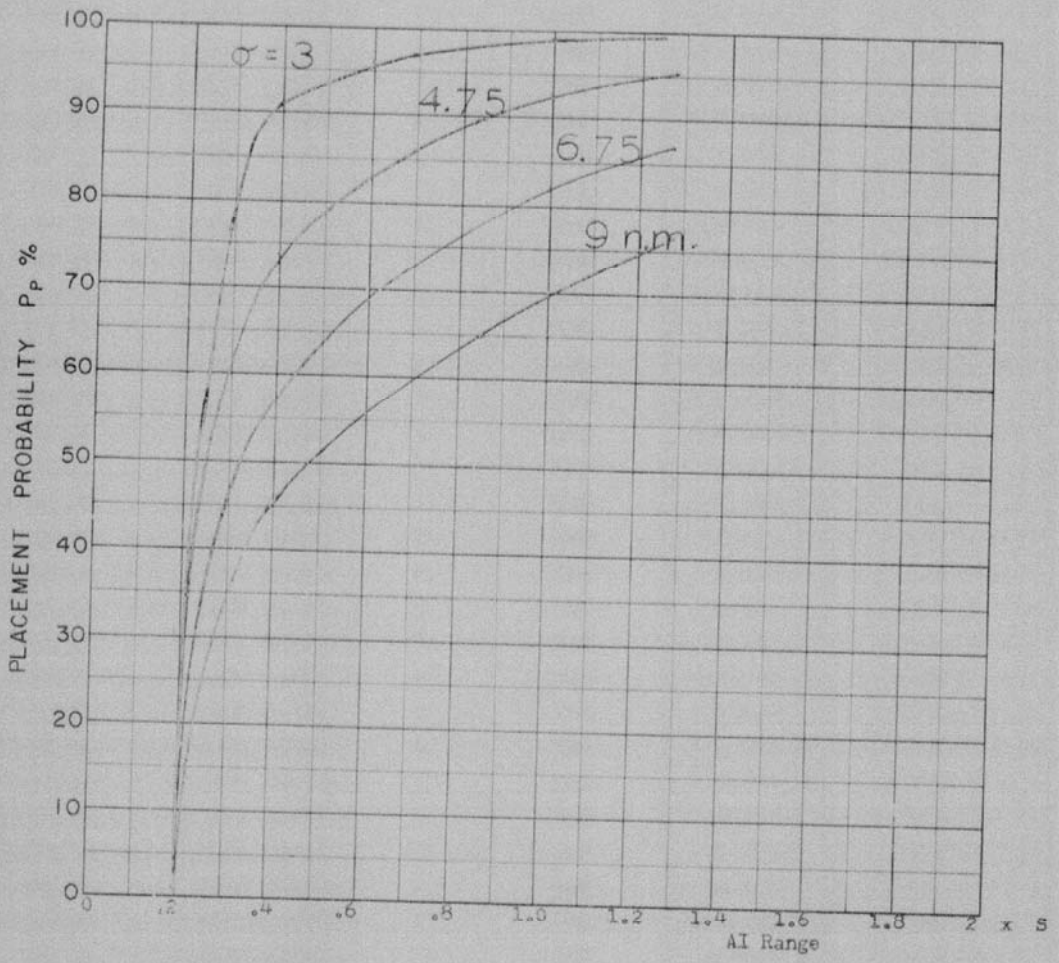

COURSE DIFFERENCE: 90°
TARGET EVASION: 0
TARGET MACH NO: 2.0
INTERCEPTOR LATERAL G's: 3.35
INTERCEPTOR MACH NO.: 1.5
σ OF G.C.I. ACCURACY: Four values
A.I. DETECTION RANGE AS FRACTION OF SPECIFICATION RANGE, S: Abscissa
A.I. DETECTION RANGE CONTOUR: Delta
ALTITUDE: 60 K

D105d

Launch zone of figure L-6, missile launched at maximum range with 15° heading error allowance.

13 b x d p r

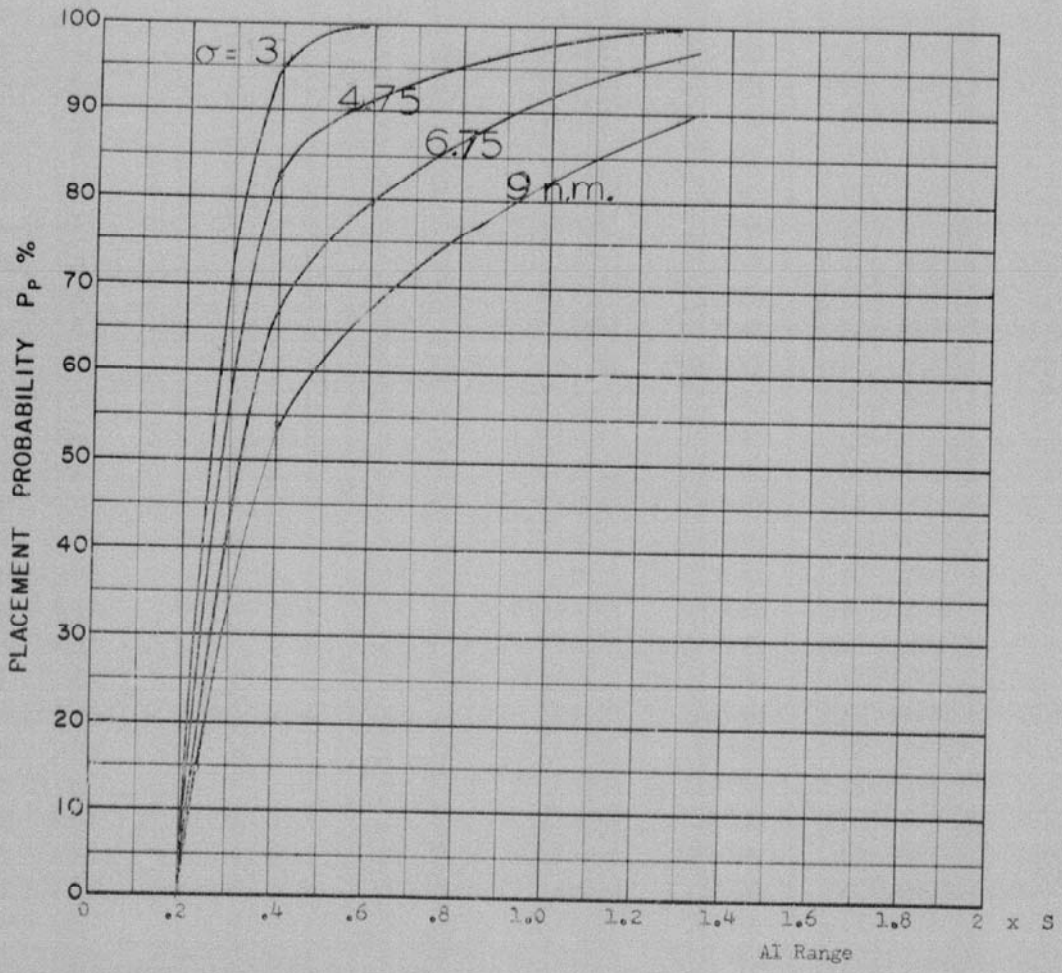

COURSE DIFFERENCE: 100°
TARGET EVASION: 0
TARGET MACH NO.: 2.0
INTERCEPTOR LATERAL G's: 3.35
INTERCEPTOR MACH NO.: 1.5
σ OF G.C.I. ACCURACY: Five values
A.I. DETECTION RANGE AS FRACTION OF SPECIFICATION RANGE, S: Abscissa
A.I. DETECTION RANGE CONTOUR: Delta
ALTITUDE: 60 K

D106a

Launch zone of figure L-9, missile launched at maximum range with 8° heading error allowance.

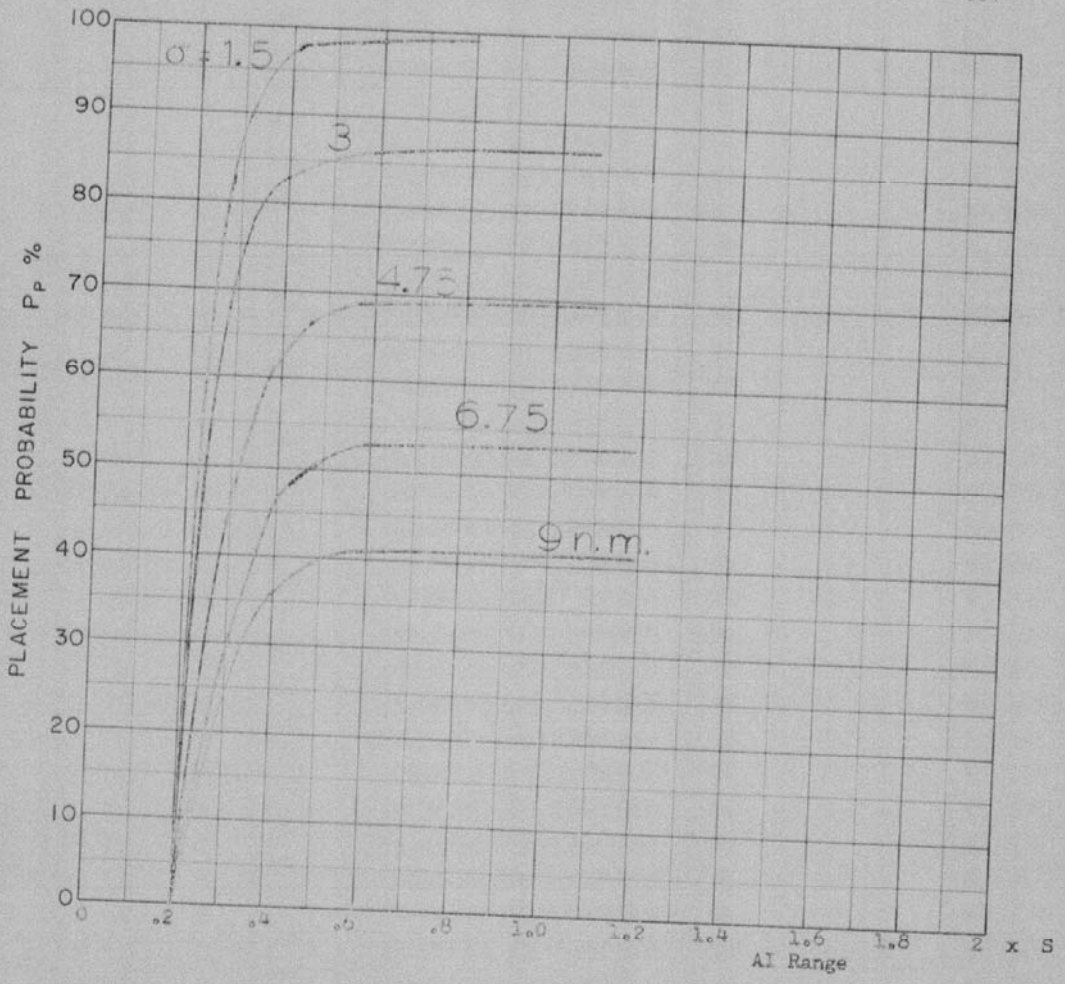

COURSE DIFFERENCE: 100°
TARGET EVASION: 0
TARGET MACH NO: 2.0
INTERCEPTOR LATERAL G's: 3.35
INTERCEPTOR MACH NO: 1.5
σ OF G.C.I. ACCURACY: Five values
A.I. DETECTION RANGE AS FRACTION OF SPECIFICATION RANGE, S: Abscissa
A.I. DETECTION RANGE CONTOUR: Delta
ALTITUDE: 60 K

(D1061)

Launch zone of figure L-5, missile launched at minimum range with 8° heading error allowance.

6 b d p r

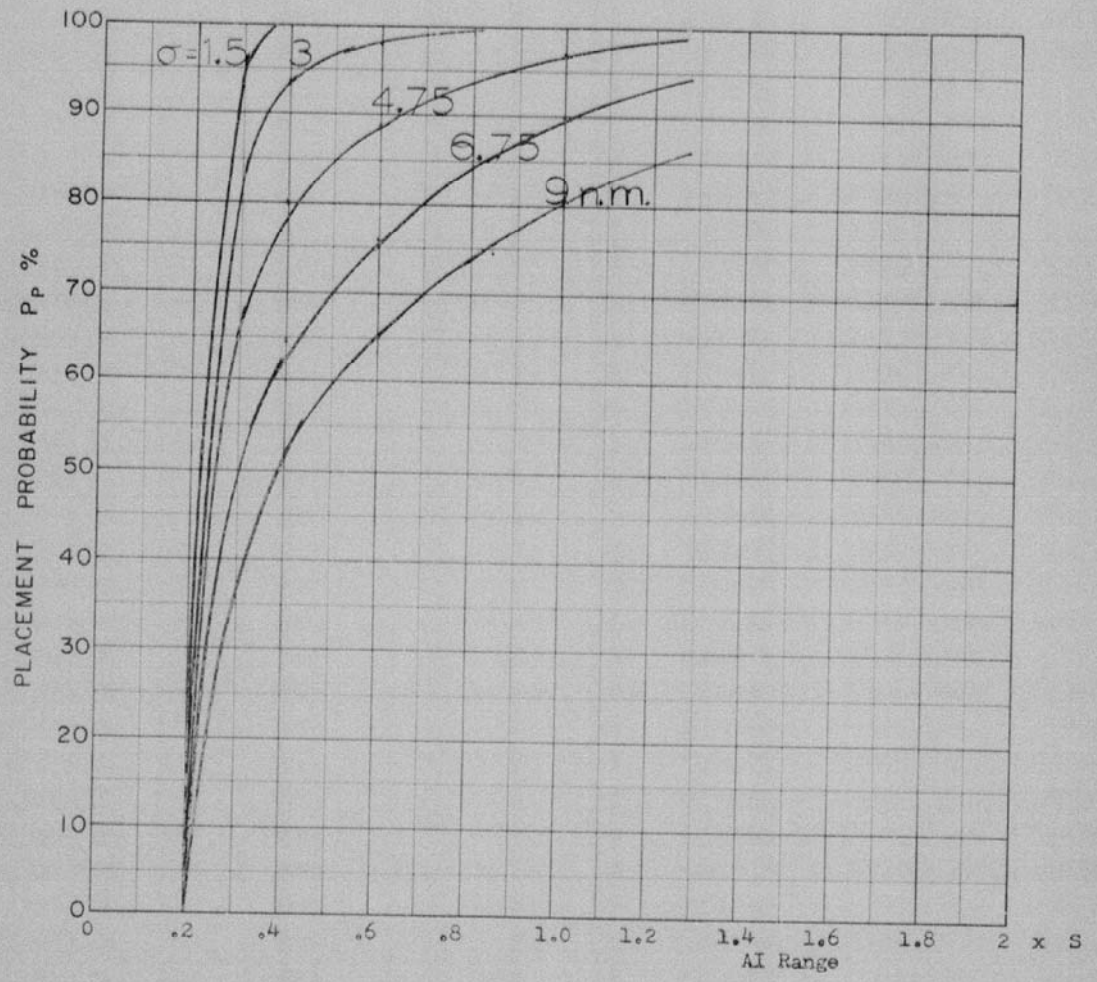

COURSE DIFFERENCE: 100°
TARGET EVASION: 0
TARGET MACH NO.: 2.0
INTERCEPTOR LATERAL G's: 3.35
INTERCEPTOR MACH NO.: 1.5
σ OF G.C.I. ACCURACY: Five values
A.I. DETECTION RANGE AS FRACTION OF SPECIFICATION RANGE, S: Abscissa
A.I. DETECTION RANGE CONTOUR: Delta
ALTITUDE: 60 K

D106c

Launch zone of figure L-5, missile launched at minimum range with 15° heading error allowance.

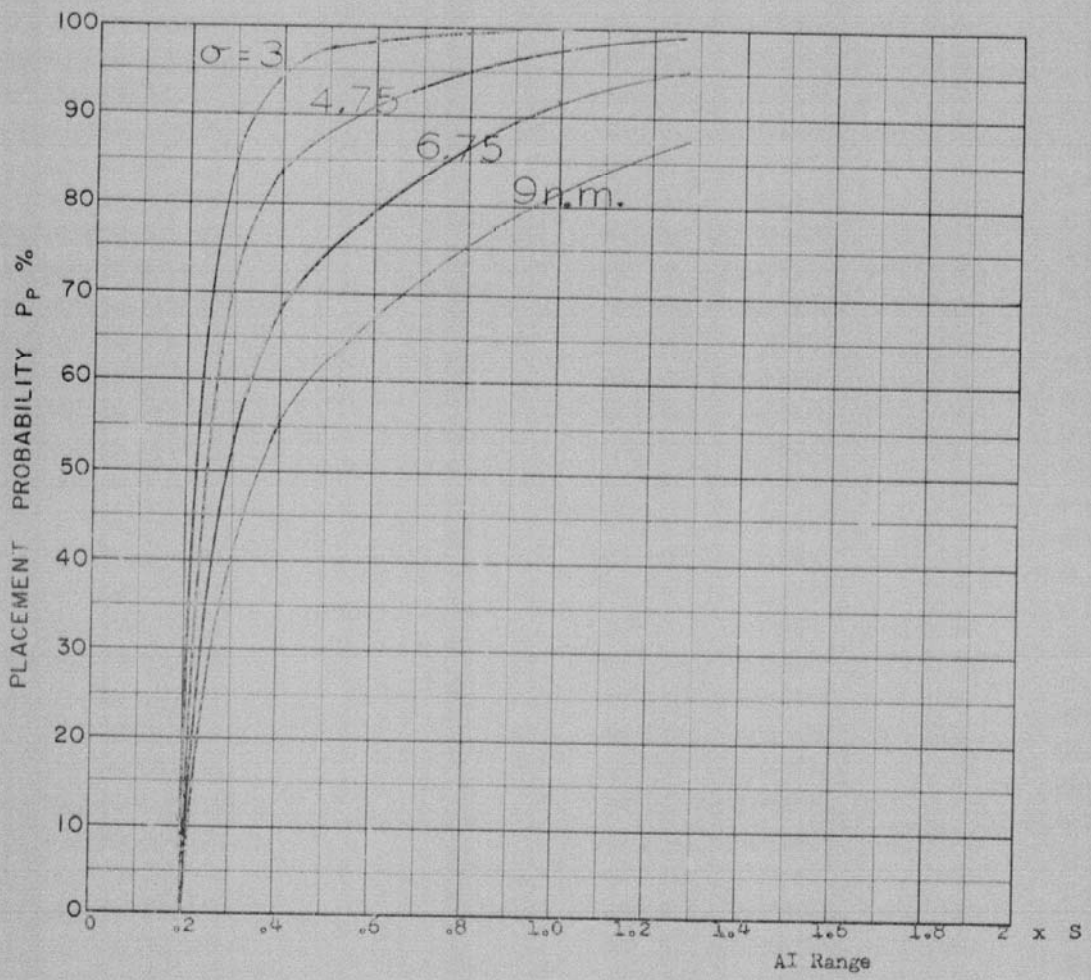

COURSE DIFFERENCE: 100°
TARGET EVASION: 0
TARGET MACH NO.: 2.0
INTERCEPTOR LATERAL G's: 3.35
INTERCEPTOR MACH NO.: 1.5
σ OF G.C.I. ACCURACY: Four values
A.I. DETECTION RANGE AS FRACTION OF SPECIFICATION RANGE, S: Abscissa
A.I. DETECTION RANGE CONTOUR: Delta
ALTITUDE: 60 K

D106d

Launch zone of figure L-6, missile launched at maximum range with 15° heading error allowance.

13 c x d p r

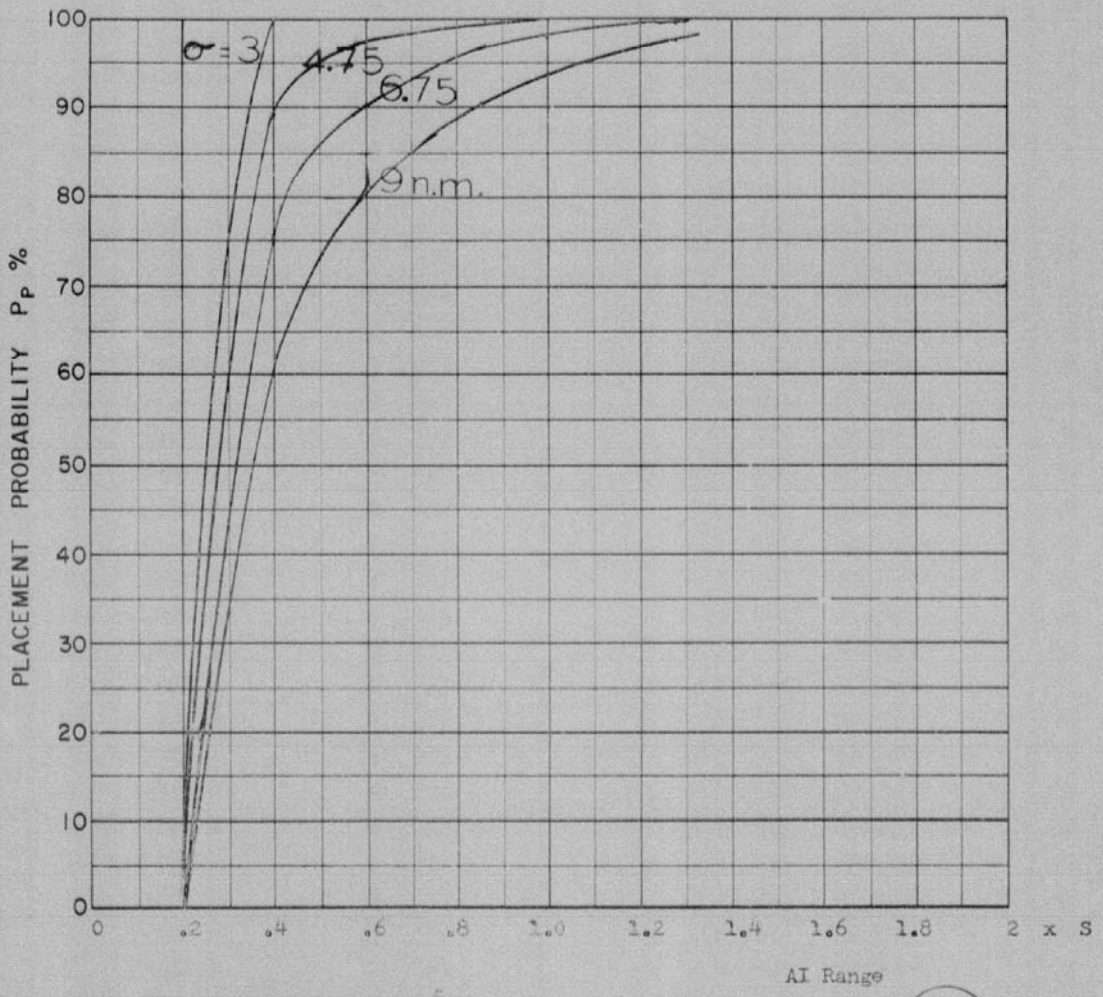

COURSE DIFFERENCE: 120°
TARGET EVASION: 0
TARGET MACH NO.: 2.0
INTERCEPTOR LATERAL G's: 3.35
INTERCEPTOR MACH NO.: 1.5
σ OF G.C.I. ACCURACY: Four values
A.I. DETECTION RANGE AS FRACTION OF SPECIFICATION RANGE, S: Abscissa
A.I. DETECTION RANGE CONTOUR: Delta
ALTITUDE: 60 K

(D107a)

Launch zone of figure L-9, missile launched at maximum range with 8° heading error allowance.

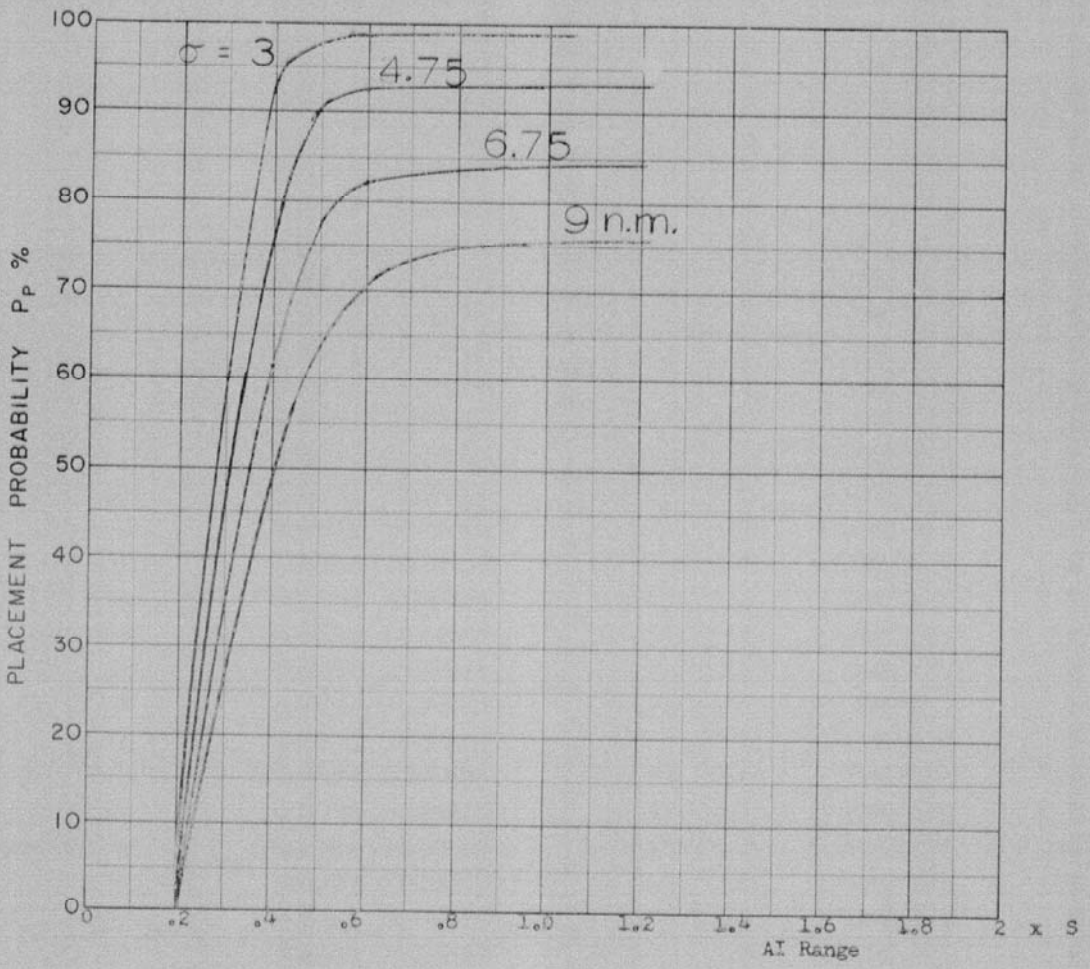

COURSE DIFFERENCE: 120°
TARGET EVASION: 0
TARGET MACH NO.: 2.0
INTERCEPTOR LATERAL G's: 3.35
INTERCEPTOR MACH NO.: 1.5
σ OF G.C.I. ACCURACY: Four values
A.I. DETECTION RANGE AS FRACTION OF SPECIFICATION RANGE, S: Abscissa
A.I. DETECTION RANGE CONTOUR: Delta
ALTITUDE: 60 K

(D1076)

Launch zone of figure L-5, missile launched at minimum range with 8° heading error allowance.

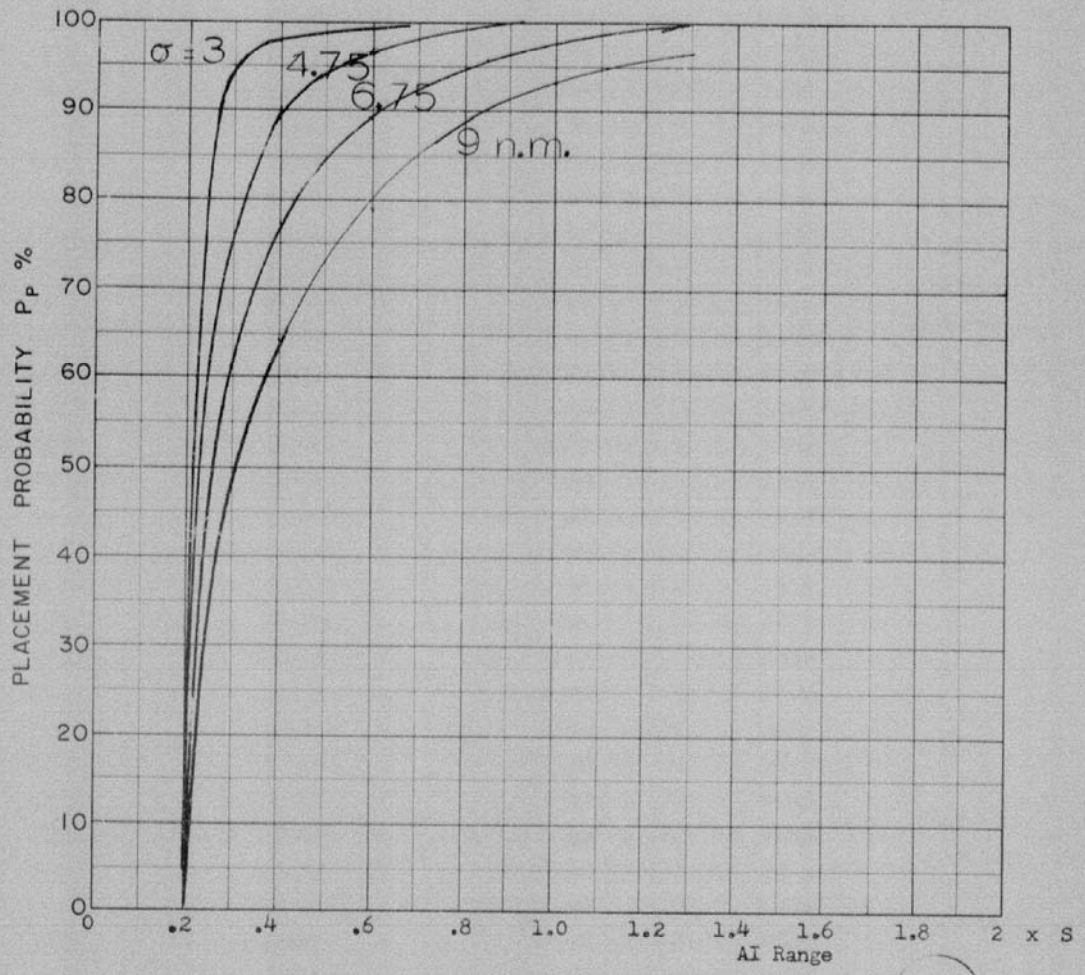

(D107c)

COURSE DIFFERENCE: 120°
TARGET EVASION: 0
TARGET MACH NO.: 2.0
INTERCEPTOR LATERAL G's: 3.35
INTERCEPTOR MACH NO.: 1.5
σ OF G.C.I. ACCURACY: Four values
A.I. DETECTION RANGE AS FRACTION OF SPECIFICATION RANGE, S: Abscissa
A.I. DETECTION RANGE CONTOUR: Delta
ALTITUDE: 60 K

Launch zone of figure L-5, missile launched at minimum range with 15° heading error allowance.

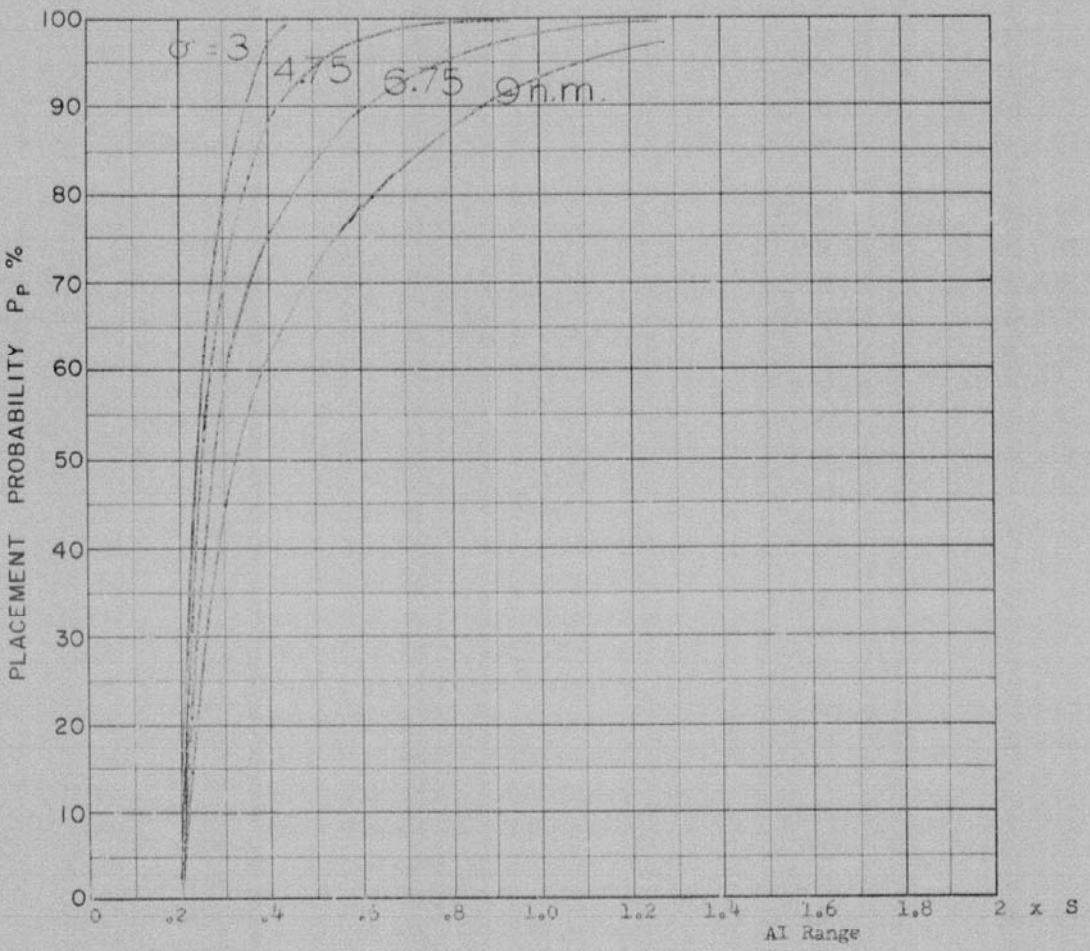

COURSE DIFFERENCE: 120°
TARGET EVASION: 0
TARGET MACH NO.: 2.0
INTERCEPTOR LATERAL G's: 3.35
INTERCEPTOR MACH NO.: 1.5
σ OF G.C.I. ACCURACY: Four values
A.I. DETECTION RANGE AS FRACTION OF SPECIFICATION RANGE, S: Abscissa
A.I. DETECTION RANGE CONTOUR: Delta
ALTITUDE: 60 K

(D107d)

Launch zone of figure L-6, missile launched at maximum range with 15° heading error allowance.

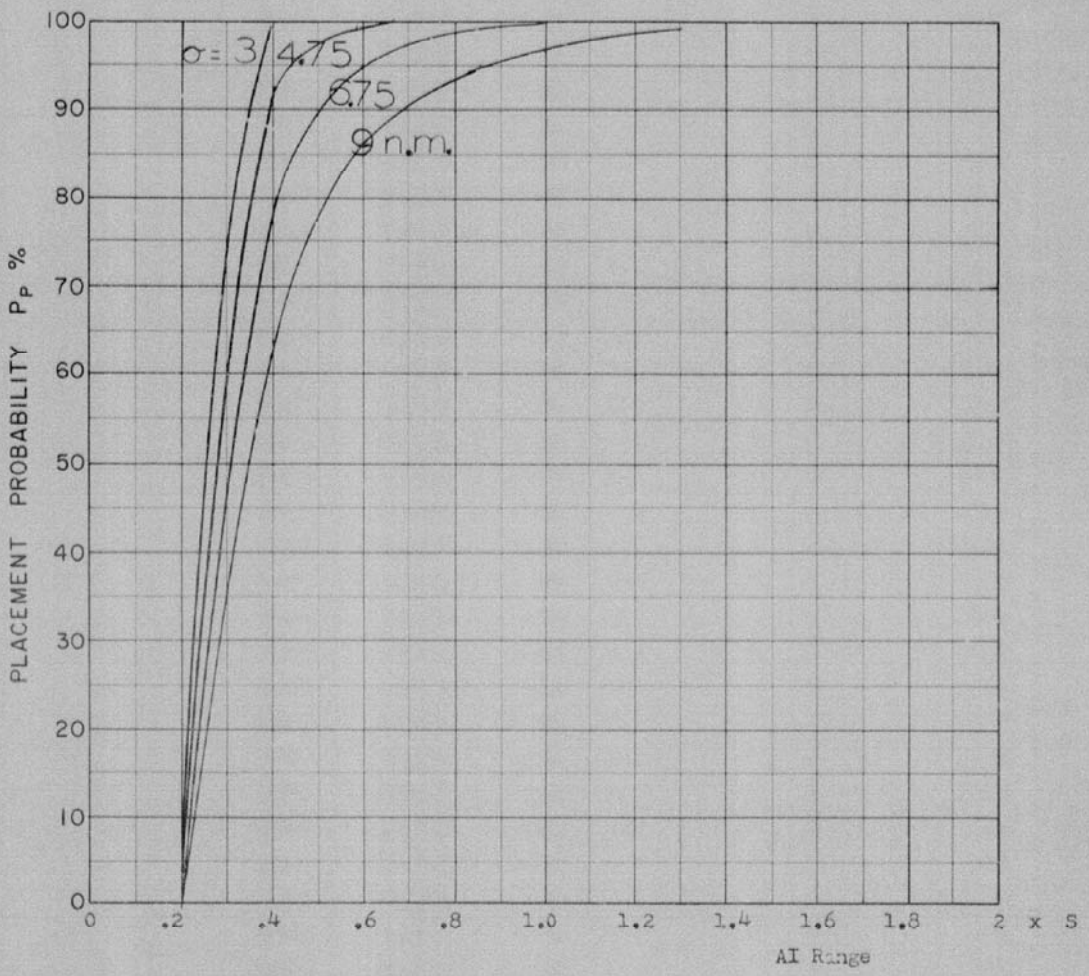

COURSE DIFFERENCE: 135°
TARGET EVASION: 0
TARGET MACH NO.: 2.0
INTERCEPTOR LATERAL G's: 3.35
INTERCEPTOR MACH NO.: 1.5
σ OF G.C.I. ACCURACY: Four values
A.I. DETECTION RANGE AS FRACTION OF SPECIFICATION RANGE, S: Abscissa
A.I. DETECTION RANGE CONTOUR: Delta
ALTITUDE: 60 K

D108a

Launch zone of figure L-9, missile launched at maximum range with 8° heading error allowance.

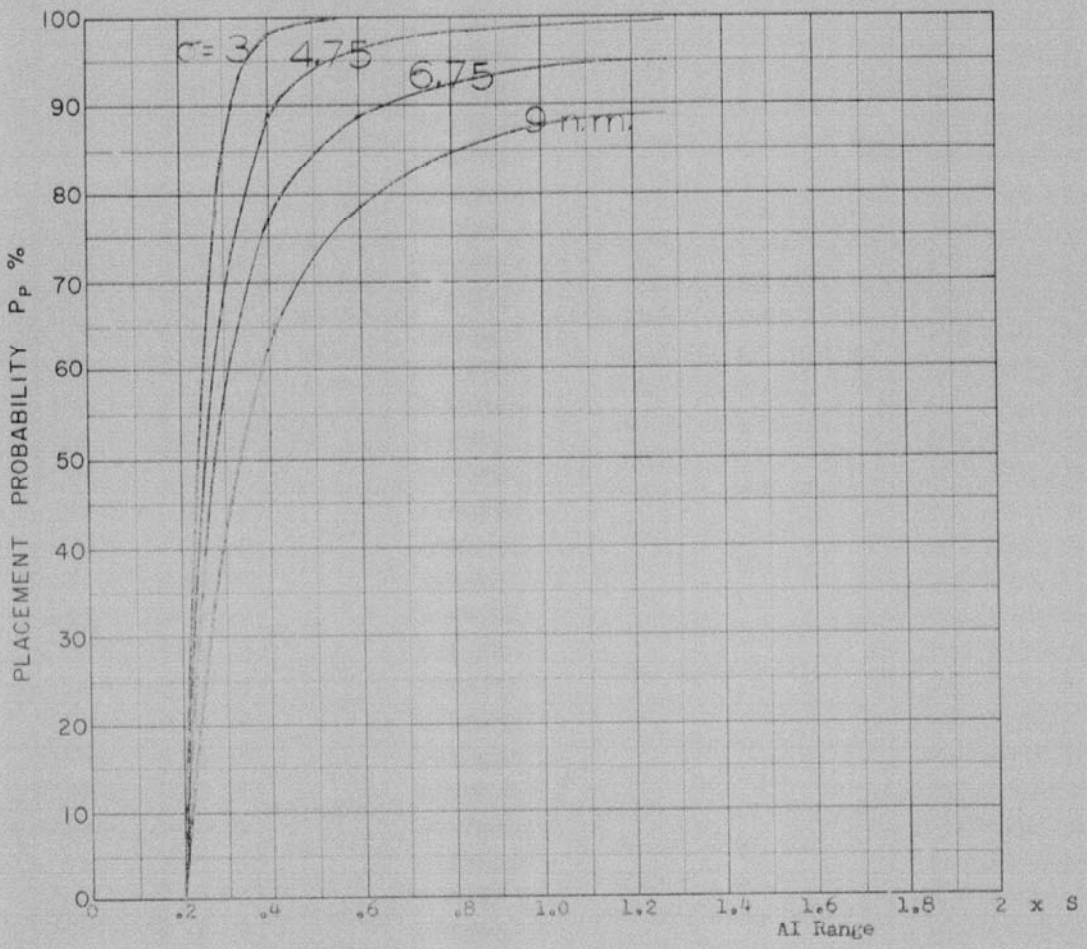

COURSE DIFFERENCE: 135°
TARGET EVASION: 0
TARGET MACH NO.: 2.0
INTERCEPTOR LATERAL G's: 3.35
INTERCEPTOR MACH NO.: 1.5
σ OF G.C.I. ACCURACY: Four values
A.I. DETECTION RANGE AS FRACTION OF SPECIFICATION RANGE, S: Abscissa
A.I. DETECTION RANGE CONTOUR: Delta
ALTITUDE: 60 K

(D108b)

Launch zone of figure L-5, missile launched at minimum range with 8° heading error allowance.

6 d d p r

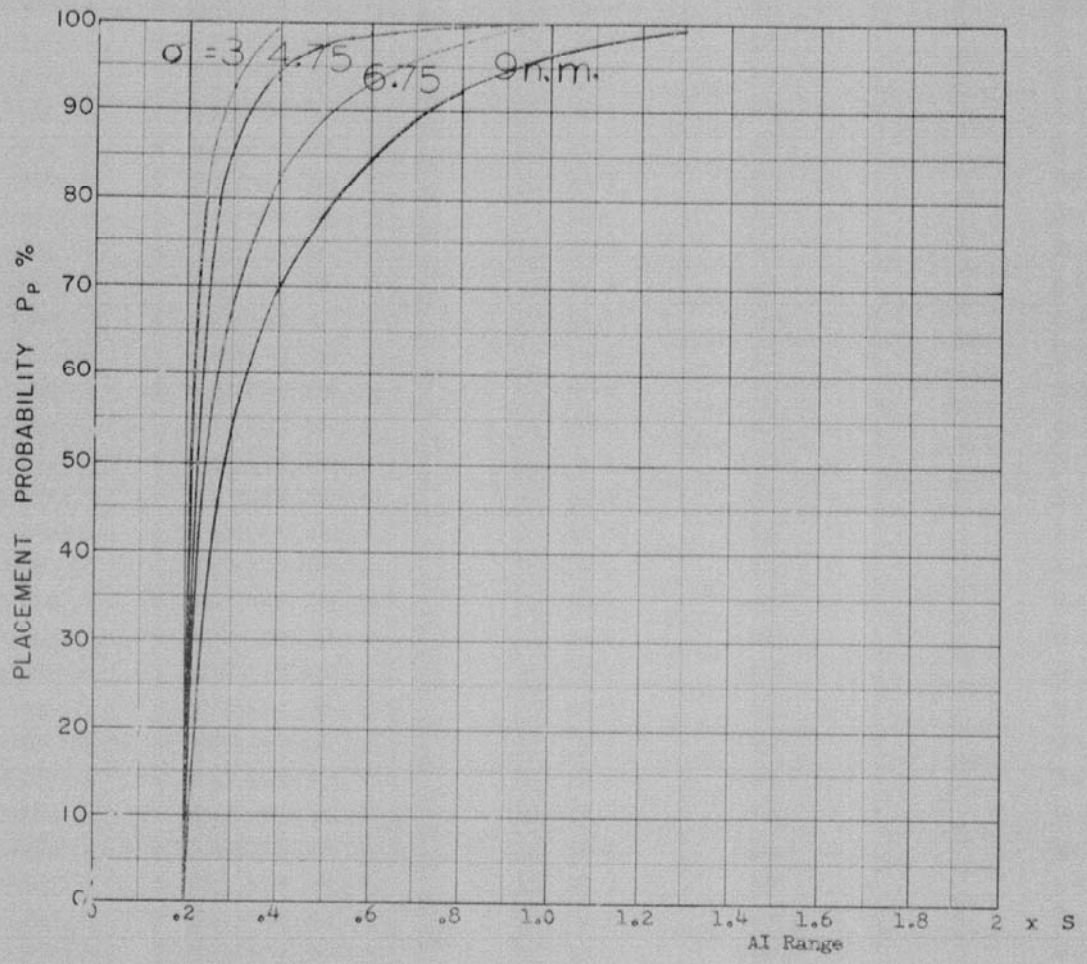

COURSE DIFFERENCE: 135°
TARGET EVASION: 0
TARGET MACH NO.: 2.0
INTERCEPTOR LATERAL G's: 3.35
INTERCEPTOR MACH NO.: 1.5
σ OF G.C.I. ACCURACY: Four values
A.I. DETECTION RANGE AS FRACTION OF SPECIFICATION RANGE, S: Abscissa
A.I. DETECTION RANGE CONTOUR: Delta
ALTITUDE: 60 K

(D108c)

Launch zone of figure L-5, missile launched at minimum range with ±5° heading error allowance.

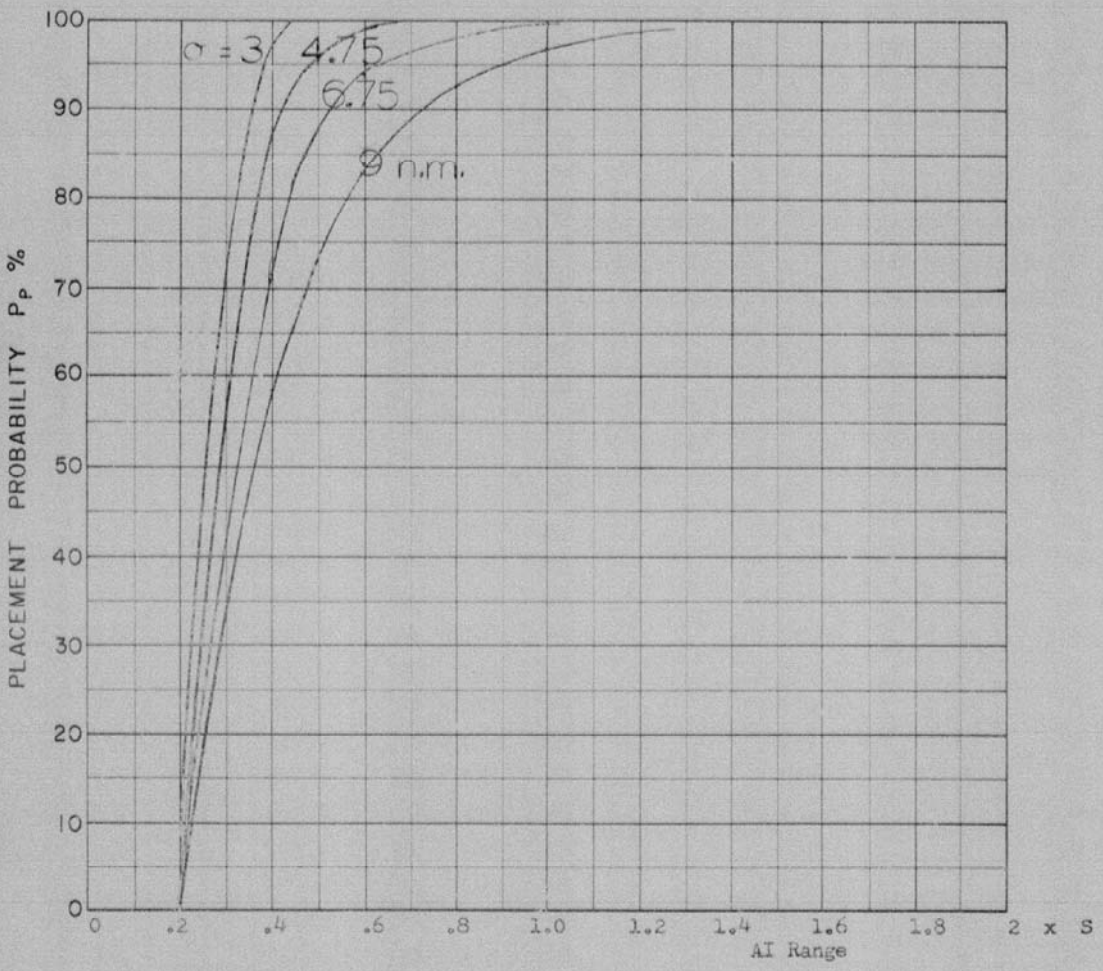

COURSE DIFFERENCE: 135°
TARGET EVASION: 0
TARGET MACH NO.: 2.0
INTERCEPTOR LATERAL G's: 3.35
INTERCEPTOR MACH NO.: 1.5
σ OF G.C.I. ACCURACY: Four values
A.I. DETECTION RANGE AS FRACTION OF SPECIFICATION RANGE, S: Abscissa
A.I. DETECTION RANGE CONTOUR: Delta
ALTITUDE: 60 K

D 108d

Launch zone of figure L-6, missile launched at maximum range with 15° heading error allowance.

13 e x d p r

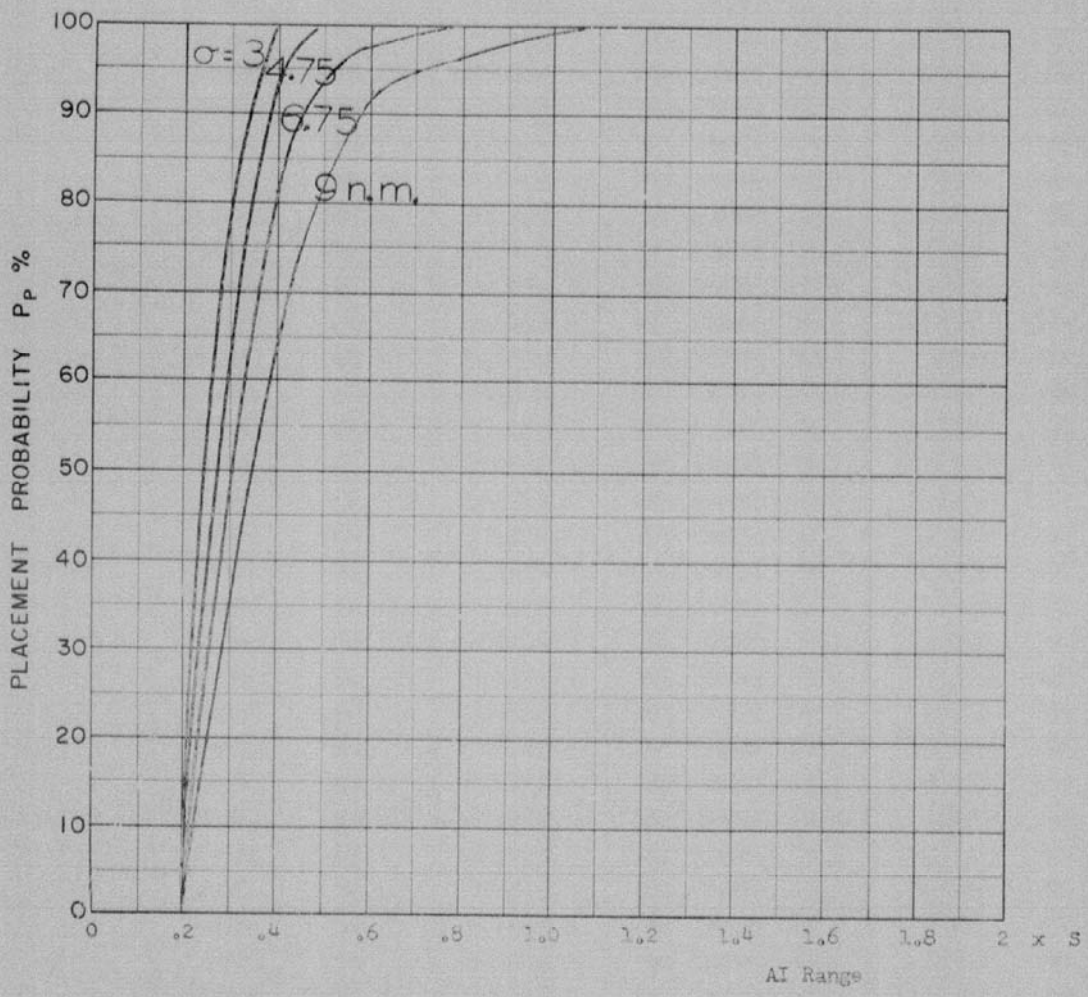

COURSE DIFFERENCE: 160°
TARGET EVASION: 0
TARGET MACH NO.: 2.0
INTERCEPTOR LATERAL G's: 3.35
INTERCEPTOR MACH NO.: 1.5
σ OF G.C.I. ACCURACY: Four values
A.I. DETECTION RANGE AS FRACTION OF SPECIFICATION RANGE, S: Abscissa
A.I. DETECTION RANGE CONTOUR: Delta
ALTITUDE: 60 K

D109a

Launch zone of figure L-9, missile launched at maximum range with 8° heading error allowance.

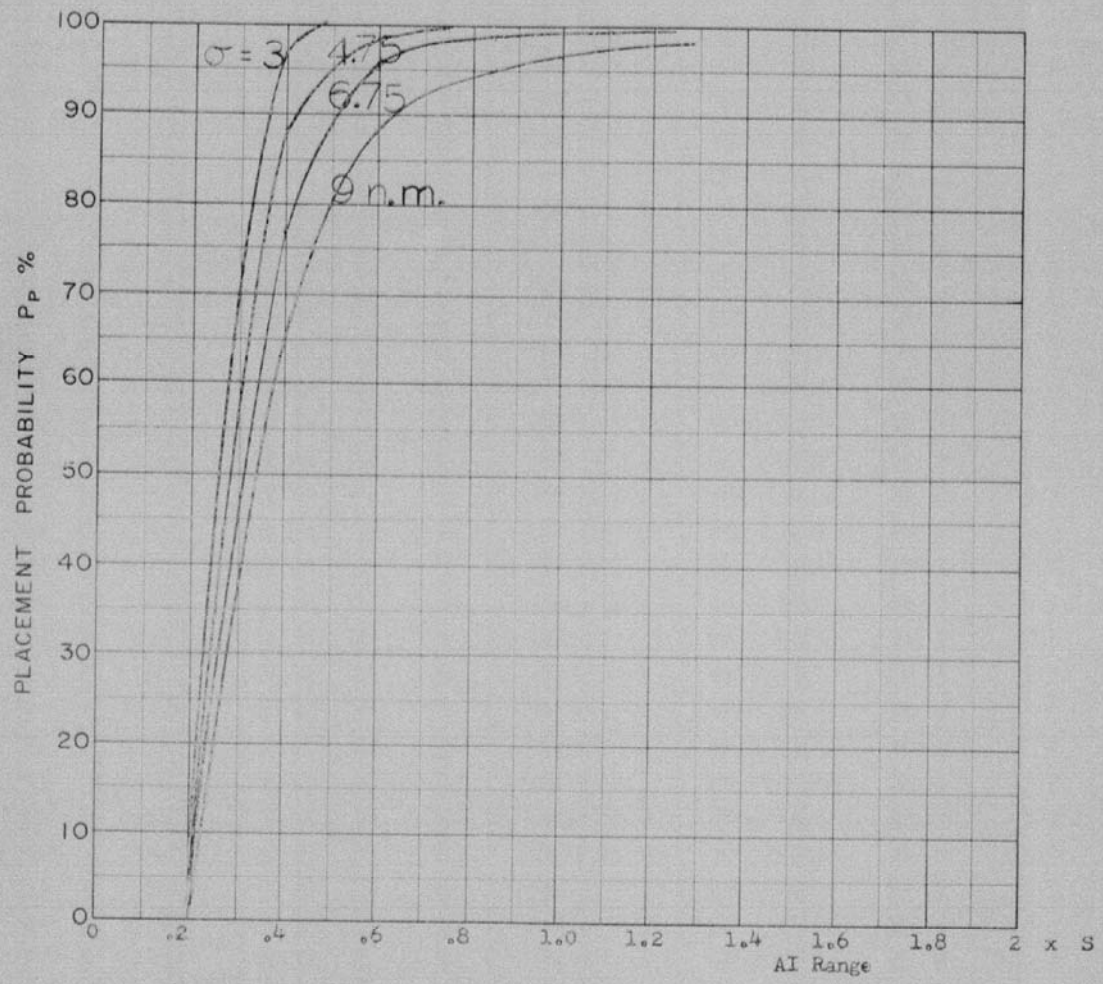

COURSE DIFFERENCE: 160°
TARGET EVASION: 0
TARGET MACH NO.: 2.0
INTERCEPTOR LATERAL G's: 3.35
INTERCEPTOR MACH NO.: 1.5
σ OF G.C.I. ACCURACY: Four values
A.I. DETECTION RANGE AS FRACTION OF SPECIFICATION RANGE, S: Abscissa
A.I. DETECTION RANGE CONTOUR: Delta
ALTITUDE: 60 K

D1096

Launch zone of figure L-5, missile launched at minimum range with 8° heading error allowance.

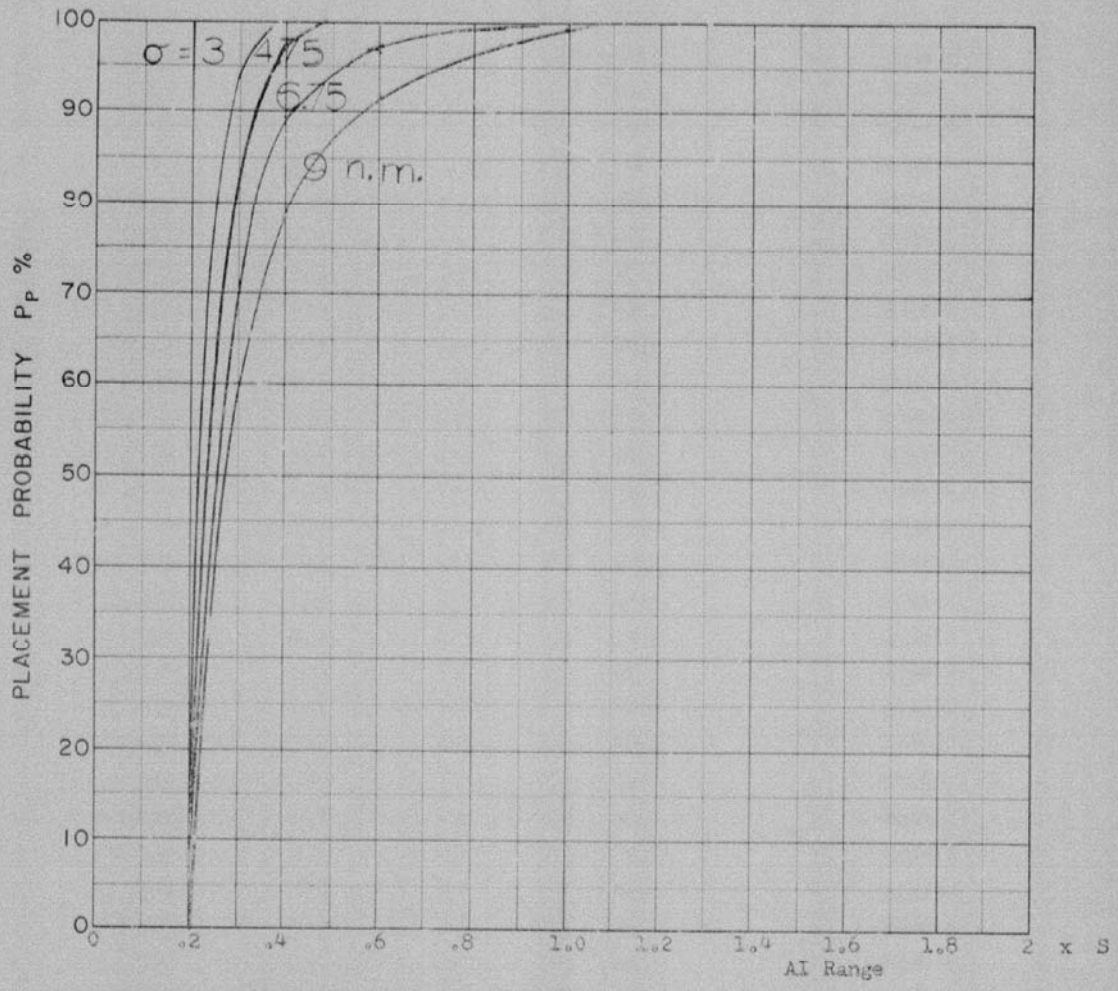

COURSE DIFFERENCE: 160°
TARGET EVASION: 0
TARGET MACH NO.: 2.0
INTERCEPTOR LATERAL G's: 3.35
INTERCEPTOR MACH NO.: 1.5
σ OF G.C.I. ACCURACY: Four values
A.I. DETECTION RANGE AS FRACTION OF SPECIFICATION RANGE, S: Abscissa
A.I. DETECTION RANGE CONTOUR: Delta
ALTITUDE: 60 K

(D109c)

Launch zone of figure L-5. missile launched at minimum range with 5° heading error allowance.

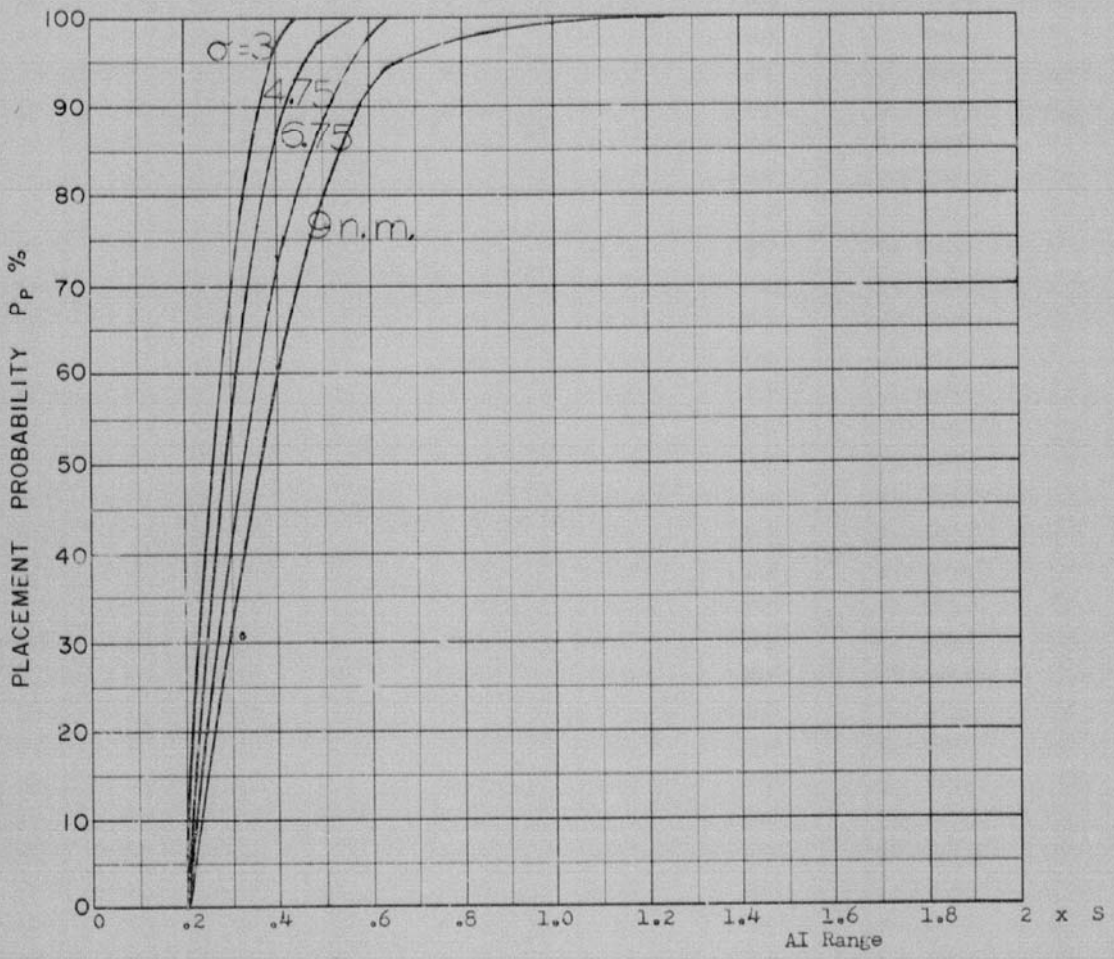

COURSE DIFFERENCE: 160°
TARGET EVASION: 0
TARGET MACH NO.: 2.0
INTERCEPTOR LATERAL G's: 3.35
INTERCEPTOR MACH NO.: 1.5
σ OF G.C.I. ACCURACY: Four values
A.I. DETECTION RANGE AS FRACTION OF SPECIFICATION RANGE, S: Abscissa
A.I. DETECTION RANGE CONTOUR: Delta
ALTITUDE: 60 K

D109d

Launch zone of figure L-6, missile launched at maximum range with 15° heading error allowance.

10 A x d p r

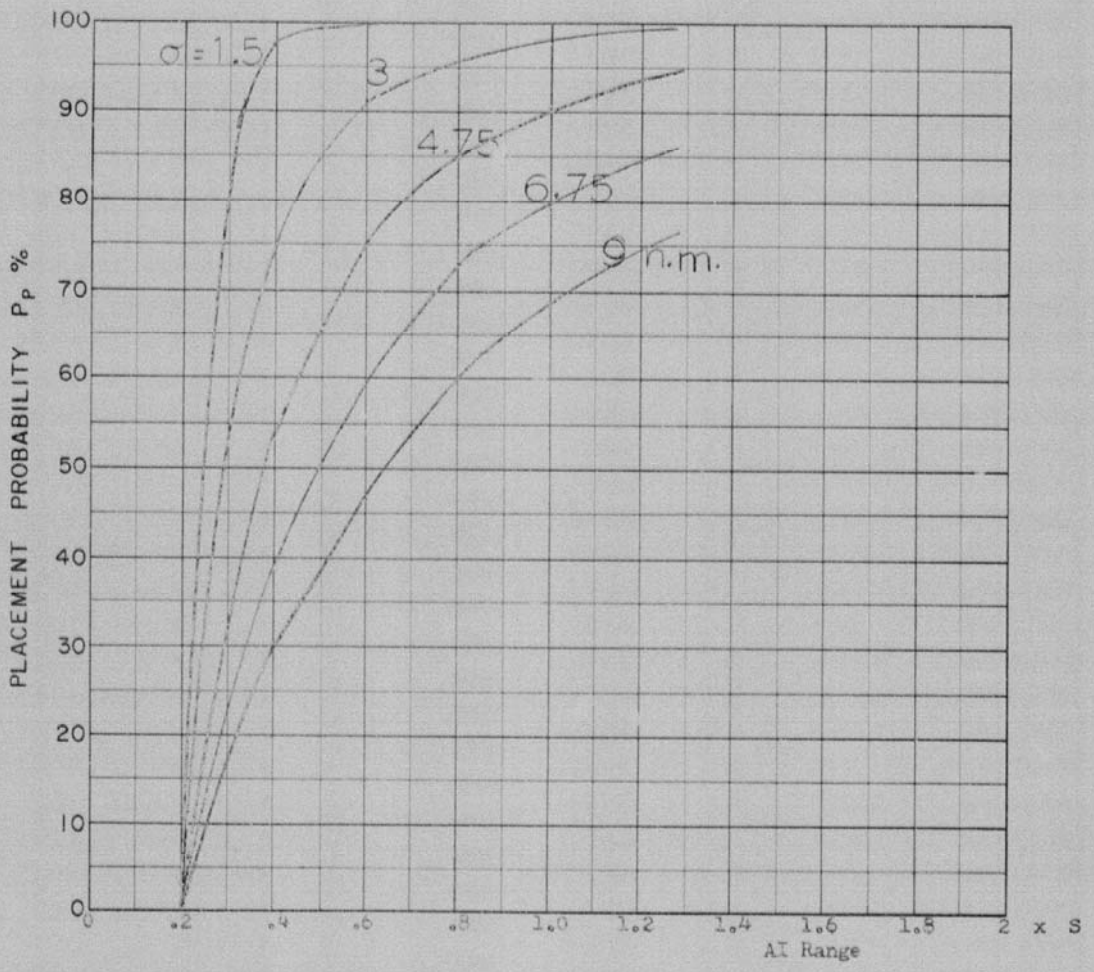

COURSE DIFFERENCE: 90°
TARGET EVASION: 0
TARGET MACH NO.: 2.0
INTERCEPTOR LATERAL G's: 1.12
INTERCEPTOR MACH NO.: 1.3
σ OF G.C.I. ACCURACY: Five values
A.I. DETECTION RANGE AS FRACTION OF SPECIFICATION RANGE, S: Abscissa
A.I. DETECTION RANGE CONTOUR: Delta
ALTITUDE: 60 K

D110b

Launch zone of figure L.5. missile launched at maximum range with 8° heading error allowance.

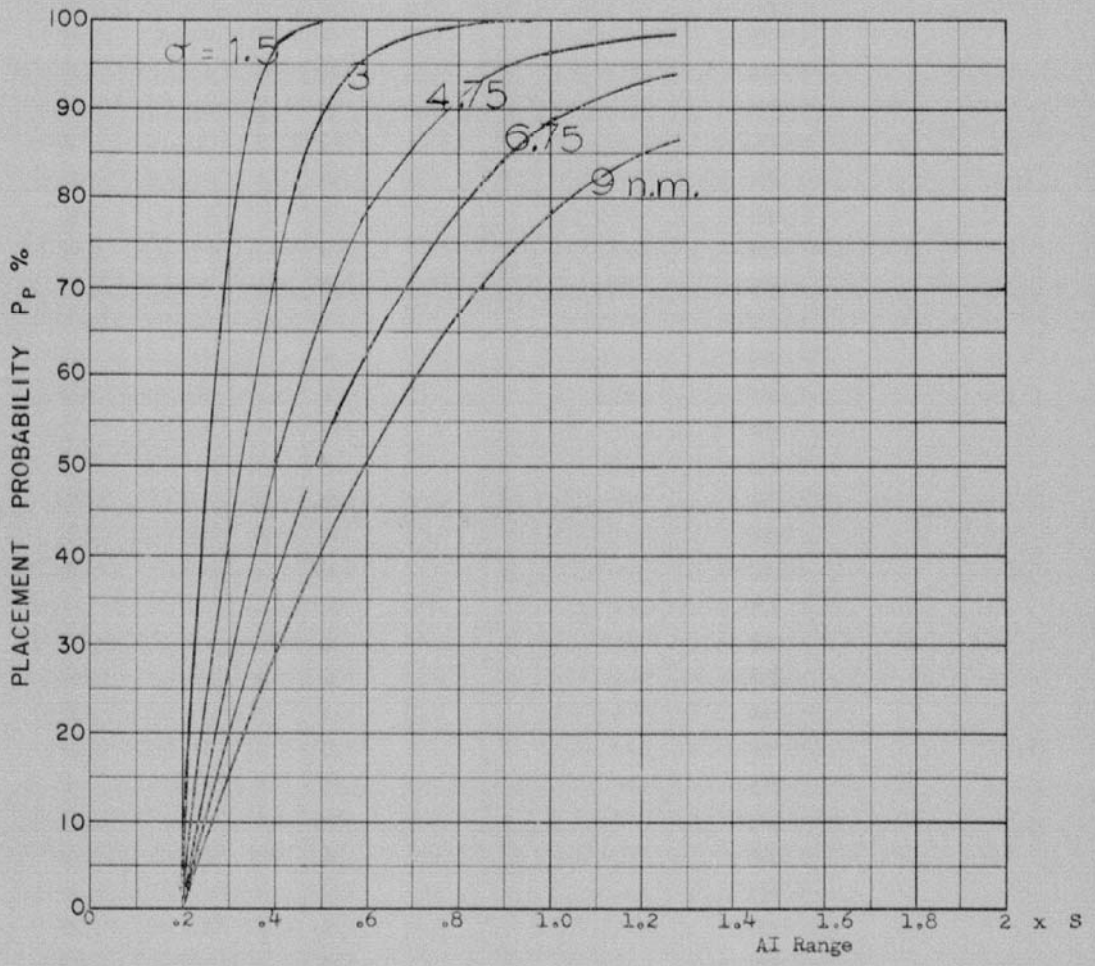

COURSE DIFFERENCE: 100°
TARGET EVASION: 0
TARGET MACH NO.: 2.0
INTERCEPTOR LATERAL G's: 1.12
INTERCEPTOR MACH NO.: 1.5
σ OF G.C.I. ACCURACY: Five values
A.I. DETECTION RANGE AS FRACTION OF SPECIFICATION RANGE, S: Abscissa
A.I. DETECTION RANGE CONTOUR: Delta
ALTITUDE: 60 K

(D111 b)

Launch zone of figure L-5, missile launched at maximum range with 8° heading error allowance.

-374-

15 b d p r

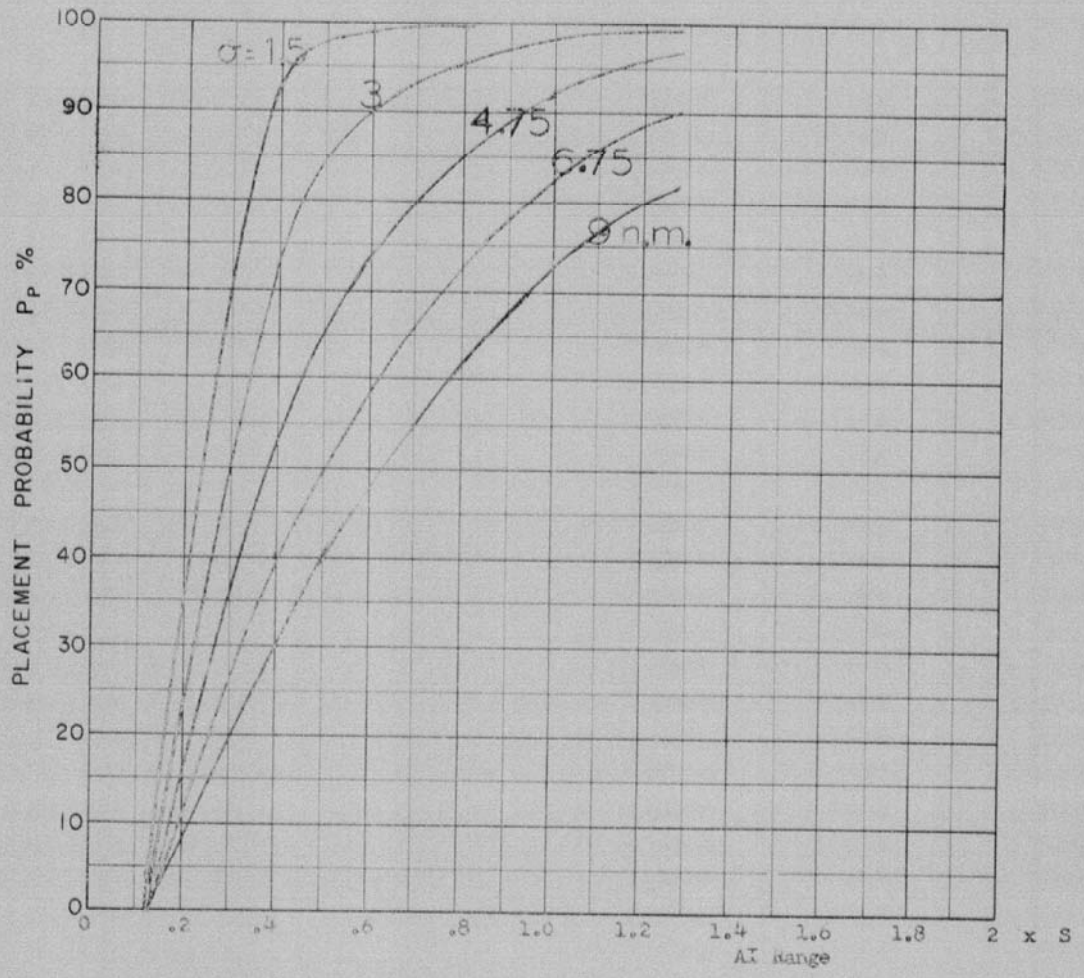

COURSE DIFFERENCE: 100°
TARGET EVASION: 0
TARGET MACH NO.: 2.0
INTERCEPTOR LATERAL G's: 1.12
INTERCEPTOR MACH NO.: 1.5
σ OF G.C.I. ACCURACY: Five values
A.I. DETECTION RANGE AS FRACTION OF SPECIFICATION RANGE, S: Abscissa
A.I. DETECTION RANGE CONTOUR: Delta
ALTITUDE: 60 K

D111c

Missile launch zone of figure L-2, missile launched at minimum range with 8° heading error allowance.

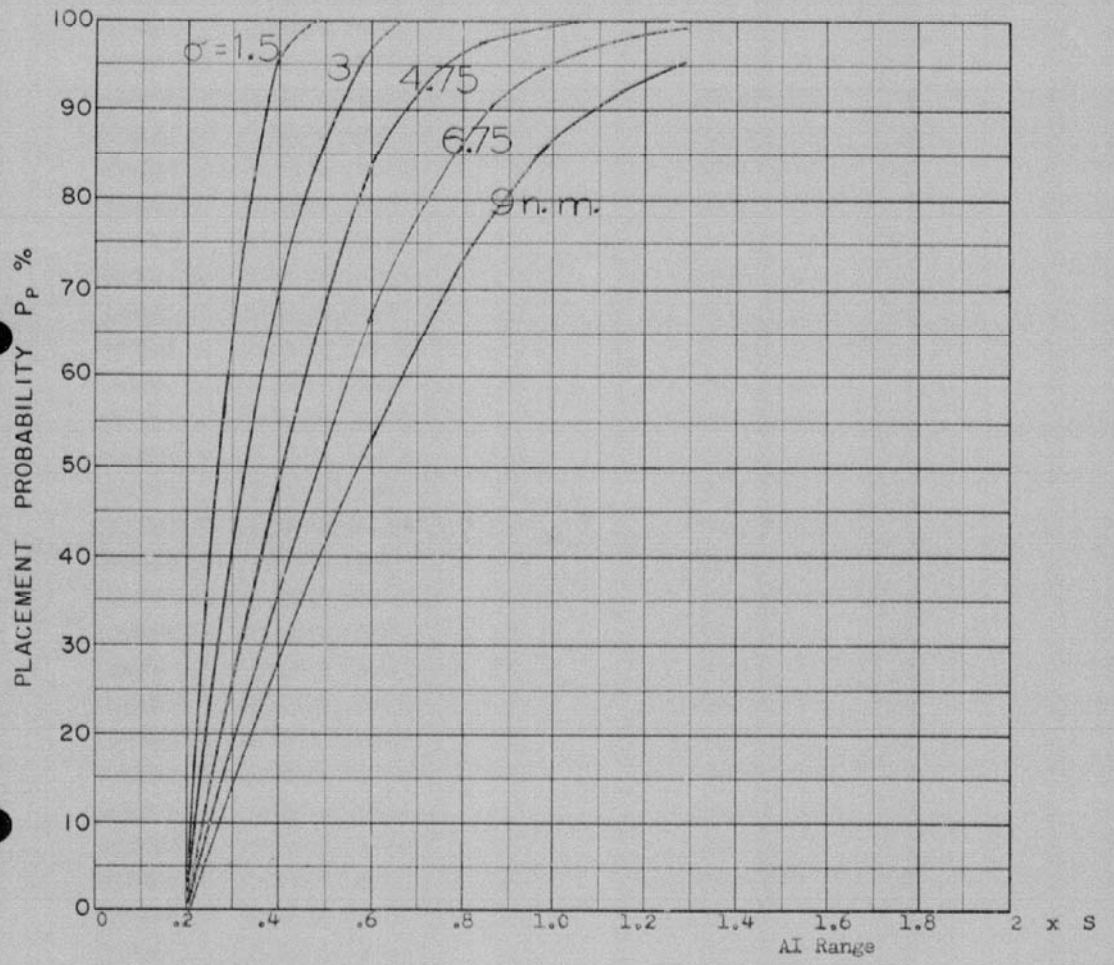

COURSE DIFFERENCE: 120°
TARGET EVASION: 0
TARGET MACH NO.: 2.0
INTERCEPTOR LATERAL G's: 1.12
INTERCEPTOR MACH NO.: 1.5
σ OF G.C.I. ACCURACY: Five values
A.I. DETECTION RANGE AS FRACTION OF SPECIFICATION RANGE, S: Abscissa
A.I. DETECTION RANGE CONTOUR: Delta
ALTITUDE: 60 K

D112b

Launch zone of figure L-5. missile launched at maximum range with 8° heading error allowance.

10 d x d p r

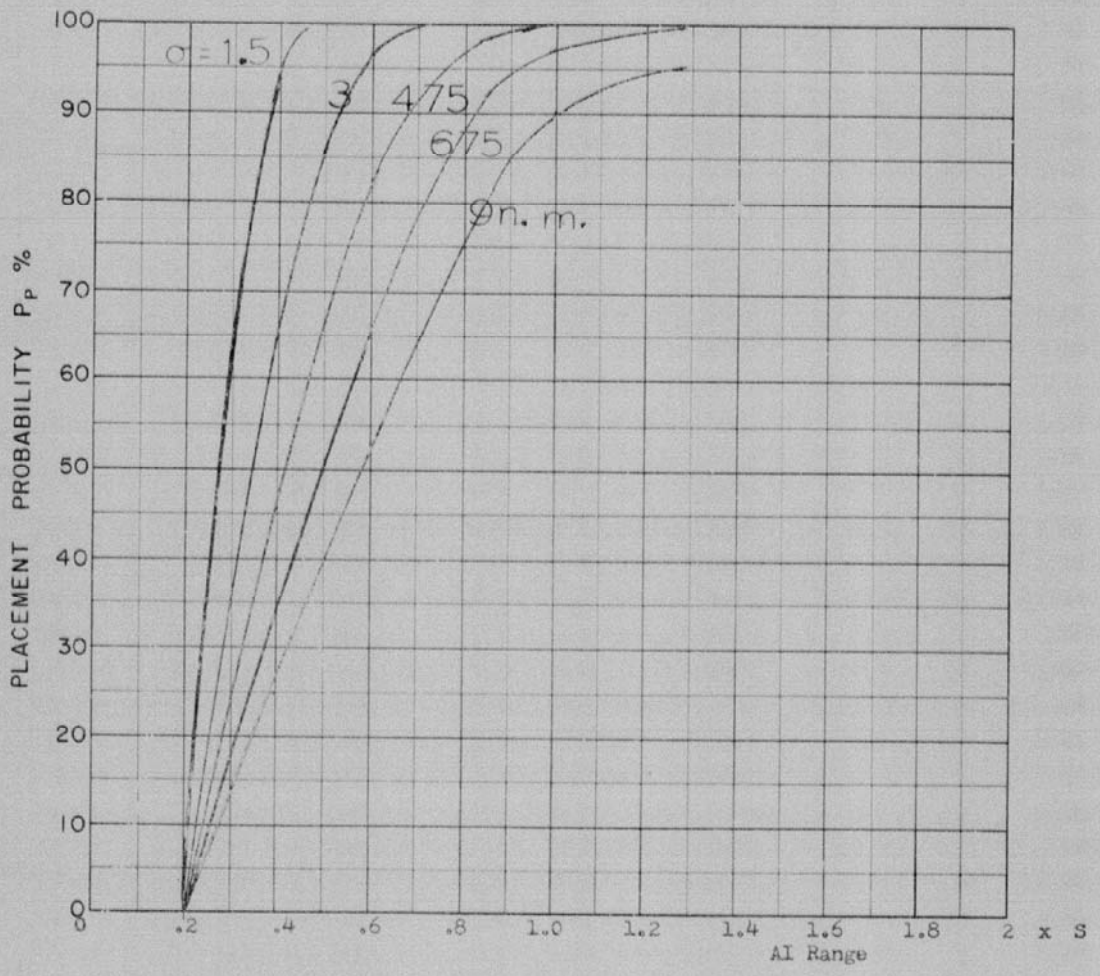

COURSE DIFFERENCE: 135°
TARGET EVASION: 0
TARGET MACH NO.: 2.0
INTERCEPTOR LATERAL G's: 1.12
INTERCEPTOR MACH NO.: 1.5
σ OF G.C.I. ACCURACY: Five values
A.I. DETECTION RANGE AS FRACTION OF SPECIFICATION RANGE, S: Abscissa
A.I. DETECTION RANGE CONTOUR: Delta
ALTITUDE: 60 K

D1136

Launch zone of figure L-5, missile launched at maximum range with 8° heading error allowance.

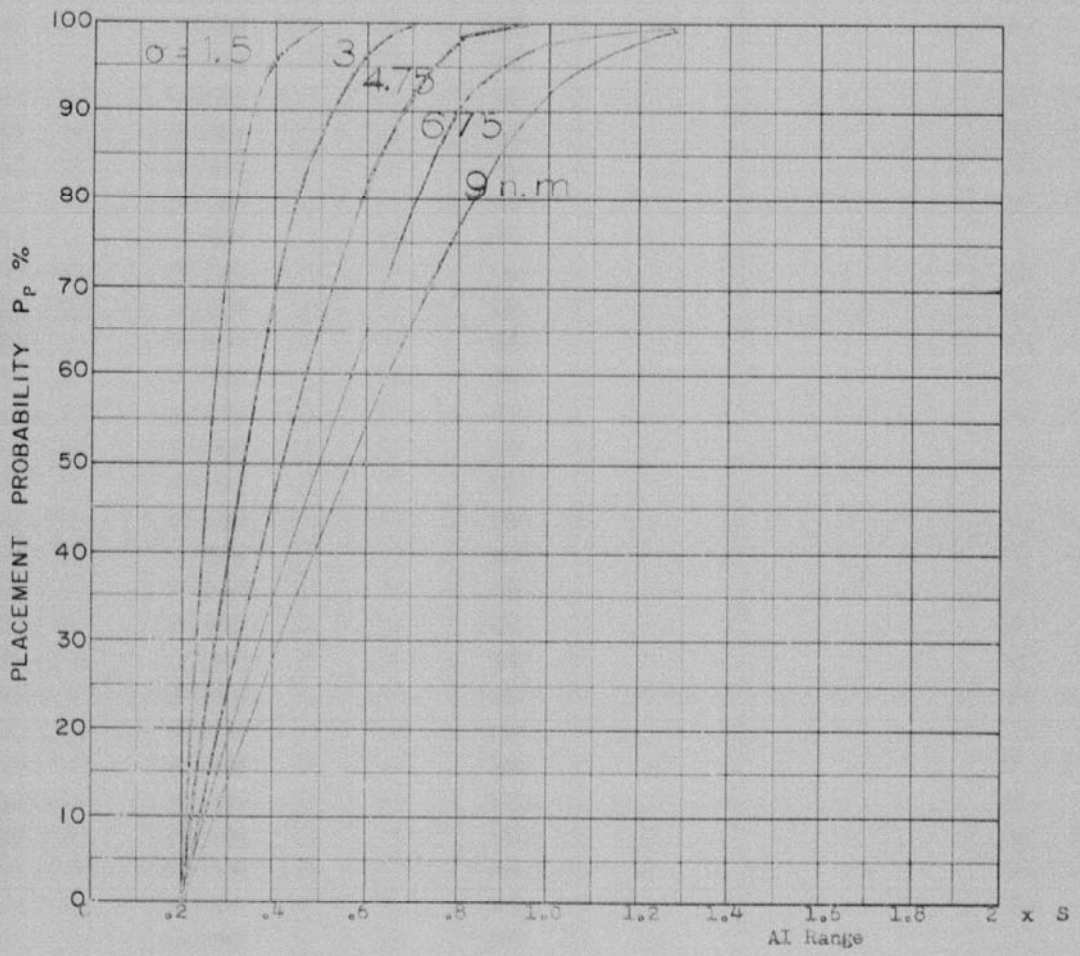

COURSE DIFFERENCE: 160°
TARGET EVASION: C
TARGET MACH NO.: 2.0
INTERCEPTOR LATERAL G's: 2.12
INTERCEPTOR MACH NO.: 1.5
σ OF G.C.I. ACCURACY: Five values
A.I. DETECTION RANGE AS FRACTION OF SPECIFICATION RANGE, S: Abscissa
A.I. DETECTION RANGE CONTOUR: Delta
ALTITUDE: 60 K

D1146

Launch zone of figure L-5, missile launched at maximum range with 8° heading error allowance.

127 dpr

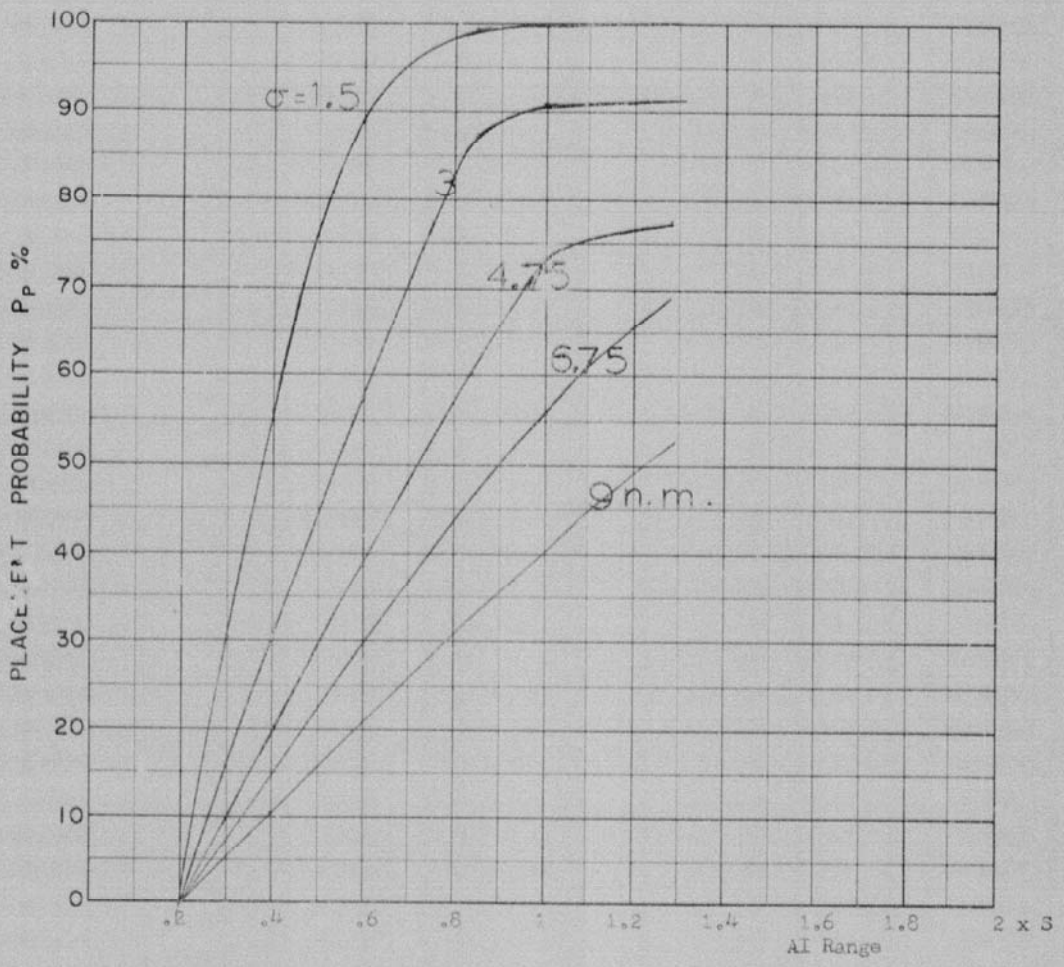

COURSE DIFFERENCE: 110°
TARGET EVASION: 0.1 lateral g's
TARGET MACH NO.: 2.0
INTERCEPTOR LATERAL G's: 0.66
INTERCEPTOR MACH NO.: 1.5
σ OF G.C.I. ACCURACY: 5 values
A.I. DETECTION RANGE AS FRACTION OF SPECIFICATION RANGE, S: Abscissa
A.I. DETECTION RANGE CONTOUR: Delta
ALTITUDE: 60 K

Missile launch zone L-1!

D115

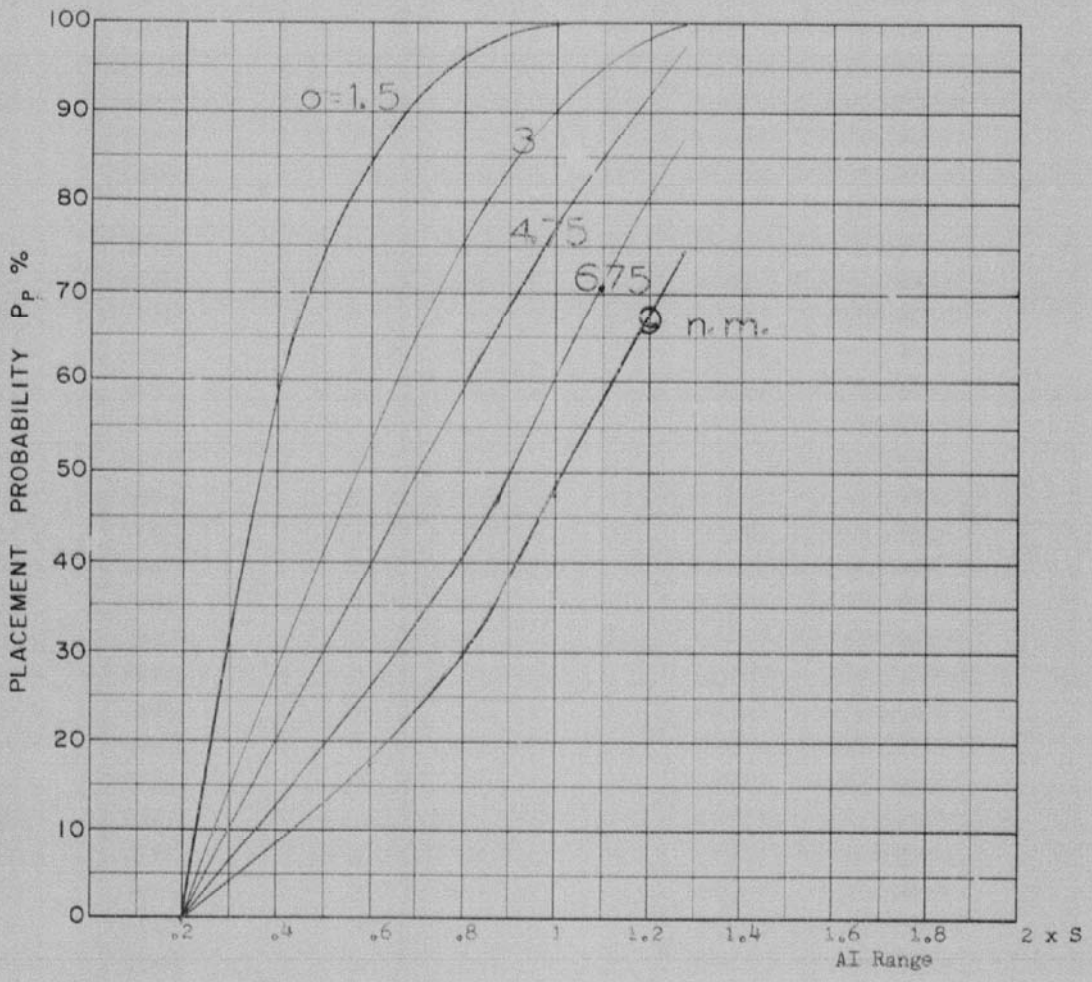

COURSE DIFFERENCE: 135°
TARGET EVASION: 0.1 lateral g's
TARGET MACH NO.: 2.0
INTERCEPTOR LATERAL G's: 0.66
INTERCEPTOR MACH NO.: 1.5
σ OF G.C.I. ACCURACY: 5 values
A.I. DETECTION RANGE AS FRACTION OF SPECIFICATION RANGE, S: Abscissa
A.I. DETECTION RANGE CONTOUR: Delta
ALTITUDE: 60 K

Missile launch zone L-11

D116

131 dpr

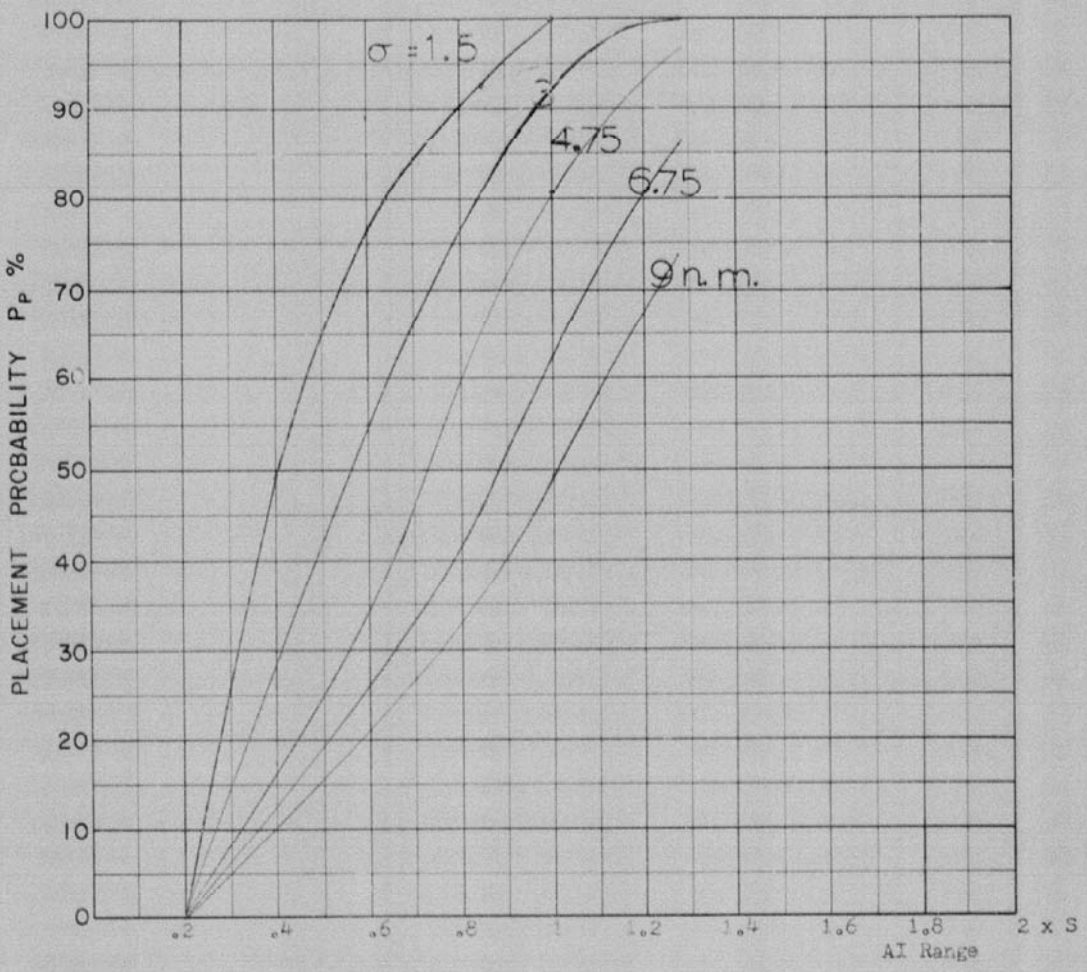

COURSE DIFFERENCE: 160°
TARGET EVASION: 0.1 lateral g's
TARGET MACH NO.: 2.0
INTERCEPTOR LATERAL G's: 0.66
INTERCEPTOR MACH NO.: 1.5
σ OF G.C.I. ACCURACY: 5 values
A.I. DETECTION RANGE AS FRACTION OF SPECIFICATION RANGE, S: Abscissa
A.I. DETECTION RANGE CONTOUR: Delta
ALTITUDE: 60 K

Missile launch zone L-11

D117

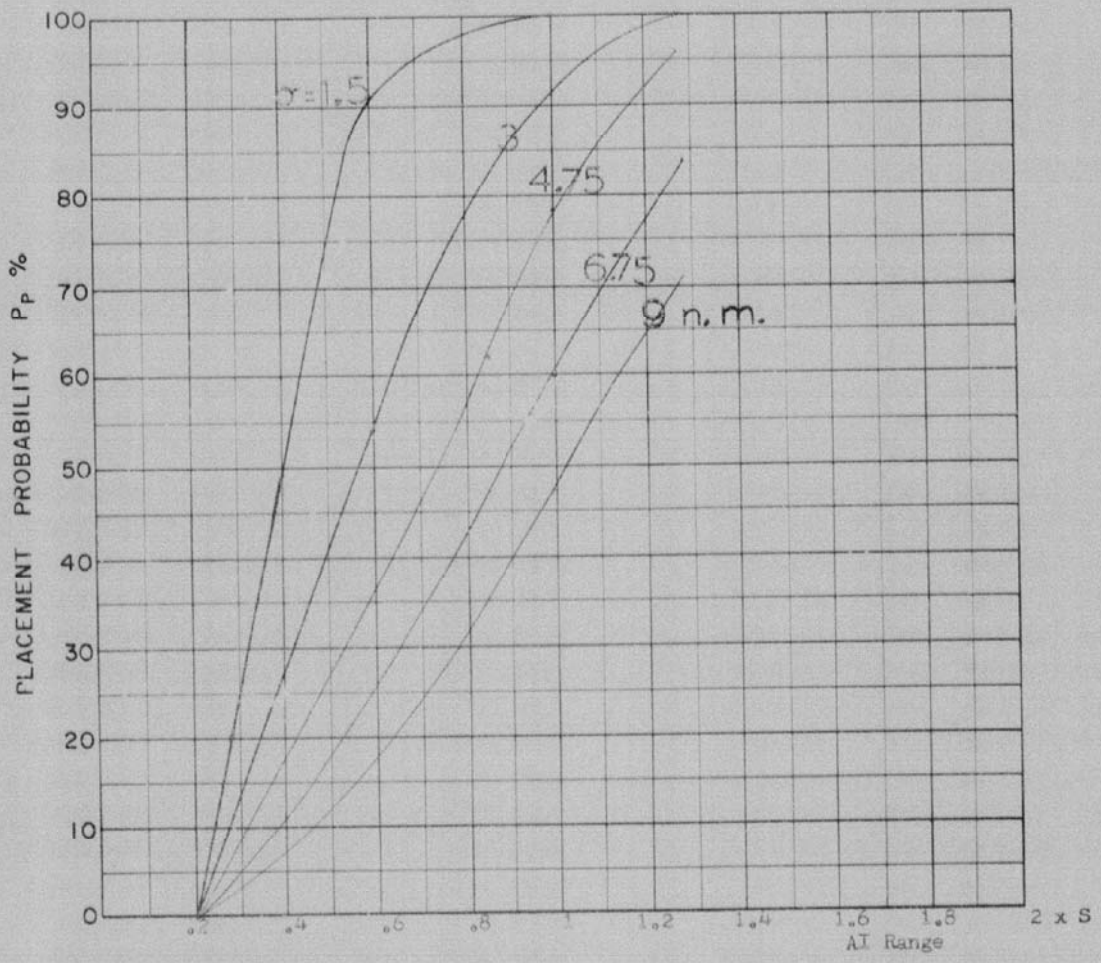

COURSE DIFFERENCE: 180°
TARGET EVASION: 0.1 lateral g's
TARGET MACH NO.: 2.0
INTERCEPTOR LATERAL G's: 0.66
INTERCEPTOR MACH NO.: 1.5
σ OF G.C.I. ACCURACY: 5 values
A.I. DETECTION RANGE AS FRACTION OF SPECIFICATION RANGE, S: Abscissa
A.I. DETECTION RANGE CONTOUR: Delta
ALTITUDE: 60 K

D118

Missile launch zone figure L-11

138 dpr

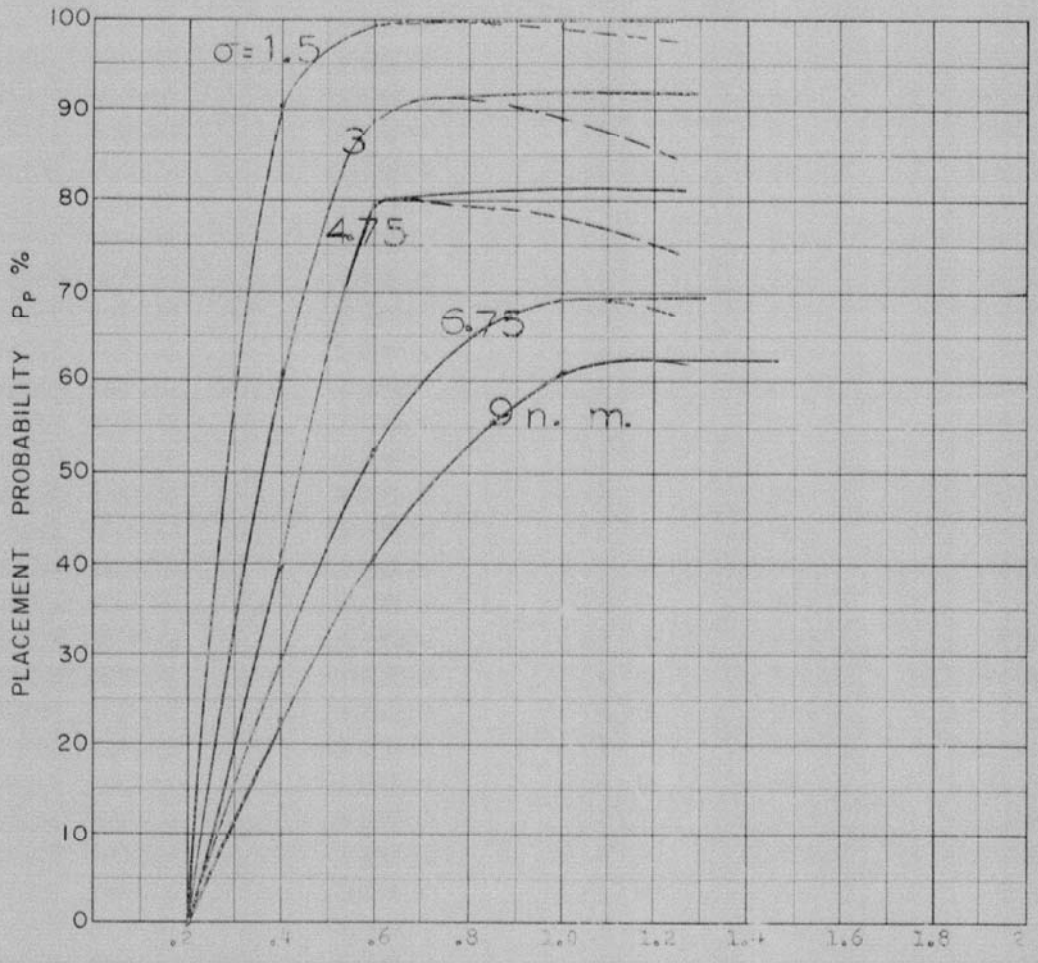

COURSE DIFFERENCE: 110°
TARGET EVASION: 0.1 lateral g's
TARGET MACH NO.: 2.0
INTERCEPTOR LATERAL G's: 1.5
INTERCEPTOR MACH NO.: 1.5
σ OF G.C.I. ACCURACY: five values
A.I. DETECTION RANGE AS FRACTION OF SPECIFICATION RANGE, S: Abscissa
A.I. DETECTION RANGE CONTOUR: Delta
ALTITUDE: 60K

D119a

Missile launch zone figure L11

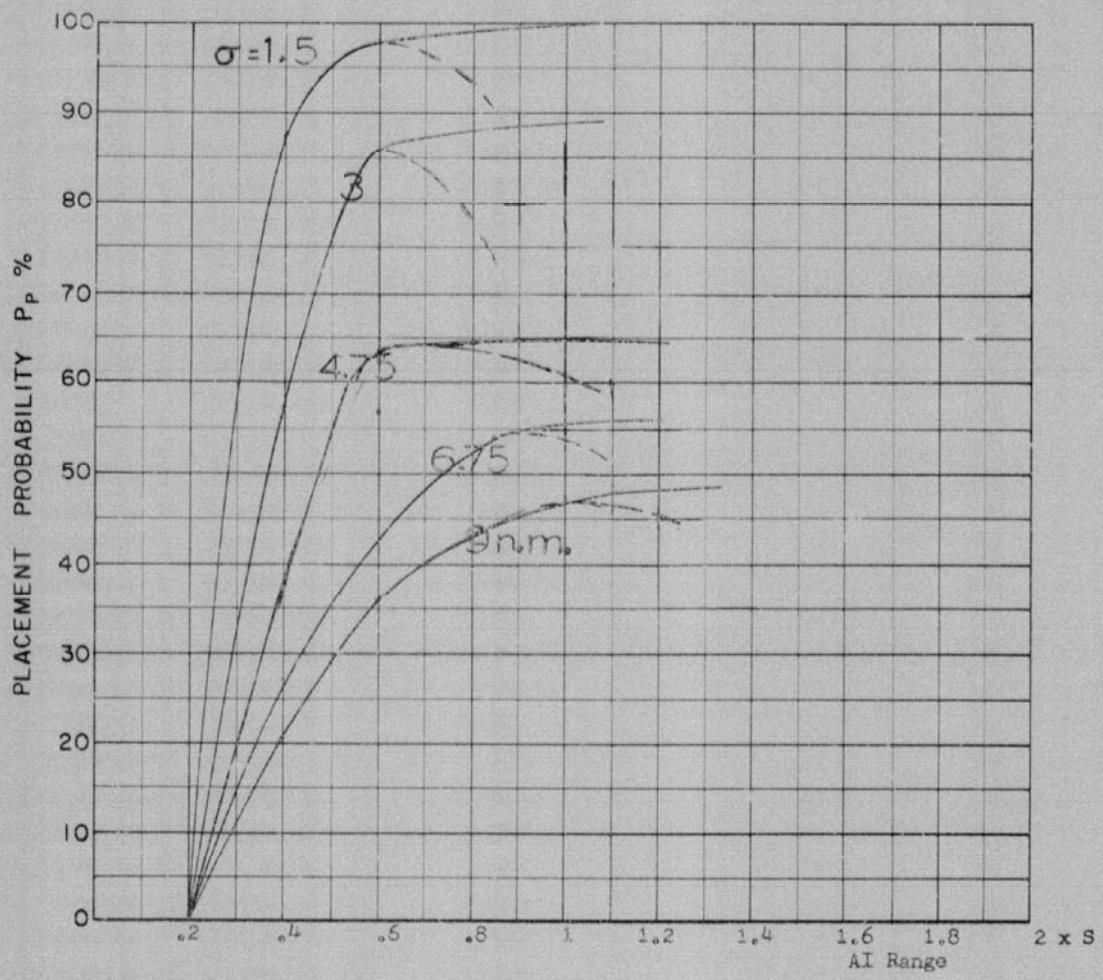

COURSE DIFFERENCE: 110°
TARGET EVASION: 0.2 lateral g's
TARGET MACH NO.: 2.0
INTERCEPTOR LATERAL G's: 1.5
INTERCEPTOR MACH NO.: 1.5
σ OF G.C.I. ACCURACY: Five values
A.I. DETECTION RANGE AS FRACTION OF SPECIFICATION RANGE, S Abscissa
A.I. DETECTION RANGE CONTOUR: Delta
ALTITUDE: 60 K

D1196

Missile launch zone figure L-11

140 dpr

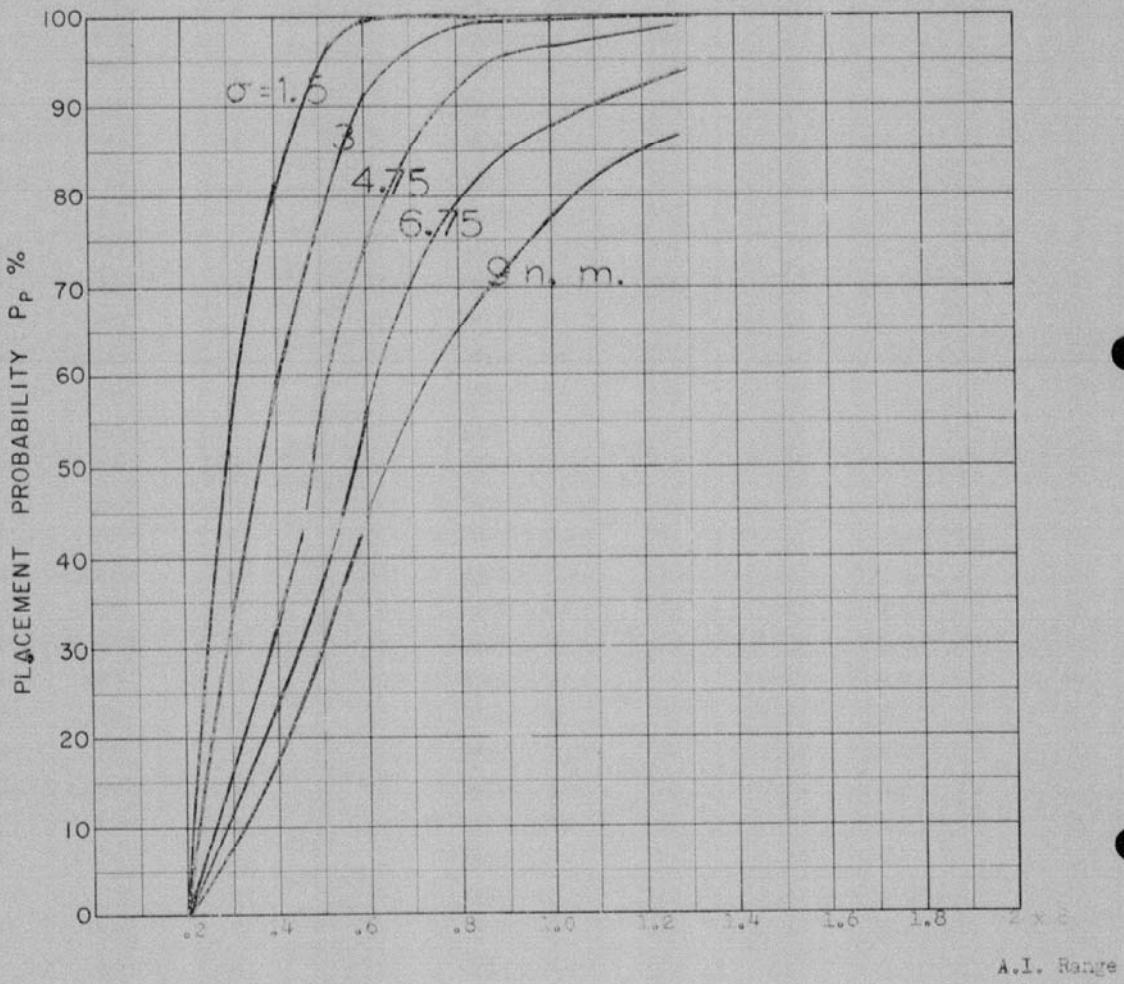

COURSE DIFFERENCE: 140°
TARGET EVASION: 0.1 lateral g's
TARGET MACH NO.: 2.0
INTERCEPTOR LATERAL G's: 1.5
INTERCEPTOR MACH NO.: 1.5
σ OF G.C.I. ACCURACY: 5 values
A.I. DETECTION RANGE AS FRACTION OF SPECIFICATION RANGE, S: abscissa
A.I. DETECTION RANGE CONTOUR: Delta
ALTITUDE: 60K

D120

Missile launch zone L 11

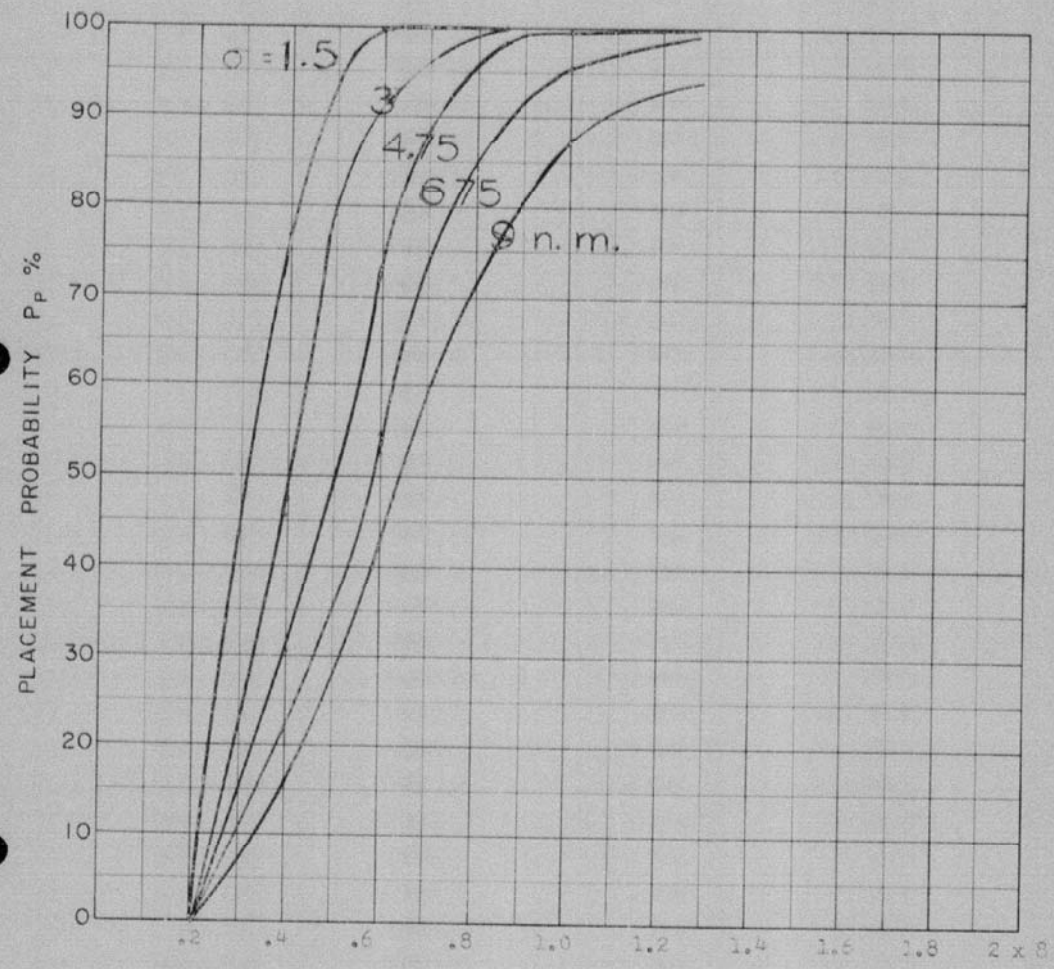

COURSE DIFFERENCE: 160°
TARGET EVASION: 0.1 lateral g's
TARGET MACH NO.: 2.0
INTERCEPTOR LATERAL G's: 1.5
INTERCEPTOR MACH NO.: 1.5
σ OF G.C.I. ACCURACY: five values
A.I. DETECTION RANGE AS FRACTION OF SPECIFICATION RANGE, S: abscissa
A.I. DETECTION RANGE CONTOUR: Delta
ALTITUDE: 60K

D121a

Missile launch zone L 11

136 dpr

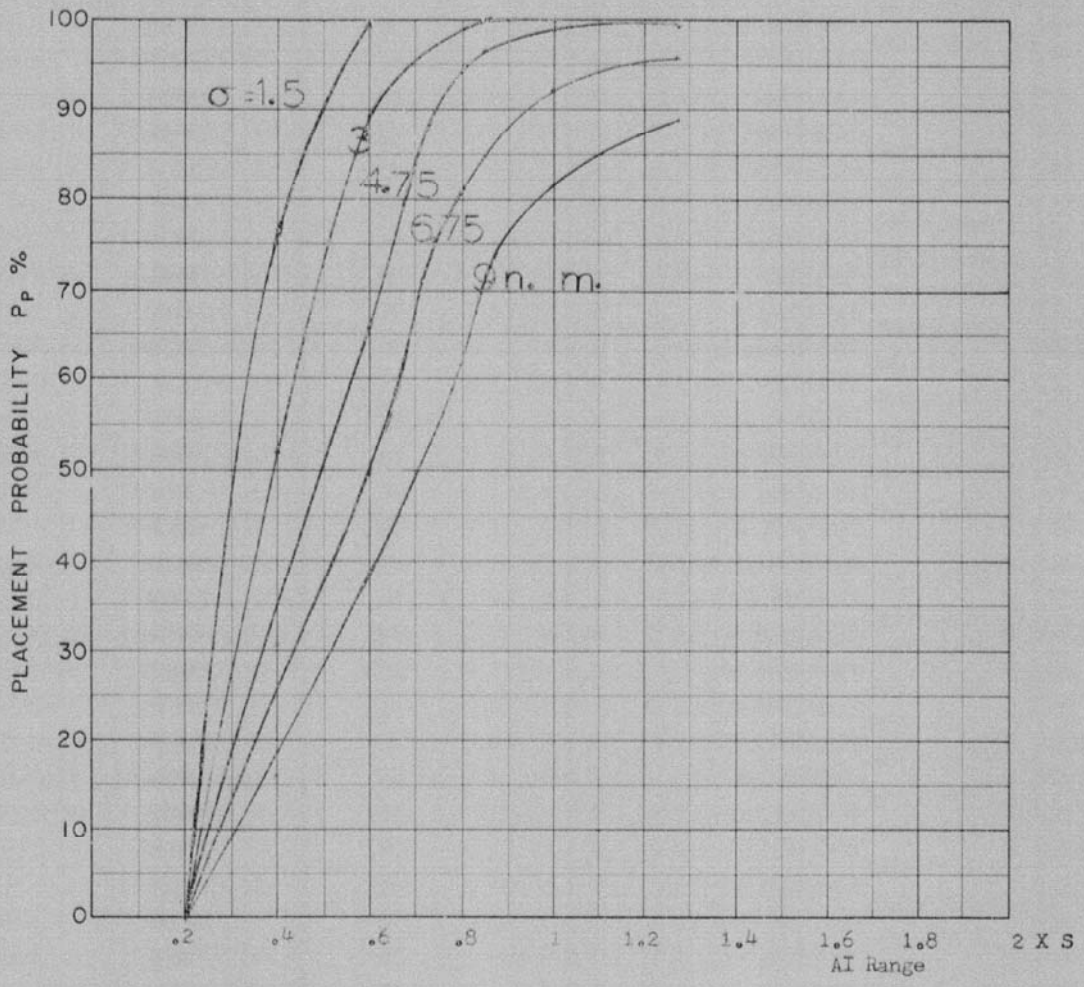

COURSE DIFFERENCE: 160°
TARGET EVASION: 0.2 lateral g's
TARGET MACH NO.: 2.0
INTERCEPTOR LATERAL G's: 1.5
INTERCEPTOR MACH NO.: 1.5
σ OF G.C.I. ACCURACY: Five values
A.I. DETECTION RANGE AS FRACTION OF SPECIFICATION RANGE, S: Abscissa
A.I. DETECTION RANGE CONTOUR: Delta
ALTITUDE: 60 K

D121b

Missile launch zone figure L-11

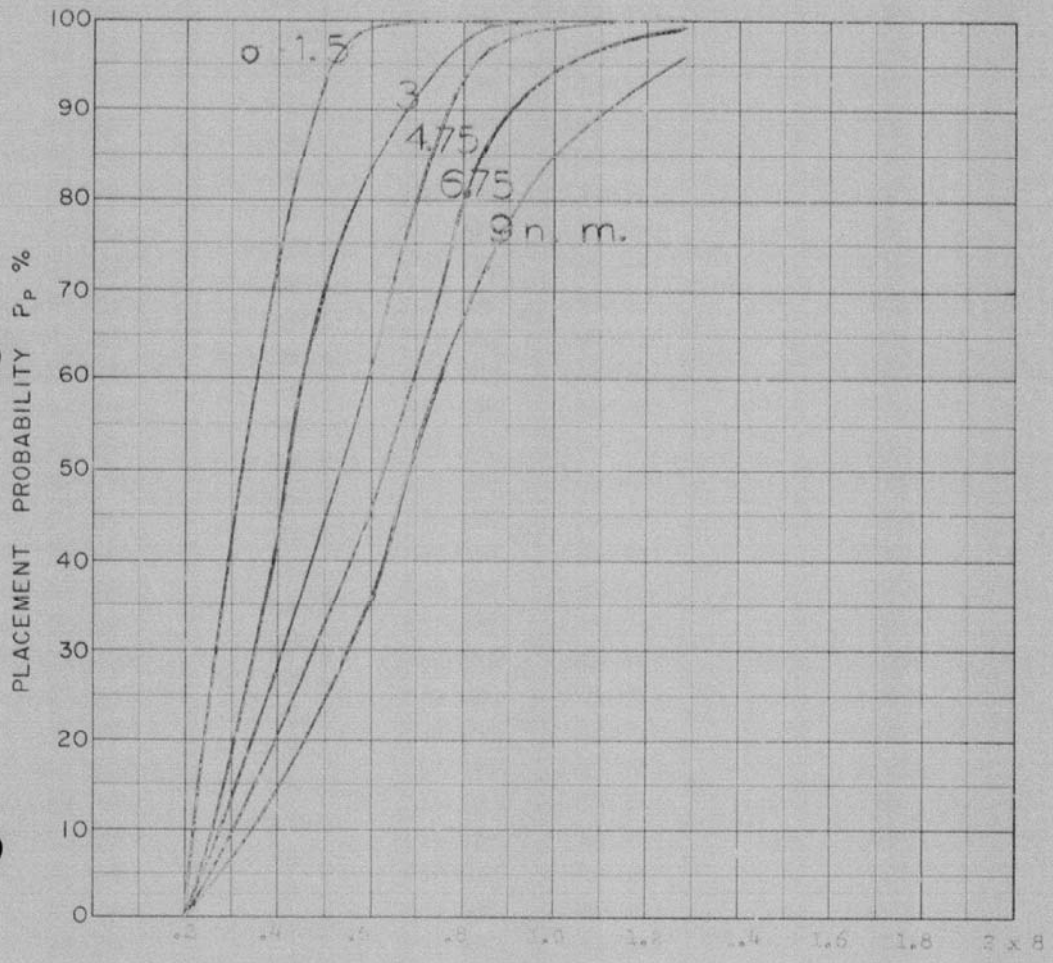

COURSE DIFFERENCE: 180°
TARGET EVASION: 0.1 lateral g's
TARGET MACH NO.: 2.0
INTERCEPTOR LATERAL G's: 4.5
INTERCEPTOR MACH NO.: 1.5
σ OF G.C.I. ACCURACY: five values
A.I. DETECTION RANGE AS FRACTION OF SPECIFICATION RANGE, S: abscissa
A.I. DETECTION RANGE CONTOUR: Delta
ALTITUDE: 60K

Missile launch zone L 11

D122

145 dpr

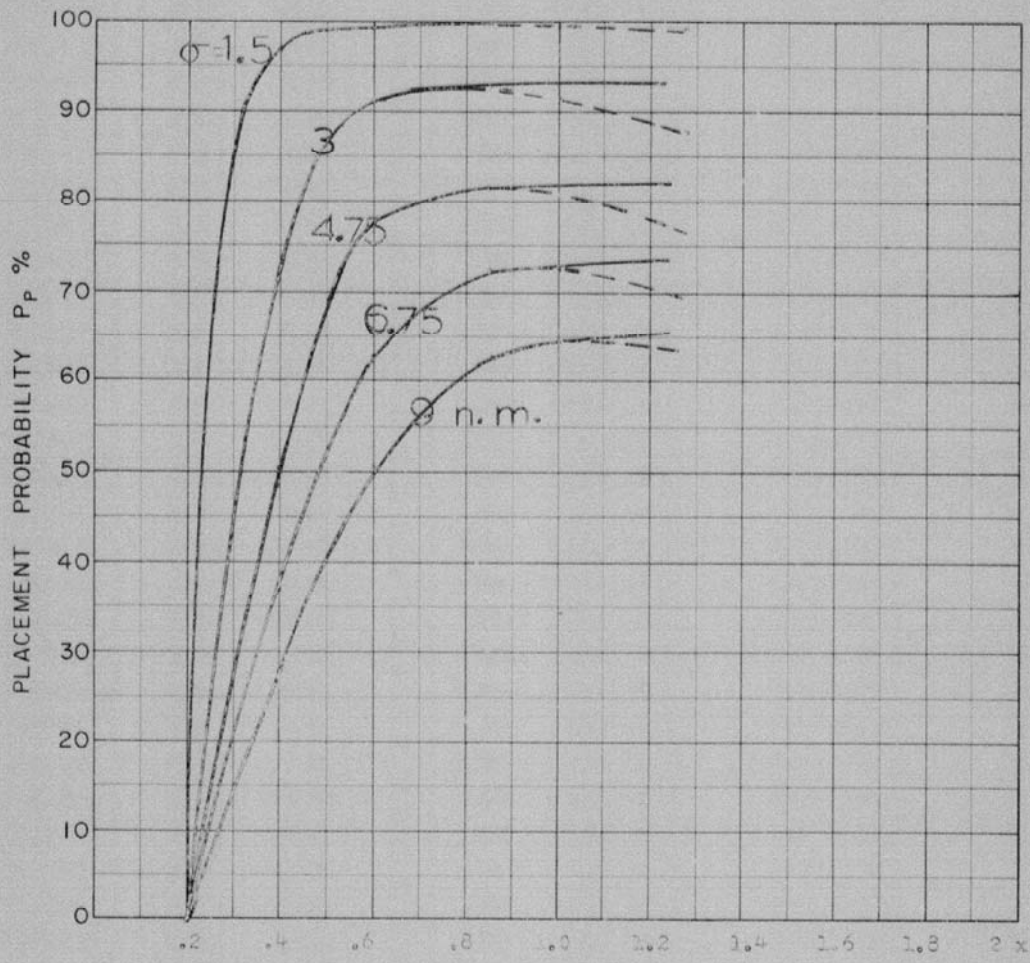

COURSE DIFFERENCE: 110°
TARGET EVASION: 0.1 lateral g's
TARGET MACH NO.: 2.0
INTERCEPTOR LATERAL G's: 2.4
INTERCEPTOR MACH NO.: 1.5
σ OF G.C.I. ACCURACY: Five values
A.I. DETECTION RANGE AS FRACTION OF SPECIFICATION RANGE, S: abscissa
A.I. DETECTION RANGE CONTOUR: Delta
ALTITUDE: 60K

D123

Missile launch zone L 11

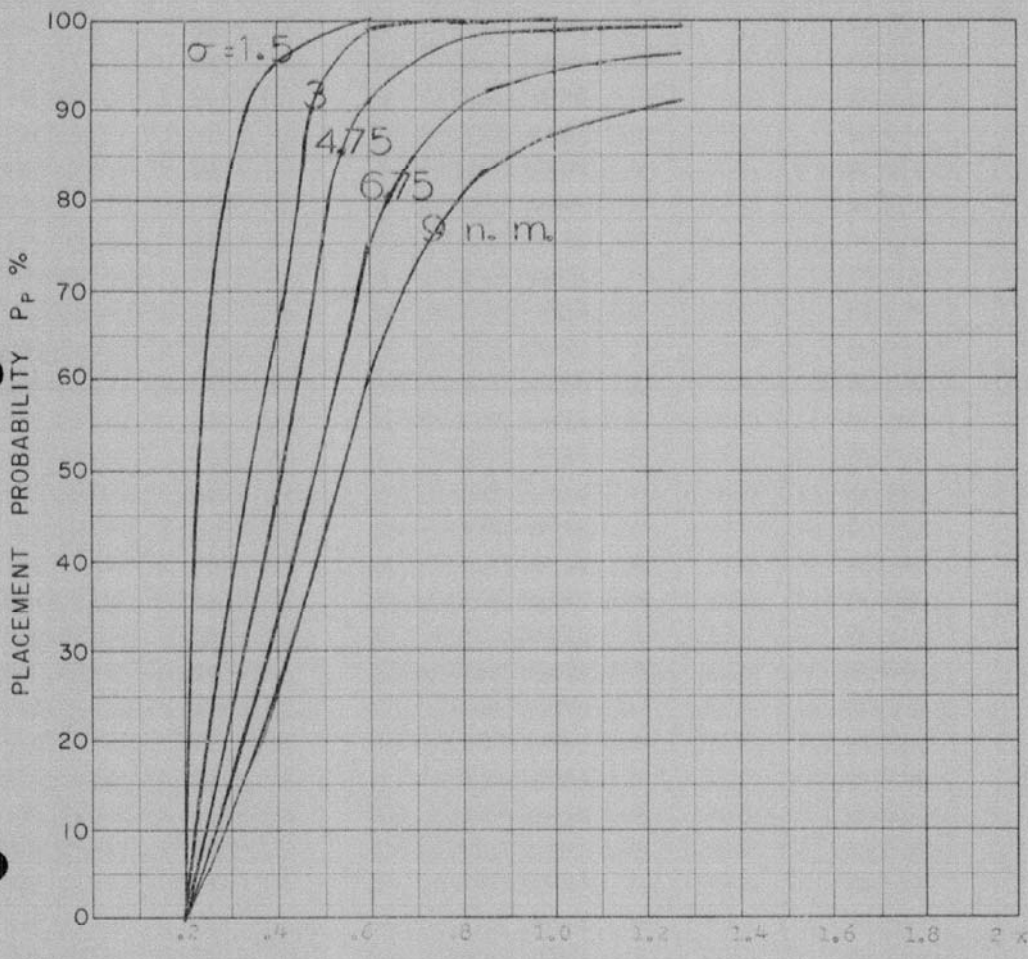

COURSE DIFFERENCE: 135°
TARGET EVASION: 0.2 lateral g's
TARGET MACH NO.: 1.0
INTERCEPTOR LATERAL G's: 2.4
INTERCEPTOR MACH NO.: 1.5
σ OF G.C.I. ACCURACY: Five values
A.I. DETECTION RANGE AS FRACTION OF SPECIFICATION RANGE, S: abscissa
A.I. DETECTION RANGE CONTOUR: Delta
ALTITUDE: 60K

D124

Missile launch zone L 11

149 dpr

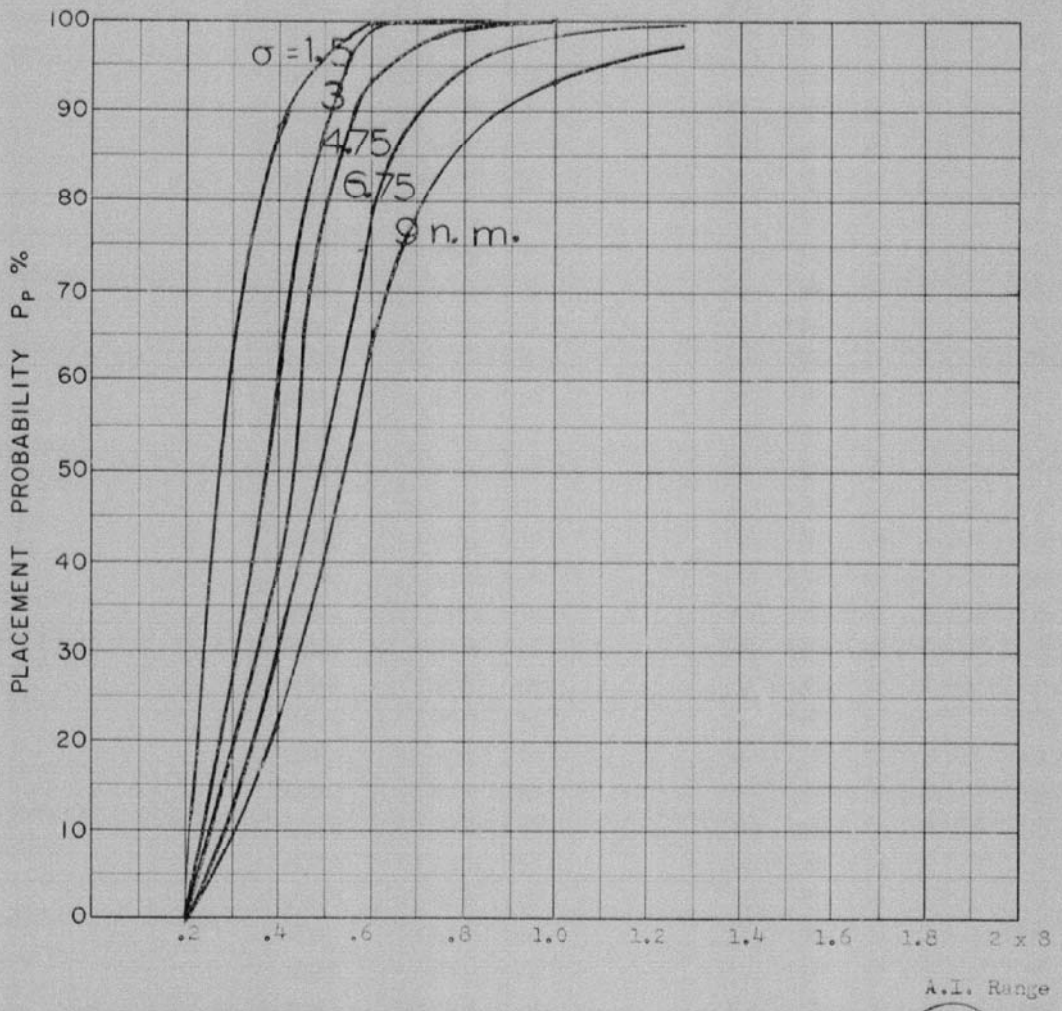

COURSE DIFFERENCE: 160°
TARGET EVASION: 0.1
TARGET MACH NO.: 2.0
INTERCEPTOR LATERAL G's: 2.4
INTERCEPTOR MACH NO.: 1.5
σ OF G.C.I. ACCURACY: five values
A.I. DETECTION RANGE AS FRACTION OF SPECIFICATION RANGE, S: abscissa
A.I. DETECTION RANGE CONTOUR: Delta
ALTITUDE: 60K

D125

Missile launch zone L 11

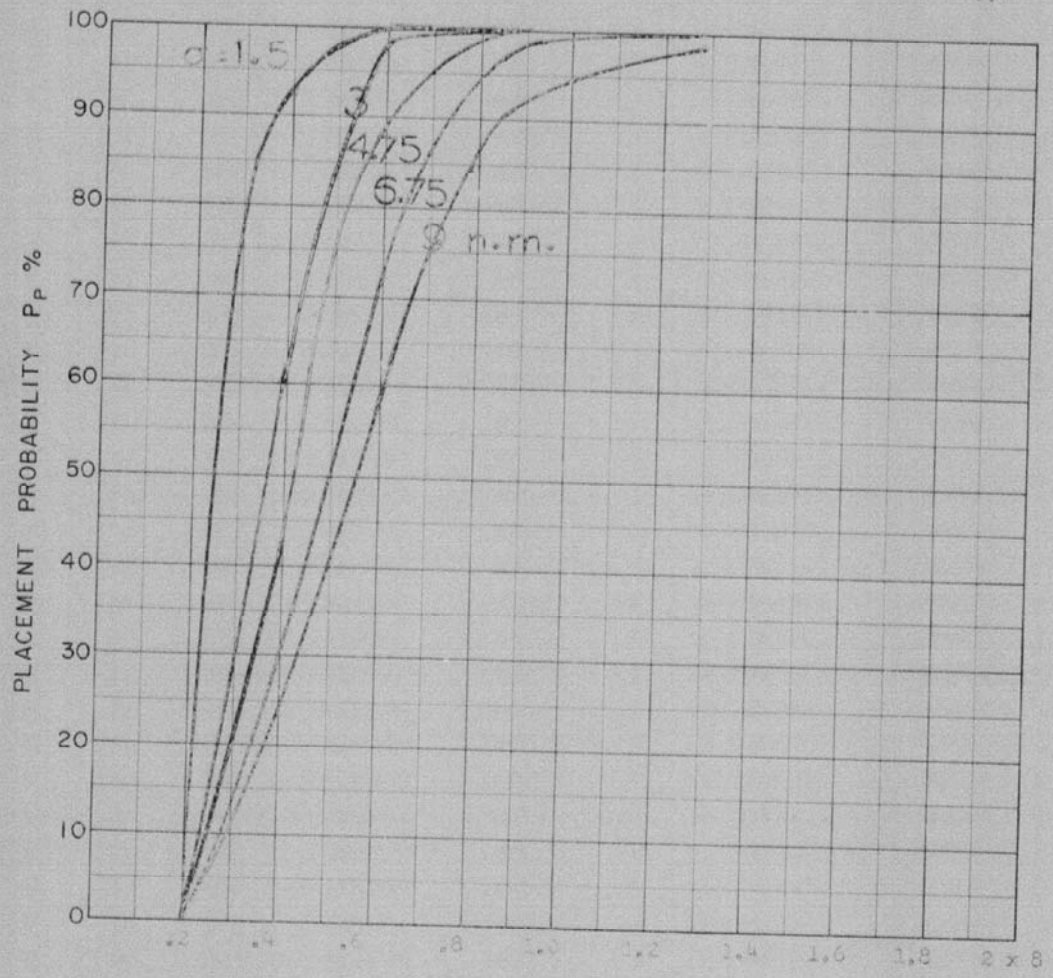

COURSE DIFFERENCE: 180°
TARGET EVASION: 0.1 lateral g's
TARGET MACH NO.: 2.0
INTERCEPTOR LATERAL G's: 2.4
INTERCEPTOR MACH NO.: 1.5
σ OF G.C.I. ACCURACY: five values
A.I. DETECTION RANGE AS FRACTION OF SPECIFICATION RANGE, S: abscissa
A.I. DETECTION RANGE CONTOUR: Del-a
ALTITUDE: 60K

Missile launch zone L 11

D126

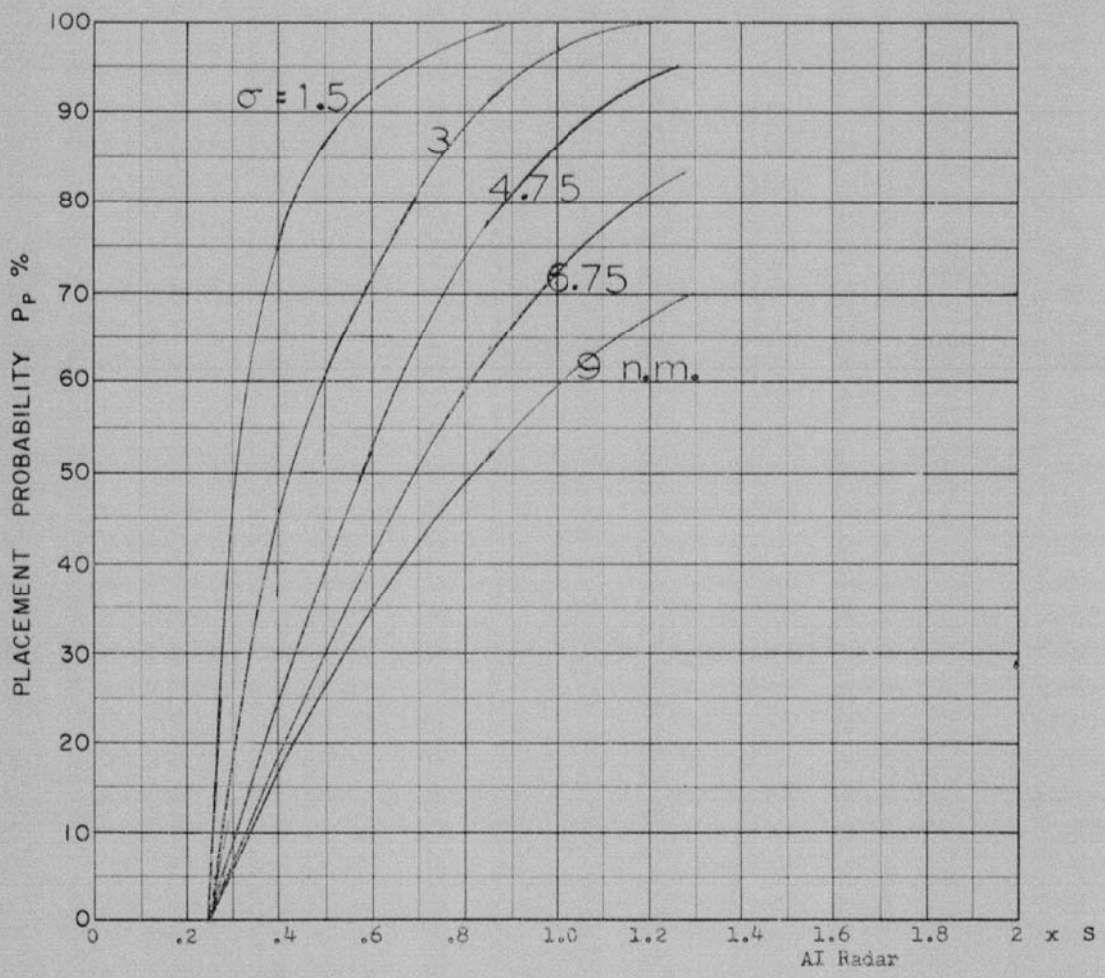

COURSE DIFFERENCE: 75°
TARGET EVASION: 0
TARGET MACH NO.: 2.0
INTERCEPTOR LATERAL G's: 0.66
INTERCEPTOR MACH NO.: 1.8
σ OF G.C.I. ACCURACY: Five values
A.I. DETECTION RANGE AS FRACTION OF SPECIFICATION RANGE, S: Abscissa
A.I. DETECTION RANGE CONTOUR: Delta
ALTITUDE: 60 K

D127a

Launch zone figure L-8, missile launched at minimum range with 8° heading error allowance.

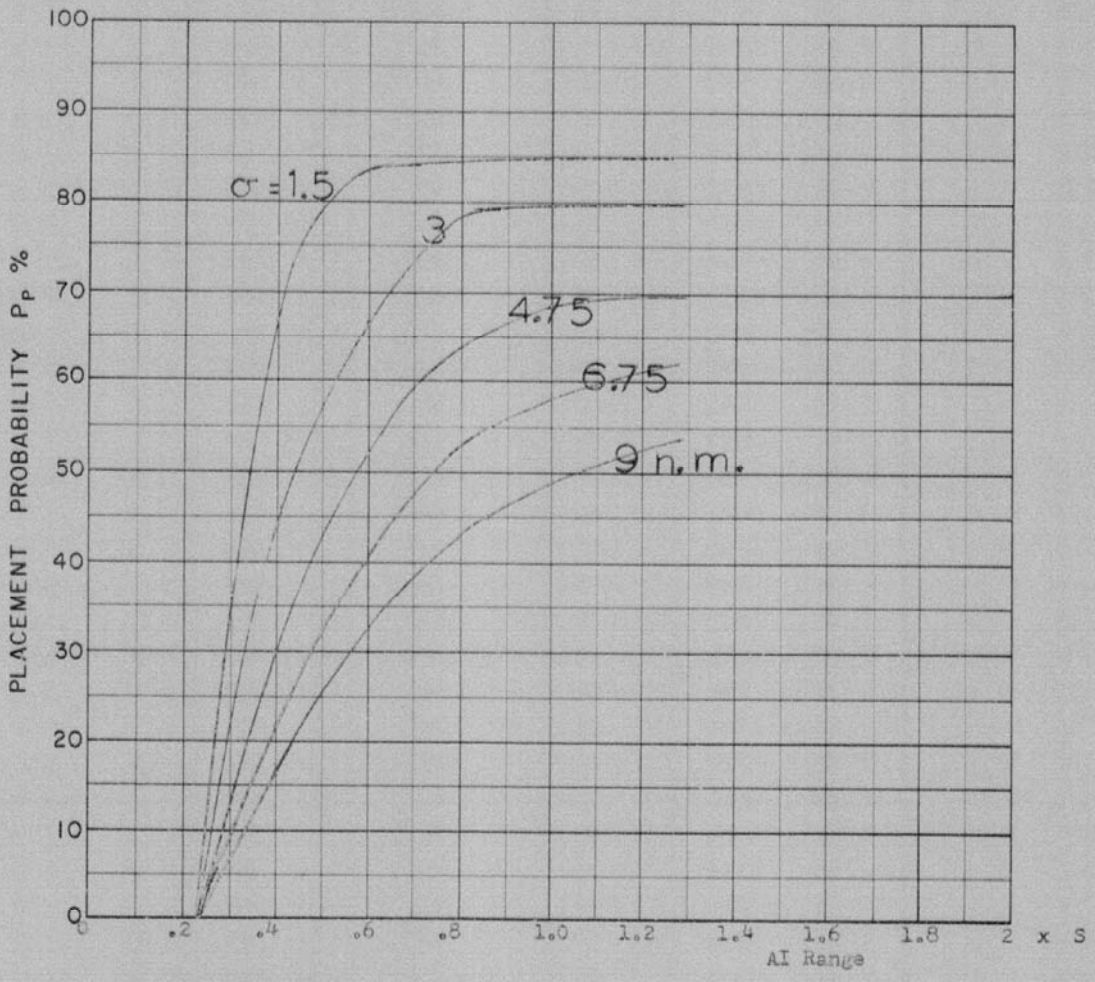

COURSE DIFFERENCE: 75°
TARGET EVASION: 0
TARGET MACH NO.: 2.0
INTERCEPTOR LATERAL G's: 0.66
INTERCEPTOR MACH NO.: 1.8
σ OF G.C.I. ACCURACY: Five values
A.I. DETECTION RANGE AS FRACTION OF SPECIFICATION RANGE, S: Abscissa
A.I. DETECTION RANGE CONTOUR: Delta
ALTITUDE: 60 K

D1276

Launch zone figure I-8, missile launched at medium range with 8° heading error allowance.

24hspr

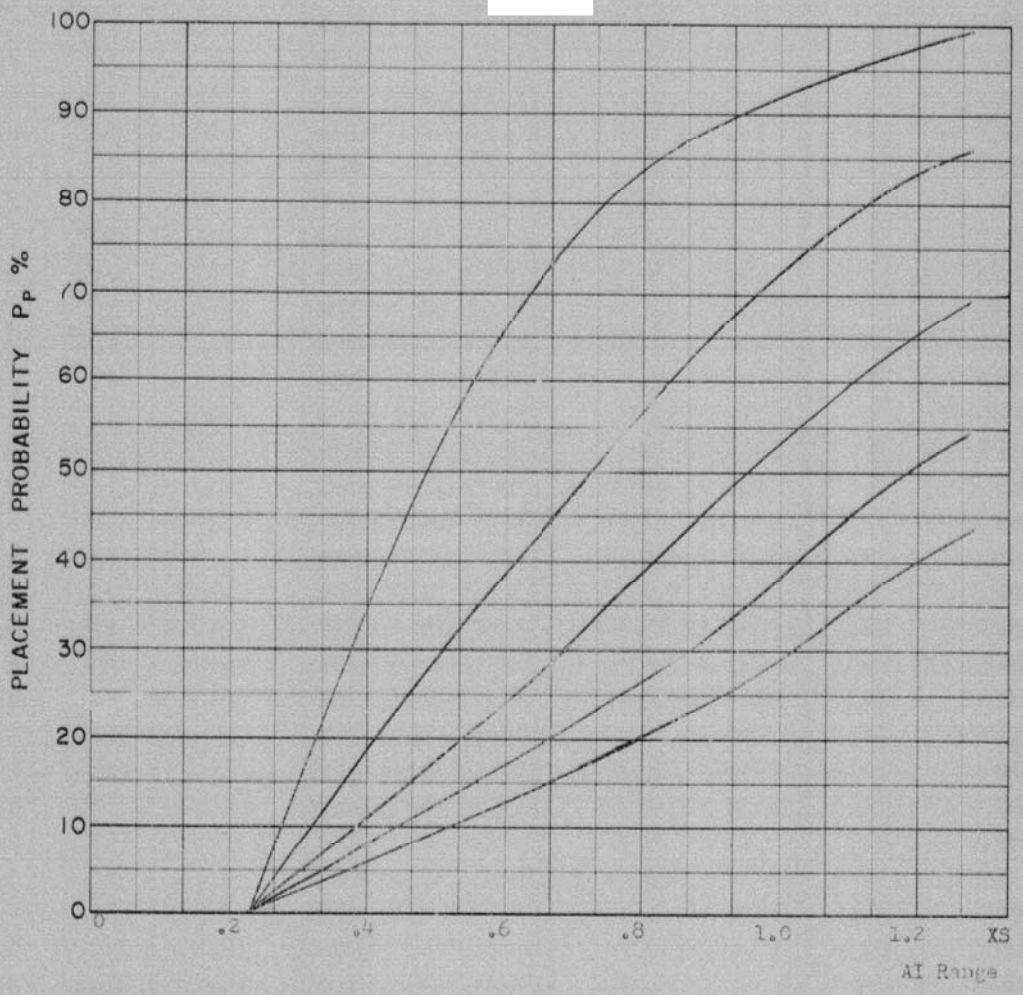

COURSE DIFFERENCE: 90°
TARGET EVASION: 0
TARGET MACH NO.: 2.0
INTERCEPTOR LATERAL G's: 0.66
INTERCEPTOR MACH NO.: 1.8
σ OF G.C.I. ACCURACY: Five values
A.I. DETECTION RANGE AS FRACTION OF SPECIFICATION RANGE, S: Abscissa
A.I. DETECTION RANGE CONTOUR: Straight Wing
ALTITUDE: 60K

S128a

Missile launch zone L-8, minimum range, 8° heading error.

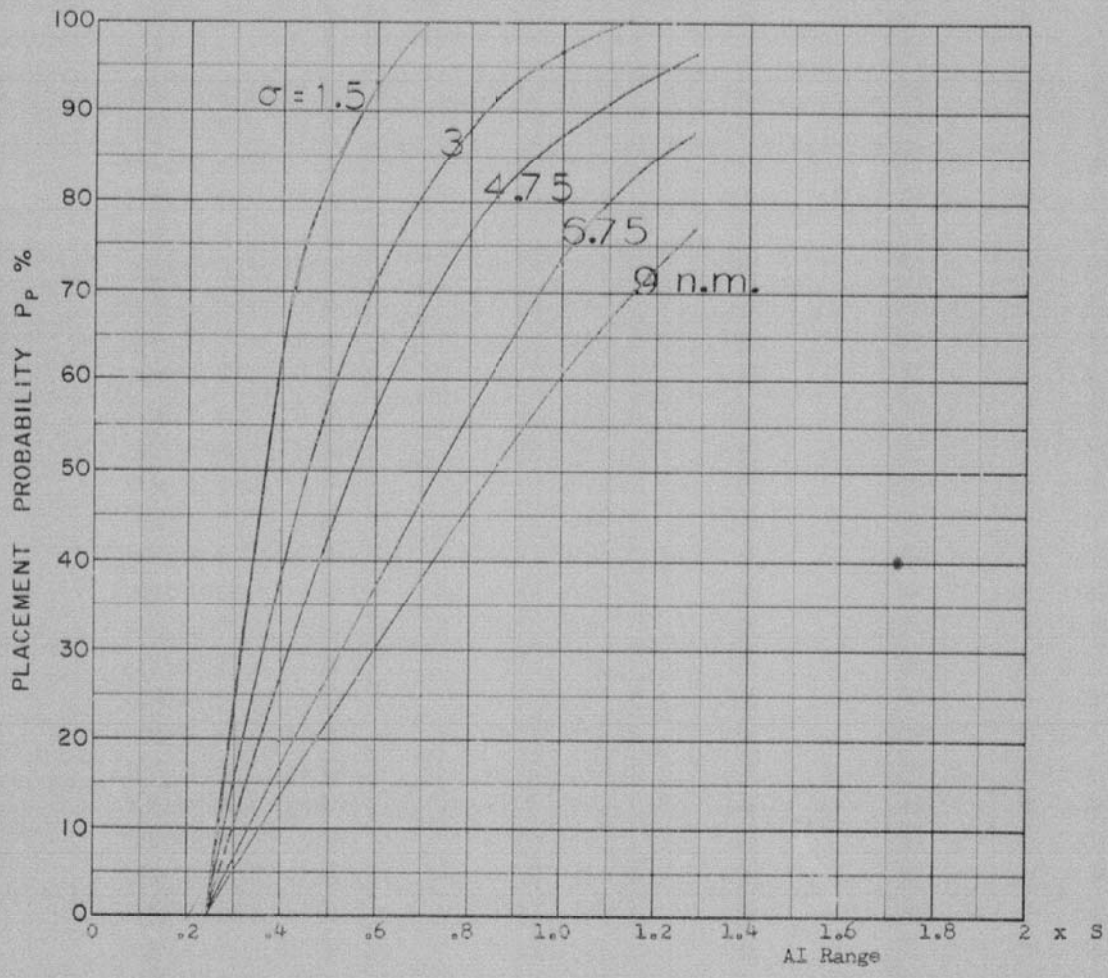

COURSE DIFFERENCE: 90°
TARGET EVASION: 0
TARGET MACH NO.: 2.0
INTERCEPTOR LATERAL G's: 0.66
INTERCEPTOR MACH NO.: 1.8
σ OF G.C.I. ACCURACY: Five values
A.I. DETECTION RANGE AS FRACTION OF SPECIFICATION RANGE, S: Abscissa
A.I. DETECTION RANGE CONTOUR: Delta
ALTITUDE: 60 K

D128a

Launch zone figure L.8, missile launched at minimum range with 8° heading error allowance.

23 b m d p r

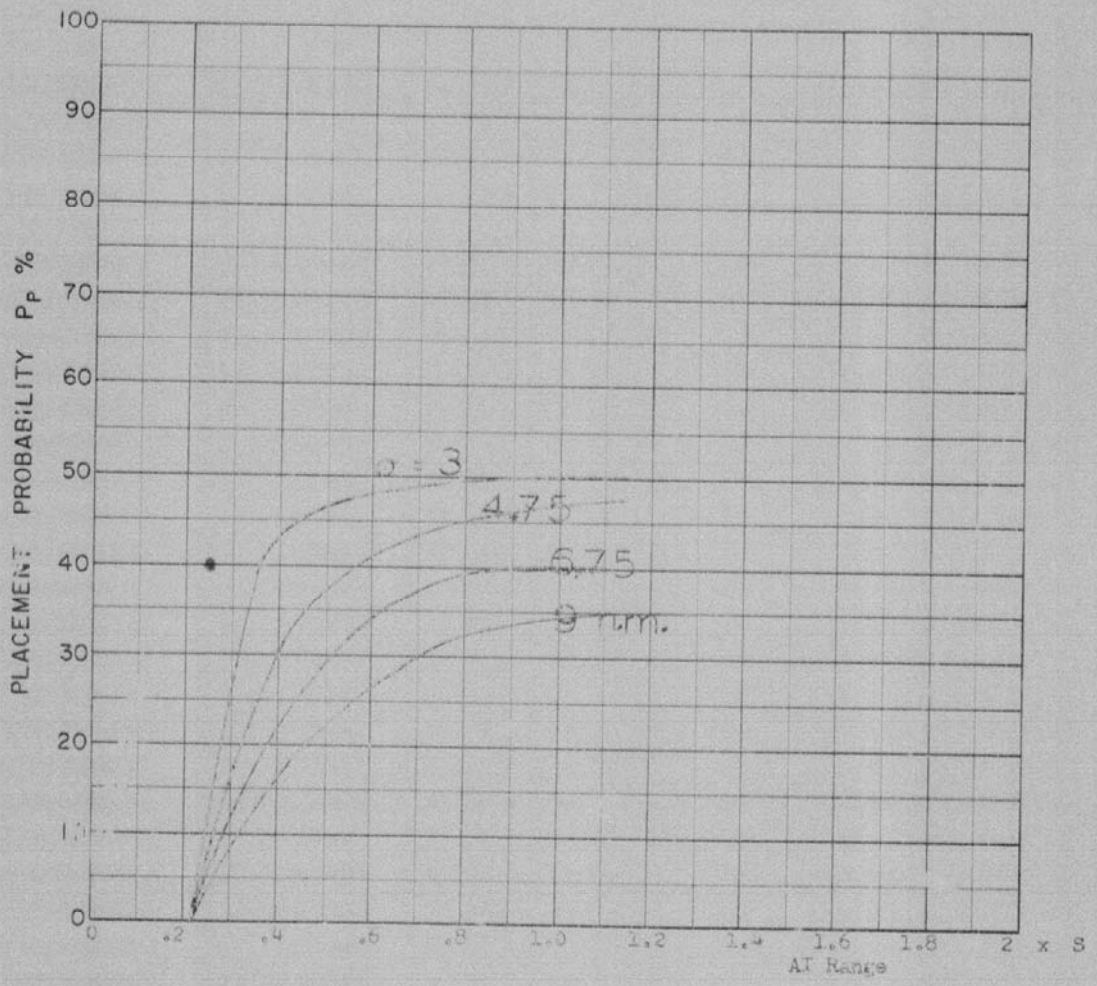

COURSE DIFFERENCE: 90°
TARGET EVASION: 0
TARGET MACH NO.: 2.0
INTERCEPTOR LATERAL G's: 0.66
INTERCEPTOR MACH NO.: 1.8
σ OF G.C.I. ACCURACY: Four values
A.I. DETECTION RANGE AS FRACTION OF SPECIFICATION RANGE, S: Abscissa
A.I. DETECTION RANGE CONTOUR: Delta
ALTITUDE: 60 K

D128b

Launch zone figure 4-8, missile launched at medium range with 8° heading error allowance.

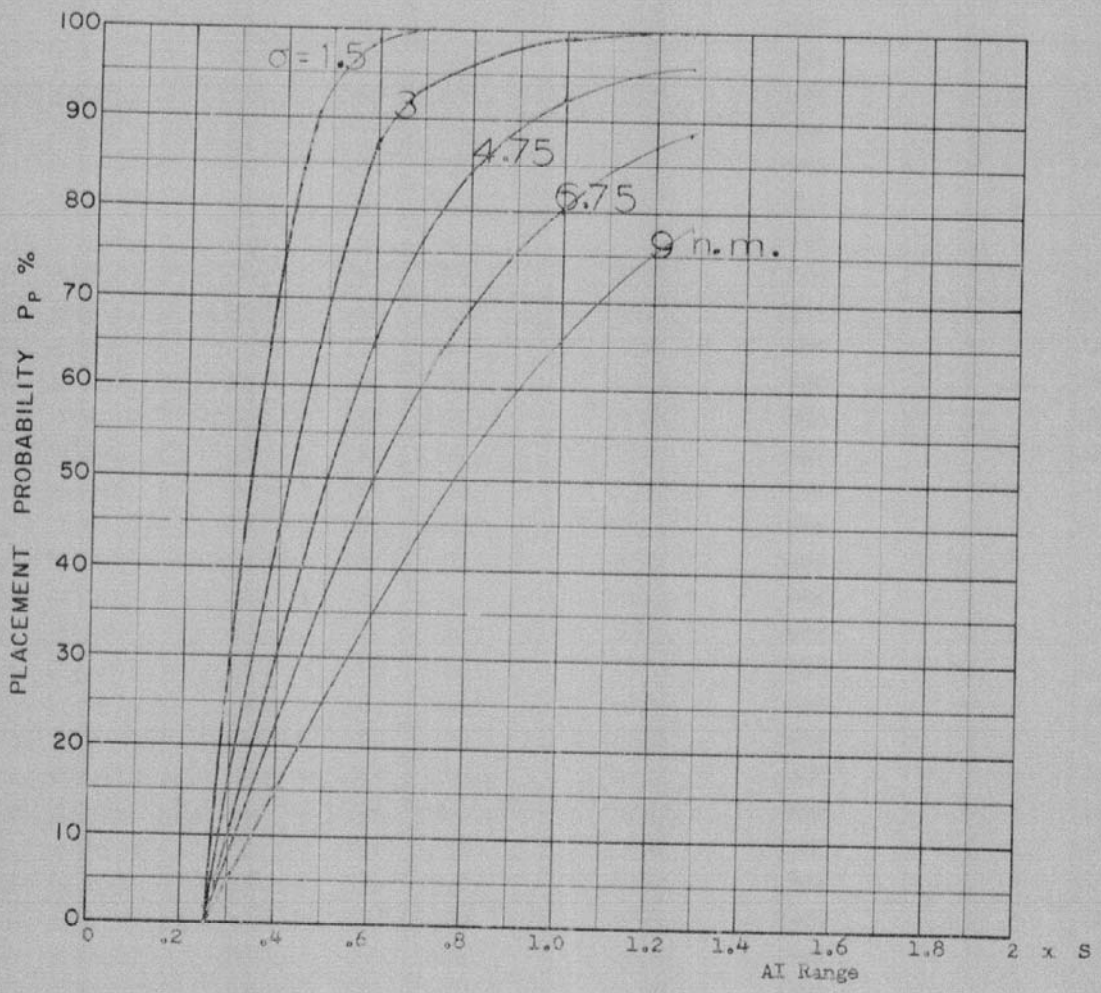

COURSE DIFFERENCE: 100°
TARGET EVASION: 0
TARGET MACH NO.: 2.0
INTERCEPTOR LATERAL G's: 0.66
INTERCEPTOR MACH NO.: 1.8
σ OF G.C.I. ACCURACY: Five values
A.I. DETECTION RANGE AS FRACTION OF SPECIFICATION RANGE, S: Abscissa
A.I. DETECTION RANGE CONTOUR: Delta
ALTITUDE: 60 K

D129a

Launch zone figure L-8. missile launched at minimum range with 8° heading error allowance.

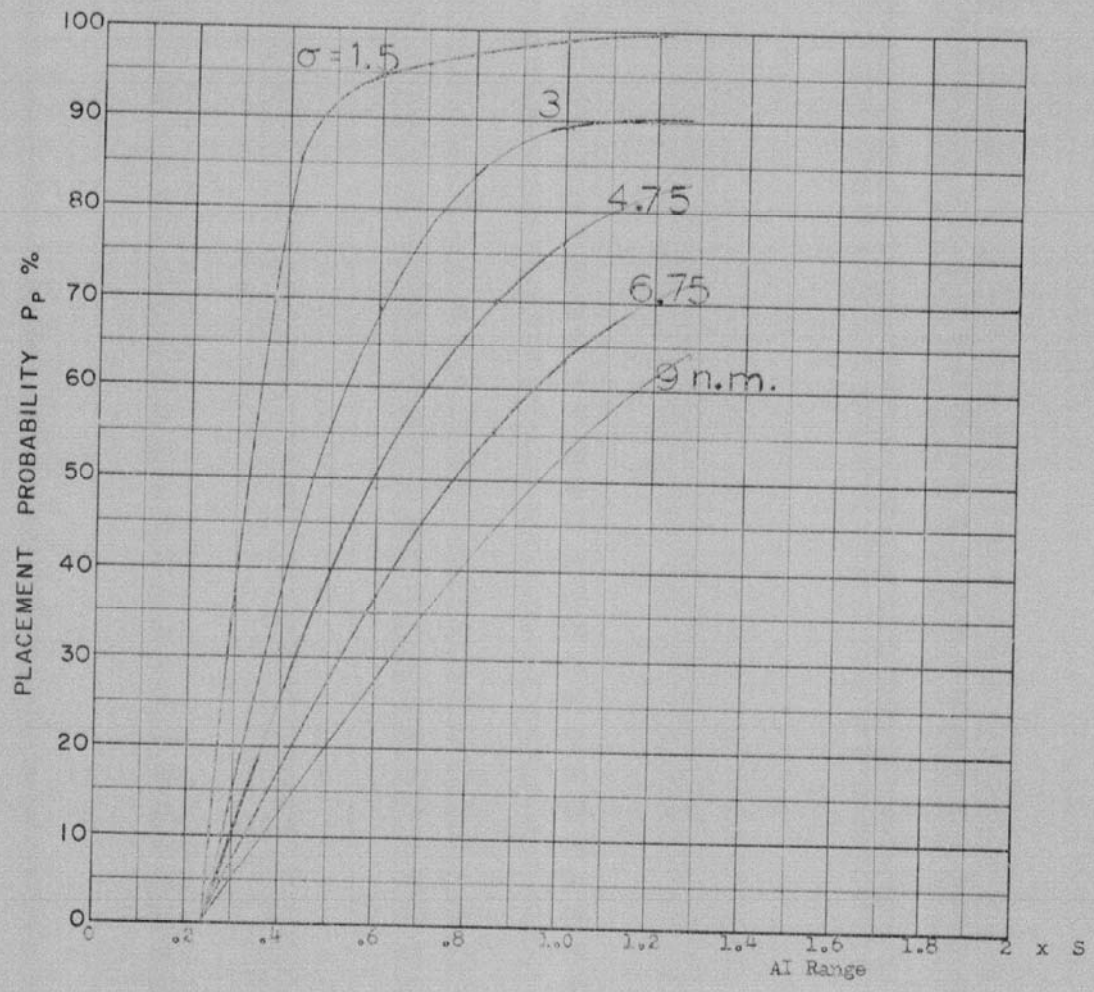

COURSE DIFFERENCE: 120°
TARGET EVASION: 0
TARGET MACH NO.: 2.0
INTERCEPTOR LATERAL G's: 0.66
INTERCEPTOR MACH NO.: 1.8
σ OF G.C.I. ACCURACY: Five values
A.I. DETECTION RANGE AS FRACTION OF SPECIFICATION RANGE, S: Abscissa
A.I. DETECTION RANGE CONTOUR: Delta
ALTITUDE: 60 K

(130a)

Launch zone figure 1-8, missile launched at minimum range with 8° heading error allowance.

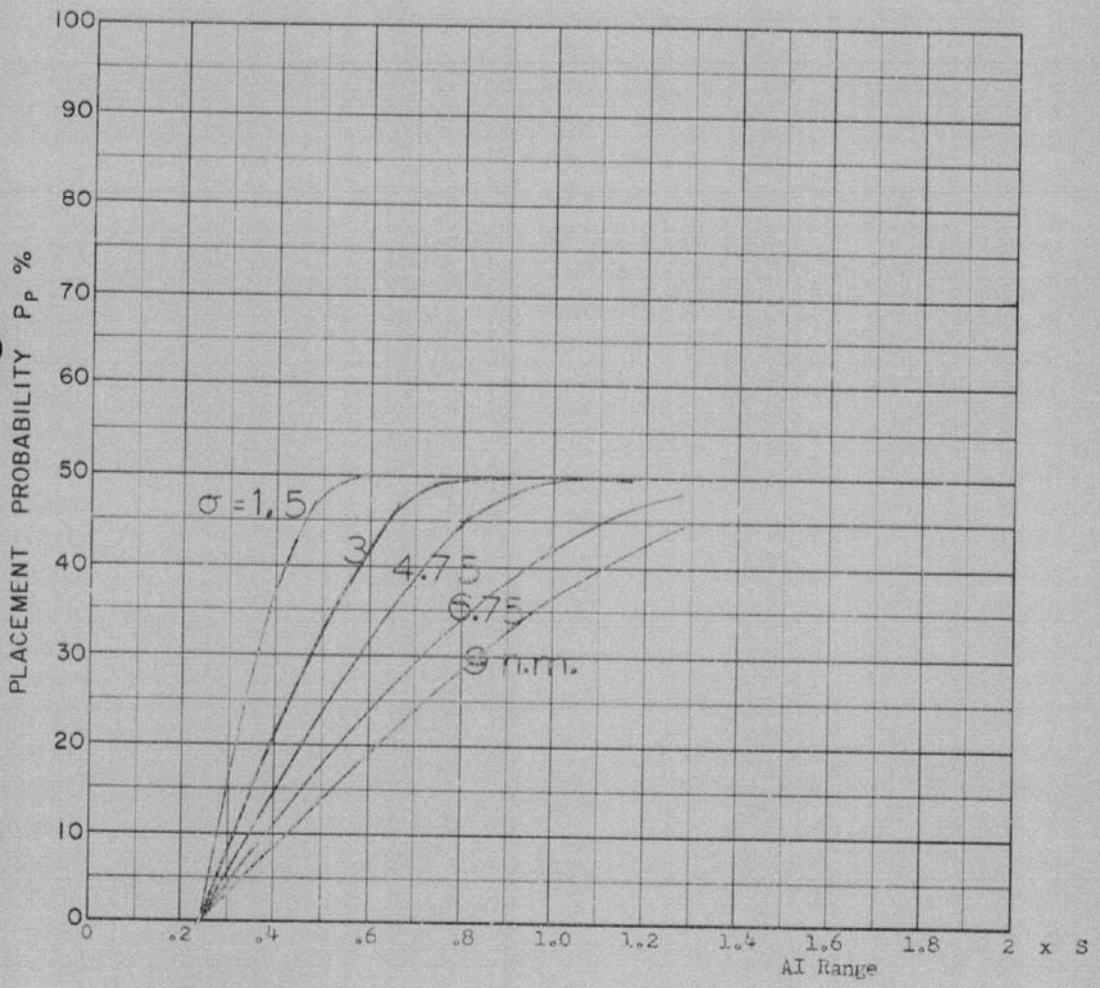

COURSE DIFFERENCE: 120°
TARGET EVASION: 0
TARGET MACH NO.: 2.0
INTERCEPTOR LATERAL G's: 0.66
INTERCEPTOR MACH NO.: 1.8
σ OF G.C.I. ACCURACY: Four values
A.I. DETECTION RANGE AS FRACTION OF SPECIFICATION RANGE, S: Abscissa
A.I. DETECTION RANGE CONTOUR: Delta
ALTITUDE: 60 K

1306

Launch zone figure L 8, missile launched at medium range with 8° heading error allowance.

24 e n d p r

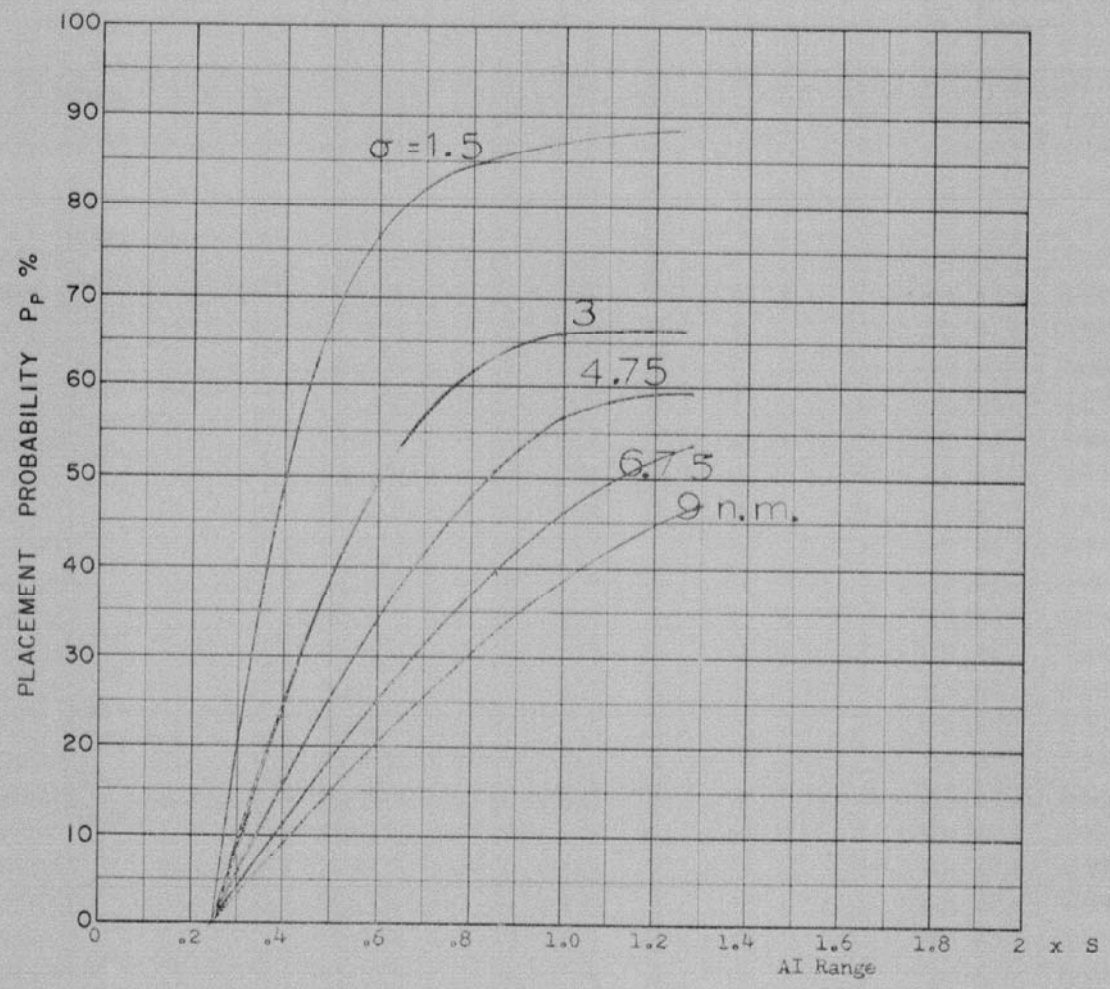

COURSE DIFFERENCE: 135°
TARGET EVASION: 0
TARGET MACH NO.: 2.0
INTERCEPTOR LATERAL G's: 0.66
INTERCEPTOR MACH NO.: 1.8
σ OF G.C.I. ACCURACY: Five values
A.I. DETECTION RANGE AS FRACTION OF SPECIFICATION RANGE, S: Abscissa
A.I. DETECTION RANGE CONTOUR: Delta
ALTITUDE: 60 K

(131a)

Launch zone figure L-8, missile launched at minimum range with 8° heading error allowance.

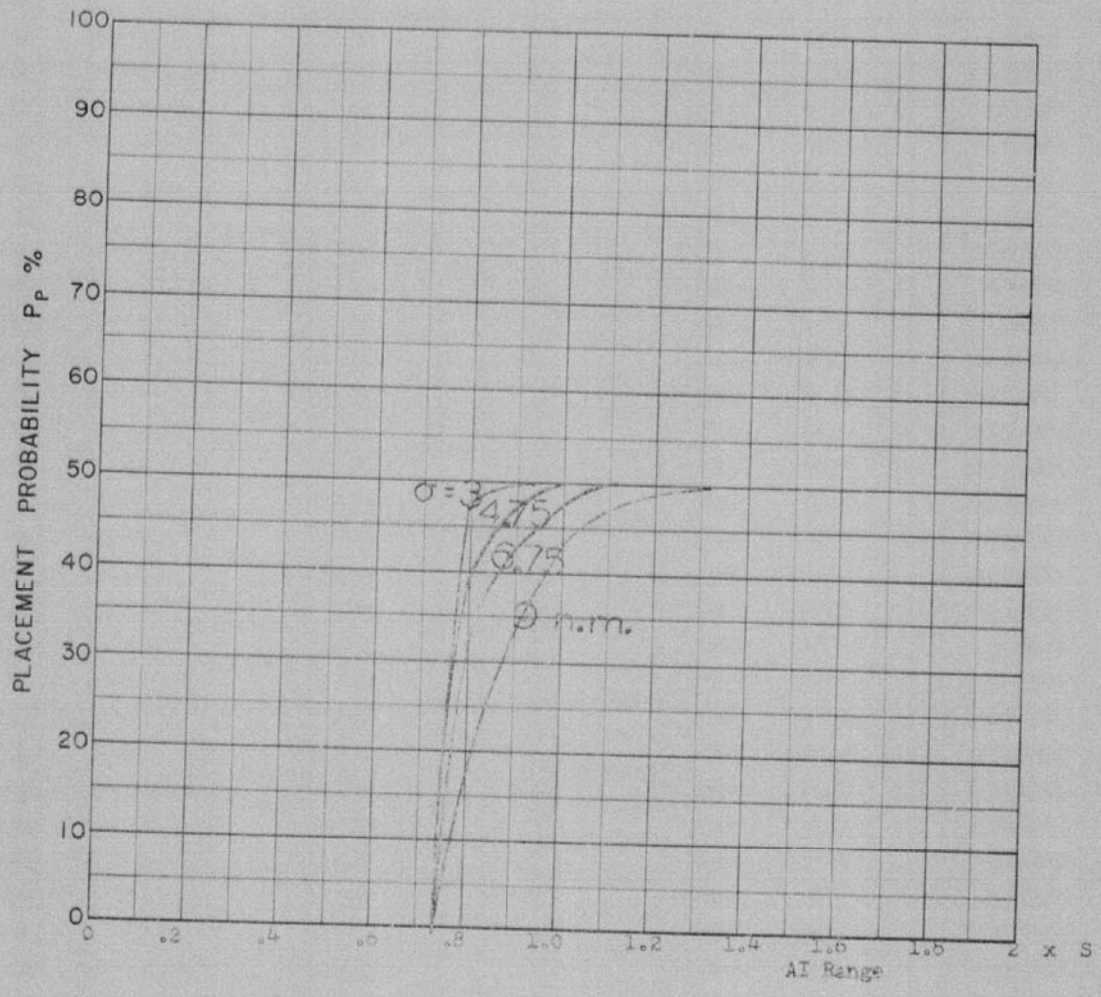

COURSE DIFFERENCE: 135°
TARGET EVASION: 0
TARGET MACH NO.: 2.0
INTERCEPTOR LATERAL G's: 0.66
INTERCEPTOR MACH NO.: 1.8
σ OF G.C.I. ACCURACY: Four values
A.I. DETECTION RANGE AS FRACTION OF SPECIFICATION RANGE, S: Abscissa
A.I. DETECTION RANGE CONTOUR: Delta
ALTITUDE: 50 K

(1316)

Launch zone figure 1-8, missile launched at medium range with 8° heading error allowance.

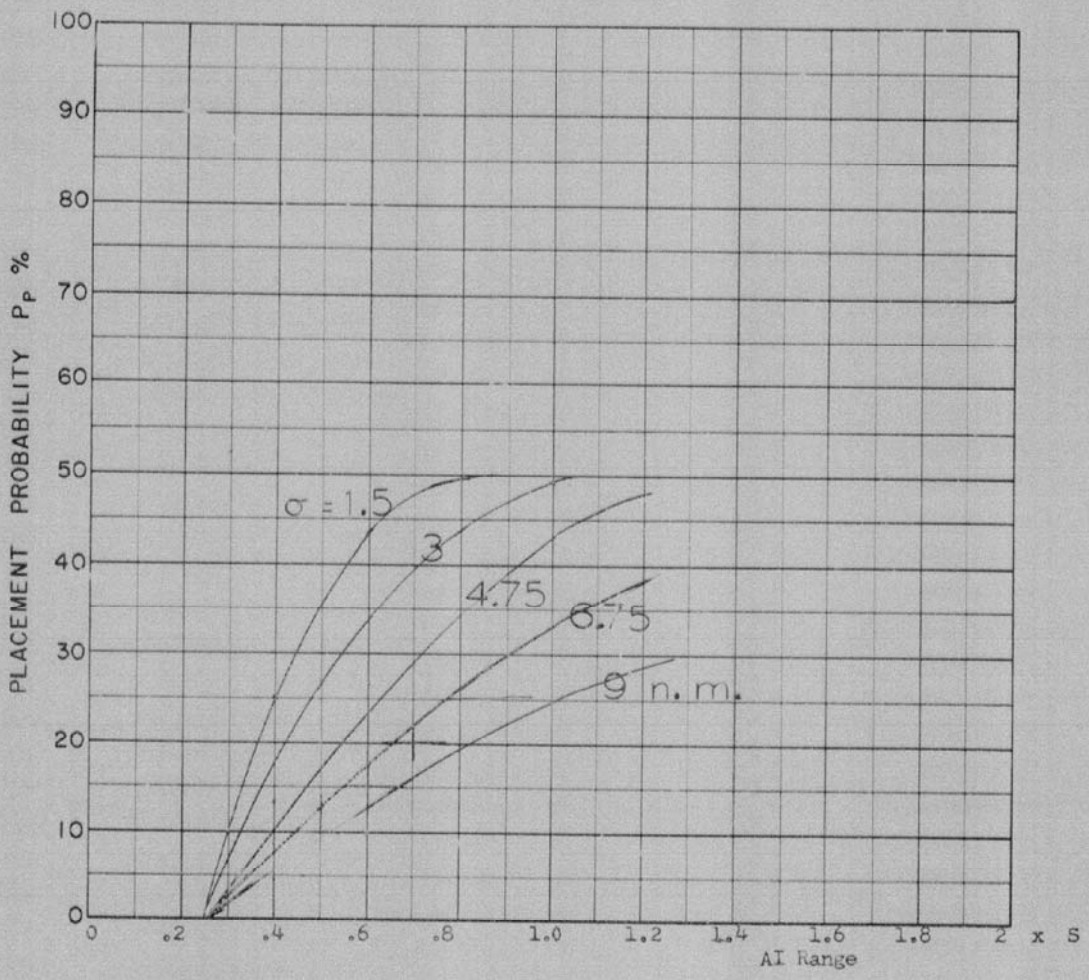

COURSE DIFFERENCE: 160°
TARGET EVASION: 0
TARGET MACH NO.: 2.0
INTERCEPTOR LATERAL G's: 0.66
INTERCEPTOR MACH NO.: 1.8
σ OF G.C.I. ACCURACY: Five values
A.I. DETECTION RANGE AS FRACTION OF SPECIFICATION RANGE, S: Abscissa
A.I. DETECTION RANGE CONTOUR: Delta
ALTITUDE: 60 K

(132)

Launch zone figure L-8, missile launched at minimum range with 8° heading error allowance.

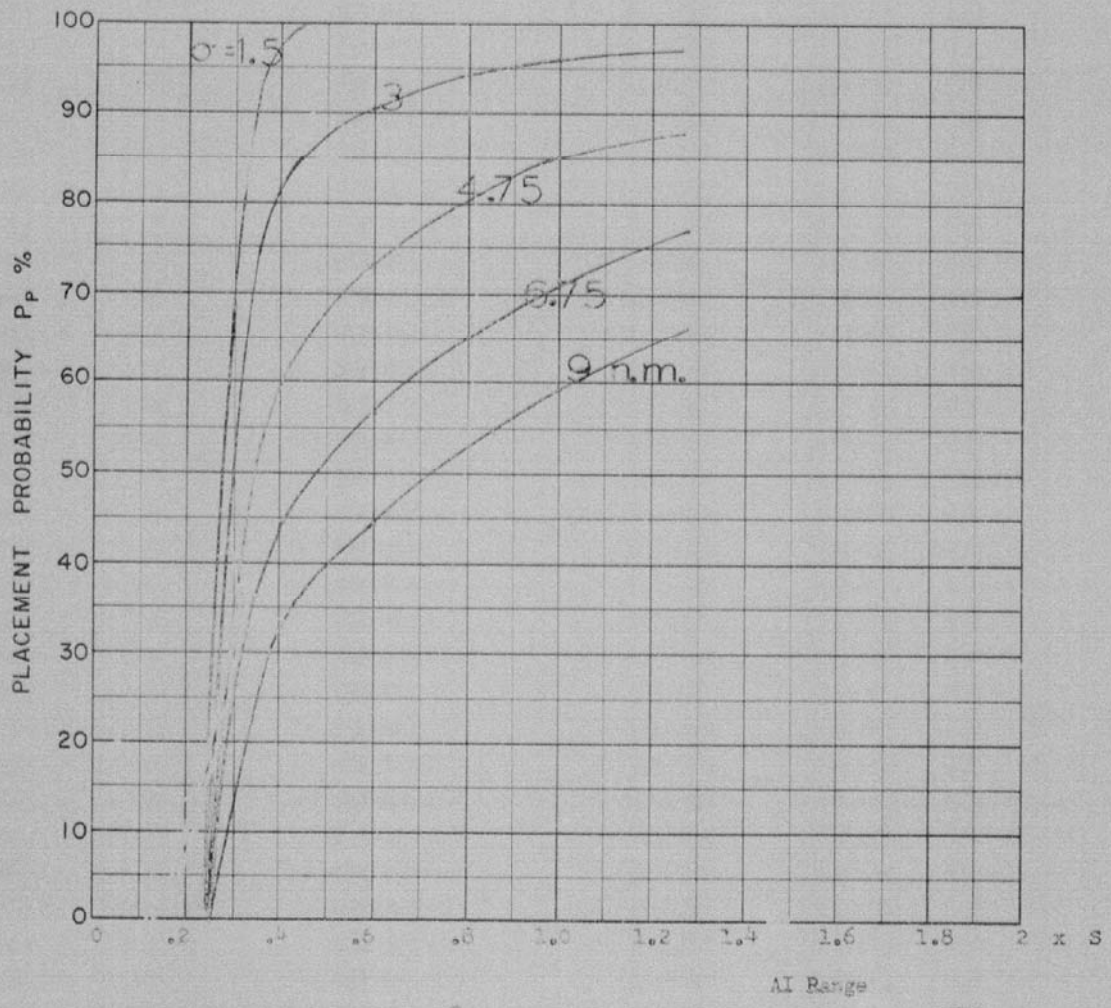

COURSE DIFFERENCE: 75°
TARGET EVASION: 0
TARGET MACH NO.: 2.0
INTERCEPTOR LATERAL G's: 2.0
INTERCEPTOR MACH NO.: 1.8
σ OF G.C.I. ACCURACY: Five values
A.I. DETECTION RANGE AS FRACTION OF SPECIFICATION RANGE, S: Abscissa
A.I. DETECTION RANGE CONTOUR: Delta
ALTITUDE: 60 K

D133a

Launch zone of figure 8. Missile launched at minimum range with 8° heading error allowance.

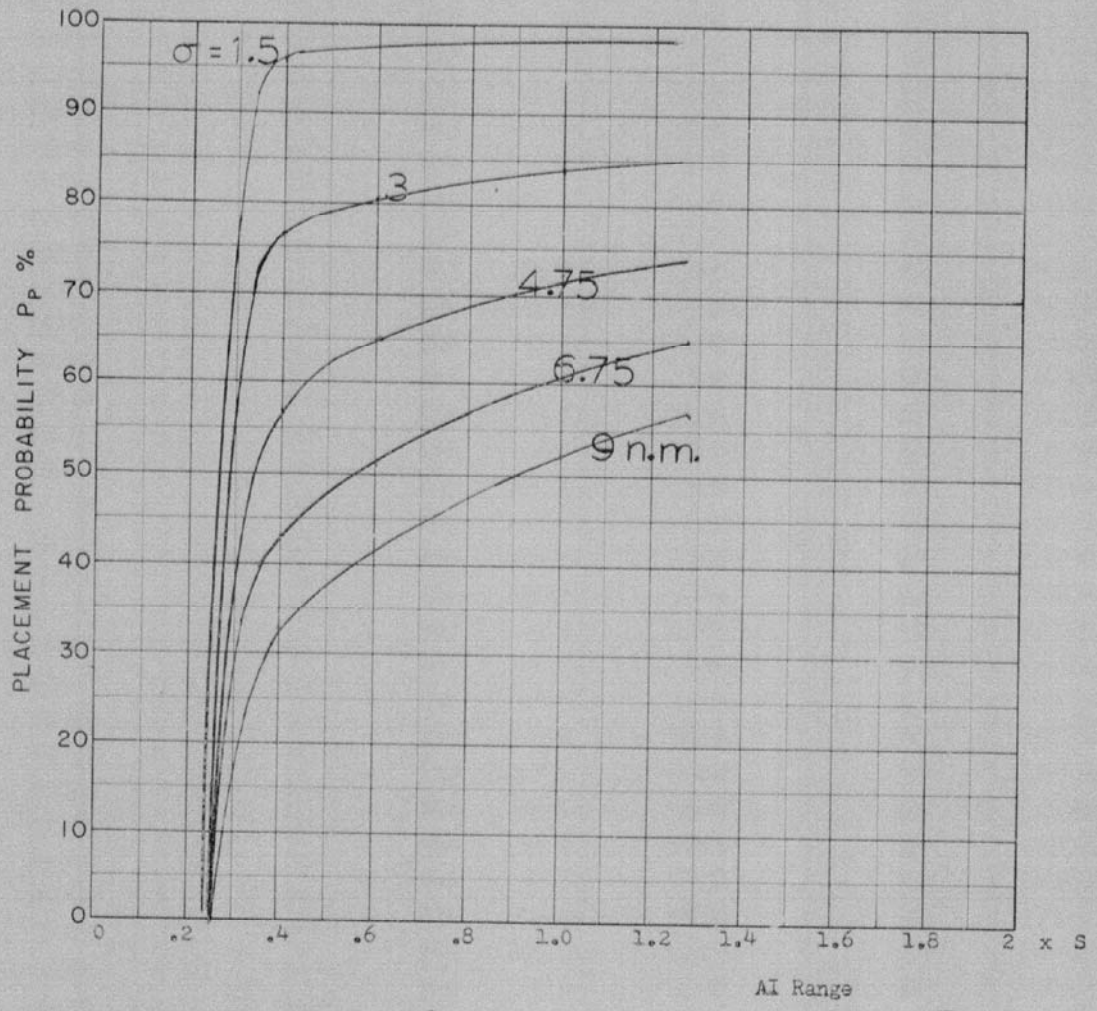

COURSE DIFFERENCE: 75°
TARGET EVASION: 0
TARGET MACH NO.: 2.0
INTERCEPTOR LATERAL G's: 2.0
INTERCEPTOR MACH NO.: 1.8
σ OF G.C.I. ACCURACY: Five values
A.I. DETECTION RANGE AS FRACTION OF SPECIFICATION RANGE, S: Abscissa
A.I. DETECTION RANGE CONTOUR: Delta
ALTITUDE: 60 K

(D133b)

Launch zone figure L-8, missile launched at medium range with 8° heading error allowance.

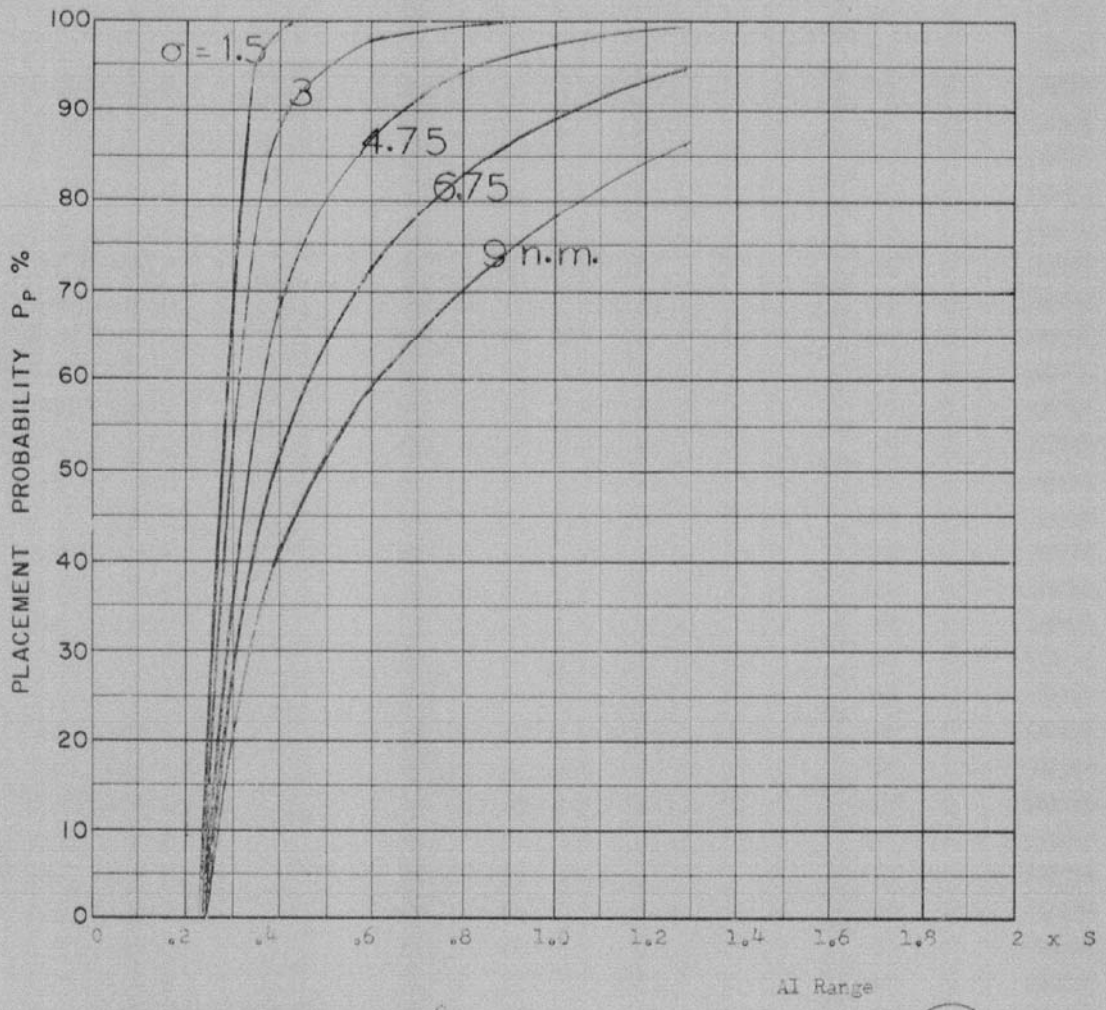

COURSE DIFFERENCE: 90°
TARGET EVASION: 0
TARGET MACH NO.: 2.0
INTERCEPTOR LATERAL G's: 2.0
INTERCEPTOR MACH NO.: 1.8
σ OF G.C.I. ACCURACY: Five values
A.I. DETECTION RANGE AS FRACTION OF SPECIFICATION RANGE, S: Abscissa
A.I. DETECTION RANGE CONTOUR: Delta
ALTITUDE: 60 K

D134a

Launch zone of figure 8. Missile launched at minimum range with 8° heading error allowance.

22 b m d p r

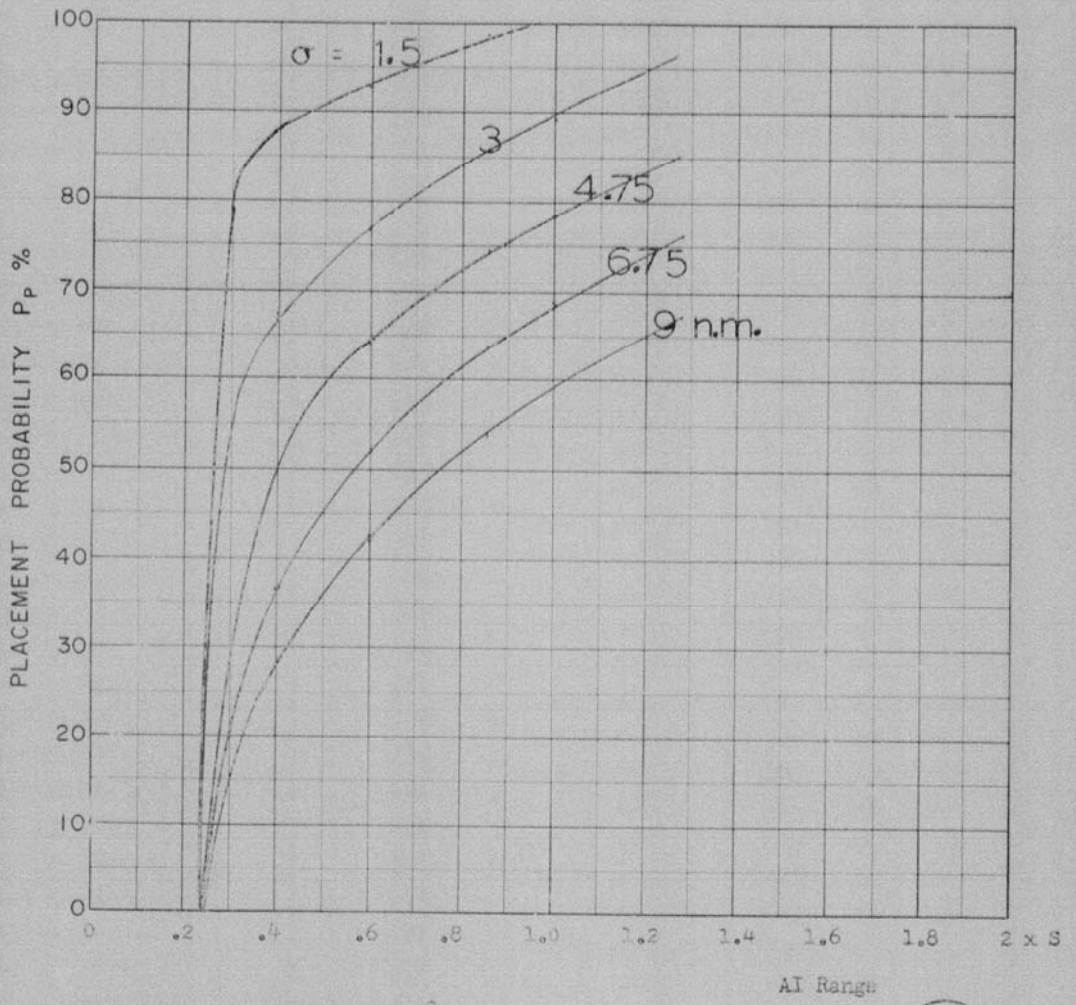

COURSE DIFFERENCE: 90°
TARGET EVASION: 0
TARGET MACH NO.: 2.0
INTERCEPTOR LATERAL G's: 2.0
INTERCEPTOR MACH NO.: 1.8
σ OF G.C.I. ACCURACY: Five values
A.I. DETECTION RANGE AS FRACTION OF SPECIFICATION RANGE, S: Abscissa
A.I. DETECTION RANGE CONTOUR: Delta
ALTITUDE: 60 K

D1346

Launch zone figure L-8, missile launched at medium range with 8° heading error allowance.

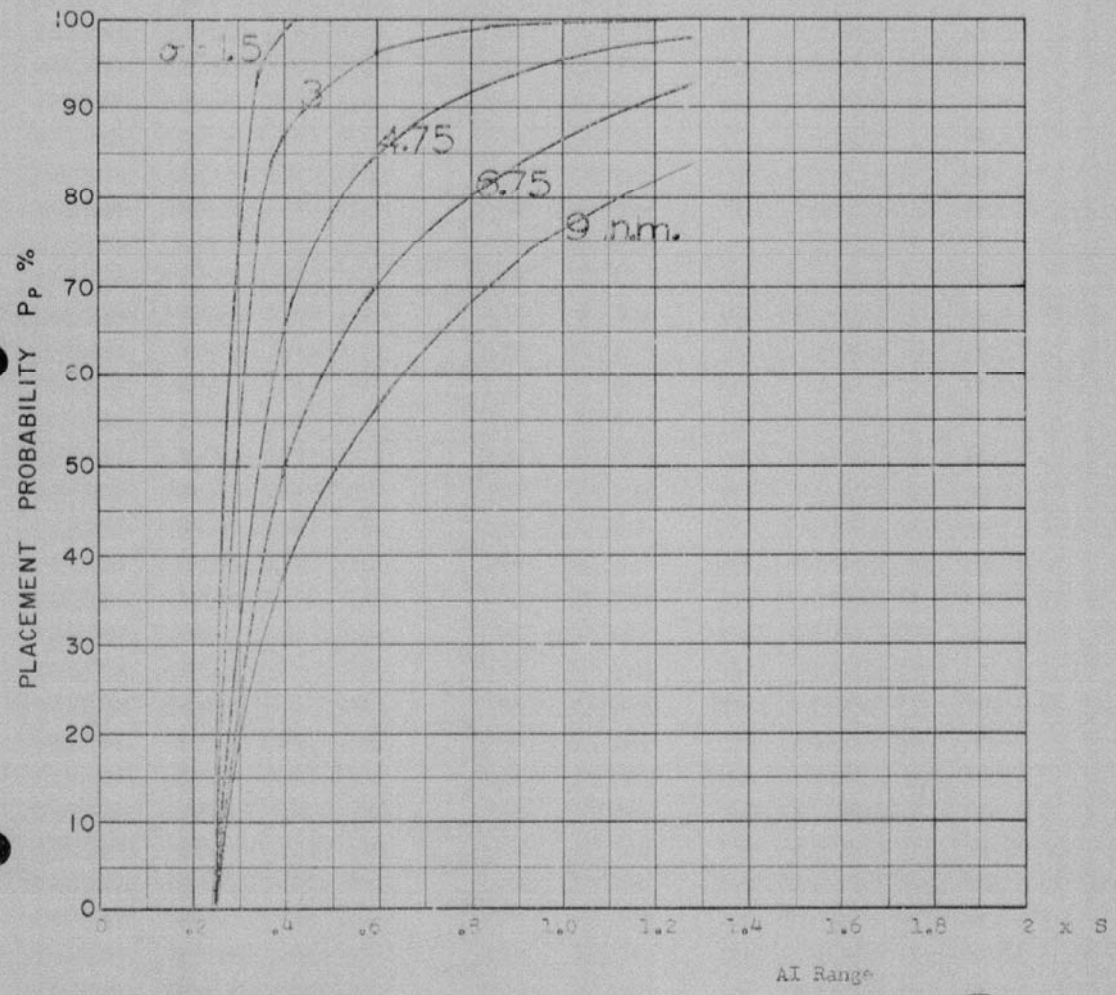

COURSE DIFFERENCE: 180°
TARGET EVASION: 0
TARGET MACH NO.: 2.0
INTERCEPTOR LATERAL G's: 2.0
INTERCEPTOR MACH NO.: 1.8
σ OF G.C.I. ACCURACY: Five values
A.I. DETECTION RANGE AS FRACTION OF SPECIFICATION RANGE, S: Abscissa
A.I. DETECTION RANGE CONTOUR: Delta
ALTITUDE: 60 K

D135

Launch zone of figure 8. Missile launched at minimum range with 8° heading error allowance.

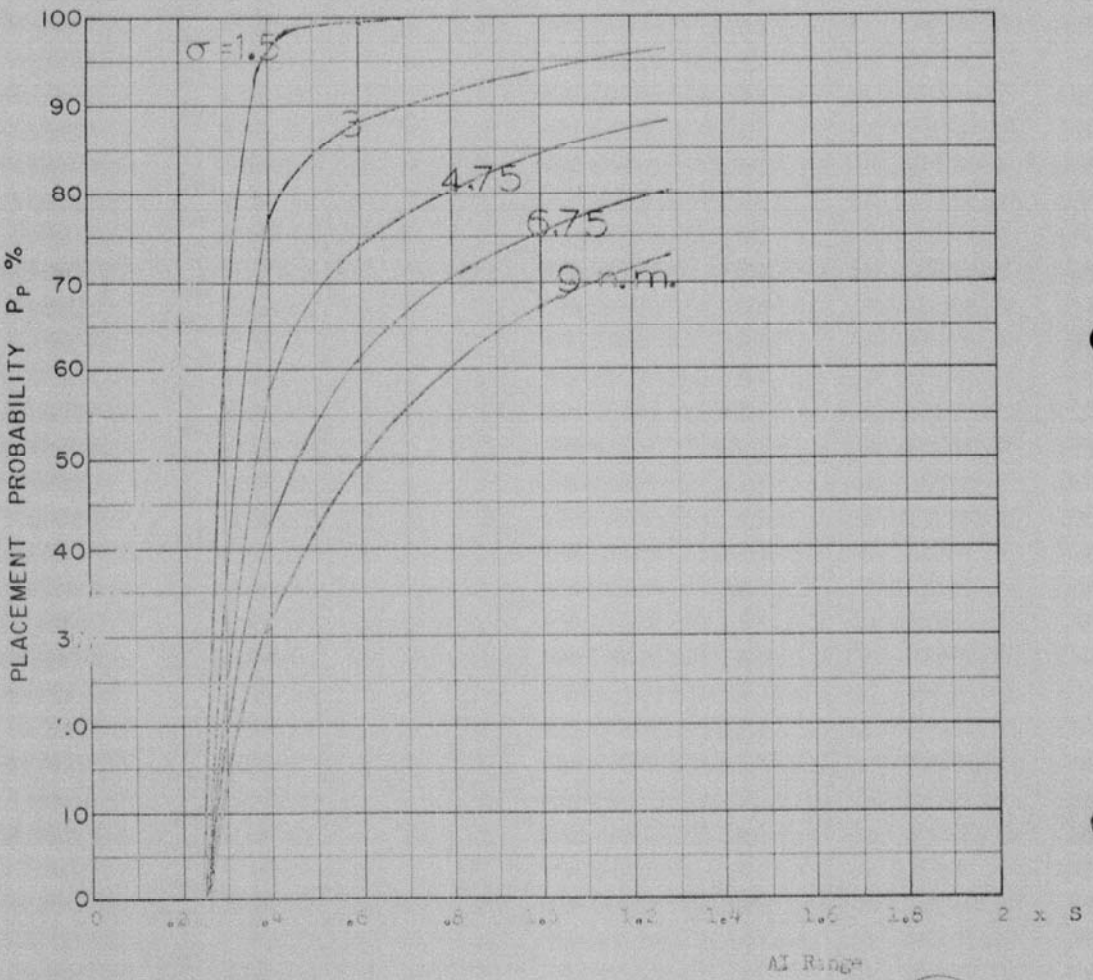

D136

COURSE DIFFERENCE: 120°
TARGET EVASION: 0
TARGET MACH NO.: 2.0
INTERCEPTOR LATERAL G's: 2.0
INTERCEPTOR MACH NO.: 1.8
σ OF G.C.I. ACCURACY: Five values
A.I. DETECTION RANGE AS FRACTION OF SPECIFICATION RANGE, S: Abscissa
A.I. DETECTION RANGE CONTOUR: Delta
ALTITUDE: 60 K

Launch zone of figure 8. Missile launched at minimum range with 8° heading error allowance.

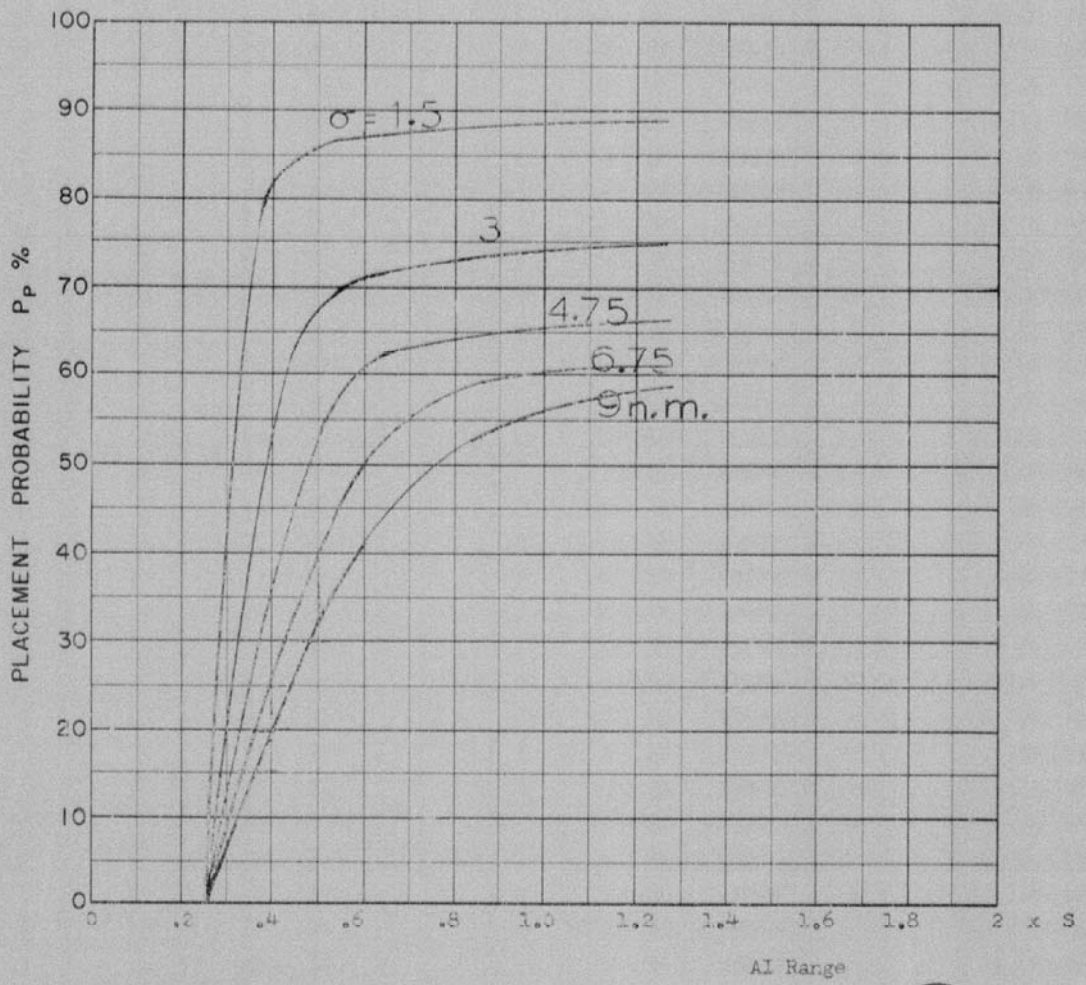

COURSE DIFFERENCE: 135°
TARGET EVASION: 0
TARGET MACH NO.: 2.0
INTERCEPTOR LATERAL G's: 2.0
INTERCEPTOR MACH NO.: 1.8
σ OF G.C.I. ACCURACY: Five values
A.I. DETECTION RANGE AS FRACTION OF SPECIFICATION RANGE, S: Abscissa
A.I. DETECTION RANGE CONTOUR: Delta
ALTITUDE: 60 K

D137

Launch zone of figure 8. Missile launched at minimum range with 8° heading error allowance.

22 f n d p r

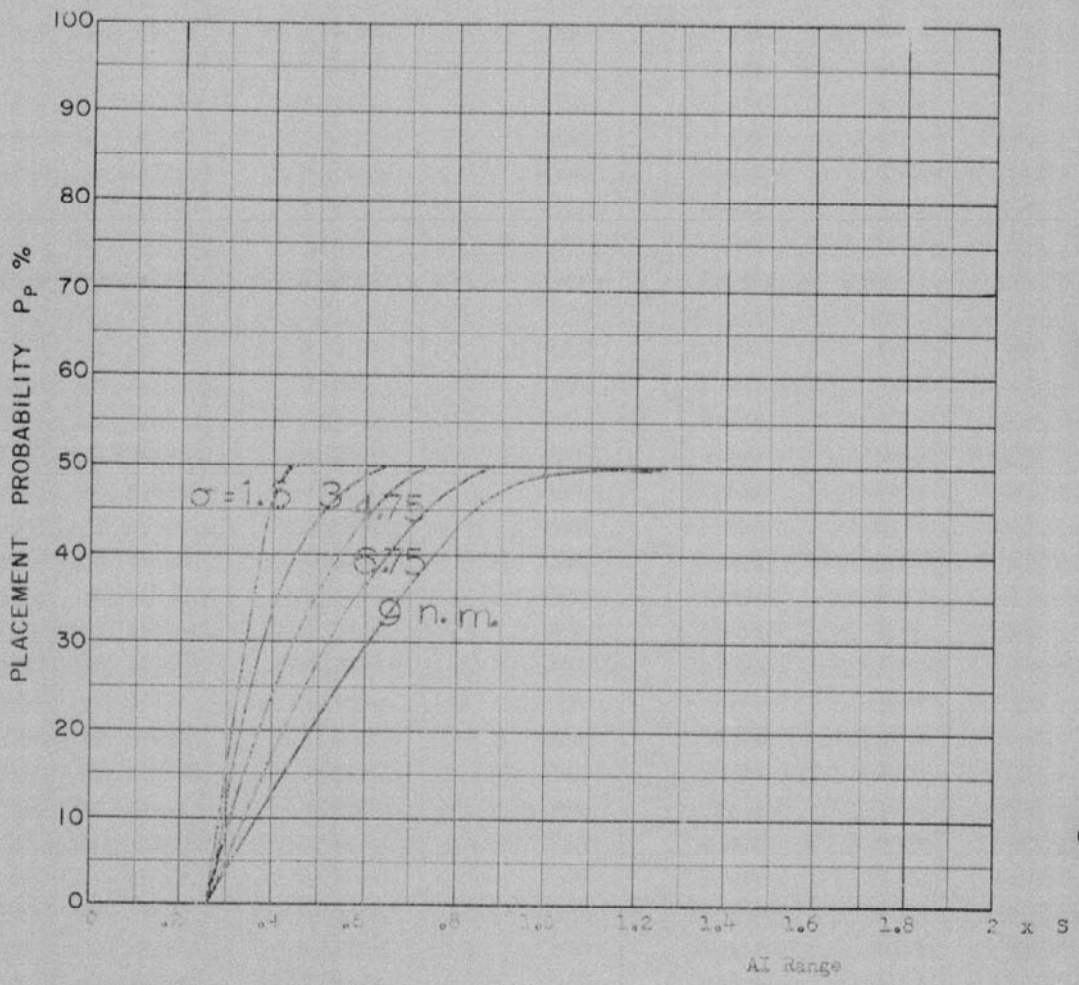

COURSE DIFFERENCE: 160°
TARGET EVASION: 0
TARGET MACH NO.: 2.0
INTERCEPTOR LATERAL G's: 2.0
INTERCEPTOR MACH NO.: 1.8
σ OF G.C.I. ACCURACY: Five values
A.I. DETECTION RANGE AS FRACTION OF SPECIFICATION RANGE, S: Abscissa
A.I. DETECTION RANGE CONTOUR: Delta
ALTITUDE: 60 K

(D138)

Launch zone of figure 8. Missile launched at minimum range with 8° heading error allowance.

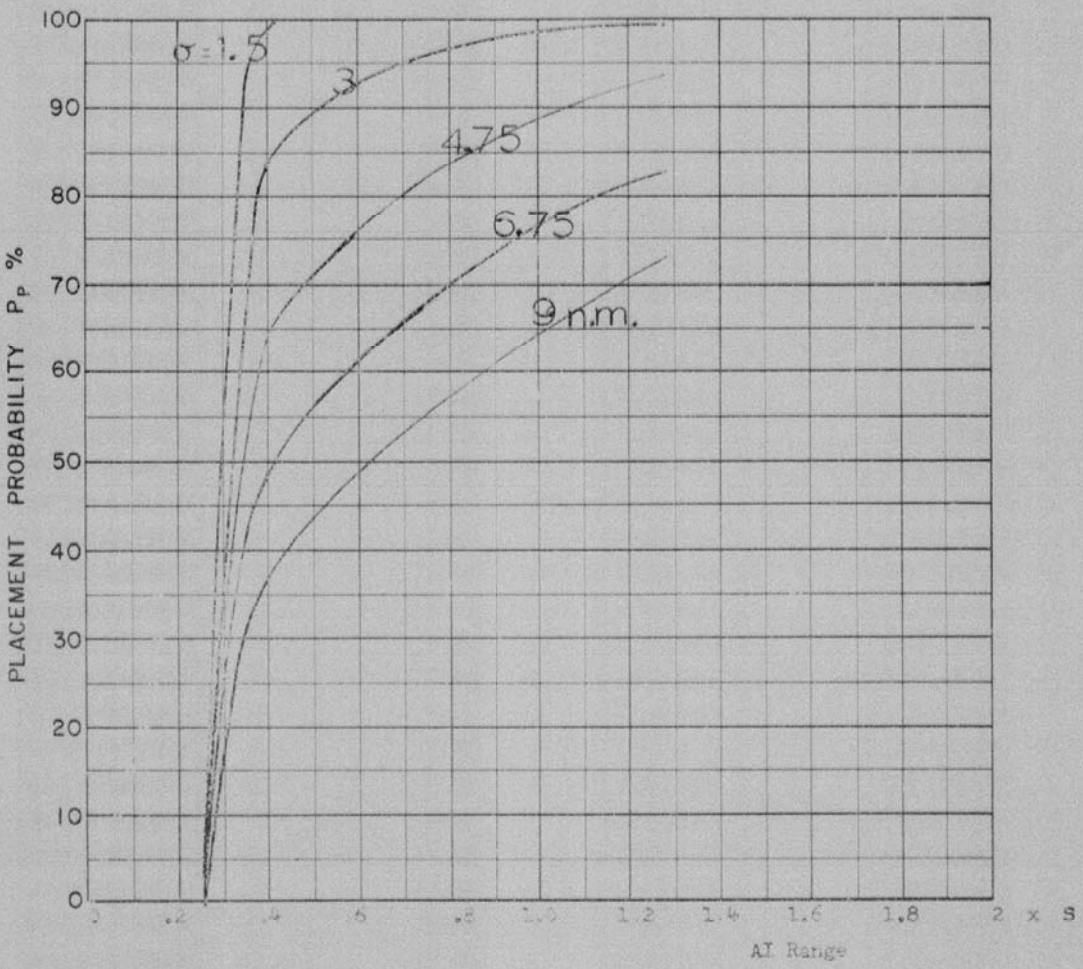

COURSE DIFFERENCE: 75°
TARGET EVASION: 0
TARGET MACH NO.: 2
INTERCEPTOR LATERAL G's: 3.60
INTERCEPTOR MACH NO.: 1.8
σ OF G.C.I. ACCURACY: Five values
A.I. DETECTION RANGE AS FRACTION OF SPECIFICATION RANGE, S: Abscissa
A.I. DETECTION RANGE CONTOUR: Delta
ALTITUDE: 60 K

D139a

Launch zone of figure 1-8 missile launched at minimum range with 8° heading error allowance.

18 a m d p r

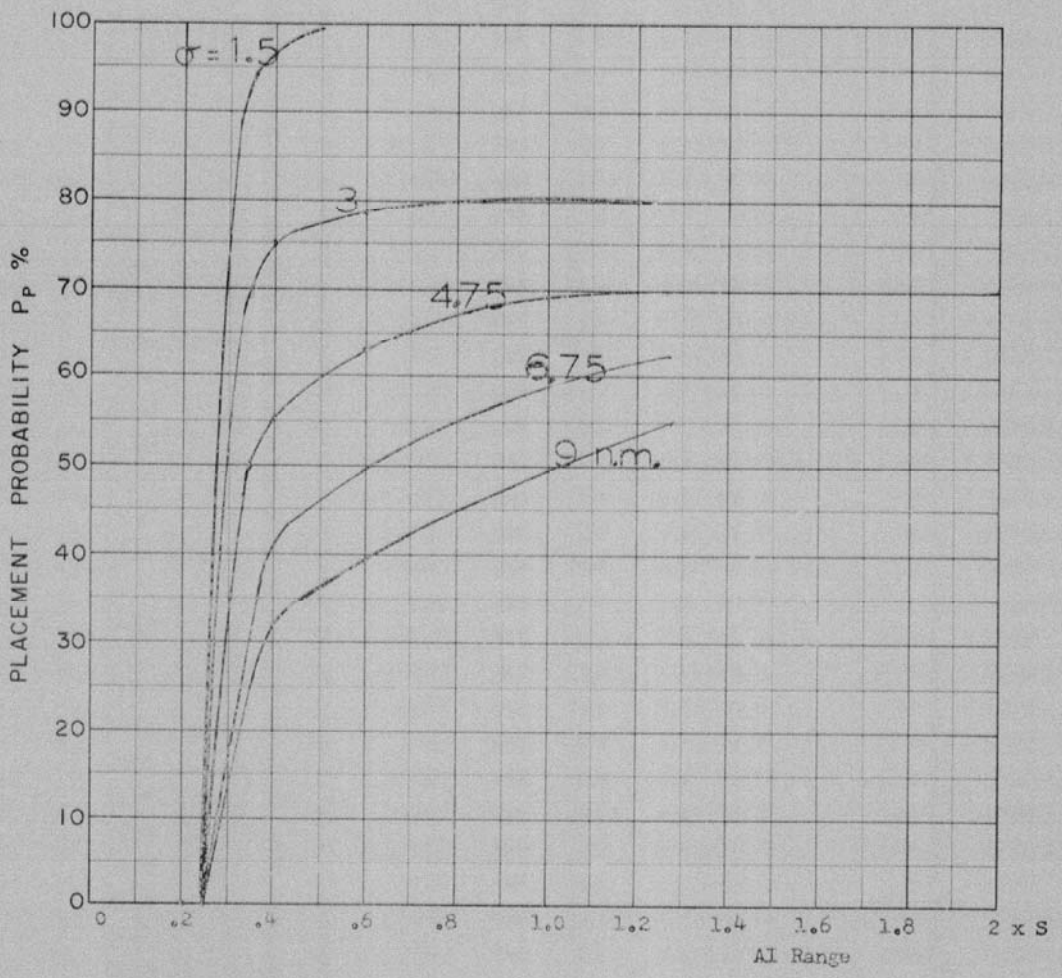

COURSE DIFFERENCE: 75°
TARGET EVASION: 0
TARGET MACH NO.: 2.0
INTERCEPTOR LATERAL G's: 3.60
INTERCEPTOR MACH NO.: 1.8
σ OF G.C.I. ACCURACY: Five values
A.I. DETECTION RANGE AS FRACTION OF SPECIFICATION RANGE, S: Abscissa
A.I. DETECTION RANGE CONTOUR: Delta
ALTITUDE: 60 K

D1396

Launch zone figure L-8. Missile launched at medium range with 8° heading error allowance.

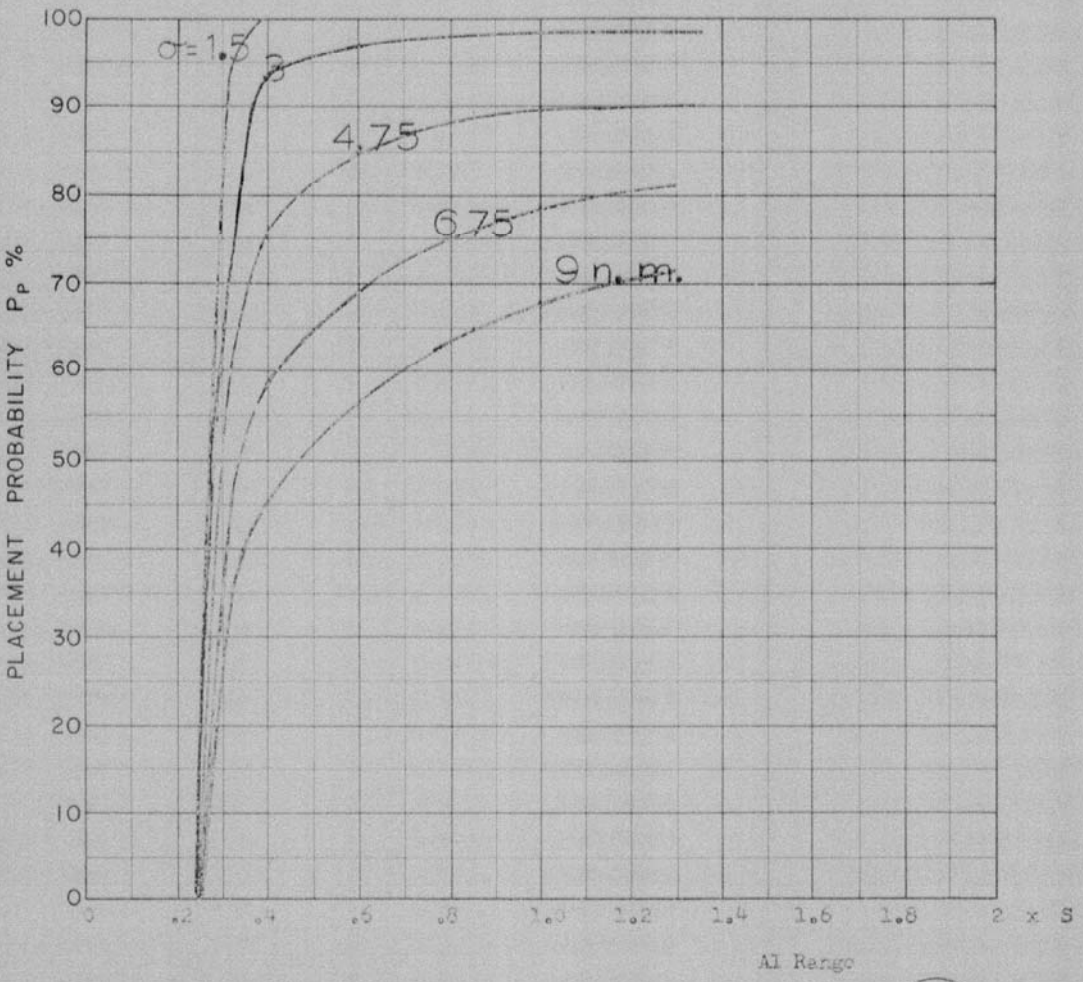

COURSE DIFFERENCE: 90°
TARGET EVASION: 0
TARGET MACH NO.: 2
INTERCEPTOR LATERAL G's: 3.60
INTERCEPTOR MACH NO.: 1.8
σ OF G.C.I. ACCURACY: Five values
A.I. DETECTION RANGE AS FRACTION OF SPECIFICATION RANGE, S: Abscissa
A.I. DETECTION RANGE CONTOUR: Delta
ALTITUDE: 60 K

D140a

Launch zone of figure L-8, missile launched at minimum range with 8° heading error allowance.

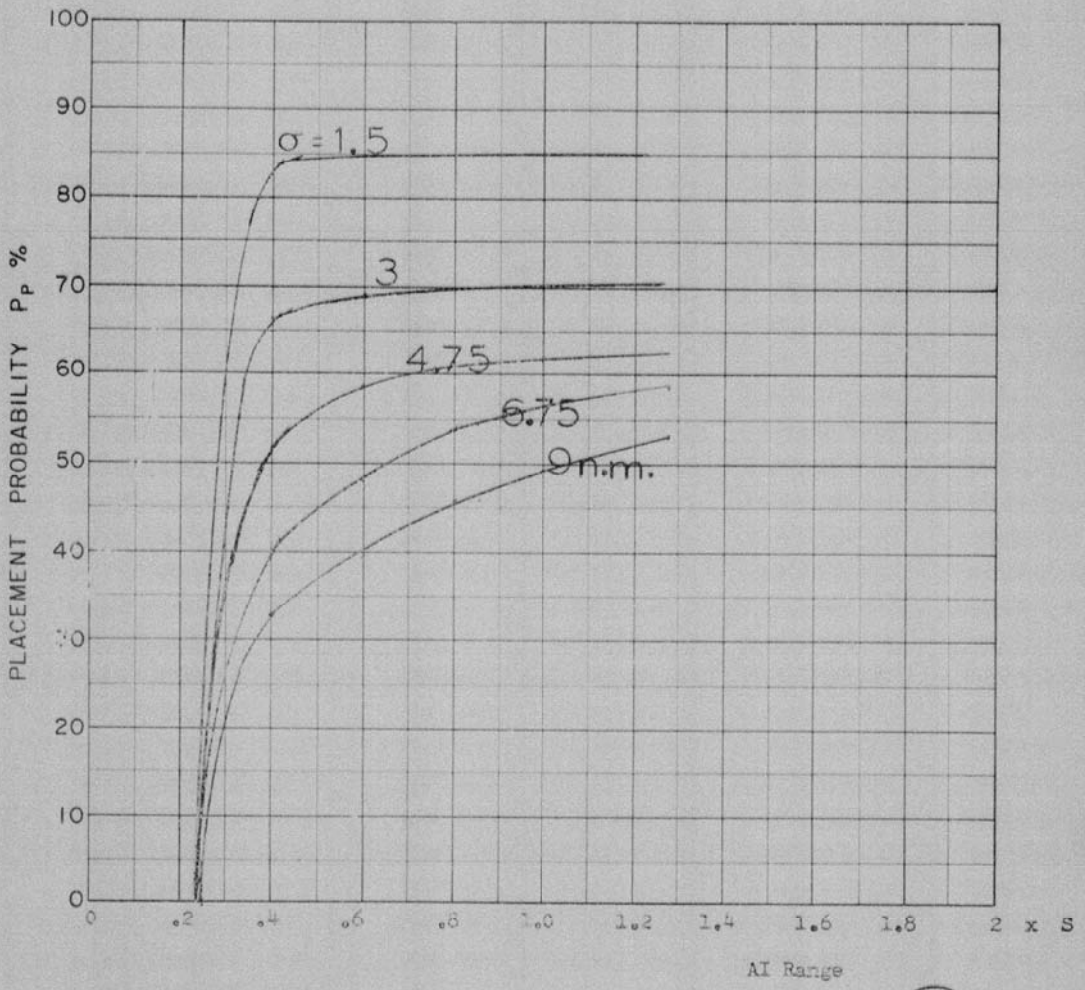

COURSE DIFFERENCE: 90°
TARGET EVASION: 0
TARGET MACH NO.: 2.0
INTERCEPTOR LATERAL G's: 3.60
INTERCEPTOR MACH NO.: 1.8
σ OF G.C.I. ACCURACY: Five values
A.I. DETECTION RANGE AS FRACTION OF SPECIFICATION RANGE, S: Abscissa
A.I. DETECTION RANGE CONTOUR: Delta
ALTITUDE: 60 K

D1406

Launch zone figure L-8. Missile launched at medium range with 8° heading error allowance.

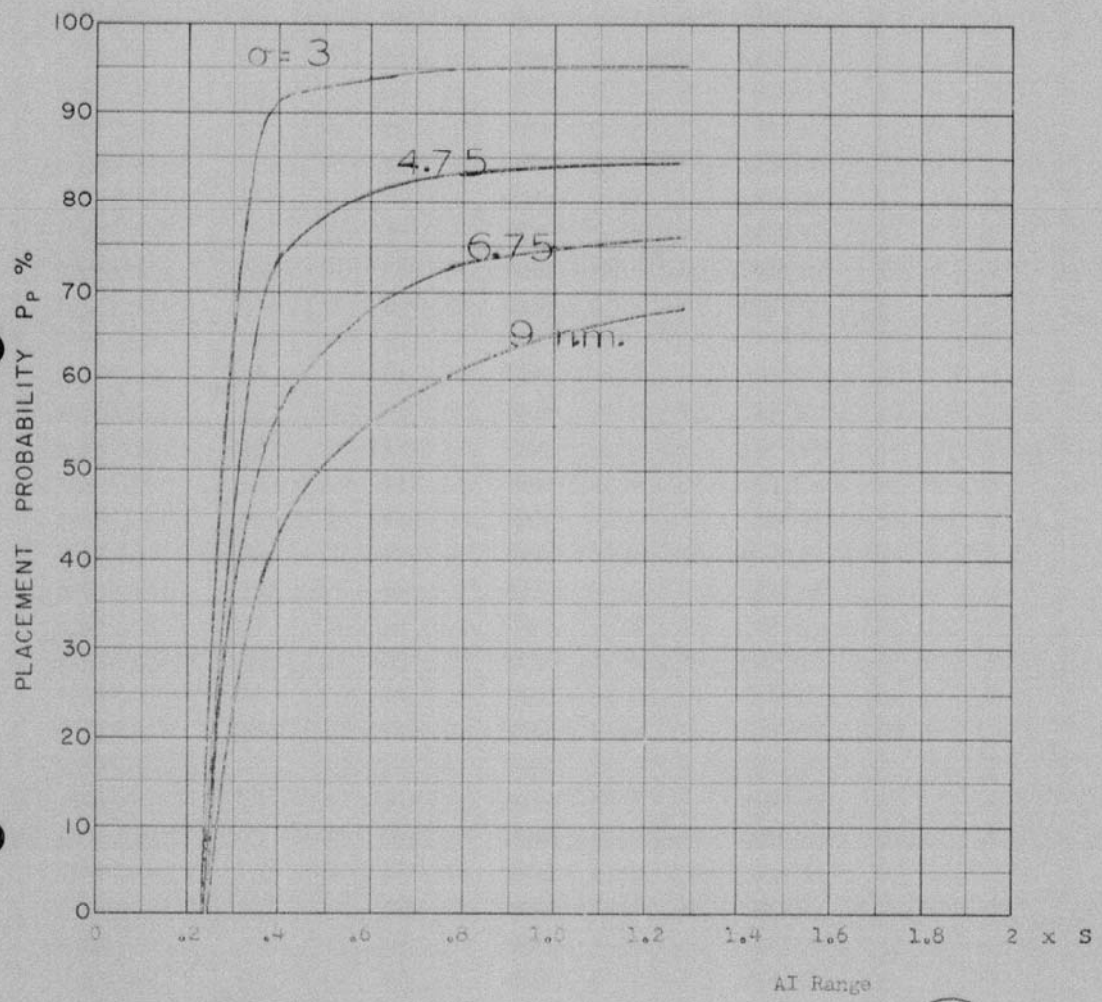

COURSE DIFFERENCE: 180°
TARGET EVASION: 0
TARGET MACH NO.: 2
INTERCEPTOR LATERAL G's: 3.60
INTERCEPTOR MACH NO.: 1.8
σ OF G.C.I. ACCURACY: Four values
A.I. DETECTION RANGE AS FRACTION OF SPECIFICATION RANGE, S: Abscissa
A.I. DETECTION RANGE CONTOUR: Delta
ALTITUDE: 60 K

D141a

Launch zone of figure L-8, missile launched at minimum range with 9° heading error allowance.

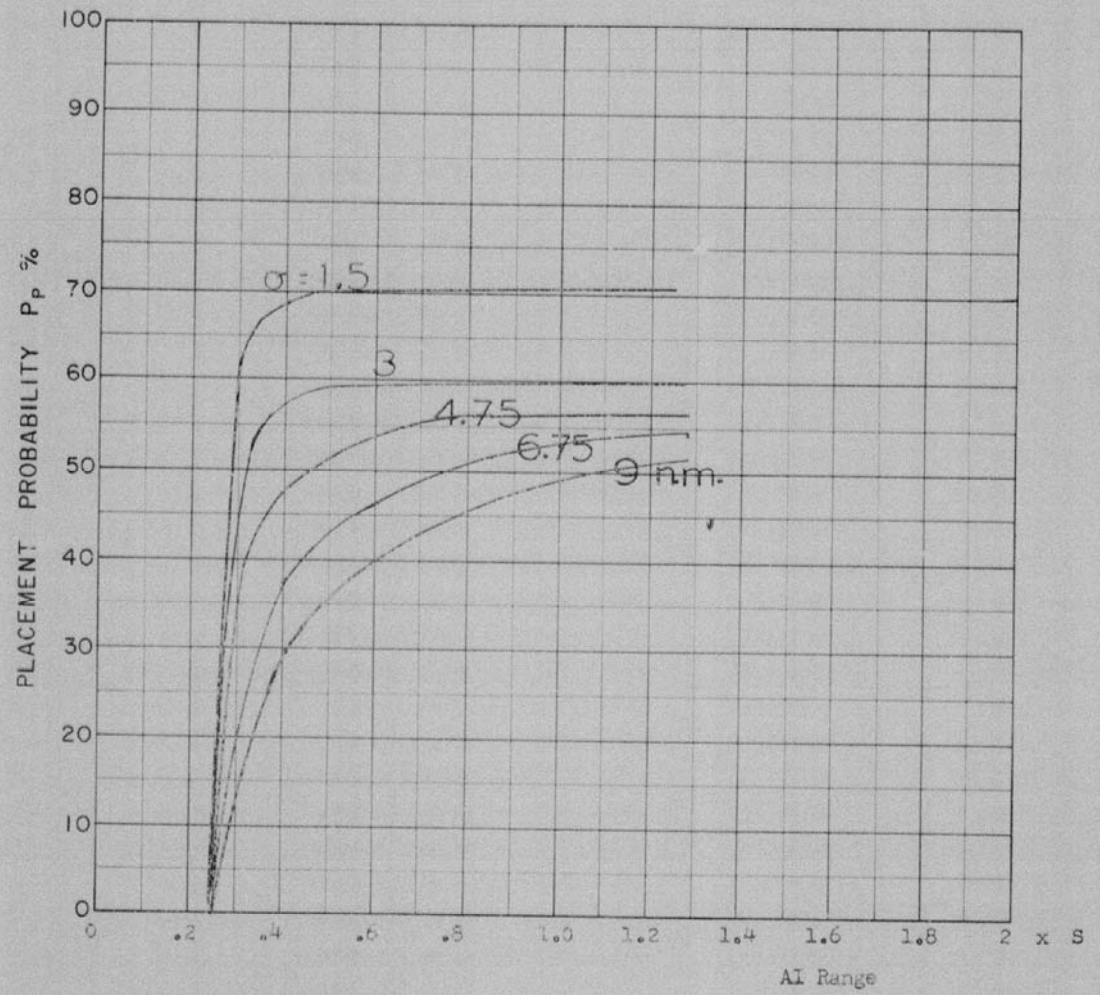

COURSE DIFFERENCE: 100°
TARGET EVASION: 5
TARGET MACH NO.: 2.0
INTERCEPTOR LATERAL G's: 3.60
INTERCEPTOR MACH NO.: 1.8
σ OF G.C.I. ACCURACY: Five values
A.I. DETECTION RANGE AS FRACTION OF SPECIFICATION RANGE, S: Abscissa
A.I. DETECTION RANGE CONTOUR: Delta
ALTITUDE: 60 K

D141b

Launch zone figure L-8. Missile launched at medium range with 8° heading error allowance.

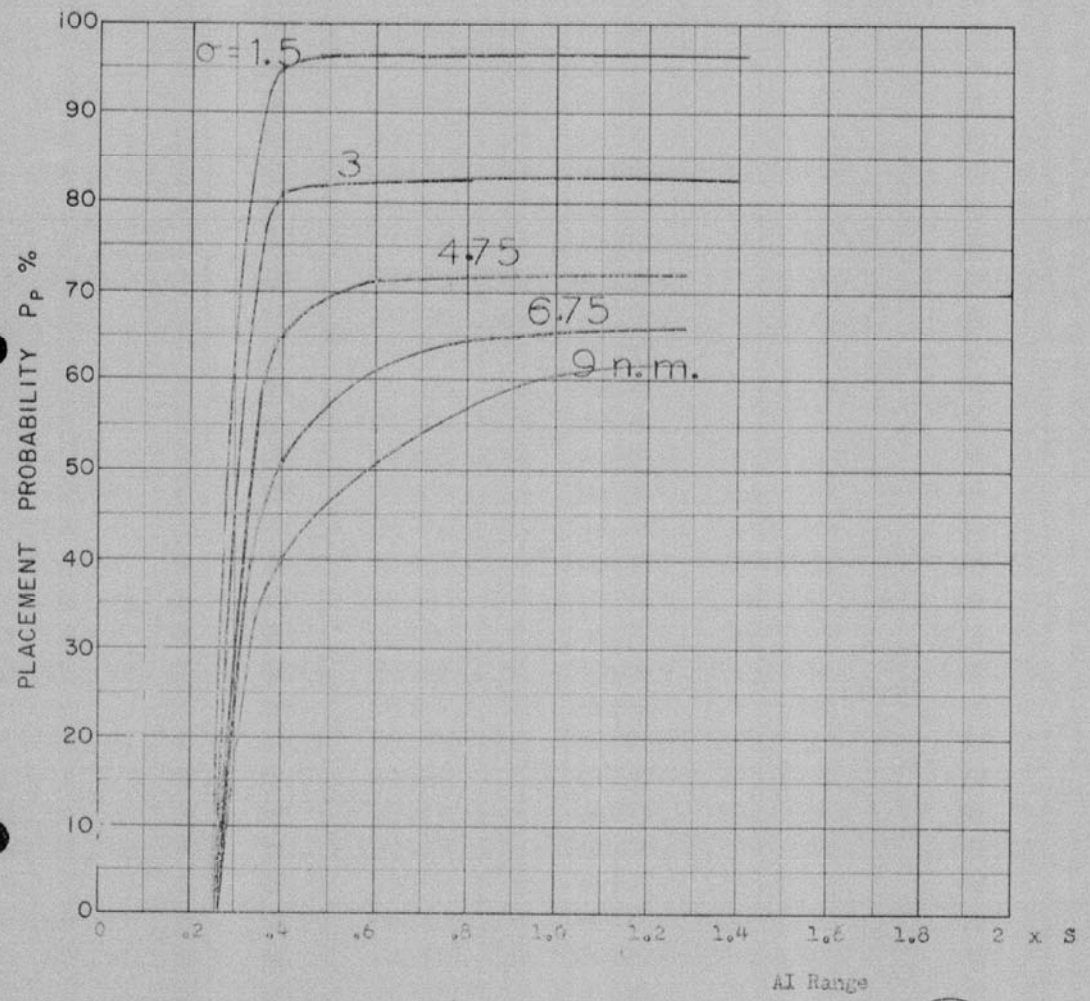

COURSE DIFFERENCE: 120°
TARGET EVASION: 0
TARGET MACH NO.: 2
INTERCEPTOR LATERAL G's: 3.60
INTERCEPTOR MACH NO.: 1.5
σ OF G.C.I. ACCURACY: Five values
A.I. DETECTION RANGE AS FRACTION OF SPECIFICATION RANGE, S: Abscissa
A.I. DETECTION RANGE CONTOUR: Delta
ALTITUDE: 60 K

D14

Launch zone of figure L-8, missile launched at minimum range with 8° heading error allowance.

18 e n d p r

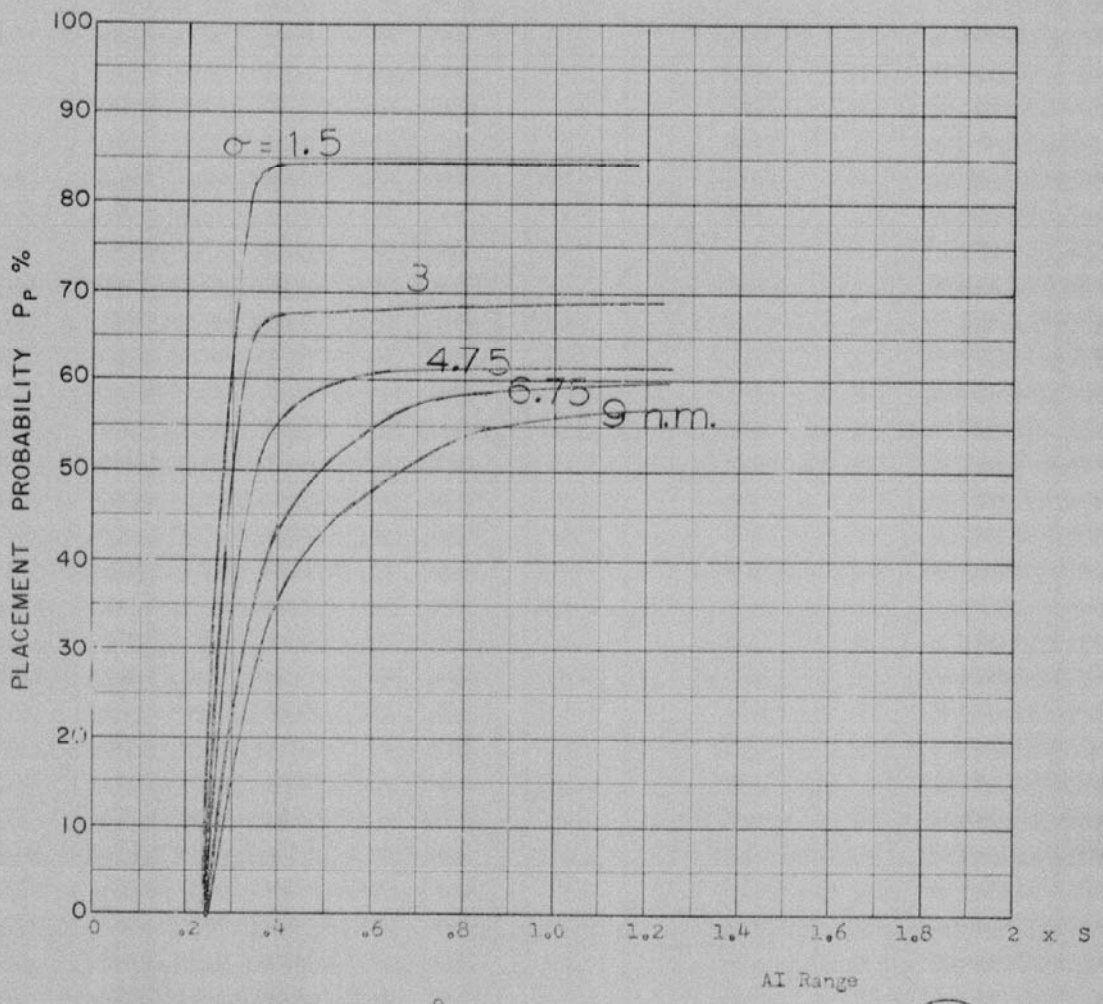

COURSE DIFFERENCE: 135°
TARGET EVASION: 0
TARGET MACH NO.: 2
INTERCEPTOR LATERAL G's: 3.60
INTERCEPTOR MACH NO.: 1.5
σ OF G.C.I. ACCURACY: Five values
A.I. DETECTION RANGE AS FRACTION OF SPECIFICATION RANGE, S: Abscissa
A.I. DETECTION RANGE CONTOUR: Delta
ALTITUDE: 60 K

D143

Launch zone of figure L-8, missile launched at minimum range with 8° heading error allowance.

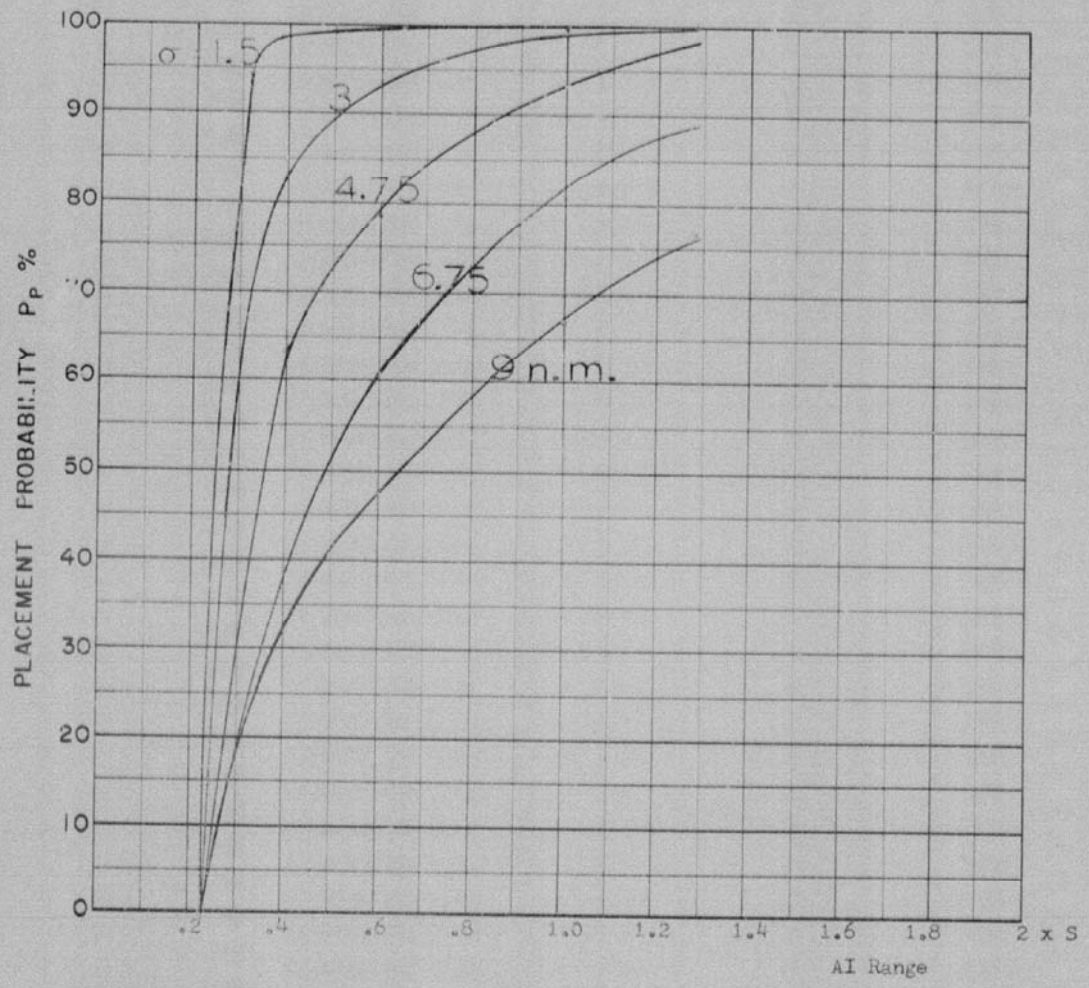

COURSE DIFFERENCE: 110°
TARGET EVASION: 0.1 lateral g's
TARGET MACH NO.: 2.0
INTERCEPTOR LATERAL G's: 3.0
INTERCEPTOR MACH NO.: 1.5
σ OF G.C.I. ACCURACY: Five values
A.I. DETECTION RANGE AS FRACTION OF SPECIFICATION RANGE, S: Abscissa
A.I. DETECTION RANGE CONTOUR: Delta
ALTITUDE: 50 K

(D 96)

Missile launch zone L-10

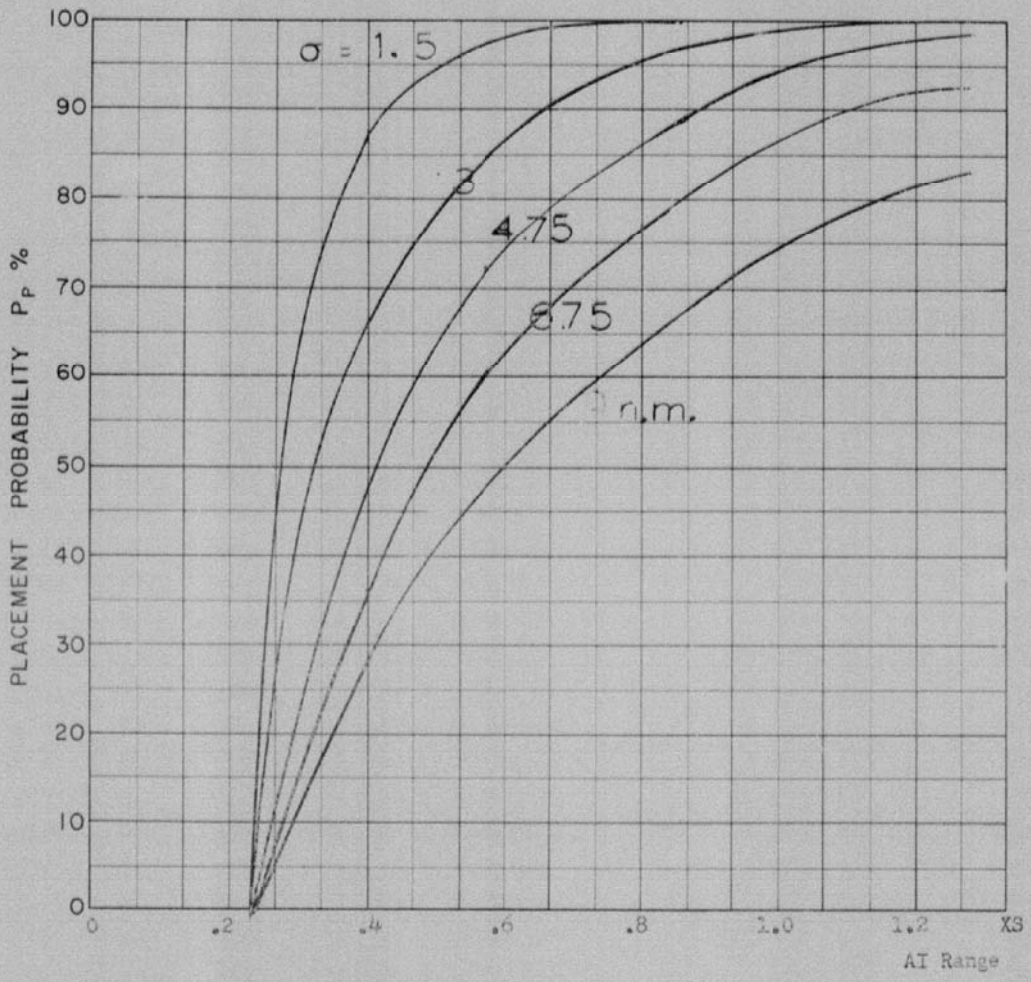

COURSE DIFFERENCE: 80°
TARGET EVASION: 0
TARGET MACH NO.: 1.5
INTERCEPTOR LATERAL G's: 0.85
INTERCEPTOR MACH NO.: 1.5
σ OF G.C.I. ACCURACY: Five values
A.I. DETECTION RANGE AS FRACTION OF SPECIFICATION RANGE, S: Abscissa
A.I. DETECTION RANGE CONTOUR: Straight Wing
ALTITUDE: 50K

S1

Launch zone L-1, maximum range, 15° heading error.

34bxspr

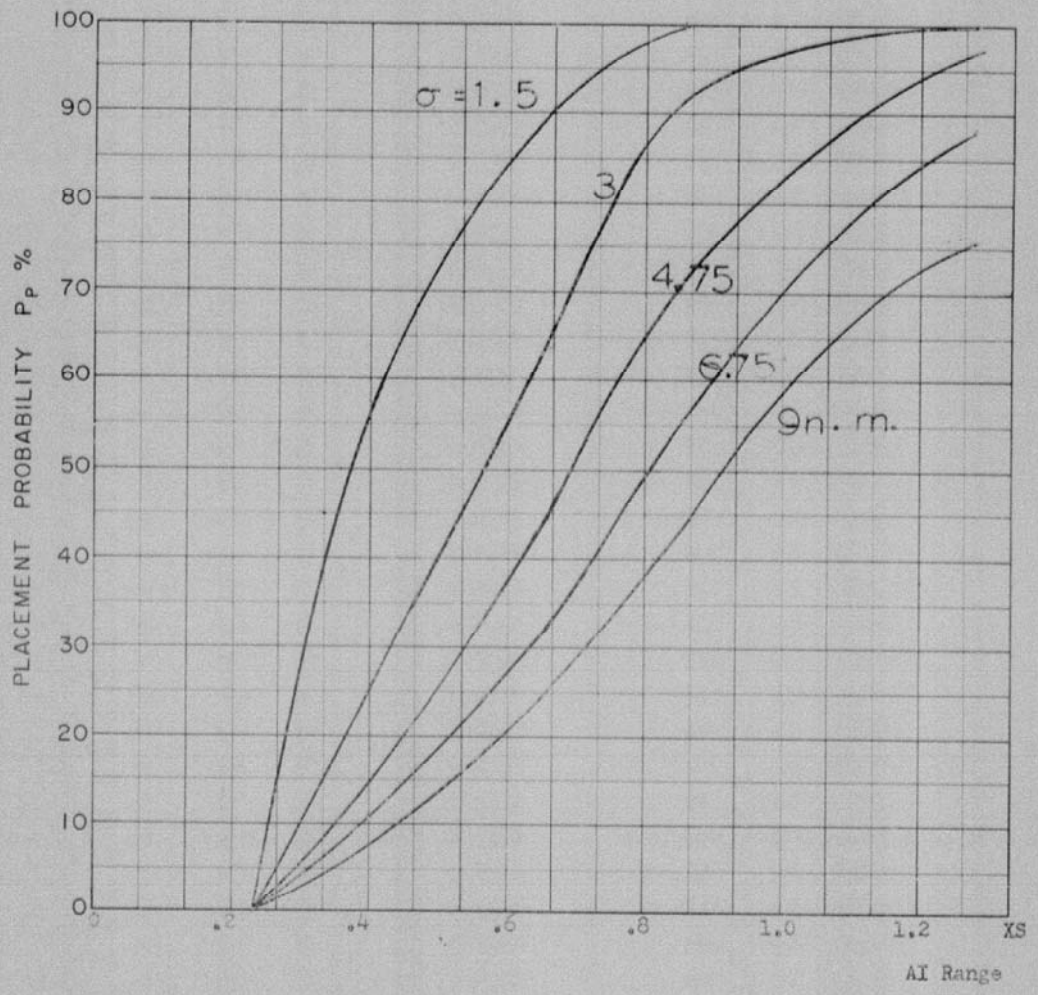

S-2a

COURSE DIFFERENCE: 100°
TARGET EVASION: 0
TARGET MACH NO.: 1.5
INTERCEPTOR LATERAL G's: 0.85
INTERCEPTOR MACH NO.: 1.5
σ OF G.C.I. ACCURACY: Five values
A.I. DETECTION RANGE AS FRACTION OF SPECIFICATION RANGE, S: Abscissa
A.I. DETECTION RANGE CONTOUR: Straight Wing
ALTITUDE: 50K

Launch zone L-1, maximum range, 15° heading error.

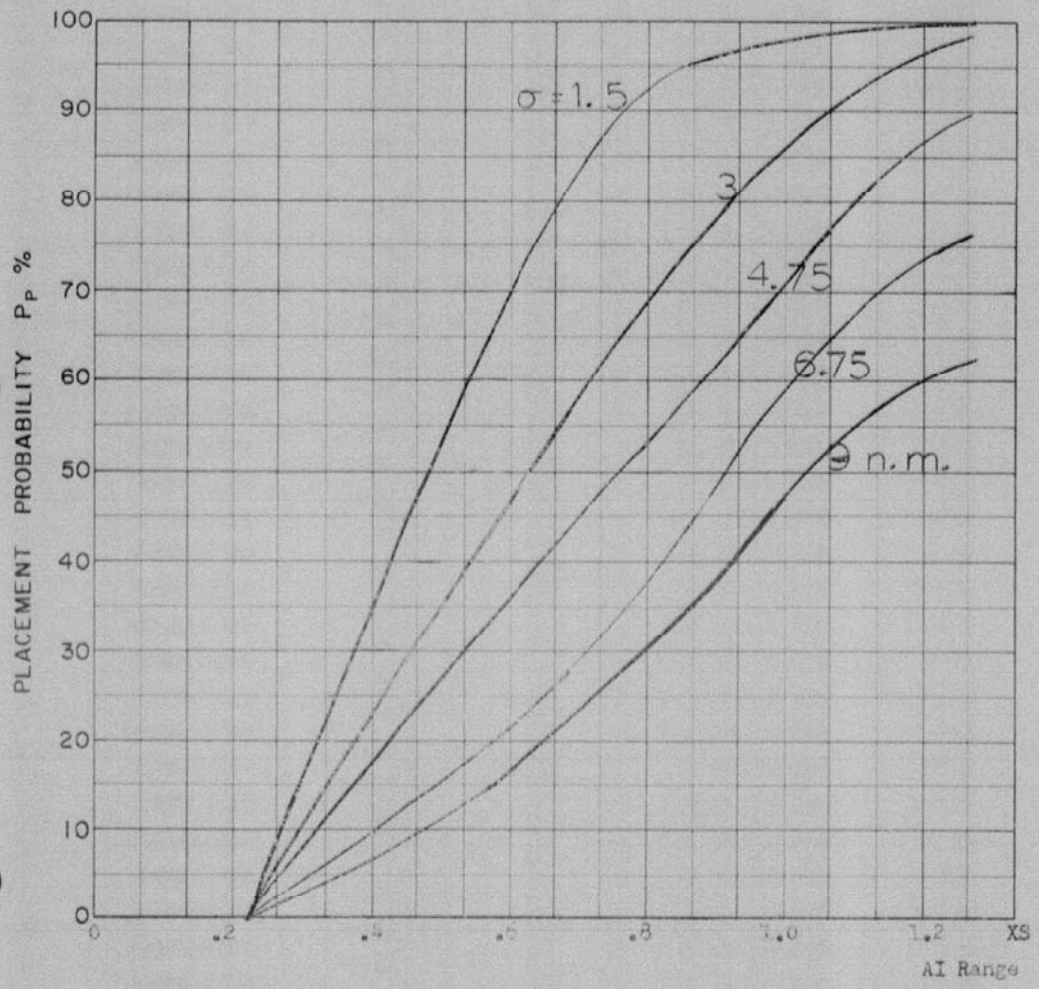

COURSE DIFFERENCE: 100°
TARGET EVASION: 0
TARGET MACH NO.: 1.5
INTERCEPTOR LATERAL G's: 0.85
INTERCEPTOR MACH NO.: 2.5
σ OF G.C.I. ACCURACY: Five values
A.I. DETECTION RANGE AS FRACTION OF SPECIFICATION RANGE, S: Abscissa
A.I. DETECTION RANGE CONTOUR: Straight Wing
ALTITUDE: 50K

(S2b)

Launch zone L-1, minimum range, 10° heading error.

3Mcxspr

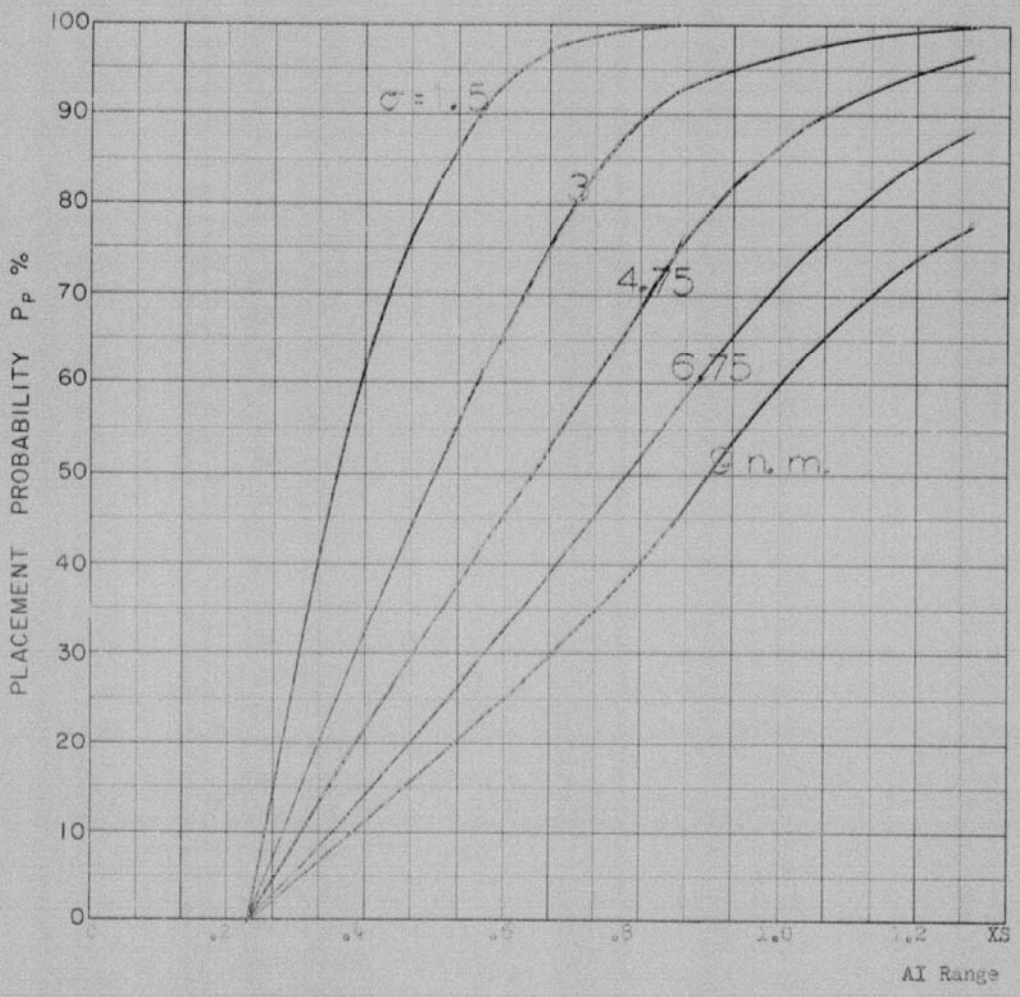

COURSE DIFFERENCE: 120°
TARGET EVASION: 0
TARGET MACH NO.: 2.5
INTERCEPTOR LATERAL G's: 0.85
INTERCEPTOR MACH NO.: 1.5
σ OF G.C.I. ACCURACY: Five values
A.I. DETECTION RANGE AS FRACTION OF SPECIFICATION RANGE, S: Abscissa
A.I. DETECTION RANGE CONTOUR: Straight Wing
ALTITUDE: 50K

S 3

Launch zone L-1, maximum range, 15° heading error.

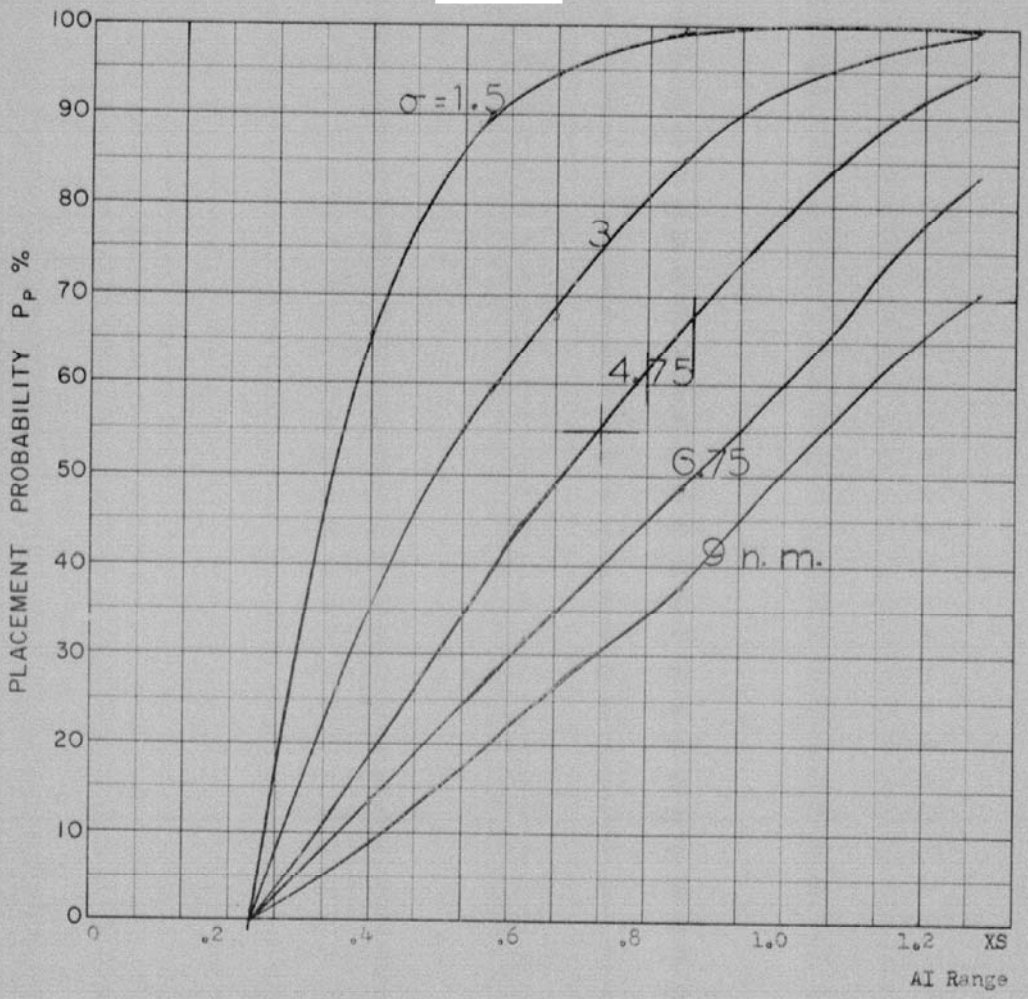

COURSE DIFFERENCE: 140°
TARGET EVASION: 0
TARGET MACH NO.: 1.5
INTERCEPTOR LATERAL G's: 0.85
INTERCEPTOR MACH NO.: 1.5
σ OF G.C.I. ACCURACY: Five values
A.I. DETECTION RANGE AS FRACTION OF SPECIFICATION RANGE, S: Abscissa
A.I. DETECTION RANGE CONTOUR: Straight Wing
ALTITUDE: 50K

(S-4)

Launch zone L-1, maximum range, 15° heading error.

34exspr

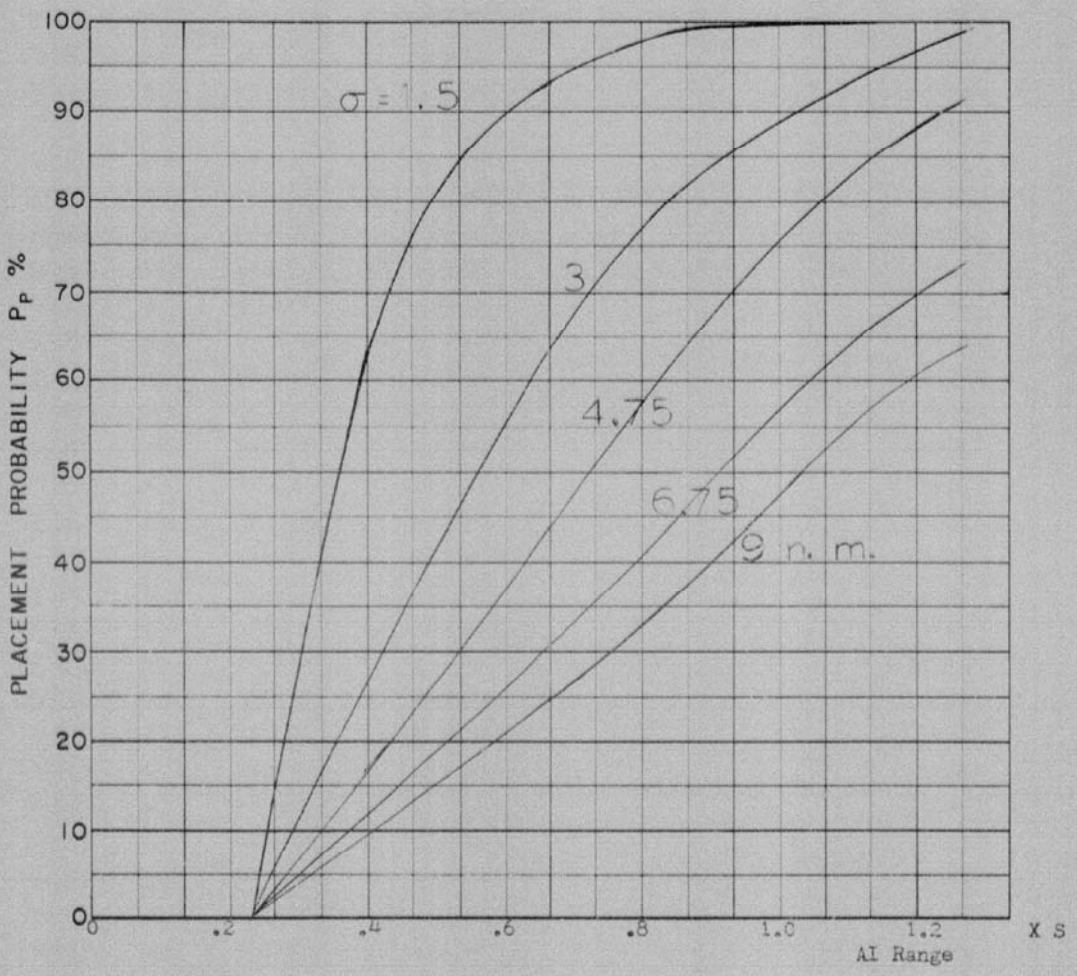

S.5

COURSE DIFFERENCE: 160°
TARGET EVASION: 0
TARGET MACH NO.: 1.5
INTERCEPTOR LATERAL G's: 0.85
INTERCEPTOR MACH NO.: 1.5
σ OF G.C.I. ACCURACY: Five values
A.I. DETECTION RANGE AS FRACTION OF SPECIFICATION RANGE, S: Abscissa
A.I. DETECTION RANGE CONTOUR: Straight wing
ALTITUDE: 50 K

Launch zone L-1, maximum range, 15° heading error.

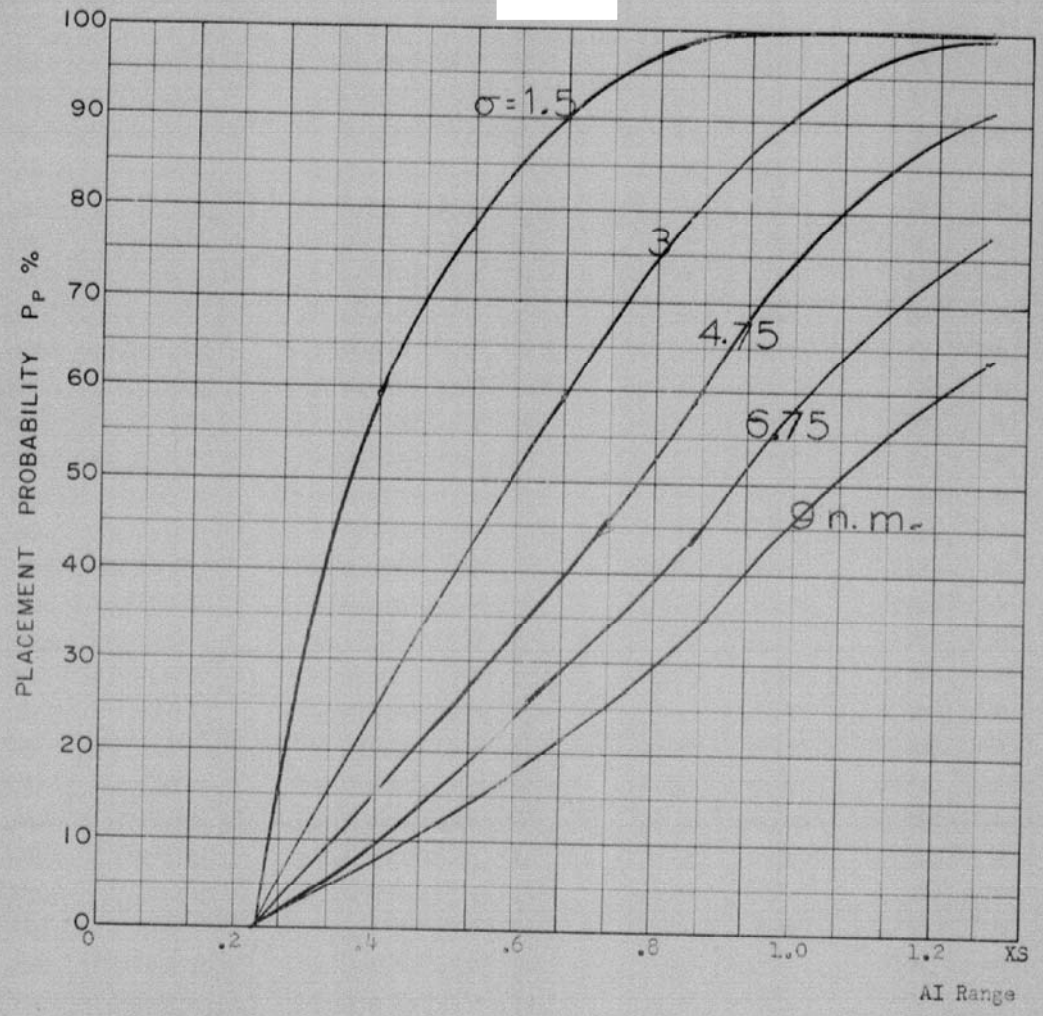

COURSE DIFFERENCE: 180°
TARGET EVASION: 0
TARGET MACH NO.: 1.5
INTERCEPTOR LATERAL G's: 0.85
INTERCEPTOR MACH NO.: 1.5
σ OF G.C.I. ACCURACY: Five values
A.I. DETECTION RANGE AS FRACTION OF SPECIFICATION RANGE, S: Abscissa
A.I. DETECTION RANGE CONTOUR: Straight Wing
ALTITUDE: 50K

S-6

Launch zone L-1, maximum range, 15° heading error.

35axspr

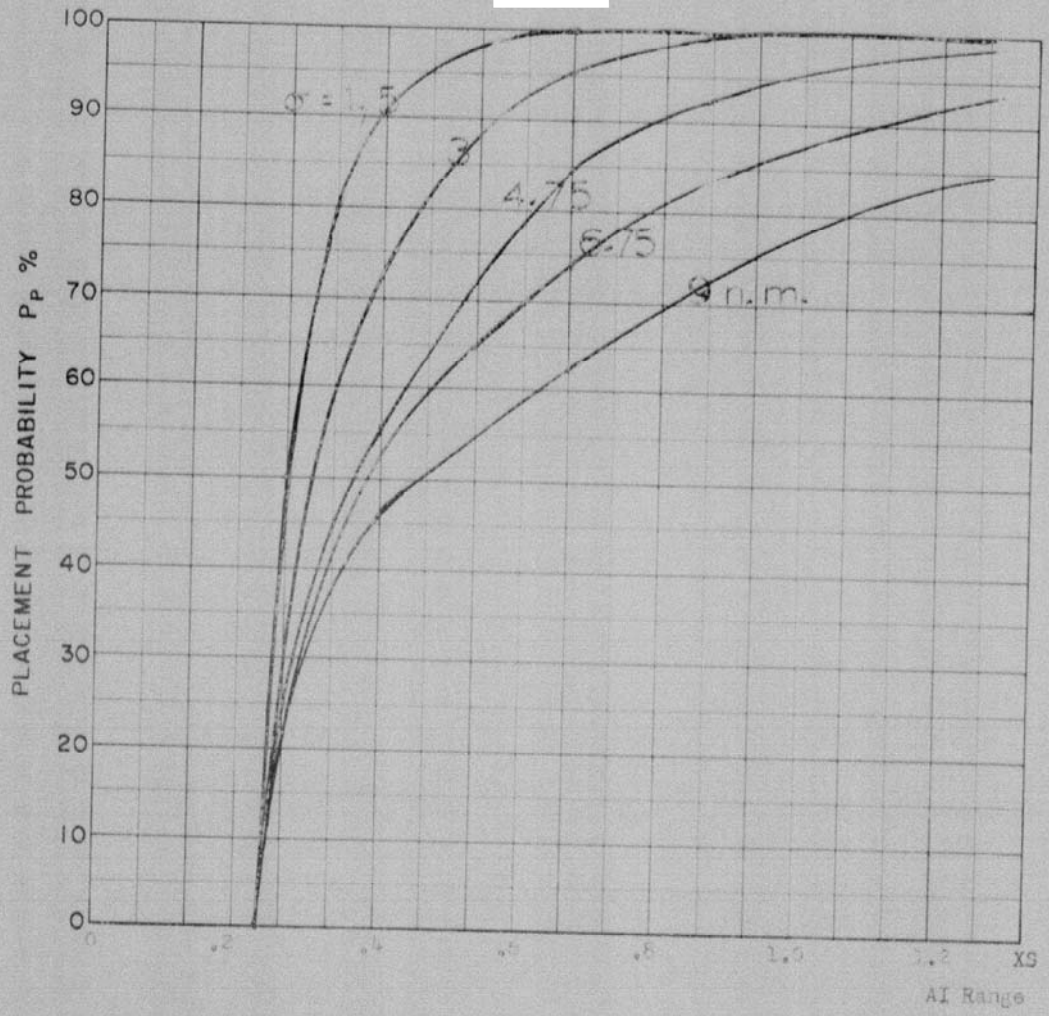

COURSE DIFFERENCE: 80°
TARGET EVASION: 0
TARGET MACH NO.: 1.5
INTERCEPTOR LATERAL G's: 0.25
INTERCEPTOR MACH NO.: 1.5
σ OF G.C.I. ACCURACY: Five values
A.I. DETECTION RANGE AS FRACTION OF SPECIFICATION RANGE, S: Abscissa
A.I. DETECTION RANGE CONTOUR: Straight Wing
ALTITUDE: 50K

S-7

Missile launch zone L-1, maximum range, 15° heading error.

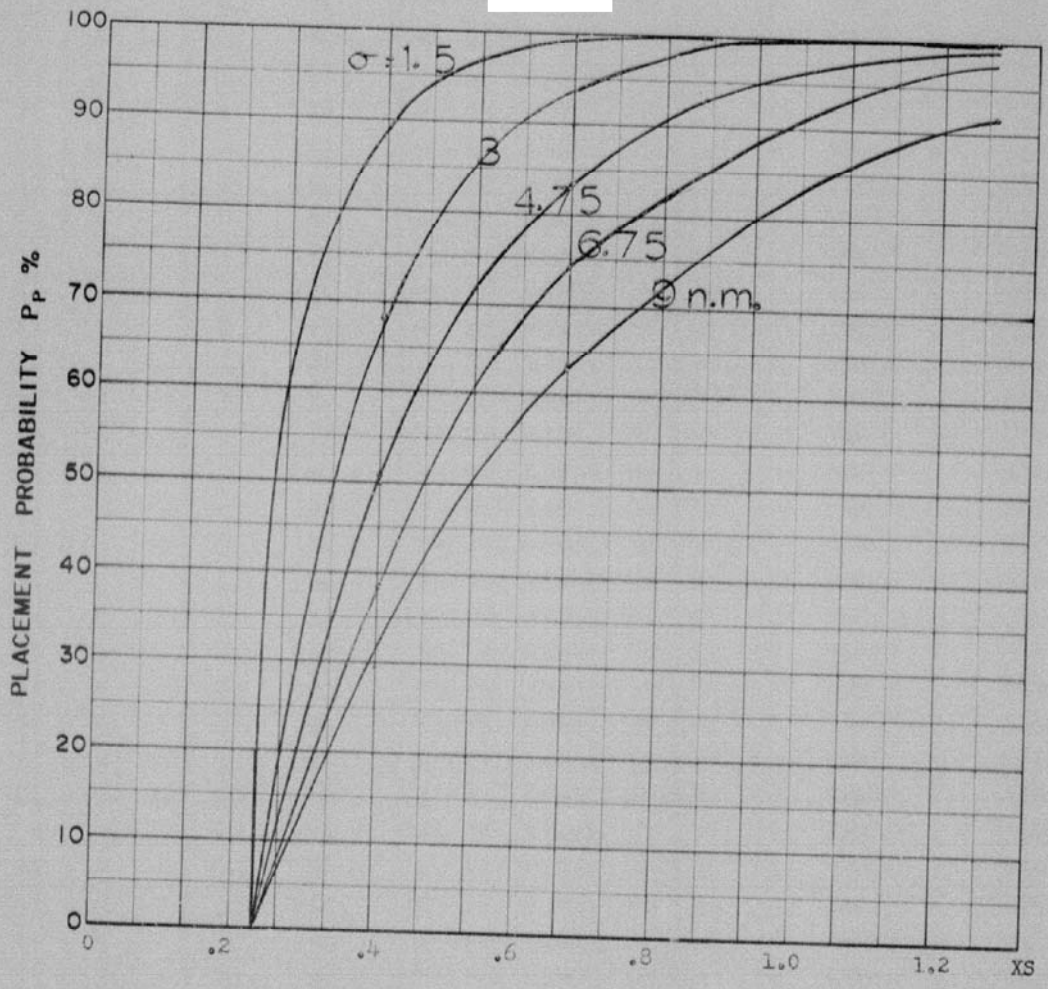

COURSE DIFFERENCE: 100°
TARGET EVASION: 0
TARGET MACH NO.: 1.5
INTERCEPTOR LATERAL G's: 1.25
INTERCEPTOR MACH NO.: 1.5
σ OF G.C.I. ACCURACY: Five values
A.I. DETECTION RANGE AS FRACTION OF SPECIFICATION RANGE, S: Abscissa
A.I. DETECTION RANGE CONTOUR: Straight Wing
ALTITUDE: 50K

S8a

Missile launch zone L-1, maximum range, 15° heading error.

35bnspr

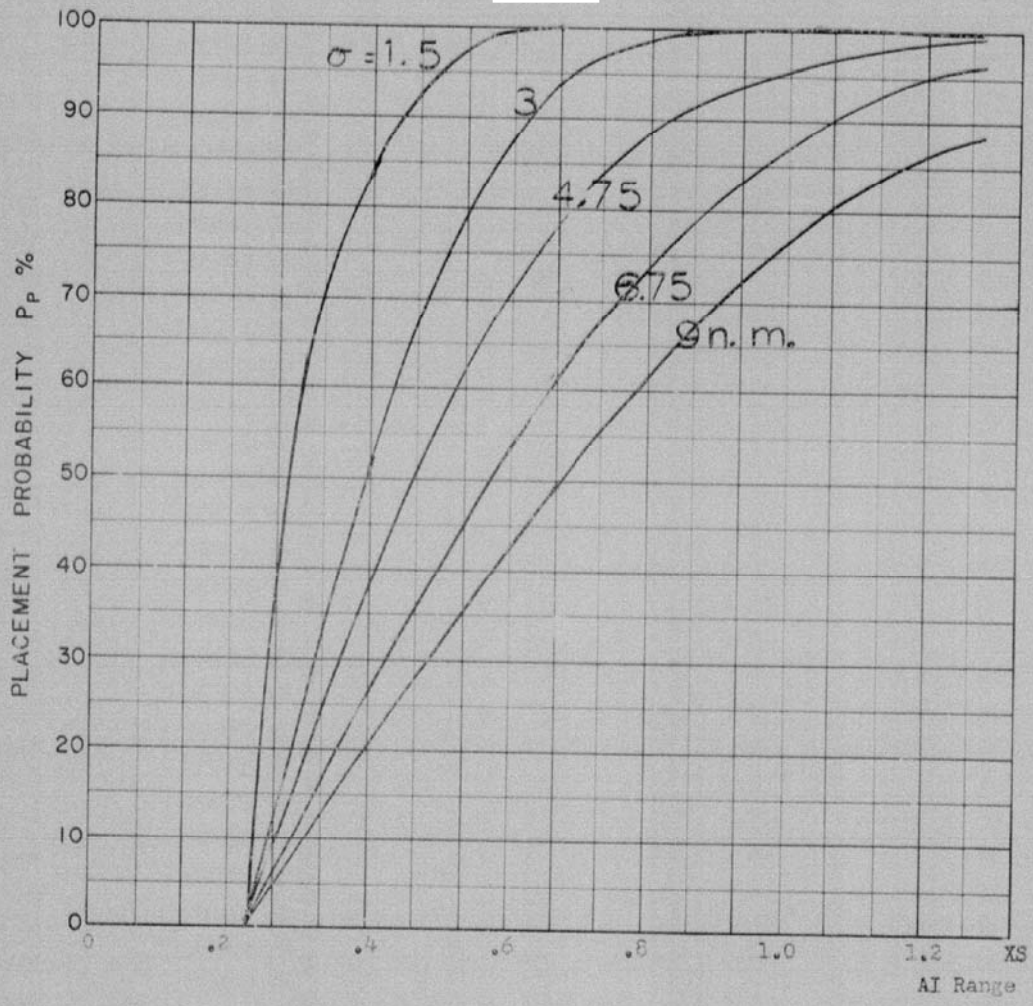

COURSE DIFFERENCE: 100°
TARGET EVASION: 0
TARGET MACH NO.: 1.5
INTERCEPTOR LATERAL G's: 1.25
INTERCEPTOR MACH NO.: 1.5
σ OF G.C.I. ACCURACY: Five values
A.I. DETECTION RANGE AS FRACTION OF SPECIFICATION RANGE, S: Abscissa
A.I. DETECTION RANGE CONTOUR: Straight Wing
ALTITUDE: 50K

S8b

Missile launch zone L-1, minimum range, 10° heading error.

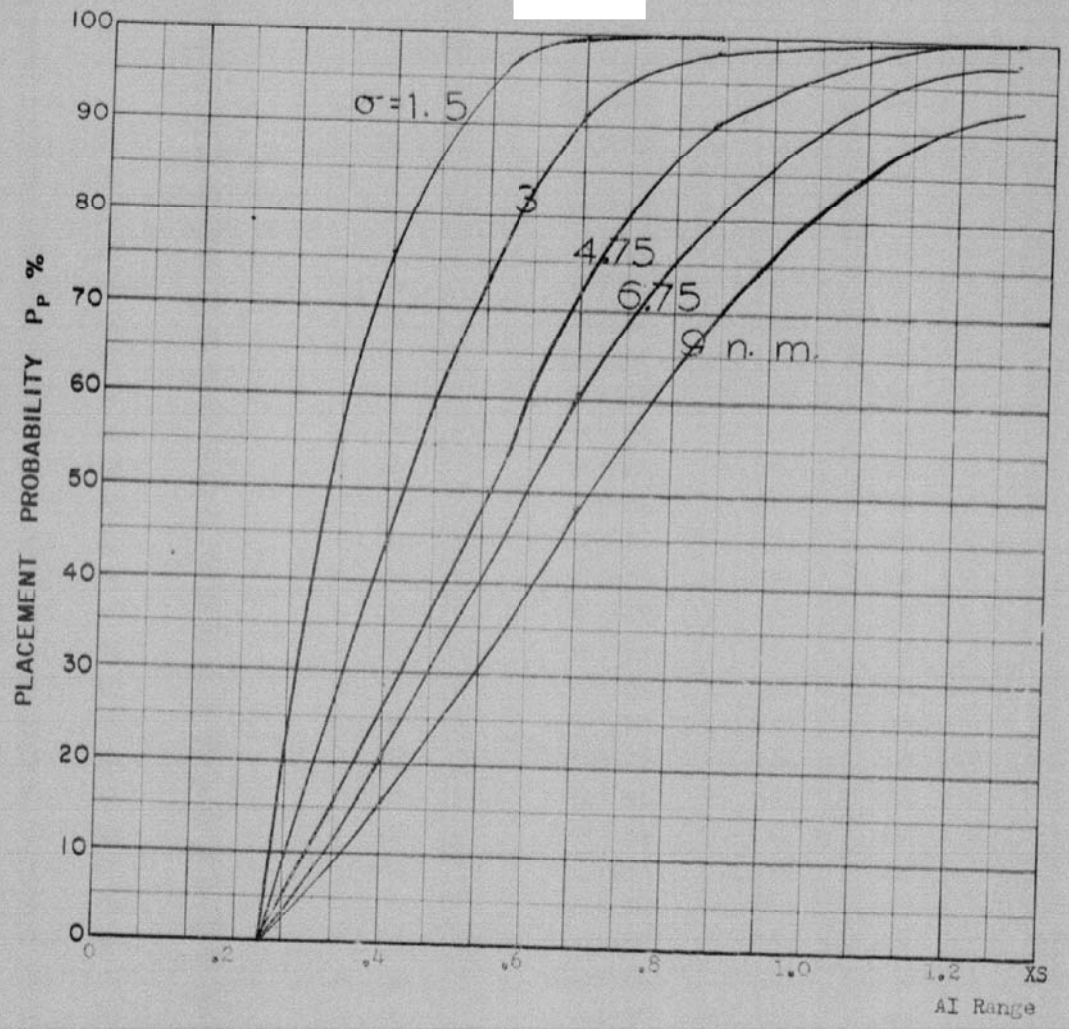

COURSE DIFFERENCE: 120°
TARGET EVASION: 0
TARGET MACH NO.: 1.5
INTERCEPTOR LATERAL G's: 1.25
INTERCEPTOR MACH NO.: 1.5
σ OF G.C.I. ACCURACY: Five values
A.I. DETECTION RANGE AS FRACTION OF SPECIFICATION RANGE, S: Abscissa
A.I. DETECTION RANGE CONTOUR: Straight Wing
ALTITUDE: 30K

S9

Missile launch zone L-1, maximum range 15° heading error.

35dxspr

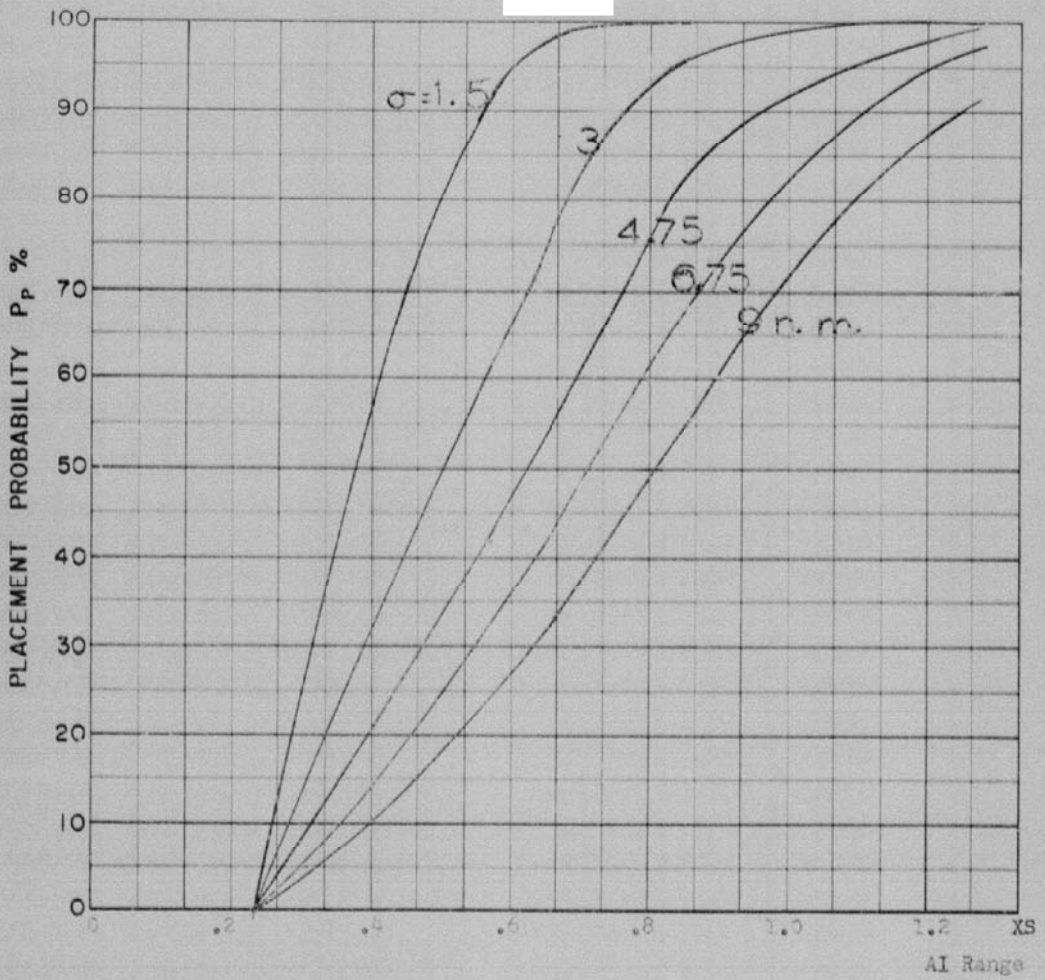

S.10

COURSE DIFFERENCE: 140°
TARGET EVASION: 0
TARGET MACH NO.: 1.5
INTERCEPTOR LATERAL G's: 3.25
INTERCEPTOR MACH NO.: 1.5
σ OF G.C.I. ACCURACY: Five values
A.I. DETECTION RANGE AS FRACTION OF SPECIFICATION RANGE, S: Abscissa
A.I. DETECTION RANGE CONTOUR: Straight Wing
ALTITUDE: 50K

Missile launch zone L-1, maximum range, 15° heading error.

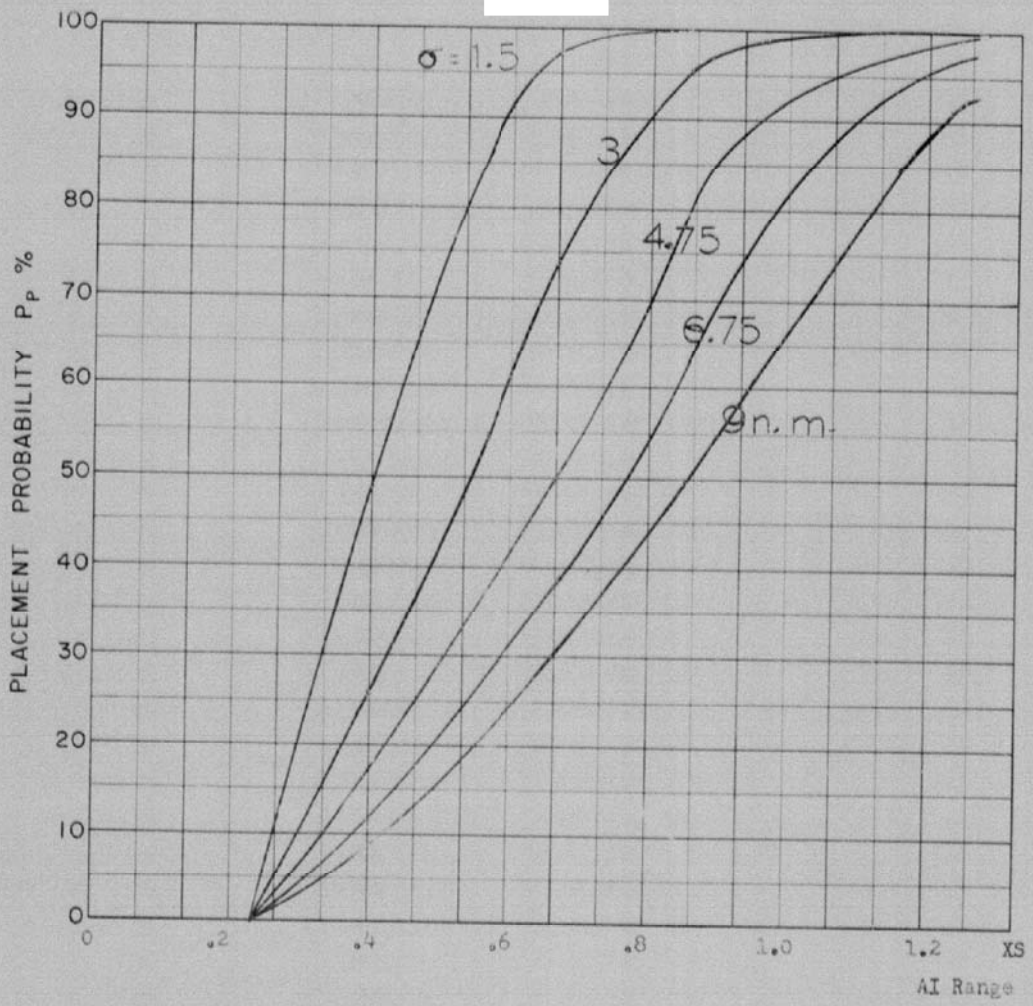

COURSE DIFFERENCE: 160°
TARGET EVASION: 0
TARGET MACH NO.: 1.5
INTERCEPTOR LATERAL G's: 1.25
INTERCEPTOR MACH NO.: 1.5
σ OF G.C.I. ACCURACY: Five values
A.I. DETECTION RANGE AS FRACTION OF SPECIFICATION RANGE, S: Abscissa
A.I. DETECTION RANGE CONTOUR: Straight Wing
ALTITUDE: 50K

Missile launch zone L-1, maximum range, 15° heading error.

3510xspr

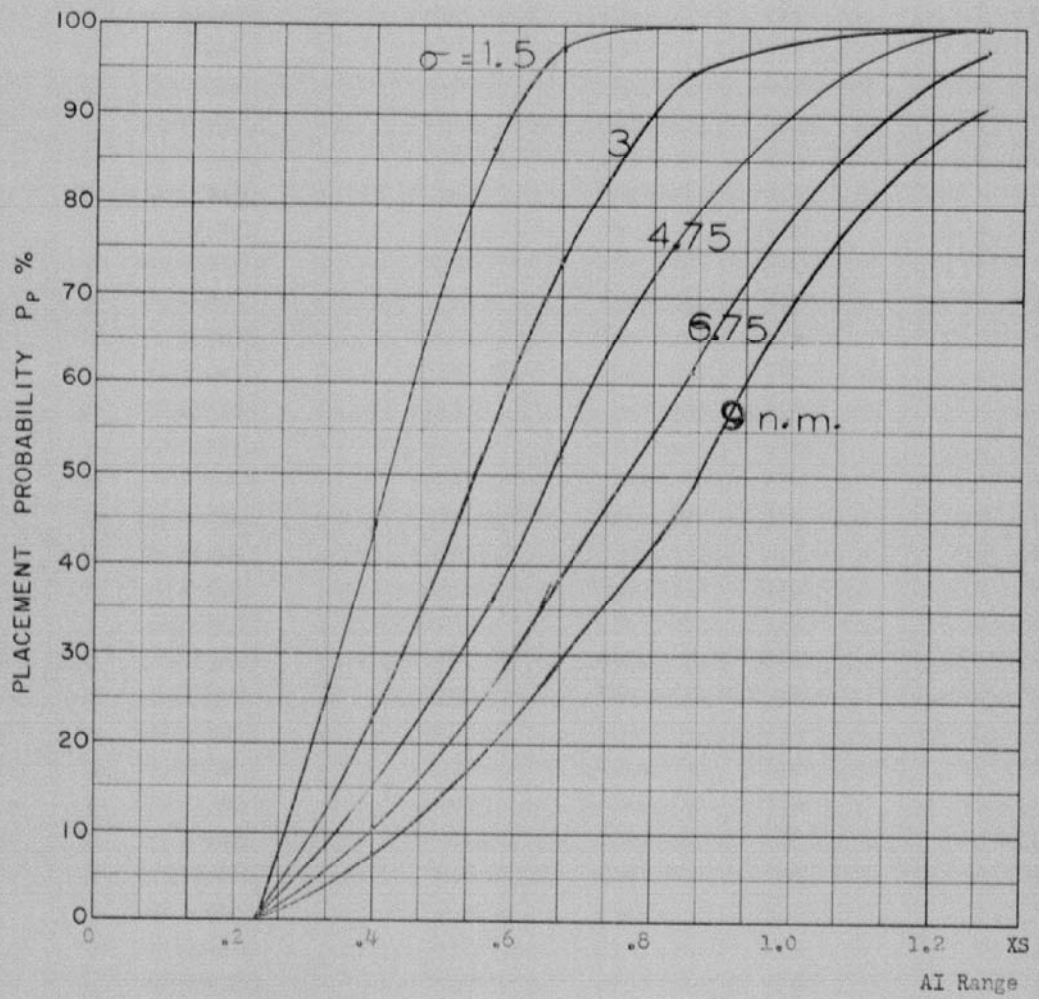

COURSE DIFFERENCE: 180°
TARGET EVASION: 0
TARGET MACH NO.: 1.5
INTERCEPTOR LATERAL G's: 1.25
INTERCEPTOR MACH NO.: 1.5
σ OF G.C.I. ACCURACY: Five values
A.I. DETECTION RANGE AS FRACTION OF SPECIFICATION RANGE, S: Abscissa
A.I. DETECTION RANGE CONTOUR: Straight Wing
ALTITUDE: 50K

S12

Missile launch zone L-1, maximum range, 15° heading error.

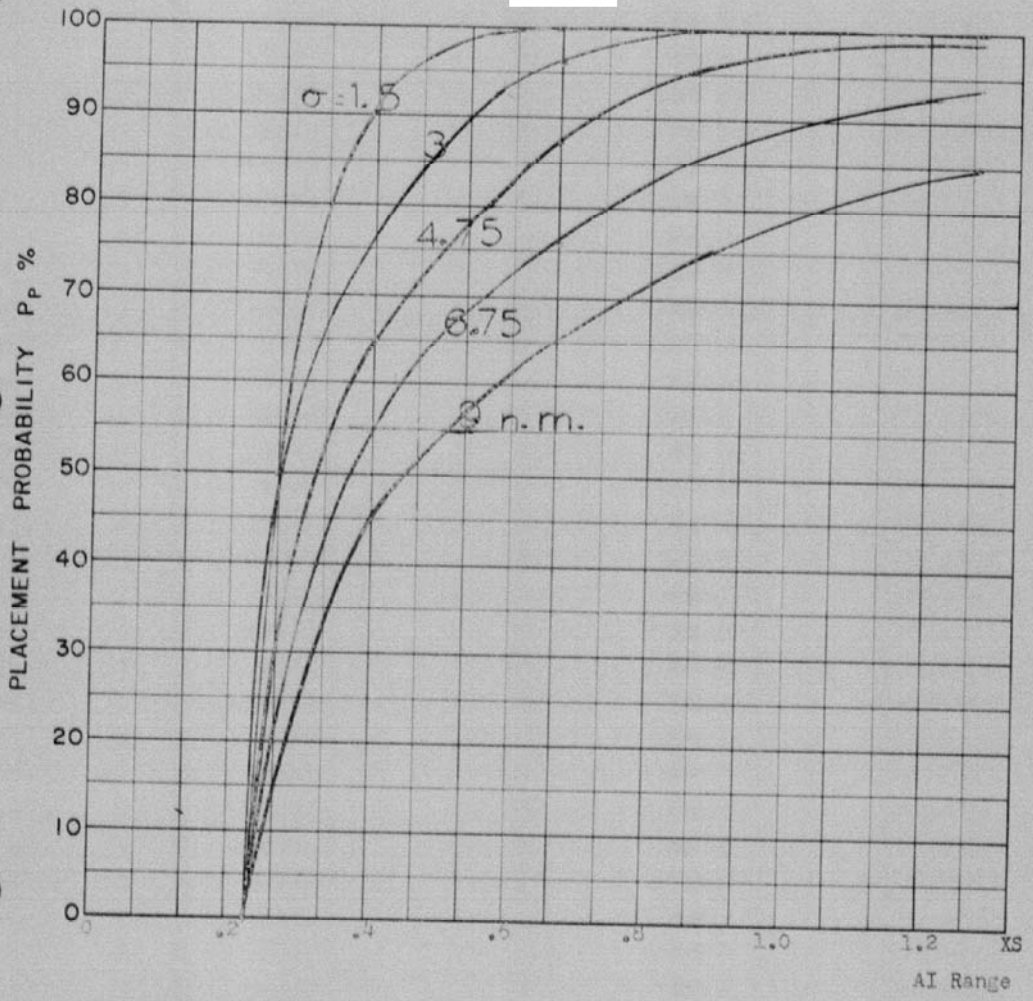

COURSE DIFFERENCE: 80°
TARGET EVASION: 0
TARGET MACH NO.: 1.5
INTERCEPTOR LATERAL G's: 1.60
INTERCEPTOR MACH NO.: 1.5
σ OF G.C.I. ACCURACY: Five values
A.I. DETECTION RANGE AS FRACTION OF SPECIFICATION RANGE, S: Abscissa
A.I. DETECTION RANGE CONTOUR: Straight Wing
ALTITUDE: 50K

S13a

Missile launch zone L-1, maximum range, 15° heading error.

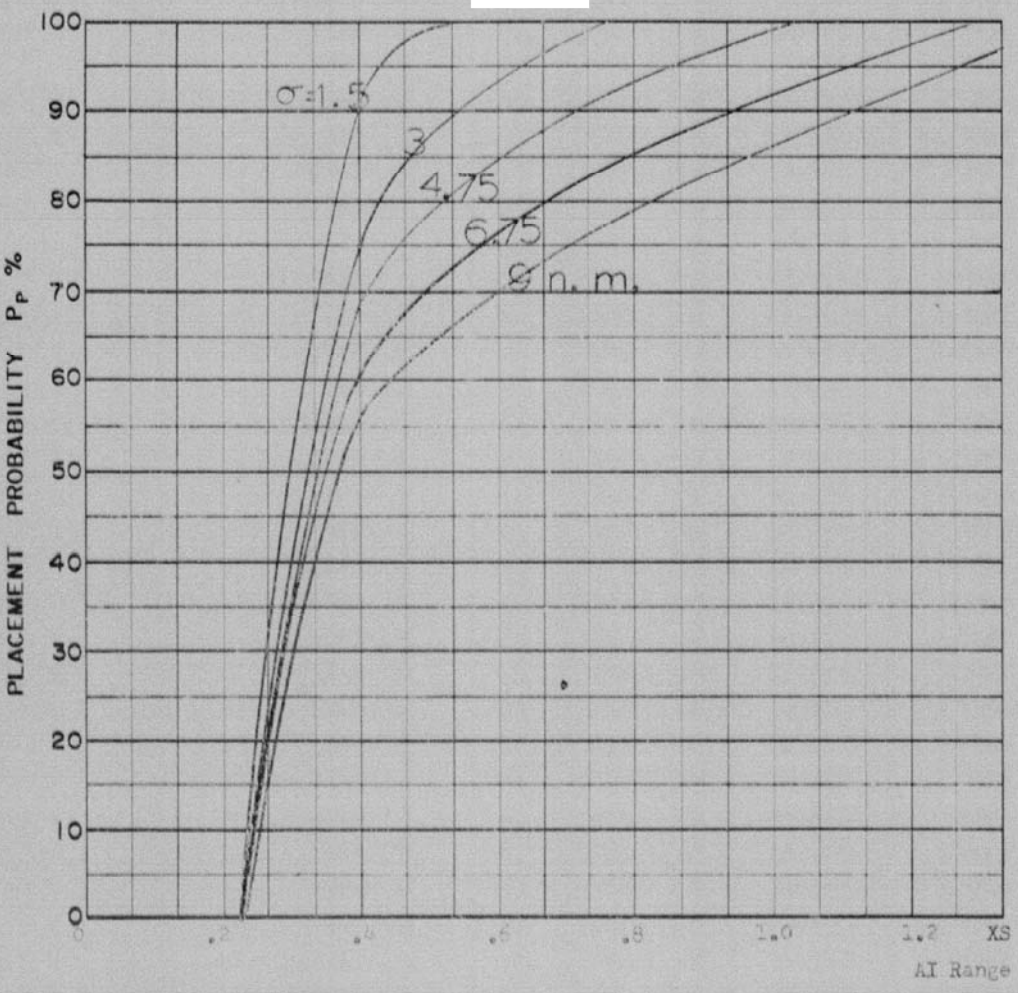

COURSE DIFFERENCE: 80°
TARGET EVASION: 0
TARGET MACH NO.: 1.5
INTERCEPTOR LATERAL G's: 1.60
INTERCEPTOR MACH NO.: 1.5
σ OF G.C.I. ACCURACY: Five values
A.I. DETECTION RANGE AS FRACTION OF SPECIFICATION RANGE, S: Abscissa
A.I. DETECTION RANGE CONTOUR: Straight Wing
ALTITUDE: 50K

S13c

Missile launch zone L-1, maximum range, 15° heading error, Look angle limit 80°.

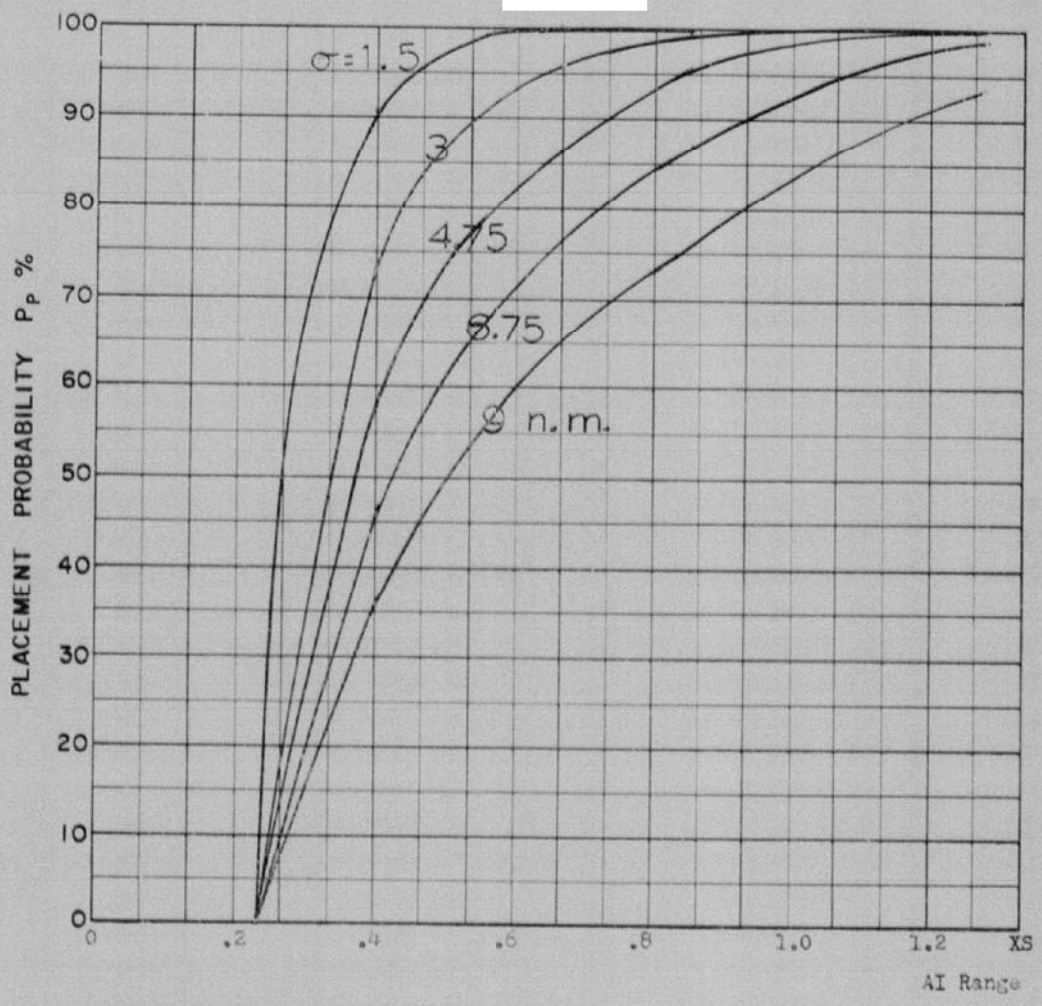

COURSE DIFFERENCE: 100°
TARGET EVASION: 0
TARGET MACH NO.: 1.5
INTERCEPTOR LATERAL G's: 1.60
INTERCEPTOR MACH NO.: 1.5
σ OF G.C.I. ACCURACY: Five values
A.I. DETECTION RANGE AS FRACTION OF SPECIFICATION RANGE, S: Abscissa
A.I. DETECTION RANGE CONTOUR: Straight Wing
ALTITUDE: 50K

Missile launch zone L-1, maximum range, 15° heading error.

S14a

36bnspr

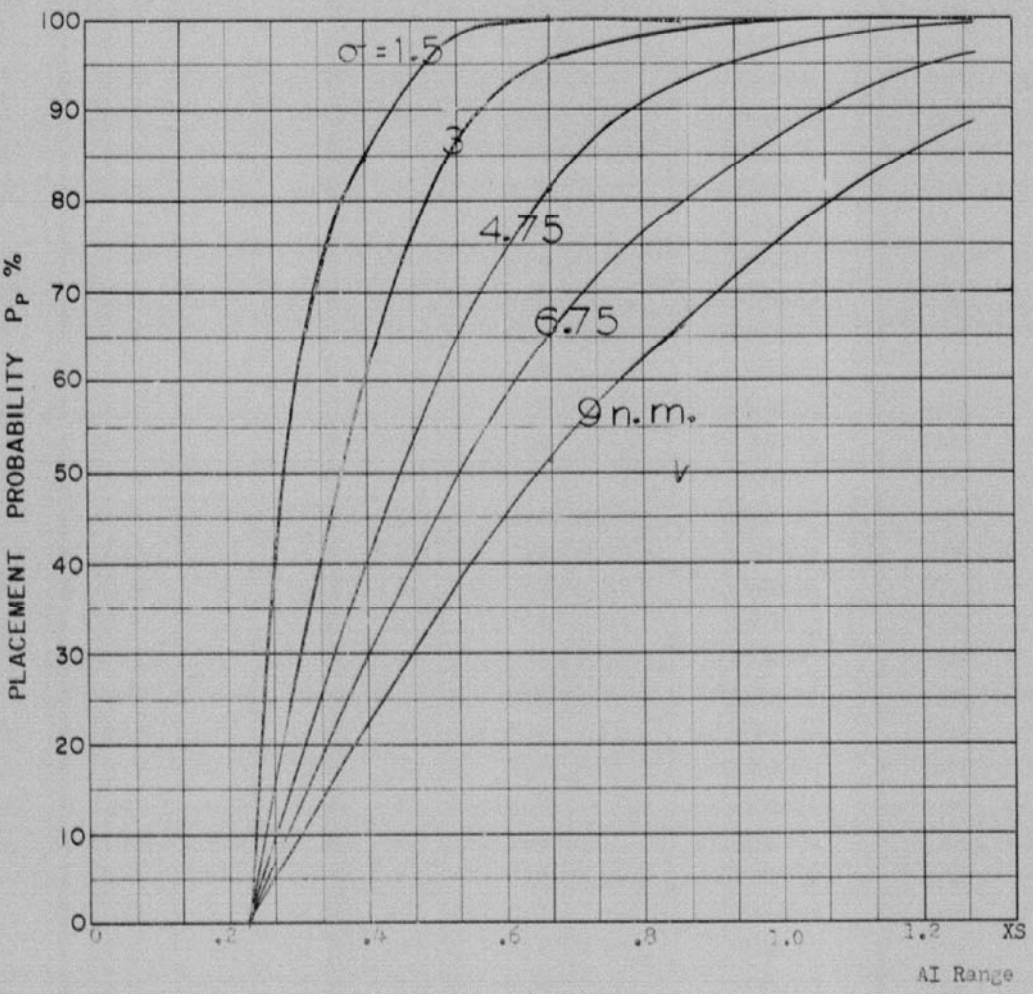

S14b

COURSE DIFFERENCE: 100°
TARGET EVASION: 0
TARGET MACH NO.: 1.5
INTERCEPTOR LATERAL G's: 1.60
INTERCEPTOR MACH NO.: 1.5
σ OF G.C.I. ACCURACY: Five values
A.I. DETECTION RANGE AS FRACTION OF SPECIFICATION RANGE, S: Abscissa
A.I. DETECTION RANGE CONTOUR: Straight Wing
ALTITUDE: 50K

Missile launch zone L-1, minimum range, 10° heading error.

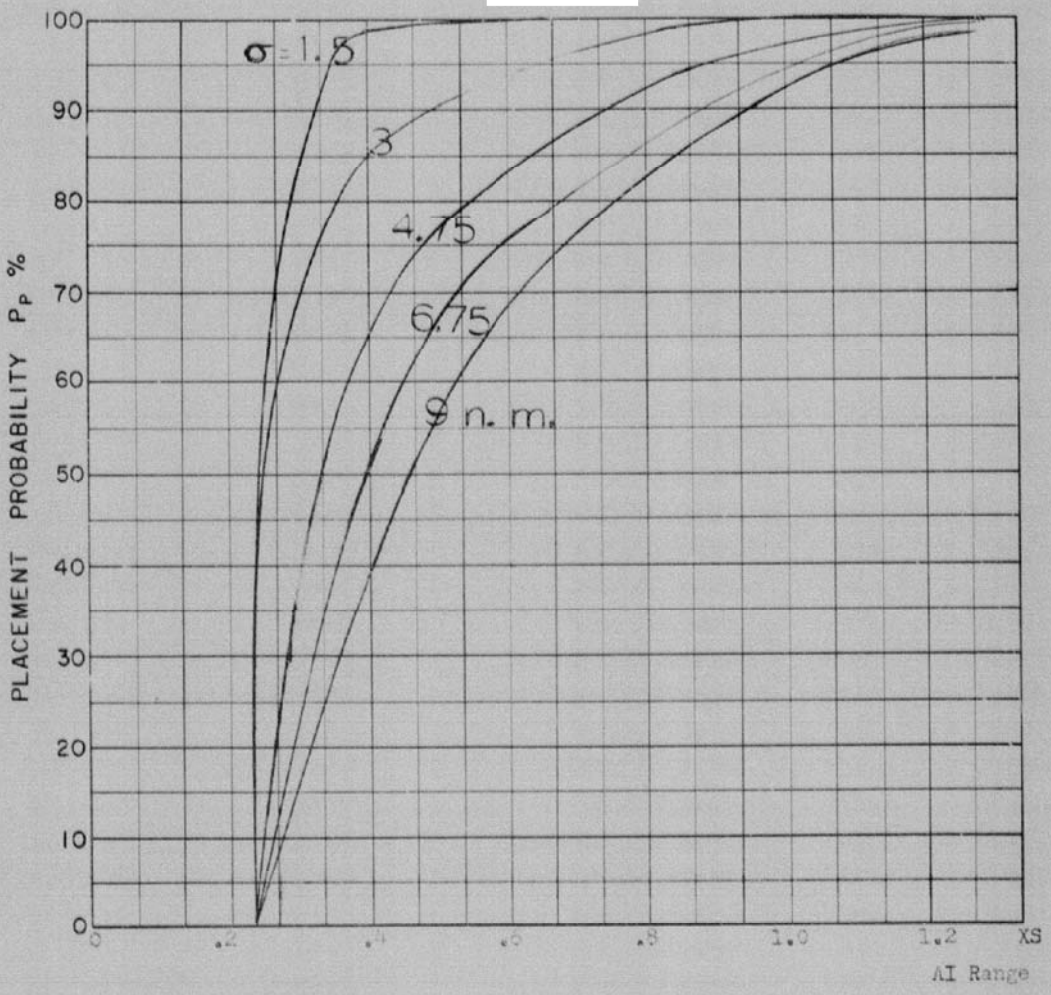

COURSE DIFFERENCE: 100°
TARGET EVASION: 0
TARGET MACH NO.: 1.5
INTERCEPTOR LATERAL G's: 1.60
INTERCEPTOR MACH NO.: 1.5
σ OF G.C.I. ACCURACY: Five values
A.I. DETECTION RANGE AS FRACTION OF SPECIFICATION RANGE, S: Abscissa
A.I. DETECTION RANGE CONTOUR: Straight Wing
ALTITUDE: 50K

S14c

Missile launch zone L-1, maximum range, 15° heading error, Look angle limit 80°.

37bnspr

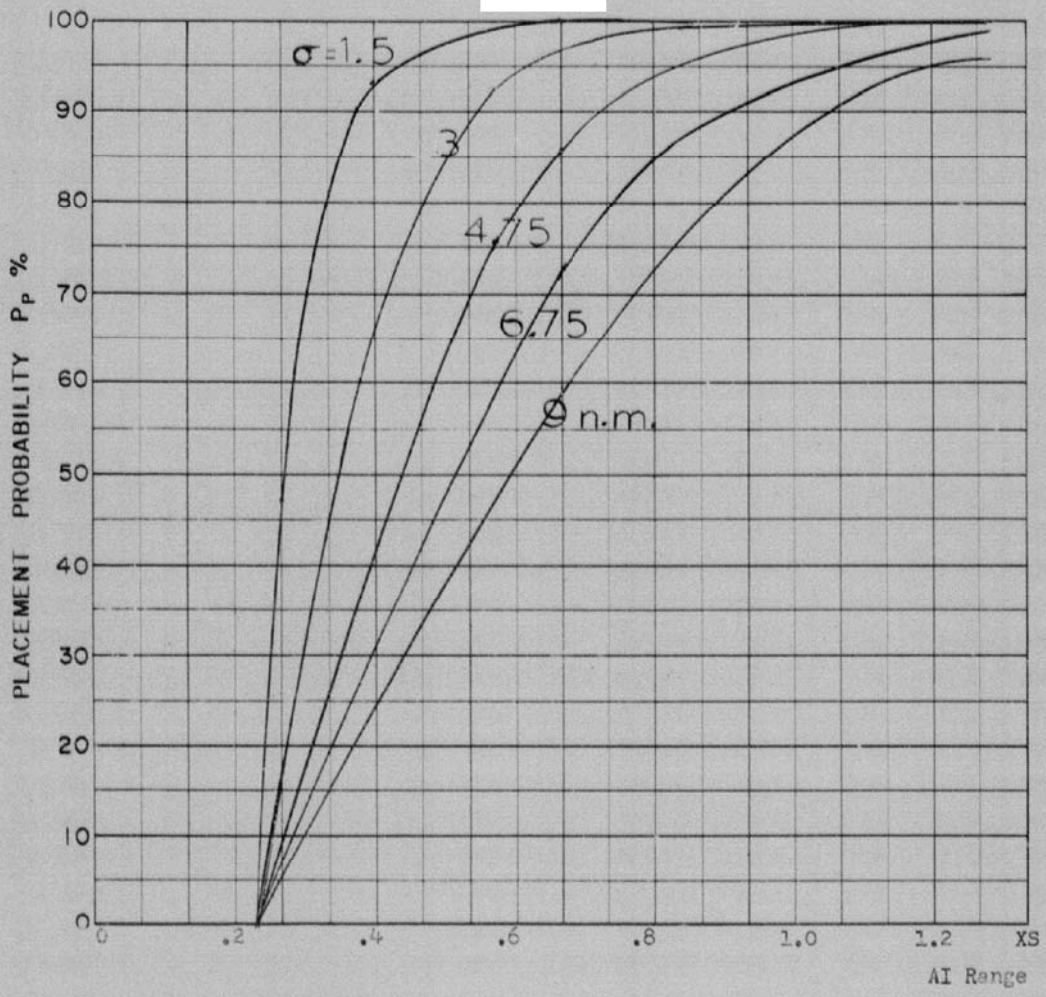

COURSE DIFFERENCE: 100°
TARGET EVASION: 0
TARGET MACH NO.: 1.5
INTERCEPTOR LATERAL G's: 1.60
INTERCEPTOR MACH NO.: 1.5
σ OF G.C.I. ACCURACY: Five values
A.I. DETECTION RANGE AS FRACTION OF SPECIFICATION RANGE, S: Abscissa
A.I. DETECTION RANGE CONTOUR: Straight Wing
ALTITUDE: 50K

S14d

Missile launch zone L-1, minimum range 10° heading error, Look angle limit 80°.

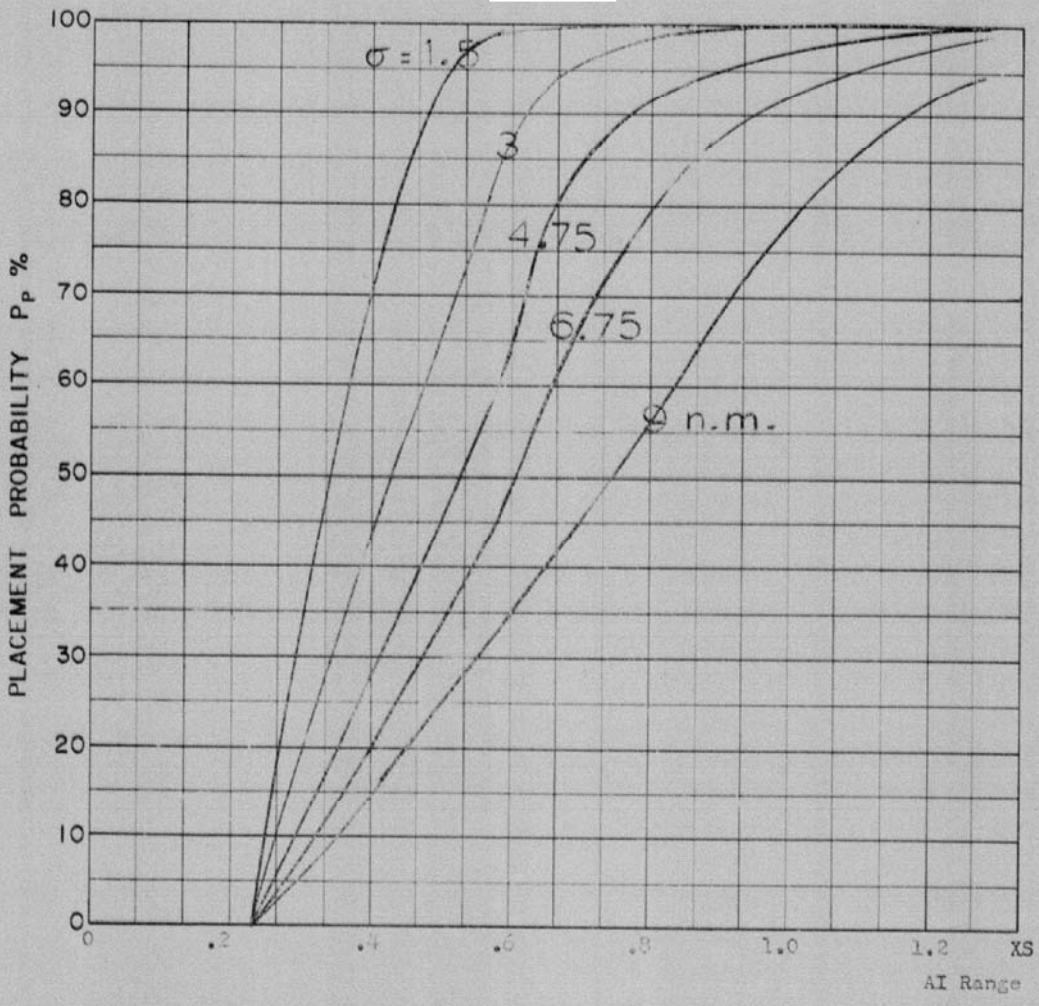

COURSE DIFFERENCE: 120°
TARGET EVASION: 0
TARGET MACH NO.: 1.5
INTERCEPTOR LATERAL G's: 1.60
INTERCEPTOR MACH NO.: 1.5
σ OF G.C.I. ACCURACY: Five values
A.I. DETECTION RANGE AS FRACTION OF SPECIFICATION RANGE, S: Abscissa
A.I. DETECTION RANGE CONTOUR: Straight
ALTITUDE: 50K

S15a

Missile launch zone L-1, maximum range, 15° heading error.

37cxspr

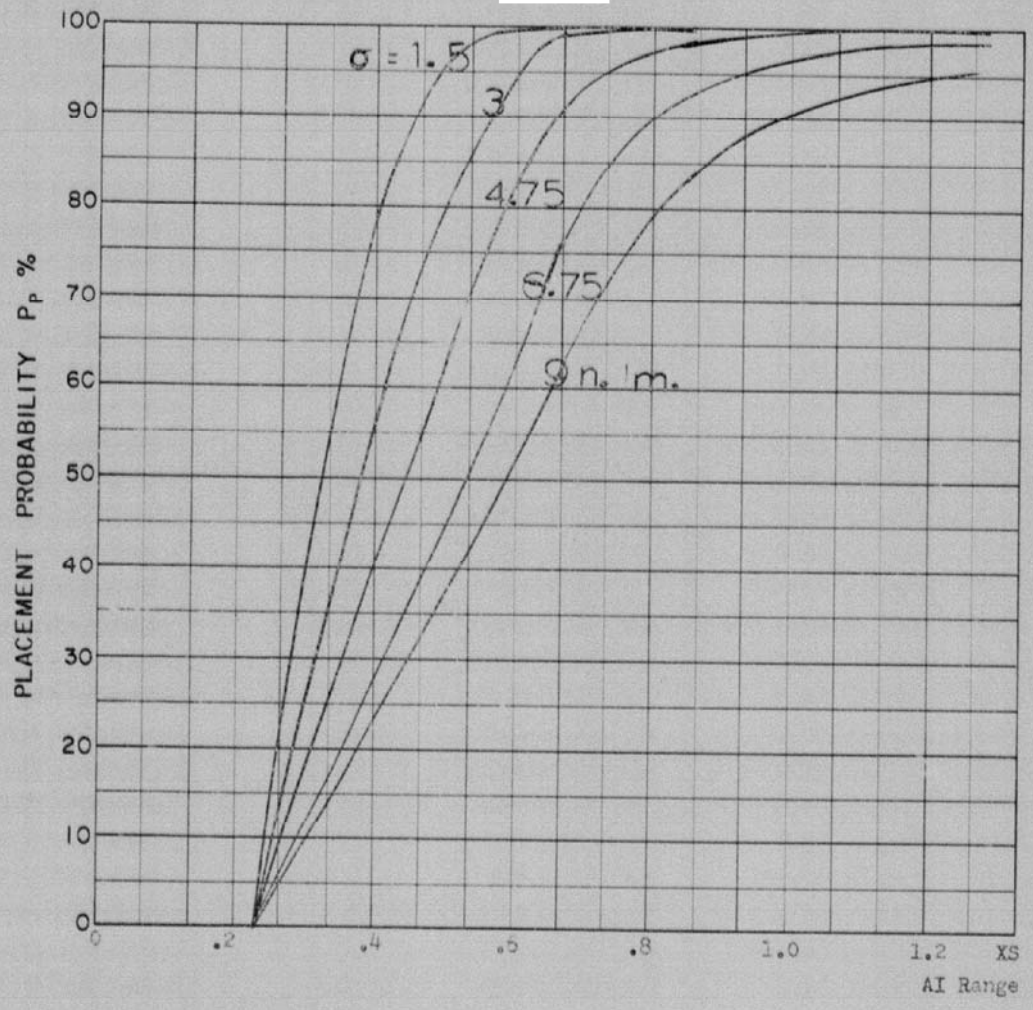

COURSE DIFFERENCE: 120°
TARGET EVASION: 0
TARGET MACH NO.: 1.5
INTERCEPTOR LATERAL G's: 1.60
INTERCEPTOR MACH NO.: 1.5
σ OF G.C.I. ACCURACY: Five values
A.I. DETECTION RANGE AS FRACTION OF SPECIFICATION RANGE, S: Abscissa
A.I. DETECTION RANGE CONTOUR: Straight Wing
ALTITUDE: 50K

S15c

Missile launch zone L-1, maximum range, 15° heading error, Look angle limit 80°.

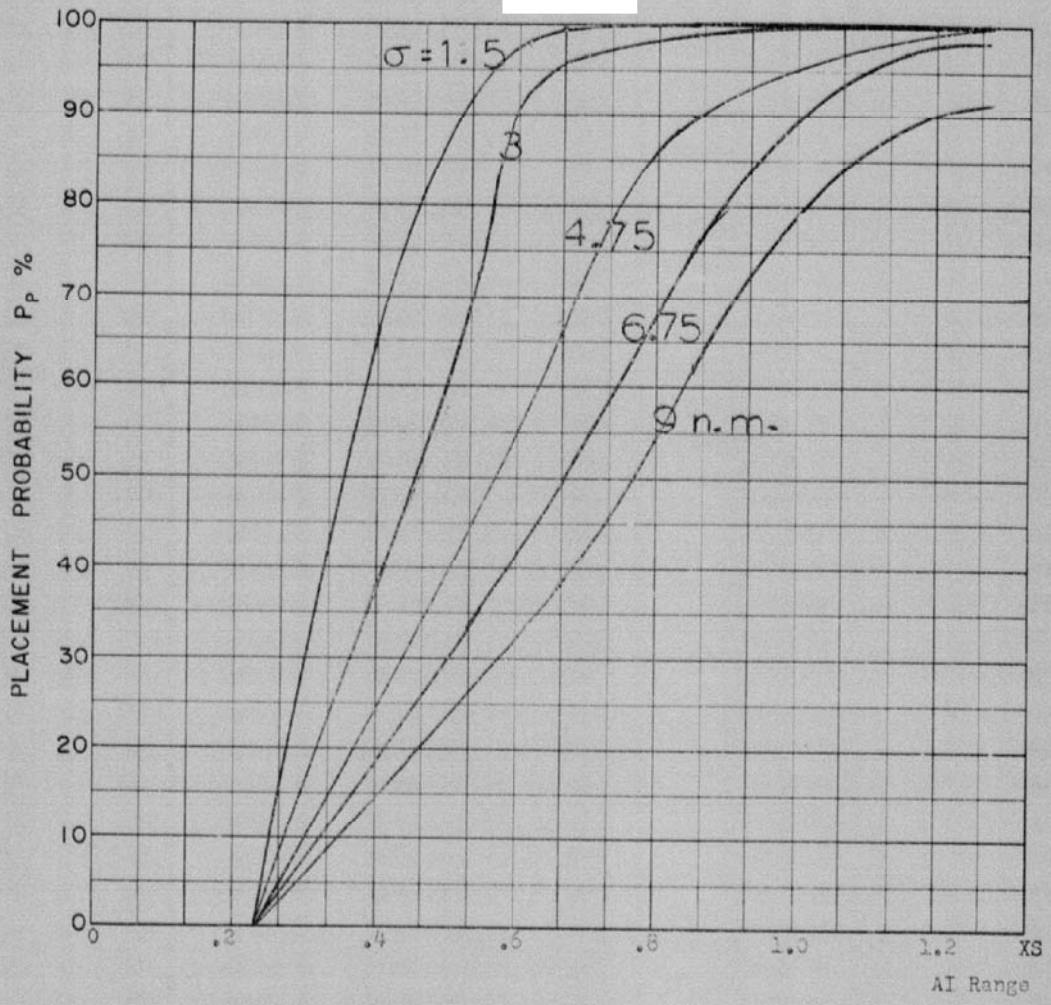

COURSE DIFFERENCE: 140°
TARGET EVASION: 0
TARGET MACH NO.: 1.5
INTERCEPTOR LATERAL G's: 1.50
INTERCEPTOR MACH NO.: 1.5
σ OF G.C.I. ACCURACY: Five values
A.I. DETECTION RANGE AS FRACTION OF SPECIFICATION RANGE, S: Abscissa
A.I. DETECTION RANGE CONTOUR: Straight Wing
ALTITUDE: 50K

S16a

Missile launch zone L-1, maximum range, 15° heading error.

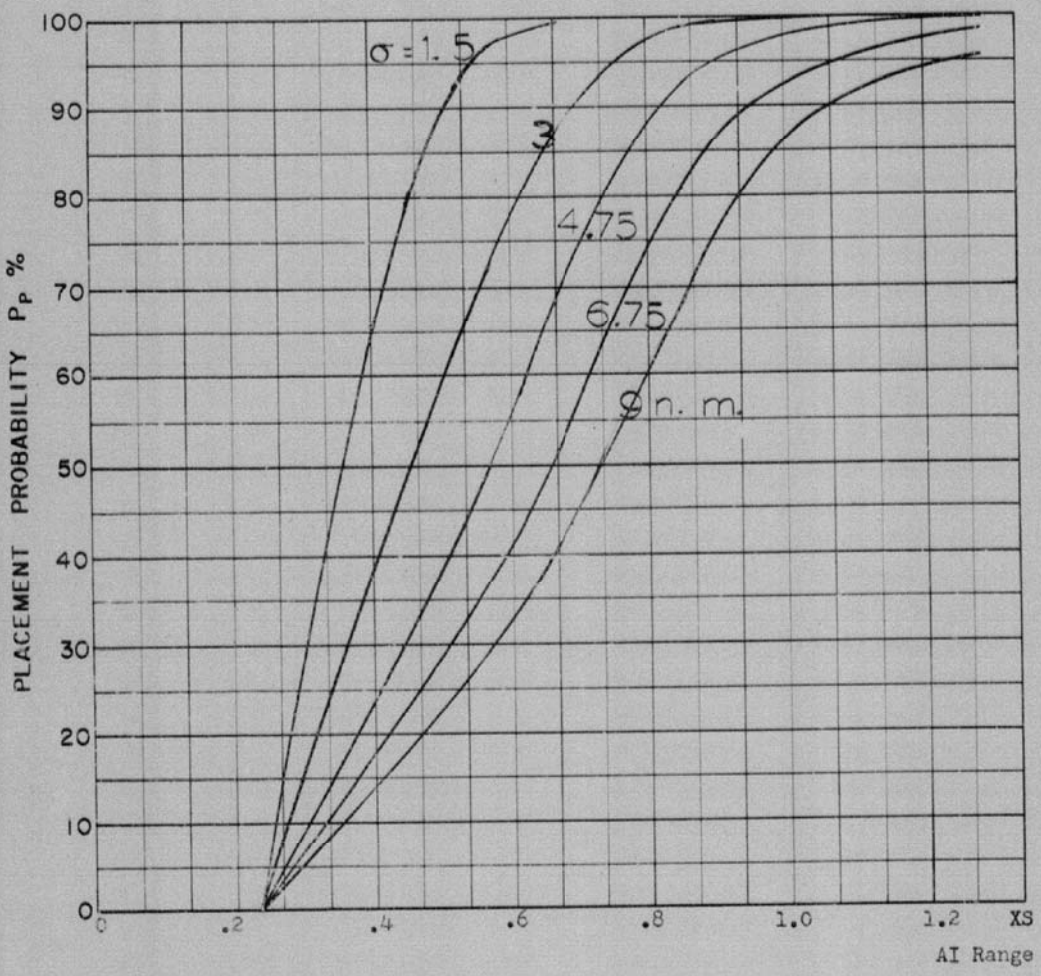

S16c

COURSE DIFFERENCE: 140°
TARGET EVASION: 0
TARGET MACH NO.: 1.5
INTERCEPTOR LATERAL G's: 1.60
INTERCEPTOR MACH NO.: 1.5
σ OF G.C.I. ACCURACY: Five values
A.I. DETECTION RANGE AS FRACTION OF SPECIFICATION RANGE, S: Abscissa
A.I. DETECTION RANGE CONTOUR: Straight Wing
ALTITUDE: 50K

Missile launch zone L-1, maximum range, 15° heading error, Look angle limit 80°.

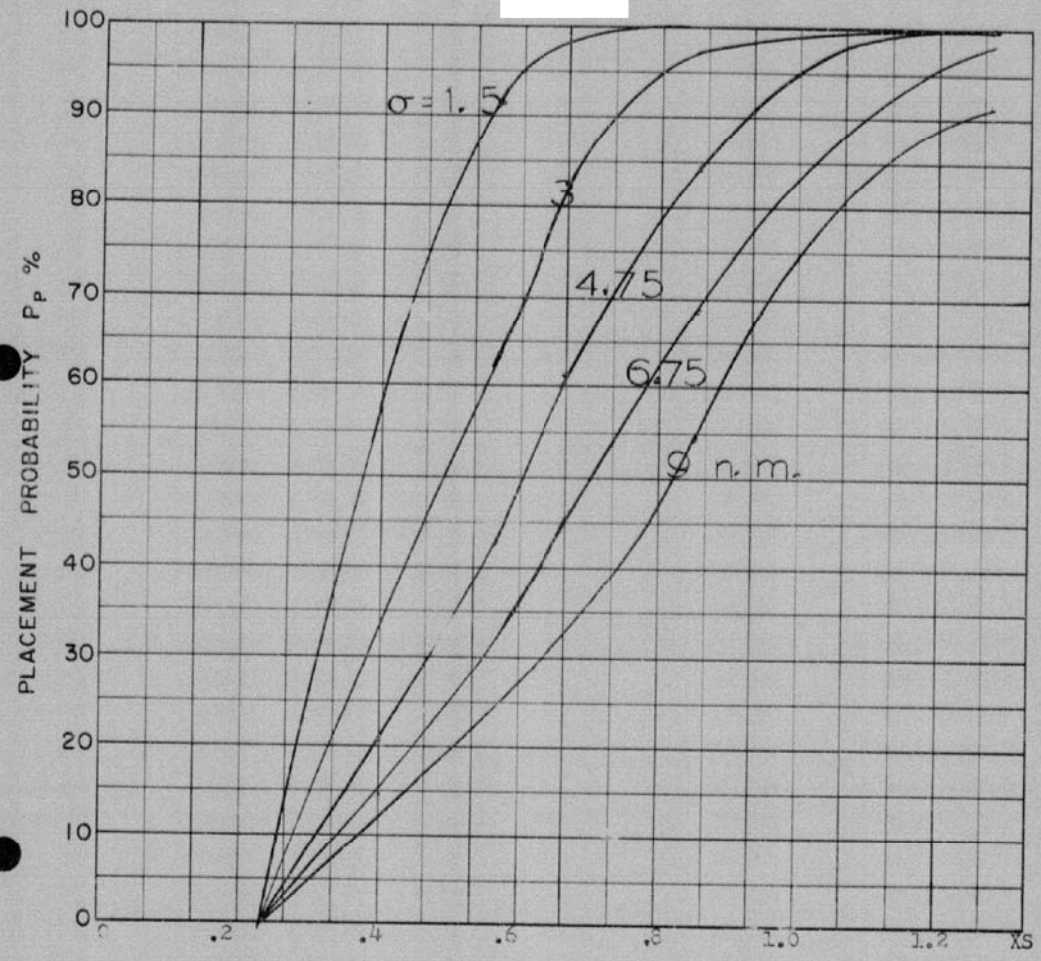

COURSE DIFFERENCE: 160°
TARGET EVASION: 0
TARGET MACH NO.: 1.5
INTERCEPTOR LATERAL G's: 1.60
INTERCEPTOR MACH NO.: 1.5
σ OF G.C.I. ACCURACY: Five values
A.I. DETECTION RANGE AS FRACTION OF SPECIFICATION RANGE, S: Abscissa
A.I. DETECTION RANGE CONTOUR: Straight Wing
ALTITUDE: 50K

Missile launch zone L-1, maximum range, 15° heading error.

(S17a)

37exspr

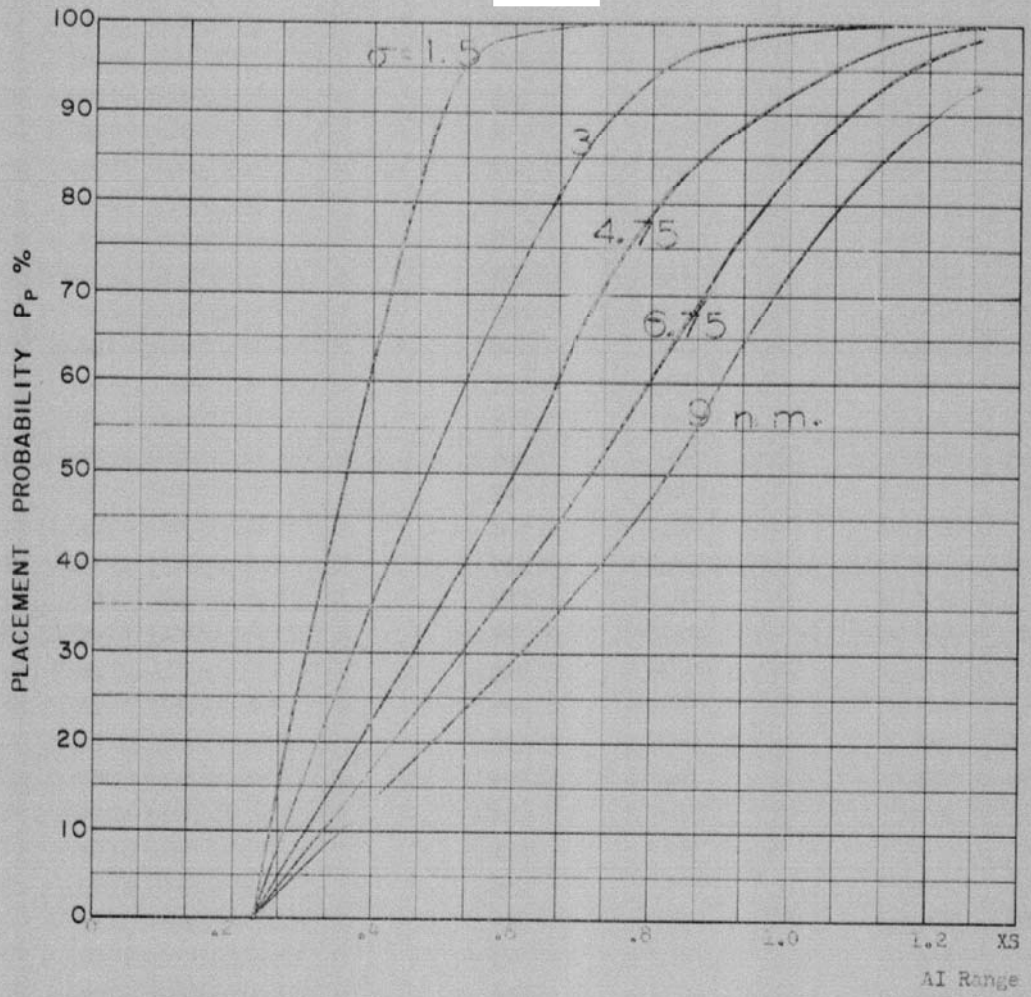

COURSE DIFFERENCE: 160°
TARGET EVASION: 0
TARGET MACH NO.: 1.5
INTERCEPTOR LATERAL G's: 1.60
INTERCEPTOR MACH NO.: 1.5
σ OF G.C.I. ACCURACY: Five values
A.I. DETECTION RANGE AS FRACTION OF SPECIFICATION RANGE, S: Abscissa
A.I. DETECTION RANGE CONTOUR: Straight Wing
ALTITUDE: 50K

S17c

Missile launch zone L.I. maximum range, 15° heading error, Look angle limit 80°.

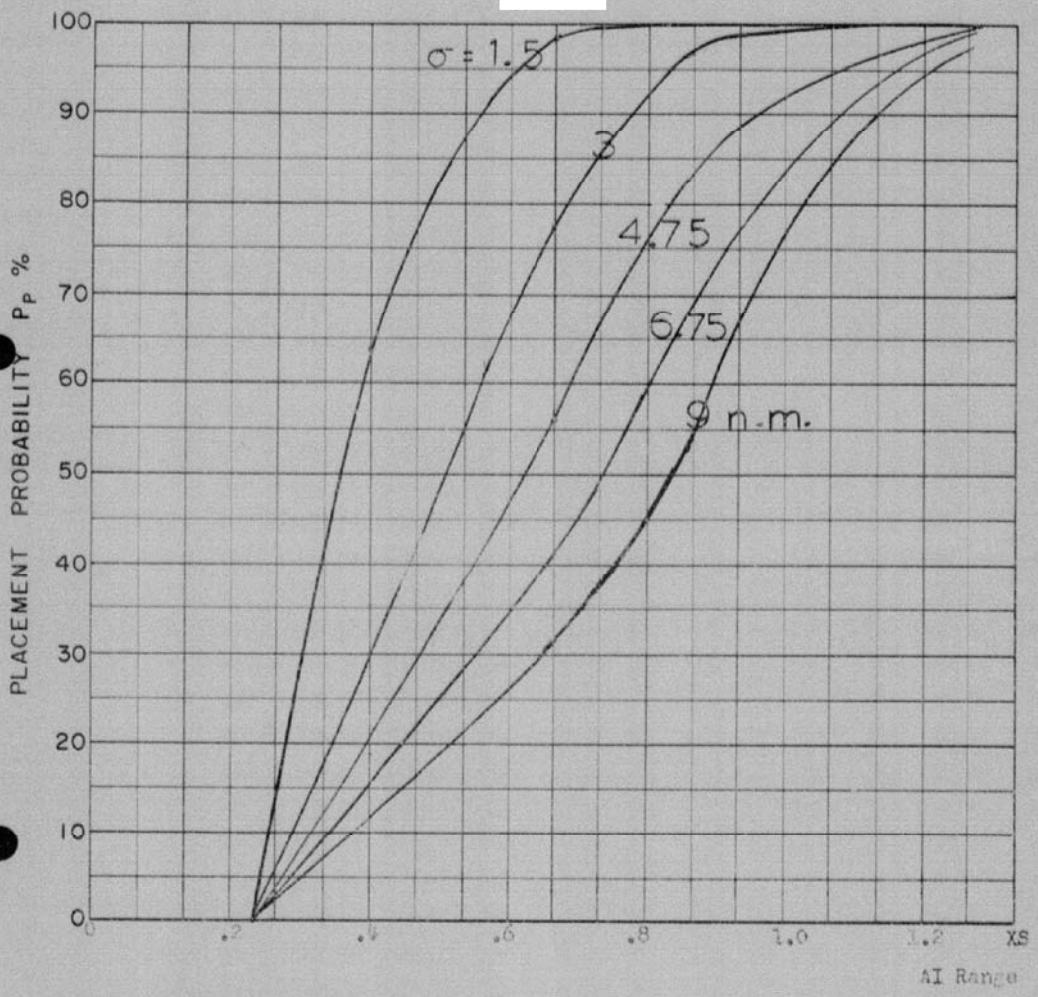

COURSE DIFFERENCE: 180°
TARGET EVASION: 0
TARGET MACH NO.: 1.5
INTERCEPTOR LATERAL G's: 1.60
INTERCEPTOR MACH NO.: 1.5
σ OF G.C.I. ACCURACY: Five Values
A.I. DETECTION RANGE AS FRACTION OF SPECIFICATION RANGE, S: Abscissa
A.I. DETECTION RANGE CONTOUR: Straight Wing
ALTITUDE: 50K

Missile launch zone L-1, maximum range, 15° heading error.

(S18a)

37fxspr

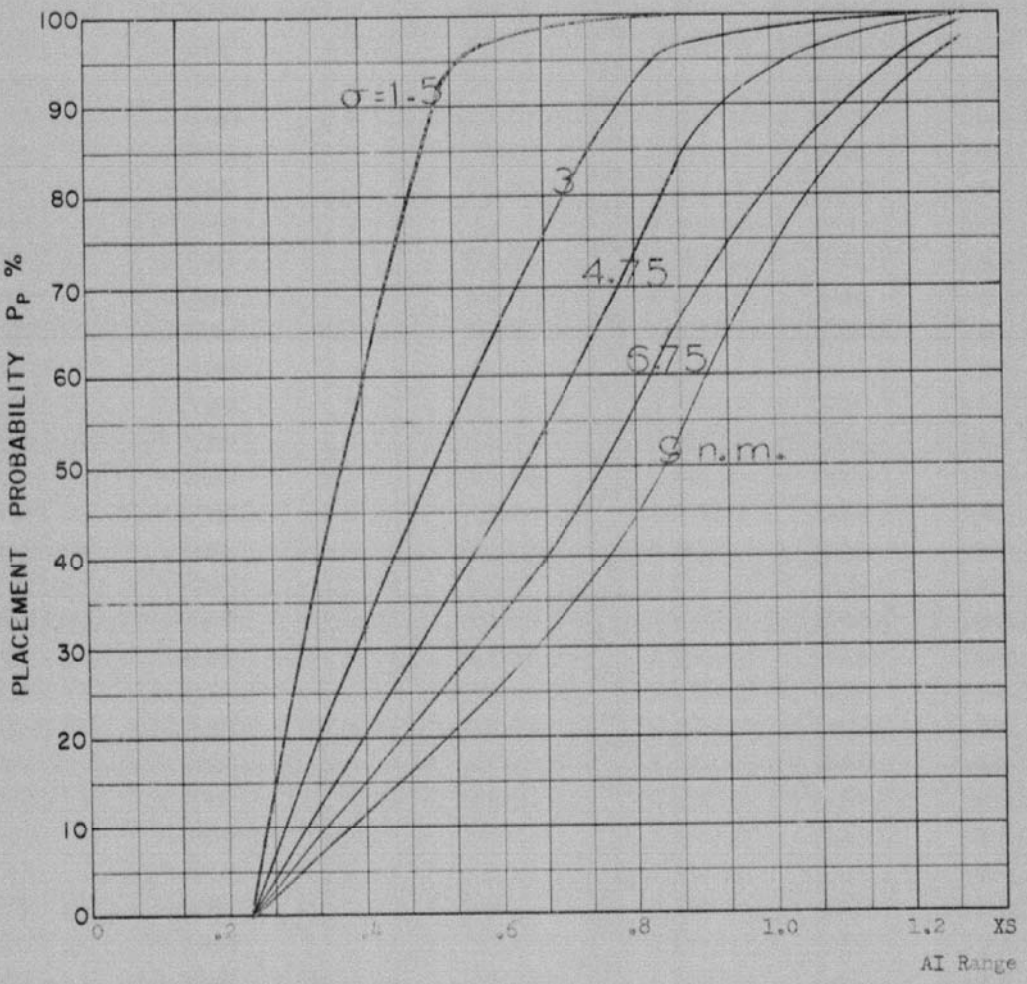

S18c

COURSE DIFFERENCE: 180°
TARGET EVASION: 0
TARGET MACH NO.: 1.5
INTERCEPTOR LATERAL G's: 1.60
INTERCEPTOR MACH NO.: 1.5
σ OF G.C.I. ACCURACY: Five values
A.I. DETECTION RANGE AS FRACTION OF SPECIFICATION RANGE, S: Abscissa
A.I. DETECTION RANGE CONTOUR: Straight Wing
ALTITUDE: 50K

Missile launch zone L.I. maximum range. 15° heading error. Look angle limit 80°.

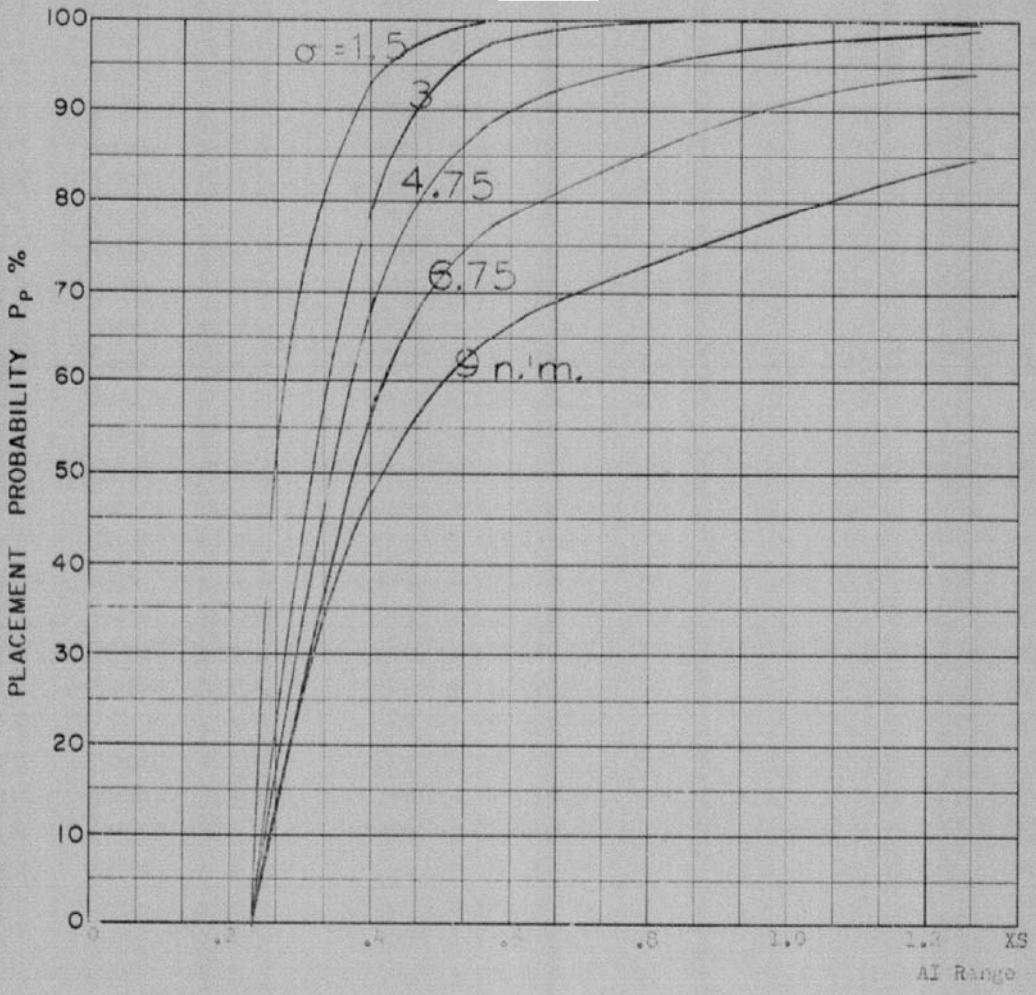

COURSE DIFFERENCE: 80°
TARGET EVASION: 2
TARGET MACH NO.: 1.5
INTERCEPTOR LATERAL G's: 5.0
INTERCEPTOR MACH NO.: 1.5
σ OF G.C.I. ACCURACY: Five values
A.I. DETECTION RANGE AS FRACTION OF SPECIFICATION RANGE, S: Abscissa
A.I. DETECTION RANGE CONTOUR: Straight Wing
ALTITUDE: 50K

S 19

Missile launch zone L-1, maximum range, 15° heading error.

38mspr

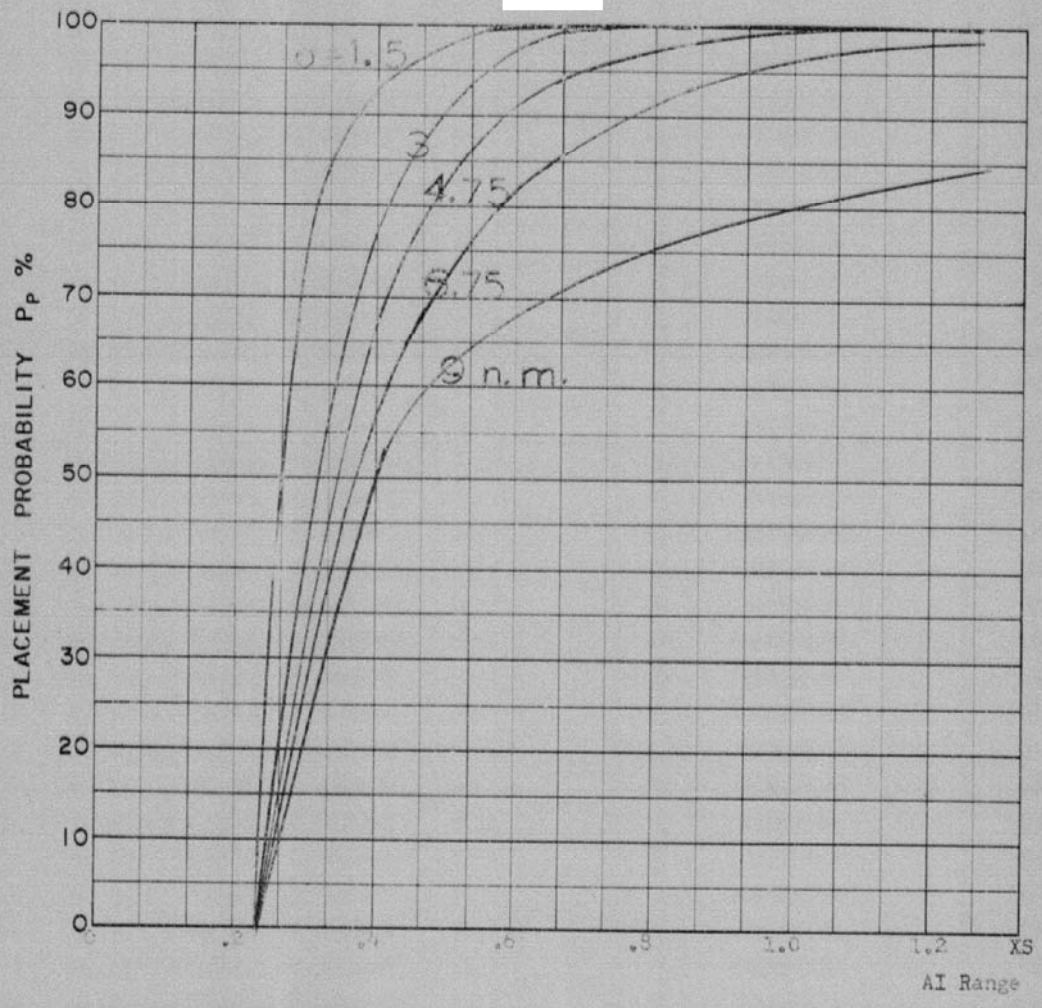

COURSE DIFFERENCE: 100°
TARGET EVASION: 0
TARGET MACH NO.: 1.5
INTERCEPTOR LATERAL G's: 3.0
INTERCEPTOR MACH NO.: 1.5
σ OF G.C.I. ACCURACY: Five values
A.I. DETECTION RANGE AS FRACTION OF SPECIFICATION RANGE, S: Abscissa
A.I. DETECTION RANGE CONTOUR: Straight Wing
ALTITUDE: 50K

S20a

Missile launch zone L-1, maximum range, 15° heading error.

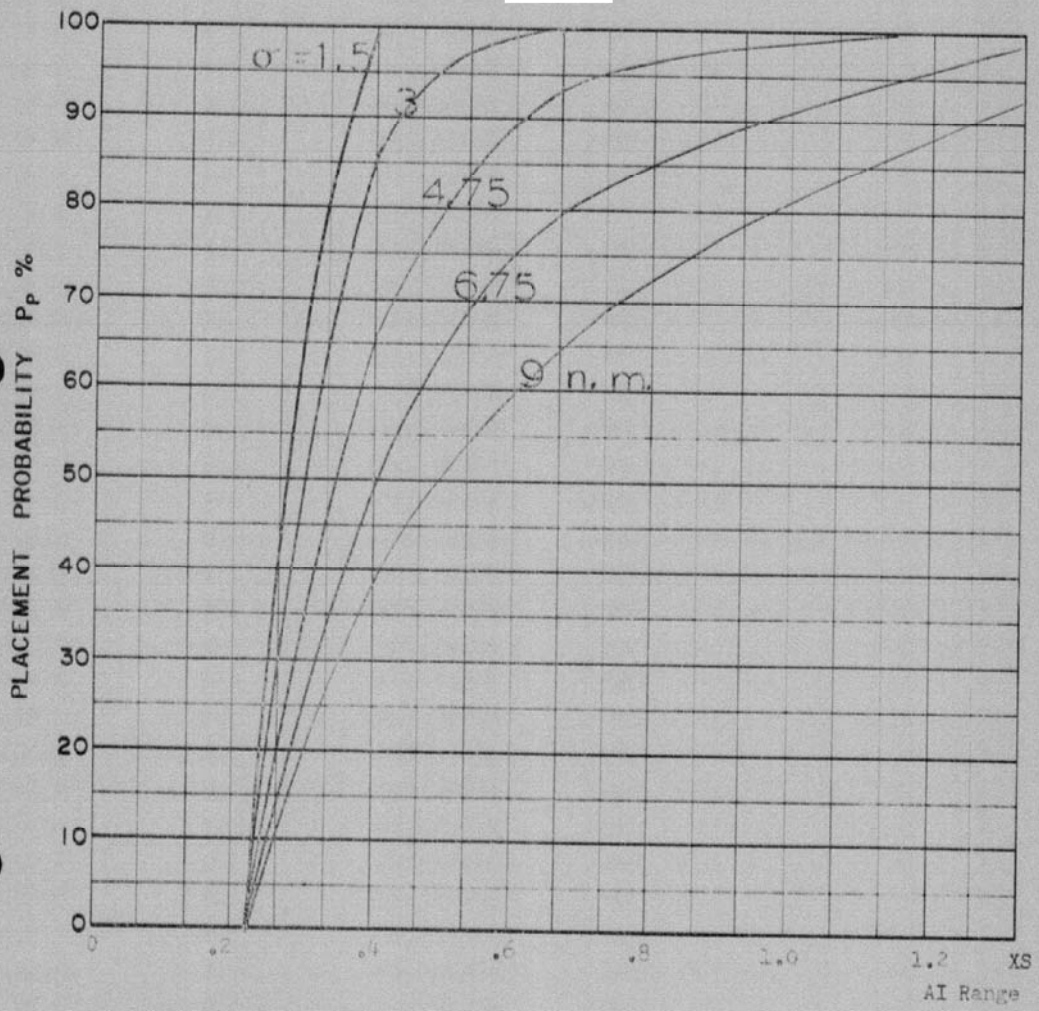

COURSE DIFFERENCE: 100°
TARGET EVASION: 0
TARGET MACH NO.: 1.5
INTERCEPTOR LATERAL G's: 3.0
INTERCEPTOR MACH NO.: 1.5
σ OF G.C.I. ACCURACY: Five values
A.I. DETECTION RANGE AS FRACTION OF SPECIFICATION RANGE, S: Abscissa
A.I. DETECTION RANGE CONTOUR: Straight Wing
ALTITUDE: 50K

S20b

Missile launch zone L-2, minimum range, 10° heading error.

38cxspr

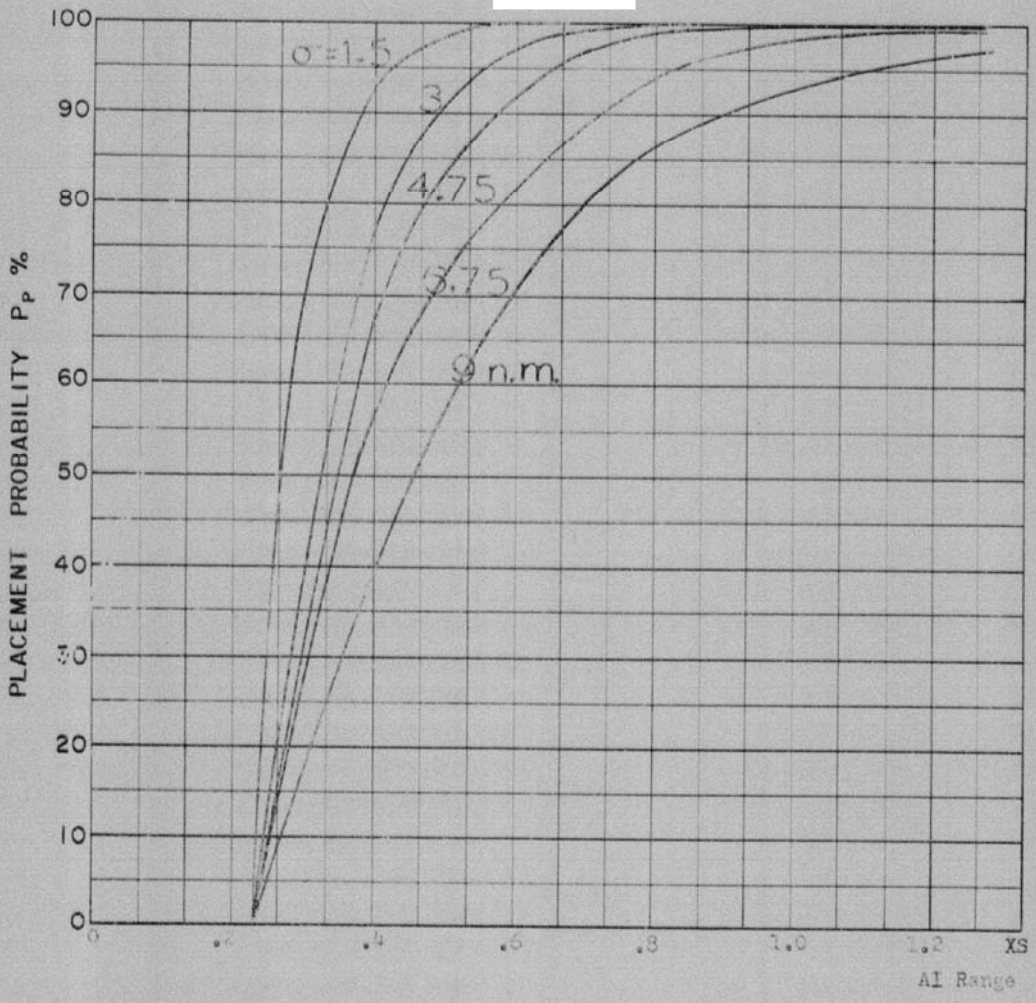

COURSE DIFFERENCE: 120°
TARGET EVASION: 0
TARGET MACH NO.: 1.5
INTERCEPTOR LATERAL G's: 3.0
INTERCEPTOR MACH NO.: 1.5
σ OF G.C.I. ACCURACY: Five Values
A.I. DETECTION RANGE AS FRACTION OF SPECIFICATION RANGE, S: Abscissa
A.I. DETECTION RANGE CONTOUR: Straight Wing
ALTITUDE: 50K

S2.1

Missile launch zone L-1, maximum range, 15° heading error.

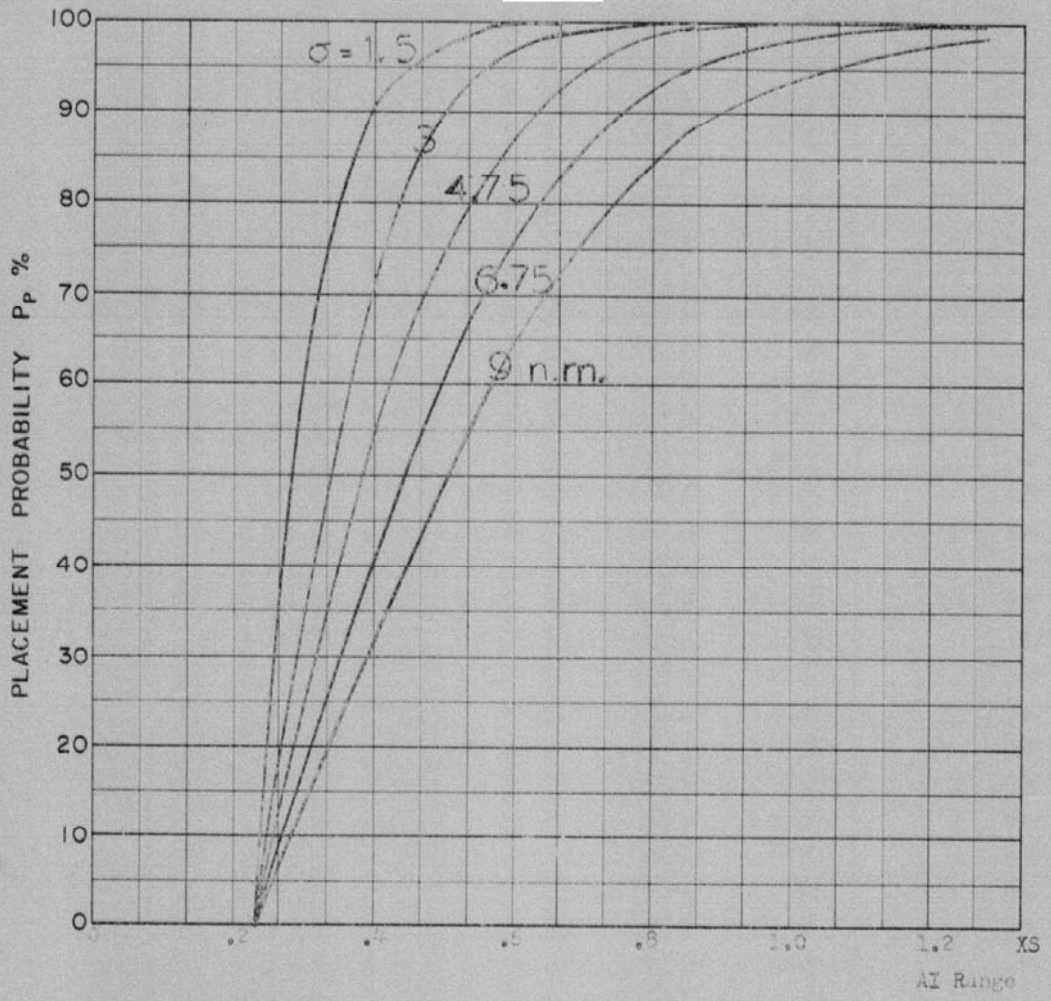

COURSE DIFFERENCE: 140°
TARGET EVASION: 0
TARGET MACH NO.: 1.5
INTERCEPTOR LATERAL G's: 3.0
INTERCEPTOR MACH NO.: 1.5
σ OF G.C.I. ACCURACY: Five values
A.I. DETECTION RANGE AS FRACTION OF SPECIFICATION RANGE, S: Abscissa
A.I. DETECTION RANGE CONTOUR: Straight Wing
ALTITUDE: 50K

(S22)

Missile launch zone L-1, maximum range, 15° heading error.

38exsgr

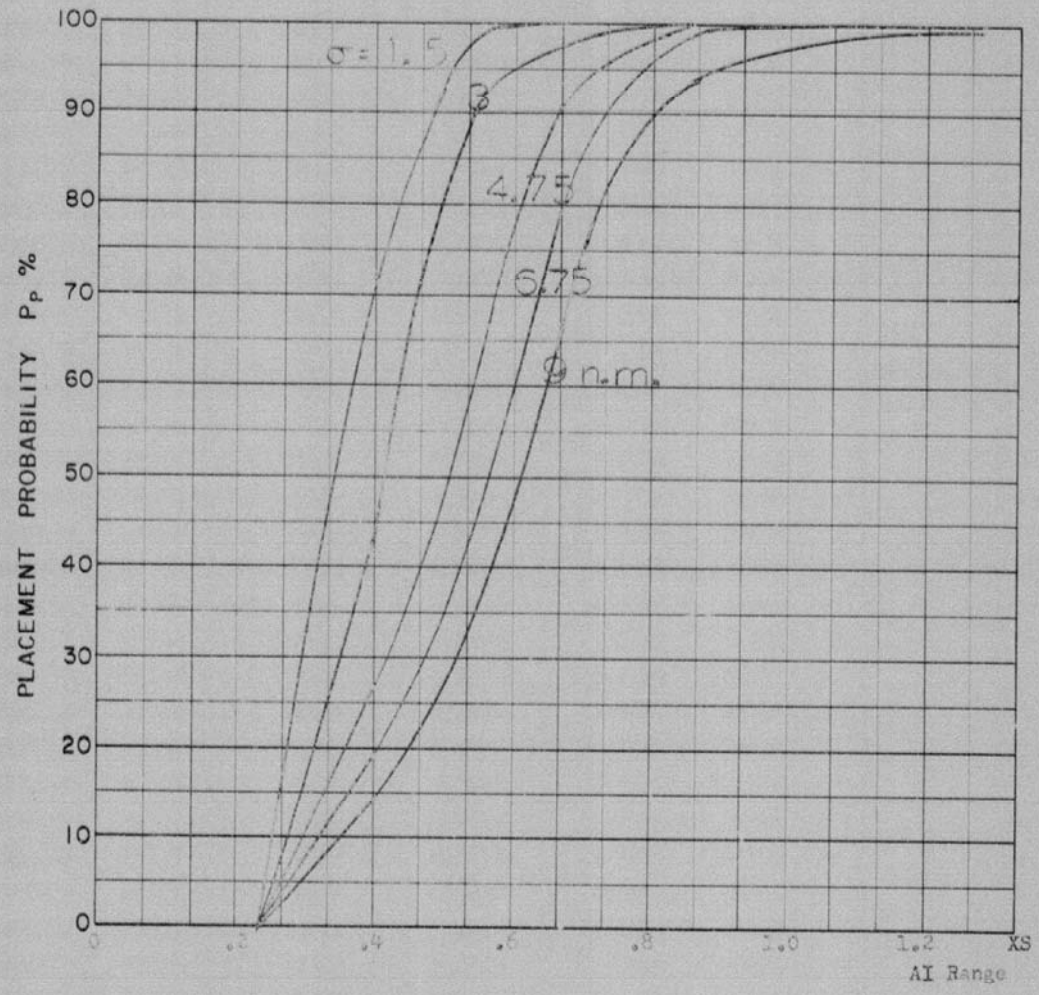

COURSE DIFFERENCE: 360°
TARGET EVASION: 0
TARGET MACH NO.: 2.5
INTERCEPTOR LATERAL G's: 3.0
INTERCEPTOR MACH NO.: 1.3
σ OF G.C.I. ACCURACY: Five values
A.I. DETECTION RANGE AS FRACTION OF SPECIFICATION RANGE, S: Abscissa
A.I. DETECTION RANGE CONTOUR: Straight Wing
ALTITUDE: 50K

S23

Missile launch zone L-1, maximum range, 15° heading error.

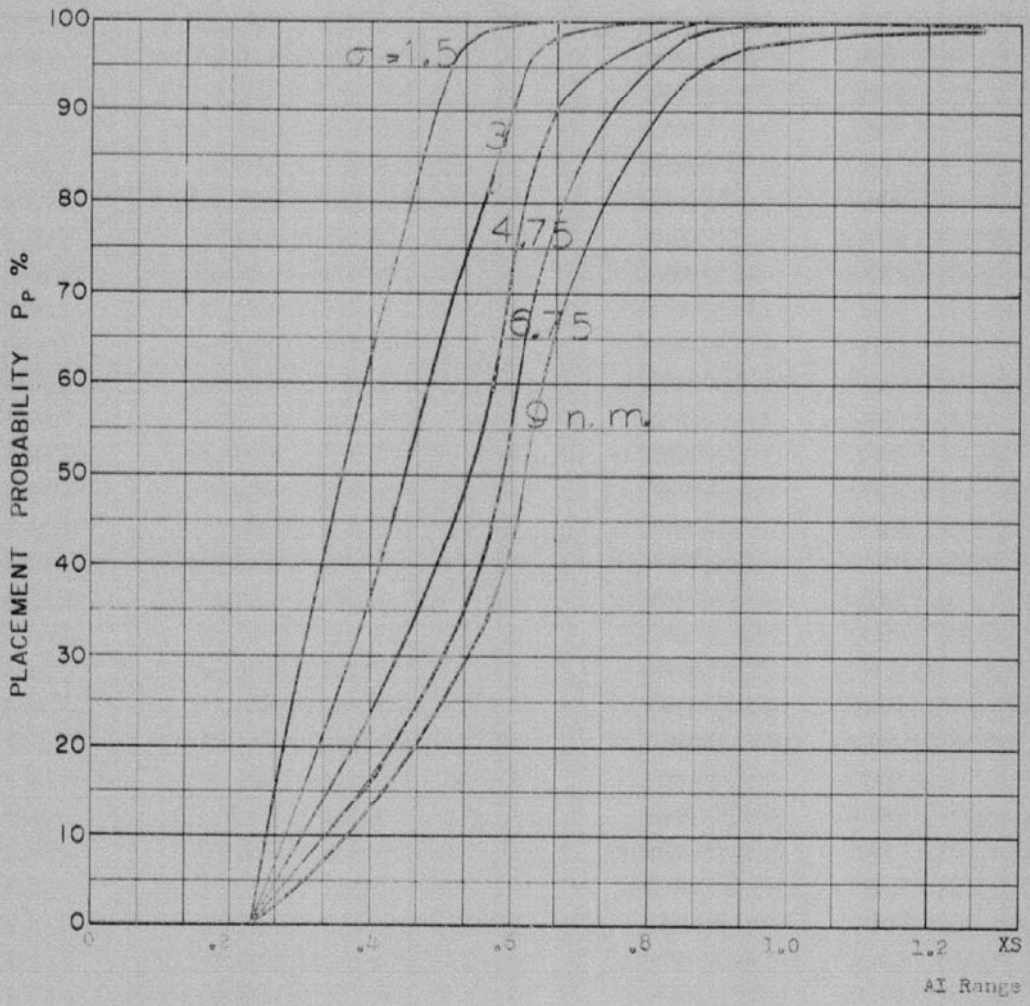

S24

COURSE DIFFERENCE: 180°
TARGET EVASION: 0
TARGET MACH NO.: 1.5
INTERCEPTOR LATERAL G's: 3.0
INTERCEPTOR MACH NO.: 2.5
σ OF G.C.I. ACCURACY: Five values
A.I. DETECTION RANGE AS FRACTION OF SPECIFICATION RANGE, S: Abscissa
A.I. DETECTION RANGE CONTOUR: Straight Wing
ALTITUDE: 50K

Missile launch zone L-1, maximum range, 15° heading error.

32 axspr

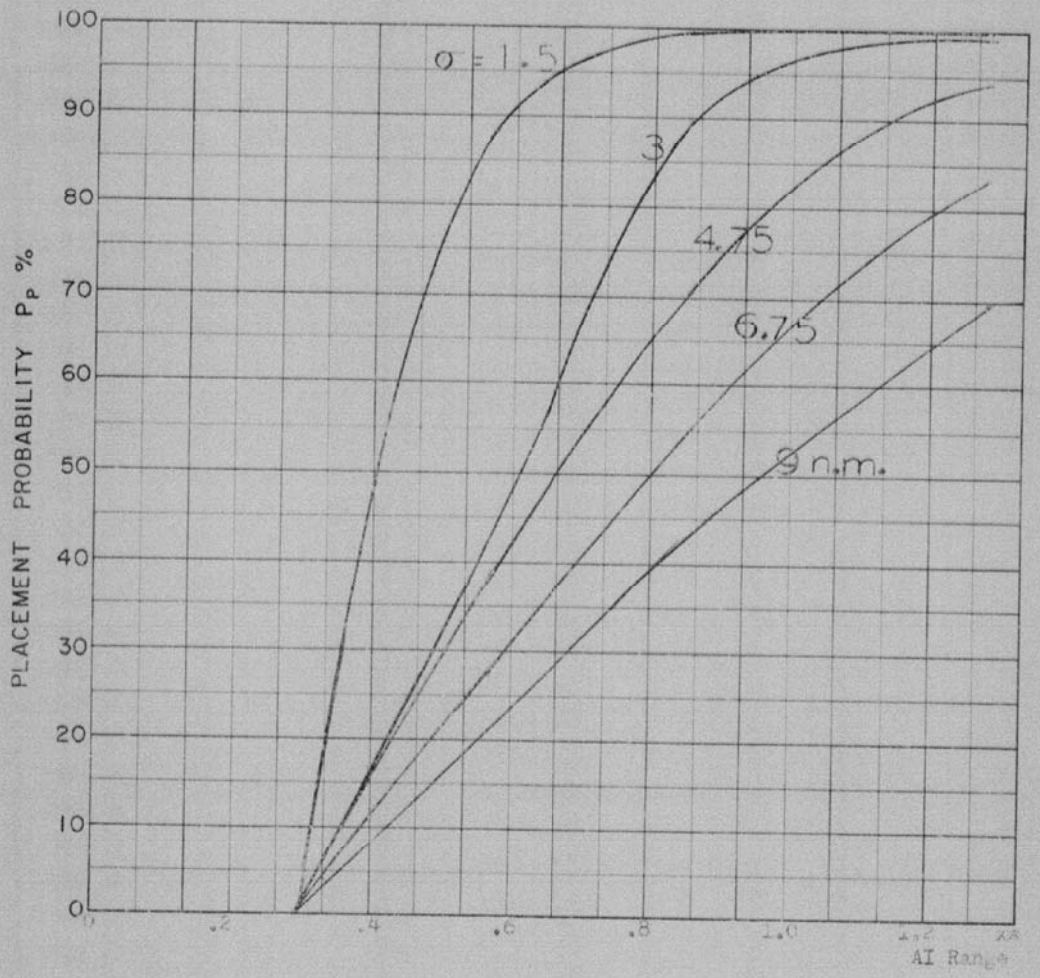

COURSE DIFFERENCE: 80°
TARGET EVASION: 0
TARGET MACH NO.: 1.5
INTERCEPTOR LATERAL G's: 0.66
INTERCEPTOR MACH NO.: 1.5
σ OF G.C.I. ACCURACY: Five values
A.I. DETECTION RANGE AS FRACTION OF SPECIFICATION RANGE, S: Abscissa
A.I. DETECTION RANGE CONTOUR: Straight Wing
ALTITUDE: 60 K

S25

Launch zone of figure L-2, maximum range, 10° heading error.

32 bxspr

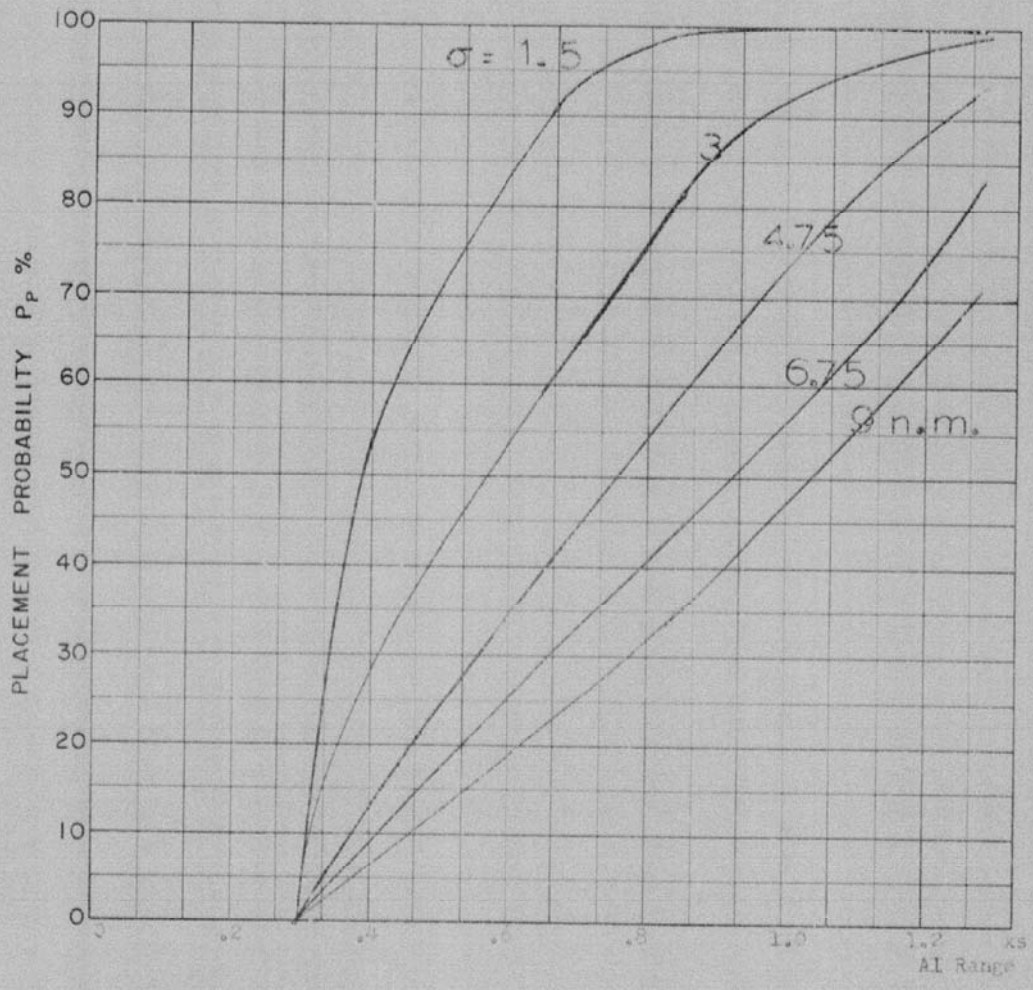

COURSE DIFFERENCE: 100°
TARGET EVASION: 0
TARGET MACH NO.: 1.5
INTERCEPTOR LATERAL G's: 0.66
INTERCEPTOR MACH NO.: 1.5
σ OF G.C.I. ACCURACY: Five values
A.I. DETECTION RANGE AS FRACTION OF SPECIFICATION RANGE, S: Abscissa
A.I. DETECTION RANGE CONTOUR: Straight Wing
ALTITUDE: 60 K

(S26)

Launch zone L-2, maximum range,
10° heading error.

32 cxspr

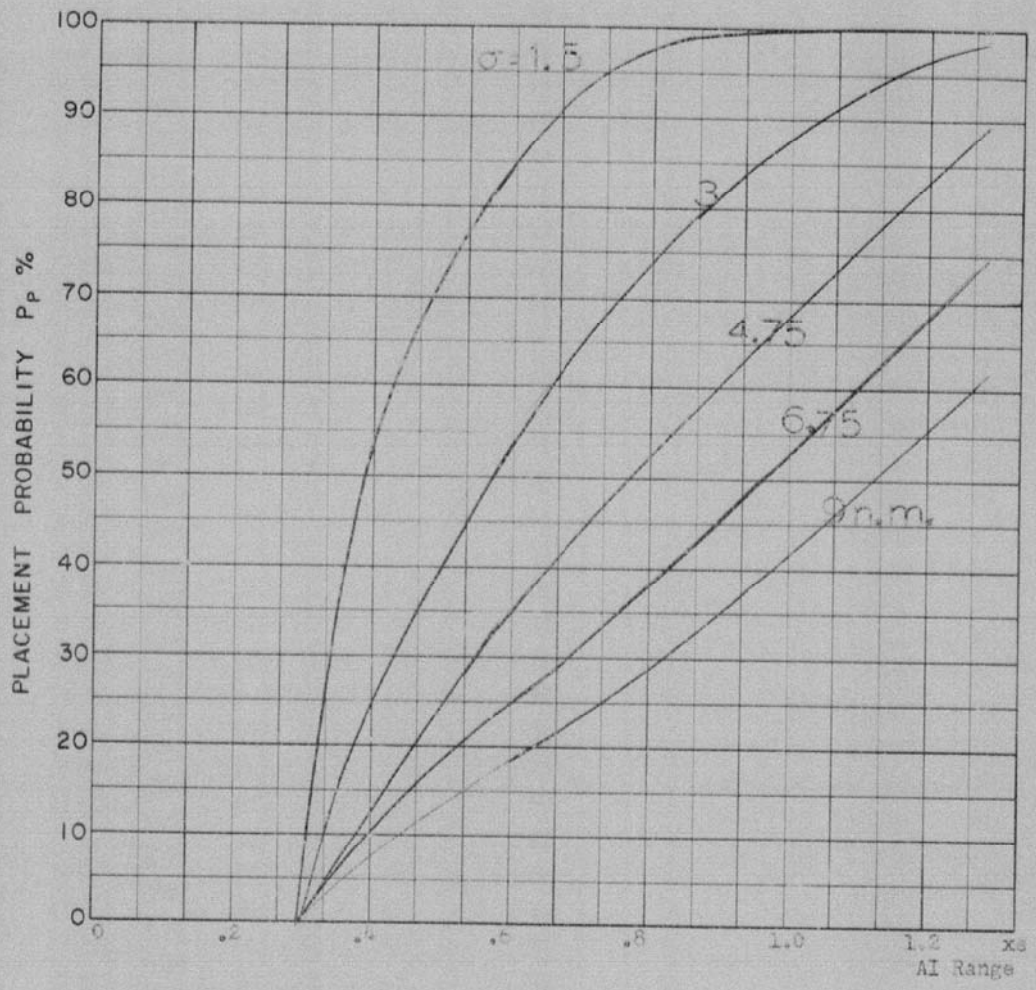

COURSE DIFFERENCE: 120°
TARGET EVASION: 0
TARGET MACH NO.: 1.5
INTERCEPTOR LATERAL G's: 0.66
INTERCEPTOR MACH NO.: 1.5
σ OF G.C.I. ACCURACY: Five values
A.I. DETECTION RANGE AS FRACTION OF SPECIFICATION RANGE, S Abscissa
A.I. DETECTION RANGE CONTOUR: Straight Wing
ALTITUDE: 60 K

S27

Launch zone of figure L-2, maximum range, 10° heading error.

32 dxspr

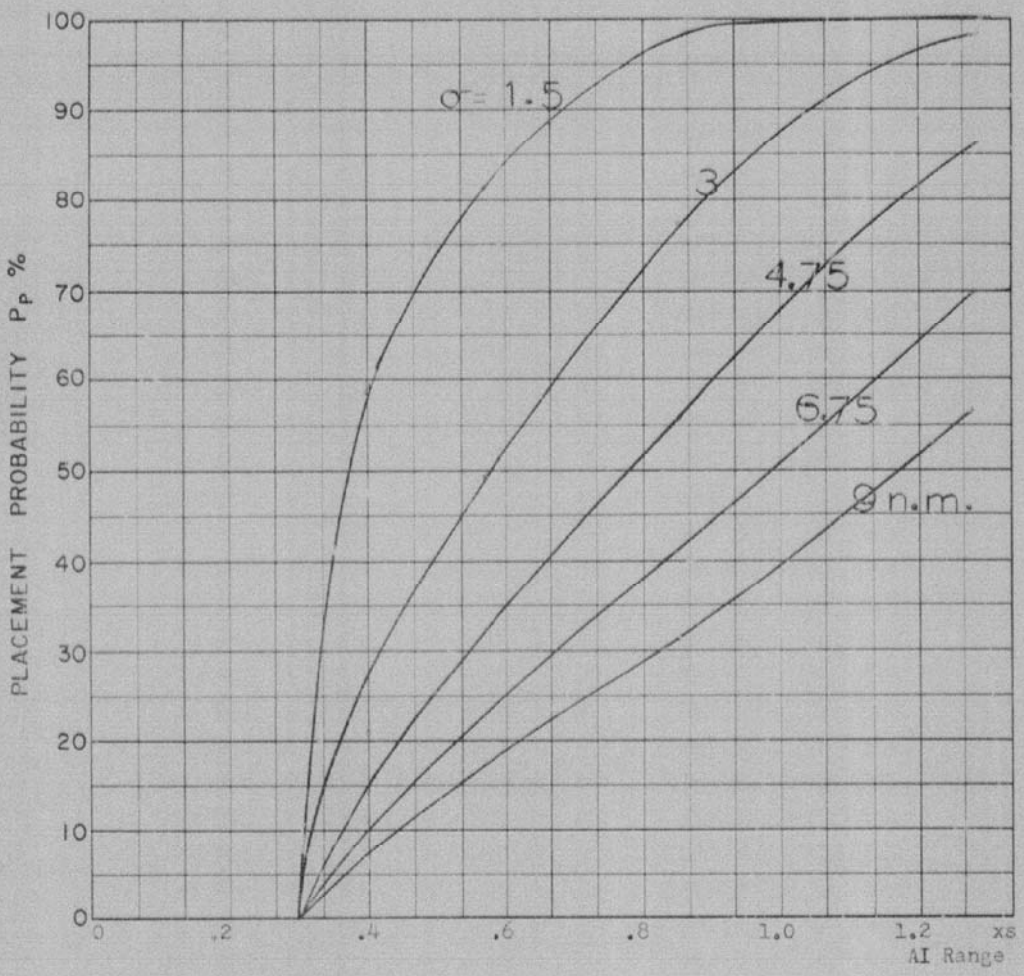

COURSE DIFFERENCE: 140°
TARGET EVASION: 0
TARGET MACH NO.: 1.5
INTERCEPTOR LATERAL G's: 0.66
INTERCEPTOR MACH NO.: 1.5
σ OF G.C.I. ACCURACY: Five values
A.I. DETECTION RANGE AS FRACTION OF SPECIFICATION RANGE, S: Abscissa
A.I. DETECTION RANGE CONTOUR: Straight Wing
ALTITUDE: 60 K

S 28

Launch zone figure L-2, maximum range, 10° heading error.

32 exspr

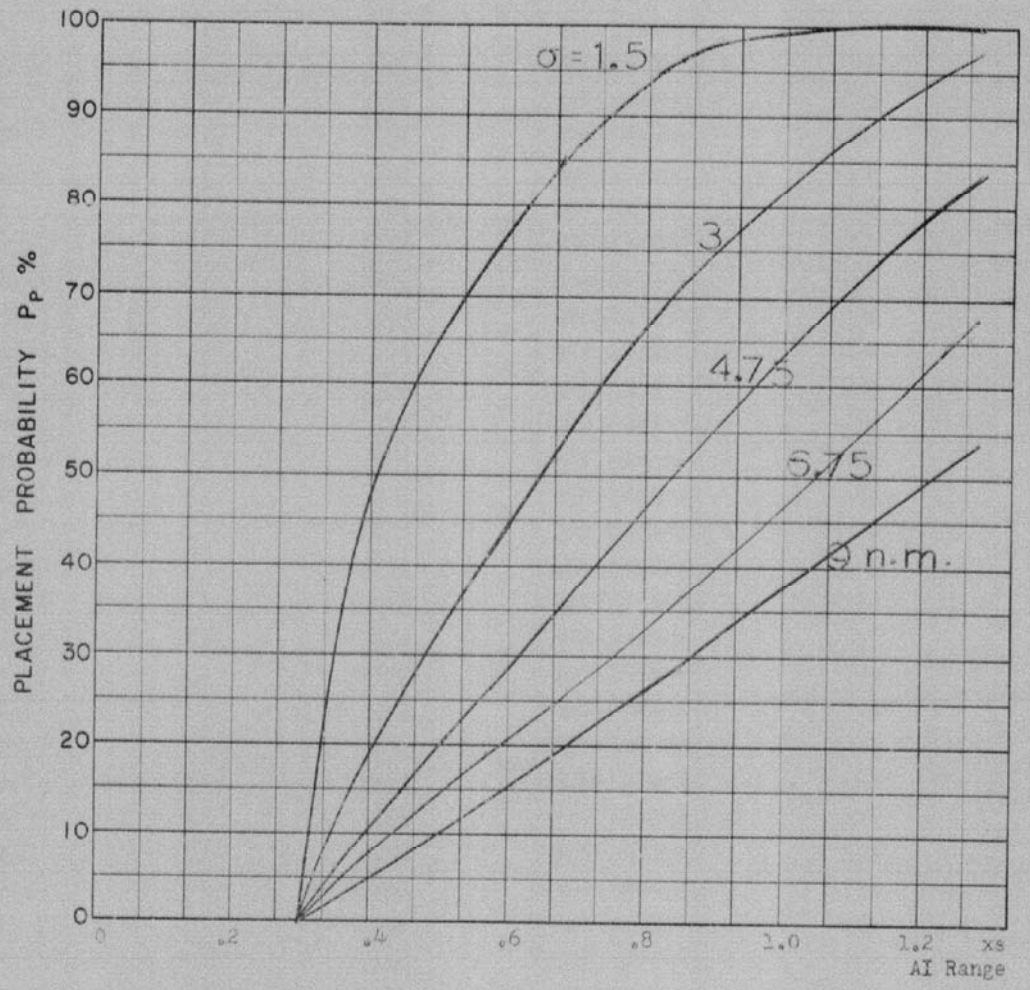

COURSE DIFFERENCE: 160°
TARGET EVASION: 0
TARGET MACH NO.: 1.5
INTERCEPTOR LATERAL G's: 0.66
INTERCEPTOR MACH NO.: 1.5
σ OF G.C.I. ACCURACY: Five values
A.I. DETECTION RANGE AS FRACTION OF SPECIFICATION RANGE, S: Abscissa
A.I. DETECTION RANGE CONTOUR: Straight Wing
ALTITUDE: 60 K

S-29

Launch zone figure L-2, maximum range,
10° heading error.

32 fxspr

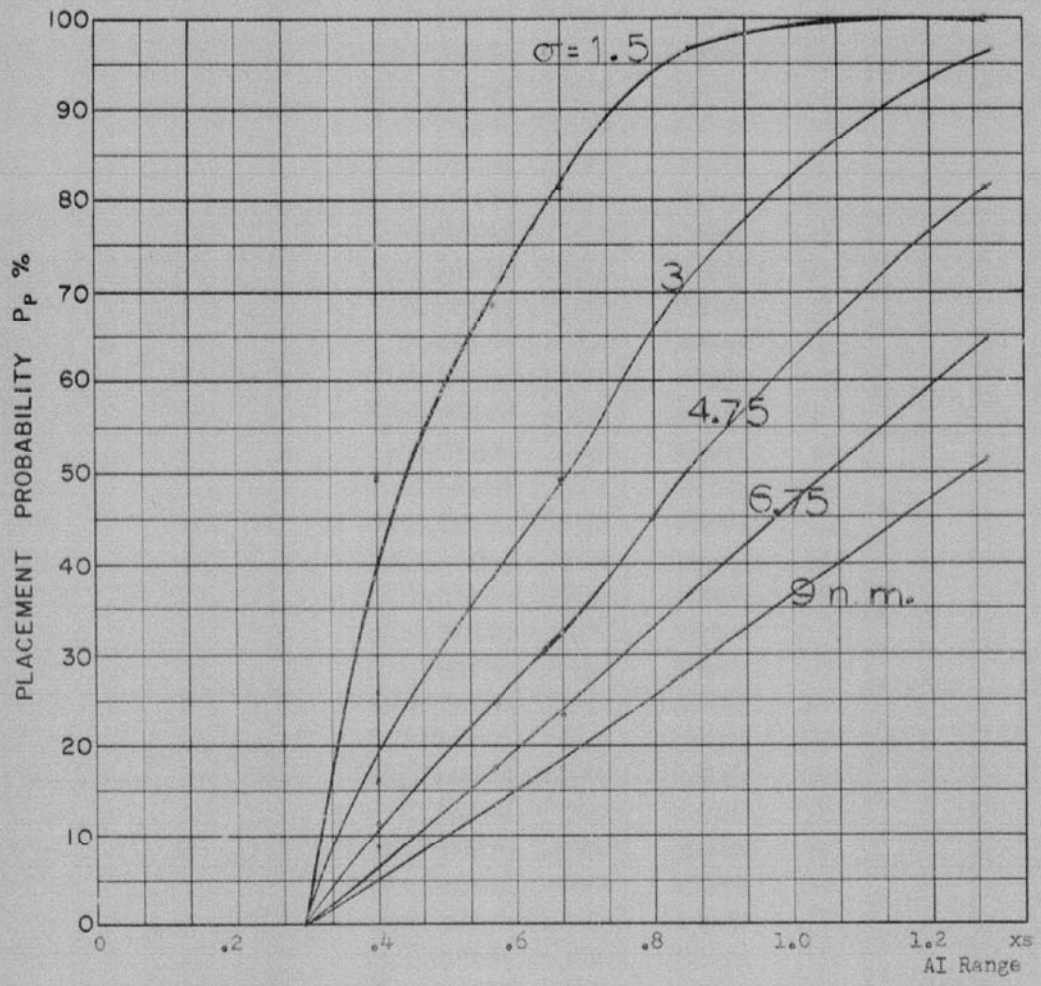

COURSE DIFFERENCE: 180°
TARGET EVASION: 0
TARGET MACH NO.: 1.5
INTERCEPTOR LATERAL G's: 0.66
INTERCEPTOR MACH NO.: 1.5
σ OF G.C.I. ACCURACY: Five values
A.I. DETECTION RANGE AS FRACTION OF SPECIFICATION RANGE, S: Abscissa
A.I. DETECTION RANGE CONTOUR: Straight Wing
ALTITUDE: 60 K

S 30

Launch zone figure L-2, maximum range, 10° heading error.

33 excpt

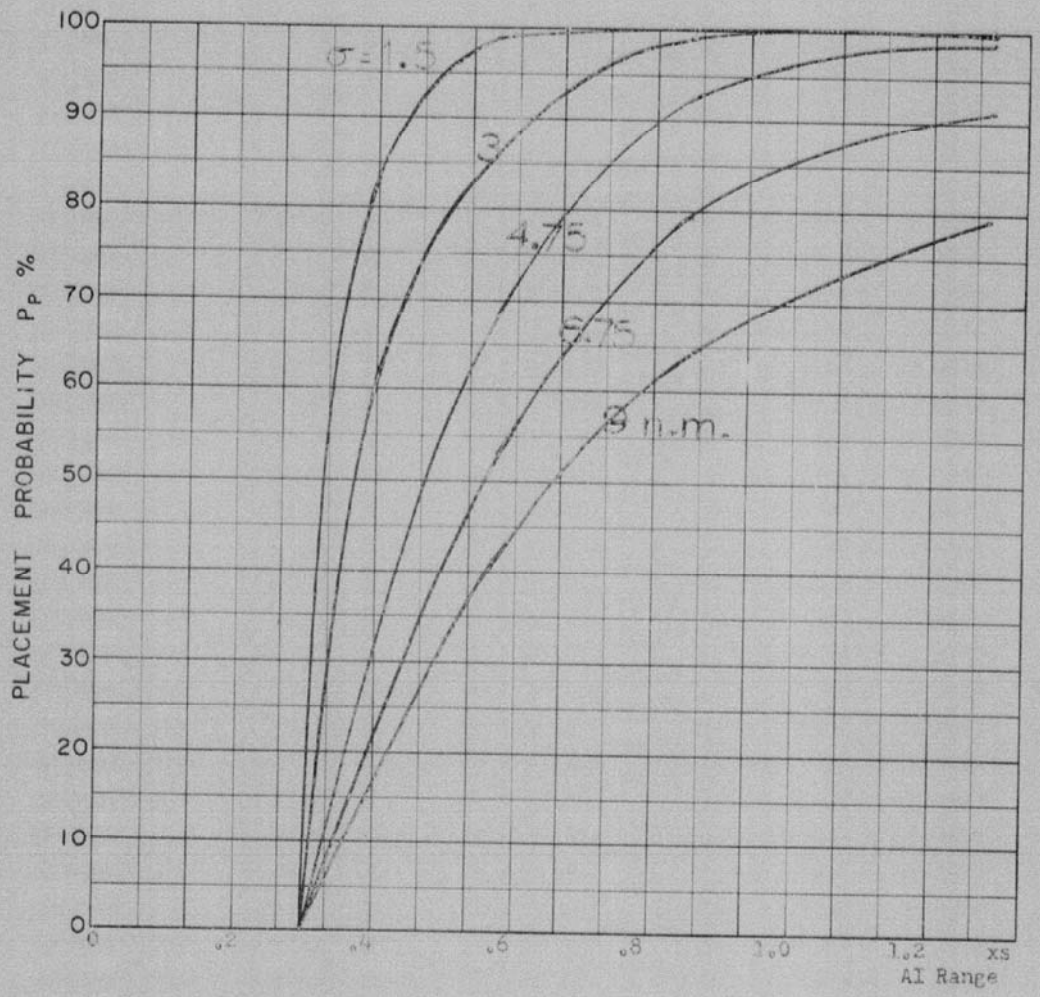

COURSE DIFFERENCE: 80°
TARGET EVASION: 0
TARGET MACH NO.: 1.5
INTERCEPTOR LATERAL G's: 1.6
INTERCEPTOR MACH NO.: 1.5
σ OF G.C.I. ACCURACY: Five values
A.I. DETECTION RANGE AS FRACTION OF SPECIFICATION RANGE, S: Abscissa
A.I. DETECTION RANGE CONTOUR: Straight Wing
ALTITUDE: 60 K

(S-31)

Missile launch zone L-2, maximum range, 10° heading error.

33 bxspr

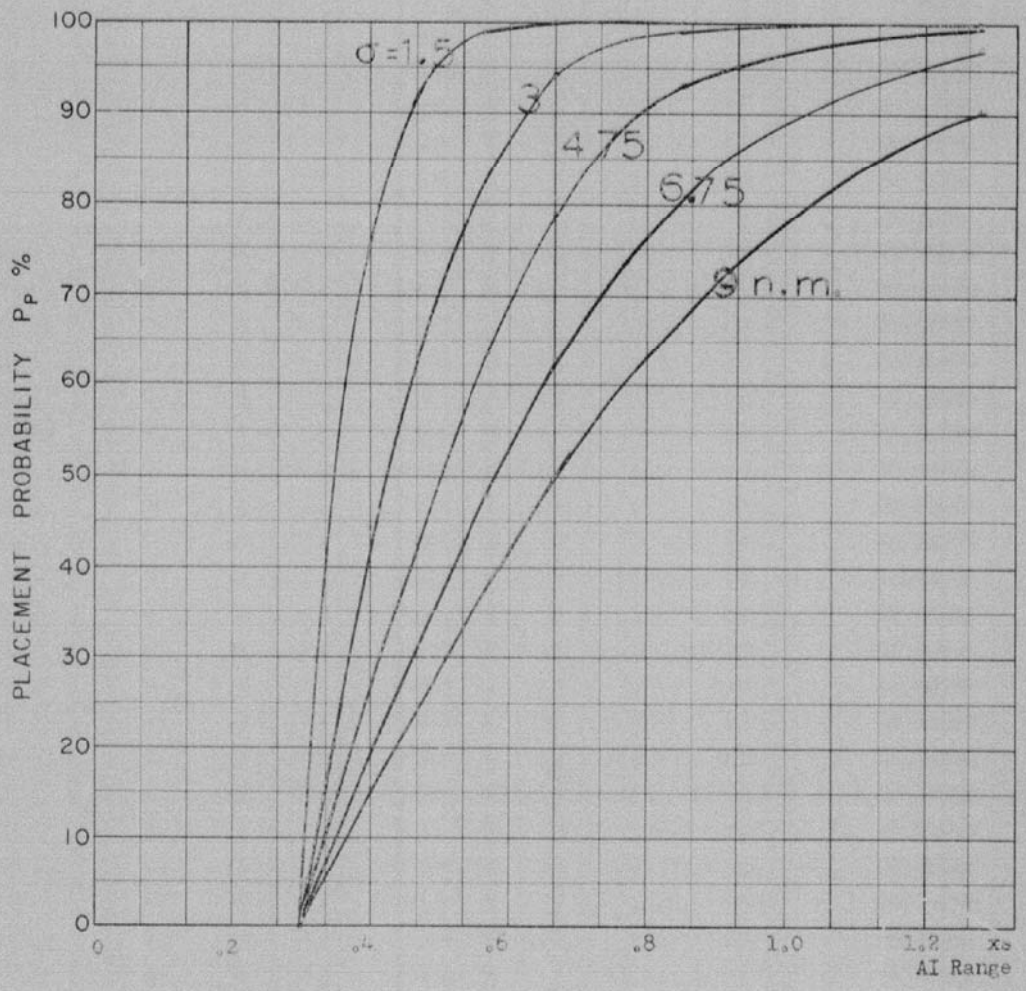

COURSE DIFFERENCE: 100°
TARGET EVASION: 0
TARGET MACH NO.: 1.5
INTERCEPTOR LATERAL G's: 1.6
INTERCEPTOR MACH NO.: 1.5
σ OF G.C.I. ACCURACY: Five values
A.I. DETECTION RANGE AS FRACTION OF SPECIFICATION RANGE, S: Abscissa
A.I. DETECTION RANGE CONTOUR: Straight Wing
ALTITUDE: 60 K

(S-32)

Launch zone L-2, maximum range,
10° heading error.

33 cxspr

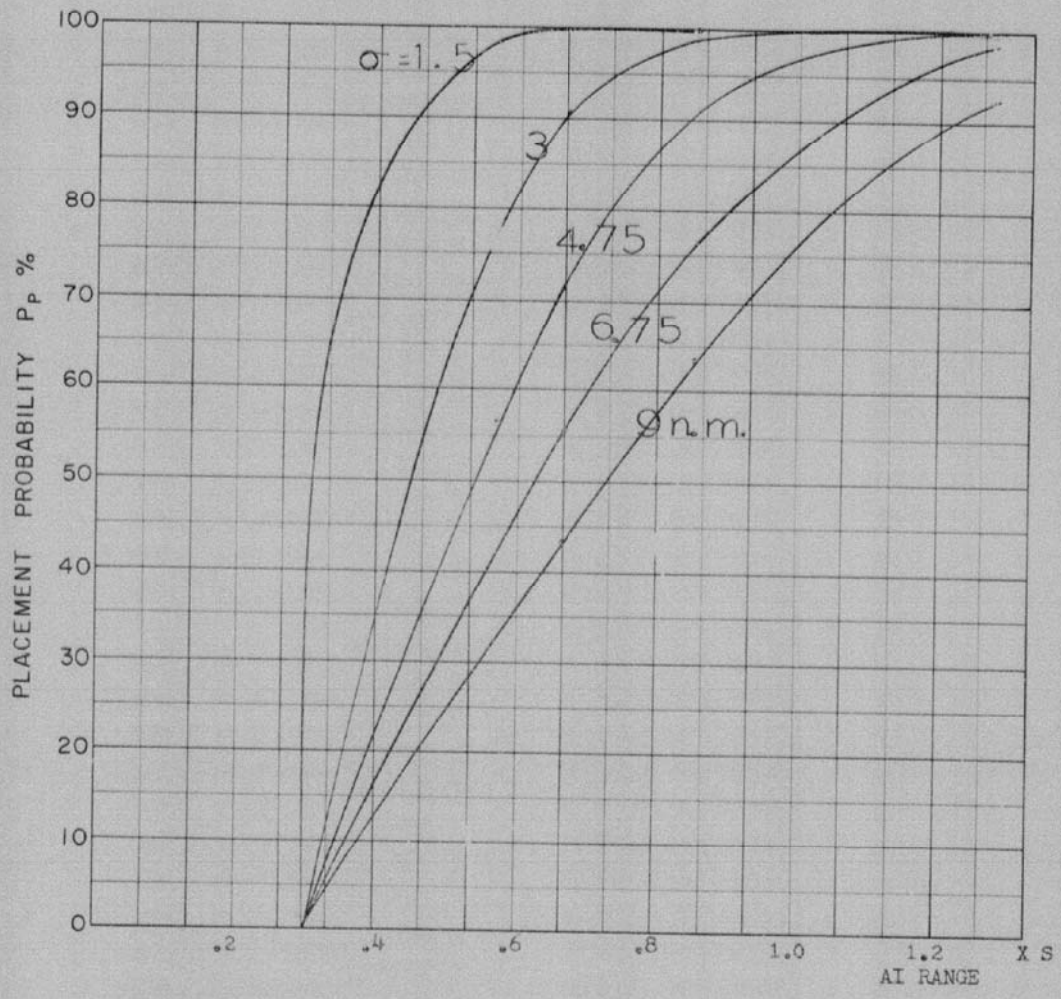

COURSE DIFFERENCE: 120°
TARGET EVASION: 0
TARGET MACH NO.: 1.5
INTERCEPTOR LATERAL G's: 1.6
INTERCEPTOR MACH NO.: 1.5
σ OF G.C.I. ACCURACY: Five values
A.I. DETECTION RANGE AS FRACTION OF SPECIFICATION RANGE, S: Abscissa
A.I. DETECTION RANGE CONTOUR: Straight wing
ALTITUDE: 60 K

S 33

Launch zone L-2, maximum range, 10° heading error

33 dxspr

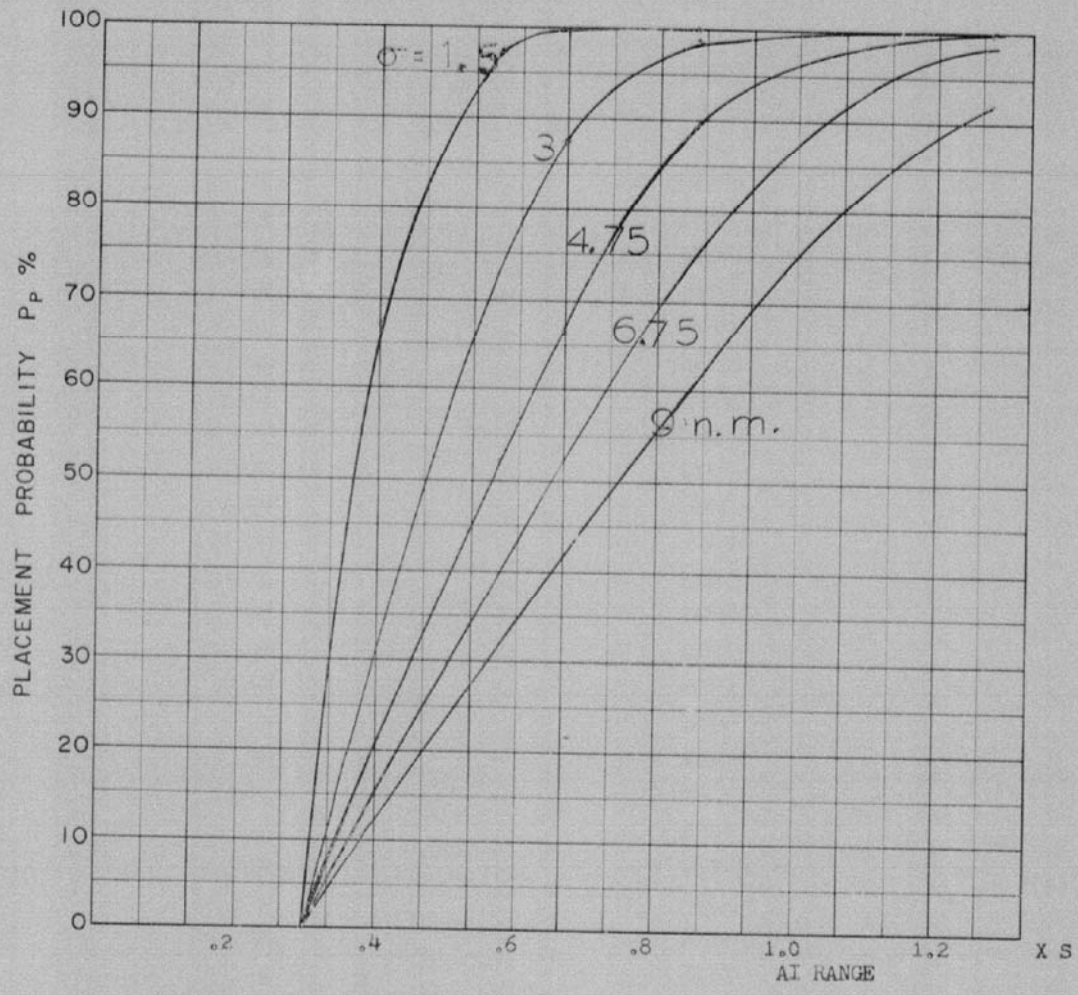

COURSE DIFFERENCE: 140°
TARGET EVASION: 0
TARGET MACH NO.: 1.5
INTERCEPTOR LATERAL G's: 1.6
INTERCEPTOR MACH NO.: 1.5
σ OF G.C.I. ACCURACY: Five values
A.I. DETECTION RANGE AS FRACTION OF SPECIFICATION RANGE, S: Abscissa
A.I. DETECTION RANGE CONTOUR: Straight wing
ALTITUDE: 60 K

S34

Launch zone L-2, maximum range, 10° heading error

33exspr

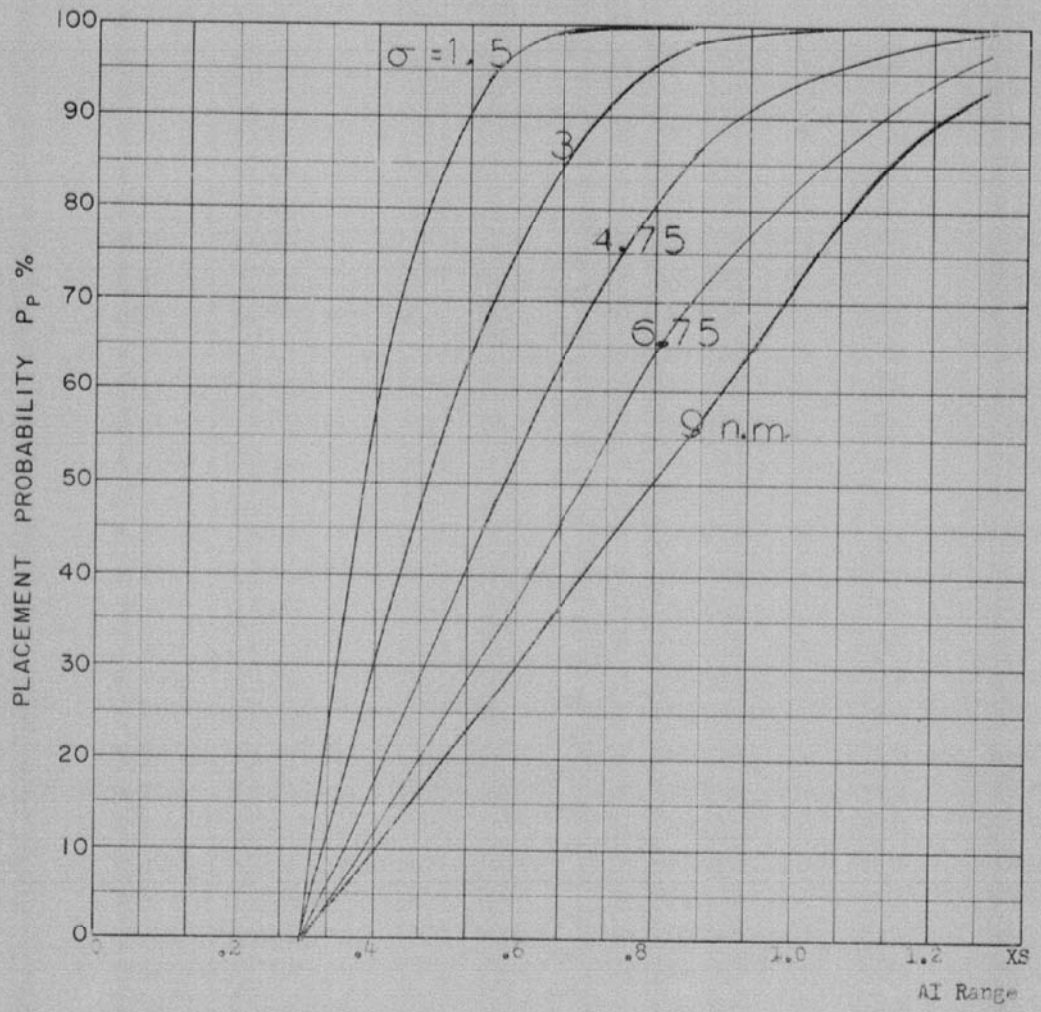

COURSE DIFFERENCE: 160°
TARGET EVASION: 0
TARGET MACH NO.: 1.5
INTERCEPTOR LATERAL G's: 1.6
INTERCEPTOR MACH NO.: 1.5
σ OF G.C.I. ACCURACY: Five values
A.I. DETECTION RANGE AS FRACTION OF SPECIFICATION RANGE, S: Abscissa
A.I. DETECTION RANGE CONTOUR: Straight Wing
ALTITUDE: 60K

S-35

Launch zone L-2, maximum range, 10° heading error.

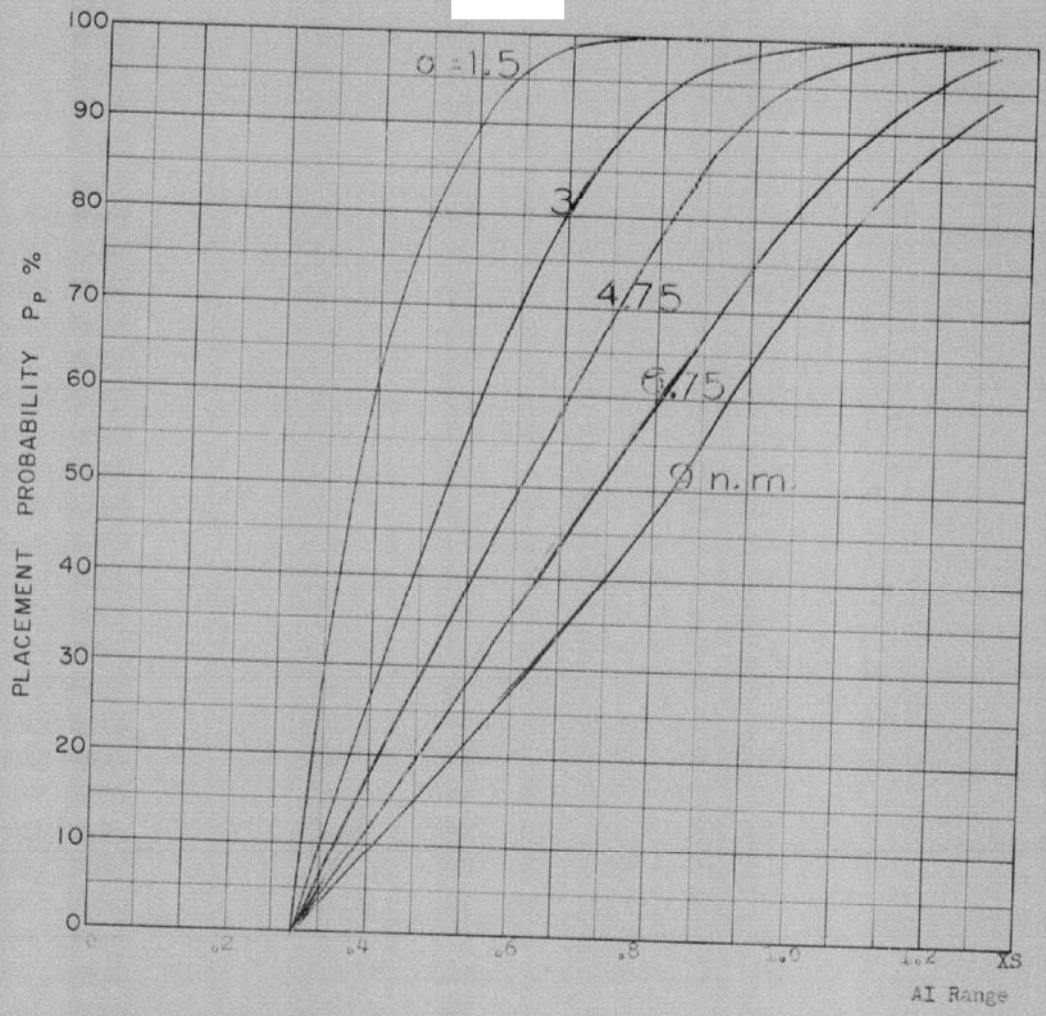

COURSE DIFFERENCE: 180°
TARGET EVASION: 0
TARGET MACH NO.: 1.5
INTERCEPTOR LATERAL G's: 1.6
INTERCEPTOR MACH NO.: 1.5
σ OF G.C.I. ACCURACY: Five values
A.I. DETECTION RANGE AS FRACTION OF SPECIFICATION RANGE, S: Abscissa
A.I. DETECTION RANGE CONTOUR: Straight Wing
ALTITUDE: 60K

S36

Launch zone L 2, maximum range, 10° heading error.

31 aspr

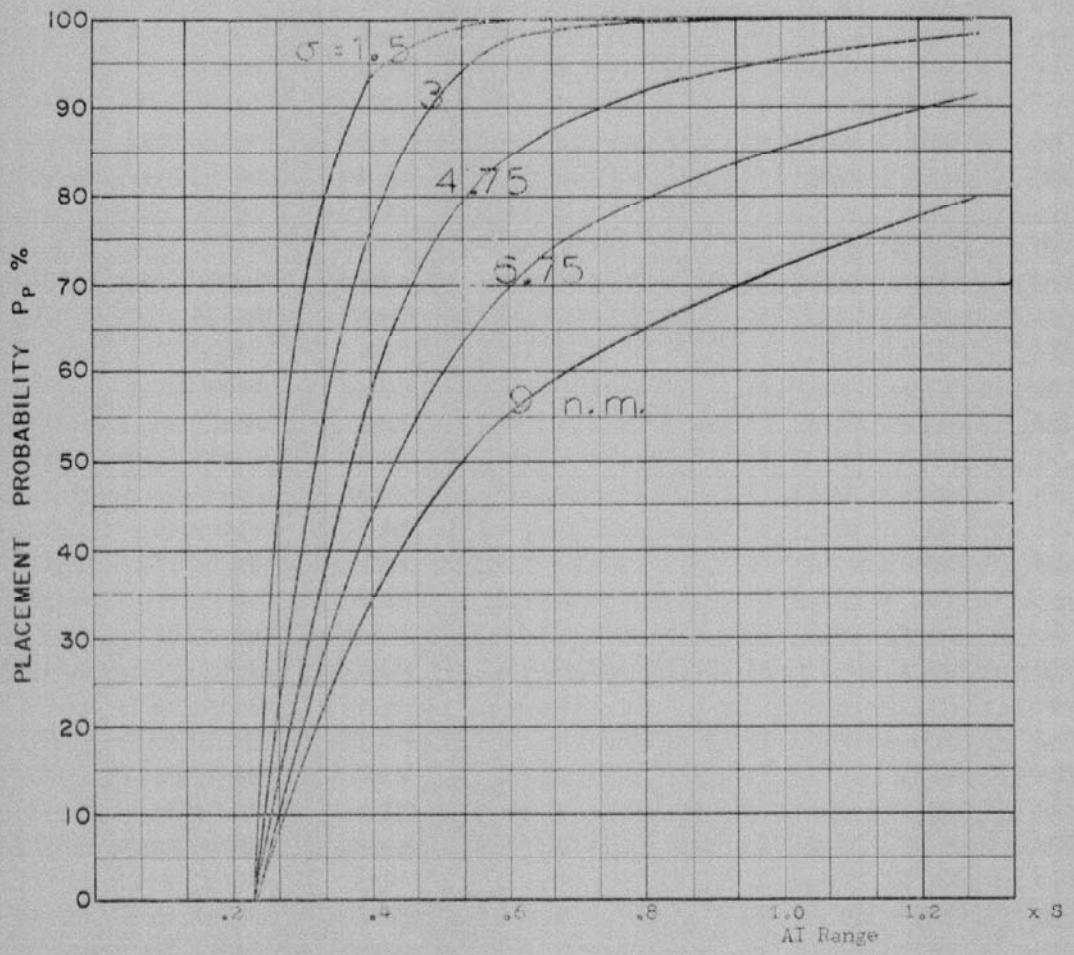

COURSE DIFFERENCE: 80°
TARGET EVASION: 0
TARGET MACH NO.: 1.5
INTERCEPTOR LATERAL G's: 3.0
INTERCEPTOR MACH NO.: 1.5
σ OF G.C.I. ACCURACY: Five values
A.I. DETECTION RANGE AS FRACTION OF SPECIFICATION RANGE, S: Abscissa
A.I. DETECTION RANGE CONTOUR: Straight wing
ALTITUDE: 60 K

Missile launch zone L-2

(S 37)

31 Dapr

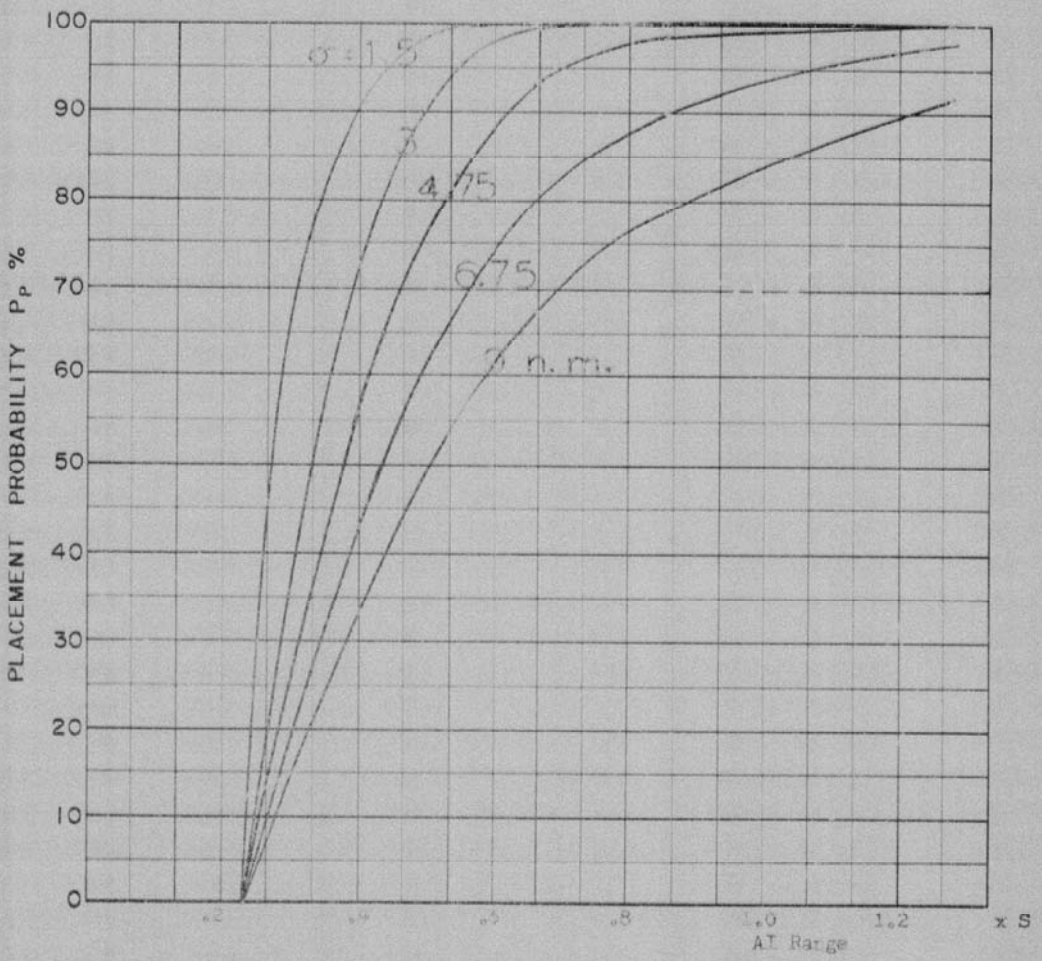

COURSE DIFFERENCE: 180°
TARGET EVASION: 0
TARGET MACH NO.: .85
INTERCEPTOR LATERAL G's: 3.0
INTERCEPTOR MACH NO.: 1.85
σ OF G.C.I. ACCURACY: Five values
A.I. DETECTION RANGE AS FRACTION OF SPECIFICATION RANGE, S: Abscissa
A.I. DETECTION RANGE CONTOUR: Straight wing
ALTITUDE: 60 K

S-38

Missile launch zone L-2

31 cspr

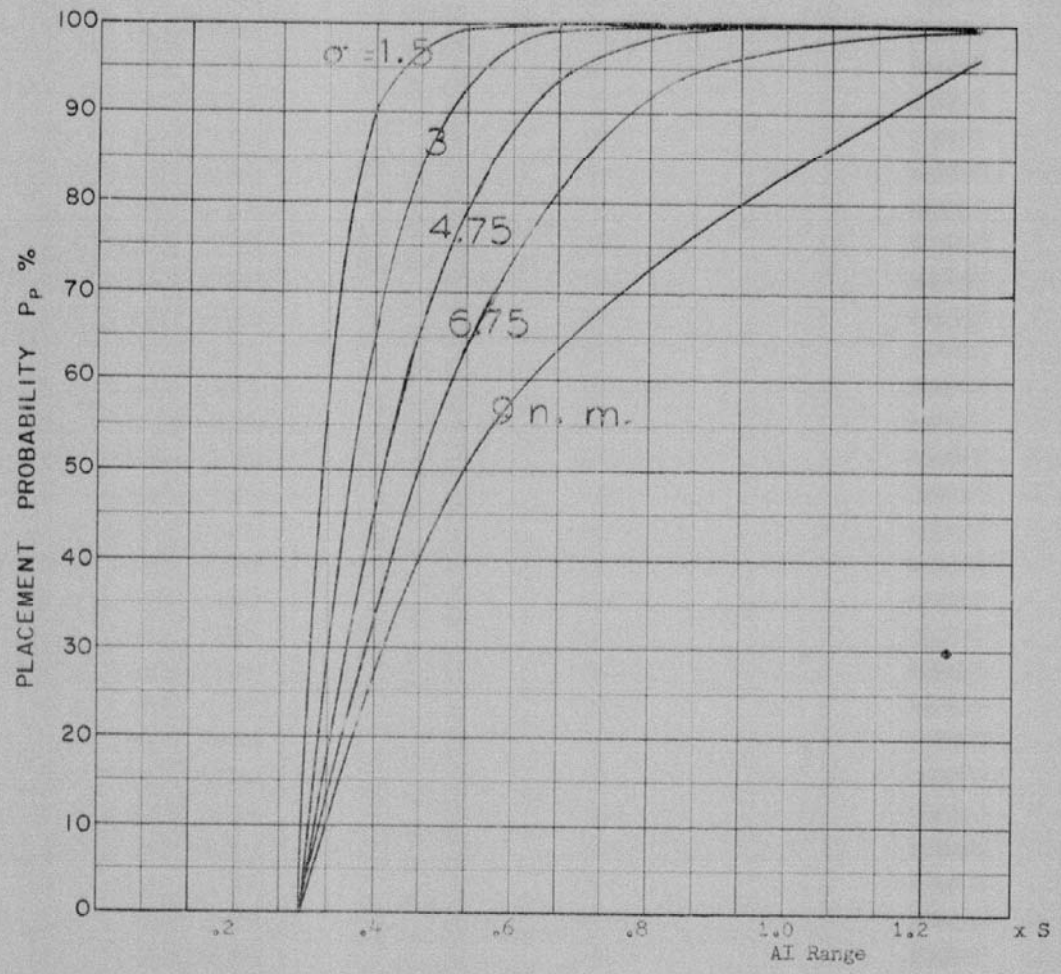

COURSE DIFFERENCE: 120°
TARGET EVASION: 0
TARGET MACH NO.: 1.5
INTERCEPTOR LATERAL G's: 3.0
INTERCEPTOR MACH NO.: 1.5
σ OF G.C.I. ACCURACY: Five values
A.I. DETECTION RANGE AS FRACTION OF SPECIFICATION RANGE, S: Abscissa
A.I. DETECTION RANGE CONTOUR: Straight wing
ALTITUDE: 60 K

Missile launch zone L-2

(S 39)

31 dspr

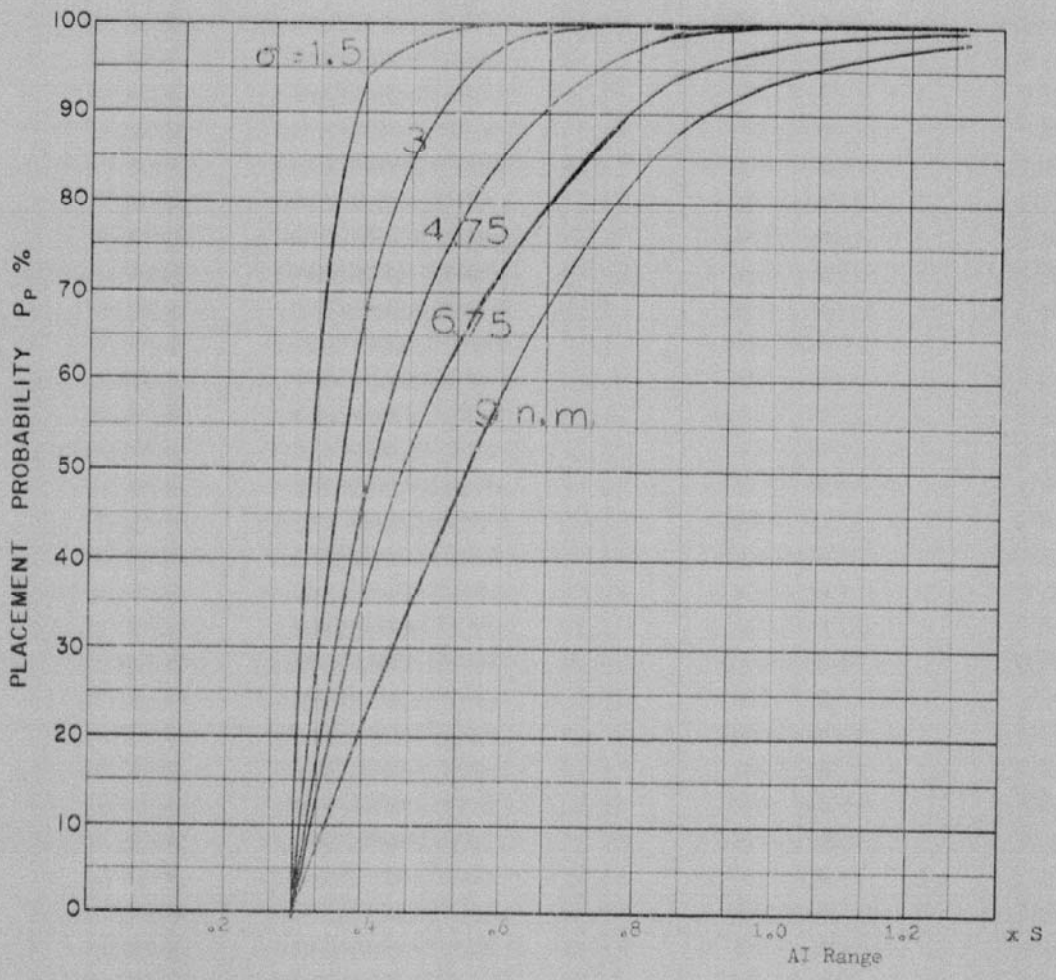

COURSE DIFFERENCE: 140°
TARGET EVASION: 0
TARGET MACH NO.: 1.5
INTERCEPTOR LATERAL G's: 3.0
INTERCEPTOR MACH NO.: 1.5
σ OF G.C.I. ACCURACY: Five values
A.I. DETECTION RANGE AS FRACTION OF SPECIFICATION RANGE, S: Abscissa
A.I. DETECTION RANGE CONTOUR: Straight wing
ALTITUDE: 60 K

Missile launch zone L-2

S 40

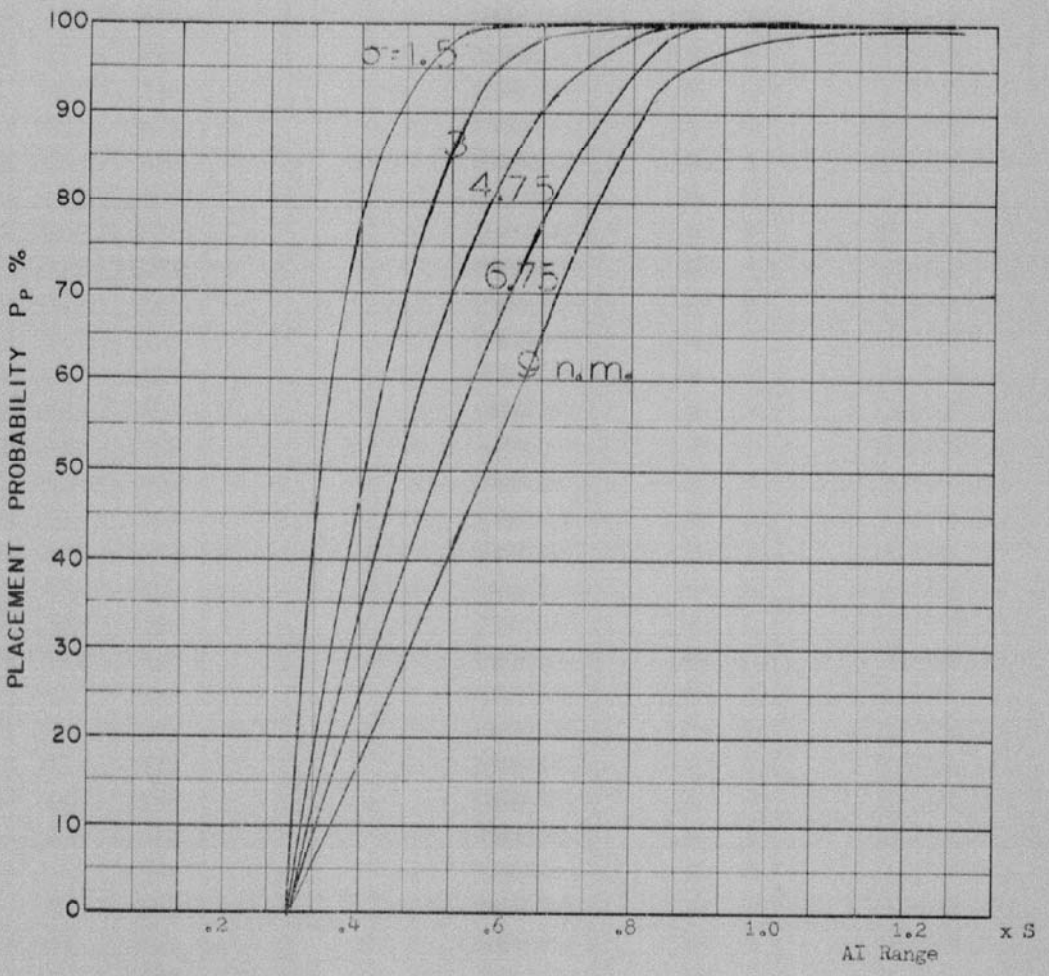

COURSE DIFFERENCE: 160°
TARGET EVASION: 0
TARGET MACH NO.: 1.5
INTERCEPTOR LATERAL G's: 3.0
INTERCEPTOR MACH NO.: 1.5
σ OF G.C.I. ACCURACY: Five values
A.I. DETECTION RANGE AS FRACTION OF SPECIFICATION RANGE, S: Abscissa
A.I. DETECTION RANGE CONTOUR: Straight wing
ALTITUDE: 60 K

S 41

Missile launch zone L-2

31 fspr

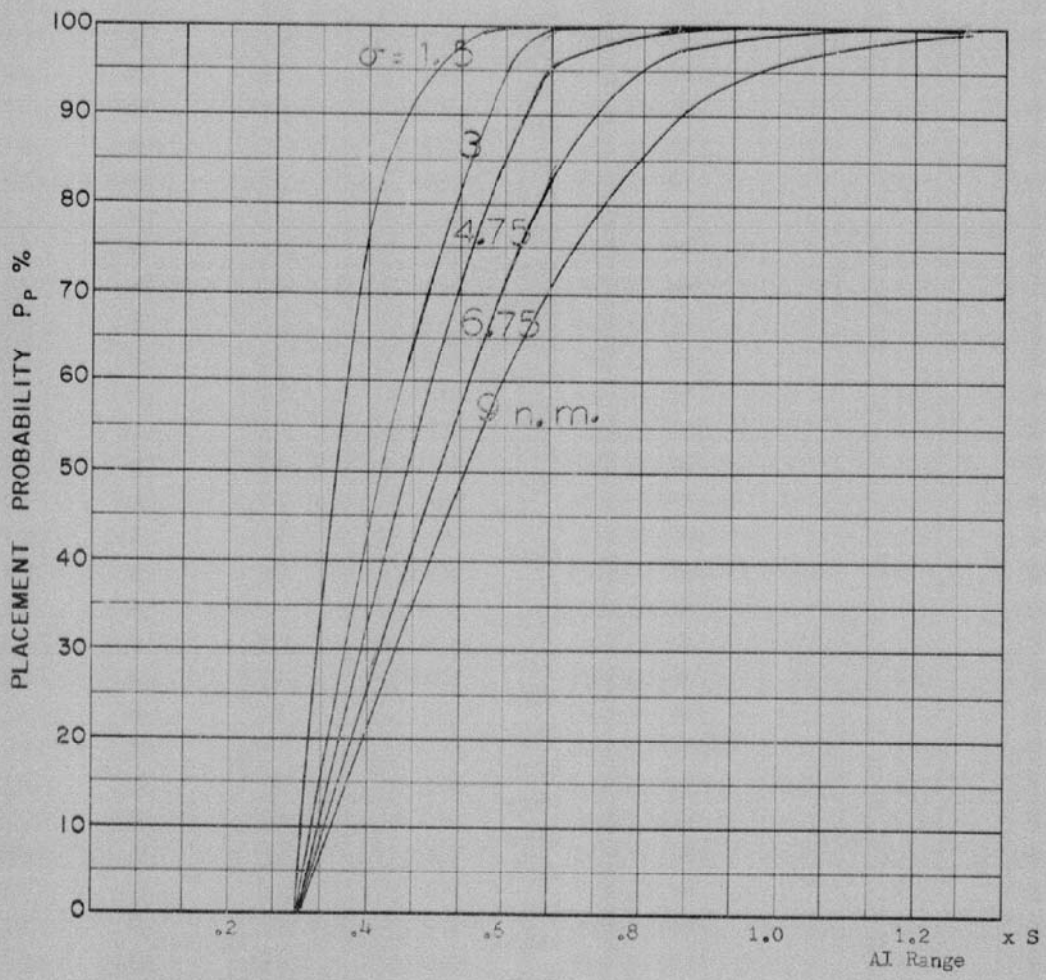

COURSE DIFFERENCE: 180°
TARGET EVASION: 0
TARGET MACH NO.: 1.5
INTERCEPTOR LATERAL G's: 3.0
INTERCEPTOR MACH NO.: 1.5
σ OF G.C.I. ACCURACY: Five values
A.I. DETECTION RANGE AS FRACTION OF SPECIFICATION RANGE, S Abscissa
A.I. DETECTION RANGE CONTOUR: Straight wing
ALTITUDE: 60 K

S 42

Missile launch zone L-2

155 spr

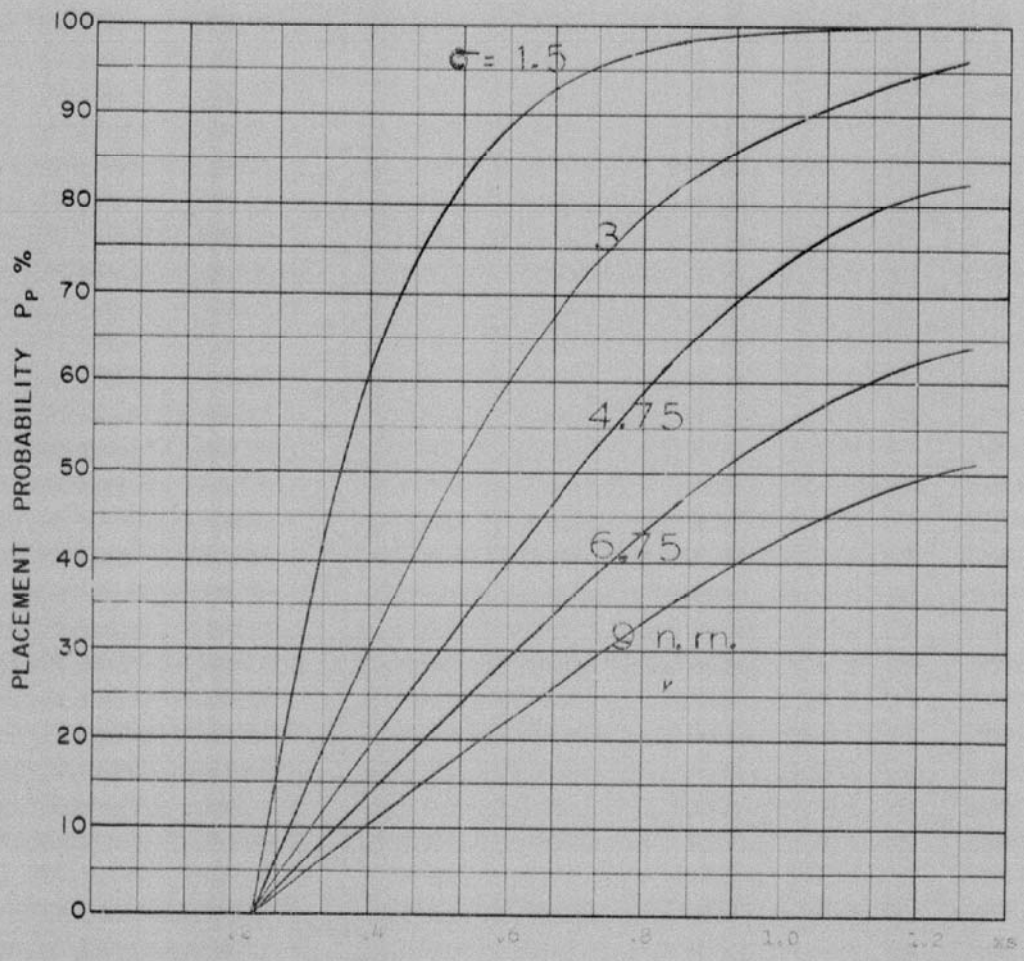

(543)

COURSE DIFFERENCE: 210°
TARGET EVASION: 0.35 lateral g's
TARGET MACH NO.: 1.5
INTERCEPTOR LATERAL G's: 0.85
INTERCEPTOR MACH NO.: 2.5
σ OF G.C.I. ACCURACY: five values
A.I. DETECTION RANGE AS FRACTION OF SPECIFICATION RANGE, S: abscissa
A.I. DETECTION RANGE CONTOUR: Straight wing
ALTITUDE: 50K

Missile Launch zone I 12

157 apr

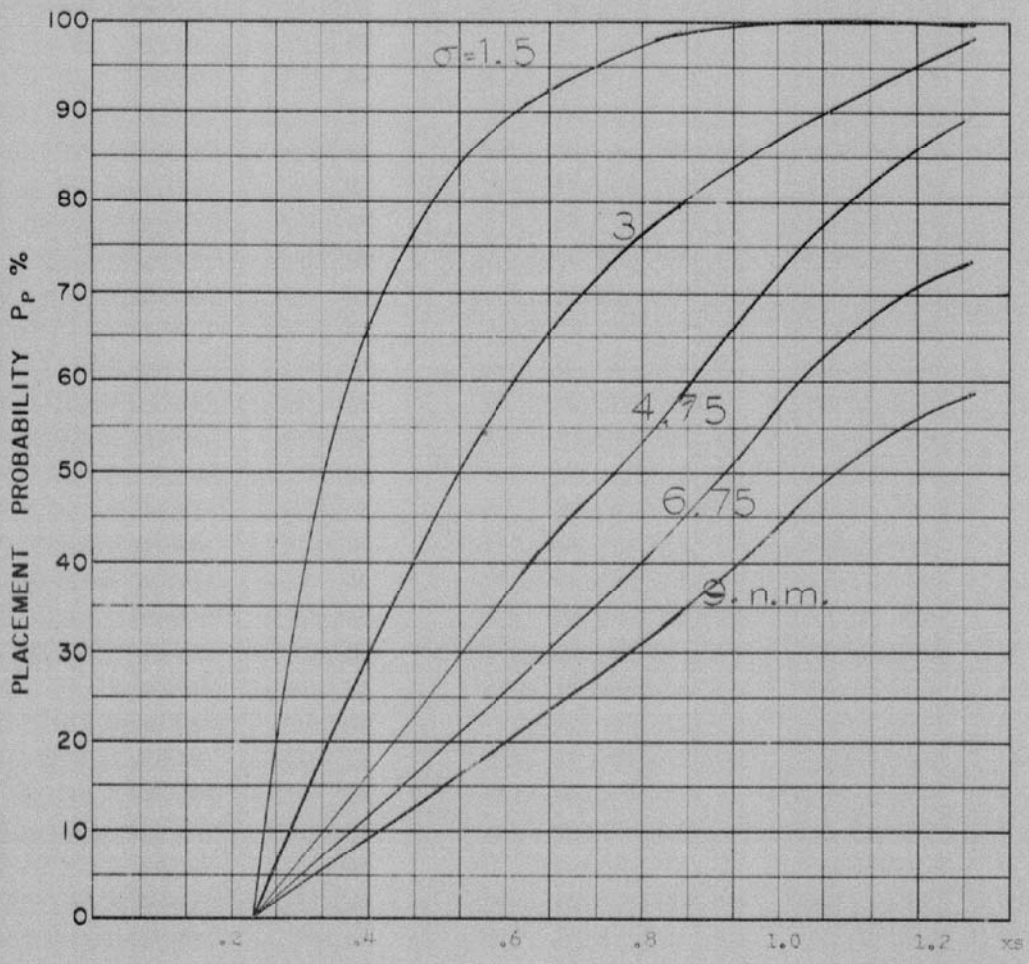

COURSE DIFFERENCE: 135°
TARGET EVASION: 0.15 lateral g's
TARGET MACH NO.: 1.5
INTERCEPTOR LATERAL G's: 0.85
INTERCEPTOR MACH NO.: 1.5
σ OF G.C.I. ACCURACY: five values
A.I. DETECTION RANGE AS FRACTION OF SPECIFICATION RANGE, S: abscissa
A.I. DETECTION RANGE CONTOUR: Straight wing
ALTITUDE: 50K

S44

Missile launch zone L 12

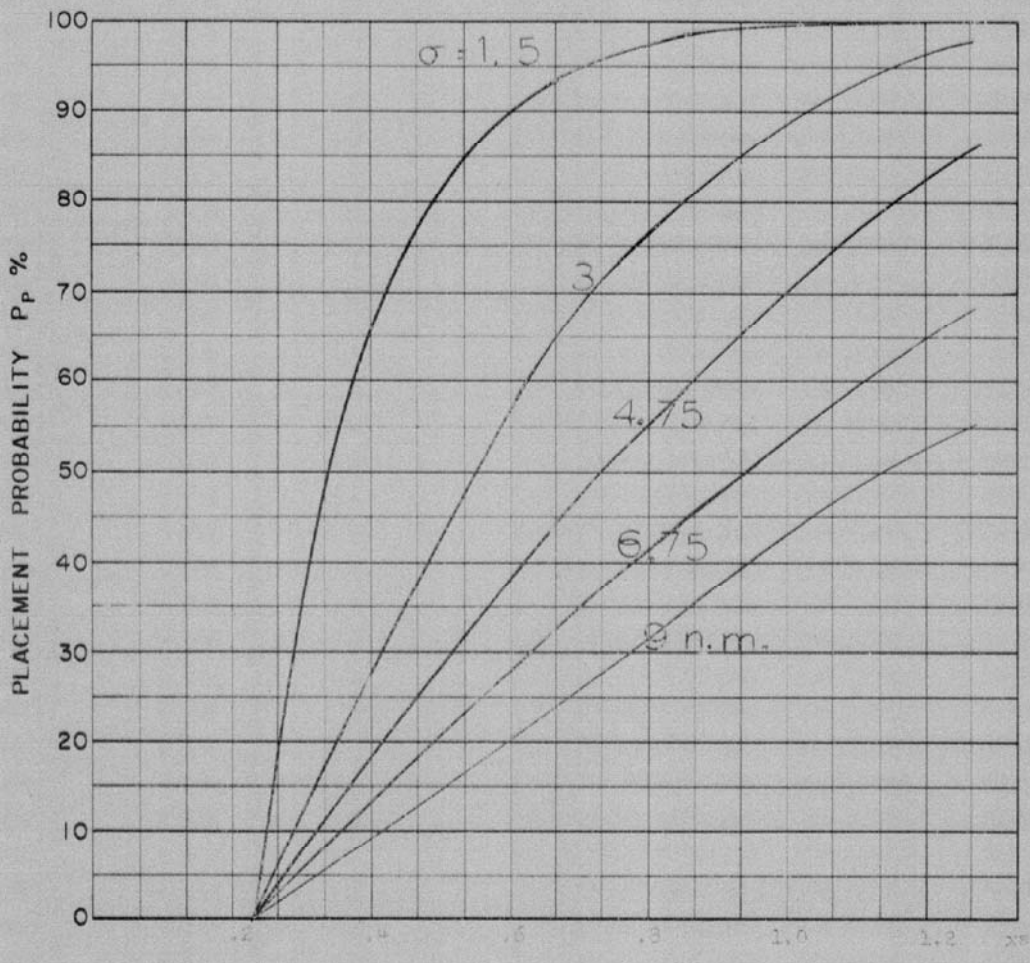

COURSE DIFFERENCE:
TARGET EVASION:
TARGET MACH NO.:
INTERCEPTOR LATERAL G's:
INTERCEPTOR MACH NO.:
σ OF G.C.I. ACCURACY:
A.I. DETECTION RANGE AS FRACTION OF SPECIFICATION RANGE, S:
A.I. DETECTION RANGE CONTOUR:
ALTITUDE:

161 spr

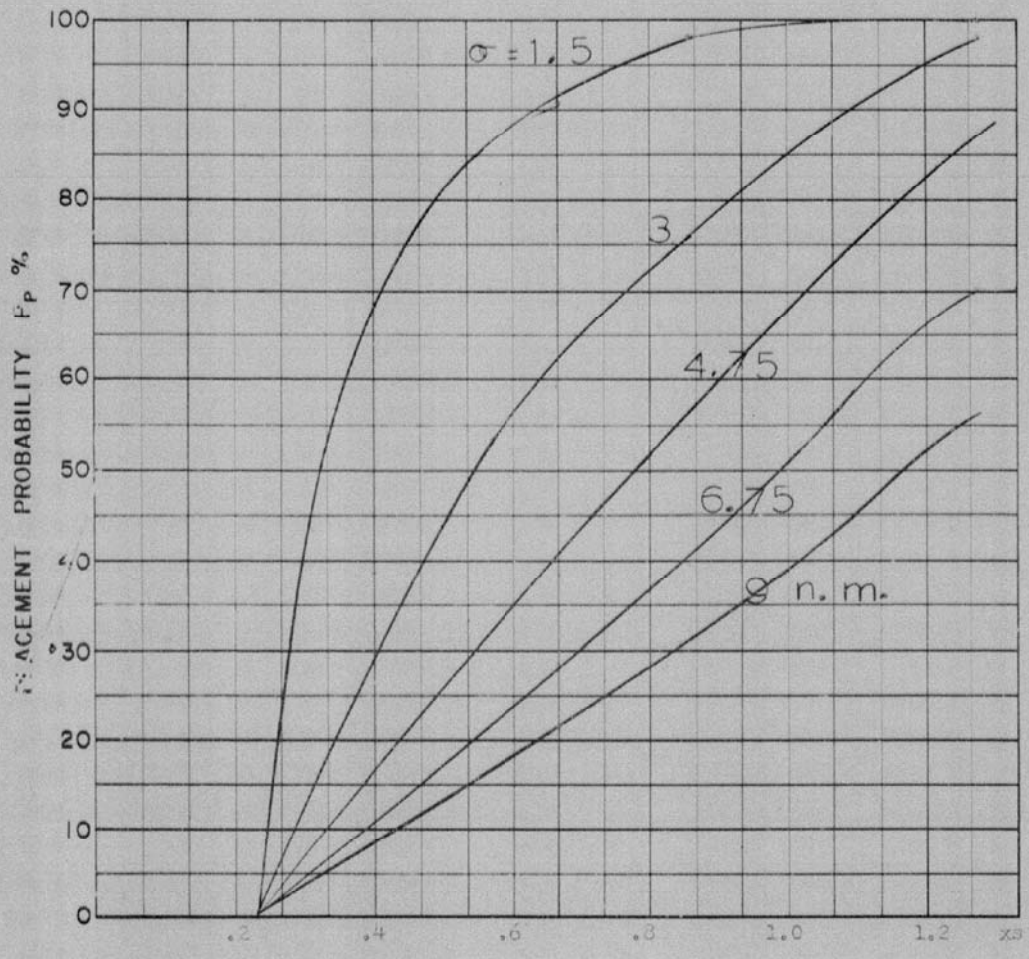

ACEMENT PROBABILITY P_p %

S46

COURSE DIFFERENCE: 180°
TARGET EVASION: 0.15 lateral g's
TARGET MACH NO.: 1.5
INTERCEPTOR LATERAL G's: 0.85
INTERCEPTOR MACH NO.: 1.5
σ OF G.C.I. ACCURACY: five values
A.I. DETECTION RANGE AS FRACTION OF SPECIFICATION RANGE, S: abscissa
A.I. DETECTION RANGE CONTOUR: Straight wing
ALTITUDE: 50K

Missile launch zone L 12

162 spr

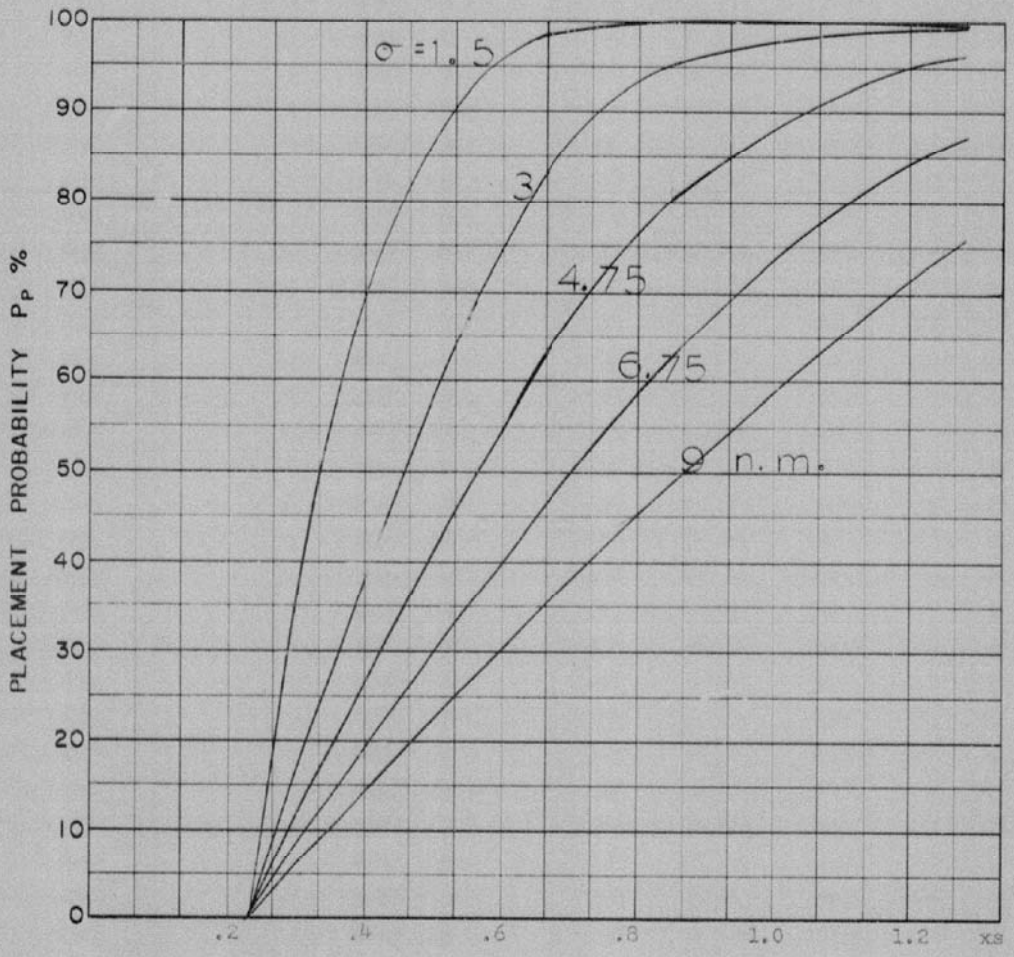

A.I. Range

S47a

COURSE DIFFERENCE: 110°
TARGET EVASION: 0.15 lateral g's
TARGET MACH NO.: 1.5
INTERCEPTOR LATERAL G's: 1.6
INTERCEPTOR MACH NO.: 1.5
σ OF G.C.I. ACCURACY: five values
A.I. DETECTION RANGE AS FRACTION OF SPECIFICATION RANGE, S: abscissa
A.I. DETECTION RANGE CONTOUR: Straight wing
ALTITUDE: 50K

Missile launch zone L 12

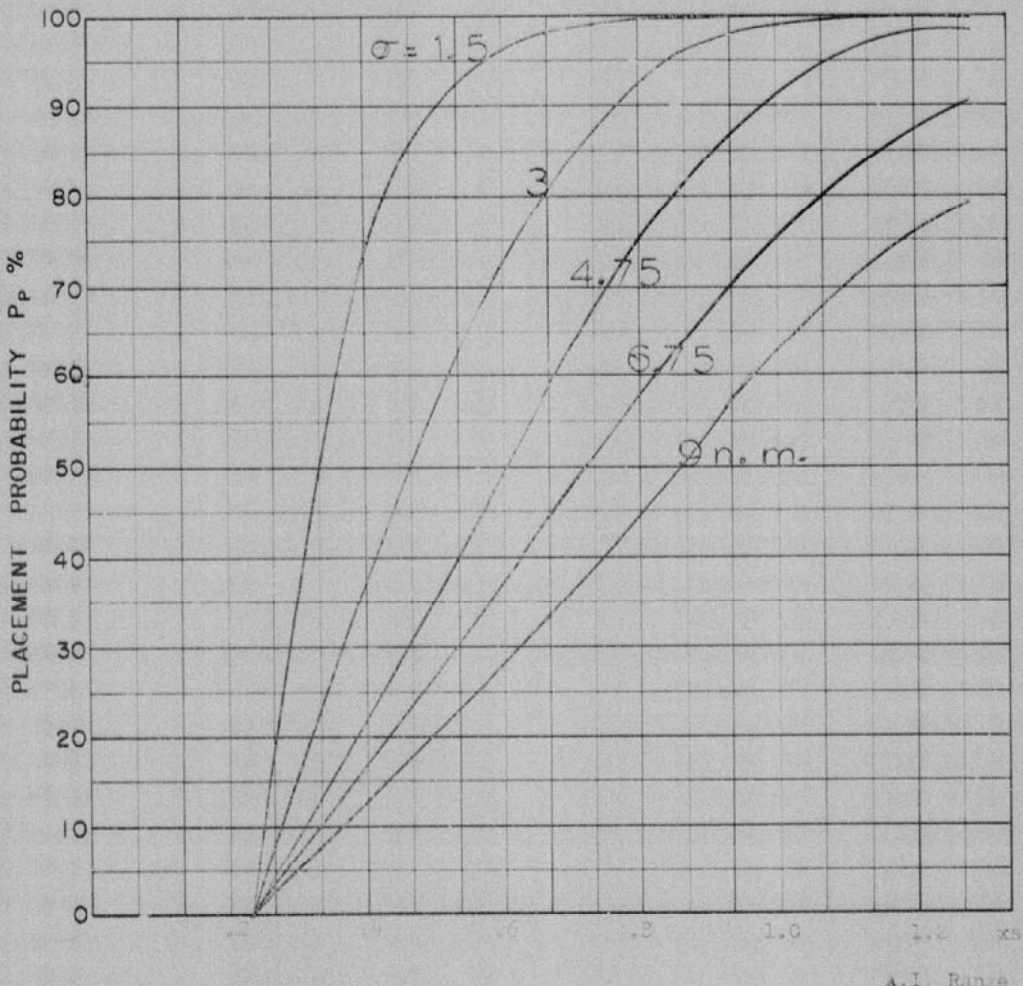

COURSE DIFFERENCE:
TARGET EVASION:
TARGET MACH NO.:
INTERCEPTOR LATERAL G's:
INTERCEPTOR MACH NO.:
σ OF G.C.I. ACCURACY:
A.I. DETECTION RANGE AS FRACTION OF SPECIFICATION RANGE, S:
A.I. DETECTION RANGE CONTOUR:
ALTITUDE:

S48

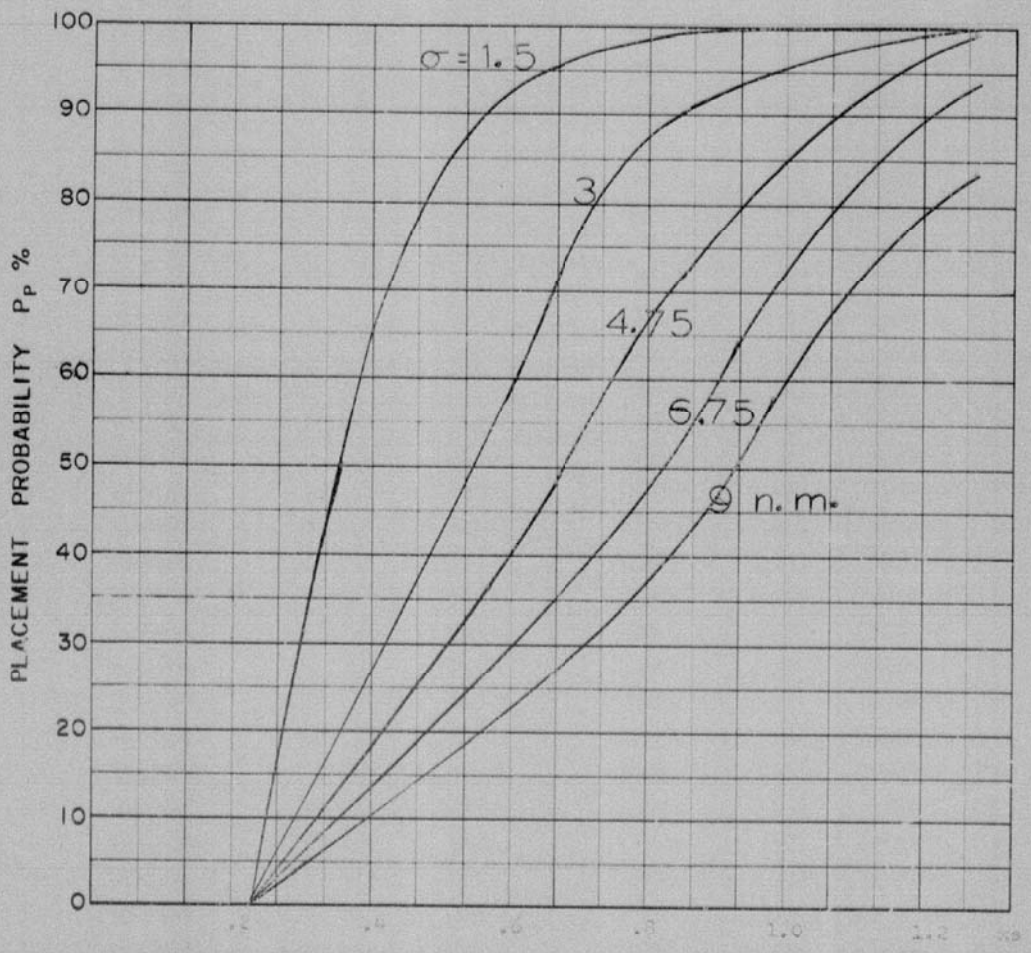

COURSE DIFFERENCE: 160°
TARGET EVASION: 0.15 lateral g's
TARGET MACH NO.: 1.5
INTERCEPTOR LATERAL G's: 1.6
INTERCEPTOR MACH NO.: 1.5
σ OF G.C.I. ACCURACY: Five values
A.I. DETECTION RANGE AS FRACTION OF SPECIFICATION RANGE, S: abscissa
A.I. DETECTION RANGE CONTOUR: Straight wing
ALTITUDE: 50K

S49a

Missile launch zone L 12

171 aspr

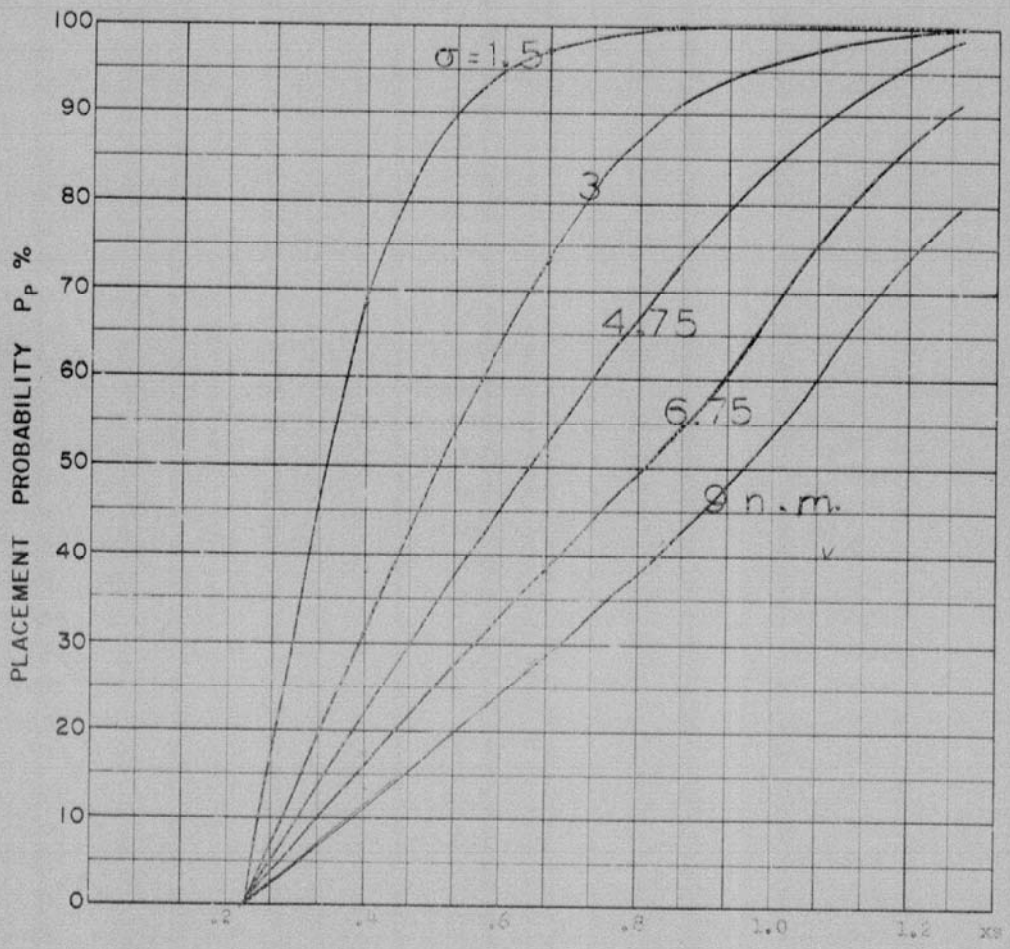

(S50a)

COURSE DIFFERENCE: 180°
TARGET EVASION: 0.15 lateral g's
TARGET MACH NO.: 1.5
INTERCEPTOR LATERAL G's: 1.6
INTERCEPTOR MACH NO.: 1.5
σ OF G.C.I. ACCURACY: five values
A.I. DETECTION RANGE AS FRACTION OF SPECIFICATION RANGE, S: abscissa
A.I. DETECTION RANGE CONTOUR: Straight wing
ALTITUDE: 50K

Missile launch zone L 12

173 spr

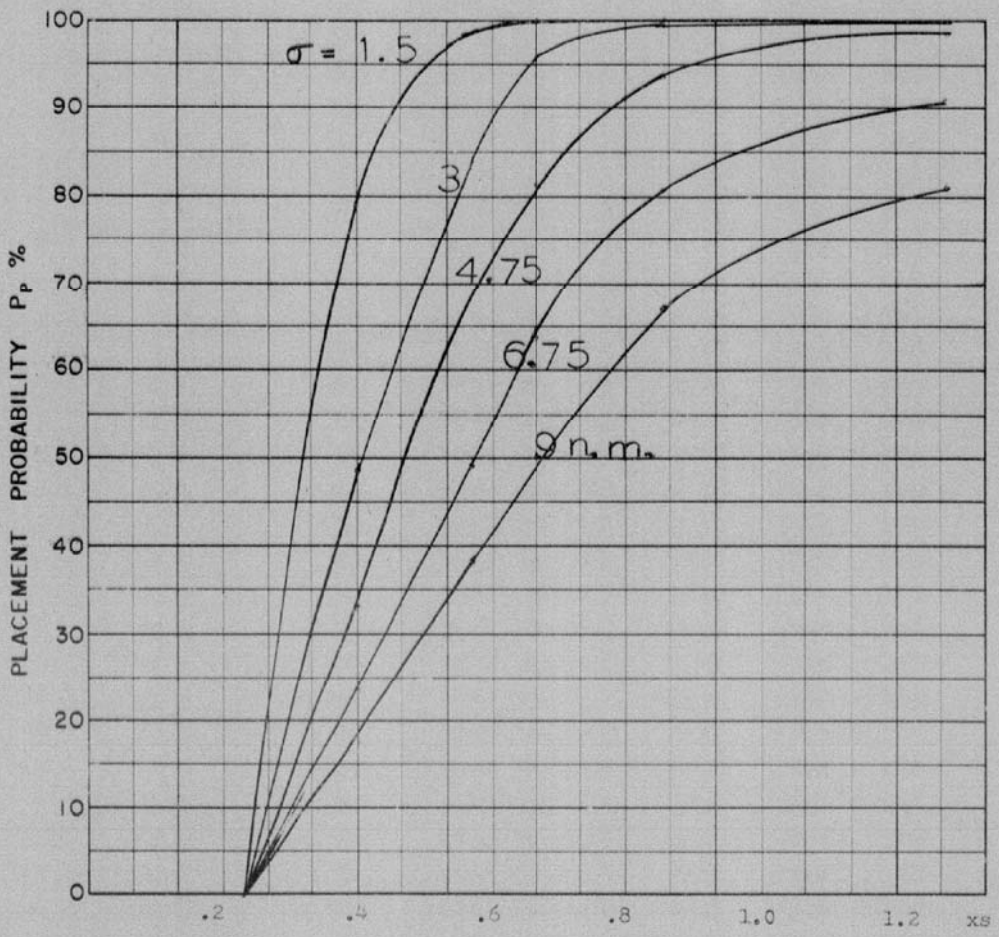

COURSE DIFFERENCE: 110°
TARGET EVASION: 0.15 lateral g's
TARGET MACH NO.: 1.5
INTERCEPTOR LATERAL G's: 3.0
INTERCEPTOR MACH NO.: 1.5
σ OF G.C.I. ACCURACY: five values
A.I. DETECTION RANGE AS FRACTION OF SPECIFICATION RANGE, S: abscissa
A.I. DETECTION RANGE CONTOUR: Straight wing
ALTITUDE: 50K

S51

Missile launch zone L 12

175 spr

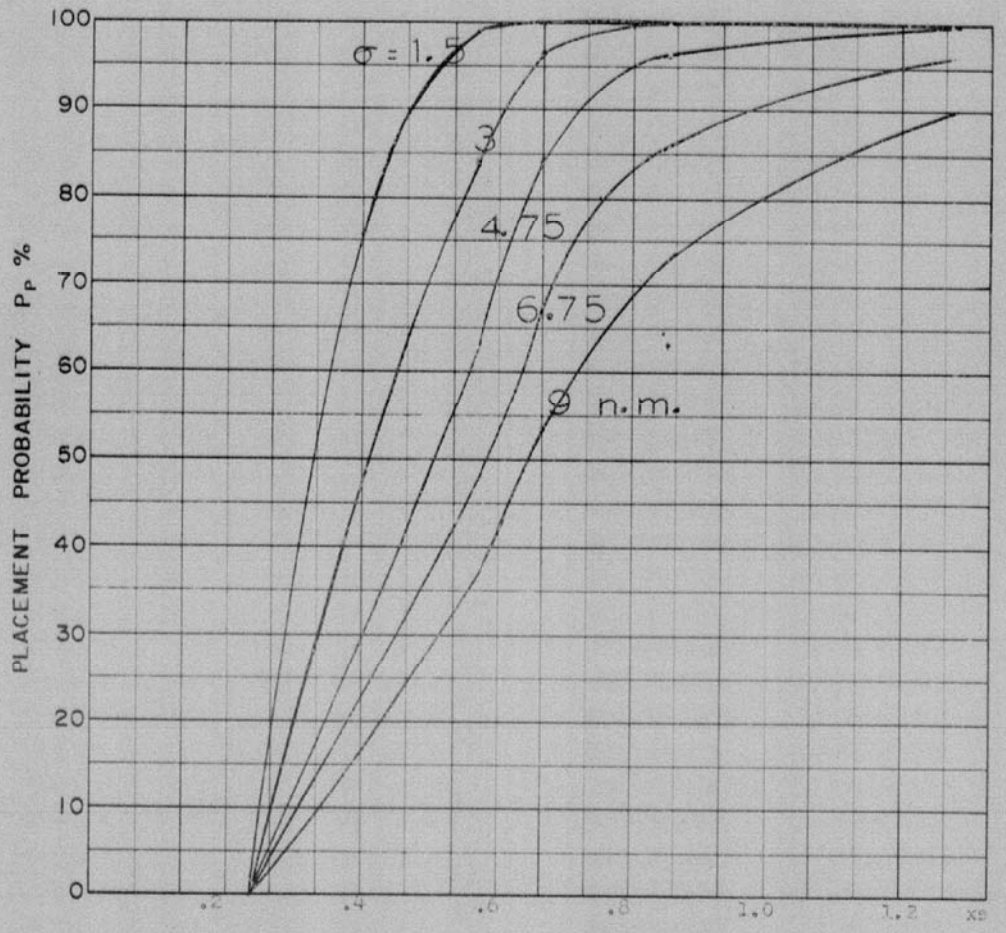

A.I. Range

S52

COURSE DIFFERENCE: 135°
TARGET EVASION: 0.15 lateral g's
TARGET MACH NO.: 1.5
INTERCEPTOR LATERAL G's: 3.0
INTERCEPTOR MACH NO.: 1.5
σ OF G.C.I. ACCURACY: five values
A.I. DETECTION RANGE AS FRACTION OF SPECIFICATION RANGE, S: abscissa
A.I. DETECTION RANGE CONTOUR: Straight wing
ALTITUDE: 50K

Missile launch zone L 12

177 spr

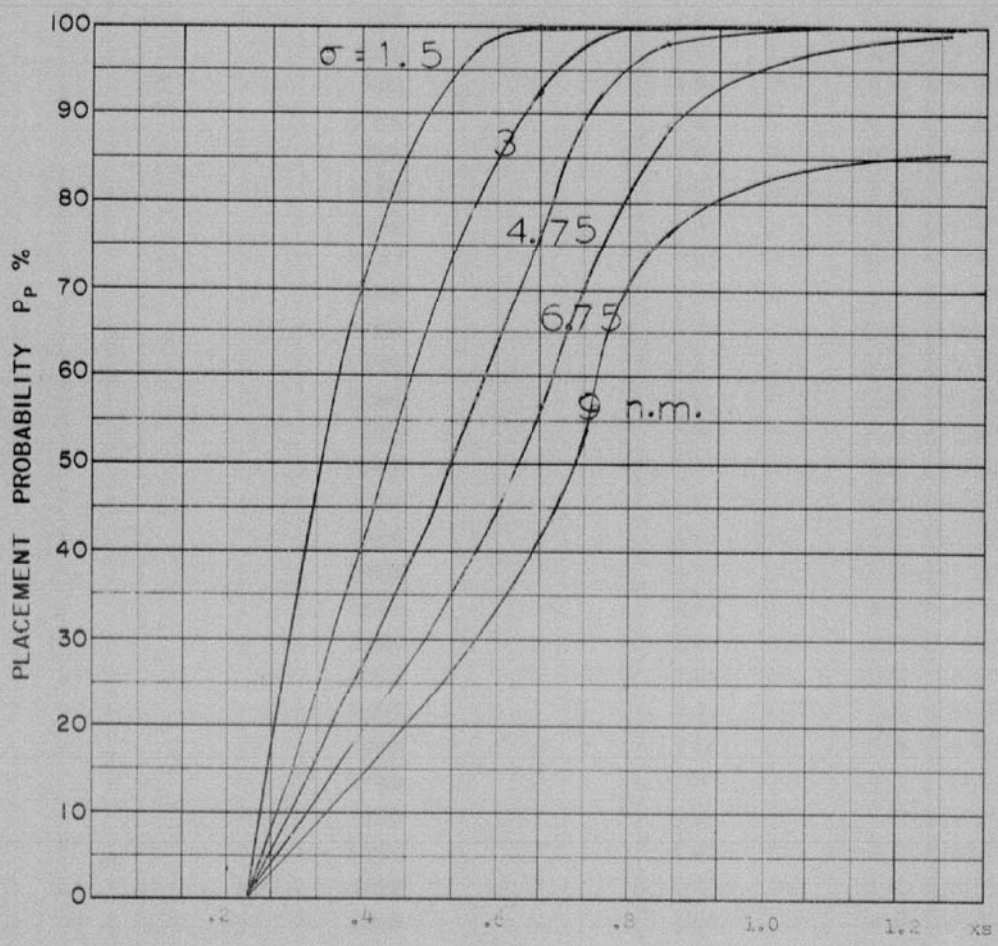

A.I. Range

S53

COURSE DIFFERENCE: 160°
TARGET EVASION: 0.15 lateral g's
TARGET MACH NO.: 1.5
INTERCEPTOR LATERAL G's: 3.0
INTERCEPTOR MACH NO.: 1.5
σ OF G.C.I. ACCURACY: Five values
A.I. DETECTION RANGE AS FRACTION OF SPECIFICATION RANGE, S: abscissa
A.I. DETECTION RANGE CONTOUR: Straight wing
ALTITUDE: 50K

Missile launch zone L 12

179 sp:

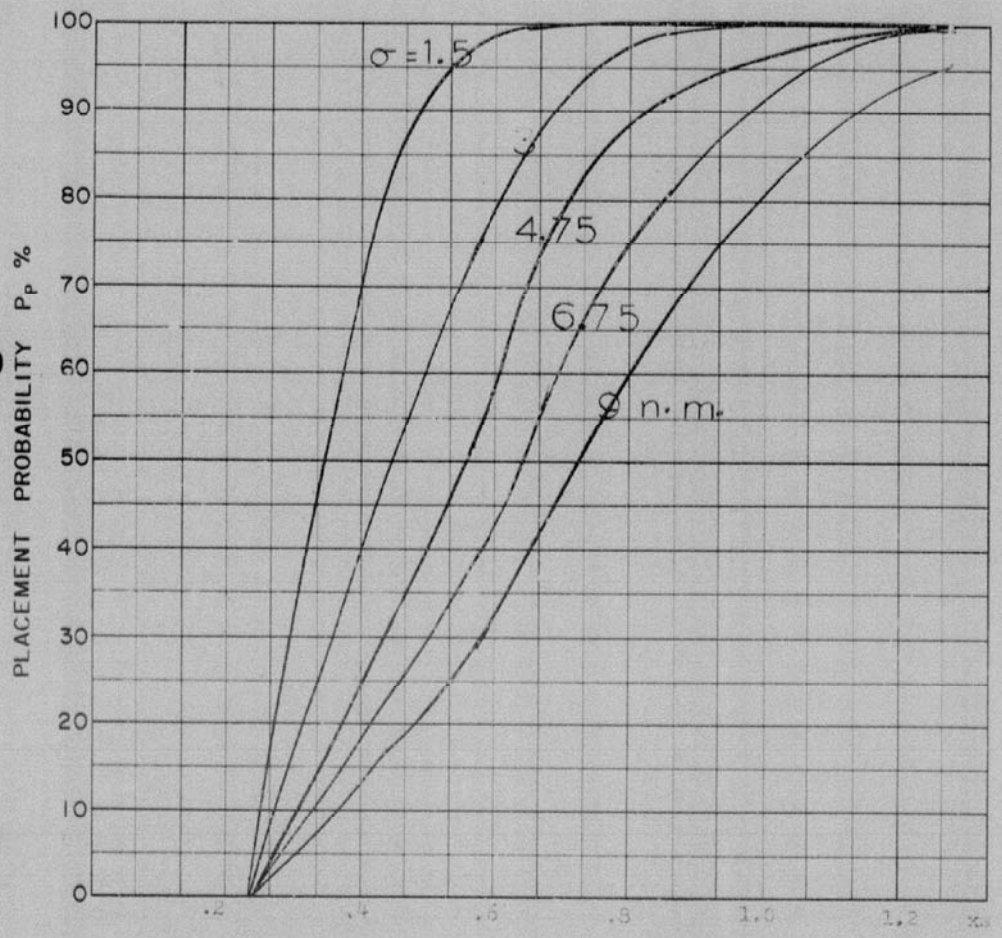

A.I. Range

COURSE DIFFERENCE: 180°
TARGET EVASION: 0.15 lateral g's
TARGET MACH NO.: 1.5
INTERCEPTOR LATERAL G's: 3.0
INTERCEPTOR MACH NO.: 1.5
σ OF G.C.I. ACCURACY: five values
A.I. DETECTION RANGE AS FRACTION OF SPECIFICATION RANGE, S: abscisse
A.I. DETECTION RANGE CONTOUR: Straight wing
ALTITUDE: 50k

S 54

Missile launch zone L 12

180 spr

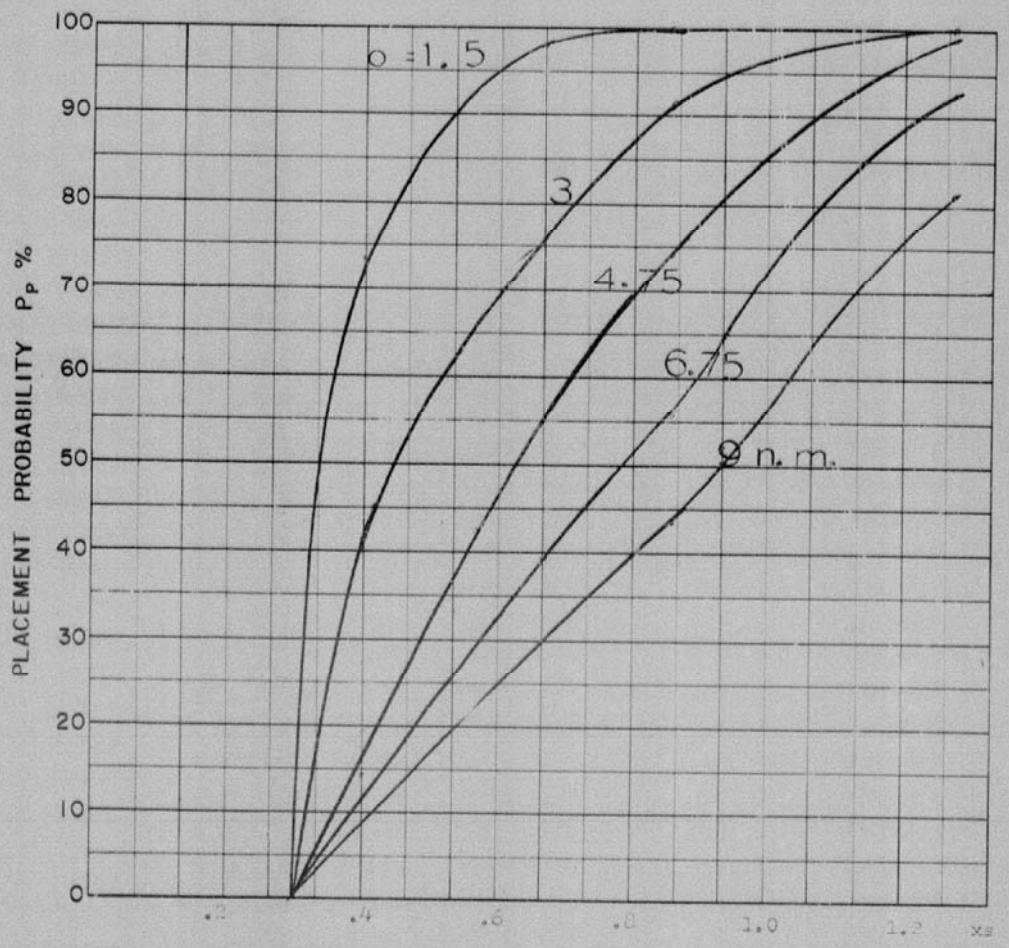

A.I. Range

COURSE DIFFERENCE: 180°
TARGET EVASION: 0.15 lateral g's
TARGET MACH NO.: 1.5
INTERCEPTOR LATERAL G's: 1.6
INTERCEPTOR MACH NO.: 1.5
σ OF G.C.I. ACCURACY: five values
A.I. DETECTION RANGE AS FRACTION OF SPECIFICATION RANGE, S: abscissa
A.I. DETECTION RANGE CONTOUR: Straight wing
ALTITUDE: 50K

S-55

Missile Launch zone L 12

181 spr

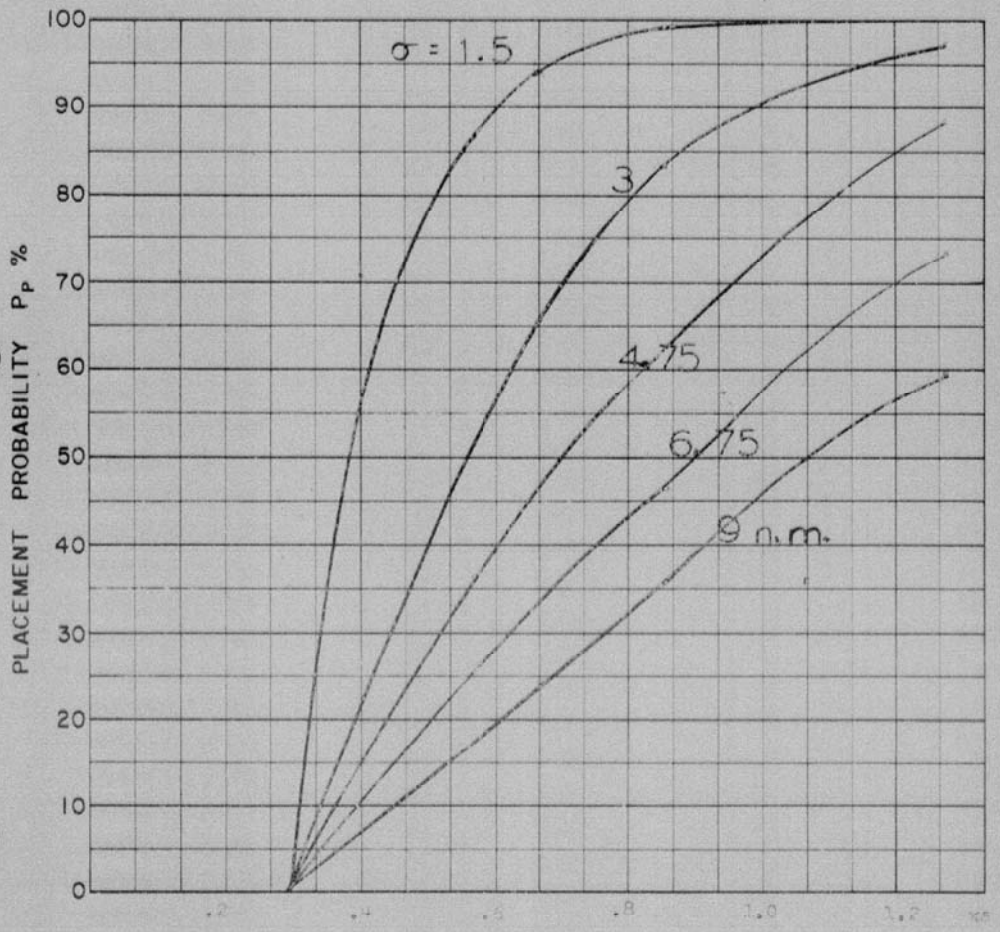

COURSE DIFFERENCE: 110°
TARGET EVASION: 0.25 lateral g's
TARGET MACH NO.: 1.8
INTERCEPTOR LATERAL G's: 0.66
INTERCEPTOR MACH NO.: 1.5
σ OF G.C.I. ACCURACY: five values
A.I. DETECTION RANGE AS FRACTION OF SPECIFICATION RANGE, S: abscissa
A.I. DETECTION RANGE CONTOUR: Straight wing
ALTITUDE: 60K

S-56

Missile launch zone L 13

183 spr

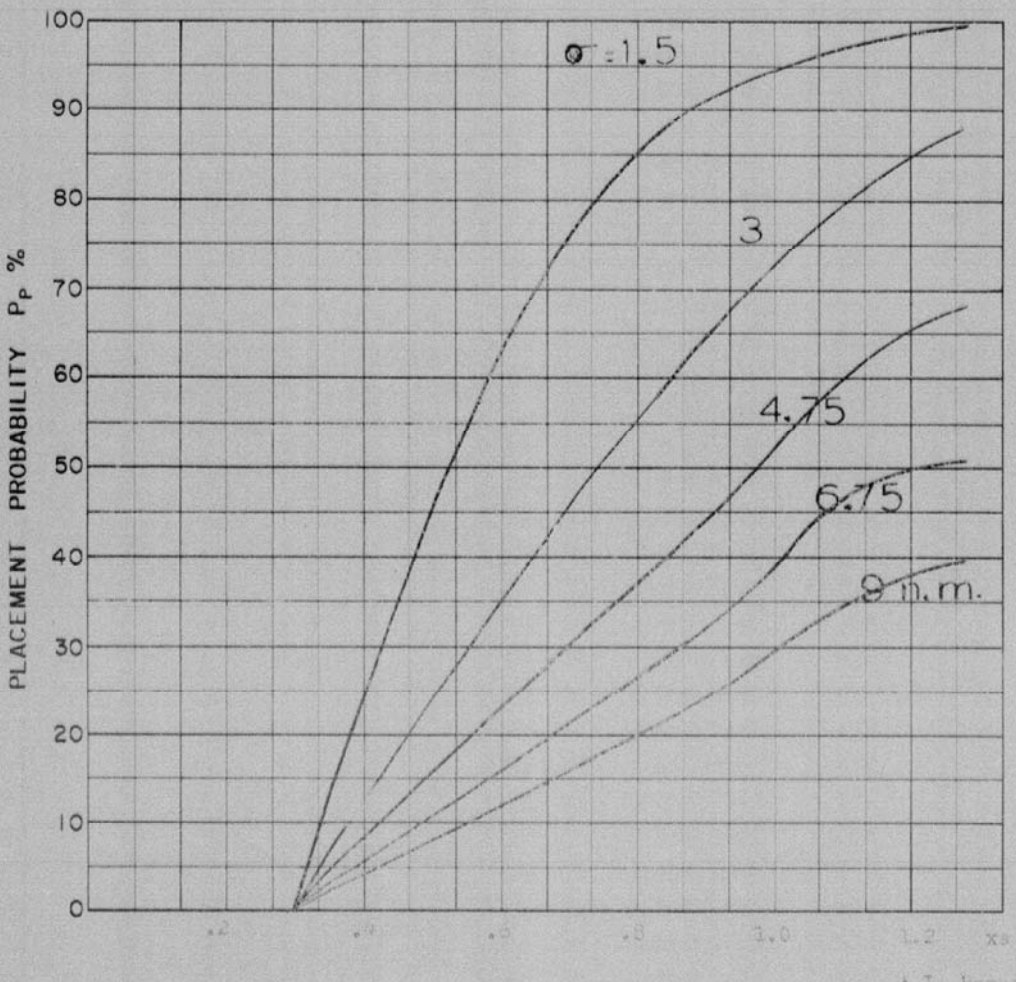

COURSE DIFFERENCE: 135°
TARGET EVASION: 0.15 lateral g's
TARGET MACH NO.: 1.5
INTERCEPTOR LATERAL G's: 0.66
INTERCEPTOR MACH NO.: 1.5
σ OF G.C.I. ACCURACY: five values
A.I. DETECTION RANGE AS FRACTION OF SPECIFICATION RANGE, S: abscissa
A.I. DETECTION RANGE CONTOUR: Straight wing
ALTITUDE: 60K

S57

Missile launch zone L 13

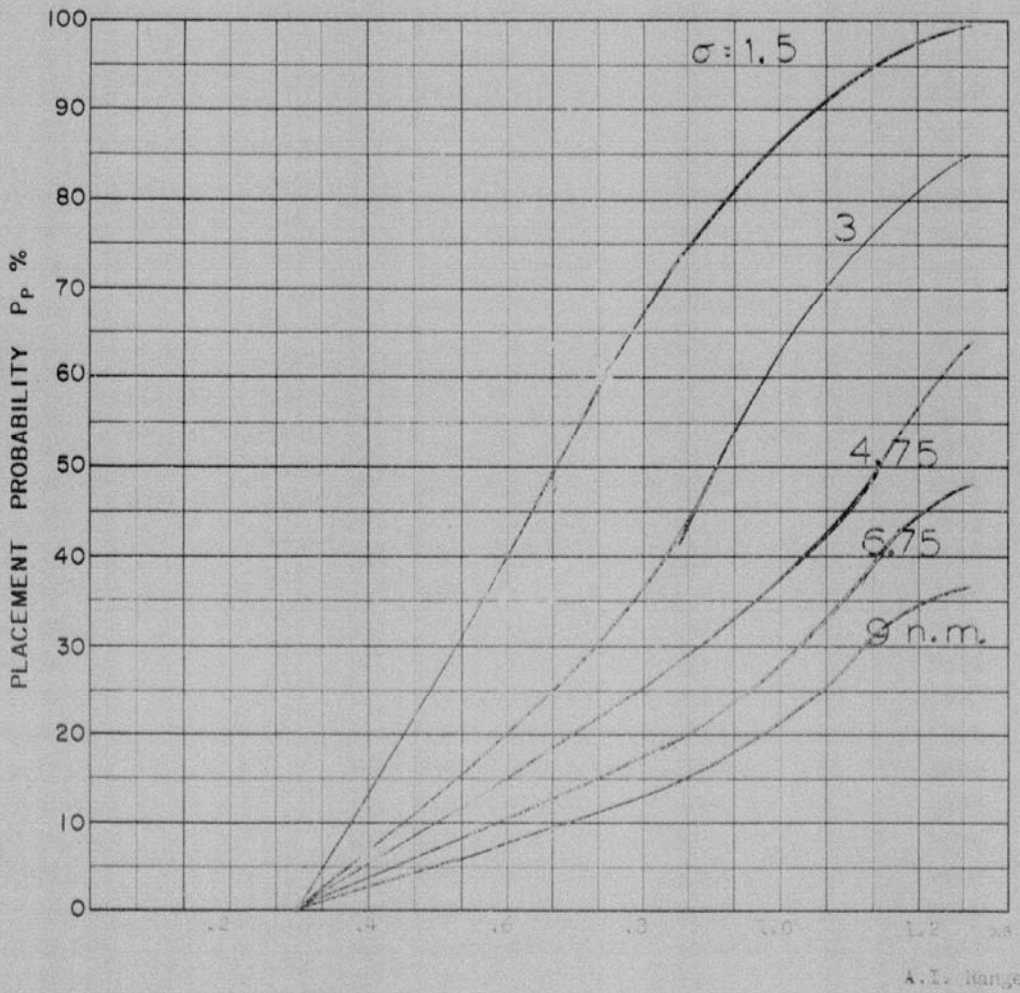

COURSE DIFFERENCE: 180°
TARGET EVASION: 0.15 lateral g's
TARGET MACH NO.: 1.5
INTERCEPTOR LATERAL G's: 0.66
INTERCEPTOR MACH NO.: 1.5
σ OF G.C.I. ACCURACY: five values
A.I. DETECTION RANGE AS FRACTION OF SPECIFICATION RANGE, S: abscissa
A.I. DETECTION RANGE CONTOUR: Straight wing
ALTITUDE: 60K

S 58

Missile launch zone L 13

187 spr

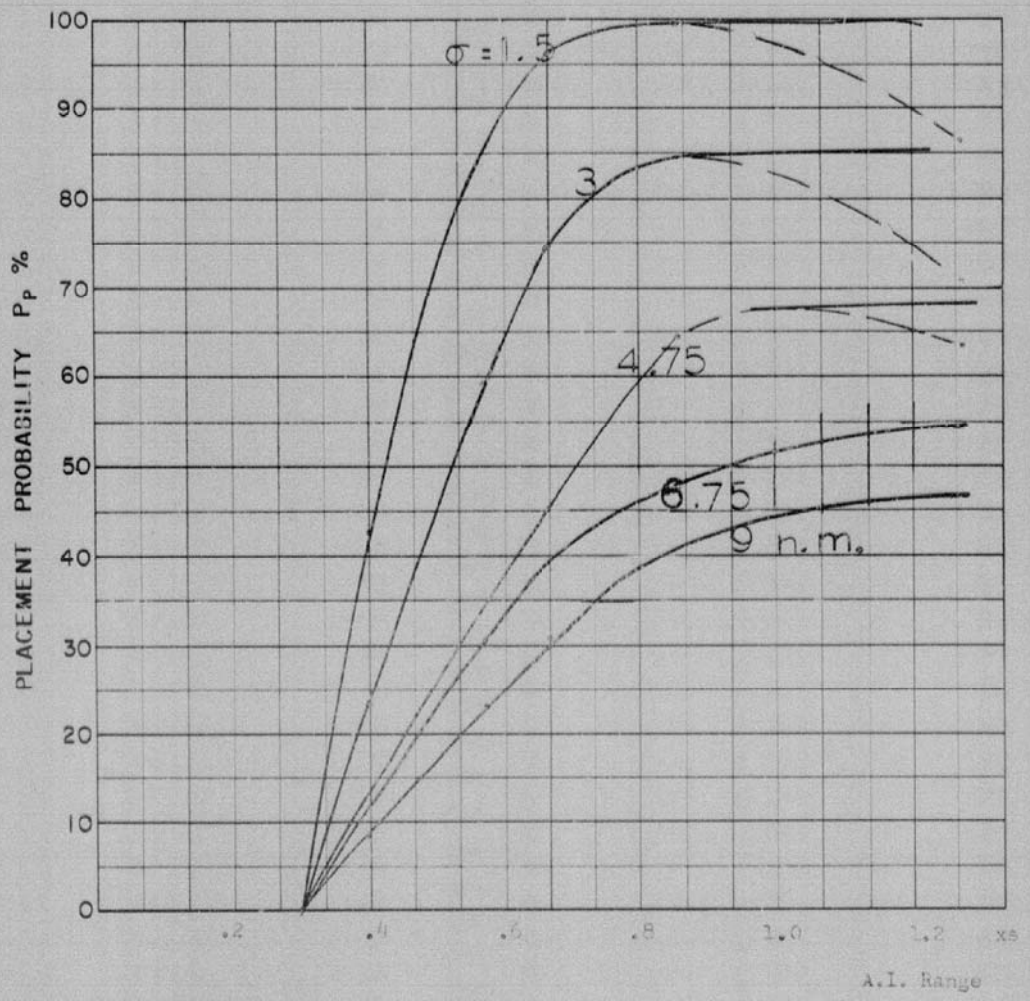

COURSE DIFFERENCE: 110°
TARGET EVASION: 0.15 lateral g's
TARGET MACH NO.: 1.5
INTERCEPTOR LATERAL G's: 1.5
INTERCEPTOR MACH NO.: 1.5
σ OF G.C.I. ACCURACY: five values
A.I. DETECTION RANGE AS FRACTION OF SPECIFICATION RANGE, S: abscissa
A.I. DETECTION RANGE CONTOUR: Straight wing
ALTITUDE: 60K

S59

Missile launch zone L 13

189 spr

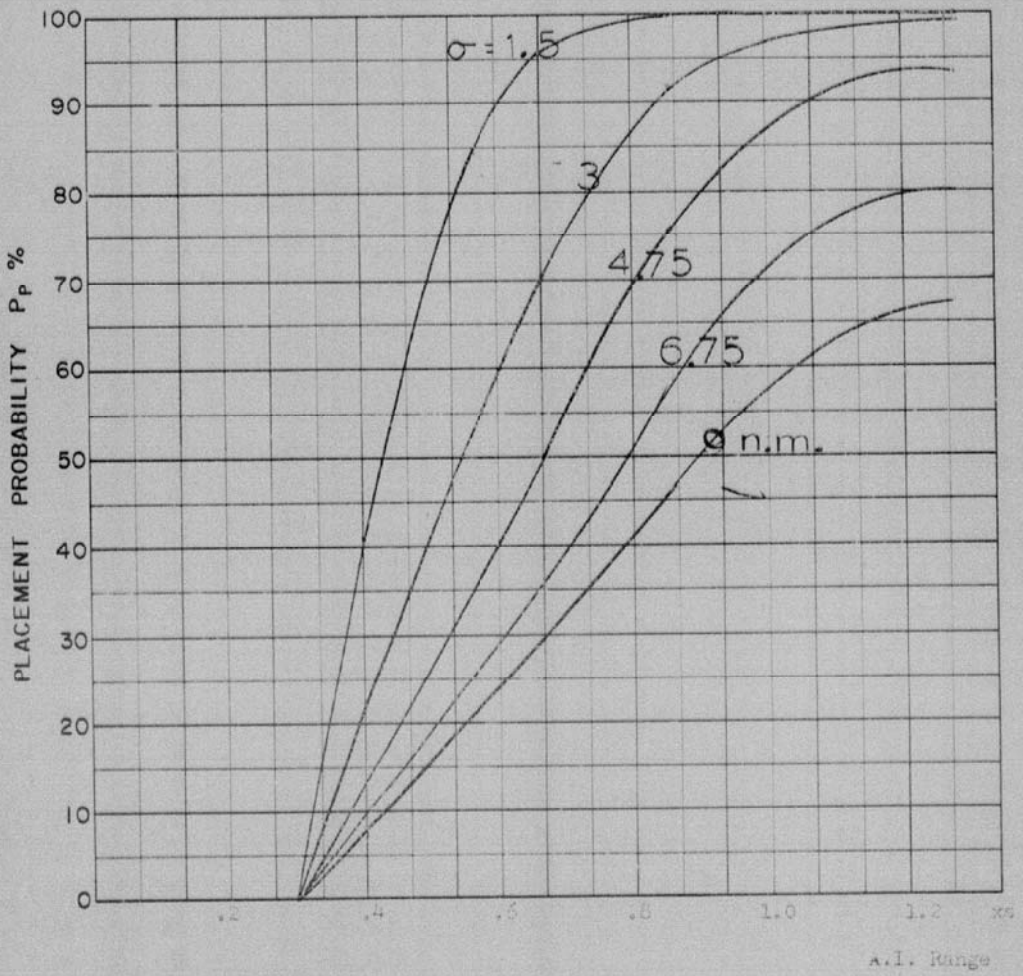

COURSE DIFFERENCE: 135°
TARGET EVASION: 0.15 literal g's
TARGET MACH NO.: 1.5
INTERCEPTOR LATERAL G's: 1.5
INTERCEPTOR MACH NO.: 1.5
σ OF G.C.I. ACCURACY: five values
A.I. DETECTION RANGE AS FRACTION OF SPECIFICATION RANGE, S: abscissa
A.I. DETECTION RANGE CONTOUR: Straight wing
ALTITUDE: 60K

S 60

Missile launch zone L 13

191 spr

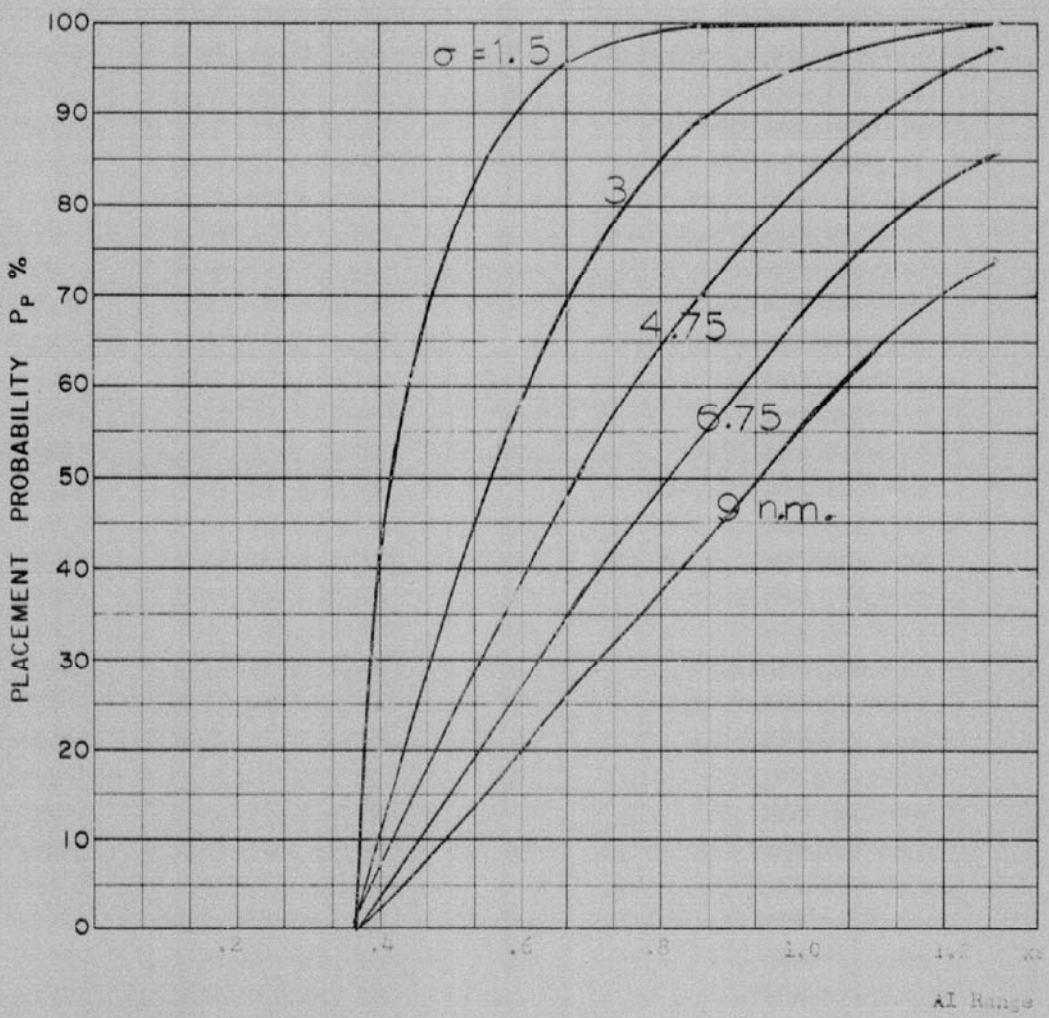

COURSE DIFFERENCE: 160°
TARGET EVASION: 0.15 lateral g's
TARGET MACH NO.: 1.5
INTERCEPTOR LATERAL G's: 1.5
INTERCEPTOR MACH NO.: 1.5
σ OF G.C.I. ACCURACY: five values
A.I. DETECTION RANGE AS FRACTION OF SPECIFICATION RANGE, S: abscissa
A.I. DETECTION RANGE CONTOUR: Straight wing
ALTITUDE: 60K

S 61

Missile launch zone L 13

193 spr

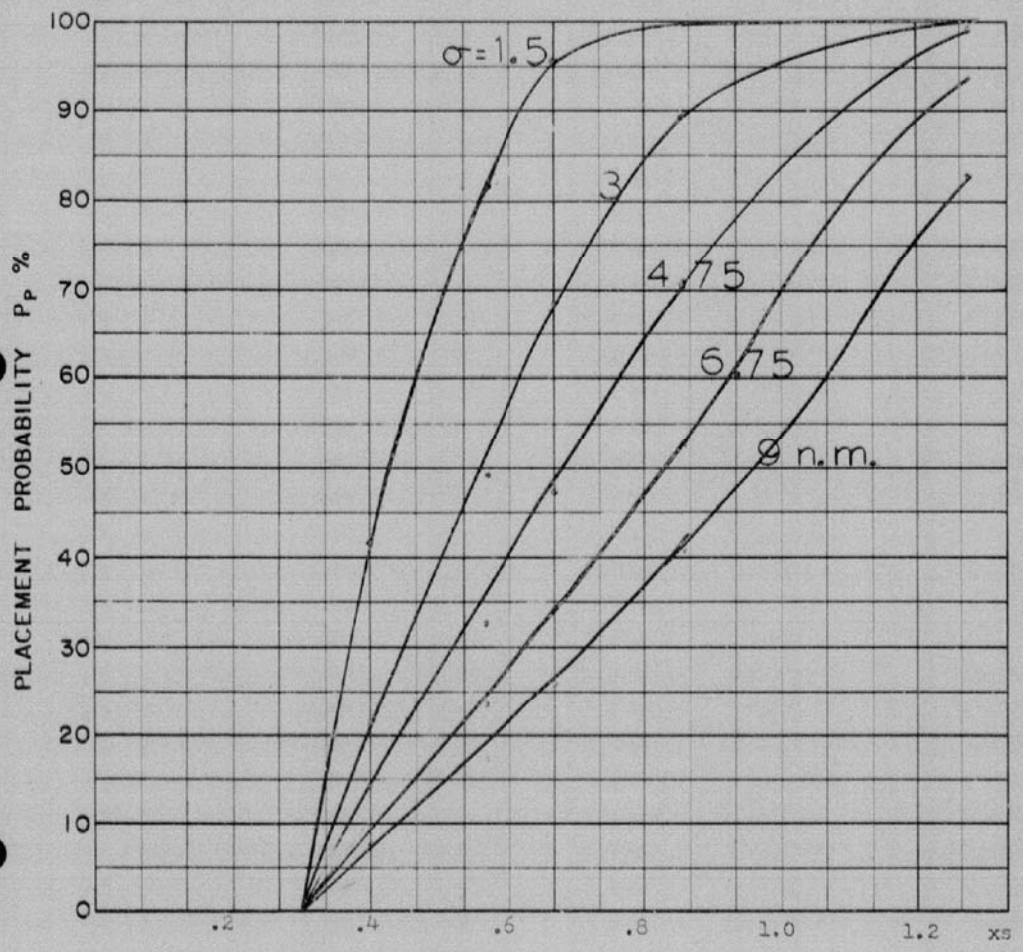

A.I. Range

S 62

COURSE DIFFERENCE: 180°
TARGET EVASION: 0.15 lateral g's
TARGET MACH NO.: 1.5
INTERCEPTOR LATERAL G's: 1.5
INTERCEPTOR MACH NO.: 1.5
σ OF G.C.I. ACCURACY: five values
A.I. DETECTION RANGE AS FRACTION OF SPECIFICATION RANGE, S: abscissa
A.I. DETECTION RANGE CONTOUR: Straight wing
ALTITUDE: 60K

Missile launch zone L 13

194 spr

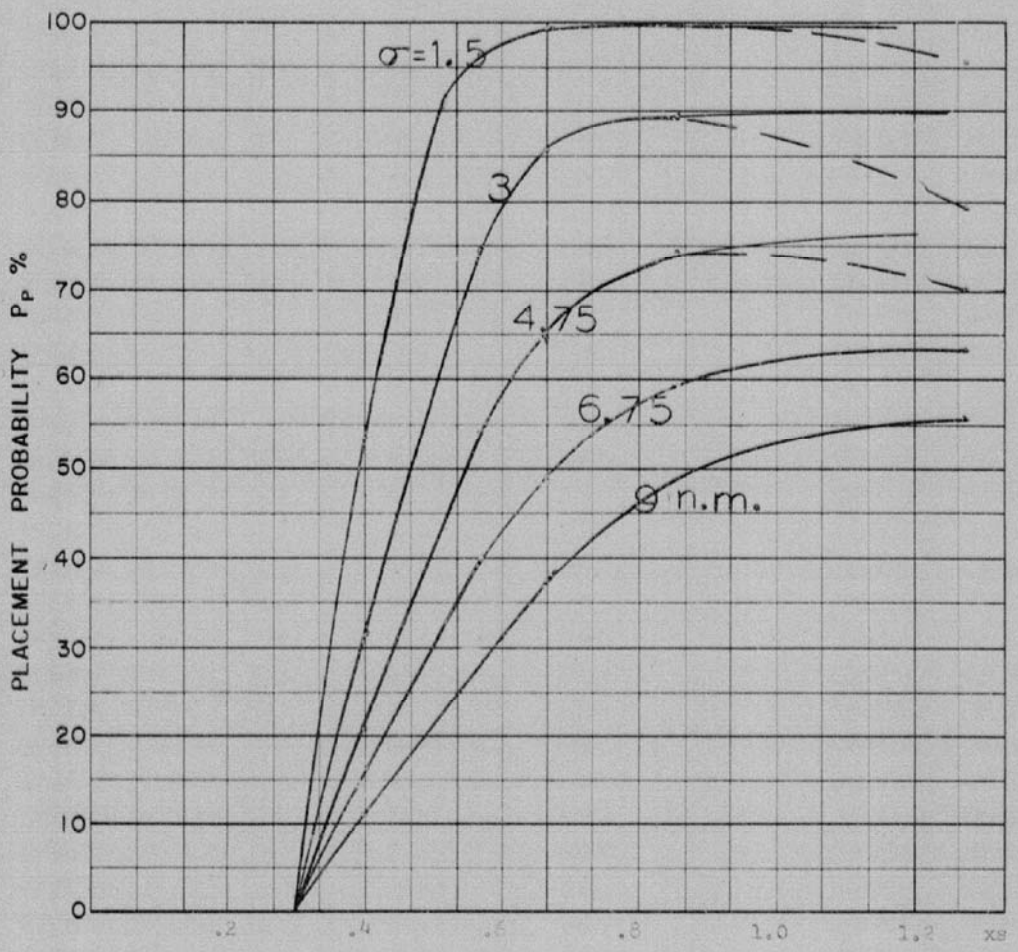

COURSE DIFFERENCE: 110°
TARGET EVASION: 0.15 lateral g's
TARGET MACH NO.: 1.5
INTERCEPTOR LATERAL G's: 2.4
INTERCEPTOR MACH NO.: 1.5
σ OF G.C.I. ACCURACY: five values
A.I. DETECTION RANGE AS FRACTION OF SPECIFICATION RANGE, S: abscissa
A.I. DETECTION RANGE CONTOUR: Straight wing
ALTITUDE: 60K

(S63)

Missile launch zone L 13

196 apr

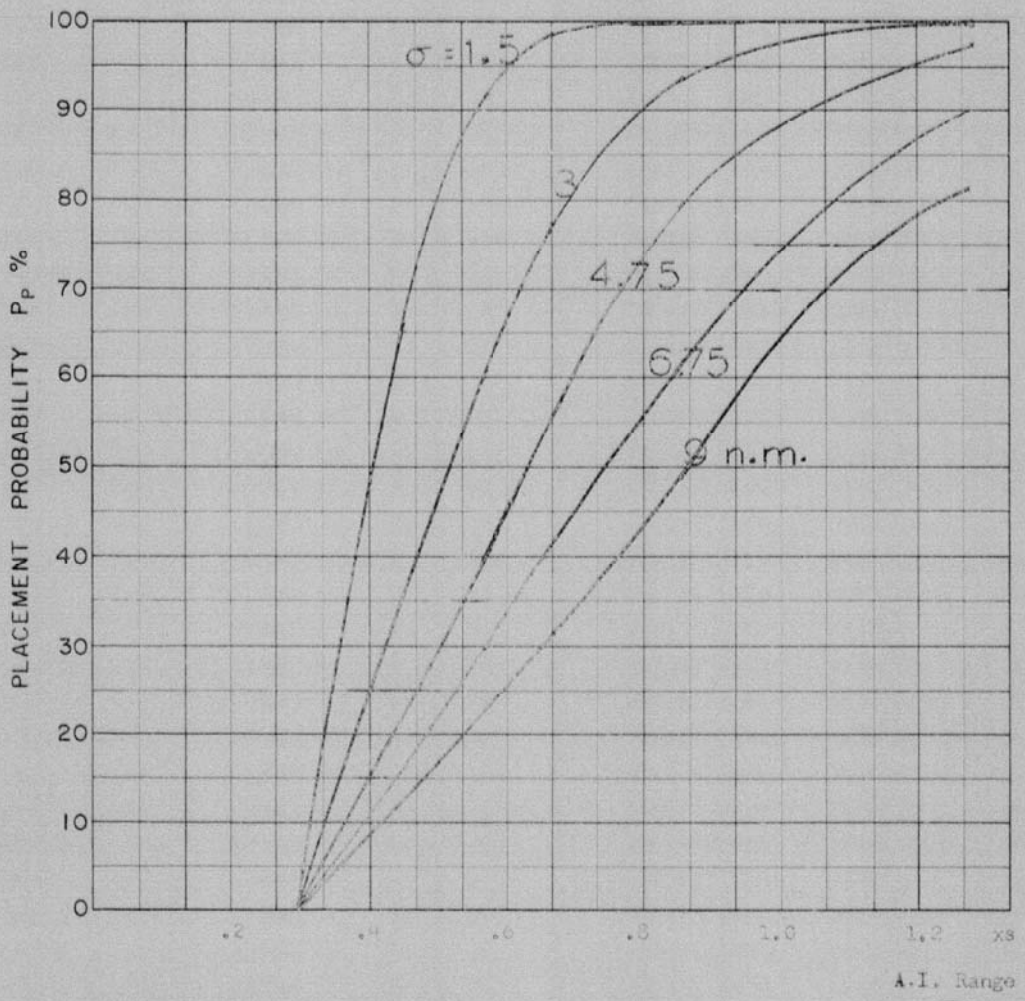

COURSE DIFFERENCE: 135°
TARGET EVASION: 0.15 lateral g's
TARGET MACH NO.: 1.5
INTERCEPTOR LATERAL G's: 2.4
INTERCEPTOR MACH NO.: 1.5
σ OF G.C.I. ACCURACY: five values
A.I. DETECTION RANGE AS FRACTION OF SPECIFICATION RANGE, S: abscissa
A.I. DETECTION RANGE CONTOUR: Straight wing
ALTITUDE: 60K

(564)

Missile launch area I 23

198 spr

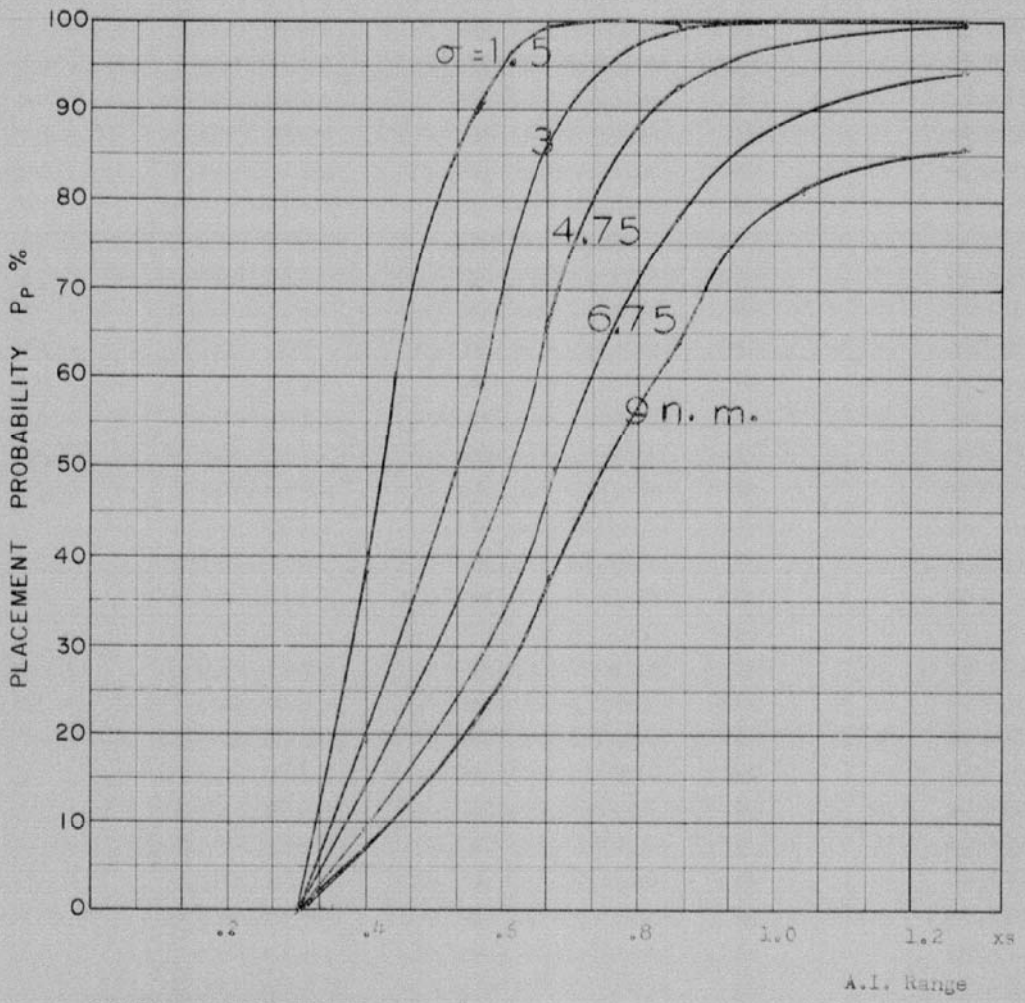

COURSE DIFFERENCE: 160°
TARGET EVASION: 0.15 lateral g's
TARGET MACH NO.: 1.2
INTERCEPTOR LATERAL G's: 2.4
INTERCEPTOR MACH NO.: 1.5
σ OF G.C.I. ACCURACY: five values
A.I. DETECTION RANGE AS FRACTION OF SPECIFICATION RANGE, S: abscissa
A.I. DETECTION RANGE CONTOUR: Straight wing
ALTITUDE: 60K

(565)

Missile launch zone L 13

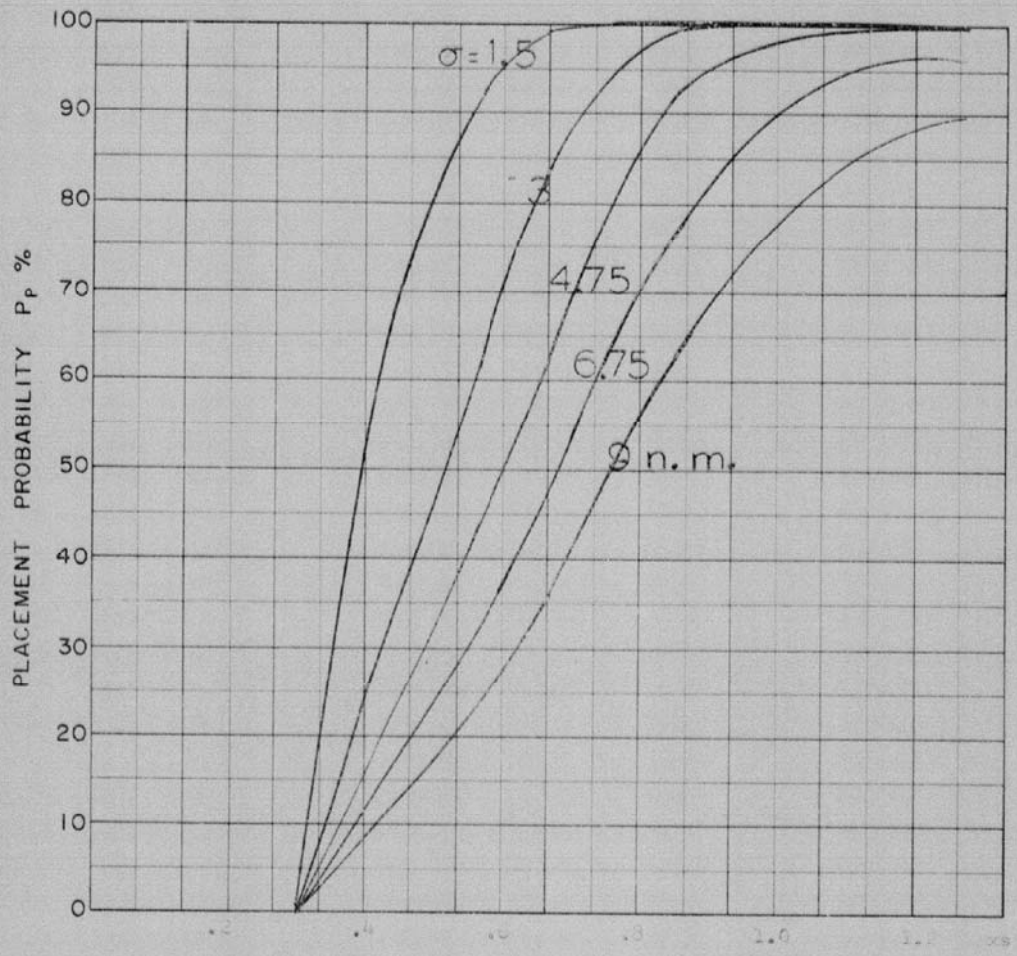

COURSE DIFFERENCE: 180°
TARGET EVASION: 0.15 lateral g's
TARGET MACH NO.: 1.5
INTERCEPTOR LATERAL G's: 2.4
INTERCEPTOR MACH NO.: 1.4
σ OF G.C.I. ACCURACY: five values
A.I. DETECTION RANGE AS FRACTION OF SPECIFICATION RANGE, S: alcofssa
A.I. DETECTION RANGE CONTOUR: Straight wing
ALTITUDE: 60K

Missile launch zone L 13

S66

29 aspr

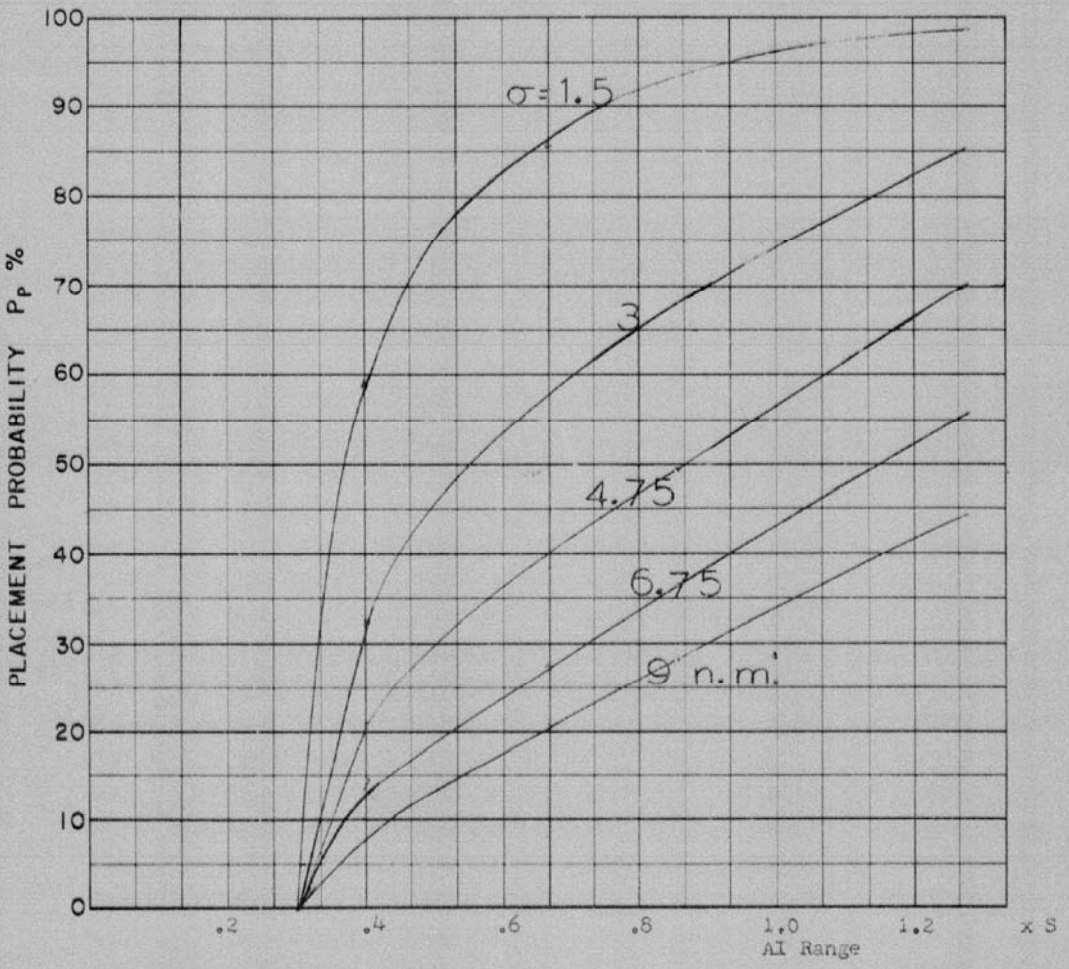

COURSE DIFFERENCE: 75°
TARGET EVASION: 0
TARGET MACH NO.: 2.0
INTERCEPTOR LATERAL G's: 0.85
INTERCEPTOR MACH NO.: 1.5
σ OF G.C.I. ACCURACY: 5 values
A.I. DETECTION RANGE AS FRACTION OF SPECIFICATION RANGE, S: Abscissa
A.I. DETECTION RANGE CONTOUR: Straight wing
ALTITUDE: 50 K

Missile launch zone L-3
Maximum range 10° heading error

567

29 bspr

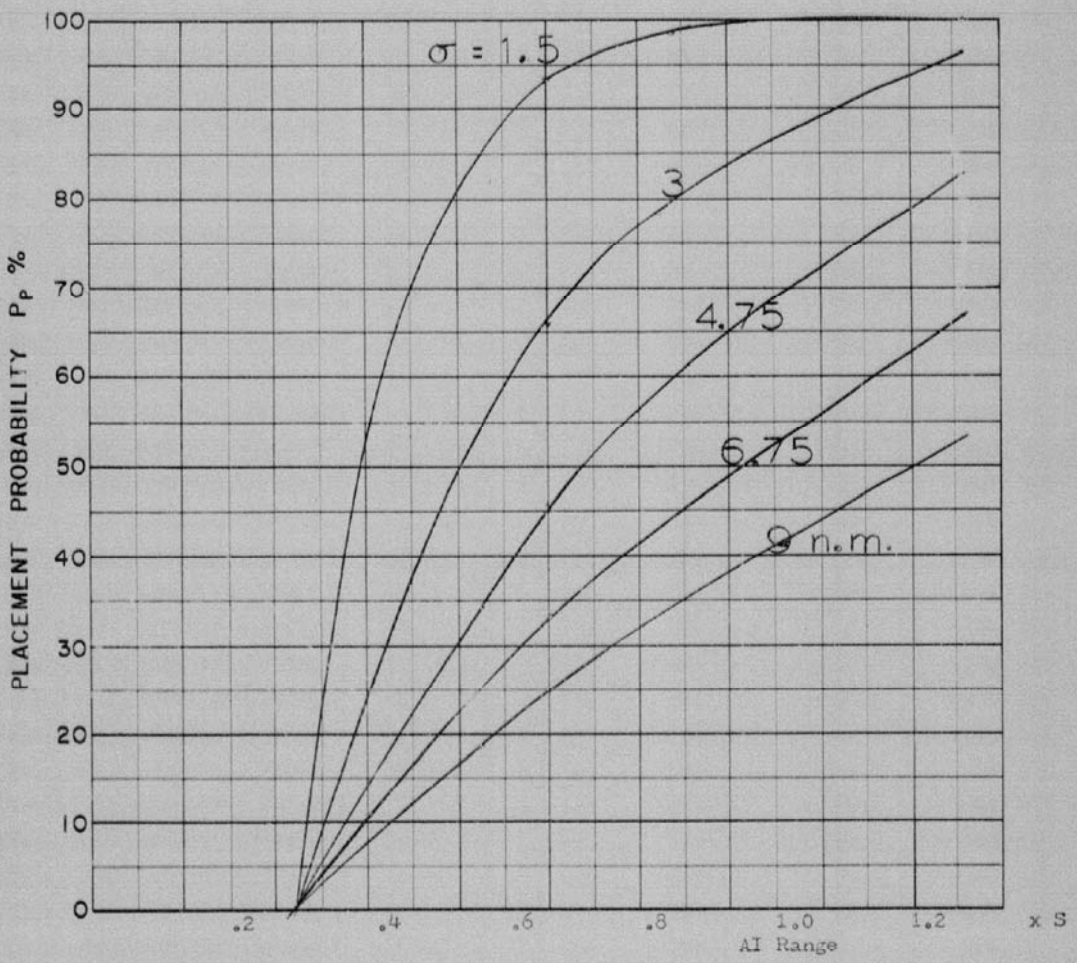

COURSE DIFFERENCE: 90°
TARGET EVASION: 0
TARGET MACH NO.: 2.0
INTERCEPTOR LATERAL G's: 0.85
INTERCEPTOR MACH NO.: 1.5
σ OF G.C.I. ACCURACY: 5 values
A.I. DETECTION RANGE AS FRACTION OF SPECIFICATION RANGE, S: Abscissa
A.I. DETECTION RANGE CONTOUR: Straight wing
ALTITUDE: 50 K

Missile launch zone L-3
Maximum range 10° heading error

(568a)

29 aspr

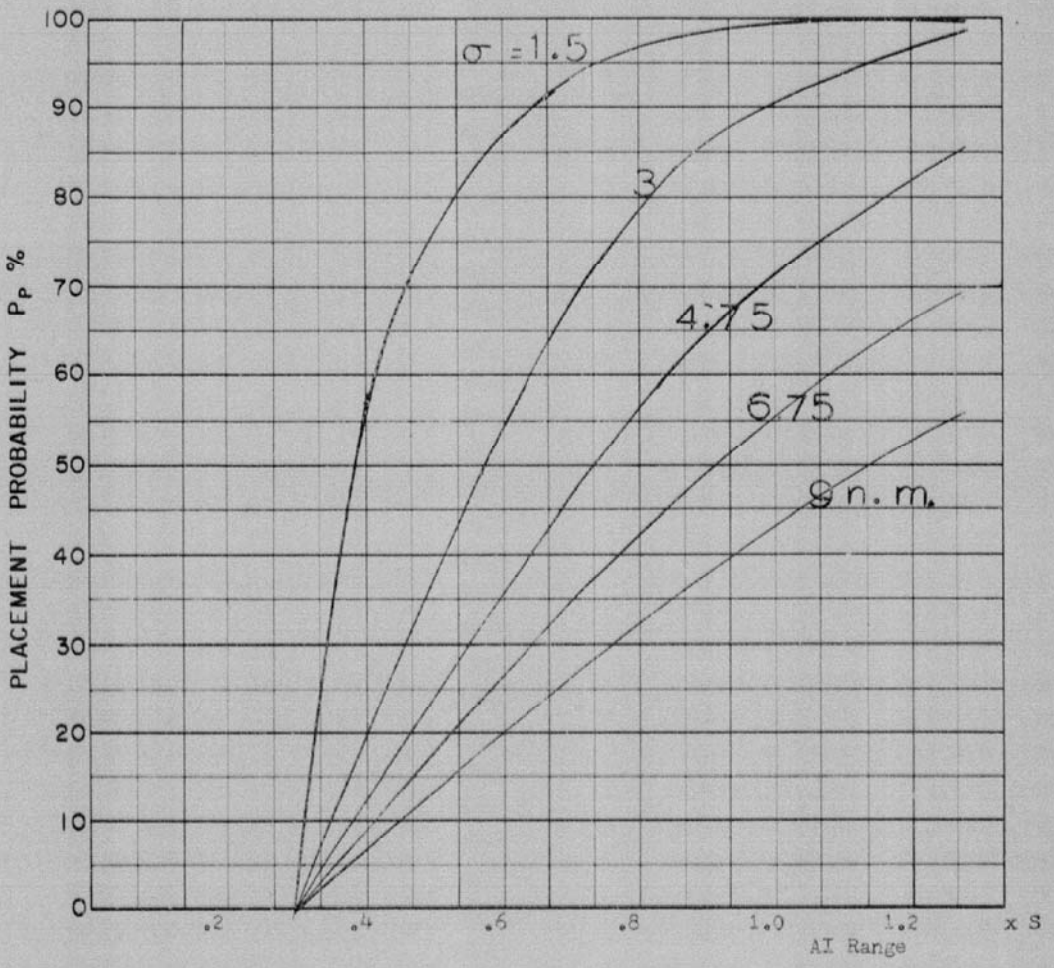

COURSE DIFFERENCE: 100°
TARGET EVASION: 0
TARGET MACH NO.: 2.0
INTERCEPTOR LATERAL G's: 0.85
INTERCEPTOR MACH NO.: 1.5
σ OF G.C.I. ACCURACY: 5 values
A.I. DETECTION RANGE AS FRACTION OF SPECIFICATION RANGE, S: Abscissa
A.I. DETECTION RANGE CONTOUR: Straight wing
ALTITUDE: 50 K

Missile launch zone L-3
Maximum range 10° heading error

(S69)

29 depr

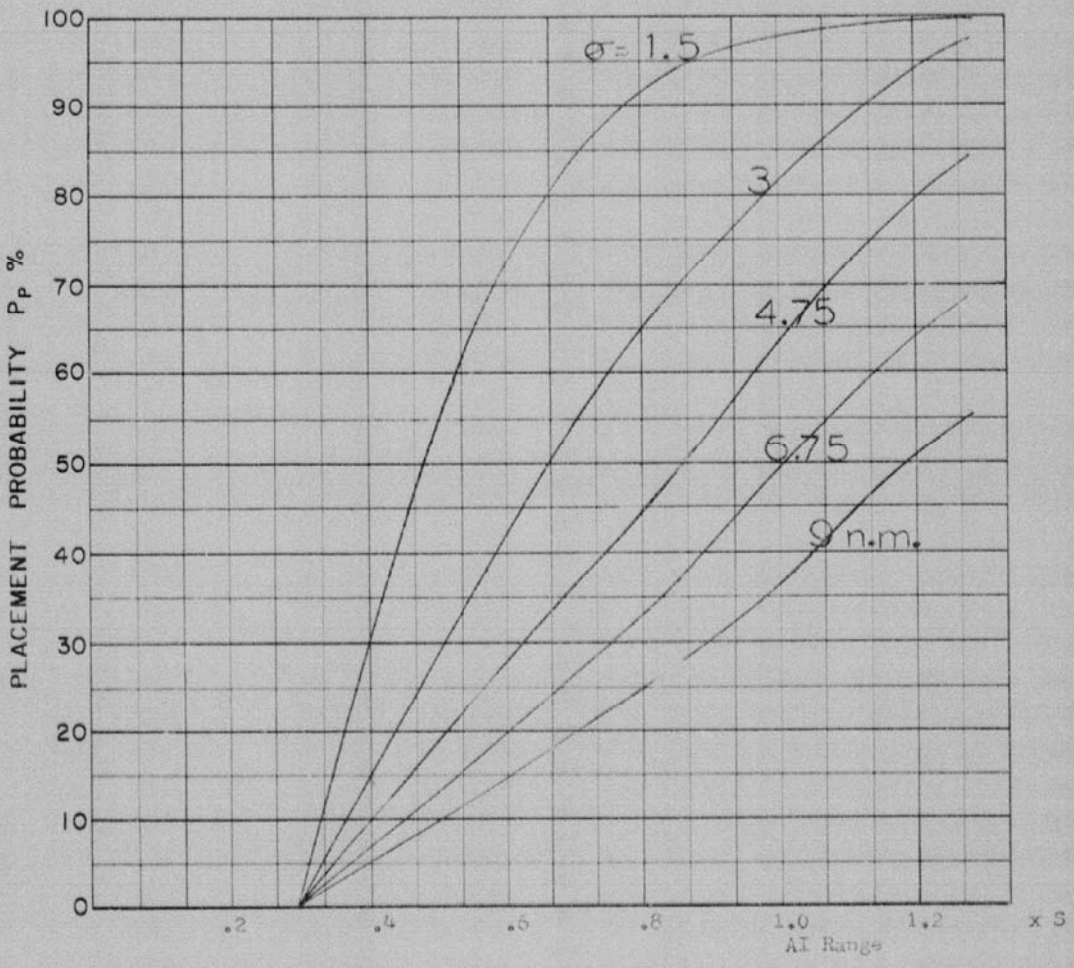

COURSE DIFFERENCE: 120°
TARGET EVASION: 0
TARGET MACH NO.: 2.0
INTERCEPTOR LATERAL G's: 0.85
INTERCEPTOR MACH NO.: 1.5
σ OF G.C.I. ACCURACY: Five values
A.I. DETECTION RANGE AS FRACTION OF SPECIFICATION RANGE, S Abscissa
A.I. DETECTION RANGE CONTOUR: Straight wing
ALTITUDE: 50 K

Missile launch zone L-3
Maximum range 10° heading error

S 70

29 espr

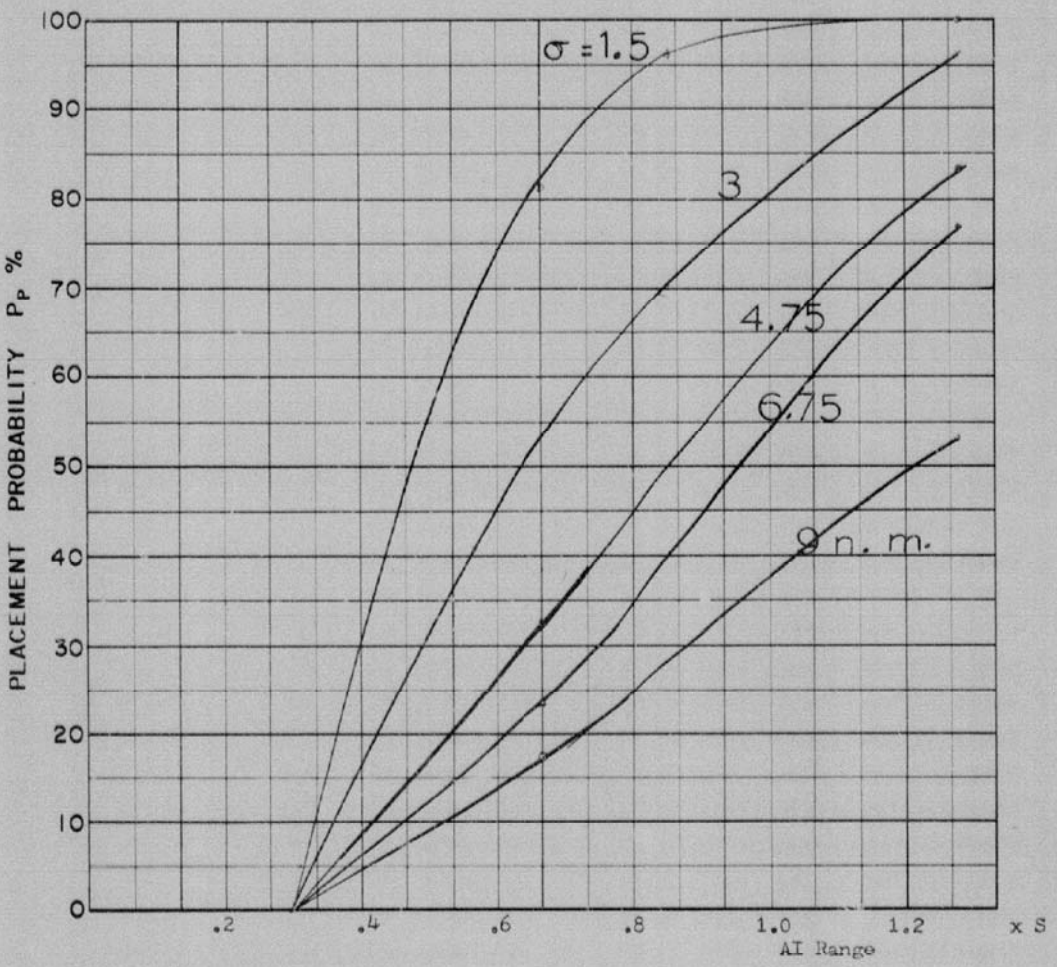

COURSE DIFFERENCE: 135°
TARGET EVASION: 0
TARGET MACH NO.: 2.0
INTERCEPTOR LATERAL G's: 0.85
INTERCEPTOR MACH NO.: 1.5
σ OF G.C.I. ACCURACY: Five values
A.I. DETECTION RANGE AS FRACTION OF SPECIFICATION RANGE, S: Abscissa
A.I. DETECTION RANGE CONTOUR: Straight wing
ALTITUDE: 50 K

Missile launch zone L-3
Maximum range 10° heading error

S71

29 fspr

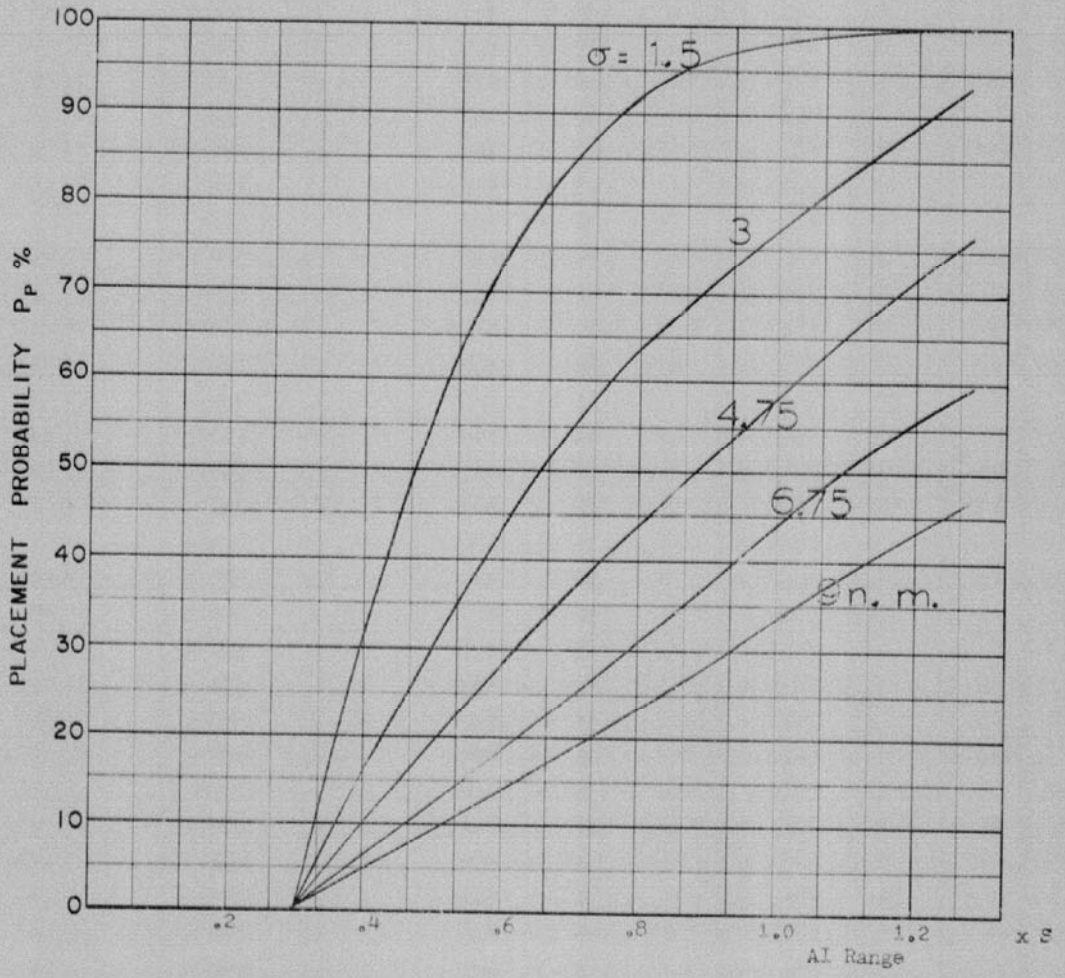

COURSE DIFFERENCE: 160°
TARGET EVASION: 0
TARGET MACH NO.: 2.0
INTERCEPTOR LATERAL G's: 0.85
INTERCEPTOR MACH NO.: 1.5
σ OF G.C.I. ACCURACY: Five values
A.I. DETECTION RANGE AS FRACTION OF SPECIFICATION RANGE, S: Abscissa
A.I. DETECTION RANGE CONTOUR: Straight wing
ALTITUDE: 50 K

S72

Missile launch zone L-3
Maximum range 10° heading error

27 aspr

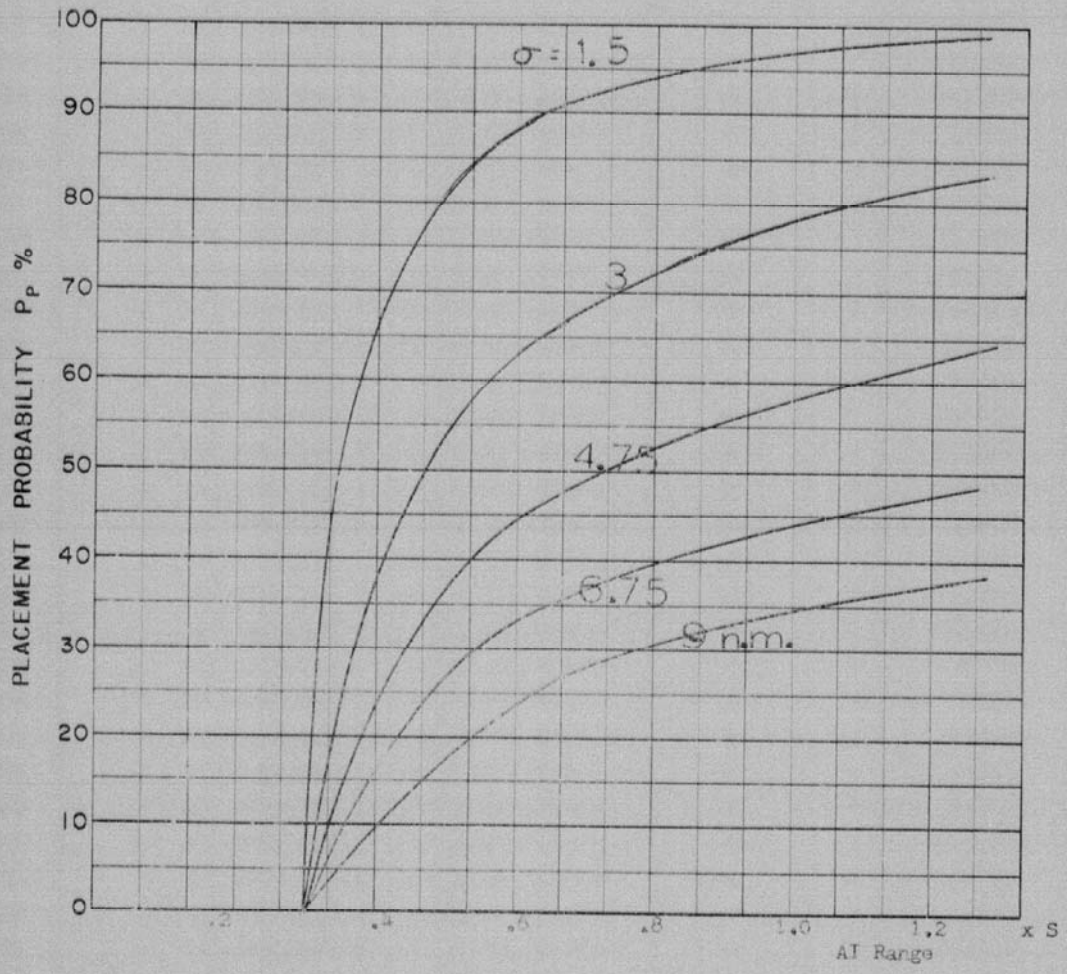

COURSE DIFFERENCE: 75°
TARGET EVASION: 0
TARGET MACH NO.: 2.0
INTERCEPTOR LATERAL G's: 1.6
INTERCEPTOR MACH NO.: 1.5
σ OF G.C.I. ACCURACY: Five values
A.I. DETECTION RANGE AS FRACTION OF SPECIFICATION RANGE, S: Abscissa
A.I. DETECTION RANGE CONTOUR: Straight Wing
ALTITUDE: 50 K

Missile launch zone L-3
Maximum range 10° heading error

S73

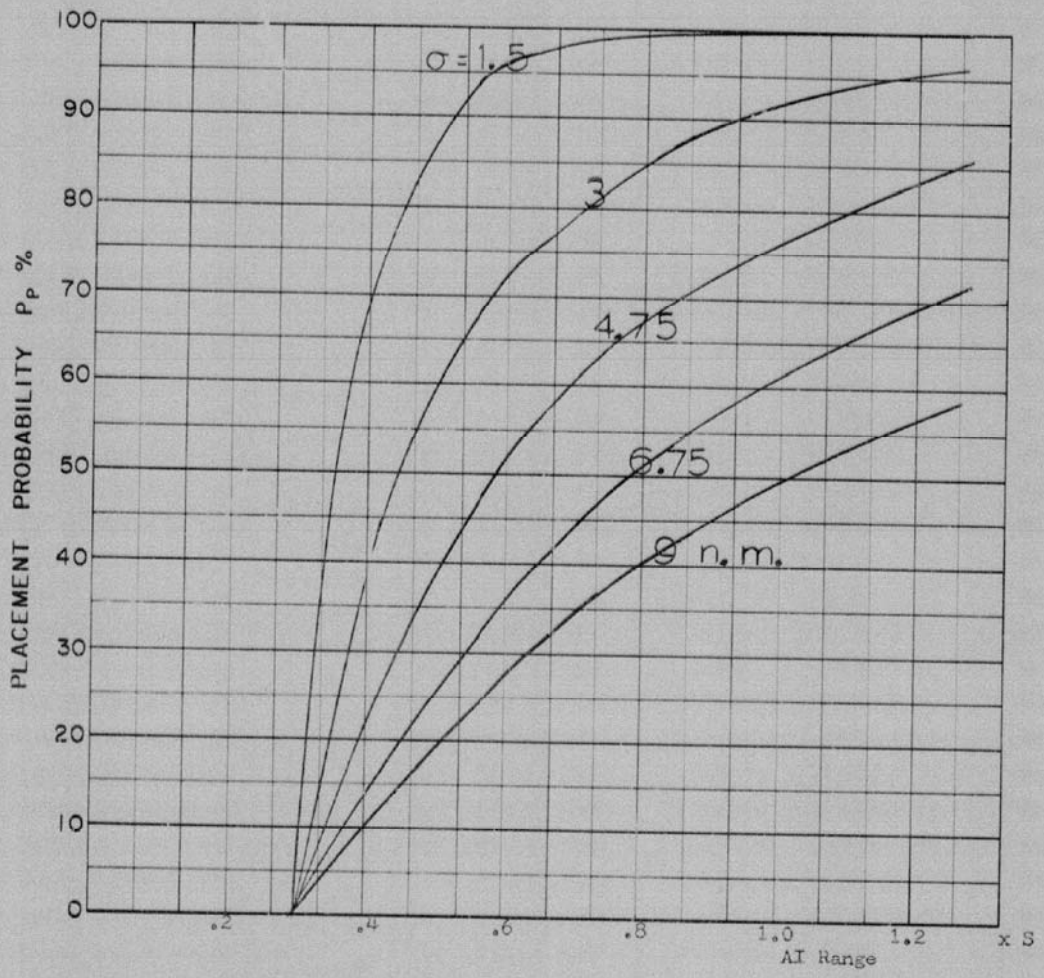

COURSE DIFFERENCE: 90°
TARGET EVASION: 0
TARGET MACH NO.: 2.0
INTERCEPTOR LATERAL G's: 1.6
INTERCEPTOR MACH NO.: 1.5
σ OF G.C.I. ACCURACY: 5 values
A.I. DETECTION RANGE AS FRACTION OF SPECIFICATION RANGE, S: Abscissa
A.I. DETECTION RANGE CONTOUR: Straight Wing
ALTITUDE: 50 K

S74a

Missile launch zone L-3
Maximum range 10° heading error

27 cspr

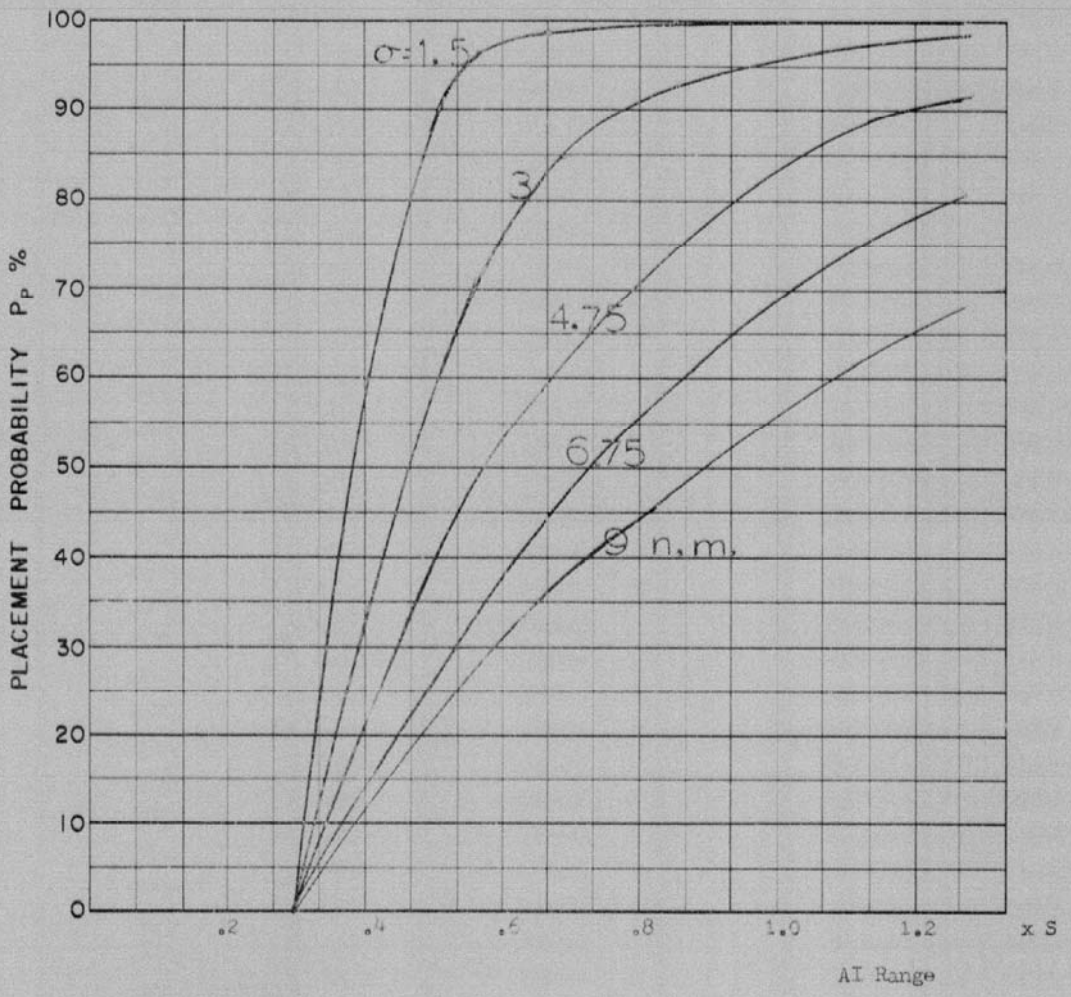

S75

COURSE DIFFERENCE: 100°
TARGET EVASION: 0
TARGET MACH NO.: 2.0
INTERCEPTOR LATERAL G's: 1.6
INTERCEPTOR MACH NO.: 1.5
σ OF G.C.I. ACCURACY: Five values
A.I. DETECTION RANGE AS FRACTION OF SPECIFICATION RANGE, S: Abscissa
A.I. DETECTION RANGE CONTOUR: Straight Wing
ALTITUDE: 50 K

Missile launch zone L-3
Maximum range 10° heading error

27 dspr

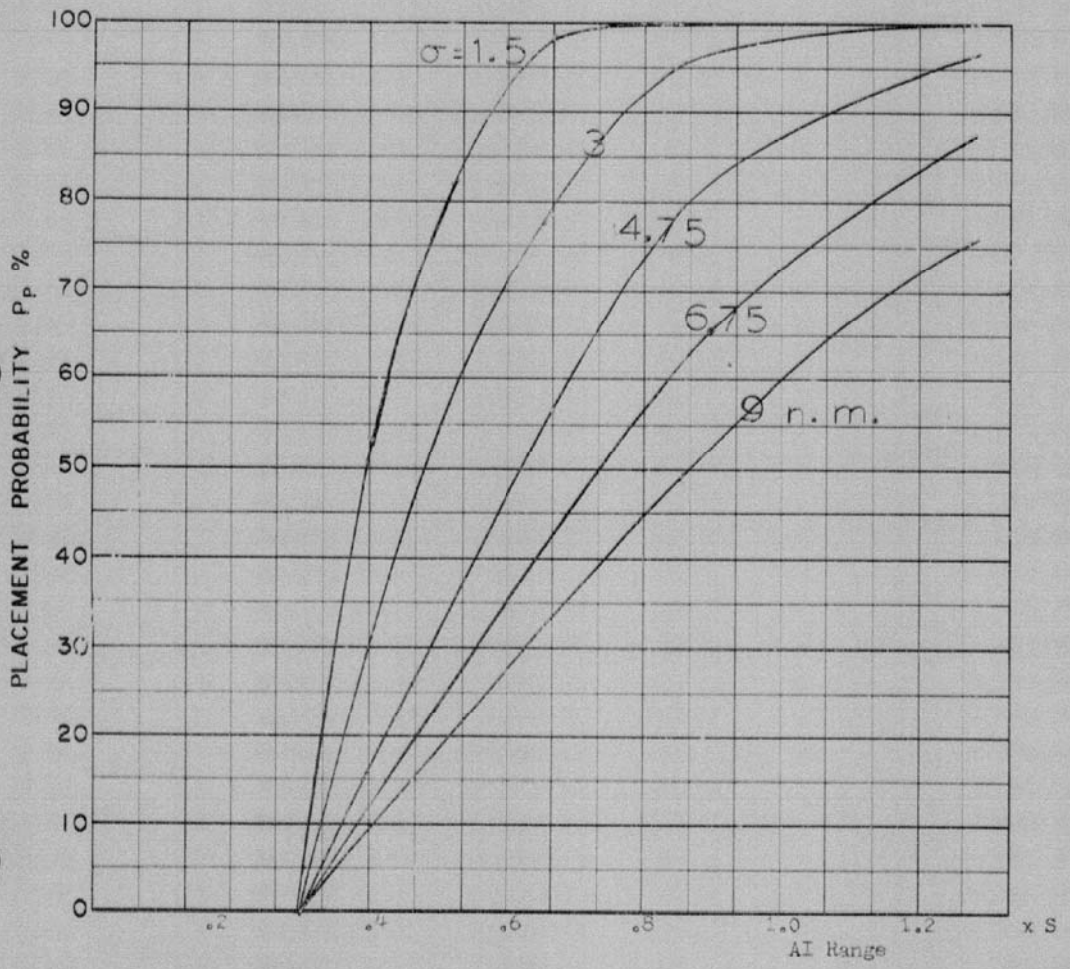

COURSE DIFFERENCE: 120°
TARGET EVASION: 0
TARGET MACH NO.: 2.0
INTERCEPTOR LATERAL G's: 1.6
INTERCEPTOR MACH NO.: 1.5
σ OF G.C.I. ACCURACY: 5 values
A.I. DETECTION RANGE AS FRACTION OF SPECIFICATION RANGE, S: Abscissa
A.I. DETECTION RANGE CONTOUR: Straight wing
ALTITUDE: 50 K

Missile launch zone L-3
Maximum range 10° heading error

S76a

27 espr

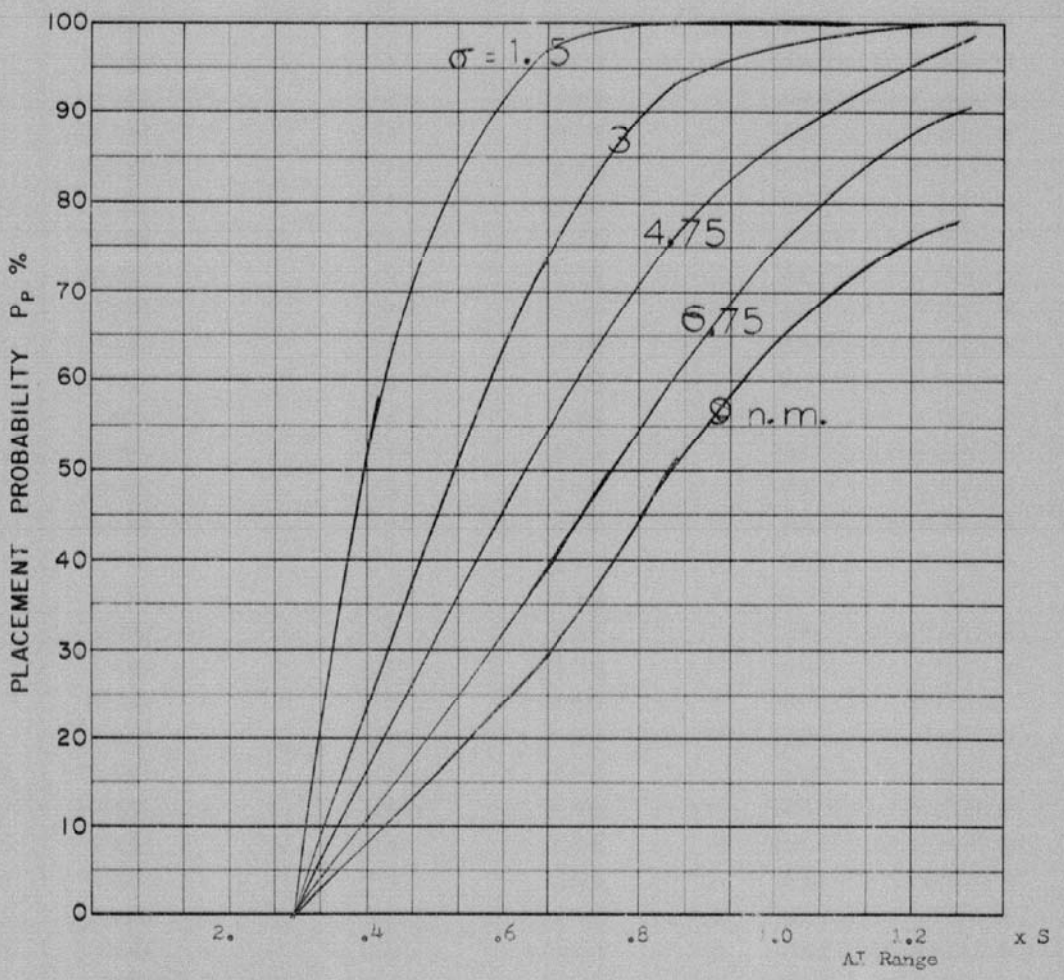

COURSE DIFFERENCE: 135°
TARGET EVASION: 0
TARGET MACH NO.: 2.0
INTERCEPTOR LATERAL G's: 1.6
INTERCEPTOR MACH NO.: 1.5
σ OF G.C.I. ACCURACY: Five values
A.I. DETECTION RANGE AS FRACTION OF SPECIFICATION RANGE, S Abscissa
A.I. DETECTION RANGE CONTOUR: Straight wing
ALTITUDE: 50 K

S77

Missile launch zone L-3
Maximum range 10° heading error

27 fspr

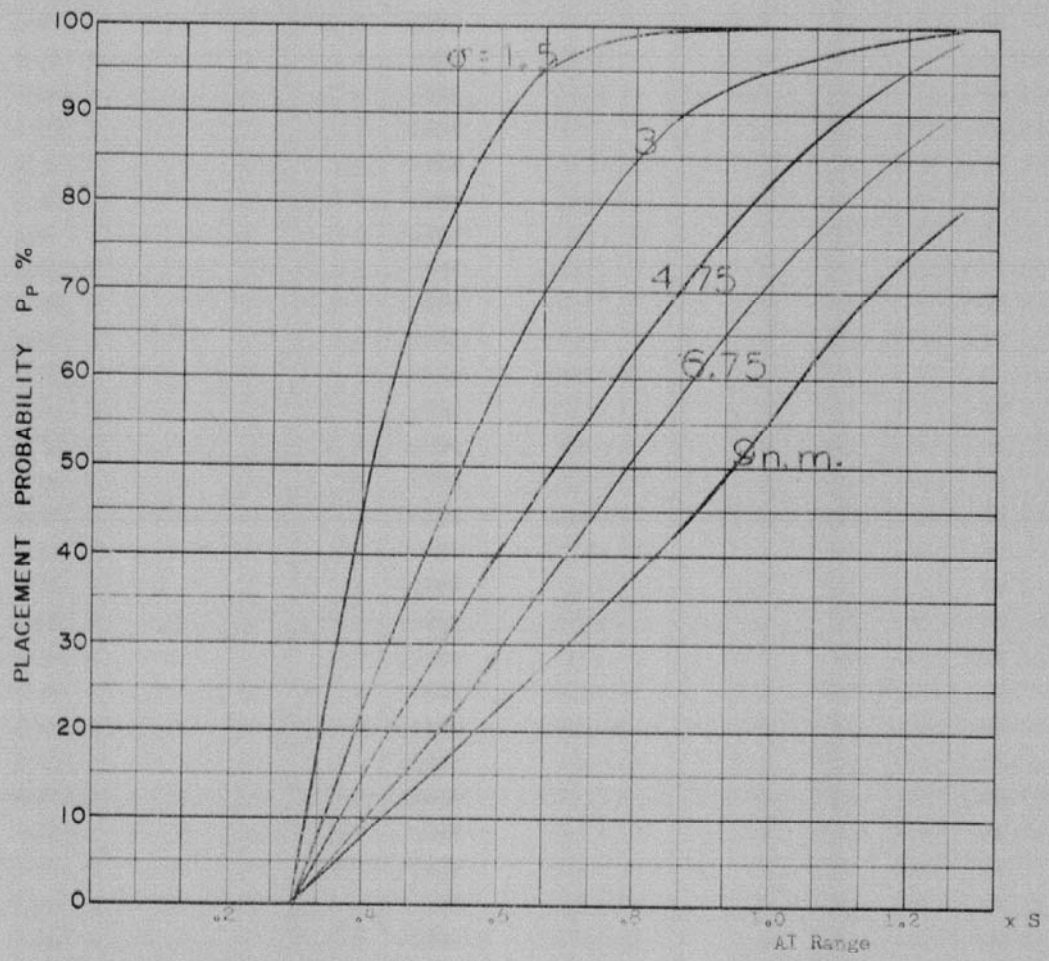

COURSE DIFFERENCE: 160
TARGET EVASION: 0
TARGET MACH NO.: 2.0
INTERCEPTOR LATERAL G's: 1.6
INTERCEPTOR MACH NO.: 1.5
σ OF G.C.I. ACCURACY: 5 values
A.I. DETECTION RANGE AS FRACTION OF SPECIFICATION RANGE, S: Abscissa
A.I. DETECTION RANGE CONTOUR: Straight wing
ALTITUDE: 50 K

Missile launch zone L-3
Maximum range 10° heading error

578

25 aspr

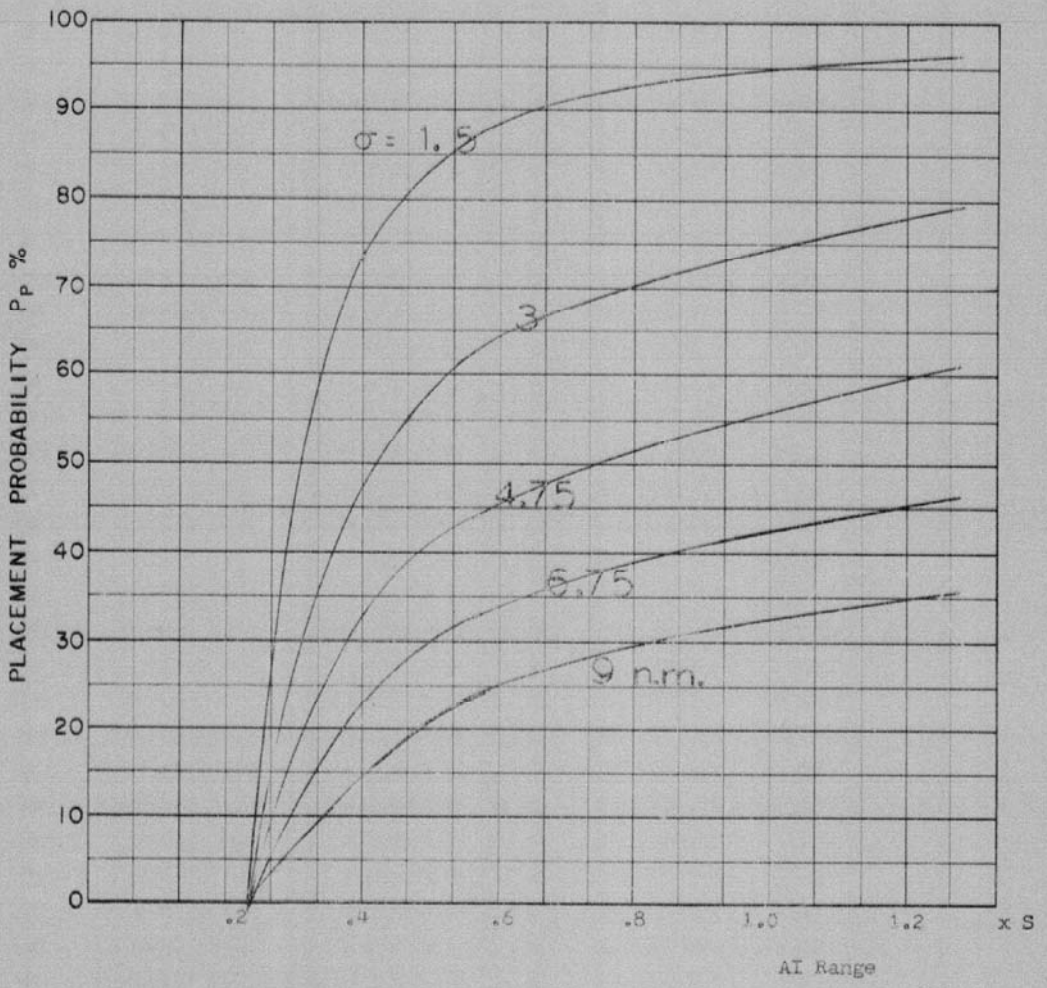

COURSE DIFFERENCE: 75°
TARGET EVASION: 0
TARGET MACH NO.: 2.0
INTERCEPTOR LATERAL G's: 3.0
INTERCEPTOR MACH NO.: 1.5
σ OF G.C.I. ACCURACY: 5 values
A.I. DETECTION RANGE AS FRACTION OF SPECIFICATION RANGE, S: Abscissa
A.I. DETECTION RANGE CONTOUR: Straight Wing
ALTITUDE: 50 K

S80a

Missile Launch Zone L-3
Maximum range, 10° heading error

25 bspr

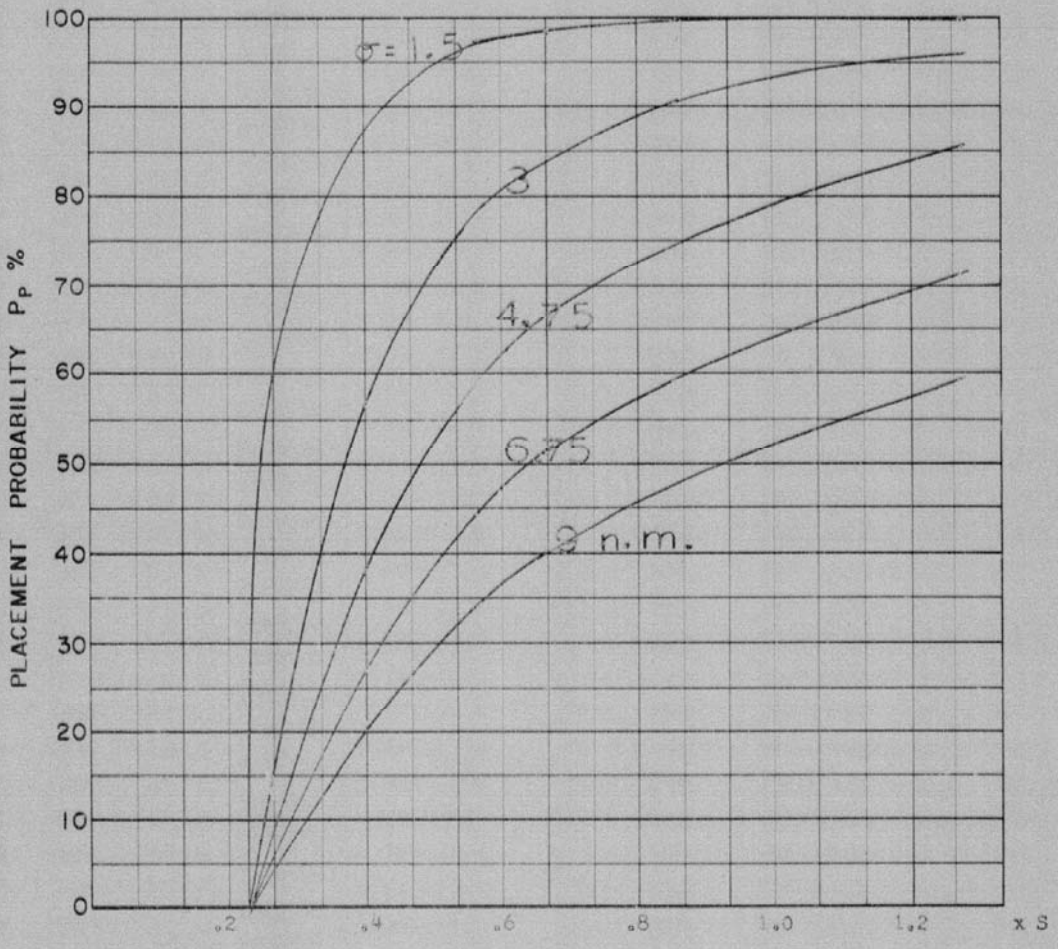

COURSE DIFFERENCE: 90°
TARGET EVASION: 0
TARGET MACH NO.: 2.0
INTERCEPTOR LATERAL G's: 3.0
INTERCEPTOR MACH NO.: 1.5
σ OF G.C.I. ACCURACY: 5 values
A.I. DETECTION RANGE AS FRACTION OF SPECIFICATION RANGE, S: Abscissa
A.I. DETECTION RANGE CONTOUR: Straight Wing
ALTITUDE: 50 K

Missile launch zone L-3
Maximum range, 10° heading error

S806

25 cspr

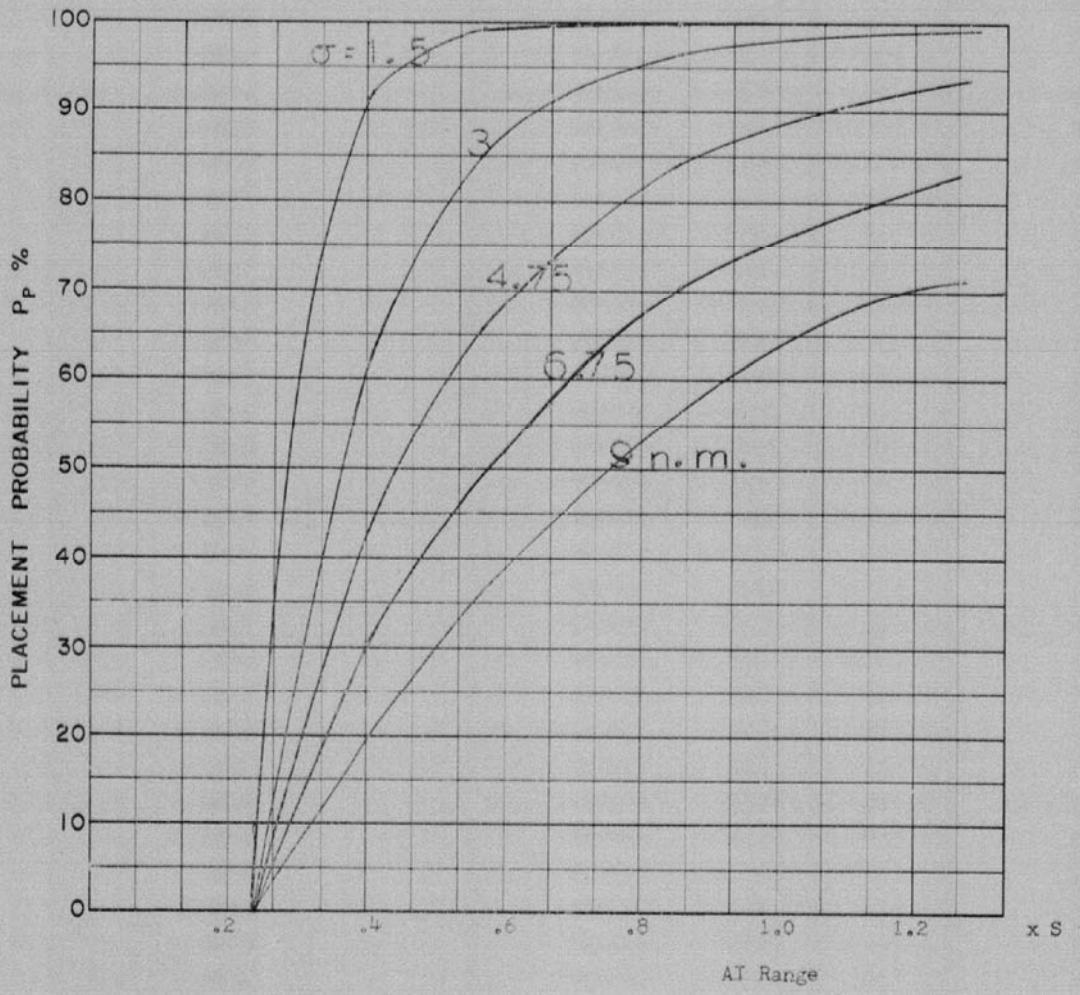

COURSE DIFFERENCE: 100°
TARGET EVASION: 0
TARGET MACH NO.: 2.0
INTERCEPTOR LATERAL G's: 3.0
INTERCEPTOR MACH NO.: 1.5
σ OF G.C.I. ACCURACY: 5 values
A.I. DETECTION RANGE AS FRACTION OF SPECIFICATION RANGE, S: Abscissa
A.I. DETECTION RANGE CONTOUR: Straight Wing
ALTITUDE: 50 K

Missile launch zone L-3
Maximum range 10° heading error

(581)

25 dapr

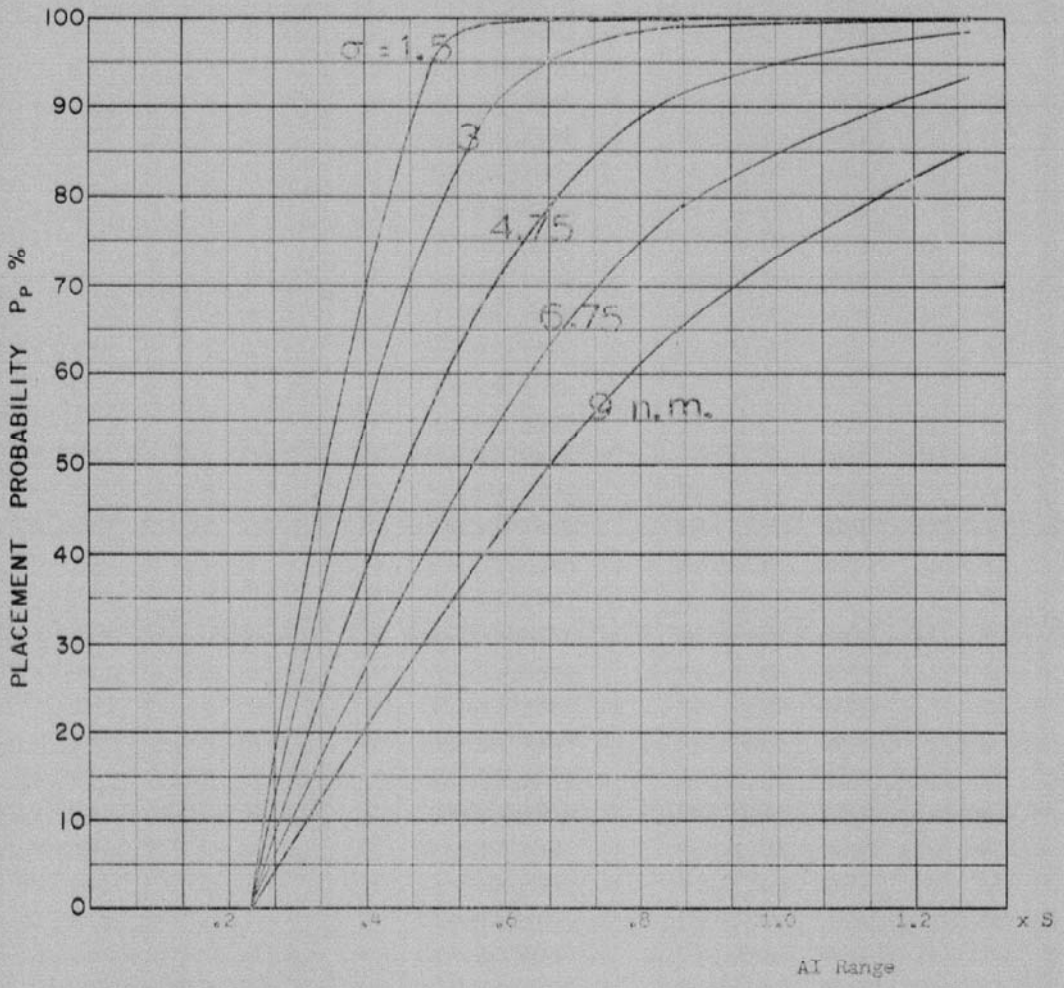

COURSE DIFFERENCE: 120°
TARGET EVASION: 0
TARGET MACH NO.: 2.0
INTERCEPTOR LATERAL G's: 3.0
INTERCEPTOR MACH NO.: .85
σ OF G.C.I. ACCURACY: Five values
A.I. DETECTION RANGE AS FRACTION OF SPECIFICATION RANGE, S: Abscissa
A.I. DETECTION RANGE CONTOUR: Straight Wing
ALTITUDE: 50 K

Missile launch zone L-3
Maximum range 10° heading error

582

25 espr

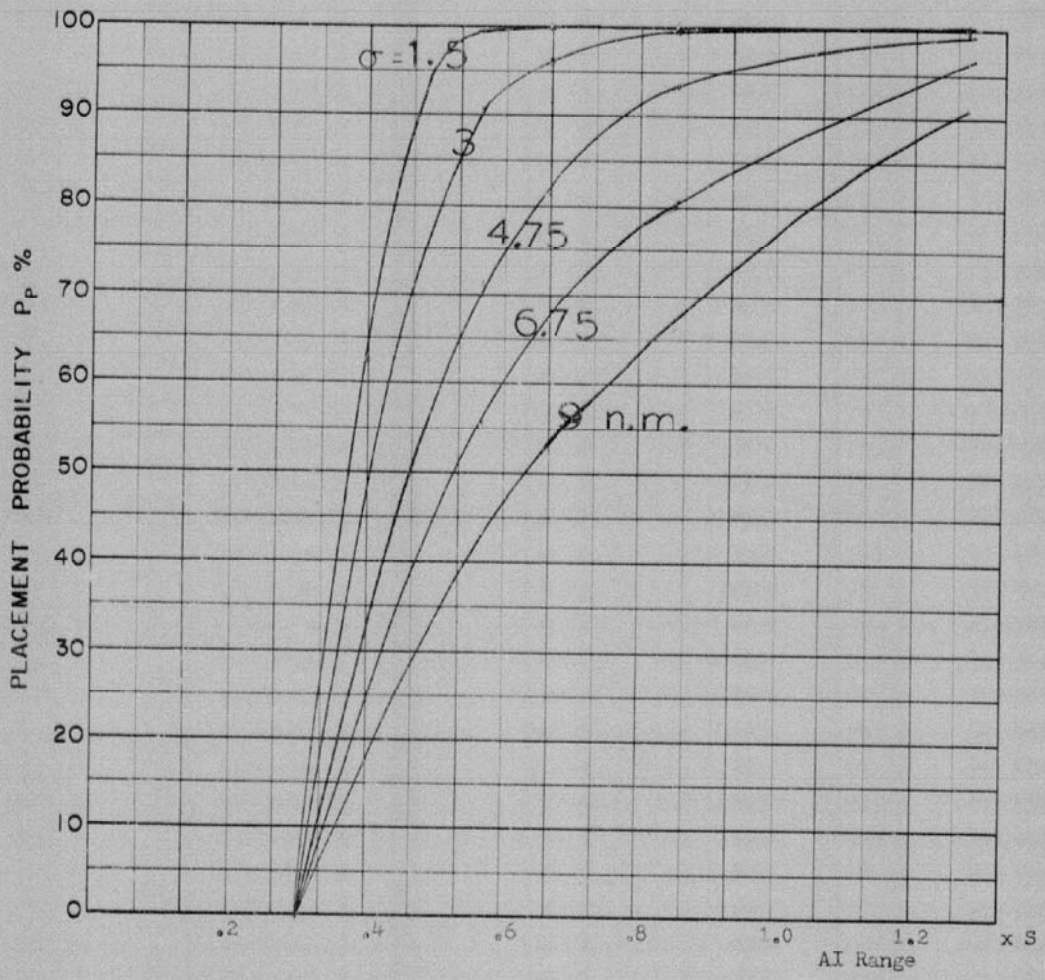

COURSE DIFFERENCE: 135°
TARGET EVASION: 0
TARGET MACH NO.: 2.0
INTERCEPTOR LATERAL G's: 3.0
INTERCEPTOR MACH NO.: 1.6
σ OF G.C.I. ACCURACY: 5 values
A.I. DETECTION RANGE AS FRACTION OF SPECIFICATION RANGE, S: Abscissa
A.I. DETECTION RANGE CONTOUR: Straight Wing
ALTITUDE: 50 K

Missile launch zone L-3
Maximum range 10° heading error

S83

25 fspr

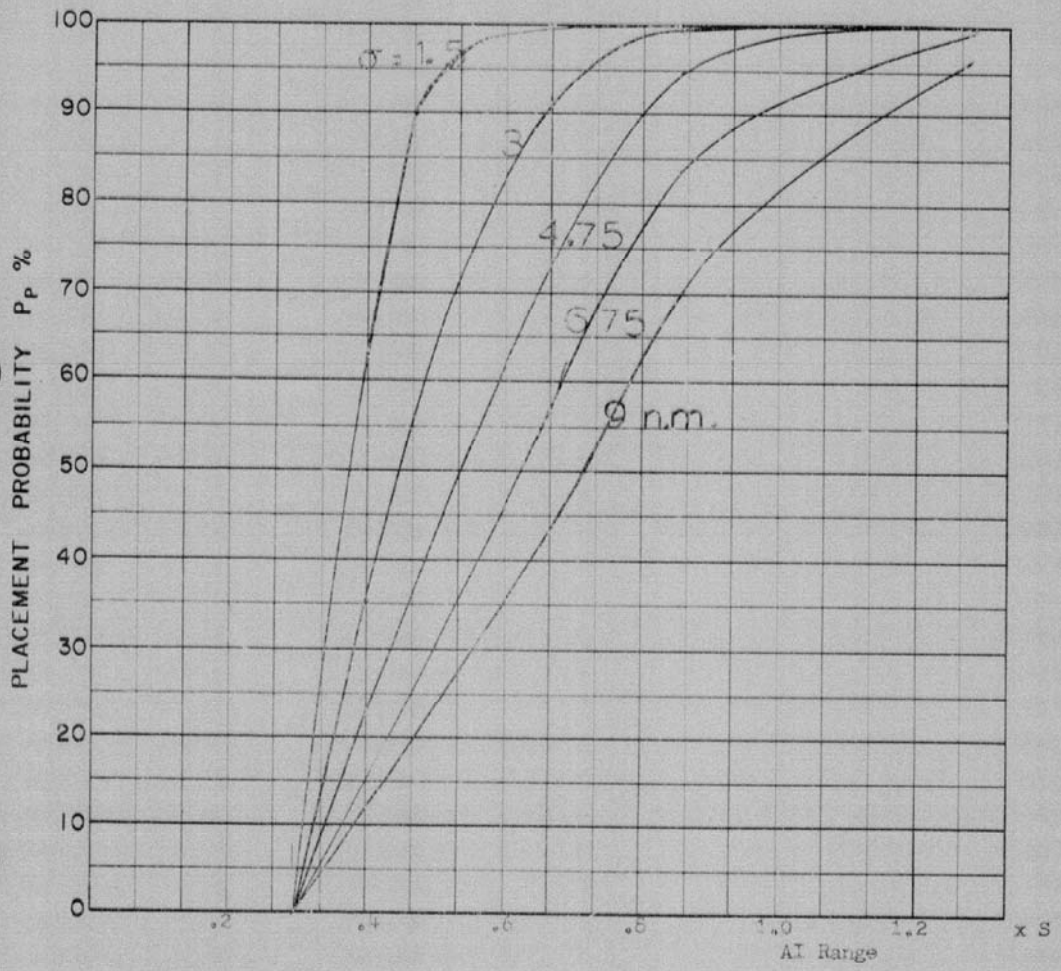

COURSE DIFFERENCE: 160°
TARGET EVASION: 0
TARGET MACH NO.: 2.0
INTERCEPTOR LATERAL G's: 3.0
INTERCEPTOR MACH NO.: 1.5
σ OF G.C.I. ACCURACY: 5 values
A.I. DETECTION RANGE AS FRACTION OF SPECIFICATION RANGE, S Abscissa
A.I. DETECTION RANGE CONTOUR: Straight Wing
ALTITUDE: 50 K

S84

Missile launch zone L-3
Maximum range 10° heading error

110 spr

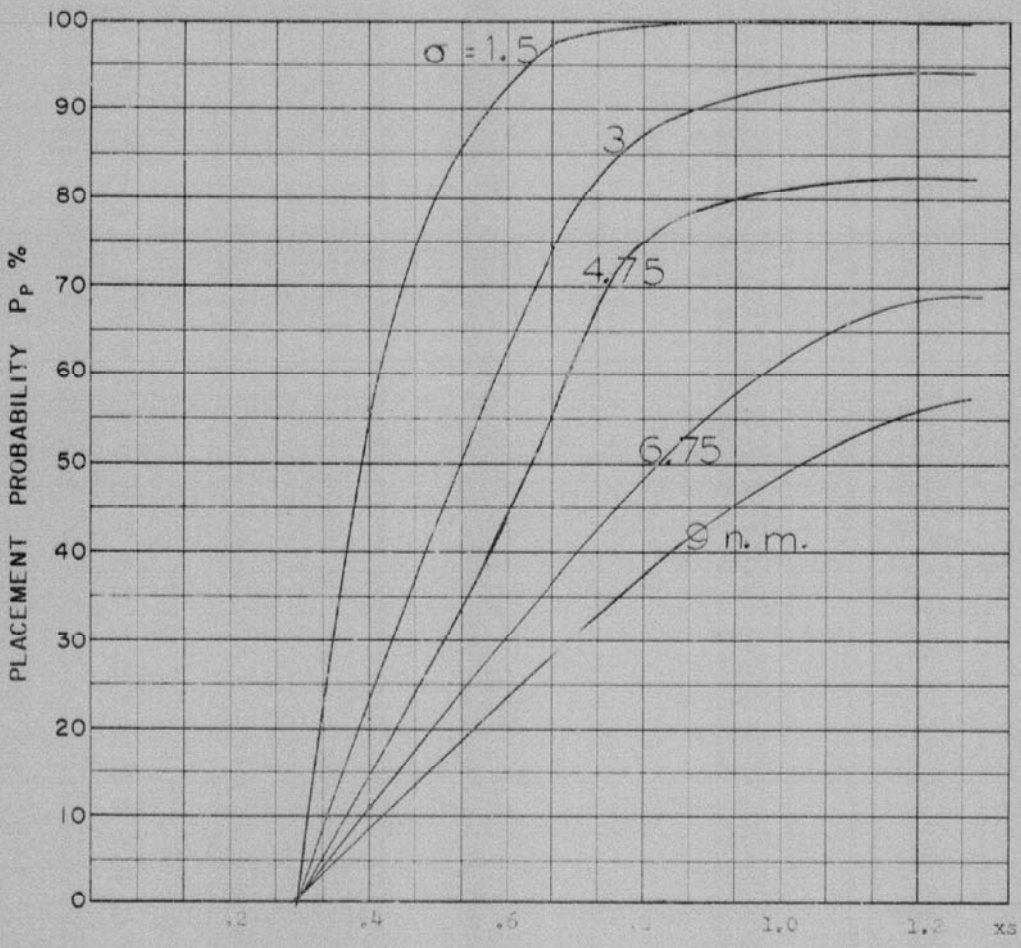

COURSE DIFFERENCE: 110°
TARGET EVASION: 0.1 lateral g's
TARGET MACH NO.: 2.0
INTERCEPTOR LATERAL G's: 1.6
INTERCEPTOR MACH NO.: 1.5
σ OF G.C.I. ACCURACY: five values
A.I. DETECTION RANGE AS FRACTION OF SPECIFICATION RANGE, S: abscissa
A.I. DETECTION RANGE CONTCUR: Straight wing
ALTITUDE: 50K

S91a

Launch zone L 10

103 asp

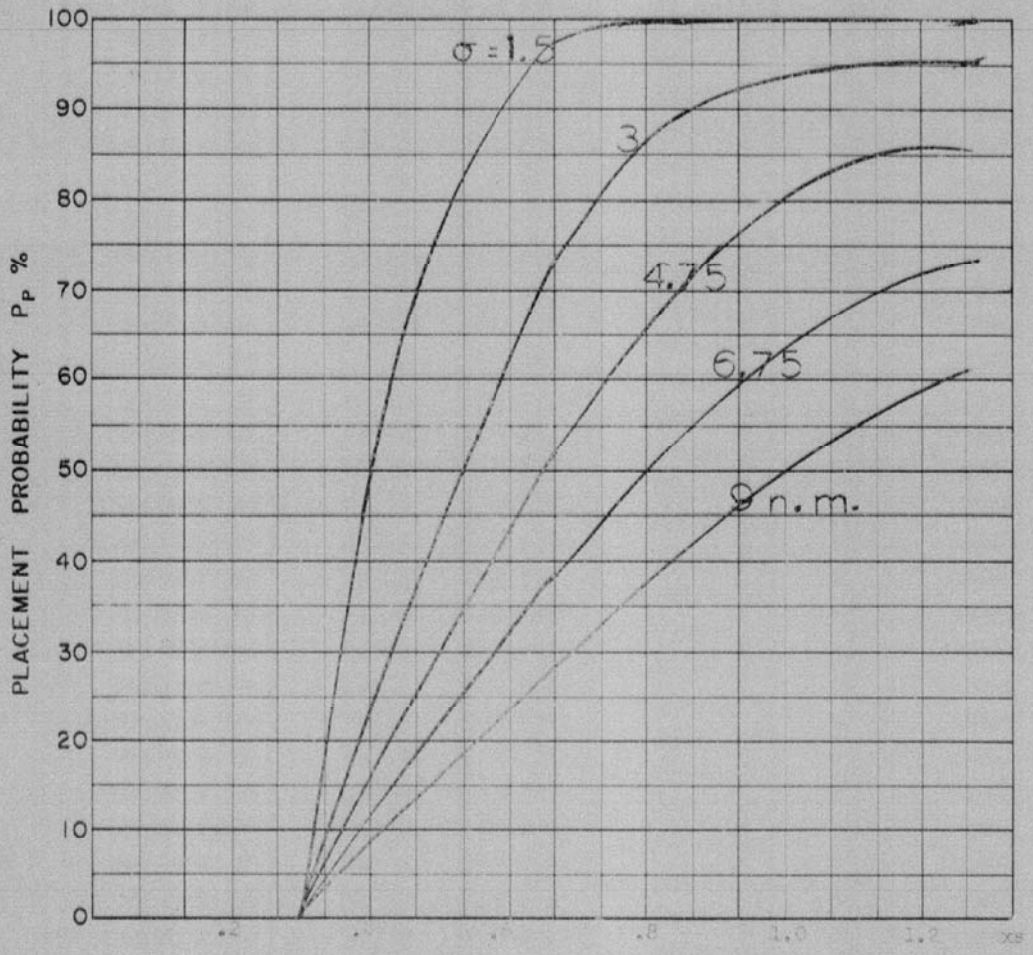

COURSE DIFFERENCE: 120°
TARGET EVASION: 0.1 lateral g's, towards interceptor only
TARGET MACH NO.: 2.0
INTERCEPTOR LATERAL G's: 1.6
INTERCEPTOR MACH NO.: 1.5
σ OF G.C.I. ACCURACY: five values
A.I. DETECTION RANGE AS FRACTION OF SPECIFICATION RANGE, S: abscissa
A.I. DETECTION RANGE CONTOUR: Straight wing
ALTITUDE: 50K

S91b

Missile launch zone L 10

104 spr

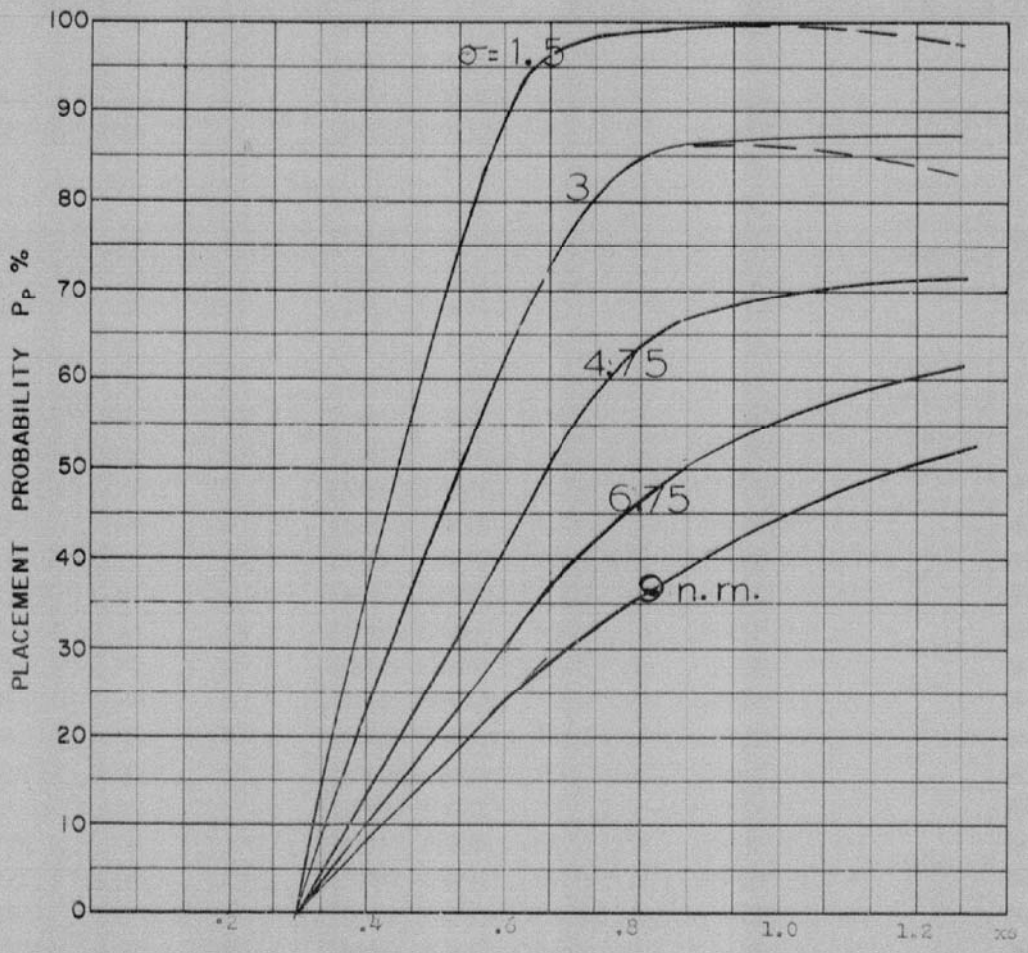

A.I. Range

COURSE DIFFERENCE: 110°
TARGET EVASION: 0.2 lateral g's, towards interceptor only (S92)
TARGET MACH NO.: 2.0
INTERCEPTOR LATERAL G's: 1.6
INTERCEPTOR MACH NO.: 1.5
σ OF G.C.I. ACCURACY: five values
A.I. DETECTION RANGE AS FRACTION OF SPECIFICATION RANGE, S: abscissa
A.I. DETECTION RANGE CONTOUR: Straight wing
ALTITUDE: 50K

Missile launch zone L 10

105 spr

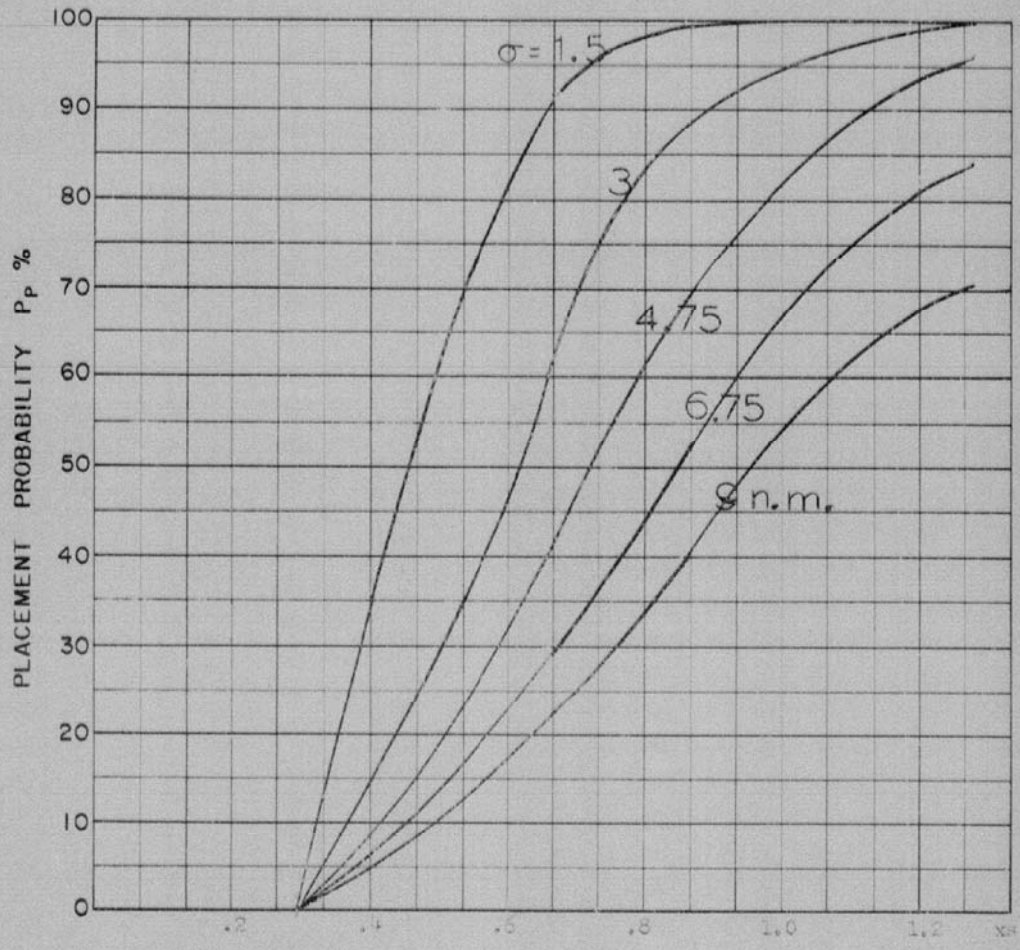

A.I. Range

COURSE DIFFERENCE: 135°
TARGET EVASION: 0.1 lateral g's
TARGET MACH NO.: 2.0
INTERCEPTOR LATERAL G's: 1.6
INTERCEPTOR MACH NO.: 1.5
σ OF G.C.I. ACCURACY: five values
A.I. DETECTION RANGE AS FRACTION OF SPECIFICATION RANGE, S: abscissa
A.I. DETECTION RANGE CONTOUR: Straight wing
ALTITUDE: 50K

S93

Missile launch zone L 10

11¼ spr

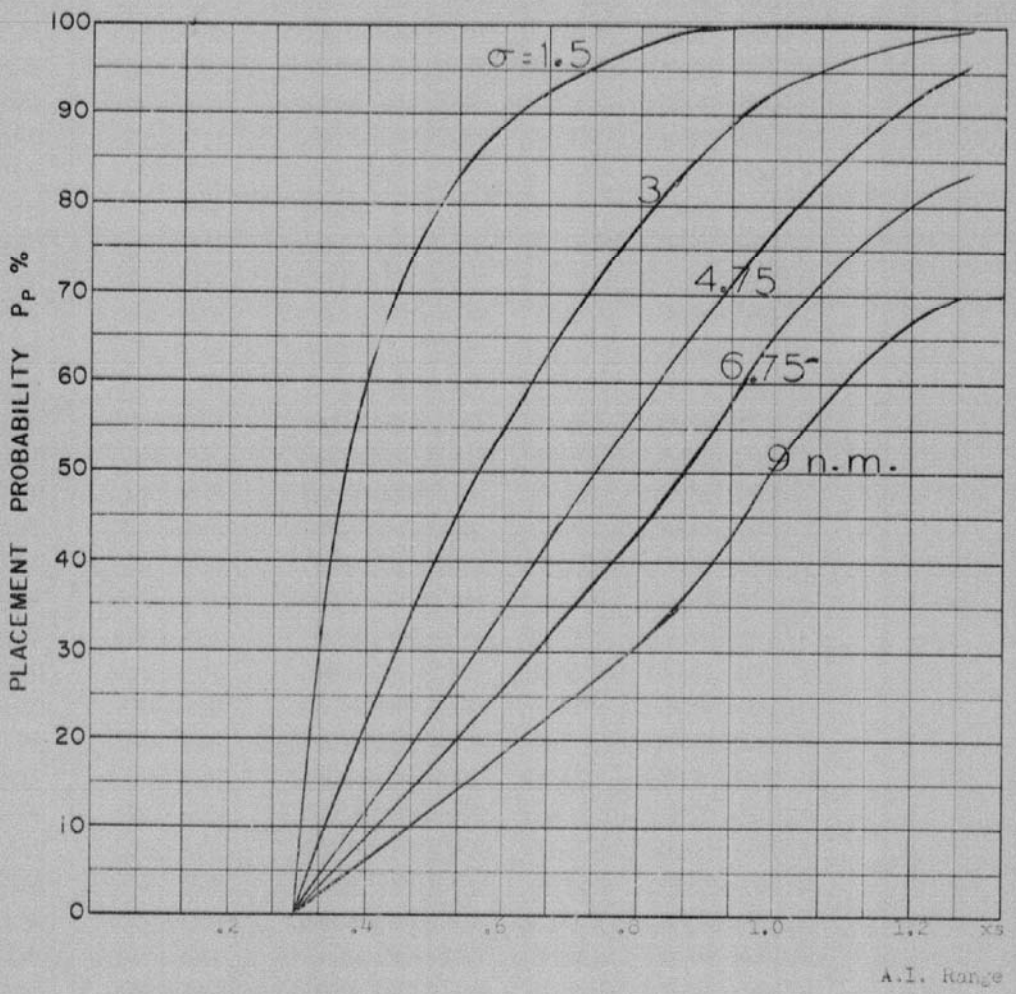

COURSE DIFFERENCE: 160°
TARGET EVASION: 0.1 lateral g's
TARGET MACH NO.: 2.0
INTERCEPTOR LATERAL G's: 1.6
INTERCEPTOR MACH NO.: 1.5
σ OF G.C.I. ACCURACY: five values
A.I. DETECTION RANGE AS FRACTION OF SPECIFICATION RANGE, S: abscissa
A.I. DETECTION RANGE CONTOUR: Straight wing
ALTITUDE: 50K

S94a

Missile launch zone L 10

102 aspr

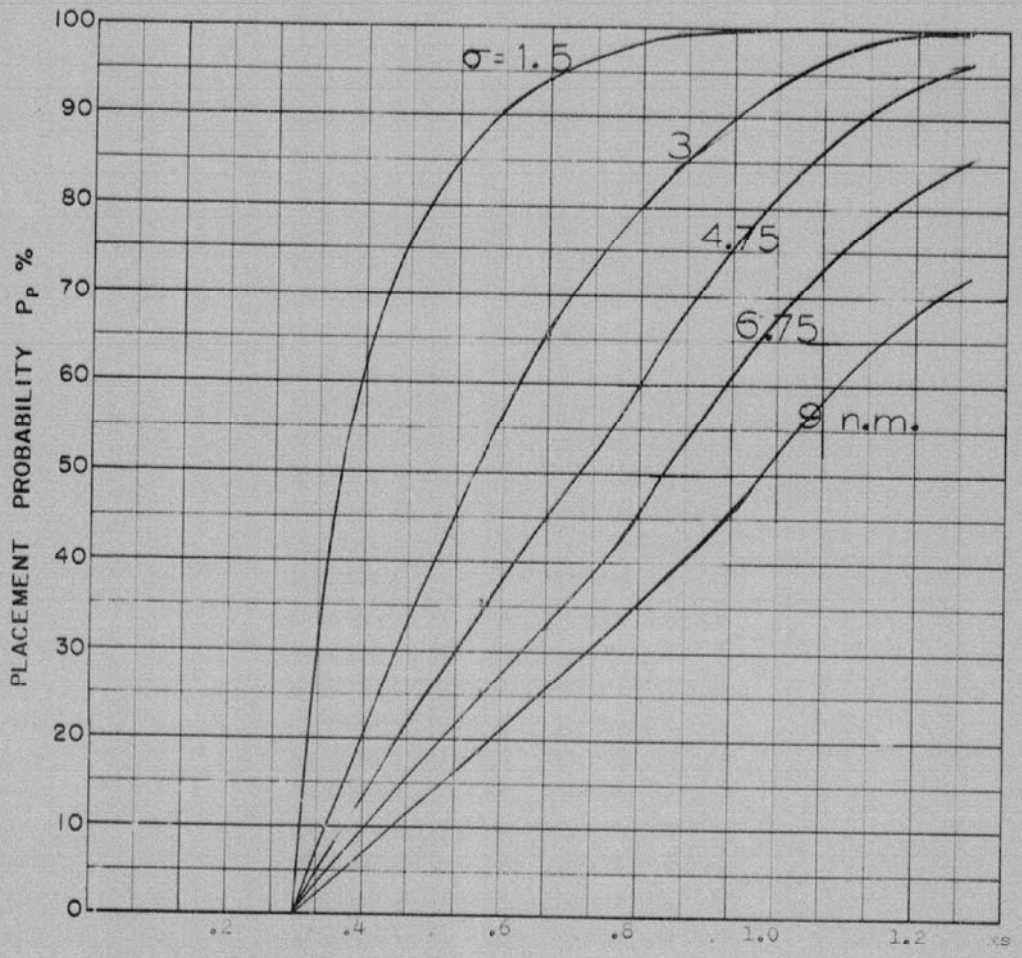

A.I. Range

COURSE DIFFERENCE: 160°
TARGET EVASION: 0.1 lateral g's, towards interceptor only
TARGET MACH NO.: 2.0
INTERCEPTOR LATERAL G's: 1.6
INTERCEPTOR MACH NO.: 1.5
σ OF G.C.I. ACCURACY: five values
A.I. DETECTION RANGE AS FRACTION OF SPECIFICATION RANGE, S: abscissa
A.I. DETECTION RANGE CONTOUR: Straight wing
ALTITUDE: 50K

S94b

Missile launch zone L 10

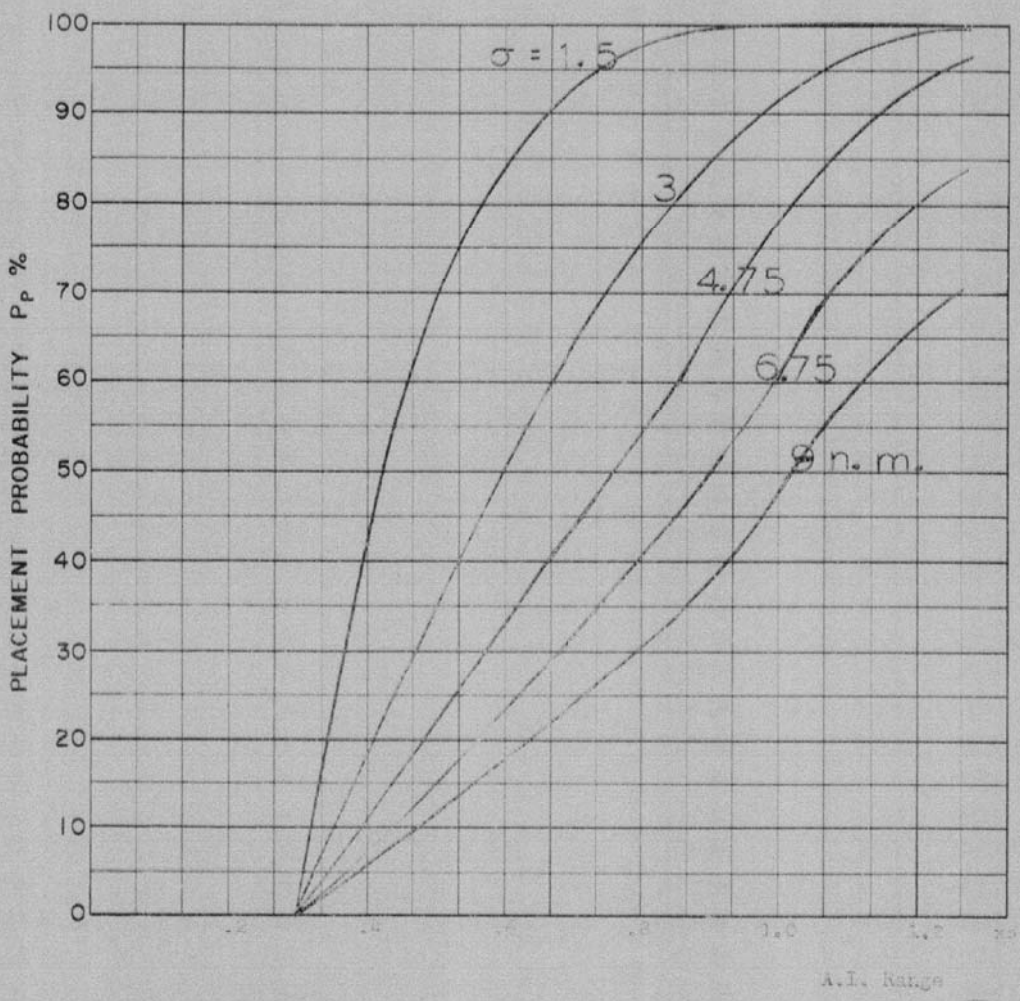

COURSE DIFFERENCE:
TARGET EVASION:
TARGET MACH NO.:
INTERCEPTOR LATERAL G's:
INTERCEPTOR MACH NO.:
σ OF G.C.I. ACCURACY:
A.I. DETECTION RANGE AS FRACTION OF SPECIFICATION RANGE, S:
A.I. DETECTION RANGE CONTOUR:
ALTITUDE:

S95

106 bspr

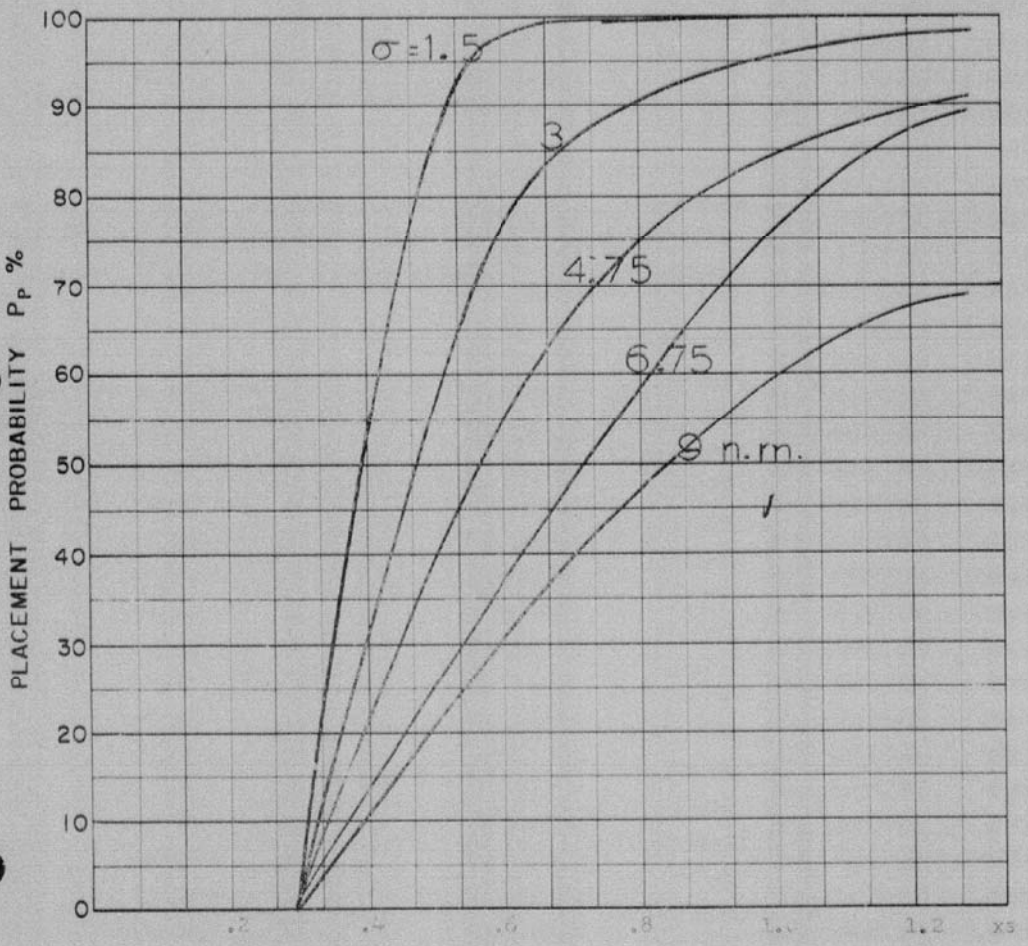

COURSE DIFFERENCE: 110°
TARGET EVASION: 0.1 lateral g's
TARGET MACH NO.: 2.0
INTERCEPTOR LATERAL G's: 3.0
INTERCEPTOR MACH NO: 1.5
σ OF G.C.I. ACCURACY: five values
A.I. DETECTION RANGE AS FRACTION OF SPECIFICATION RANGE, S: abscissa
A.I. DETECTION RANGE CONTOUR: Straight wing
ALTITUDE: 50K

(596)

Missile launch zone L 10

108 spr

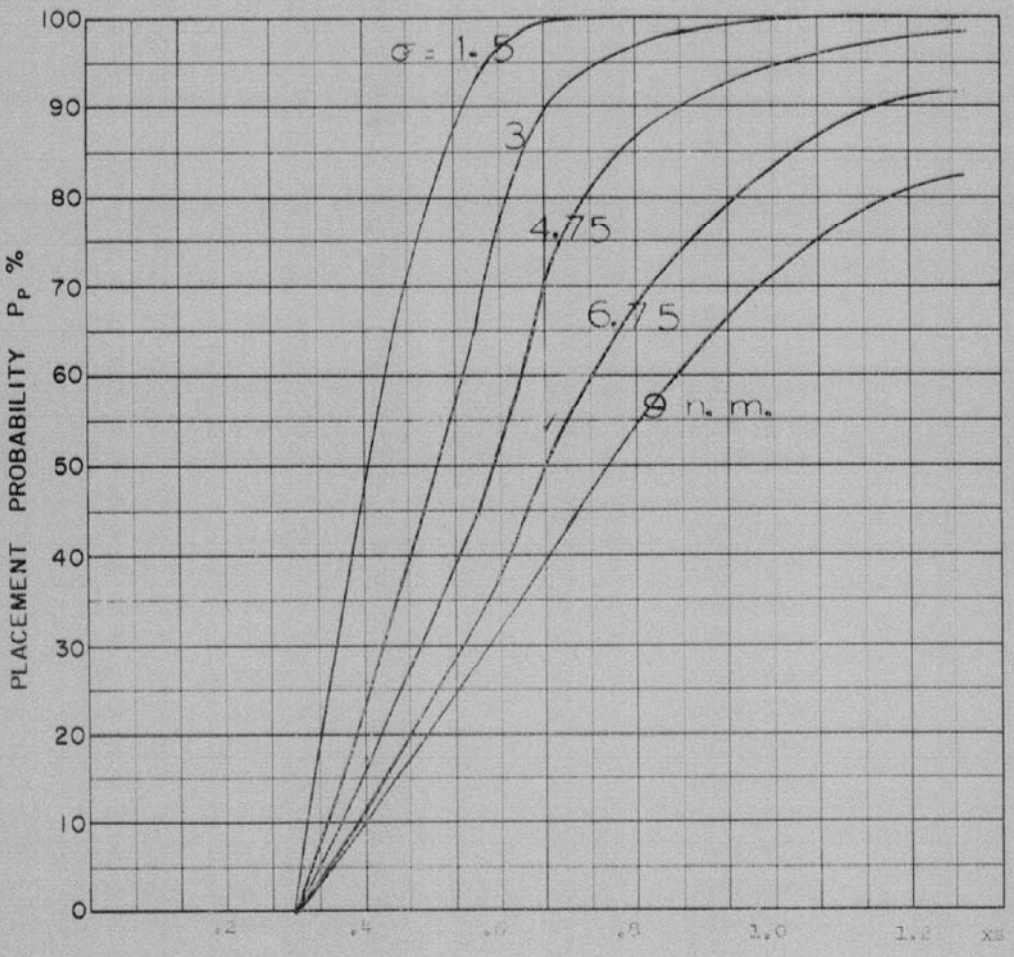

COURSE DIFFERENCE: 135°
TARGET EVASION: 0.1 lateral g's
TARGET MACH NO.: 2.0
INTERCEPTOR LATERAL G's: 3.0
INTERCEPTOR MACH NO.: 1.5
σ OF G.C.I. ACCURACY: five values
A.I. DETECTION RANGE AS FRACTION OF SPECIFICATION RANGE, S: abscissa
A.I. DETECTION RANGE CONTOUR: Straight wing
ALTITUDE: 50K

(S97a)

Missile launch zone L 10

Look angle 75°

107 spr

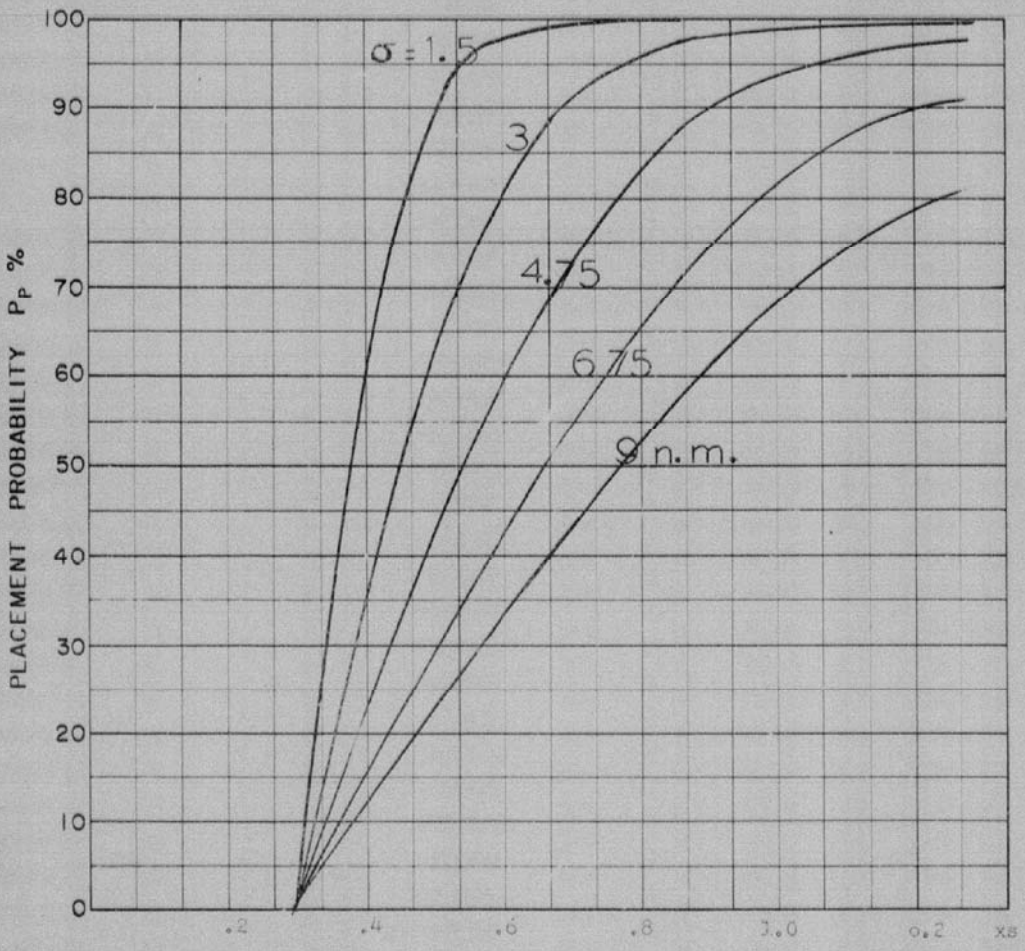

COURSE DIFFERENCE: 135°
TARGET EVASION: 0.1 lateral g's
TARGET MACH NO.: 2.0
INTERCEPTOR LATERAL G's: 3.0
INTERCEPTOR MACH NO.: 1.5
σ OF G.C.I. ACCURACY: five values
A.I. DETECTION RANGE AS FRACTION OF SPECIFICATION RANGE, S: abscissa
A.I. DETECTION RANGE CONTOUR: Straight wing
ALTITUDE: 50K

S976

Missile launch zone L 10

111 spr

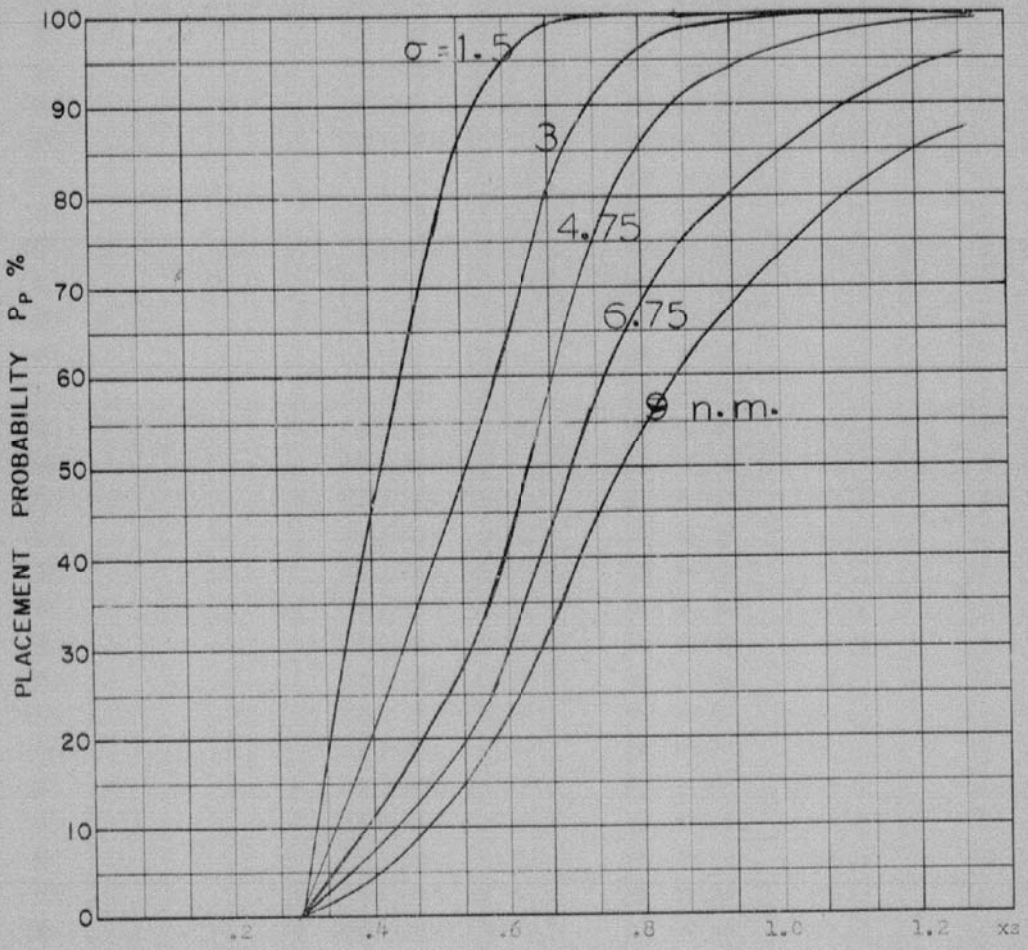

COURSE DIFFERENCE: 160°
TARGET EVASION: 0.1 lateral g's
TARGET MACH NO.: 2.0
INTERCEPTOR LATERAL G's: 3.0
INTERCEPTOR MACH NO.: 1.5
σ OF G.C.I. ACCURACY: five values
A.I. DETECTION RANGE AS FRACTION OF SPECIFICATION RANGE, S: abscissa
A.I. DETECTION RANGE CONTOUR: Straight wing
ALTITUDE: 50K

S98a

Missile launch zone L10

101 spr

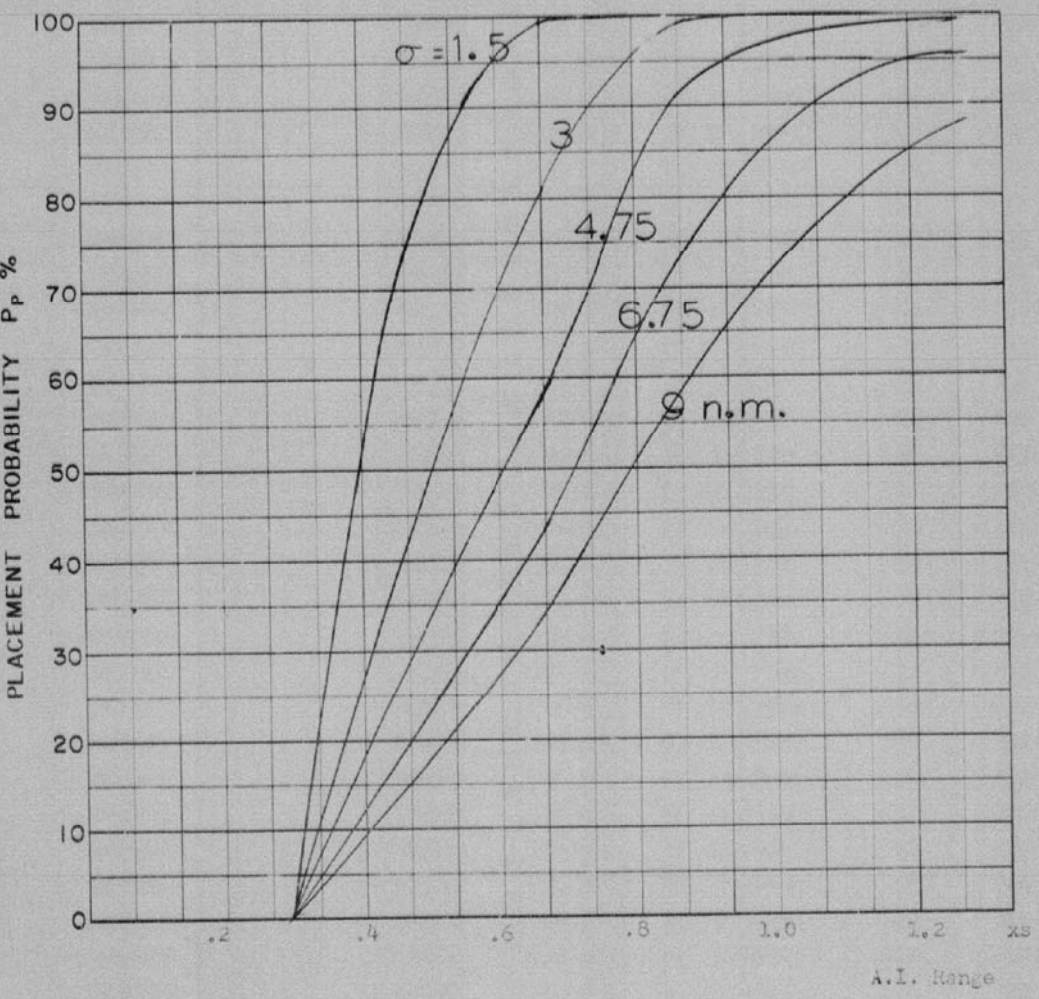

COURSE DIFFERENCE: 160°
TARGET EVASION: 0.1 lateral g's, towards interceptor only
TARGET MACH NO.: 2.0
INTERCEPTOR LATERAL G's: 3.0
INTERCEPTOR MACH NO.: 1.5
σ OF G.C.I. ACCURACY: five values
A.I. DETECTION RANGE AS FRACTION OF SPECIFICATION RANGE, S: abscissa
A.I. DETECTION RANGE CONTOUR: Straight wing
ALTITUDE: 50K

S986

Missile launch zone L 10

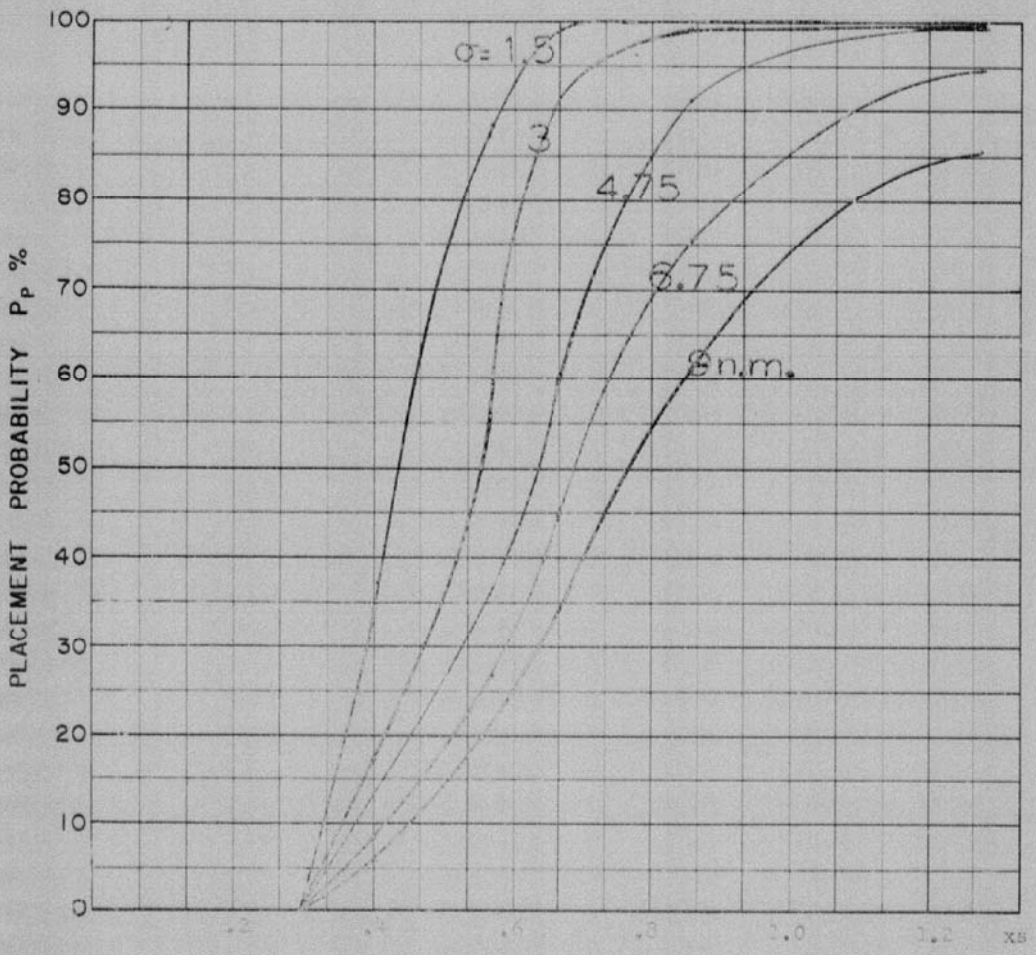

COURSE DIFFERENCE:
TARGET EVASION:
TARGET MACH NO.:
INTERCEPTOR LATERAL G's:
INTERCEPTOR MACH NO.:
σ OF G.C.I. ACCURACY:
A.I. DETECTION RANGE AS FRACTION OF SPECIFICATION RANGE, S: abscissa
A.I. DETECTION RANGE CONTOUR:
ALTITUDE:

S99

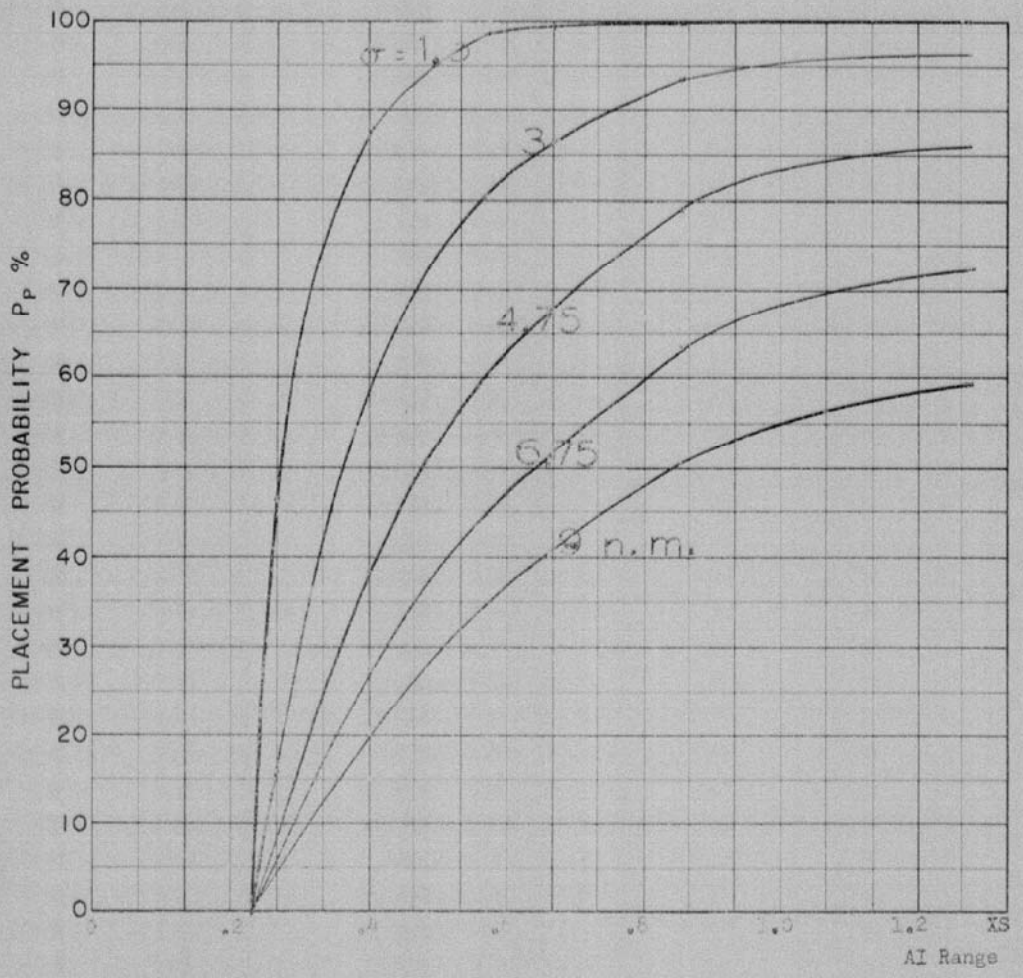

COURSE DIFFERENCE: 90°
TARGET EVASION: 0
TARGET MACH NO.: 2.0
INTERCEPTOR LATERAL G's: 2.0
INTERCEPTOR MACH NO.: 1.5
σ OF G.C.I. ACCURACY: Five values
A.I. DETECTION RANGE AS FRACTION OF SPECIFICATION RANGE, S: Abscissa
A.I. DETECTION RANGE CONTOUR: Straight Wing
ALTITUDE: 60K

S100a

Missile launch zone L-6, maximum range, 8° heading error.

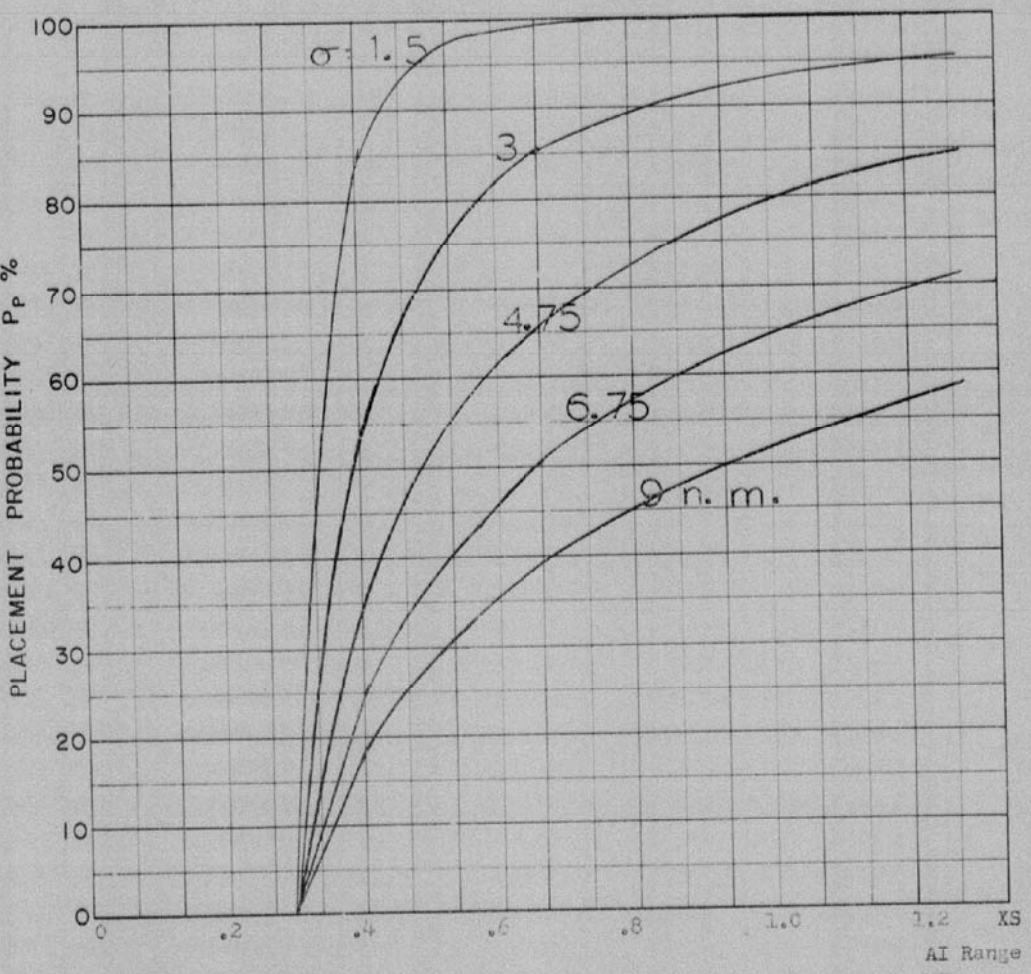

(S100b)

COURSE DIFFERENCE: 90°
TARGET EVASION: 0
TARGET MACH NO.: 2.0
INTERCEPTOR LATERAL G's: 2.0
INTERCEPTOR MACH NO.: 1.5
σ OF G.C.I. ACCURACY: Five values
A.I. DETECTION RANGE AS FRACTION OF SPECIFICATION RANGE, S: Abscissa
A.I. DETECTION RANGE CONTOUR: Straight Wing
ALTITUDE: 60K

Missile launch zone L-5, maximum range, 8° heading error.

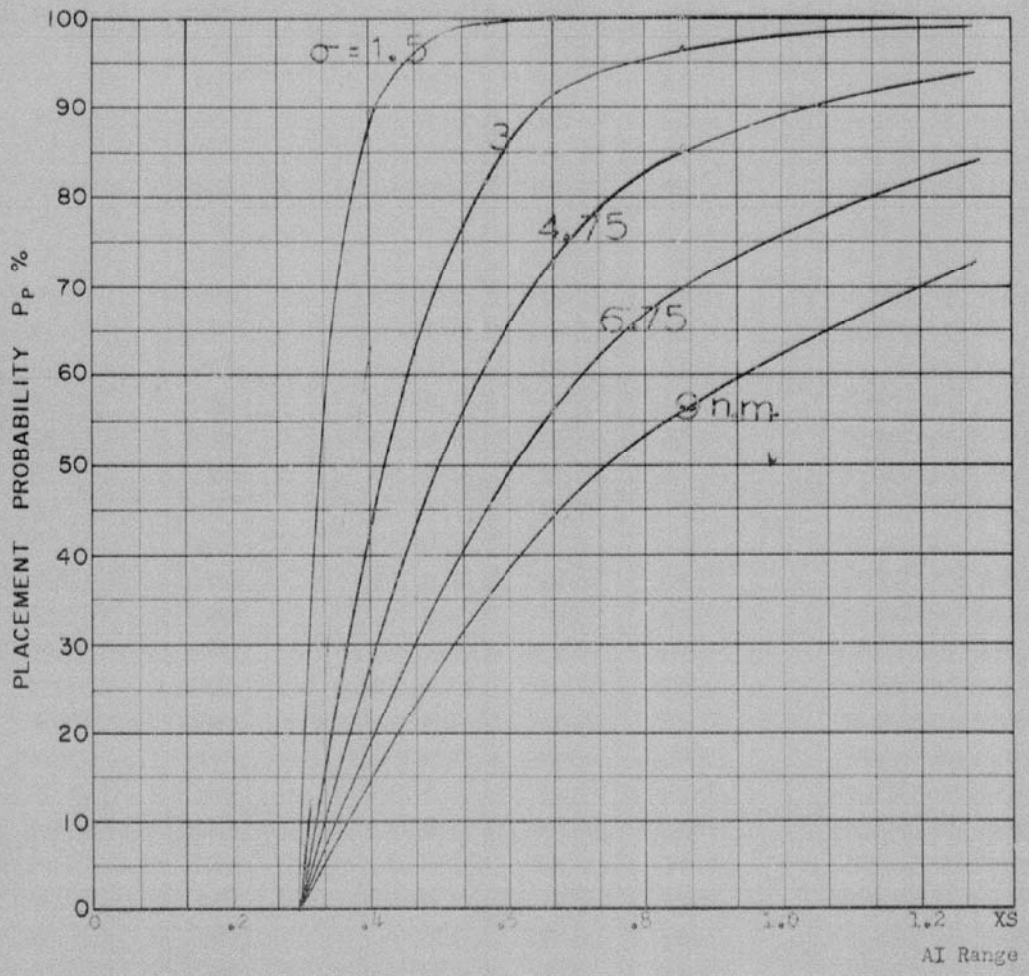

COURSE DIFFERENCE: 180°
TARGET EVASION: 0
TARGET MACH NO.: 2.0
INTERCEPTOR LATERAL G's: 2.0
INTERCEPTOR MACH NO.: 1.6
σ OF G.C.I. ACCURACY: Five values
A.I. DETECTION RANGE AS FRACTION OF SPECIFICATION RANGE, S: Abscissa
A.I. DETECTION RANGE CONTOUR: Straight Wing
ALTITUDE: 60K

S101a

Missile launch zone L-9, maximum range, 8° heading error.

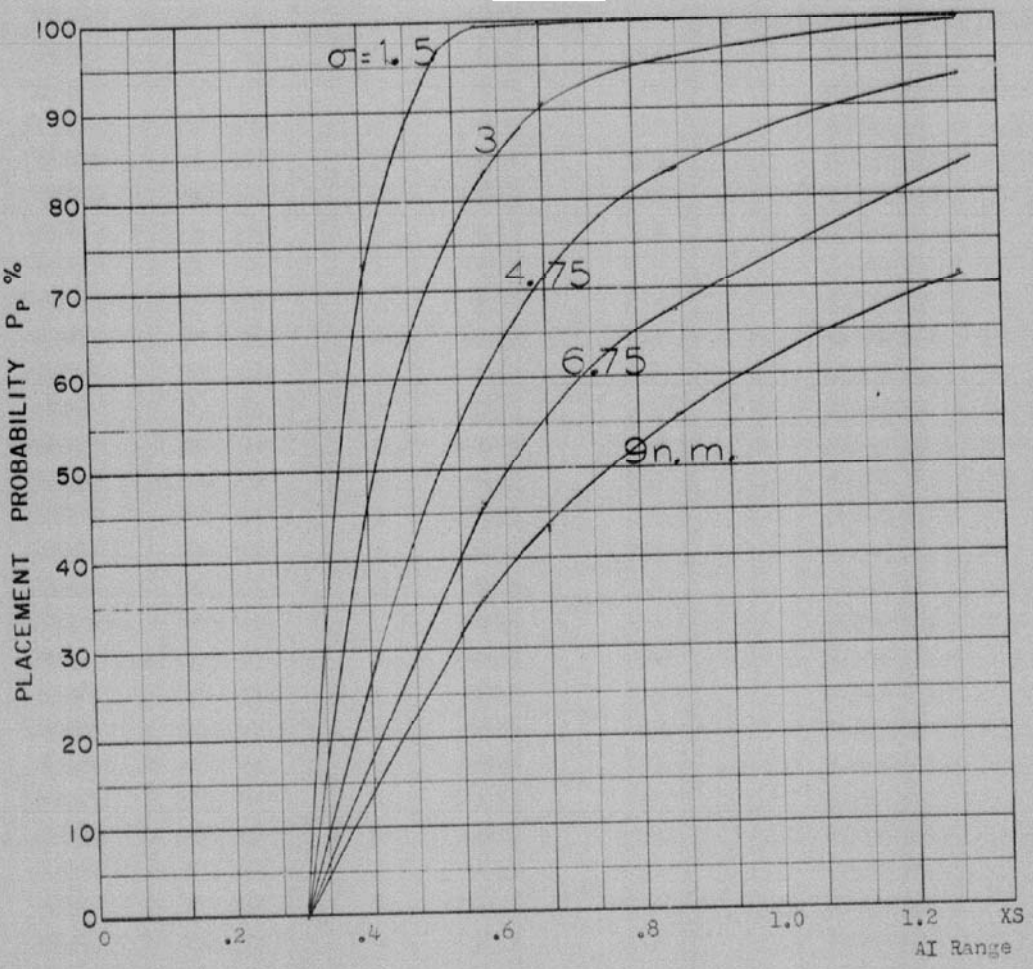

COURSE DIFFERENCE: 100°
TARGET EVASION: 0
TARGET MACH NO.: 2.0
INTERCEPTOR LATERAL G's: 2.0
INTERCEPTOR MACH NO.: 1.5
σ OF G.C.I. ACCURACY: Five values
A.I. DETECTION RANGE AS FRACTION OF SPECIFICATION RANGE, S: Abscissa
A.I. DETECTION RANGE CONTOUR: Straight Wing
ALTITUDE: 60K

S1011b

Missile launch zone L-5, maximum range, 8° heading error.

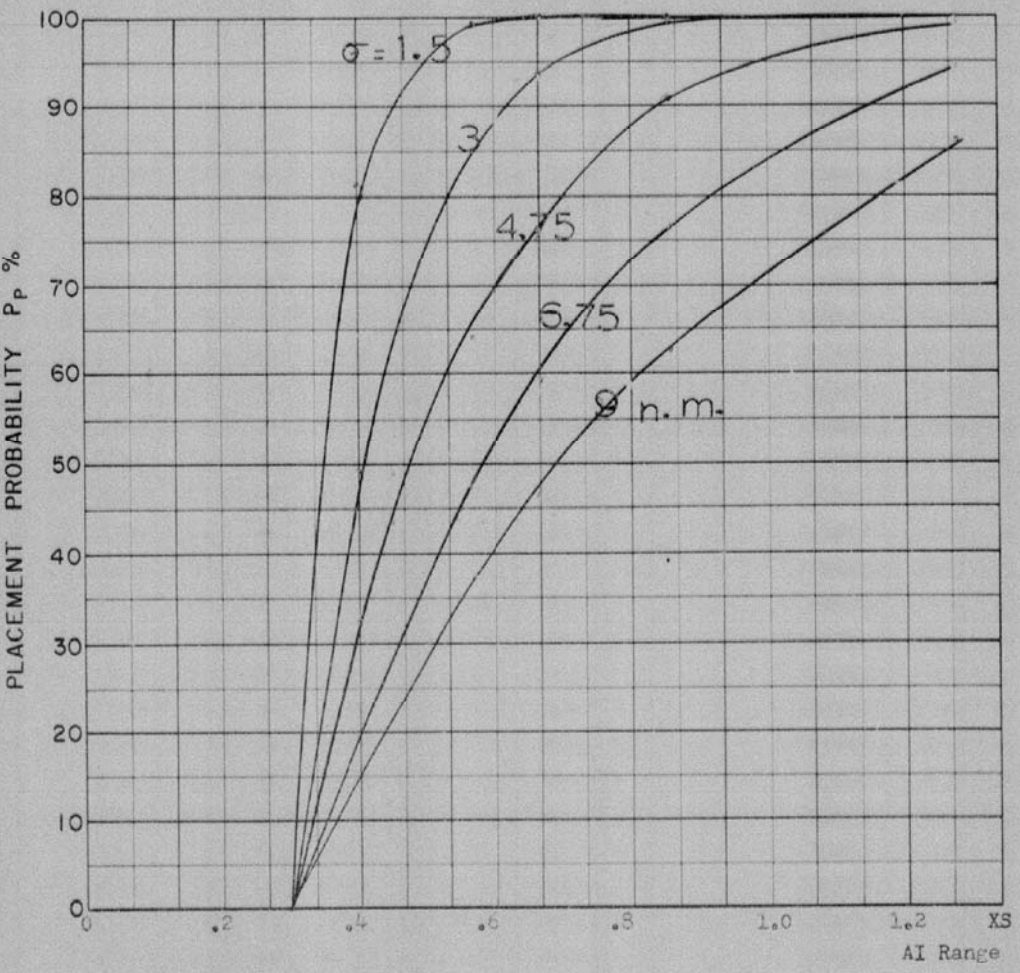

COURSE DIFFERENCE: 120°
TARGET EVASION: 0
TARGET MACH NO.: 2.0
INTERCEPTOR LATERAL G's: 2.0
INTERCEPTOR MACH NO.: 1.5
σ OF G.C.I. ACCURACY: Five values
A.I. DETECTION RANGE AS FRACTION OF SPECIFICATION RANGE, S: Abscissa
A.I. DETECTION RANGE CONTOUR: Straight Wing
ALTITUDE: 60K

S102a

Missile launch zone L-9, maximum range, 8° heading error.

11espr

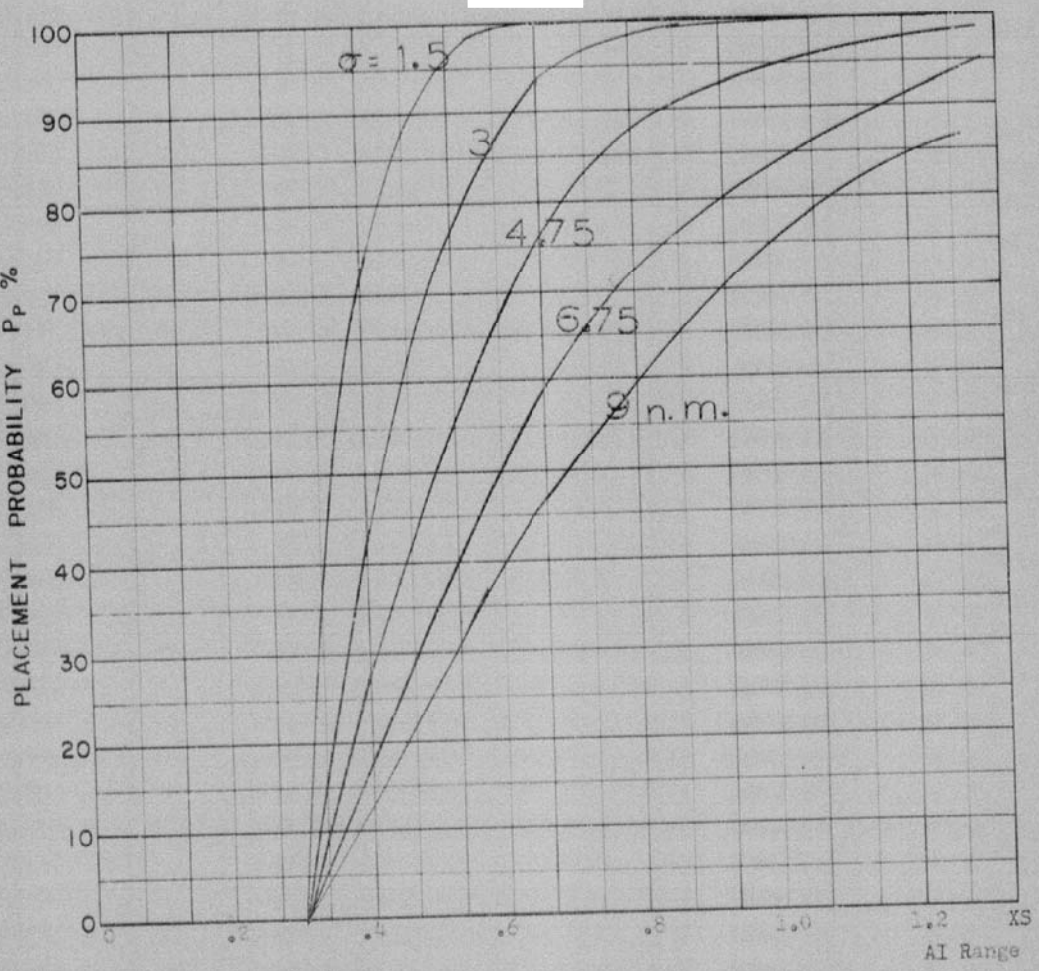

S102b

COURSE DIFFERENCE: 120°
TARGET EVASION: 0
TARGET MACH NO.: 2.0
INTERCEPTOR LATERAL G's: 2.0
INTERCEPTOR MACH NO.: 1.5
σ OF G.C.I. ACCURACY: Five values
A.I. DETECTION RANGE AS FRACTION OF SPECIFICATION RANGE, S: Abscissa
A.I. DETECTION RANGE CONTOUR: Straight Wing
ALTITUDE: 60K

Missile launch zone L-5, maximum range, 8° heading error.

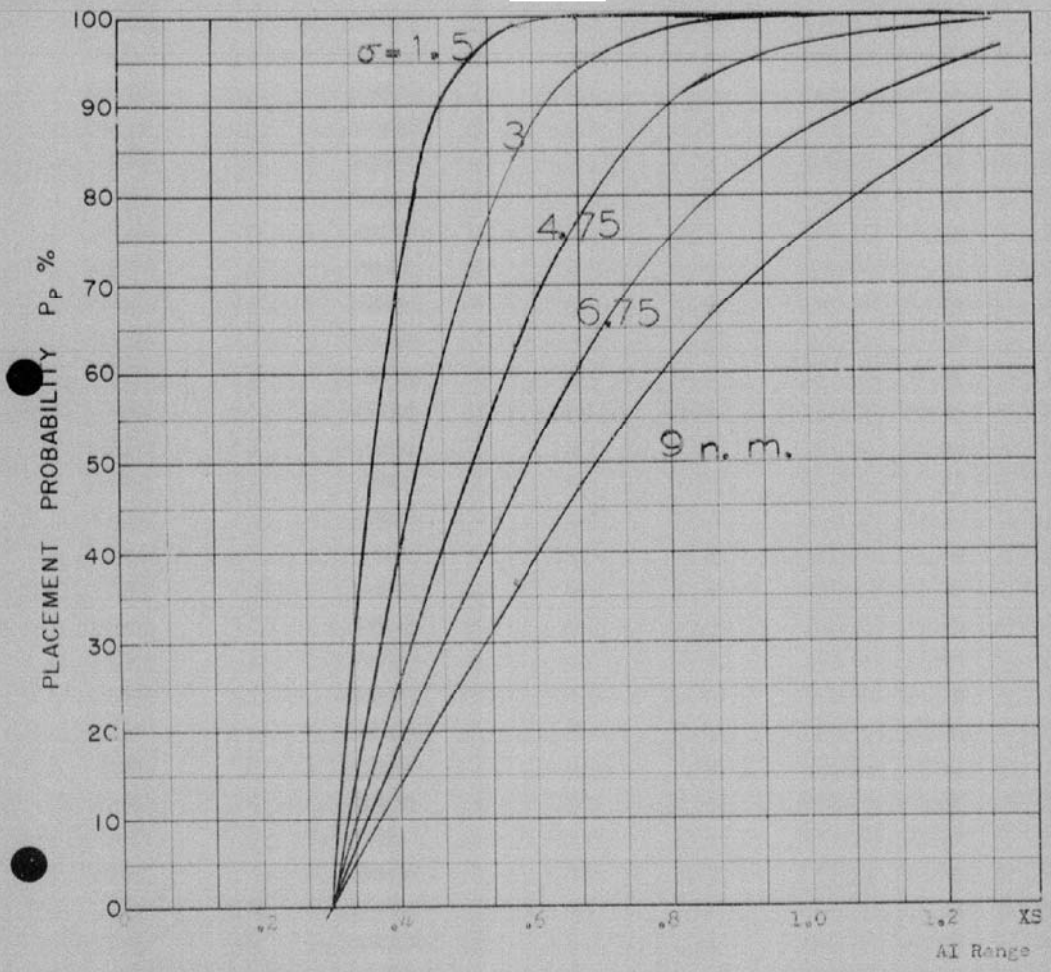

COURSE DIFFERENCE: 135°
TARGET EVASION: 0
TARGET MACH NO.: 2.0
INTERCEPTOR LATERAL G's: 2.0
INTERCEPTOR MACH NO.: 1.5
σ OF G.C.I. ACCURACY: Five values
A.I. DETECTION RANGE AS FRACTION OF SPECIFICATION RANGE, S: Abscissa
A.I. DETECTION RANGE CONTOUR: Straight Wing
ALTITUDE: 60K

S103a

Missile launch zone L-9, maximum range, 8° heading error.

11dspr

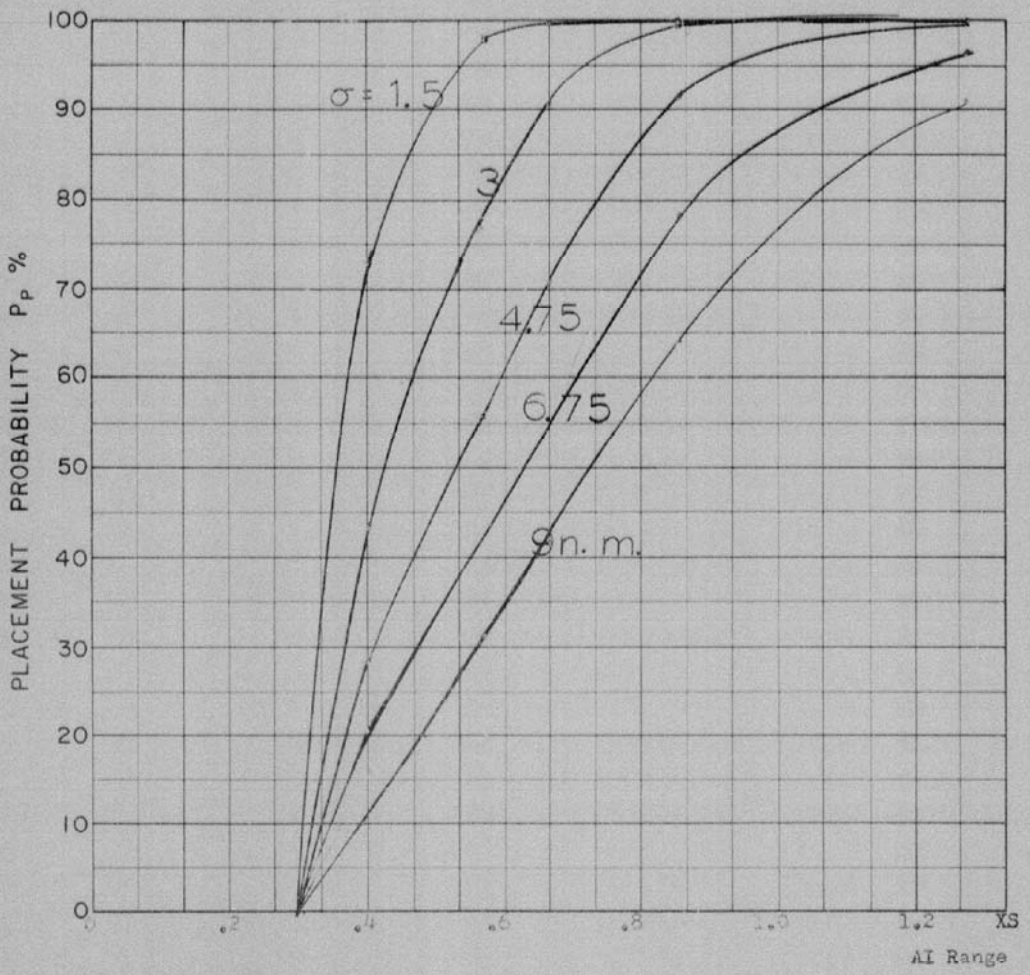

COURSE DIFFERENCE: 135°
TARGET EVASION: 0
TARGET MACH NO.: 2.0
INTERCEPTOR LATERAL G's: 2.0
INTERCEPTOR MACH NO.: 1.5
σ OF G.C.I. ACCURACY: Five values
A.I. DETECTION RANGE AS FRACTION OF SPECIFICATION RANGE, S: Abscissa
A.I. DETECTION RANGE CONTOUR: Straight Wing
ALTITUDE: 60K

S103b

Missile launch zone L-5, maximum range, 8° heading error.

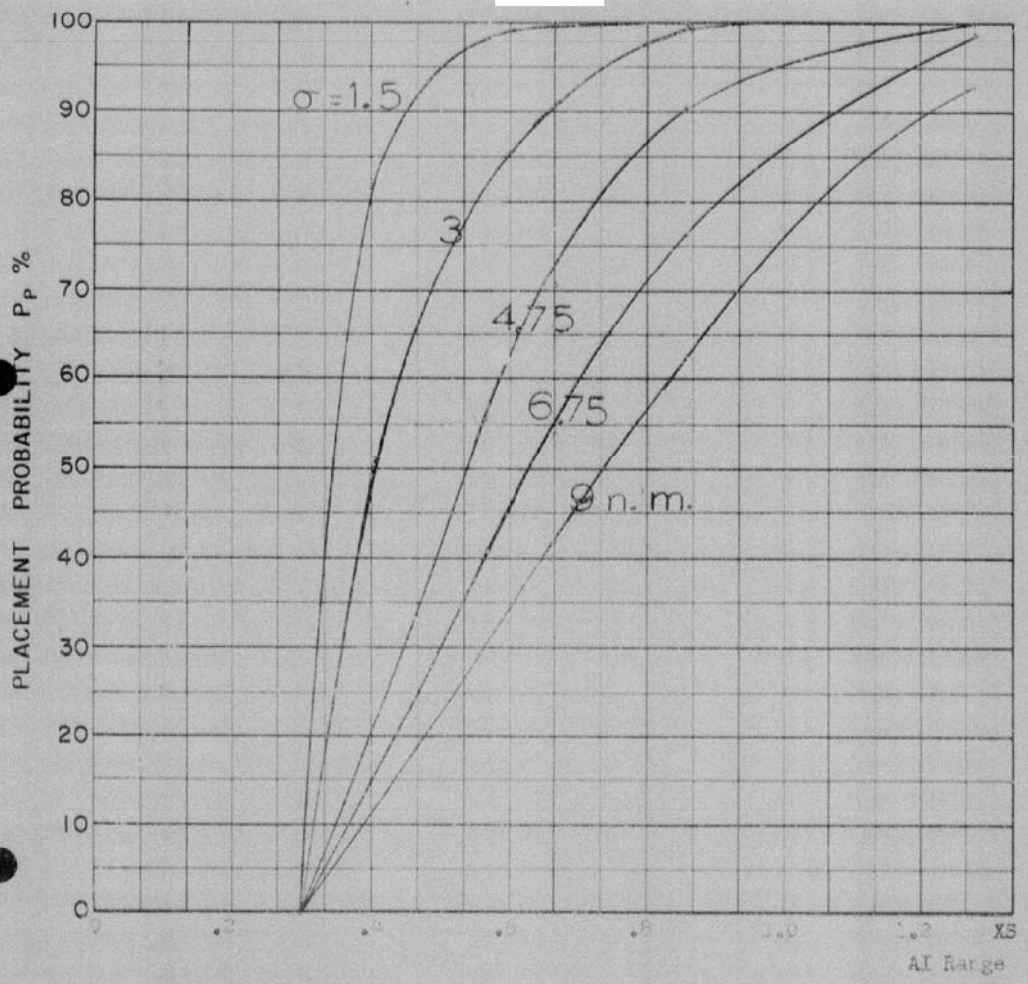

COURSE DIFFERENCE:
TARGET EVASION:
TARGET MACH NO.:
INTERCEPTOR LATERAL G's:
INTERCEPTOR MACH NO.:
σ OF G.C.I. ACCURACY:
A.I. DETECTION RANGE AS FRACTION OF SPECIFICATION RANGE, S: Abscissa
A.I. DETECTION RANGE CONTOUR: Straight Wing
ALTITUDE:

S104a

Missile-launch zone I-9, maximum range, 8° heading error.

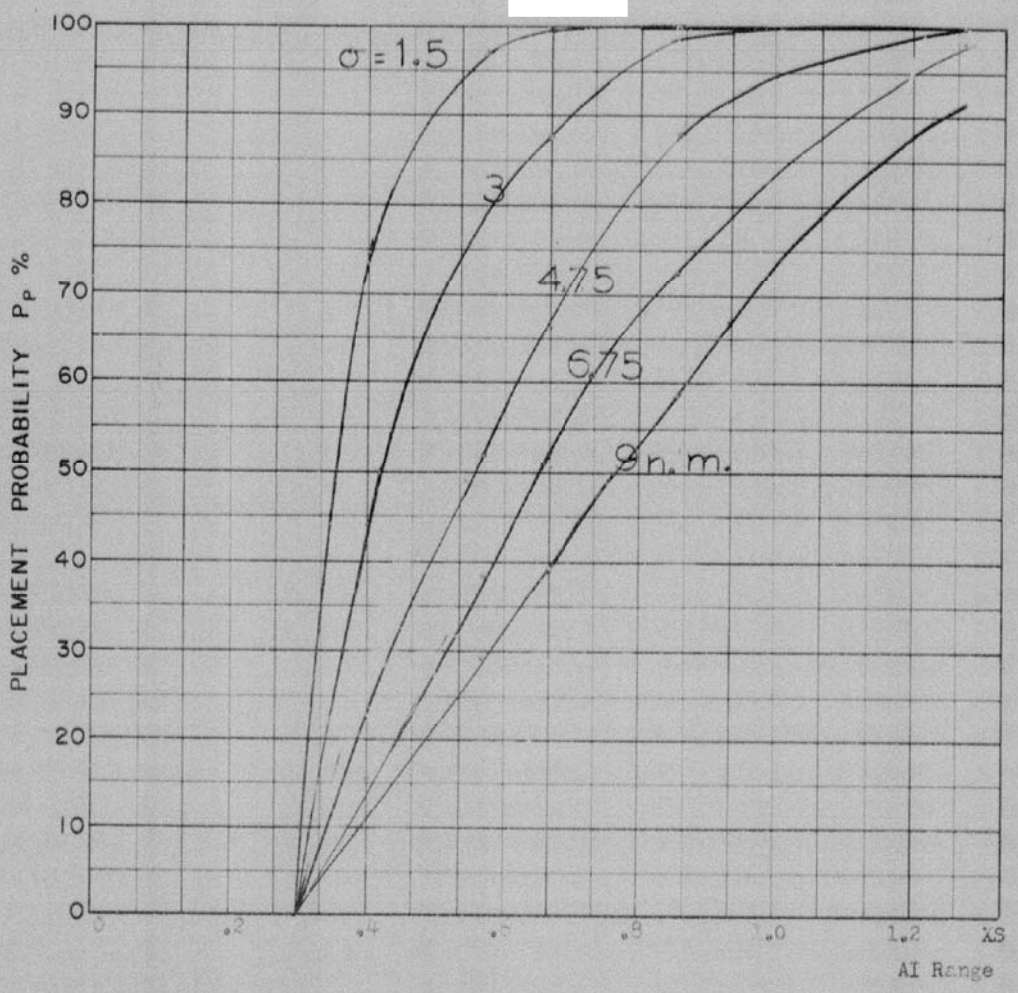

COURSE DIFFERENCE: 180°
TARGET EVASION: 0
TARGET MACH NO.: 2.0
INTERCEPTOR LATERAL G's: 2.0
INTERCEPTOR MACH NO.: 1.8
σ OF G.C.I. ACCURACY: Five values
A.I. DETECTION RANGE AS FRACTION OF SPECIFICATION RANGE, S: Abscissa
A.I. DETECTION RANGE CONTOUR: Straight Wing
ALTITUDE: 60K

S104b

Missile launch zone L-5, maximum range, 8° heading error.

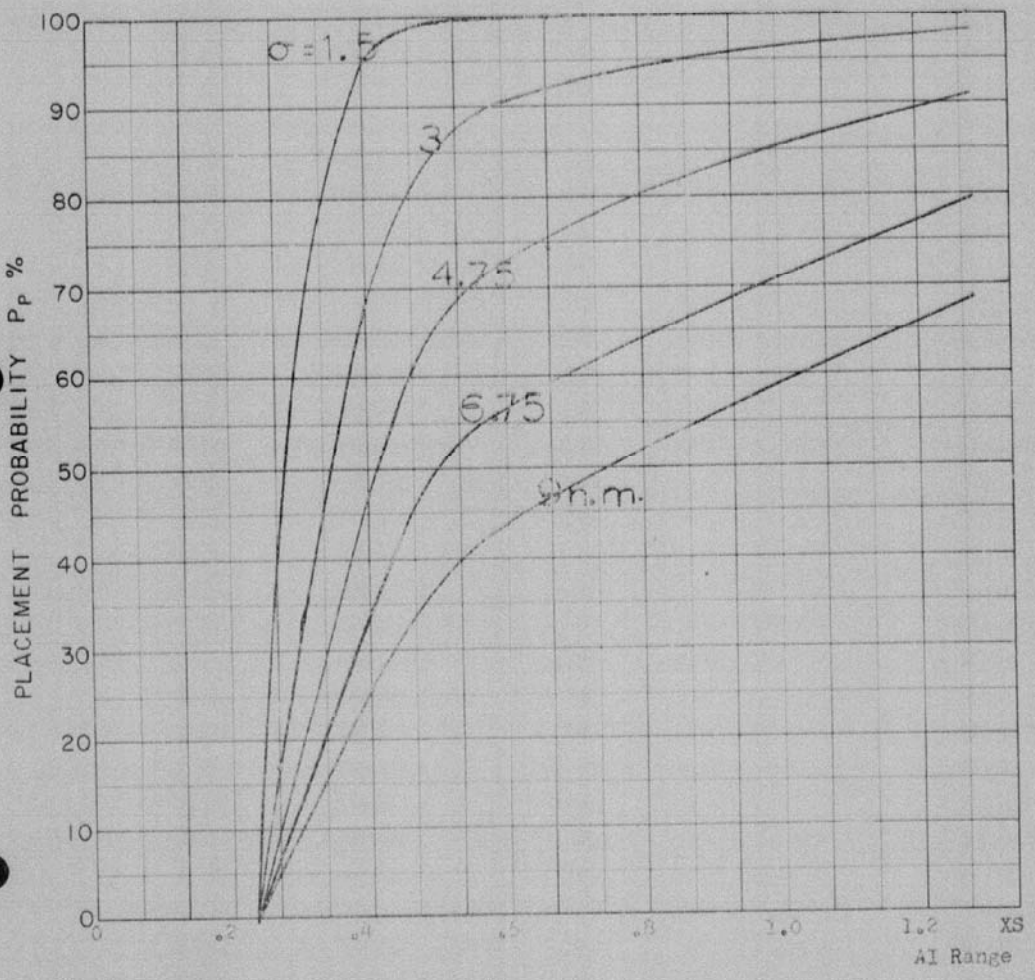

COURSE DIFFERENCE: 90°
TARGET EVASION: 2
TARGET MACH NO.: 2.7
INTERCEPTOR LATERAL G's: 3.35
INTERCEPTOR MACH NO.: .9
σ OF G.C.I. ACCURACY: Five values
A.I. DETECTION RANGE AS FRACTION OF SPECIFICATION RANGE, S: Abscissa
A.I. DETECTION RANGE CONTOUR: Straight Wing
ALTITUDE: 60K

S105a

Missile launch zone L-9, maximum range, 8° heading error.

6aspr

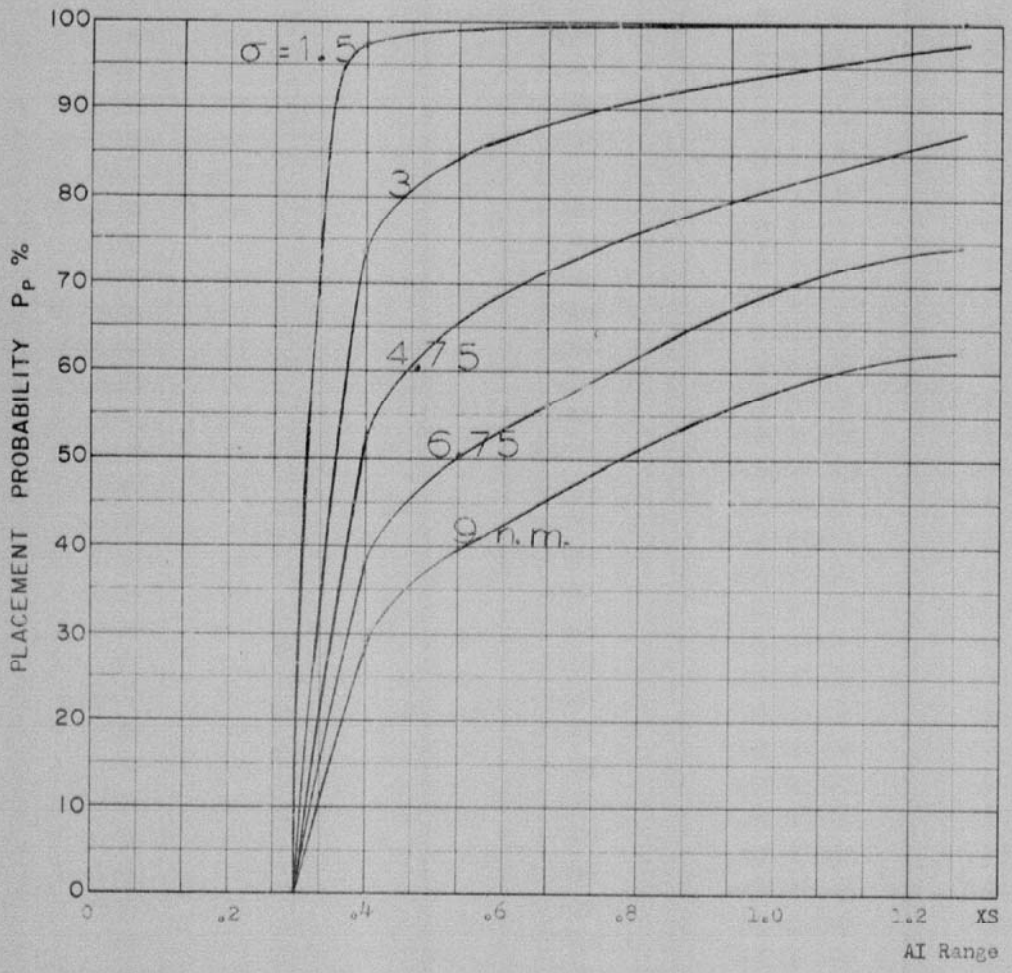

COURSE DIFFERENCE: 90°
TARGET EVASION: 0
TARGET MACH NO.: 2.0
INTERCEPTOR LATERAL G's: 3.35
INTERCEPTOR MACH NO: 1.5
σ OF G.C.I. ACCURACY: Five values
A.I. DETECTION RANGE AS FRACTION OF SPECIFICATION RANGE, S: Abscissa
A.I. DETECTION RANGE CONTOUR: Straight Wing
ALTITUDE: 60K

S105c

Missile launch zone L-5, maximum range, 15° heading error.

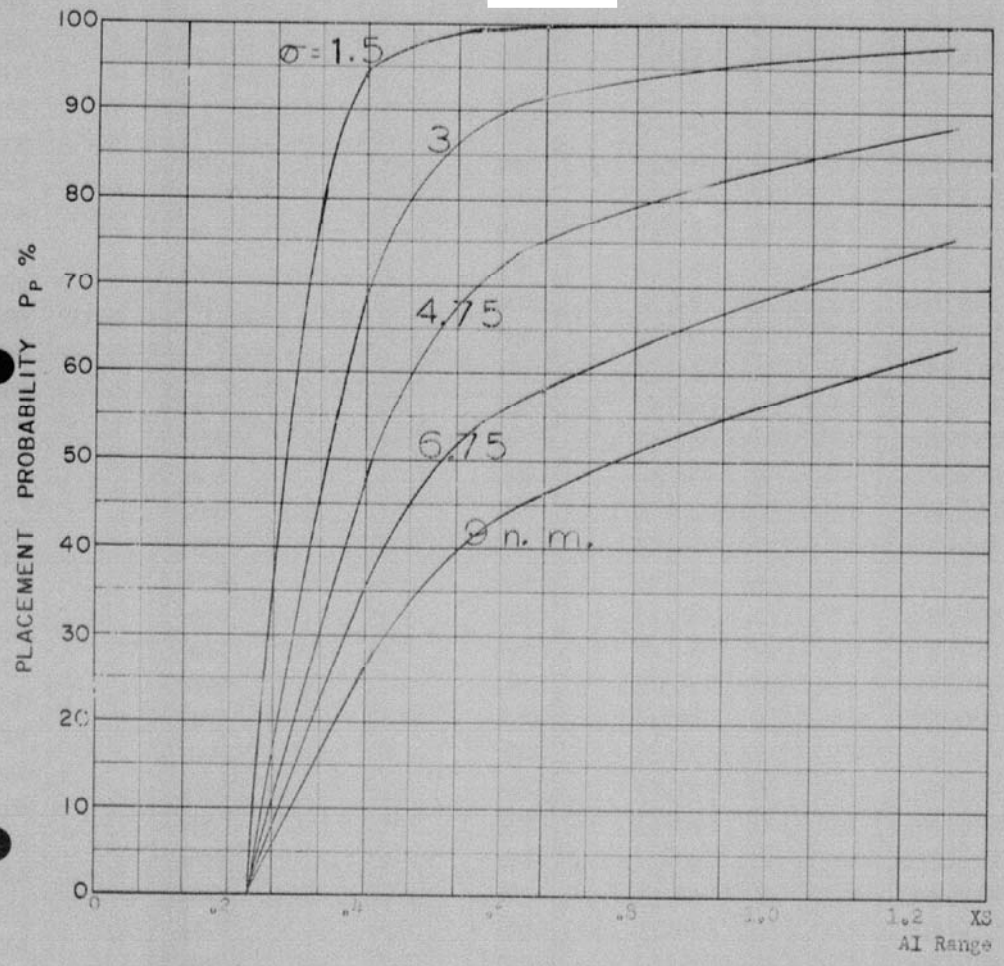

COURSE DIFFERENCE: 90°
TARGET EVASION: 0
TARGET MACH NO.: 2.0
INTERCEPTOR LATERAL G's: 3.35
INTERCEPTOR MACH NO.: 2.5
σ OF G.C.I. ACCURACY: Five values
A.I. DETECTION RANGE AS FRACTION OF SPECIFICATION RANGE, S: Abscissa
A.I. DETECTION RANGE CONTOUR: Straight Wing
ALTITUDE: 60K

Missile launch zone 1.6.

(S105d)

13bspr

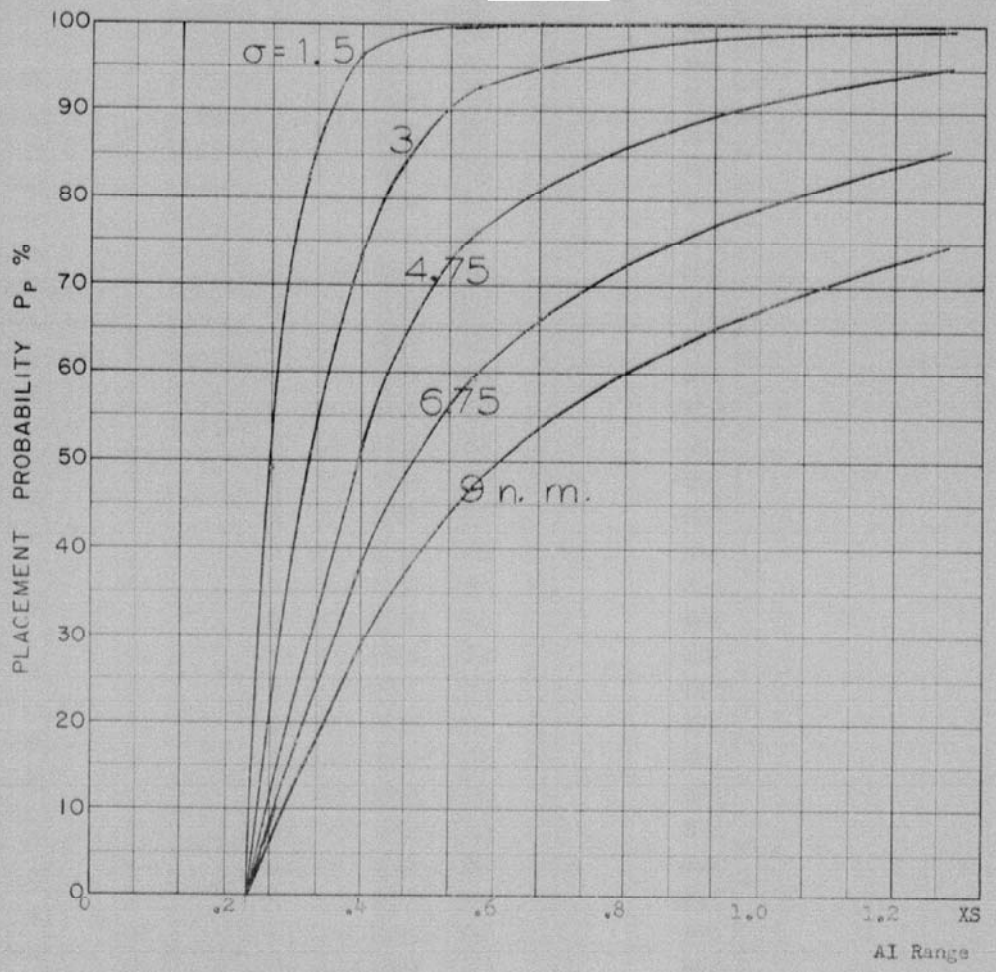

COURSE DIFFERENCE: 100°
TARGET EVASION: 0
TARGET MACH NO.: 2.0
INTERCEPTOR LATERAL G's: 3.35
INTERCEPTOR MACH NO.: 1.5
σ OF G.C.I. ACCURACY: Five values
A.I. DETECTION RANGE AS FRACTION OF SPECIFICATION RANGE, S: Abscissa
A.I. DETECTION RANGE CONTOUR: Straight Wing
ALTITUDE: 60K

S106a

Missile launch zone L-9, maximum range, 8° heading error.

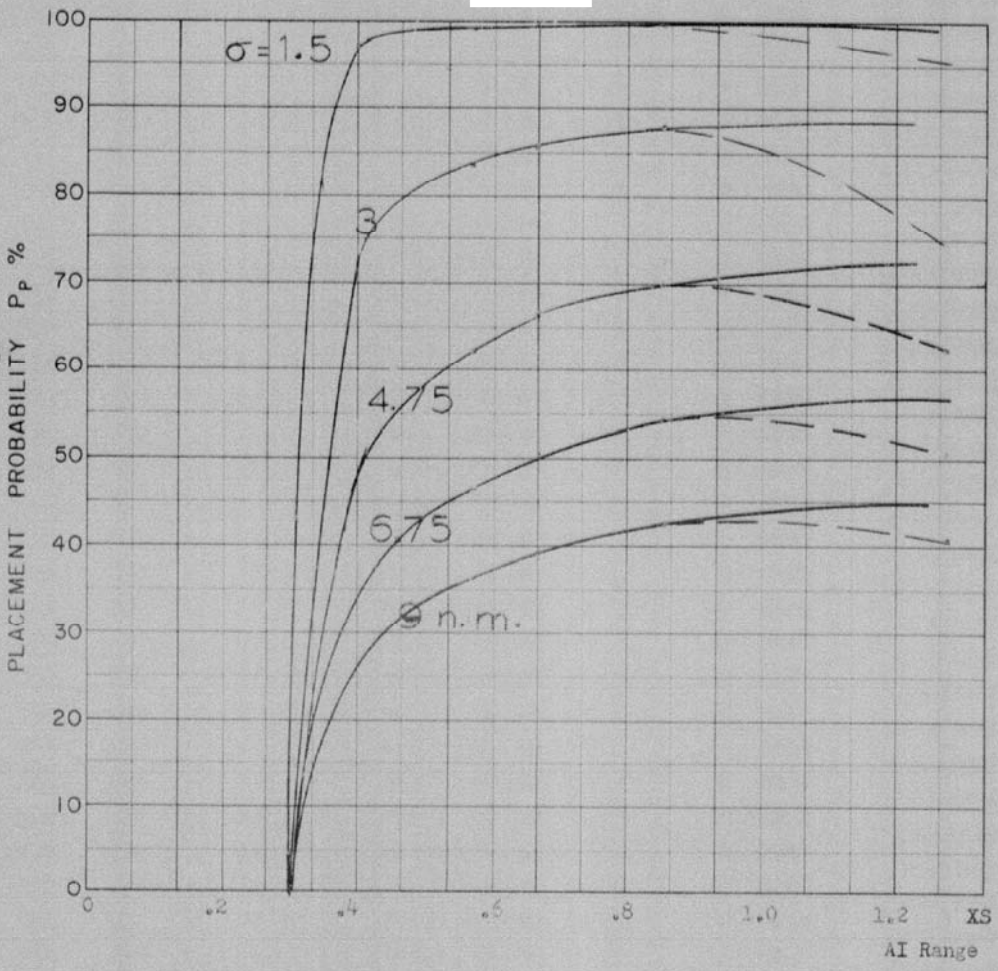

COURSE DIFFERENCE: 100°
TARGET EVASION: 0
TARGET MACH NO.: 2.0
INTERCEPTOR LATERAL G's: 3.35
INTERCEPTOR MACH NO.: 1.5
σ OF G.C.I. ACCURACY: Five values
A.I. DETECTION RANGE AS FRACTION OF SPECIFICATION RANGE, S: Abscissa
A.I. DETECTION RANGE CONTOUR: Straight Wing
ALTITUDE: 60K

S1066

Missile launch zone L-3, minimum range, 8° heading error.

6bspr

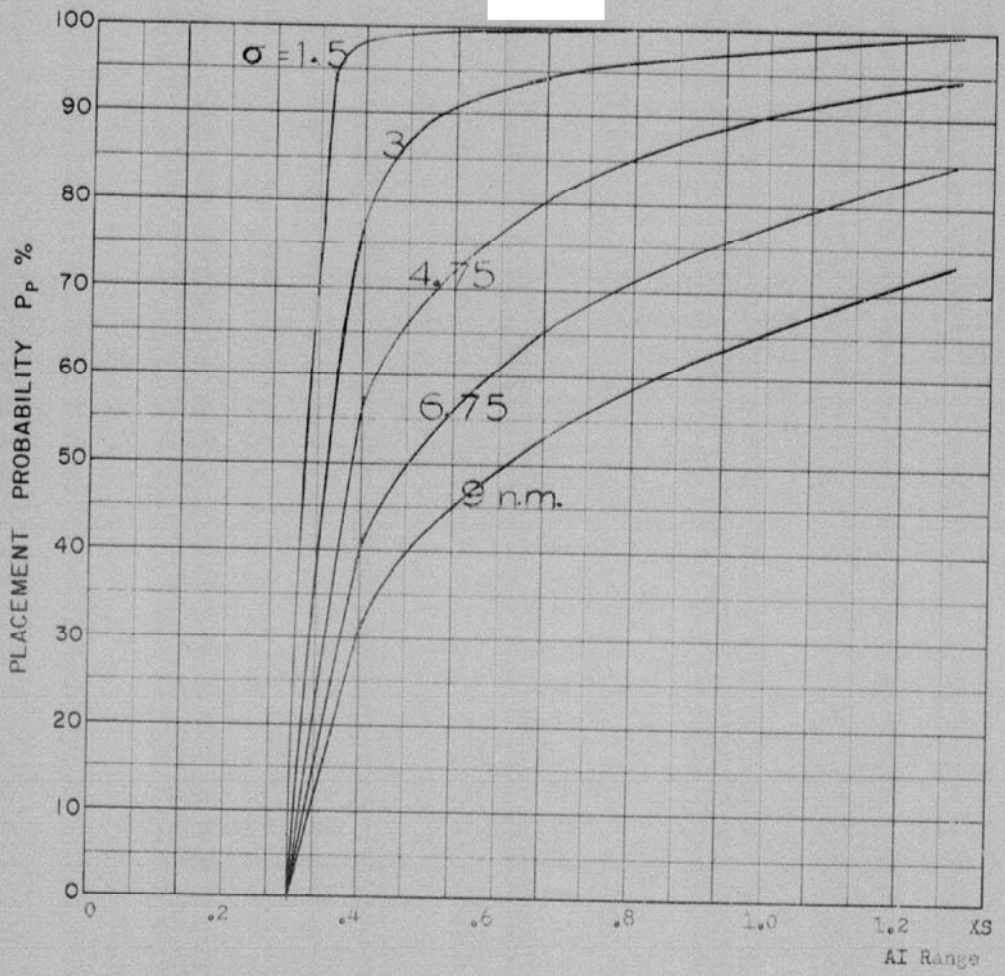

COURSE DIFFERENCE: 100°
TARGET EVASION: 0
TARGET MACH NO.: 2.0
INTERCEPTOR LATERAL G's: 3.35
INTERCEPTOR MACH NO.: 1.5
σ OF G.C.I. ACCURACY: Five values
A.I. DETECTION RANGE AS FRACTION OF SPECIFICATION RANGE, S: Abscissa
A.I. DETECTION RANGE CONTOUR: Straight Wing
ALTITUDE: 60K

S106d

Missile launch zone L-5, maximum range, 15° heading error.

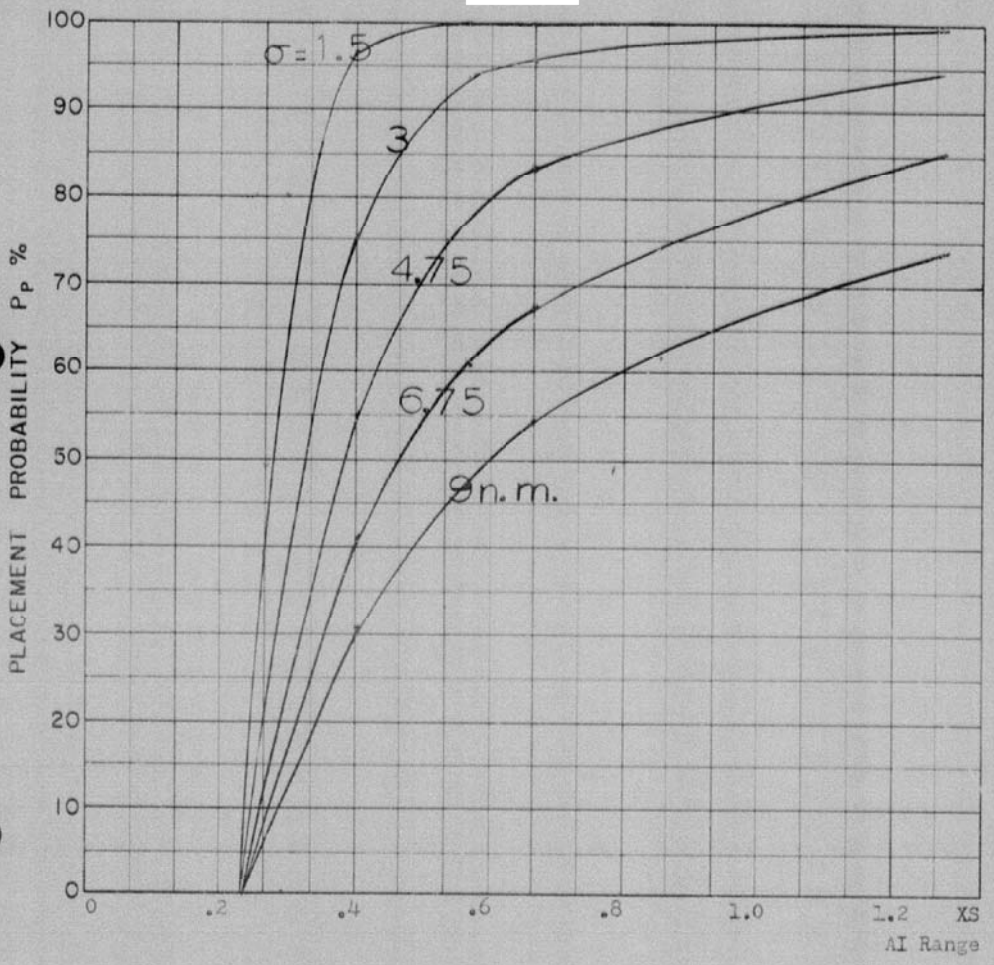

COURSE DIFFERENCE: 100°
TARGET EVASION: 0
TARGET MACH NO.: 2.0
INTERCEPTOR LATERAL G's: 3.35
INTERCEPTOR MACH NO.: 1.5
σ OF G.C.I. ACCURACY: Five values
A.I. DETECTION RANGE AS FRACTION OF SPECIFICATION RANGE, S: Abscissa
A.I. DETECTION RANGE CONTOUR: Straight Wing
ALTITUDE: 60K

S106d

Missile launch zone L-6.

23espr

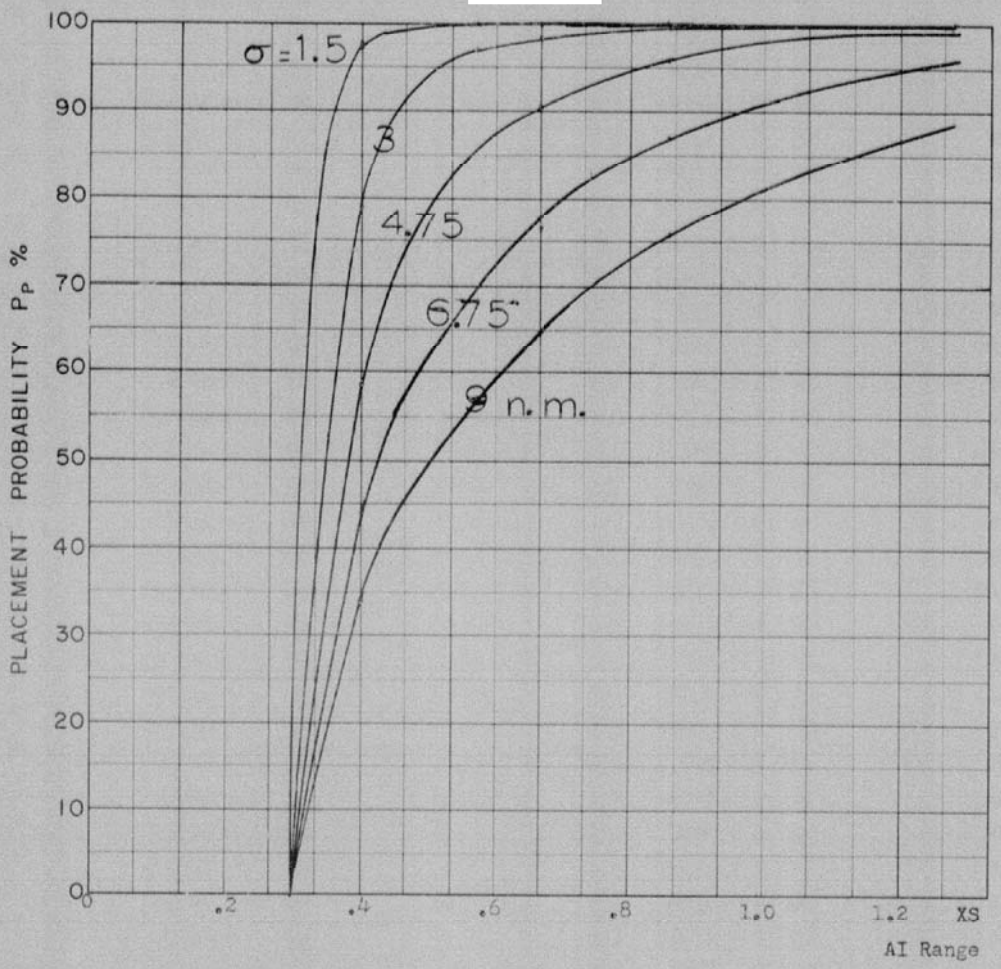

COURSE DIFFERENCE: 120°
TARGET EVASION: 0
TARGET MACH NO.: 2.0
INTERCEPTOR LATERAL G's: 3.35
INTERCEPTOR MACH NO.: 1.5
σ OF G.C.I. ACCURACY: Five values
A.I. DETECTION RANGE AS FRACTION OF SPECIFICATION RANGE, S: Abscissa
A.I. DETECTION RANGE CONTOUR: Straight Wing
ALTITUDE: 60K

S107a

Missile launch zone L-9, maximum range, 8° heading error.

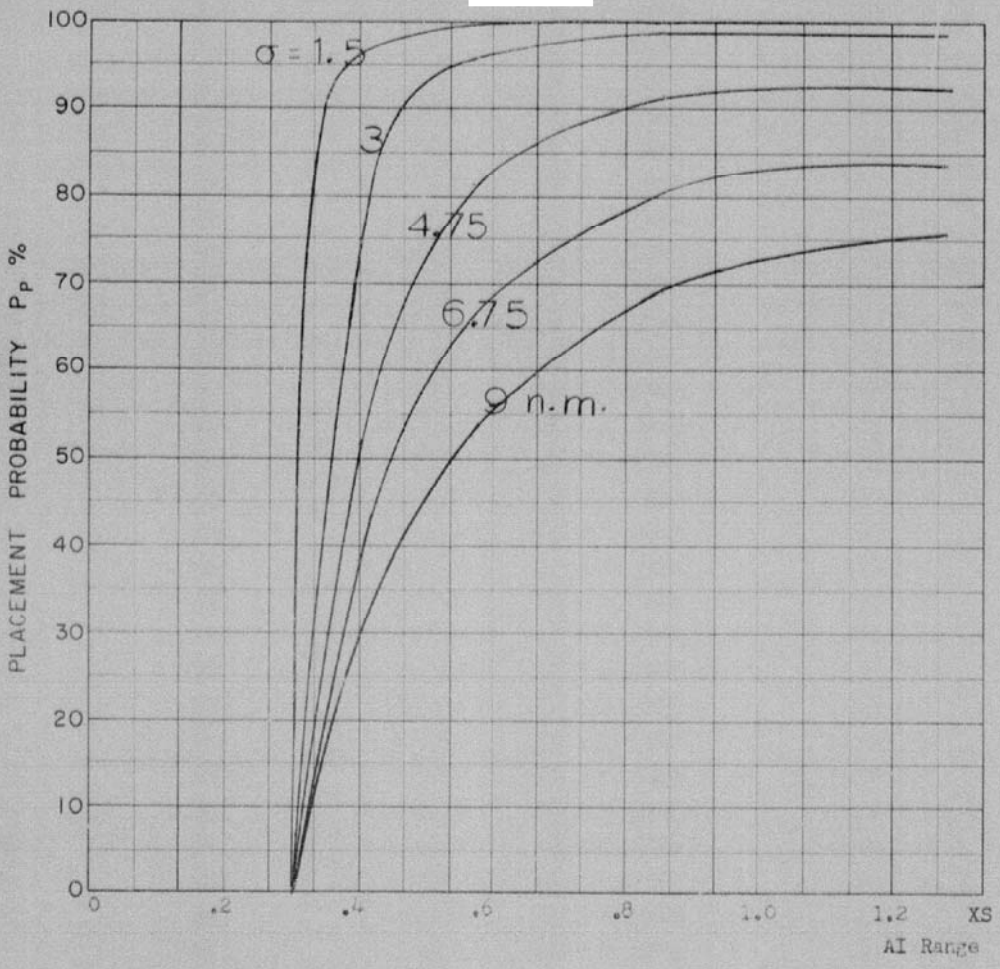

COURSE DIFFERENCE: 120°
TARGET EVASION: 0
TARGET MACH NO.: 2.0
INTERCEPTOR LATERAL G's: 3.35
INTERCEPTOR MACH NO.: 1.5
σ OF G.C.I. ACCURACY: Five values
A.I. DETECTION RANGE AS FRACTION OF SPECIFICATION RANGE, S: Abscissa
A.I. DETECTION RANGE CONTOUR: Straight Wing
ALTITUDE: 60K

(S107b)

Missile launch zone L-5, minimum range, 8° heading error.

6dspr

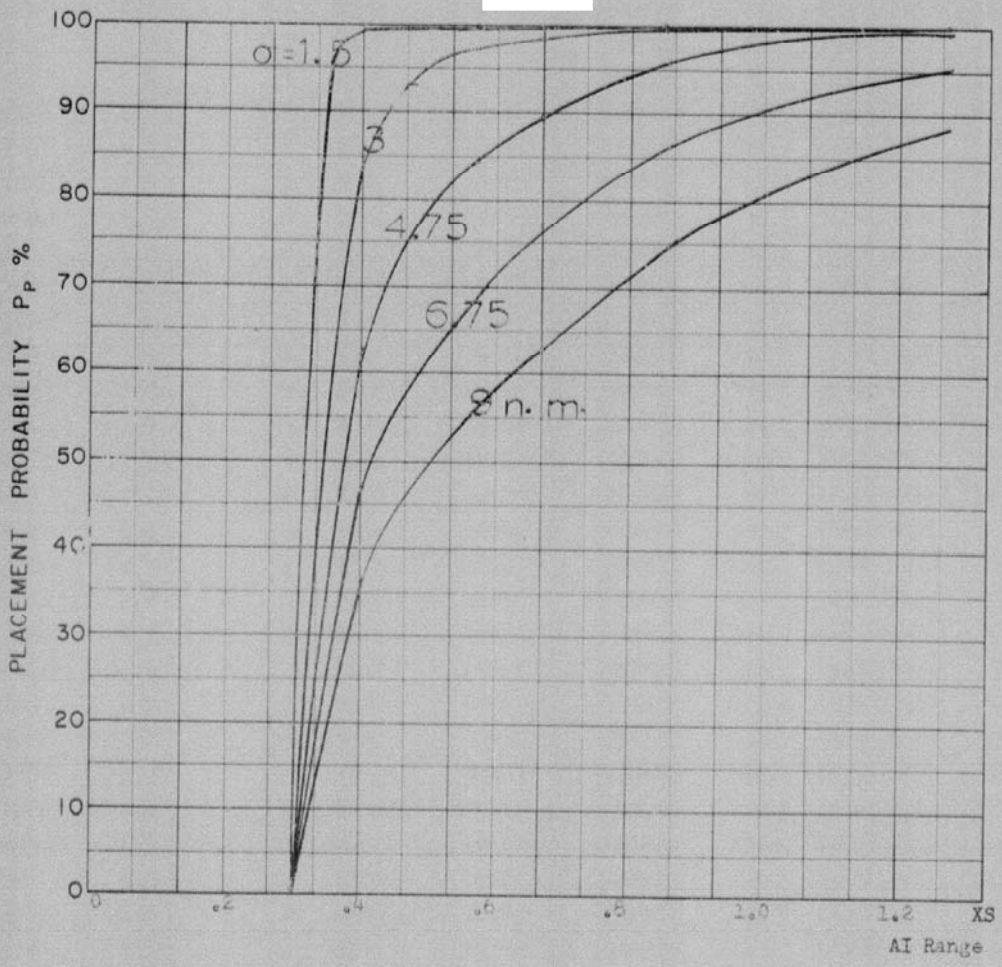

COURSE DIFFERENCE: 120°
TARGET EVASION: 0
TARGET MACH NO.: 2.0
INTERCEPTOR LATERAL G's: 3.35
INTERCEPTOR MACH NO.: 1.5
σ OF G.C.I. ACCURACY: Five values
A.I. DETECTION RANGE AS FRACTION OF SPECIFICATION RANGE, S: Abscissa
A.I. DETECTION RANGE CONTOUR: Straight Wing
ALTITUDE: 60K

(S107c)

Missile launch zone L-5, maximum range, 15° heading error.

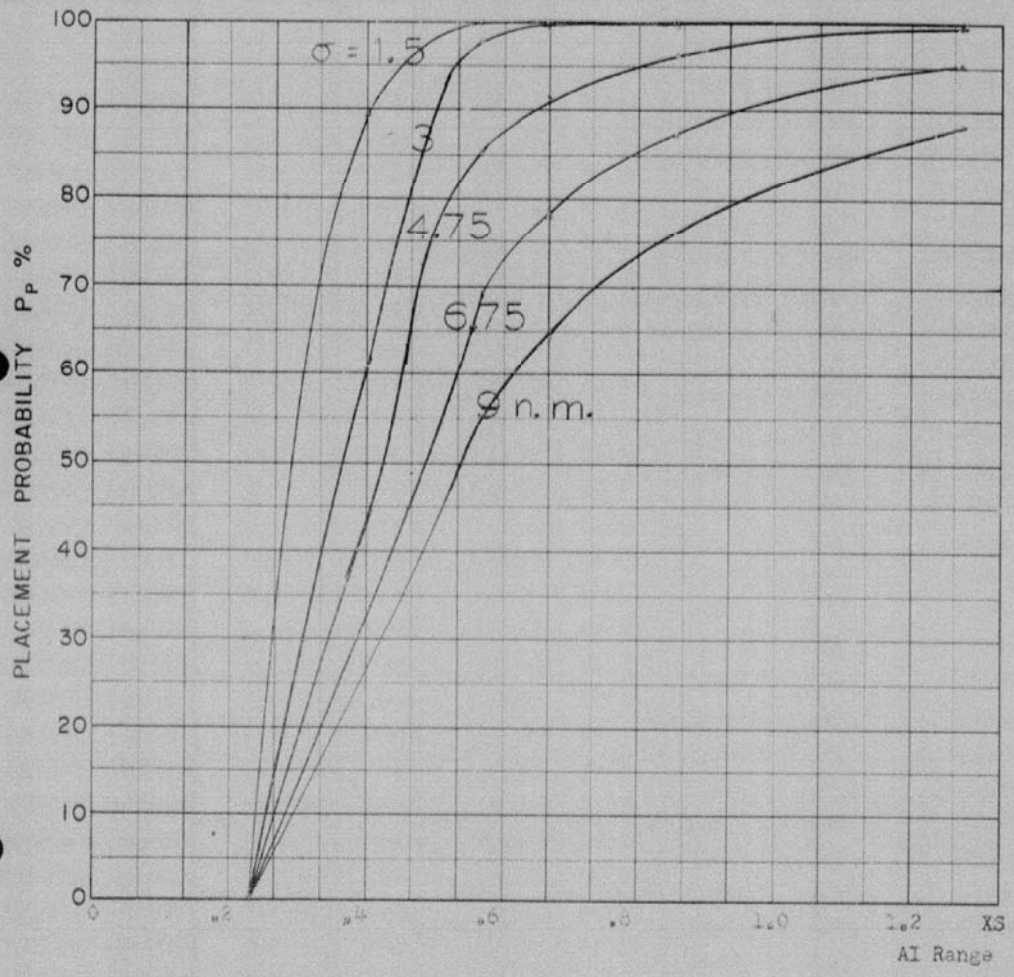

COURSE DIFFERENCE: 120°
TARGET EVASION: 0
TARGET MACH NO.: 2.0
INTERCEPTOR LATERAL G's: 3.35
INTERCEPTOR MACH NO.: 1.5
σ OF G.C.I. ACCURACY: Five values
A.I. DETECTION RANGE AS FRACTION OF SPECIFICATION RANGE, S: Abscissa
A.I. DETECTION RANGE CONTOUR: Straight Wing
ALTITUDE: 60K

(S107d)

Missile Launch zone L-6.

13dspr

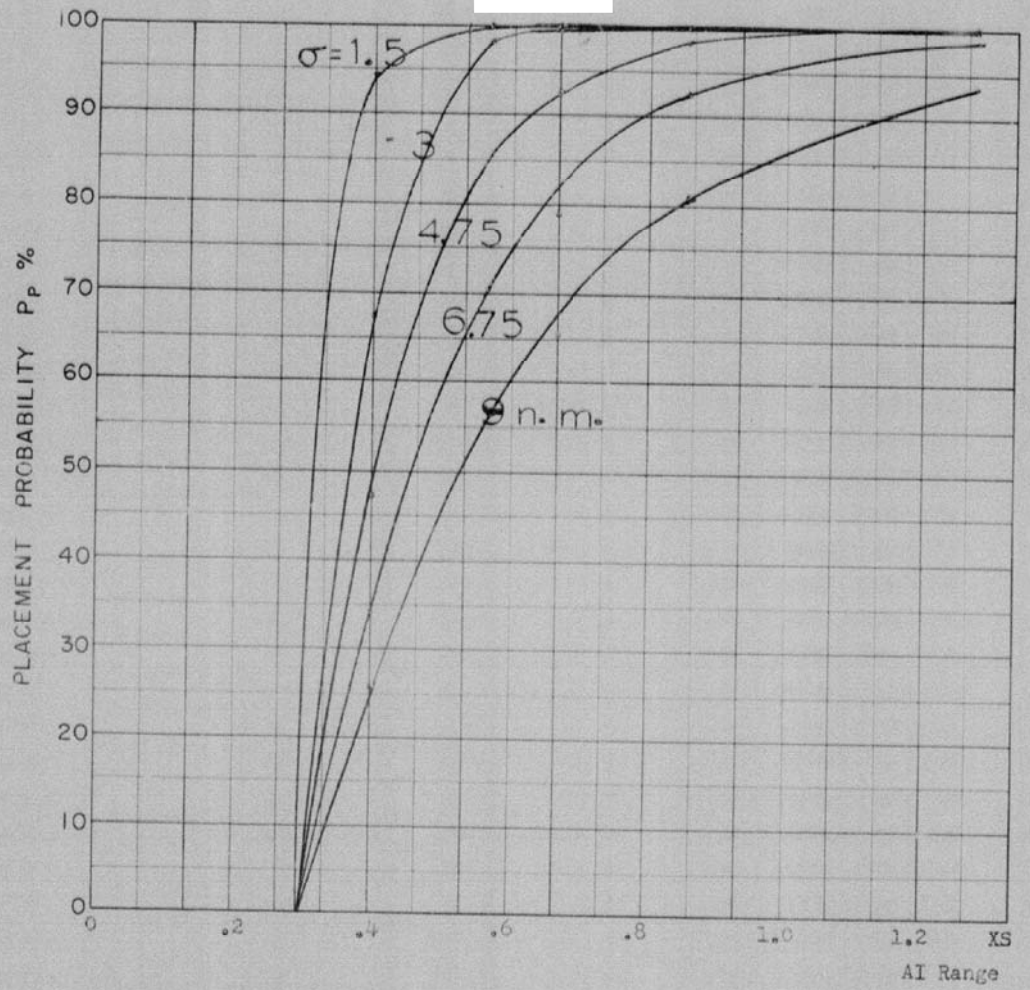

COURSE DIFFERENCE: 135°
TARGET EVASION: 0
TARGET MACH NO.: 2.0
INTERCEPTOR LATERAL G's: 3.35
INTERCEPTOR MACH NO.: 1.5
σ OF G.C.I. ACCURACY: Five values
A.I. DETECTION RANGE AS FRACTION OF SPECIFICATION RANGE, S: Abscissa
A.I. DETECTION RANGE CONTOUR: Straight Wing
ALTITUDE: 60K

S108a

Missile launch zone L-9, maximum range, 8° heading error.

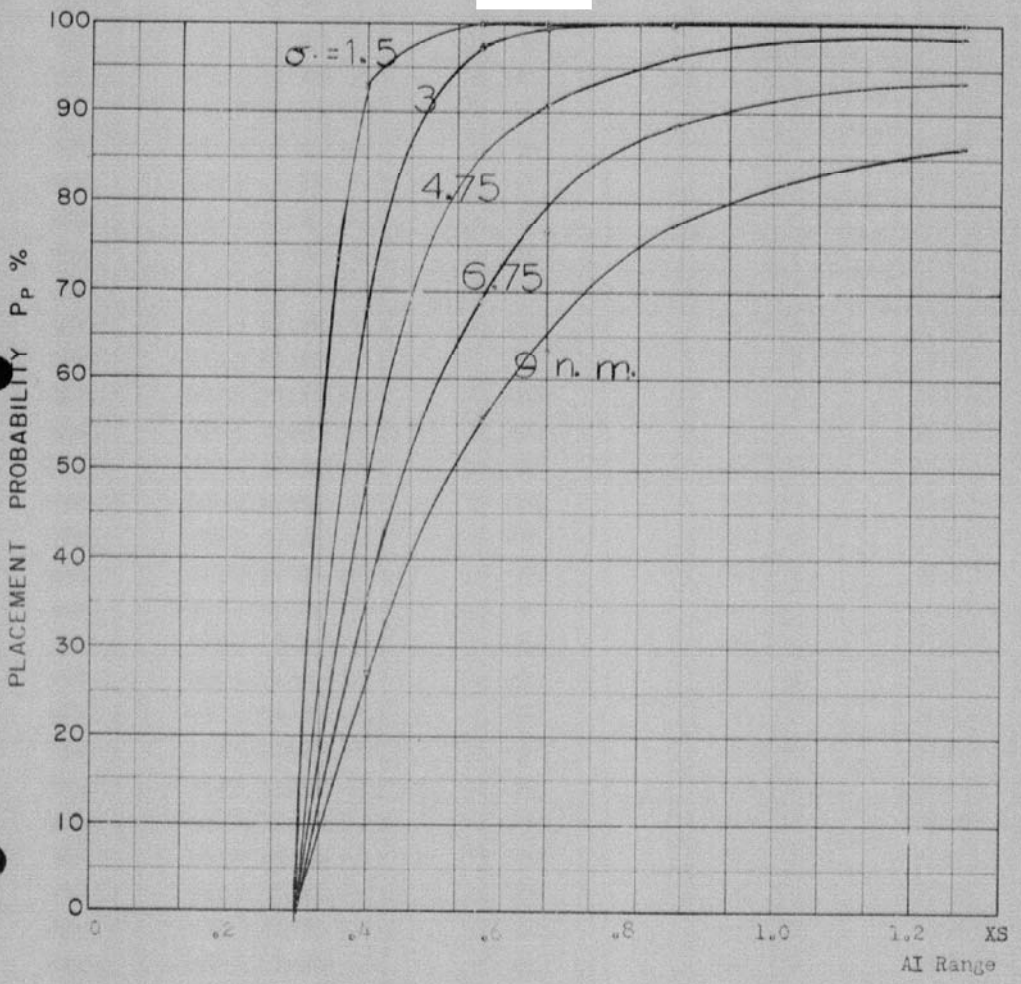

COURSE DIFFERENCE: 135°
TARGET EVASION: 0
TARGET MACH NO.: 2.0
INTERCEPTOR LATERAL G's: 3.35
INTERCEPTOR MACH NO.: 1.5
σ OF G.C.I. ACCURACY: Five values
A.I. DETECTION RANGE AS FRACTION OF SPECIFICATION RANGE, S: Abscissa
A.I. DETECTION RANGE CONTOUR: Straight Wing
ALTITUDE: 60K

S1086

Missile launch zone L-5 minimum range, 8° heading error.

6dspr

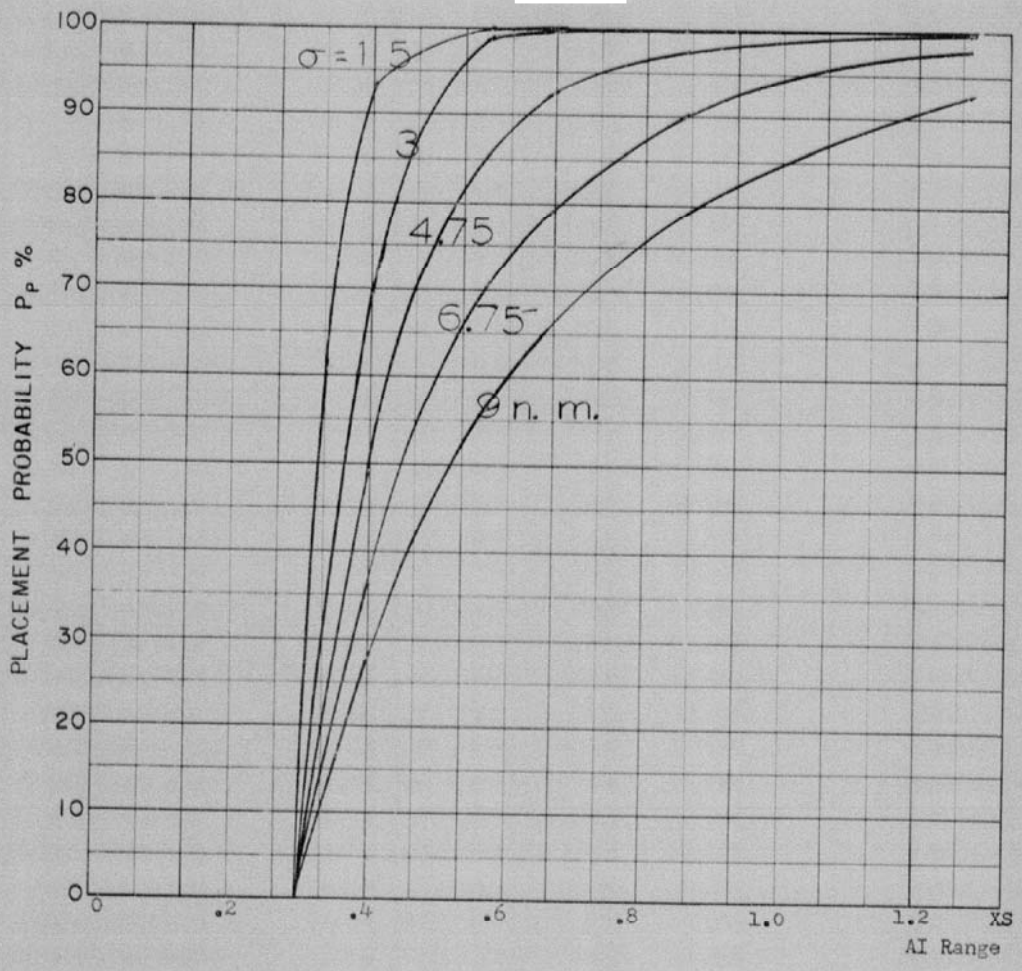

COURSE DIFFERENCE: 135°
TARGET EVASION: 0
TARGET MACH NO.: 2.0
INTERCEPTOR LATERAL G's: 3.35
INTERCEPTOR MACH NO.: 1.5
σ OF G.C.I. ACCURACY: Five values
A.I. DETECTION RANGE AS FRACTION OF SPECIFICATION RANGE, S: Abscissa
A.I. DETECTION RANGE CONTOUR: Straight Wing.
ALTITUDE: 60K

S108c

Missile Launch zone I-5, maximum range, 15° heading error.

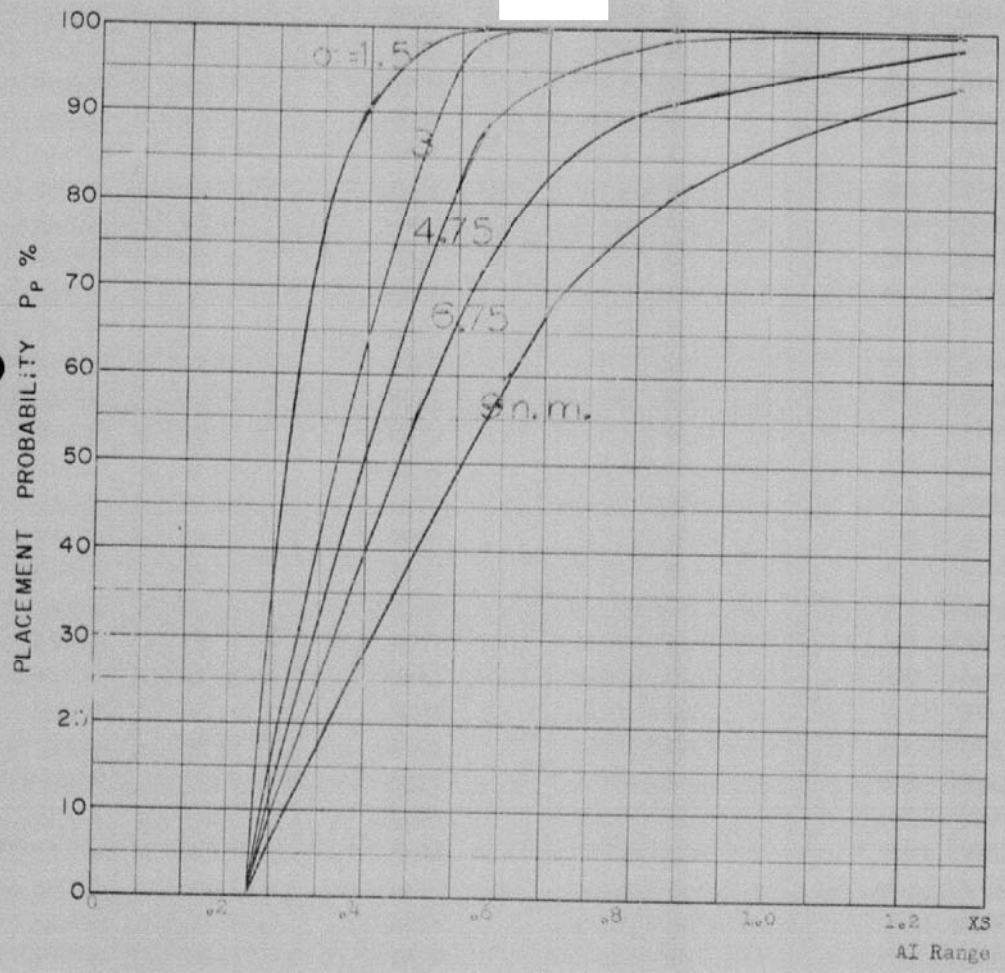

COURSE DIFFERENCE: 135°
TARGET EVASION: 0
TARGET MACH NO.: 2.0
INTERCEPTOR LATERAL G's: 3.35
INTERCEPTOR MACH NO.: 1.5
σ OF G.C.I. ACCURACY: Five values
A.I. DETECTION RANGE AS FRACTION OF SPECIFICATION RANGE, S: Abscissa
A.I. DETECTION RANGE CONTOUR: Straight Wing
ALTITUDE: 60K

Missile Launch Zone L.G.

S108d

13espr

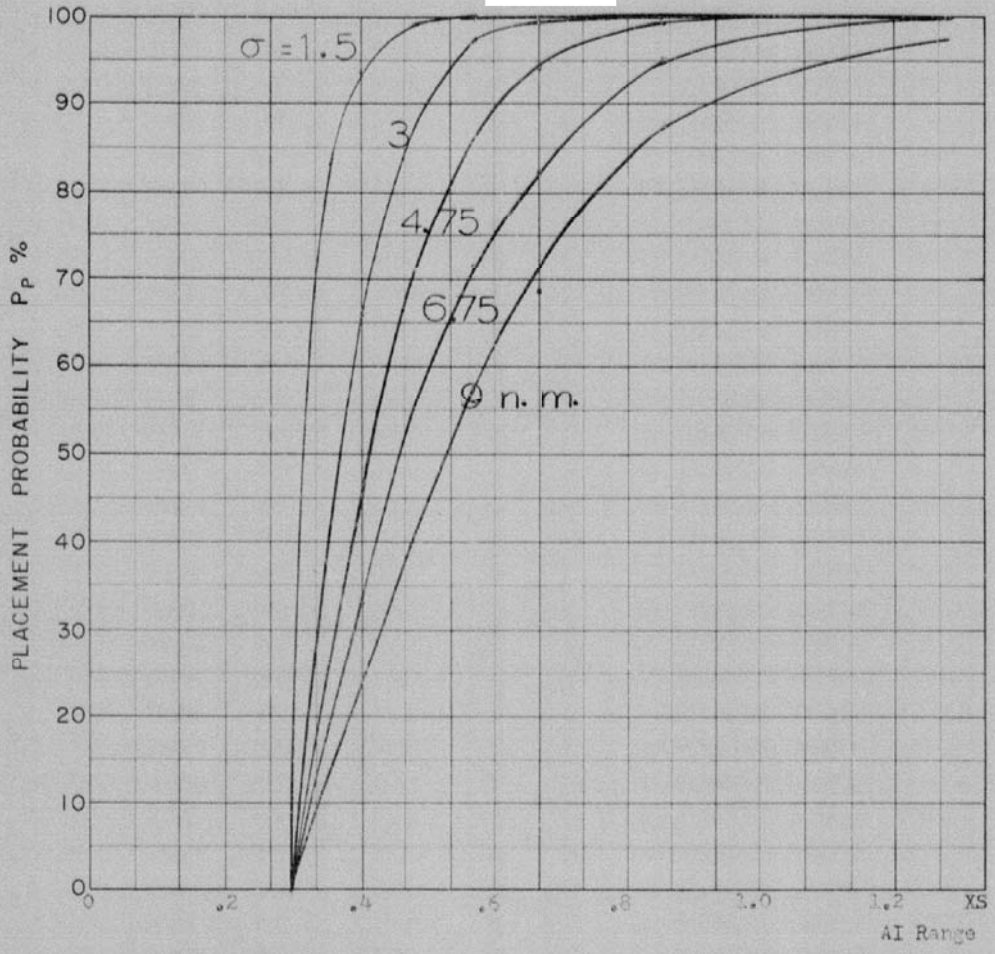

COURSE DIFFERENCE: 160°
TARGET EVASION: 0
TARGET MACH NO.: 2.0
INTERCEPTOR LATERAL G's: 3.35
INTERCEPTOR MACH NO.: 1.5
σ OF G.C.I. ACCURACY: Five values
A.I. DETECTION RANGE AS FRACTION OF SPECIFICATION RANGE, S: Abscissa
A.I. DETECTION RANGE CONTOUR: Straight Wing
ALTITUDE: 60K

S109a

Missile launch zone L-9, maximum range, 8° heading error.

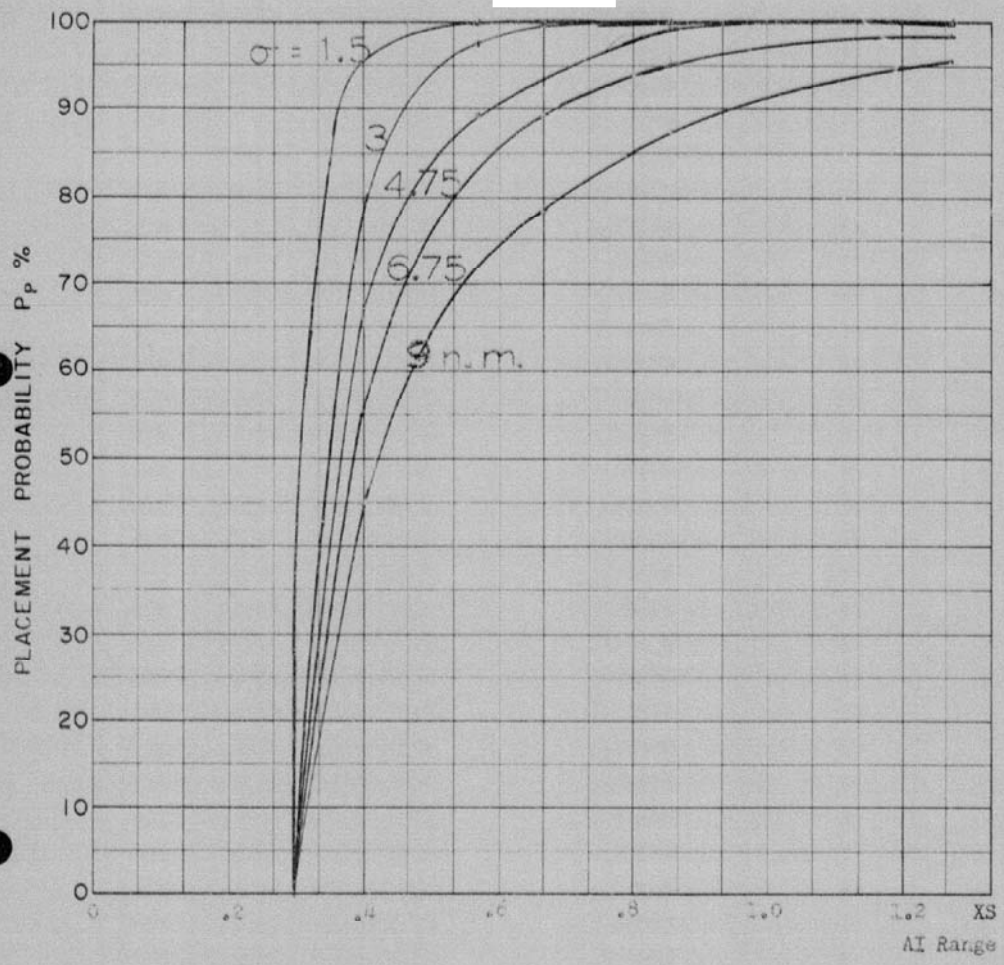

COURSE DIFFERENCE: 160°
TARGET EVASION: 0
TARGET MACH NO.: 2.0
INTERCEPTOR LATERAL G's: 3.05
INTERCEPTOR MACH NO.: 1.5
σ OF G.C.I. ACCURACY: Five values
A.I. DETECTION RANGE AS FRACTION OF SPECIFICATION RANGE, S: Abscissa
A.I. DETECTION RANGE CONTOUR: Straight Wing
ALTITUDE: 60K

S109b

Missile launch zone L-5, minimum range, 8° heading error.

6espr

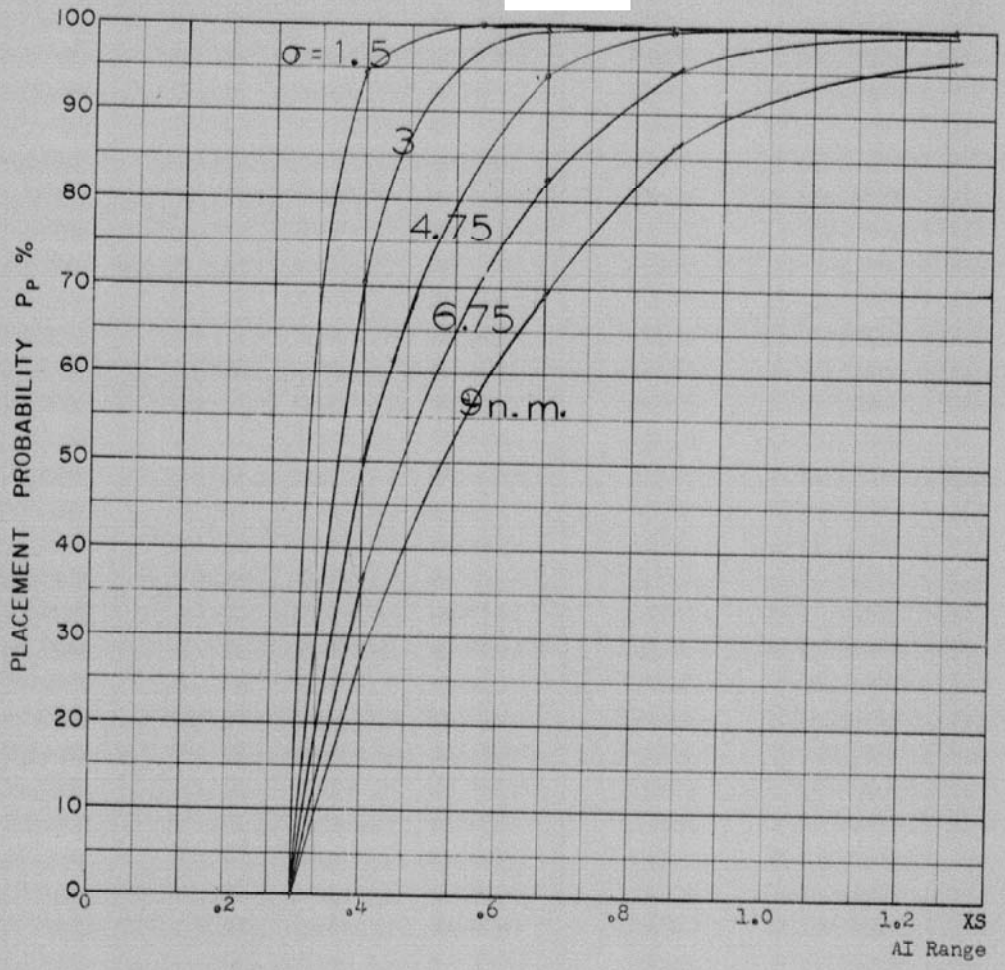

COURSE DIFFERENCE: 160°
TARGET EVASION: 0
TARGET MACH NO.: 2.0
INTERCEPTOR LATERAL G's: 3.35
INTERCEPTOR MACH NO.: 1.5
σ OF G.C.I. ACCURACY: Five values
A.I. DETECTION RANGE AS FRACTION OF SPECIFICATION RANGE, S: Abscissa
A.I. DETECTION RANGE CONTOUR: Straight Wing
ALTITUDE: 60K

S109c

Missile launch zone L-5, maximum range, 15° heading error.

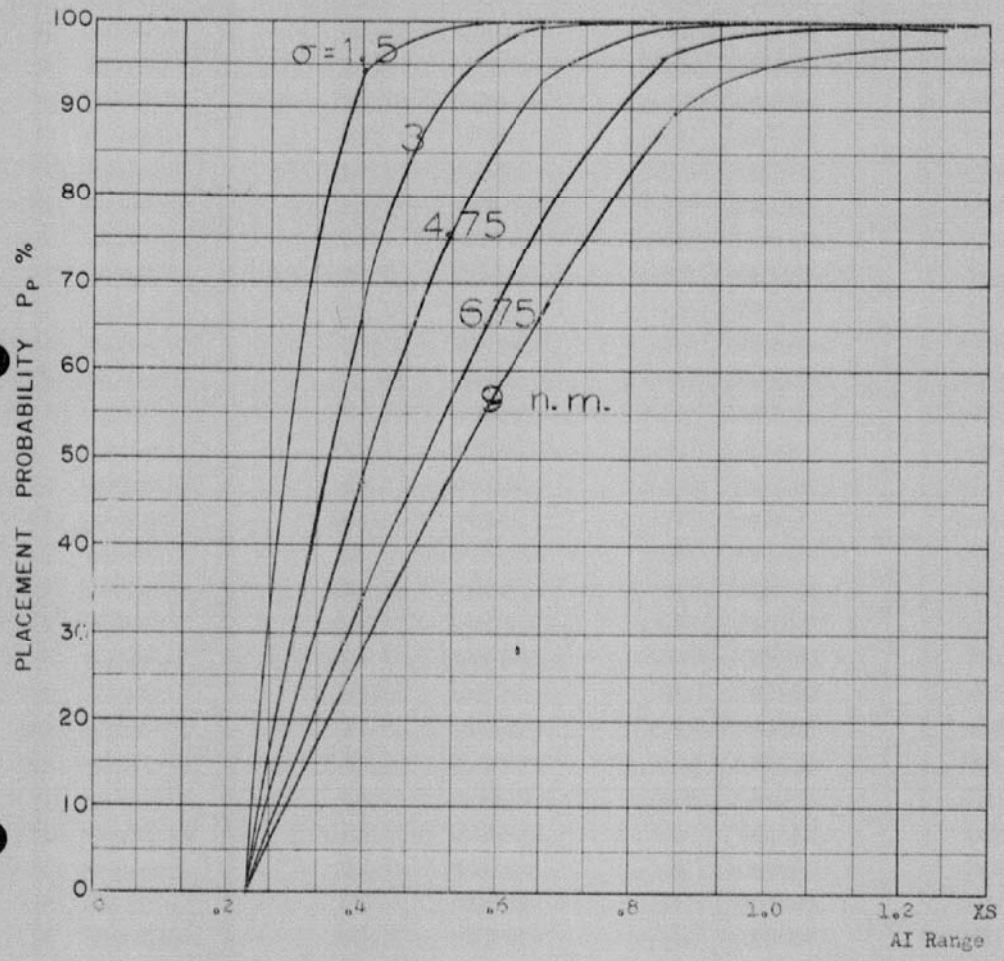

COURSE DIFFERENCE: 160°
TARGET EVASION: 0
TARGET MACH NO.: 2.0
INTERCEPTOR LATERAL G's: 3.35
INTERCEPTOR MACH NO.: 1.5
σ OF G.C.I. ACCURACY: Five values
A.I. DETECTION RANGE AS FRACTION OF SPECIFICATION RANGE, S: Abscissa
A.I. DETECTION RANGE CONTOUR: Straight Wing
ALTITUDE: 60K

Missile Launch zone L-6.

(S109d)

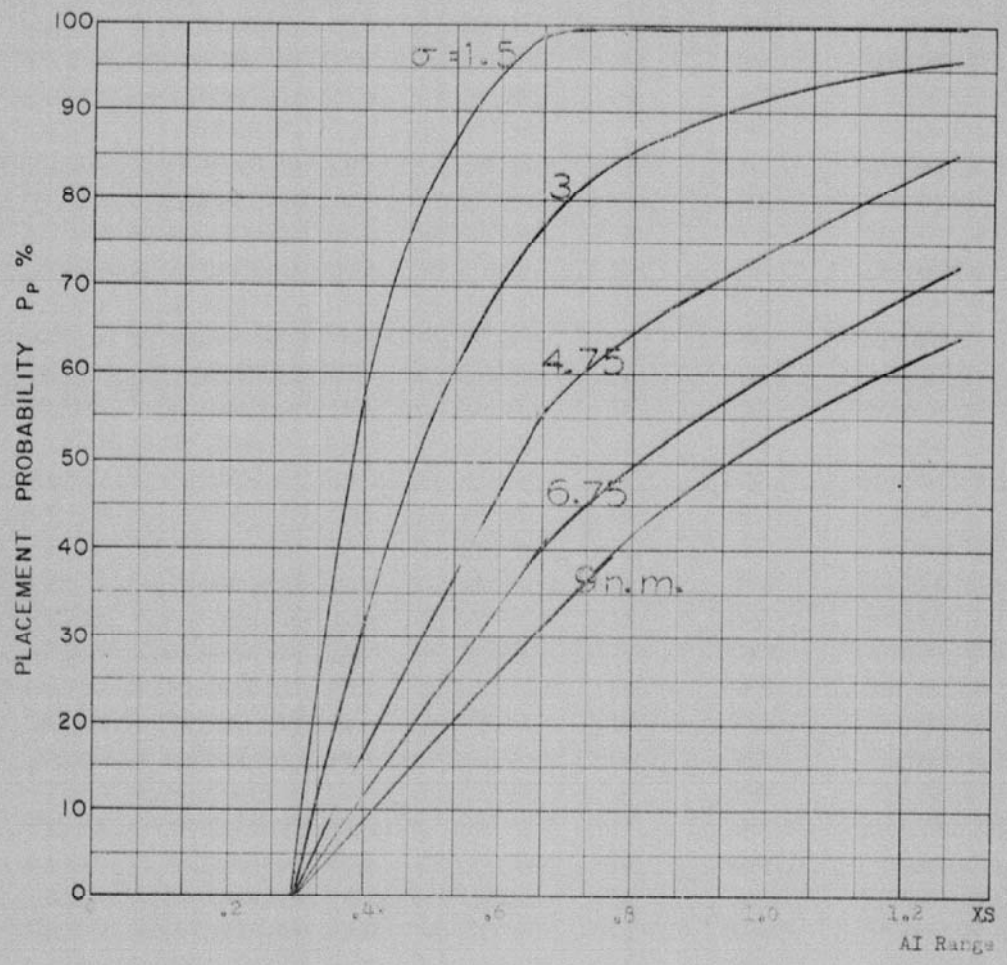

COURSE DIFFERENCE: 90°
TARGET EVASION: 0
TARGET MACH NO.: 2.0
INTERCEPTOR LATERAL G's: 1.12
INTERCEPTOR MACH NO.: .85
σ OF G.C.I. ACCURACY: Five values
A.I. DETECTION RANGE AS FRACTION OF SPECIFICATION RANGE, S: Abscissa
A.I. DETECTION RANGE CONTOUR: Strai ht Wing
ALTITUDE: 60K

S110b

Missile Launch Zone L-6, maximum range, 8° heading error.

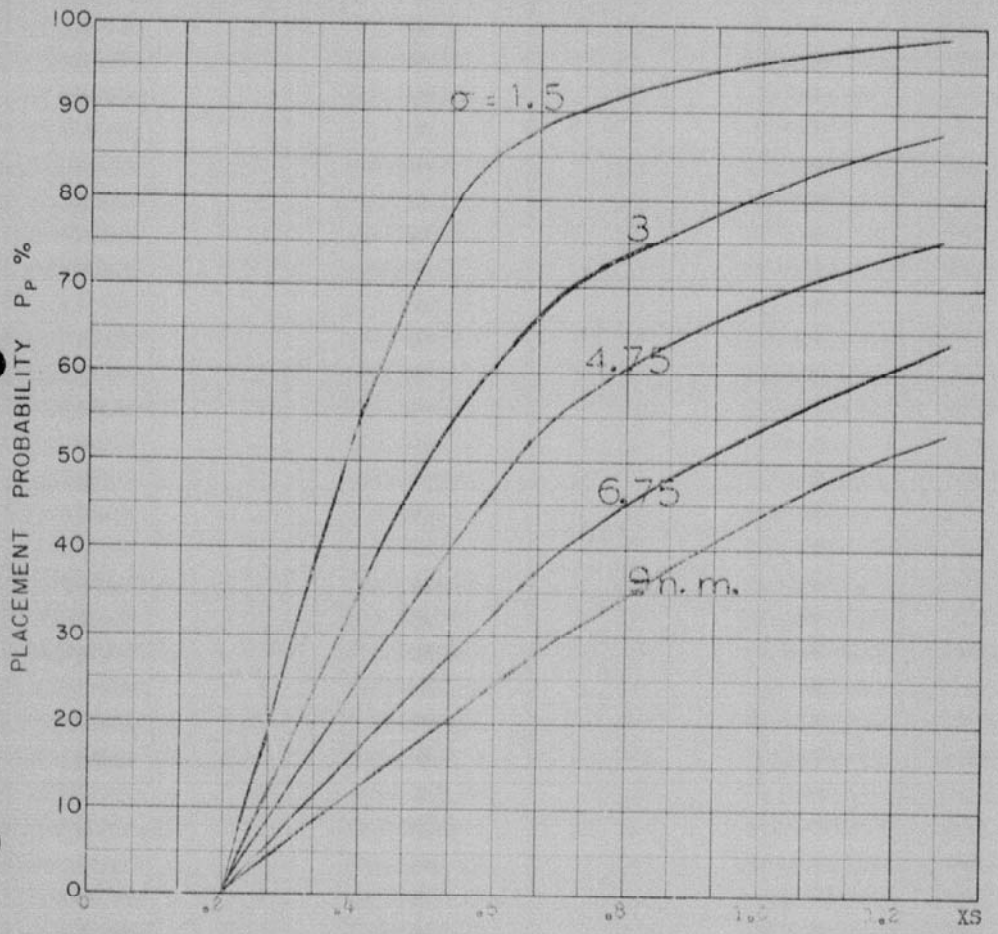

COURSE DIFFERENCE: 90°
TARGET EVASION: 0
TARGET MACH NO.: 2.0
INTERCEPTOR LATERAL G's: 1.2
INTERCEPTOR MACH NO.: .85
σ OF G.C.I. ACCURACY: Five values
A.I. DETECTION RANGE AS FRACTION OF SPECIFICATION RANGE, S: Abscissa
A.I. DETECTION RANGE CONTOUR: Straight Wing
ALTITUDE: 60K

S110 c

Launch time I-7.

10bspr

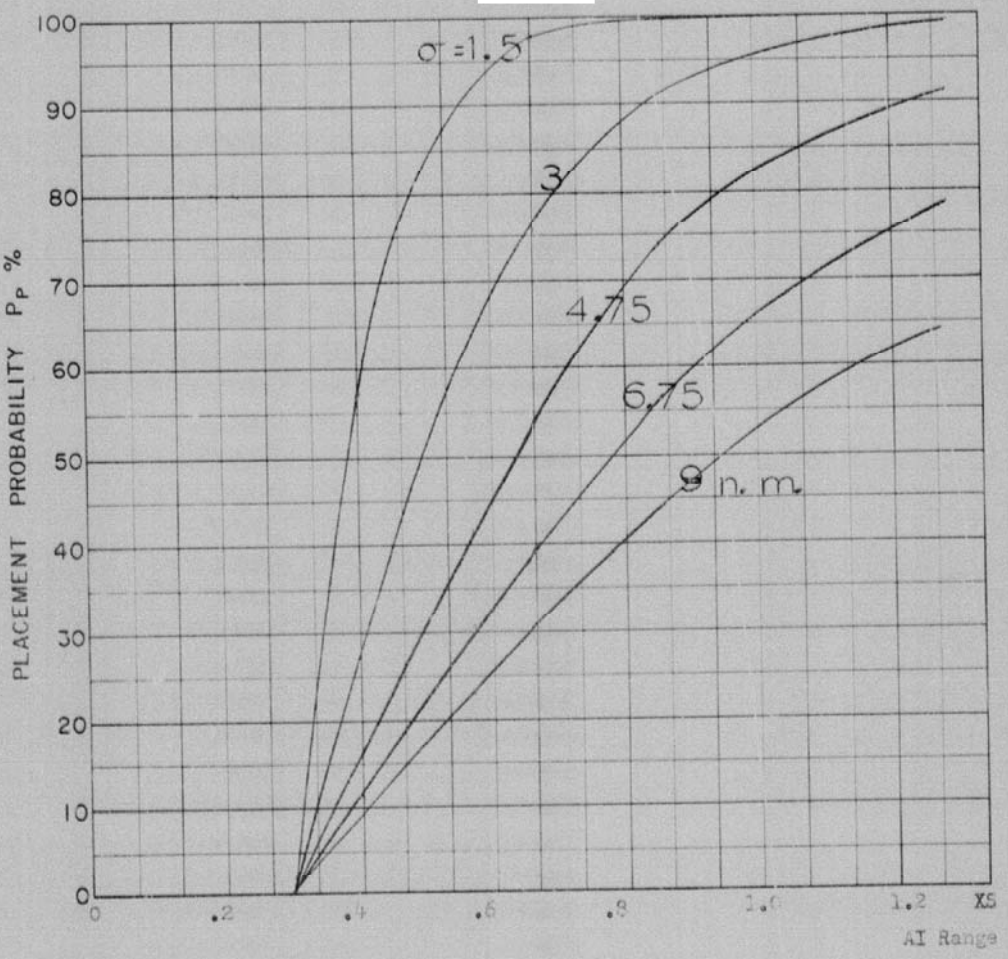

COURSE DIFFERENCE: 100°
TARGET EVASION: 0
TARGET MACH NO.: 2.0
INTERCEPTOR LATERAL G's: 1.12
INTERCEPTOR MACH NO.: 1.5
σ OF G.C.I. ACCURACY: Five values
A.I. DETECTION RANGE AS FRACTION OF SPECIFICATION RANGE, S: Abscissa
A.I. DETECTION RANGE CONTOUR: Straight Wing
ALTITUDE: 60K

S111b

Missile launch zone L-6, maximum range, 8° heading error.

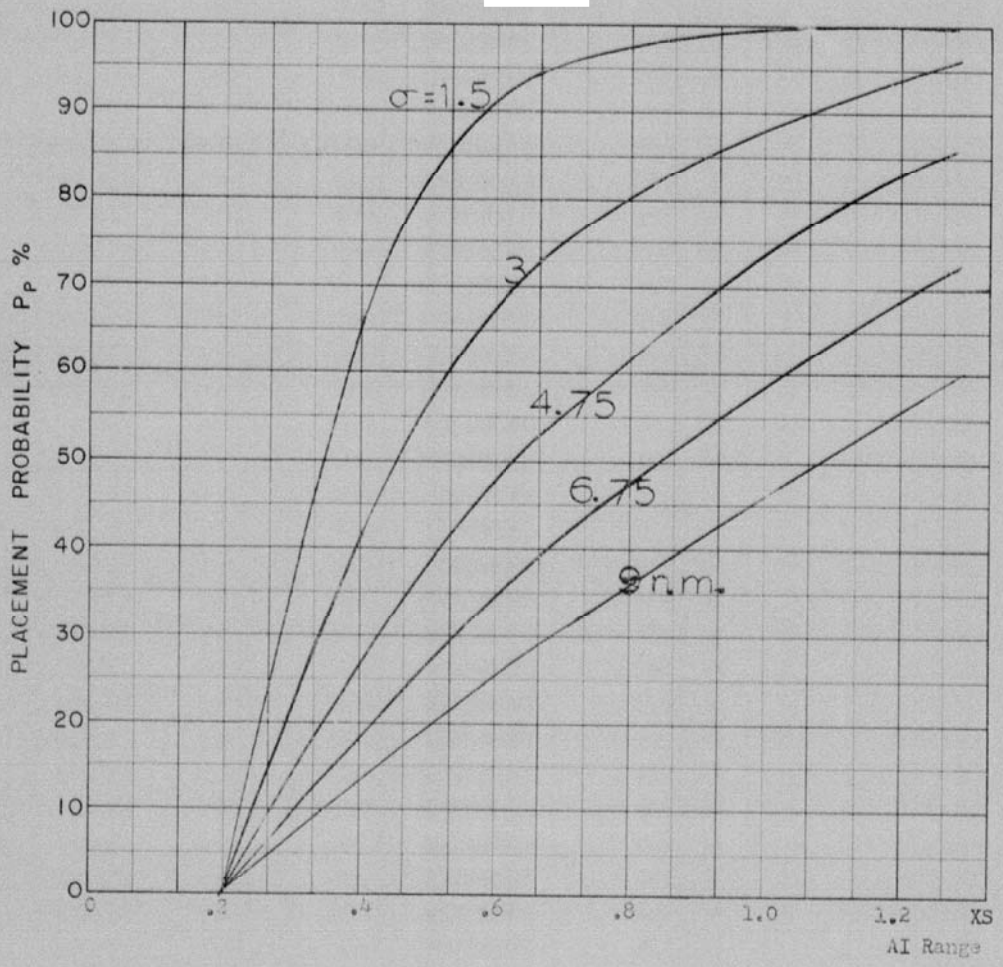

COURSE DIFFERENCE: 100°
TARGET EVASION: 0
TARGET MACH NO.: 2.0
INTERCEPTOR LATERAL G's: 1.12
INTERCEPTOR MACH NO.: 1.5
σ OF G.C.I. ACCURACY: Five values
A.I. DETECTION RANGE AS FRACTION OF SPECIFICATION RANGE, S: Abscissa
A.I. DETECTION RANGE CONTOUR: Straight Wing
ALTITUDE: 60K

S111c

Launch zone L-7.

10cspr

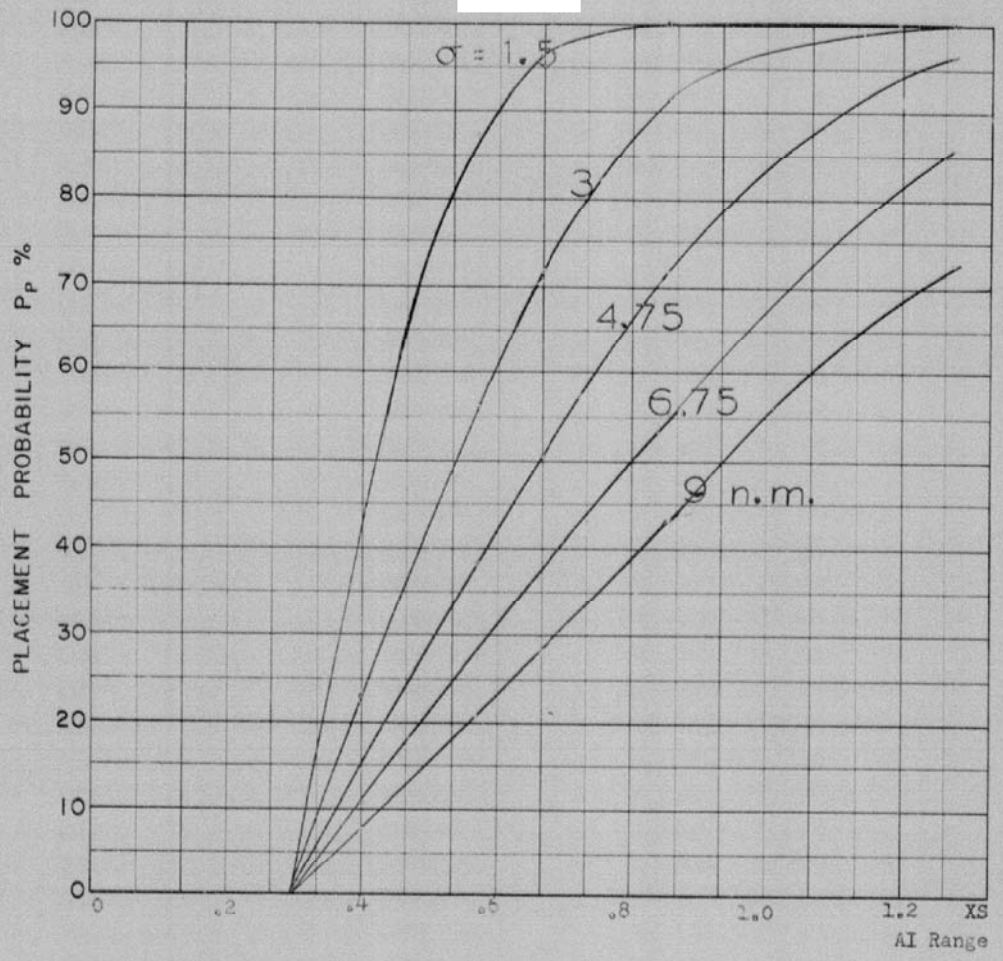

COURSE DIFFERENCE: 120°
TARGET EVASION: 0
TARGET MACH NO.: 2.0
INTERCEPTOR LATERAL G's: 1.12
INTERCEPTOR MACH NO.: 1.5
σ OF G.C.I. ACCURACY: Five values
A.I. DETECTION RANGE AS FRACTION OF SPECIFICATION RANGE, S: Abscissa
A.I. DETECTION RANGE CONTOUR: Straight Wing
ALTITUDE: 60K

S112b

Missile Launch zone L-6, maximum range, 8° heading error.

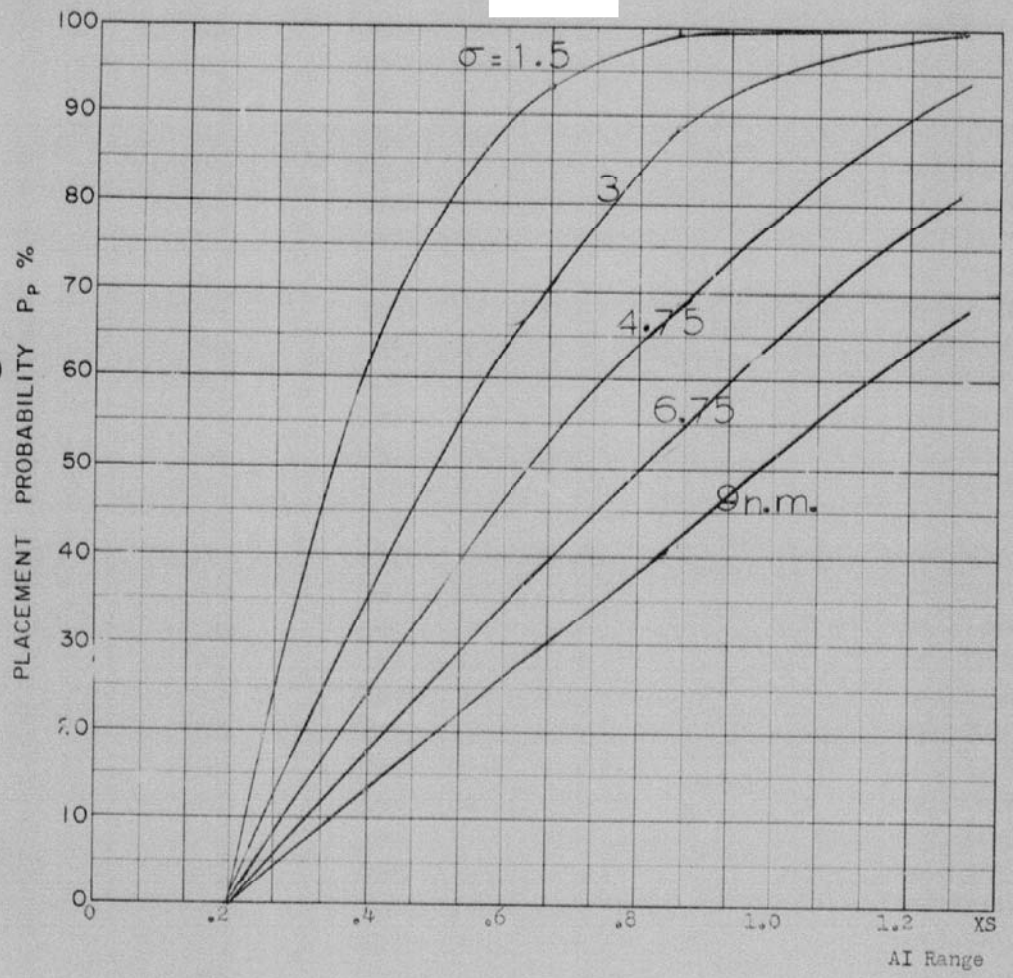

COURSE DIFFERENCE: 110°
TARGET EVASION: 0
TARGET MACH NO.: 2.0
INTERCEPTOR LATERAL G's: 1.12
INTERCEPTOR MACH NO.: 1.5
σ OF G.C.I. ACCURACY: Five values
A.I. DETECTION RANGE AS FRACTION OF SPECIFICATION RANGE, S: Abscissa
A.I. DETECTION RANGE CONTOUR: Straight Wing
ALTITUDE: 60K

S112c

Launch zone L-7.

10dspr

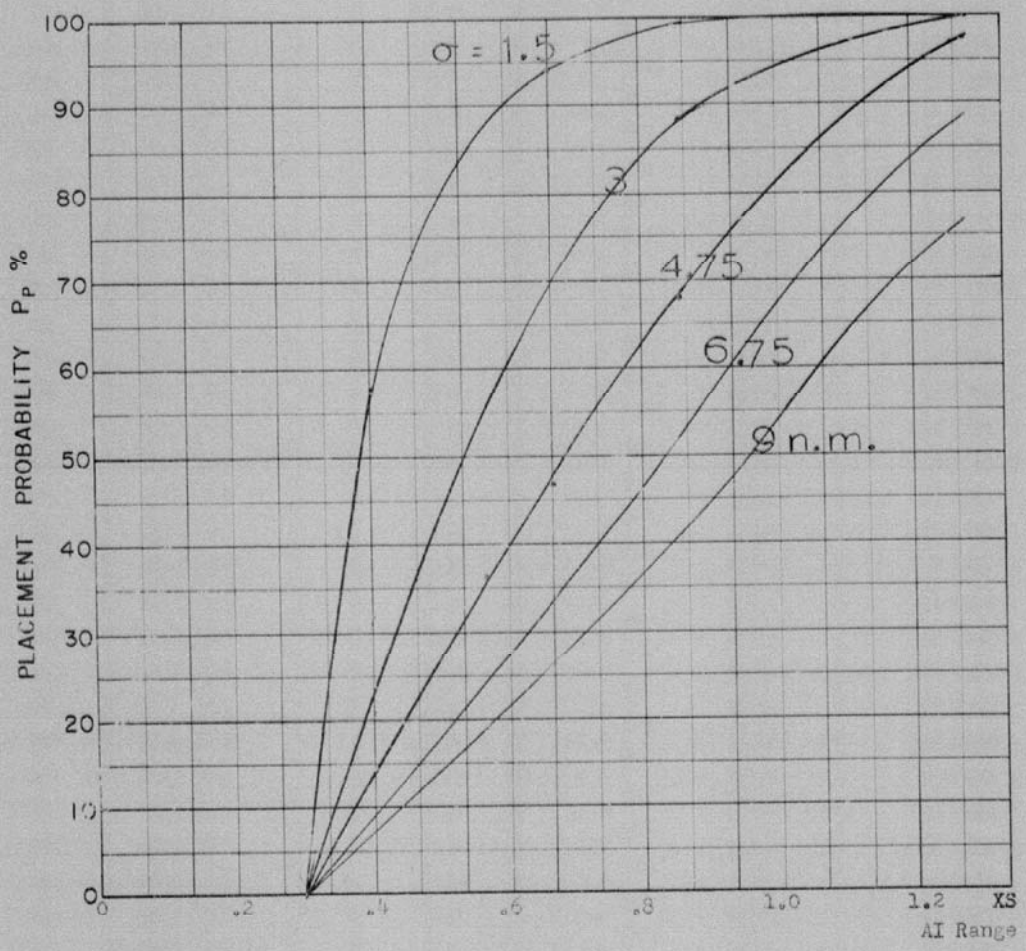

COURSE DIFFERENCE: 135°
TARGET EVASION: 0
TARGET MACH NO.: 2.0
INTERCEPTOR LATERAL G's: 1.12
INTERCEPTOR MACH NO.: 1.5
σ OF G.C.I. ACCURACY: Five values
A.I. DETECTION RANGE AS FRACTION OF SPECIFICATION RANGE, S: Abscissa
A.I. DETECTION RANGE CONTOUR: Straight Wing
ALTITUDE: 60K

(SII36)

Missile launch zone L-6, maximum range, 8° heading error.

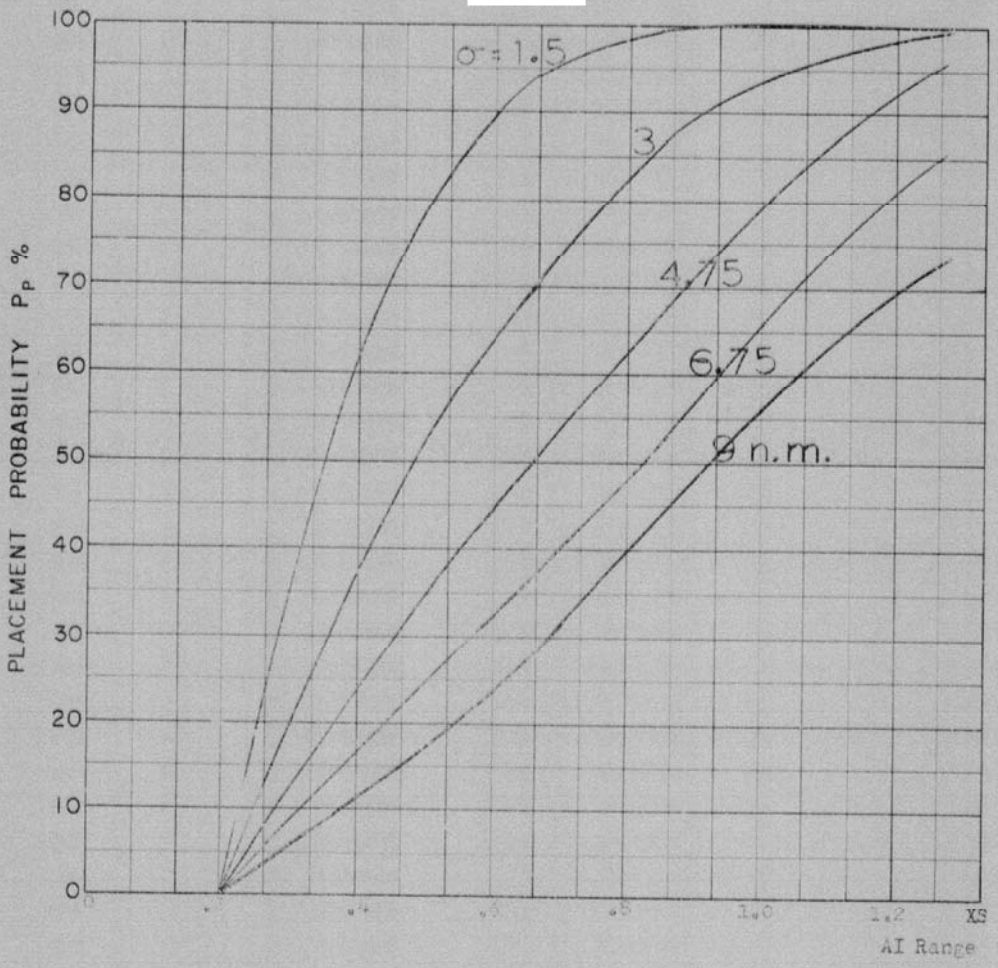

COURSE DIFFERENCE: [illegible]
TARGET EVASION: [illegible]
TARGET MACH NO.: [illegible]
INTERCEPTOR LATERAL G's: [illegible]
INTERCEPTOR MACH NO.: [illegible]
σ OF G.C.I. ACCURACY: Five values
A.I. DETECTION RANGE AS FRACTION OF SPECIFICATION RANGE, S: Abscissa
A.I. DETECTION RANGE CONTOUR: Straight Wing
ALTITUDE: 60K

S113c

Launch zone [illegible]

10espr

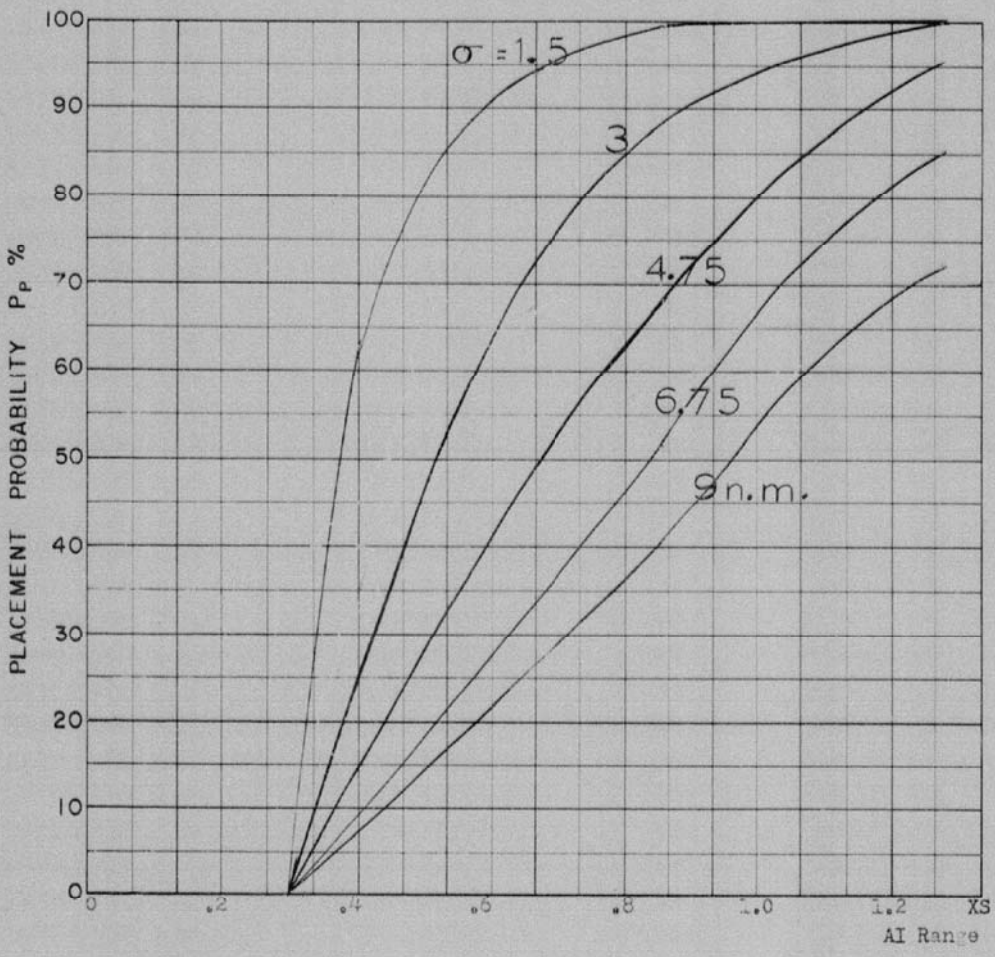

COURSE DIFFERENCE: 160°
TARGET EVASION: 0
TARGET MACH NO.: 2.0
INTERCEPTOR LATERAL G's: 1.12
INTERCEPTOR MACH NO.: 1.5
σ OF G.C.I. ACCURACY: Five values
A.I. DETECTION RANGE AS FRACTION OF SPECIFICATION RANGE, S: Abscissa
A.I. DETECTION RANGE CONTOUR: Straight Wing
ALTITUDE: 60K

S1146

Missile launch zone L-6, maximum range, 8° heading error.

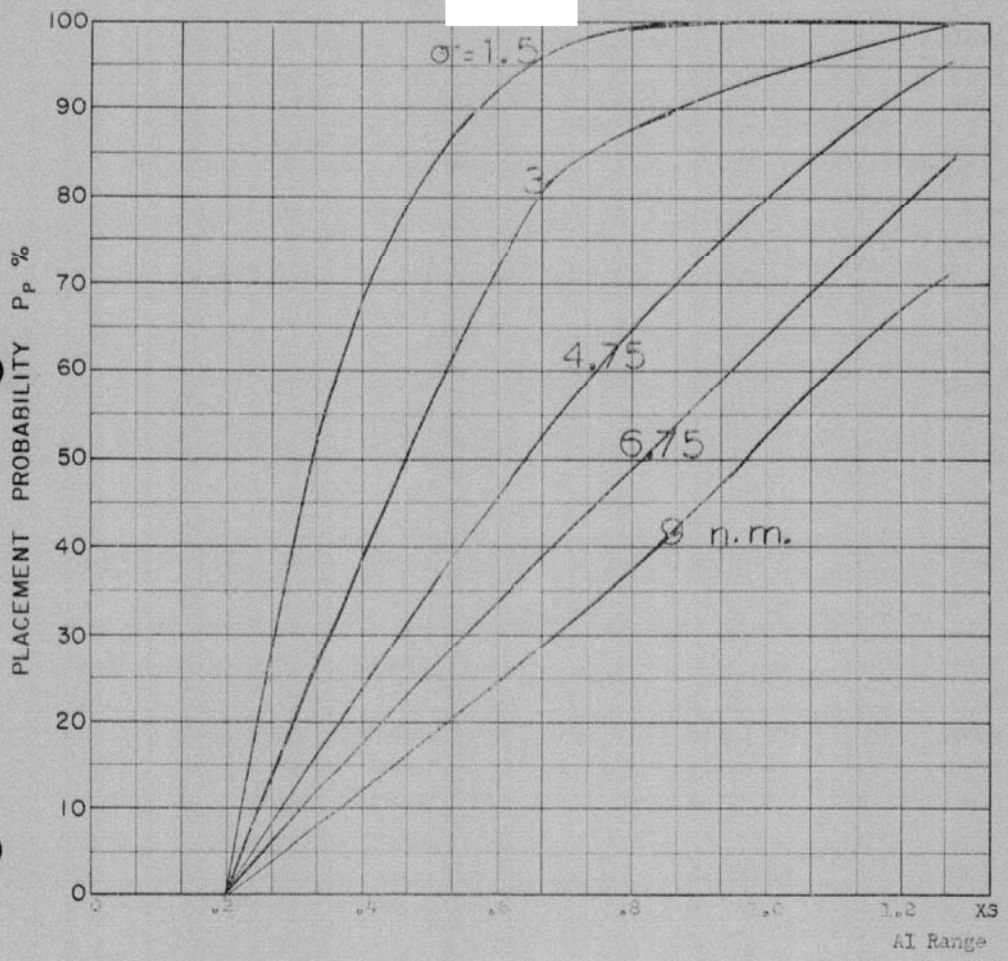

COURSE DIFFERENCE: 150°
TARGET EVASION: 0
TARGET MACH NO.: 2.0
INTERCEPTOR LATERAL G's: 1.12
INTERCEPTOR MACH NO.: .85
σ OF G.C.I. ACCURACY: Five values
A.I. DETECTION RANGE AS FRACTION OF SPECIFICATION RANGE, S: Abscissa
A.I. DETECTION RANGE CONTOUR: Straight Wing
ALTITUDE: 50K

S114c

Lauren zone L-7.

127 spr

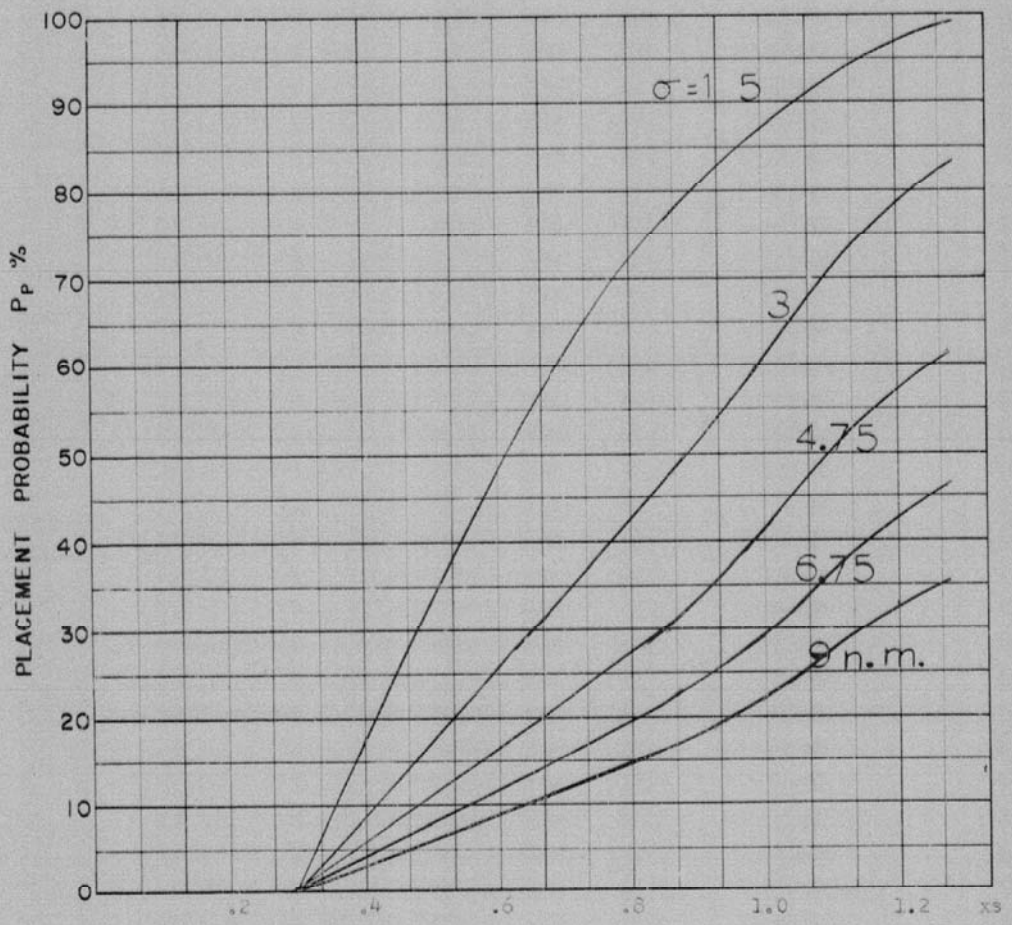

COURSE DIFFERENCE: 110°
TARGET EVASION: 0.1 lateral g's
TARGET MACH NO.: 2.0
INTERCEPTOR LATERAL G's: 0.66
INTERCEPTOR MACH NO.: 1.5
σ OF G.C.I. ACCURACY: five values
A.I. DETECTION RANGE AS FRACTION OF SPECIFICATION RANGE, S: abscissa
A.I. DETECTION RANGE CONTOUR: Straight wing
ALTITUDE: 60K

S115

Missile launch zone L 11

129 spr

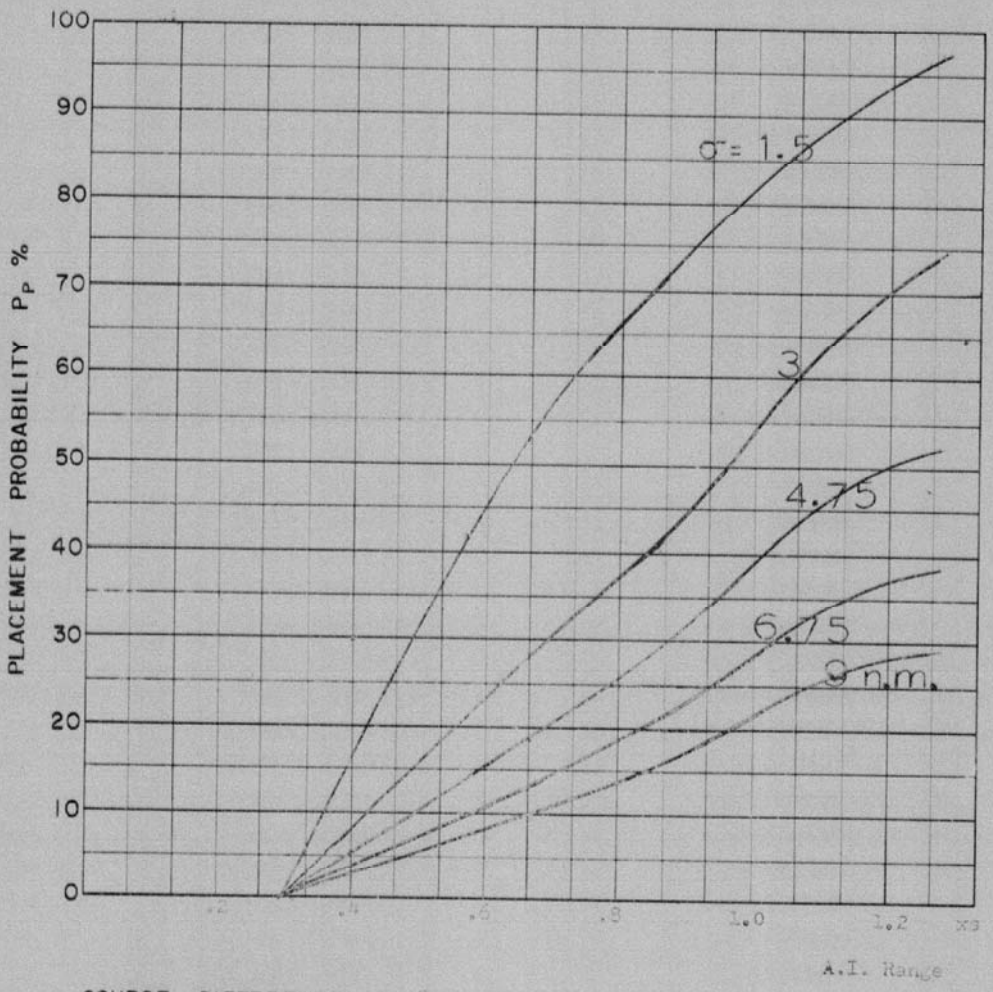

COURSE DIFFERENCE: 120°
TARGET EVASION: 0.1 lateral g's
TARGET MACH NO.: 2.0
INTERCEPTOR LATERAL G's: 0.66
INTERCEPTOR MACH NO.: 1.5
σ OF G.C.I. ACCURACY: five values
A.I. DETECTION RANGE AS FRACTION OF SPECIFICATION RANGE, S: abscissa
A.I. DETECTION RANGE CONTOUR: Straight wing
ALTITUDE: 60K

S116

Missile launch zone L 11

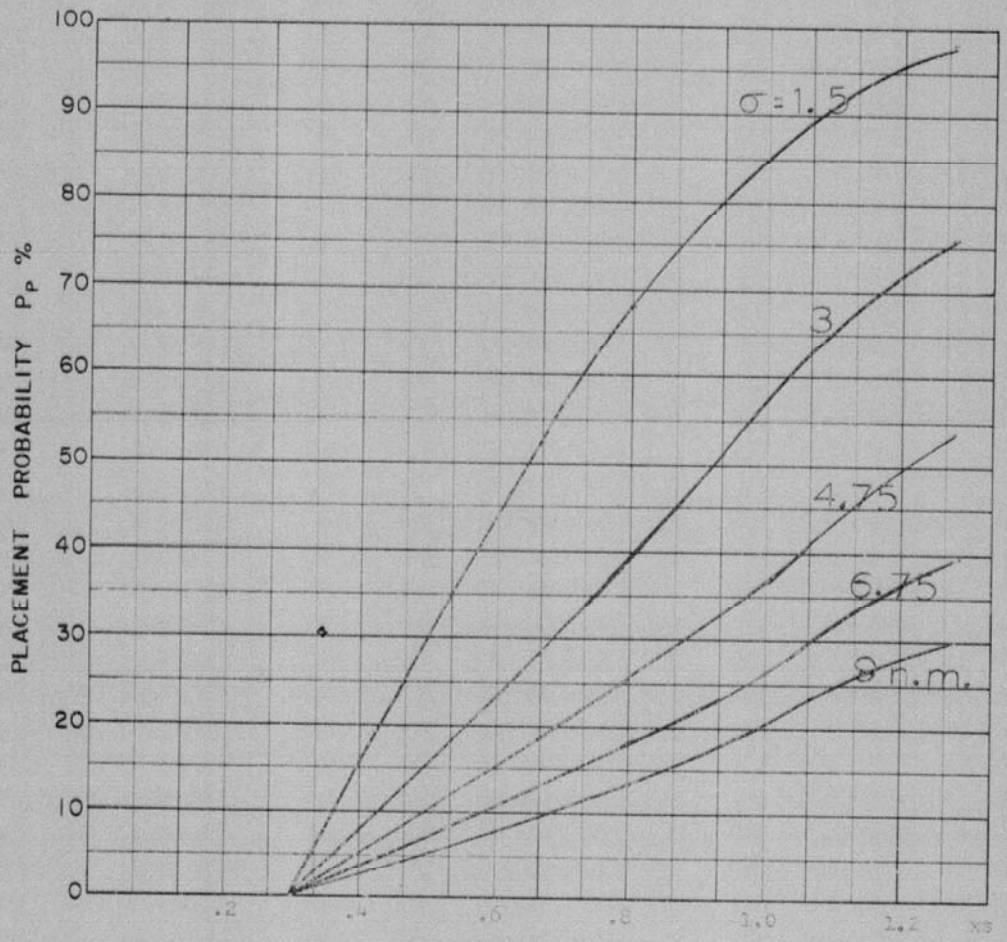

A.I. Range

COURSE DIFFERENCE:
TARGET EVASION:
TARGET MACH NO.:
INTERCEPTOR LATERAL G's:
INTERCEPTOR MACH NO.:
σ OF G.C.I. ACCURACY:
A.I. DETECTION RANGE AS FRACTION OF SPECIFICATION RANGE, S: abscissa
A.I. DETECTION RANGE CONTOUR:
ALTITUDE:

S117

133 spr

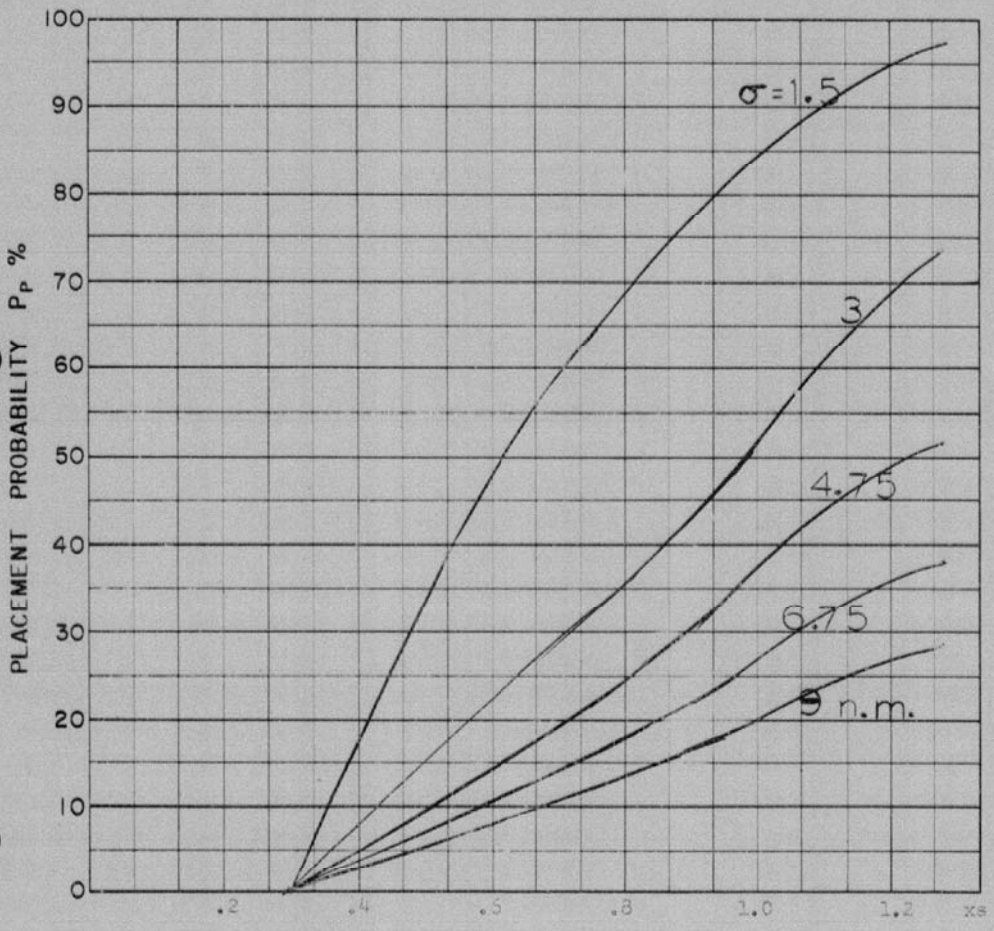

COURSE DIFFERENCE: 180°
TARGET EVASION: 0.1 lateral g's
TARGET MACH NO.: 2.0
INTERCEPTOR LATERAL G's: 0.66
INTERCEPTOR MACH NO.: 1.5
σ OF G.C.I. ACCURACY: five values
A.I. DETECTION RANGE AS FRACTION OF SPECIFICATION RANGE, S: abscissa
A.I. DETECTION RANGE CONTOUR: Straight wing
ALTITUDE: 60K

S118

Missile launch zone L11

138 spr

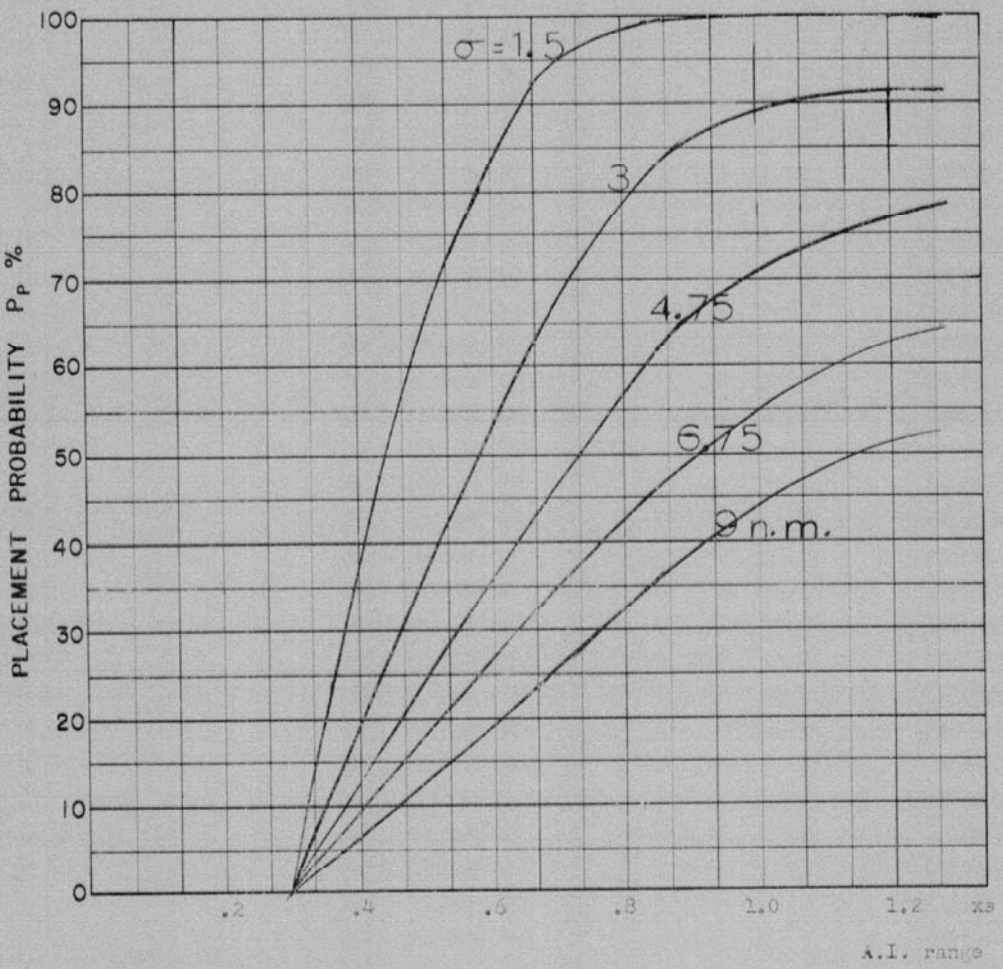

COURSE DIFFERENCE: 110°
TARGET EVASION: 0.1 lateral g's
TARGET MACH NO.: 2.0
INTERCEPTOR LATERAL G's: 1.5
INTERCEPTOR MACH NO.: 1.5
σ OF G.C.I. ACCURACY: five values
A.I. DETECTION RANGE AS FRACTION OF SPECIFICATION RANGE, S: abscissa
A.I. DETECTION RANGE CONTOUR: Straight wing
ALTITUDE: 60K

S119a

Missile launch zone L 11

134 spr

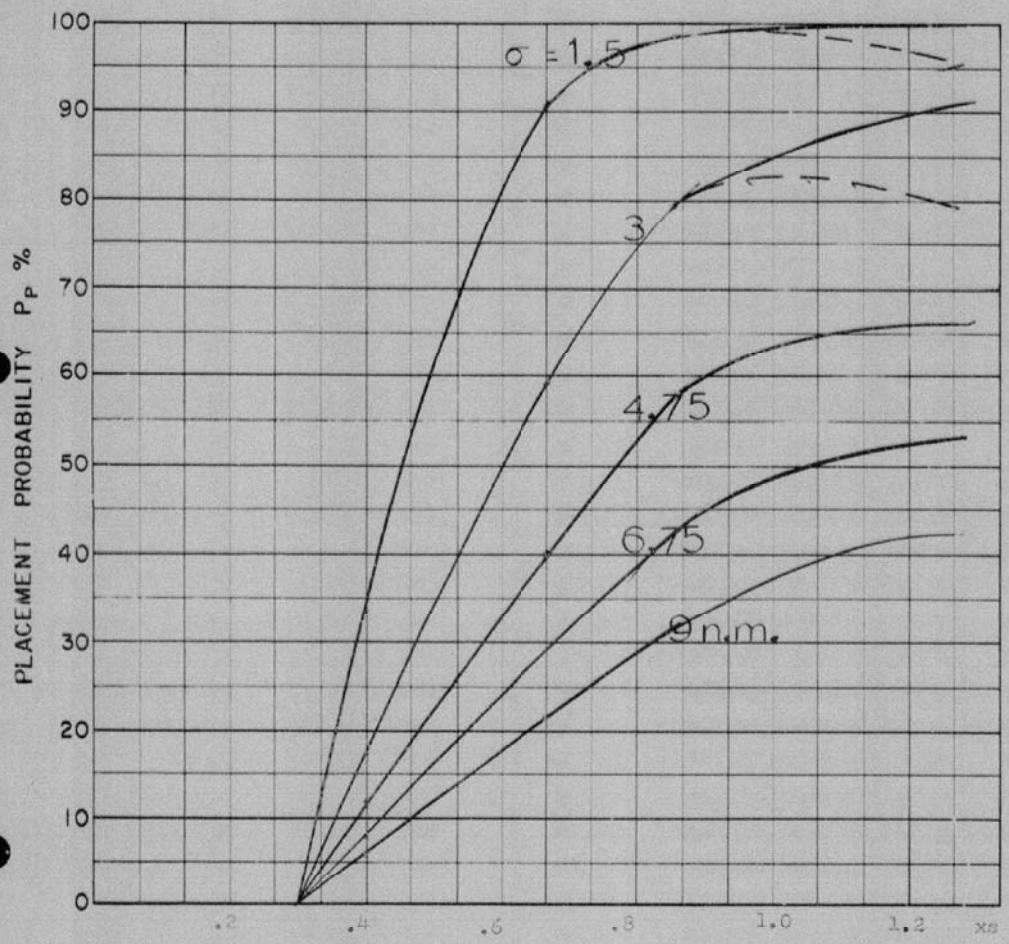

COURSE DIFFERENCE: 110°
TARGET EVASION: 0.2 lateral g's
TARGET MACH NO.: 2.0
INTERCEPTOR LATERAL G's: 1.5
INTERCEPTOR MACH NO.: 1.5
σ OF G.C.I. ACCURACY: five values
A.I. DETECTION RANGE AS FRACTION OF SPECIFICATION RANGE, S: abscissa
A.I. DETECTION RANGE CONTOUR: Straight wing
ALTITUDE: 60K

S1196

Missile law : zone L 11

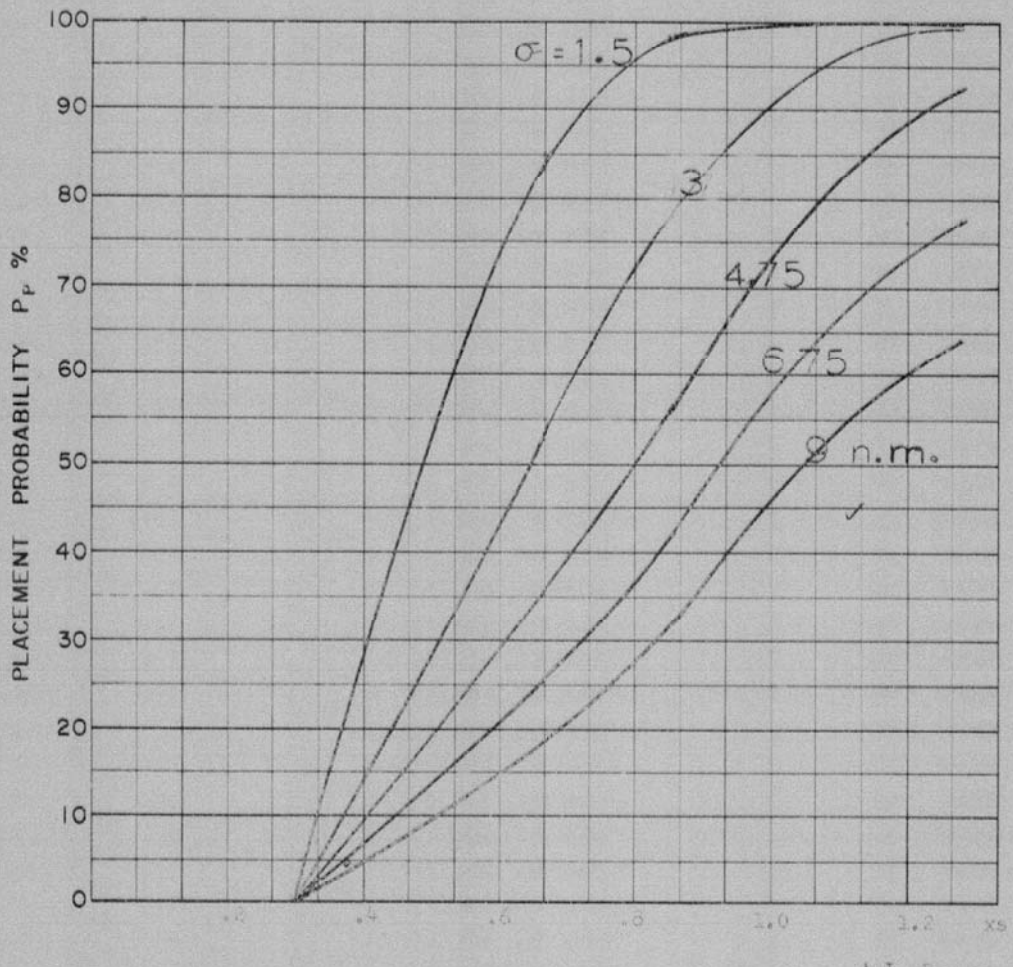

COURSE DIFFERENCE: 135°
TARGET EVASION: 0.1 lateral g's
TARGET MACH NO.: 2.0
INTERCEPTOR LATERAL G's: 1.5
INTERCEPTOR MACH NO.: 1.5
σ OF G.C.I. ACCURACY: five values
A.I. DETECTION RANGE AS FRACTION OF SPECIFICATION RANGE, S: abscissa
A.I. DETECTION RANGE CONTOUR: Straight wing
ALTITUDE: 60K

Missile launch zone L 11

S120

142 spr

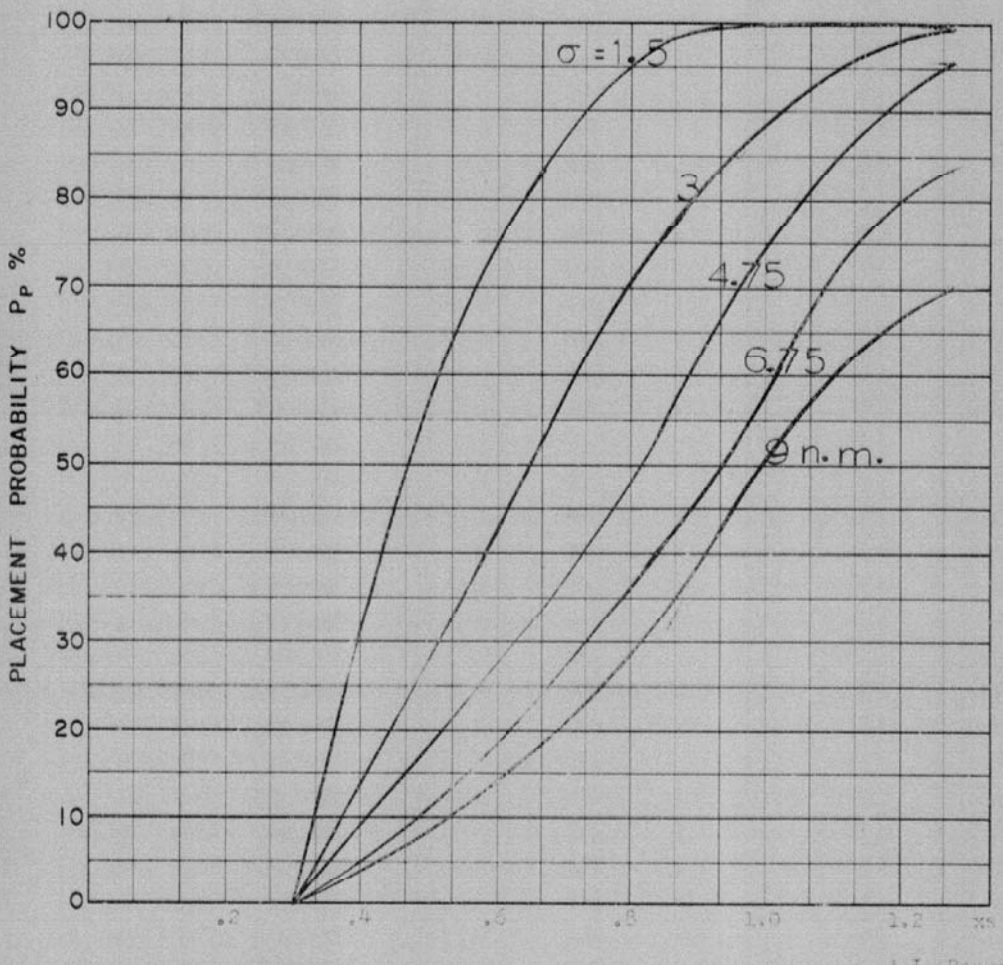

COURSE DIFFERENCE: 160°
TARGET EVASION: 0.1 lateral g's
TARGET MACH NO.: 2.0
INTERCEPTOR LATERAL G's: 1.5
INTERCEPTOR MACH NO.: 1.5
σ OF G.C.I. ACCURACY: five values
A.I. DETECTION RANGE AS FRACTION OF SPECIFICATION RANGE, S: abscissa
A.I. DETECTION RANGE CONTOUR: Straight wing
ALTITUDE: 60K

S12a

Missile launch zone L 11

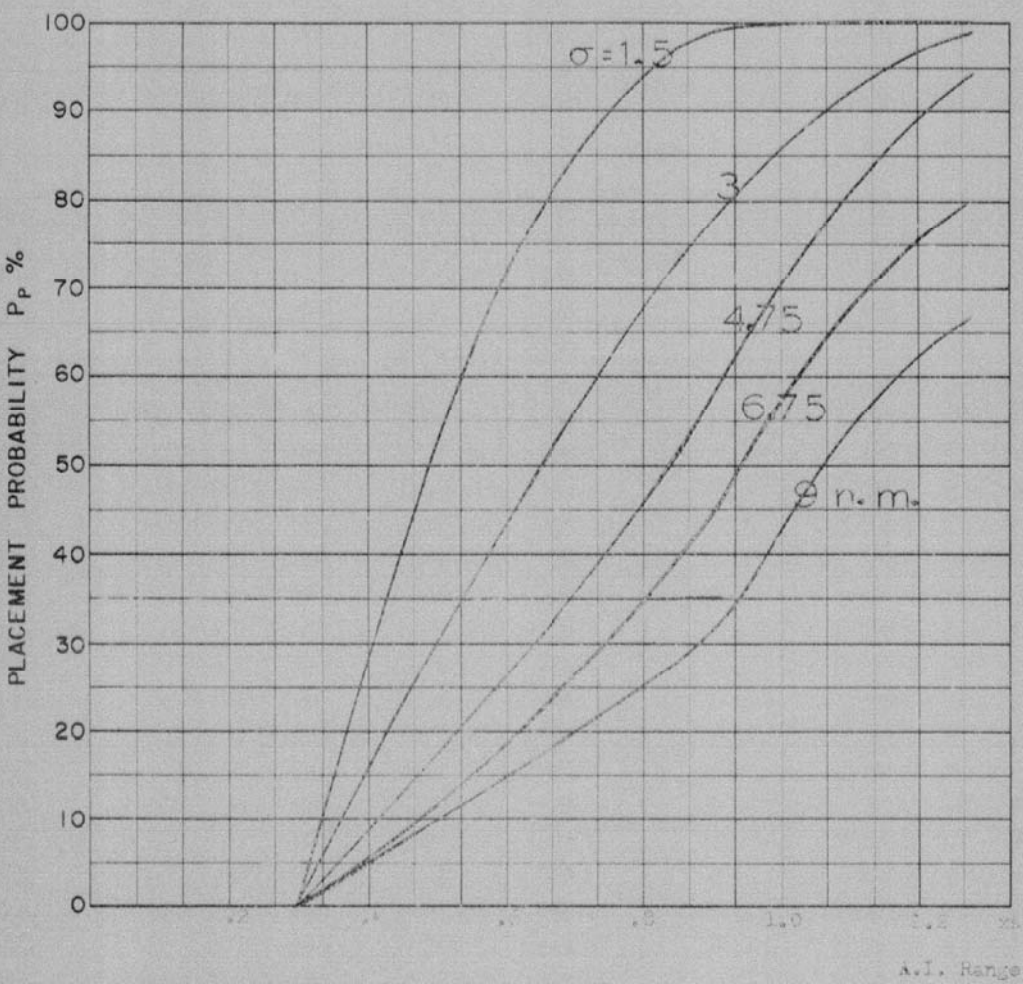

COURSE DIFFERENCE:
TARGET EVASION:
TARGET MACH NO.:
INTERCEPTOR LATERAL G's:
INTERCEPTOR MACH NO.:
σ OF G.C.I. ACCURACY:
A.I. DETECTION RANGE AS FRACTION OF SPECIFICATION RANGE, S:
A.I. DETECTION RANGE CONTOUR:
ALTITUDE:

S1216

144 spr

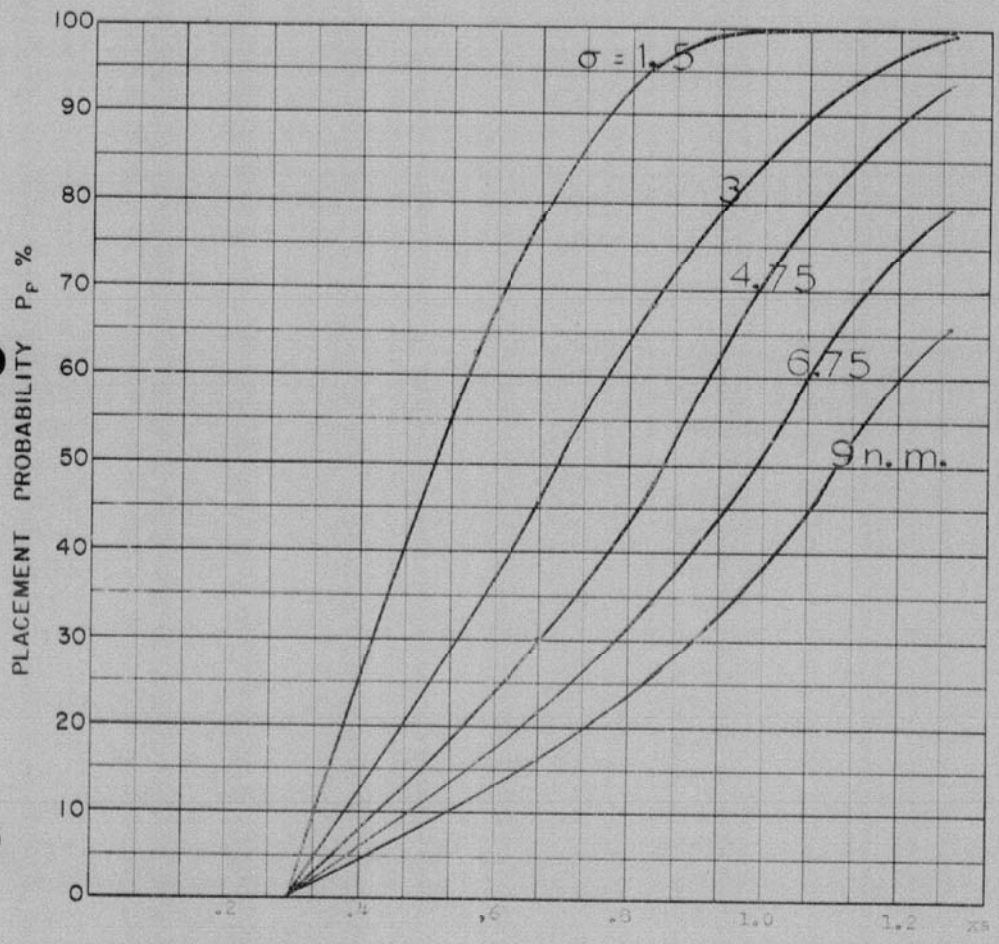

COURSE DIFFERENCE: 180°
TARGET EVASION: 0.1 lateral g's
TARGET MACH NO.: 2.0
INTERCEPTOR LATERAL G's: 1.5
INTERCEPTOR MACH NO.: 1.5
σ OF G.C.I. ACCURACY: Five values
A.I. DETECTION RANGE AS FRACTION OF SPECIFICATION RANGE, S: abscissa
A.I. DETECTION RANGE CONTOUR: Straight wing
ALTITUDE: 60K

S122

Missile Launch none L11

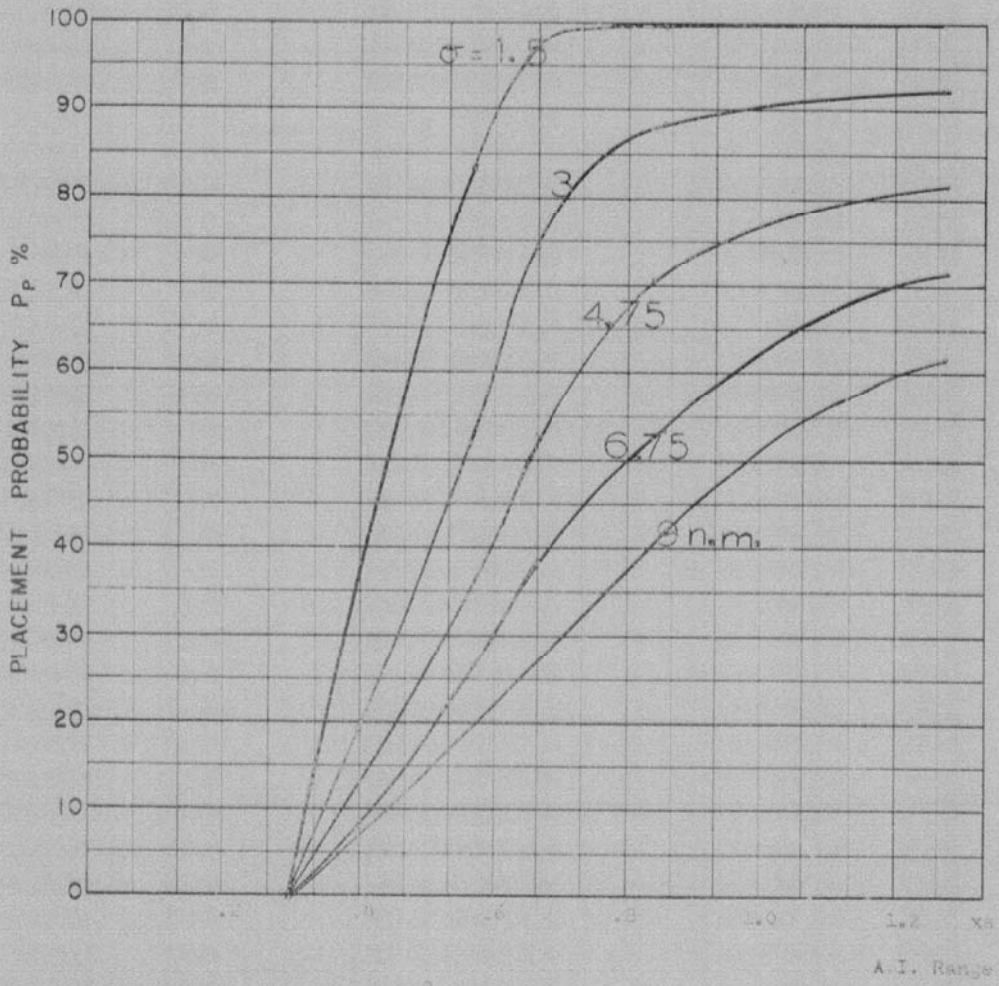

COURSE DIFFERENCE:
TARGET EVASION:
TARGET MACH NO.:
INTERCEPTOR LATERAL G's
INTERCEPTOR MACH NO.:
σ OF G.C.I. ACCURACY:
A.I. DETECTION RANGE AS FRACTION OF SPECIFICATION RANGE, S:
A.I. DETECTION RANGE CONTOUR:
ALTITUDE:

S123

147 spr

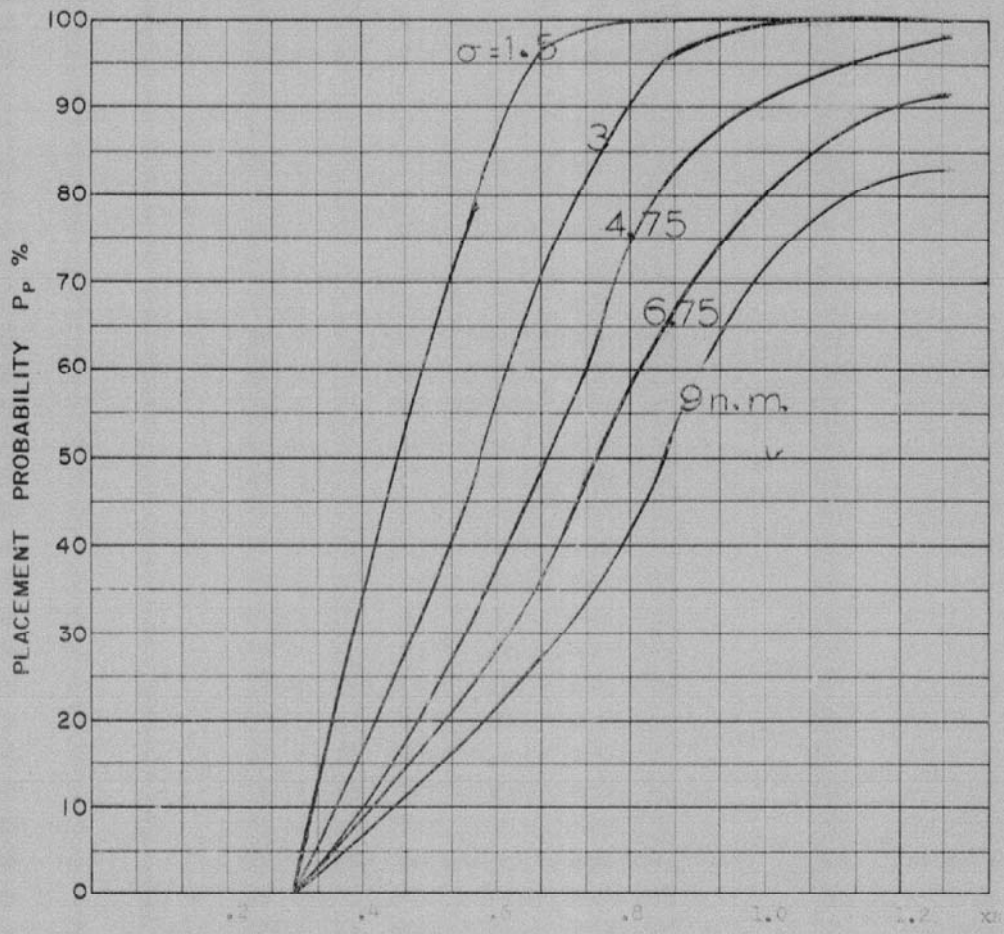

COURSE DIFFERENCE: 135°
TARGET EVASION: 0.1 lateral g's
TARGET MACH NO.: 2.0
INTERCEPTOR LATERAL G's: 2.4
INTERCEPTOR MACH NO.: 1.5
σ OF G.C.I. ACCURACY: five values
A.I. DETECTION RANGE AS FRACTION OF SPECIFICATION RANGE, S: abscissa
A.I. DETECTION RANGE CONTOUR: Straight wing
ALTITUDE: 60K

(S124)

Missile launch zone L-11

149 sgr

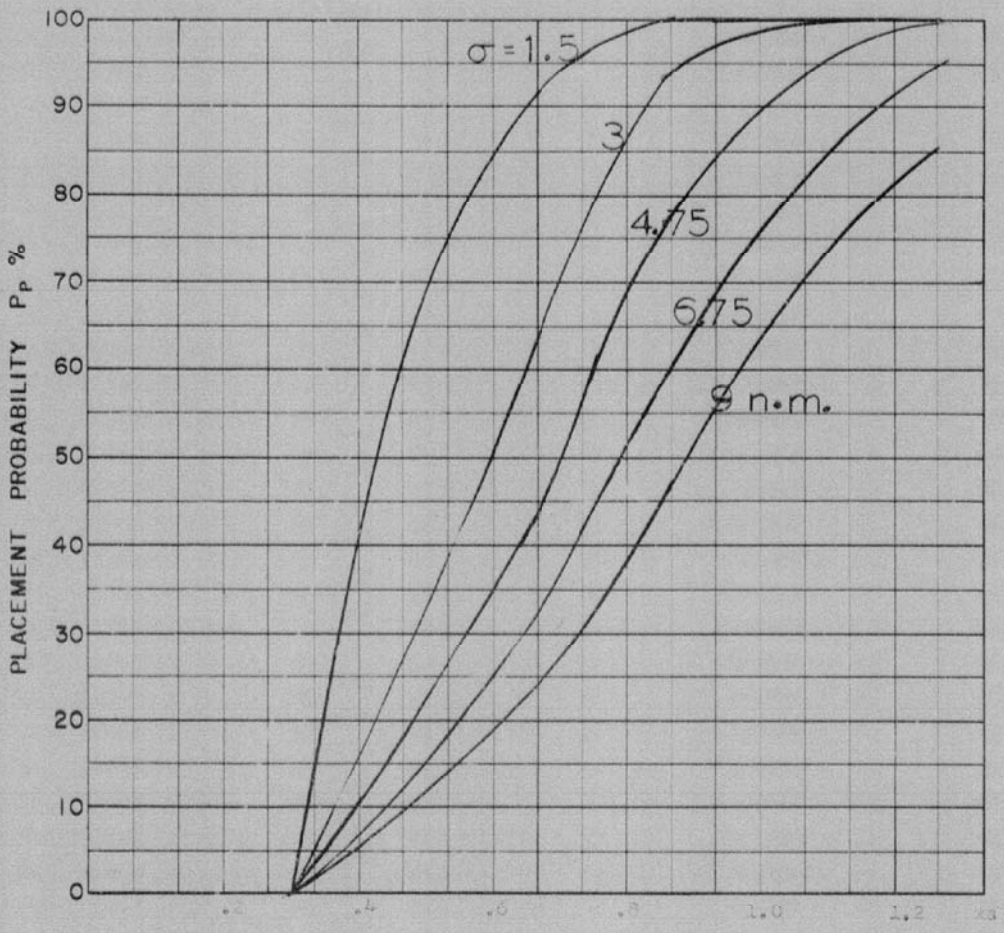

COURSE DIFFERENCE: 180°
TARGET EVASION: 0.1 lateral g's
TARGET MACH NO.: 2.0
INTERCEPTOR LATERAL G's: 2.4
INTERCEPTOR MACH NO.: 1.5
σ OF G.C.I. ACCURACY: five values
A.I. DETECTION RANGE AS FRACTION OF SPECIFICATION RANGE, S: Abscissa
A.I. DETECTION RANGE CONTOUR: Straight wing
ALTITUDE: 60K

S125

Missile Launch zone L 11

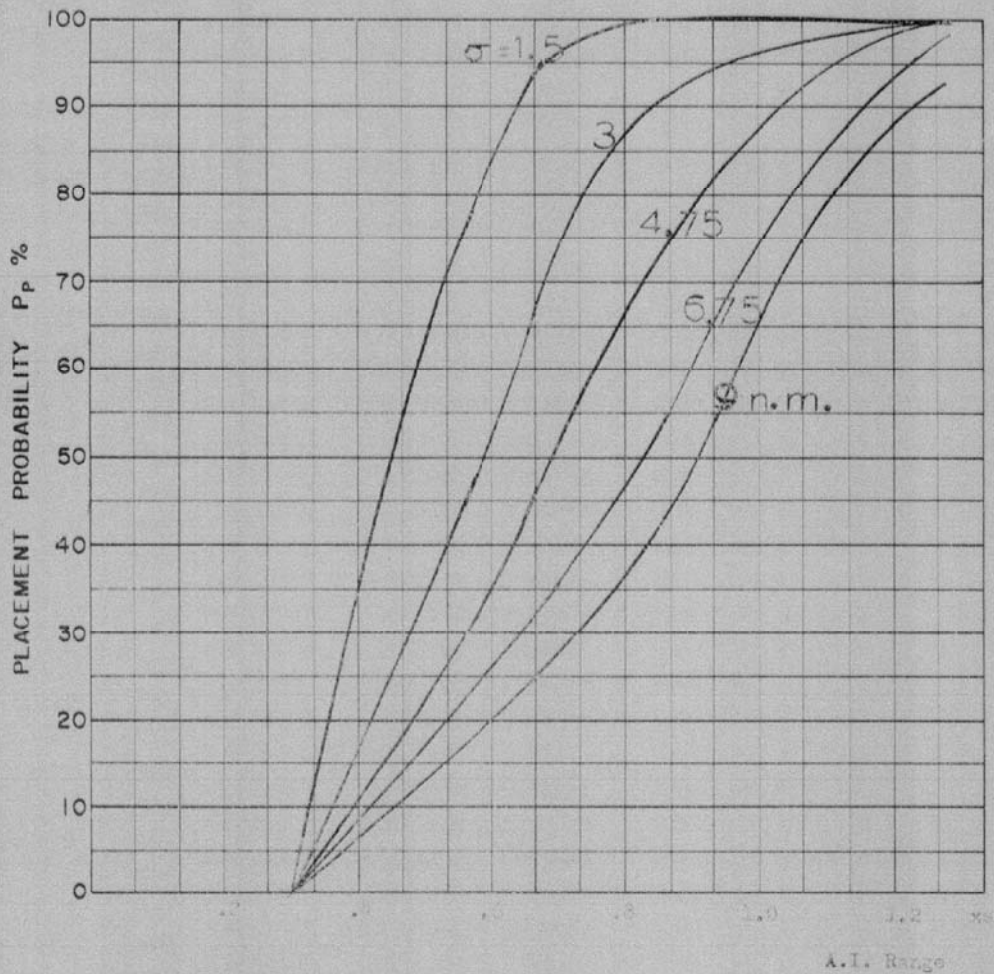

COURSE DIFFERENCE:
TARGET EVASION:
TARGET MACH NO.:
INTERCEPTOR LATERAL G's:
INTERCEPTOR MACH NO.:
σ OF G.C.I. ACCURACY:
A.I. DETECTION RANGE AS FRACTION OF SPECIFICATION RANGE, S: abscissa
A.I. DETECTION RANGE CONTOUR:
ALTITUDE:

S126

24aspr

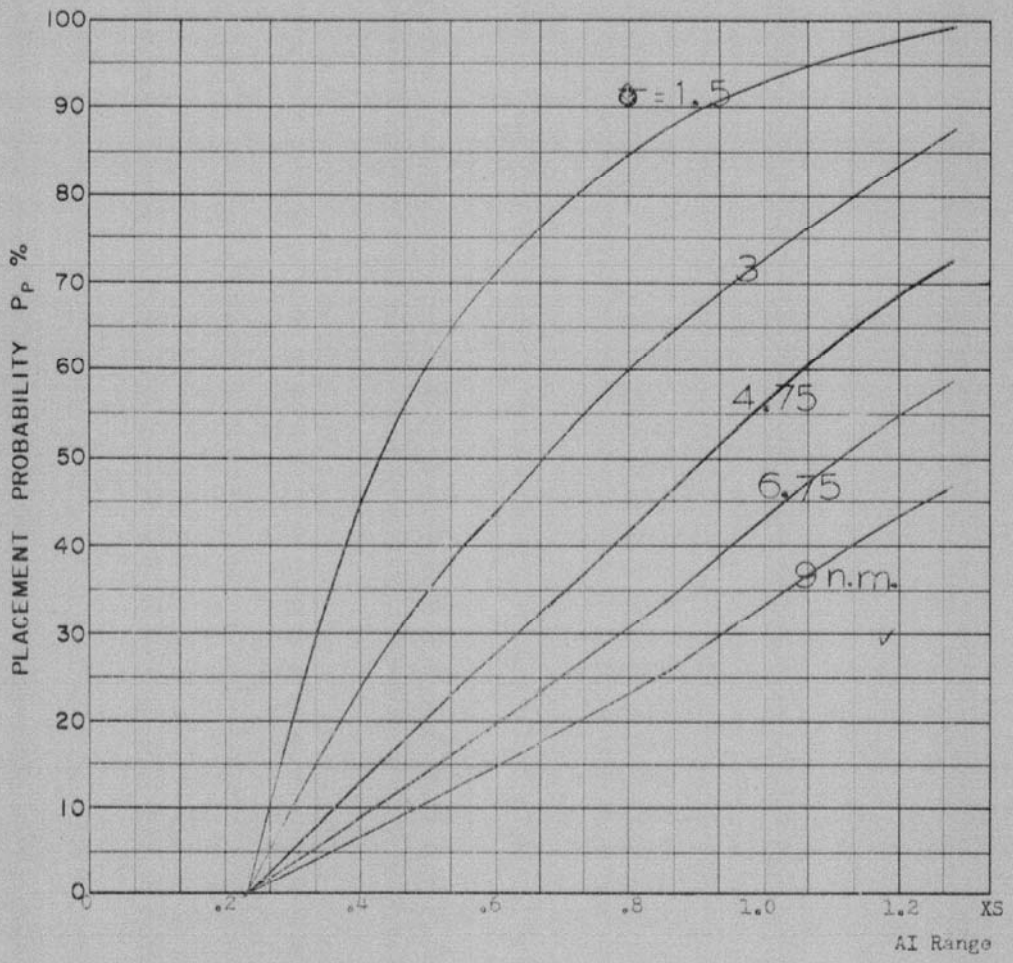

COURSE DIFFERENCE: 75°
TARGET EVASION: 0
TARGET MACH NO.: 2.0
INTERCEPTOR LATERAL G's: 0.66
INTERCEPTOR MACH NO.: 1.8
σ OF G.C.I. ACCURACY: Five values
A.I. DETECTION RANGE AS FRACTION OF SPECIFICATION RANGE, S: Abscissa
A.I. DETECTION RANGE CONTOUR: Straight Wing
ALTITUDE: 60K

S127a

Missile launch zone L-3, minimum range, 8° heading error.

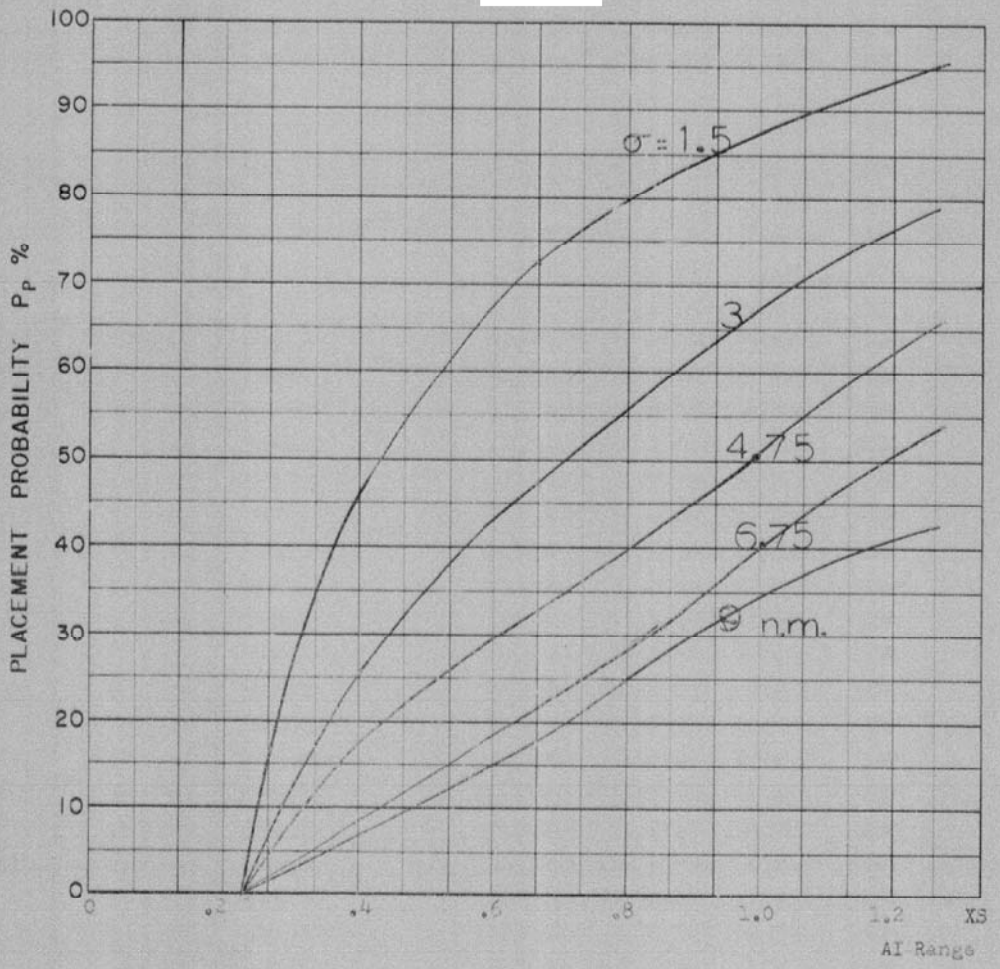

COURSE DIFFERENCE: 75°
TARGET EVASION: 0
TARGET MACH NO.: 2.0
INTERCEPTOR LATERAL G's: 0.66
INTERCEPTOR MACH NO.: 1.8
σ OF G.C.I. ACCURACY: Five values
A.I. DETECTION RANGE AS FRACTION OF SPECIFICATION RANGE, S: Abscissa
A.I. DETECTION RANGE CONTOUR: Straight Wing
ALTITUDE: 60K

S1276

Missile launch zone L-8, medium range, 8° heading error.

23bspr

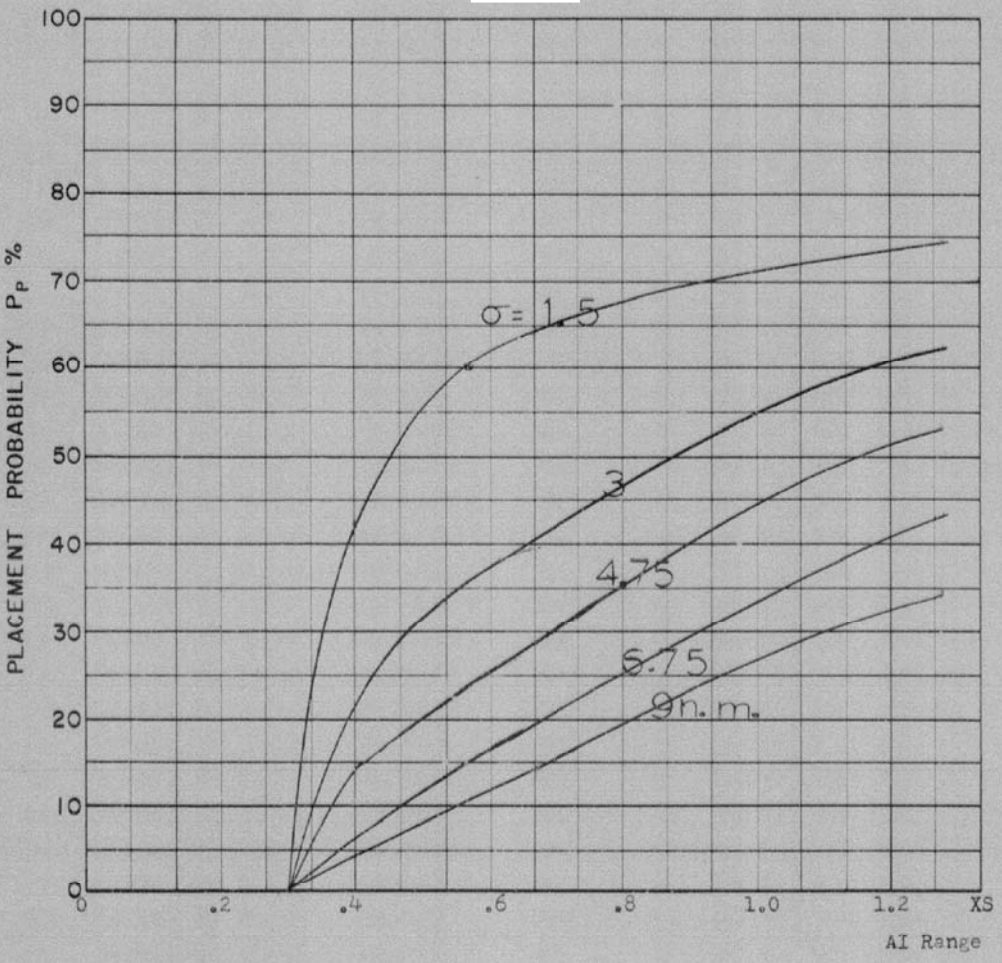

COURSE DIFFERENCE: 90°
TARGET EVASION: 0
TARGET MACH NO.: 2.0
INTERCEPTOR LATERAL G's: 0.66
INTERCEPTOR MACH NO.: 1.8
σ OF G.C.I. ACCURACY: Five values
A.I. DETECTION RANGE AS FRACTION OF SPECIFICATION RANGE, S: Abscissa
A.I. DETECTION RANGE CONTOUR: Straight Wing
ALTITUDE: 60K

S128 b

Missile launch zone L-8, medium range, 8° heading error.

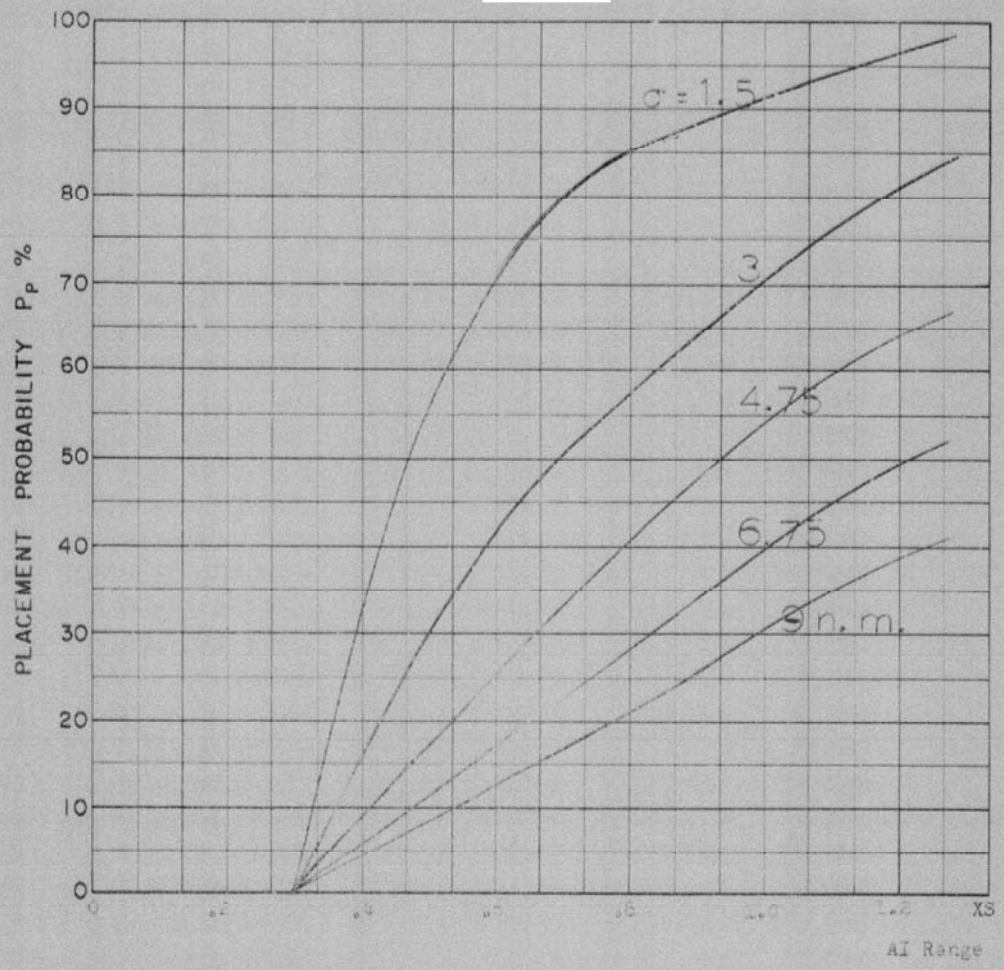

COURSE DIFFERENCE: 180°
TARGET EVASION: 0
TARGET MACH NO.: 2.0
INTERCEPTOR LATERAL G's: 0.66
INTERCEPTOR MACH NO.: 1.8
σ OF G.C.I. ACCURACY: Five values
A.I. DETECTION RANGE AS FRACTION OF SPECIFICATION RANGE, S: Abscissa
A.I. DETECTION RANGE CONTOUR: Straight Wing
ALTITUDE: 60K

S-29a

Missile Launch Zone 1.8, minimum range, 8° heading error.

23cspr

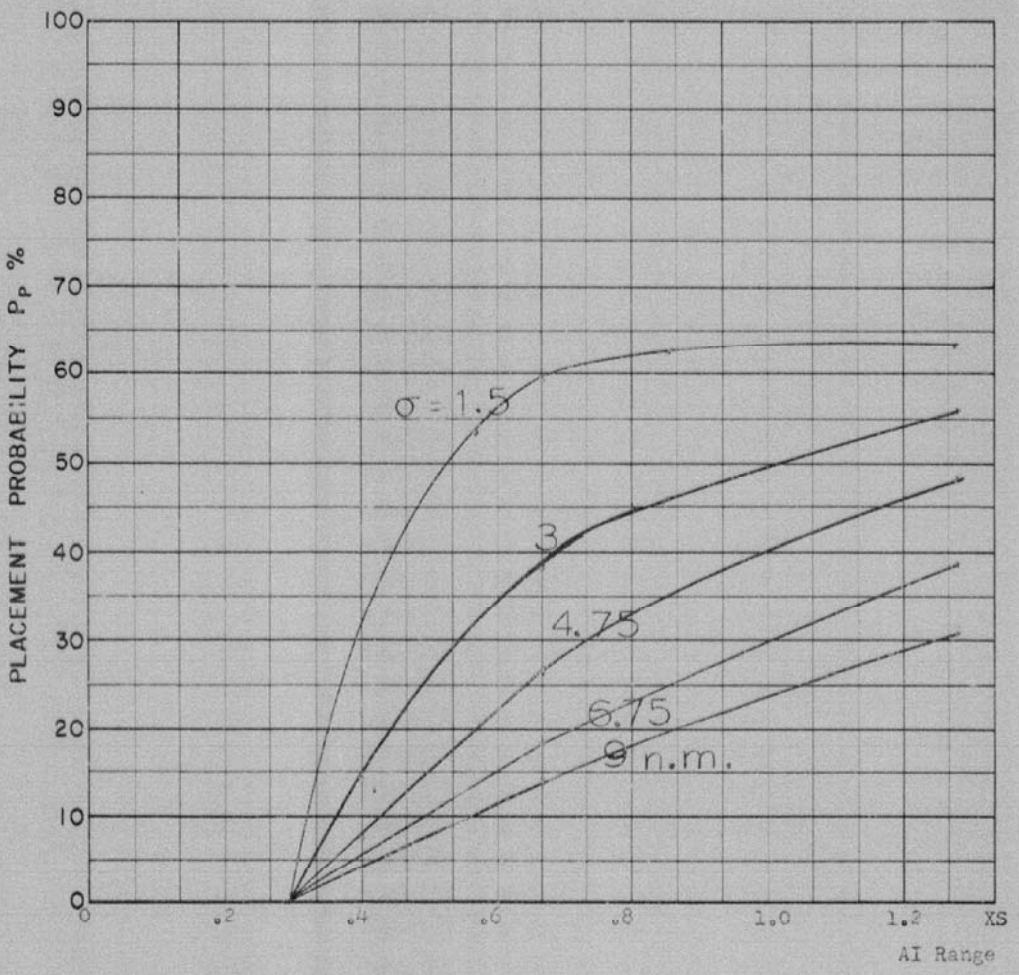

COURSE DIFFERENCE: 100°
TARGET EVASION: 0
TARGET MACH NO.: 2.0
INTERCEPTOR LATERAL G's: 0.66
INTERCEPTOR MACH NO.: 1.8
σ OF G.C.I. ACCURACY: Five values
A.I. DETECTION RANGE AS FRACTION OF SPECIFICATION RANGE, S: Abscissa
A.I. DETECTION RANGE CONTOUR: Straight Wing
ALTITUDE: 60K

S1296

Missile launch zone L-3, medium range, 8° heading error.

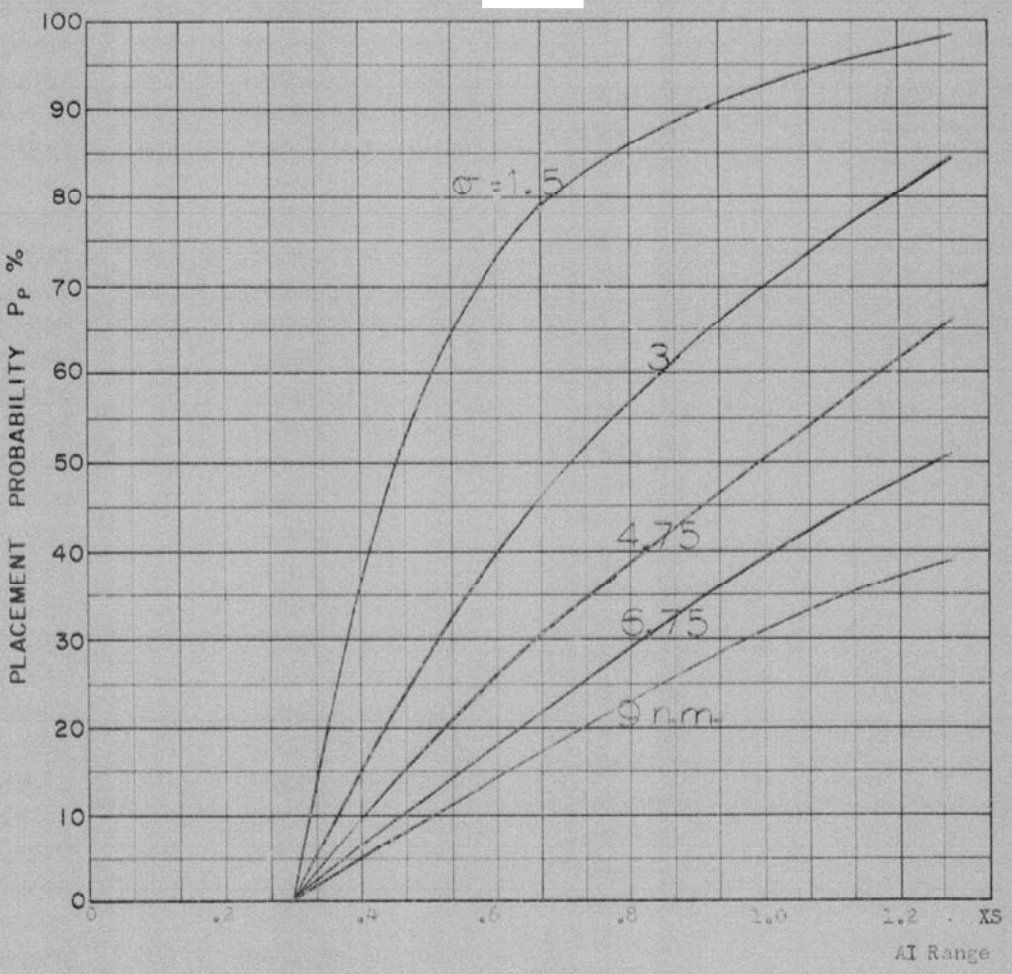

COURSE DIFFERENCE: 120°
TARGET EVASION: 0
TARGET MACH NO.: 2.0
INTERCEPTOR LATERAL G's: 0.66
INTERCEPTOR MACH NO.: 1.8
σ OF G.C.I. ACCURACY: Five values
A.I. DETECTION RANGE AS FRACTION OF SPECIFICATION RANGE, S: Abscissa
A.I. DETECTION RANGE CONTOUR: Straight Wing
ALTITUDE: 60K

S130a

Missile launch zone L-8, minimum range, 8° heading error.

24espr

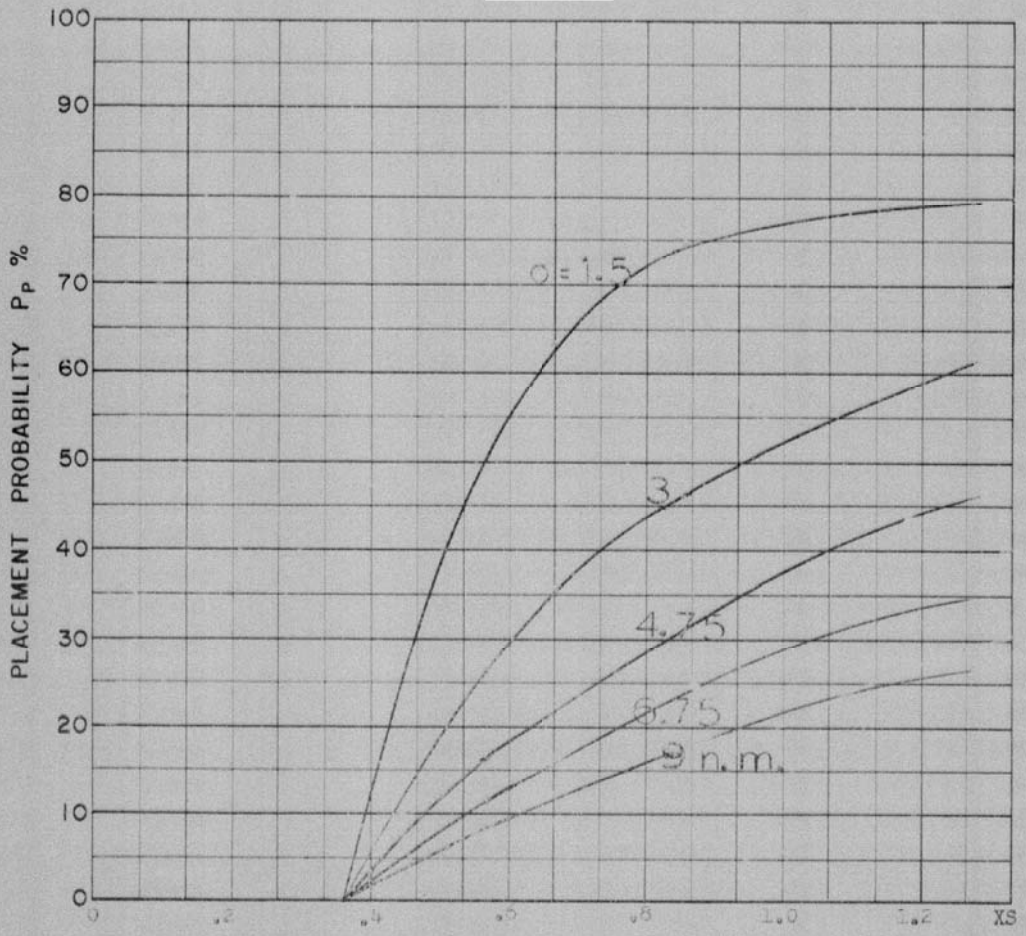

COURSE DIFFERENCE: 135°
TARGET EVASION: 0
TARGET MACH NO.: 2.0
INTERCEPTOR LATERAL G's: 0.56
INTERCEPTOR MACH NO.: 1.8
σ OF G.C.I. ACCURACY: Five values
A.I. DETECTION RANGE AS FRACTION OF SPECIFICATION RANGE, S: Abscissa
A.I. DETECTION RANGE CONTOUR: Straight Wing
ALTITUDE: 60K

S131a

Missile launch zone L-8, minimum range, 8° heading error.

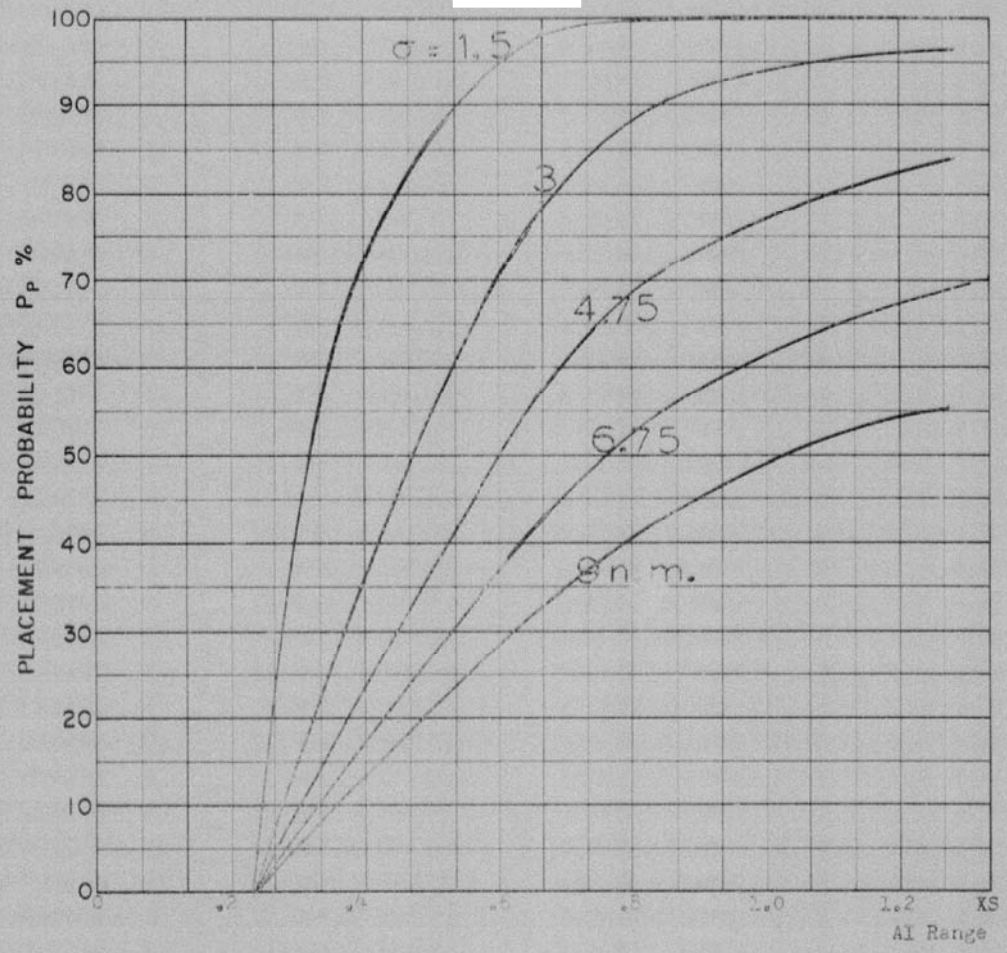

COURSE DIFFERENCE:
TARGET EVASION: 0
TARGET MACH NO.: 2.0
INTERCEPTOR LATERAL G's: 2.0
INTERCEPTOR MACH NO.:
σ OF G.C.I. ACCURACY: Five values
A.I. DETECTION RANGE AS FRACTION OF SPECIFICATION RANGE, S Abscissa
A.I. DETECTION RANGE CONTOUR: Straight Wing
ALTITUDE: 60K

S133a

Missile launch zone L-8, minimum range, 8° heading error.

22axspr

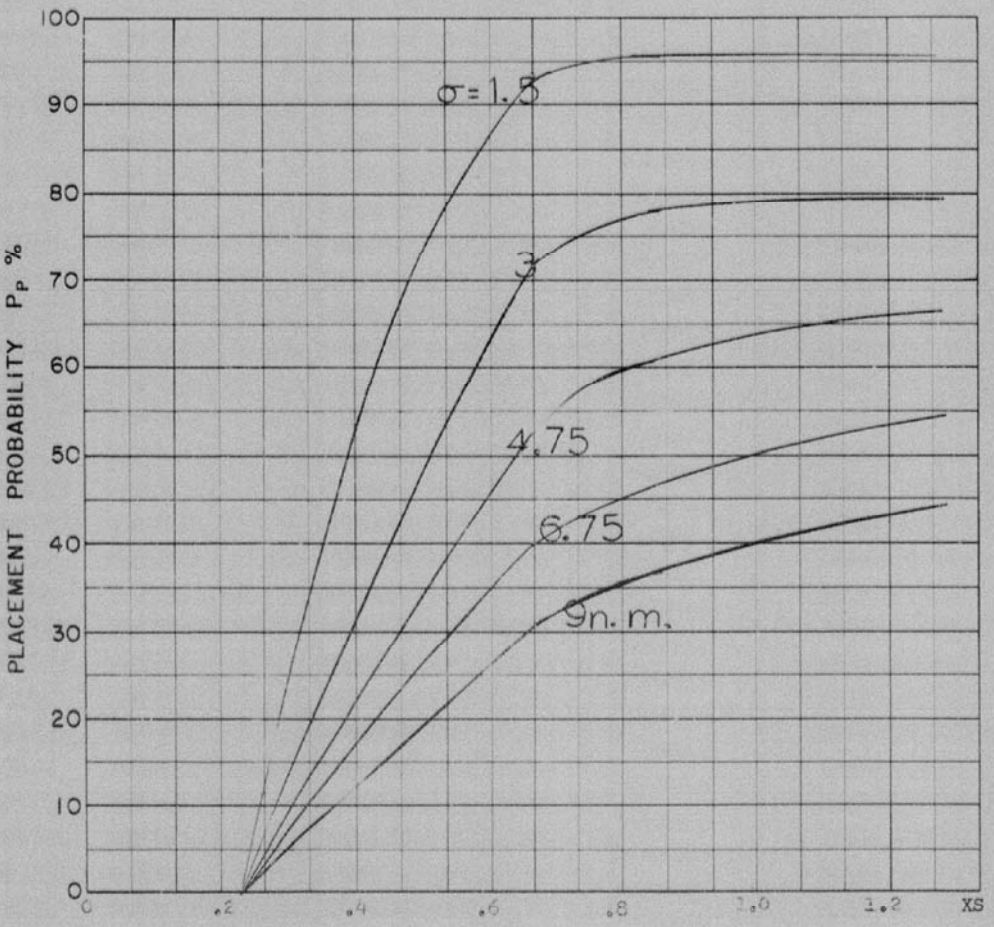

S1336

COURSE DIFFERENCE: 75°
TARGET EVASION: 0
TARGET MACH NO.: 2.0
INTERCEPTOR LATERAL G's: 2.0
INTERCEPTOR MACH NO.: 1.8
σ OF G.C.I. ACCURACY: Five values
A.I. DETECTION RANGE AS FRACTION OF SPECIFICATION RANGE, S: Abscissa
A.I. DETECTION RANGE CONTOUR: Straight Wing
ALTITUDE: 60K

Missile launch zone L-8, medium range, 8° heading error.

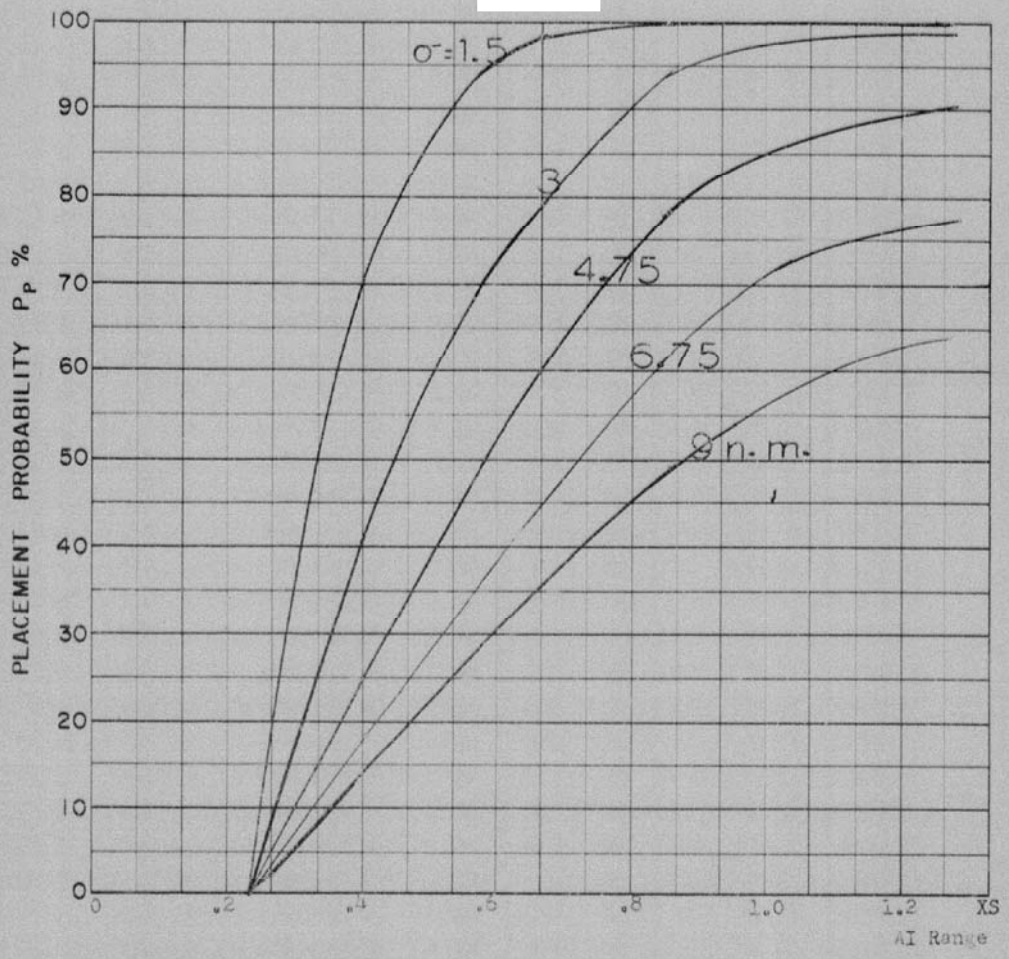

COURSE DIFFERENCE: 90°
TARGET EVASION: 0
TARGET MACH NO.: 2.0
INTERCEPTOR LATERAL G's: 2.0
INTERCEPTOR MACH NO.: 1.8
σ OF G.C.I. ACCURACY: Five values
A.I. DETECTION RANGE AS FRACTION OF SPECIFICATION RANGE, S: Abscissa
A.I. DETECTION RANGE CONTOUR: Straight Wing
ALTITUDE: 60K

S134a

Missile launch zone L-8, minimum range, 8° heading error.

22bxspr

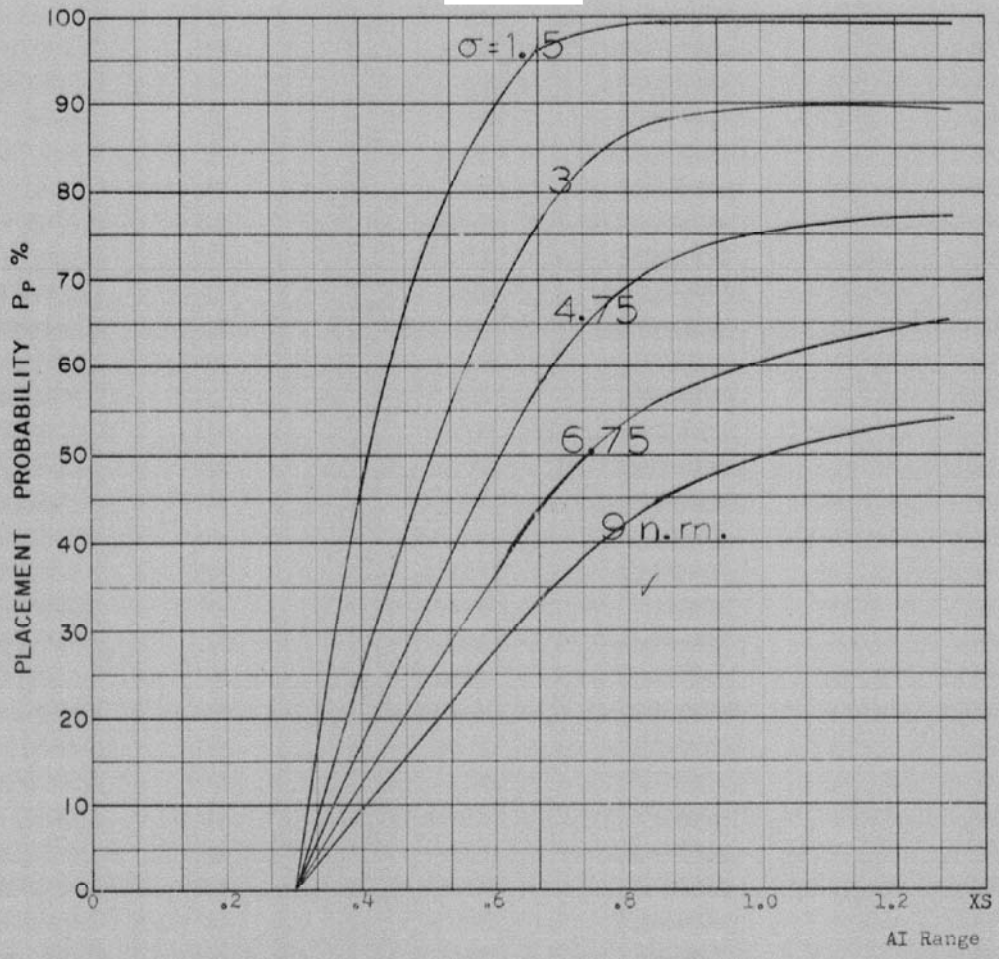

COURSE DIFFERENCE: 90°
TARGET EVASION: 0
TARGET MACH NO.: 2.0
INTERCEPTOR LATERAL G's: 2.0
INTERCEPTOR MACH NO.: 1.8
σ OF G.C.I. ACCURACY: Five values
A.I. DETECTION RANGE AS FRACTION OF SPECIFICATION RANGE, S: Abscissa
A.I. DETECTION RANGE CONTOUR: Straight Wing
ALTITUDE: 60K

S1346

Missile launch zone L-8, medium range, 8° heading error.

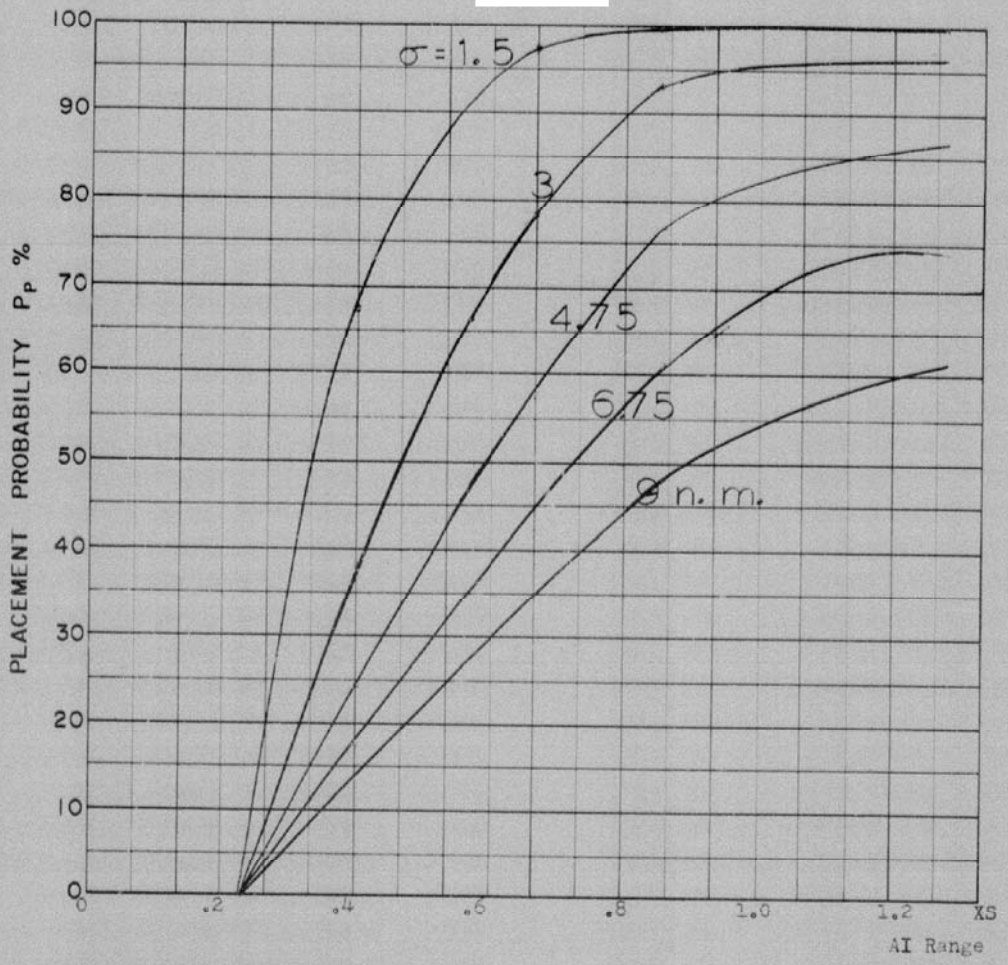

COURSE DIFFERENCE: 100°
TARGET EVASION: 0
TARGET MACH NO.: 2.0
INTERCEPTOR LATERAL G's: 2.0
INTERCEPTOR MACH NO.: 1.8
σ OF G.C.I. ACCURACY: Five values
A.I. DETECTION RANGE AS FRACTION OF SPECIFICATION RANGE, S: Abscissa
A.I. DETECTION RANGE CONTOUR: Straight Wing
ALTITUDE: 60K

S135a

Missile launch zone L-8, minimum range, 8° heading error.

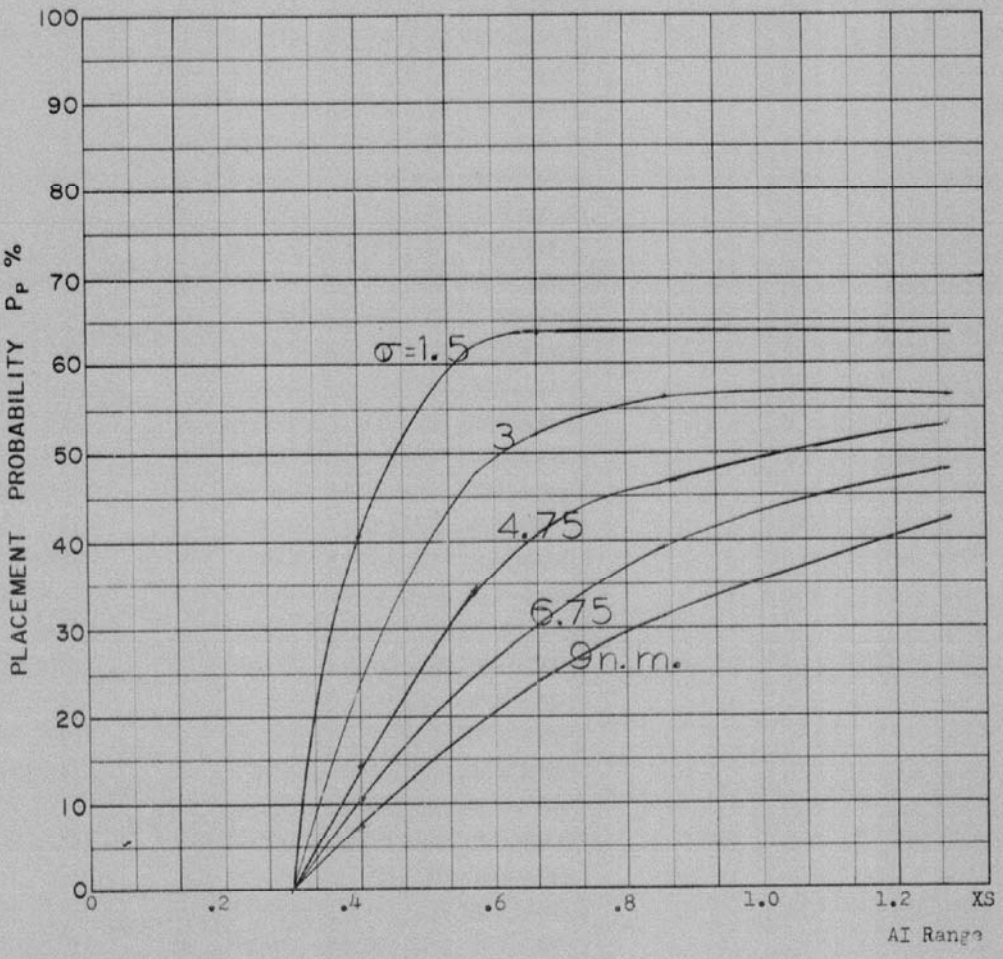

COURSE DIFFERENCE: 100°
TARGET EVASION: 0
TARGET MACH NO.: 2.0
INTERCEPTOR LATERAL G's: 2.0
INTERCEPTOR MACH NO.: 1.8
σ OF G.C.I. ACCURACY: Five values
A.I. DETECTION RANGE AS FRACTION OF SPECIFICATION RANGE, S Abscissa
A.I. DETECTION RANGE CONTOUR: Straight Wing
ALTITUDE: 60K

S1356

Missile launch zone L-8, medium range, 8° heading error.

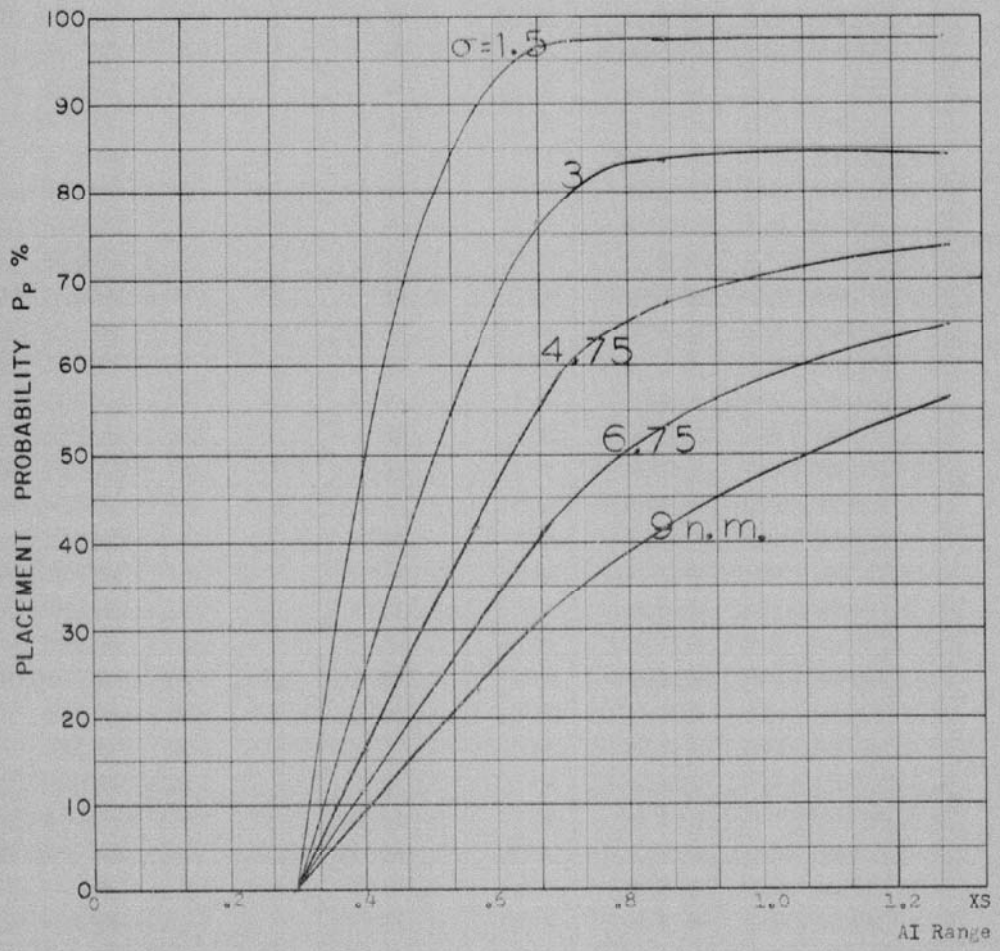

S136

COURSE DIFFERENCE: 120°
TARGET EVASION: 0
TARGET MACH NO.: 2.0
INTERCEPTOR LATERAL G's: 2.0
INTERCEPTOR MACH NO.: 1.8
σ OF G.C.I. ACCURACY: Five values
A.I. DETECTION RANGE AS FRACTION OF SPECIFICATION RANGE, S: Abscissa
A.I. DETECTION RANGE CONTOUR: Straight Wing
ALTITUDE: 60K

Missile launch zone L 8, minimum range, 8° heading error.

22espr

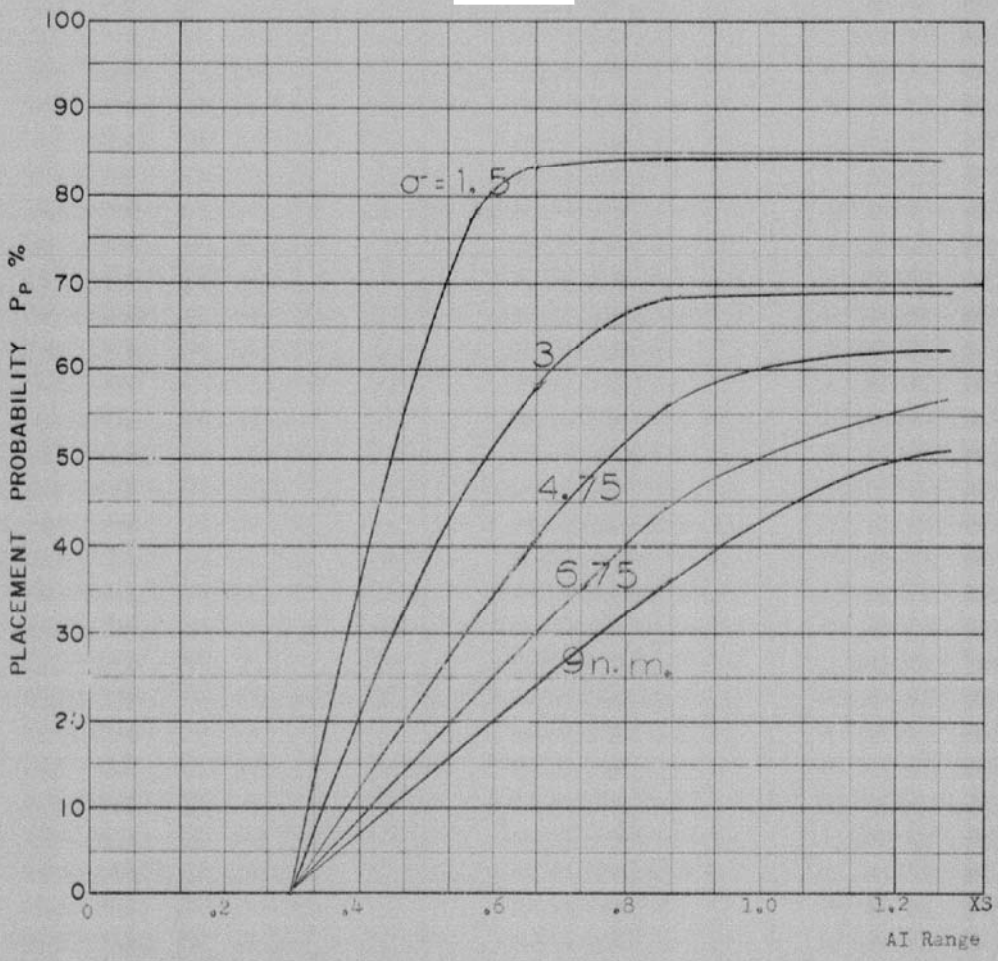

COURSE DIFFERENCE: 135°
TARGET EVASION: 0
TARGET MACH NO.: 2.0
INTERCEPTOR LATERAL G's: 2.0
INTERCEPTOR MACH NO.: 1.8
σ OF G.C.I. ACCURACY: Five values
A.I. DETECTION RANGE AS FRACTION OF SPECIFICATION RANGE, S: Abscissa
A.I. DETECTION RANGE CONTOUR: Straight Wing
ALTITUDE: 60K

S137

Missile launch zone L-8, minimum range, 8° heading error.

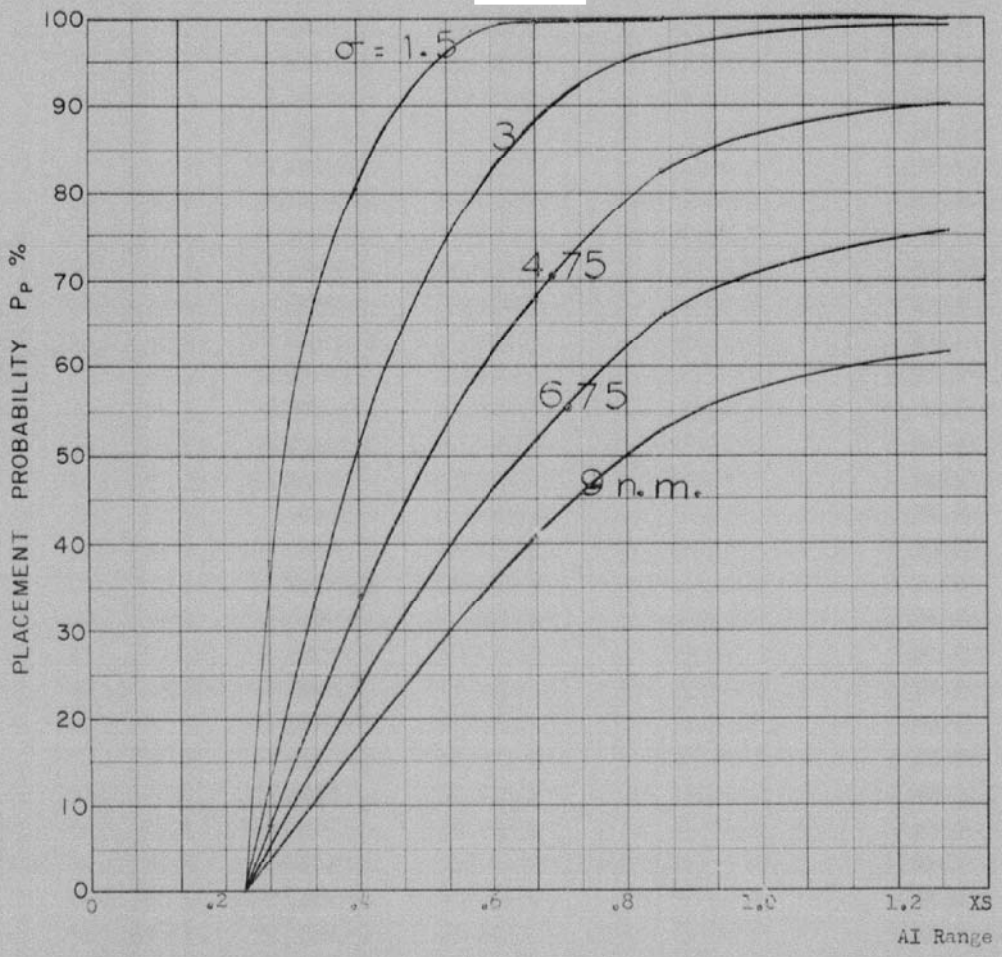

COURSE DIFFERENCE: 75°
TARGET EVASION: 0
TARGET MACH NO.: 2.0
INTERCEPTOR LATERAL G's: 3.6
INTERCEPTOR MACH NO.: 1.8
σ OF G.C.I. ACCURACY: Five values
A.I. DETECTION RANGE AS FRACTION OF SPECIFICATION RANGE, S: Abscissa
A.I. DETECTION RANGE CONTOUR: Straight Wing
ALTITUDE: 60K

S139a

Missile launch zone L-8, minimum range, 8° heading error.

18axspr

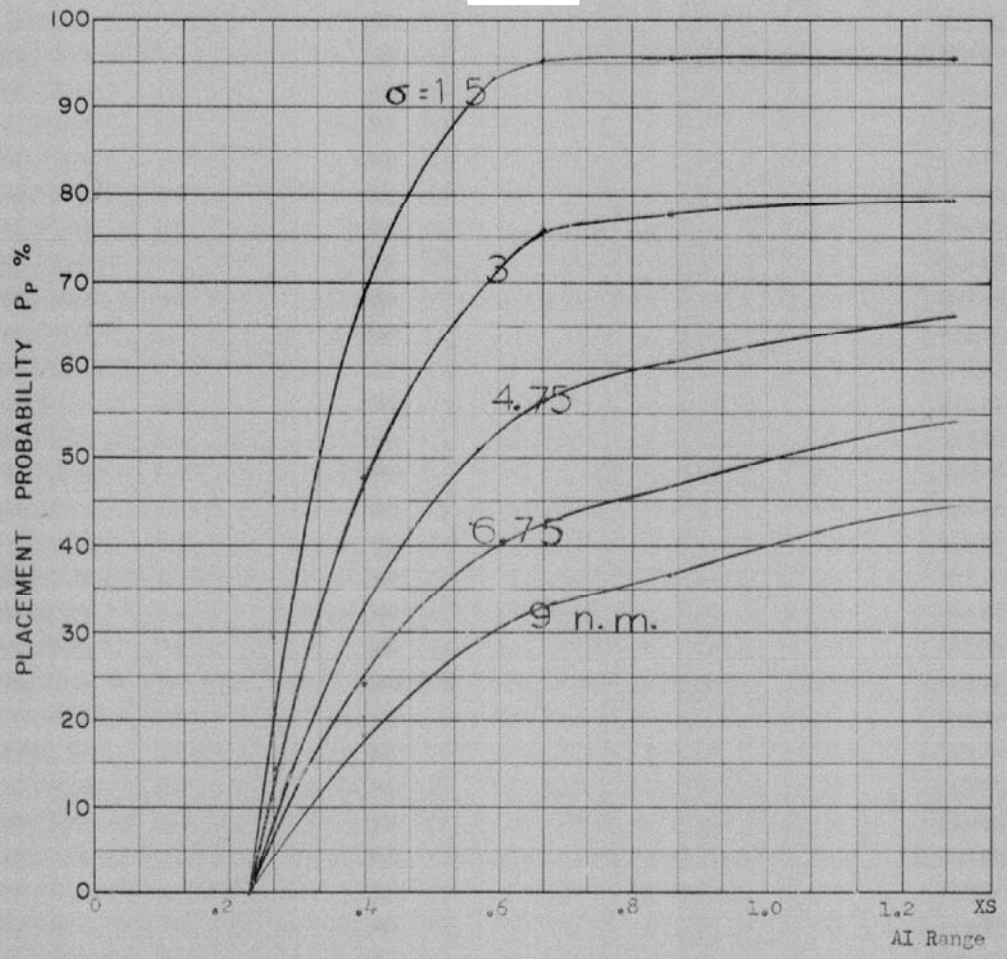

COURSE DIFFERENCE: 75°
TARGET EVASION: 0
TARGET MACH NO.: 2.0
INTERCEPTOR LATERAL G's: 3.6
INTERCEPTOR MACH NO.: 1.8
σ OF G.C.I. ACCURACY: Five values
A.I. DETECTION RANGE AS FRACTION OF SPECIFICATION RANGE, S: Abscissa
A.I. DETECTION RANGE CONTOUR: Straight Wing
ALTITUDE: 60K

S1396

Missile launch zone L-8, medium range, 0° heading error.

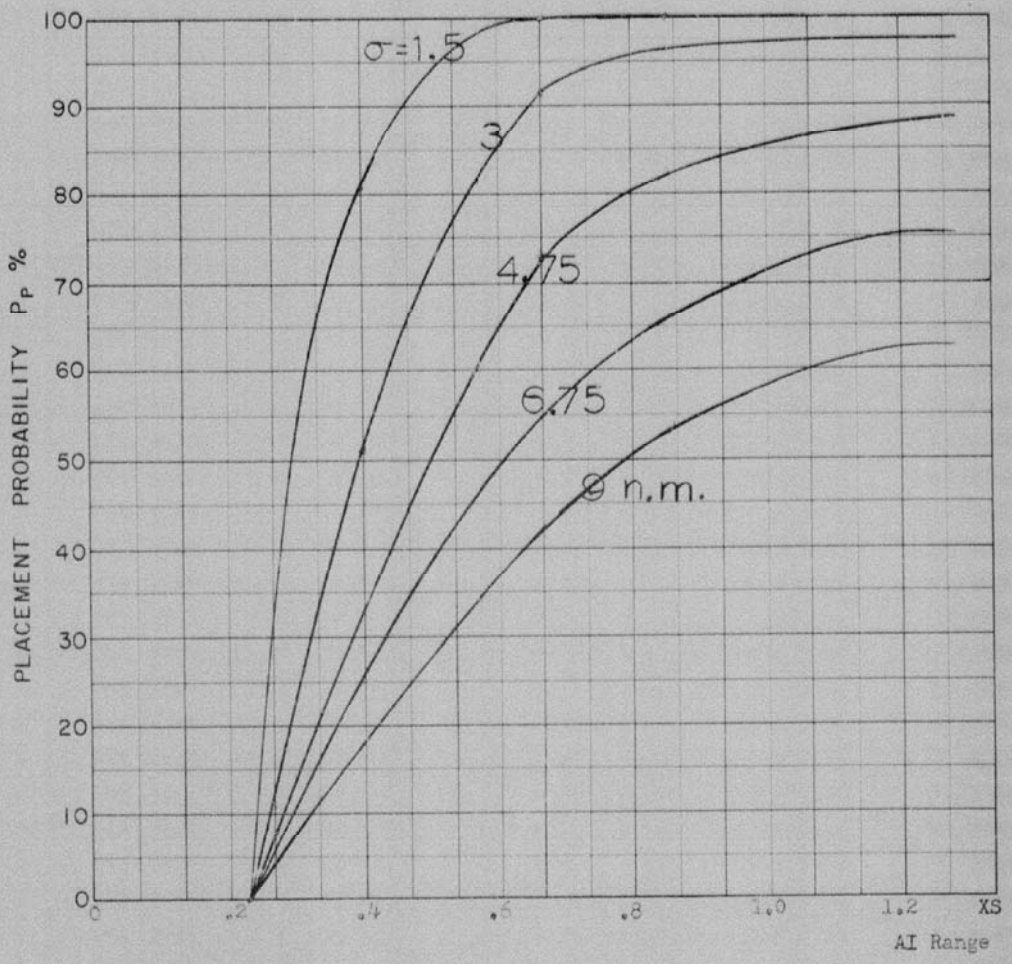

S140a

COURSE DIFFERENCE: 90°
TARGET EVASION: 0
TARGET MACH NO.: 2.0
INTERCEPTOR LATERAL G's: 3.6
INTERCEPTOR MACH NO.: 1.8
σ OF G.C.I. ACCURACY: Five values
A.I. DETECTION RANGE AS FRACTION OF SPECIFICATION RANGE, S: Abscissa
A.I. DETECTION RANGE CONTOUR: Straight Wing
ALTITUDE: 60K

Missile launch zone L-8, minimum range, 8° heading error.

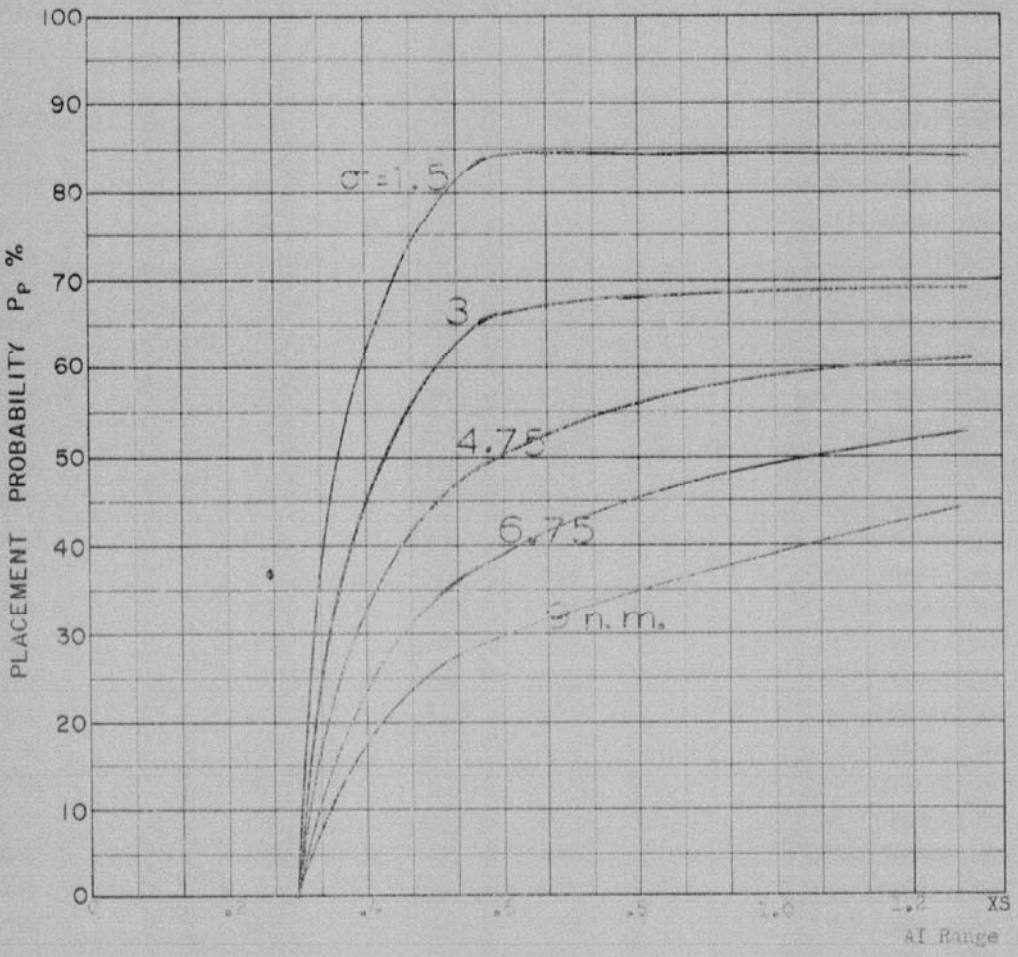

COURSE DIFFERENCE: 90
TARGET EVASION: 0
TARGET MACH NO.: 2.
INTERCEPTOR LATERAL G's: 3.6
INTERCEPTOR MACH NO.: 1.8
σ OF G.C.I. ACCURACY: Five values
A.I. DETECTION RANGE AS FRACTION OF SPECIFICATION RANGE, S Abscissa
A.I. DETECTION RANGE CONTOUR: Straight Wing
ALTITUDE: 60K

(Stu06)

Missile launch zone L-S, medium range, 8° heading error.

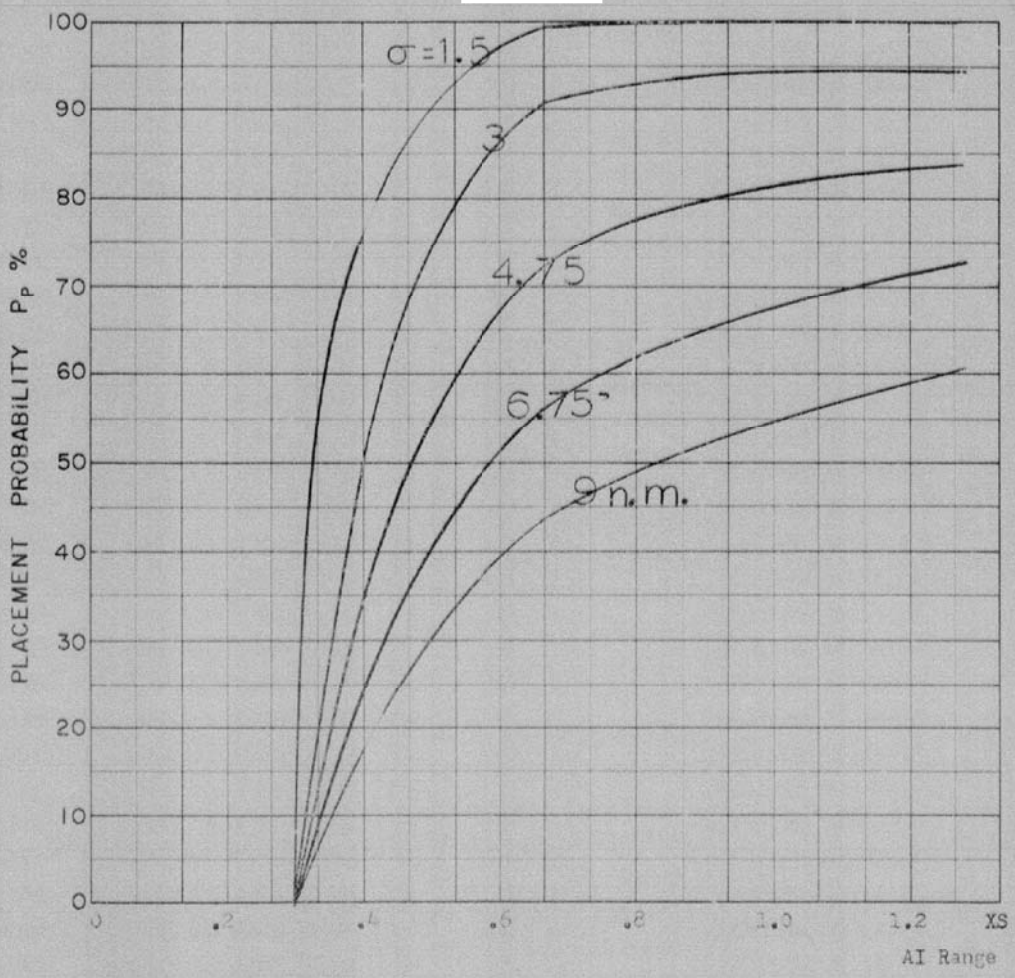

COURSE DIFFERENCE: 100°
TARGET EVASION: 0
TARGET MACH NO.: 2.0
INTERCEPTOR LATERAL G's: 3.6
INTERCEPTOR MACH NO.: 1.8
σ OF G.C.I. ACCURACY: Five values
A.I. DETECTION RANGE AS FRACTION OF SPECIFICATION RANGE, S: Abscissa
A.I. DETECTION RANGE CONTOUR: Straight Wing
ALTITUDE: 60K

S141a

Missile launch zone L-3, minimum range, 8° heading error.

18xxepr

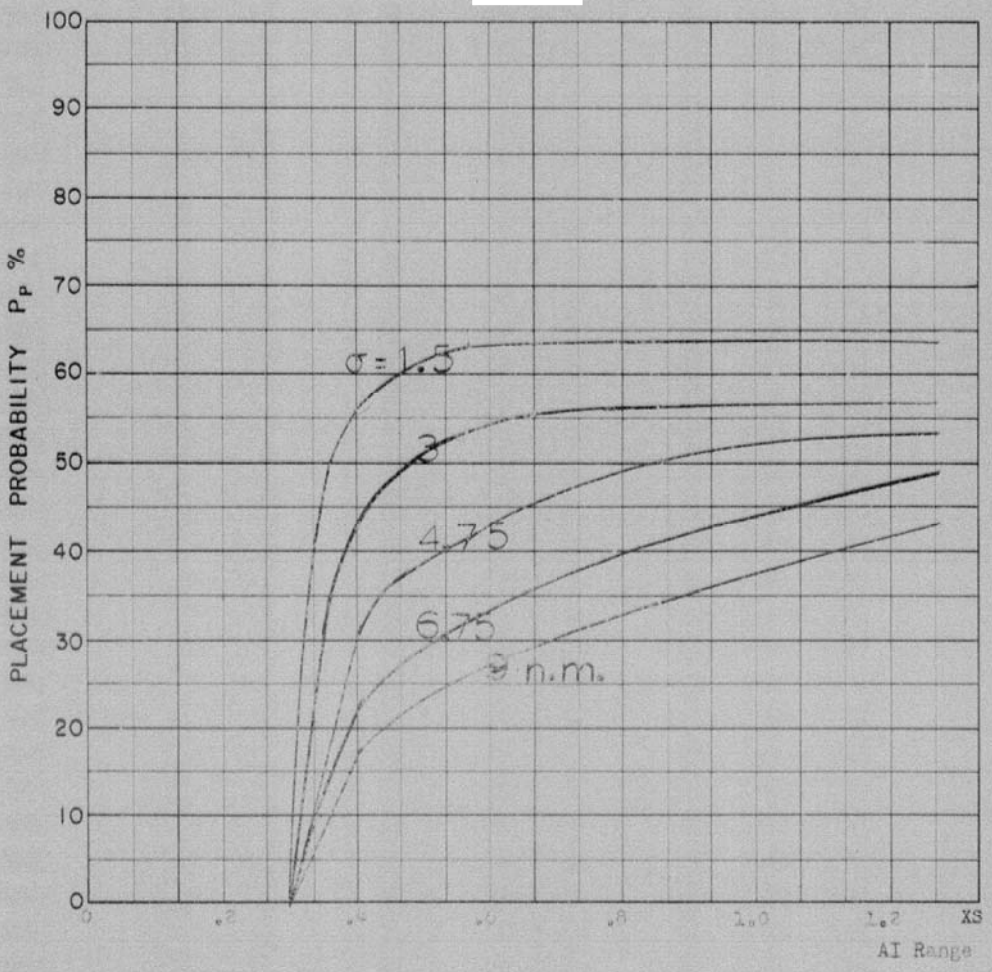

COURSE DIFFERENCE: 180°
TARGET EVASION: 0
TARGET MACH NO.: 2.0
INTERCEPTOR LATERAL G's: 3.6
INTERCEPTOR MACH NO.: 1.8
σ OF G.C.I. ACCURACY: Five values
A.I. DETECTION RANGE AS FRACTION OF SPECIFICATION RANGE, S: Abscissa
A.I. DETECTION RANGE CONTOUR: Straight Wing
ALTITUDE: 60K

S1416

Missile launch zone L-8, minimum range, 8° heading error.

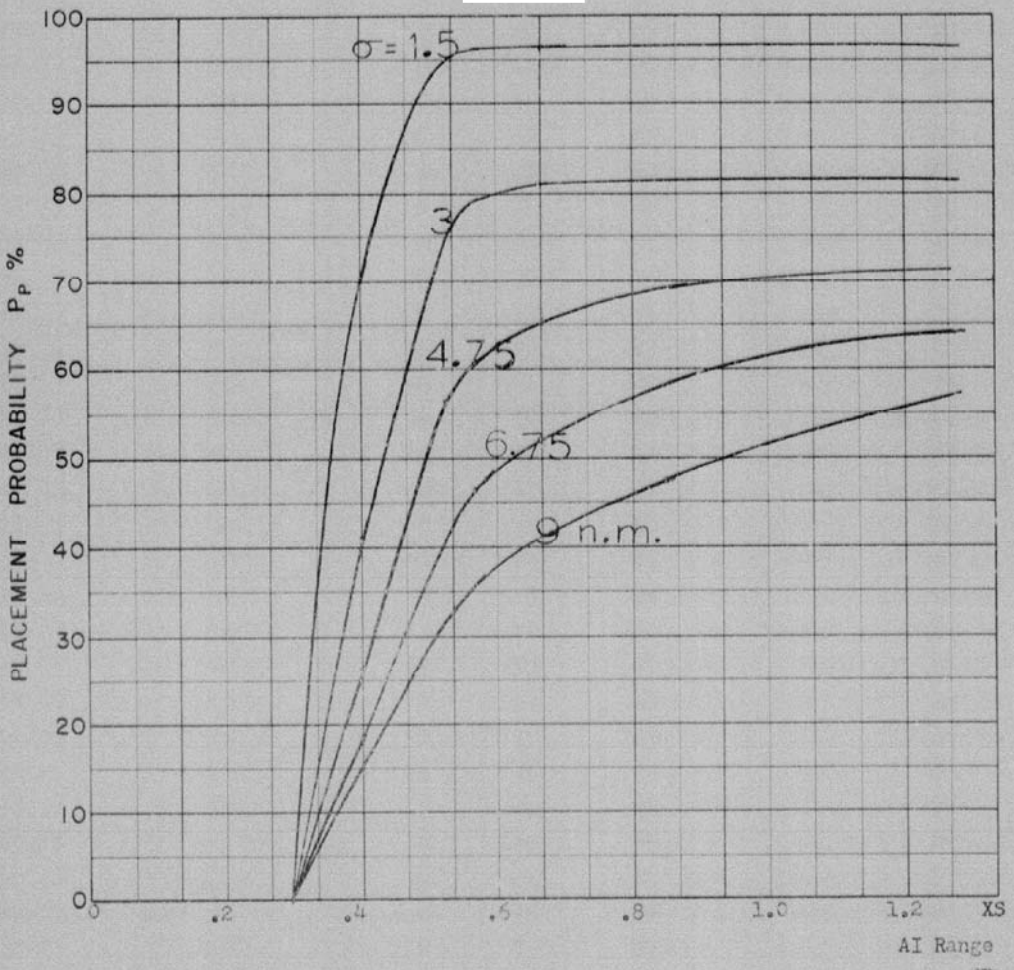

COURSE DIFFERENCE: 120°
TARGET EVASION: 0
TARGET MACH NO.: 2.0
INTERCEPTOR LATERAL G's: 3.6
INTERCEPTOR MACH NO.: 1.8
σ OF G.C.I. ACCURACY: Five values
A.I. DETECTION RANGE AS FRACTION OF SPECIFICATION RANGE, S: Abscissa
A.I. DETECTION RANGE CONTOUR: Straight Wing
ALTITUDE: 60K

(S142)

Missile Launch zone L-8, minimum range, 8° heading error.

18sept

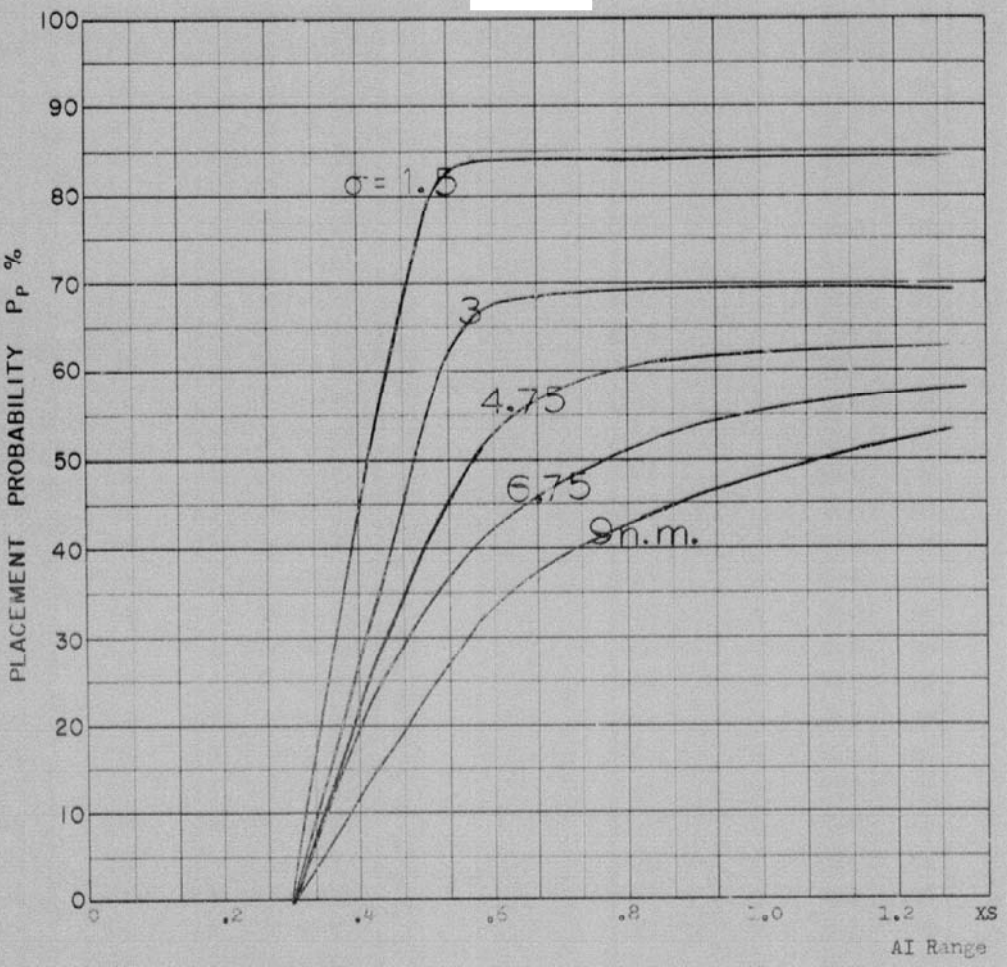

COURSE DIFFERENCE: 135°
TARGET EVASION: 0
TARGET MACH NO.: 2.0
INTERCEPTOR LATERAL G's: 3.6
INTERCEPTOR MACH NO.: 1.8
σ OF G.C.I. ACCURACY: Five values
A.I. DETECTION RANGE AS FRACTION OF SPECIFICATION RANGE, S: Abscissa
A.I. DETECTION RANGE CONTOUR: Straight Wing
ALTITUDE: 60K

S143

Missile launch zone L-8, minimum range, 8° heading error.

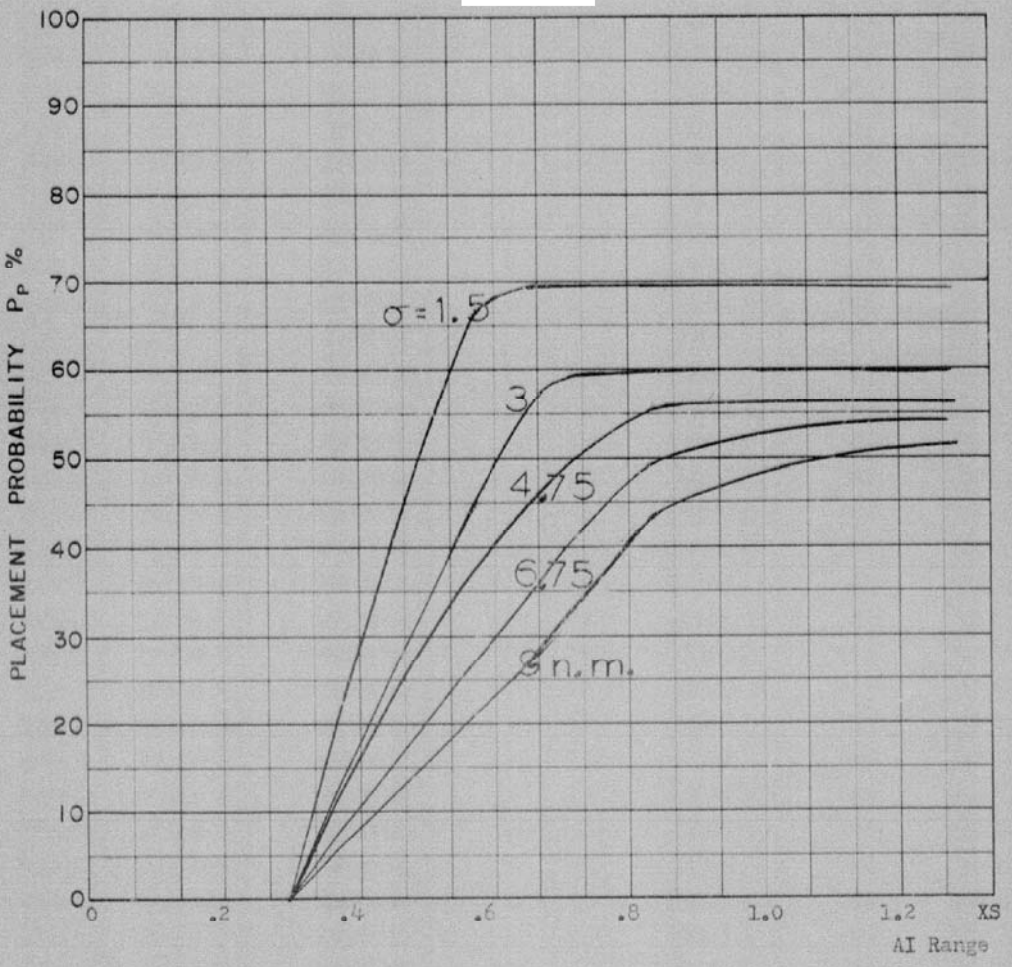

S144

COURSE DIFFERENCE: 160°
TARGET EVASION: 0
TARGET MACH NO.: 2.0
INTERCEPTOR LATERAL G's: 3.6
INTERCEPTOR MACH NO.: 1.8
σ OF G.C.I. ACCURACY: Five values
A.I. DETECTION RANGE AS FRACTION OF SPECIFICATION RANGE, S: Abscissa
A.I. DETECTION RANGE CONTOUR: Straight Wing
ALTITUDE: 60K

Missile launch zone L-8, minimum range, 8° heading error.

36 e

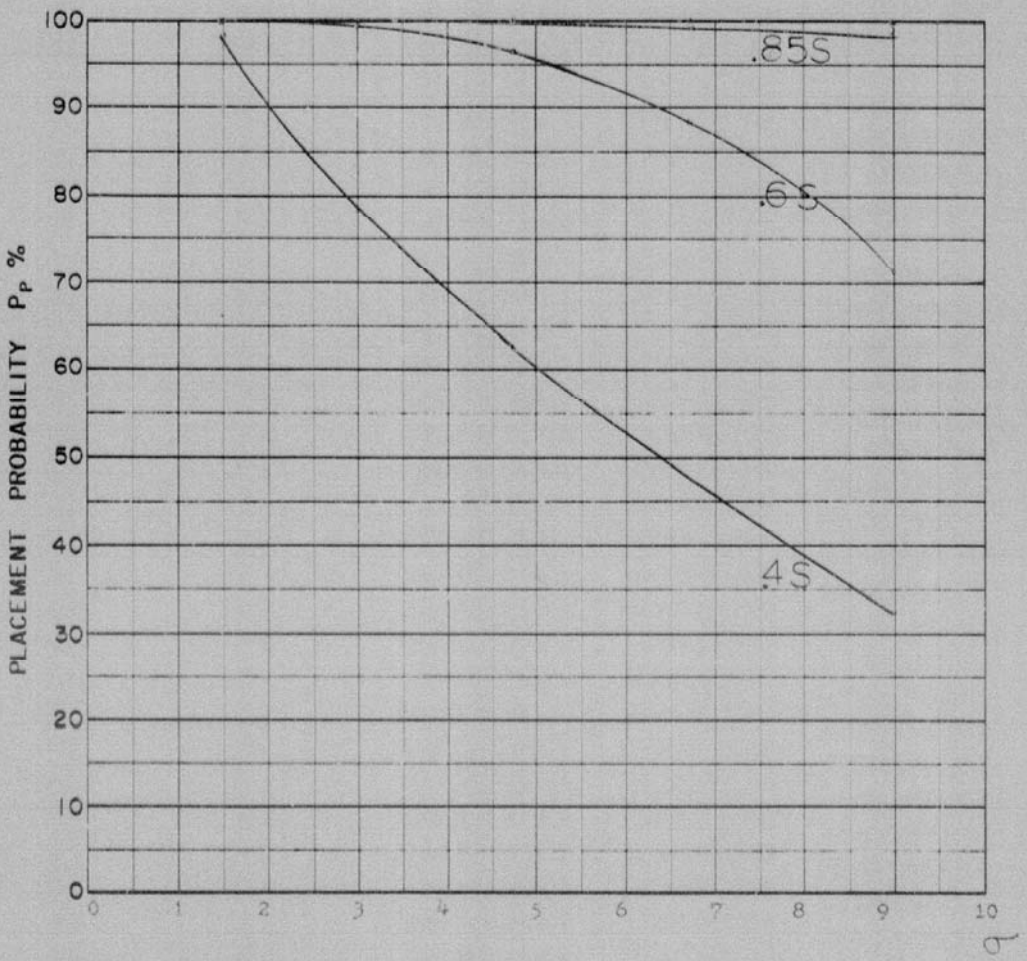

COURSE DIFFERENCE: 160°
TARGET EVASION: 0
TARGET MACH NO.: 1.5
INTERCEPTOR LATERAL G's: 1.6
INTERCEPTOR MACH NO.: 1.5
σ OF G.C.I. ACCURACY: Abscissa
A.I. DETECTION RANGE AS FRACTION OF SPECIFICATION RANGE, S: 3 values
A.I. DETECTION RANGE CONTOUR: Delta
ALTITUDE: 50 K

A-1

Missile launch zone L-1, maximum range 15° heading error

36 c

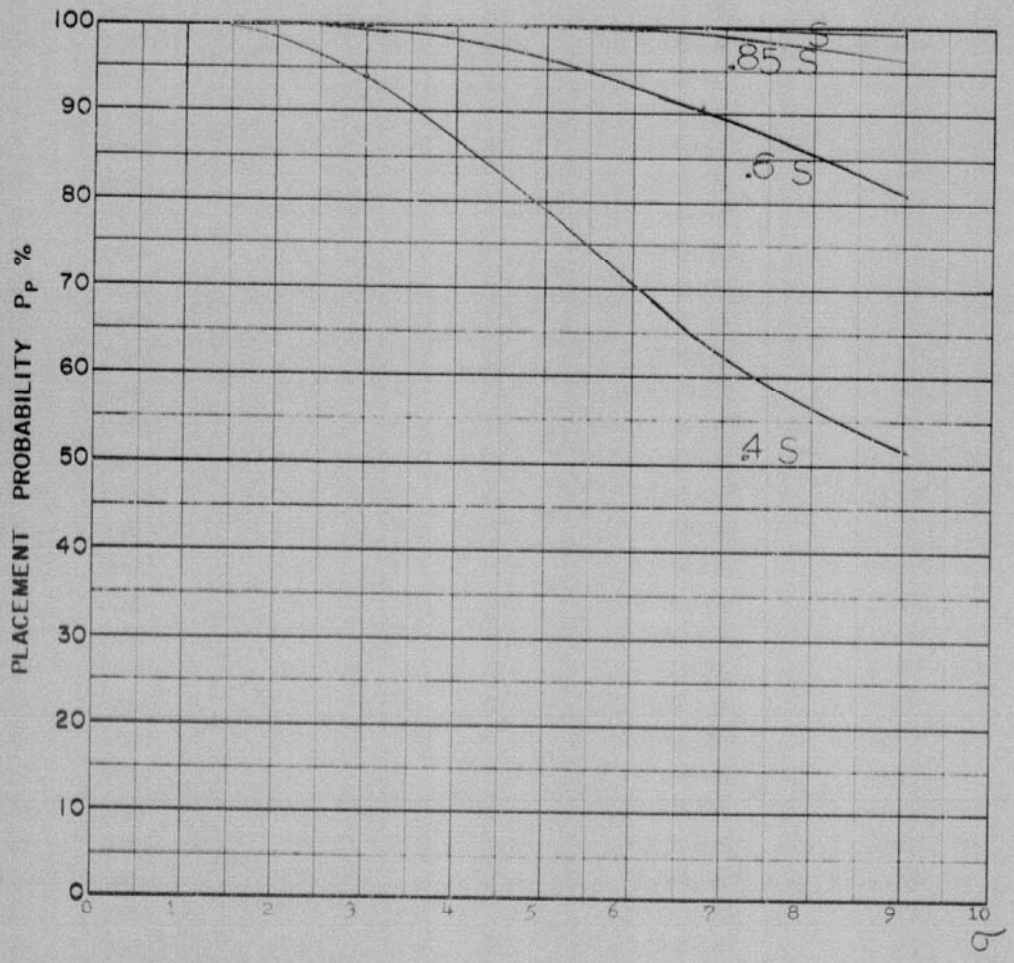

COURSE DIFFERENCE: 120°
TARGET EVASION: 0
TARGET MACH NO.: 1.5
INTERCEPTOR LATERAL G's: 1.6
INTERCEPTOR MACH NO.: 1.5
σ OF G.C.I. ACCURACY: Abscissa
A.I. DETECTION RANGE AS FRACTION OF SPECIFICATION RANGE, S: 4 values
A.I. DETECTION RANGE CONTOUR: Delta
ALTITUDE: 50 K

(A-2)

Missile launch zone L-1, maximum range,
15° heading error

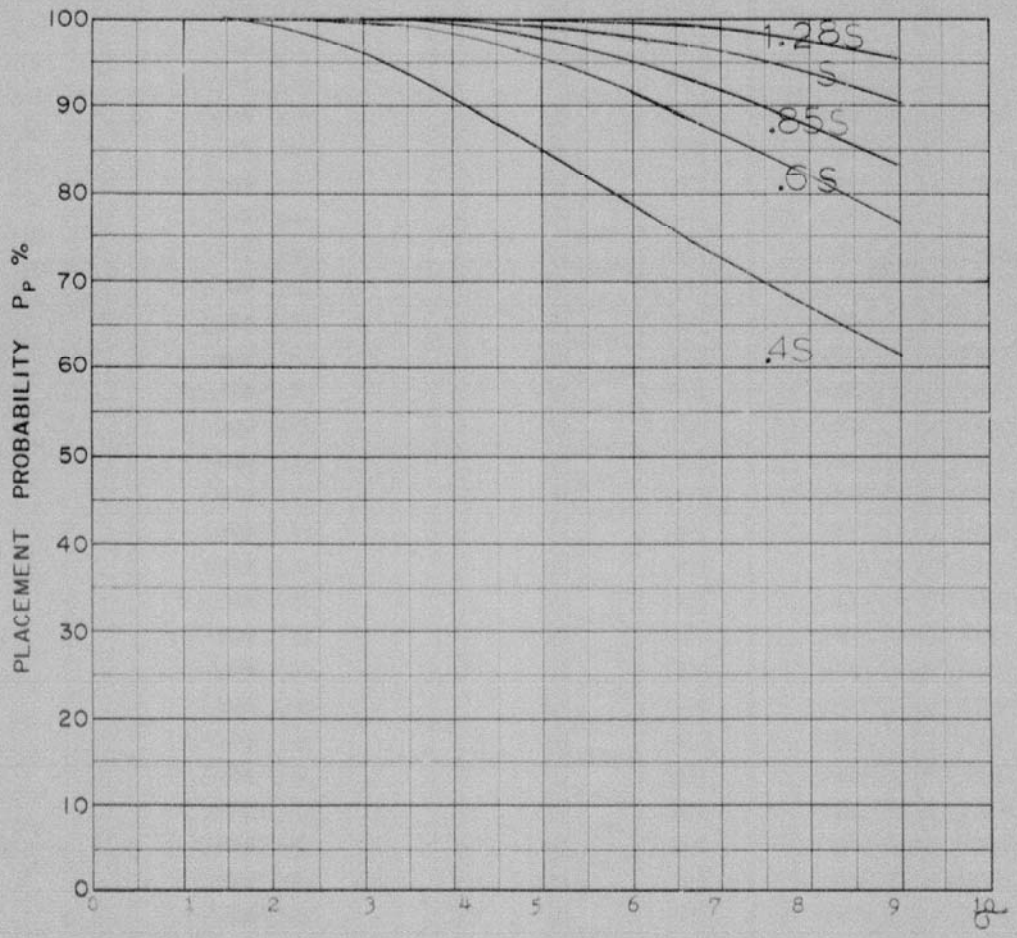

COURSE DIFFERENCE: 80°
TARGET EVASION: 0
TARGET MACH NO.: 1.5
INTERCEPTOR LATERAL G's: 1.6
INTERCEPTOR MACH NO.: 1.5
σ OF G.C.I. ACCURACY: Abscissa
A.I. DETECTION RANGE AS FRACTION OF SPECIFICATION RANGE, S: 5 values
A.I. DETECTION RANGE CONTOUR: Delta
ALTITUDE: 50 K

Missile launch zone L-1
Maximum range, 15° heading error

A3

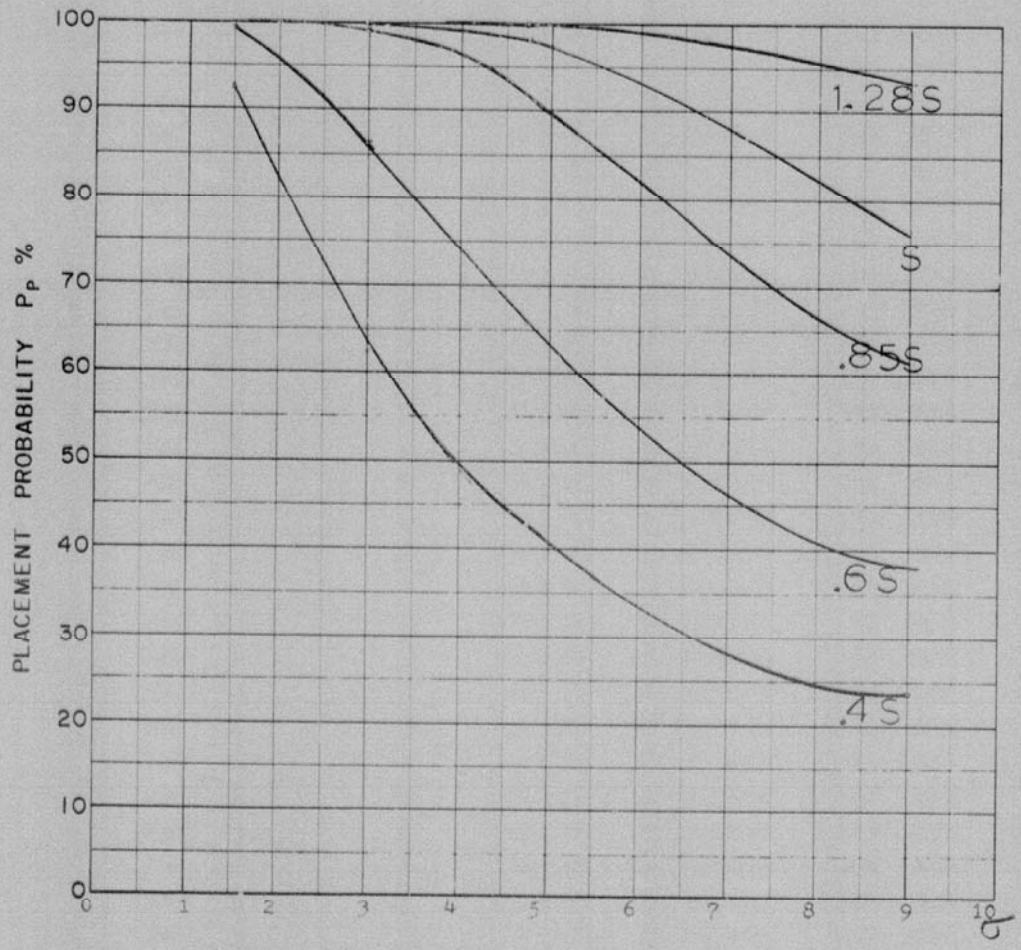

COURSE DIFFERENCE: 160°
TARGET EVASION: 0.15 lateral g's
TARGET MACH NO.: 1.5
INTERCEPTOR LATERAL G's: 0.85
INTERCEPTOR MACH NO.: 1.5
σ OF G.C.I. ACCURACY: Abscissa
A.I. DETECTION RANGE AS FRACTION OF SPECIFICATION RANGE, S Four values
A.I. DETECTION RANGE CONTOUR: Delta
ALTITUDE: 50 K

(A-4)

Missile launch zone L-12

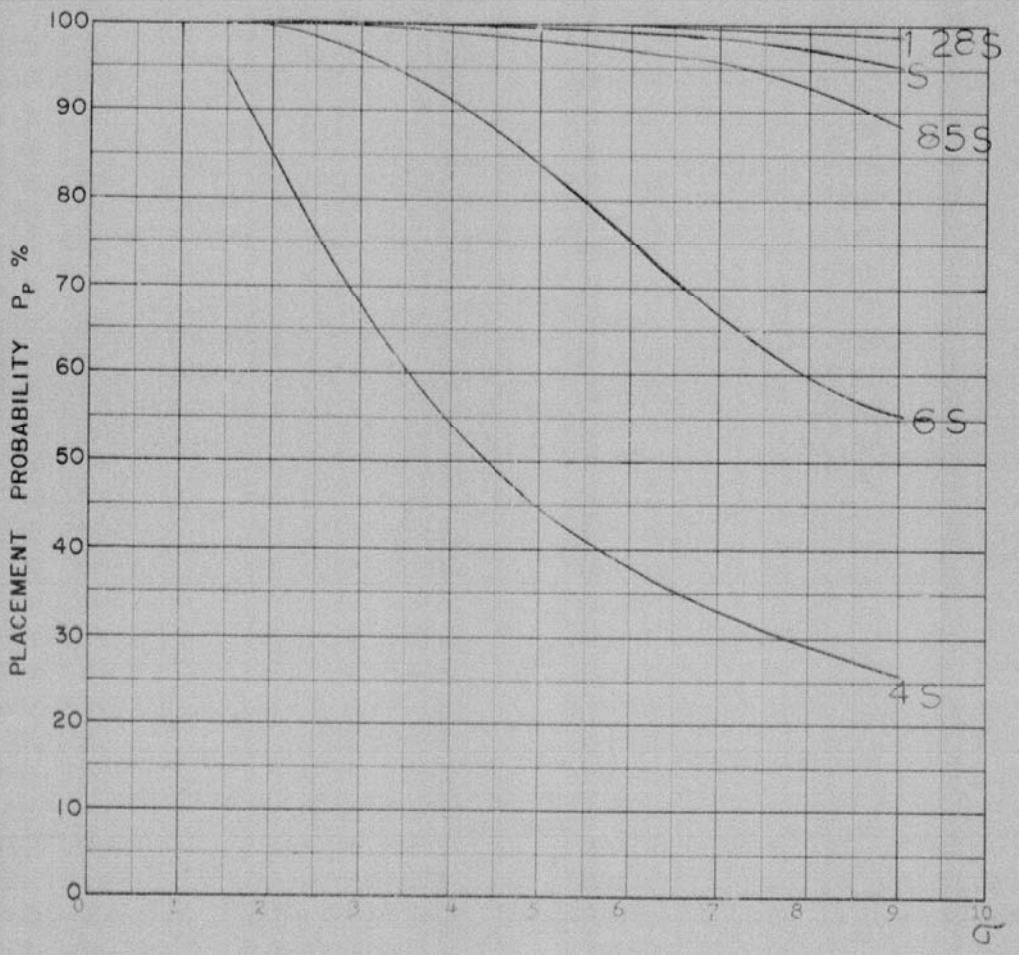

COURSE DIFFERENCE: 160°
TARGET EVASION: 0.15 lateral g's
TARGET MACH NO.: 1.5
INTERCEPTOR LATERAL G's: 1.6
INTERCEPTOR MACH NO.: 1.5
σ OF G.C.I. ACCURACY: Abscissa
A.I. DETECTION RANGE AS FRACTION OF SPECIFICATION RANGE, S: 5 values
A.I. DETECTION RANGE CONTOUR: Delta
ALTITUDE: 50 K

(A-5)

Missile launch zone L-12

29 e

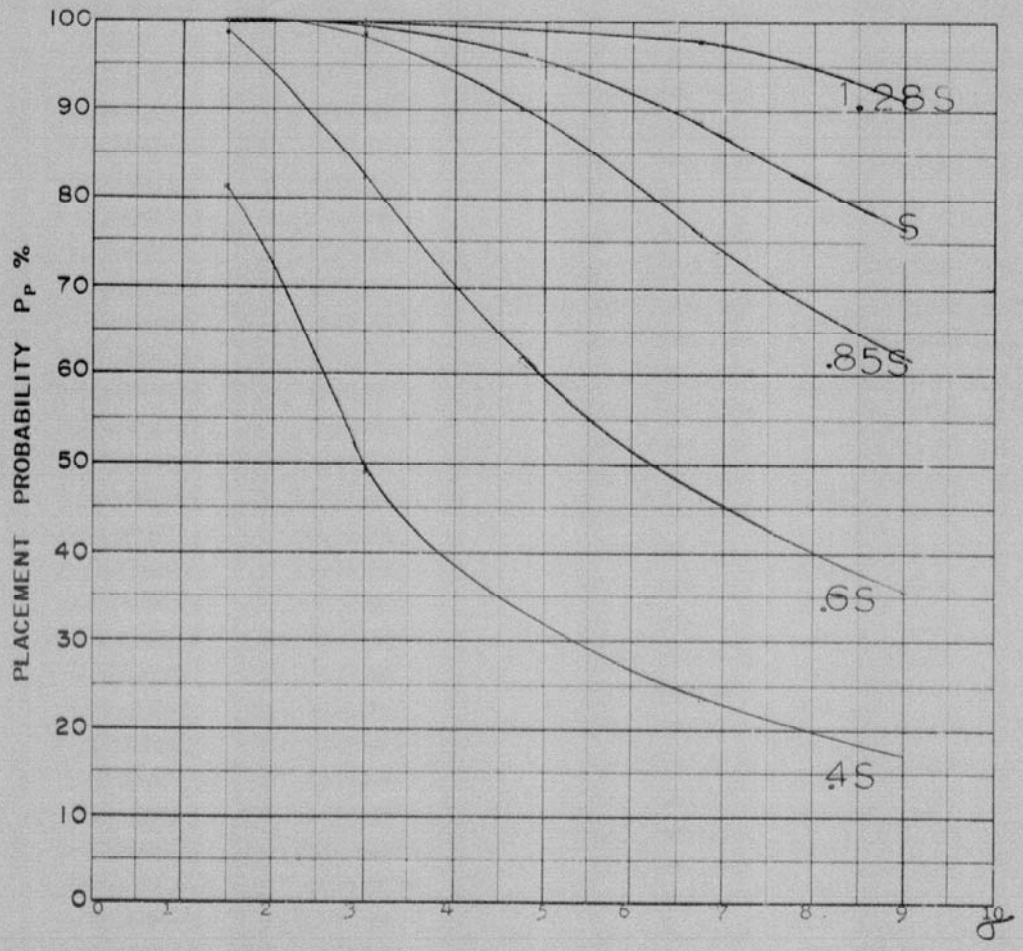

COURSE DIFFERENCE: 135°
TARGET EVASION: 0
TARGET MACH NO.: 2.0
INTERCEPTOR LATERAL G's: 0.85
INTERCEPTOR MACH NO.: 1.5
σ OF G.C.I. ACCURACY: Abscissa
A.I. DETECTION RANGE AS FRACTION OF SPECIFICATION RANGE, S: 5 values
A.I. DETECTION RANGE CONTOUR: Delta
ALTITUDE: 50 K

Missile launch zone L-3
Maximum range 10° heading error

(A-6)

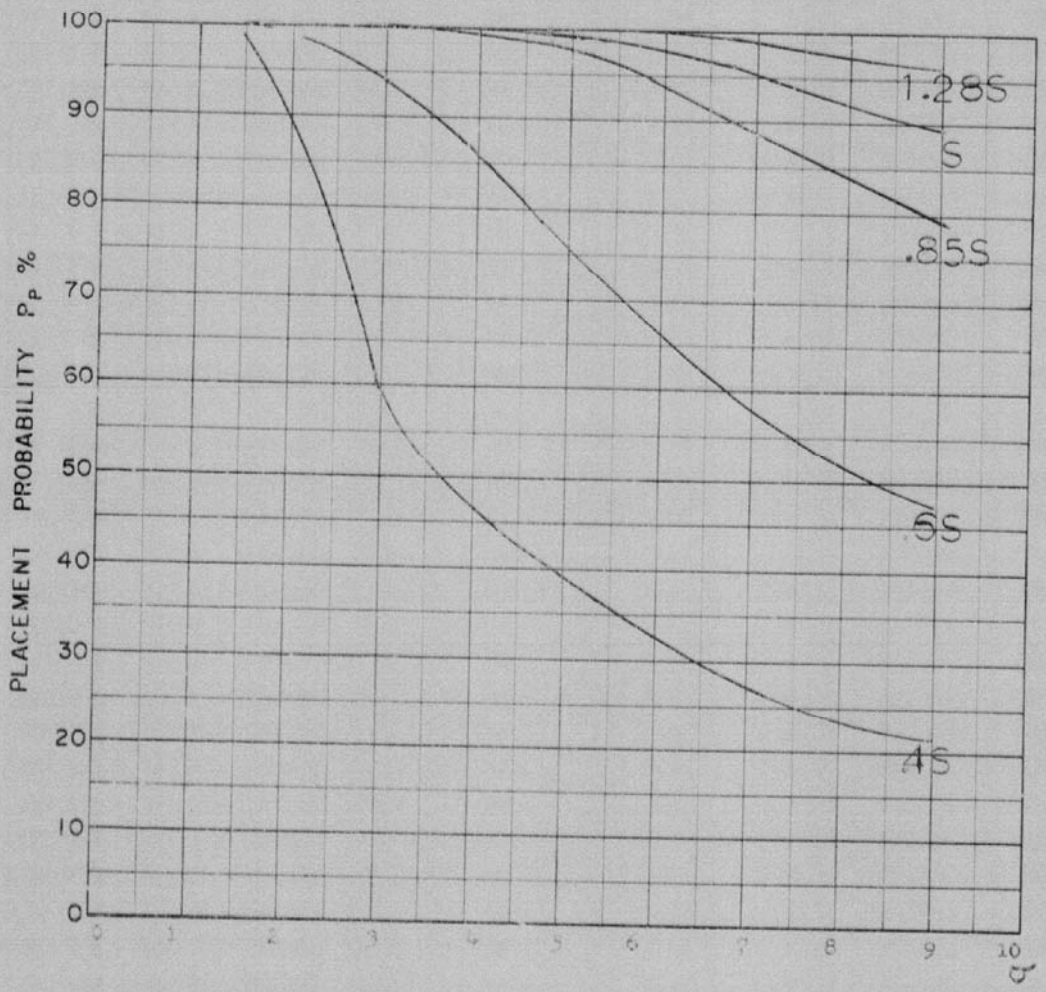

COURSE DIFFERENCE: 160°
TARGET EVASION: 0.1 lateral g's, towards interceptor only
TARGET MACH NO.: 2.0
INTERCEPTOR LATERAL G's: 1.6
INTERCEPTOR MACH NO.: 1.5
σ OF G.C.I. ACCURACY: Abscissa
A.I. DETECTION RANGE AS FRACTION OF SPECIFICATION RANGE, S: 4 values
A.I. DETECTION RANGE CONTOUR: Delta
ALTITUDE: 50 K

A-7

Missile launch zone L-10

38b dpn3

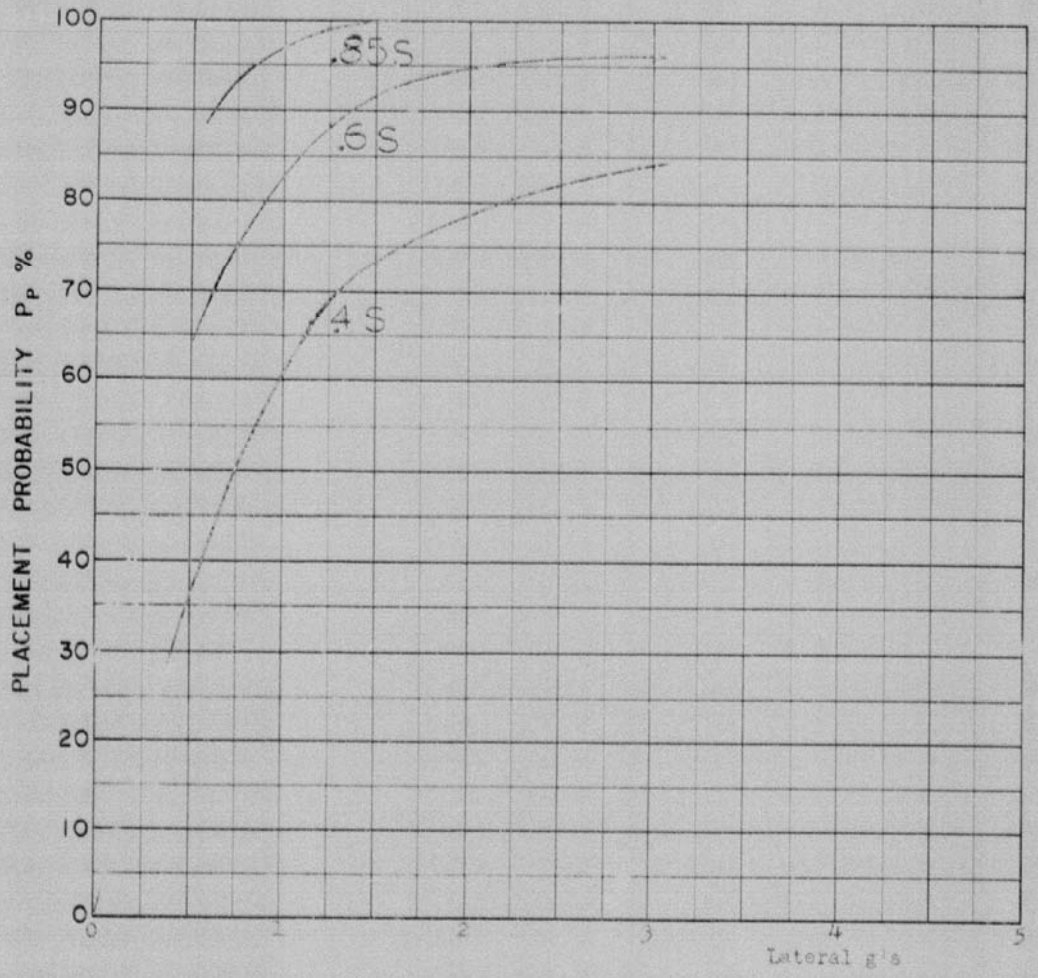

COURSE DIFFERENCE: 100°
TARGET EVASION: 0
TARGET MACH NO.: 1.5
INTERCEPTOR LATERAL G's: Abscissa
INTERCEPTOR MACH NO.: 2.5
σ OF G.C.I. ACCURACY: 6.75 N.M.
A.I. DETECTION RANGE AS FRACTION OF SPECIFICATION RANGE, S: 3 values
A.I. DETECTION RANGE CONTOUR: Delta
ALTITUDE: 50 K

G-1

Launch zone figure L-1, maximum range 15° heading error.

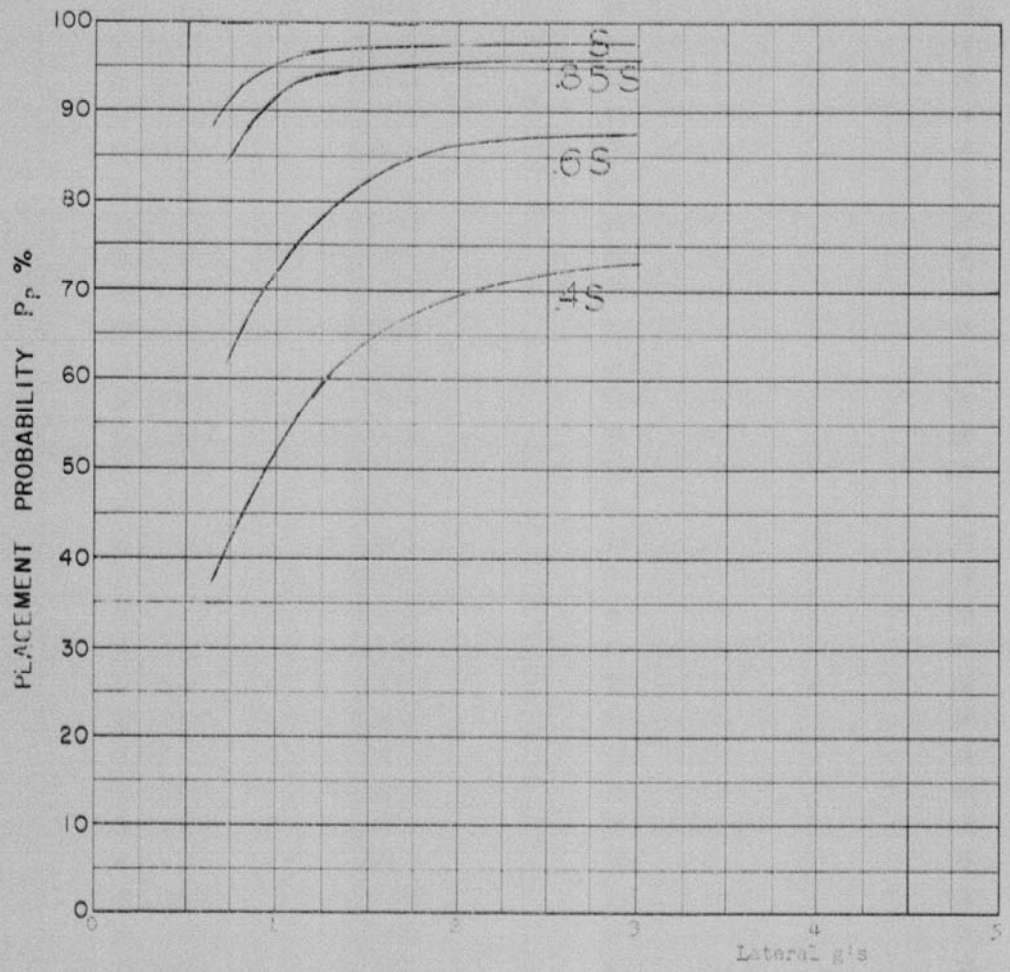

COURSE DIFFERENCE: 200°
TARGET EVASION: 0
TARGET MACH NO.: 1.5
INTERCEPTOR LATERAL G's: Abscissa
INTERCEPTOR MACH NO.: 1.5
σ OF G.C.I. ACCURACY: 9 n.m.
A.I. DETECTION RANGE AS FRACTION OF SPECIFICATION RANGE, S: 4 values
A.I. DETECTION RANGE CONTOUR: Delta
ALTITUDE: 50 K

G-2

Launch zone L.I. maximum range, 35° heading error.

38e dpn3

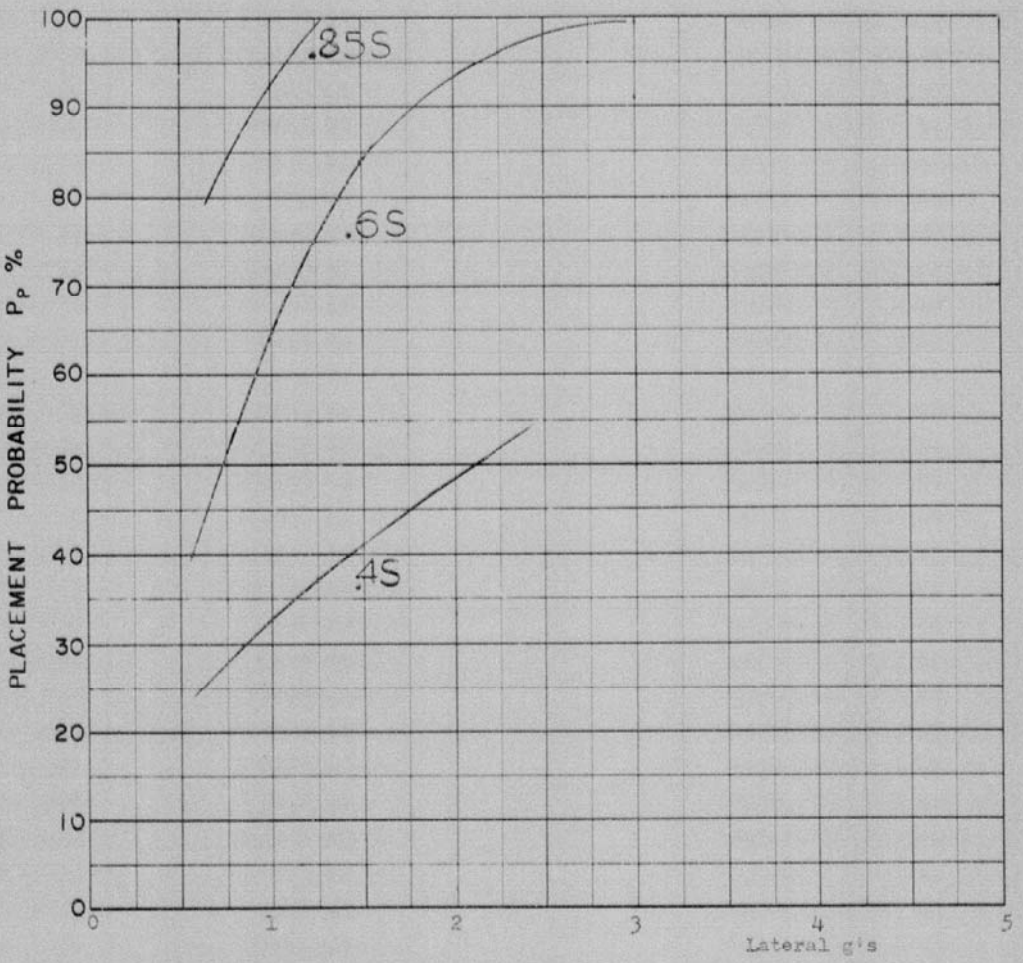

COURSE DIFFERENCE: 160°
TARGET EVASION: 0
TARGET MACH NO.: 1.5
INTERCEPTOR LATERAL G's: Abscissa
INTERCEPTOR MACH NO.: 1.5
σ OF G.C.I. ACCURACY: 6.75 n.m.
A.I. DETECTION RANGE AS FRACTION OF SPECIFICATION RANGE, S: 3 values
A.I. DETECTION RANGE CONTOUR: Delta
ALTITUDE: 50 K

G-3

Launch zone L-1, maximum range, 15° heading error.

38e dpn/4

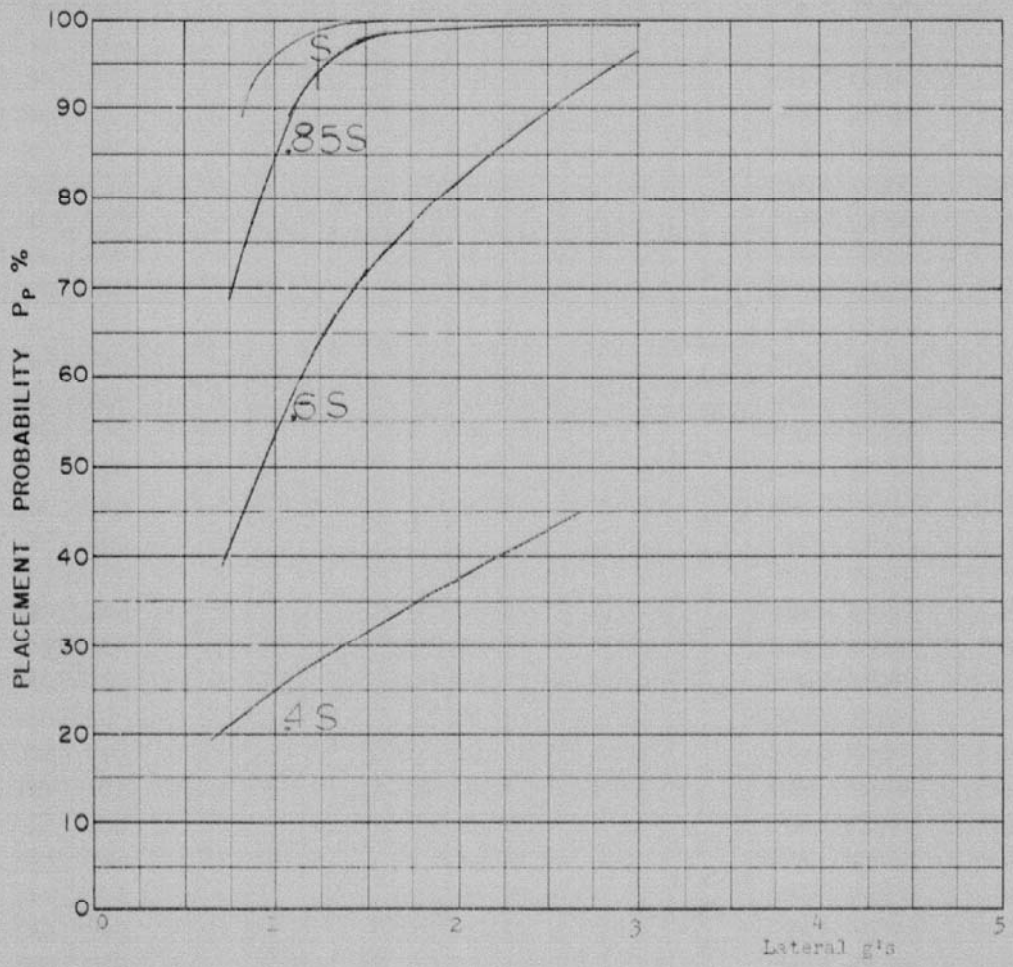

COURSE DIFFERENCE: 160°
TARGET EVASION: 0
TARGET MACH NO.: 1.5
INTERCEPTOR LATERAL G's: Abscissa
INTERCEPTOR MACH NO.: 1.5
σ OF G.C.I. ACCURACY: 9 n.m.
A.I. DETECTION RANGE AS FRACTION OF SPECIFICATION RANGE, S: 4 values
A.I. DETECTION RANGE CONTOUR: Delta
ALTITUDE: 50 K

G-4

Launch zone L-1, maximum range, 15° heading error.

181 dpnJ

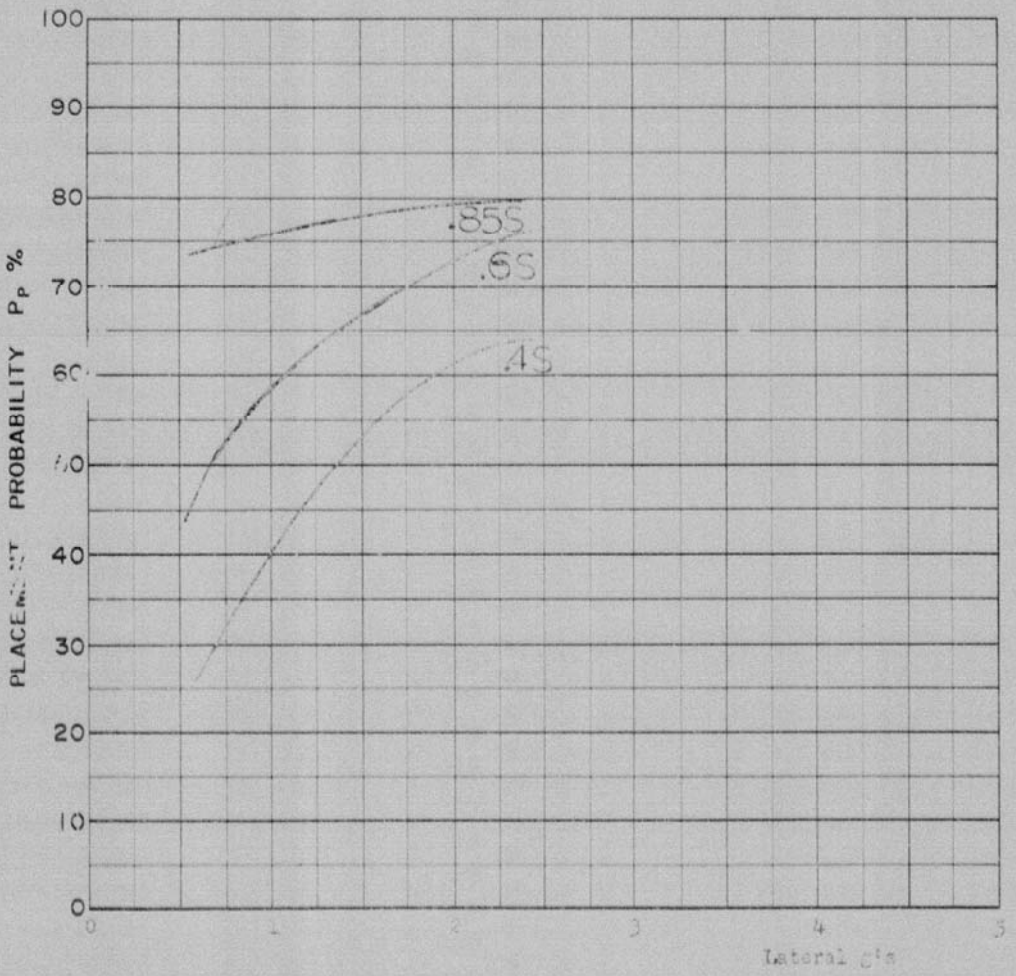

COURSE DIFFERENCE: 110°
TARGET EVASION: 0.15 Lateral g's
TARGET MACH NO.: 1.5
INTERCEPTOR LATERAL G's: Abscissa
INTERCEPTOR MACH NO.: 1.6
σ OF G.C.I. ACCURACY: 4.75 N.M.
A.I. DETECTION RANGE AS FRACTION OF SPECIFICATION RANGE, S β values
A.I. DETECTION RANGE CONTOUR: Delta
ALTITUDE: 60 K

G-5

Missile launch zone L-13

181 dpn

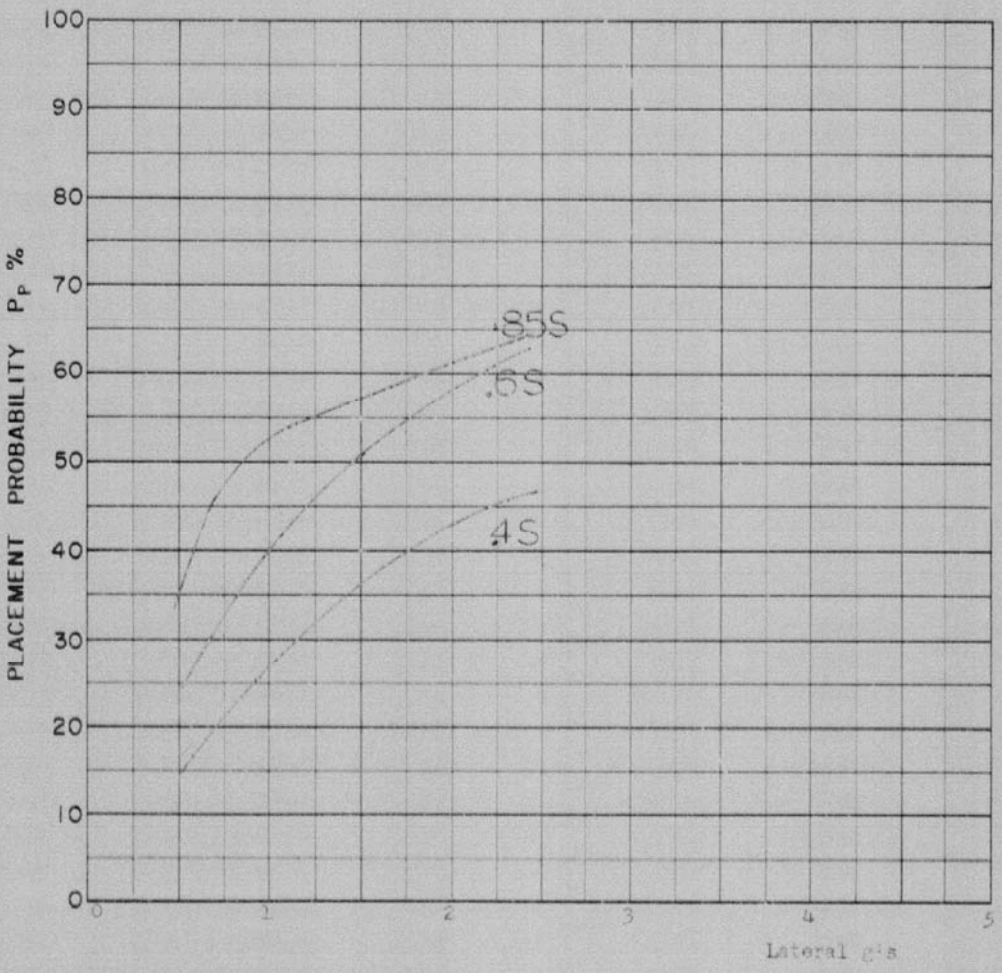

COURSE DIFFERENCE: 110°
TARGET EVASION: 0.15 lateral g's
TARGET MACH NO.: 1.5
INTERCEPTOR LATERAL G's: Abscissa
INTERCEPTOR MACH NO.: 1.5
σ OF G.C.I. ACCURACY: 6.75 n.m.
A.I. DETECTION RANGE AS FRACTION OF SPECIFICATION RANGE, S: values
A.I. DETECTION RANGE CONTOUR: Delta
ALTITUDE: 50 K

G-6

Missile launch zone L-13

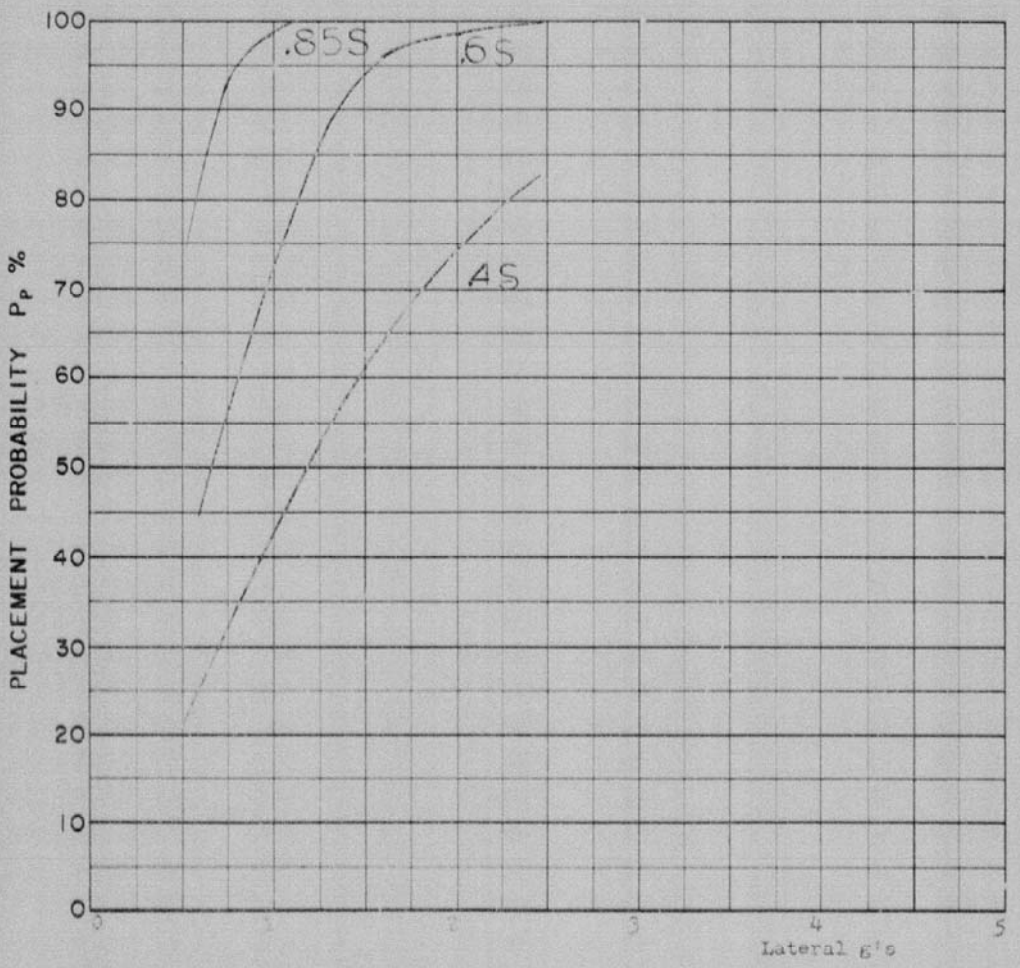

COURSE DIFFERENCE: 180°
TARGET EVASION: 0.15 lateral g's
TARGET MACH NO.: 1.5
INTERCEPTOR LATERAL G's: Abscissa
INTERCEPTOR MACH NO.: 2.5
σ OF G.C.I. ACCURACY: 3 n.m.
A.I. DETECTION RANGE AS FRACTION OF SPECIFICATION RANGE, S: 2 values
A.I. DETECTION RANGE CONTOUR: Delta
ALTITUDE: 60 K

Missile launch zone L-13

G-7

186 dpn3

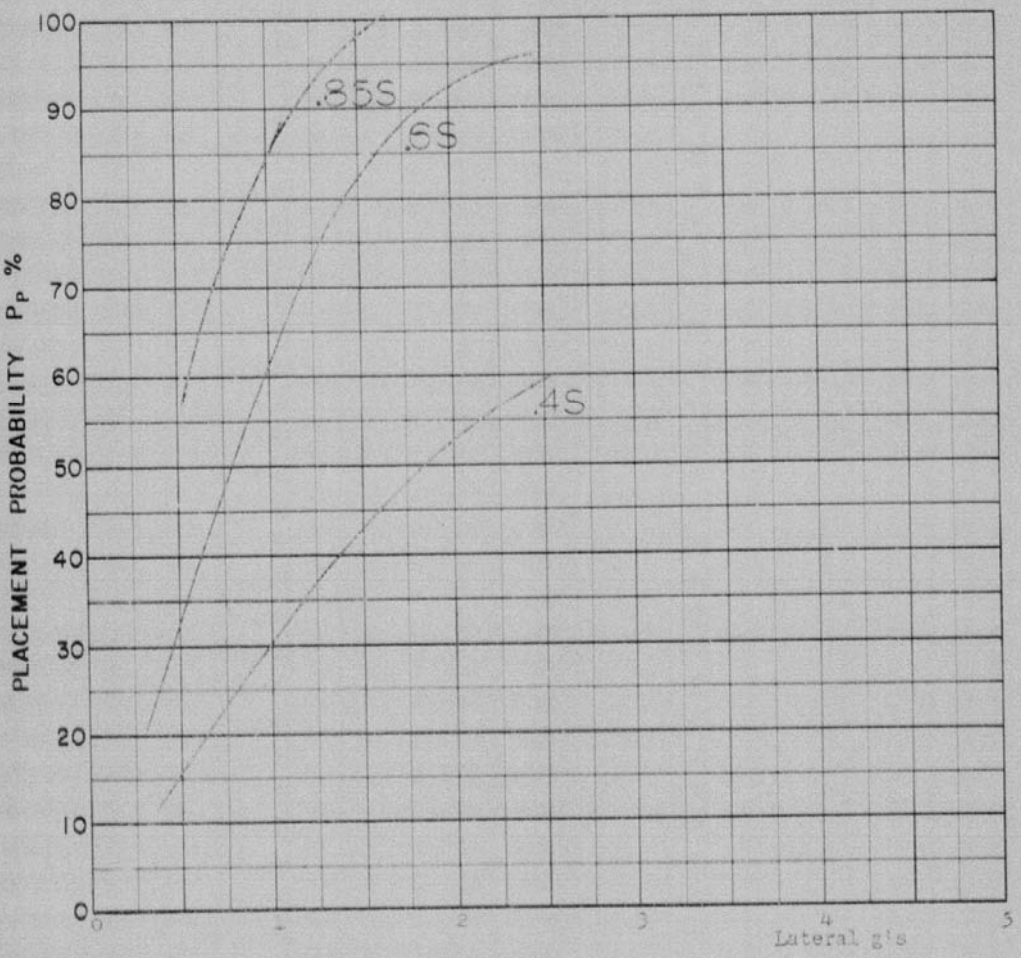

COURSE DIFFERENCE: 180°
TARGET EVASION: 0.15 lateral g's
TARGET MACH NO.: 2.5
INTERCEPTOR LATERAL G's: Abscissa
INTERCEPTOR MACH NO.: 1.5
σ OF G.C.I. ACCURACY: 4.75 n.m.
A.I. DETECTION RANGE AS FRACTION OF SPECIFICATION RANGE, S: 3 values
A.I. DETECTION RANGE CONTOUR: Delta
ALTITUDE: 60 K

G-8

Missile launch zone L-13

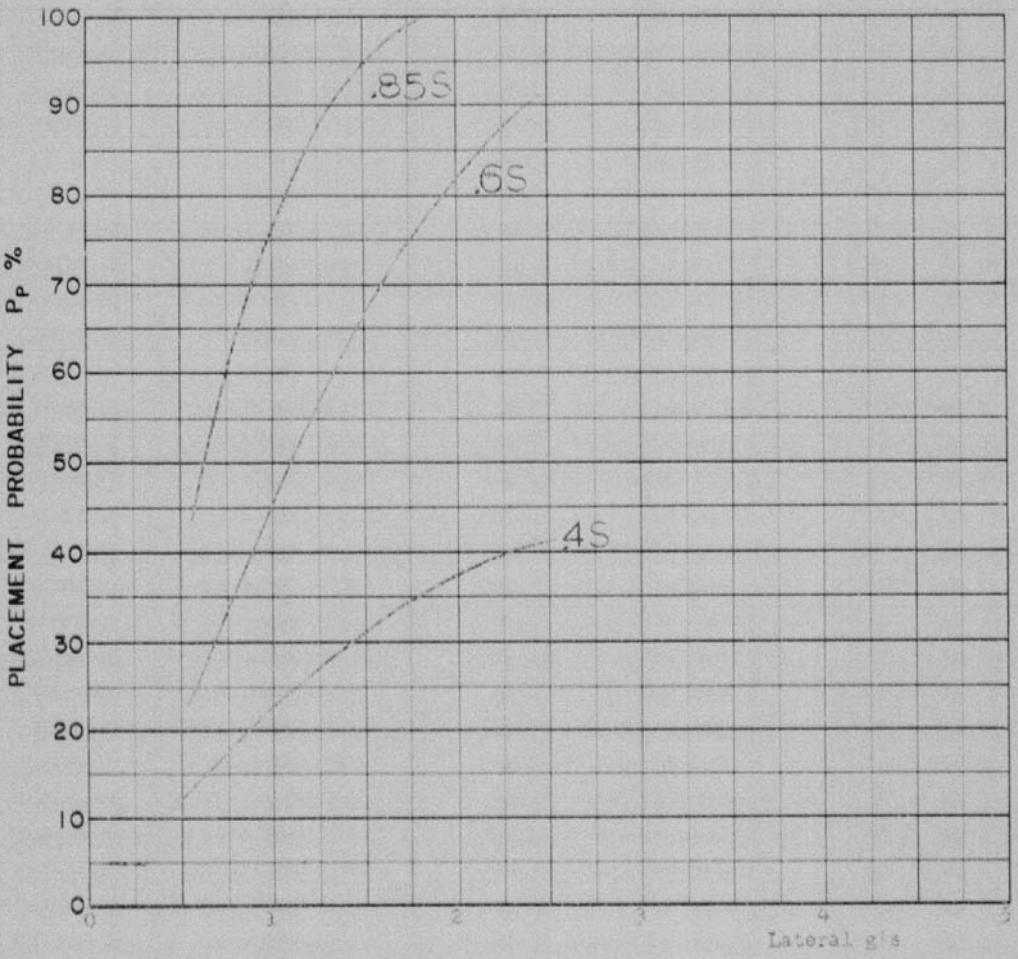

COURSE DIFFERENCE: 180°
TARGET EVASION: 0.15 lateral g's
TARGET MACH NO.: 1.5
INTERCEPTOR LATERAL G's: Abscissa
INTERCEPTOR MACH NO.: 1.8
σ OF G.C.I. ACCURACY: 0.75 n.m.
A.I. DETECTION RANGE AS FRACTION OF SPECIFICATION RANGE, S: 3 values
A.I. DETECTION RANGE CONTOUR: Delta
ALTITUDE: 60 K

Missile launch zone L-13

G-9

4 axipnl

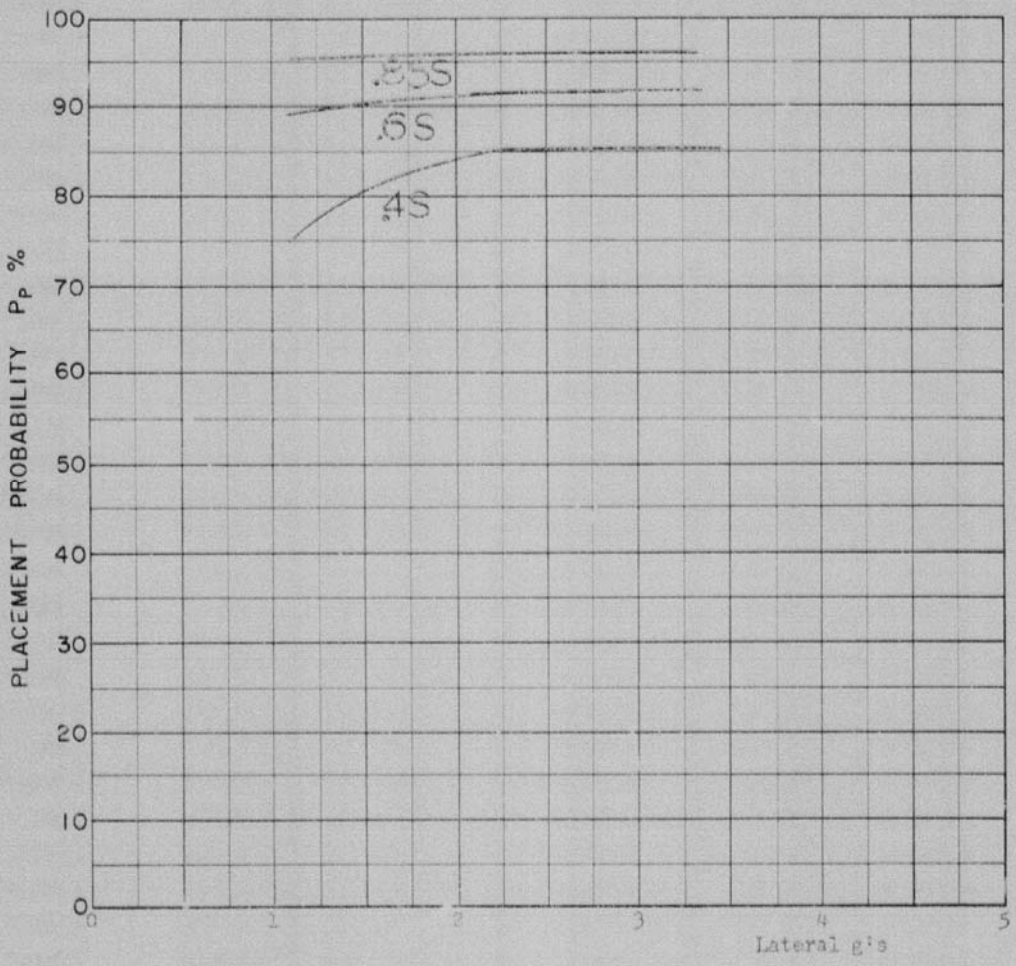

COURSE DIFFERENCE: 90°
TARGET EVASION: 0
TARGET MACH NO.: 2.0
INTERCEPTOR LATERAL G's: Abscissa
INTERCEPTOR MACH NO.: 1.5
σ OF G.C.I. ACCURACY: 3 n.m.
A.I. DETECTION RANGE AS FRACTION OF SPECIFICATION RANGE, S: 3 values
A.I. DETECTION RANGE CONTOUR: Delta
ALTITUDE: 60 K

G-10

Missile launch zone L-5 maximum range, 8° heading error.

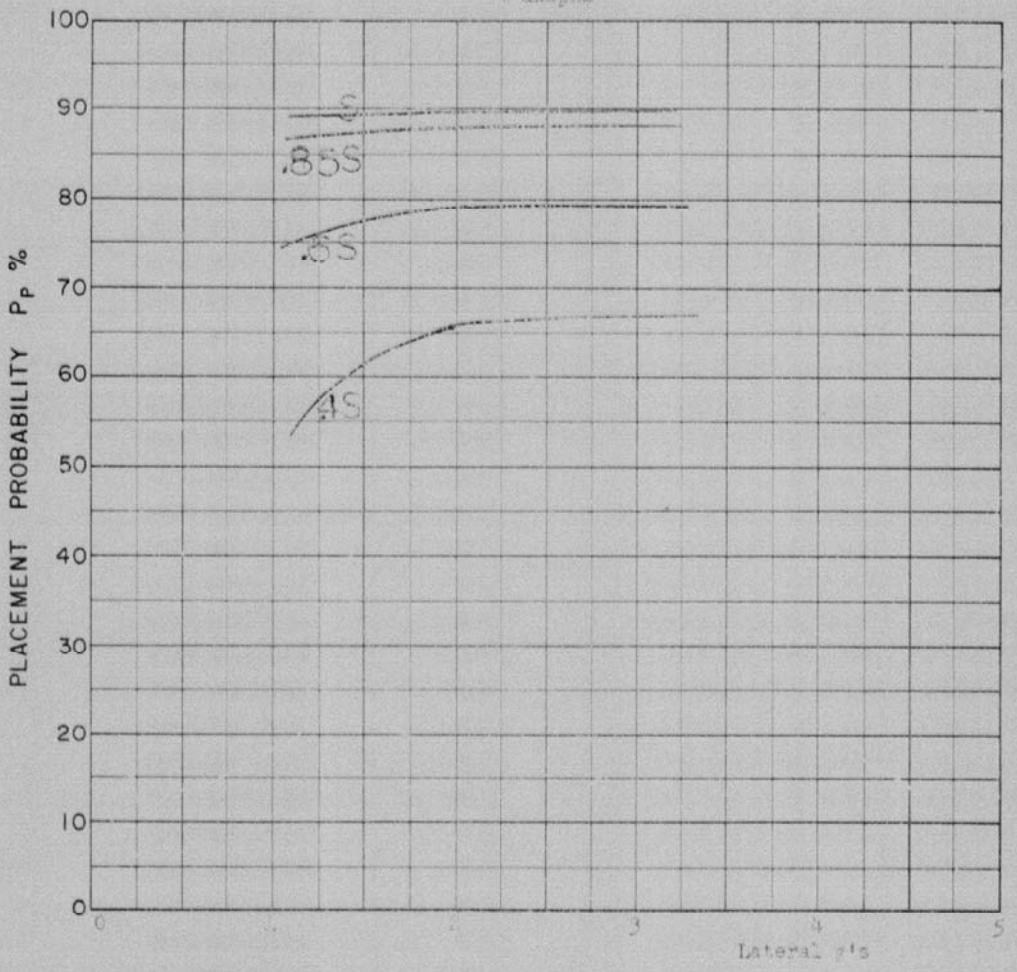

COURSE DIFFERENCE: 90°
TARGET EVASION: 0
TARGET MACH NO.: 2.0
INTERCEPTOR LATERAL G's: Abscissa
INTERCEPTOR MACH NO.: 2.2
σ OF G.C.I. ACCURACY: 4.75 n.m.
A.I. DETECTION RANGE AS FRACTION OF SPECIFICATION RANGE, S: 4 values
A.I. DETECTION RANGE CONTOUR: Delta
ALTITUDE: 60 K

(G-11)

Missile launch zone L.S maximum range, 5° heading error.

4 axdpn3

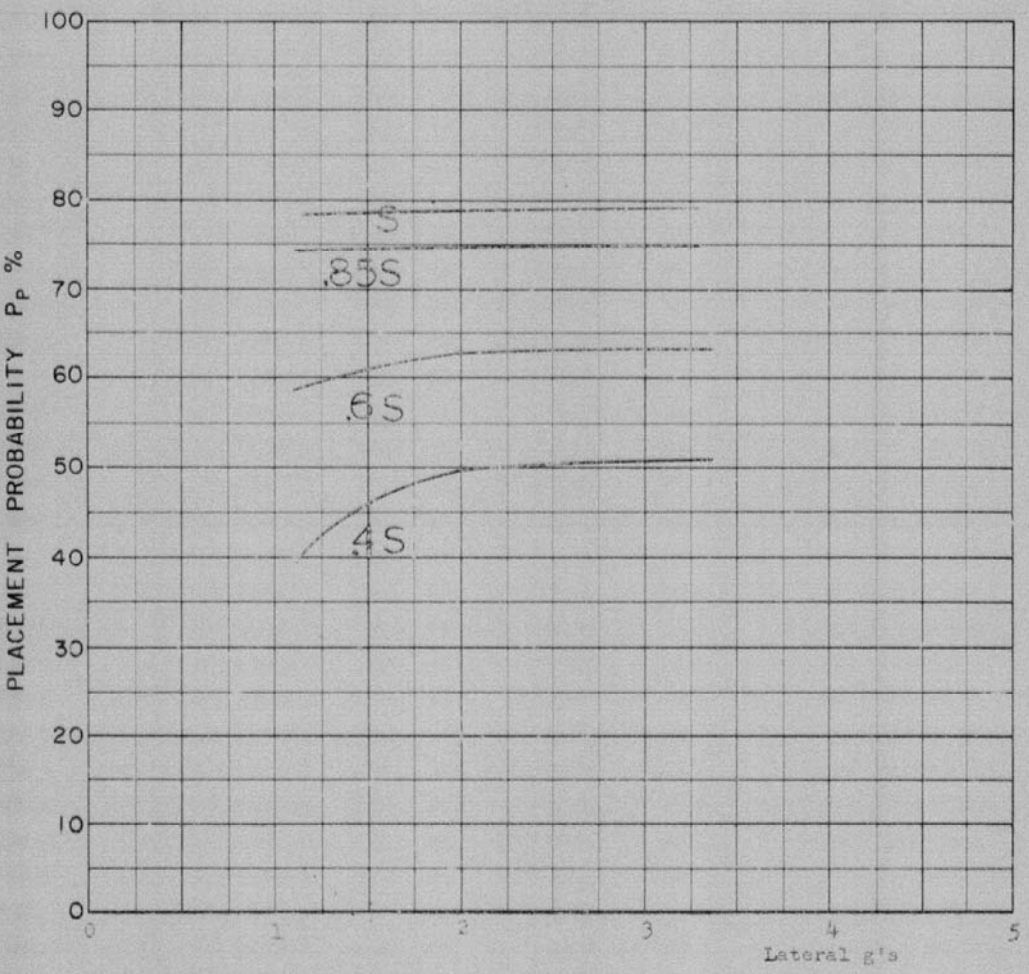

COURSE DIFFERENCE: 90°
TARGET EVASION: 0
TARGET MACH NO.: 2.0
INTERCEPTOR LATERAL G's: Abscissa
INTERCEPTOR MACH NO.: 1.5
σ OF G.C.I. ACCURACY: 6.25 n.m.
A.I. DETECTION RANGE AS FRACTION OF SPECIFICATION RANGE, S: 4 values
A.I. DETECTION RANGE CONTOUR: Delta
ALTITUDE: 60 K

G-12

Missile launch zone L-5, maximum range, 8° heading error.

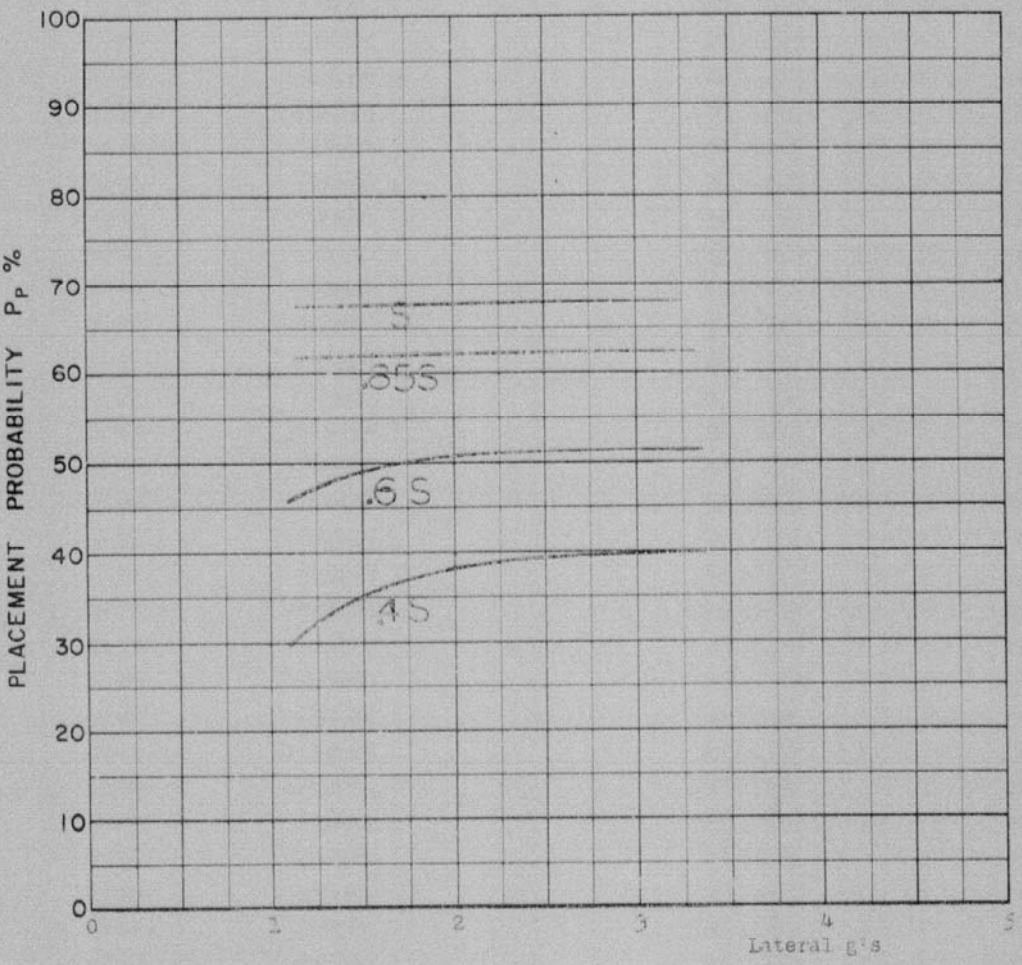

COURSE DIFFERENCE: 90°
TARGET EVASION: 0
TARGET MACH NO.: 2.0
INTERCEPTOR LATERAL G's: Abscissa
INTERCEPTOR MACH NO.: 1.5
σ OF G.C.I. ACCURACY: 9 n.m.
A.I. DETECTION RANGE AS FRACTION OF SPECIFICATION RANGE, S: 4 values
A.I. DETECTION RANGE CONTOUR: Delta
ALTITUDE: 60 K

G-13

Missile launch zone L.E. maximum range, 8° heading error.

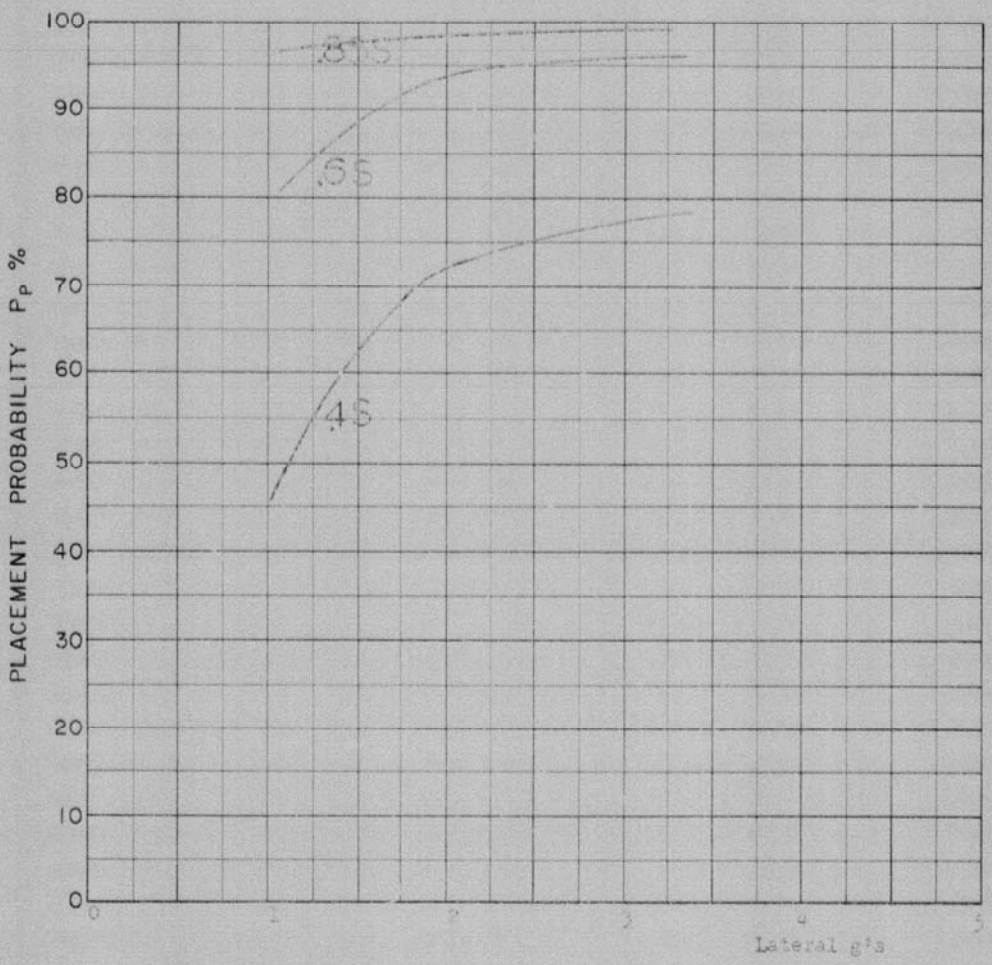

COURSE DIFFERENCE: 120°
TARGET EVASION: 0
TARGET MACH NO.: 2.0
INTERCEPTOR LATERAL G's: Abscissa
INTERCEPTOR MACH NO.: 2.5
σ OF G.C.I. ACCURACY: 4.75 n.m.
A.I. DETECTION RANGE AS FRACTION OF SPECIFICATION RANGE, S: 3 values
A.I. DETECTION RANGE CONTOUR: Delta
ALTITUDE: 60 K

(G-14)

Launch zone of figure L-5 missile launched at maximum range with 8° heading error allowance.

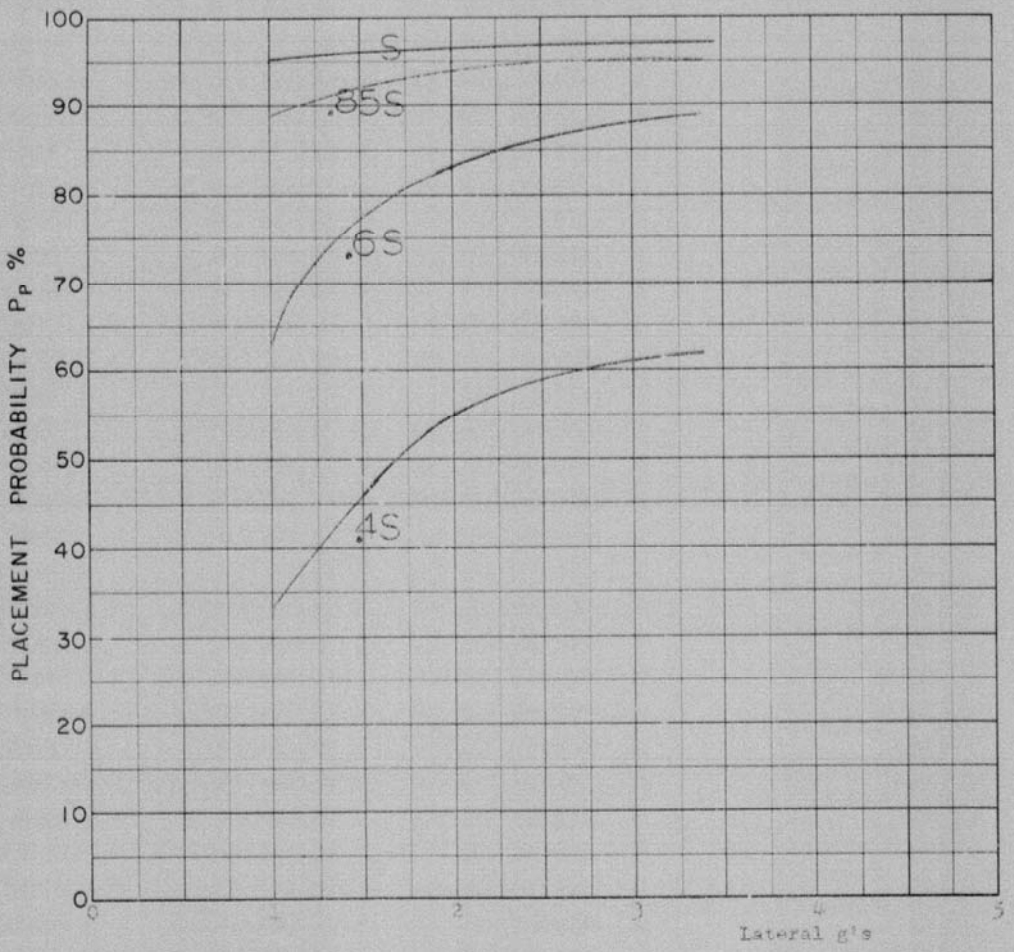

COURSE DIFFERENCE: 120°
TARGET EVASION: 0
TARGET MACH NO.: 2.0
INTERCEPTOR LATERAL G's: Abscissa
INTERCEPTOR MACH NO.: 1.5
σ OF G.C.I. ACCURACY: 6.75 n.m.
A.I. DETECTION RANGE AS FRACTION OF SPECIFICATION RANGE, S # values
A.I. DETECTION RANGE CONTOUR: Delta
ALTITUDE: 60 K

G-15

Launch zone of figure L-5, missile launched at maximum range with 8° heading error allowance.

4 cxdpn4

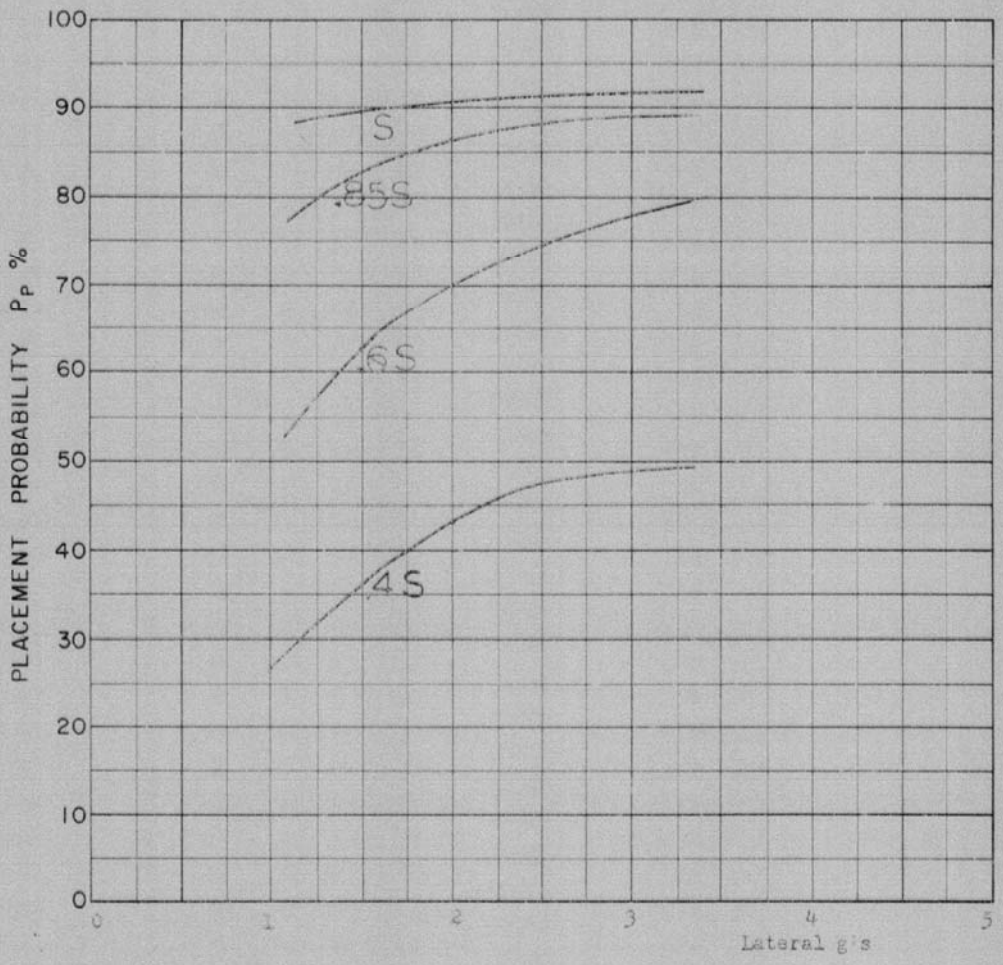

COURSE DIFFERENCE: 120°
TARGET EVASION: 0
TARGET MACH NO.: 2.0
INTERCEPTOR LATERAL G's: Abscissa
INTERCEPTOR MACH NO.: 1.5
σ OF G.C.I. ACCURACY: 9 n.m.
A.I. DETECTION RANGE AS FRACTION OF SPECIFICATION RANGE, S: 4 values
A.I. DETECTION RANGE CONTOUR: Delta
ALTITUDE: 60 K

G-16

Launch zone of figure L-5, missile launched at maximum range with 8° heading error allowance.

4 exdpnl

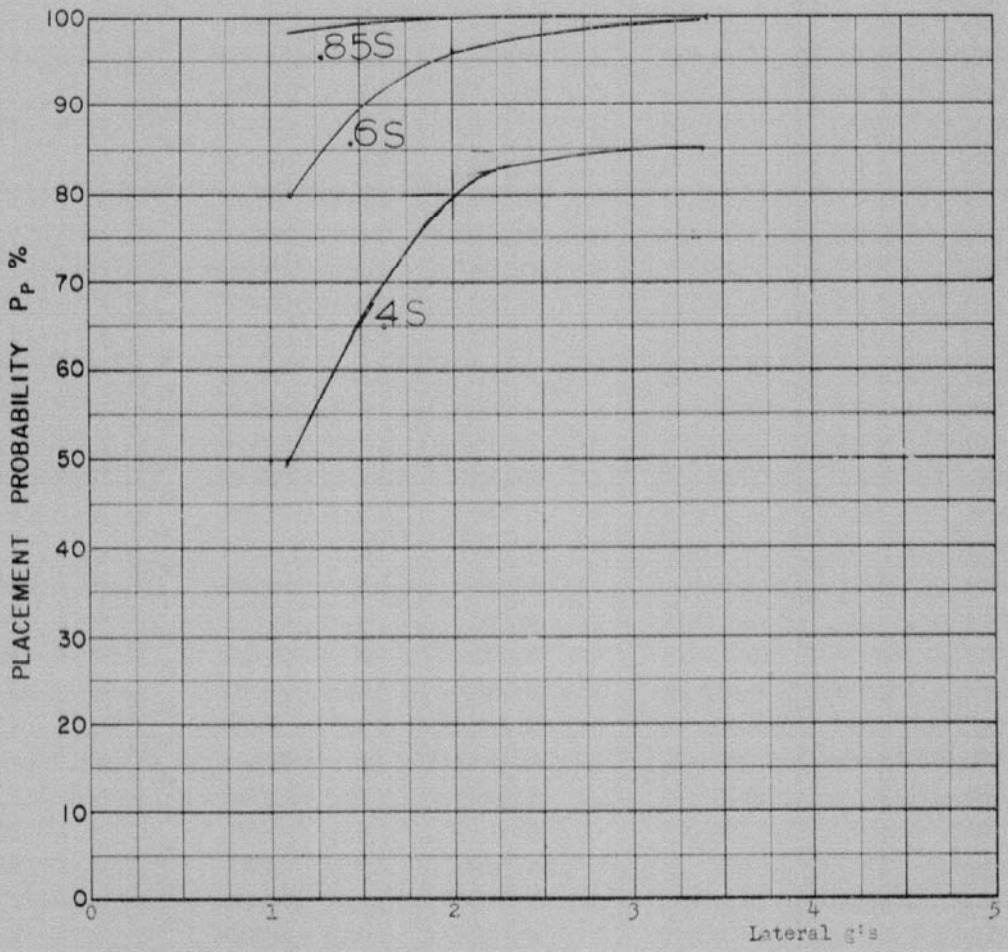

COURSE DIFFERENCE: 160°
TARGET EVASION: 0
TARGET MACH NO.: 2.0
INTERCEPTOR LATERAL G's: Abscissa
INTERCEPTOR MACH NO.: 1.5
σ OF G.C.I. ACCURACY: 4.75 n.m.
A.I. DETECTION RANGE AS FRACTION OF SPECIFICATION RANGE, S: 3 values
A.I. DETECTION RANGE CONTOUR: Delta
ALTITUDE: 60 K

G-17

Launch zone of figure L-5, missile launched at maximum range, with 8° heading error allowance.

4 cxdpn2

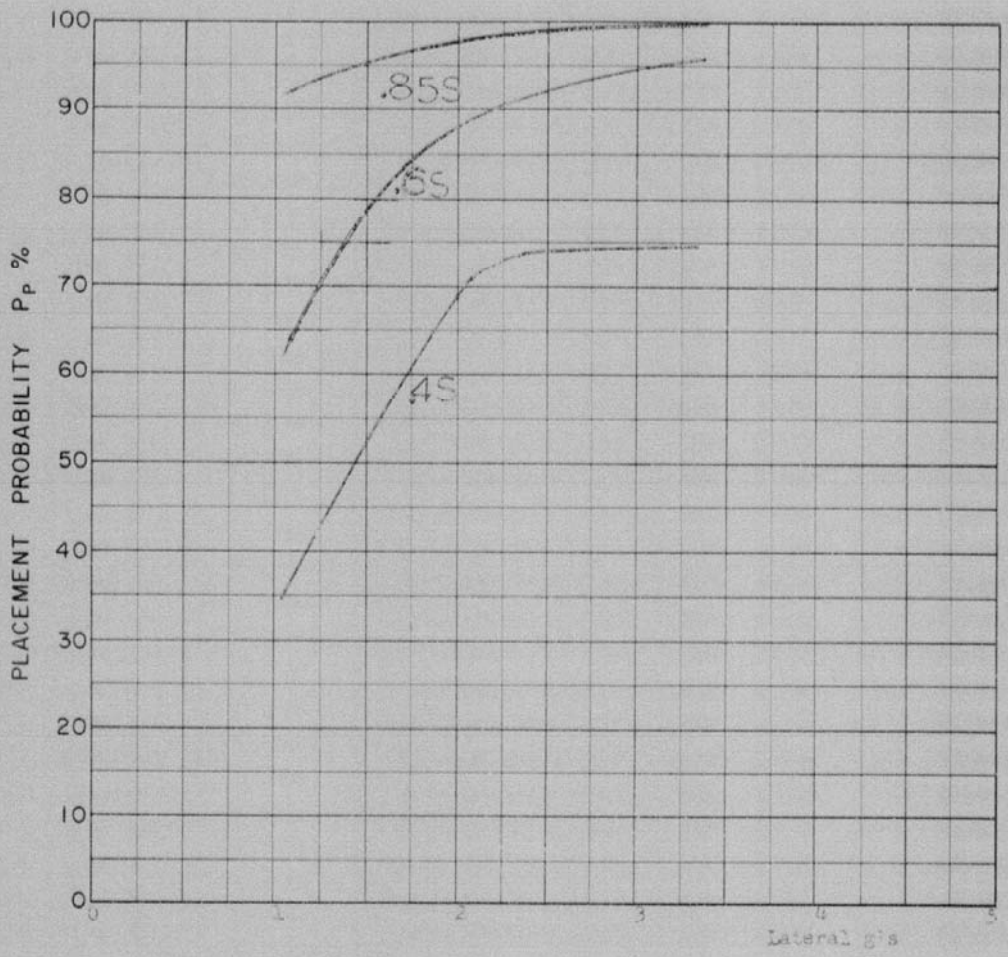

COURSE DIFFERENCE: 160°
TARGET EVASION: 0
TARGET MACH NO.: 2.0
INTERCEPTOR LATERAL G's: Abscissa
INTERCEPTOR MACH NO.: 1.5
σ OF G.C.I. ACCURACY: 6.25 n.m.
A.I. DETECTION RANGE AS FRACTION OF SPECIFICATION RANGE, S: 3 values
A.I. DETECTION RANGE CONTOUR: Delta
ALTITUDE: 60 K

G-18

Launch zone of figure L S, missile launched at maximum range with 8° heading error allowance.

4 expon.

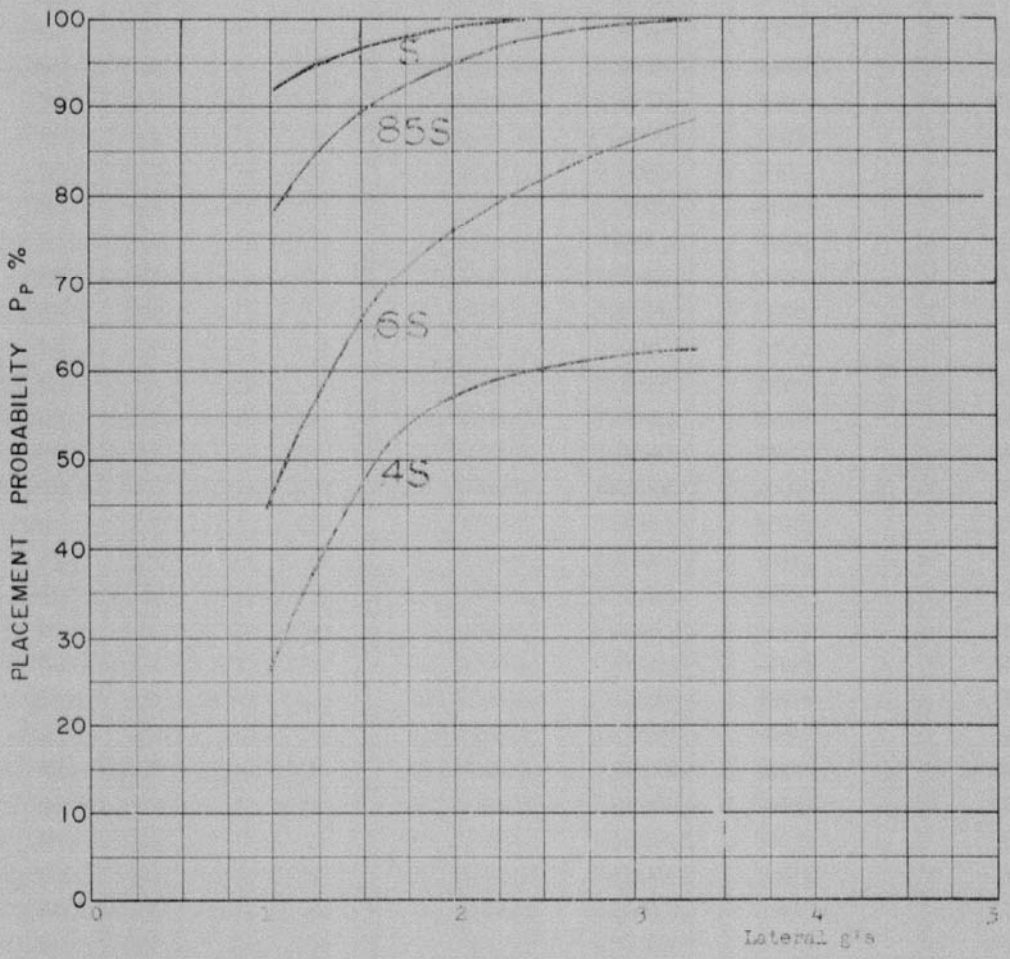

COURSE DIFFERENCE: 180°
TARGET EVASION: 0
TARGET MACH NO.: 2.0
INTERCEPTOR LATERAL G's: Abscissa
INTERCEPTOR MACH NO.: 1.5
σ OF G.C.I. ACCURACY: 9 n.m.
A.I. DETECTION RANGE AS FRACTION OF SPECIFICATION RANGE, S: 4 values
A.I. DETECTION RANGE CONTOUR: Delta
ALTITUDE: 60 K

Launch zone of figure L5, missile launched at maximum range with 8° heading error allowance.

G-19

138 dpn2

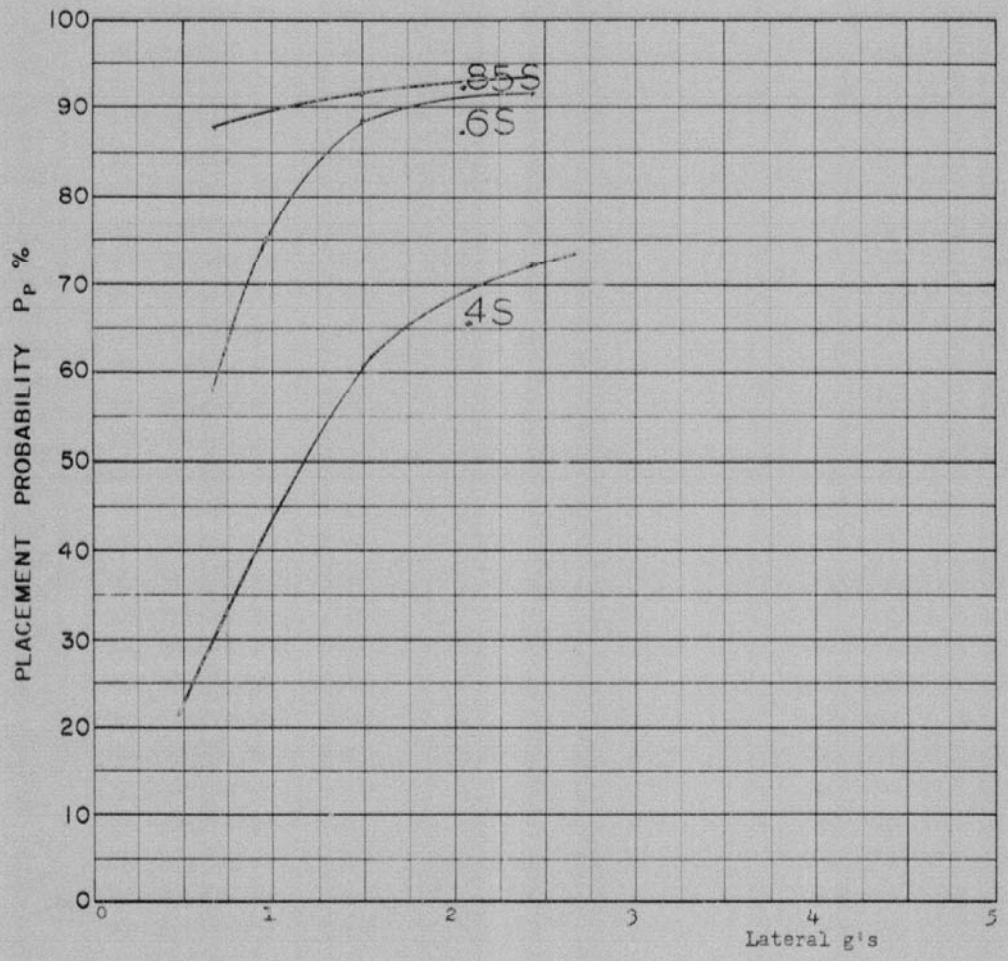

COURSE DIFFERENCE: 110°
TARGET EVASION: 0.1 lateral g's
TARGET MACH NO.: 2.0
INTERCEPTOR LATERAL G's: Abscissa
INTERCEPTOR MACH NO.: 1.5
σ OF G.C.I. ACCURACY: 30 n.m.
A.I. DETECTION RANGE AS FRACTION OF SPECIFICATION RANGE, S: 3 values
A.I. DETECTION RANGE CONTOUR: Delta
ALTITUDE: 60 K

Launch zone L-11

G-20

138 dpn3

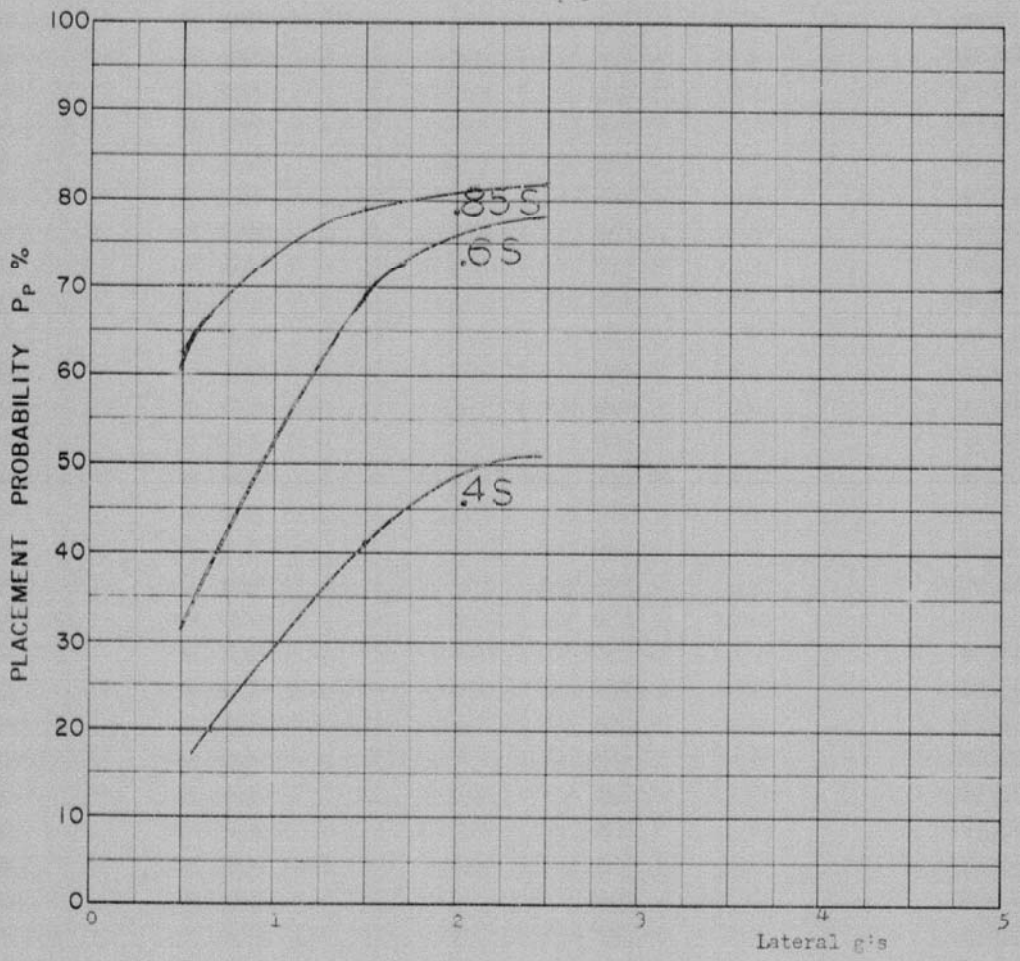

COURSE DIFFERENCE: 110°
TARGET EVASION: 0.1 lateral g's
TARGET MACH NO.: 2.0
INTERCEPTOR LATERAL G's: Abscissa
INTERCEPTOR MACH NO.: 1.5
σ OF G.C.I. ACCURACY: 4.75 n.m.
A.I. DETECTION RANGE AS FRACTION OF SPECIFICATION RANGE, S: 3 values
A.I. DETECTION RANGE CONTOUR: Delta
ALTITUDE: 60 K

G-21

138 dpn4

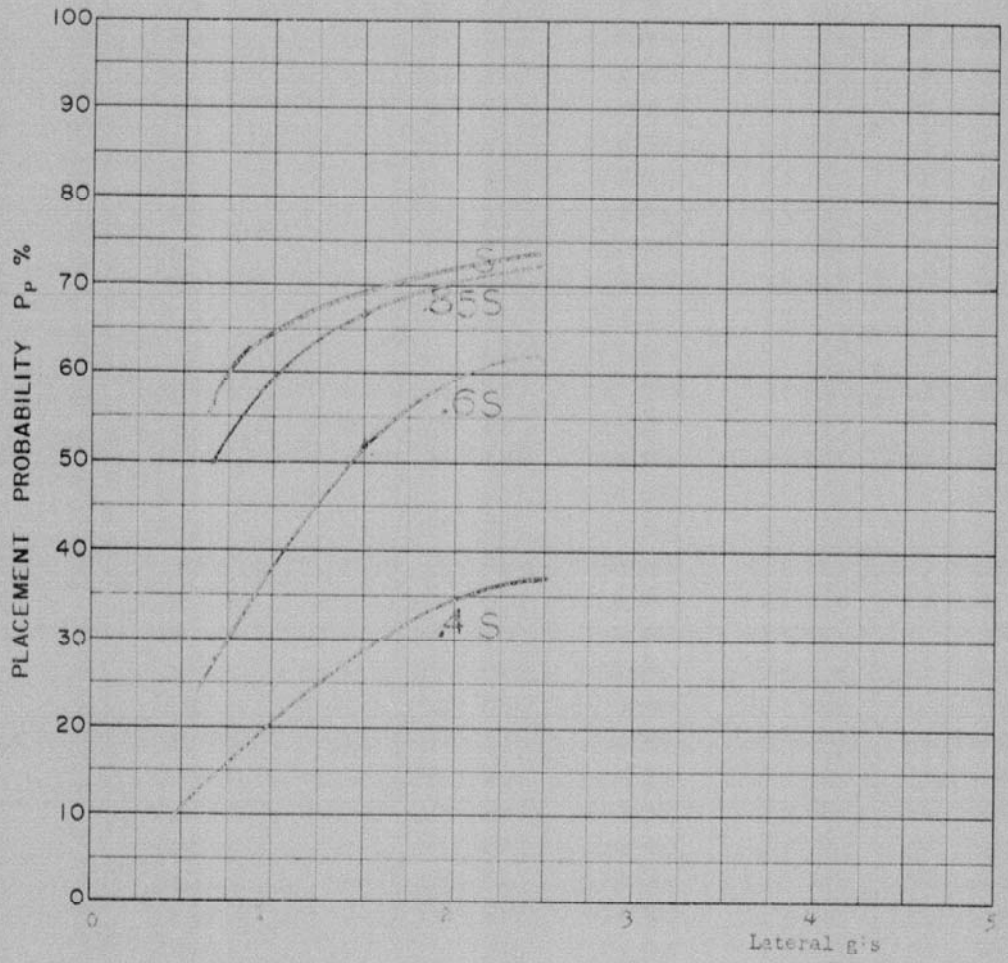

COURSE DIFFERENCE: 110°
TARGET EVASION: 0.7 lateral g's
TARGET MACH NO.: 2.0
INTERCEPTOR LATERAL G's: Abscissa
INTERCEPTOR MACH NO.: 1.5
σ OF G.C.I. ACCURACY: 6.75 n.m.
A.I. DETECTION RANGE AS FRACTION OF SPECIFICATION RANGE, S: .4 values
A.I. DETECTION RANGE CONTOUR: Delta
ALTITUDE: 60 K

G-22

Launch zone figure L-11

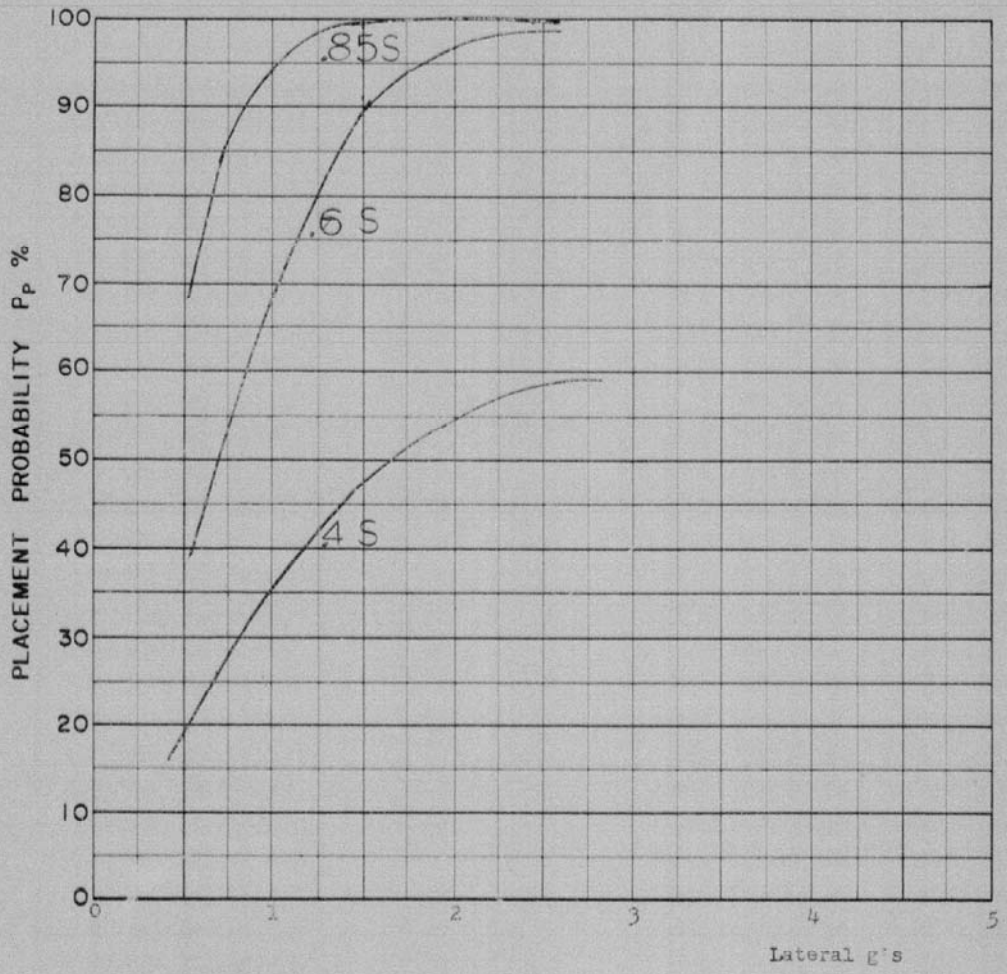

COURSE DIFFERENCE: 160°
TARGET EVASION: 0.1 lateral g's
TARGET MACH NO.: 2.0
INTERCEPTOR LATERAL G's: Abscissa
INTERCEPTOR MACH NO.: 1.5
σ OF G.C.I. ACCURACY: 3 n.m.
A.I. DETECTION RANGE AS FRACTION OF SPECIFICATION RANGE, S: 3 values
A.I. DETECTION RANGE CONTOUR: Delta
ALTITUDE: 60 K

G-23

Missile launch zone L-11

L42 dpn3

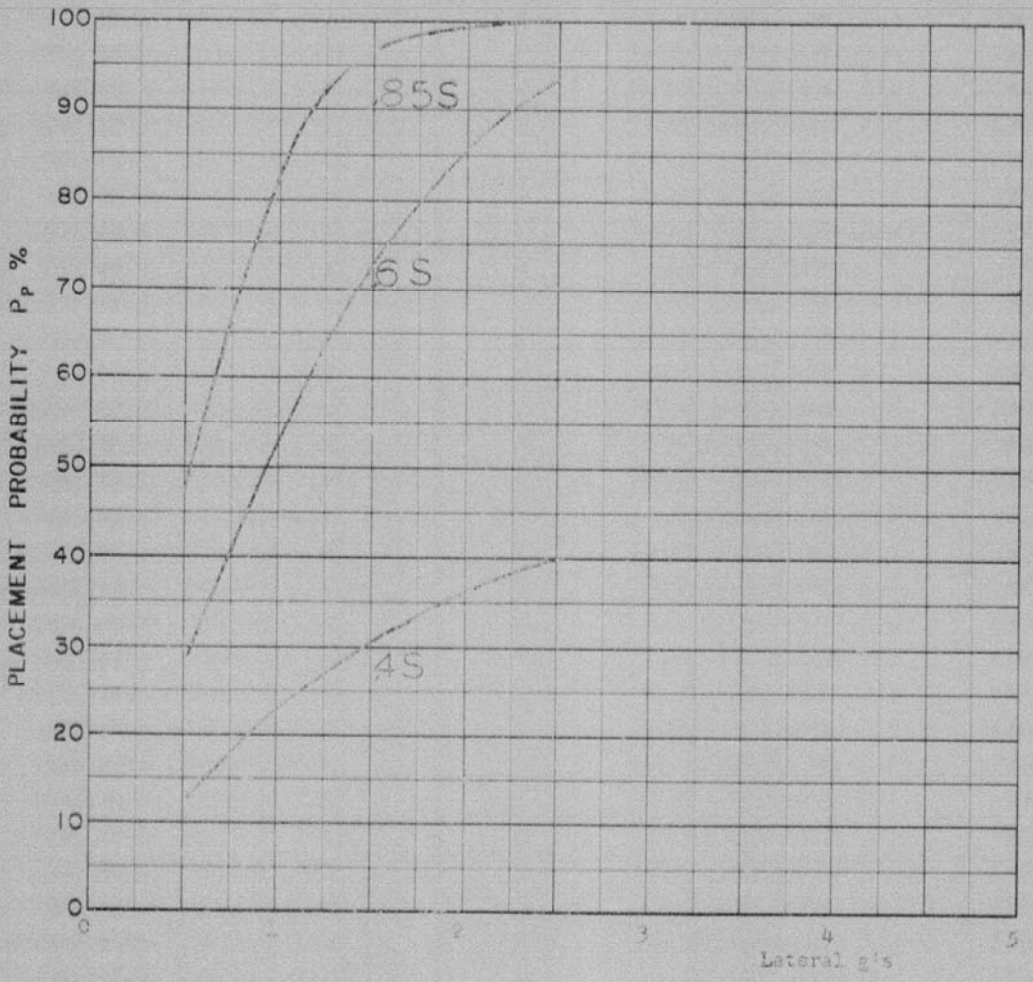

COURSE DIFFERENCE: 160°
TARGET EVASION: 0.3 lateral g's
TARGET MACH NO.: 2.0
INTERCEPTOR LATERAL G's: Abscissa
INTERCEPTOR MACH NO.: 1.5
σ OF G.C.I. ACCURACY: 4.75 n.m.
A.I. DETECTION RANGE AS FRACTION OF SPECIFICATION RANGE, S: 3 values
A.I. DETECTION RANGE CONTOUR: Delta
ALTITUDE: 60 K

G24

Missile launch zone L-11

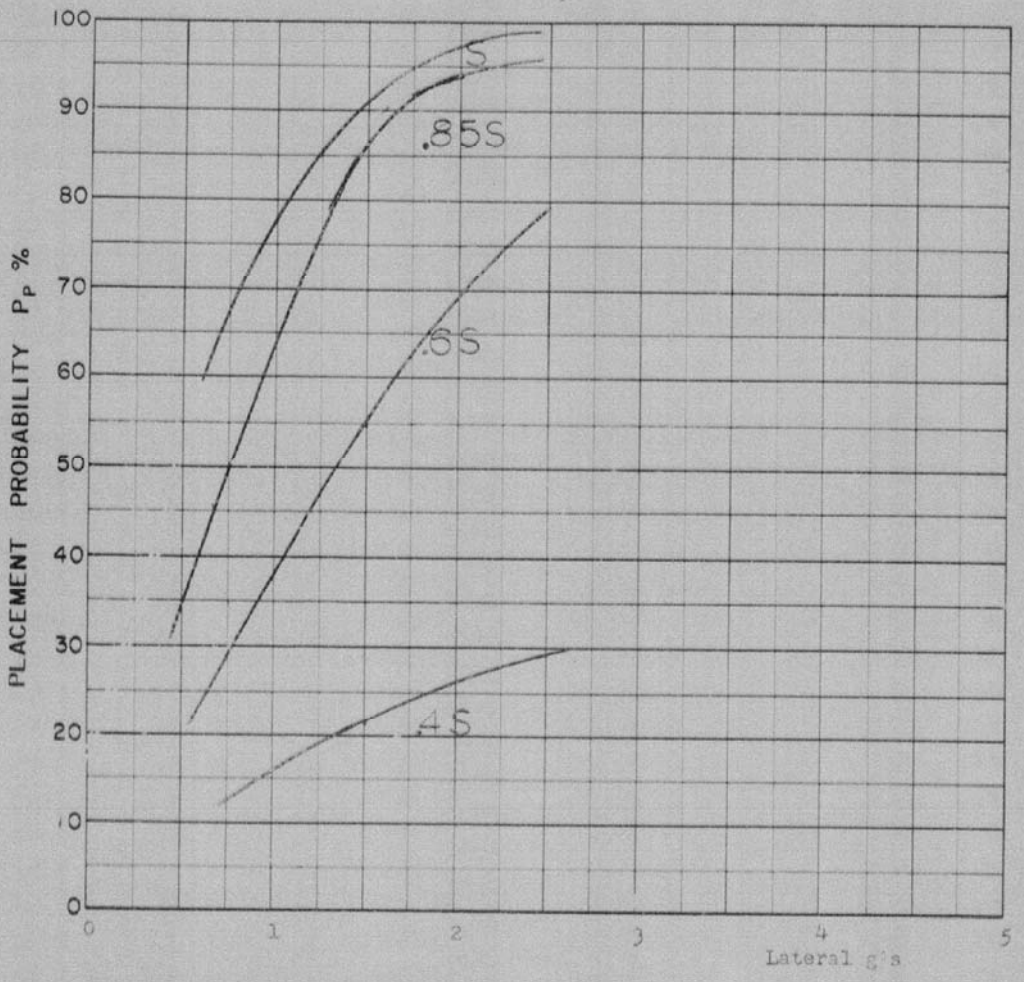

COURSE DIFFERENCE: 160°
TARGET EVASION: 0.1 lateral g's
TARGET MACH NO.: 2.0
INTERCEPTOR LATERAL G's: Abscissa
INTERCEPTOR MACH NO.: 1.5
σ OF G.C.I. ACCURACY: 6.75 n.m.
A.I. DETECTION RANGE AS FRACTION OF SPECIFICATION RANGE, S: 4 values
A.I. DETECTION RANGE CONTOUR: Delta
ALTITUDE: 50 K

Missile launch zone L.11

G-25

18 anpn2

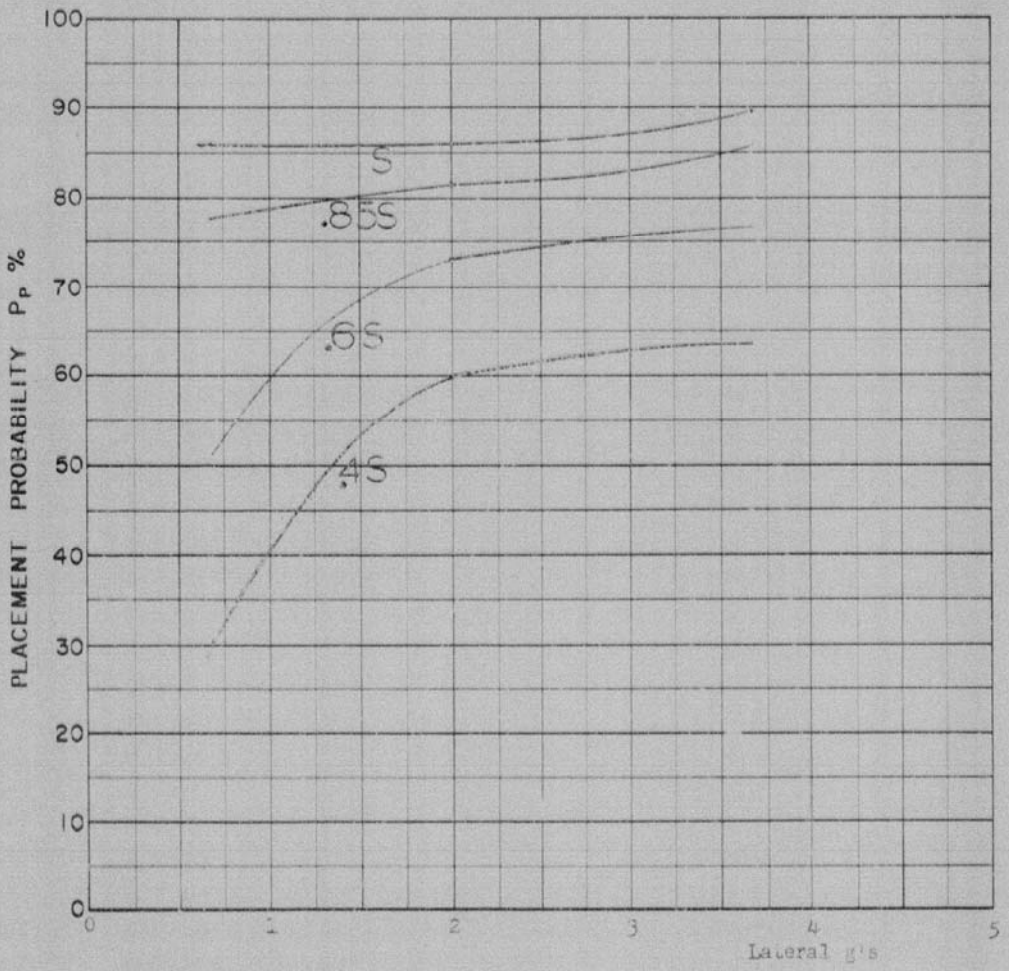

COURSE DIFFERENCE: 75°
TARGET EVASION: 0
TARGET MACH NO.: 2.0
INTERCEPTOR LATERAL G's: Abscissa
INTERCEPTOR MACH NO.: 1.8
σ OF G.C.I. ACCURACY: 4.75 n.m.
A.I. DETECTION RANGE AS FRACTION OF SPECIFICATION RANGE, S: 4 values
A.I. DETECTION RANGE CONTOUR: Delta
ALTITUDE: 60 K

G-26

Missile launch zone L.8.

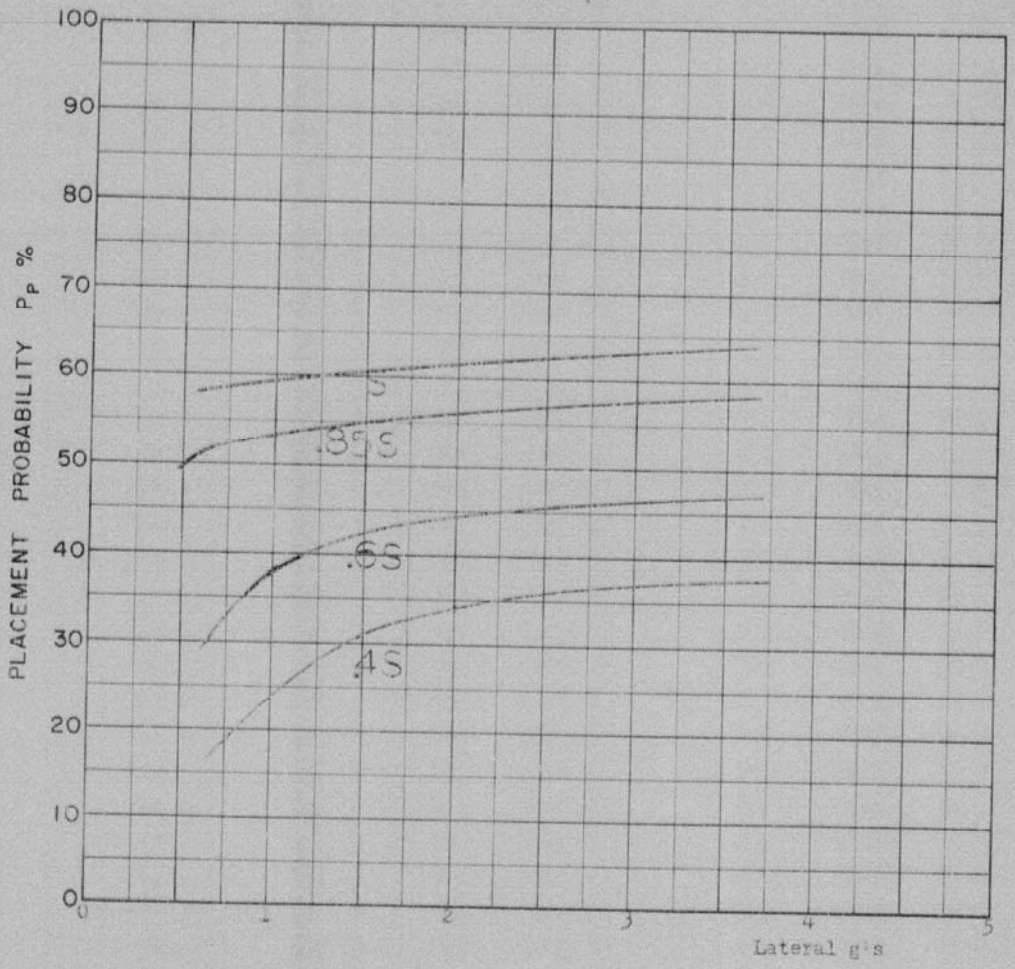

COURSE DIFFERENCE: 75°
TARGET EVASION: 0
TARGET MACH NO.: 2.0
INTERCEPTOR LATERAL G's: Abscissa
INTERCEPTOR MACH NO.: 1.8
σ OF G.C.I. ACCURACY: 9 n.m.
A.I. DETECTION RANGE AS FRACTION OF SPECIFICATION RANGE, S: 4 values
A.I. DETECTION RANGE CONTOUR: Delta
ALTITUDE: 50 K

G-27

Missile launch zone L-8, missile launched at minimum range with 8° heading error.

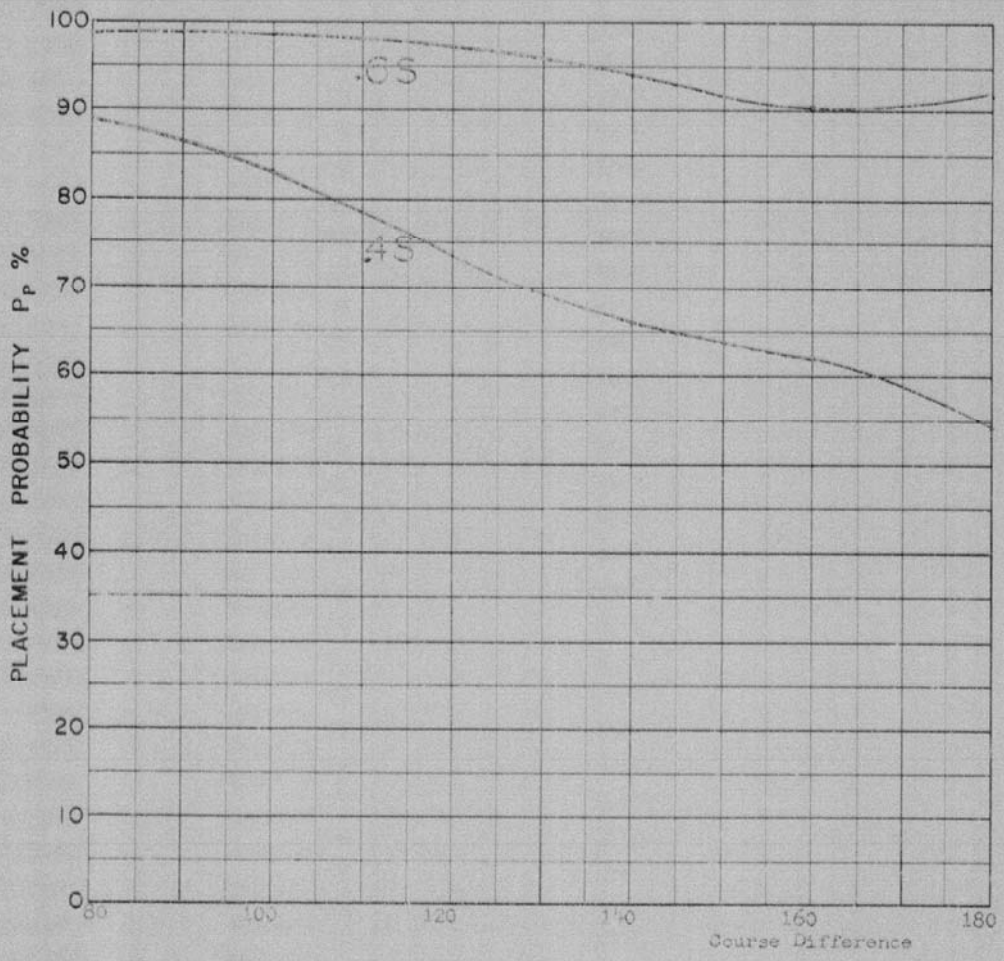

COURSE DIFFERENCE: Abscissa
TARGET EVASION: 0
TARGET MACH NO.: 1.5
INTERCEPTOR LATERAL G's: 0.85
INTERCEPTOR MACH NO.: 1.5
σ OF G.C.I. ACCURACY: 3.0
A.I. DETECTION RANGE AS FRACTION OF SPECIFICATION RANGE, S: 2 values
A.I. DETECTION RANGE CONTOUR: Delta
ALTITUDE: 50 K

C-1

Launch zone figure L-1

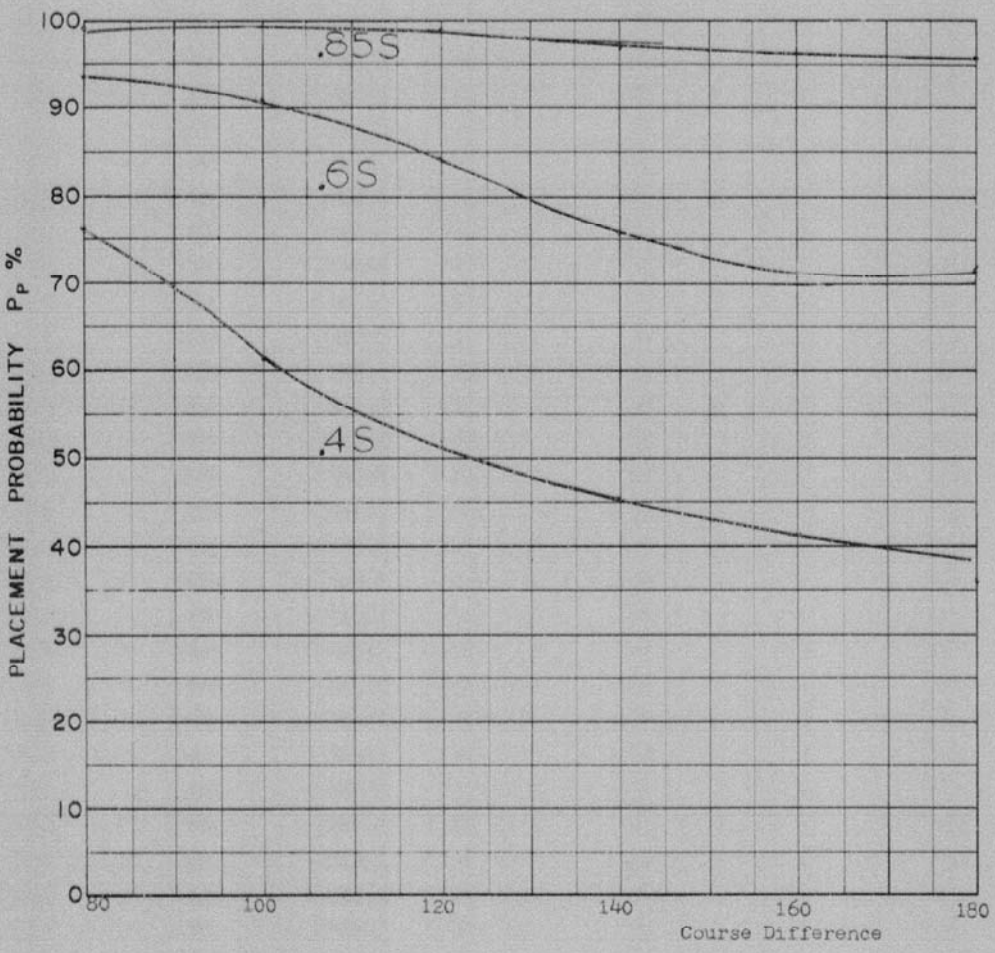

COURSE DIFFERENCE: Abscissa
TARGET EVASION: 0
TARGET MACH NO.: 1.5
INTERCEPTOR LATERAL G's: 0.85
INTERCEPTOR MACH NO.: 1.5
σ OF G.C.I. ACCURACY: 4.75 n.m.
A.I. DETECTION RANGE AS FRACTION OF SPECIFICATION RANGE, S: 3 values
A.I. DETECTION RANGE CONTOUR: Delta
ALTITUDE: 50 K

(C-2)

Launch zone figure L-1

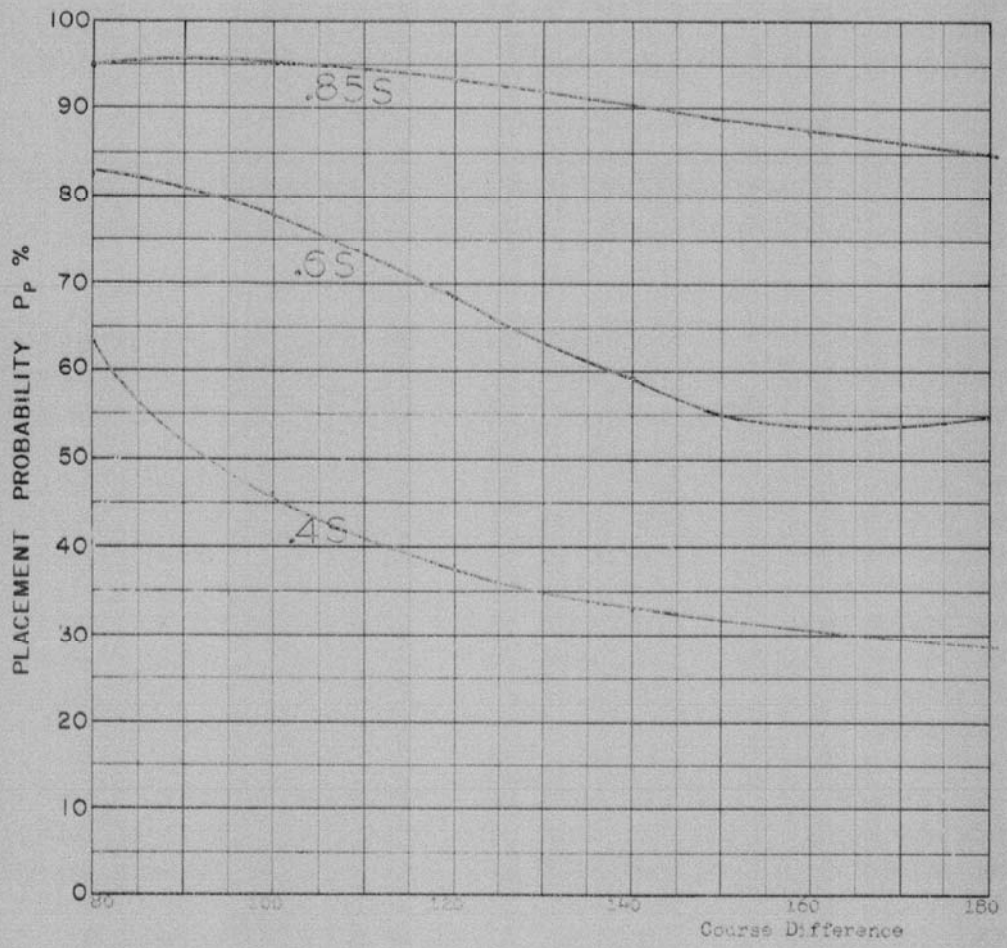

COURSE DIFFERENCE: Abscissa
TARGET EVASION: 0
TARGET MACH NO.: 1.5
INTERCEPTOR LATERAL G's: 0.85
INTERCEPTOR MACH NO.: 1.5
σ OF G.C.I. ACCURACY: 6.75 n.m.
A.I. DETECTION RANGE AS FRACTION OF SPECIFICATION RANGE, S : 3 values
A.I. DETECTION RANGE CONTOUR: Delta
ALTITUDE: 50 K

C-3

Launch zone figure L-1

35 dpa2

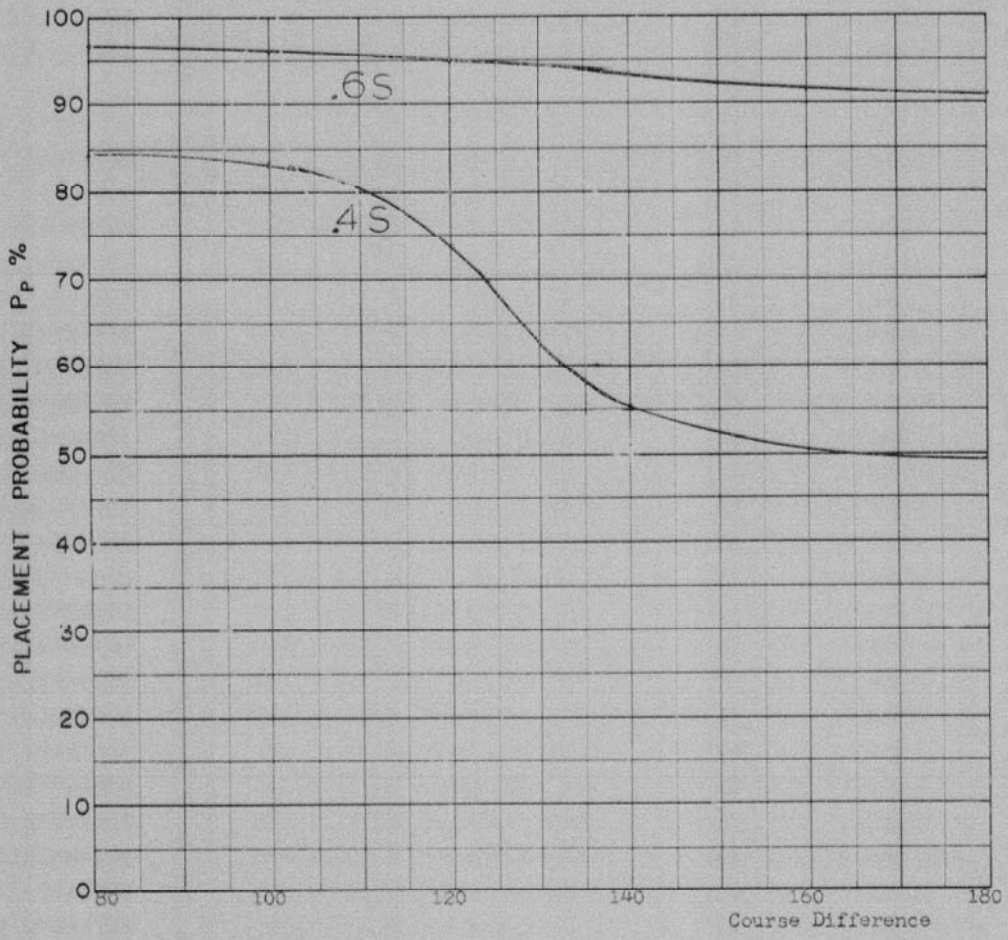

C-4

COURSE DIFFERENCE: Abscissa
TARGET EVASION: 0
TARGET MACH NO.: 1.5
INTERCEPTOR LATERAL G's: 1.25
INTERCEPTOR MACH NO.: 1.5
σ OF G.C.I. ACCURACY: 4.75 n.Mi.
A.I. DETECTION RANGE AS FRACTION OF SPECIFICATION RANGE, S: 2 values
A.I. DETECTION RANGE CONTOUR: Delta
ALTITUDE: 50 K

Launch zone figure L-1

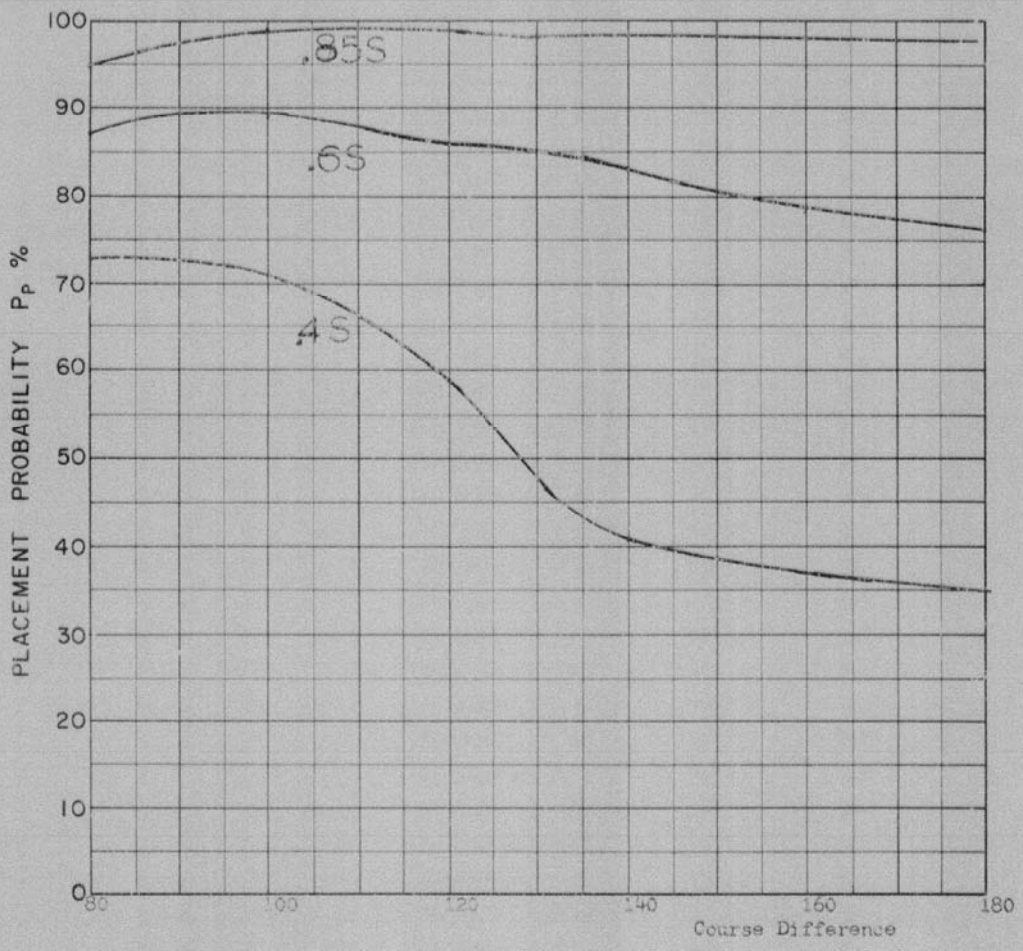

COURSE DIFFERENCE: Abscissa
TARGET EVASION: 0
TARGET MACH NO.: 1.5
INTERCEPTOR LATERAL G's: 1.25
INTERCEPTOR MACH NO.: 1.5
σ OF G.C.I. ACCURACY: 6.75 n.m.
A.I. DETECTION RANGE AS FRACTION OF SPECIFICATION RANGE, S: values
A.I. DETECTION RANGE CONTOUR: Delta
ALTITUDE: 50 K

C-5

Launch zone figure L-1

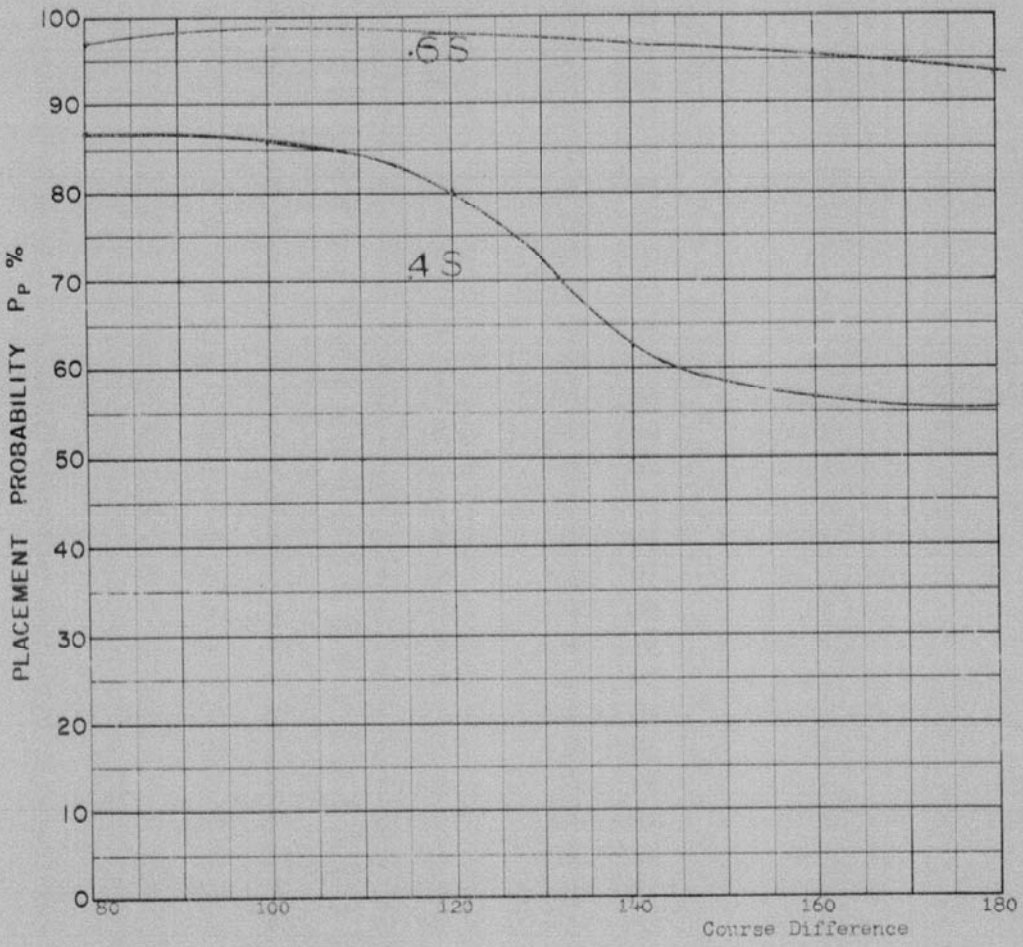

C-6

COURSE DIFFERENCE: Abscissa
TARGET EVASION: 0
TARGET MACH NO.: 1.5
INTERCEPTOR LATERAL G's: 1.6
INTERCEPTOR MACH NO.: 1.5
σ OF G.C.I. ACCURACY: 4.75 n.m.
A.I. DETECTION RANGE AS FRACTION OF SPECIFICATION RANGE, S: 2 values
A.I. DETECTION RANGE CONTOUR: Delta
ALTITUDE: 50 K

Launch zone figure L-1

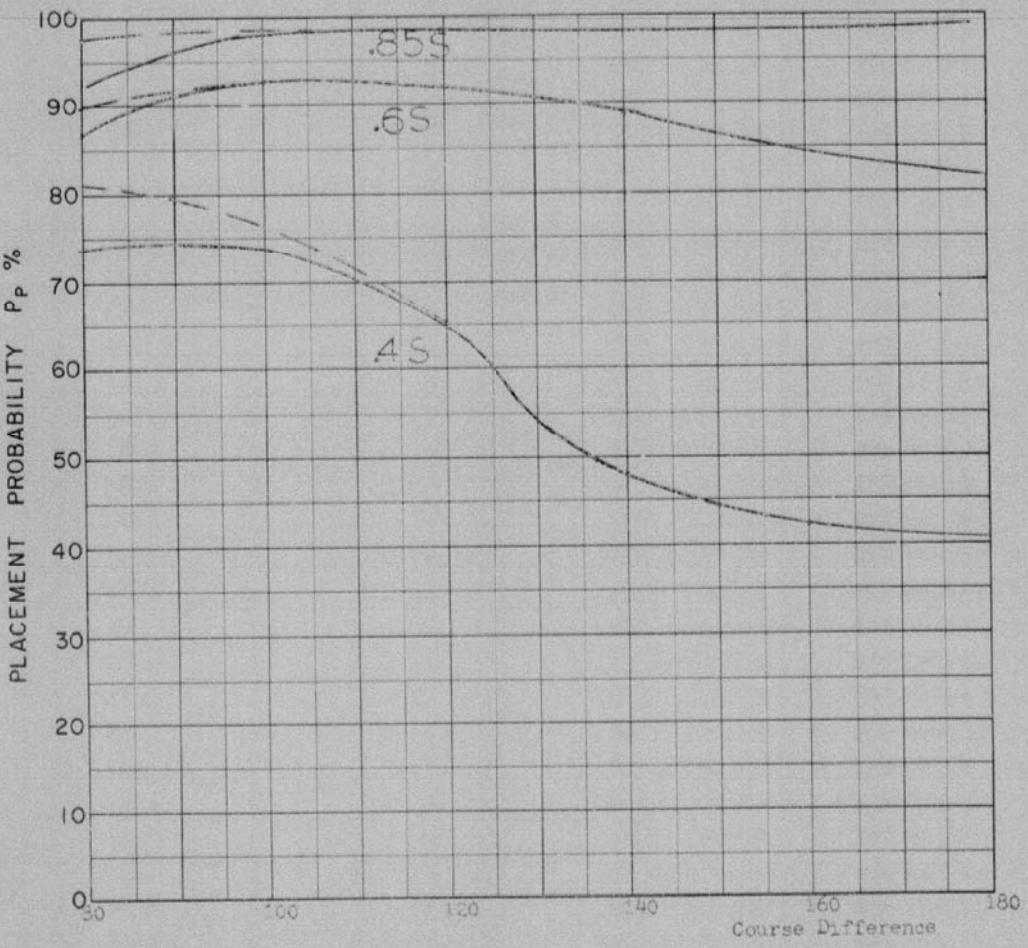

C-7

COURSE DIFFERENCE: Abscissa
TARGET EVASION: 0
TARGET MACH NO.: 1.5
INTERCEPTOR LATERAL G's: 1.6
INTERCEPTOR MACH NO.: 1.5
σ OF G.C.I. ACCURACY: 6.75 n.m.
A.I. DETECTION RANGE AS FRACTION OF SPECIFICATION RANGE, S: 3 values
A.I. DETECTION RANGE CONTOUR: Delta
ALTITUDE: 50 K

Launch zone figure L-1
(Dashed curve show improvement obtained with 80° Look Angle Limit)

38 dpa4

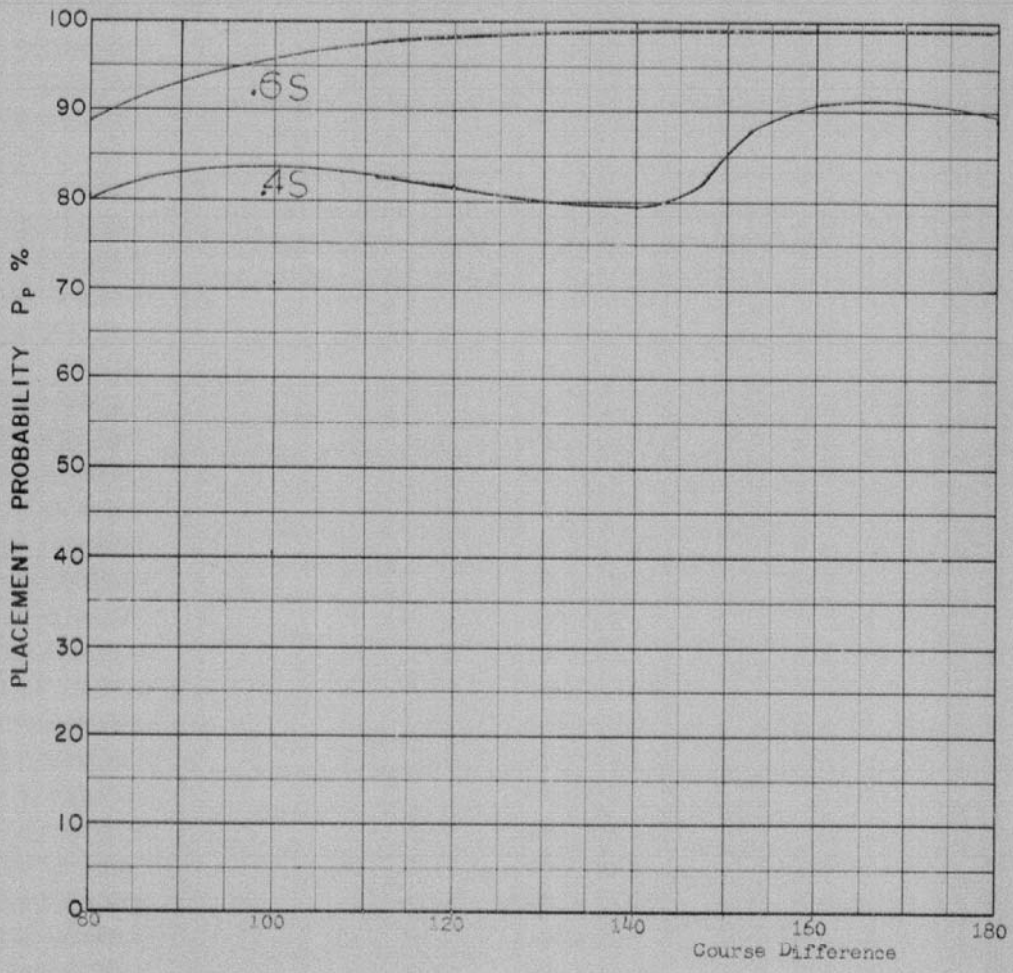

COURSE DIFFERENCE: Abscissa
TARGET EVASION: 0
TARGET MACH NO.: 1.5
INTERCEPTOR LATERAL G's: 3.0
INTERCEPTOR MACH NO.: 1.5
σ OF G.C.I. ACCURACY: 6.25 n.m.
A.I. DETECTION RANGE AS FRACTION OF SPECIFICATION RANGE, S: 2 values
A.I. DETECTION RANGE CONTOUR: Delta
ALTITUDE: 50 K

Missile launch zone L-1

C-8

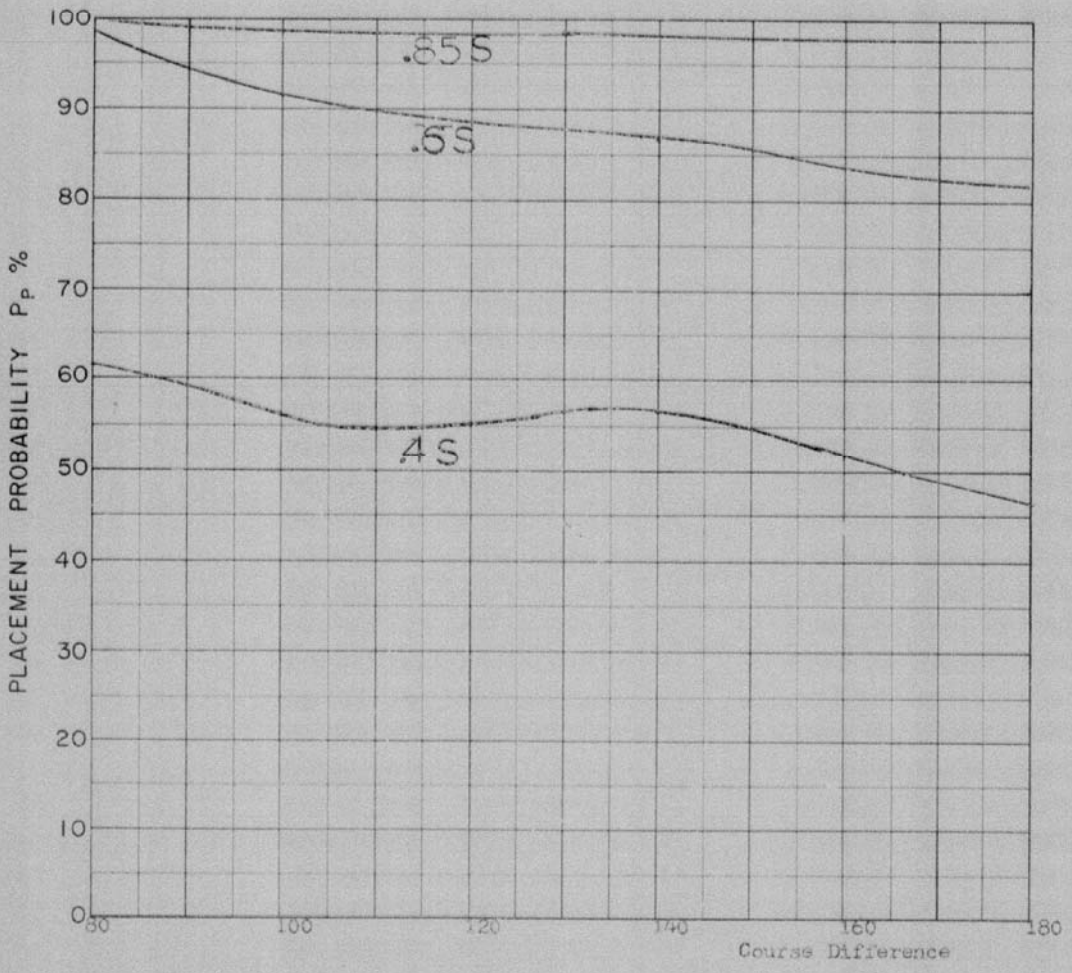

COURSE DIFFERENCE: Abscissa
TARGET EVASION: 0
TARGET MACH NO.: 1.5
INTERCEPTOR LATERAL G's: 0.66
INTERCEPTOR MACH NO.: 1.5
σ OF G.C.I. ACCURACY: 3 n.m.
A.I. DETECTION RANGE AS FRACTION OF SPECIFICATION RANGE, S: 3 values
A.I. DETECTION RANGE CONTOUR: Delta
ALTITUDE: 60 K

C-9

Launch zone figure L-2

32 dpa3

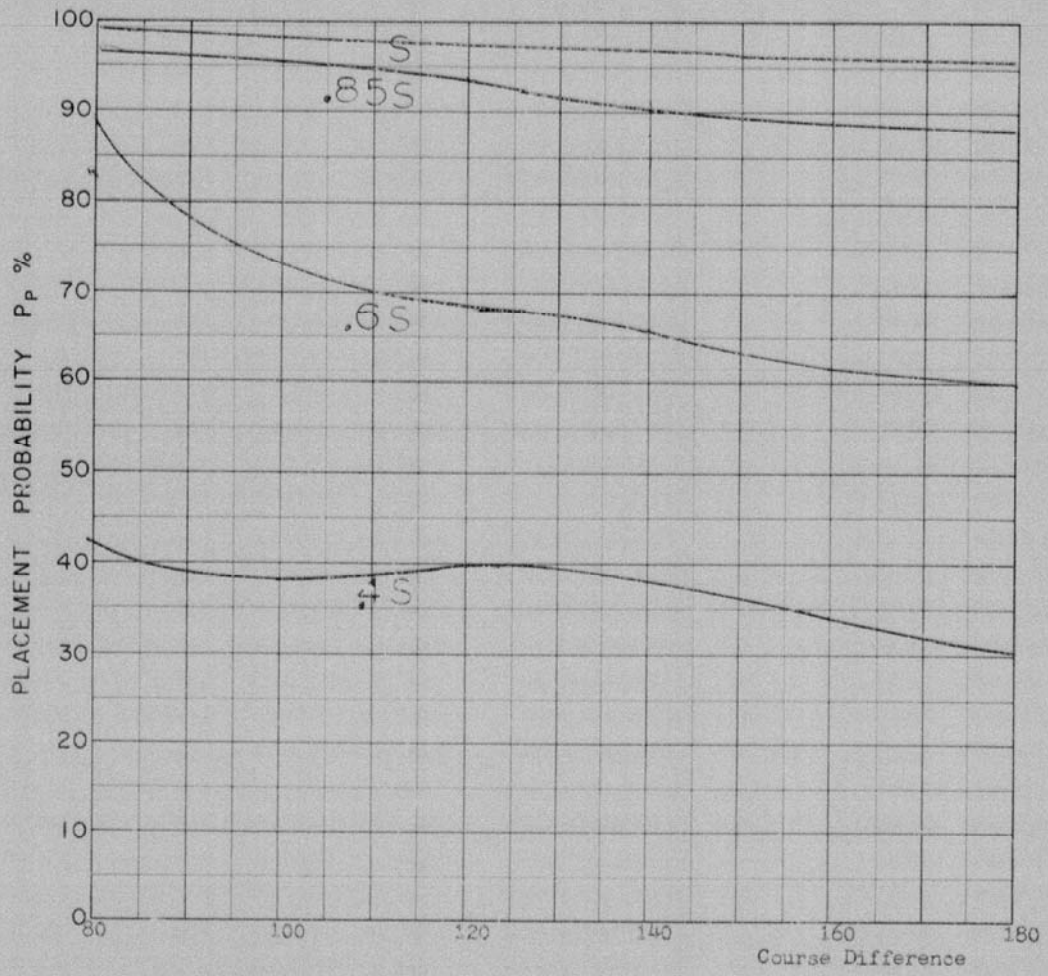

COURSE DIFFERENCE: Abscissa
TARGET EVASION: 0
TARGET MACH NO.: 1.5
INTERCEPTOR LATERAL G's: 0.66
INTERCEPTOR MACH NO.: 1.5
σ OF G.C.I. ACCURACY: 4.75 n.m.
A.I. DETECTION RANGE AS FRACTION OF SPECIFICATION RANGE, S: 4 values
A.I. DETECTION RANGE CONTOUR: Delta
ALTITUDE: 60 K

C-10

Launch zone figure L-2

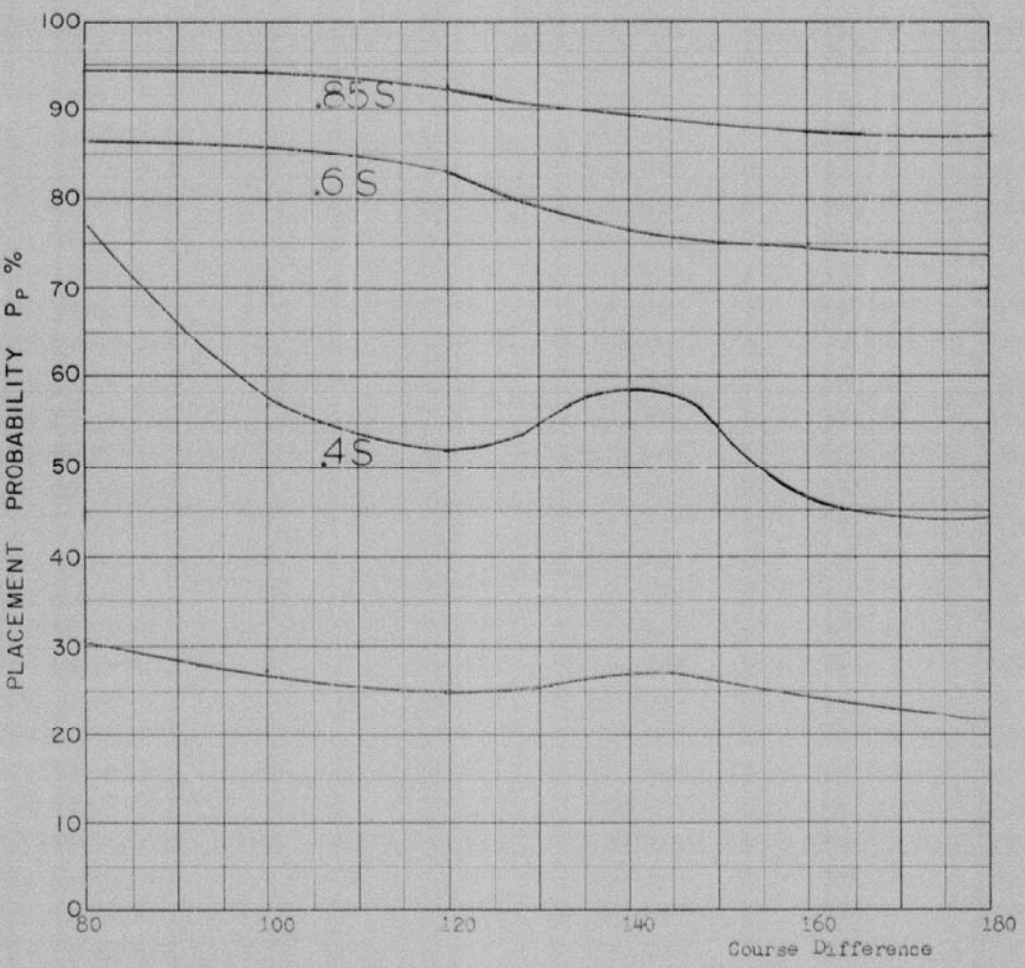

COURSE DIFFERENCE: Abscissa
TARGET EVASION: 0
TARGET MACH NO.: 1.5
INTERCEPTOR LATERAL G's: 0.66
INTERCEPTOR MACH NO.: 1.5
σ OF G.C.I. ACCURACY: 6.75 n.m.
A.I. DETECTION RANGE AS FRACTION OF SPECIFICATION RANGE, S 4 values
A.I. DETECTION RANGE CONTOUR: Delta
ALTITUDE: 60 K

C-11

Launch zone figure L-2

32 dpa5

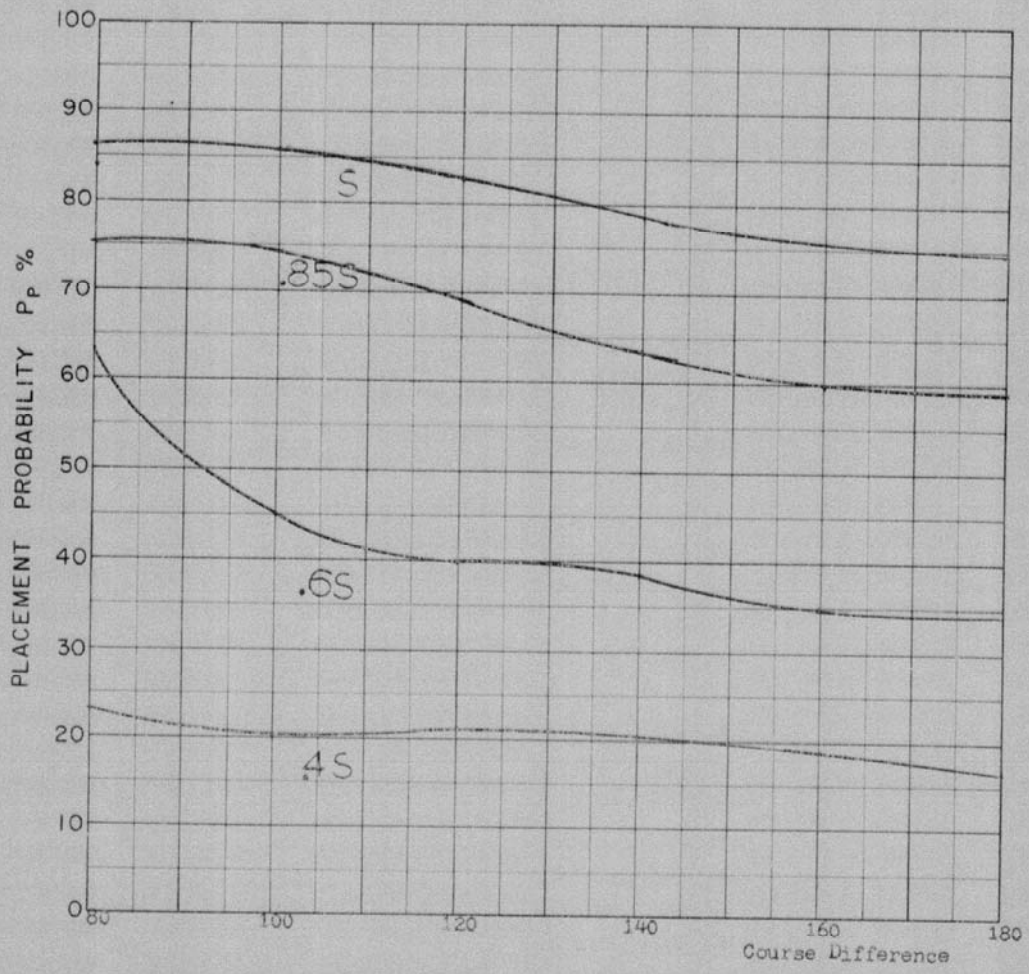

COURSE DIFFERENCE: Abscissa
TARGET EVASION: 0
TARGET MACH NO.: 1.5
INTERCEPTOR LATERAL G's: 0.66
INTERCEPTOR MACH NO.: 1.5
σ OF G.C.I. ACCURACY: 9 n.m.
A.I. DETECTION RANGE AS FRACTION OF SPECIFICATION RANGE, S: 4 values
A.I. DETECTION RANGE CONTOUR: Delta
ALTITUDE: 60 K

C-12

Launch zone figure L-2

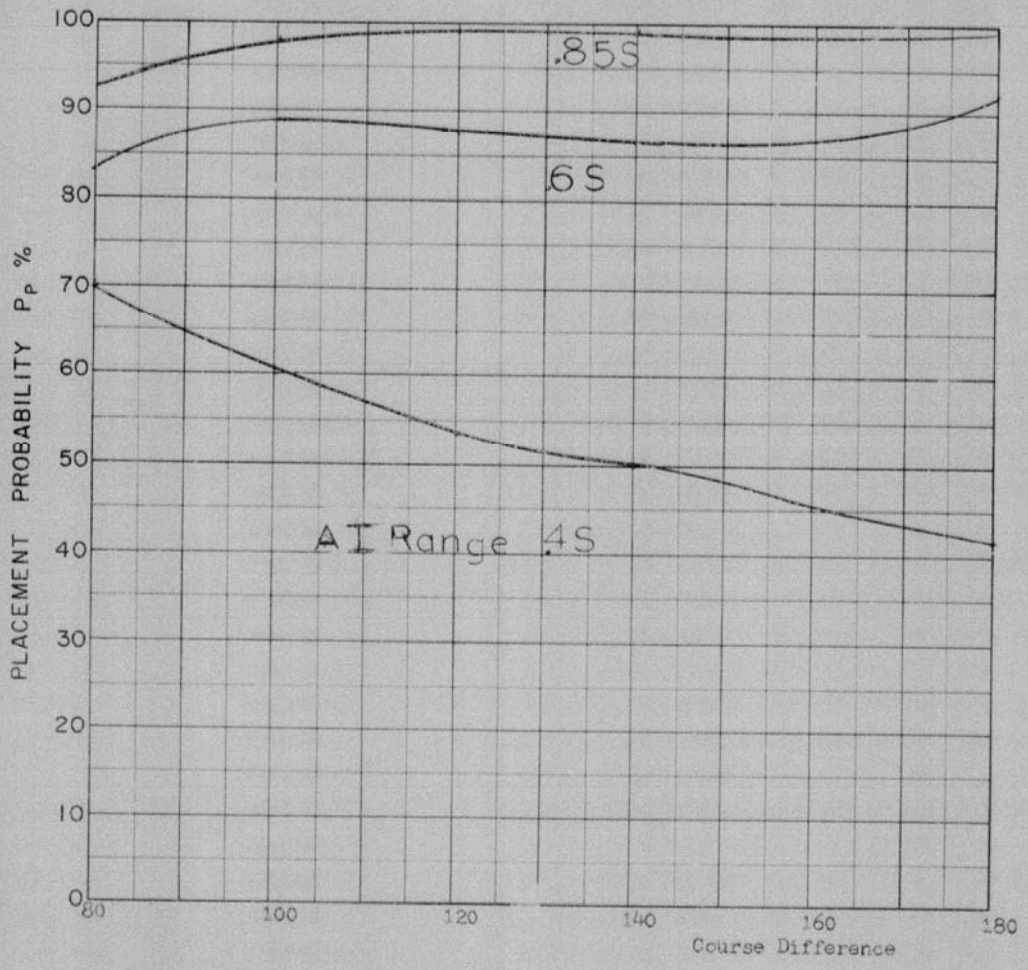

COURSE DIFFERENCE: Abscissa
TARGET EVASION: 0
TARGET MACH NO.: 1.5
INTERCEPTOR LATERAL G's: 1.6
INTERCEPTOR MACH NO.: 1.5
σ OF G.C.I. ACCURACY: 6.75 n.m.
A.I. DETECTION RANGE AS FRACTION OF SPECIFICATION RANGE, S: 3 values
A.I. DETECTION RANGE CONTOUR: Delta
ALTITUDE: 60 K

C-13

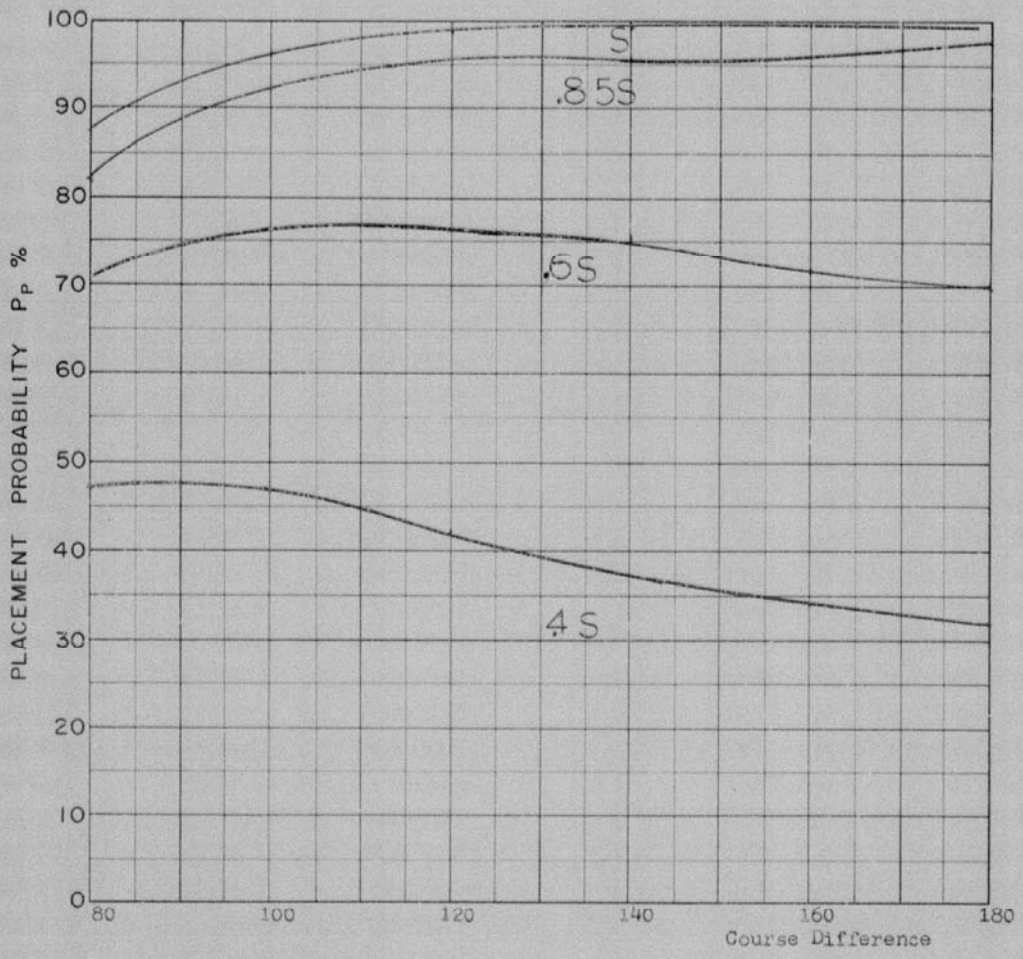

COURSE DIFFERENCE: Abscissa
TARGET EVASION: 0
TARGET MACH NO.: 1.5
INTERCEPTOR LATERAL G's: 1.6
INTERCEPTOR MACH NO.: 1.5
σ OF G.C.I. ACCURACY: 9 n.m.
A.I. DETECTION RANGE AS FRACTION OF SPECIFICATION RANGE, S: 4 values
A.I. DETECTION RANGE CONTOUR: Delta
ALTITUDE: 60 K

C-14

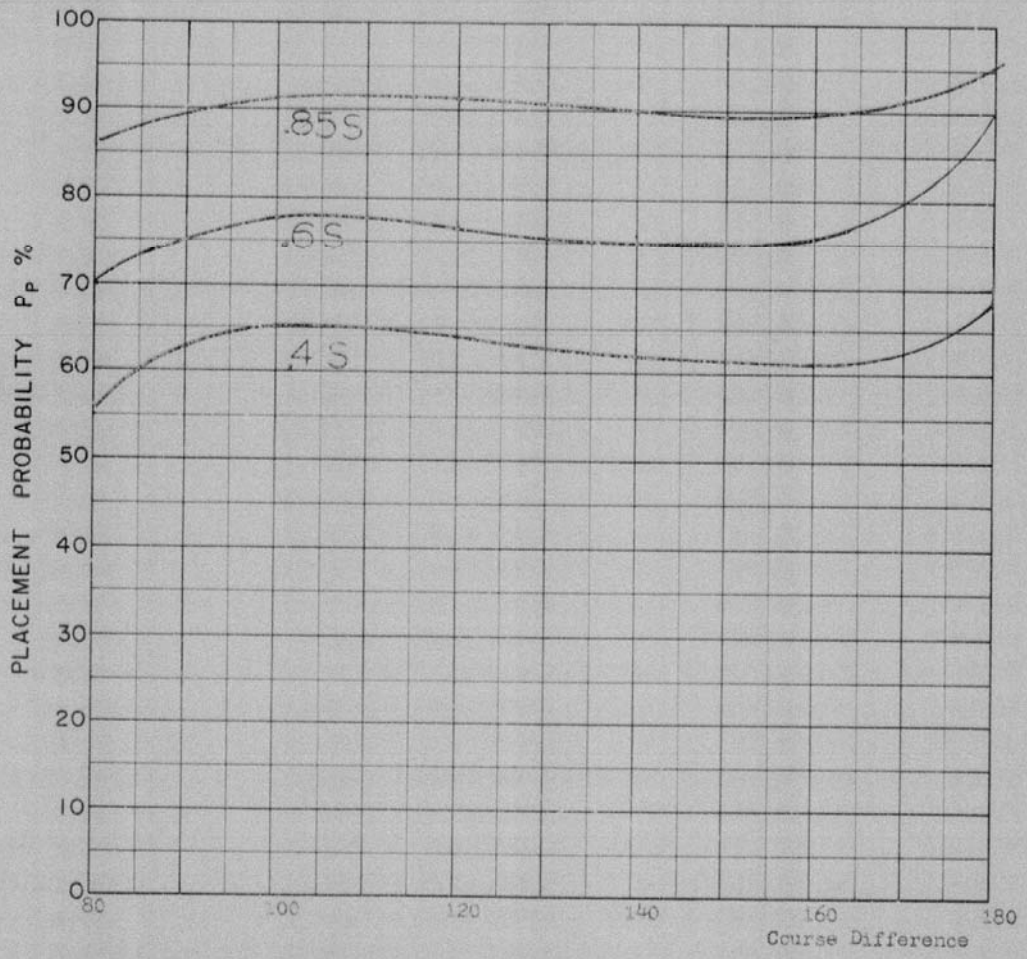

COURSE DIFFERENCE: Abscissa
TARGET EVASION: 0
TARGET MACH NO.: 1.5
INTERCEPTOR LATERAL G's: 3.0
INTERCEPTOR MACH NO.: 1.5
σ OF G.C.I. ACCURACY: 3 values
A.I. DETECTION RANGE AS FRACTION OF SPECIFICATION RANGE, S: 0.4
A.I. DETECTION RANGE CONTOUR: Delta
ALTITUDE: 60 K

C-15

Launch zone figure L-2

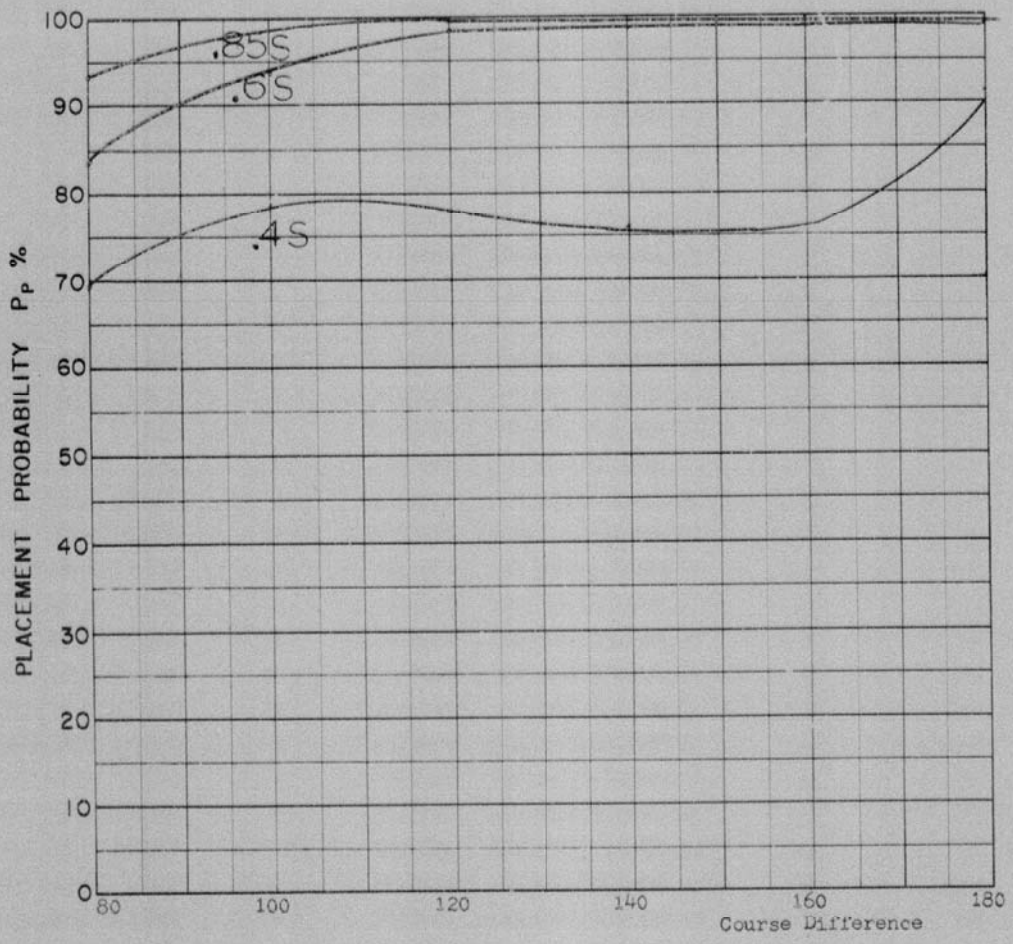

COURSE DIFFERENCE: Abscissa
TARGET EVASION: 0
TARGET MACH NO.: 1.5
INTERCEPTOR LATERAL G's: 3.0
INTERCEPTOR MACH NO.: 1.5
σ OF G.C.I. ACCURACY: 6.75 n.m.
A.I. DETECTION RANGE AS FRACTION OF SPECIFICATION RANGE, S: 3 values
A.I. DETECTION RANGE CONTOUR: Delta
ALTITUDE: 60 K

C-16

Launch zone figure L-2

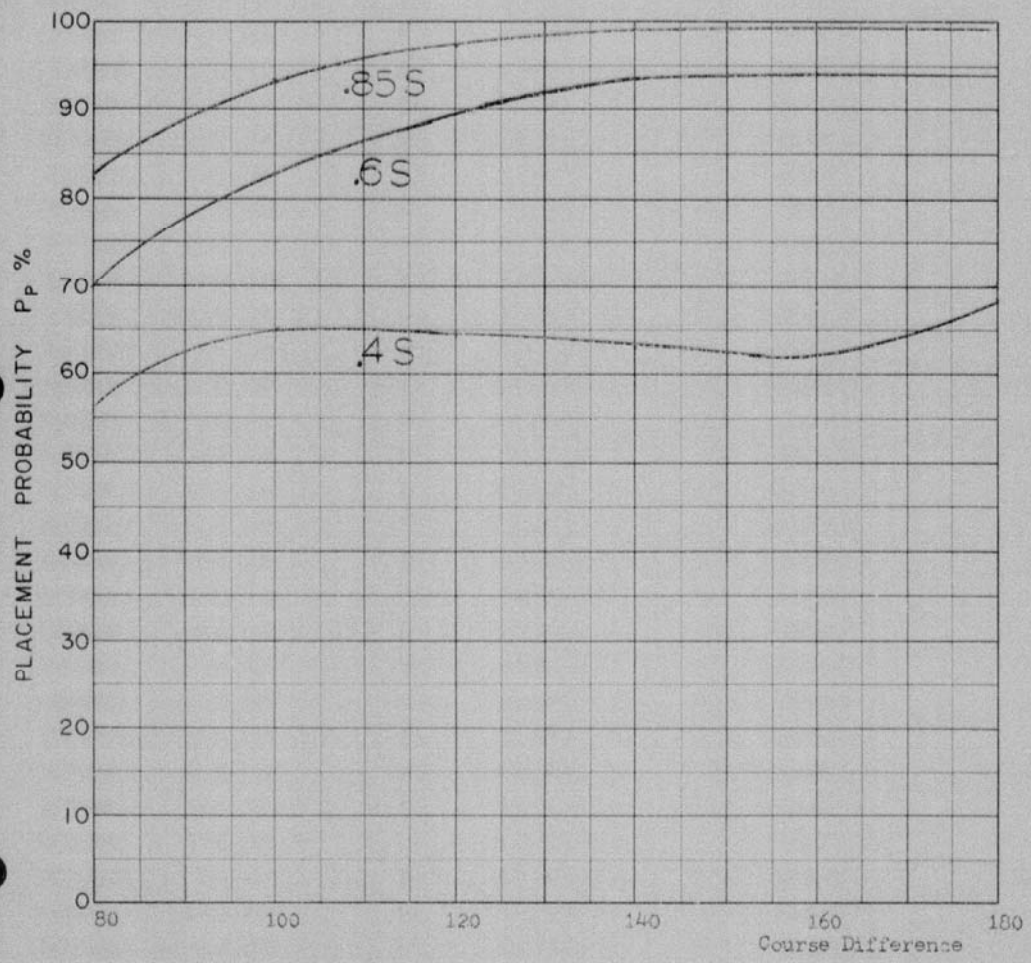

COURSE DIFFERENCE: Abscissa
TARGET EVASION: 0
TARGET MACH NO.: 1.5
INTERCEPTOR LATERAL G's: 3.0
INTERCEPTOR MACH NO.: 1.5
σ OF G.C.I. ACCURACY: .9 n.m.
A.I. DETECTION RANGE AS FRACTION OF SPECIFICATION RANGE, S: 3 values
A.I. DETECTION RANGE CONTOUR: Delta
ALTITUDE: 60 K

C-17

Launch zone figure L-2

187 dpa3

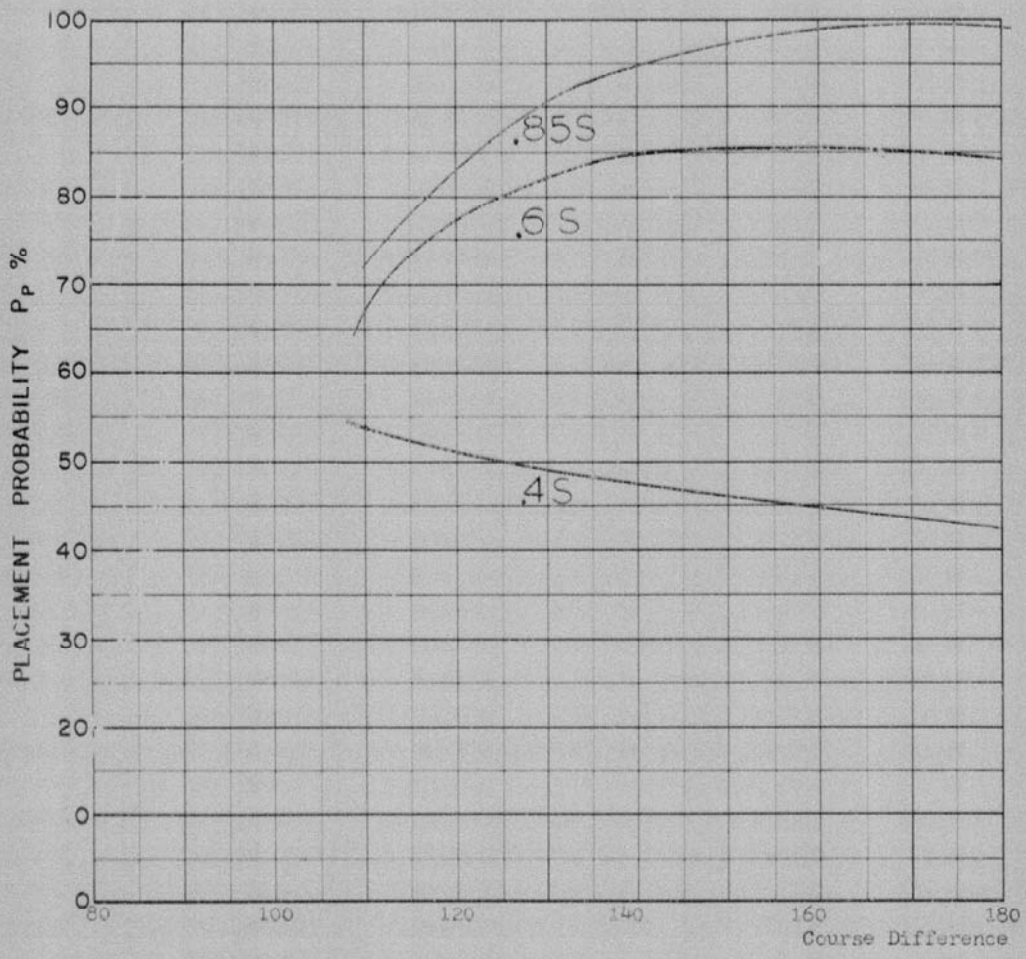

COURSE DIFFERENCE: Abscissa
TARGET EVASION: 0.15 lateral g's
TARGET MACH NO.: 1.5
INTERCEPTOR LATERAL G's: 1.5
INTERCEPTOR MACH NO.: 1.5
σ OF G.C.I. ACCURACY: 4.75 n.m.
A.I. DETECTION RANGE AS FRACTION OF SPECIFICATION RANGE, S: 3 values
A.I. DETECTION RANGE CONTOUR: Delta
ALTITUDE: 60 K

Missile launch zone L-13

C-18

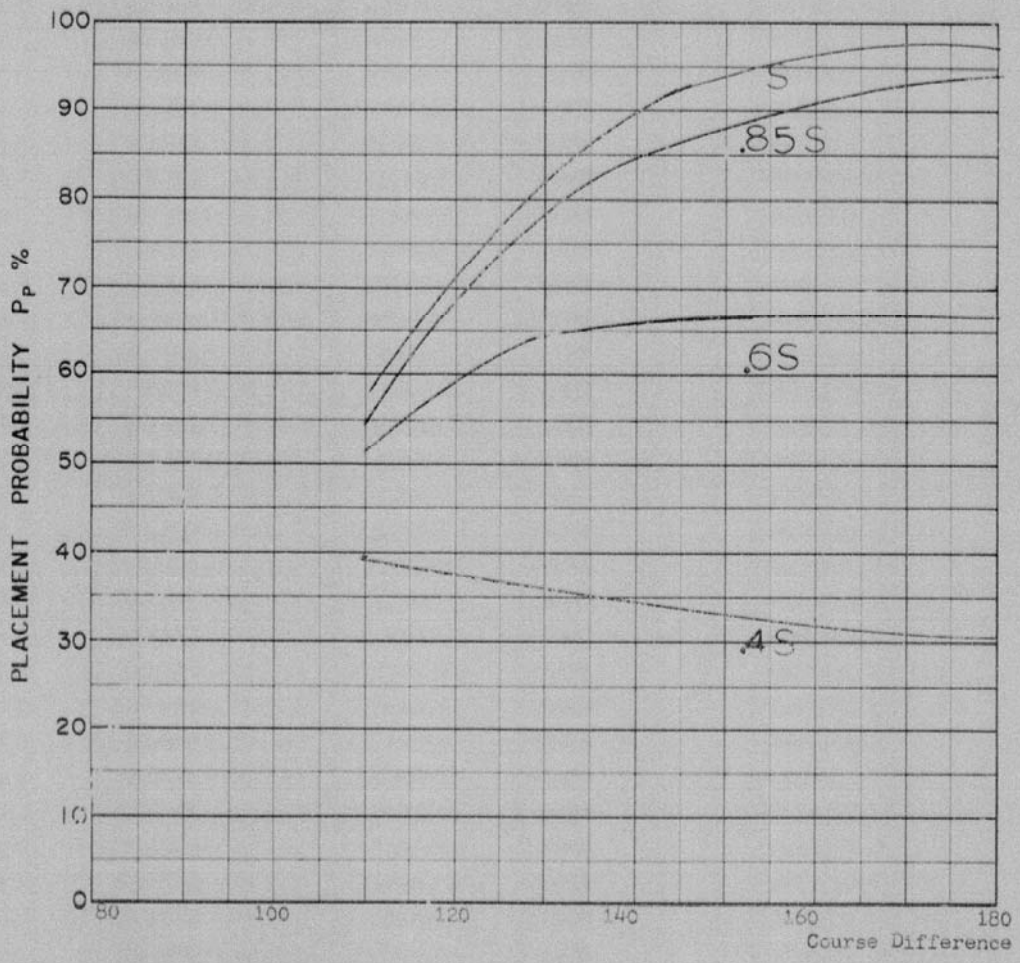

COURSE DIFFERENCE: Abscissa
TARGET EVASION: 0.15 lateral g's
TARGET MACH NO.: 1.5
INTERCEPTOR LATERAL G's: 1.5
INTERCEPTOR MACH NO.: 1.5
σ OF G.C.I. ACCURACY: 6.75 n.m.
A.I. DETECTION RANGE AS FRACTION OF SPECIFICATION RANGE, S: 4 values
A.I. DETECTION RANGE CONTOUR: Delta
ALTITUDE: 60 K

Missile launch zone L-13

C-19

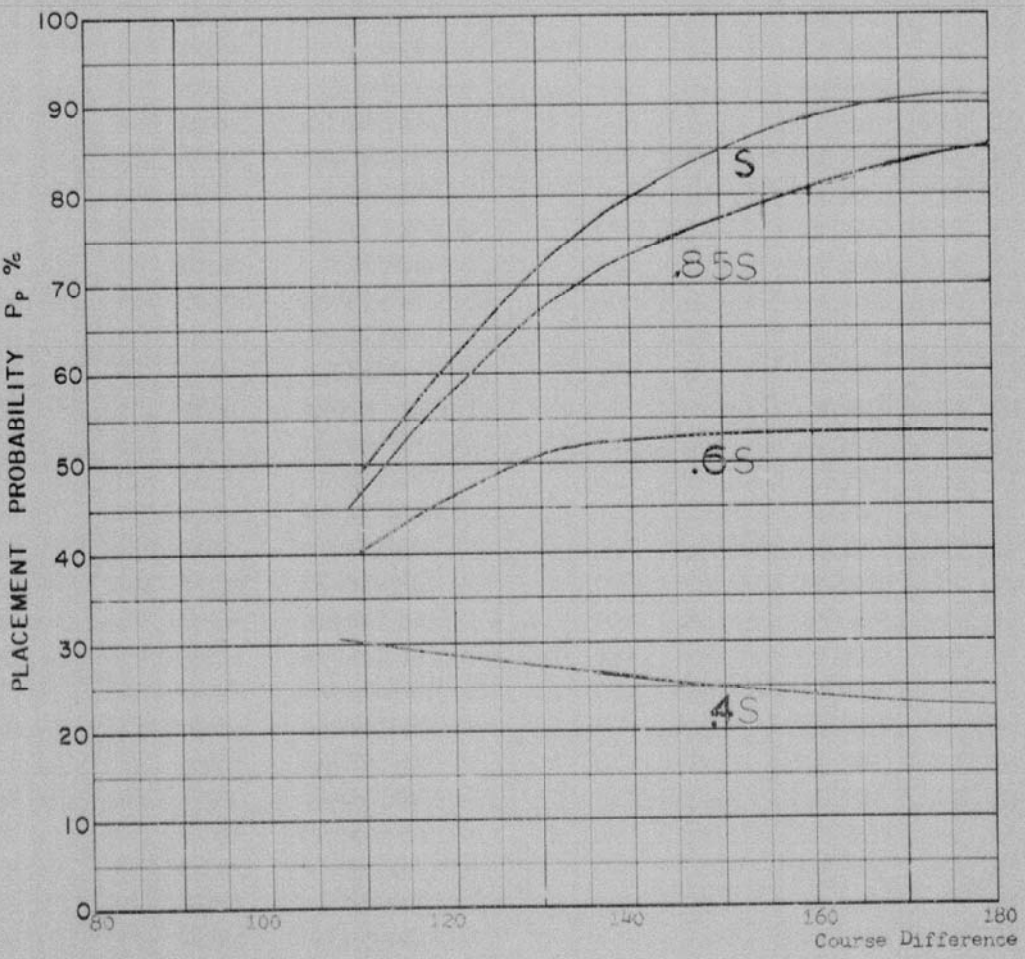

COURSE DIFFERENCE: Abscissa
TARGET EVASION: 0.15 lateral g's
TARGET MACH NO.: 1.5
INTERCEPTOR LATERAL G's: 1.5
INTERCEPTOR MACH NO.: 1.5
σ OF G.C.I. ACCURACY: 9 n.m.
A.I. DETECTION RANGE AS FRACTION OF SPECIFICATION RANGE, S: 4 values
A.I. DETECTION RANGE CONTOUR: Delta
ALTITUDE: 60 K
Missile launch zone L-13

C-20

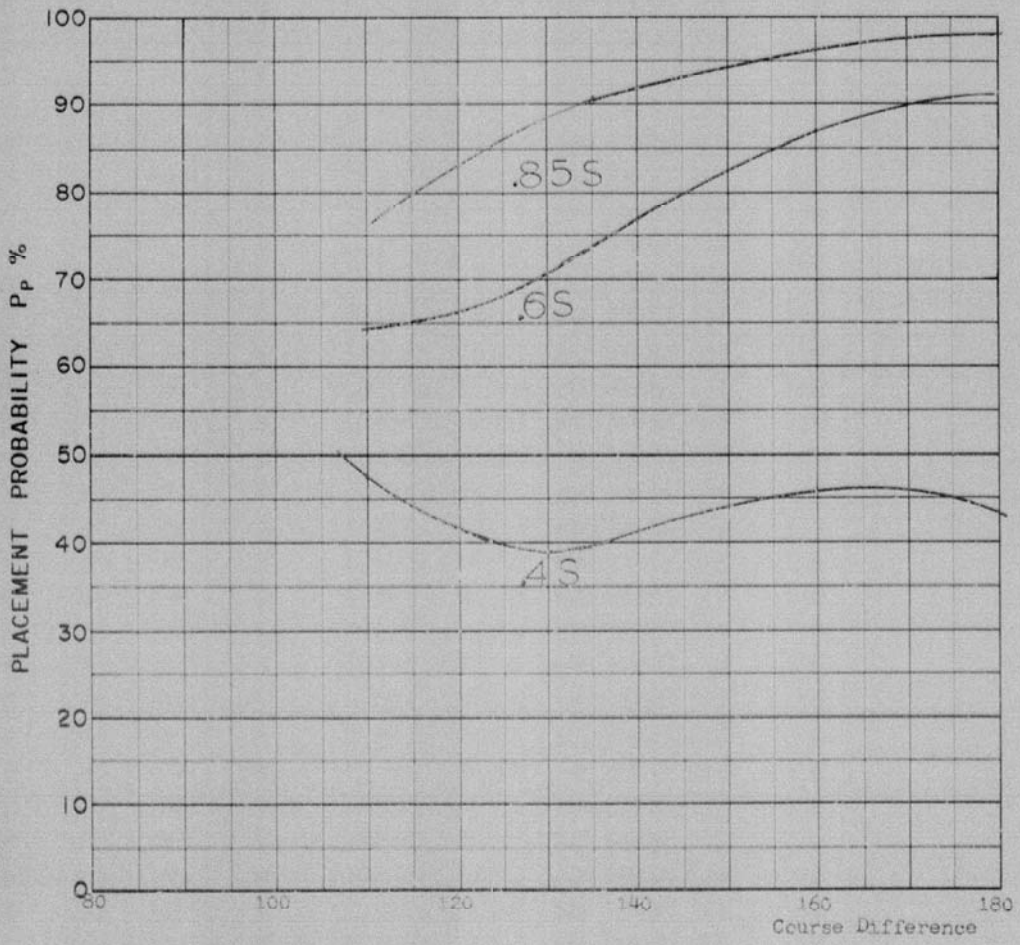

COURSE DIFFERENCE: Abscissa
TARGET EVASION: 0.15 lateral g's
TARGET MACH NO.: 1.5
INTERCEPTOR LATERAL G's: 2.4
INTERCEPTOR MACH NO.: 1.6
σ OF G.C.I. ACCURACY: 6.75
A.I. DETECTION RANGE AS FRACTION OF SPECIFICATION RANGE, S: 3 values
A.I. DETECTION RANGE CONTOUR: Delta
ALTITUDE: 60 K

Missile launch zone L-13

(C-21)

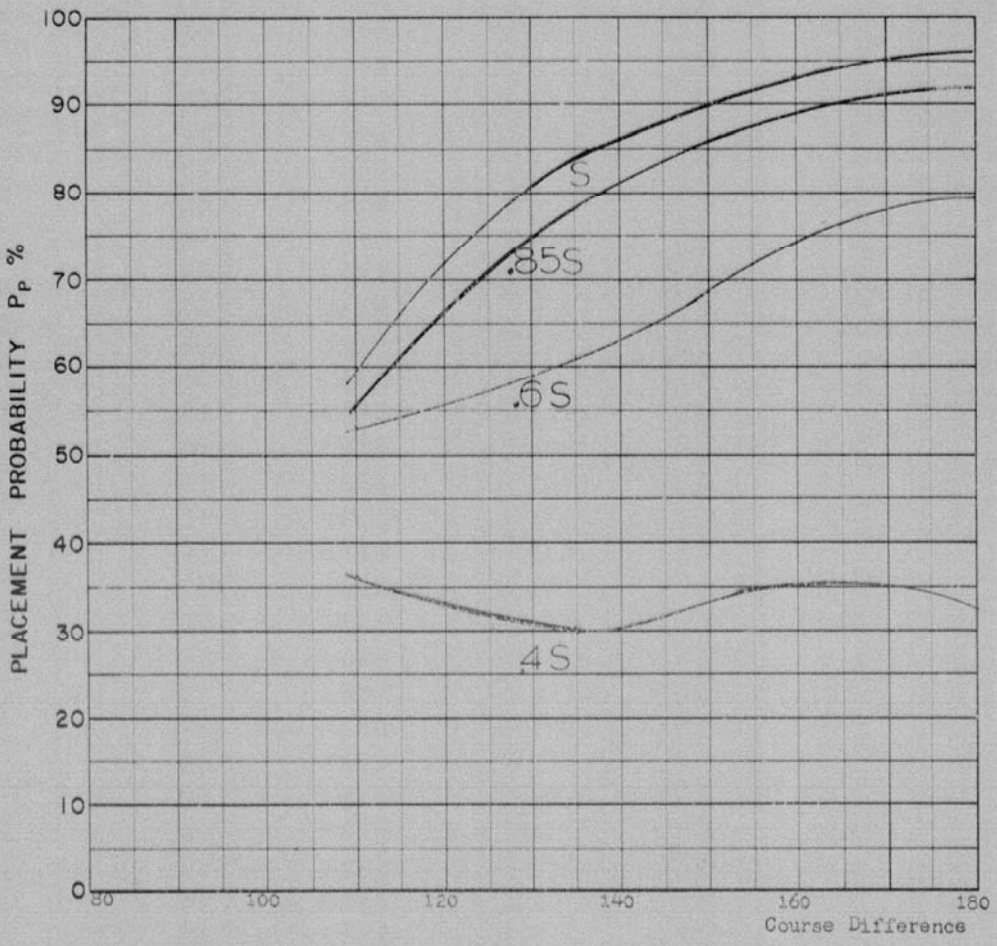

COURSE DIFFERENCE: Abscissa
TARGET EVASION: 0.15 lateral g's
TARGET MACH NO.: 1.5
INTERCEPTOR LATERAL G's: 2.4
INTERCEPTOR MACH NO.: 1.5
σ OF G.C.I. ACCURACY: 9 n.m.
A.I. DETECTION RANGE AS FRACTION OF SPECIFICATION RANGE, S: 4 values
A.I. DETECTION RANGE CONTOUR: Delta
ALTITUDE: 60 K

Missile launch zone L-13

C-22

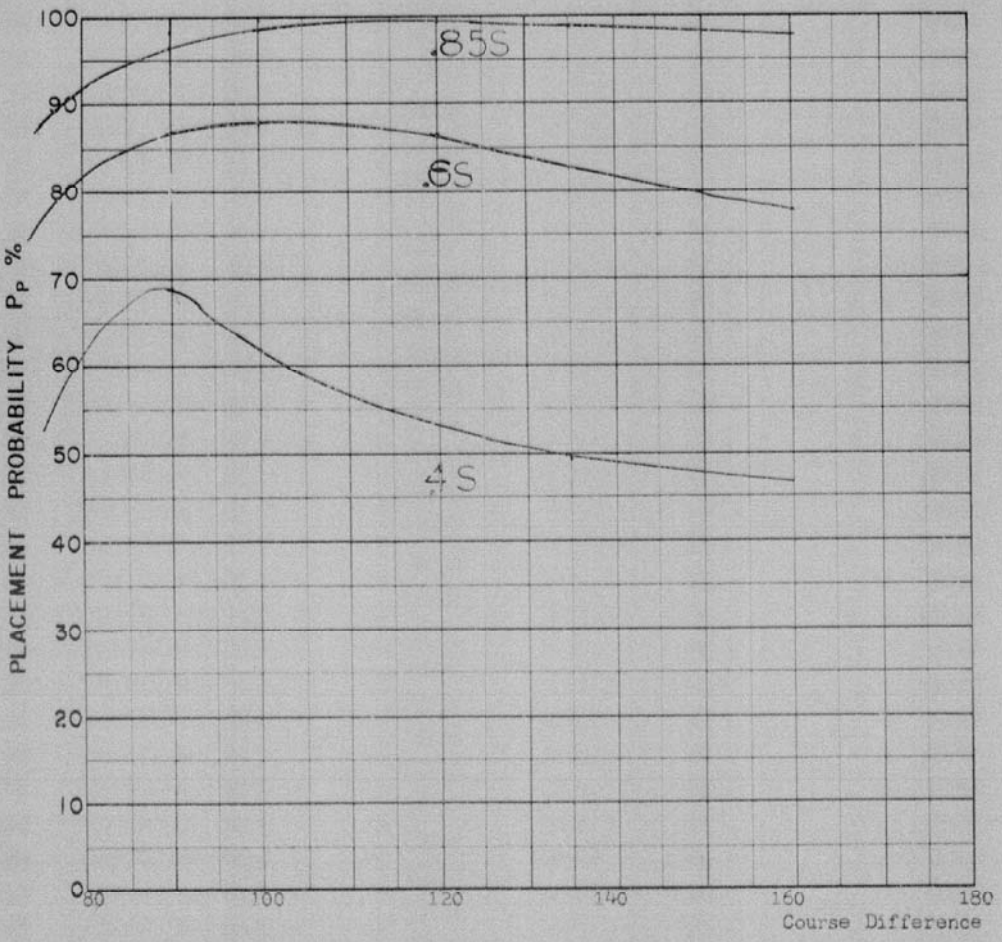

COURSE DIFFERENCE: Abscissa
TARGET EVASION: 0
TARGET MACH NO.: 2.0
INTERCEPTOR LATERAL G's: 0.85
INTERCEPTOR MACH NO.: 1.5
σ OF G.C.I. ACCURACY: 3.nm
A.I. DETECTION RANGE AS FRACTION OF SPECIFICATION RANGE, S 3 values
A.I. DETECTION RANGE CONTOUR: Delta
ALTITUDE: 50 K

Missile launch zone L-3 (Maximum range 10° heading error)

C-23

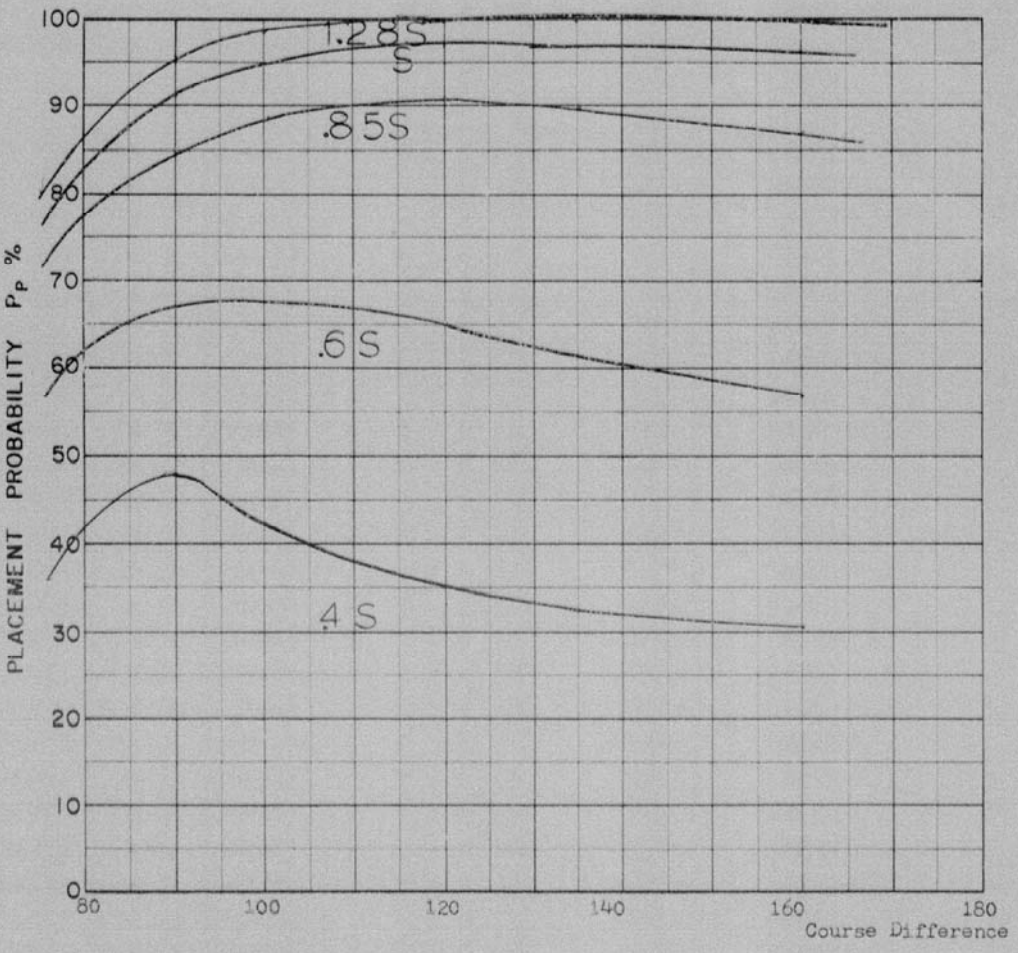

COURSE DIFFERENCE: Abscissa
TARGET EVASION: 0
TARGET MACH NO.: 2.0
INTERCEPTOR LATERAL G's: 0.85
INTERCEPTOR MACH NO.: 1.5
σ OF G.C.I. ACCURACY: 4.75 nm
A.I. DETECTION RANGE AS FRACTION OF SPECIFICATION RANGE, S: 5 values
A.I. DETECTION RANGE CONTOUR: Delta
ALTITUDE: 50 K

Missile launch zone L-3

C-24

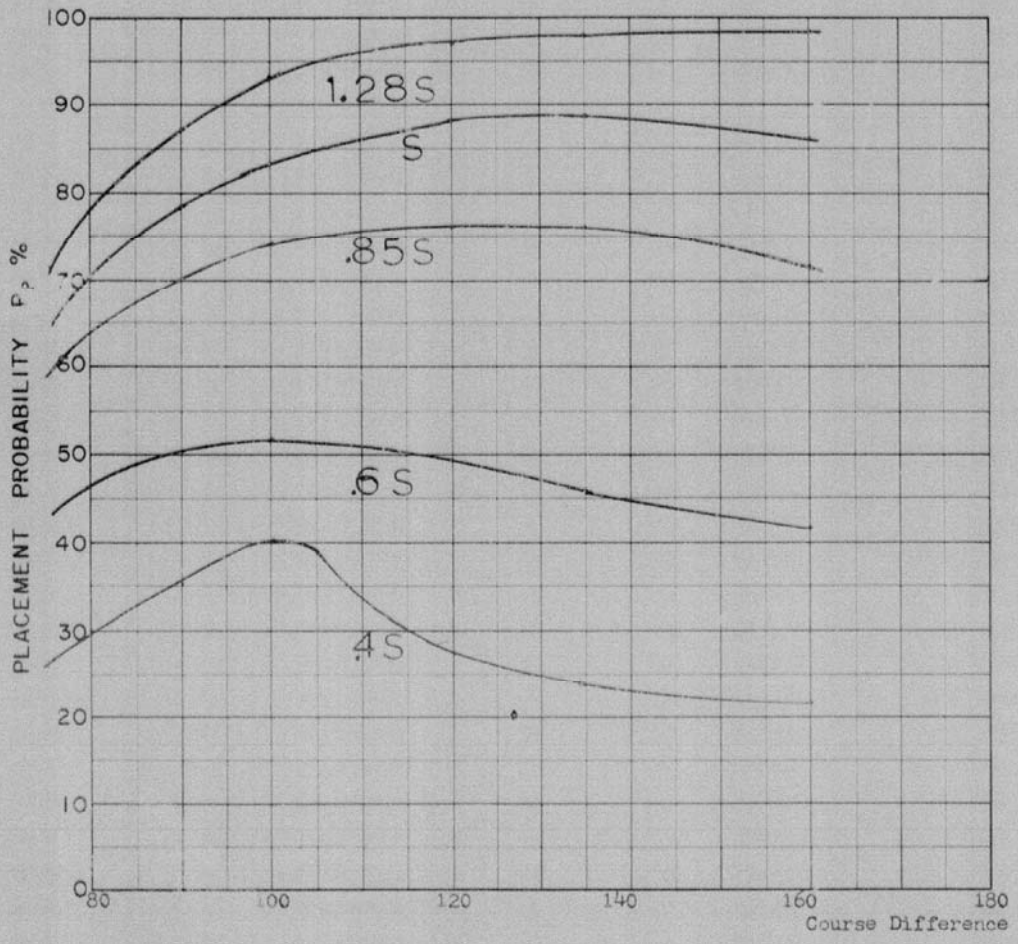

COURSE DIFFERENCE: Abscissa
TARGET EVASION: 0
TARGET MACH NO.: 2.0
INTERCEPTOR LATERAL G's: 0.85
INTERCEPTOR MACH NO: 1.5
σ OF G.C.I. ACCURACY: 6.75 nm
A.I. DETECTION RANGE AS FRACTION OF SPECIFICATION RANGE, S: 5 values
A.I. DETECTION RANGE CONTOUR: Delta
ALTITUDE: 50 K

Missile launch zone L-3

C-25

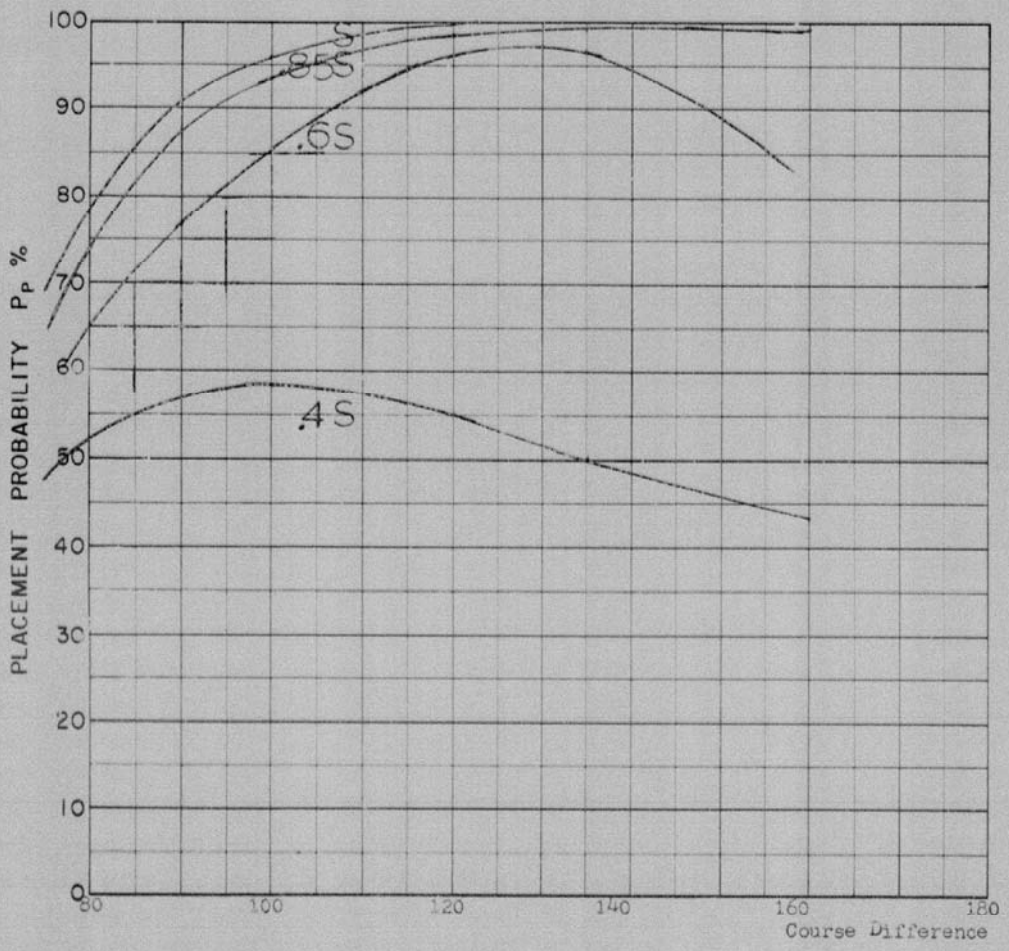

COURSE DIFFERENCE: Abscissa
TARGET EVASION: 0
TARGET MACH NO.: 2.0
INTERCEPTOR LATERAL G's: 1.6
INTERCEPTOR MACH NO.: 1.5
σ OF G.C.I. ACCURACY: 4.75 nm
A.I. DETECTION RANGE AS FRACTION OF SPECIFICATION RANGE, S: 4 values
A.I. DETECTION RANGE CONTOUR: Delta
ALTITUDE: 50 K

Missile launch zone L-3

C-26

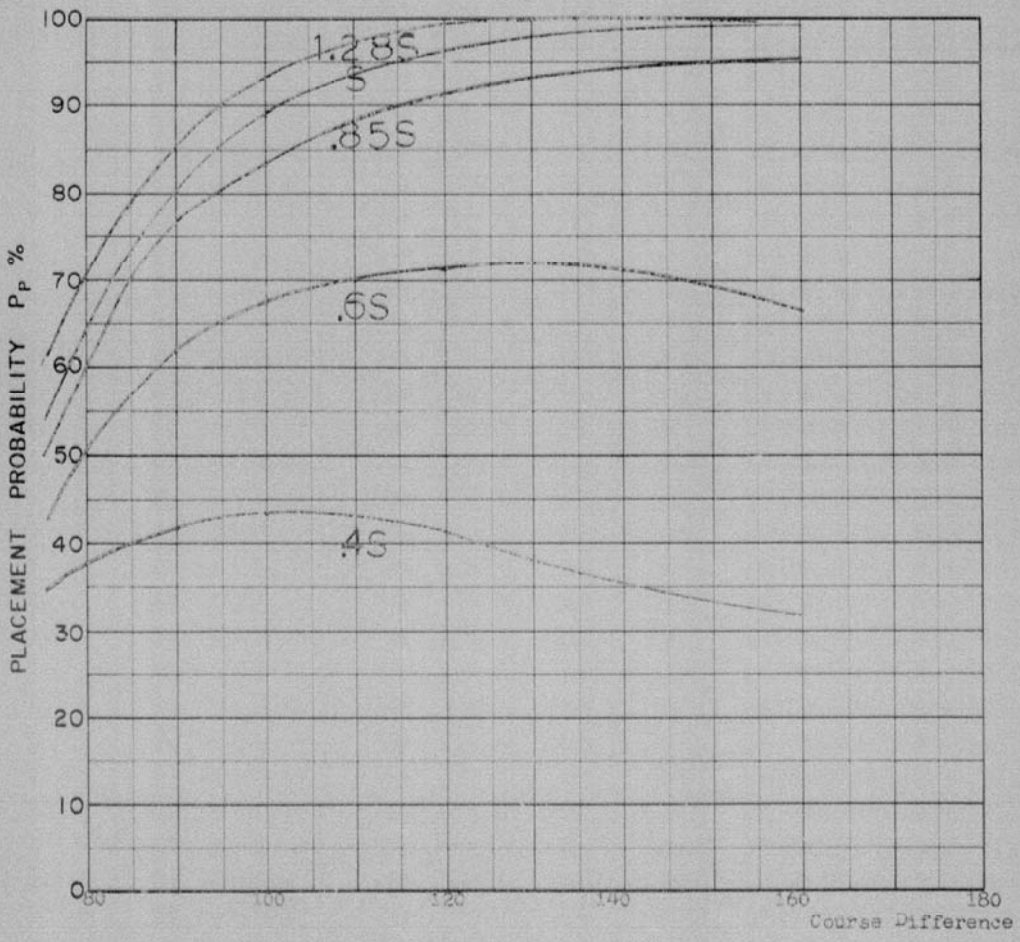

COURSE DIFFERENCE: Abscissa
TARGET EVASION: 0
TARGET MACH NO.: 2.0
INTERCEPTOR LATERAL G's: 1.6
INTERCEPTOR MACH NO.: 1.5
σ OF G.C.I. ACCURACY: 6.25 nm
A.I. DETECTION RANGE AS FRACTION OF SPECIFICATION RANGE, S: 5 values
A.I. DETECTION RANGE CONTOUR: Delta
ALTITUDE: 50 K

Missile launch zone L-3

C-27

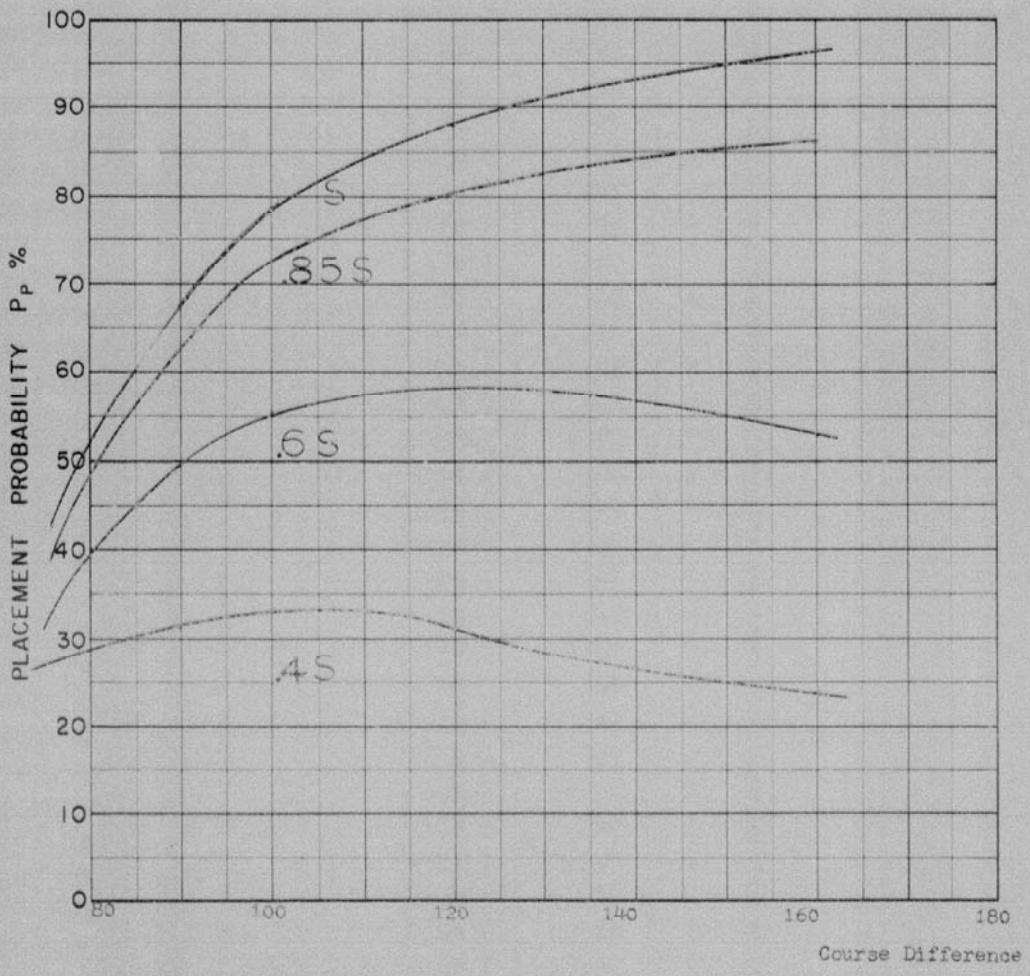

COURSE DIFFERENCE: Abscissa
TARGET EVASION: 0
TARGET MACH NO.: 2.0
INTERCEPTOR LATERAL G's: 1.6
INTERCEPTOR MACH NO.: 2.5
σ OF G.C.I. ACCURACY: 9 nm
A.I. DETECTION RANGE AS FRACTION OF SPECIFICATION RANGE, S: 4 values
A.I. DETECTION RANGE CONTOUR: Delta
ALTITUDE: 50 K

Missile launch zone L-3

C-28

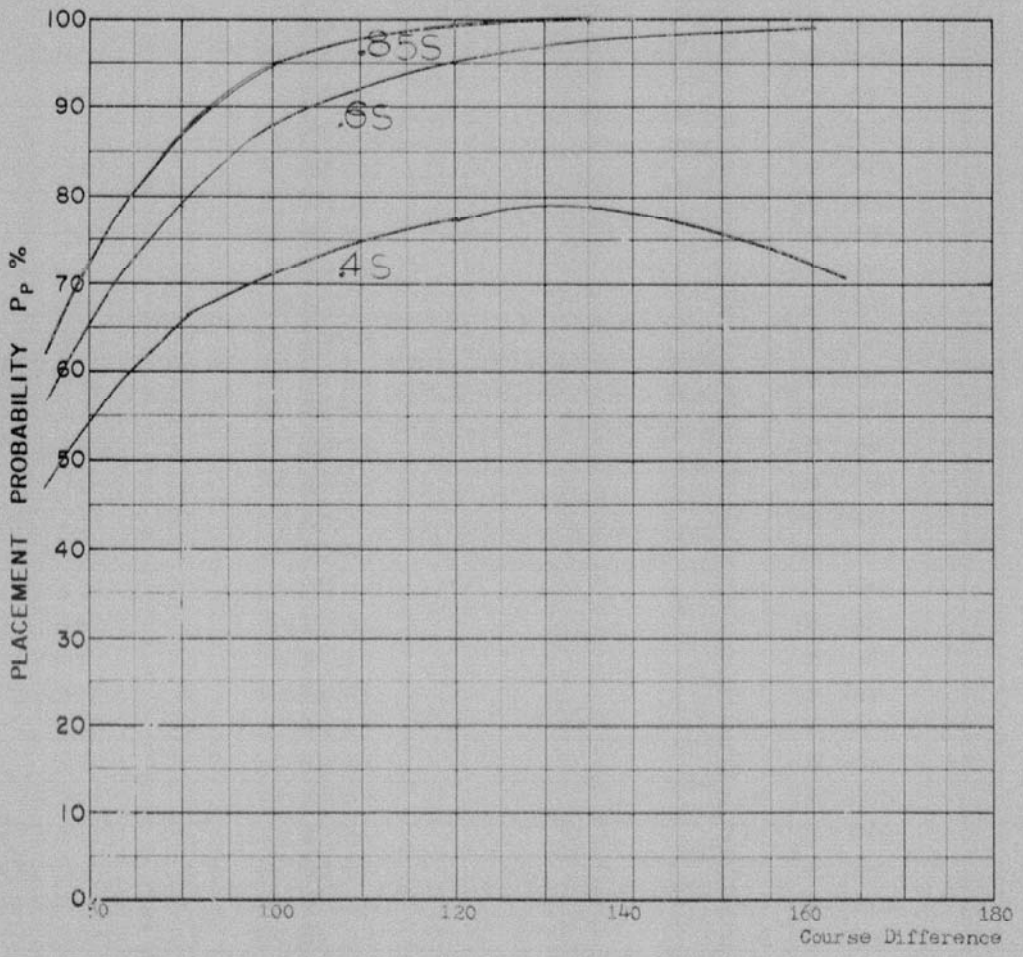

COURSE DIFFERENCE: Abscissa
TARGET EVASION: 0
TARGET MACH NO.: 2.0
INTERCEPTOR LATERAL G's: 3.0
INTERCEPTOR MACH NO.: 1.5
σ OF G.C.I. ACCURACY: 4.75 nm
A.I. DETECTION RANGE AS FRACTION OF SPECIFICATION RANGE, S: 3 values
A.I. DETECTION RANGE CONTOUR: Delta
ALTITUDE: 50 K

Missile launch zone L-3

(C-29)

10 xdpa3

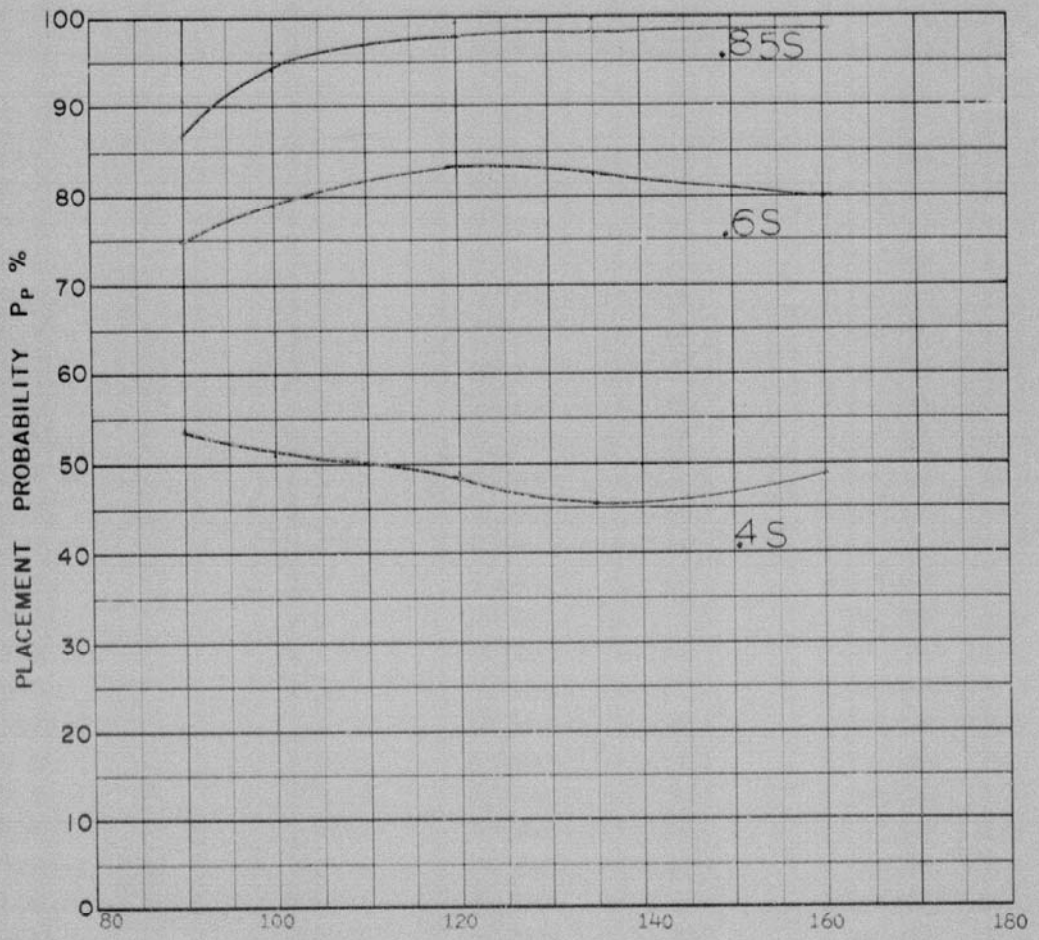

COURSE DIFFERENCE: Abscissa
TARGET EVASION: 0
TARGET MACH NO.: 2.0
INTERCEPTOR LATERAL G's: 1.12
INTERCEPTOR MACH NO.: 1.5
σ OF G.C.I. ACCURACY: 4.75 nm
A.I. DETECTION RANGE AS FRACTION OF SPECIFICATION RANGE, S: 3 values
A.I. DETECTION RANGE CONTOUR: Delta
ALTITUDE: 60 K
Missile launch zone L-5. (Maximum range 8° heading Error)

C-30

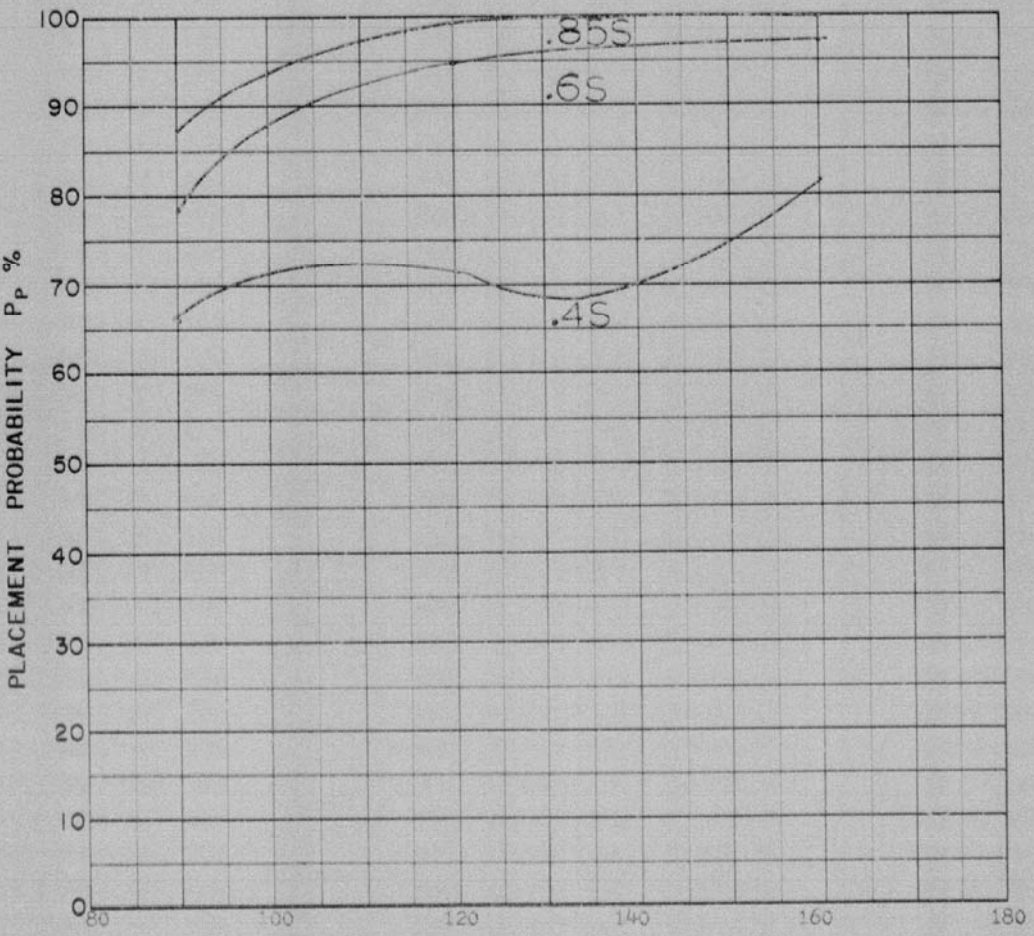

COURSE DIFFERENCE: Abscissa
TARGET EVASION: 0
TARGET MACH NO.: 2.0
INTERCEPTOR LATERAL G's: 2.0
INTERCEPTOR MACH NO.: 1.5
σ OF G.C.I. ACCURACY: 4.25 nm
A.I. DETECTION RANGE AS FRACTION OF SPECIFICATION RANGE, S: 3 values
A.I. DETECTION RANGE CONTOUR: Delta
ALTITUDE: 60 K

Missile launch zone L-5.

C-31

110 adpal

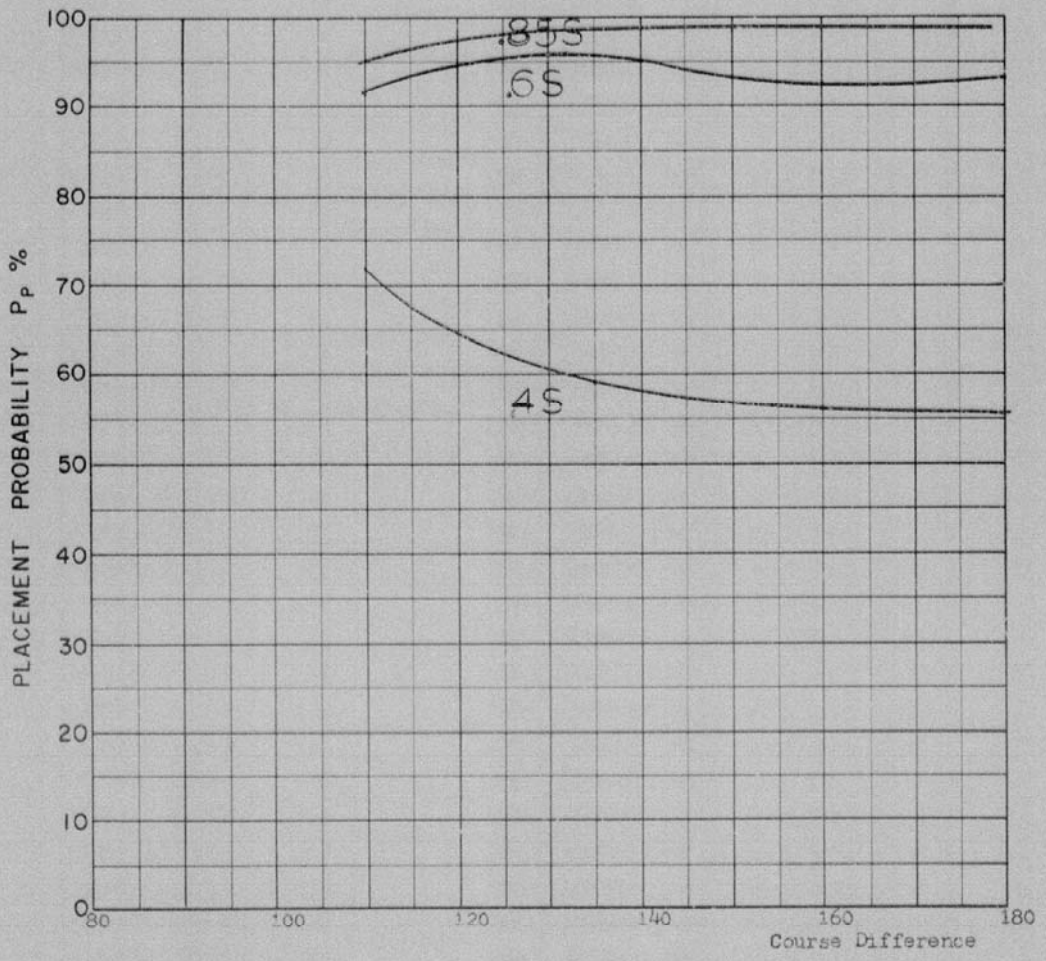

COURSE DIFFERENCE: Abscissa
TARGET EVASION: 0.1
TARGET MACH NO.: 2.0
INTERCEPTOR LATERAL G's: 1.6
INTERCEPTOR MACH NO.: 1.5
σ OF G.C.I. ACCURACY: 3 n.m.
A.I. DETECTION RANGE AS FRACTION OF SPECIFICATION RANGE, S: 3 values
A.I. DETECTION RANGE CONTOUR: Delta
ALTITUDE: 50 K

C-32

Launch zone figure L-10

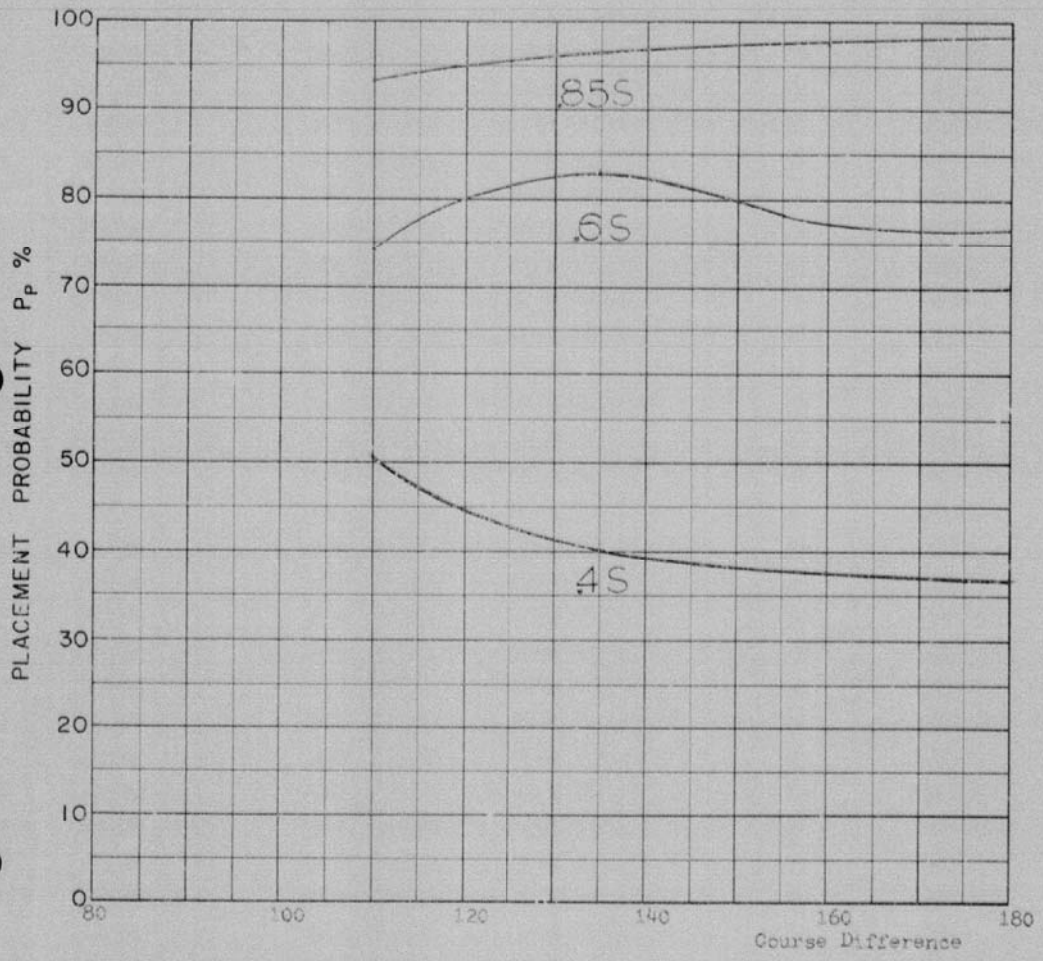

COURSE DIFFERENCE: Abscissa
TARGET EVASION: 0.1
TARGET MACH NO.: 2.0
INTERCEPTOR LATERAL G's: 1.6
INTERCEPTOR MACH NO.: 1.5
σ OF G.C.I. ACCURACY: 4.75 n.m.
A.I. DETECTION RANGE AS FRACTION OF SPECIFICATION RANGE, S: 3 values
A.I. DETECTION RANGE CONTOUR: Delta
ALTITUDE: 50 K

C-33

Launch zone figure L-10

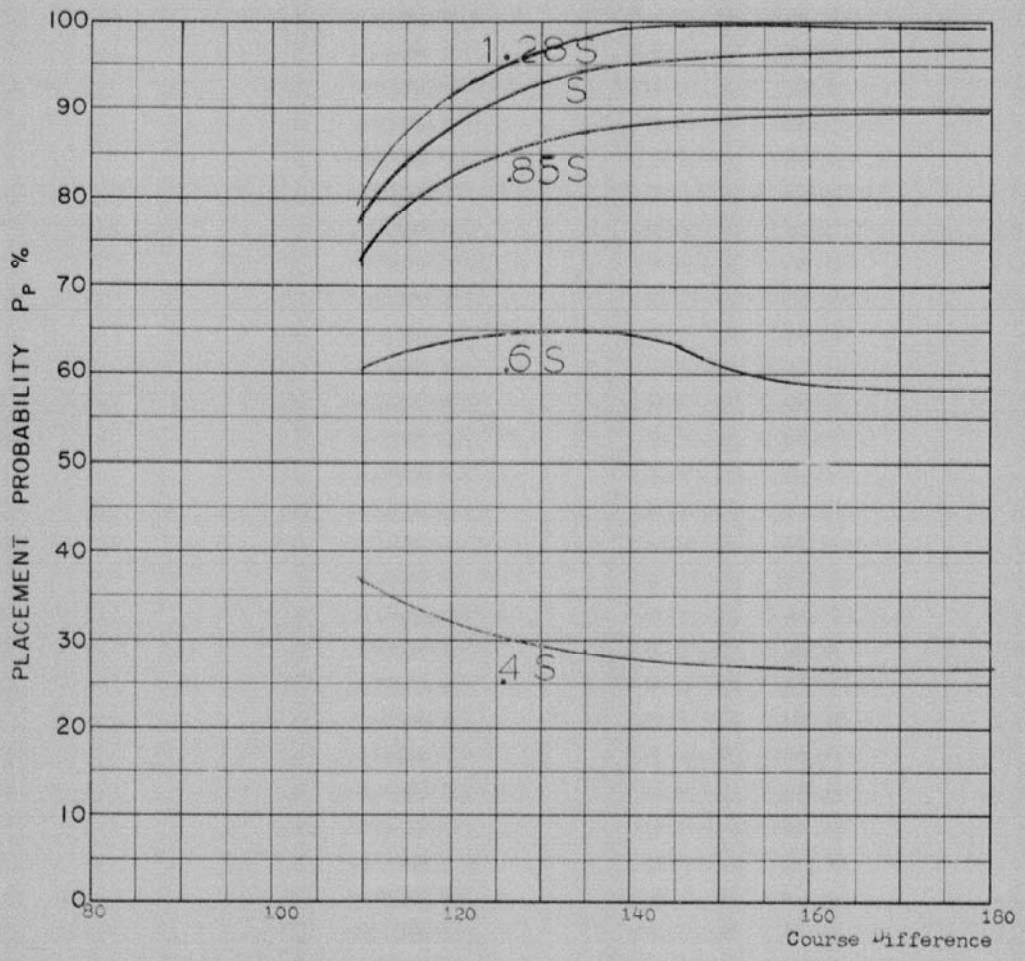

COURSE DIFFERENCE: Abscissa
TARGET EVASION: 0.1
TARGET MACH NO.: 2.0
INTERCEPTOR LATERAL G's: 1.6
INTERCEPTOR MACH NO.: 1.5
σ OF G.C.I. ACCURACY: 6.75 n.m.
A.I. DETECTION RANGE AS FRACTION OF SPECIFICATION RANGE, S: 5 values
A.I. DETECTION RANGE CONTOUR: Delta
ALTITUDE: 50 K

C-34

Launch zone figure L-10

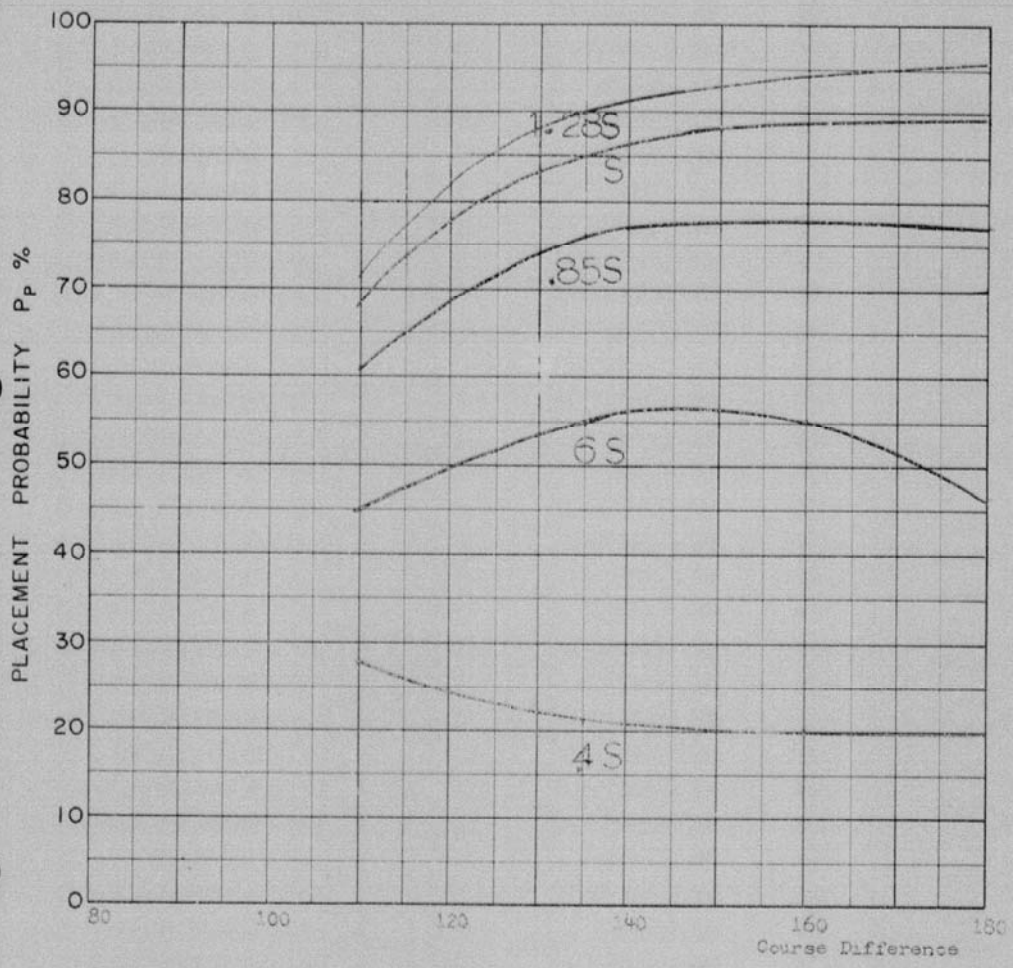

COURSE DIFFERENCE: Abscissa
TARGET EVASION: 0.1
TARGET MACH NO.: 2.0
INTERCEPTOR LATERAL G's: 1.6
INTERCEPTOR MACH NO.: 1.5
σ OF G.C.I. ACCURACY: 9 n.m.
A.I. DETECTION RANGE AS FRACTION OF SPECIFICATION RANGE, S: 5 values
A.I. DETECTION RANGE CONTOUR: Delta
ALTITUDE: 50 K

C-35

Launch zone figure L-10

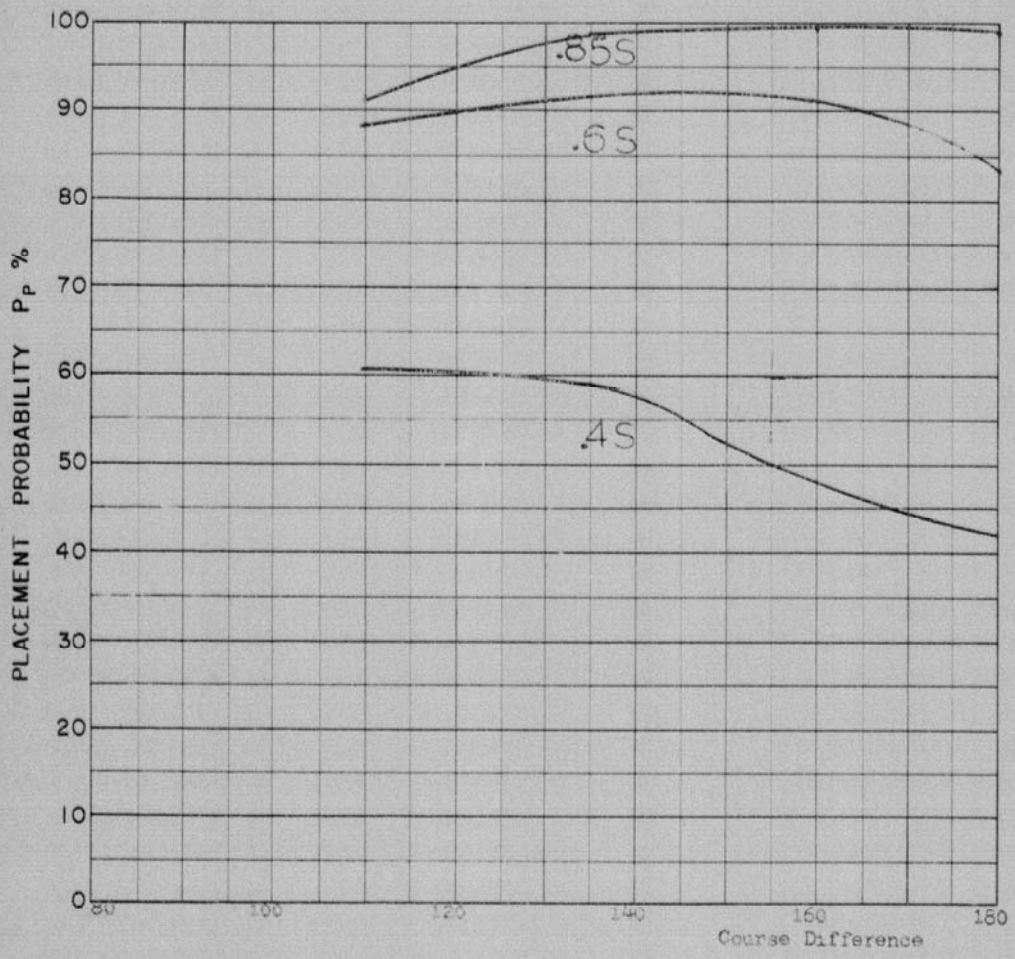

COURSE DIFFERENCE: Abscissa
TARGET EVASION: 0.1 lateral g's
TARGET MACH NO.: 2.0
INTERCEPTOR LATERAL G's: 1.5
INTERCEPTOR MACH NO.: 1.5
σ OF G.C.I. ACCURACY: 3 n.m.
A.I. DETECTION RANGE AS FRACTION OF SPECIFICATION RANGE, S: 3 values
A.I. DETECTION RANGE CONTOUR: Delta
ALTITUDE: 60 K

C-36

Launch zone figure L-11

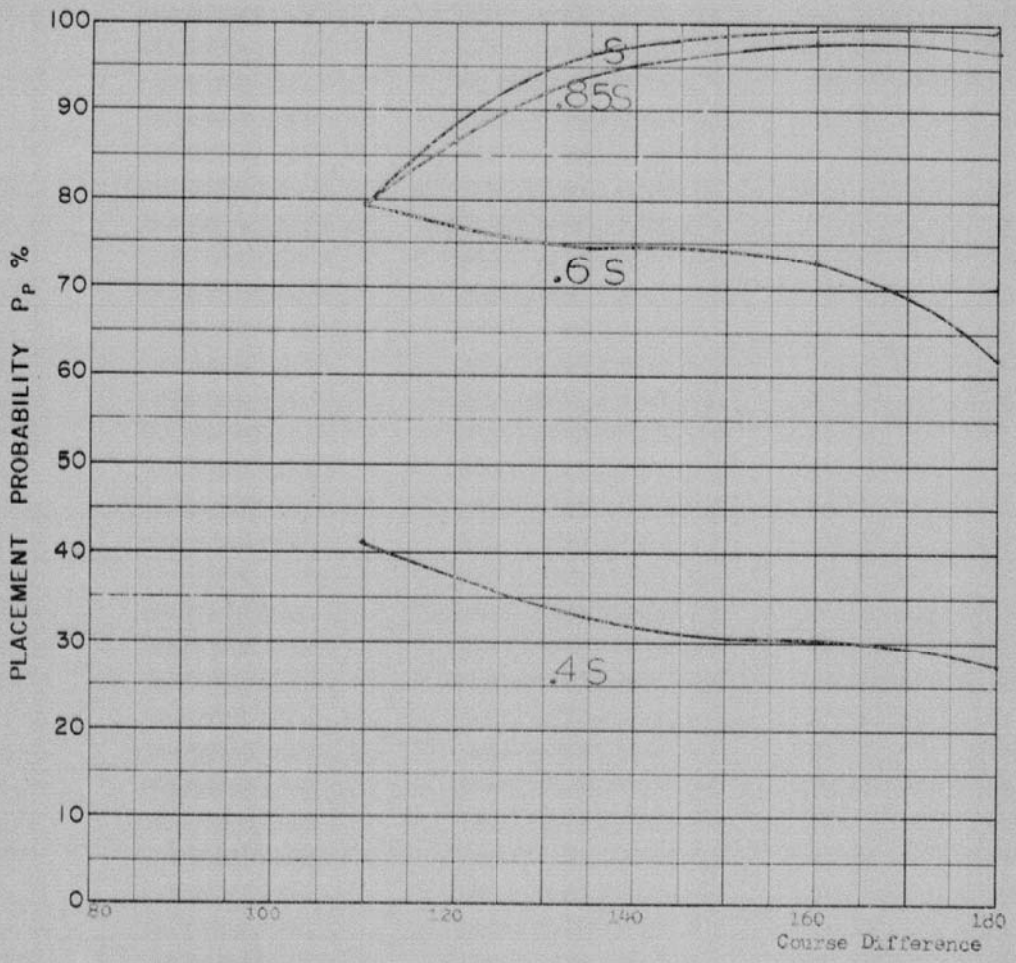

COURSE DIFFERENCE: Abscissa
TARGET EVASION: 0.1 lateral g's
TARGET MACH NO.: 2.0
INTERCEPTOR LATERAL G's: 1.5
INTERCEPTOR MACH NO.: 1.5
σ OF G.C.I. ACCURACY: 4.75 n.m.
A.I. DETECTION RANGE AS FRACTION OF SPECIFICATION RANGE, S: 4 values
A.I. DETECTION RANGE CONTOUR: Delta
ALTITUDE: 60 K

C-37

Launch zone figure L-11

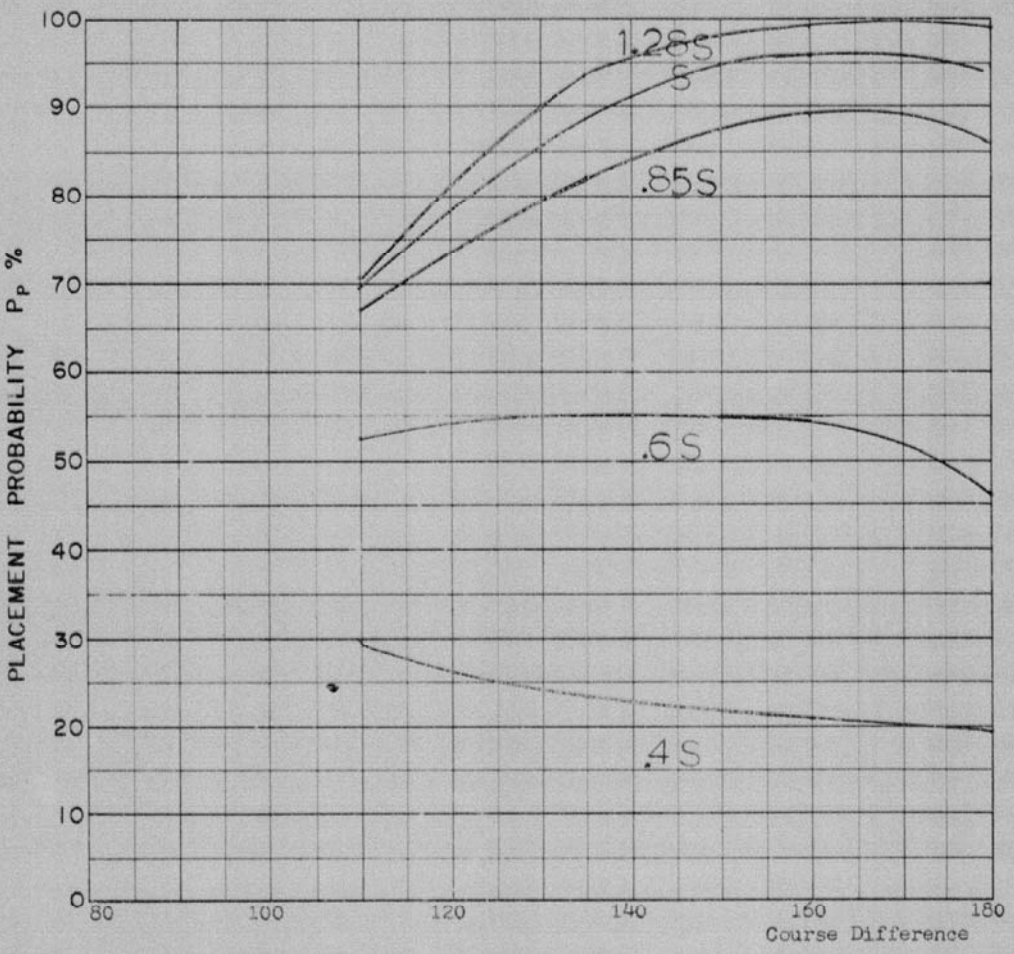

COURSE DIFFERENCE: Abscissa
TARGET EVASION: 0.1 lateral g's
TARGET MACH NO.: 2.0
INTERCEPTOR LATERAL G's: 1.5
INTERCEPTOR MACH NO.: 1.5
σ OF G.C.I. ACCURACY: 6.75 n.m.
A.I. DETECTION RANGE AS FRACTION OF SPECIFICATION RANGE, S: 5 values
A.I. DETECTION RANGE CONTOUR: Delta
ALTITUDE: 60 K

Launch zone L-11

C-38

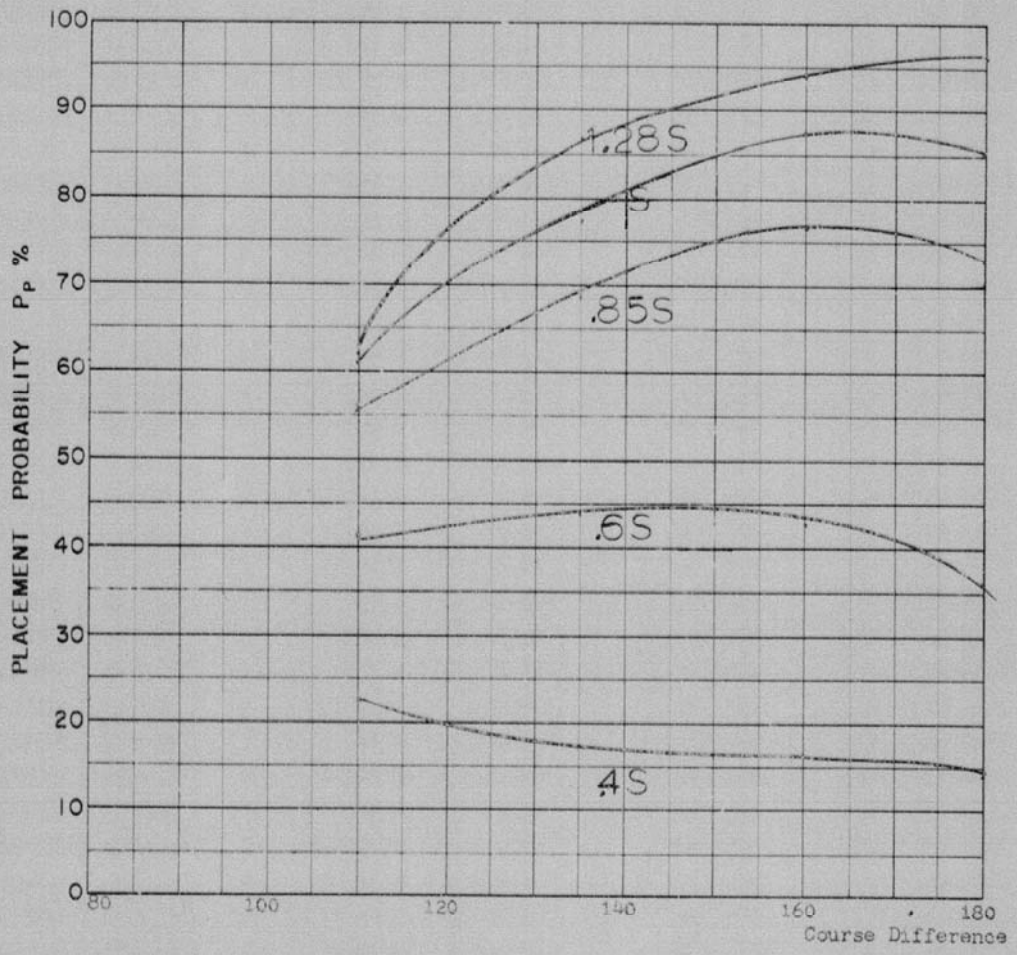

COURSE DIFFERENCE: Abscissa
TARGET EVASION: 0.1 lateral g's
TARGET MACH NO.: 2.0
INTERCEPTOR LATERAL G's: 1.5
INTERCEPTOR MACH NO.: 1.5
σ OF G.C.I. ACCURACY: 9 n.m.
A.I. DETECTION RANGE AS FRACTION OF SPECIFICATION RANGE, S: 5 values
A.I. DETECTION RANGE CONTOUR: Delta
ALTITUDE: 60 K

Launch zone L-11

C-39

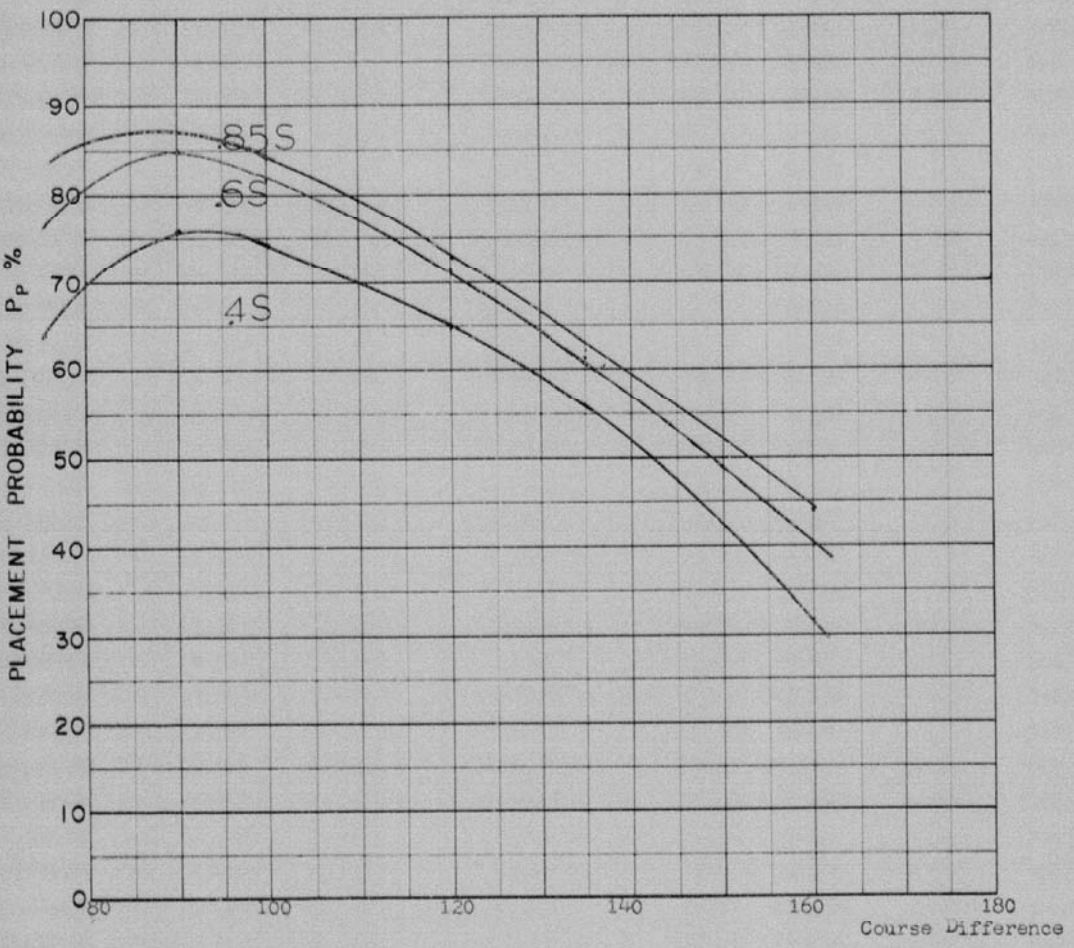

COURSE DIFFERENCE: Abscissa
TARGET EVASION: 0
TARGET MACH NO.: 2.0
INTERCEPTOR LATERAL G's: 3.6
INTERCEPTOR MACH NO.: 1.8
σ OF G.C.I. ACCURACY: 4.75 nm
A.I. DETECTION RANGE AS FRACTION OF SPECIFICATION RANGE, S: Delta
A.I. DETECTION RANGE CONTOUR: 3 values
ALTITUDE: 60 K

Missile launch zone L-8

C-40

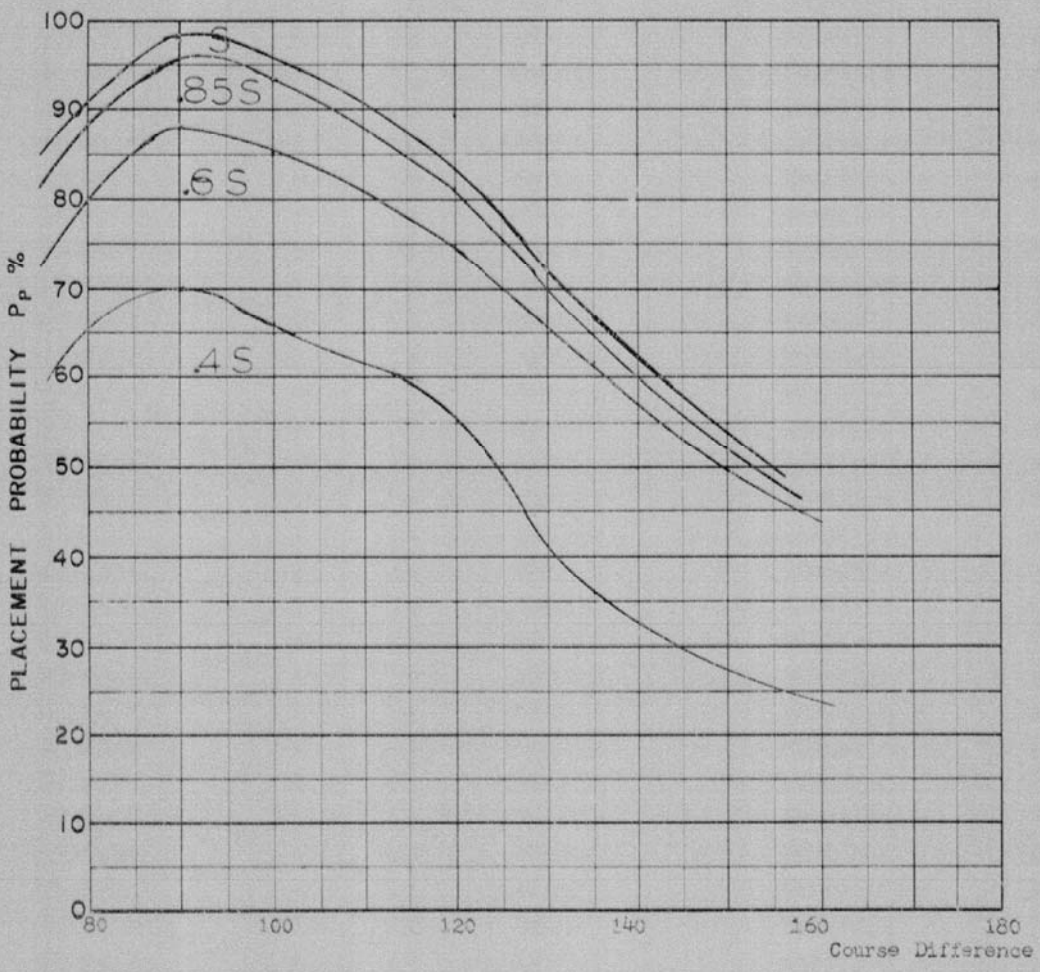

COURSE DIFFERENCE: Abscissa
TARGET EVASION: 0
TARGET MACH NO.: 2.0
INTERCEPTOR LATERAL G's: 2.0
INTERCEPTOR MACH NO.: 1.8
σ OF G.C.I. ACCURACY: 4.75 nm
A.I. DETECTION RANGE AS FRACTION OF SPECIFICATION RANGE, S: Delta
A.I. DETECTION RANGE CONTOUR: 4 values
ALTITUDE: 60 K

Missile launch zone L-8

C-41

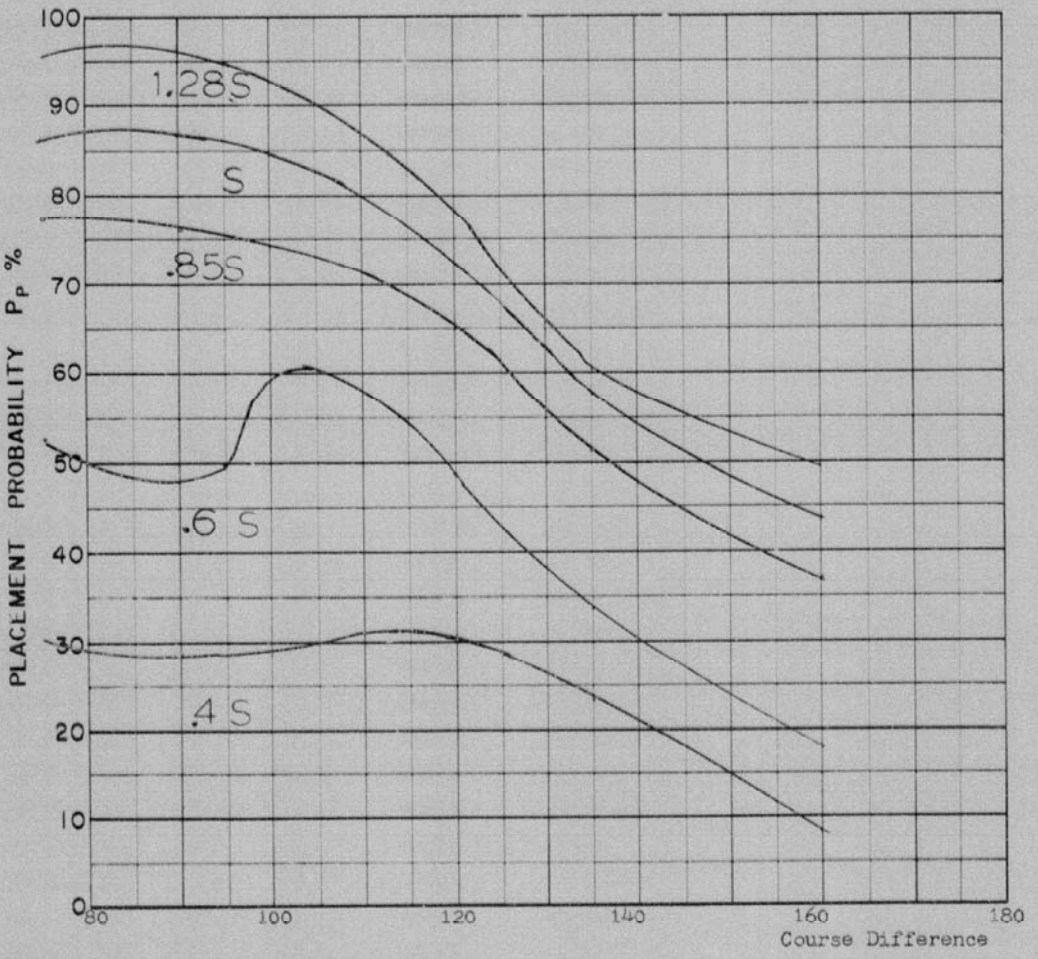

COURSE DIFFERENCE: Abscissa
TARGET EVASION: 0
TARGET MACH NO.: 2.0
INTERCEPTOR LATERAL G's: 0.66
INTERCEPTOR MACH NO.: 1.8
σ OF G.C.I. ACCURACY: 4.75 nm
A.I. DETECTION RANGE AS FRACTION OF SPECIFICATION RANGE, S: 5 values
A.I. DETECTION RANGE CONTOUR: Delta
ALTITUDE: 60 K

Missile launch zone L-8 (minimum range, 8° heading error)

(C-42)

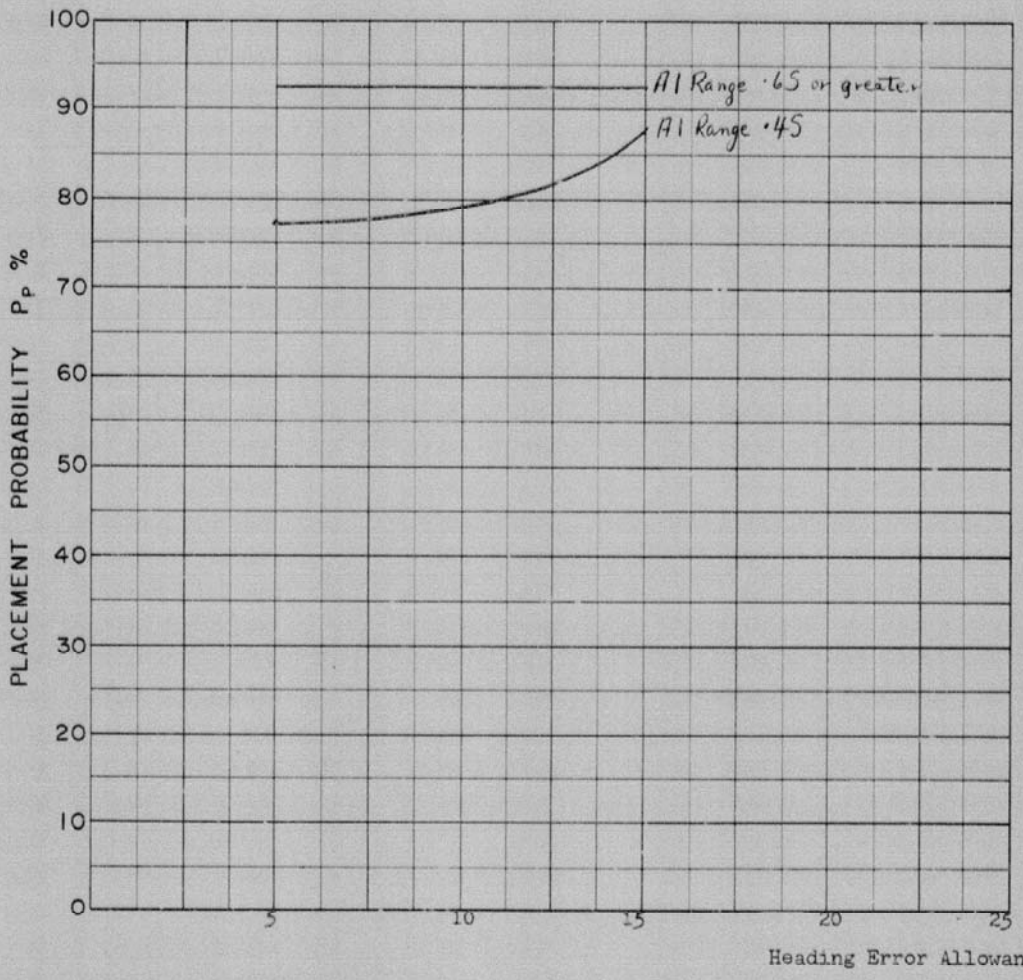

COURSE DIFFERENCE: 120°
TARGET EVASION: 0
TARGET MACH NO.: 2.0
INTERCEPTOR LATERAL G's: 3.35
INTERCEPTOR MACH NO.: 1.5
σ OF G.C.I. ACCURACY: 4.75 n.m.
A.I. DETECTION RANGE AS FRACTION OF SPECIFICATION RANGE, S: 2 values
A.I. DETECTION RANGE CONTOUR: Delta
ALTITUDE: 60 K

E-1

Launch zone of figure L-5

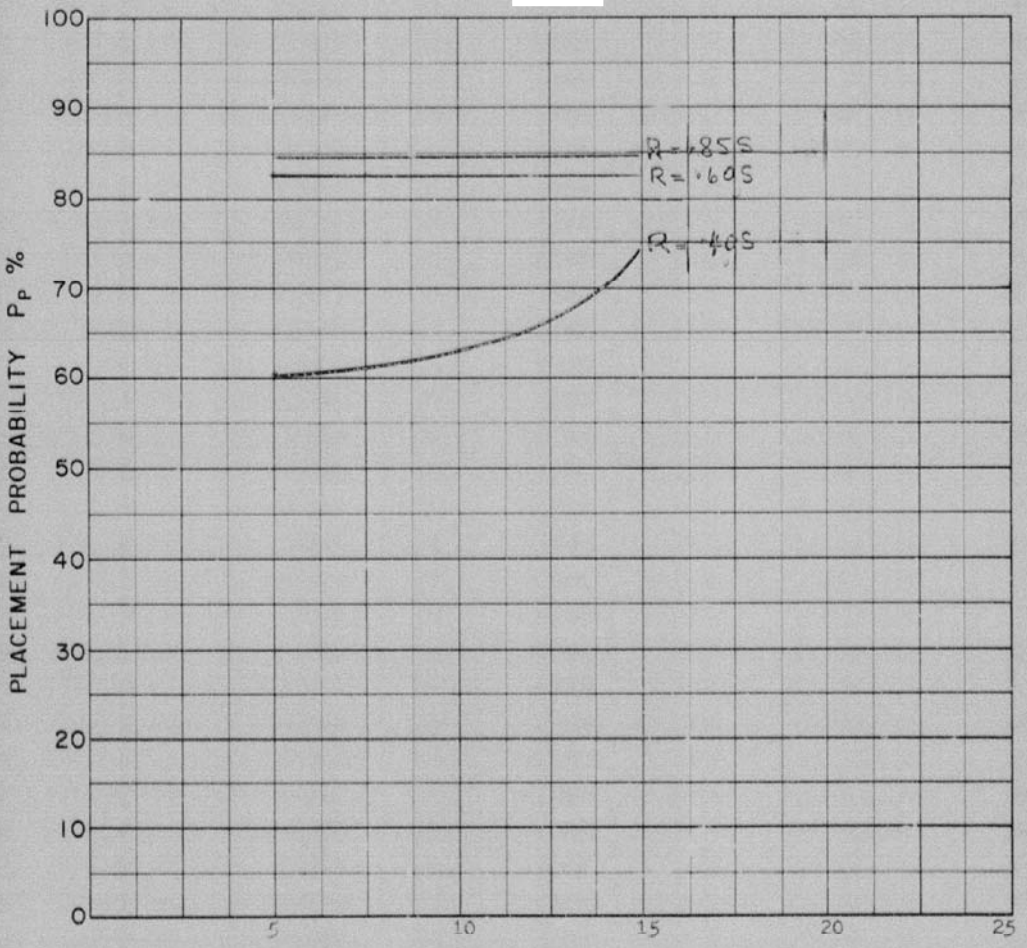

COURSE DIFFERENCE: 120°
TARGET EVASION: 0
TARGET MACH NO.: 2.0
INTERCEPTOR LATERAL G's: 3.35
INTERCEPTOR MACH NO.: 1.5
σ OF G.C.I. ACCURACY: 6.75 n.m.
A.I. DETECTION RANGE AS FRACTION OF SPECIFICATION RANGE, S: 3 values
A.I. DETECTION RANGE CONTOUR: Delta
ALTITUDE: 60 K

E-2

Launch zone of figure L-5

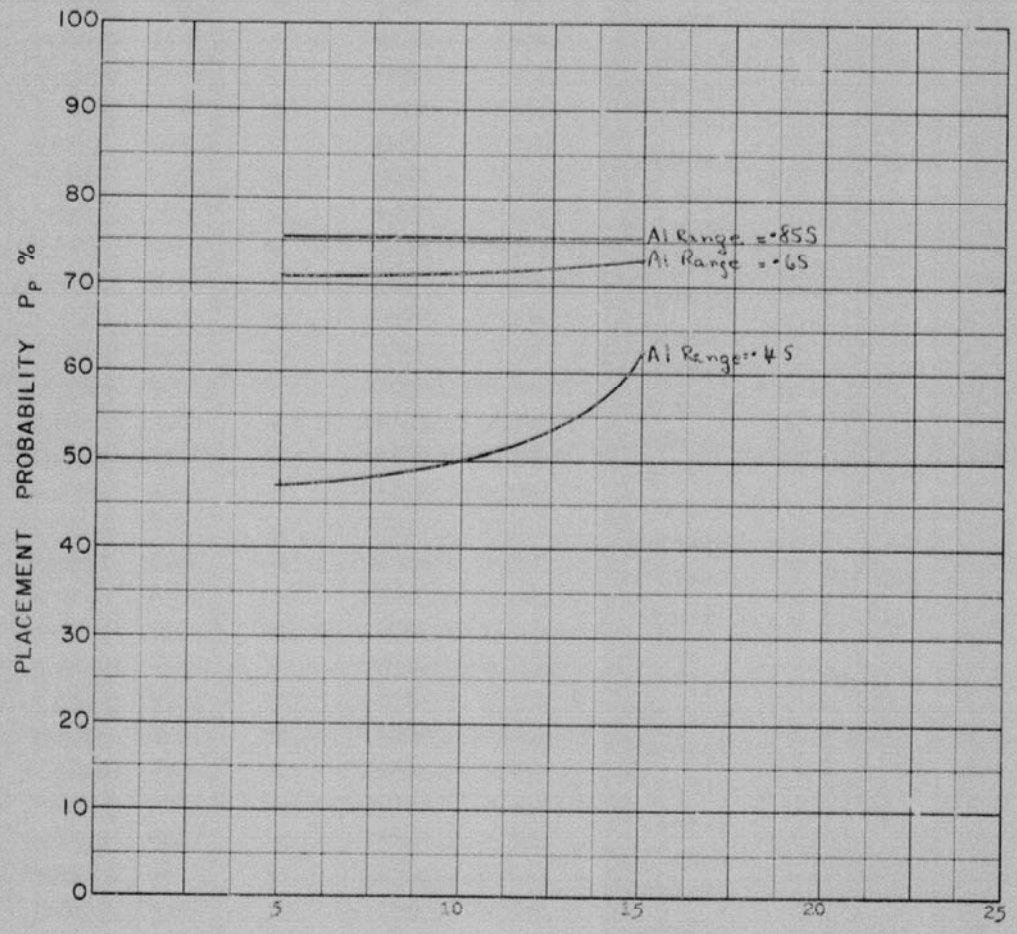

COURSE DIFFERENCE: 120°
TARGET EVASION: 0
TARGET MACH NO.: 2.0
INTERCEPTOR LATERAL G's: 3.35
INTERCEPTOR MACH NO.: 1.5
σ OF G.C.I. ACCURACY: 9 n.m.
A.I. DETECTION RANGE AS FRACTION OF SPECIFICATION RANGE, S: 3 values
A.I. DETECTION RANGE CONTOUR: Delta
ALTITUDE: 60 K

E-3

Launch zone of figure L-5

PRECEDING PAGE BLANK

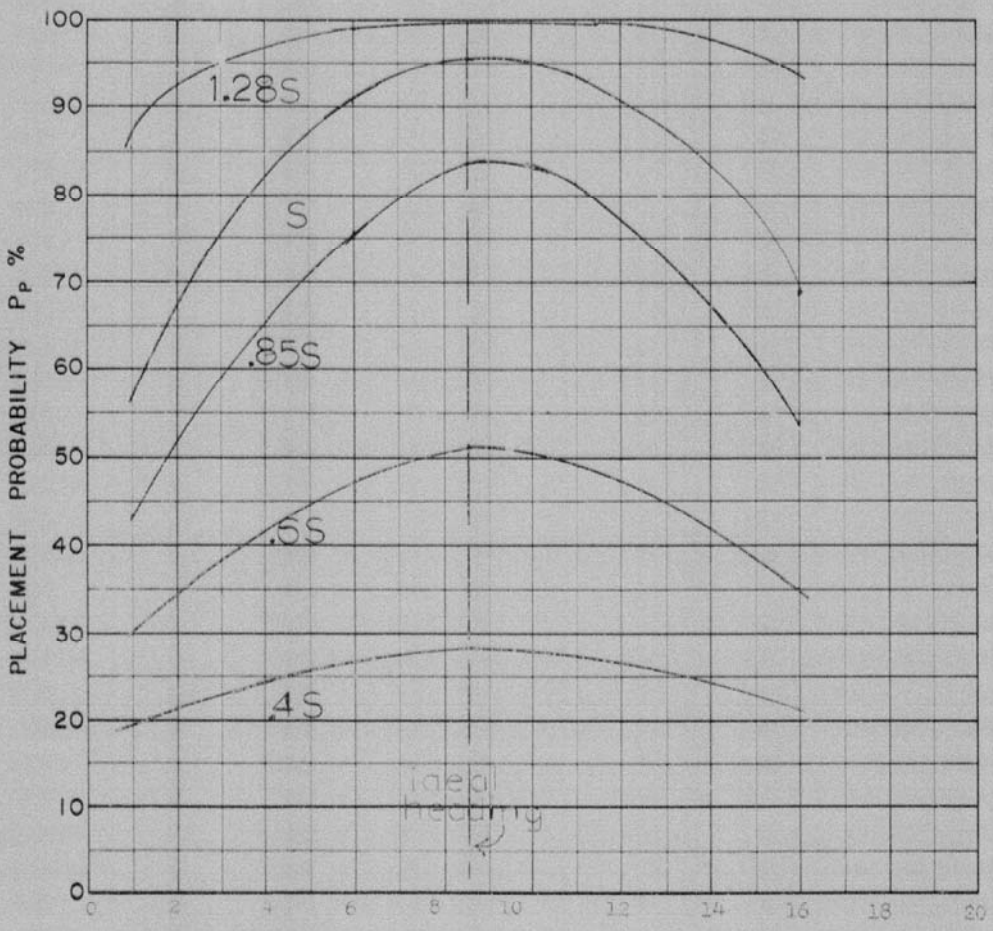

COURSE DIFFERENCE: 160°
TARGET EVASION: 0.1 lateral g's
TARGET MACH NO.: 2.0
INTERCEPTOR LATERAL G's: 0.66
INTERCEPTOR MACH NO.: 1.5
σ OF G.C.I. ACCURACY: 3 n.m.
A.I. DETECTION RANGE AS FRACTION OF SPECIFICATION RANGE, S: five values
A.I. DETECTION RANGE CONTOUR: Delta
ALTITUDE: 60K

F-1

Missile launch zone L 11

Abscissa: Angle off target path of attempted approach line.

1543

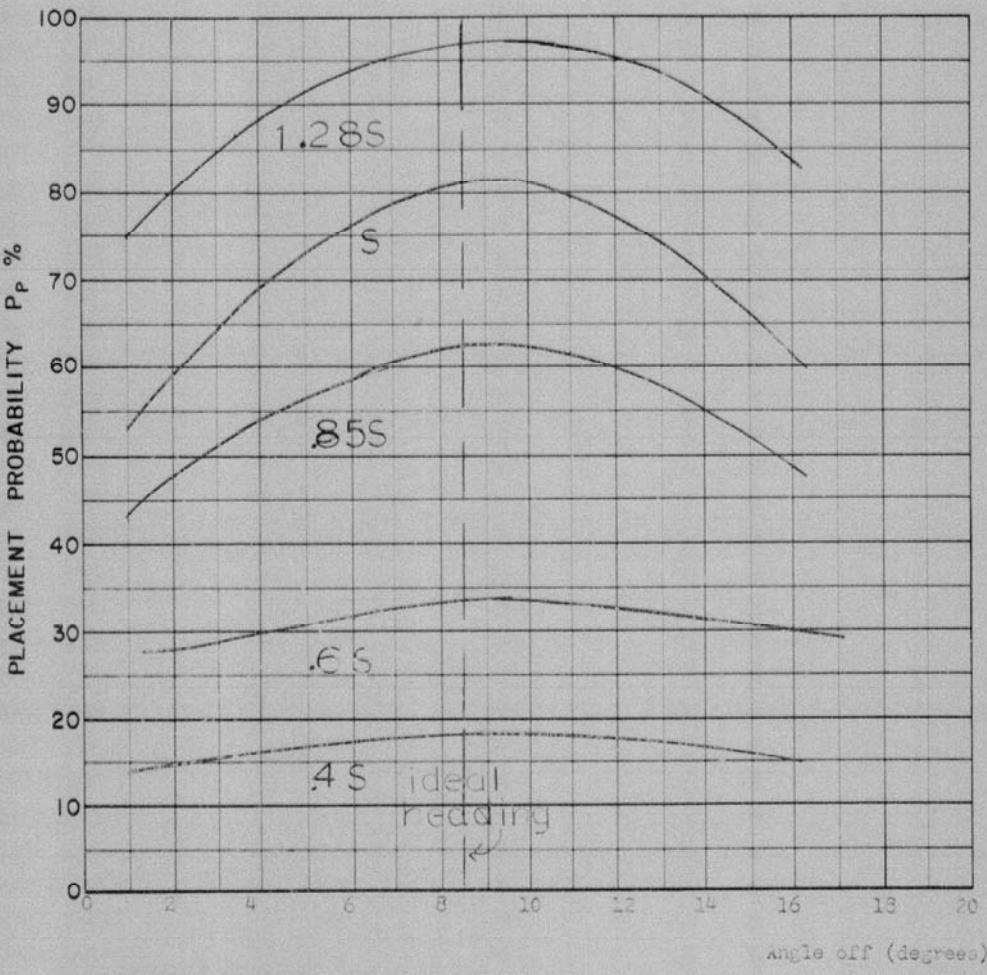

COURSE DIFFERENCE: 160°
TARGET EVASION: 0.1 lateral g's
TARGET MACH NO.: 2.0
INTERCEPTOR LATERAL G's: 0.66
INTERCEPTOR MACH NO.: 1.5
σ OF G.C.I. ACCURACY: 4.75 N.M.
A.I. DETECTION RANGE AS FRACTION OF SPECIFICATION RANGE, S: 5 values
A.I. DETECTION RANGE CONTOUR: Delta
ALTITUDE: 60K

(F-2)

Missile launch zone L 11

Abscissa: Angle off target path of attempted approach line.

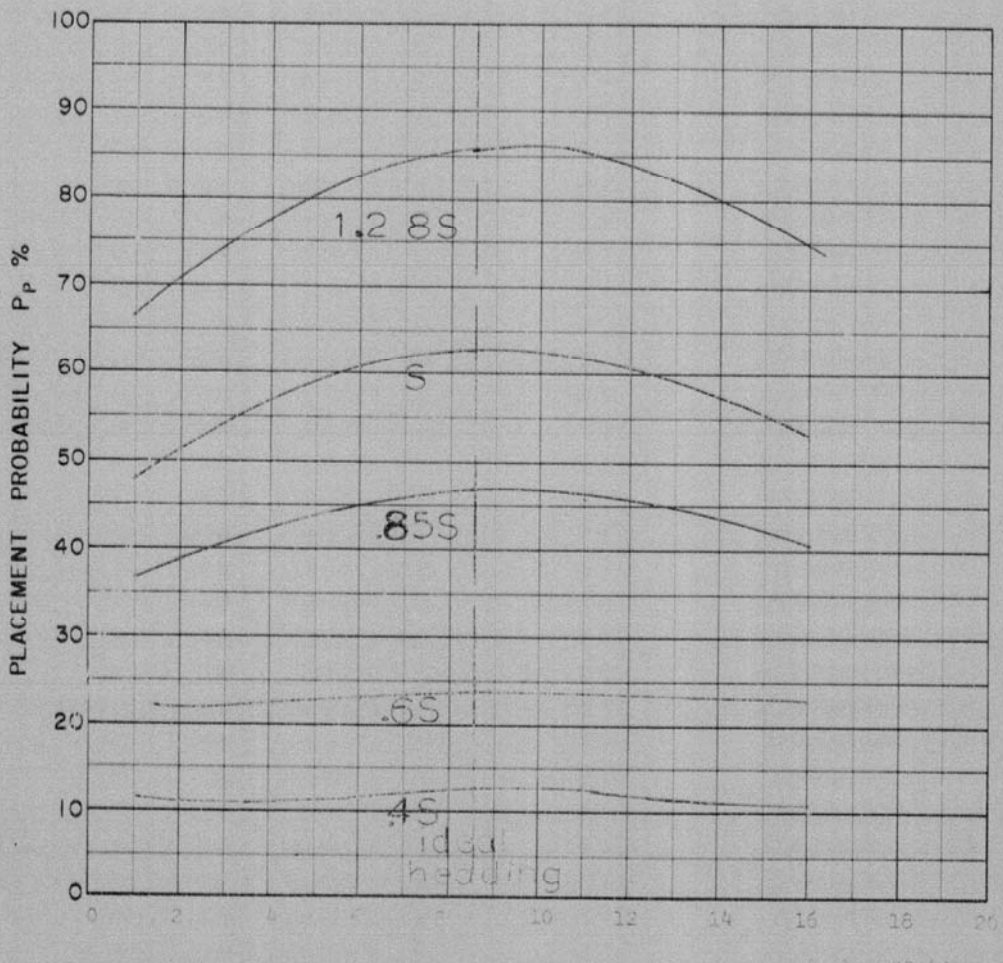

COURSE DIFFERENCE: 180°
TARGET EVASION: 0.4 lateral g's
TARGET MACH NO.: 2.0
INTERCEPTOR LATERAL G's: 0.65
INTERCEPTOR MACH NO.: 1.5
σ OF G.C.I. ACCURACY: 0.75 n.m.
A.I. DETECTION RANGE AS FRACTION OF SPECIFICATION RANGE, S: 5 value
A.I. DETECTION RANGE CONTOUR: Delta
ALTITUDE: 60K

(F-3)

Missile launch zone 1 11

Abscissa: Angle off target path of attempted approach line

154-5

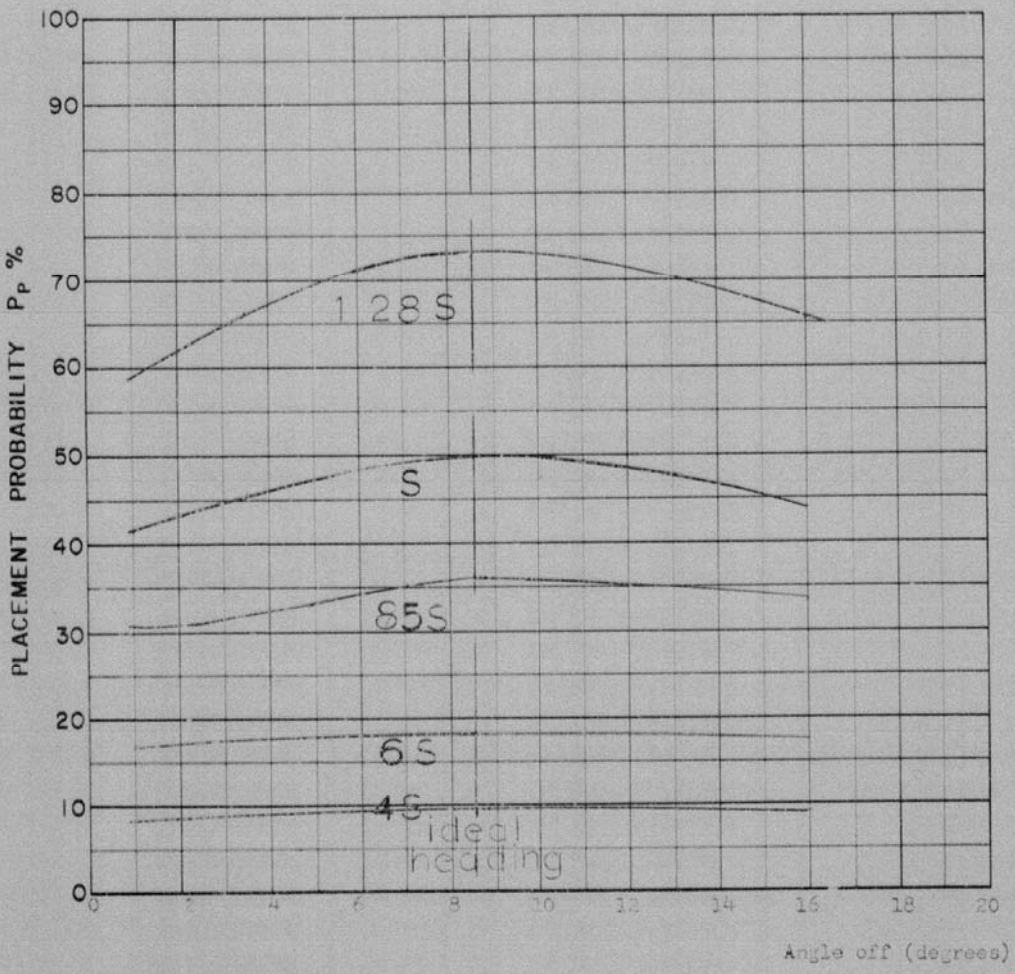

COURSE DIFFERENCE: 160°
TARGET EVASION: 0.1 lateral g's
TARGET MACH NO.: 2.0
INTERCEPTOR LATERAL G's: 0.66
INTERCEPTOR MACH NO.: 1.5
σ OF G.C.I. ACCURACY: 9 n.m.
A.I. DETECTION RANGE AS FRACTION OF SPECIFICATION RANGE, S: five values
A.I. DETECTION RANGE CONTOUR: Delta
ALTITUDE: 60K

F-4

Missile launch zone L 11

Abscissa: Angle off target path of attempted approach line.

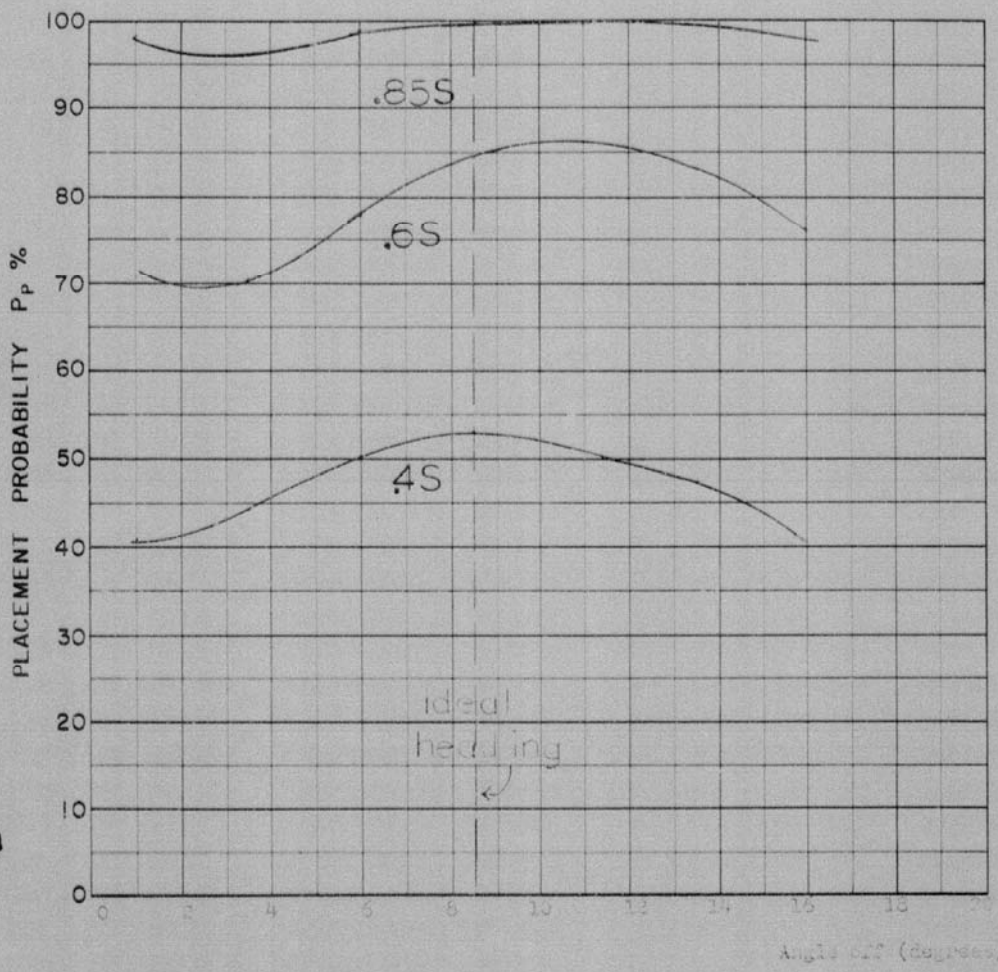

COURSE DIFFERENCE: 160°
TARGET EVASION: 0.1 lateral g's
TARGET MACH NO.: 2.0
INTERCEPTOR LATERAL G's: 1.5
INTERCEPTOR MACH NO.: 1.2
σ OF G.C.I. ACCURACY: 3 n.m.
A.I. DETECTION RANGE AS FRACTION OF SPECIFICATION RANGE, S: 3 values
A.I. DETECTION RANGE CONTOUR: Delta
ALTITUDE: 60K

F-5

Missile Launch Zone L 11

Abscissa: Angle off target path of attempted approach line

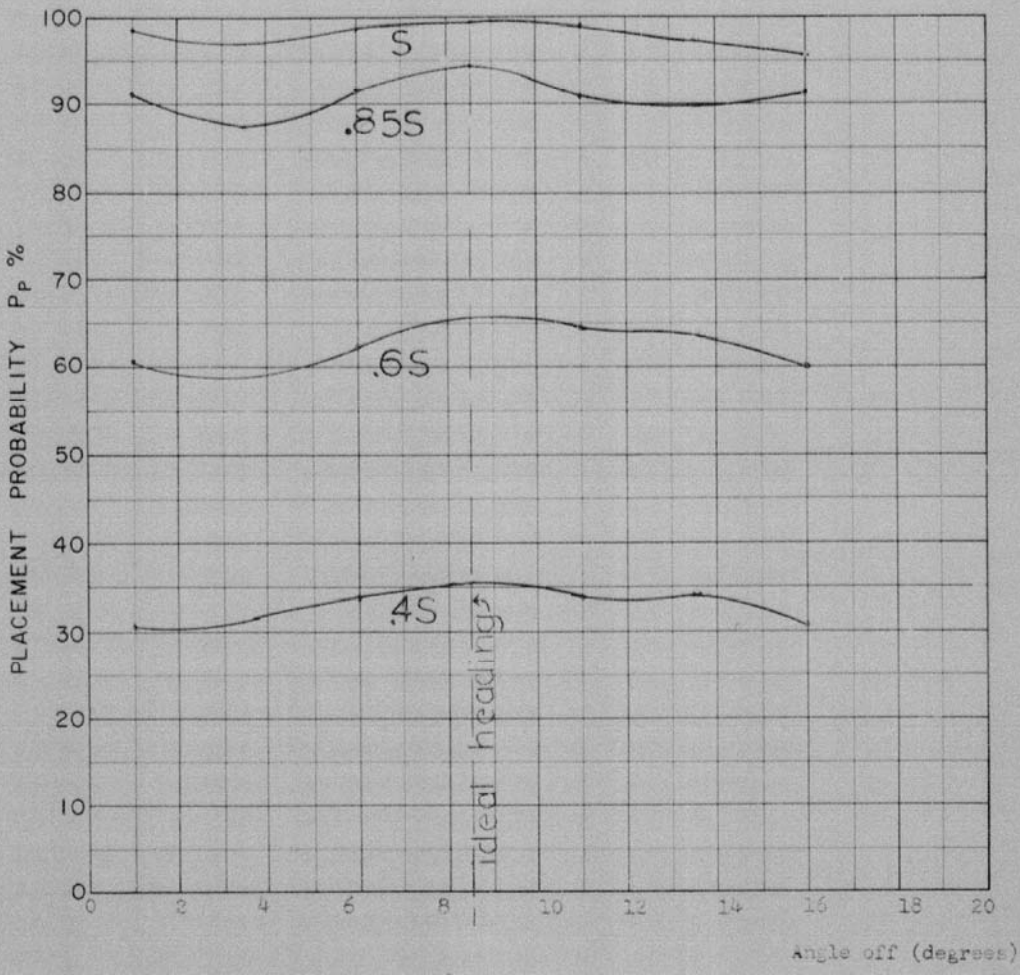

COURSE DIFFERENCE: 160°
TARGET EVASION: 0.1 lateral g's
TARGET MACH NO.: 2.0
INTERCEPTOR LATERAL G's: 1.5
INTERCEPTOR MACH NO.: 1.5
σ OF G.C.I. ACCURACY: 4.75 n.m.
A.I. DETECTION RANGE AS FRACTION OF SPECIFICATION RANGE, S: 4 values
A.I. DETECTION RANGE CONTOUR: Delta
ALTITUDE: 60K

(F-6)

Missile launch zone L 11

Abscissa: Angle off target path of attempted approach line

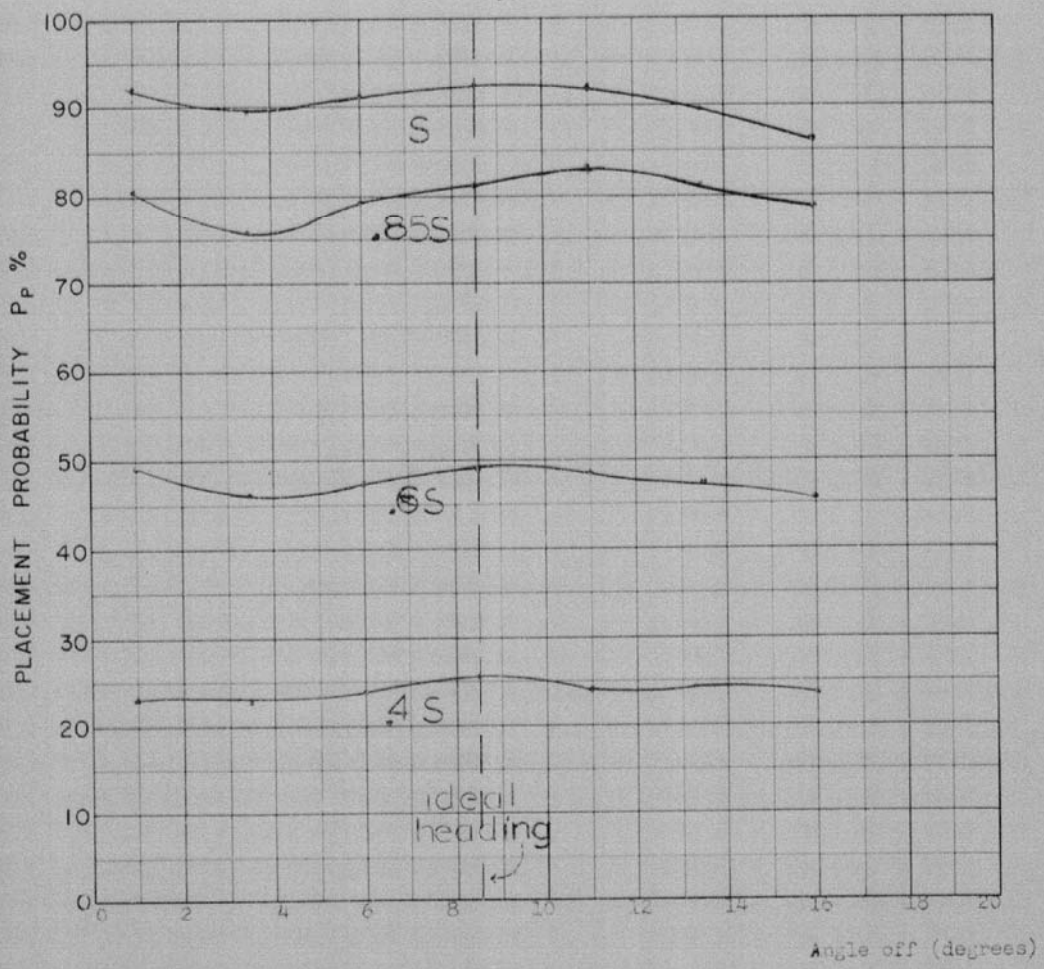

COURSE DIFFERENCE: 160°
TARGET EVASION: 0.1 lateral g's
TARGET MACH NO.: 2.0
INTERCEPTOR LATERAL G's: 1.5
INTERCEPTOR MACH NO.: 1.5
σ OF G.C.I. ACCURACY: 6.75 n.m.
A.I. DETECTION RANGE AS FRACTION OF SPECIFICATION RANGE, S: 4 values
A.I. DETECTION RANGE CONTOUR: Delta
ALTITUDE: 60K

F-7

Missile launch zone L 11

Abscissa: Angle off target path of attempted approach line

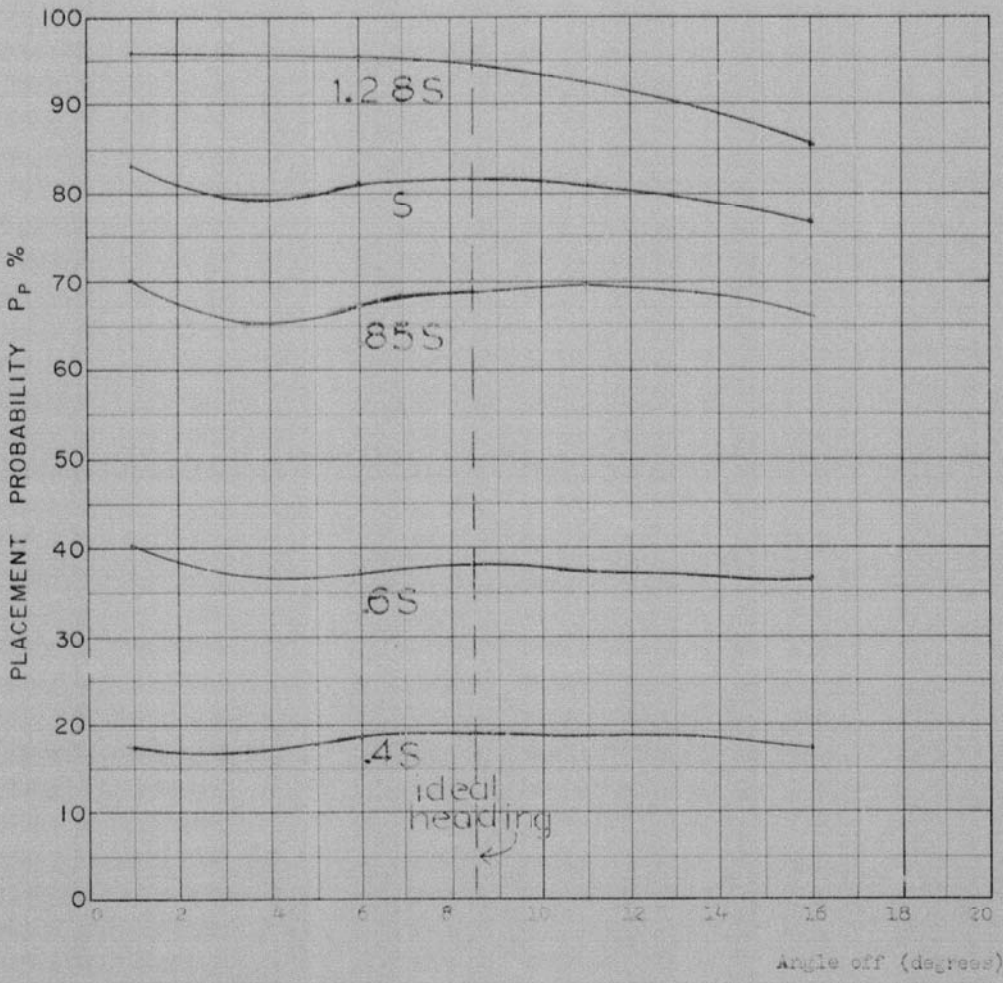

COURSE DIFFERENCE: 160°
TARGET EVASION: 0.5 lateral g's
TARGET MACH NO.: 2.0
INTERCEPTOR LATERAL G's: 1.5
INTERCEPTOR MACH NO.: 1.5
σ OF G.C.I. ACCURACY: 0.1 n.m.
A.I. DETECTION RANGE AS FRACTION OF SPECIFICATION RANGE, S: 5 values
A.I. DETECTION RANGE CONTOUR: Delta
ALTITUDE: 60k

F-8

Missile launch zone & ll

Abscissa: Angle off target path of attempted approach line

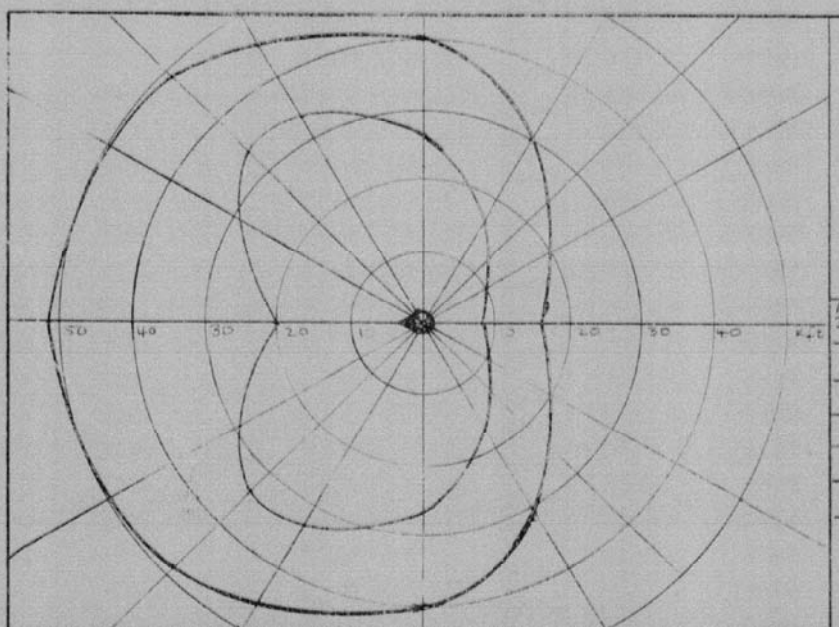

$M_T = 1.5$
$M_I = 1.5$
$H = 50K$

Ideal Course Difference at Launch	Aspect off Target
60	32
90	57
120	87
135	108
150	130

L-1

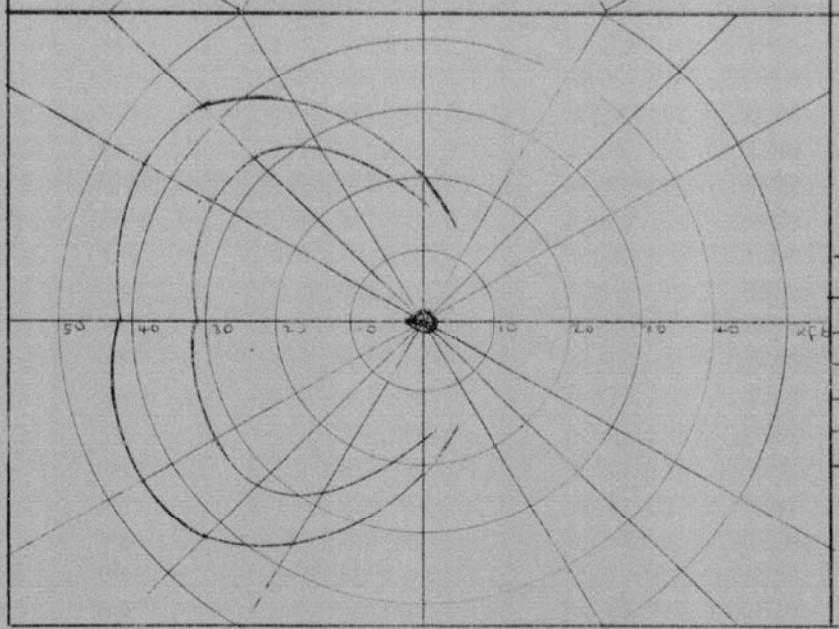

$M_T = 1.5$
$M_I = 1.5$
$H = 60K$

Course Diff at Launch	Aspect
60	32
90	57
120	87
135	108
150	130

L-2

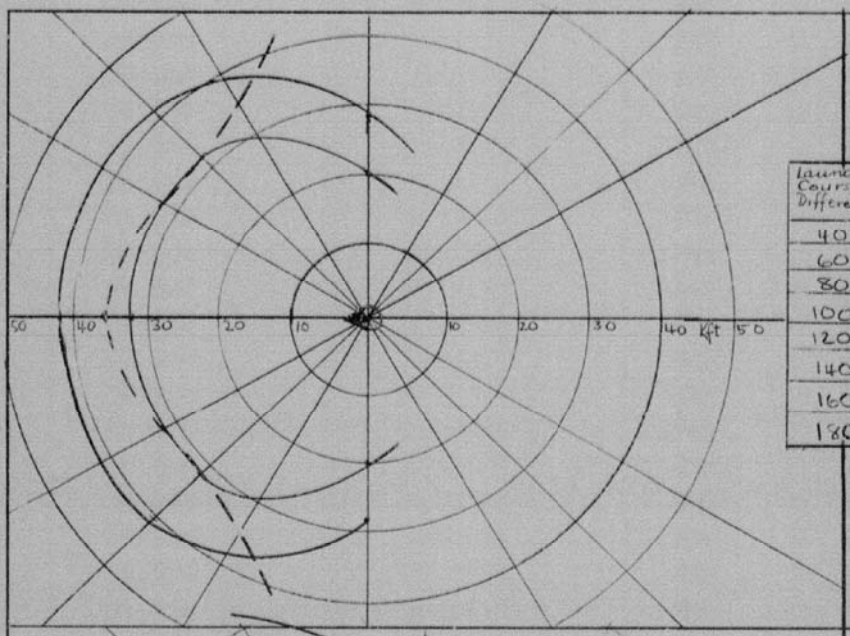

$M_T = 2.0$
$M_I = 1.5$
$H = 50K$

Launch Course Difference	Aspect off Target
40°	87°
60°	107°
80°	122°
100°	135°
120°	148°
140°	160°
160°	170°
180°	180°

L-3

L-4 - Dashed contour represents degraded seeker range in front zone

L-4

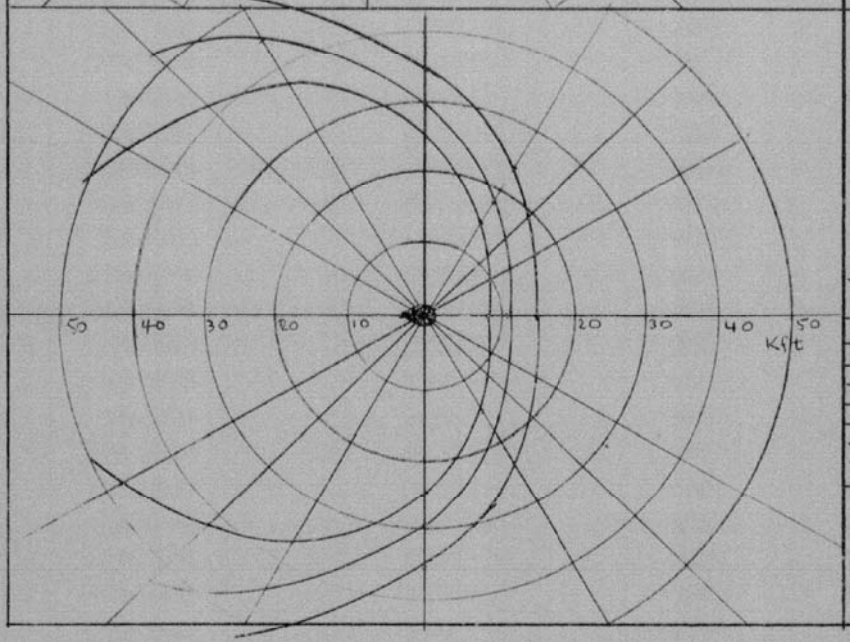

$M_T = 2.0$
$M_I = 1.8$
$H = 60K$

Front zone restricted by expected seeker range

Course Diff at Launch	Aspect off Target
10°	30°
17.5°	45°
25°	60°
37.5°	75°
52.5°	90°
68°	105°
87°	120°
106°	135°

L-8

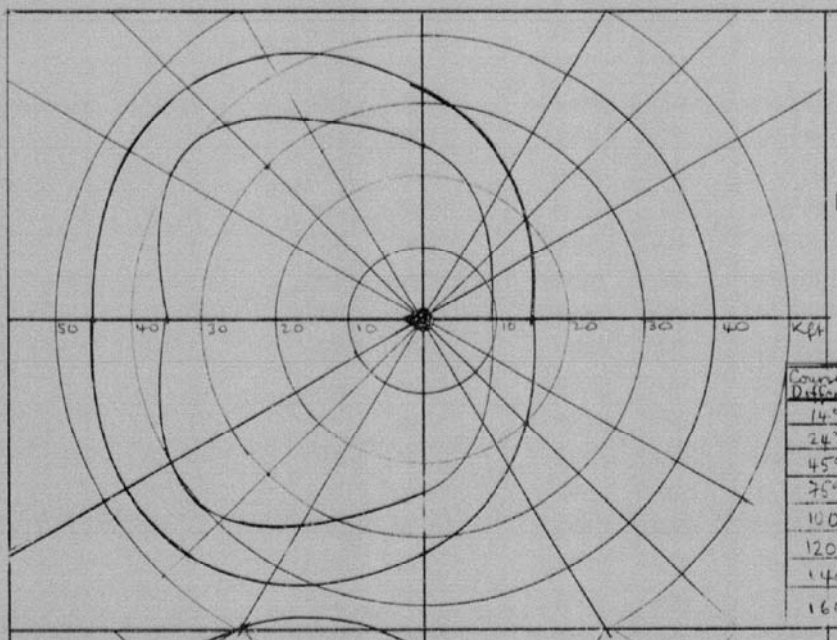

$M_T = 2.0$
$M_I = 1.5$
$H = 60K$

L5: same values of ideal course difference as L6, 7

L-5

Course Difference	Aspect
14°	45°
24°	60°
45°	95°
75°	115°
100°	132°
120°	144°
140°	158°
160°	168°

L-9

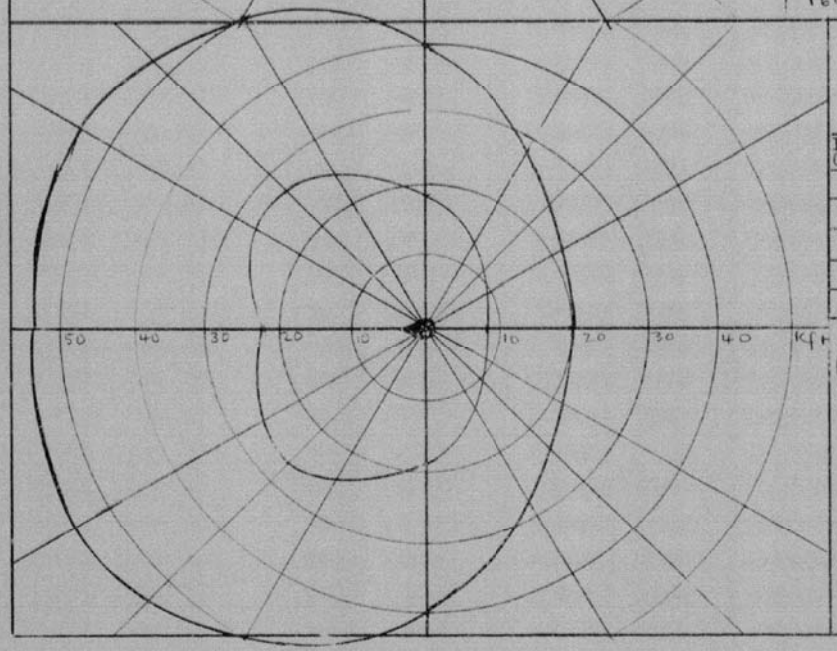

Same Kinematics as L5, L9

Ideal Launch Course Difference	Aspect
32°	90°
72°	120°
85°	135°
118°	150°
142°	160°

L-6 Maximum Range Contour Only

L-7 Minimum Range Contour Only

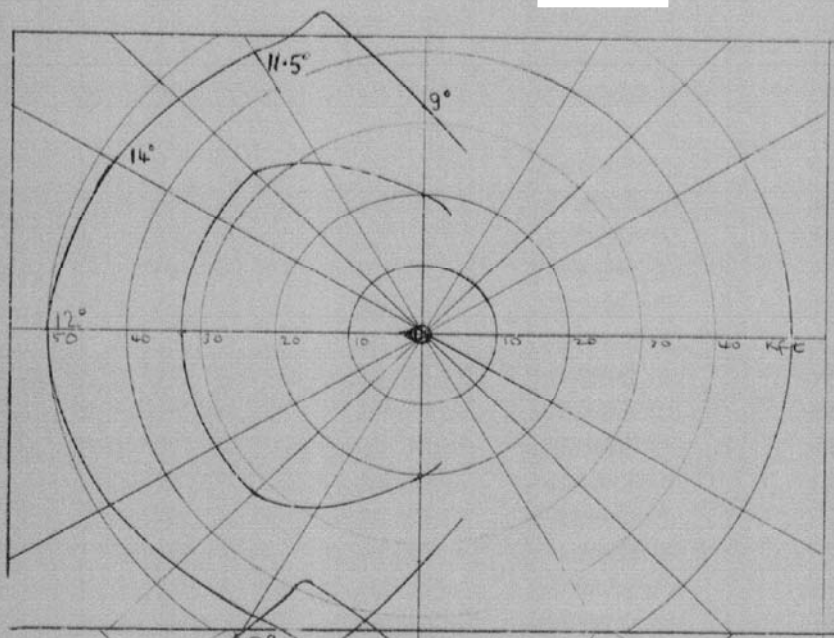

$M_T = 2 \cdot 0$
$M_I = 1 \cdot 5$
$H = 50K$

Heading error at minimum range ±5°, at maximum range as marked

Launch Course Difference vs Aspect off Target as for L·3

L·10

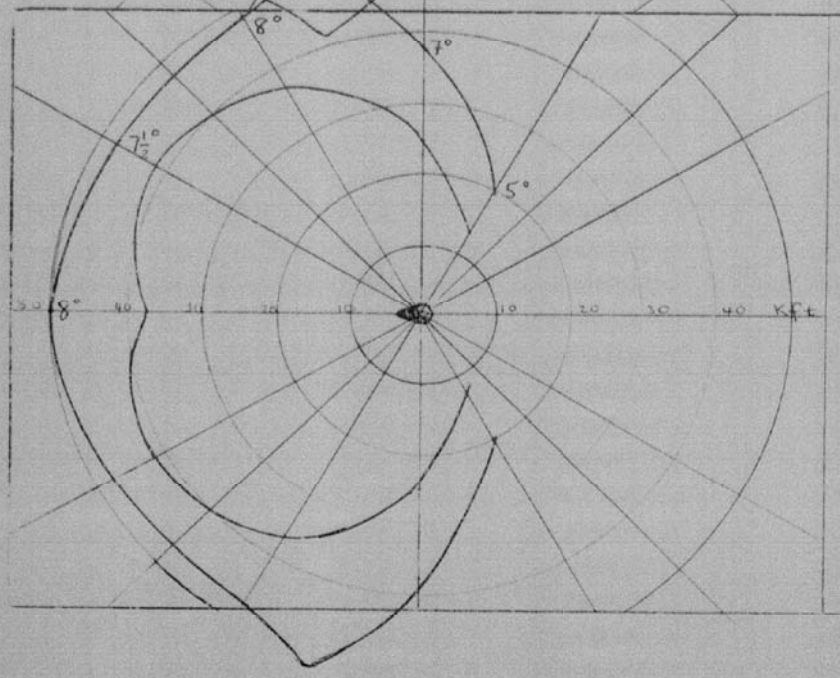

$M_T = 2 \cdot 0$
$M_I = 1 \cdot 5$
$H = 60K$

Heading error at minimum range 5°, at maximum range as marked

L·11

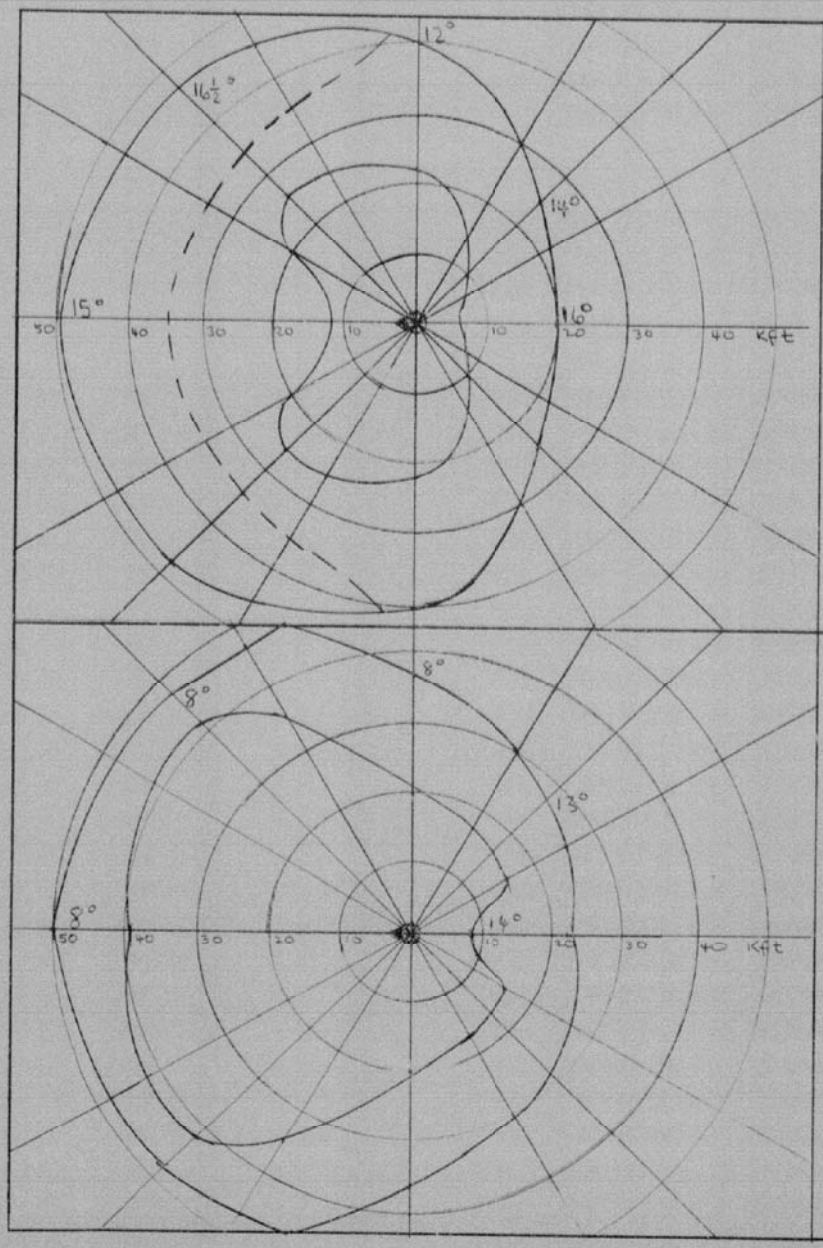

$M_T = 1 \cdot 5$
$M_L = 1 \cdot 5$
$H = 50K$

Heading error at minimum range = 5°, at maximum range as marked

Ideal Course Difference at Launch vs Aspect off target as for L-1

L-12

$M_T = 1 \cdot 5$
$M_L = 1 \cdot 5$
$H = 60\ K$

Heading error at minimum range = 5°, at maximum range as marked

Ideal Course difference at Launch as for L-2

L-13